

---

# Peptides

---

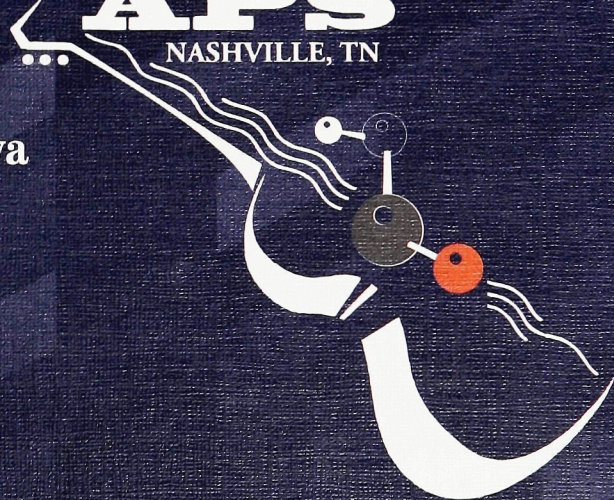
## Frontiers of Peptide Science

---

Proceedings of the Fifteenth  
American Peptide Symposium

Edited by  
James P. Tam and  
Pravin T.P. Kaumaya

15<sup>th</sup>  
**APS**  
NASHVILLE, TN



**KLUWER/ESCOM**



Peptides  
Frontiers of Peptide Science



# Peptides

## Frontiers of Peptide Science

Proceedings of the Fifteenth American Peptide Symposium  
June 14-19, 1997, Nashville, Tennessee, U.S.A.

Edited by

**James P. Tam**

*Department of Microbiology and Immunology,  
Vanderbilt University Medical School,  
Nashville, Tennessee, U.S.A.*

and

**Pravin T. P. Kaumaya**

*Departments of Ob/Gyn, Medical Biochemistry and Microbiology and  
The Comprehensive Cancer Center,  
The Ohio State University,  
Columbus, Ohio, U.S.A.*



**KLUWER ACADEMIC PUBLISHERS**

DORDRECHT / BOSTON / LONDON

## Library of Congress Cataloging-in-Publication Data

Peptides : frontiers of peptide science / edited by James P. Tam and Pravin T.P. Kaumaya.

p. cm.

"The Fifteenth American Peptide Symposium was held in Nashville, Tennessee, on June 14-19, 1997"--Pref.

Includes index.

ISBN 0-7923-5160-6 (hbk. : alk. paper)

1. Peptides--Congresses. I. Tam, James P. II. Kaumaya, Pravin T. P. III. American Peptide Symposium (15th : 1997 : Nashville, Tenn.)

QP552.P4P478 1998

572'.65--dc21

98-26533

ISBN 0-7923-5160-6

---

Published by Kluwer Academic Publishers,  
P.O. Box 17, 3300 AA Dordrecht, The Netherlands.

Sold and distributed in North, Central and South America  
by Kluwer Academic Publishers,  
101 Philip Drive, Norwell, MA 02061, U.S.A.

In all other countries, sold and distributed  
by Kluwer Academic Publishers,  
P.O. Box 322, 3300 AH Dordrecht, The Netherlands.

*Printed on acid-free paper*

All Rights Reserved

© 1999 Kluwer Academic Publishers and copyright holders  
as specified on appropriate pages within.

No part of the material protected by this copyright notice may be reproduced or utilized in any form or by any means, electronic or mechanical, including photocopying, recording or by any information storage and retrieval system, without written permission from the copyright owner.

Printed in the Netherlands

## Contents

Preface	xliii
Fifteenth American Peptide symposium Committees	xlvi
Acknowledgments - Benefactors, Sponsors, Donors, and Contributors	xlviii
The First Merrifield Award and Past Alan E. Pierce Awards	1
American Peptide Symposia	li
1997 Young Investigators Poster Competition Awards	liii
American Peptide Society Travel Grant Recipients	liv
Abbreviations	lvi
<b>First Merrifield Award Lecture-Makineni Lecture</b>	
Fifty Years of My Protein Synthesis <i>Shumpei Sakakibara</i>	1
<b>Keynote Lecture</b>	
“The time has come,” the walrus said, “to talk of many things...” -Lewis Carroll, Through the Looking Glass <i>Ralph Hirschmann</i>	11
<b>Session I. Peptide Diversity/Chemical Libraries</b>	
Novel Concept for the Synthesis of Cyclic Peptide Libraries <i>Lianshan Zhang, and James P. Tam</i>	19
Combinatorics, Peptide Mimetics, and Combizymes <i>Hyunsoo Han, Anthony M. Vandersteen and Kim D. Janda</i>	22
Peptides as Precursors in the Synthesis of Heterocyclic Positional Scanning Combinatorial Libraries <i>Jean-Philippe Meyer, John M. Ostresh, Adel Nefzi, Vince T. Hamashin, Christa C. Schoner, Marc A. Giulianotti, Amy L. Hannah, and Richard A. Houghten</i>	25

Expanding Molecular Diversity with Pseudopeptides and Macrotoxins. Synthesis, Characterization and Biological Activities of Macrocyclic Combinatorial Libraries	28
<i>Arno F. Spatola, Yvon Crozet, Peteris Romanovskis, and David Vogel</i>	
Solid Phase Synthesis of Peptidomimetics	31
<i>J. P. Mayer, D. Bankaitis-Davis, G. Beaton, K. Bjergarde, J. J. Gaudino, B. A. Goodman, C. J. Herrera, D. M. Lenz, G. S. Lewis, C. M. Tarlton, J. Zhang</i>	
Determination of the Amino Acid Composition of the Bioactive Components in Peptide Libraries	34
<i>Árpád Furka, Eugen Câmpian, Hans R. Tanner, and Hossain H. Saneii</i>	
Backbone Amide Linker (BAL) for Solid-Phase Synthesis of 2,5- Piperazinediones (DKP), Useful Scaffolds for Combinatorial Chemistry	37
<i>Fernando Albericio, Montse del Fresno, Ariadna Frieden, Miriam Royo, Jordi Alsina, Knud J. Jensen, Steven A. Kates, and George Barany</i>	
Fluorescent Quenched Substrates for Protein Disulfide Isomerase (PDI) Defined By the Use of Disulfide Bridge Containing Libraries	40
<i>J. C. Spetzler, V. Westphal, J.R. Winther, and M. Meldal</i>	
Solid Phase Synthesis of Cyclic Homodetic Peptide Libraries Utilizing a Novel Intraresin Chain Transfer	42
<i>Michael L. Moore, Kenneth A. Newlander, Heidemarie Bryan, William M. Bryan and William F. Huffman</i>	
Analysis of O-And N-Linked Glycopeptide Libraries by MALDI-TOF MS: Application in Solid Phase Assays of Carbohydrate-Binding-Proteins	45
<i>Phaedria M. St.Hilaire, Morten Meldal, and Klaus Bock</i>	
Unsymmetrically Functionalized Polyamine Libraries by a Solid Phase Strategy Starting from their Symmetrical Polyamine-Counterparts	47
<i>Gerardo Byk, Marc Frederic and Daniel Scherman</i>	
Development of DNA-Encoded Library Containing 10 <sup>9</sup> Backbone Cyclic Peptides on 7 µm Glass Beads	49
<i>Anna Balanov, Eran Hadas, Ilana Cohen</i>	
Introduction of Bulky Betidamino Acids in Thyrotropin Releasing Hormone (TRH)	51
<i>Dean A. Kirby, Marvin C. Gershengorn, and Jean E. Rivier</i>	

Combinatorial Libraries and Polyamines in the Battle against Third World Trypanosomes <i>Helen K. Smith, and Mark Bradley</i>	53
Hybrid Resin for Synthesis and Screening of Synthetic Peptide Libraries <i>Hoebert S. Hiemstra, Willemien E. Benckhuijsen, Wolfgang E. Rapp, and Jan W. Drijfhout</i>	55
Combinatorial Libraries: Equimolar Incorporation of Benzaldehyde Mixtures in Reductive Alkylation Reactions <i>John M. Ostresh, Christa C. Schoner, Marc A. Giulianotti, Michael J. Kurth, Barbara Dörner and Richard A. Houghten</i>	57
Potential Cancer Vaccine: Anti-Idiotypic Antibody Developed from Antigen Binding Peptides Bind to Human Breast Cancer Antigen <i>John Mark Carter, Judy Singleton, Phoebe Strome, Cindy Coleman, Vernon Alvarez</i>	59
Studying Receptor-Ligand Interactions Using Encoded Amino Acid Scanning <i>Julio A. Camarero, Joanna Pavel, Tom W. Muir</i>	61
A Double-Bond-Containing Angiotensin and Its Derivatization into Linear vs. Branched Analogs <i>Kun-hwa Hsieh, and Garland R. Marshall</i>	63
Synthesis and Application of Tyrosine Kinase Substrate Libraries <i>Song Zheng, Richard Cummings, Rose Cubbon, Young-Whan Park, Patricia Cameron, Patrick Griffin, Jeffrey Hermes</i>	65
Encoding Schemes for Application with Polyethylene Glycol-Polystyrene Graft (PEG-PS) Supports in Solid-Phase Peptide and Small Molecule Synthesis <i>Steven A. Kates, Wade Hines, Michael A. Kelley, Paul Lynch, Fernando Albericio, and George Barany</i>	67
Use of Phage Display and Cellulose-Bound Peptide Libraries for the Identification of Urea Herbicide Binding Peptides <i>Ulrich Hoffmüller, Christine Rottenberger, Günter Wellnhofer, Leodevico L. Ilag, Jürgen Spindler, and Jens Schneider-Mergener</i>	69
High Affinity Binding Peptides for Phosphatase <i>Stefan Vetter, and Holger Schmid</i>	71
<b>Session II. De Novo Design of Peptides &amp; Proteins</b>	
Five Axioms for Protein Engineering: Keys for Understanding Protein Structure/Function? <i>Dan W. Urry</i>	75

Novel Collagen-Mimetic Structures <i>Elizabeth A. Jefferson, and Murray Goodman</i>	79
<i>De Novo</i> Design of $\alpha$ -Helical Coiled-Coils: the Effect on Stability of Amino Acid Substitution in the Hydrophobic Core <i>Kurt C. Wagschal, Brian Tripet, Pierre Lavigne, and Robert S. Hodges</i>	82
Towards Full Mimics of Antibodies: A 37-aa Mini-protein with Two Independent Activities <i>Antonello Pessi, Elisabetta Bianchi, Jaques Neyton, Eugenia Drakopolou, and Claudio Vita</i>	85
Optical Holographic Data Storage Using Peptides <i>Rolf H. Berg, Palle H. Rasmussen, Soren Hvilsted, P.S. Ramanujam</i>	88
Developing Synthetic Hemoprotein Mimetics: Design, Synthesis and Characterization of Heme-Peptides Conjugates <i>Angela Lombardi, Flavia Nastri, Luca D. D'Andrea, Ornella Maglio, Gabriella D'Auria, Carlo Pedone, Vincenzo Pavone</i>	91
A Novel Class of Calmodulin Mimetics: <i>De Novo</i> Designed Proteins in Molecular Recognition <i>Angela Lombardi, Giovanna Ghirlanda, Laura Zaccaro, Vincenzo Pavone, and William F. DeGrado</i>	94
Non native Architectures in Protein Design: Four Helix Bundles as Locked-in Tertiary Fold <i>Marc Mathieu, and Gabriele Tuchscherer</i>	97
Synthesis and <i>In Vivo</i> Pharmacological Profile of Dimeric HOE 140 Bradykinin antagonists <i>Muriel Amblard, Isabelle Daffix, Gilbert Bergé, Pierre Dodey, Didier Pruneau, Jean-Luc Paquet, Pierre Béliard, Jean-Michel Luccarini, and Jean Martinez</i>	100
Conformations and Use of Beta-Amino Acid Residues <i>Isabella L. Karle</i>	103
Modular Design of Synthetic Redox and Light-Absorbing Proteins <i>Wolfgang Haehnel, Harald K. Rau, Heike Snigula, and Hugo Scheer</i>	106
Synthesis of Semicaged Ruthenium(II) Complexes of a Branched Peptide Containing Three Bipyridine Ligands <i>Barney M. Bishop, Matthew C. Foster, Richard W. Vachet, and Bruce W. Erickson</i>	108

Design of New Tentoxin Analogues: Study of the ATP-Synthase Catalytic Mechanism	110
<i>Florine Cavelier, Christine Enjalbal, Jérôme Santolini, Francis Haraux, Claude Sigalat, Jean Verducci, and François André</i>	
Investigation of conformational Properties of Calcium-binding Peptides in the Cell Adhesion Molecules	112
<i>Wei Yang and Jenny J. Yang</i>	
End Capping and Helix Stabilization in Short Peptides	114
<i>Hemender K. Reddy, and Krishnan P. Nambiar</i>	
Novel $\alpha,\alpha$ -Disubstituted Amino Acids for Peptide Secondary Structure Control	116
<i>Christopher L. Wysong, Muna K. Thalji, Thad A. Labbe, and Robert P. Hammer</i>	
Design of Antimicrobial Peptides Based on Sequence Analogy and Amphipathicity	118
<i>A. Tossi, C. Tarantino, N. Mitaritonna, G. Rocco, D. Romeo</i>	
Synthesis and Structural Characterization of the Ligand Binding Site of Macrophage Scavenger Receptor	120
<i>Hironobu Hojo, Yoshiko Akamatsu, Yu Nakamura, Shunji Miki, Kiyoshi Yamauchi, and Masayoshi Kinoshita</i>	
Enantiomeric Structural Libraries of Unnatural Peptides Which Bind DNA and Alter Enzymatic Activity	122
<i>L. M. Martin, B-H Hu, and C. Li</i>	
Interplay of Hydrophobic and Electrostatics in Peptide-bilayer Interactions	124
<i>Li-Ping Liu and Charles M. Deber</i>	
An Investigation of Position 3 in Arginine Vasopressin (AVP)	126
<i>M. Manning, S. Stoev, L.L. Cheng, A. Olma, W.A. Klis, W.H. Sawyer, N.C. Wo, and W.Y. Chan</i>	
Design and Expression of Recombinant Rop Protein Analogs Which Have Metal Binding Ability	128
<i>Takahisa Nakai, Osamu Odawara, Takemune Yasuda, and Nobutaka Tani</i>	
Combination of $\alpha$ -Helix Peptides with Intercalator Anthracene for Reporting Peptide-DNA Interactions	130
<i>Tsuyoshi Takahashi, Akihiko Ueno, Hisakazu Mihara</i>	

Macroitorials: Concept and Synthetic Examples Using PTH(1-34) <i>Wanli Ma, Jeffrey A. Dodge, and Arno F. Spatola</i>	132
Metal Ion-induced Folding of a <i>De Novo</i> Designed (-Helical Coiled-coil <i>W. D. Kohn, C. M. Kay, and R. S. Hodges</i>	134
$\alpha$ to $\beta$ Transitions of Peptides Caused by Hydrophobic Defects <i>Yuta Takahashi, Akihiko Ueno, Hisakazu Mihara</i>	136
A Natural Motif Approach to Protein Folding and Design [1] <i>Daniel J. Butcher, M. Anna Kowalska, Song Li, Zhaowen Luo, Simei Shan, Zhixian Lu, Stefan Niewiarowski, and Ziwei Huang</i>	138
Engineering of a Cationic Coiled-Coil Protein Bearing RGD-Like Ligands on Proline-II Helical Spacers <i>Harold D. Graham Jr., Deborah M. John, and Bruce W. Erickson</i>	140
Conformational Comparison of Peptide Templates and Their Folding Enhancements on TASP <i>Zhenwei Miao, Guangzhong Tu, Xiaojie Xu, Riqing Zhang, and Youqi Tang</i>	142
Use of a Potent and Selective Highly Constrained Peptide Agonist to Design <i>De Novo</i> an Equally Potent and Selective Non-Peptide Mimetic for the $\delta$ Opioid Receptor <i>Victor J. Hruby, Subo Liao, Mark D. Shenderovich, Josue Alfaro-Lopez, Keiko Hosohata, Peg Davis, Frank Porreca, and Henry I. Yamamura</i>	144
Engineering of the Deltoid Protein: A Model for the Four Corners of Quadrin, a Square Octamer from the Hepatitis delta Antigen <i>Matthew J. Saderholm, Gopal K. Balachandran, Stanley M. Lemon, and Bruce W. Erickson</i>	146
Engineering of Helical Oligoproline Redox Assemblies That Undergo Photoinduced Electron Transfer <i>Cheryl A. Slate, Durwin R. Striplin, Robert A. Binstead, Thomas J. Meyer, and Bruce W. Erickson</i>	148
The Use of 5-tert-Butylproline to Study Nucleation of Polyproline Type I Conformation <i>Eric Beausoleil, and William D. Lubell</i>	150
Structure-Activity Relationships in Cyclic $\beta$ -Sheet Antibacterial Peptides <i>Leslie H. Kondejewski, Masood Jelokhani-Niaraki, Robert E.W. Hancock, and Robert S. Hodges</i>	152

Chimeric TASP Molecules as Biosensors <i>Lukas C. Scheibler, Pascal Dumy, Mila Bontcheva, Horst Vogel, and Manfred Mutter</i>	154
Topologies of Consolidated Ligands for the SRC Homology (SH)3 and SH2 Domains of Abelson Protein-Tyrosine Kinase <i>Qinghong Xu, Jie Zhang, George Barany, and David Cowburn</i>	156
Toward Design of a Triple Stranded Antiparallel $\beta$ -Sheet <i>Heather L. Schenck, and Samuel H. Gellman</i>	158
Copper(II)-Induced Folding of Betabellin 15D, a Designed Beta-Sheet Protein <i>Amareth Lim, Mattias Kroll, Yibing Yan, Matthew J. Saderholm, Alexander M. Makhov, Jack D. Griffith, and Bruce W. Erickson</i>	160
Engineering of an Iron(II)-Braced Tripod Protein Containing Proline-II Helical Legs <i>Bassam M. Nakhle, Tracie L. Vestal, Matthew J. Saderholm, and Bruce W. Erickson</i>	162
<i>De Novo</i> Design and Synthesis of a Heme-binding Four-helix TASP Capable of Light-induced Electron Transfer <i>Harald K. Rau, Niels de Jonge, and Wolfgang Haehnel</i>	164
Inhibition of Nitric Oxide Synthase with Calmodulin Binding Peptides <i>Karen S. Gregson, Michael A. Marletta, and Henry I. Mosberg</i>	166
Improved Peptides for Holographic Data Storage <i>Palle H. Rasmussen, P.S. Ramanujam, Søren Hvilsted, and Rolf H. Berg</i>	168
<b>Session III. Peptide Mimetics</b>	
Structure-Based <i>De Novo</i> Design and Discovery of Novel Peptidomimetic and Nonpeptide Antagonists of the pp60 <sup>src</sup> (Src) SH2 Domain <i>K. S. Para, E. A. Lunney, M.S. Plummer, C. J. Stankovic, A. Shahripour, D. Holland, J. R. Rubin, C. Humblet, J. Fergus, J. Marks, S. Hubbell, R. Herrera, A. R. Saltiel, and T. K. Sawyer</i>	173
New RGDamphiphilic Cyclic Peptide and New RGD-Mimetic Constrained Diketopiperazines <i>Jean-François Pons, Mamadou Sow, Frédéric Lamaty, Jean-Luc Fauchère, Annie Molla, Philippe Viallefont, and René Lazaro</i>	176

A Pharmacophore Model of a Novel Hematopoietic Peptide, SK&F 107647 and Design of Peptidomimetic Analogs	178
<i>P. K. Bhatnagar, E. K. Agner, D. Alberts, J. Briand, L. J. F. Callahan, A. S. Cuthbertson, H. Fjordingstad, D. Heerding, J. Hiebl, W. F. Huffman, M. Hybsen, A. G. King, S. LoCastro, D. Lovhug, L. M. Pelus, G. Seibel, J. S. Takata</i>	
Design and Synthesis of Potent and Selective Peptidomimetic Vitronectin Receptor Antagonists	181
<i>Jochen Knolle, Roland Baron, Gerhard Breipohl, Pierre Broto, Tom Gadek, Jean F. Gourvest, Glenn R. Hammonds, Anusch Peyman, Karl H. Scheunemann, Hans U. Stilz, and Volkmar Wehner</i>	
Structure-Based Design of Small Molecule Protein-Tyrosine Phosphatase Inhibitors	183
<i>Zhu-Jun Yao, Bin Ye, He Zhao, Xinjian Yan, Li Wu, David Barford, Shaomeng Wang, Zhong-Yin Zhang, and Terrence R. Burke, Jr.</i>	
Structure-Activity Relationships and Spectroscopic Insights into a Series of Retro-Inverso Tachykinin NK-1 Receptor Antagonists	186
<i>A. Sisto, R. Cirillo, B. Conte, C. I. Fincham, E. Monteagudo, E. Potier, R. Terracciano, F. Cavalieri, M. Venanzi, and B. Pispisa</i>	
Immunologically - Active Mimetics of Muramyl Dipeptide	188
<i>Danijel Kikelj, Alenka Rutar, Irena Merslavic, Lucka Povsic, and Anton Stalc</i>	
Peptidomimetic Tyrosine Kinase Inhibitors Induce Non Apoptotic Clarke III Type Programmed Cell Death	190
<i>György Kéri, László Orfi, Gergely Szántó, Judit Érchegeyi, Ferenc Hollósy, Miklós Idei, Anikó Horváth, István Teplán, Aviv Gazit, Zsolt Szegedi, Béla Szende</i>	
SAR of a series of Related Peptidomimetics Derived from a Novel Hematopoietic Peptide, SK&F 107647	192
<i>J. F. Callahan, D. Alberts, J. L. Burgess, L. Chen, W. F. Huffman, A. G. King, S. LoCastro, L. M. Pelus, and P. K. Bhatnagar</i>	
Applications of Tropane-Based Peptidomimetics	194
<i>Philip E. Thompson, David L. Steer, Kerry A. Higgins, Marie-Isabel Aguilar, and Milton T.W. Hearn</i>	
Structure-Activity Relationship Studies of Dialkylamine Derivatives Exhibiting Wide Spectrum Antimicrobial Activities	196
<i>U. P. Kari, S.R. Maddukuri, M.T. MacDonald, L.M. Jones, D.L. MacDonald, W.L. Maloy</i>	

Identification of Prototype Peptidomimetic Agonists at the Human Melanocortin Receptors, MC1R and MC4R	198
<i>Carrie Haskell-Luevano, Tomi K. Sawyer, Mac E. Hadley, Victor J. Hruby, and Ira Gantz</i>	
Cyclic Somatostatins Containing $\alpha$ -Benzyl-O-AMPA as a Cis Peptide Bond Mimic	200
<i>Dirk A. Tourwe, Valerie Brex, Jo Van Betsbrugge, and Patricia Verhcyden</i>	
Alpha-Helix Nucleation Between Peptides Using a Covalent Hydrogen Bond Mimic	202
<i>Elena Z. Dovalsantos, Edelmira Cabezas, Arnold C. Satterthwait</i>	
Development of Inhibitors of MAdCAM-1/ $\alpha_4\beta_7$ Interactions	204
<i>H. N. Shroff, C. F. Schwender, A. D. Baxter, N. Hone, N. A. Cochran, D.L. Gallant, M.J. Briskin</i>	
Synthesis of Cyclic RGD-Tetra-Peptoids and Optimization of the Submonomer Solid Phase Coupling Protocol	206
<i>Jorg Schmitt, S. L. Goodman, A. Jonczyk and Horst Kessler</i>	
Reduced Amide Bond Pseudopeptides Induce Antibodies Against Native Proteins of <i>Plasmodium falciparum</i>	208
<i>José-Manuel Lozano, Fabiola Espejo, Diana Diaz, Fanny Guzmán, Julio C. Calvo, Luz M. Salazar, Manuel Elkin Patarroyo</i>	
Inhibition of Ras Farnesyl Transferase by Histidine-(N-Benzylglycinamide) Type Molecules	210
<i>Kevon R. Shuler, Daniele M. Leonard, Dennis J. McNamara, Jeffrey D. Scholten, Judith S. Sebolt-Leopold, Annette M. Doherty</i>	
Synthesis of Dipeptide Secondary Structure Mimetics	212
<i>Masakatsu Equchi, Hwa-Ok Kim, Benjamin S. Gardner, P. Douglas Boatman, Min S. Lee, Hiroshi Nakanishi, and Michael Kahn</i>	
Design and Synthesis of Nanomolar $\delta$ -Opioid Selective Non-Peptide Mimetic Agonists Based on Peptide Leads	214
<i>Subo Liao, Mark D. Shenderovich, Josue Alfaro-Lopez, Dagmar Stropova, Kaiko Hosohata, Peg Davis, Kevin A. Jernigan, Frank Porreca, Henry I. Yamanura, and Victor J. Hruby</i>	

Development of the New Potent Non-Peptide GpIIb/IIIa Antagonist NSL-95301 by Utilizing Combinatorial Idea	216
<i>Yoshio Hayashi, Takeo Harada, Jun Katada, Akira Tachiki, Kiyoko Iijima, Tohru Asari, Isao Uno, and Iwao Ojima</i>	
A flexible Strategy for the Incorporation of Ureas into Peptide Linkages	218
<i>J. A. Kowalski and M. A. Lipton</i>	
<b>Session IV. Synthetic Methods</b>	
On-resin N-methylation circumvents a Deletion Peptide Formed during the Synthesis of Cyclosporin Analogs	223
<i>Prakash Raman, Yvonne M. Angell, George R. Flentke, and Daniel H. Rich</i>	
Synthetic Approaches to Elucidate Roles of Disulfide Bridges in Peptides and Proteins	226
<i>George Barany</i>	
Synthesis of Cyclopsychotride by Orthogonal Ligation Using Unprotected Peptide Precursor	229
<i>Yi-An Lu and James P. Tam</i>	
Methionine as the Ligation Site in the Orthogonal Ligation of Unprotected Peptides	231
<i>Qitao Yu and James P. Tam</i>	
Low Scale Multiple Array Synthesis and DNA Hybridization of Peptide Nucleic Acids	233
<i>Ralf Hoffmann, Hildegund C.J. Ertl, Anne Marie Pease, Zhenning He, Giovanni Rovera, and Laszlo Otvos, Jr.</i>	
Intramolecular Orthogonal Ligation for the Synthesis of Cyclic Peptides	235
<i>Chuan-Fa Liu, Chang Rao, and James P. Tam</i>	
A New Approach to Phosphonopeptide Analogs	237
<i>Maria de Fatima Fernandez, Joseph C. Kappel, and Robert P. Hammer</i>	
Protected amino acid chlorides: Coupling reagents suitable for the most highly hindered systems	239
<i>Michael Beyermann, Dumitru Ionescu, Petra Henklein, Ayman El-Faham, Holger Wenschuh, Michael Bienert and Louis A. Carpino</i>	
Stereoselective synthesis of highly topographically constrained $\beta$ -isopropyl substituted aromatic amino acids	241
<i>Yinglin Han, Jun Lin, Subo Liano, Wei Qiu, Chaozhong Cai and Victor J. Hruby</i>	

Development of a New Class of Protecting Groups for Use in Solid Phase Peptide Synthesis. <i>Amelie H. Karlstrom and Anders E. Uden</i>	244
Sequential Orthogonal Ligation for the Synthesis of $\beta$ Defensin <i>Christophe Hennard and James P. Tam</i>	247
A Facile Metal Ion-Assisted Amidation on Solid Supports <i>Kalle Kaljuste and James P. Tam</i>	249
Sequence Assisted Peptide Synthesis (SAPS - a Structural Evaluation of the Technology) <i>B. Due Larsen, A. Holm, D.H. Christensen, and O. Faurskov Nielsen</i>	251
The Design of Congener Breaking Sets to Determine the Function of Amino Acid Residues in Biologically Active Peptides <i>James A. Burton, Timothy B. Frigo, Bore G. Raju</i>	253
Application of Different Coupling and Deprotection Conditions in the Synthesis of "Difficult Sequences" <i>M. Villain, P. L. Jackson, N. R. Krishna, and J. E. Blalock</i>	255
An Artificial Receptor for a Tri(Histidine) Ligand <i>Sanku Mallik, Suguang Sun, Jennifer Saltmarsh and Ipsita Mallik</i>	257
Comparative Studies of Racemization during Peptide Synthesis <i>Todd T. Romoff, Thuy-Anh Tran and Murray Goodman</i>	259
A Novel Approach for SPPS of Compounds with an Amidino-Group in the C-Terminal Residue Using Trityl Resins <i>Torsten Steinmetzer, Andrea Schweinitz, Lydia Seyfarth, Siegmund Reißmann, and Jörg Stürzebecher</i>	261
Mild Method for the Synthesis of Peptide Aldehydes Directly from Thioester Resin <i>Aleksandra Wyslouch-Cieszynska and James P. Tam</i>	263
Synthesis of Cyclic Ureas and Cyclic Thioureas from Acyl Dipeptides <i>Adel Nefzi, Marc A. Giulianotti, Edward Brehm, Christa C. Schoner, Vince T. Hamashin, and Richard A. Houghten</i>	265
Tri-t-Butyl DTPA: a Versatile Synthone for the Preparation of DTPA-Containing Peptides by Solid Phase <i>Ananth Srinivasan and Michelle A. Schmidt</i>	267

Intramolecular Migration of the $\beta$ -Dde Protecting Group of Diaminopropionyl to the $\alpha$ -Position During Fmoc Solid Phase Synthesis <i>Ananth Srinivasan, R. Randy Wilhelm, and Michelle A. Schmidt</i>	269
Intentional Syntheses of Disulfide-Mispaired Isomers of $\alpha$ -Conotoxin SI and SIA <i>Balazs Hargittai and George Barany</i>	271
S-Xanthenyl Side-Chain Anchoring for Solid-Phase Synthesis of Cysteine-Containing Peptides <i>Balazs Hargittai, Yongxin Han, Steven A. Kates, and George Barany</i>	273
Isolation, Characterization and Synthesis of a Trisulfide Related to the Somatostatin Analog Lanreotide <i>Lin Chen, Steven R. Skinner, Thomas D. Gordon, John E. Taylor, George Barany, and Barry A. Morgan</i>	275
Novel Safety-Catch Protecting Groups and Handles Cleavable by Intramolecular Cyclization <i>Chongxi Yu and George Barany</i>	277
Synthesis of Conformationally Constrained Peptides Using the Heck Reaction <i>David E. Wright</i>	279
A Facile Synthesis of 3-Substituted Pípecolic Acids <i>Gergely M. Makara and Garland Marshall</i>	281
Rapid Thioester Couplings Mediated by New Uronium Salts <i>Hartmut Echner and Wolfgang Voelter</i>	283
Chemical Synthesis, Purification and Characterization of a 107 Residue Fragment of the Prion Protein <i>Hayden L. Ball, Michael A. Baldwin, Tatiana Bekker, Paolo Mascagni, David King, and Stanley B. Prusiner</i>	285
Problems Encountered with the Synthesis of a Glycosylated Hydroxylysine Derivative Suitable for Fmoc-Solid Phase Peptide Synthesis <i>Henriette A. Remmer and Gregg B. Fields</i>	287
Efficient Assembly of Stable Site-Directed Fluorescence Labeled Peptides <i>Holger Wenschuh, Ulrich Schaible, Stephanie Lamer, Michael Bienert, and Eberhard Krause</i>	289
Solid Phase Synthesis of Lanthionine Peptides <i>J. P. Mayer, J. Zhang, S. Gröger, and C.F. Liu</i>	291

Synthesis of (-methyl Aspartic Acids <i>Guoxia Han, Andrew Burritt, Jung-Mo Ahn, and Victor Hruby</i>	293
Total Solid-Phase Synthesis of Human Cholecystokinin (CCK) -39 <i>K. Kitagawa, C. Aida, H. Fujiwara, T. Yagami and S. Futaki</i>	295
Studies on Synthesis of Peptides with C-Terminal Glutamine Para- nitroanilide <i>Lili Guo, Dongxia Wang, Patrick J. Edwards, Navayath Shobana, and Roger W. Roeske</i>	297
Solid Phase Synthesis of Peptide Nucleic Acids - Peptide Conjugates <i>Lynn D. Mayfield, Revathi R. Katipally, Carla G. Simmons, and David R. Corey</i>	299
Solid Phase Protein Synthesis by Chemical Ligation of Unprotected Peptide Segments in Aqueous Solution <i>Lynne E. Canne, Darren A. Thompson, Reyna J. Simon, Stephen B.H. Kent</i>	301
Amino Acids with Alkyloxy-Aryl-Keto Function in their Side Chains <i>Maria A. Bednarek</i>	303
Solid Phase Synthesis via 5-Oxazolidinones. Ring Opening Reactions with Amines and Reaction Monitoring by Single Bead FT-IR Microspectroscopy <i>Roger E. Marti, Mary Sue Martin, Bing Yan, and Mark A. Jarosinski</i>	305
Synthesis and Applications of a Bis-Sulfonyl Handle for Solid-Phase Synthesis of Peptides <i>Marta Planas, Susumu Funakoshi, Eduard Bardaji, and Fernando Albericio</i>	307
Side Reactions During Synthesis of p-Benzoyl-Phenylalanine Scanned Analog of the Yeast Tridecapeptide Pheromone <i>Michael Breslav, Boris Arshava, Jeffrey M. Becker, and Fred Naider</i>	309
Diaminopimelate-Containing Isopeptides are Cleaved by Leucine Aminopeptidase and Metalloproteinases in Tumors <i>Yoshimitsu Yamazaki, Michael Savva, and Michael Mokotoff</i>	311
Synthesis and Optical Properties of Cyclic Bis-CysteinyI-Peptides and their Linear Precursors with a Built-In Light-Switches <i>Michaela Schenk, Sabine Rudolph-Böhner, Josef Wachtveitl, Thomas Nägele, Dieter Oesterhelt, and Luis Moroder</i>	313

Cyclodextrin as Carrier of Bioactive Peptides <i>Norbert Schaschke, Stella Fiori, Daniel Fourmy, and Luis Moroder</i>	315
Facile Stereoselective Synthesis of $\gamma$ -Amino Acids from the Corresponding $\alpha$ -Amino Acids <i>Pavel Majer, Martin Smrcina, Eva Majerova, Tatiana A. Guerassina, and Michael Eissenstat</i>	317
Unnatural Peptide Synthesis (UPS): a Positional Scan Study <i>Peteris Romanovskis, David Mendel, Martin J. O'Donnell, William C. Scott, Arno F. Spatola, and Changyou Zhou</i>	319
Preparation of Peptide Thioester Segments Using Fmoc-Solid-Phase Peptide Synthesis and Application of the Thioester Ligation Strategy to the Construction of TASP Molecules <i>Shiroh Futaki, Koji Sogawa, Masayuki Fukuda, Mineo Niwa, and Hironobu Hojo</i>	321
Racemization Induced by Excess Base During Activation with Uronium Salts <i>Jo-Ann Jablonski, Russel Shpritzer, and Stephen P. Powers</i>	323
Synthesis and Characterization of a Novel Tryptophan Derivative <i>Ted J. Gauthier, Bo Liu, Guillermo Morales, and Mark L. McLaughlin</i>	325
On Resin Preparation of C-Terminal Peptide Amides, Analogs of the Nematode Neuropeptide PF1, SDPNFLRF-NH <sub>2</sub> , by Application of a Cysteine-Specific Precursor Clavage <i>Teresa M. Kubiak, Alan R. Freidman, and Martha J. Larsen</i>	327
Synthesis of a Series of "Cationic", Orthogonally Protected, $\alpha,\alpha$ -Disubstituted Amino Acids <i>T. S. Yokum, M. G. Bursavich, S. A. Piha-Paul, D. A. Hall, and M. L. McLaughlin</i>	329
Synthesis of $N\alpha$ - <i>t</i> -Boc-Benz[f]Tryptophan: An Intrinsic/Extrinsic Fluorescent Probe <i>T. S. Yokum, P. K. Tungaturthi, and M. L. McLaughlin</i>	331
Synthesis of HIV-1 Protease Analog by Ligation of Bromoacetyl and Mercaptoethylamide Peptide Prepared Using Disulfide Linkage to Solid-Support <i>Yoshiaki Kiso, Tooru Kimura, Yoichi Fujiwara, Naoki Nishizawa, Hikaru Matsumoto, Masamichi Kishida, Kenichi Akaji, and Haruo Takaku</i>	333

- An Efficient Preparation of the Potent and Selective Pseudopeptide Thrombin Inhibitor, Inogatran 335  
*Wayne L. Cody, John X. He, Patrice Preville, Micheline Tarazi, M. Arshad Siddiqui and Annette M. Doherty*
- Application of Novel Organophosphorus Compounds as Coupling Reagents for the Synthesis of Bioactive Peptides 337  
*Yun-hua Ye, Chong-xu Fan, De-yi Zhang, Hai-bo Xie, Xiao-lin Hao, and Gui-lin Tian*
- Minimization of Cysteine Racemization During Stepwise Solid-Phase Peptide Synthesis 339  
*Yvonne M. Angell, Yongxin Han, Fernando Albericio, and George Barany*
- Solid Phase Synthesis of *N*-Methyl Amino Acids: Application of the Fukuyama Amine Synthesis 340  
*Lihu Yang and Kuenley Chiu*
- Novel Solid-Phase Reagents for Facile Formation of Intramolecular Disulfide Bonds in Peptides Under Mild Conditions 343  
*Ioana Annis and George Barany*
- Fmoc-2-Aminopalmitic Acid for the Synthesis of Lipopeptides with an Hydrophobic Chain on a C-C Bond 345  
*Anna M. Papini, Silvia Mazzucco, Elena Nardi, Mario Chelli, Mauro Ginanneschi, and Gianfranco Rapi*
- Session V. Structure, Folding and Conformational Analysis**
- Folding of a Predominantly  $\beta$  Sheet Protein with a Central Cavity 349  
*P.L. Clark, M. Sukumar, Z. P. Liu, J. Rizo, B.F. Weston, K.S. Rotondi, and L. M. Gierasch*
- Insights into the Molecular Mechanisms of Protein Folding and Misfolding 352  
*Sheena E. Radford*
- Prediction of Protein Transmembrane Segments Using a Hydrophobicity Scale Derived from Hydrophobic Peptides 355  
*Li-Ping Liu, Chen Wang, Charles M. Deber*
- Structure, Function and Modeling of Human Endothelin and Its Precursor Polypeptide, BigET: Targets for Rational Drug Design 358  
*Bonnie A. Wallace and R.W. Janes*
- 3D Modeling for TM Receptors: Problems and Perspectives 361  
*Gregory V. Nikiiforovich, Stan Galaktionov, Vladimir M. Tseitin, David R. Lowis, Mark D. Shenderovich and Garland R. Marshall*

Multicyclic Side-Chain Bridged Peptides Designed for $\alpha$ -Helix Stabilization <i>John W. Taylor, Guihua Guo, and Chongxi Yu</i>	364
Natural Selection with Self Replicating Peptides <i>S.Q. Yao, I. Ghosh, and J.A. Chmielewski</i>	366
Exploring the Foldability and Function of Insulin by Combinatorial Peptide Chemistry <i>Ming Zhao, Satoe Nakagawa, Qingxin Hua, and Michael A. Weiss</i>	369
Characterization of Transforming Growth Factor Alpha Binding to Epidermal Growth Factor Receptor Through NMR Structure Determination and NOE Analysis Methods <i>Campbell McInnes, David W. Hoyt, Maureen O'Connor-McCourt, and Brian D. Sykes</i>	372
Vibrational and Electronic Circular Dichroism Study of $3_{10}$ -Helical Stabilization in Blocked ( $\alpha$ -Me)-Val Peptides <i>Gorm Yoder, T.A. Keiderling, Alessandra Polese, Fernando Formaggio, Marco Crisma, Claudio Toniolo, Q.B. Broxterman, and Johan Kamphuis</i>	375
First Peptide-Based System of Rigid Donor, Rigid Acceptor, and Rigid Interchromophore Spacer: a Conformational and Photophysical Study <i>Claudio Toniolo, Fernando Formaggio, Marco Crisma, Jean-Paul Mazaleyrat, Michel Wakselman, Clifford George, Judith L. Flippen-Anderson, Basilio Pispisa, Mariano Venanzi, and Antonio Palleschi</i>	378
Correlation of Kinetic Data with Crystallographic Structures of Aspartic Proteinases <i>Ben M. Dunn, Kohei Oda, Marina Bukhtiyarova, Deepa Bhatt, Chetana Rao-Naik, W. Todd Lowther, Paula E. Scarborough, Brian M. Beyer, Jennifer Westling John Kay, Nora Cronin, and Tom Blundell</i>	381
Structural Characterization of Two-Stranded Anti-Parallel $\beta$ -Sheet Peptides for DNA Major Groove Recognition[1] <i>Bing Y. Wu and Laurence H. Hurley</i>	383
Conformation and Activity of Antimicrobial Peptides Related to PGLa <i>Jack Blazyk, Janet Hammer, Amy E. Kearns, U. Prasad Kari, and W. Lee Maloy</i>	385
Structure-Activity Studies on a Circular Protein Domain <i>Julio A. Camarero, Joanna Pavel and Tom W. Muir</i>	387

- Folding and Aggregation in Mixed Dimers of Gramicidin D 389  
*William L. Duax, Brian M. Burkhardt, David A. Langs, and Walter A. Pangborn*
- RS-66271, a Clinical Candidate Derived from Parathyroid Hormone Related Protein: the Role of Enhanced Amphiphilic Helicity 392  
*Maria Pellegrini, Alessandro Bisello, Michael Rosenblatt, Michael Chorev and Dale F. Mierke*
- Identification of a Minimal Peptide Sequence of Islet Amyloid Polypeptide (IAPP) with Amyloidogenic and Cytotoxic Properties  $\beta$  394  
*Aphrodite Kapurniotu, Jurgen Bernhagen, Wolfgang Fischle, Saul Teichberg, Wolfgang Voelter, and Richard Bucala*
- Substrate Specificity and Mechanism of Activation of Hepatitis C Virus Protease 396  
*Elisabetta Bianchi, Andrea Urbani, Raffaele De Francesco, Christian Steinkühler, and Antonello Pessi*
- The Allosteric-type Mechanism of Tetanus Toxin Metalloprotease Activity Determines Its Substrate Specificity 398  
*Fabrice Cornille, Loïc Martin, Christine Lenoir, Didier Cussac, Bernard P. Roques, and Marie-Claude Fournié-Zaluski*
- Structure Activity Studies of Macrophage Migration Inhibitory Factor Show a Functional Role for Cysteine Residues 400  
*Jürgen Bernhagen, Robert Kleemann, Aphrodite Kapurniotu, Richard Bucala, and Herwig Brunner*
- Secondary and Tertiary Fold of the Human Parathyroid Hormone 1-34 in Different Environments as a Pathway to Bioactive Conformation 402  
*Maria Pellegrini, Stefano Maretto, Miriam Royo, Michael Rosenblatt, Michael Chorev, and Dale F. Mierke*
- Three-Dimensional Models of  $\delta$  Opioid Pharmacophore: Molecular Modeling and QSAR Study of Peptide and Non-Peptide Ligands 404  
*Mark D. Shenderovich, Subo Liao, Xinhua Qian, Victor J. Hruby*
- A Chromophoric Study of Zinc Coordination and Conformer Selectivity of the Human Insulin Hexamer in Solution 406  
*Mark L. Brader*
- Amide NH Shift Gradients: Quantitating Peptide Structure/Disorder Transitions 408  
*Jonathan W. Neidigh, Scott M. Harris, Hui Tong, Gregory M. Lee, Zhihong Liu, and Niels H. Andersen*

Predicting Conductance Properties for Ion Channel Structural Models Using the HOLE Program <i>Oliver S. Smart</i>	410
Molecular Dynamics Simulation of Epidermal Growth Factors in Aqueous Solution <i>Charles R. Watts, Sándor Lovas, and Richard F. Murphy</i>	412
Engineering of Snake Venom Cardiotoxin by Computer Modeling and Chemical Synthesis Approach <i>Shui-Tein Chen, Chi-Yue Wu, Kung-Tsung Wang</i>	414
In Search of the Earliest Events of hCG Folding: Structural Studies of the 60-87 Peptide Fragment <i>S. Sherman, L. Kirnarsky, O. Prakash, H.M. Rogers, R.A.G.D. Silva, T.A. Keiderling, D.D. Smith, A.M. Hanly, F. Perini, and R. W. Ruddon</i>	416
Synthetic Peptides from Putative Amphipathic $\beta$ Strand Sequences of Apolipoprotein B-100 Associate with Lipid in the $\beta$ Strand Conformation <i>Vinod K. Mishra, Manjula Chaddha, G.M. Anantharamaiah, Mayakonda N. Palgunachari, Krishnan K. Chittur, Sissel Lund-Katz, Michael C. Phillips, and Jere P. Segrest</i>	418
Proline Puckering and a <i>cis-trans</i> Isomerization of Proline-Containing Peptides <i>Young Kee Kang, Seong Jun Han, and Jong Suk Jhon</i>	420
Retention of <i>Cis</i> -Proline Rotamer in a Small Fragment of RNase A Containing a Non-Natural Proline Analog - an NMR Study <i>Yue-Jin Li, Cathy C. Lester, David M. Rothwarf, Jin-Lin Peng Theodore W. Thannhauser, Lianshan Zhang, James Tam, and Harold A. Scheraga</i>	422
Phosphorylation Alters the Three Dimensional Structure of the Carboxyl Terminal of Bovine Rhodopsin <i>Arlene D. Albert, Phillip L. Yeagle, James L. Alderfer, Marc Dorey, Todd Vogt, Nilaya Bhawsar, Paul A. Hargrave, J. Hugh McDowell, and Anatol Arendt</i>	424
Conformational Calculations Restrained by NMR and Fluorescence Data on Functionalized Aib-Based Peptides <i>Basilio Pispisa, Maria E. Amato, Antonio Palleschi, Mariano Venanzi, Giancarlo Zanotti, and Anna L. Segre</i>	426

- Long-Distance REDOR NMR Measurements for Determination of Secondary Structure and Conformational Heterogeneity in Peptides 428  
*Boris Arshava, Michael Breslav, Octavian Antohi, Ruth E. Stark, Joel R. Garbow, Jeffrey M. Becker, and Fred Naider*
- Interpretation of the Fluorescence Decay Characteristics of Cyclic  $\beta$ -Casomorphin Analogs Based on Theoretically Calculated Ensembles of their Low Energy Conformers 430  
*B. C. Wilkes, B. Zelent, H. Malake, R. Schmidt and P. W. Schiller*
- Synthesis of the Putative Sixth Transmembrane Helix of the Neurokinin-1 Receptor and its Structural Analysis in Phospholipid Bilayer Vesicles 432  
*Chinchi C. Chen, and Garland R. Marshall*
- Distinguishing  $\alpha/3_{10}$ -Helices in a Lipopeptaibol Antibiotic Using the Amino Acid TOAC and ESR. 435  
*Vania Monaco, Claudio Toniolo, Fernando Formaggio, Marco Crisma, Paul Hanson, Glenn L. Millhauser, Clifford George, Judith L. Flippen-Anderson, Sylvie Rebuffat, and Bernard Bodo*
- 3D Structure of the Anti-AChR Fv Antibody Fragment Complexed to the [A<sup>76</sup>]MIR Antigen: A Homology and Molecular Modelling Approach 437  
*Piotr Orlewski, Jens Kleinjung, Avgi Mamalaki, Christos Liolitsas, Socrates J. Tzartos, Vassilios Tsikaris, Maria Sakarellos-Daitsiotis, Constantinos Sakarellos, and Manh-Thong Cung*
- Parathyroid Hormone-Related Protein Derived Mono- and Bi-Cyclic Agonists and Antagonists: A Conformational Comparison 439  
*Stefano Maretto, Elisabetta Schievano, Evaristo Peggion, Stefano Mammi, Alessandro Bisello, Michael Chorev, Michael Rosenblatt, and Dale F. Mierke*
- The NMR Structure of a Cyclic V3 Loop Peptide that Binds Tightly to a Monoclonal Antibody that Potently Neutralizes HIV-1 441  
*Edelmira Cabezas, and Arnold C. Satterthwait*
- Folding of the Second Extracellular Loop of the Myelin Proteolipid Protein (PLP). Effect of a Point Mutation Found in Pelizaeus-Merzbacher Disease 443  
*Ingrid Dreveny and Elisabeth Trifilieff*
- An Improved Template for the Initiation of Peptide Helices 445  
*Evan T. Powers, Peter Renold, Sherri Oslick, D.S. Kemp*

Conformational Studies of a PTH/PTHrP Hybrids <i>Stefano Mammi, Lara Pauletto, Evaristo Peggion, Vered Behar, M. Rosenblatt, Michael Chorev</i>	447
Synthesis and Conformational Analysis of C- and N-Glycopeptides <i>Fred Burkhart, Gerhard Hessler and Horst Kessler</i>	449
Lactam Cyclization [i to(i+4)] for Nucleation/Stabilization of $\alpha$ -Helices? <i>Gal Bitan, Maria Pellegrini, Michael Chorev, and Dale F. Mierke</i>	451
Molecular Modeling and Design of Metal Binding Template Assembled Synthetic Proteins (TASP) <i>Gregory V. Nikiforovich, Christian Lehmann, and Manfred Mutter</i>	453
Synthesis, Conformational Analysis and the Bioactivities of the Lanthionine Analogs of a Cell Adhesion Modulator <i>Haitao Li, Xiaohui Jiang, and Murray Goodman</i>	455
Utilization of a Reporting Conformational Template in Probing the Phe-His Interaction in the Short Alanine-Rich Peptide Helices <i>Kwok Yin Tsang, and Daniel S. Kemp</i>	457
Structure-Activity Studies on the Abl-SH2 Domain <i>Maria C. Pietanza and Tom W. Muir</i>	459
Design and Use of Amphiphilic Peptides in Liposomes as pH-Triggered Releasing Agents <i>M. L. Brickner, C. Yusuf, K. M. Vogel, and J. A. Chmielewski</i>	461
NMR Structure Determination and DNA Binding Properties of GCN4 Peptidomimetics Designed for $\alpha$ -Helix Initiation and Stabilization <i>Min Zhang, Bingyuan Wu, Jean Baum, and John W. Taylor</i>	463
Synthesis and Conformational Analysis of Axinastatin 5 and Derivatives <i>Oliver Mechnich, Gerhard Hessler, Michael Bernd, Bernhard Kutscher, and Horst Kessler</i>	465
On the Energetics of the Heterodimerization of the Max and c-Myc Leucine Zippers <i>P. Lavigne, L.H. Kondejewski, M.E. Houston Jr., R. S. Hodges, and C. M. Kay</i>	467
Synthesis and Conformational Analysis of Cyclic-Hexapeptides Related to Somatostatin Incorporating Novel Peptoid Structures <i>Thuy-Anh Tran, Ralph-Heiko Mattern, and Murray Goodman</i>	469

The Importance of Residue B8 in Insulin Activity, Structure and Folding <i>Satoe H. Nakagawa, Ming Zhao, Qin Xin Hua, and Michael A. Weiss</i>	471
Opioidmimetic Peptides Containing $\alpha$ -Aminoisobutyric Acid <i>Sharon D. Bryant, Remo Guerrini, Severo Salvadori, Clementina Bianchi, Roberto Tomatis, Martti Attila, and Lawrence H. Lazarus</i>	473
Circular Dichroism Study of the Interaction of Synthetic J Protein of Bacteriophage $\phi$ K with Single-Stranded DNA <i>Shin Ono, Takayuki Okada, Saburo Aimoto, Ken-Ichi Kodaira, Takayoshi Fujii, Choichiro Shimasaki, and Toshiaki Yoshimura</i>	475
V3 Loop of HIV gp120 Protein: Molecular Modeling of 3D Structures Interacting with Cell Proteins <i>Stan Galaktionov, Gregory V. Nikiforovich, and Garland R. Marshall</i>	477
Conformational Studies of a D-Trp <sup>12</sup> -substituted PTHrP-derived Antagonist Containing Lactam-Bridged Side-Chains <i>Stefano Maretto, Elisabetta Schievano, Stefano Mammi, Alessandro Bisello, Chizu Nakamoto, Michael Rosenblatt, Michael Chorev, and Evaristo Peggion</i>	479
Cold Denaturation Studies of (LKELPKEL) <sub>n</sub> Peptide Using Vibrational and Electronic Circular Dichroism Spectroscopic Techniques <i>R.A.G.D.Silva, Vladimir Baumruk, Petr Pancoska, T.A. Keiderling, Eric Lacassie and Yves Trudelle</i>	481
Solution Structure of Human Salivary Statherin <i>Tarikere L. Gururaja, Gowda A. Naganagowda, and Michael J. Levine</i>	483
Interaction of Melittin with Phospholipid Monolayer Modified Silica Support <i>Tzong-Hsien Lee, Hans-Jürgen Wirth, Patrick Perlmutter, and Marie-Isabel Aguilar</i>	485
Predictions of Intramembrane Regions in Transmembrane Helices <i>Vladimir M. Tseitin, and Gregory V. Nikiforovich</i>	487
Synthesis of Gramicidin Analogs with Conformational Constrained Dipeptides <i>Wei Jun Zhang, Jeff Kao, Eduardo Groissman and Garland R. Marshall</i>	489
Conformational Studies of Rat Brain Sodium Ion Channel Segment IS4 in Different Mediums <i>Xiaojie Xu, Zhenwei Miao, Yun Jiang, Youqi Tang, and Saburo Aimoto</i>	491

Identification of a Novel Human CD8 Surface Region Involved in MHC Class I Binding <i>Song Li, Swati Choksi, Simei Shan, Jimin Gao, Robert Korngold, and Ziwei Huang</i>	493
Surveying the Protein Folding Landscape: Equilibrium Models for Partially Folded Intermediates of Bovine Pancreatic Trypsin Inhibitor (BPTI) <i>Christopher M. Gross, Clare Woodward, and George Barany</i>	495
Structure Activity Studies of Normal and Retro Pig Cecropin- Melittin Hybrids <i>Padmaja Juvvadi, Satyanarayana Vunnam, Barney Yoo, and R. B. Merrifield</i>	497
<b>Session VI. Receptor-Ligand interactions</b>	
A Peptide Mimetic of Erythropoietin: Critical Residues and Description of a Minimal Functional Epitope <i>Dana L. Johnson, Francis X. Farrell, Frank J. McMahon, Jennifer Tullai, Francis P. Barbone, Steven A. Middleton, Kenay Hoey, Oded Livnah, Nicholas C. Wrighton, William J. Dower, Linda S. Mulcahy, Enrico A. Stura, Ian A. Wilson, and Linda K. Jolliffe</i>	501
Structure of Rhodopsin-Bound C-Terminal $\alpha$ -Peptide of Transducin <i>Oleg G. Kisselev, Yang C. Fann, N. Gautam, and Garland R. Marshall</i>	504
Molecular Dissection of the GABA <sub>A</sub> Receptor: the N-Terminal Domain of the $\gamma 2$ Subunit is Essential for Benzodiazepine Binding and Subunit Assembly <i>Andrew J. Boileau, Amy Kucken, Amy R. Evers, and Cynthia Czajkowski</i>	508
Glucagon Receptor Structure and Function: Probing the Putative Hormone Binding Site with Receptor Chimeras <i>Cecilia G. Unson, Aaron M. Cypess, Cui-Rong Wu, Connie P. Cheung, and R.B. Merrifield</i>	511
A New Class of Dipeptide Derivatives that are Potent and Selective $\delta$ Opioid Agonists <i>P. W. Schiller, G. Weltrowska, I. Berezowska, C. Lemieux, N. N. Chung, K.A. Carpenter, and B. C. Wilkes</i>	514
Discovery of Small Non-Peptidic CD4 Inhibitors as Novel Immunotherapeutics <i>Song Li, Jimin Gao, Takashi Satoh, Thea M. Friedman, Andrea E. Edling, Ute Koch, Swati Choksi, Xiaobing Han, Robert Korngold, and Ziwei Huang</i>	517

Biochemistry and Biology of Phospholipase C- $\gamma$ 1 <i>Graham Carpenter, Qun-sheng Ji, and Debra Horstman</i>	520
Tumor Cell Interactions with Type IV Collagen: Synthetic Peptide Dissection of Post-Adhesion Signal Transduction Mechanisms <i>Janelle L. Lauer, and Gregg B. Fields</i>	523
Somatostatin Receptor Antagonists Based on a Mixed Neuromedin B Antagonist/Somatostatin Agonist <i>David H. Coy, Rahul Jain, William a Murphy, Wojciech J. Rossowski, Joseph Fuselier, and John E. Taylor</i>	526
The Origin of Specificity in the Opioid Receptor Family <i>Irina D. Pogozheva, Andrei L. Lomize, and Henry L. Mosberg</i>	530
Mapping of the Interleukin-10/Interleukin-10 Receptor Combining Site Using Structurally Different Peptide Scans <i>Ulrich Reineke, Robert Sabat, Hans-D. Volk and Jens Schneider- Mergener</i>	533
Design and Synthesis of Specific Proline-Rich Peptides with High Affinity for GRB2 <i>Didier Cussac, Fabrice Cornille, Gilles Tiraboschi, Christine Lenoir, Bernard Roques, and Christiane Garbay</i>	535
N-Terminal Myristoylation Of HBV Pre-S1 Domain Affects Folding and Receptor Recognition <i>Menotti Ruvo, Sandro De Falco, Antonio Verdoliva, Angela Scarallo, and Giorgio Fassina</i>	537
High Affinity IgE-Receptor- $\alpha$ -Subunit-Derived Peptides as Antagonists of Human IgE Binding <i>Waleed Danho, Raymond Makofske, Joseph Swistok, Michael Mallamaci, Mignon Nettleton, Vincent Madison, David Greeley, David Fry and Jarko Kochan</i>	539
Highly Potent Human Parathyroid Hormone Analogs <i>Jesse Z. Dong, Chizu Nakamoto, Michael Chorev, Barry A. Morgan, Michael Rosenblatt, and Jacques-Pierre Moreau</i>	541
Monitoring Binding Interactions of Peptide-Peptide, Peptide-Protein, Ligand- Protein and Substrate-Enzyme by NILIA-CD Spectroscopy <i>Giuliano Siligardi, and Rohanah Hussain</i>	543

Peptide Libraries with Free Carboxy-Terminus Used to Characterize Epitopes Recognized by PDZ-Domains <i>Ulrich Hoffmüller, Rudolf Volkmer-Engert, Mark Kelly, Hartmut Oschkinat, and Jens Schneider-Mergener</i>	545
Functional Site Studies with Peptide Segments of Cdk Inhibitory Proteins <i>Peter P. Roller, Feng-Di T. Lung, Masato Mutoh, and Patrick M. O'Connor</i>	547
Expression of C5a Receptors (CD88) on Human Bronchial Epithelial Cells (HBEC): C5a-Mediated Release of IL-8 upon HBEC Exposure to Cigarette Smoke <i>Anthony A. Floreani, Art J. Heires, Laurel Clark-Pierce, Lisbeth Welniak, Amanda Miller-Lindholm, Stephen I. Rennard, Edward L. Morgan, and Sam D. Sanderson</i>	549
Mapping and Characterization of Epitopes Recognized by WW Domains Using Cellulose-Bound Peptide Libraries <i>Ulrich Hoffmüller, Hartmut Oschkinat, and Jens Schneider-Mergener</i>	551
Biological and Physicochemical Properties of Urocortin <i>Andreas Rühmann, Ines Bonk, Andreas K. E. Köpke and Joachim Spiess</i>	553
Towards a Rational Approach in the Finding of Potent Peptide Ligands for Grb2 SH2 <i>C. García-Echeverría, B. Gay, P. Furet, J. Rahuel, H. Fretz, J. Schoepfer, and G. Caravatti</i>	555
Multivalent Carbohydrate-Linked Peptides Interfere with Adherence of <i>Candida albicans</i> to Asialo-GM1 Receptor: Toward the Design of Anti-Adhesin Therapeutics <i>C.M. Charles Yang, Wah Y. Wong, Ole Hindsgaul, Randall T. Irvin, and Robert S. Hodges</i>	557
Development of Somatostatin Agonists with High Affinity and Specificity for the Human and Rat Type 5 Receptor Subtype <i>David H. Coy and John E. Taylor</i>	559
Properties of GnRH Conjugates <i>In Vivo</i> <i>Imze Mezö, B. Vincze, G. Tóth, J. Patá, D. Gaál, T. Kremmer, A. Kálnay, E. Gulyás, I. Teplán, F. Ötvös, S. Lovas, R.F. Murphy, I. Pályi</i>	561
Phospholipid Vesicle Binding by an Amphiphilic $\beta$ -Sheet Structure from Serum Apolipoprotein B-100 <i>Jinliang Lu and John W. Taylor</i>	563

Stability and Binding of SH3 Domain of Bruton's Tyrosine Kinase <i>Jya-Wei Cheng, Himatkumar V. Patel, Shiou-Ru Tzeng, Chen-Yee Liao</i>	565
The Interaction Between Monoclonal Antibody 4A5 and Fibrinogen Gamma Chain Peptides Studied by Nuclear Magnetic Resonance <i>Michael Blumenstein and Gary R. Matsueda</i>	567
A Potent Synthetic Dimeric Peptide Agonist of the Erythropoietin Receptor <i>Palaniappan Balasubramanian, Qun Yin, Surekha Podduturi, Nicholas C. Wrighton, and William J. Dower</i>	569
Binding Studies of Cytokines rhGM-CSF and rhIL-3 with a Peptide Fragment of hGM-CSF Receptor $\alpha$ -Chain by Non-Immobilised Ligand Interaction Assay (NILIA) Using Circular Dichroism(CD) <i>Rohanah Hussain, Paolo Rovero, Claudia Galoppini, and Giuliano Siligardi</i>	571
Synthesis, Bioactivity, 2D NMR and ESR of Angiotensin II and Its Spin Labelled Derivative <i>Xiaoyu Hu, Rui Wang, Xiaoxu Li, and Jianheng Shen</i>	573
Structure-Function Studies on Synthetic Tetrapeptide Analogs of AVP(4-8) <i>Ke-Yin Ma and Yu-Cang Du</i>	575
Development of Feeding and Y-1 NPY Receptor Antagonists <i>Z. Tao, F. Peng, S. Sheriff, P. Eden, J. Taylor, W.T. Chance, and A. Balasubramaniam</i>	578
Receptor 3D Homology Molecular Modeling and <i>In Vitro</i> Mutagenesis Identify Putative Melanocortin (hMC1R) Agonist Ligand-Receptor Interactions and a Proposed Mechanism for Receptor Activation <i>Carrie Haskell-Luevano, Ying-kui Yang, Chris Dickinson, and Ira Gantz</i>	580
Novel Non-Phosphorylated Peptide Binding to the Grb2-SH2 Domain <i>Feng-Di T. Lung, Lakshimi Sastry, Shaomeng Wang, Bih-Show Lou, Joseph J. Barchi, C. Richter King, and Peter P. Roller</i>	582
A Endothelin-A/Lutropin Chimeric Receptor Exhibits Ligand-Mediated Internalization in the Absence of Signaling <i>Neil Bhowmick, Prema Narayan and David Puett</i>	584
Examination of the Role of TMH VII in Subtype-Selective Ligand Binding Using Semi-Synthetic Muscarinic Receptors <i>Carol B. Fowler, Harry LeVine, and Henry I. Mosberg</i>	586

Modeling Somatostatin Receptor-Ligand Complexes <i>Xiaohui Jiang, and Murray Goodman</i>	588
 <b>Session VII. Neuro-, Endocrino-, and Bioactive Peptides</b>	
Solution Synthesis and Structure Revision of Dendrotoxin I <i>Hideki Nishio, Tatsuya Inui, Yuji Nishiuchi, Edward G. Rowan, Alan L. Harvey, Terutoshi Kimura, and Shumpei Sakakibara</i>	593
Amphipathic $\alpha$ - and $3_{10}$ -Helical Peptides with <i>in Vitro</i> and <i>in Vivo</i> Bioactivity <i>Mark L. McLaughlin, T. Scott Yokum, Ted J. Gauthier, Robert P. Hammer, and Philip H. Elzer</i>	595
[D-Pen <sup>2,7</sup> ]-Human- $\alpha$ Calcitonin Gene-Related Peptide: a Novel CGRP Antagonist <i>D. David Smith, Shankar Saha, David J.J. Waugh, Peter W. Abel</i>	597
Improved Parathyroid Hormone Analogue for the Treatment of Osteoporosis <i>J.R. Barbier, V. Ross, P. Morley, J. F. Whitfield, and G. E. Willick</i>	599
Multifunctional Chimeric Analogs of Small Peptide Hormones: Agonists and Receptor-Selective Antagonists <i>John Howl and Mark Wheatley</i>	601
Generation of New Dmt-Tic $\delta$ Opioid Antagonists: N-Alkylation <i>Lawrence H. Lazarus, Severo Salvadori, Gianfranco Balboni, Remo Guerrini, Clementina Bianchi, Peter S. Cooper, and Sharon D. Bryant</i>	603
Novel D-Amino Acid Hexapeptide Calmodulin Antagonists Identified from Synthetic Combinatorial Libraries <i>Sylvie E. Blondelle, Ema Takahashi, Ed Brehm, Rosa Aligue, Richard A. Houghten, Enrique Pérez-Payá</i>	605
Pseudopeptides and Cyclic Peptides Analogues of Osteogenic Growth Peptide (OGP): Synthesis and Biological Evaluation <i>Yuchen Chen, Itai Bab, Andras Muhrad, Arye Shteyer, Marina Vidson, Zvi, Greenberg, Dan Gazit, Michael Chorev</i>	607
A Cyclic Heptapeptide Mimics CD4 Domain 1 CC' Loop and Inhibits CD4 Biological Function [1-4] <i>Takashi Satoh, James M. Aramini, Song Li, Thea M. Friedman, Jimin Gao, Andrea E. Edling, Robert Townsend, Ute Koch, Swati Choksi, Markus W. Germann, Robert Korngold, and Ziwei Huang</i>	609

- Analogues of Main Autophosphorylation Site of PP60<sup>src</sup> PTK as Substrates for Syk and Src PTKs 611  
*Paolo Ruzza, Andrea Calderan, Barbara Biondi, Arianna Donella-Deana, Lorenzo A. Pinna, and Gianfranco Borin*
- Positively Charged Residues of Glucagon: Role in Glucagon Action 613  
*Cecilia Unson, Cui-Rong Wu, Connie P. Cheung, and R. B. Merrifield*
- Synthesis and Activity of Proteolysis-Resistant GLP-1 Analogues 615  
*D. L. Smiley, R.D. Stucky, V.J. Chen, D.B. Flora, A. Kriauciunas, B.M. Hine, J. A. Hoffmann, W.T. Johnson, R.A. Owens, F.E. Yakubu-Madus, and R.D. DiMarchi*
- Homo-Oligomeric Opioid Analogues and Incorporation of 4-Trans-Aminomethylcyclohexanecarboxylic Acid (Amcca) 617  
*DeAnna L. Wiegandt Long, Peg Davis, Frank Porreca, and Arno F. Spatola*
- Replacement at Positions 17, 18, and 21 of Glucagon Leads to Formation of a New Salt Bridge and to an Increase in Binding Affinities 619  
*Dev Trivedi, Jung-Mo Ahn, Ying Lin, John L. Krstenansky, Stephen K. Burley, and Victor J. Hruby*
- Design and Synthesis of Novel GnRH-Endothelin Chimeras 621  
*Dror Yahalom, Yitzhak Koch, Nurit Ben-Aroya, Mati Fridkin*
- Receptor Specificity of [2,3-Cyclopropane Amino Acids] - fMLP Analogues 623  
*Hiroaki Kodama, Eiichi Hirano, Takahiro Yamaguchi, Satoshi Osada, Masaya Miyazaki, Ichiro Fujita, Sumio Miyazaki, and Michio Kondo*
- Synthesis of Short Analogues of Neuropeptide Y Specific for the Y2 Receptor Using the TASP Concept 625  
*Eric Grouzmann, Alain Razaname, Gabriele Tuchscherer, Maria Martire, and Manfred Mutter*
- Interaction with Membranes of Peptides Related to the Fusogenic Region of PH-30 $\alpha$ , a Sperm-Egg Fusion Protein 627  
*Haruhiko Aoyagi, Miyuki Kimura, Takuro Niidome, Tomomitsu Hatakeyama, and Hisakazu Mihara*
- Elucidation of the Conformational Features within a Series of Tetrapeptides Which Determine the Selective Recognition of  $\mu$  Versus  $\delta$  Opioid Receptors 629  
*Jeffrey C. Ho, Carol A. Mousigian, Henry I. Mosberg*

- Structure Activity Relationship of NDF Isoforms 631  
*T. J. Zamborelli, G.S. Elliot, S. Hara, D. L. Lacy, D. M. Lenz, N. Lu, S.K. Pakar, B.Ratzkin, J. E. Tarpley, J. S. Whoriskey, S. K. Yoshinaga, and J. P. Mayer*
- Solid State Conformation of Constrained Somatostatin Analogues with High Potency and Specificity for the  $\mu$  Opioid Receptor 633  
*Judith L. Flippen-Anderson, Jeffrey R. Deschamps, Christi Moore, Clifford George, Victor J. Hruby, Wieslaw Kazmierski, and G. Gregg Bonner*
- Design, Synthesis and Biology Activity of Cyclic GHRP-6 Analogues 635  
*Kjeld Madsen, Peter H. Andersen, Birgit Sehested Hansen, Nils L. Johansen, and Henning Thøgersen*
- Systematic Lactam Scan of hGRF<sub>1-29</sub>-NH<sub>2</sub> Yields Potent Agonists and Antagonists 637  
*L. Cervini, C. J. Donaldson, S. Koerber, W. Vale, and J. Rivier*
- The Interaction Between Gramicidin-S and Lipid Bilayers. Evidence for Cholesterol Attenuation of Phospholipid-Peptide Interactions 639  
*T. P.W. McMullen, E. J. Prenner, R.N.A.H. Lewis, L. H. Kondejewski, R. S. Hodges, and R. N. McElhaney*
- New Synthetic Peptides Derived from Human Fibroblast Growth Factor-1: Search for Agonists and Inhibitors 641  
*S. Kiyota, A.G. Gambarini, W. Viviani, S. Oyama, B.D. Sykes, and M.T.M. Miranda*
- Rapid Modular Total Chemical Synthesis of Chemokines Based on Genome Sequence Data 643  
*Michael A. Siani, Darren A. Thompson, Lynne E. Canne, Jill Wilken, Gianine M. Figliozzi, Stephen B.H. Kent, and Reyna J. Simon*
- Synthesis and Study of All-L and All-D Normal and Retro Isomers of Cecropin A - Melittin Hybrids and Selective Enzyme Inactivation 645  
*Satyanarayana Vunnam, Padmaja Juvvadi, Kenneth S. Rotondi and R. B. Merrifield*
- Characterization of Neurokinin Receptor Types and Their Intracellular Signal Transduction in C1300 Cells 648  
*Shigetomo Fukuhara, Hidehito Mukai, and Eisuke Munekata*

- Influence of Different Types of Cyclization on Certain Biological Activities of Three Structural Types of Bradykinin Antagonists 650  
*Siegmund Reissmann, Inge Agricola, Torsten Steinmetzer, Lydia Seyfarth, George Greiner, and Inge Paegelow*
- Antimicrobial Peptides with Activity Against an Intracellular Pathogen 652  
*T. S. Yokum, P. H. Elzer, and M. L. McLaughlin*
- Properties of Cyclic Peptides Having Inhibitory Site of  $\alpha$ -Amylase Inhibitor Tendamistat 654  
*Tomiya Hirano, Shin Ono, Hiroyuki Morita, Toshiaki Yoshimura, Hiroki Yasutake, Tetsuo Kato, and Choichiro Shimasaki*
- Solid-Phase Synthesis of Caged Peptides Containing Photolabile Derivatives of Aspartic Acid 656  
*Yoshiro Tatsu, Yasushi Shigeri, Shinji Sogabe, Noboru Yumoto, and Susumu Yoshikawa*
- Induction of Erectogenic Activity in the Human Male by Systemic delivery of a Melanotropic Peptide 658  
*M. Hadley and V. J. Hruby*
- Design and Synthesis of Opioid Mimetics Containing Pyrazinone Ring and Examination of Their Opioid Receptor Binding Activity 660  
*Yoshio Okada, Masaki Tsukatani, Hiroaki Taguchi, Toshio Yokoi, Sharon D. Bryant and Larry H. Lazarus*
- Intracellular Third Loop of Galanin Receptor as G-Protein Interaction Site 662  
*Ursel Soomets, Ülo Langel*
- Session VIII. Protease Inhibitors**
- Potent Dipeptide HIV Protease Inhibitors Containing the Hydroxymethylcarbonyl Isostere as an Ideal Transition-State Mimetic 667  
*Yoshiaki Kiso, Satoshi Yamaguchi, Hikaru Matsumoto, Tsutomu Mimoto, Ryohei Kato, Satoshi Nojima, Haruo Takaku, Tominaga Fukazawa, Tooru Kimura, and Kenichi Akaji*
- Rational Design and Synthesis of Conformationally Constrained Inhibitors of Human Cathepsin D 670  
*Pavel Majer, Jack R. Collins, Wenxi Pan, Sergei V. Gulnik, Angela Lee, Alena Gustchina, and John W. Erickson*

- Discovery of a Novel, Selective, and Orally Bioavailable Class of Thrombin Inhibitors Incorporating Aminopyridyl Moieties at the P1 Position 672  
*Dong-Mei Feng, Roger M. Freidinger, S. Dale Lewis, Stephen J. Gardell, Mark G. Bock, Zhonggo Chen, Adel Naylor-Olsen, Richard Woltmann, Elizabeth P. Baskin, Joseph J. Lynch, Robert Lucas, Jules A. Shafer, Kimberley B. Dancheck, I-Wu Chen, Joseph P. Vacca*
- Aminopeptidase A: Selective Inhibition and Physiological Involvement in CCK<sub>8</sub> Metabolism 674  
*Laurent Bischoff, Christelle David, Tarik Khaznadar, Valérie Daugé, Bernard Pierre Roques, and Marie-Claude Fournié-Zaluski*
- Synthetic Proregion-related Peptides of Proprotein Convertases, PC1 and Furin, Represent Potent Inhibitors of Each Protease 676  
*Ajoy Basak, Dany Gauthier, Nabil G. Seidah, and Claude Lazure*
- “O, N-Acyl Migration” - Type Prodrugs of Dipeptide HIV Protease Inhibitors 678  
*Yoshiaki Kiso, Satoshi Yamaguchi, Hikaru Matsumoto, Tooru Kimura, and Kenichi Akaji*
- The Crystal Structure of  $\alpha$ -Thrombin with Retro-Binding Inhibitor SEL2711 680  
*Igor Mochalkin and Alexander Tulinsky*
- Novel Peptide Inhibitors for Interleukin-1 $\beta$  Processing in Monocytes 682  
*Sándor Bajusz, Irén Fauszt, Klára Németh, Eva Barabás, Attila Juhász, and Miklós Pathy*
- Synthetic Route to P<sub>1</sub>-Argininals Suitable for Radiolabeling Studies 684  
*Susan Y. Tamura, J. Edward Semple, David C. Rowley, Paul McNamara, Ruth F. Nutt, and William C. Ripka*
- Peptide Vinyl Sulfones: Inhibitors and Active Site Probes for the Study of Proteasome Function *In Vivo* 686  
*Matthew Bogyo, John S. McMaster, Rickard Glas, Maria Gaczynska, Domenico Tortorella, and Hidde Ploegh*
- Synthesis of 3-(3-Pyrrolidinyl)alanine and its Derivatives as Arginine Peptidomimetics for Incorporation into Serine Protease Inhibitors 688  
*Darin R. Kent, Wayne L. Cody, and Annette M. Doherty*
- Design of a Protein-Based Inhibitor For Proprotein Convertase Furin: Expression, Purification and Inhibition of Furin Substrates *In Vivo* by an Epitope-tag Recombinant Serpin  $\alpha_1$ -PDX/hf 690  
*Francois Jean, Kori Stella, Craig J. Lipps, James B. Hicks, and Gary Thomas*

## Session IX. Glyco/Lipo/Phospho Peptides

- Multiphosphorylated Synthetic Peptides as Antigens and Immunogens in Alzheimer's Disease Paired Helical Filaments 695  
*Laszlo Otvos, Jr., Virginia M. Lee, Susan Leight, Peter Davies, and Ralf Hoffmann*
- Synthesis of Fluoroalkylated Muramyl Dipeptide Analogs with Lipophilic Character 698  
*Zheng-Fu Wang and Jie-Cheng Xu*
- Lipoderivatives of an Immunodominant Epitope of Myelin Basic Protein Increased T Cell Responsiveness in Lewis Rats 700  
*Anna M. Papini, Silvia Mazzucco, Daniela Pinzani, Massimo Biondi, Mario Chelli, Mauro Ginanneschi, Gianfranco Rapi, Benedetta Mazzanti, Marco Vergelli, Luca Massacesi, and Luigi Amaducci*
- Antibacterial Insect Glycopeptides: Synthesis, Structure and Activity 703  
*Laszlo Otvos, Jr., Philippe Bulet, Istvan Varga, and Ralf Hoffmann*
- 1997 ABRF Peptide Synthesis Research Committee Study on a Peptide Containing a Phosphorylated Tyrosine 705  
*Lynda F. Bonewald, Lisa Bibbs, Steven A. Kates, Ashok Khatri, Katalin F. Medzihradszky, John S. McMurray, and Susan Weintraub*
- Targeting a Hydrophobic Patch on the Surface of the Grb2-SH2 Domain Leads to High-Affinity Phosphotyrosine-Containing Peptide Ligands 707  
*H. Fretz, P. Furet, J. Schoepfer, C. Garcia-Echeverria, B. Gay, J. Rahuel, and G. Caravatti*
- Synthesis and Purification of Unphosphorylated and Phosphorylated Phospholamban 709  
*Holger B. Schmid, Sjouke Hoving, Stefan Vetter, Thomas Vorherr, and Ernesto Carafiol*
- Design and Synthesis of Controlled Oligomeric Neo-C-Glycopeptides as Multivalent Inhibitors of Carbohydrate-Protein Interactions 711  
*Johanne Roby, Robert N. Ben, Kristina Kutterer, Huiping Qin, George K.H. Shimizu, Michael Barnes, and Prabhat Arya*
- Structural Analysis of Peptide Substrates for O-Glycosylation 713  
*L. Kirnarsky, O. Prakash, S.M. Vogen, Y. Ikematsu, N. Johnson Kaufman, S. D. Sanderson, H. Clausen, M. A. Hollingsworth, and S. Sherman*

Phosphopeptide Models of the C-Terminal Basic Domain of p53 <i>Ralf Hoffmann, Randall E. Bolger, Zhi Q. Xiang, Magdalena Blaszczyk-Thurin, Hildegund C.J. Ertl, and Laszlo Otvos, Jr.</i>	715
Solid Phase Synthesis of N- and O-Glycopeptide by Boc-Strategy <i>Tadashi Teshima, Saeko Oikawa, Kumiko Y. Kumagaye, Kiichiro Nakajima, and Tetsuo Shiba</i>	717
Novel Dde-Protected Glycoamino Acids and Glycoazido Acids in Saccharopeptide Synthesis <i>Gyula Dekany, Bruno Drouillat, Barrie Kellam, Istvan Toth</i>	719
<b>Session X. Peptide Biology</b>	
Design of Novel Melanotropin Antagonists and Agonists for the Recently Discovered MC3, MC4 and MC5 Receptors and Their Use to Determine New Biological Roles <i>Victor J. Hruby, Guoxia Han, Wei Yuan, Sejin Lim, Carrie Haskell-Luevano, Roger D. Cone, Gergo Kunos, and Mac E. Hadley</i>	723
Cellular Import of Founctional Peptides <i>Jacek Hawiger</i>	726
Novel Highly Potent Bradykinin Antagonists Containing Pentafluorophenylalanine <i>Lajos Gera and John M. Stewart</i>	730
Application of Cell-Permeable Peptides to the Functional Analysis of EGF-Induced Mitogenic Signaling Pathways <i>Mauricio Rojas, Song Yi Yao, John P. Donahue, and Yao-Zhong Lin</i>	733
Biological Functions of Synthetic Peptides Derived from the Laminin Alpha 1 Chain G Domain <i>Motoyoshi Nomizu, Yuichiro Kuratomi, Woo Ho Kim, Sang-Yong Song, Matthew P. Hoffman, Hynda K. Kleinman, and Yoshihiko Yamada</i>	735
Competitive Antagonists of the Corticotropin Releasing Factor (CRF) Scanned with an i-(i+3) Glu_Lys Bridge <i>A. Miranda, S. Lahrachi, J. Gulyas, C. Rivier, S. Koerber, C. Miller, A. Corrigan, S. Sutton, A. Craig, W. Vale, and J. Rivier</i>	737
Cytocidal Effect of Custom Antibacterial Peptides on Leukemia Cancer Cells <i>Hueih Min Chen, Wei Wang, David Smith, and Siu-Chiu Chan</i>	739

- In Vitro and in Vivo* Properties of NSL-9511, a Novel Anti-Platelet Hexapeptide without an RGD Sequence 741  
*Jun Katada, Yoshio Hayashi, Yoshimi Sato, Michiko Muramatsu, Yoshimi Takiguchi, Takeo Harada, Toshio Fujiyoshi and Isao Uno*
- Model Peptides of Interstitial Collagens: Hydrolysis by Matrix Metalloproteinases 743  
*Kathleen A. Tuzinski, Ken-ichi Shimokawa, Hideaki Nagase, and Gregg B. Fields*
- Serum Amyloid A and its Related Peptide Modulate Endothelial Cells Proliferation and Prostaglandin I<sub>2</sub> Production 745  
*Liana Preciado-Patt, Ruth Shainkin-Kestenbaum, and Mati Fridkin*
- A New Paradigm for Fish Antifreeze Protein Binding to Ice 747  
*Michael Houston, Jr., Heman Chao, Michele C. Loewen, Frank D. Sönnichsen, Cyril M. Kay, Brian D. Sykes, Peter L. Davies, and Robert S. Hodges*
- Neuropeptides and Skin Cell Function: VIP and Stearyl-[Nle<sup>17</sup>]VIP Effects on HaCaT Cells 749  
*Ruth Granoth, Mati Fridkin, and Illana Gozes*
- Inhibiting Dimerization and DNA Binding of c-Jun 751  
*S. Q. Yao, E.I. Pares-Matos, M.L. Brickner and J.A. Chmielewski*
- Inhibition of E-Cadherin-Mediated Cell-Cell Adhesion by Cadherin Peptides 753  
*K.L. Lutz, D.Pal, K.L. Audus, and T. J. Siahaan*
- Discovery and Structure-Activity Relationship Study of a Novel and Specific Peptide Motif, Pro-X-X-X-Asp-X, for Platelet Fibrinogen Receptor Recognition 755  
*Yoshio Hayashi, Jun Katada, Yoshimi Sato, Katsuhide Igarashi, Takeo Harada, Michiko Muramatsu, Emiko Yasuda, and Isao Uno*
- Session XI. Peptide Vaccines/Immunology/Viruses**
- Synthetic Combinatorial Libraries for the Study of Molecular Mimicry: Identification of an All D-Amino Acid Peptide Recognized by an Anti-carbohydrate Antibody 761  
*Clemencia Pinilla, Jon R. Appel, Jaime Buencamino, Gretchen D. Campbell, Jutta Eichler, Neil Greenspan, and Richard A. Houghten*
- Processing of Peptide Antigens in EBV-Transformed B Cells and in an *in Vitro* System 763  
*Hubert Kalbacher, Hermann Beck, Christian Schröter, Martin Deeg, Helmut E. Meyer, and Thomas Halder*

New Ligands for MHC Molecules Based on Activity Patterns of Peptide Libraries	766
<i>Karl-Heinz Wiesmüller, Burkhard Fleckenstein, Peter Walden, Roland Martin, Günther Jung</i>	
Transformation of L-Peptide Epitopes into D-Peptide Analog	769
<i>Achim Kramer and Jens Schneider-Mergener</i>	
Production of Potent-Specific Antigens and Effective Immunogens Using Sequential Oligopeptide Carriers (SOC <sub>n</sub> )	771
<i>Constantinos Sakarellos, Vassilios Tsikaris, Eugenia Panou-Pomonis, Charalampos Alexopoulos, Maria Sakarellos-Daitsiotis, Constantinos Petrovas, Panagiotis G. Vlachoyiannopoulos, and Haralampos M. Moutsopoulos</i>	
Cross-Immunogenicity of Topological Mimics of Peptide Antigens	773
<i>Maria Rossi, Antonio Verdoliva, Menotti Ruvo, and Giorgio Fassina</i>	
Searching for Dominant Linear Antigenic Region of Hepatitis B Surface Antigen with Human Immune Sera Against Phage-Displayed Random Peptide Library	775
<i>Zhi-Jian Yao, Lay-Hain Ong, Lily Chan, and Maxey C.M. Chung</i>	
Comparative Immunological Properties of Lipidated HIV-1 gp41 Fragments on Various Structural Templates	777
<i>Artur Pedyczak, Dave McLeod, Olive James, Michel Klein, and Pele Chong</i>	
Biological Effects of Peptide Antibodies Raised to HER-2/neu. Implications for Therapy of Human Breast Cancer	779
<i>Donna-Beth Woodbine, Naveen Dakappagari, Pierre Triozzi, Vern Stevens, and Pravin T.P. Kaumaya</i>	
A Multiple Branch Peptide Construction Derived from a Conserved Sequence of the Envelope Glycoprotein gp41 Inhibits Human Immunodeficiency Virus Infection	781
<i>Jean-Marc Sabatier, Maxime Moulard, Emmanuel Fenouillet, Herve Rochat, Jurphaas Van Rietschoten, and Kamel Mabrouk</i>	
Antigenic Domains of Shigella Virulence Proteins	783
<i>Kevin R. Turbyfill and Edwin V. Oaks</i>	
Characterization and Immune Response of a Novel Synthetic Peptide Vaccine for HTLV-I	785
<i>Melanie Frangione and Pravin T.P. Kaumaya</i>	

Mapping of the Immunodominant B- and T-Cell Epitopes of the Outer Membrane Protein D15 of <i>H. influenzae</i> Type b Using Overlapping Synthetic Peptides	787
<i>Pele Chong, Olive James, Yan-Ping Yang, Charles Sia, Sheena Loosmore, Dave McLeod and M. Klein</i>	
A Novel Bovine Antimicrobial Peptide of the Cathelicidin Family	789
<i>Renato Gennaro, Marco Scocchi, Laura Merluzzi, Shenglun Wang, and Margherita Zanetti</i>	
On the Reaction Kinetics of Peptide: Antibody Binding in the "BIAcore™" Biosensor	791
<i>Robert M. Wohlhueter, Sunan Fang, Thomas W. Wells, and Danny L. Jue</i>	
V3-Mediated Neutralisation of Primary Isolates. Serology with Synthetic V3 Peptides Demonstrates Deficiencies in Anti-V3 Response	793
<i>R. Pipkorn, A. Lawoko, B. Johansson, B. Christenson, B. Ljungberg, U. Dietrich, L. Alkhalili, E-M Fenyö, J. Blomberg</i>	
Conformational Mapping of a Neutralizing Epitope on the C4 Region of HIV-1 gp120 with Cyclic And Bicyclic Peptides	795
<i>Ruoheng Zhang, Yuan Xu, Gerald R. Nakamura, Philip W. Berman, and Arnold C. Satterthwait</i>	
Further Characterization of Anchor and Non-Anchor Residues on Deca- and Undeca-Peptides in Addition to Nona-Peptides, Which Bind to HLA Class I Molecules (HLA-B*3501)	797
<i>Kiyoshi Nokihara, Christian Schonbach and Masafumi Takiguchi</i>	
Delivery of Peptide Epitopes for HTLV-1 Using Biodegradable Microspheres	799
<i>Melanie Frangione, Travis Rose, Steven P. Schwendeman, Vernon C. Stevens, and Pravin T.P. Kaumaya</i>	
<b>Session XII. Analytical Methods</b>	
Differences in Encephalitogenicity in MBP Peptide 68-88 Due to Histidine Racemization	803
<i>P.L. Jackson, M. Villain, F.S. Galin, N.R. Krishna, and J.E. Blalock</i>	
TFA/HCl Mixture as an Alternative to the Standard Propionic Acid/HCl Mixture for Aminoacyl- and Peptidyl-Resin Hydrolysis	805
<i>G. N. Jubilot, A.Miranda, E. Oliveira, E. M. Cilli, M. Tominaga, and C. R. Nakaie</i>	
Investigation of Aggregation and Binding of $\beta(12-28)$ Using NMR Spectroscopy	807
<i>Dimuthu A. Jayawickrama and Cynthia K. Larive</i>	

ESI-MS & MALDI-MS Analysis, and Amino Acid Sequencing of Three Multiple-Antigen Peptides (MAPs) <i>Robert R. Becklin and Dominic M. Desiderio</i>	809
Stability Studies on Peptide Aldehyde Enzyme Inhibitors <i>Patricia A. Messina, John P. Mallamo, and Mohamed A. Iqbal</i>	811
The Selectivity of C18 Reversed-Phase for Peptides Depends on the Type of Silanes Linked to the Silica Matrix <i>Paul J. Kostel, Yan-Bo Yang, and William H. Campbell</i>	813
Purification of a Crude Synthetic Peptide by Strong Cation Exchange: Breaking Up Hydrophobic Complexes Prior to Reversed-Phase <i>Paul J. Kostel</i>	815
Molecular Recognition Using a Peptide Combinatorial Library and Its Detection by Surface Plasmon Resonance Spectroscopy <i>Hiroshi Taniguchi, Koji Inai, Takahisa Taguchi, and Susumu Yoshikawa</i>	817
Preliminary Mapping of Conformational Epitopes on the HPV-16 E7 Oncoprotein <i>Julio C. Calvo, Katia C. Choconta, Diana Diaz, Oscar Orozco, Fabiola Espejo, Fanny Guzman, and Manuel E. Patarroyo</i>	819
<b>Session XIII. Drug Delivery</b>	
Synthesis, Characterization and Use of Novel Non Viral Vectors for Gene Delivery <i>Gerardo Byk, Catherine Dubertret, Bertrand Schwartz, Marc Frederic, Gabrielle Jaslin, and Daniel Scherman</i>	823
Prodrug Strategies to Enhance the Permeation of Peptides Through the Intestinal Mucosa <i>Ronald T. Borchardt</i>	825
Characterization of a Stable Leuprolide Formulation for One Year in an Implantable Device <i>Cynthia L. Stevenson, Cynthia A. Corley, Matt Cukierski, Corinne A. Falender, Steven C. Hall, Paul Johnson, J. Joe Leonard, Mandy M. Tan and Jeremy C. Wright</i>	828
Oligopeptide Transport Systems in Eukaryotes <i>Jeffrey M. Becker, Mark Lubkowitz and Fred Naidler</i>	831

Brain Delivery and Targeting of Thyrotropin-Releasing Hormone Analogs by Covalent Packaging and Sequential Metabolism	834
<i>Laszlo Prokai, Katalin Prokai-Tatrai, Wei-Mei Wu, Jiaxiang Wu, Xudong Ouyang, Ho-Seung Kim, Alevtina Zharikova, James Simpkins, and Nicholas Bodor</i>	
A Novel Lipoamino Acid Based System for Delivery of Leu-Enkephalinamide Derivatives Through the Blood-Brain Barrier	837
<i>Barrie Kellam, Mike Starr, Temitope G. Lamidi, and Istvan Toth</i>	
Hydrophobic Peptides: Synthesis and Interaction with Model Membranes	839
<i>Francesca Reig, Isabel Haro, Patricia Sospedra and M.Asunción Alsina</i>	
Importance of Hydrophobic Region in Cationic Peptides on Gene Transfer	841
<i>Naoya Ohmori, Takuro Niidome, Taira Kiyota, Sannamu Lee, Gohsuke Sugihara, Akihiro Wada, Toshiya Hirayama, Tomomitsu Hatakeyama, and Haruhiko Aoyagi</i>	
A Novel Lipoamino Acid Based System for Peptide Delivery: Application for Administering Tumour Selective Somatostatin Analogues	843
<i>Nicholas S. Flinn, Judit Erchegyi, Aniko Horvath, Gyorgy Keri, and Istvan Toth</i>	
Aerosol Delivery of Peptide Immuno-Modulators to Rodent Lungs	845
<i>Ronald J. Pettis and Anthony J. Hickey</i>	
Indexes	
Author Index	847
Subject Index	861



## Preface

The Fifteen American Peptide Symposium (15APS) was held in Nashville, Tennessee, on June 14-19, 1997. This biennial meeting was jointly sponsored by the American Peptide Society and Vanderbilt University. The attendance of 1,081 participants from 37 countries was lower than the two previously held Symposia. However, the number of participating countries was the largest. Thus, it was gratifying to see that this meeting retained both its international flavor and participant loyalty at a time when there are many more symposia held each year on similar subjects.

The scientific program, thanks to the insights and efforts of the Program Committee as well as Dr. Peter Schiller, the President of the American Peptide Society, was extraordinarily rich, diverse, and exciting. It was comprised of 124 oral and 550 poster presentations. Three prominent format changes were installed. First, the Symposium started on Saturday instead of Sunday. Second, the program opened on Saturday afternoon with a Mini-symposium by the Young Investigators to give them an early start and attention. Finally, 40 short and definitive reports were given in two parallel sessions. The expanded format permitted an unprecedented number of lectures and enabled wider participation by the attending delegates.

Dr. Ralph Hirschmann, Makineni Professor of Bioorganic Chemistry at the University of Pennsylvania, officially opened the Symposium on Sunday morning with an exciting lecture entitled "‘The time has come,’ the walrus said, ‘to talk of many things.’" His lecture focused on past achievements and contributions of peptide chemistry and biology to science and health care.

Sessions I and II covered the frontiers and novel concepts of peptide science. Sessions III to VI dealt with the problems in minimizing proteins to peptides and peptides to drugs.

Sessions VII, VIII and XIX dealt with the increasing importance of peptide mimetics and diversity, including combinatorial libraries, in drug design. Specific problems of peptide and drug designs were also addressed in sessions IV and XX. The problems of drug delivery were explored in Session XVIII.

Other sessions dealt with protein folding, receptor-ligand interactions, peptide biology, peptide immunology and conformational analysis.

This symposium marked the first official presentation of the Merrifield Award, newly endowed by Dr. Rao Makineni. The Alan E. Pierce Award was discontinued. The Merrifield Award recognizes outstanding contributions to the chemistry and biology of peptides and represents the most prestigious award given by the American Peptide Society. This year's recipient was Dr. Shumpei Sakakibara of the Peptide Institute, Inc., Protein Research Foundation, Japan. Dr. Sakakibara delivered the Makineni lecture entitled "Fifty Years of My Protein Synthesis" in which he succinctly described his experience in the arts and methods of protein synthesis.

The success of the 15<sup>th</sup> APS was largely due to the dedication, enthusiasm and hard work of the local organizing committee, who for the most part consisted of volunteers. As Symposium Chair, I am deeply indebted to the postdoctoral fellows in my laboratory at Vanderbilt University. They worked tirelessly, often past midnight, to meet deadlines, and there were many such deadlines. They each spent nearly two months of their time correcting, collating, typing, editing, and proofreading all printed materials, including this proceeding volume. I am also indebted to Ms. Vicki Bryant, my secretary, for her patience in handling administrative matters. Most of all, I am forever grateful to my wife, Sylvaine who shouldered the enormous task of creating the symposium database, keeping track of the correspondence, abstracts, registrations, and

manuscripts as well as maintaining the book-keeping on financial matters and audits.

We are especially grateful for the generous financial support by the Benefactors, Sponsors, Donors and Contributors who are listed on the following pages. Their support enabled the excellence expected of this meeting. Special thanks goes to Polypeptide, Inc. for providing the funds for the purchase of the symposium bags. The Chairman would also like to acknowledge the Department of Microbiology and Immunology, particularly its chairman, Dr. Jacek Hawiger. I also thank Vanderbilt University for their support for holding the 15th American Peptide Symposium in Nashville.

Finally, I would like to acknowledge Ms. Victoria Shaw and her band for their wonderful performance at the closing banquet and for providing a fond memory for all 15<sup>th</sup> APS attendees.

James P. Tam

Pravin T.P. Kaumaya

June 14-19, 1997

Chairman - James P. Tam, *Vanderbilt University*

### **PROGRAM COMMITTEE MEMBERS**

George Barany	<i>University of Minnesota</i>
Richard DiMarchi	<i>Eli Lilly &amp; Company</i>
Annette Doherty	<i>Park-Davis</i>
Gregg B. Fields	<i>University of Minnesota</i>
Roger M. Freidinger	<i>Merck, Sharp &amp; Dohme</i>
Murray Goodman	<i>University of California</i>
Jacek Hawiger	<i>Vanderbilt University</i>
William Heath	<i>Eli Lilly &amp; Company</i>
Richard A. Houghten	<i>Torrey Pines Institute</i>
Isabelle Karle	<i>Naval Research Center</i>
Garland R. Marshall	<i>University of Washington</i>
John P. Mayer	<i>Amgen, Inc.</i>
Daniel Rich	<i>University of Wisconsin</i>
Arno Spatola	<i>University of Louisville</i>
James A. Well	<i>Genetech, Inc.</i>

### **AMERICAN PEPTIDE SOCIETY**

#### *Officers*

Peter W. Schiller	President	Clinical Research Inst. of Montreal
Robert S. Hodges	President-Elect	University of Alberta
Ruth F. Nutt	Secretary	
Teresa M. Kubiak	Treasurer	Pharmacia & Upjohn, Inc.

***Councilors***

George Barany	Lila M. Gierasch	Tomi K. Sawyer
David H. Coy	Richard A. Houghten	James P. Tam
Richard D. DiMarchi	Kenneth D. Kopple	Daniel F. Veber
William F. DeGrado	Daniel H. Rich	Janis D. Young

***Honorary Members***

Elkan R. Blout	Ralph F. Hirschmann	Andrew V. Schally
Miklos Bodanszky	Victor J. Hruby	Harold A. Scheraga
Gerald D. Fasman	Isabella L. Karle	Robert Schwyzer
Joseph S. Fruton	Rao Makineni	John M. Stewart
Murray Goodman	Bruce R. Merrifield	Daniel F. Veber
Roger Guillemin	Shumpei Sakakibara	

***Local Planning Committee***

James P. Tam	<i>Chair</i>
Vicki Bryant	<i>Symposium Secretary</i>
Traci Castleman	<i>Registration</i>
Faith Chan	<i>Registration</i>
Przemyslaw Cieszynski	<i>Operational Manager</i>
John Donahue	<i>Transportation Coordinator</i>
Christophe Hennard	<i>Hospitality Committee</i>
A. Kasia Jarzecka	<i>Registration</i>
Kalle Kaljuste	<i>Vanderbilt Accommodation's Coordinator</i>
Alan Kilpatrick	<i>Computer Applications Consultant</i>
Yao-Zhong Lin	<i>Hospitality Coordinator</i>
Yi-An Lu	<i>Hospitality Committee</i>
Dale McClendon	<i>Exhibit Assistant</i>
Steven Muhle	<i>Hospitality Committee</i>
Gosia Pawlak	<i>Registration</i>
Sue Rowlinson	<i>Registration</i>
Greta Tam	<i>Registration</i>
Jonathan Tam	<i>Registration</i>
Sylvaine Tam	<i>Data Manager</i>
Sheila Timmons	<i>Hotel Accommodations Coordinator</i>
Carol Water	<i>Manuscript Editor</i>
Deborah West	<i>Registration</i>
Ola Wyslouch-Cieszynska	<i>Abstract/Program Book Coordinator</i>
Qitao Yu	<i>Audio Visual Coordinator</i>
Lianshan Zhang	<i>Child Care/AV Coordinator</i>

## **ACKNOWLEDGMENTS**

The Fifteenth American Peptide Symposium organizing committee is grateful for the financial and administrative support of the host institution:

### **VANDERBILT UNIVERSITY**

***Medical School, Department of Microbiology & Immunology***

The Fifteenth American Peptide Symposium organizing committee also greatly appreciates the support and generous financial assistance of the following organizations:

## **BENEFACTORS**

### ***PolyPeptide Laboratories Group***

***PolyPeptide Laboratories, Inc., USA***

***PolyPeptide Laboratories AB, Sweden***

***PolyPeptide Laboratories A/S, Denmark***

## **SPONSORS**

***Hoffman-LaRoche***

***Amgen***

***C S Bio Co.***

***Eli Lilly & Company***

***Genzyme Pharmaceuticals***

***Synthetech***

***Abbott Laboratories***

***Mallinckrodt Chemical***

## DONORS

*Pfizer*

*Bio-Synthesis*

*Biomeasure*

*Multiple Peptide Systems*

*Peninsula Laboratories*

*SmithKline Beecham*

*UCB-Bioproducts S. A.*

*Biogen*

*GlaxoWellcome*

*Merck Research Laboratories*

*Neuropeptide Dynamics*

*Orpegen Pharma*

*Parke-Davis Pharmaceutical Research*

*Pharmacia & Upjohn*

## CONTRIBUTORS

*Alza*

*Bio-Mega*

*Bristol-Myers Squibb*

*Dupont-Merck*

*Waters*

*Zeneca Pharmacetuticals*

*Sigma-Aldrich*

# **The Merrifield Award 1997**

**(Generously endowed by Dr. Rao Makineni)**

## **Shumpei Sakakibara**

The first recipient of the newly created Merrifield Award is Dr. Shumpei Sakakibara, founder and long-time chairman of Peptide Institute Inc., Protein Research Foundation, Osaka, Japan. This award has recently been created through the effort of Dr. James P. Tam and with a generous endowment from Dr. Rao Makineni who retired from Bachem California last year. The Merrifield Award represents the most prestigious APS award and continues under a new title the Society's previous Alan E. Pierce Award.

Dr. Sakakibara is one of the world's foremost leaders in peptide chemistry. One of his major scientific contributions was the development of the hydrogen fluoride cleavage reaction in solid-phase peptide synthesis. Another great achievement of his illustrious career is the synthesis, by solid-phase or fragment condensation methods, of large, complex biologically active peptides, including human parathyroid hormone-(1-84), omega-conotoxin GIVA, omega-agatoxin IVA, porcine C5a anaphylatoxin, angiogenin-(1-123), calciseptine and human midkine.

Dr. Sakakibara started his career as research associate in the laboratory of Professor Shiro Akabori at Osaka University (1951-60) and received his Ph. D degree from the same university. He was a research associate at Cornell University, Ithaca (1960-63). He then returned to Japan to assume a position as associate professor in the Institute for Protein Research at Osaka University. In 1971, he founded the Peptides Institute (Protein Research Foundation) in Osaka and served as its director (1971-76), president (1976-91) and Chairman of the Board (1991-96). From 1990-1992, he was the president of the Japanese Peptide Society. His other awards include the Chemical Technology Award from the Kinki Chemical Company, the Scoffone Medal, and the Hirschmann Award. Dr. Sakakibara is the second non-American recipient of the American Peptide Society's most prestigious award.

## Alan E. Pierce Award

(Sponsored by Pierce Chemical Company, 1977-1995)

The recipient is an individual who has made outstanding contributions to techniques and methodology in the chemistry of amino acids, peptides and proteins.

<b>1995</b>	<b>John M. Stewart</b>	<b>1993</b>	<b>Victor J. Hruby</b>
<b>1991</b>	<b>Daniel Veber</b>	<b>1989</b>	<b>Murray Goodman</b>
<b>1987</b>	<b>Choh Hao Li</b>	<b>1985</b>	<b>Robert Schwyzer</b>
<b>1983</b>	<b>Ralph Hirschmann</b>	<b>1981</b>	<b>Klaus Hofmann</b>
<b>1979</b>	<b>Bruce Merrifield</b>	<b>1977</b>	<b>Miklos Bodanszky</b>

## American Peptide Symposia

<b>Symposium</b>	<b>Chair(s)</b>	<b>Location</b>
First 1968	<b>Saul Lande</b> <i>Yale University</i> <b>Boris Weinstein</b> <i>University of Washington, Seattle</i>	Yale University New Haven, CT USA
Second 1970	<b>F. Merlin Bumpus</b> <i>Cleveland Clinic, Cleveland</i>	Cleveland Clinic Cleveland, OH, USA
Third 1972	<b>Johannes Meienhofer</b> <i>Harvard Medical School</i> <i>Boston</i>	Children's Cancer Research Foundation Boston, MA, USA
Fourth 1975	<b>Roderich Walter</b> <i>University of Illinois</i> <i>Medical Center, Chicago</i>	The Rockefeller University and Barbizon Plaza Hotel New York, NY, USA
Fifth 1977	<b>Murray Goodman</b> <i>University of California-</i> <i>San Diego</i>	University of California- San Diego, San Diego, CA USA

Sixth 1979	<b>Erhard Gross</b> <i>National Institute of Health Bethesda</i>	Georgetown University Washington, DC, USA
Seventh 1981	<b>Daniel H. Rich</b> <i>University of Wisconsin Madison</i>	University of Wisconsin- Madison, Madison, WI. USA
Eighth 1983	<b>Victor J. Hruby</b> <i>University of Arizona Tucson</i>	University of Arizona Tucson, AZ, USA
Ninth 1985	<b>Kenneth D. Kopple</b> <i>Illinois Institute of Technology Chicago</i> <b>Charles M. Deber</b> <i>University of Toronto, Toronto</i>	University of Toronto Toronto, Ontario Canada
Tenth 1987	<b>Garland R. Marshall</b> <i>Washington University School of Medicine, St. Louis</i>	Washington University St. Louis, MO, USA
Eleventh 1989	<b>Jean E. Rivier</b> <i>The Salk Institute for Biological Studies, La Jolla</i>	University of California- San Diego, CA, USA
Twelfth 1991	<b>John A. Smith</b> <i>Massachusetts General Hospital, Boston</i>	Massachusetts Institute of Technology, Cambridge, MA, USA
Thirteenth 1993	<b>Robert S. Hodges</b> <i>University of Alberta, Edmonton</i>	Edmonton Convention Centre, Edmonton, Alberta, Canada
Fourteenth 1995	<b>Pravin T.P. Kaumaya</b> <i>Ohio State University, Columbus</i>	Ohio State University Columbus, OH, USA
Fifteenth 1997	<b>James P. Tam</b> <i>Vanderbilt University Medical School, Nashville</i>	Nashville Convention Center, Nashville, TN, USA
Sixteenth 1999	<b>George Barany &amp; Gregg Fields</b> <i>University of Minnesota,</i>	Minneapolis, MN, USA

Seventeenth 2001 **Richard A. Houghten**  
*Torrey Pines Institute*

San Diego, CA, USA

## **1997 Young Investigator Poster Competition Awards**

### **First Place**

Harald K. Rau

*Albert-Ludwigs Universitat, Germany*

### **Second Place**

Xiaohui Jiang  
Li-Ping Liu

*University of California - San Diego  
Hospital for Sick Children and  
University of Tonoton, Canada*

### **Third Place**

Ioana Annis  
Carrie Haskell-Luevano  
Matthew J. Sandeholm  
Cheryl A. Slate  
Lukas C. Scheibler

*University of Minnesota  
University of Michigan  
University of North Carolina, Chapel Hill  
University of North Carolina, Chapel Hill  
University of Lausanne, Switzerland*

### **Honorable Mentions**

Matthew Bogyo  
Margaret L. Falcone  
Melanie Frangione  
Carol B. Fowler  
Wenli Ma  
Michael Randall  
Michael D. Schultz  
Sandra C. Vigil-Cruz

*Massachusetts Institute of Technology  
University of Maryland  
Ohio State University  
University of Michigan  
University of Michigan  
Ohio State University  
Purdue University  
University of Maryland, Baltimore*

### Poster Competition Judges

Jane Aldrich (Chair, Student Affairs Committee)		
Art Felix (Co-chair, Student Affairs Committee)		
Fernando Albericio	Michael Chorev	Wayne Cody
Ben Dunn	Gregg Fields	Deborah Heyl-Clegg
Richard Houghton	Rodney Johnson	Steve Kates
Lenore Martin	Tom Muir	Kerry Spear
John Taylor	Janis Young	

## American Peptide Society 15th American Peptide Symposium Travel Grant Recipients

Jung-Mo Ahn, USA	Kristin Jauch, German
Ludmila Gennadyevna Alekseeva, Russia	Francois Jean, USA
Lorenzo Josue Alfaro-Lopez, USA	Xiaohui Jiang, USA
Yvonne M. Angell, USA	Michael B. Keller, Switzerland
Ioana Annis, USA	Wayne D. Kohn, Canada
Jordi Bacardit, Spain	Jennifer A. Kowalski, USA
Bari A. Barwis, USA	Haitao Li, USA
Eric Beausoleil, Canada	Subo Liao, USA
Vered Behar, USA	Inta Liepina, Latvia
Marta Del Rosario Benites, USA	Amareth Lim, USA
Alessandro Bisello, USA	Li-Ping Liu, Canada
Barney M. Bishop, USA	Ralph-Heiko Mattern, USA
Gal Bitan, USA	Kristofer K. Moffett, USA
Matthew S. Bogyo, USA	Bassam M. Nakhle, USA
Michelle L. Brickner, USA	Svetlana S. Pantchcva, Bulgaria
Lin Chen, USA	Maria M. Pellegrini, USA
Guzin Dogruyol, USA	Liana Preciado-Patt, Israel
Amanda L. Doherty-Kirby, Canada	Marketa Rinnova, Czech Republic
Margaret L. Falcone, USA	Johanne Roby, Canada
Hong Fan, USA	Jaimie K. Rueter, USA
Ted J. Gauthier, USA	Sheila D. Rushing, USA
Ruth Granoth, Israel	Matthew J. Saderholm, USA
Karen S. Gregson, USA	Seiji Sakamoto, Japan
Christopher M. Gross, USA	Mohamed D. Salamoun, USA
Guoxia Han, USA	Lukas C. Scheibler, Switzerland
Yinglin Han, USA	Cheryl A. Slate, USA
Balazs Hargittai, USA	Tsuyoshi Takahashi, Japan
Bernd Henkel, Germany	Yuta Takahashi, Japan
Hoebert S. Hiemstra, The Netherlands	Andreas Tholey, Japan

Kin-ya Tomizaki, Japan  
Shawn M. Vogen, USA  
Qiang Wan, USA  
Kevin R. Wyckoff, USA  
Christopher L. Wysong, USA  
Qinghong Xu, USA  
Dror Yahalom, Isreal  
Thomas Scott Yokum, USA  
Chongxi Yu, USA  
Natalya I. Zaitseva, Russia

## Abbreviations

Abbreviations of common amino acids and units of measurements based on the IUPAC nomenclature are not enumerated. However, other abbreviations used in this proceedings volume are defined below:

$\mu$	hydrophobic moment		Bal)-Apn-Abc-Gly-NH <sub>2</sub>
[ $\theta$ ]	mean residue ellipticity	AMBER	assisted model building and energy refinement
Abc	4'-aminomethyl-2,2'-bipyridine-4-carboxylic acid	AMC	aminomethylcoumaride
Abh	azabicyclo[2.2.1]heptane-2-carboxylic acid	AMCA	7-amino-4-methylcoumarin-
Abl	abelson kinase		3-acetic acid
Abu	$\alpha$ -amino- <i>n</i> -butyric acid	Amn	8-(aminomethyl)naphth-2-oic acid
Abz	2-amino-benzoic acid; 2-aminobenzoyl	APB	(4-amino)phenylazobenzoic acid
AC	adenylyl cyclase	APC	antigen presenting cell
Ac	acetyl; acyl	Apn	5-aminopentanoic acid
Ac <sub>6</sub> C	1-amino-cyclohexyl-1-carboxylic acid	Arg-al	argininal
Aca	adamantanecarboxyl-	Arg-ol	argininol
Acc	1-aminocyclopropane-1-carboxylic acid	ATP	adenosine triphosphate
Acm	acetamidomethyl	AUC	area under the curve
AEDI	aminoethyldithio-2-isobutyric acid	AVP	vasopressin
AHA	6-aminohexanoic acid	B	$\alpha$ -aminobutyric acid
Ahp	2-amino-heptanoic acid	BAL	backbone amide linker; broncho-alveolar lavage
$\Delta^6$ Ahp	6-dehydro-2-amino-heptanoic acid	bApG	<i>N,N</i> -bis(3-aminopropyl)-glycine
Ahx	6-aminohexanoic acid	BBB	blood brain barrier
$\epsilon$ Ahx	aminohexanoic acid	BK	bradykinin
Aib	$\alpha$ -aminoisobutyric acid	BMAP	bovine myeloid antimicrobial peptide
AI	angiotensin II	BME	$\beta$ -mercaptoethanol
Al	allyl	Bn	benzyl
Alloc	allyloxycarbonyl	Boc, BOC	<i>tert</i> -butyloxycarbonyl
AM	alveolar macrophage		
ama	Ac-Abc-Ahx-Orn(Mbc-		

Boc-ON	2- <i>tert</i> -butyloxy-carbonylamino-2-phenylacetoneitrile	DB[DMAP]	2,6-di- <i>tert</i> -butyl-4-(dimethylamino)pyridine
Boc <sub>2</sub> O	di- <i>tert</i> butyl dicarbonate	DBU	1,8-diazabicyclo [5.4.0]-undec-7-ene
BOP	(benzotriazol-1-yloxy)-tris(dimethylamino) phosphonium hexafluorophosphate	DCCI; DCC	dicyclohexylcarbodiimide
Bpa	p-benzoylphenylalanine	DCM	dichloromethane
BPTI	bovine Pancreatic trypsin inhibitor	Dde	1-(4,4-dimethyl-2,6-dioxocyclohexylidene)ethyl
bpy	2,2'-bipyridine	Ddz	$\alpha,\alpha$ -dimethyl-3,5-dimethoxybenzyloxycarbonyl
Bzl	benzyl	DHT	1,4-Dihydrotrigonellyl
CaM	calmodulin	DIC	diisopropylcarbodiimide
CAMM	computer assisted molecular modeling	DIEA	<i>N,N</i> -diisopropylethylamine;
CBA	carboxymethyl	DIPCDI	<i>N,N'</i> -diisopropylcarbodiimide
Cbz	carbobenzyloxy; benzyloxycarbonyl	DMAP	4-dimethylaminopyridine
CCK	cholecystokinin	DMER-Plot	difference minimum energy ramachandran plot
CCK-B	cholecystokinin-B	DMF	dimethylformamide
CD	circular dichroism	DMSO	dimethyl sulfoxide
$\beta$ -CD	$\beta$ -cyclodextrin	DNP	dinitrophenyl
CED3	<i>cenorhabditis elegans</i> cell-death protein	DOF-COSY	double quantum field
CF	5(6)-carboxyfluorescein	COSY	
CFU	colony forming units	DOPC	dioleoyl-DL- $\alpha$ -phosphatidylcholine
Cha	cyclohexylalanine	DOPG	dioleoyl-DL- $\alpha$ -phosphatidylglycerol
Chg	$\alpha$ -cyclohexylglycine	DPC	dodecyl phosphocholine
Cho	cholesteryl	DPDPE	<i>cyclo</i> [DPen <sup>2</sup> -DPen <sup>5</sup> ]enkephalin
Clt-resin	2-chlorotrityl resin	DPPA	diphenylphos-phorylazide
Cl-Trt	2-Cl-trityl	DPPC	dipalmitoyl-DL- $\alpha$ -phosphatidylcholine
Cl-Z	2-chlorobenzyloxycarbonyl	DPPG	dipalmitoyl-DL- $\alpha$ -phosphatidylglycerol
Cpg	$\alpha$ -cyclopentylglycine	DTT	dithiothreitol
Cpg→Arg	pseudo (CH <sub>2</sub> NH) Cpg-Arg	EAE	experimental allergic encephalomyelitis
CRF	corticotropin releasing factor	EBP	erythropoietin binding
CTL	cytotoxic T-lymphocyte	EBV	Epstein-Barr virus
d.e.	diastereomeric excess		
Da	Dalton		
DAMGO	[Dala <sup>3</sup> ,MePhe <sup>4</sup> ,Glyal <sup>5</sup> ]enkephalin		

ED50	median effective dose		bound protein 2
EDT	1,2-ethanedithiol	GRF	growth hormone releasing factor
EDTA	ethylenediamine-tetraacetic acid	GS	gramicidin S
EGF	epidermal growth factor	GSH	reduced glutathione
EGFR	EGF receptor	GSSG	oxidized glutathione
EGS	ethylene glycol <i>bis</i> -	GuHCl	guanidine hydrochloride
succinyl-		H	hydrophobicity
ELISA	enzyme linked immunosorbance assay	Hat	2-amino-6-hydroxytetralin-2-carboxylic acid
EMP	erythropoietin mimetic protein	HATU	O-(7-azabenzotriazol-1-yl)- <i>N,N,N',N'</i> -tetramethyluronium hexafluorophosphate
EPO	erythropoietin		
ES-MS	electrospray mass spectrometry	HBTU	2-(1 <i>H</i> -benzotriazol-1-yl)-1,1,3,3-tetramethyluronium hexafluorophosphate
ESI	electrospray ionization		
ESR	electron spin resonance	HBV	hepatitis B virus
ESTs	expressed sequence tags	hCG	human chorionadotropin
ET-1	endothelin-1	HCV	hepatitis C virus
Et <sub>3</sub> N	triethylamine	HDAG	hepatitis delta antigen
ET <sub>A</sub> R	endothelin-A receptor	HDV	hepatitis delta virus
F <sub>2</sub> Pmp	difluorophosphonomethyl phenylalanine	HFIP	hexafluoroisopropanol
f5f	pentafluorophenylalanine	HG	human gastrin
FAB-MS	fast atom bombardment mass spectrometry	HIV	human immunodeficiency virus
FceRI	IgE-receptor	HLA	human leukocyte antigen
FceRI $\alpha$	IgE-receptor- $\alpha$ -subunit	hm	human muscarinic receptor
FITC	fluorescein isothiocyanate	hm1 trune	truncated muscarinic receptor
fMLP	formyl-Met-Leu-Phe	HMC	hydroxymethylcarbonyl
Fmoc; Fmoc	9-fluorenylmethoxycarbonyl	HMPA	<i>p</i> -hydroxymethylphenoxy acetic acid
Fmoc-Cl	9-fluorenylmethoxy chloroformate	HMPA	hexamethylphosphoramide
FTIR	Fourier transform infrared	HMPB	4-(4-hydroxymethyl-3-methoxyphenoxy)-butyric acid
GalR	galanin receptor		
GdnHCl	guanidinium hydrochloride	<sup>1</sup> H-NMR	protein nuclear magnetic resonance
GFC	gel filtration chromatography	<sup>3</sup> H-NMS	tritiated <i>N</i> -methyl scopalamine
GlcNAc	<i>N</i> -acetylgalactosamine	HOAt	1-hydroxy-7-azabenzotriazole
GPCR	G-protein-coupled receptor		
GpIIb/IIIa	glycoprotein IIb/IIIa		
Grb <sub>2</sub>	growth factor receptor-		

HOBt	1- hydroxybenzotriazole	IP <sub>3</sub>	inositol trisphosphate;
HPLC	high performance liquid chromatography	1,4,5-	trisphosphate
Hpp	3-(4-hydroxyphenyl)proline	ITC	isothermal titration calorimery
HPV	human papilloma virus	LAH	lithium aluminum hydride
HSBtU	(2-mercaptobenzoxazol-2-yl)-1,1,3,3-tetramethyluronium-hexafluorophosphate	LDL	low density lipoprotei
HSBtU	2-(1-mercaptobenzoxazol-1-yl)-1,1,3,3-tetramethyluronium-hexafluorophosphate	LHR	lutropin receptor
1-		Lol	leucinol
		LPS	lipopolysaccharide
		LUV	large unilamellar vesicle
		MAb	monoclonal antibody
		MAdCAM-1	mucosal addressin cell adhesion molecule-1
HSF	hematopoietic synergistic factor	MALDI	matrix-assisted laser desorption/ionization
HSNPtU	2-(1-mercapto-4-nitrophenyl-1-yl)-1,1,3,3-tetramethyluronium-hexafluorophosphate	MALDI-MS	MALDI mass spectrometry
HSDNPtU	2-(1-mercapto-2,4-dinitrophenyl-1-yl)-1,1,3,3-tetramethyluronium-hexafluorophosphate	MALDI-TOF MS	MALDI time-of-flight mass spectrometry
HTLV virus	human T cell leukemia	MAP	mitogen-activated protein; multiple antigen peptide
Inogatran	glycine, N-{2-[2-[[[3-(aminoiminomethyl)amino]propyl]amino]-carbonyl]-1-piperidinyl]1-(cyclohexylmethyl)-2-oxoethyl]-[2 <i>R</i> -[2 <i>S</i> ]]	Mbc	4'-methyl-2,2'-bipyridine-4-carboxylic acid
i.v.	intravenous	MBHA	<i>para</i> -methylbenzhydrylamine
IAPP	islet amyloid polypeptide	MBHA	methylbenzhydrylamine
iBoc	isobutyloxycarbonyl	MBP	myelin basic protein
IC <sub>50</sub>	50% inhibition concentration	MC1R	melanocortin-1 receptor
ICE	interleukin-1 $\beta$ converting enzyme	MCR	melanocortin receptor
IFN	interferon	MD	molecular dynamics
Igl	$\alpha$ -(2-indanyl)-glycine	MDP	muramyl dipeptide
IL-1 $\beta$	interleukin-1 $\beta$	Me	methyl
		MeCN	acetonitrile
		MeOBzl	<i>para</i> -methoxybenzyl
		MeOH	methanol
		MER-Plot	minimum energy ramachandran plot
		MHC	major histocompatibility complex
		MIC	minimum inhibitory concentration

MIF	macrophage migration inhibitory factor	Ntc <sup>2α</sup>	nortropane-2α-carboxylic acid
MMP	matrix metalloproteinase	Ntc <sup>2β</sup>	nortropane-2β-carboxylic acid
Mmt	4-methoxytrityl		
MS	mass spectrometry	Ntc <sup>3</sup>	nortropane-3-carboxylic acid
MSH	melanocyte stimulating hormone, melanotropin		
MT-I	[Nle <sup>4</sup> ,Dphe <sup>7</sup> ]α-MSH	O	defined sequence position in peptide libraries
MT-II	Ac-Nle <sup>4</sup> -c[Asp <sup>5</sup> ,Dphe <sup>7</sup> ,Lys <sup>10</sup> ]α-MSH(4-10)-NH <sub>2</sub> ; Ac-Nle-e[Asp <sup>5</sup> , Dphe <sup>7</sup> , Lys <sup>10</sup> ]α-MSH(4-10)-NH <sub>2</sub>	O/X <sub>10</sub>	the complete set of 220 sublibraries
Mtr	2,3,6-trimethyl-4-methoxybenzenesulfonyl	o-AMPA	o-aminomethylphenylacetic acid
Mtt	4-methyltrityl	Ochx	cyclohexyl ester
NADPH	nicotinamide adenine dinucleotide phosphate, reduced form	OHA	octahydroacridine
Nal	naphthylalanine	Oic	octahydroindole-2-carboxylic acid
Nc7g	<i>N</i> -cycloheptylglycine	Ome	methoxy
Nchg	<i>N</i> -cyclohexylglycine	OMI	oxomorphindole
Nec	norecgonidine	OPT	oligopeptide transport
Nip	nipecotinic acid	Orn	ornithine
NIR-FT	near-infrared, fourier-transform	Orn-ol	ornithinol
NK-1	neurokinin -1 receptor (substance P receptor)	OVX	ovariectomy
NKA	neurokinin A	PAL	tris(alkoxy)benzylamide; peptide amide linker, 5-(4-Fmoc-aminomethyl-3,5-dimethoxyphenoxy)valeric acid
NKB	neurokinin B	PAM	peptidyl glycine α-amidating
NKR cells	normal rat kidney cells		
NMePhe;		PBMC	monoxygenase peripheral blood mononuclear cells
NMF	<i>N</i> -methyl phenylalanine		
NMM	<i>N</i> -methylmorpholine	PBS	phosphate-buffered saline
NMP	<i>N</i> -methylpyrrolidinone	PC	phosphatidylcholine
NMR	nuclear magnetic resonance	PCR	polymerase chain reaction
NO	nitric oxide	Pd/C	palladium on carbon
nOct	<i>n</i> -octanoyl	PDI	protein disulfide isomerase
NOE	nuclear overhauser effect	PEG	polyethylene glycol
NOESY	nuclear overhauser enhanced spectroscopy	PEG-PS	Polyethylene glycol-polystyrene
NPY	Neuropeptide Y	PEGA	polyethylene glycol pole-

	acrylamide copolymer	PyAOP	(7-azabenzotriazol-1-
Pen	penicillamine	yl oxy)-	
Pfp	pentafluorophenyl ester		tris(pyrrolidino)
Phe	phenylalanine		phosphonium
Phe(4-CH <sub>2</sub> OH)	4-		hexafluorophosphate
	hydroxymethylphenylalanine	PyBOP	(benzotriazol-1-yloxy)-
Phe(4-Et)	4-ethylphenylalanine		tris(pyrrolidino)
			phosphonium
ΔPhe	dehydrophenylalanine; α,β-	QSAR	hexafluorophosphate
	dehydrophenylalanine		quantitative structure-
∇Phe	cyclopropylphenylalanine	relC	activity relationships
PI	phosphatidylinositol	RGD	relative competition
PLC	phospholipase C	RMSD	Arg-Gly-Asp
PLN	phospholamban	RNA	root mean square deviation
PLP	proteolipid protein	RP	ribonucleic acid
PM	plasma membranes	RP-HPLC	reversed-phase
Pmc	2,2,5,7,8-		reversed-phase high
	pentamethylchroman-		performance liquid
	6-sulfonyl	RuCl <sub>2</sub> (dmsO) <sub>4</sub>	chromatography
PMD	Pelizaesus-Merzbacher		dichloro tetrakis(dimethyl
	disease	Ru <sup>II</sup>	sulfoxide)ruthenium(II)
pNA	p-nitroaniline	Ru <sup>II</sup> (ama)	ruthenium(II)
Pnc	3β-phenylnorepinephrine-2-	SAPS	ama complexed with Ru <sup>II</sup>
	carboxylic acid		sequence assisted peptide
pNpys	5-nitro-2-pyridinesulfonyl	SAR	synthesis
PPCE	post-proline cleaving		structure activity
	enzyme	SCLs	relationships
PS	polystyrene		synthetic combinatorial
PSD/CID	post source decay/collision-	SD	libraries
	induced dissociation	SH(32)	standard deviation
PS-SCL	positional scanning SCL		dual domains with SH2 and
PTH	parathyroid hormone	SH2	SH3
PTHrP	parathyroid hormone related	SH3	src homology domain 2
	protein	SHU-9119	src homology domain 3
PTK	protein tyrosine kinase		Ac-Nle <sup>4</sup> -c[Asp <sup>5</sup> ,Dnal(2') <sup>7</sup> ,
PTP	protein-tyrosine	SNC-80	Lys <sup>10</sup> ]α-MSH(4-10)-NH <sub>2</sub>
	phosphatase		(+)-4-[(αR-α-((2S',5R)-4-
PTR	peptide transport		allyl-2,5-dimethyl-1-
pTyr	phosphotyrosine		piperazinyl)-3-
pY	phosphotyrosine	SIOM	methoxybenzyl]-N,N-
			diethylbenzamide
			7-spiroindolyloxymorphone

SP	substance P		potential 3 point water
SPPS	solid phase peptide	TLC	thin layer chromatography
synthesis		TMH	transmembrane helix
SPR	surface plasma resonance	Tmob	<i>S</i> -2,4,6-trimethoxybenzyl
SR-Ca <sup>2+</sup> -	sarcoplasmic reticulum	TMP	2,4,6-trimethylpyridine
ATPase	Ca <sup>2+</sup> - ATPase	TMS-Cl	trimethylsilyl chloride
ss-DNA	single-stranded DNA	TMSI	iodotrimethylsilane
Sub	(2 <i>S</i> ,7 <i>S</i> )-2,7 diaminosuberic acid	TMT	$\beta$ -methyl-2',6'-dimethyltyrosine
SUV	small unilamellar vesicle	TOAC	2,2,6,6-tetramethylpiperidine-1-oxyl-4-amino-4-carboxylic acid
SynJ	synthetic J protein		
TAN-67	2-methyl-4a $\alpha$ -(3-hydroxyphenyl)-1,2,3,4,4a,5,12,12a $\alpha$ -octahydroquinolino[2,3,3-g]isoquinoline	TOCSY	total correlation spectroscopy
TASP	template-assembled synthetic protein(s)	Tos	<i>p</i> -toluenesulfonyl
TBDMS	<i>tert</i> -butyldimethylsilyl	TPTU	2-(2-oxo-1(2 <i>H</i> )-pyridyl)-1,1,3,3-tetramethyluronium
<sup>t</sup> BU	<i>tert</i> -butyl		tetrafluorophosphate; 2-(2-pyridon-1-yl))-1,1,3,3-tetramethyluronium
TCEP	tris(carboxyethyl)phosphine	TRH	thyrotropin-releasing hormone
Tea	triethylamine	Tris	tris(hydroxymethyl)aminomethane
TEMP	2,3,5,6-tetramethylpyridine	Trt	trityl
TFA	trifluoroacetic acid	TsOH	toluenesulfonic acid
TFE	trifluoroethanol	Tyr(NO <sub>2</sub> )	3-nitrotyrosine
TFFH	tetramethylfluoro-formamidinium hexafluorophosphate	W13	<i>N</i> -(4-aminobutyl)-5-chloro-2-naphthalenesulfonamide
TFMSA	trifluoromethylsulfonic acid	X	randomized sequence
TGF $\alpha$	transforming growth factor alpha	XAL	position in peptide libraries
THF	tetrahydrofuran		5-(9-aminoxanthen-2-oxy)valeric acid
Thi	$\beta$ -(2-thienyl)-alanine	Xan	<i>S</i> -9 <i>H</i> -xanthen-9-yl
THP	triple-helical peptide	Z	benzyloxycarbonyl
Tic	1,2,3,4-tetrahydroisoquinoline-3-carboxylic acid		
TIP3P	transferable inter-molecular		

# Fifty years of my protein synthesis

**Shumpei Sakakibara**

*Peptide Institute, Inc., Protein Research Foundation  
Minoh-shi, Osaka 562, Japan*

I am greatly honored to have been selected as the recipient of the first Bruce Merrifield Award. I am grateful to those who nominated me for this Award and supported me during the selection process. I am particularly honored to receive this award named after a great scientist who showed the possibility of the chemical synthesis of ribonuclease A by the solid phase method in early 1969. It is an additional pleasure to know that my nomination for this Award was sponsored by one of my friends, Rao Makineni, who must be the most successful and generous man in the peptide business. My thanks are also extended to each of my colleagues who worked with me through every stage of my research over the past 50 years. Without their contributions, I know I could not have realized my life-long dream. Now, I would like to thank the organizing committee of this symposium for giving me an opportunity to give a talk on the background leading to the establishment of the methodology for our solution synthesis of proteins.

## 1951 to 1960

I graduated from Osaka University in 1951, and started my research career as a peptide chemist in the same University. My first project under my instructor was the synthesis of poly- $\alpha$ -amino acids. In 1953, I tried to synthesize a copolymer of Lys, Glu, and Cys by the polymerization of a mixture of the respective *N*-carboxy anhydrides in a ratio of 20:20:1, but the synthetic product was far different from the natural protein [1]. In that year, 1953, almost all peptide chemists around the world were very much excited on hearing the announcement by du Vigneaud of the total synthesis of oxytocin. I tried to reproduce his oxytocin synthesis in my laboratory, but I could only synthesize the N-terminal tripeptide, Z-Pro-Leu-Gly-OEt, in a crystalline form.

In 1955, Morris Huggins of Eastman Kodak visited Osaka University and gave a lecture on the structure of collagen. He suggested that if someone could synthesize a sequential polymer having a unit of (Gly-Pro-X), it should be useful for studying the three-dimensional structure of collagen by X-ray. I thought that the C-terminal tripeptide of oxytocin could be used as the starting material. I had the additional idea of polymerizing the free tripeptide, Pro-Leu-Gly, by heating with Anderson's reagent, tetraethylpyrophosphite, in diethylphosphite, which I had prepared myself for the synthesis of oxytocin. Finally, I got a product, (Pro-Leu-Gly)<sub>n</sub>, which had an average molecular weight of 3000 ( $n \approx 10$ ), but it was just an amorphous powder and not as useful as had been expected for X-ray analysis [2]. Later, however, this material was found to be digestible by a bacterial collagenase, and after examining the structure of the digested peptides, the substrate

specificity of the collagenase as well as the smallest size of the substrate could be determined [3].

### 1960 to 1970

After receiving a Ph.D. in 1960, I had a chance to work with Professor George Hess at Cornell University for two years. His interest was in using liquid HF as a solvent for proteins and in elucidating the mechanism of the inactivation of proteins in HF. This phenomenon was originally reported by Joseph Katz of the Argonne National Laboratory in 1954. He had tried to dissolve various biologically active peptides or proteins in HF and found that the recovered materials showed only diminished biological activities although some of them gradually regained their original activity when kept in a buffer solution for a while. Professor Hess considered that such a reversible inactivation of peptides could be explained by *N* to *O* acyl migration of the peptide bonds at the Ser or Thr residue. To elucidate the mechanism, I was asked to synthesize several Ser- or Thr-containing peptides and put them in HF under various conditions. I was able to confirm that *N*-Gly-Ser was converted to *O*-Gly-Ser in HF after 2 or 3 weeks at room temperature. On the other hand, the *O*-Gly-Ser formed reverted to the original *N*-Gly-Ser instantly in an aqueous sodium hydrogencarbonate solution [4]. While repeating these experiments, a Z-peptide happened to be added to the HF, and it was observed that the Z-group decomposed immediately at below 0°. I reported this fact to my superior, but no interest in this phenomenon was shown because the Z-group was known to decompose in anhydrous HBr in acetic acid at room temperature. I, therefore, decided to continue this work after returning to Japan. However, I am grateful to Professor Hess for having given me a chance to work with liquid HF in his laboratory.

After returning to Japan, I assembled the HF-reaction apparatus in my laboratory and tried to dissolve various protected amino acids or peptides in HF. I found that almost all benzyl-type protecting groups as well as the nitro group of Arg were removable at room temperature [5]. My major interest was to discover whether the S-Bzl group could be removed by HF because it was known to be stable even in HBr/AcOH. In 1959, Micros Bodanszky reported a new synthesis of oxytocin by elongating the peptide bonds one by one using Z-amino acid p-nitrophenylesters as building blocks followed by removal of the Z-group by HBr/AcOH. By using his procedure, I was finally able to synthesize oxytocin. This gave me a small amount of fully protected oxytocin containing one Z group and two Cys(Bzl) groups in the sequence. The protected peptide was treated with HF at room temperature, and after aeration for several hours, the product was found to show oxytocic activity. I reported this in a short communication in 1965 [6]. The next year, I reported the behavior of various protecting groups in HF and the new synthesis of Arg-vasopressin by the HF method at the 8th European Peptide Symposium held in Holland [7]. At the same symposium, Bruce Merrifield reported the synthesis of insulin by his solid phase method. After the meeting, I visited his laboratory in New York, and we discussed the usefulness of the HF method in peptide synthesis. This procedure was then adopted by Merrifield as the

standard method for removing products from his peptide resins, and finally he succeeded in synthesizing an enzyme, ribonuclease A, by applying the method [8]. Independently, the Merck research group headed by Ralph Hirschmann also synthesized ribonuclease S by applying the same HF method at the final stage of deprotection [9]. As you know, both syntheses were published in the same issue of JACS in early 1969.

The solid phase technology is, no doubt, extremely useful and convenient for synthesizing peptides within a short time period, but the formation of a small amount of truncated side products was unavoidable. Thus, success in the synthesis of peptides by the solid phase method totally depends on success in the isolation of the desired peptide from the reaction products. Until the middle of the 1970's, only limited techniques were available for detecting or removing those side products having very similar structures. In such a situation, I thought that if a fragment condensation technique could be applied to the solid phase method, it should be possible to extend the limitation in the size of peptides to be synthesized. In 1968, I tried to couple a tripeptide unit, Pro-Pro-Gly (an intermediate for the synthesis of bradykinin) on a Merrifield resin, for a definite number of times such as 10 or 20 for the synthesis of poly(Pro-Pro-Gly) having definite molecular weights [10]. During simple dialysis of the product, (Pro-Pro-Gly)<sub>10</sub>, using a cellophane dialysis bag, the formation of several crystals was observed in the bag. When a crystal was subjected to X-ray analysis, it was found to be composed of a typical collagen-like triple-helical structure [11]. This was the first successful example of the fragment condensation of peptides on solid support.

## 1970 to 1980

One of the drawbacks of HF as a reagent for the removal of protecting groups was the formation of stable carbonyl cations, which attack aromatic groups in peptides to form alkylated side products. In most cases, this could be suppressed by adding anisole to the reaction mixture, but it was still unavoidable in some cases. Various improvements were made by many workers not only in the reaction conditions, but also in the structure of the protecting groups, and the formation of almost all major side products were eliminated one by one. Nevertheless, if formation of unexpected side products was found during the solid phase synthesis, many workers frequently attributed this to the use of HF. We therefore decided to synthesize such questionable peptides by classical solution procedures to observe whether or not the same side reactions would occur. In the meantime, HPLC had been introduced for peptide synthesis and could be used to detect and remove almost all those side products. Using HPLC, we checked the conditions for forming such side products, and established the conditions suitable for eliminating the side reactions. This finally gave us confidence in obtaining peptides by the HF method in a highly homogeneous form. Then, we designed our own strategy suitable for the synthesis of large peptides by the solution procedure under the principles summarized below [12].

- 1) A large peptide is assembled from several smaller segments of about 10 amino acid residues each.
- 2) Each segment is synthesized with Boc-amino acids in a form of Boc-A<sub>1</sub>-A<sub>2</sub>-A<sub>3</sub>--A<sub>n</sub>-OPac (n is around 10; Pac: phenacyl), in which all side-chain functional groups are protected by suitable protecting groups removable by HF.
- 3) After removal of either the Boc or Pac group, those segments are coupled one by one using WSCI as the coupling reagent in the presence of HOBt or HOObt as an additive. [WSCI: 1-ethyl-3-(3-dimethylaminopropyl)-carbodiimide]
- 4) After completion of the entire segment condensation reactions, the remaining protecting groups are removed by the HF method.

The strategy is characterized by the use of Boc to protect  $\alpha$ -amino groups and the Pac ester to protect the  $\alpha$ -carboxyl group. The biggest advantage of our procedure is being able to use the same fully protected peptide segment as not only a carboxyl component but also as an amino component since the Boc or Pac group can be removed selectively without disturbing any other protecting groups in the same segment. By applying this principle, we could overcome almost all major problems which were apt to arise in the synthesis of large peptides.

### 1980-1990

In 1981, we tested the usefulness of our strategy in the synthesis of an 84-residue peptide, human parathyroid hormone (PTH). The 84-residue peptide was assembled from four large segments, (1-22), (23-38), (39-68), and (69-84). Each segment was assembled from two or four smaller size segments. All of the side chain functional groups were protected by a set of groups which are shown in Table 1 as the 1980 version .

*Table 1. Type of Protecting Groups for the Side-Chain Functional Groups Used in our Peptide Synthesis.*

Version	Asp, Glu	Ser, Thr	Lys	Arg	His	Cys	Tyr	Trp
1965	OBzl	Bzl	Z	NO <sub>2</sub>	---	Bzl	Bzl	---
1980	OBzl	Bzl	ClZ	Tos	Tos	Acm, MeB	BrZ	---
1990	OcHx	Bzl	ClZ	Tos	Bom	Acm, MeB	BrZ	For
1995	OcHx	Bzl	ClZ	Tos	Bom	Acm, MeB	BrZ	Hoc

During the segment coupling reactions, we encountered an insolubility problem in two steps; the first in the synthesis of Boc-(39-68)-OPac and the second in the last coupling reaction of Boc-(1-22)-OH with H-(23-84)-OBzl. In the synthesis of Boc-(39-68)-OPac,

assembly was attempted from four smaller segments, (39-43), (44-51), (52-59), and (60-68), which were coupled from the C-terminus one by one, but the first intermediate, Boc-(52-68)-OPac, was extremely insoluble in ordinary solvents suitable for the coupling reactions and we were forced to give up the synthesis at this point. However, when the N-terminal Boc-(39-59)-OPac was synthesized first, and then the barely soluble segment, Boc-(60-68)-OPac, was coupled to the C-terminus, the product was found to be extremely soluble in DMF, giving the desired product, Boc-(39-68)-OPac, in a highly soluble form [12]. This taught us that the solubility of protected peptides is not length-dependent, but sequence-dependent. Thus, the elongation of three larger segments was achieved smoothly using a mixture of DMF/NMP as the coupling solvent. In the final coupling reaction between Boc-(1-22)-OH and H-(23-84)-OBzl, the product precipitated as a gel. After treating the precipitated product with HF, we were able to isolate human PTH, although the yield was not very high [13]. From this experiment, we grasped that our present strategy could be applied to the synthesis of peptides much larger than PTH if we could overcome the insolubility problems.

Applying this principle, we synthesized many peptides having two or more disulfide bonds that were mainly smaller than 100 residues. They are listed in Table 2.

*Table 2. Biologically active peptides synthesized by applying the present strategy.*

Year	Name	Number of	
		Amino acids	SS-bonds
1982	Conotoxin G1	13	2
1985	h-ANP	28	1
1986	$\omega$ -Conotoxin GVIA	27	3
1988	C5a Anaphylatoxin	74	3
1988	Endothelin I	21	2
1990	Angiogenin	123	3
1990	Charybdotoxin	37	3
1992	Calciseptine	60	4
1992	Elafin	57	4
1992	$\mu$ -Conotoxin GIIIB	22	3
1992	Na,K-ATPase Inhibitor I	49	4
1992	rat Interleukin-8	72	2
1993	h-Adrenomedulin	52	1
1993	$\omega$ -Agatoxin IVA	48	4
1994	h-Osteocalcin	49	1

From the synthesis of those peptides, we learned that the yield of the desired products in the folding reactions is strongly affected by changes in the peptide concentration, reaction temperature, type of buffer, presence or absence of a denaturing agent, redox agents, and water-soluble organic solvent in the folding reaction systems [14]. Such a

phenomenon was typically observed in the synthesis of  $\omega$ -conotoxin MVII C [15].

### 1990-1997

The low yield in the earlier synthesis of h-PTH was due to an aggregate formation during the final coupling reaction in an ordinary solvent such as DMF or NMP. The aggregate may be formed by inter- or intra-chain hydrogen bonds as well as van der Waals interaction between alkyl groups of side-chains. To dissolve such aggregates, powerful solvent systems are required. TFE is known as a solvent capable of converting molecules from  $\beta$ -sheet to helical, but neat TFE was completely ineffective in dissolving the aggregate. We next examined the effect of various organic solvents as the additive in TFE and found that the mixture of CHL or DCM in TFE in a ratio of 3:1 had a miraculous potential for dissolving those sparingly soluble protected peptides. However, in the case of using a CHL/TFE mixture as a solvent, we had to check the tendency for the formation of TFE-esters or racemization of the carboxyl components under the conditions of their coupling reactions. Thus, we examined the possibility of forming such side products using a model system. From this experiment, we realized that TFE ester formation could be suppressed in a range of less than 0.1% when WSCI/HOObt was used as the coupling reagent. HFIP was known to be a much more powerful solvent for the same purpose, but the extent of ester formation increased to 2-3% since its nucleophilicity is stronger than that of TFE. Thus, CHL/TFE(3:1) was found to be a much more suitable solvent system for the synthesis of peptides when WSCI/HOObt was used as the coupling reagent [16]. This technique was successfully applied to the synthesis of a 121-residue protein, human midkine (MK), having five intramolecular disulfide bonds.

The fully protected MK precursor molecule was assembled from two large domains. The N-terminal half was assembled from six segments, and the C-terminal portion from seven segments, all of which were synthesized in a form of Boc-peptide-OPac, except for the C-terminal segment which was protected by the benzyl ester, as in the case of our PTH synthesis. The type of protecting groups applied to the synthesis is shown in Table 1 as the 1990 version. Almost all solubility problems could be overcome by using CHL/TFE(3:1) as the solvent. The final coupling reaction between the two large segments, Boc-(1-59)-OH and H-(60-121)-OBzl, proceeded quite smoothly within 1 hr. Thus, the fully protected peptide, Boc-(1-121)-OBzl, could be obtained in an almost quantitative yield. Next, all the protecting groups were removed by the HF method except for Ac groups. The (10 Ac)-peptide (1-121) thus isolated in a homogeneous form was further treated with  $\text{Hg}(\text{AcO})_2$  to obtain the completely unprotected peptide. The folding reaction proceeded smoothly as in the case of small peptides, and we were finally able to isolate a homogeneous product, which showed a single peak not only on RP-HPLC or IEX-HPLC but also on CEZ. All analytical data

supported the formation of human MK in a highly homogeneous form as was reported in our paper [17].

In order to confirm the reproducibility of the present strategy, we also synthesized a slightly larger protein, human pleiotrophin (PTN), a 136-residue protein having five disulfide bonds [18]. The structure of the segments and the routes of their condensation reactions are shown in Fig. 1. The types of protecting groups are shown in Table 1 in the 1996 version. In the final coupling reaction, a large carboxyl component, Boc-(1-64)-OH, was found to react quite smoothly with a large amino component, H-(65-136)-OBzl, in CHL/TFE(3:1) as in the case of the MK synthesis. All the protecting groups were removed by HF except ten AcM groups, which were then removed by treatment

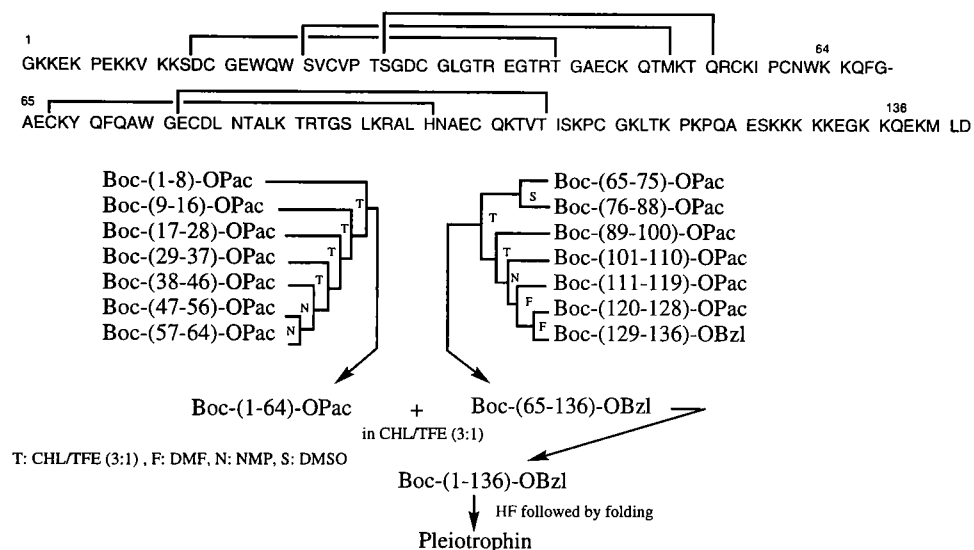


Fig. 1. Primary structure and route for the synthesis of pleiotrophin.

with  $\text{Hg}(\text{AcO})_2$ . After the folding reaction, we could isolate the product by HPLC in a highly homogeneous form, which showed full biological activity equivalent to that of a recombinant product. Thus, we can state with confidence that our segment condensation procedure using maximum protection strategy should be useful and convenient for the synthesis of proteins having more than 130 residues.

In order to confirm the limitations of our strategy, we are trying to synthesize the so-called "green fluorescent protein" (GFP), which has 238 residues including two uncoupled Cys residues. This protein is assumed to be an auto-catalytic enzyme for forming a unique dehydro-imidazolidone structure from its own sequence, -Ser-Tyr-Gly-, at position (65-67), which is essential for emitting a green fluorescence when the molecule is stimulated by UV light [19]. Since its three-dimensional structure had

already been determined [20], we decided to synthesize this protein to elucidate the mechanism of the auto-catalytic cyclization reaction. In order to speed up the synthesis, we decided to combine a solid phase method to obtain all the fully protected segments, because the size of each segment is relatively small and they are considered to be purified in a homogeneous form before being subjected to the segment condensation reactions. For the synthesis of the segments, we decided to apply the Boc strategy on a 9-hydroxymethyl-fluorenyl resin. This idea was originally reported by Rabanal *et al.* in 1992 [21], but we found it necessary to modify the reaction conditions in several ways because some of the side-chain protecting groups are not so stable under the conditions for removing a protected segment from the resin. By applying our improved reaction conditions, we were able to synthesize a fully protected segment of 10 to 12 residues within a day or two. We started the project this March, and have now already finished the synthesis of all 23 necessary protected segments. I am optimistic about the total synthesis of the 238-residue protein GFP and plan to report the preliminary results at the First International Peptide Symposium to be held in Kyoto late this year.

## References

1. Tani, H., Yuki, H., Sakakibara, S. and Taki, T., *J. Am. Chem. Soc.*, 75(1953)3042.
2. Kitaoka, H., Sakakibara, S. and Tani, H., *Bull. Chem. Soc. Japan*, 31(1958)802.
3. Nagai, Y. and Noda, H., *Biochim. Biophys. Acta*, 34(1959)298 ; Nagai, Y., Sakakibara, S., Noda, H. and Akabori, S., *Biochim. Biophys. Acta*, 37(1960)567.
4. Sakakibara, S., Shin, K.H. and Hess, G.P., *J. Am. Chem. Soc.*, 84(1962)4921.
5. Sakakibara, S., Shimonishi, Y., Kishida, Y., Okada, M. and Sugihara, H., *Bull. Chem. Soc. Japan*, 40(1967)2164.
6. Sakakibara, S. and Shimonishi, Y., *Bull. Chem. Soc. Japan*, 38(1965)1412.
7. Sakakibara, S., Shimonishi, Y., Okada, M. and Kishida, Y., In Beyerman, H.C., van de Linde, A. and van den Brink, W.M. (Eds.), *Peptide (Proceedings of the Eighth European Peptide Symposium)*, North-Holland, Amsterdam, 1967, p. 44.
8. Gutte, B. and Merrifield, R.B., *J. Am. Chem. Soc.*, 91(1969)501.
9. Hirschmann, R., Nutt, R.F., Veber, D.F., Vitali, R.A., Varga, S.L., Jacpb, T.A., Holly, F.W. and Denkwalter, R.G., *J. Am. Chem. Soc.*, 91(1969)507.
10. Sakakibara, S., Kishida, Y., Kikuchi, Y., Sakai, R. and Kakiuchi, K., *Bull. Chem. Soc. Japan*, 41(1968)1273.
11. Sakakibara, S., Kishida, Y., Okuyama, K., Tanaka, N., Ashida, T. and Kakudo, M., *J. ol. Biol.*, 65(1972)371; Okuyama, K., Okuyama, K., Arnott, S., Takayanagi, M and Kakudo, J. *Mol. Biol.*, 152(1981)427.
12. Kimura, T., Takai, M., Masui, Y., Morikawa, T. and Sakakibara, S. *Biopolymers*, 20(1981)1823.
13. Kimura, T., Morikawa, T., Takai, M. and Sakakibara, S., *J. Chem. Soc. Chem. Commun.*, (1982), 340; Kimura, T., Takai, M., Yoshizawa, K. and Sakakibara, S., *Biochem. Biophys. Res. Commun.*, 114(1983)493.
14. Sakakibara, S., *Biopolymers (Peptide Science)*, 37(1995)17.
15. Kubo, S., Chino, N., Kimura, T., Sakakibara, S., *Biopolymers*, 38(1996)733.
16. Kuroda, H., Chen, Y.N., Kimura, T. and Sakakibara, S., *Int. J. Peptide Protein Res.*, 40

(1992)294.

17. Inui, T., Bódi, J., Kubo, S., Nishio, H., Kimura, T., Kojima, S., Maruta, H., Muramatsu, and Sakakibara, S., *J. Peptide Science*, 2(1996)28.
18. Merenmies, J. and Rauvala, H., *J. Biol. Chem.*, 265(1990)16721.
19. Cody, C.W., Prssher, D.C., Westler, W.M., Prendergast, F.G. and Warad, W.W., *Biochemistry*, 32(1993)1212.
20. Brejc, K., Sixma, T.K., Kitts, P.A., Kan, S.R., Tsien, R.Y., Ormó, M. and Remington, S.J., *Proc. Natl. Acad. Sci. USA*, 94(1997)2306.
21. Rabanal, F., Giralt, E. and Albericio, F., *Tetrahedron*, 51(1995)1449.



# **“The time has come,” the Walrus said, “to talk of many things...” Lewis Carroll, Through the Looking Glass**

**Ralph Hirschmann**

*Department of Chemistry, University of Pennsylvania, 231 South 34th Street,  
Philadelphia, PA 19104, USA*

Peptide Chemistry had its beginning in 1902 at a meeting in Karlsbad when Franz Hofmeister and Emil Fischer independently reported that proteins are made up of amino acids linked *via* “peptide bonds,” a term coined by Fischer. It is fitting and proper that the international peptide community should celebrate the forthcoming centenary with pride and with confidence about the future.

## **Selected Major Milestones Achieved During the Past 95 Years**

Consider some arbitrarily selected achievements which have collectively had a seminal impact on both biology and chemistry:

(1) *Protection and Activation of Amino Acids and Peptides* The invention of the carbobenzoxy protecting group in 1932 made possible the practical synthesis of chiral peptides (1932). As is well-known, this urethane N-protecting group allows activation of amino acids without racemization. In addition, this group can readily be removed, making it ideal for stepwise peptide synthesis. The carbobenzoxy group surely represented one of the most important accomplishments in peptide synthesis of the first half of the century. Its counterpart, activation of the C-terminal carboxyl, was accomplished early on (1902) *via* the azide process. Azides are less stable than one might wish, a concern primarily when peptide *fragments* couple only slowly. The survival of this procedure for nearly a century is due in part to improvements introduced over the years. Its primary strength lies in the fact that it permits the activation and coupling of peptide *fragments* with minimal racemization. In the intervening years, diverse new activation procedures involving primarily anhydrides, active esters, carbodiimides and combinations of these methods, have found favor. The introduction of novel useful protecting groups, permitting an ever increasing degree of selectivity continues to this day. Still, one can only marvel at the fact that the carbobenzoxy protecting group in combination with the azide coupling procedure made chiral peptide synthesis a reality nearly 70 years ago, the former permitting stepwise chain elongation, the latter fragment condensation.

(2) *Early Biologically Important Peptides* (a) The isolation, characterization and synthesis of the peptide hormones oxytocin and vasopressin in 1953 and of ACTH in 1956 put peptides firmly on the map in physiology and medicine. One must admire the ingenuity and creativity of our forefathers. Consider that automated amino acid analysis was reported only in 1958, and that the Edman degradation was not employed in the structure determination of oxytocin and vasopressin, two nonapeptides with a cystine containing

cyclic hexapeptide linked to a C-terminal tripeptide amide. The generation of three equivalents of ammonia during acid hydrolysis showed conclusively that oxytocin contains one Gln, one Asn, and a C-terminal amide but no dibasic acids. Partial hydrolyses played a major role in the sequence determination.

Enzymatic hydrolyses, spectroscopic methods, or high resolution mass spectrometry could establish these facts now-a-days. In 1953, seemingly unsophisticated techniques succeeded in answering these same questions in a definitive manner.

(b) Among the many peptide hormones that have been isolated, characterized and synthesized, insulin deserves special mention. It became the first life-saving peptide after its isolation in 1922. The crystallization of insulin was achieved in 1926. Elucidation of the amino acid sequence of the hormone in 1950 was followed by the determination of the connectivity of the six cysteines just five years later. The X-ray structure of the hexameric zinc complex of pig insulin evolved between 1969 and 1972. Importantly, these spectacular achievements disproved the widely accepted belief that peptide hormones are mixtures (a "Gemisch") of closely related structures, and therefore not deserving the attention of organic chemists. That insulin proved to be a single chemical entity dramatically changed the way organic chemists think about peptide chemistry. Finally, insulin became the first peptide hormone to be accessible by molecular biological expression in the mid 1980s.

(3) *Peptide Chemistry, an Integral Part of Organic Chemistry* One of the curiosities of our time is the fact that it is often implied that peptides are not organic compounds. Thus, a pharmaceutical company may be reported to be increasing its efforts in the synthesis of organic compounds at the expense of peptides. This bizarre aberration is not only inconsistent with the definition of organic chemistry, but it also distorts history. Consider that Fischer gained renown for his work with purines and sugars before he initiated research with peptides. Surely, above all he was an organic chemist. Peptide chemists have developed techniques, concepts, and methods that are part of the mainstream of nonpeptide organic chemistry. Conversely, physical organic chemists have contributed immeasurably to the elucidation of, for example, the mechanism of racemization of amino acids and peptides, the design of selective protecting groups, the activation of carboxyl groups and the removal of protecting groups under acidic conditions while minimizing cation induced side reactions.

It is true, I believe, that organic chemists lacking familiarity with peptide chemistry, underestimate the complexity of our field. They perceive peptide synthesis as an extension of the synthesis of acetamide, ignoring both the problems imparted by the functionalized sidechains and the elegance of the diversities in the molecular shape of peptides induced by these sidechains. Peptide chemists, using three and one letter codes for amino acids, doubtless contribute to the erroneous notion that polypeptides lack structural elegance.

One of the most striking examples of the impact of peptide chemistry on non-peptidal organic chemistry is cited in section 4b.

(4) *The Impact of Automation on Peptide Research* (a) The invention of automated quantitative amino acid analysis reported in 1958 profoundly affected the determination of the amino acid composition of peptides, the evaluation of the purity of both synthetic and natural peptides, and - in the context of the so-called subtractive Edman degradation

method - the sequencing of peptides and proteins. In the hands of a skilled experimentalist, an accuracy of  $\pm 3\%$  is achievable in automated amino acid analysis, although most laboratories, academic and industrial, do not come close to achieving this degree of experimental sophistication now-a-days. One must fear that this cavalier attitude may reflect a certain lack of concern about the purity and, indeed, the identity of the synthetic peptides.

(b) The synthesis of peptides on solid support (1963) literally revolutionized peptide synthesis and also provided as a fringe benefit the application of support methodology to the sequencing of peptides. The usefulness of solid phase peptide synthesis benefited greatly from the introduction in the mid 70s of reverse phase high pressure liquid chromatography (RP-HPLC) as a highly resolutive chromatographic technique for the analytical, and preparative separation of unprotected peptides. The effectiveness of the RP-HPLC technique in separating diastereomers is another important plus of this technique.

Importantly, solid phase synthesis was subsequently successfully applied to nucleic acid synthesis, and in the 1990s to the synthesis of, for example, oligosaccharides, of the anti-tumour agents epothilones A and B, and of other natural and unnatural (designed) nonpeptides. Thus the solid phase methodology is "not just for peptides anymore." It has, in fact, become the cornerstone of the paradigm of library synthesis. This means nothing less than that an ever-growing percentage of compounds prepared for biological evaluation are synthesized on solid support. Peptide chemists and peptide chemistry thus laid the groundwork for a revolutionary development in the synthesis of nonpeptidal organic compounds.

It is pleasing to note that peptide chemists have also been able to extend the scope of solid phase peptide synthesis to generate complex polypeptides containing non-protein amino acids. For example, analogs of the cyclic undecapeptide cyclosporin A (CsA) with its seven N-alkylated amino acids, can now be synthesized on solid support by varying solvent, temperature and synthetic strategy. Indeed, synthetic libraries of cyclosporin derivatives are now possible. The facile synthesis of CsA analogs has made a significant contribution to our understanding of the mechanism of the immunosuppressive action of this natural product. Analog synthesis has shown that it is possible to separate the immunosuppressant activity from the inhibition of the peptidyl-prolyl *cis-trans* isomerase activity, while retaining anti-HIV-activity.

(5) *Protein Synthesis* Landmark achievements in natural product synthesis include both peptide hormones and enzymes. In 1958 it was shown that ribonuclease A (Rnase A) may be cleaved at a single bond without impairment of enzymatic activity to produce ribonuclease S (Rnase S), which may be separated into a tetraheptapeptide (S-protein) and an eicosapeptide (S-peptide). Recombination of these two enzymatically inactive fragments in equimolar ratio restored full enzymatic activity. Three years later (1961) in an experiment of historic importance, it was shown that the amino acid sequence of Rnase A and even of Rnase S encode the tertiary structure of these two proteins *in vitro*. In recent years, the role of chaperones in the folding of certain proteins has been investigated. This fact does not, however, diminish the importance of the earlier, underlying discovery. Rather, I see it as just another example of a general pattern: seemingly simple phenomena

have a way of becoming more complex as we study them further. That sequence encodes tertiary structure made it reasonable to undertake the total syntheses of these enzymes with the expectation that the synthetic products will have the proper tertiary structure. The required amino acid sequence of these enzymes became known in 1963. The total syntheses of Rnase A and of Rnase S by solid phase and solution methodology, respectively, were announced simultaneously in 1969. The former, involved so-called stepwise approach, the latter, fragment condensation. Both syntheses employed anhydrous HF for the removal of protecting groups. Eleven years later synthetic and purification techniques had progressed sufficiently to make possible the total synthesis of crystalline ribonuclease A using the fragment condensation method.

In 1987, the total chemical synthesis of HIV-1 protease was achieved before this important AIDS-related enzyme became available by molecular biological expression, making possible the initiation of screening for inhibitors of this enzyme. The significance of this achievement has not received the attention which it deserves.

More recently, different new approaches for the synthesis of unprotected peptides through selective acylations of  $\alpha$ -amino groups have been described. Among them, the use of ligases obtained from proteases by site-directed mutagenesis has already achieved success in protein synthesis. Catalytic antibodies have generated small peptides with good turn-over numbers.

(6) *Conformational Analysis* At about the same time, enormous strides were being made in the conformational analysis of peptides both by computational methods and by crystallographic and spectroscopic techniques. Advances in the understanding of the relationship between conformation and structure were both invaluable from a theoretical and from a practical point of view. For example, the importance of intramolecular hydrogen bonds for c-(Gly)<sub>6</sub> was proven in 1963 by X-ray crystallography. Such understanding has become the cornerstone in the design of both peptides and peptidomimetics possessing targeted biological properties. The ever growing number of peptide hormones and neurotransmitters that have been isolated and characterized both chemically and biologically has fueled an understanding of the relationship between chemical structure and biological activity. Somatostatin, one of the hypothalamic releasing factors isolated in the 60s and 70s, is a tetradecapeptide which has a half-life of such short duration that its therapeutic potential could not be determined. A speculation about its bioactive conformation was validated *via* the synthesis of rigid bicyclic analogs. This led eventually to the design and synthesis of a highly potent cyclic hexapeptide which retains the critical  $\beta$ -turn of the hormone. This research carried out in the 70s represented the first time that a major pharmaceutical company was willing to make a significant chemical and biological commitment to converting a peptide hormone having no practical medical value into a peptide that does. This goal was subsequently realized by another pharmaceutical company.

The understanding of the importance of solvent-driven hydrophobic interactions in protein folding has advanced impressively in recent years. In addition, creative experiments have been devised to determine the relative importance of hydrophobic interactions and of

hydrogen bonding, as well as of torsional effects on protein folding. More recently *de novo* design has been successfully employed in attempts to mimic protein folding by using diverse template-assembled secondary structures. Helical bundles have often been the target of such *de novo* design.

Multidimensional NMR spectroscopy is proving invaluable in providing information about solution conformations of both peptides and proteins. It has become an important alternative to X-ray crystallography in the determination of tertiary structures.

Because inhibitors of many enzymes, especially proteolytic enzymes, are of therapeutic interest, cocrystallization of such enzymes with inhibitors has been a highly useful tool for the design of more potent and more selective inhibitors. The angiotensin converting enzyme inhibitors and the inhibitors of HIV-1 protease, an enzyme required by the AIDS virus, are all peptide-related compounds. They are excellent examples of rationally designed, orally bioavailable therapeutic agents of great clinical value. These protease inhibitors followed into the clinic such earlier injectable peptide drugs as the hormones oxytocin, ACTH, insulin and the antibiotic penicillin.

(7) *Peptidomimetics* Peptidomimetics have emerged as a broad field including both natural and unnatural molecules. The former category includes morphine, a peptidomimetic known since antiquity, which is known today to bind the receptor for which the enkephalins are the endogenous ligands. Another natural product, statine, is a dipeptide mimetic transition state analog. Unnatural peptidomimetics, on the other hand, include pseudopeptides, peptoids,  $\beta$ -peptides and so forth. Peptidomimetics have come to play an important role in the pharmaceutical industry which screens hundreds of thousands of compounds from chemical sample collections, fermentation broths, and libraries generated by combinatorial chemistry, for their ability to bind either receptors whose endogenous ligands are peptides, or enzymes such as proteases. The search for such ligands is generally guided by two distinct strategies. One of these builds on the knowledge that certain scaffolds, the so-called privileged or promiscuous platforms, have a remarkably good track record in their ability to bind different receptors, the specificity resulting from the substituents attached to these scaffolds. Although it is widely thought that such platforms tend to bind only proteins that have much in common structurally (such as G-protein coupled receptors), this belief is not consistent with the reports that benzodiazepines (a well established class of privileged platforms) can also inhibit, for example, the enzymes farnesyl transferase and reverse transcriptases. The second strategy, instead of relying on a common scaffold and common structural features, seeks to emphasize diversity in three-dimensional space. Polycyclic peptides, peptoids and  $\beta$ -peptides, and so forth, permit one to achieve such structural diversity also with unnatural peptides.

Peptidomimetics are discovered today both *via* random screening and by design. Unexpectedly, peptidomimetics have been able to reveal similarities between different receptors which were not disclosed by the endogenous ligands. Further, the creative use of site-directed mutagenesis of receptors has made it possible in several instances to determine whether or not peptides and their peptidomimetic counterparts bind a receptor in a similar manner. Incorporation of conformational constraints into both peptides and

peptidomimetics has provided valuable information about the bioactive conformation of ligands.

## Summary

Taken together, even the above, limited, highly subjective selection of the achievements of peptide chemists and biologists amply demonstrate that peptide research has benefitted both science and therapy, and thus mankind. More often than not, these advances were made possible through synergistic interaction between biologists and synthetic, physical and bioorganic chemists.

## Future Directions

As Niels Bohr pointed out, "Prediction is a very difficult art, especially when it involves the future." Nevertheless, it is tempting to make some prognostications, especially since we are approaching the end of the first 100 years of peptide chemistry.

I believe that the continuing importance of peptides and peptide-derived research is all but a certainty for two reasons.

(1) Life, as we know it, would not exist without peptides and proteins and biochemists are isolating and characterizing new such peptidal structures at a bewildering rate. The evolution of biotechnology is regarded to have been one of the most important developments of the past twenty years, but it is becoming increasingly clear that molecular biology cannot fulfill its promise without structural biology. Thus, physical measurements, including X-ray crystallography, NMR spectroscopy and mass spectrometry are likely to assume an ever-increasing importance in peptide-related research.

(2) The other reason for optimism about the future of peptide and peptide-derived research is that while we *know* an enormous amount, I believe that we really *understand* very little. This is probably generally true in science; I'm confident that it applies to peptide research. Even without the isolation of new peptides, there is much work to be done to increase our understanding. Let me cite two unrelated examples of important areas of research which are only now picking up steam: (1) the interactions between macromolecules and (2) factors affecting transport of molecules across membranes. That there is a problem with the oral bioavailability of most peptides has been known for a very long time, but the *causes* of this problem started to receive scientific scrutiny only during the past twenty years. This trend will surely accelerate.

Taken together, this perspective suggests that it probably doesn't matter whether combinatorial chemistry or genomics or structural biology, or some other, as yet unknown discovery, will be the dominant force in the early 21st century; peptide chemistry and biology are sure to flourish.

**Session I**

**Peptide Diversity and Chemical Libraries**



# Novel concepts for the synthesis of cyclic peptide libraries

**Lianshan Zhang and James P. Tam**

Department of Microbiology and Immunology, A 5119 MCN, Vanderbilt University,  
Nashville, TN 37232-2363, USA

Our laboratory has previously reported various methods for orthogonal ligation and cyclization of unprotected peptides [1-3]. These methods differ both in concept and mechanism from conventional coupling and cyclization methods and have two key features: (1) amide bond formation proceeds through a proximity-driven intramolecular acyl migration without the need for an activation agent, and (2) in cyclization, the ring formation is governed by ring-chain tautomerization through reversible interaction of two reactive ends under aqueous conditions. The former feature eliminates multi-tiered protecting groups in the reaction scheme while the latter removes the requirement for high dilution to favor monomeric products. In addition, the final products can be used directly for bioassays without further chemical steps. These features are also attractive for preparing peptide libraries by orthogonal ligation strategies.

Cyclic peptide libraries have recently received much attention because of the advantages of their constrained structures in facilitating drug development. To meet this challenge we have developed novel concepts for peptide cyclization with unprotected peptide precursors that exploit orthogonal ligation strategies and the principle of ring-chain tautomerization to give monomeric products. Here we describe two strategies based on thiolactone and Ag<sup>+</sup> ion-assisted peptide cyclization.

## Results and Discussion

**Thiolactone cyclization through thioester ligation.** Thiolactone cyclization produces an end-to-end cyclic peptide containing a Cys which is also the ligation site (Fig. 1). It requires a free peptide containing an N-terminal Cys and a thioester. Under aqueous conditions, ring-chain tautomerization through transthioesterification of the sulfhydryl of the N-terminal cysteine and the C-terminal thioester yields a covalent thiolactone **1** which spontaneously undergoes an S to N acyl migration via a 5-membered ring transition state to give a cyclic peptide. The entropic factor favors thiolactone formation rather than the intersegmental thioester ligation under the influence of ring-chain tautomerization.

Peptide thioesters were prepared directly by solid-phase peptide synthesis using Boc chemistry according to Aimoto et al. [4]. Crude peptides were used directly for cyclizations at ~ pH 7 in phosphate buffer after cleavage from the resin support. Tris(carboxyethyl)phosphine (TCEP) was added to prevent disulfide formation and to accelerate the desired reaction. Cyclizations occurred cleanly and were complete within 4 hr as shown by RP-HPLC in yields ranging from 78 to 92%. The cyclization was regioselective. No side reactions were observed with side-chain functionalities such as the N<sup>ε</sup>-amine of lysine, thiol of internal cysteine, or imidazole

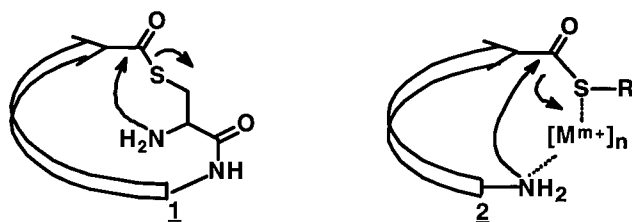


Fig. 1. Cyclic intermediates derived from ring-chain tautomerization in peptide cyclization.

of histidine. More importantly, no oligomerization was observed at concentrations of 1 to 10 mM as monitored by RP-HPLC.

**Ag<sup>+</sup> ion-assisted cyclization.** For cyclization of non-cysteinyll peptides, we used the thiophilic Ag<sup>+</sup> ion to coordinate the reactive functionalities of the N- and C-termini of a flexible linear peptide thioester to form a cyclic intermediate **2** for facilitating the intramolecular cyclization through entropic activation. Similar to the thiolactone cyclization method, the Ag<sup>+</sup> ion assisted in the formation of a reversible cyclic intermediate through a non-classical ring-chain tautomerization to promote intramolecular cyclization rather than intermolecular ligation (Fig. 1). However, the Ag<sup>+</sup> ion plays an additional role in the enthalpic activation of the C-terminal carbonyl to accelerate the amide bond formation.

Using Xaa-Lys-Tyr-Gly-Gly-Phe-Leu-SCH<sub>2</sub>CH<sub>2</sub>CONH<sub>2</sub> where Xaa represents all proteogenic amino acids except Cys, we determined the selectivity of Xaa for the formation of end-to-end cyclic peptides. We found that > 85% of products were end-to-end cyclic peptides if Xaa was Gly, Ser, and Asp/Asn. End-to-sidechain cyclic peptides as major products were obtained if sterically hindered amino acids such as Ile, Pro were placed at the N-terminus. In addition, this method could generate molecular diversity from a single peptide chain by varying the reaction buffer pH and by adding DMSO as a cosolvent. End-to-end cyclization of Ala-Lys-Tyr-Gly-Gly-Phe-Leu-SCH<sub>2</sub>CH<sub>2</sub>CONH<sub>2</sub> was obtained in 67% yield in 5 hr at pH 5.7 and in the presence of 10% DMSO. By increasing the pH to 6.7, the end-to-sidechain cyclized peptide through lysine was obtained in 72% yield. However, when the pH was lowered to 5 in the absence of DMSO, a lactonization product was obtained in 60% yield. In all cases, no dimerization or oligomerization was detected. These results confirm the usefulness of ring-chain tautomerization in suppressing unwanted competing oligomerization and the versatility of producing a library of cyclic lactams and lactones through a single precursor.

**On-resin synthesis of cyclic peptide libraries.** In addition to off-resin cyclization, these methods can be used for the preparation of cyclic peptide libraries by on-resin cyclization. Thioester resin was obtained by directly derivatizing 3-mercaptopropionic acid to TentaGel (Fig. 2). A peptide library with the core sequence, Tyr-Gly-Xaa-Yaa-Leu, was synthesized according to the procedure by Ostresh *et al.* [5]. For cyclization mediated through thioester ligation, cysteine was introduced to the resin at the  $\alpha$ -amino terminus. After HF treatment, the resin was incubated with 0.2 M phosphate buffer at pH 7 in the presence of TCEP for 1 h. The products were desalted by RP-HPLC. No dimerization via amide bond was detected by MALDI-

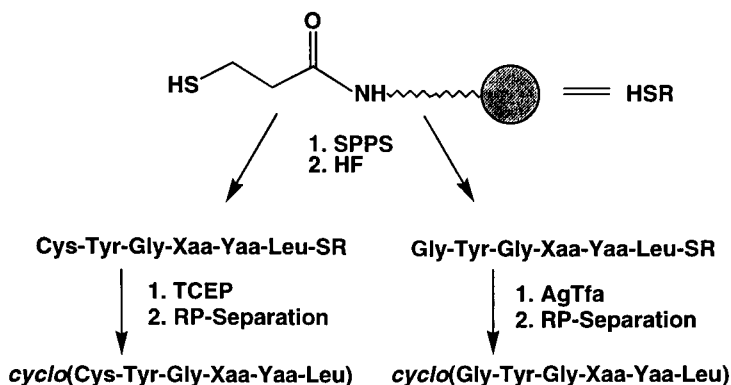


Fig. 2. Synthesis of cyclic peptide libraries using polymer-bound peptide thioesters. TentaGel™ was used for the assembly of peptides.

MS, showing the high efficiency of the formation of monomeric cyclic peptides. For  $\text{Ag}^+$  ion-assisted cyclization, glycine was introduced at the  $\alpha$ -amino terminus as the cyclization site. After HF treatment, the cyclization was conducted in 0.2 M acetate buffer at pH 5.7 in the presence of 10% DMSO. After precipitation of  $\text{Ag}^+$ , the products were separated from DMSO and NaOAc by RP-HPLC. MALDI-MS indicated no oligomerization had occurred in the cyclization process.

In conclusion, the orthogonal ligation strategy has been exploited to form cyclic peptide libraries from a single or mixture of unprotected precursors through covalent or noncovalent cyclic intermediates derived from the process of ring-chain tautomerization which favors the formation of monomeric cyclic peptides. Use of unprotected peptides also eliminates further chemical steps after cyclization and the products can be used directly for bioassays.

## References

1. Pallin, T. D. and Tam, J. P. J. Chem. Soc., Chem. Commun., 19(1995)2021
2. Botti, P. Pallin, D. P. and Tam, J. P. J. Am. Chem. Soc., 118(1996)10018.
3. Zhang, L. and Tam, J. P., J. Am. Chem. Soc., 119(1997)2363.
4. Hojo, H. and Aimoto, S., Bull. Chem. Soc. Jpn., 64(1991)111.
5. Ostresh, J.M., Winkle, J.H., Hamashin, V.T. and Houghten, R.A., Biopolymers, 34(1994)1681

# Combinatorics, peptide mimetics, and combizymes

**Hyunsoo Han, Anthony M. Vandersteen and Kim D. Janda**

*Department of Chemistry, The Scripps Research Institute, 10550 N. Torrey Pines Rd.,  
La Jolla, CA 92037, USA*

Combinatorial chemistry has grown to be one of the most popular tools in the drug discovery arena [1]. Founded upon peptide and oligonucleotide libraries [2,3], combinatorics has funneled most synthetic efforts down the path of solid phase synthesis in which excess reagent may be engaged and tedious purification of products avoided. However, with these advantages also come limitations as solid phase synthesis has yet to be generalized to the synthesis of complex molecules which classic solution phase synthesis permits [4]. We have advocated the use of soluble polymer supports (liquid phase synthesis) with which the advantages of both solid and solution phase synthesis may be applied with equal vigor [5].

We have developed a combinatorial library strategy known as recursive deconvolution [6]. The essence of this method is to apply split synthesis [7] for the library construction but to hold back and categorize partially synthesized libraries in the building process. The amount saved and cataloged depends on the type of library; for a final library consisting of pentapeptides, five sublibraries are required. These partial libraries are later utilized in the screening process to identify library members with targeted properties. We have examined this recursive deconvolution technique using liquid phase synthesis to create a peptide library tailored to contain pentapeptide sequences that display binding to an anti- $\beta$ -endorphin monoclonal antibody (3E7). In the final analysis, the native epitope YGGFL was found to be the most extensive binder; however, other weaker binders were also deduced through this strategy. We have termed this general methodology liquid phase combinatorial synthesis (LPCS) [6].

We and others have been interested in applying combinatorial chemistry to the area of *de novo* peptide catalyst design or what we term "combizymes"[8]. As a starting point for such studies, we reinvestigated two linear pentapeptides: L-threonyl-L-alanyl-L-seryl-L-histidyl-L-aspartic acid (TASHD) [9,10] and L-seryl- $\gamma$ -aminobutyryl-L-aspartic acid (Ser-Gaba-His-Gaba-Asp)[9]. These peptides had been reported by Sheehan and co-workers to catalyze the hydrolysis of p-nitrophenyl acetate (p-NPA) with second order rate constants 3 to 25 times greater than imidazole and L-histidine, respectively, to show catalytic stereoselectivity and to be subject to inhibition by the serine protease inhibitor DFP. What the authors had concluded from their studies was that polyfunctional effects associated with enzyme active sites might be operative in these two peptides.

Peptidomimetics have become immensely important for both organic and medicinal chemists [11]. Synthetic interest in these surrogate peptide structures has been driven by the pharmaceutical industry's needs for molecules with improved pharmacokinetic properties [12]. The alteration of peptides to peptidomimetics has included peptide side chain manipulations, amino acid extensions, deletions, substitutions, and backbone

modifications [13]. We have been interested in exploiting this latter development. Azapeptides are peptides in which one (or more) of the  $\alpha$ -carbon(s) has been replaced by a trivalent nitrogen atom (Fig. 1) [14]. This transformation results in a loss of asymmetry associated with the  $\alpha$ -carbon and yields a structure that can be considered intermediate in configuration between D- and L-amino acids. While the synthesis of azapeptides has been reported, the synthesis of a pure azapeptide or what we term an azatide (Fig. 1) was only recently accomplished by our group using a liquid phase strategy [15].

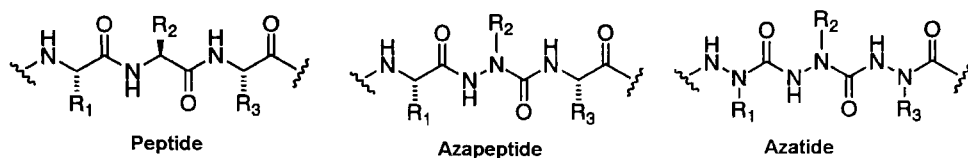


Fig. 1. General structures of a peptide, azapeptide and azatide.

## Results and Discussion

We have investigated [16] the two pentapeptides and the claims put forth by Sheehan and co-workers. Second order rate constants for the hydrolysis of p-NPA were investigated with both pentapeptides. Generally speaking, the second order rate constants we obtained were approximately five to twenty times smaller than was originally reported. A Brønsted plot was constructed using our data and available second order rate constants for the hydrolysis of p-NPA. The second order rate constants for both peptides fell closely on the calculated Brønsted line (gradient = 0.64). From this we concluded that both peptides were acting as substituted imidazoles and were not exhibiting any enhanced catalytic acceleration connected with the presence of the "catalytic triad" of chymotrypsin.

To synthesize oligoazatides an alphabet of suitably protected aza-amino acid constituents was prepared. Shown in Fig. 2 are the two general tactics that we have employed in our preparation of these monomers [15]. To convert these Boc-protected aza-amino acids into acylating agents that would allow stepwise chain lengthening, the hydrazine portion of the molecule had to be activated.

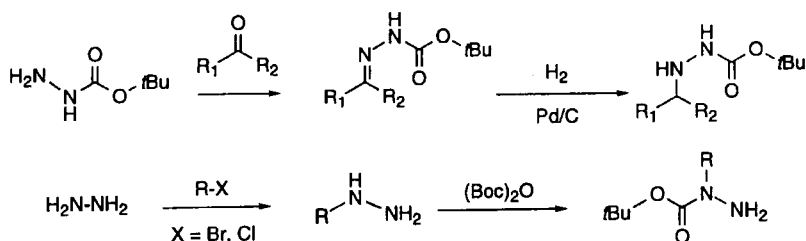


Fig. 2. Preparation of aza-amino acid monomers.

Activation of the hydrazine portion of the molecule is a challenging problem since Boc-alkylhydrazines are rather poor nucleophiles. To resolve this problem we have used bis(pentafluorophenyl) carbonate as the carbonyl activation element. This reagent was successful in coupling the weakly nucleophilic hydrazine terminus both in solution and liquid phase synthesis. The versatility of this chemistry has been proven by the successful synthesis of azatide dimers that were both unhindered (Gly) and hindered (Val-Val) [15]. An oligoazatide analog of the leucine enkephalin peptide sequence was synthesized using liquid phase supported synthesis (Fig. 3) and the structural integrity of the product confirmed by tandem mass spectrometry using electrospray ionization [15].

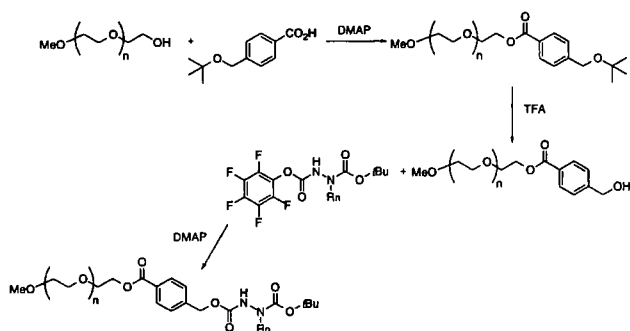


Fig. 3. General scheme for liquid phase synthesis of oligoazatides.

## References

1. Chaiken, I.M. and Janda, K.D. (eds.) *Molecular Diversity and Combinatorial Chemistry*, American Chemical Society, Washington, D.C., 1996, pp. 328.
2. Geysen, H.M., Rodda, S.J. and Mason, T.S., *Mol. Immunol.*, 23 (1986) 709.
3. Tuerk, C. and Gold, L., *Science*, 249 (1990) 505.
4. Boger, D.L., Tarby, C.M., Myers, P.L. and Caporale, L.H., *J. Am. Chem. Soc.*, 118 (1996) 2109.
5. Gravert, D.J. and Janda, K.D., *Chem. Rev.*, 97 (1997) 489.
6. Erb, E., Janda, K.D. and Brenner, S., *Proc. Natl. Acad. Sci. USA.*, 91 (1994) 11422.
7. Furka, A., Sebastyen, F., Asgedom, M. and Dibo, G., *Int. J. Pept. Protein Res.*, 37 (1991) 487.
8. Vandersteen, A.M., Han, H. and Janda, K.D., *Mol. Div.*, 2 (1996) 89.
9. Sheehan, J.C., Bennett, G.B. and Schneider, J.A., *J. Am. Chem. Soc.*, 88 (1996) 3455.
10. Cruickshank, P. and Sheehan, J.C., *J. Am. Chem. Soc.*, 86 (1993) 7070.
11. Spatola, A.F., In Weinstein, BN. (Ed.) *Chemistry and Biochemistry of Amino Acids, Peptides, and Proteins*, Marcel Dekker, New York, 1983, p. 267.
12. Hodgson, J., *Bio/Technology*, 11 (1993) 683.
13. Cho, C.Y., Moran, E.J., Cherry, S.R., Stephans, J.C. Foder, S.P.A., Adams, C.L., Sundaaram, A., Jacobs, J.W. and Schultz, P.G., *Science*, 261 (1993) 1303.
14. Gante, J. *Synthesis*, (1989) 405.
15. Han, H. and Janda, K.D., *J. Am. Chem. Soc.*, 118 (1996) 2539.
16. Vandersteen, A.M. and Janda, K.D., *J. Am. Chem. Soc.*, 118 (1996) 8787.

# Peptides as precursors in the synthesis of heterocyclic positional scanning combinatorial libraries

Jean-Philippe Meyer, John M. Ostresh, Adel Nefzi, Vince T. Hamashin,  
Christa C. Schoner, Marc A. Giulianotti,  
Amy L. Hannah and Richard A. Houghten

Torrey Pines Institute for Molecular Studies, 3550 General Atomics Ct.,  
San Diego, CA 92121, USA

Peptide combinatorial libraries [1] have been employed as precursors in the synthesis of both polyamine [2] and peralkylated peptide [3] combinatorial libraries using the "libraries from libraries" concept [3] (Fig. 1). The application of this concept to the generation of heterocyclic libraries [4] is described here. Well-characterized resin-bound peptide combinatorial libraries, synthesized in the positional scanning format [5] using isokinetic ratios [6], generated well-characterized heterocyclic combinatorial libraries in one or two clean transformations. The resultant indole-imidazole, bicyclic guanidine, cyclic urea, and hydantoin libraries in positional scanning format are readily deconvoluted following a single screening of the libraries (Fig. 1).

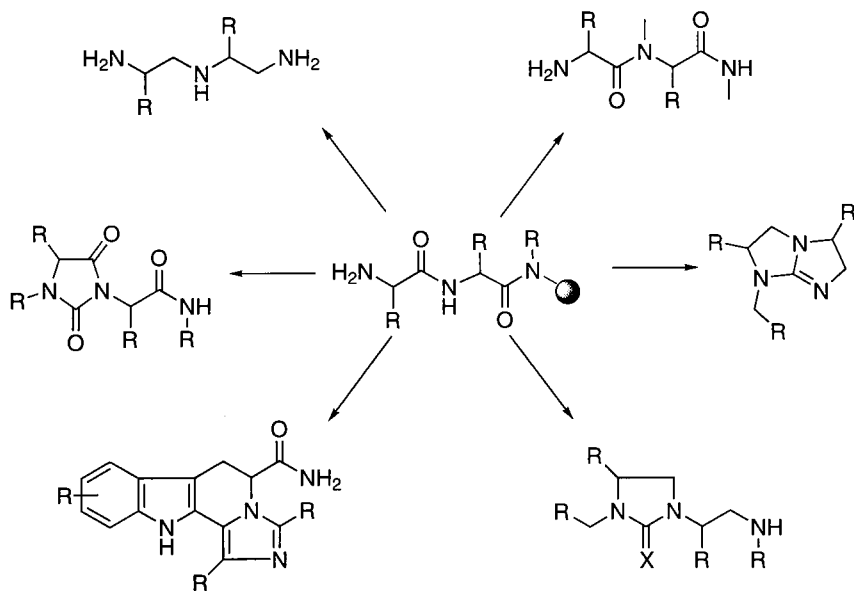


Fig. 1. Positional scanning heterocyclic combinatorial libraries derived from dipeptides.

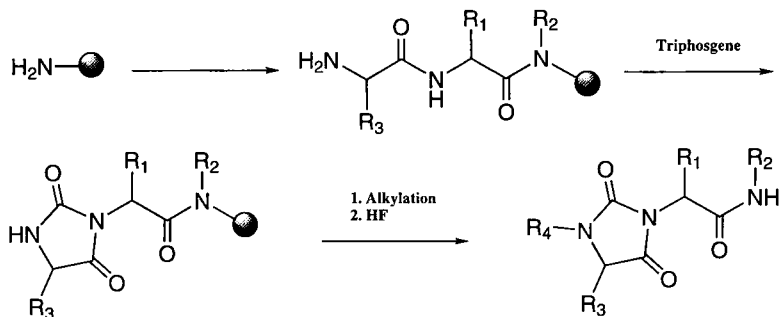


Fig. 2. Reaction scheme for the synthesis of an alkylated hydantoin library from dipeptides.

Since the lengthy iterative process is unnecessary, the time and labor expended on screening and synthesis are drastically reduced. In one case, the synthetic strategy is outlined and analytical data from a model compound is shown.

## Results and Discussion

Expanding the "libraries from libraries" approach, we designed and synthesized four heterocyclic libraries by modifying short resin-bound peptide libraries. In one library, acylated dipeptides containing a C-terminal tryptophan residue were treated with phosphorus oxychloride to generate an indole-imidazole library. In a second library, a reduced, acylated dipeptide library was treated with thiocarbonyldiimidazole to form a bicyclic guanidine library. In a third library, the same reduced, acylated dipeptide library, which had the C-terminal amino group blocked, was treated with either carbonyldiimidazole or thiocarbonyldiimidazole to generate cyclic urea and cyclic thiourea libraries. The reaction scheme for the synthesis of an alkylated hydantoin library is presented in Fig 2. This library was prepared by reacting a resin-bound dipeptide library with triphosgene. In all cases, model compounds were synthesized and analyzed by HPLC-MS. Fig. 3 shows the HPLC-MS for a purified control compound synthesized for the hydantoin library.

We have successfully synthesized many positional scanning combinatorial libraries using the "libraries from libraries" concept. With numerous transformations available, the concept is a valuable tool in the search for biologically active compounds.

In conclusion, small peptides are versatile precursors for heterocyclic compounds. Heterocyclic libraries are readily deconvoluted using the positional scanning format. The "libraries from libraries" concept leverages the diversity found in existing combinatorial libraries.

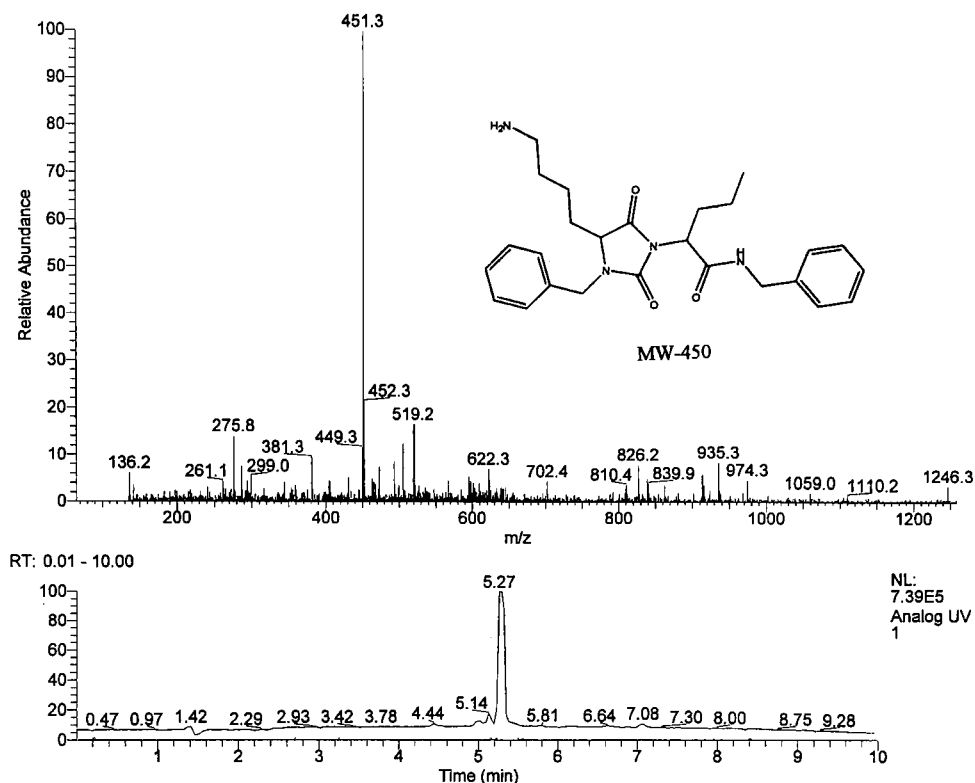


Fig. 3. LC-MS of a purified alkylated hydantoin.

## Acknowledgments

This work was funded by N.S.F. Grant CHE-9520142 and by Trega Biosciences, Inc.

## References

1. Houghten, R.A., Pinilla, C., Blondelle, S.E., Appel, J.R., Dooley, C.T., and Cuervo, J. H., *Nature*, 354(1991)84.
2. Cuervo, J.H., Weilt, F., Ostresh, J.M., Hamashin, V.T., Hannah, A.L., and Houghten, R.A., In Maia, H.L.S. (Ed.), *Peptides 1994 (Proceedings of the Twenty-Third European Peptide Symposium)*, ESCOM, Leiden, The Netherlands, 1995, p.465.
3. Ostresh, J.M., Husar, G.M., Blondelle, S.E., Dörner, B., Weber, P.A., and Houghten, R.A., *Proc. Natl. Acad. Sci. U.S.A.*, 91(1994)11138.
4. Nefzi, A., Ostresh, J.M., Meyer, J.-P., and Houghten, R.A., *Tetrahedron Lett.*, 38(1997)931.
5. Pinilla, C., Appel, J.R., Blanc, P., and Houghten, R.A., *Biotechniques*, 13(1992)901.
6. Ostresh, J.M., Winkle, J.H., Hamashin, V.T., and Houghten, R.A., *Biopolymers*, 34(1994)1681.

# Expanding molecular diversity with pseudopeptides and macrotorials: Synthesis, characterization, and biological activities of macrocyclic combinatorial libraries

Arno F. Spatola, Yvon Crozet, Peteris Romanovskis  
and David Vogel

*Department of Chemistry, University of Louisville, Louisville, KY 40292, USA*

Combinatorial mixtures represent a potentially rich source of drug leads if problems involving deconvolution and structure optimization can be overcome. Cyclic peptides and their analogs are partially constrained systems that reduce the complexities inherent with linear macromolecules. Through careful optimization of synthetic procedures, we have been able to prepare, test, and interpret biological results from both small and large (>1000 component) cyclic peptide libraries.

## Results and Discussion

The synthesis and testing of mixtures seems appropriate when all the following criteria can be met: 1) the synthetic procedure is sound and well-precedented; 2) the synthesis of individual components is rendered unexpectedly tedious due to the complexity of the synthesis, and 3) there is a straightforward method for deconvolution of the mixture. From our work with cyclic peptides, pseudopeptides, and macrotorials, we concluded that the above three conditions were being met. This has led us to prepare relatively large mixtures of each of the structural types above. Representative examples of a cyclic pseudopeptide library are given in Table 1.

The cyclic pseudohexa-, hepta-, and octapeptides were prepared using a side chain attachment strategy [1,2]: Fifteen syringes (Multiblock, Coshisoft) were each loaded with 100 mg of Boc-Asp(Merrifield resin)-OFm, with a substitution level of 0.53 mmol/g. The pseudodipeptide Proψ[CH<sub>2</sub>S]Gly was incorporated as its Boc-protected form using BOP/HOBt reagent, exactly as performed with standard amino acids. The flexible pseudodipeptide shares with glycine a greater propensity to facilitate cyclization when incorporated within linear sequences. Cyclizations were performed using HATU/HOBt while the linear pseudopeptides were still attached to the resin. When representative mixture cyclizations were judged complete (ninhydrin testing), the resin-bound cyclic products were cleaved and deprotected with anhydrous hydrogen fluoride/anisole in a multiple compartment HF apparatus. Following cleavage, the crude products were extracted with acetic acid, subjected to solid phase extraction to wash out salts, and then lyophilized. As seen in Table 1, overall yields were relatively constant, and no clear trends were observed with ring size or with amide bond replacement position. Yields ranged from 33-57% with the cyclic pseudohexapeptides, 33-54% with cyclic pseudoheptapeptides, and 40-45% with cyclic pseudooctapeptides.

The above compound types, along with several examples of linear pseudopeptides, have

been subjected to a variety of bioassays including a full set of antitumor and anti-AIDS tests by the National Cancer Institute. To date, promising leads have been developed against several tumor lines and antimicrobials, including leads to methicillin-resistant *Staphylococcus aureus*.

As previously reported, the positional scan approach was validated in a cyclic peptide library for the first time using a known endothelin antagonist, BQ-123, as a test case [2]. Several other laboratories have reported increased potency when comparing cyclic peptide candidates with

*Table 1. Cyclic pseudopeptide libraries incorporating a pseudodipeptide (Proψ[CH<sub>2</sub>S]Gly) scan*

number	# cmpds	yield mg (%)	structure
L-1	216	23.5 (57%)	cyclo(Xxx-Xxx-Xxx-Proψ[CH <sub>2</sub> S]Gly-Asp)
L-2	216	13.7 (33%)	cyclo(Xxx-Xxx-Proψ[CH <sub>2</sub> S]Gly-Xxx-Asp)
L-3	216	16.3 (39%)	cyclo(Xxx-Proψ[CH <sub>2</sub> S]Gly-Xxx-Xxx-Asp)
L-4	216	22.3 (54%)	cyclo(Proψ[CH <sub>2</sub> S]Gly-Xxx-Xxx-Xxx-Asp)
L-5	1296	22.0 (45%)	cyclo(Xxx-Xxx-Xxx-Xxx-Proψ[CH <sub>2</sub> S]Gly-Asp)
L-6	1296	19.1 (39%)	cyclo(Xxx-Xxx-Xxx-Proψ[CH <sub>2</sub> S]Gly-Xxx-Asp)
L-7	1296	16.1 (33%)	cyclo(Xxx-Xxx-Proψ[CH <sub>2</sub> S]Gly-Xxx-Xxx-Asp)
L-8	1296	17.1 (35%)	cyclo(Xxx-Proψ[CH <sub>2</sub> S]Gly-Xxx-Xxx-Xxx-Asp)
L-9	1296	18.9 (38%)	cyclo(Proψ[CH <sub>2</sub> S]Gly-Xxx-Xxx-Xxx-Asp)
L-10	7776	28.8 (50%)	cyclo(Xxx-Xxx-Xxx-Xxx-Xxx-Proψ[CH <sub>2</sub> S]Gly-Asp)
L-11	7776	26.9 (47%)	cyclo(Xxx-Xxx-Xxx-Xxx-Proψ[CH <sub>2</sub> S]Gly-Xxx-Asp)
L-12	7776	30.7 (54%)	cyclo(Xxx-Xxx-Xxx-Proψ[CH <sub>2</sub> S]Gly-Xxx-Xxx-Asp)
L-13	7776	26.2 (46%)	cyclo(Xxx-Xxx-Proψ[CH <sub>2</sub> S]Gly-Xxx-Xxx-Xxx-Asp)
L-14	7776	23.7 (42%)	cyclo(Xxx-Proψ[CH <sub>2</sub> S]Gly-Xxx-Xxx-Xxx-Xxx-Asp)
L-15	7776	22.6 (40%)	cyclo(Proψ[CH <sub>2</sub> S]Gly-Xxx-Xxx-Xxx-Xxx-Xxx-Asp)

*Xxx = Leu, Lys, Arg, Tyr, Ser, Glu*

less active linear counterparts [3,4]. These studies suggest that when cyclic peptides, pseudopeptides, and macrocyclics [5] are carefully selected and prepared according to a synthetic scheme that has been perfected using small mixtures or individual compounds, then the combinatorial approach appears to be both valid and potentially powerful in combination with traditional methods of drug design.

One concern regarding the testing of large mixtures involves the concentration of individual components. With a medium-sized cyclic peptide library (average MW of 500 Daltons), a 1.5 mg sample with 10<sup>6</sup> components dissolved in 1 mL of solvent yields a concentration of 3 nM for any one given species. But compared to linear peptides, cyclic peptides are more constrained and can thus present a structural motif, such as a specific

tripeptide sequence, in a relatively well-defined, constant orientation. The net result is an *effective* concentration of a potential pharmacophore that can be several orders of magnitude higher than the individual species. Our approach to cyclic peptide libraries also features a single functional group (or closely related structures) at the side chain attachment point. This fixes two positions and thus further reduces the ambiguities from "frame shifting" when combined with the positional scan mode of deconvolution [6].

In summary, the constraints and solubility parameters achievable with cyclic peptides, pseudopeptides, and related macrocycles provide a compelling middle ground between linear peptides and rigid organic peptidomimetics.

### Acknowledgements

Supported by NIH GM33376. Mass spectral data was provided by Dr. Phil Andrews and Dr. Rachel Loo at the University of Michigan Protein and Carbohydrate Structure Facility. We thank Dr. V. Narayanan at NCI for tumor assays and Dr. Richard Houghten and Dr. Sylvie Blondelle at Torrey Pines Institute for Molecular Studies for antibacterial assays.

### References

1. Darlak, K., Romanovskis, P. and Spatola, A.F., In Hodges, R.S. and Smith, J.A. (Eds.), *Peptides: Chemistry, Structure and Biology*, ESCOM, Leiden, The Netherlands, 1994, p. 981.
2. Spatola, A.F., Crozet, Y., DeWit, D. and Yanagisawa, M., *J. Med. Chem.*, 39 (1996) 3842.
3. Eichler, J., Lucka, A. W., Pinilla, C. and Houghten, R.A., *Molecular Diversity*, 1 (1996) 233.
4. Giebel, L.B., Cass, R., Milligan, D.L., Young, D., Rafael, A., and Johnson, C., *Biochemistry*, 34 (1995) 15430.
5. Ma, W., Dodge, J. and Spatola, A.F., In Tam, J.P. and Kaumaya, P.T.P. (Eds.), *Proceedings of the 15th American Peptide Symposium*, in press.
6. Pinilla, C., Appel, J.R., Blanc, P. and Houghten, R.A., *Biotechniques*, 13 (1992) 901.

## Solid phase synthesis of peptidomimetics

**J. P. Mayer, D. Bankaitis-Davis, G. Beaton, K. Bjergarde, J. J. Gaudino,  
B. A. Goodman, C. J. Herrera, D. M. Lenz, G. S. Lewis, C. M. Tarlton  
and J. Zhang**

*Amgen Inc., 3200 Walnut St., Boulder, CO, 80301, USA*

The characteristic peptide properties of low bioavailability and short half life present significant problems in their development as therapeutic agents. One approach to overcoming these problems has been the identification of non-peptide structures whose topological features enable them to mimic binding of the native peptide at the receptor level. These compounds are collectively known as peptidomimetics and have been the subject of several extensive reviews [1, 2, 3].

Recent advances in solid phase organic synthesis have the potential to accelerate the discovery and lead optimization phases of medicinal chemistry, including the area of peptidomimetic research. While much peptidomimetic chemistry has traditionally been performed by solution phase methods, the application of solid phase methodology can offer many of the same inherent advantages with respect to speed and ease of automation which have been realized in solid phase peptide synthesis. Our initial efforts have centered around the development of solid phase methods for two well established peptidomimetic scaffolds shown in Fig.1, the 1,4-benzodiazepine-2,5-diones **1** [4], and the 4-(3H)-quinazolinones **2** [5].

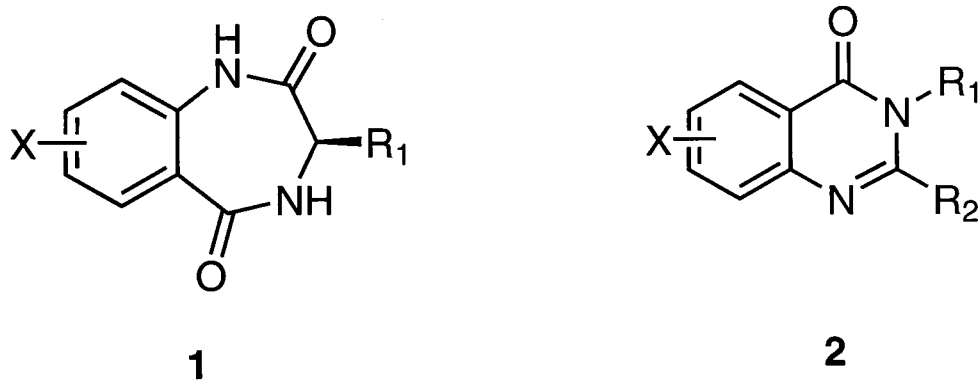


*Fig.1. General structures of 1,4-Benzodiazepine-2,5-diones **1**, and 4-(3H)-quinazolinones **2**.*

## Results and Discussion

The overall synthetic scheme to obtain 1,4-benzodiazepine-2,5-diones and 4-(3H)-quinazolinones is outlined in Fig. 2. Commercially available Fmoc amino acid derivatized Wang resins were deprotected with piperidine in DMF and converted to the anthranilamide intermediate **3**. This conversion was either accomplished directly, by treatment with an isatoic anhydride or through a two step sequence using utilizing DCC/HOBt mediated coupling of an *o*-nitrobenzoic acid, followed by tin (II) chloride reduction. The use of *o*-nitrobenzoic acids and isatoic anhydrides permitted a wider diversity of aromatic substituents than would have been possible through a single route. The intermediate **3** was then used directly in route **a** to yield 1,4-benzodiazepine-2,5-diones **1**, or route **b** to prepare 4-(3H)-quinazolinones **2**.

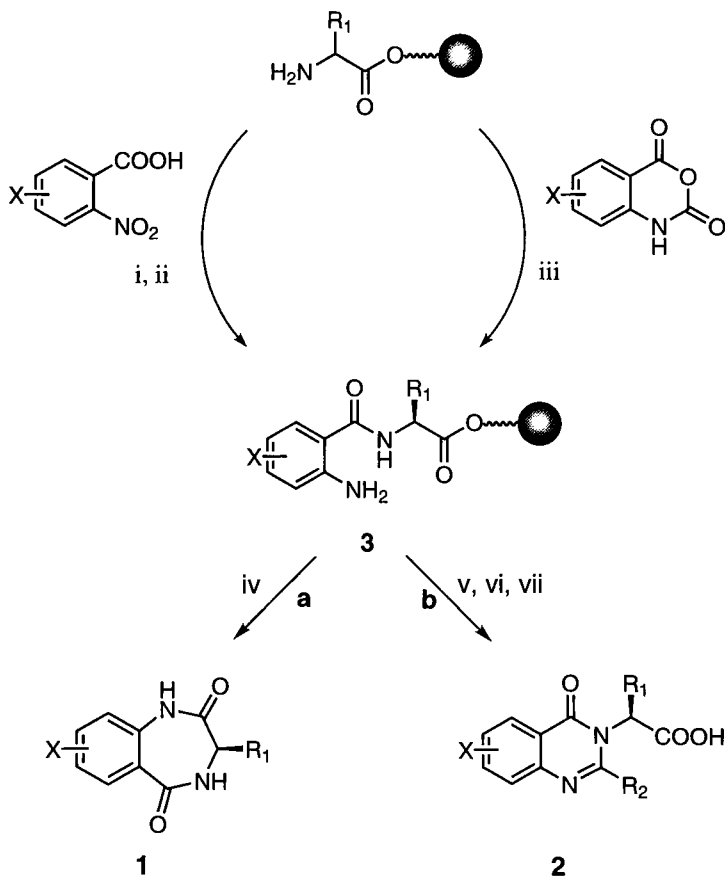


Fig. 2. (i) DCC, HOBt; (ii)  $\text{SnCl}_2$ , DMF; (iii) 55°C, DMF; (iv) NaOtBu, THF; (v) RCHO, 5% AcOH, DMA, 100°C; (vi)  $\text{KMnO}_4$ , acetone; (vii) 50% TFA, DCM.

Route **a** involved heating the resin in tetrahydrofuran at 60° C for 24 hours in the presence of sodium t-butoxide and resulted in highly efficient cyclization and release of the desired 1,4-benzodiazepine-2,5-diones **1** with purities in the 80-95% range as determined by HPLC analysis [6]. An advantageous feature to this approach is the simultaneous heterocyclization and release mechanism of the final step which ensures that only the desired material is released and the accumulated sideproducts of the previous steps remain bound to the polymer. The general utility of this route was validated through the use of various amino acids, including N-methylamino acids, proline, and a number of anthranilic acid derivatives.

Route **b** utilized aldehyde synthons in 5% acetic acid / dimethylacetamide at 100°C for 18-24 hours followed by potassium permanganate oxidation to convert intermediate **3** to the polymer bound 4-(3H)-quinazolinones. Standard TFA treatment was then used to release the final materials **2**, which were obtained in purities ranging from 65-85%. The chemistry was validated for both electron withdrawing and donating aromatic substituents as well as a wide range of aldehyde inputs.

## Conclusion

Peptidomimetic structures such as the 1,4-benzodiazepine-2,5-diones and 4-(3H)-quinazolinones can be synthesized using polymer supports, linkers and protecting groups which are commonly employed in solid phase peptide synthesis. The inherent advantages associated with the application of solid phase methods can result in dramatic improvements in speed and efficiency with respect to conventional solution phase chemistry.

## References

1. Freidinger, R. M., *Prog. Drug Res.*, 40 (1993) 33.
2. Giannis, A., Kolter, T., *Angew. Chem. Int. Ed. Engl.*, 32 (1993) 1244.
3. Wiley, R. A., Rich, D. H., *Med. Res. Rev.*, 13 (1993) 327.
4. McDowel, R. S., Blackburn, B. K., Gadek, T. R., McGee, L. R., Rawson, T., Reynolds, M. E., Robarge, K. D., Somers, T. C., Thorsett, E. D., Tischler, M., Webb, R. R., II, Venuti, M.C., *J. Am Chem Soc.*, 118 (1994) 5077.
5. Yu, M. J., Thrasher, K. J. McCowan, J. R., Mason, N. R., Mendelsohn, L. R., *J. Med. Chem.*, 34 (1991) 1508.
6. Mayer, J. P., Zhang, J., Bjergarde, K., Lenz, D. M., Gaudino, J. J., *Tetrahedron Lett.*, 37 (1996) 8081.

# Determination of the amino acid composition of the bioactive components in peptide libraries

Árpád Furka, Eugen Câmpian, Hans R. Tanner and Hossain H. Saneii

*Advanced ChemTech Inc., Louisville, KY 40228, USA*

In order to facilitate deconvolution of soluble peptide libraries [1] we developed different sets of partial libraries [2]. These include omission libraries (OLs) which proved to be useful tools in determining the amino acid composition of bioactive components in peptide libraries [3]. In this paper we show that sets of amino acid tester mixtures can be successfully used for the same purpose.

## Results and Discussion

An amino acid tester mixture (AATM) comprises all peptides in which a particular amino acid is present in any position and, as such, can be applied to determine whether or not the amino acid is present in the active peptide.

*Table 1. Complexity of omission and amino acid tester libraries.*

	Tri	Tetra	Penta	Hexa
OL	6859	130321	2476099	47045881
AATM	1141	29679	723901	16954119

OLs and AATMs are expected to give opposing results in screening since exactly those peptides that are found in AATMs are missing from OLs. The number of peptides in AATMs is less than that in the corresponding omission libraries (Table 1).

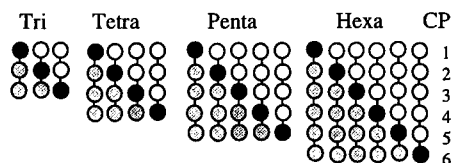


*Fig. 1. Component libraries of amino acid tester mixtures. Black, white and gray circles symbolize couplings with one, 19 and 20 amino acids, respectively. CP1-CP6: coupling positions.*

The low complexity of AATMs is advantageous in screening. A lower quantity of peptide mixture has to be dissolved, for example, to achieve the required molar concentration of the individual peptides. Preparation of an AATM is more complicated, however, than that of an OL. Each AATM is composed of several partial libraries. The number of component libraries is the same as the number of amino acid building blocks in the peptides (Fig. 1). As the figure shows, the non-varied amino acid (e.g. Ala if the alanine

tester mixture is prepared) symbolized by a black circle occupies a different position in these libraries. In lower coupling positions (white circles) the non-varied amino acid is omitted from and in the higher positions (gray circles) is included into the set of varied amino acids. The number of peptides in the component libraries is listed in Table 2.

*Table 2. Number of peptides in the component libraries of the amino acid tester mixtures.*

Length	Coupling position of the amino acid to be tested					
	1	2	3	4	5	6
Tri	400	380	361			
Tetra	8,000	7,600	7,220	6,859		
Penta	160,000	152,000	144,400	137,180	130,321	
Hexa	3,200,000	3,040,000	2,888,000	2,743,600	2,606,420	2,476,099

According to our optimized procedure (Fig. 2), any AATM, regardless of the number of its component libraries, can be prepared in a single run on an automatic synthesizer if it has at least 40 reaction vessels (e.g. ACT 357). If the full library is composed from 20 amino acids, the coupling reaction in one position is executed on a maximum of 40 samples.

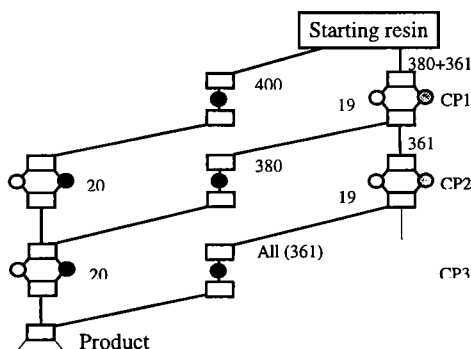


*Fig. 2. General scheme of the optimized synthesis of amino acid (alanine) tester mixtures. CP1-CP3: coupling positions. Black circle: coupling only with alanine. White and gray circle: coupling with all amino acids except alanine (19). White and black circle: coupling with all amino acids including alanine (20). It can be continued in the same manner.*

Beginning with the starting resin, samples are sequentially removed to couple with the non-varied amino acid. The quantity of these samples corresponds to the number of peptides in the component libraries (Table 2). The remaining part of the resin is submitted to coupling with 19 amino acids. The samples after coupling with the non-varied amino acid are sequentially pooled for coupling with 20 amino acids. The quantities of the samples are exemplified in Fig. 2 for tripeptides.

Applicability in screening was tested by determining the competitive inhibition of binding of radiolabeled LH-RH to its polyclonal antibody. The results of the experiments, using a full set of tripeptide amide AATMs synthesized from 19 amino acids (Cys omitted) are shown in Fig. 3. The glycine, proline and arginine tester mixtures show outstanding inhibition activity which allow us to conclude that these three amino acids are present in the active tripeptide. These results are in complete agreement with those obtained previously with tripeptide OLs and thus, the sets of AATMs offer themselves as reliable tools applicable in deconvolution experiments.

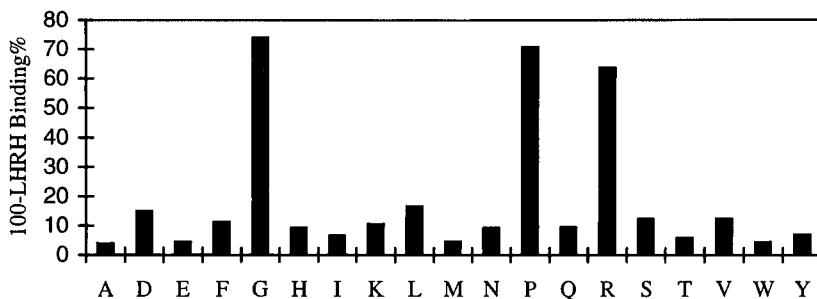


Fig. 3. Binding experiment with 19 amino acid tester mixtures.

### Acknowledgment

We thank Joanne Chou for the binding experiments.

### References

1. Furka, Á., Sebestyén, F., Asgedom, M. and Dibó G., In Abstr. 14th Int Congr Biochem, Prague, Czechoslovakia, 1988 , Vol 5, p 47.
2. Sebestyén, F., Dibó, G., Furka, Á., In Schneider, C. H., Eberle, A. N. 1992 (Proceedings of the 22nd European Peptide Symposium), ESCOM Leiden, 1993,p. 63.
3. Furka, Á., Câmpian, E., Peterson, M. L. and Saneii, H. H., In Kaumaia, P. T. P. and Hodges, R. S. (Eds.), Peptides. Chemistry, Structure and Biology (Proceedings of the 14th American Peptide Symposium), Mayflower Scientific Ltd. England, 1996, p. 317.

# Backbone amide linker (BAL) for solid-phase synthesis of 2,5-piperazinediones (DKP), useful scaffolds for combinatorial chemistry

Fernando Albericio,<sup>a</sup> Montse del Fresno,<sup>a</sup> Ariadna Frieden,<sup>a</sup> Miriam Royo,<sup>a</sup> Jordi Alsina,<sup>a</sup> Knud J. Jensen,<sup>b,c</sup> Steven A. Kates<sup>d</sup> and George Barany<sup>b</sup>

<sup>a</sup>*Department of Organic Chemistry, University of Barcelona, 08028 Barcelona, Spain,*

<sup>b</sup>*Department of Chemistry, University of Minnesota, Minneapolis, MN 55455, USA,*

<sup>c</sup>*Technical University of Denmark, 2800-Lyngby, Denmark,* <sup>d</sup>*PerSeptive Biosystems, Framingham, MA 10701, USA.*

Most current methods of solid-phase peptide synthesis rely on the  $\alpha$ -carboxyl function of the eventual C-terminal amino acid residue to achieve anchoring to the solid support. This allows either stepwise or fragment elongation in the  $C \rightarrow N$  direction. These strategies easily permit modification of the N-terminal amino acid residue, but preclude modification at the C-terminus. Our laboratories have been working on the development of new strategies that allow the attachment of peptides through other functional groups. These approaches have been applied successfully for the syntheses of peptide acids with C-terminal Asn or Gln, and for on-resin head-to-tail cyclizations [1]. However, side-chain anchoring is inherently limited to trifunctional amino acids, and target sequences of interest may lack appropriate attachment sites.

Building on chemistry that we developed previously for the preparation and use of the tris(alkoxy)benzylamide (PAL) handle [2], we have recently described the Backbone Amide Linker (BAL) approach (Fig. 1) for Fmoc SPPS, whereby the growing peptide is anchored through a backbone nitrogen instead of the C-terminal carboxyl [3]. In the present communication, we report further extensions of the applications of the BAL approach for the preparation of peptides containing unusual termini (e.g., *N,N*-disubstituted amides, alcohols, esters, aldehydes, hydrazides, etc.), as well as for the solid-phase preparation of small heterocyclic molecules, such as pyrazoles and 2,5-piperazinediones (diketopiperazines, DKP).

## Results and Discussion

The BAL anchor is established by  $\text{NaBH}_3\text{CN}$ -mediated reductive amination reactions in DMF or MeOH, involving amino acid residues (or appropriately modified derivatives) with 4-formyl-tris(alkoxy)benzyl derivatives linked to PEG-PS or PS solid supports. Key to further progress was the development of effective *N*-acylation conditions, since the hindered secondary amines formed from reductive amination were found to be less reactive than comparable unsubstituted amines. High yields for such acylations are obtained by

using symmetrical anhydrides, HATU/DIEA (1:2), PyAOP/DIEA (1:2), and TFFH/DIEA (1:2). Preformed acid fluorides, in the presence of DIEA (1.1 equiv.), are also effective. In all cases, the optimal solvent is  $\text{CH}_2\text{Cl}_2$ -DMF (9:1), always preferred over neat DMF or NMP. Further acylations to continue chain growth proceed normally.

Reductive amination with monoprotected hydrazine gives rise to a resin for the preparation of peptide hydrazides (Fig. 2). The use of protected hydrazine is mandatory for

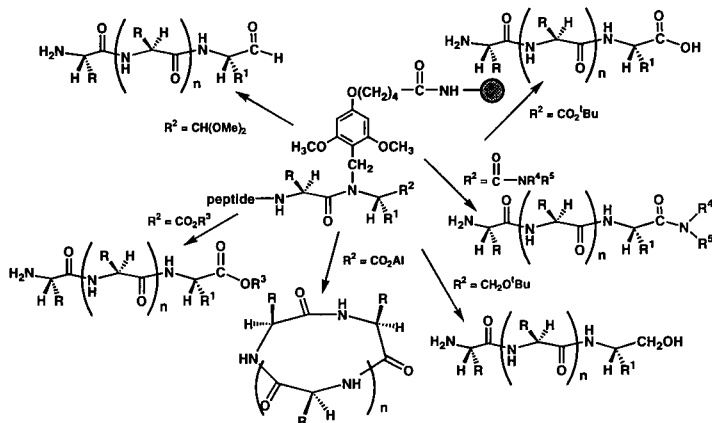


Fig. 1. Some applications of BAL anchoring.

two reasons. First, hydrazine has two nucleophilic nitrogens, one of which should be blocked. Second, the peptide chain should be grown through the  $\alpha$ -nitrogen (see arrow), because acidolytic cleavage of the bond between the BAL methylene and the peptide acylated hydrazine  $\alpha$ -nitrogen can occur in good yields, in contrast to the difficulty in cleaving the unacylated hydrazine  $\alpha$ -nitrogen bond when the peptide chain has been grown through the  $\beta$ -nitrogen. As an added benefit, use of a selectively removable hydrazine protecting group, e.g., Ddz or Trt, will make it possible to grow a second peptide chain off the  $\beta$ -nitrogen to ultimately prepare two-chain tail-to-tail linked peptides. Furthermore, the described hydrazine-resin reacts with dicarbonyl compounds to pyrazoles, which are later released from the resin by treatment with TFA.

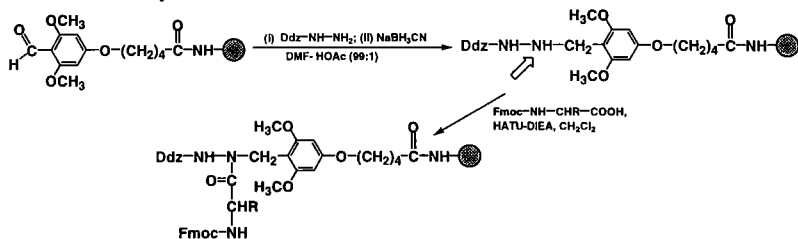


Fig. 2. BAL hydrazine linker.

In working with BAL-anchored amino acyl allyl and *n*-alkyl esters towards the goal of preparing peptide intermediates of some length, we observed that removal of the Fmoc group at the dipeptidyl level was accompanied by almost quantitative diketopiperazine formation. The DKPs thus formed remain covalently attached to the solid support, and can be released later by TFA. DKP formation can be circumvented by (i) incorporation of the second residue as its Trt or Ddz derivative; (ii) selective removal of Trt or Ddz with dilute TFA solutions; and (iii) incorporation of the third residue as its Fmoc derivative under *in situ* neutralization/coupling conditions mediated by PyAOP in DMF in the presence of DIEA [4]. However, it is possible to intentionally take advantage of the facile formation of DKPs to prepare resin-bound as well as soluble DKPs. The rigid DKP scaffolds are useful to display a wide range of pendant functionalities (Fig. 3).

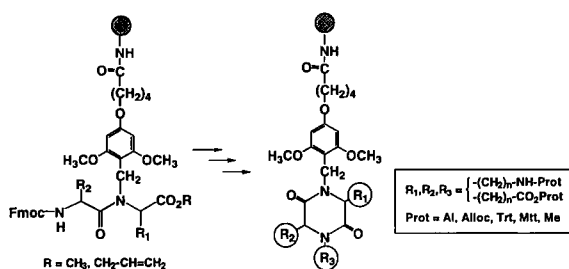


Fig. 3. BAL anchoring of DKPs.

In conclusion, chemistry developed for preparation of the PAL handle has been adapted successfully to the BAL system. This approach promises to overcome limitations inherent to C-terminal or side-chain anchoring, and allows for SPS of C-terminal modified peptides. A new hydrazine linker allows the preparation of hydrazide peptides and heterocyclic compounds such as pyrazoles. Finally, BAL is used to prepare DKPs attached to the solid support.

## References

1. (a) Alsina, J., Chiva, C., Ortíz, M., Rabanal, F., Giralt, E., and Albericio, F. *Tetrahedron Lett.* 38(1997)883; (b) Kates S. A., Solé, N. A., Albericio F., and Barany G., In Basava, C. and Anantharamaiah G. M. (Eds.), *Peptide: Design, Synthesis and Biological Activity*, Birkhäuser, Boston, MA, USA, 1994, p.39, and references cited therein.
2. Albericio F., Kneib-Cordonier N., Biancalana S., Gera L., Masada R. I., Hudson, D., and Barany G., *J. Org. Chem.*, 55(1990)3730.
3. Jensen, K.J., Songster, M.F., Alsina, J., Vágner, J., Albericio, F., and Barany, G. In Kaumaya, P.T.P and Hodges, R.S. (Eds.). *Peptides: Chemistry, Structure and Biology*. Proceedings of the Fourteenth American Peptide Symposium. Mayflower Worldwide Ltd., Kingswinford, England, 1996, p.30.
4. Alsina, J., Giralt, E., and Albericio, F. *Tetrahedron Lett.* 37(1996)4195.

# Fluorescent quenched substrates for protein disulfide isomerase (PDI) defined by the use of disulfide bridge containing libraries

J.C. Spetzler,<sup>a</sup> V. Westphal,<sup>b</sup> J.R. Winther<sup>b</sup> and M. Meldal<sup>a</sup>

<sup>a</sup>Carlsberg Laboratory, Department of Chemistry, <sup>b</sup>Department of Yeast Genetics, Gamle Carlsberg Vej 10, DK-2500 Valby, Copenhagen, Denmark

Protein disulfide isomerase (PDI) is essential for the correct folding of many proteins and catalyzes disulfide rearrangements [1]. It contains two thioredoxin-like domains. However, assays for direct measurement of PDI activity are not available and the mechanism of PDI is not well understood. Therefore, a peptide library [2-4] containing well-defined disulfide bridges and the internally quenched fluorogenic donor-acceptor pair ((2-aminobenzoyl (Abz)/Tyr(NO<sub>2</sub>)) [5] have been constructed [6,7] in order to develop substrates suitable for PDI. Prior to construction of the library model substrates were synthesized and applied in the study of chemical disulfide reducing reagents such as thiols, phosphines and silanes in solution and on solid phase [6]. The library has been screened using the enzyme hPDI expressed from *E. coli*. Peptides on the collected beads were identified by amino acid sequencing and fluorescence quenched substrates for PDI were synthesized. The design and preparation of the library and substrates will be discussed. The enzymatic screening as well as the study of PDI using the synthetic substrates will be described elsewhere.

## Results and Discussion

The design of the library is presented in Fig. 1, where R = PEGA-resin [8]. It consists of two peptide chains linked together through an inter-chain disulfide bridge. One of the peptide chains contains the fluorogenic Abz-group at the N-terminal and the library is generated by variation of the amino acids around the Cys residue (all the natural amino acids except Cys were used). The peptide chain is attached to the PEGA-resin via a Met residue selectively cleavable by CNBr. The quencher chromophore Tyr(NO<sub>2</sub>) is incorporated into the other peptide chain and the distance between the donor-acceptor pair is four amino acid residues including the S-S bond. Generation of the quenched library was achieved in two steps. First, the two peptide chains were synthesized separately on solid phase using the Fmoc strategy. Then, they were combined through an inter-chain disulfide bond formed by the reaction between the free thiol of Cys on the solid phase bound peptide generated upon TFA cleavage and the *p*Npys protected and activated Cys residue [9] of a peptide in solution. The library was generated on the PEGA-resin using the split synthesis-method [2] to yield one peptide on each bead. In the synthesis of the peptide chain containing Tyr(NO<sub>2</sub>), the Rink linker was employed to generate  $\alpha$ -carboxamide after treatment with 95% aq. TFA. In order to establish a complete reaction, the disulfide bond formation was monitored under a fluorescent microscope where the beads turned dark blue. Cleavage with CNBr followed by MALDI-MS

of a few beads proved that the quenched library had been generated. Peptide sequences were identified by amino acid sequencing

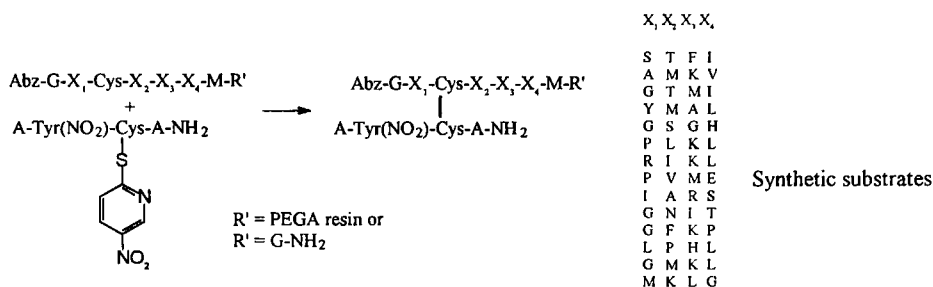


Fig. 1. Formation of the quenched library and the synthetic substrates.

after screening the library with hPDI. The corresponding substrates available for enzymatic studies in solution were synthesized (Fig. 1, R = Gly-NH<sub>2</sub>). In the generation of the substrates, the same synthetic strategy has been applied as for the library. An average yield of 51% was achieved for the synthetic substrates.

In conclusion, a strategy for synthesis of a peptide library as well as substrates suitable for the study of PDI specificity have been developed. Furthermore, the specificity of hPDI towards the synthetic substrates is currently under investigation.

## Acknowledgements

We thank Dr. Ib Svendsen for sequencing the beads.

## References

1. Freedman, R.B., Hirst, T.R. and Tuite, M.F. *TIPS*, 19 (1994) 331.
2. Lam, K.S., Salmon, S.E., Hersh, E.M., Hruby, V.J., Kazmierski, W.M. and Knapp, R.J. *Nature*, 354 (1991) 82.
3. Houghten, R.A., Pinilla, C., Blondelle, S.E., Appel, J.R., Dooley, C.T. and Cuervo, J.H. *Nature*, 354 (1991) 84.
4. Furka, A., Sebestyen, F., Asgedom, M. and Dibo, G. *Int. J. Pept. Prot. Res.*, 37 (1991) 487.
5. Meldal, M. and Breddam, K. *Analytical Biochemistry*, 195 (1991) 141.
6. Spetzler, J.C., V. Westphal, J.R. Winther and Meldal, M. in *Proceedings of the 4th Chinese Peptide Symposium, 1996* (in press).
7. Spetzler, J.C., Westphal, V. Winther J.R. and Meldal, M. *J. Pept. Science* (submitted).
8. Meldal, M. *Tetrahedron Lett.*, 33 (1992) 3077.
9. Rabanal, F., DeGrado, W.F. and Dutton, L. *Tetrahedron Lett.*, 37 (1996) 1347.

# Solid phase synthesis of cyclic homodetic peptide libraries utilizing a novel intraresin chain transfer

Michael L. Moore, Kenneth A. Newlander, Heidemarie Bryan, William M. Bryan and William F. Huffman

*SmithKline Beecham Pharmaceuticals, King of Prussia, PA 19406, USA*

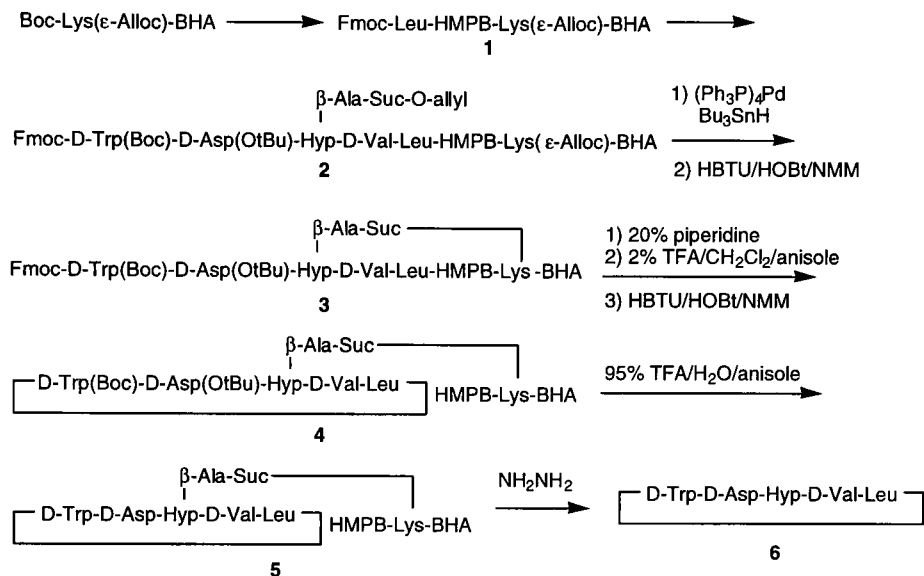
BQ-123, cyclo[D-Trp-D-Asp-Pro-D-Val-Leu], a potent endothelin receptor antagonist [1], is a member of the important class of G-protein coupled receptor ligands. In addition, its solution conformation is quite constrained both in polar and nonpolar solvents, adopting a  $\gamma$ -turn about the Pro<sup>3</sup> residue and a  $\beta$ -turn involving the other four residues [2].

During the course of synthesis of a variety of BQ-123 analogs, we noted an extremely facile ring closure for the linear sequence D-Trp-D-Asp-Pro-D-Val-Leu compared to the sequence D-Val-Leu-D-Trp-D-Asp-Pro. This facile cyclization occurred with the Hyp<sup>3</sup>, MeAla<sup>3</sup> and Aib<sup>3</sup> substitutions as well. Since all these amino acids share a low energy  $\gamma$ -turn conformation, we hypothesize that a  $\gamma$ -turn in the linear peptide facilitates the cyclization by bringing the N- and C-terminal residues into proximity. This cyclization was largely independent of the side chain or chirality of the remaining residues and suggested cyclo[X-X-Pro-X-X] as a template for a combinatorial peptide library [3].

We designed a solid phase approach in which all four residues could be randomized and in which the peptide could be synthesized by normal stepwise addition, cyclized on the resin, side chain protecting groups removed and the free peptide released from the resin.

## Results and Discussion

As shown in Scheme 1, a differentially-protected bifunctional resin was prepared using Boc-Lys( $\epsilon$ -Alloc) attached to BHA resin. The super acid labile hydroxymethylmethoxyphenoxybutyryl (HMPB) linker was attached to the  $\alpha$ -amino group and used as the handle to build the linear peptide by conventional Fmoc chemistry. The Pro<sup>3</sup> residue was substituted with a hydroxyproline bearing a differentially protected linker, succinyl- $\beta$ -alanine monoallyl ester. After construction of the linear peptide, the allyl ester and Alloc groups were selectively removed by palladium(0) and the resulting free amino and carboxyl groups were coupled together [3]. This was extremely facile and gave a negative ninhydrin test after a single HBTU coupling. The Leu-HMPB bond was then selectively cleaved by treatment with 2% TFA/anisole in CH<sub>2</sub>Cl<sub>2</sub>, to give the linear peptide now tethered to the resin via the Hyp<sup>3</sup> residue. There was no loss of nitrogen content on the resin at this step. Removal of the Fmoc group and cyclization gave the resin-bound cyclic peptide.



*Scheme 1. Synthetic design.*

The side chain protecting groups were removed by treatment with 95% TFA/anisole/H<sub>2</sub>O. The free peptide was finally released from the resin by treatment with hydrazine. The HPLC trace of the crude peptide released from the resin is shown in Fig 1. The peptide was obtained in 97% crude yield based on the nitrogen content of the linear pentapeptide resin **2** and its identity was confirmed by mass spectrometry.

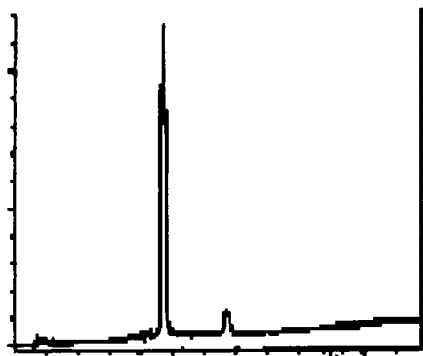


*Fig. 1. HPLC of crude cyclic peptide.*

Based on these results, an eight-membered test library was constructed using the split-and-combine approach, with either D-Trp or D-Gln at position 1, D-Asp or D-Ala at position 2 and D-Val or D-Thr at position 4. HPLC traces of the resulting peptide mixture are shown in Fig 2. All eight peptides were identified by LC-MS. In the UV trace, the Trp-containing peptides give much stronger responses due to their larger extinction coefficients. In the total ion current trace, all peptides are present in approximately equal amounts.

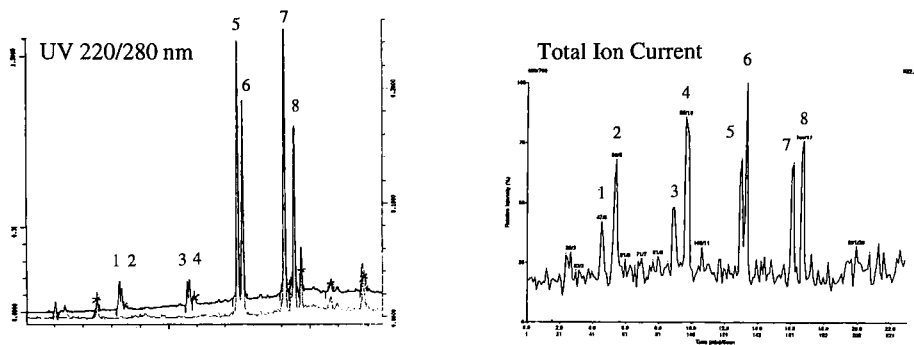


Fig. 2. HPLC traces of 8-membered test library.

## References

1. Ishikawa, K., Fukami, T., Nagase, T., Fujita, K., Hayama, T., Niiyama, K., Mase, T., Ihara, M. and Yano, M., *J. Med. Chem.*, 35 (1992) 2139.
2. Peishoff, C., Bean, J., unpublished results; Coles, M., Sowemimo, V., Scanlon, D., Munro, S. L. A. and Craik, D. J., *J. Med. Chem.*, 36 (1993) 2658; Reily, M. D., Thanabal, V., Omecinsky, D. O., Dunbar, Jr., J. B.; Doherty, A. M. and DePue, P. L., *FEBS Lett.*, 300 (1992) 136.
3. BQ-123 has been used by others as a template for cyclic peptide libraries. Spatola, A. F., Crozet, Y., deWit, D. and Yanagisawa, M., *J. Med. Chem.*, 39 (1996) 3842.
4. A similar approach, applied to chain reversal on the solid support, has been published. Holmes, C. P. and Rybak, C. M., In R. S. Hodges and J. A. Smith (Eds), *Peptides: Chemistry, Structure and Biology*, Proceedings of the 13th American Peptide Symposium, ESCOM, Leiden, 1994, pp. 992.

# Analysis of *O*- and *N*-linked glycopeptide libraries by MALDI-TOF MS: Application in solid phase assays of carbohydrate-binding-proteins

Phaedria M. St. Hilaire, Morten Meldal and Klaus Bock

Department of Chemistry, Carlsberg Laboratory, Gamle Carlsberg Vej 10, DK-2500 Valby, Denmark.

The glycopeptide building block approach in portion mixing library synthesis allows the expedient formation of numerous glycopeptides as putative ligands in protein binding assays. However, rapid and unambiguous analysis of modified peptides on solid phase remains challenging. It has been recently demonstrated that peptide libraries can be analyzed using *ladder synthesis*, an analytical technique which involves capping a small portion of the growing peptide during synthesis [1]. The “ladder” of peptide fragments generated is subsequently evaluated by MALDI-TOF mass spectrometry. Previously, we reported the analysis of a glycopeptide using a similar strategy in which *in situ* capping with Boc-amino acids was successfully used to generate the “ladder” [2]. In the present work, we extend the methodology to include 1) an *encoded in situ capping* methodology that allows immediate distinction between peptide residues of identical masses and 2) rapid *on-bead* mass analysis facilitated by use of a photolabile linker [3]. The library generated was screened against *Lathyrus Odoratus*, a mannose/glucose specific lectin.

## Results and Discussion

*Library Ladder Synthesis With Encoded In situ Capping:* The non-glycosylated amino acid building blocks were incorporated into the library using Fmoc/TBTU/NEM methodology while the glycosylated amino acid building blocks and their labels were coupled using the pentafluorophenol ester strategy. To ensure similar reactivity of the capping agent and reacting amino acid, we utilized the Boc-protected counterpart (10%) of each amino acid as the capping agent. The library was synthesized using a high loading PEG-Sarcosine resin (0.46 meq/g) equipped with a photolabile linker for rapid cleavage and an “ionization/mass spacer”, APRPPRV, for moving the fragment mass peaks beyond the matrix mass region and for facilitating flight of protected peptide fragments during monitoring of the library synthesis. The three glycosylated amino acid building blocks and their carboxylic acid labels incorporated into the library were as follows:  $\beta$ -D-GlcNAc-Asn (Ng)-2-phenylpropionic acid (Ppa, mass: 132.2),  $\alpha$ -D-Man-Thr (Tm)-lauric acid (Lau, mass: 182.3), and  $\alpha$ -D-Man(1-3) $\alpha$ -D-Man-Thr (Tm3)-2-naphthoic acid (Nap, mass: 154.2).

*Solid Phase Assay of Lathyrus Odoratus:* A portion of the library was incubated with FITC labelled sweet pea lectin, *Lathyrus Odoratus*, and beads with varying degrees of fluorescence were removed and sequenced by MALDI-MS (Fig.1). Both non-glycosylated

and glycosylated peptides were detected. The following active peptides were synthesized and tested for binding to the lectin on solid phase: **1.** TmFHFVENgV, **2.** TmTNgSLENgV, **3.** PHGNgGTEV, **4.** VYYGNgFLV, **5.** TEVSFWTmV, **6.** TmFFFVNKV, **7.** DTmPENgYKV, **8.** TWFNgGFSV, **9.** TmLFKGFHV, **10.** EFPWLSEV, **11.** TLDTTFHV, and **12.** YGEASTTV. Peptides **6** and **9** showed the most intense fluorescence followed by peptides **7**, **5** and **2**. This result is in agreement with the mannose specificity of the lectin. Peptides which contained only  $\beta$ -D-GlcNAc as the carbohydrate moiety showed little fluorescence. Of the non-glycosylated peptides, **10** and **12** demonstrated no fluorescence but peptide **11** showed a brightness equivalent to that of peptide **2**. Interestingly, peptide **1** showed very little or no binding. Inhibition of lectin binding to the resin-bound peptides with  $\alpha$ -D-methyl mannose and yeast mannan resulted in reduction of binding at concentrations of 100 mM and 0.1 mg/mL, respectively.

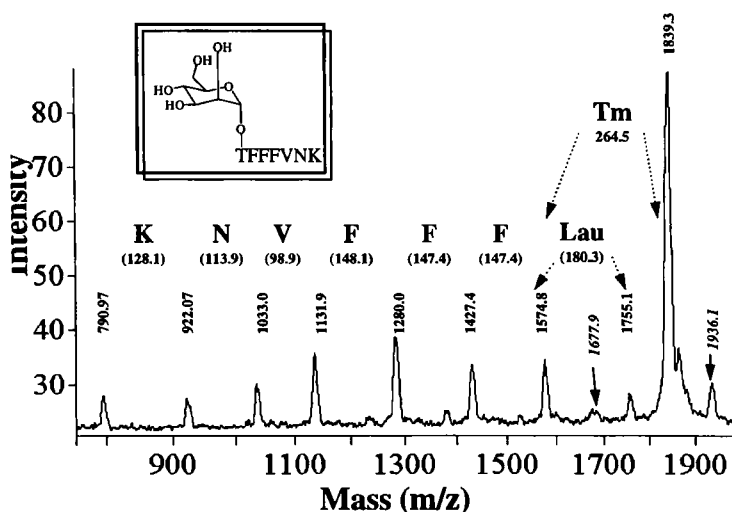


Fig. 1. Mass spectrum of peptide 6 fragments showing peptide sequence. 1936.1: peptide-TFA adduct, 1677.9: loss of mannose from peptide during MALDI.

## References

1. Youngquist, R., Fuentes, G., Lacey, M. and Keough, T., *J. Am. Chem. Soc.*, 117 (1995) 3900.
2. St.Hilaire, P., Lowary, T., Bock, K. and Meldal, M. In *Peptides 1996: Proceedings of the Twentyfourth European Peptide Symposium, ESCOM in press.*
3. Fitzgerald, M., Harris, K., Shelvin, C., and Siuzdak, G., *Bioorg. Med. Chem. Lett.*, 6 (1996) 979.

# Unsymmetrically functionalized polyamine libraries by a solid phase strategy starting from their symmetrical polyamine-counterparts

**Gerardo Byk, Marc Frederic and Daniel Scherman**

*UMR-133 Rhône-Poulenc Rorer Gencell/CNRS, 13 Quai Jules Guesde B.P. 14,  
94403-Vitry sur Seine, France*

The synthesis of unsymmetrically substituted polyamines commonly involves tedious multistep reaction synthesis [1]. In the context of our gene therapy program, we were challenged to synthesize novel and varied lipopolyamines as non-viral vectors for DNA delivery [2]. Thus, we have developed a solid phase methodology which allows quick and easy access to a large number of mono-functionalized polyamines starting from their symmetrical counterparts.

## Results and Discussion

Using this approach, the alkylating reagent is covalently attached to the polymeric support through esterification. The principle of the method is the use of solid phase synthesis to give rise to a "high dilution effect" in the proximity of the alkylating reagent. This dilution effect prevents poly-alkylation of the polyamine once the first alkylation has taken place. The symmetrical polyamine reacts with the alkylating reagent on the solid phase to yield the unsymmetrically mono-functionalized polyamine attached to the support. The free amines of the product can be protected on the solid phase with groups such as Boc (see Fig. 1 products 1-2, 5-7) or orthogonally protected with DdeOH [3] for the primary amines from one side and Boc for the secondary amines on the other side (see in Fig. 1 products 3-4). In the absence of primary amines, secondary amines will react to give the unsymmetrically functionalized polyamine as assessed by the synthesis of a derivative of the cryptand 1,4,8,11-tetraazacyclotetradecane (see product 7).

When polyamines contain primary as well as secondary symmetrical polyamines, a mini-combinatorial library composed of the primary and secondary amino-functionalized derivatives is obtained (see products 1-2 and 3-4). The secondary functionalized polyamines are easily separated from their primary counterparts after protection. Finally, non-acidic cleavage of products from Cl-trityl chloride solid phase support using  $\text{CH}_2\text{Cl}_2$ /trifluoroethanol leads to protected products, thus allowing further modification of the acidic function by classical solution methodologies.

In conclusion, combining the unsymmetrical functionalization of polyamines and orthogonal amine protection with DdeOH [4] significantly extends the solid phase chemistry of polyamines, allowing novel applications such as the use of polyamines for the synthesis of polyamine-combinatorial libraries, synthesis of novel analogs of polyamine-containing toxins [5], introduction of polyamines into peptides [6], synthesis of

functionalized metal-complexing cryptands [7] suitable for introduction into peptides, or synthesis of novel cationic lipids for gene delivery, which is currently being investigated in our laboratory.

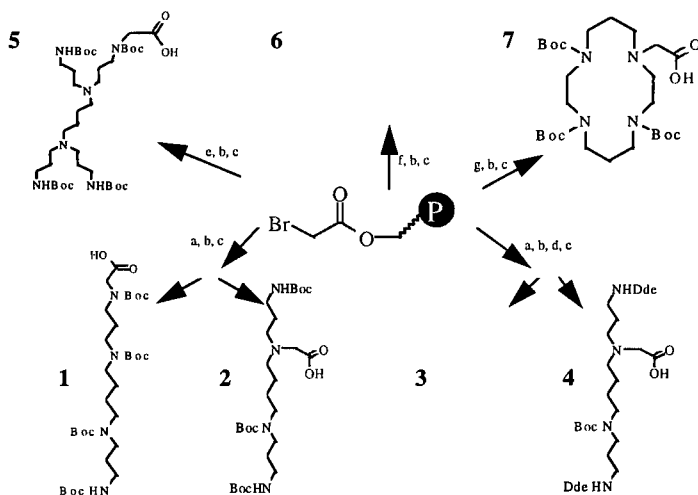


Fig. 1. a: Spermine in  $\text{CH}_2\text{Cl}_2$ , b:  $(\text{Boc})_2\text{CO}_2$  in  $\text{CH}_2\text{Cl}_2$ , c: Cleavage with trifluoroethanol/ $\text{CH}_2\text{Cl}_2$ , d: DdeOH, e: Tetra-(3-aminopropyl)-diaminobutane, f: Tris (2-aminoethyl)amine, g: 1,4,8,11-tetraazacyclotetradecane.

## References

1. Ganem, B. *Acc. Chem. Res.*, 15 (1982) 290.
2. Byk, G., Dubertret, C., Schwartz, B., Frederic, M., Jaslin, G., Rangara, R. and Scherman D. *Lett. Pept. Sci.*, (1997) in press.
3. Bycroft, B.W.; Chan, W.C., Chhabra, S.R.; Hone, N.D. *J. Chem. Commun.*, (1993) 778.
4. (a) Nash, I.A.; Bycroft, B.W., Chan, W.C. *Tetrahedron Lett.*, 15 (1996) 2625. (b) Bycroft, B.W., Chan, W.C., Hone, N.D., Millington, S., Nash, I.A. *J. Am. Chem. Soc.*, 116 (1994) 7415.
5. Aramaki, Y., Yasuhara, T., Higashijima, T., Yoshioka, M., Miwa, A., Kawai, N., Nakajima, T. *Proc. Japan Acad. Sci.*, 62B (1986) 359.
6. Toki, T., Yasuhara, T., Aramaki, Y., Osowa, K., Miwa, A., Kawai, N., Nakashima, T. *Biomedical Res.*, 9 (1988) 421.
7. (a) Granier, C., Guilard, R. *Tetrahedron*, 51 (1995) 1197. (b) Kaden, T.A., Studer, M. *Helv. Chim. Acta*, 69 (1986) 2081. (c) Yamamoto, H., Maruoka, K. *J. Am. Chem. Soc.*, 103 (1981) 6133.

# Development of DNA-encoded library containing $10^9$ backbone cyclic peptides on 7 $\mu\text{m}$ glass beads

Anna Balanov, Eran Hadas and Ilana Cohen

Peptor Ltd., Kiryat Weizmann, 76326 Rehovot, Izrael

Combinatorial synthetic libraries have become a powerful tool in high-throughput screening of peptides and an important starting point in the search for lead compounds for the development of new pharmaceutical agents. Difficulties in deconvolution of such large libraries brought about the invention of various tagging methods. Only a few examples of DNA-tagged libraries of linear peptides have been reported. [1] The size of these libraries is quite limited due to the relatively low capacity of the bead sorting techniques.

Peptor Ltd. has developed a proprietary technology known as backbone cyclization (Fig.1) which permits the creation of conformationally constrained peptides without modification of their side chains or terminal groups [2]. Each linear peptide can give rise to a great variety of backbone cyclic peptides having the same amino acid sequence but different conformations and therefore different biological activity.

The very large number of different peptides afforded by the backbone cyclization technology prompted the development of peptide libraries capable of screening a very large number of peptides per experiment. A DNA-tagged immobilized library approach is described that is capable of screening about  $10^9$  backbone cyclic peptides per experiment for binding activity.

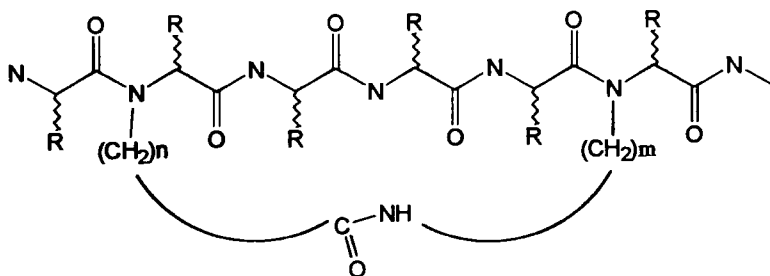


Fig. 1. Peptor's backbone cyclic peptides.

## Results and Discussion

We found 7  $\mu\text{m}$  glass bead supports to be useful solid carriers both for cyclic peptide synthesis and for screening binding activities. The small size of the beads provides a highly dense library (more than  $10^9$  peptides in 1 ml) and the glass is compatible with all the reagents used in peptide and DNA synthesis. The glass bead surface was modified with aminopropyl-triethoxy silane,

and all the remaining free OH-groups were protected as trimethylsilyl ethers. Two linkers were coupled to the free amino groups in a 4:1 mixture of Fmoc- $\beta$ -Ala (for peptide synthesis) and Fmoc-Ser(Trt) (for DNA synthesis). The synthetic procedure includes parallel peptide assembly and encoding of DNA sequences (Fig. 2), which is followed by peptide backbone cyclization. It was found that conditions of peptide assembly as well as backbone cyclization do not affect the DNA molecules; DNA synthesis in turn did not cause any problems in the peptides.

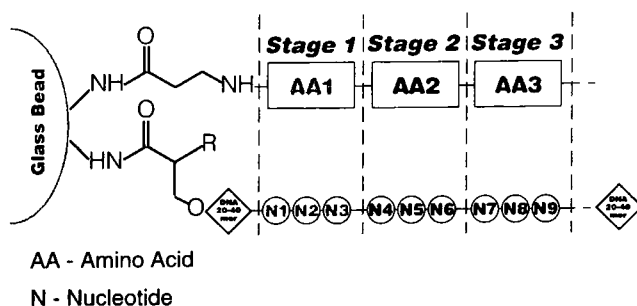


Fig. 2. Parallel assembly of peptide and DNA.

Peptide combinatorial synthesis is achieved using a special mix and split strategy, designed for the libraries of backbone cyclic peptides that enables the creation of cyclic peptides with various bridge positions (cycloscan) within the same library. Beads are blocked by incorporation of biotin after each amino acid coupling step so that all deletion sequences are capped with biotin at the N-terminal. DNA synthesis is performed by an automated synthesizer using standard phosphoramidite derivatives of four nucleosides.

Following DNA and peptide global deprotection, the beads are first blocked with avidin, washed and stained with murine monoclonal antibody to human interleukin-6 receptor (hIL-6R, gp80), followed by Texas red conjugated anti-mouse immunoglobulin second antibody. Selection of highly fluorescent beads is performed by a computerized image analysis procedure using an inverted microscope. "Positive" beads are retrieved by a CellSelector (Cell Robotics, USA). DNA of the "positive" beads are amplified by PCR and sequenced. Known DNA sequences enable us to determine the sequence of the cyclic peptide attached to the same bead. In model experiments many beads containing the same peptide were prepared and the correspondence of the peptide sequence to the encoding DNA was proven.

## References

1. Brener, S. and Lerner, R.A., Proc. Natl. Acad. Sci. USA, 89 (1992) 5381.
2. Gilon, C., Halle, D., Chorev, M., Selinger, Z. and Byk, G., Biopolymers, 31 (1991) 745.

# Introduction of bulky betidamino acids in thyrotropin releasing hormone (TRH)

Dean A. Kirby,<sup>a</sup> Marvin C. Gershengorn<sup>b</sup> and Jean E. Rivier<sup>a</sup>

<sup>a</sup>Clayton Foundation Laboratories for Peptide Biology, The Salk Institute, 10010 N. Torrey Pines Rd., La Jolla, CA 92037 ; <sup>b</sup>Division of Molecular Medicine, Cornell University Medical Center, New York, NY 10021, USA

Recently, much attention has been directed to the development of new methods for introducing chemical diversity into peptide or peptidomimetic lead structures. Orthogonally protected monoacylated aminoglycine (Agl) derivatives, referred to as betidamino acids (bAaa), have been identified as useful scaffolds for the introduction of chemical diversity into bioactive polypeptides [1] A variety of novel and high potency analogs of gonadotropin-releasing hormone (GnRH) [2] and somatostatin (SRIF) [3] have recently been presented in which betidamino acids were generated by acylation of one of the two amino functions of aminoglycine. In the present study we synthesized TRH analogs that incorporated novel aromatic and heterocyclic functionalities (Fig. 1 and Table 1) using a number of acylating agents to derivatize the resin-bound tripeptide pGlu-(D/L)Agl(Fmoc)-Pro-MBHA after deprotection of the Fmoc group.

## Results and Discussion

TRH (pGlu-His-Pro-NH<sub>2</sub>) is the smallest hypothalamic releasing factor and has been found to have very strict structural requirements for activation of its pituitary receptor. With the exception of two modifications of the histidine residue at position 2 (i.e. [N<sup>im</sup>-3Me-His<sup>2</sup>]TRH and [Pyr(1)Ala<sup>2</sup>]TRH are 8 and 3 times more potent than TRH [4, 5]), all other reported modifications to this tripeptide resulted in analogs with reduced binding affinity or low potency. In particular, the introduction of a bulky indole side-chain at position 2 led to [Trp<sup>2</sup>]TRH which was found inactive at doses up to 5000 times the effective TRH dosage [6].

Using the versatile pGlu-Agl-Pro-MBHA scaffold, we tested the influence of steric as well as charge requirements at position 2. Functionalities at position 2 ranged from [Pyr(1)Ala]-like (expected to be active) to [Trp]-like (expected to be inactive) (See Table 1). TRH analogs did not bind to mouse pituitary AtT-20 cells stably expressing TRH-Rs nor to COS-1 cells transiently expressing TRH-Rs [7]. These negative results were unexpected in the cases where the substitutions of the Agl scaffold were conservative in both charge and/or steric hindrance, thus emphasizing the strict structural requirements of TRH for recognition by and activation of its receptor.

Fig. 1. Structure of betidamino acid-containing TRH analogs.

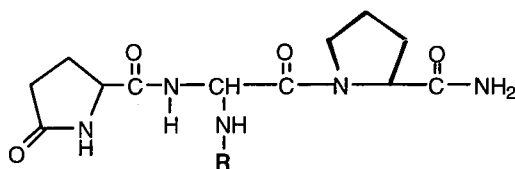


Table 1. Selected heterocyclic and aromatic betidamino acid structures.

Symbol	acylating agent	Structure (R)	Symbol	acylating agent	Structure (R)
b-Atz	not applicable		b-Trp	indole-3-carboxylyl	
b-Pca	2-pyrazine-carboxylyl		b-homo Trp	indole-3-acetyl	
b-Apc	3-amino-4-pyrazole carboxylyl		b-iso Trp	indole-2-carboxylyl	

## Acknowledgments

The authors thank C. Miller for HPLC and CZE analysis, Dr. A. G. Craig and T. Goedken for mass spectral analysis and D. Johns for manuscript preparation. This work was supported by NIH grants DK 26741 (JER) and DK 43036 (MCG).

## References

- Rivier, J. E., Jiang, G.-C., Koerber, S. C., Porter, J., Craig, A. G. and Hoeger, C., Proc. Natl. Acad. Sci. USA, 93 (1996) 2031.
- Jiang, G., Miller, C., Koerber, S. C., Porter, J., Craig, A. G., Rivier, C. L. and Rivier, J. E., J. Med. Chem., (1997) submitted.
- Hoeger, C. A., Jiang, G.-C., Koerber, S. C., Reisine, T., Liapakis, G. and Rivier, J. E., In P. T. P. Kaumaya and R. S. Hodges (Eds.) Betide based strategy for the design of selective somatostatin analogs, Proceedings of the 14th American Peptide Symposium, Mayflower Scientific Ltd., England, 1996, p. 635.
- Rivier, J., Vale, W., Monahan, M., Ling, N. and Burgus, R., J. Med. Chem. 15 (1972) 479.
- Coy, D. H., Hirotsu, Y., Redding, T. W., Coy, E. J. and Schally, A. V., J. Med. Chem., 18 (1975) 948.
- Sievertsson, H., Chang, J.-K. and Folkers, K., J. Med. Chem., 15 (1972) 219-221.
- Laakkonen, L., Li, W., Perlman, J. H., Guarnieri, F., Osman, R., Moeller, K. D. and Gershengorn, M. C., Mol. Pharmacol., 49 (1996) 1092.

# Combinatorial libraries and polyamines in the battle against Third World trypanosomes

Helen K. Smith and Mark Bradley

Department of Chemistry, University of Southampton, Highfield, Southampton SO17 1BJ, UK

Tropical diseases such as African Sleeping Sickness and Chagas' disease result from infection by the trypanosome and leishmania parasites. Trypanothione reductase [1] is an essential enzyme in these organisms, responsible for oxidative stress management. The natural substrate  $N^1, N^8$ -bis(glutathionyl)spermidine (trypanothione) [2] has been prepared on the solid phase in our laboratory, using a polyamine linker [3,4]. This method of synthesis has enabled us to apply a combinatorial approach to the preparation of trypanothione analogues. In addition, the modification of our linker has led to the synthesis of two identical 576 member libraries of polyamine-peptide conjugates for screening both in solution and on the solid phase against trypanothione reductase. This has resulted in the identification of several potent enzyme inhibitors, with both screening methods providing identical 'hits'.

## Results and Discussion

The resin bound polyamines **1** and **2** were prepared as described [3,4] by selective protection of the primary amines of spermidine, followed by urethane formation. After tethering to the solid phase, libraries of polyamine-dipeptide conjugates were synthesized using 'split and mix' methodology (Fig. 1). After Fmoc removal, side chain deprotection was achieved using a TFA cleavage cocktail. The differing acid labilities of the two linkers ensured that while linker **1** remained attached to the resin support during TFA deprotection, linker **2** was cleaved, releasing the 576 member library into solution.

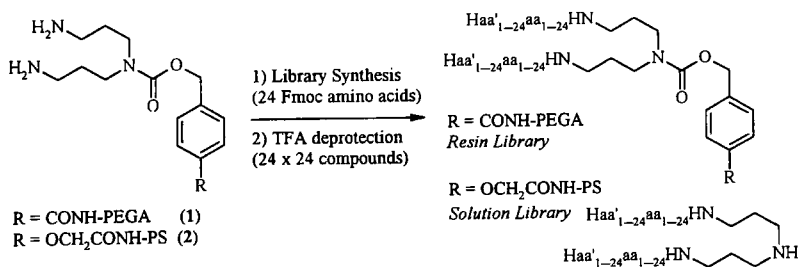


Fig. 1. Preparation of solution phase and resin bound polyamine-dipeptide libraries.

Both libraries were screened against trypanothione reductase using an iterative approach. The solution screen gave Trp as the most potent residue in the second position, giving rise to three potent inhibitors after deconvolution: TrpArg ( $K_i = 16\mu\text{M}$ ), TrpTrp ( $K_i = 3.1\mu\text{M}$ ) and TrpPhg ( $K_i = 83\mu\text{M}$ ). Upon resynthesis it was observed that an impurity in the arginine containing compound was the most active component. This was shown to be TrpArg(Pmc). Hence, two further compounds were prepared containing either one ( $K_i = 100\text{ nM}$ ) or two ( $K_i = 185\text{ nM}$ ) Pmc protected arginines. In order to investigate any shielding effect of the resin linker during solid phase screening, a Cbz protecting group was attached to the secondary amine of spermidine in the TrpArg containing compound ( $K_i = 1.6\mu\text{M}$ ). Interestingly, all the compounds tested proved to be classic noncompetitive inhibitors.

Screening of the resin-bound library was achieved by incubating the sub-libraries overnight in trypanothione reductase. The residual enzyme activity was determined after resin filtration, giving an approximate indication of protein binding. The terminal residues in the least active pots were again tryptophan, but also arginine. Deconvolution resulted in the identification of the identical hit from the solution library; TrpArg. In addition, there was a tendency for the two residues required for binding to be positively charged and hydrophobic.

## Conclusion

Linkers designed for the solid phase synthesis of polyamines have been employed for the generation of two identical libraries of polyamine-peptide conjugates. These libraries have been screened against trypanothione reductase both in solution and on the solid phase. This has resulted in the identification of the *same* potent inhibitors containing both Trp and Arg (+ or - Pmc). Interestingly, a depletion screen of the same library on a TentaGel support gave no diminution in enzyme activity.

## Acknowledgements

We would like to thank the Wellcome Trust for an equipment grant (039094/Z/93/Z) and for a Project Grant 043503/PMG/AH (MB) and EPSRC for a quota award (H.K.S.). This investigation received financial support from the UNDP/WORLD BANK/WHO Special Programme for Research and Training in Tropical Diseases.

## References

1. Schirmer, R.H., Müller, J.G. and Krauth-Siegel, R.L., *Angew. Chem. Int. Ed. Engl.*, 34(1995)141.
2. Fairlamb, A.H., Blackburn, P., Ulrich, P., Chait, B. and Cerami, A., *Science*, 227(1985)1485.
3. Marsh, I.R., Smith, H. and Bradley, M., *J. Chem. Soc., Chem. Commun.*, (1996)941.
4. Marsh I.R., Smith, H.K., Leblanc, C. and Bradley, M., *Mol. Div.*, 2(1996)165.

## Hybrid resins for synthesis and screening of synthetic peptide libraries

Hoebert S. Hiemstra,<sup>a</sup> Willemien E. Benckhuijsen,<sup>a</sup> Wolfgang E. Rapp<sup>b</sup> and Jan W. Drijfhout<sup>a</sup>

<sup>a</sup>Department of Immunohematology and Blood Bank, Leiden University Hospital, POBox 9600, 2300 RC Leiden, The Netherlands, <sup>b</sup>Rapp Polymere GmbH, Tübingen, Germany

A convergent library approach using peptides in solution for screening and peptides on beads for selection has been proposed using orthogonal cleavage conditions [1]. We present hybrid resins that offer possibilities for this type of library screening, but use only one type of cleavable linker together with non-cleavable linking. After several screening rounds, the identity of single active beads is determined by Edman bead sequencing.

### Results and Discussion

A mixture of Fmoc-5(4'-aminomethyl-3',5'-dimethoxyphenoxy) valeric acid (Fmoc-linker) and Fmoc-Nle was coupled (PyBOP/NMM in NMP, three hours, three times molar excess) to TentaGelS-NH<sub>2</sub>, yielding an amide hybrid resin. After performing peptide synthesis on the hybrid resin, each bead contained both acid-labile and acid-stabile attached peptides (Fig. 1). The ratio of acid-stabile versus acid-labile attached peptides depends on the ratio of Fmoc-Nle and Fmoc-linker in the mixture that is used for synthesis of the hybrid resin. Since the cleavage rate from the hybrid resin of acid-labile attached peptides depends on the composition of the cleavage mix and time, but not on the peptide sequence, the peptide can be partially cleaved using defined cleavage conditions. Using TFA/CH<sub>3</sub>CN/H<sub>2</sub>O, 10/9/1 (v/v/v) (16% acid-stable peptide), for 90 minutes 25 % of the acid-labile attached peptide is cleaved off. Cleaving off a second 25% takes 180 minutes. This cleavage procedure allows for stepwise screening of 'one-bead-one-structure' libraries in which screening for bioactivity is performed with solubilized peptides. Selection is done on the bead level. The peptide sequence on an active bead can be deduced by Edman bead sequencing with high repetitive yield. Using this newly developed method several CD4+ T-cell epitopes were identified from HLA class II binding synthetic peptide libraries with a complexity of 8,000,000 (data not shown). CD8+ T cell clones, however, recognize HLA class I bound peptides, which require a free carboxy terminus for binding. Therefore we also developed a hybrid resin yielding C-terminal Val carboxy-peptides after cleavage.

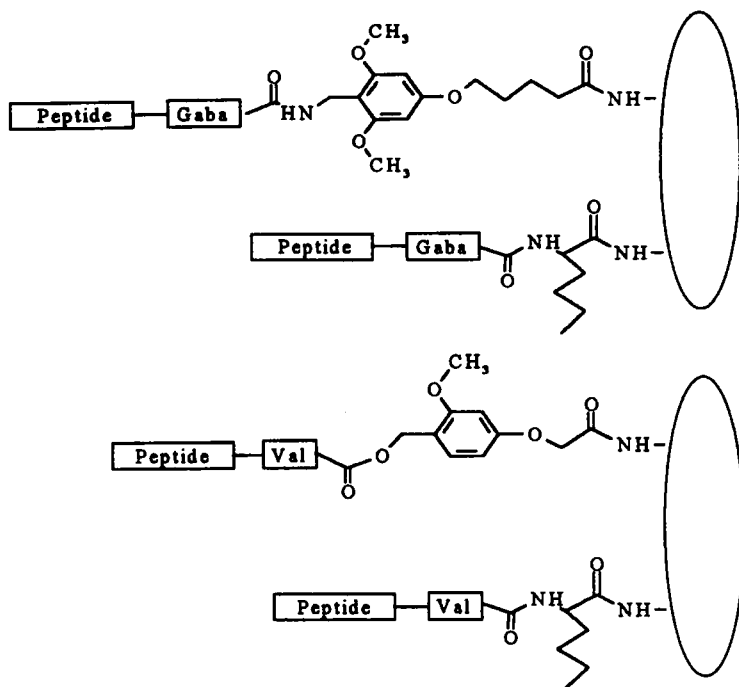


Fig. 1. Hybrid resins after peptide synthesis. The upper hybrid resin yields peptide-amides after acid cleavage. The lower hybrid resin yields carboxy-peptides after acid cleavage. Peptides contain either a C-terminal Gaba residue or a C-terminal Val residue to make cleavage rates independent of the C-terminal amino acid. Part of the peptide material on both hybrid resins is attached in an acid-stable manner and can be used for sequence identification by Edman bead sequencing.

A mixture of 2-methoxy-4-hydroxymethylphenoxyacetic acid (acid labile linker) and Fmoc-Nle-OH was coupled to TentaGelS-NH<sub>2</sub>. After deprotection (piperidine) Fmoc-Val-OH was coupled (DIC/DMAP/HOBT) yielding a carboxy hybrid resin (Fig. 1). Cleavage rates from this hybrid resin were found to be dependent on the peptide sequence, probably due to the hyper acid-lability of the linker, which might make cleavage sequence dependent and diffusion controlled (inside the bead). This implies that library screening using this hybrid resin is impaired.

## References

1. Lebl, M., Patek, M., Kocis, P., Krchnak, V., Hruby, V.J., Salmon, S.E., Lam, K.S. *Int. J. Pept. Protein Res.*, 41 (1993) 201.

# Combinatorial libraries: Equimolar incorporation of benzaldehyde mixtures in reductive alkylation reactions

John M. Ostresh, Christa C. Schoner, Marc A. Giulianotti,  
Michael J. Kurth, Barbara Dörner and Richard A. Houghten

Torrey Pines Institute for Molecular Studies, 3550 General Atomics Ct.,  
San Diego, CA 92121, USA

In order to facilitate the synthesis of combinatorial libraries [1] in the positional scanning format [2], a method was developed for determining the relative incorporation of benzaldehyde derivatives in the reductive alkylation of peptides (Fig. 1). By comparing 60 different benzaldehydes with 4-fluorobenzaldehyde as an internal reference control, we were able to calculate the isokinetic ratios [3] necessary for equimolar incorporation in a competitive reagent mixture. Individual component concentrations were adjusted based on the absorbance normalized peak area of the alkylated peptides in RP-HPLC. Mixtures obtained by this method are comparable to the equimolar mixtures generated using the split-resin method [1]. Syntheses were performed using the tea-bag method [4] and reagents were used in excesses large enough for observing pseudo first-order reaction kinetics.

## Results and Discussion

For each of 60 benzaldehyde derivatives, a control resin mixture was prepared by synthesizing and combining equivalent molar amounts of a standard resin, 4-fluorobenzyl-Ala-Phe-Lys(2ClZ)-mBHA, with O-Ala-Phe-Lys(2ClZ)-mBHA resin, where O represents one benzaldehyde reductively alkylated to the N-terminus of the alanine residue. Following cleavage, the control resin mixture was used to determine the relative RP-HPLC absorbance of the two components in the equimolar mixture. In addition, an equimolar

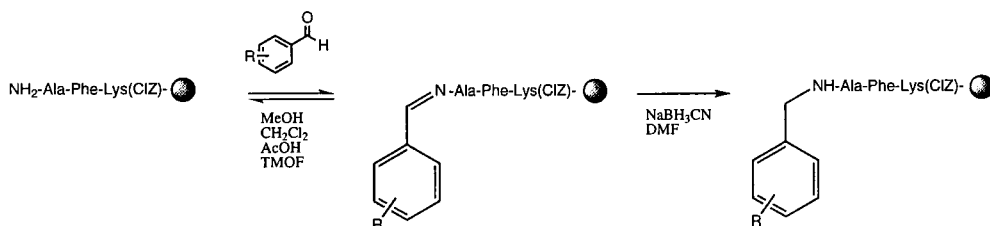


Figure 1. Reaction scheme for the reductive alkylation of peptides using benzaldehydes.  
Table 1. Isokinetic ratios of six benzaldehydes necessary for equimolar incorporation during a competitive reductive alkylation reaction and the actual percent incorporation found. Isokinetic ratios were calculated from the RP-HPLC peak areas of compounds synthesized using a mixture of six different benzaldehydes during the reductive alkylation step and from control mixtures

prepared using the split-resin technique.

<i>Benzaldehyde derivative</i>	<i>Isokinetic Ratio</i>	<i>Percent Incorporation</i>
4-fluorobenzaldehyde	1.000	100%
3-hydroxybenzaldehyde	0.557	83%
3-cyanobenzaldehyde	0.556	110%
2-chloro-5-nitrobenzaldehyde	1.153	107%
3-bromobenzaldehyde	0.501	112%
4-phenoxybenzaldehyde	1.347	91%

mixture of each benzaldehyde with the 4-fluorobenzaldehyde standard was then reacted with the Ala-Phe- Lys(2ClZ)-mBHA resin, followed by cleavage of the peptide. The RP-HPLC peak areas, normalized using the absorbance of the standard, were used to determine the relative incorporation of the benzaldehydes during the competitive reaction. It should be noted that an inverse relationship exists between the isokinetic ratio and the overall reaction rate for each benzaldehyde, and thus their incorporation into the peptide (Table 1).

## Conclusion

In conclusion, relative incorporation of reagents can be determined using RP-HPLC. Resin mixtures synthesized using isokinetic ratios are comparable to mixtures made by the split-resin method. Calculation of isokinetic ratios using RP-HPLC can be applied to many other reactions.

## Acknowledgments

This work was funded by National Science Foundation Grant No. CHE-9520142 and by Trega Biosciences, Inc. of San Diego, California.

## References

1. Houghten, R.A., Pinilla, C., Blondelle, S.E., Appel, J.R., Dooley, C.T., and Cuervo, J. H., *Nature*, 354(1991)84.
2. Pinilla, C., Appel, J.R., Blanc, P., and Houghten, R.A., *Biotechniques*, 13(1992)901.
3. Ostresh, J.M., Winkle, J.H., Hamashin, V.T., and Houghten, R.A., *Biopolymers*, 34(1994)1681.
4. Houghten, R.A., *Proc. Natl. Acad. Sci. U.S.A.*, 82(1985)5131.

# **Potential cancer vaccine: Anti-idiotypic antibodies developed from antigen binding peptides bind to human breast cancer antigen**

**John Mark Carter, Judy Singleton, Phoebe Strome,  
Cindy Coleman and Vernon Alvarez**

*CYTOGEN Corporation, 201 College Road East, Princeton, NJ 08540-5237, USA*

We have developed phage libraries for displaying large (38- and 45-mer) peptides [1,2]. It has previously been shown that such large peptides can fold into functional domains [3]. Panning with these peptide libraries can thus produce peptides with antibody-like binding activity. We call such molecules Abtide™ peptides.

In this study we panned our phage libraries against a 23-residue peptide derived from the well-characterized human breast cancer mucin antigen known as MUC-1 [4]. This antigen results from aberrant glycosylation of the normal mucin glycoprotein by cancer cells and the subsequent unmasking of the peptide epitope. It has been shown to elicit a functional immune response against experimental mammary adenocarcinoma [5]. We then immunized mice with the MUC-1 peptide (Muc1a) and compared ELISA reactivity of the antigen binding peptides developed via panning and the antigen binding Ab developed via the humoral immune response of the mice.

## **Results and Discussion**

Panning the phage libraries with a MUC-1 synthetic peptide (Muc1a, PDTRPAPGSTAPP-AHGVT SAPDTR) yielded several MUC-1 binding peptides. We found that these Abtide™ peptides bound Muc1a with binding comparable to that of several MAb known to bind to MUC-1, including HMFG1 [6] (data not shown). We selected one of the MUC-1 binding molecules (MP1, GAPAPVWRGNPRWRGPGGFKWPGCGNGPMCNT-FTPARGGSRNNGPGG) for further study, in which MP1 was a substrate for phage panning to develop a series of MP1 binding molecules. The best of these was MPB5 (proprietary sequence). Remarkably, a biotinylated version of MPB5 bound to the HMFG1 MAb with strength similar to that of the original Muc1a peptide antigen (Fig. 1A).

We then used both MP1 and MPB5 as experimental vaccines in mice, and studied the responses of the animals to both peptides via ELISA. Serum Ab against MP1 bound strongly to MP1 (Fig. 1B), and serum Ab against MPB5 also bound strongly to that peptide (Fig. 1C). When we tested the sera for the presence of anti-idiotypic Ab, we found that the MP1 antiserum contained reactivity against Muc1a (Fig. 1D), and the MPB5 antisera contained reactivity against MP1 (Fig. 1E), confirming the anti-idiotypic response.

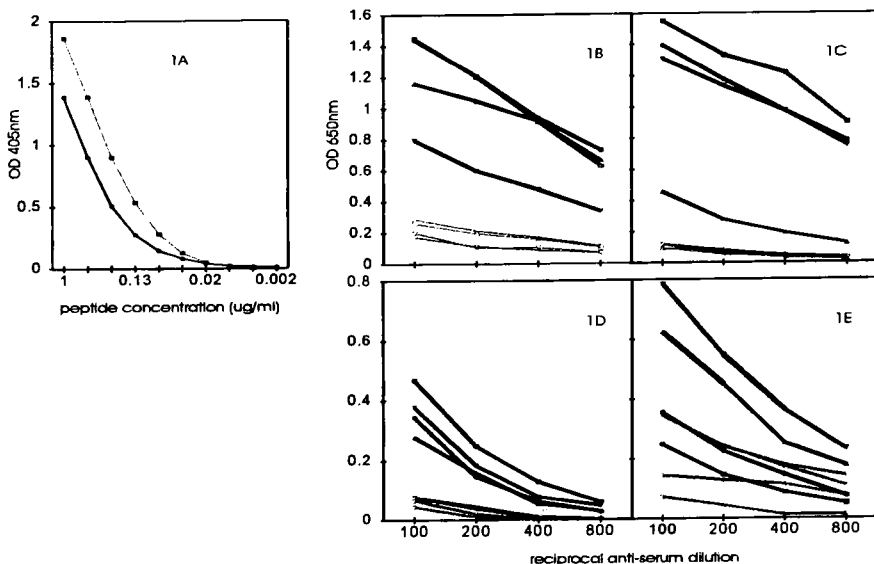


Fig. 1. ELISA data. A) binding of biotinylated MPB5 ● and MUC1 ■ to HMFG1, B) binding of MP1 antisera to MP1, C) binding of MPB5 antisera to MPB5, D) binding of MP1 antisera to Muc1a, E) binding of MPB5 antisera to MP1 (binding of pre-bleed controls shown in gray).

## Conclusion

We have shown that phage panning can produce large Ab-like peptides (called Abtide™ peptides) that are capable of binding small antigens. Through subsequent panning, these peptides, in turn, can be used to generate new molecules that bear the image of the original antigen. This process is analogous and equivalent to the generation of anti-idiotypic Ab molecules bearing the image of an antigen via *in vivo* immunogenicity.

## References

1. McConnell, S.J., Uveges, A.V., Fowlkes, D.M. and Spinella, D.G., *Mol. Diversity*, 1 (1995) 165.
2. Cramer, R. and Suter, M., *Gene*, 137 (1993) 69.
3. Davidson, A.R. and Sauer, R.T., *Proc. Nat. Acad. Sci., USA*, 91 (1994) 2146.
4. Taylor-Papadimitriou, J., Gendler, S.J., In Hilgers, J. and Zotter, S., (Eds.) *Cancer Reviews*, Munksgaard, Copenhagen, 1988, Vol. 11, p. 11.
5. Ding, L., Lalani, E.N., Koganty, R., Wong, T., Samuel, J., Yacyshyn, M.B., Meikle, A., Fung, P.Y.S., Taylor-Papadimitriou, J. and Longenecker, B.M., *Cancer Immunol. Immunother.*, 36 (1993) 9.
6. Taylor-Papadimitriou, J., Peterson, J., Arklie, J., Burchell, J., Ceriani, R.L. and Bodmer, W.F., *Int. J. Cancer*, 28 (1981) 17.

# Studying receptor-ligand interactions using encoded amino acid scanning

Julio A. Camarero, Joanna Pavel and Tom W. Muir

Synthetic Protein Chemistry Laboratory, The Rockefeller University, 1230 York Avenue  
New York, 10021 NY, USA

Investigation into the molecular basis of protein structure and function typically requires modification of the chemical structure of the protein, and subsequent evaluation of the effects of such modification(s). Although this goal can be achieved by synthesis and analysis of individual compounds, this process is time-consuming and costly. Recently, the development of combinatorial techniques has provided a more rapid means of extensively modifying the chemical structure of a parent molecule [1]. Despite the obvious synthetic advantages of these strategies, they are often handicapped by the difficulties associated with the identification of the active compounds resolved during the screening process. In order to facilitate identification of "hit" compounds, several innovative approaches that rely on different encoding-decoding systems have been developed [1,2]. However, they typically provide only a qualitative readout.

In the present work we introduce a new and simple solution-based encoding-decoding system that allows the quantitative analysis of small to medium sized polypeptide libraries (Fig. 1). In order to test this methodology, we have synthesized a small library based on the poly-Pro peptide derived from the exchange factor C3G, the natural ligand for the N-terminal SH3 domain of the oncogene c-Crk [3]. The peptide library has been designed so that the positions XX<sup>5</sup> (P-0) and XX<sup>8</sup> (P-3), involved in key interactions in the complex [4], have been systematically changed (Fig. 2) in order to quantify their importance.

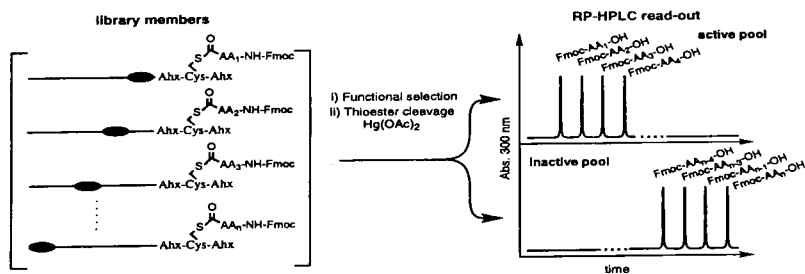


Fig. 1. Description of the "Encoded Amino Acid Scanning" approach. The ellipsoid represents the mutation being scanned through the native sequence (here represented as a black line).

## Results and Discussion

The synthesis of the peptide library (12 members, Fig. 2) was carried out using optimized Boc-solid phase chemistry in conjunction with a modified split-resin approach [2]. The C-terminal Cys residue was protected as Cys(Fm) to allow the orthogonal introduction of the corresponding Fmoc-AA-OH tags as thioesters. Once the synthesis was complete, the

library was deprotected and cleaved using HF. Functional selection was achieved by running the self-encoded library over an c-Crk SH3-N affinity column. The resulting pools, both inactive (washes with PBS) and active (washes with 50% MeCN in H<sub>2</sub>O containing 0.1% TFA), were submitted to Hg(OAc)<sub>2</sub> cleavage and analyzed by RP-HPLC. The results (Fig. 2) indicate that the residue in the position XX<sup>8</sup> (P-3) must be charged and that mutations containing isosteric residues with H-bonding capabilities (Cit, Gln) or hydrophobic residues (Nle) are not tolerated. This indicates the interaction at XX<sup>8</sup> is mainly electrostatic. On the other hand, the results obtained from changing the residue XX<sup>5</sup> (P-0) clearly show that as the hydrophobic surface of the side-chain increases, the binding is tighter.

XX <sup>5</sup>				XX <sup>8</sup>				Tag	Bound to c-Crk SH3-N (%)
P	P	P	A	Leu	P	Lys	K R X C X	Fmoc-Ser-OH	82 (+)
-	-	-	-	-	-	Orn	- - - - -	Fmoc-Asp-OH	39 (±)
-	-	-	-	-	-	Gln	- - - - -	Fmoc-Gly-OH	7 (-)
-	-	-	-	-	-	Arg	- - - - -	Fmoc-Ala-OH	77 (+)
-	-	-	-	-	-	Cit	- - - - -	Fmoc-Aib-OH	3 (-)
-	-	-	-	-	-	Nle	- - - - -	Fmoc-Abu-OH	7 (-)
-	-	-	-	Ala	-	-	- - - - -	Fmoc-Val-OH	41 (±)
-	-	-	-	Abu	-	-	- - - - -	Fmoc-Nva-OH	88 (+)
-	-	-	-	Nva	-	-	- - - - -	Fmoc-Ile-OH	89 (+)
-	-	-	-	Ile	-	-	- - - - -	Fmoc-Leu-OH	89 (+)
-	-	-	-	Nle	-	-	- - - - -	Fmoc-Phe-OH	95 (+)

Fig. 2. Functional activity of the C3G peptide library used in this study. The bound percentage was calculated by UV detection at 300 nm from the chromatographic peaks corresponding to the cleaved Fmoc-AA-OH tags.

## Conclusion

A novel encoding-decoding system has been developed which allows a quantitative read-out of polypeptides in solution. This approach is ideal for studying protein-ligand interactions and will provide a rapid means of determining the relative contributions of individual residues to biological function.

## References

1. Lam, K.S., Lebl, M. and Krchnak, V., *Chem. Rev.*, 97 (1997) 411.
2. Muir, T.W., Dawson, P.E., Fitzgerald, M.C. and Kent, S.B.H., *Chemistry & Biology*, 3 (1996) 817.
3. Knudsen, B.S., Feller, S.M. and Hanafusa, H., *J. Biol. Chem.*, 269 (1994) 32781.
4. Wu, X., Knudsen, B., Meller, S.M., Zheng, J., Sali, A., Cowburn, D., Hanafusa, H. and Kuriyan, J., *Structure*, 3 (1995) 215.

# A double-bond-containing angiotensin and its derivatization into linear vs. branched analogs

Kun-hwa Hsieh<sup>a</sup> and Garland R. Marshall<sup>b</sup>

<sup>a</sup>*Department of Veterinary and Comparative Anatomy, Pharmacology and Physiology, Washington State University, Pullman, WA 99164-6520, USA and* <sup>b</sup>*Center for Molecular Design, Washington University, St. Louis, MO 63110, USA*

The alkene side-chain offers a versatile means of generating structural diversity. In addition to the diol and dibromide via, respectively, KMnO<sub>4</sub> and Br<sub>2</sub> addition [1], the double bond can react with peracid to form epoxide, with ozone to form aldehyde, and with H<sub>2</sub>/Pd to form alkane [2-4]. Because angiotensin (AII) antagonism is induced by replacing 8-Phe with branched residues [5, 6], this study used [Sar<sup>1</sup>, DL-Δ<sup>6</sup>Ahp<sup>8</sup>]AII to generate different inhibitors with diverse activities, and examined the stability of Δ<sup>6</sup>Ahp (6-dehydro-2-amino-heptanoic acid) double bond during peptide synthesis.

## Results and Discussion

Synthesis of DL-Δ<sup>6</sup>Ahp, Boc-DL-Δ<sup>6</sup>Ahp and Boc-Δ<sup>3</sup>Pro has been reported [3, 4]. The double bonds appeared to be stable to alkaline hydrolysis, and to Boc-deprotection by 85% HCOOH, 4 N HCl/THF, or 25% TFA/CH<sub>2</sub>Cl<sub>2</sub>. We prepared the benzyl ester by refluxing (80°C, 24 h) DL-Δ<sup>6</sup>Ahp, Bz-ol, and TsOH in benzene. The tosylate salt was separated on silica gel (2 x 50 cm, CHCl<sub>3</sub>-CH<sub>3</sub>OH elution), and acidified (HCl/dioxane) to yield DL-Δ<sup>6</sup>Ahp-OBzl·HCl (mp 92.5-93.5°C, 61% yield), which gave the appropriate C, H, N analysis and the characteristic CH<sub>2</sub>=CH- bands in NMR (Table 1).

Cleavage of DL-Δ<sup>6</sup>Ahp-OBzl·HCl by HF (°C, 1 h), CF<sub>3</sub>SO<sub>2</sub>H/TFA-CH<sub>2</sub>Cl<sub>2</sub> (°C, 1 h), HBr/TFA, (rt, 2 h), BBr<sub>3</sub>/CH<sub>2</sub>Cl<sub>2</sub> (0°C, 1 h) or H<sub>2</sub>/Pd-C (rt, 15 min), followed by amino acid analyses, allowed a rapid assessment of the stability of the double bond. For example, DL-Δ<sup>6</sup>Ahp was eluted from the short column at 14 min, and its reduction by H<sub>2</sub>/Pd led to a different product (18.5 min). As <sup>1</sup>H NMR of the reduced product showed a methyl, but no benzyl group, DL-Δ<sup>6</sup>Ahp appeared to be rapidly reduced to the linear Ahp (2-amino-heptanoic acid). Similarly, HBr/TFA and BBr<sub>3</sub> generated multiple products with different elution times, and CF<sub>3</sub>SO<sub>2</sub>H generated two products beside a major band (13.5 min).

Although HF cleavage of DL-Δ<sup>6</sup>Ahp-OBzl gave an amino acid eluted at 13.9 min, further studies indicated HF addition to the double bond. In these studies, [Boc-Sar<sup>1</sup>, des-Phe<sup>8</sup>]AII and DL-Δ<sup>6</sup>Ahp-OBzl·HCl in DMF were coupled by DCC/HOBt (60°C, overnight). The resulting [Boc-Sar<sup>1</sup>, DL-Δ<sup>6</sup>Ahp<sup>8</sup>-OBzl]AII was partially purified (CM 52 ion-change), treated with HF (0°C, 1 h), and separated by countercurrent distribution (CCD in 8:1:2:9 of 1-butanol:pyridine:AcOH:water) into two fractions. Both fractions gave the correct amino acid analyses except for Δ<sup>6</sup>Ahp, which was decomposed during acid

Table 1.  $\Delta^6$ Ahp-OBzl and its derivatization into HF and formate adducts during synthesis.

Amino acid/Peptide	(FAB-MS)	Spectral characteristics
DL- $\Delta^6$ Ahp-OBzl·HCl		for CH <sub>2</sub> =CH- 116 & 138 ppm ( <sup>13</sup> C NMR); 5.0 & 5.75 ppm ( <sup>1</sup> H NMR)
[Sar <sup>1</sup> , DL- $\Delta^6$ Ahp]AII-HF	(987)	Amino acid analysis of CPY digest did not show $\Delta^6$ Ahp
[Sar <sup>1</sup> , DL- $\Delta^6$ Ahp]AII-HCOOH	(1013)	Amino acid analysis of CPY digest did not show $\Delta^6$ Ahp Tyr <sup>4</sup> , His <sup>6</sup> ring C at 116, 119, 128, 131, 135 ppm, but no C=CH- in <sup>13</sup> C NMR (138 ppm) or in <sup>1</sup> H NMR (5.75 ppm)

hydrolysis (6 N HCl, 120°C, 48 h). FAB-MS (Table 1) indicated no m+1 967 band for [Sar<sup>1</sup>, DL- $\Delta^6$ Ahp<sup>8</sup>]AII. Instead, the lipophilic fraction (K=0.43, 23% yield) appeared to contain a HF adduct, and the polar fraction (K=0.23, 33% yield) a formate adduct. Digestion of the former by carboxypeptidase Y (CPY, 37°C, 48 h) followed by amino acid analysis gave Tyr<sup>4</sup>, Val<sup>3,5</sup>, His<sup>6</sup>, Pro<sup>7</sup>, and a new amino acid eluted ahead of the position for  $\Delta^6$ Ahp. CPY digest of the latter gave a new amino acid with a Gly-like elution time. The absence of  $\Delta^6$ Ahp in HF and HCOOH adducts was verified by peptide reduction (H<sub>2</sub>/Pd, overnight), from whose hydrolysates no Ahp was found.

The HCOOH adduct suggests DMF formylation of  $\Delta^6$ Ahp during coupling. A similar formylation of His/Lys side-chains has been reported, and could be avoided by replacing DMF with N-methyl-2-pyrrolidinone [7]. Because  $\Delta^6$ Ahp reacted with HF and other cleavage agents, alternative TMAH/*t*-butanol cleavage [7] may be useful to retain the double bond.

In rat assays, [Asn<sup>1</sup>, Ahp<sup>8</sup>]AII with the linear 8-Ahp exhibited considerable (11.5%) pressor activity [6]. In contrast, 17.5-20  $\mu$ g of branch-chained HF and HCOOH adducts blocked the pressor effect of AII for 30 min. In rabbit aorta and rat stomach assays, the HF adduct was, respectively, 160- and 10-fold more inhibitory than the HCOOH adduct.

## References

1. Shriner, R.L., Fuson, R.C. and Curtin, D.Y., *The Systematic Identification of Organic Compounds*. Wiley, New York, 1965.
2. Stotter, P.L. and Eppner, J.B., *Tetrahedron Lett.*, 26(1973)2417.
3. Karwoski, G., Galione, M. and Starcher, B., *Biopolymers*, 17(1978)1119.
4. Felix, A.M., Wang, C.T., Liebman, A.A., Delaney, C.M., Mowles, T., Burghardt, B.A., Charnecki, A.M. and Meienhofer, J., *Int. J. Peptide Protein Res.*, 10(1977)299.
5. Bumpus, M. and Khosla, M.C., In Genest, J., Koiw, E. and Kuchel, O. (Eds.), *Hypertension: Physiology and treatment*, McGraw-Hill, New York, 1977, p. 183.
6. Hsieh, K.H., Jorgensen, E.C. and Lee T.C., *J. Med. Chem.*, 22(1979)1038.
7. Hsieh, K.H., DeMaine, M.M. and Gurusidaiah, S., *Int. J. Peptide Protein Res.*, 48(1996)292.

# Synthesis and application of tyrosine kinase substrate libraries

Song Zheng,<sup>a</sup> Richard Cummings,<sup>a</sup> Rose Cubbon,<sup>b</sup> Young-Whan Park,<sup>a</sup>  
Patricia Cameron,<sup>a</sup> Patrick Griffin,<sup>a</sup> and Jeffrey Hermes<sup>b</sup>

<sup>a</sup>Dept. of Molecular Design & Diversity, <sup>b</sup>Dept. of Autoimmune Disease Research, Merck & Co, Inc., P.O. Box 2000, Rahway, NJ 07065-0900, USA

Kinase assays often utilize peptide substrates and development of maximally sensitive assays requires substrate optimization. Previously this has been carried out in a variety of ways including individual peptide synthesis [1] and peptide library approaches such as on-bead screening [2], solution phase reactions [3], or phage display [4]. In this paper, we present a new method which utilizes the power of the combinatorial approach while allowing identification of the optimal residues through standard enzymatic assays.

## Results And Discussion

Our target for substrate optimization was the T-cell specific tyrosine kinase ZAP-70 [5]. Starting from the known tyrosine kinase substrate HS1<sub>386-402</sub> [6] a series of biotinylated HS1 derivatives were synthesized and analyzed with ZAP-70 in a <sup>33</sup>P-based scintillation proximity assay (SPA) in order to find the shortest substrate that gave an acceptable S/N ratio. The HS1<sub>394-402</sub> derivative, ((LCB)EGDYEEVLE(NH<sub>2</sub>)) (LCB = aminohexanoyl biotin), was found to be optimal and was selected as a basis for library construction.

The first library varied the Y<sub>+1-3</sub> positions of the substrate (EGDYXXXLE). Construction up to the Y<sub>+3</sub> residue was carried out on an ABI 430A peptide synthesizer using FastMoc™ chemistry. After that, syntheses were performed manually using the same reagents and the 'split and recombine' library strategy [7]. Ten amino acids were chosen for the library in order to maximize structural diversity and binding characteristics while minimizing the number of individual amino acids: Nle, Phe, Trp, Val, Pro, His, Arg, Gln, Glu, Lys, and Ser. After the first round of library synthesis, one third of the individual resins were removed and the remaining HS1<sub>394-402</sub> sequence was coupled to them (10 samples). The remaining resin was mixed, redistributed, and the next round carried out. The resulting materials were split with the parent sequence being coupled to half of the material (another 10 samples) and the remaining material recombined and treated as before. The resulting library consisted of thirty samples: ten with single peptides varying at Y<sub>+3</sub> (1 peptide/well), ten with mixtures at Y<sub>+3</sub> and defined residues at Y<sub>+2</sub> (10 peptides/well), and ten with mixtures at Y<sub>+2,+3</sub> and defined residues at Y<sub>+1</sub> (100 peptides/well). A similar library was constructed for the Y<sub>-1-3</sub> positions.

The libraries were analyzed with ZAP-70 and the results of the Y<sub>+1-3</sub> library are shown below (Fig. 1). Hydrophobic residues were preferred at all positions, particularly at Y<sub>+3</sub>. Interestingly, Glu was also a good residue at Y<sub>+1,+2</sub> suggesting that the parent sequence (EEV) was close to an optimal substrate. Consistent with this is the decreasing overall

activity of the more complex mixtures as compared to those that were less complex (more parent-like). Proline is not acceptable at  $Y_{+1}$ , an interesting result as it is well tolerated by Syk, a tyrosine kinase with  $\approx 90\%$  identity at the active site (data not shown). The second library also suggested that the parent EGDY sequence was close to an optimal substrate with the derived sequence (EREY) being similar to it.

Results from the first library suggested good substrates would be of the type  $-Y(E,W)(E,W)W-$  and a series of peptides based on this motif were tested (Table 1). Because all instances these were better substrates than the parent, this approach may be a viable method for identifying optimal substrates in a timely and efficient manner.

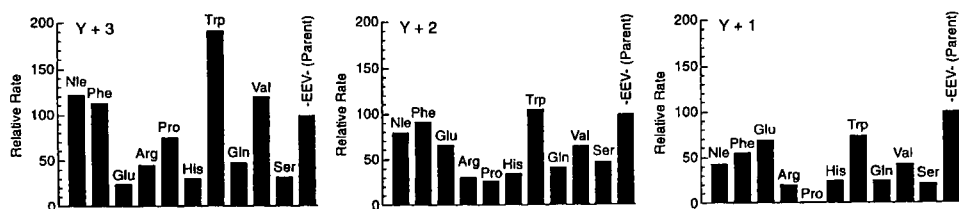


Fig. 1. Relative turnover rates for the  $Y_{+1-+3}$  library compared to the  $HSI_{394-402}$  substrate

Table 1. Results for library derived substrates

Substrate:	(LCB)EGD(YXXX)LE(NH <sub>2</sub> )	Relative Rate ( $k_{cat}/K_m$ )
-YEEV-	(Parent)	100
-YEEW-		190
-YEWW-		191
-YWEW-		177
-YWWW-		218

## References

1. Cheng, H.C., Matsuura, I., and Wang, J.H., *Mol. Cell. Biochem.*, 127/128 (1993) 103.
2. Wu, J.Z., Ma, Q.Y.N., and Lam, K.S., *Biochemistry*, 33 (1994) 14825.
3. Songyang, Z. et al, *Nature*, 373 (1995) 536.
4. Schmitz, R., Baumann, G., and Gram, H., *J. Mol. Biol.*, 260 (1996) 664.
5. Chan, A.C., Desai, D.M., and Weiss, A., *Ann. Rev. Immun.*, 12 (1994) 555.
6. Brunati, A.M., Donella-Deana, A., Ruzzene, M., Marin, O. and Pinna, L.A., *FEBS Lett.*, 367 (1995) 149.
7. Furka, A., Sebestyen, F., Asgedom, M., and Dibo, G., *Abstr. 14th Int. Congr. Biochem.*, Prague, Czechoslovakia, 5 (1988) 47.

# Encoding schemes for application with polyethylene glycol-polystyrene graft (PEG-PS) supports in solid-phase peptide and small molecule synthesis

Steven A. Kates,<sup>a</sup> Wade Hines,<sup>a</sup> Michael A. Kelley,<sup>a</sup> Paul Lynch,<sup>a</sup>  
Fernando Albericio<sup>b</sup> and George Barany<sup>c</sup>

<sup>a</sup>*PerSeptive Biosystems, Inc., 500 Old Connecticut Path, Framingham, MA 01701, USA;*

<sup>b</sup>*Department of Organic Chemistry, University of Barcelona, 08028-Barcelona, Spain;*

<sup>c</sup>*Department of Chemistry, University of Minnesota, Minneapolis, MN 55455, USA.*

Polyethylene glycol-polystyrene (PEG-PS) graft supports have been shown to be superior to conventional PS supports for the assembly of complex peptides, including structures that are cyclic, hydrophobic, or contain post-translational modifications. Both Fmoc/*t*Bu and Boc/Bzl-based strategies are compatible. Previously, different PS resins extended with PEG derivatives of various molecular weights, in conjunction with branch attachment points in the formulations, were incorporated to develop supports with increased loadings (0.35-0.45 mmol/g). These supports are compatible with a variety of organic transformations and have been applied successfully to the generation of small molecule combinatorial libraries.

The mix and split technique for the construction of combinatorial libraries produces a large collection of targets in which a single resin bead contains a single component. Unfortunately, the quantity of material prepared on a bead is too small for elucidating the structure of complex molecules. Encoded libraries represent an approach to analyzing mixtures of compounds by incorporating chemical tags associated with individual members that can specify their identities [1].

This communication focuses on further improvements in small molecule combinatorial synthesis by use of PEG-PS as an adjunct to the generation of encoded libraries. Different parent PS resins are extended with PEG derivatives and a branch point for encoding with sequences of amino acids [2]. Matrix-assisted laser desorption/ionization time-of-flight (MALDI-TOF) mass spectrometry was used as an analytical technique to characterize library members [3].

## Results and Discussion

The penultimate amino group and the side-chain amino group of the ornithine branch in PEG-PS provide attachment for two orthogonal linkers (Fig. 1) [4]. In order to examine the utility of the PEG-PS concept with an encoded strategy, Fmoc-amino acids in conjunction with the PAL handle were chosen as the tagging method since the amino acid sequences could be easily determined *via* MALDI-TOF mass spectrometry [5].

Amino acid derivatives containing basic side-chains (His, Arg, Lys) are known to ionize efficiently and provide excellent sensitivity for MALDI-TOF analysis. The following three sequences, H-LAGVXX-NH<sub>2</sub> where X = H, R, and K, were prepared on PAL-PEG-PS with Trt, Pbf, and Boc protection, respectively. A single bead was placed on



# Use of phage display and cellulose-bound peptide libraries for the identification of urea herbicide binding peptides

Ulrich Hoffmüller,<sup>a</sup> Christine Rottenberger,<sup>b</sup> Günter Wellnhofer,<sup>b</sup> Leodevico L. Ilag,<sup>b</sup> Jürgen Spindler<sup>c</sup> and Jens Schneider-Mergener<sup>a</sup>

<sup>a</sup>Institut für Medizinische Immunologie, Universitätsklinikum Charité, Humboldt-Universität zu Berlin, Schumannstr. 20-21, 10098 Berlin, Germany; <sup>b</sup>MorphoSys GmbH, Frankfurter Ring 193a, 80807 München, Germany; <sup>c</sup>Institut für Organische Chemie und Strukturanalytik, Universität Potsdam, Am Neuen Palais 10, 14415 Potsdam

Our aim was to develop peptides and peptide-mimetics that bind specifically to urea herbicides for use in biosensors. These peptides could be superior to presently used antibodies because of their higher stability, lower molecular weight and less expensive production. Since peptide hapten interactions have so far not been much studied, an investigation in this area would be of great scientific interest. To identify peptides or derivatives binding to urea herbicides, two different approaches have been compared: (I) screening of a phage display library and (II) testing chemical peptide libraries synthesized on cellulose membrane supports.

## Results and Discussion

The phage library comprises cyclic peptides of the format Cys(B)<sub>n</sub>Cys (n=6 to 16, B=19 amino acids, Cys omitted). Oligonucleotides which code for cyclic peptides were synthesized using the trinucleotide-method [1]. Three rounds of panning against immobilized N-2-aminobenzyl-N'-4-chlorophenyl urea (Fig. 1) were performed yielding an enrichment of binding phages by a factor of 920. Subsequently, several phage clones were sequenced and 20 different peptide sequences were deduced (Table 1). The cyclic peptides (6 to 12 amino acids) were rich in phenylalanine and tyrosine and some displayed sequence homologies. Nevertheless, BIAcore measurements indicated that these peptides bind only with low affinity or even nonspecifically.

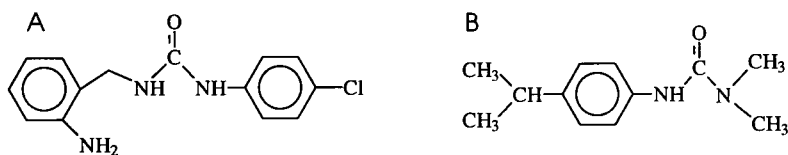


Fig. 1. Urea herbicides. (A) N-2-aminobenzyl-N'-4-chlorophenyl urea and (B) isotoproturon.

Table 1. Left: Sequences of the herbicide binding peptides. The flanking cysteine residues responsible for cyclization are not shown. Right: Homologies between sequences of identified peptides.

peptide sequences		homologies
N V S Q I T	Y S V I E Y F R	
Y G N R H D	D L G T R E N Y	F F Y A V Q F
N I P M P T Y	F Y N Y K G S M	
T T H F I Q L	I G L K S F G L	F I N A V G F
Y L I D S D F	T Q T H H F S D E	
F F Y A V Q F	V W S Y Y Y A P S (2x)	
F I N A V G F	F G F I P F N S I Y	F G F I P F N S I Y
H F T Y R F K (2x)	F T H I Q H I H I Y	.   .
Y A M L G D A D	D L G P I F D F W L	F T H I Q H I H I Y
P P D L V I R H	G L M V R P T K E S L N	

Alternatively, we tried to delineate binding peptides from the sequence of herbicide binding proteins using cellulose bound peptide scans [2]. The binding pocket of urea herbicides in plants is located on the D1 protein of photosystem II. Therefore, a peptide scan of the D1 protein was incubated with  $^{14}\text{C}$ -labelled isoproturon (Fig. 2). Several binding regions were detected which differ from the putative binding regions deduced from resistance mutations in the D1 protein. Substitutional analyses of selected peptides in which each position is substituted by all 20 amino acids indicated that the binding of these peptides is predominantly based on the hydrophobic nature of their residues.

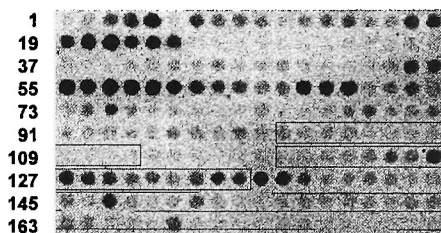


Fig. 2. Autoradiography of the peptide scan (15mer peptides, shifted by 2 residues, scanning the amino acid sequence of the D1-protein) incubated with  $^{14}\text{C}$ -labelled isoproturon. The framed regions contain positions of urea herbicide resistance mutations described in the literature.

## Acknowledgments

This work was supported by the DFG grant INK 16A1-1.

## References

- Virnekäs, B., Ge, L., Plückthun, A., Schneider, K. C., Wellenhofer, G. and Moroney, S. E., *Nucleic Acids Res.*, 22 (1994) 5600.
- Kramer, A. and Schneider-Mergener, J., *Meth. Mol. Biol.*, 87 (1997) in press.

# High affinity binding peptides for phosphatase

**Stefan Vetter and Holger Schmid**

*Department of Biochemistry, Swiss Federal Institute of Technology Zürich, ETH  
8092 Zürich, Switzerland*

Synthetic peptide libraries are useful tools in searching for biologically active peptides or for probing large numbers of diverse peptides towards a potential receptor protein. We were interested in finding a short (5-7) amino acid sequence that binds specifically and with high affinity to alkaline phosphatase (E.C.3.1.3.1). It was important to us that the peptide does not interfere with the enzyme's catalytic activity. Since it is difficult to screen libraries containing more than a million members we used a repetitive approach. A first tetrapeptide library ( $20^4$  members) allowed the identification of a lead motif after screening for phosphatase binding peptides. This consensus like motif was subsequently used to design a restricted heptapeptide library. The central position of these heptapeptides was restricted to certain amino acids, which were frequently found in the tetrapeptides identified in the first library. All 20 natural amino acids were incorporated into the outer positions. Peptide sequences showing affinity for alkaline phosphatase were resynthesized and further characterized. The stepwise screening and design of two libraries allowed the screening of virtually  $20^7$  heptapeptides.

## Results and Discussion

160,000 bead-bound tetrapeptides were assayed for phosphatase binding activity. Approximately 0.1% of the beads were recognized as positive. Microsequencing of the peptides was possible without problems under standard conditions. The obtained sequences shared certain characteristics: all peptides contained at least one cysteine accompanied by two or more basic amino acids, acidic or hydrophobic amino acids were not found (Table 1). Alignment of the sequences suggested the structure of the second, restricted heptapeptide library. The general architecture was as follows: a cysteine in the central position 4, positions 2, 3, 5 and 6 restricted to Arg, Lys, His, Ser and Trp, the outer positions 1 and 7 not restricted. It was found that the phosphatase binding assay had to be performed in the presence of specific competitors in order to decrease the number of positives and to ensure that exclusively peptides with high affinity were identified. The obtained heptapeptide sequences are relatively homogeneous (Table 1) and the hexapeptide K-K-K-C-K-K was found to be a consensus motif.

Three peptides were resynthesized and labeled with the fluorescent dansyl group. Binding affinities to phosphatase were measured for these peptides by fluorescence titration (Table 2). The observed affinities are comparable to affinities typical for antibody-antigen interactions.

*Table 1. Sequences of tetra- and heptapeptides found to bind the enzyme alkaline phosphatase by screening bead-based peptide libraries.*

Tetrapeptides	Heptapeptides
R H R C	P S K C K K P
C R R R	G K K C H K K
R C C K	K K K C K W K
R R C S	K K K C R S K
R R W C	K K K C K S K
R K C K	K K K C R K R
K C W R	K K K C R K I
R C R R	K K K C K K Y
W R R C	K K K C K K F
R R C R	
R C R W	
R C K K	
R R C H	
C S R C	
R C R H	

*Table 2. Binding constants of dansylated peptides towards phosphatase in solution.*

Peptide	$K_d$ [nM]
Dns-Abu-Arg-Arg-Cys-Gly-OH	$33 \pm 5$
Dns-Abu-Arg-Cys-Arg-Gly-OH	$36 \pm 6$
Dns-Abu-Lys-Lys-Lys-Cys-Lys-Lys-Gly-OH	$9 \pm 2$

We found a sequence of six amino acids that binds specifically and with high affinity to the enzyme alkaline phosphatase. Currently we are exploring the properties of a protein containing the phosphatase binding sequence K-K-K-C-K-K inserted into the central region of the protein as well as fused to the N-terminus. We investigate the possibility of detecting the tagged protein in a cell lysate electroblotted onto a nitrocellulose membrane using alkaline phosphatase.

## **Session II**

# ***De Novo* Design of Peptides and Proteins**



# Five axioms for protein engineering: Keys for understanding protein structure/function?

Dan W. Urry

Laboratory of Molecular Biophysics, The University of Alabama at Birmingham, VH300,  
Birmingham, AL 35294-0019, USA

Elastic protein-based polymers have been successfully used to develop a set of five experimentally based axioms for protein engineering and protein function [1]. The parent protein-based polymer, poly(GVGVP) from mammalian elastins and many isomorphous analogues thereof, exhibit hydrophobic folding and assembly transitions, referred to as inverse temperature transitions. When properly designed, they are capable of performing all of the classes of energy conversions represented by the metabolic processes of living organisms[2,3]. These protein-catalyzed free energy transductions involve the set of six free energies, the intensive variables of which are: mechanical force, temperature, pressure, chemical potential, electrochemical potential and electromagnetic radiation. Of the fifteen pairwise free energy conversions possible between the six free energies, eight have been experimentally demonstrated using engineered protein-based polymers. A sixteenth free energy transduction is chemo-chemical transduction, e.g., enzyme catalysis, the decrease in chemical energy of reactants and the increase in chemical energy of products.

## Results and Discussion

*Characterization of the Transition and a  $T_t$ -based hydrophobicity scale.* The hydrophobic folding and assembly transition is characterized by the temperature,  $T_t$ , for the onset of the transition as the temperature is raised from below to above the transition. When each of the amino acid residues are substituted in the model system, poly[ $f_v$ (GVGVP),  $f_x$ (GXGVP)] where  $f_v$  and  $f_x$  are mole fractions with  $f_v + f_x = 1$  and  $X$  is any of the naturally occurring amino acid residues or chemical modification thereof, the value of  $T_t$  is plotted vs  $f_x$  and the extrapolated values are compared at  $f_x = 1$  to provide the first hydrophobicity scale based directly on the hydrophobic folding and assembly transition [3,4]. This experimental data is the basis of **Axiom 1**. Simply raising the temperature from below to above  $T_t$  drives hydrophobic folding and assembly with the performance of mechanical work; this is the basis for **Axiom 2** for thermo-mechanical transduction.

*Dependencies of  $T_t$  and the  $\Delta T_t$ -mechanism of energy conversion.* Virtually every interaction or modification of the polymer changes the temperature,  $T_t$ , of the inverse temperature transition [1,3]. Any interaction or modification that alters the value of  $T_t$  can be used to lower the value of  $T_t$  from above to below the operating temperature to drive

hydrophobic folding and assembly with the performance of mechanical work. This is the basis for *Axiom 3* for baro-, chemo-, electro- and photo-mechanical transduction.

*Coupling of different functional groups in the same hydrophobic folding domain.* When the polymer is designed such that two different functional groups of the same hydrophobic domain are in their more-polar states and  $T_t$  is just above the operating temperature, then the conversion of either one to their more-hydrophobic state, such as

The  $\Delta T_t$  Hydrophobic Paradigm for Protein Folding and Function  
(Demonstrated and Putative Energy Conversions  
Using Molecular Machines of the  $T_t$ -type)

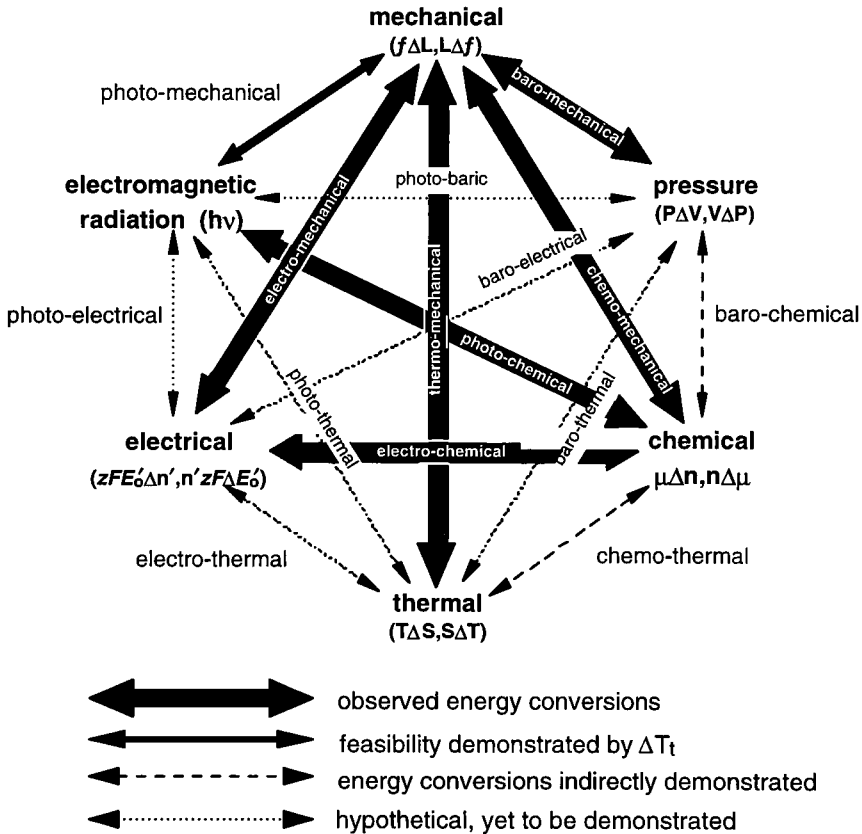


Figure 1

protonation of a carboxylate functional group or reduction of an oxidized redox function lowers  $T_t$  and changes the redox potential or the pKa, respectively, of the second coupled moiety [5]. This is the basis for *Axiom 4*, which includes ten additional pairwise energy conversions as indicated in Figure 1 and in the listing of Axioms in Table 1. In the case of the sixteenth energy conversion, chemo-chemical transduction, one type of functional group could be carboxylates and the other chemical function could be a phosphate. Protonation of the carboxylates would lower  $T_t$  and raise the free energy of the phosphate as the proton gradient of the mitochondrion may be used to drive phosphorylation.

*Table 1. Five Axioms for Protein Engineering of Protein-based Polymers Capable of Inverse Temperature Transitions of Hydrophobic Folding and Assembly.*

---

**AXIOM 1:** The manner in which a guest amino acid residue, or chemical modification thereof, alters the temperature,  $T_t$ , of a hydrophobic folding and/or assembly transition is a functional measure of its hydrophobicity. A decrease in  $T_t$  represents an increase in hydrophobicity and an increase in  $T_t$  represents a decrease in hydrophobicity.

**AXIOM 2:** Raising the temperature above  $T_t$  results in hydrophobic folding and assembly and can be used to perform useful mechanical work, e.g., of lifting weights; this is thermo-mechanical transduction.

**AXIOM 3:** At constant temperature, lowering the value of  $T_t$  from above to below an operating temperature, i.e., increasing the hydrophobicity by any of the many variables of Table IV also results in hydrophobic folding and assembly and can be used to perform useful mechanical work of building a structure, e.g., of lifting a weight.

**AXIOM 4:** Any two distinct functional groups responsive to different variables that include i) temperature, ii) pressure, iii) changes in the concentrations of chemicals, iv) changes in the redox state of a biological prosthetic group, and v) light elicited changes in chemical structure, each of which could be used to alter the value of  $T_t$  to perform mechanical work resulting from folding and assembly, can be coupled one to the other by being part of the same hydrophobic folding and assembly domain.

**AXIOM 5:** The above energy conversions can be demonstrated to be more efficient when carried out under the influence of more hydrophobic domains.

---

*Hydrophobic-induced pKa shifts and associated positive cooperativity.* Using the polymers, poly[ $f_V(\text{GVGVP}), f_X(\text{GXGVP})$ ], where X was Asp (D), Glu (E) or Lys (K) and  $f_X$  varied from 1 to 0.06, electrostatic-induced pKa shifts could be clearly delineated from hydrophobic-induced pKa shifts [6-8]. Furthermore, using a series of poly(30 mers) with one E or D per 30 mer and with 0, 2, 3, 4, and 5 Phe (F) residues per 30 mer, a supra-linear relationship was observed between the number of F residues and the  $\Delta\text{pKa}$  associated with an increase in the steepness of the acid-base titration curve [9]. The energy indicated by the

$\Delta pK_a$  was matched by the energy of interaction apparent in the increasing cooperativity. Among other things, these findings demonstrated a greater  $pK_a$  shift on going from 3 to 5 F residues per 30 mer than on going from 0 to 2 F residues per 30 mer. This finding and a similar supra-linearity for mechano-chemical transduction [10] provide the basis for **Axiom 5**: that efficiency of energy conversion increases as the hydrophobicity of the functional domain increases. The complete list of experimentally-derived Axioms is given in Table 1.

*Physical basis for the energy conversions.* The physical basis for the  $\Delta T_c$ -mechanism of energy conversion is competition for hydration between hydrophobic (apolar) groups and polar (e.g., charged) groups, termed an apolar-polar repulsive free energy of hydration. The mechanism was proposed to understand an observed stretch-induced increase in the  $pK_a$  of glutamic acid residues in cross-linked poly[ $f_V(\text{GVGIP}), f_E(\text{GEGIP})$ ] [11]. The competition was then found using differential scanning calorimetry in the decrease of the endothermic heat of the inverse temperature transition due to the formation of  $\text{COO}^-$  in poly[ $f_V(\text{GVGVP}), f_E(\text{GEGVP})$ ] [12]. Most definitively, microwave dielectric relaxation demonstrated the destruction of water of hydrophobic hydration,  $N_{hh}$ , on ionization of carboxyls in poly(30 mers) with one Glu and none or two F residues per 30 mer [13]. pH dependence of  $N_{hh}$  can be used to calculate both the  $pK_a$  shift and the associated positive co-operativity (S.Q. Peng and D.W. Urry, in preparation) [14].

## References

1. Urry, D.W., J. Phys. Chem., (1997) in press.
2. Urry, D.W., Prog. Biophys. Molec. Biol., 57 (1992) 23.
3. Urry, D.W., Angew. Chem. Int. Ed. Engl., 32 (1993) 819.
4. Urry, D.W., Gowda, D.C., Parker, T.M., Biopolymers, 32 (1992) 1243.
5. Urry, D.W., Hayes, L.C., Gowda, D.C., Biochem. Biophys. Res. Commun., 210 (1995) 1031.
6. Urry, D.W., Peng, S.-Q., Parker, T.M., J. Am. Chem. Soc., 115 (1993) 7509.
7. Urry, D.W., Peng, S.-Q., Parker, T.M., Angew. Chem. Int. Ed. Engl., 32 (1993) 1440.
8. Urry, D.W., Peng, S.-Q., Gowda, D.C., Chem. Phys. Letters, 225 (1994) 97.
9. Urry, D.W., Gowda, D.C., Peng, S.-Q., Chem. Phys. Letters, 239 (1995) 67.
10. Urry, D.W., Peng, S.-Q., J. Am. Chem. Soc., (1995) 8478.
11. Urry, D.W., Peng, S.-Q., Hayes, L.C., Biopolymers, 30 (1990) 215.
12. Urry, D.W., Luan, C.-H., Harris, R.D., Polym. Preprints, Div. Polym. Chem., 31 (1990) 188.
13. Urry, D.W., Peng, S.-Q., Xu, J., J. Am. Chem. Soc., 119 (1997) 1161.
14. Peng, S.-Q., Ph.D. Thesis, 1997, University of Alabama at Birmingham.

# Novel collagen-mimetic structures

**Elizabeth A. Jefferson and Murray Goodman**

*Department of Chemistry and Biochemistry, University of California, San Diego  
La Jolla, CA, 92093, USA*

The synthesis and biophysical study of collagen mimetics is important for the development of novel biomaterials. Collagen proteins contain large triple-helical domains composed of Gly-X-Y repeats, where X and Y are often proline and hydroxyproline, respectively. We recently introduced KTA-(Gly-OH)<sub>3</sub> (KTA represents the Kemp triacid, Fig. 1) as a template for the synthesis of triple-helical structures with relatively short chain lengths [1]. The template stabilizes triple-helical structures compared to analogous triple-helical structures formed from single-chains through intermolecular association. We also discovered that peptoid residue Nleu (N-isobutylglycine) can serve as a proline substitute in structures with (Gly-Pro-Nleu)<sub>n</sub> [2,3] and (Gly-Nleu-Pro)<sub>n</sub> [4] repeats. According to biophysical studies based on CD, optical rotation, and NMR, these compounds form triple-helical structures when chain lengths are above a critical length. These peptoid-containing structures are attractive because of their anticipated resistance to proteolytic enzymes.

We have now synthesized structures containing an achiral trimer repeat, Gly-Nleu-Nleu (Fig. 1). The achiral unit is of interest as a means of simplifying the primary structure of collagen-mimetics. The following acetyl-terminated and template-assembled structures were examined: Ac-(Gly-Pro-Hyp)<sub>2</sub>-(Gly-Nleu-Nleu)<sub>2</sub>-(Gly-Pro-Hyp)<sub>2</sub>-NH<sub>2</sub> and KTA-[Gly-(Gly-Pro-Hyp)<sub>2</sub>-(Gly-Nleu-Nleu)<sub>2</sub>-(Gly-Pro-Hyp)<sub>2</sub>-NH<sub>2</sub>]<sub>3</sub>.

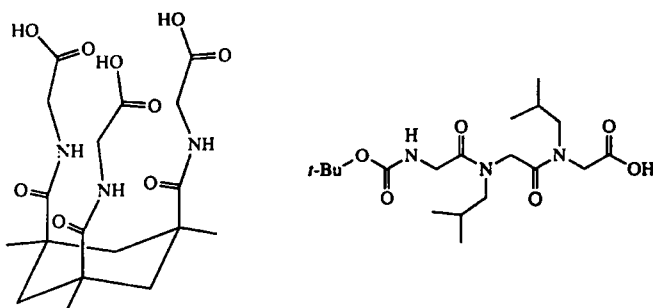


*Fig. 1. (left) KTA-based template. (right) Achiral building block, Boc-Gly-Nleu-Nleu-OH.*

## Results and Discussion

The single chain compound, Ac-(Gly-Pro-Hyp)<sub>2</sub>-(Gly-Nleu-Nleu)<sub>2</sub>-(Gly-Pro-Hyp)<sub>2</sub>-NH<sub>2</sub>, was prepared by standard solid-phase synthesis methods using Boc-Gly-Pro-Hyp(OBzl)-

OH and Boc-Gly-Nleu-Nleu-OH as the building blocks. The template-assembled compound was synthesized by coupling the N-terminus of [Gly-Pro-Hyp(OBzl)]<sub>2</sub>-(Gly-Nleu-Nleu)<sub>2</sub>-[Gly-Pro-Hyp(OBzl)]<sub>2</sub>-Resin to KTA-(Gly-OH)<sub>3</sub> in a manner similar to that described previously [5]. A novel X-ray crystal structure of a calcium complex of the achiral building block, Boc-Gly-Nleu-Nleu-OH, was obtained (Fig. 2) [6].

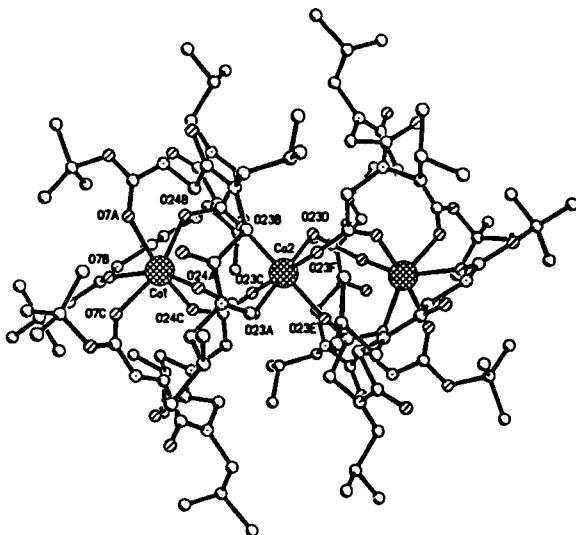


Fig. 2. The  $\text{Ca}^{2+}_3(\text{Boc-Gly-Nleu-Nleu-O}^-)_6$  entity. Calcium ions and oxygen atoms are represented as hatched and crossed circles, respectively.

We investigated the potential triple helicity of the structures using temperature dependent optical rotation measurements (melting curves) as well as CD spectroscopy. For collagen-mimetic structures, cooperative melting curves are indicative of triple-helical structure [2-5]. A cooperative melting curve was not observed for Ac-(Gly-Pro-Hyp)<sub>2</sub>-(Gly-Nleu-Nleu)<sub>2</sub>-(Gly-Pro-Hyp)<sub>2</sub>-NH<sub>2</sub>, while the template-assembled compound exhibited a cooperative melting curve with a thermal melting temperature ( $T_m$ ) of 20 °C in H<sub>2</sub>O (Fig. 3). Since ethylene glycol is known to augment weak triple helices [7], melting temperatures were determined in EG/H<sub>2</sub>O (2:1, v/v) solution, at 0.2 mg/mL.  $T_m$  values of 25 °C and 40 °C were obtained for the single-chain and the template-assembled compound, respectively (data not shown).

Collagen structures typically have CD spectra with a small positive peak near 220 nm, a crossover near 213 nm, and a large negative peak near 197 nm [7]. In H<sub>2</sub>O, the template-assembled compound gives a CD spectrum typical for a triple-helical structure while the

single chain compound does not (Fig. 4). Both compounds give CD spectra typical for triple helical structures in EG/H<sub>2</sub>O (2:1, v/v) solution (data not shown).

The effect of Gly-Nleu-Nleu incorporation on the stability of triple-helical structures is clear from the following comparisons. KTA-[Gly-(Gly-Pro-Hyp)<sub>2</sub>-(Gly-Nleu-Nleu)<sub>2</sub>-(Gly-Pro-Hyp)<sub>2</sub>-NH<sub>2</sub>]<sub>3</sub> melts at 20 °C while KTA-[Gly-(Gly-Pro-Hyp)<sub>6</sub>]<sub>2</sub>-NH<sub>2</sub> melts at 81 °C in H<sub>2</sub>O [5]. Similar in, Ac-(Gly-Pro-Hyp)<sub>2</sub>-(Gly-Nleu-Nleu)<sub>2</sub>-(Gly-Pro-Hyp)<sub>2</sub>-NH<sub>2</sub> melts at 20 °C while Ac-(Gly-Pro-Hyp)<sub>2</sub>-NH<sub>2</sub> melts at 59 °C in EG/H<sub>2</sub>O (2:1, v/v) [5]. Although substitution of Gly-Nleu-Nleu into triple-helical structures containing Gly-Pro-Hyp repeats results in a destabilized triple helix, the substitution can still accommodate triple-helical structures.

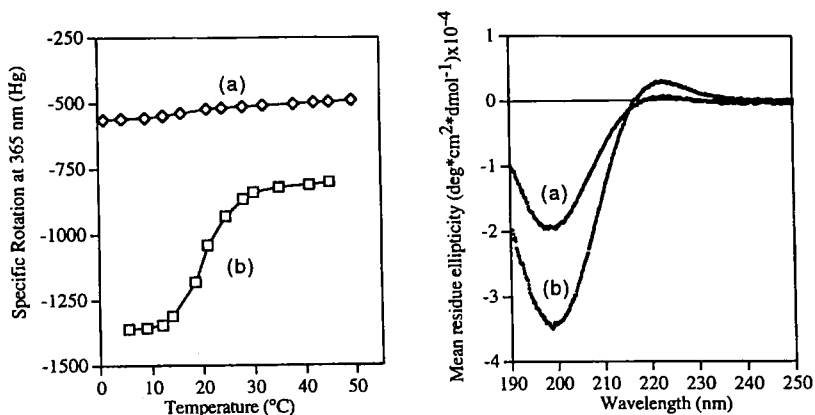


Fig. 3. (left). Melting curves for Ac-(Gly-Pro-Hyp)<sub>2</sub>-(Gly-Nleu-Nleu)<sub>2</sub>-(Gly-Pro-Hyp)<sub>2</sub>-NH<sub>2</sub> (a) and KTA-[Gly-(Gly-Pro-Hyp)<sub>2</sub>-(Gly-Nleu-Nleu)<sub>2</sub>-(Gly-Pro-Hyp)<sub>2</sub>-NH<sub>2</sub>]<sub>3</sub> (b) in H<sub>2</sub>O, at 0.2 mg/mL. Fig. 4 (right). CD spectra for Ac-(Gly-Pro-Hyp)<sub>2</sub>-(Gly-Nleu-Nleu)<sub>2</sub>-(Gly-Pro-Hyp)<sub>2</sub>-NH<sub>2</sub> (a) and KTA-[Gly-(Gly-Pro-Hyp)<sub>2</sub>-(Gly-Nleu-Nleu)<sub>2</sub>-(Gly-Pro-Hyp)<sub>2</sub>-NH<sub>2</sub>]<sub>3</sub> (b) in H<sub>2</sub>O, at 0.2 mg/mL.

## References

1. Goodman, M., Feng, Y., Melacini, G. and Taulane, J. P., J. Am. Chem. Soc., 118 (1996) 5156.
2. Goodman, M., Melacini, G. and Feng, Y., J. Am. Chem. Soc., 118 (1996) 10928.
3. Feng, Y., Melacini, G., Taulane, J. P. and Goodman, M., Biopolymers, 39 (1996) 859.
4. Feng, Y., Melacini, G. and Goodman, M., Biochemistry, (1997), in press.
5. Feng, Y., Melacini, G., Feng, Y., Taulane, J. P. and Goodman, M., J. Am. Chem. Soc., 118 (1996) 10351.
6. Jefferson, E.A., Gantzel, P., Benedetti, E. and Goodman, M., J. Am. Chem. Soc., 119 (1997) 3187.
7. Brown, F. R., III, Di Corato, A., Lorenzi, G. P. and Blout, E. R., J. Mol. Biol., 63 (1972) 85.



The relative hydrophobicity of each substituted amino acid side-chain at positions *a* and *d* was determined by reversed-phase HPLC at pH 7.0. Results of the study show that the relative hydrophobicity of each side chain correlates with the relative order of hydrophobicity previously observed in other model systems [6]. In addition, an excellent correlation ( $r=0.998$ ) of side-chain hydrophobicity at positions *a* and *d* was observed (Fig. 2), indicating that the hydrophobicity of the amino acid side-chains substituted at these positions is model independent under denaturing reversed-phase HPLC conditions.

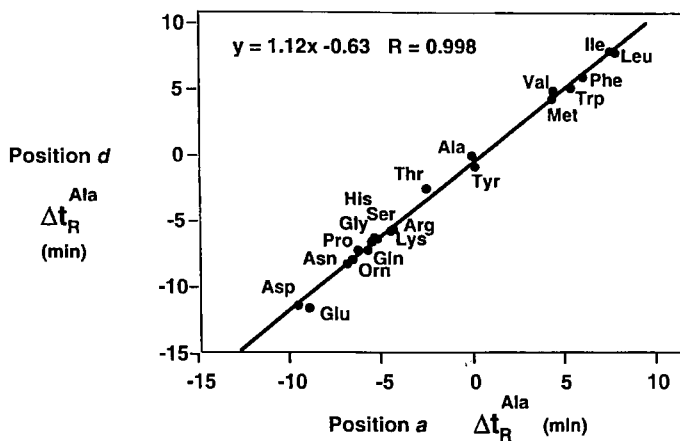


Fig. 2. Correlation of side-chain hydrophobicity at positions *a* and *d*.

The stability of each analog was determined by chemical denaturation using either guanidine hydrochloride or urea. Ellipticity was monitored at 222 nm using circular dichroism spectroscopy at 25 °C. Results of the study showed that, in general, the stability of the position *a* and *d* analogs directly correlated with hydrophobicity of the side-chain, with the exception of Pro, Asn, and Trp (Fig. 3, position *a* data only).

Peptides containing Pro in either the *a* or *d* position were unable to form coiled-coils, presumably due to the helix-breaking nature of Pro. Interestingly, it was observed that the analogs containing Trp in either the *a* or *d* position were less stable than would be predicted by relative hydrophobicity. This is likely due to negative packing effects for the large indole side-chain in a parallel two-stranded  $\alpha$ -helical model. However, it is interesting to note that Trp does in fact occur in natural coiled-coils [1], and has been shown to affect inter-helix spacing in gp41 trimers [7].

We also observed that the position *a* Asn analog was significantly (2 kcal/mol) more stable than its side-chain hydrophobicity would predict, and that it was in fact more stable than the Gln analog at 25 °C. It has been shown that Asn in position *a* of a dimeric coiled-coil forms an inter-helical side-chain-side-chain H-bond [4]. Therefore, it appears this H-bond provides stability in addition to that provided by the hydrophobicity of the Asn side-

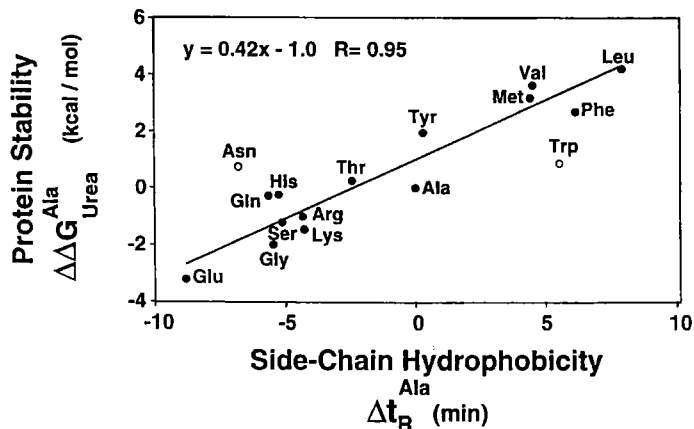


Fig. 3. Comparison of protein stability and hydrophobicity for the position *a* analogs.

chain. On the other hand, data obtained for the position *d* study revealed that the Gln analog is more stable than the Asn analog. Structural studies on GCN4 mutants revealed that the Asn side-chain can form an H-bond at the interface of a dimeric coiled-coil, but Gln cannot [8]. Preliminary molecular modeling suggests that both Asn and Gln side-chains are sterically capable of forming an inter-helical side-chain-side-chain H-bond at position *d*.

These results will be invaluable not only in *de novo* design applications but will contribute to our understanding of whether predicted coiled-coil sequences have enough stability to truly form coiled-coils *in vivo*.

### Acknowledgments

The authors thank Kim Oikawa and Lorne Burke for excellent technical assistance.

### References

1. Titus, M.A., *Curr. Opin. Cell Biol.*, 5 (1993) 77.
2. Hu, J.C. and Sauer, R.T., *Nucl. Acids Mol. Biol.*, 6 (1991) 82.
3. Littlewood, T.D. and Gerard, E.I., *Protein Profile*, 1 (1994) 642.
4. Hodges, R.S., *Biochem. Cell Biol.*, 74 (1996) 133.
5. O'Shea, E.K., Klemm, J.D., Kim, P.S. and Alber, T., *Science*, 254 (1991) 539.
6. Monera, O.D., Sereda, T.J., Zhou, N.E., Kay, C.M. and Hodges, R.S., *J. Peptide Sci.*, 1 (1995) 319.
7. Weissenhorn, W., Dessen, A., Harrison, S.C., Skehel, J.J. and Wiley, D.C., *Nature*, 387 (1997) 426.
8. Gonzales, L. Jr., Woolfson, D.N., and Alber, T., *Nature Struct. Biol.*, 13 (1996) 1011.

# Towards full mimics of antibodies: A 37-aa miniprotein with two independent activities

**Antonello Pessi,<sup>a</sup> Elisabetta Bianchi,<sup>a</sup> Jaques Neyton<sup>b</sup>  
Eugenia Drakopolou<sup>c</sup> and Claudio Vita<sup>c</sup>**

<sup>a</sup>*Istituto di Ricerche di Biologia Molecolare P. Angeletti (IRBM), 00040 Pomezia (Rome), Italy*

<sup>b</sup>*Ecole Normale Supérieure, Laboratoire de Neurobiologie, 75005 Paris, France and* <sup>c</sup>*CEA, Département d'Ingénierie et d'Etudes des Protéines, C.E. Saclay, F91191 Gif-Sur-Yvette, France*

Immunoglobulins are the prototype of the ideal designer protein, being entailed with two independent units: a selectable binding domain and an effector domain. Our attempts to reproduce these features in a much smaller motif are focused on the  $\alpha\beta$  fold common to scorpion toxins and  $C_2H_2$  zinc fingers. Selectability was previously shown for the  $\alpha$ -helix of a 27-aa consensus  $C_2H_2$  zinc-finger [CP-1, ref. 1] which was used to design a conformationally homogeneous combinatorial library [2]. Randomization of the helical site was accompanied by very limited structure perturbation [2,3]. The selection described in that work was performed with an IgA mAb (IgA-C5) reactive against the lipopolysaccharide of the human pathogen *Shigella flexneri*. We could then show that the five IgA-binding amino acids of the helix of the selected ligand (Sh-Znf) could be grafted onto another helical domain (a coiled-coil peptide) without loss of affinity [4]. We also showed that new functions could be introduced in the  $\beta$ -domain of the scorpion charybdotoxin (ChTX) without perturbation of the original  $\alpha\beta$  motif. While native ChTX acts as  $K^+$  channel inhibitor, we were able to endow it with metal binding [5] or curaremimetic [6,7] activity. Based on these results, we now have combined a "selectable"  $\alpha$  region from zinc-fingers with an "effector"  $\beta$  region from scorpion toxins, and we show here that both domains are functional in the same 37 aa chimeric miniprotein.

*Table 1. Design of the Chaybdotoxin/Zinc-finger chimera. Sequence of the peptides used.*

---

**Consensus Zinc-Finger (CP-1)**  
H-PYKCPECGKSFSQKSDLVKHQRTHTG-OH

**Shigella flexneri IgA C/5-binding Zinc-Finger (Sh-Znf)**  
H-PYKCPECGKSFSQKHFLVQHQTHTG-OH

**Charybdotoxin (ChTX)**  
H-ZFTNVSCTTSKECWSVCQRLHNTSRGKCMNKKCRCYS-OH

**Zinc-Finger/Charybdotoxin Chimera (Sh-ChTX)**  
H-ZFTNVSCTTSHFCVQVCHSLHNTSRGKCMNKKCRCYS-OH

---

*Z = 5-oxoproline (Pyroglutamic acid)*

## Results and Discussion

The design of the zinc-finger-Charybdotoxin chimera is illustrated in Table 1, where we show the sequences of all the peptides used in this study. Charybdotoxin, whose voltage-activated  $K^+$  channel “effector”  $\beta$  domain was left unaltered, was endowed with anti-*Shigella* IgA C-5 binding capability by substituting residues 11, 12, 14, 15 and 18 in the  $\alpha$ -helix (Lys, Glu, Trp, Ser and Gln, respectively) with residues 15, 16, 18, 19 and 22 of the  $\alpha$ -helix of Sh-Znf [3] (His, Phe, Val, Gln and His, respectively). Residue 19 of ChTX (Arg) was also mutated because modeling suggested the possibility of steric hindrance with His 18. The resulting chimera was named Sh-ChTX. It was synthesized by solid-phase methods using Fmoc-amino acids and HBTU activation, refolded with reduced and oxidized glutathione and purified by reversed-phase HPLC, as already described [8].

Structural integrity of the chimera was probed by circular dichroism (CD). As shown in Fig. 1, Sh-ChTX and ChTX show similar CD spectra, indicating that the six mutations did not alter the original  $\alpha\beta$  scorpion scaffold.

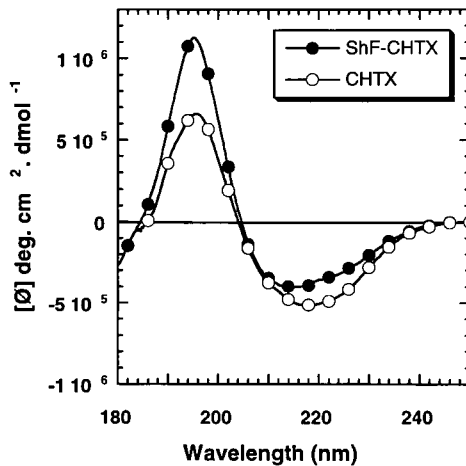


Fig. 1. CD spectra of ChTX and Sh-ChTX in 2 mM phosphate buffer, pH 7.0.

Preservation of the “effector activity” of the chimera, i.e. inhibition of voltage-activated  $K^+$  channels Kv1.3, expressed in *Xenopus* oocytes, was tested by electrophysiological recordings [9]. Sh-ChTX shows an activity ( $K_d = 2$  nM) slightly lower than ChTX ( $K_d = 0.1$  nM), being still capable of nanomolar binding to the  $K^+$  channels.

The “selected” function, i.e. binding to IgA C-5, was assessed by competition ELISA as already described [3,4]. Using 10  $\mu$ M Sh-Znf, we obtained an  $IC_{50}$  of 26  $\mu$ M for Sh-ChTX (Fig. 2) indicating a similar affinity for the parent and grafted IgA-C5 binding sites.

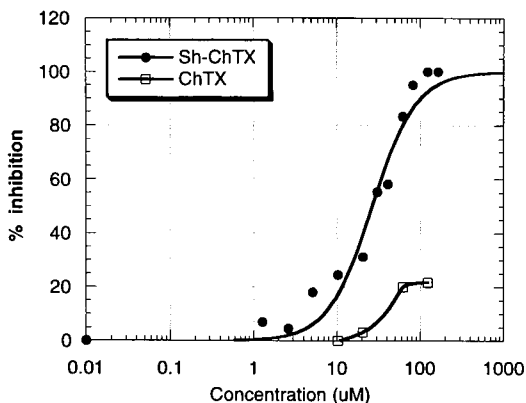


Fig. 2. ELISA Competition for IgA C-5 binding between 10  $\mu$ M Sh-Znf and increasing concentrations of Sh-ChTX or ChTX. ELISA conditions as described in ref. 3, 4.

Taken together, our results show that a peptide as small as 37-aa can be successfully endowed with two functions, one of which is the result of a selection process. With regard to antibody mimicry, we did not use for the selection the same molecule having the effector function, i.e. charybdotoxin. However we actually see the decoupling of the two functions as advantageous: while metal-dependent folding makes zinc-fingers more attractive for selection [2], the availability of many toxins structurally related to ChTX makes them collectively more attractive as sources of  $\beta$ -sheet effector domains.

## References

1. Krizek, B.A., Amann, B.T., Kilfoil, V.J., Merkle, D.L. and Berg, J.M., *J. Am. Chem. Soc.*, 113(1991) 4518.
2. Bianchi, E., Folgori, A., Wallace, A., Nicotra, M., Acali, S., Phalipon, A., Barbato, G., Bazzo, R., Cortese, R., Felici, F. and Pessi, A., *J. Mol. Biol.*, 247(1995) 154.
3. Barbato, G., Cicero, D., Bianchi, E., Pessi, A. and Bazzo, R., *J. Biomol. NMR*, 8(1996) 36.
4. Houston, M., Wallace, A., Bianchi, E., Pessi, A. and Hodges, R.C., *J. Mol. Biol.*, 262(1996) 270.
5. Vita, C., Roumestand, C., Toma, F. and Ménez, A., *Proc. Natl. Acad. Sci. USA*, 92(1995) 6404.
6. Drakopoulou, E., Zinn-Justin, S., Guenneugues, M., Gilquin, B., Ménez, A. and Vita, C., *J. Biol. Chem.*, 271(1996) 11979.
7. Zinn-Justin, S., Guenneugues, M., Drakopoulou, E., Gilquin, B., Vita, C. and Ménez, A., *Biochemistry*, 35(1996) 8535.
8. Vita, C., Bontems, F., Bouet, F., Tauc, M., Poujeol, P., Vatanpour, H., Harvey, A.L., Ménez, A. and Toma, F., *Eur. J. Biochem.*, 217(1993) 157.
9. Goldstein, A.A.M., Pheasant, D.J. and Miller, C., *Neuron*, 12(1994)1377.

# Optical holographic data storage using peptides

Rolf H. Berg, Palle H. Rasmussen, Søren Hvilsted  
and P. S. Ramanujam<sup>a</sup>

Condensed Matter Physics and Chemistry Department, <sup>a</sup>Optics and Fluid Dynamics  
Department, Risø National Laboratory, DK-4000 Roskilde, Denmark

Azobenzene-containing liquid-crystalline polymers have attracted a great deal of attention because of their potential to serve as holographic recording materials [1-4]. We report the properties of a new class of azobenzene-containing peptides which appear promising for erasable holographic data storage applications.

## Results and Discussion

When illuminated in a certain wavelength range the azobenzene undergoes random reorientations through a number of *trans-cis-trans* isomerization cycles until eventually it is aligned with its optical transition moment axis lying in the plane perpendicular to the polarization direction of the laser beam. The alignment of azobenzenes leads to a local change in the material's refractive index which forms the basis for the storage process. We designed peptides, or DNO oligomers (Fig. 1) [5], in which azobenzene side chains were incorporated in a molecular geometry similar to that of the bases in DNA or peptide nucleic acids (PNA) [6].

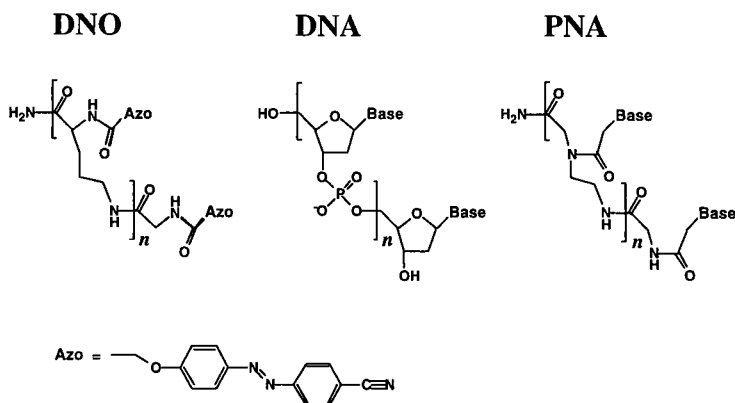


Fig. 1. Chemical structures of DNO, DNA and PNA.

The idea behind this design was to reduce the number of possible stationary orientations by imposing orientational order on the chromophores so as to achieve a high refractive index change. The particular backbone used is made up of ornithine units

oligomerized through the  $\delta$ -amino groups and with the side chains attached via the  $\delta$ -amino groups. The DNO oligomers were readily prepared by standard Merrifield synthesis.

The absorption spectrum of a DNO oligomer and the experimental set-up to record polarization holograms are shown in Fig. 2. Two orthogonally circularly polarized beams at 488 nm from an argon ion laser are used for the recording of a holographic grating. This results in a refractive index modulation because of the anisotropy created in the material. A weak, circularly polarized HeNe laser beam operating at 633 nm is used for the read-out of the diffracted light. The diffraction efficiency  $\eta$  indicates how much of the light entering the sample is diffracted by the holographic grating.

The results showed that very large first-order diffraction efficiencies (up to 80%, i. e., near the maximum achievable) can be obtained from holographic gratings of a DNO dimer or oligomer recorded in films only a few micrometers thick. The recording properties of a DNO dimer versus those of a monomer (which contains only a single azobenzene side chain) is examined in Fig. 3. For the dimer, the diffraction efficiency increases in about 300 s to about 76%, while a much lower diffraction efficiency (15%) is obtained with the monomer. The holograms can be erased with circularly polarized light and they can be rewritten and erased several times without fatigue. Furthermore, they appear to be completely stable at room temperature.

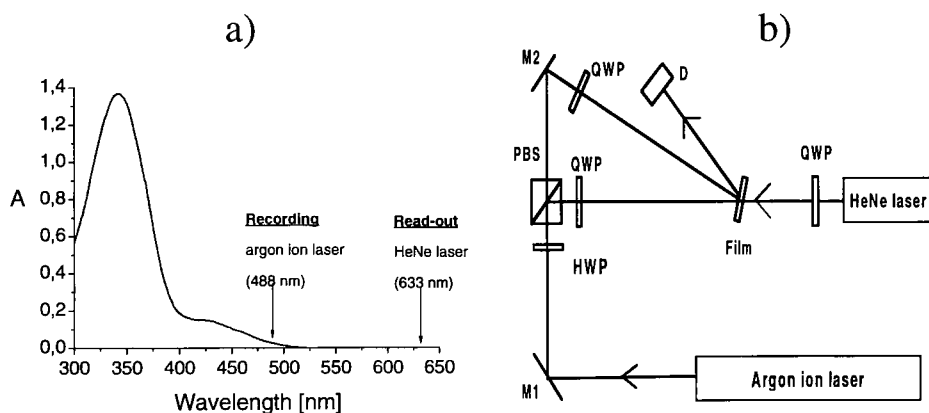


Fig. 2. (a) Absorption spectrum of a DNO oligomer. (b) Experimental set-up to record polarization holograms; M1 and M2 are mirrors, HWP is a half-wave plate, QWP's are quarter-wave plates, PBS is a polarization beam-splitter, and D is a detector.

In conclusion, a new approach to the design of potentially very useful materials for holographic data storage has been demonstrated which relies on the use of azobenzene-containing peptide oligomers.

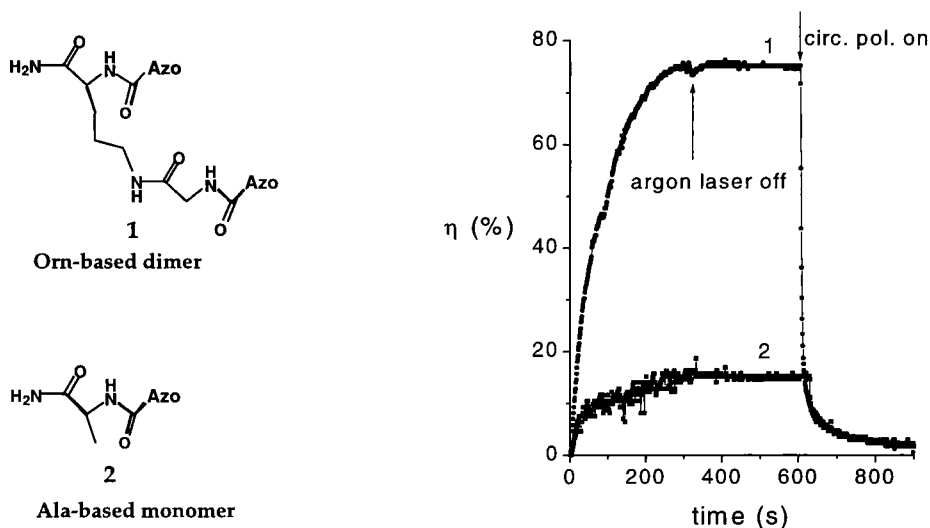


Fig. 3. First-order diffraction efficiencies as a function of time, measured during the grating formation in thin films of an ornithine-based DNO dimer (1) and an alanine-based monomer (2), respectively.

### Acknowledgements

We thank Ms. Anne Bønke Nielsen, Ms. Eva Tulin Kristensen and Tina Sonne Sonberg for skilled technical assistance. This work was supported by The Danish Research Councils and The Danish Materials Technology Development Programme.

### References

1. Eich, M., Wendorff, J. H., Reck, B. and Ringsdorf, H., *Makromol. Chem. Rapid Commun.*, 8 (1987) 59.
2. Jones, C. and Day, S., *Nature*, 351 (1991) 15.
3. Wiesner, U., Antonietti, M., Boeffel, C. and Spiess, H. W., *Makromol. Chem.*, 191 (1990) 2133.
4. Hvilsted, S., Andruzzi, F., Kulinna, C., Siesler, H. W. and Ramanujam, P. S., *Macromolecules*, 28 (1995) 2172.
5. Berg, R. H., Hvilsted, S. and Ramanujam, P. S., *Nature*, 383 (1996) 505.
6. Nielsen, P. E., Egholm, M., Berg, R. H. and Buchardt, Science, 254 (1991) 1497.

# Developing synthetic hemoprotein mimetics: Design, synthesis and characterization of heme-peptide conjugates

Angela Lombardi,<sup>a</sup> Flavia Natri,<sup>b</sup> Luca D. D'Andrea,<sup>a</sup> Ornella Maglio,<sup>b</sup>  
Gabriella D'Auria,<sup>a</sup> Carlo Pedone,<sup>b</sup> and Vincenzo Pavone<sup>a</sup>.

<sup>a</sup>*Centro Interuniversitario di Ricerca sui Peptidi Bioattivi & <sup>b</sup>Centro di Studio di Biocristallografia-CNR, University of Naples "Federico II", Via Mezzocannone 4, I-80134 Napoli, Italy*

The design of model compounds is a powerful tool for understanding the structure-function relationship in metalloproteins. Model systems are easier to study than their natural counterparts, and can lead to discovery of the minimal structural requirements for protein functions. Elaborate peptide-based metalloporphyrin molecules have been recently engineered [1-3] in order to investigate the role of the protein environment in tuning the properties of the heme center in hemoproteins.

We have recently tailored a new class of hemoprotein models, called mimochromes [4,5]. In this paper we report the design, synthesis and a preliminary characterization of mimochrome II, namely 3,7,12,17-tetramethylporphyrin-2,18-di-N<sub>9</sub>ε-(Ac-Asp<sup>1</sup>-Leu<sup>2</sup>-Ser<sup>3</sup>-Asp<sup>4</sup>-Leu<sup>5</sup>-His<sup>6</sup>-Ser<sup>7</sup>-Lys<sup>8</sup>-Lys<sup>9</sup>-Leu<sup>10</sup>-Lys<sup>11</sup>-Ile<sup>12</sup>-Thr<sup>13</sup>-Leu<sup>14</sup>-NH<sub>2</sub>)-propionamide. The present study highlights the importance of the peptide chain composition and length in controlling heme properties, and may aid in evaluating the key points in the development of highly stereo- and chemio-selective synthetic catalysts.

## Results and Discussion

Mimochromes are composed of two peptide chains that surround the heme group. They have the following two main features: *i*) the peptide chains are in  $\alpha$ -helical conformation; and *ii*) the helix - heme - helix sandwich has a covalent structure. The prototype of such peptide-heme adduct mimochrome I [4] contains deuterohemin bound through both propionyl groups to the Lys side chains of two identical N- and C-terminal protected nonapeptides. Each peptide moiety bears a His residue in the central position which acts as axial ligand of the central metal ion. The detailed structural characterization of Co(III)-mimochrome I complex [5], derived from NMR spectroscopy, gave us information about the overall structure of the model. The metallation of mimochrome I by cobalt revealed that two different orientations of the peptide chains were possible. In fact, the flexibility of the linker between the peptide and the deuteroporphyrin ring permitted a peptide chain to be positioned either above or below the porphyrin plane. This arrangement produced enantiomeric configurations around the metal center, giving rise to the formation of  $\Delta$  and  $\Lambda$  isomers for the cobalt complex [5]. Since the iron ion has a binding preference for nitrogen ligand lower than that of the cobalt, the two isomers were in a fast interconverting equilibrium in Fe(III)-mimochrome I complex. The intermediate species formed during this equilibrium may aggregate by porphyrin ring stacking. Thus, the water solubility of the

iron complex is lowered [4]. In order to obtain water soluble iron complexes, we optimized mimochrome structure's. By using the  $\beta$ -chain F helix of human deoxyhemoglobin and the three-dimensional structures of the Co(III)-mimochrome I isomers as templates, we have designed mimochrome II. Fig. 1 reports the stereo views of the molecular model of mimochrome II.

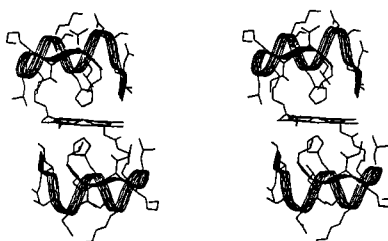


Fig. 1 Stereo view of the molecular model of mimochrome II.

In particular, the modeling analysis suggested that the addition of four residues at the C-terminal region of the nonapeptide sequence, in an extended conformation, would strongly reduce the linker flexibility. Thus, a 14 residue sequence was built based on the fragment  $\beta\text{Leu}^{88}$ - $\beta\text{Pro}^{100}$  of the hemoglobin template structure. The residues from position 1 to 10 were modeled in  $\alpha$ -helical conformation, by taking into account all the factors which contribute to  $\alpha$ -helix formation, and the C-terminal part was modeled in extended conformation. Due to the complexity of the mimochrome II molecular architecture, improvements were made in the general synthetic strategy previously reported [5]. The final procedure is schematically depicted in Fig. 2.

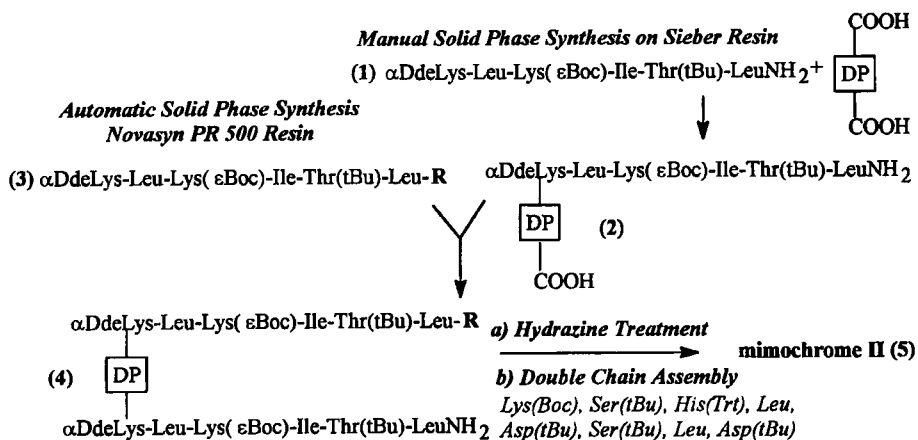


Fig. 2 Schematic presentation of the synthetic procedure employed

Table 1. CD parameters of mimochrome II, mimochrome I and their cobalt complexes.

Species	Uv-Region				Soret-	
	$[\theta]_{\min}$ (nm)	$[\theta]_{222}$	$[\theta]_{\text{ratio}}$	$\lambda_0$	$[\theta]_{190}$	$[\theta]$ (nm)
1 mimochrome II	-13335 (207)	-10463	0.78	199.7	22826	not detected
2 Co(III)-mimochrome II	-12650 (208)	-10461	0.83	200.1	23649	-10822 (415)
3 mimochrome I	-9300 (206)	-6400	0.70	199.1	18700	not detected
4 Co(III)-mimochrome I $\Delta$	-17229 (204)	-8757	0.51	197.3	24330	-54015 (416)

The first experimental evidence that the designed peptide sequence was able to fold up into a unique topology around the porphyrin was the formation of a single species upon cobalt insertion into the porphyrin. The UV-visible spectrum of Co(III)-mimochrome II showed that the expected *bis*-His axial coordination occurred. CD spectroscopy revealed that, as expected, the peptide chains were in  $\alpha$ -helical conformation and no spectral changes were observed upon metal coordination. The analysis of the Cotton effect in the Soret region of the cobalt complex gave definitive experimental evidence that only one of the two possible isomer structure's was energetically favored for mimochrome II. In fact, Co(III)-mimochrome II in TFE/buffer solution (1:1 v/v, pH 7) was characterized by a negative Cotton effect around 415 nm (see Table 1). Thus, it is possible to hypothesize, on the basis of the optical features of the Co(III)-mimochrome I isomers, that Co(III)-mimochrome II exists as a unique species whose overall structural organization corresponds to that of the  $\Delta$  isomer.

## Conclusion

Mimochrome II belongs to the second generation of a new class of low molecular weight hemoprotein models that derive from the prototype mimochrome I. The features of mimochrome II that differentiate it from mimochrome I are: *i*) a longer C-terminal tail which avoids the  $\Lambda \leftrightarrow \Delta$  interconversion; *ii*) amino acid substitutions which further stabilize the helical structure. All the experimental results obtained so far have confirmed the design hypothesis. In conclusion, our proposed structure for a stereochemically stable isomer of Co(III)-mimochrome II serves well as a template for the design of stereo- and regio-selective biomimetic catalysts.

## References

1. Choma, T., Lear, J. D., Nelson, M. J., Dutton, P. L., Robertson, D. E. and DeGrado, W. F., J. Am. Chem. Soc., 116 (1994) 856.
2. Sasaki, T. and Kaiser, E. T., J. Am. Chem. Soc., 111 (1989) 380
3. Benson, D. R., Hart, B. R., Zhu, X. and Doughty, M. B., J. Am. Chem. Soc., 117 (1995) 8502.
4. Natri, F., Lombardi, A., Morelli, G., Maglio, O., D'Auria, G., Pedone C. and Pavone, V., Chemistry. A Europ. J., 3 (1997) 340.
5. D'Auria, G., Maglio, O., Natri, F., Lombardi, A., Mazzeo, M., Morelli, G., Paolillo, L., Pedone, C. and Pavone, V., Chemistry. A Europ. J., 3 (1997) 350.

# A novel class of Calmodulin mimetics: *De Novo* designed proteins in molecular recognition

Angela Lombardi,<sup>a</sup> Giovanna Ghirlanda,<sup>b</sup> Laura Zaccaro,<sup>a</sup>  
Vincenzo Pavone,<sup>a</sup> William F. DeGrado<sup>b</sup>

<sup>a</sup>*Centro Interuniversitario di Ricerca sui Peptidi Bioattivi, University "Federico II" of Naples, Via Mezzocannone 4, I-80134 Napoli, Italy* <sup>b</sup>*Department of Biochemistry and Biophysics, Anatomy Chemistry Building 318, University of Pennsylvania, Philadelphia, PA, 19104-6059, USA*

Calmodulin (CaM) is an acidic protein of 148 amino acid residues that plays a central role in cellular regulation by relating the levels of cellular calcium to the activities of regulatory proteins, such as kinases, phosphatases, etc. Recent studies with synthetic models and natural peptides have shown that CaM recognizes positively charged, amphiphilic  $\alpha$ -helical peptides [1]. There is no exact sequence homology in the CaM binding proteins, but they frequently contain segments rich in basic residues (Arg, Lys, His) and are capable of adopting, when they bind to CaM, an amphiphilic  $\alpha$ -helical conformation. These observations demonstrated that this structural feature is important for binding, and that hydrophobic and electrostatic interactions both play a relevant role.

We report here our approach for the design of an  $\alpha$ -helical dimer covalently linked in a parallel or antiparallel orientation that is able to specifically interact with only one of the target enzymes recognized by CaM and form three stranded coiled coils. The target sequence that we chose for binding was the CaM binding domain of calcineurin. This important enzyme is the target of immunosuppressive drugs, such as cyclosporin A and FK506. A peptide that specifically binds to calcineurin could be expected to be either an immune-stimulant or an immune-suppressant, depending on whether it activates or inhibits activation of the enzyme.

## Results and Discussion

Two different approaches were used for modeling the CaM mimetics: *i*) first, a helix-loop-helix peptide, made up of two helices covalently linked in an antiparallel orientation, was designed; *ii*) secondly, parallel helices connected by a disulfide bridge were modeled.

Our initial design of calmodulin mimetics has evolved from a detailed analysis of the solid state [2] and solution behaviors of coil-Ser [3]. This 29 residue peptide is a member of a series of peptides developed in order to provide a convenient model system for investigating helix stability [4]. These peptides were expected to form parallel two stranded coiled coils, but they were actually found to form trimers in the solid state and in solution [2,3]. An antiparallel geometry was observed in the crystal structure of coil-Ser [2]. In solution this peptide exists in a relatively non-cooperative monomer/dimer/trimer equilibrium: the first step involves forming an  $\alpha$ -helical dimer from two random coil

monomers, and the second step involves adding a random coil monomer to the helical dimer. The two steps, dimerization and trimerization, are energetically equal [2]. Thus the dimer could be considered a pre-organized simple receptor for binding a random coil monomer.

Based on coil-Ser crystal structure, the CaM binding domain of calcineurin (396-414) was aligned with coil-Ser sequence, to optimize the hydrophobic interactions:

<b>Calcineurin</b>	- I - R - N - K - I - R - A - I - G - K - M - A - R - V - F - S - V - L - R -
<b>Coil-Ser</b>	- W - E - A - L - E - K - K - L - A - A - L - E - S - K - L - Q - A - L - E -

Then, a loop was built between the two antiparallel  $\alpha$ -helices and the resulting dimer sequence was mutated in order to create electrostatic interactions with the basic groups of the calcineurin sequence. Finally, using a genetic algorithm [5], the hydrophobic residues from the dimer were re-packed to be complementary to the hydrophobic residues of the calcineurin helix. The hypothetical mode of interaction between the antiparallel dimer, named CM1, and the calcineurin target peptide is schematically depicted in Fig. 1.

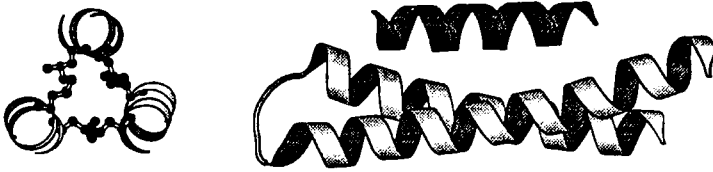


Fig. 1. Hypothetical mode of interaction of CM1 with the CaM binding domain of calcineurin.

Circular dichroism measurements showed that the CM1 dimer sequence adopts the  $\alpha$ -helical conformation and it is capable of binding to the calcineurin peptide, with a dissociation constant approximately  $1 \mu\text{M}$ . As shown in Fig. 2, the calcineurin peptide is almost entirely in a random coil conformation in diluted aqueous solution, but binding to CM1 induces the  $\alpha$ -helical conformation. In fact, the titration of CM1 with the calcineurin peptide resulted in an increasing helical content. On the other hand, no increase in ellipticity at 222 nm was observed when the CaM target peptide from myosin light chain kinase was titrated into the CM1 solution. Therefore, our first receptor model, CM1, is more specific than calmodulin, in that it is able to recognize only one of the two possible peptides.

The design of parallel receptors was based on the crystal structure of coil-Val [6,7], which adopts a trimeric state with a parallel orientation of the helices. Using the same design strategy, as illustrated above, we obtained a first disulfide bridged dimer, which specifically binds to the calcineurin target peptide with a dissociation constant of about  $1.5 \mu\text{M}$ . The design was improved by repacking the hydrophobic core [5] and creating a library of 27 asymmetric receptors. The asymmetric disulfide formation was achieved using a method recently reported in the literature [8]. Preliminary results indicate that seven of the parallel receptors specifically bind to the calcineurin peptide in a 1:1 stoichiometry, and with dissociation constants ranging from 0.1 to  $3 \mu\text{M}$ . Thus, we have

increased the affinity of the receptor for calcineurin by one order of magnitude with respect our first model CM1.

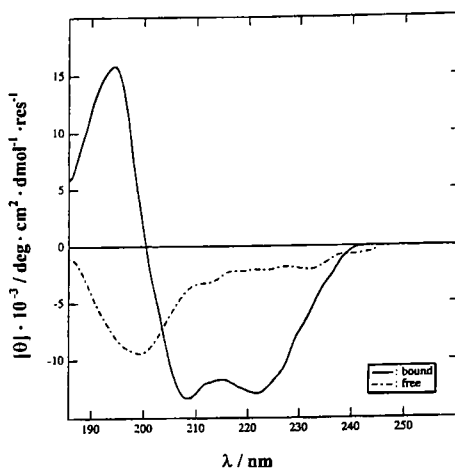


Fig. 2. CD spectra of the calcineurin peptide in the absence (---) and in the presence (—) of one equivalent of CM1; the contribution from CM1 itself has been subtracted out.

In conclusion, the design strategy that we used, allowed us to make CaM mimetics, more specific than the natural protein. Using both computational methods and synthetic procedures, it was possible to improve our initial model and obtain sequences which bind to the target peptide with higher affinity. Actually, all the designed receptors dimerize in aqueous solution and therefore, when the calcineurin target peptide interacts with them, part of the free energy of the binding is spent causing the dissociation of the dimer. Much higher affinity receptor might be obtained once the dimerization problem is overcome.

## References

1. DeGrado, W.F. and O'Neil, K., Trends in Biochemical Science, 15 (1990) 59 and references therein.
2. Lovejoy, B., Choe, S., Cascio, D., McRoie, D.K, DeGrado W.F. and Eisenberg, D., Science, 259 (1993) 1288.
3. Betz, S., Fairman, R., O'Neil, K., Lear, J. and DeGrado, W.F., Phil. Trans. R. Soc. Lond. B, 348 (1995) 81.
4. O'Neil, K. and DeGrado, W.F., Science, 250 (1990) 646.
5. Desjarlais, J.R. and Handel, T.M., Protein Science 4 (1995) 2006.
6. Boice, J.A., Dieckmann, G.R., DeGrado, W.F. and Fairman, R., Biochemistry, 35 (1996) 14480.
7. Ogihara, N.L., Weiss, M.S., DeGrado, W.F. and Eisenberg, D., Protein Science 6 (1997) 80.
8. Rabanal, F., DeGrado, W.F. and Dutton, P. L., Tetrahedron Lett., 37 (1996) 1347.

# Non native architectures in protein design : Four helix bundles as locked-in tertiary fold

Marc Mathieu and Gabriele Tuchscherer

*Institute of Organic Chemistry, University of Lausanne, BCH-Dorigny,  
CH-1015 Lausanne, Switzerland*

The concept of template assembled synthetic proteins (TASP) in protein *de novo* design aims to bypass the well known problem of protein folding by constructing tertiary folds exhibiting non-native architectures [1,2]. A topological template, i.e. a cyclic decapeptide containing spatially defined attachment sites, directs covalently linked peptide blocks to a predetermined topology, resulting in branched structures of tailored thermodynamic stability. The event of chemoselective ligation techniques [3-5] and regioselectively addressable template molecules [6] now allows us to explore the full potential of this approach.

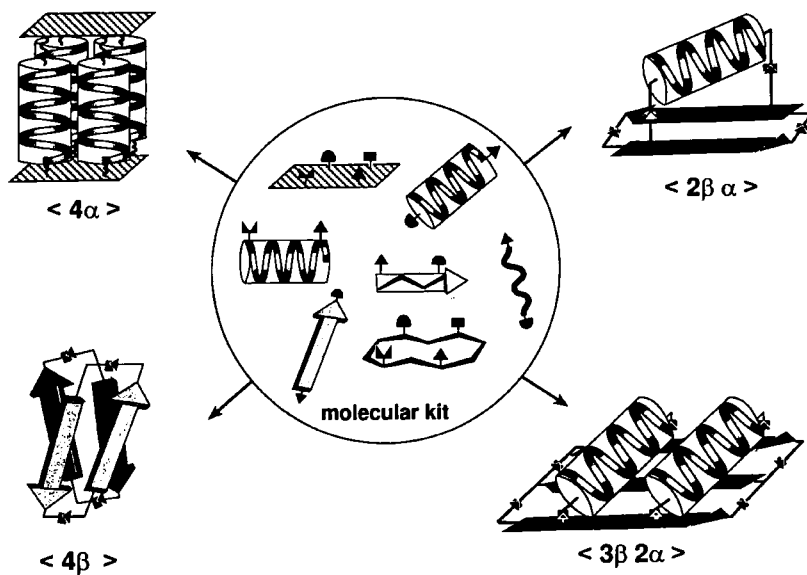


*Fig. 1. Molecular kit approach for protein de novo design : A variety of ligation methods allows for the covalent trapping of templates and peptides blocks to characteristic packing topologies.*

As depicted in Fig. 1, the envisioned structural motif is based on the principles of a molecular kit, i.e. assembly of constituent helical/ $\beta$ -sheeted peptide blocks or loops via templates or spacer molecules to crosslinked multibridged ("locked-in") tertiary folds. Most notably, the large number of alternative packing topologies as observed for linear polypeptides is drastically reduced due to the highly constrained conformational space of the locked-in structures.

## Results and Discussion

As a prototype locked-in fold, a  $4\alpha$ -helical bundle is trapped via both chain ends by two topological templates. To this end, orthogonally protected amino oxy groups attached to the C- and N-termini of a 14mer-peptide derived from hen eggwhite lysozyme [1] are sequentially ligated to the aldehyde functions of the templates (Scheme 1). The condensation reaction in aqueous solution proceeded to completion within 8 h and the resulting locked-in  $\langle 4\alpha \rangle$  molecule (Fig. 1) was characterized by ES-MS ( $M_r = 8534$ ).

CD studies in phosphate buffer reveal a significant increase in helicity of the sandwiched bundle  $T_4-(4\alpha)-T_4$  compared to the regular TASP  $T_4-(4\alpha)$  and the single helical block  $\alpha$  (Fig. 2). In addition, denaturation studies indicate a marked difference in thermodynamic stability of the TASP molecules, as documented by a two-fold increase in free energy ( $\Delta G_{T-(4\alpha)} \sim 6 \text{ Kcal M}^{-1}$ ;  $\Delta G_{T-(4\alpha)-T} \sim 12 \text{ Kcal M}^{-1}$ ; Fig. 2)

$\alpha$ : **BocAO-D-A-A-T-A-L-A-N-A-L-K-K-L-K(FmocAO)-ONH<sub>2</sub>**

**T<sub>4</sub>: c[P-G-K(CHO)-G-K(CHO)-Amhn-K(CHO)-G-K(CHO)]**

1. -Boc
2.  $\alpha + T_4$ : oxime bond formation
3. -Fmoc
4.  $T_4-(\alpha) + T_4$ : oxime bond formation

**T<sub>4</sub> - (4 $\alpha$ ) - T<sub>4</sub>**

*Scheme 1. Synthesis of the sandwiched 4-helix bundle  $T_4-(4\alpha)-T_4$  ( $\langle 4\alpha \rangle$  in Fig. 1) by sequential oxime bond formation (AO = amino oxyacetic acid).*

## Conclusion

In applying recent methodologies of peptide synthesis, the TASP concept for protein *de novo* design was extended for accessing non-native architectures with a much higher tendency for adopting a tertiary fold compared to linear polypeptides. Using oxime bond

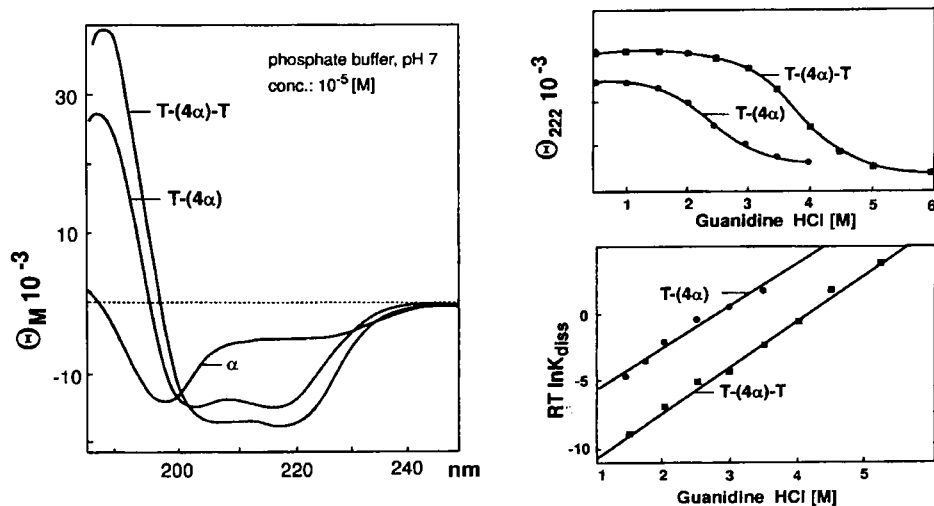


Fig. 2. Conformational properties of locked-in helical bundles (see text).

chemistry and regioselectively addressable templates for trapping helical peptide blocks in aqueous solution, a locked-in 4-helical bundle ( $\langle 4\alpha \rangle$  in Fig. 1) of increased thermodynamic stability was obtained. In a similar approach, we recently succeeded in the construction of locked-in folds mimicking native tertiary structures, e.g.  $\beta\beta\alpha$  units ( $\langle 2\beta\alpha \rangle$  in Fig. 1) derived from the zinc finger protein ZIF268 [7]. These branched architectures bypass completely the problem of protein folding and represent versatile scaffolds for mimicking protein function.

## Acknowledgements

This work was supported by the Swiss National Science Foundation.

## References

1. Mutter, M. and Tuchscherer, G., *Makromol. Chem. Rapid Commun.*, 9 (1988) 437.
2. Tuchscherer, G. and Mutter, M., *J. Biotechnol.*, 41 (1995) 197.
3. Rose, K., *J. Am. Chem. Soc.*, 116 (1994) 30.
4. Tuchscherer, G., *Tetrahedron Lett.*, 34 (1993) 8419.
5. Dawson, P.E. and Kent, S.B.H., *J. Am. Chem. Soc.*, 115 (1993) 7263.
6. Dumy, P., Eggleston, I.M., Cervigni, S., Sila. U., Sun, X. and Mutter, M., *Tetrahedron Lett.*, 36 (1995) 1255.
7. Mathieu, M., Lehmann, C., Razaname, A. and Tuchscherer, G., *Letters Pept. Sci.*, 4 (1997) 95.

# Synthesis and *in vivo* pharmacological profile of dimeric HOE 140 bradykinin antagonists

Muriel Amblard,<sup>a</sup> Isabelle Daffix,<sup>a</sup> Gilbert Bergé,<sup>a</sup> Pierre Dodey,<sup>b</sup> Didier Pruneau,<sup>b</sup> Jean-Luc Paquet,<sup>b</sup> Pierre Bélichard,<sup>b</sup>  
Jean-Michel Luccarini and Jean Martinez<sup>a</sup>

<sup>a</sup>Laboratoire des Aminoacides Peptides et Protéines (LAPP), ESA CNRS 5075, Universités de Montpellier I et II, Faculté de Pharmacie, 15 Av. C. Flahault, 34060 Montpellier, Cédex, France.

<sup>b</sup>Laboratoires de Recherche FOURNIER, Route de Dijon, 21100 Daix, France

We have been interested in the design of bradykinin B<sub>2</sub> receptor antagonists by using the so-called “bivalent ligand” approach which has been shown to increase the potency and duration of action of bioactive compounds [1, 2]. We therefore investigated the dimerization of the potent and selective bradykinin B<sub>2</sub> receptor antagonist, HOE 140 [3] (H-DArg<sup>0</sup>-Arg<sup>1</sup>-Pro<sup>2</sup>-Hyp<sup>3</sup>-Gly<sup>4</sup>-Thi<sup>5</sup>-Ser<sup>6</sup>-D-Tic<sup>7</sup>-Oic<sup>8</sup>-Arg<sup>9</sup>-OH) and of its various C-terminal fragments by introduction of a succinyl linker at their N-terminal. The dimer of the C-terminal inactive tetrapeptide of HOE 140 had a significant affinity for bradykinin B<sub>2</sub> receptors and exhibited an unexpected moderate *per os* activity in the rat. Starting from this dimer, we evaluated the influence of the linker by using different anhydrides or diacids. While corresponding monomers presented no detectable affinity up to concentrations of 10<sup>-5</sup> M, this dimerization strategy led to pseudotetrapeptide dimeric bradykinin antagonists exhibiting an affinity in the range of 80 nM on the human cloned B<sub>2</sub> receptor.

## Results and Discussion

Biological results are reported in Table 1. Dimerization of the C-terminal tripeptide and tetrapeptide of HOE-140 produced compounds (**1** and **2**) which were able to bind to the human bradykinin B<sub>2</sub> receptor with a low but significant affinity (K<sub>i</sub>, 4.09 ± 0.35 μM and 6.61 ± 0.25 μM, respectively) while the monomeric counterparts, H-DTic-Oic-Arg-OH and H-Ser-DTic-Oic-Arg-OH, presented no detectable affinity up to a 10 μM concentration. Compound **2** exhibited an antagonist activity *in vitro* on the rabbit jugular vein (RbJV). This compound was also evaluated for its *in vivo* activity in the rat. It did not alter blood pressure. By intravenous injection, however, it was able to reduce the fall of blood pressure induced by bradykinin to the same extent as HOE 140 but required a dose 300 times higher. When given orally at a dose of 30 mg/kg, dimer **2** reduced by about 50% the bradykinin-induced blood pressure decrease, while HOE 140 had no oral activity at 10 mg/kg in the same experimental conditions.

Starting from compound **2**, we have modified the linker. Only dimers having a linker containing a basic functional group (results of the most potent compounds are reported in Table 2) were able to bind with a higher affinity to the human bradykinin B<sub>2</sub> receptor (e.g.

Table 1. Pharmacological activity of dimer derivatives of HOE-140 and of its C-terminal fragments dimerized with a succinyl moiety.

Structure of dimers	Ki <sup>(1)</sup> (nM) or inhibition (%)	IC <sub>50</sub> <sup>(2)</sup> (nM) or inhibition (%)
<b>1</b> Suc[DTic-Oic-Arg-OH] <sub>2</sub>	4,096 ± 354	16,220 ± 2 875
<b>2</b> Suc[Ser-DTic-Oic-Arg-OH] <sub>2</sub>	6,609 ± 255	247 ± 94
<b>3</b> Suc[Thi-Ser-DTic-Oic-Arg-OH] <sub>2</sub>	17% (10 μM)	26% (10 μM)
<b>4</b> Suc[Gly-Thi-Ser-DTic-Oic-Arg-OH] <sub>2</sub>	30% (10 μM)	n.d.
<b>5</b> Suc[Hyp-Gly-Thi-Ser-DTic-Oic-Arg-OH] <sub>2</sub>	28% (10 μM)	n.d.
<b>6</b> Suc[Pro-Hyp-Gly-Thi-Ser-DTic-Oic-Arg-OH] <sub>2</sub>	85% (10 μM)	n.d.
<b>7</b> Suc[Arg-Pro-Hyp-Gly-Thi-Ser-DTic-Oic-Arg-OH] <sub>2</sub>	6.9 ± 0.9	n.d.
<b>8</b> Suc[HOE 140] <sub>2</sub>	0.63 ± 0.04	4.6 ± 0.8
HOE 140	0.09	1.3

(1) competition binding experiments with [<sup>3</sup>H]-bradykinin on human cloned B<sub>2</sub> receptors.

(2) inhibition of the contraction of the rabbit jugular vein (RJV) induced by bradykinin (30 nM); nd. not determined

compounds **10** and **11-2**). The spatial orientation of the basic function might play an important role since **10** was more potent than **9** and **11-2** than **11-1**. Compounds **9** and **10** were tested for their ability to inhibit bradykinin-induced contraction of human umbilical vein. They both exhibited an antagonist activity with a pK<sub>b</sub> of 5.26 and 5.48, respectively. Using compound **10** as a template, various other dimers were synthesized. Among them, compounds **12**, **13**, and **14** were the most potent (Table 2). Compound **13** inhibited the contraction of HUV induced by bradykinin with a pK<sub>B</sub> of 6.45 (Table 2). None of the dimer analogs exhibited a significant affinity for the human cloned B<sub>1</sub> receptor.

Table 2. Pharmacological activity of dimers of the C-terminal tetrapeptide of HOE-140.

Structure of dimers	Ki <sup>(1)</sup> (nM) or inhibition (%)	pK <sub>b</sub> <sup>(2)</sup> (nM) functional test
<b>9</b> L-Aspartyl-[Ser-DTic-Oic-Arg-OH] <sub>2</sub>	1,907 ± 156	5.26 ± 0.19
<b>10</b> D-Aspartyl-[Ser-DTic-Oic-Arg-OH] <sub>2</sub>	484 ± 87	5.48 ± 0.20
<b>11-1</b> D,L-2,6-diaminopimelyl-[Ser-DTic-Oic-Arg-OH] <sub>2</sub>	1,231 ± 38	n.d.
<b>11-2</b>	324 ± 1	n.d.
<b>12</b> H-Arg-DAsp-[Ser-DTic-Oic-Arg-OH] <sub>2</sub>	90.5 ± 0.3	5.49 ± 0.29
<b>13</b> H-D-Arg-DAsp-[Ser-DTic-Oic-Arg-OH] <sub>2</sub>	76 ± 2	6.45 ± 0.07
<b>14</b> NH <sub>2</sub> (CH <sub>2</sub> ) <sub>11</sub> -CO-DAsp-[Ser-DTic-Oic-Arg-OH] <sub>2</sub>	61 ± 5	n.d.

(1) competition binding experiments with [<sup>3</sup>H]-bradykinin on human cloned B<sub>2</sub> receptors.

(2) inhibition of the contraction of the human umbilical vein (HUV)\* induced by bradykinin (30nM); n.d. : not determined.

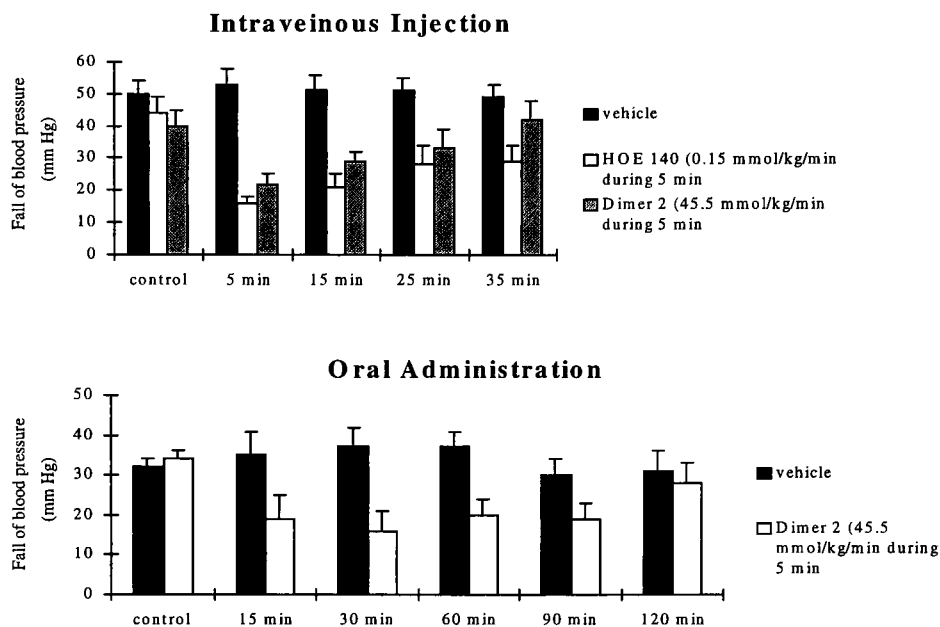


Fig. 1. *In vivo* activity of HOE 140 and dimer 2 on bradykinin induced hypotension in the rat.

## Conclusion

These results have shown that it is possible, by dimerization of the C-terminal tetrapeptide monomer of HOE-140, to obtain a compound which is able to bind to the human cloned B<sub>2</sub> receptor and which is orally active against bradykinin-mediated response in the rat. From this lead compound, we were able to synthesize dimers of increased potency. Finally, this study confirmed that dimerization is a successful strategy to enhance the affinity of a peptide monomer for a given receptor, and that this strategy applies to bradykinin analogs.

## References

1. Erez, M.; Takemori, A.E.; Portoghese, P.S. *J. Med. Chem.*, 25 (1982), 847.
2. Portoghese, P.S.; Ronsisvalle, G.; Larson, D.L.; Yim, C.B.; Sayre, L.M.; Takemori, A.E. *Life Sci.*, 31 (1982), 1283.
3. Lembeck, F.; Griesbacher, T.; Eckhardt, M.; Henke, St.; Breipohl, G.; Knolle, J. *Br. J. Pharmacol.*, (102) 1991, 297.

# Conformations and use of beta-aminoacid residues

**Isabella L. Karle**

*Laboratory for the Structure of Matter  
Naval Research Laboratory, Washington, D.C. 20375-5341, USA*

The ubiquitous occurrence in nature of alpha-aminoacid residues in peptides and proteins and their importance in biological systems have resulted in well-documented studies of their folding and twisting characteristics. Beta-aminoacid residues, containing an extra C atom in the backbone between N and C<sup>α</sup> atoms, have received very little attention until recently. The additional single bond adds a new dimension to the flexibility of the backbone and can provide new stable folds to the repertoire of folded molecular structures already known for alpha-aminoacids. Tubular [1-3] and helical [4-7] structures, most of them established by single crystal x-ray diffraction, will be described in the following paragraphs.

## Results and Discussion

Historically, (in 1975) nanotubes were shown to assemble in crystals of cyclic [L-Ser(O-tBu)-β-Ala-Gly-L-β-Asp(OMe)] [1]. The extra -HCR- moieties in β-Ala and β-Asp(OMe) allowed the 14-membered ring formed by the backbone atoms to assume a conformation such that NH<sup>⋯</sup>O=C hydrogen bonds were formed between stacked rings, thus making a tube, Fig. 1. However, only N1H and N3H participate in forming the tube while N2H<sup>⋯</sup>O2 and N4H<sup>⋯</sup>O4 hydrogen bonds are formed within each molecule. Recently, Seebach et al [2] obtained tubular structures with four H-bonds between cyclic tetrapeptide molecules in the stack by using four β-aminoacid residues that create 16-membered rings. Similar nanotube structures were prepared by Ghadiri and coworkers using only β-aminoacids but with an alternation of D and L chiralities in the sequence [3].

Perturbations of alpha or 3<sub>10</sub>-helices caused by the insertion of the β-Ala-γ-Abu segment into the middle (as residues 4 and 5) of helical peptides Boc-(Leu-Aib-Val)<sub>2</sub>OMe and Boc-(Leu-Aib-Val)<sub>2</sub>-Ala-Leu-Aib-OMe were examined by crystal structure analyses [4]. The helical nature of the altered peptides, as well as the 3<sub>10</sub>- and/or α-helical hydrogen bonds, were not significantly affected by the extra -CH<sub>2</sub>- and CH<sub>2</sub>CH<sub>2</sub>- segments that fold comfortably in the backbones with torsional angles near ±60°. Some of the hydrogen bond rings now have 12, 13 and 14 atoms, Fig. 2. Each of these rings is different from the unusual rings in cyclic (Pro-Phe-Phe-β-Ala-β-Ala) described by Pavone *et al* [5].

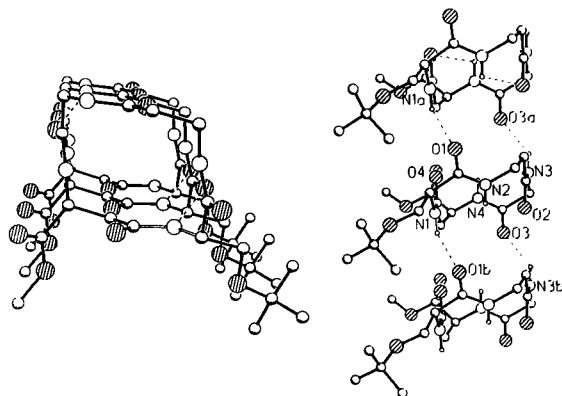


Fig. 1. Two views of tubular structure formed by stacking a cyclic  $\alpha\beta\alpha\beta$  peptide. Only N1H and N3H participate in forming the tube, while N2H and N4H [1] form intramolecular hydrogen bonds.

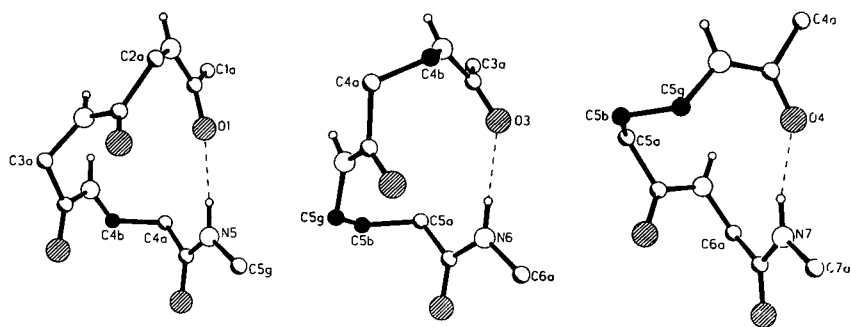
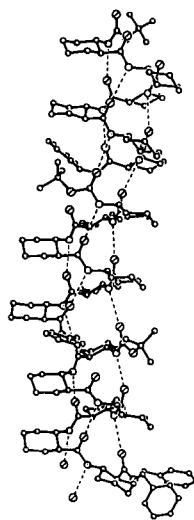


Fig. 2. Unusual hydrogen bond rings in the helical *Boc-Leu-Aib-Val- $\beta$ -Ala- $\gamma$ -Abu-Leu-Aib-Val-Ala-Leu-Aib-OMe* that contain additional methylene groups labelled C4b, C4b+C5b, C5g and C5b, C5g, respectively [4].

A homo beta-hexapeptide with the  $C^\alpha-C^\beta$  bond constrained by being incorporated into

a cyclohexyl ring,  $\text{Boc}(\text{NH}-\text{C}_6\text{H}_{10}-\text{CO})_6\text{OBzl}$ , has formed a regular helical structure with  $\beta \sim 140^\circ$ ,  $\beta \sim 130^\circ$  and  $\beta \sim 55^\circ$ , with  $\text{NH}\cdots\text{O}$  intramolecular hydrogen bonds (2.80-3.00 Å  $\text{N}\cdots\text{O}$  distances) in 14-membered rings [6]. The hydrogen bonds are formed in an opposite direction to those formed in an alpha-helix; that is,  $1\beta 3$  instead of  $5\beta 1$ . Infinite helices are formed by stacking three independent helices occurring in each asymmetric unit of the crystal, Fig. 3. A similar beta-foldamer has been deduced from solution NMR data for  $\text{H}(\beta\text{Val}-\beta\text{Ala}-\beta\text{Leu})_2\text{-OH}$  [7].



*Fig. 3. A new type of helix, called a beta-foldamer, with 14-atom hydrogen bond rings [7]. Three independent hexamer molecules stack in a column by head-to-tail hydrogen bonds, which in turn stack to form an infinite column.*

## Conclusion

Stable complex molecular structures, such as nanotubes and new types of helices, have been made by peptides synthesized from beta-amino acid residues alone or in combination with alpha-amino acid residues. These new structures may be useful in both material and biological sciences.

## References

1. Karle, I.L., Handa, B.K. and Hassall, C.H., *Acta Cryst.*, B31 (1975)555.
2. Seebach, D., Matthews, J., Meden, A., Wessels, T., Baerlocher, C. and McCusker, L., *Helv. Chim. Acta*, 80(1997)173.
3. Ghadiri, M.R., Granja, J.R., Milligan, R.A., McRee, D. E. and Kazanovich, N. *Nature*, 366(1993)324.
4. Karle, I.L., Pramanik, A., Banerjee, A., Bhattacharjya, S. and Balaram, P., *J. Am. Chem. Soc.*, submitted.
5. Pavone, V., Lombardi, A., Saviano, M., Natri, F., Maglio, O., Mazzeo, M., Pedone, C. and Isernia, C., *Biopolymers*, 38(1996)683.
6. Appella, D.H., Christianson, L.A., Karle, I.L., Powell, D.R. and Gellmann, S.H., *J. Am. Chem. Soc.*, 118(1996)13071 and to be published.
7. Seebach, D., Overhand, M., Kuhnle, F.N.M., Martinoni, C., Oberer, L., Hommel, U. and Widmer, H., *Helv. Chim. Acta*, 79(1996)913.

# Modular design of synthetic redox and light-absorbing proteins

Wolfgang Haehnel,<sup>a</sup> Harald K. Rau,<sup>a</sup> Heike Snigula<sup>b</sup> and Hugo Scheer<sup>b</sup>

<sup>a</sup>Institut für Biologie II / Biochemie, University of Freiburg, Schaenzlestr. 1, D-79104 Freiburg, Germany; <sup>b</sup>Botanisches Institut, University of Munich, Menzinger Str. 67, D-80638 Munich, Germany

An approach to a *de novo* protein having a cofactor binding site is the design of  $\alpha$ -helical bundles capable of binding heme groups [1]. Chemoselective binding of  $\alpha$ -helical peptides to predetermined positions of a cyclic template (TASP) [2] overcomes the problem of protein folding and association of single helices, allows the control of residues close to the cofactor and increases stability. The latter may be important if the design suffers from suboptimal packing of a bound cofactor. A problem in designing light absorbing chlorophyll proteins is the binding of the chlorophyll molecules. The structures of chlorophyll proteins [3] show a substantial interaction between the long hydrophobic phytol chains and the protein, which is not understood. Therefore the design of a binding pocket for the tetrapyrrol group of chlorophyll in a *de novo* protein is one of our goals. We present the design and synthesis of an antiparallel four helix TASP for binding two modified chlorophyll molecules or hemes.

## Results and Discussion

Two different amphiphilic helices (H1 and H2) were designed to form a water soluble antiparallel four-helix bundle protein and to bind in the hydrophobic interior two tetrapyrrol groups each *via* two His residues. The peptides H1, H2 and T were synthesized by automatic solid phase peptide synthesis. After modification of either the N-terminus of peptide H1 or the  $\epsilon$ -amino group of the C-terminal Lys of H2 by bromoacetylation the peptides were cleaved from the resin and purified by reversed phase HPLC. The cyclic peptide template was synthesized with four Cys being protected by Ac<sub>m</sub> and Trt protecting groups, respectively, at diagonal positions. The final molecule T(H1)<sub>2</sub>(H2)<sub>2</sub> designated MOP1 was obtained *via* thioether bond formation of the helical peptides to this orthogonally protected template T [4].

H1: BrAc-G-G-E-L-R-E-L-H-E-K-L-A-K-Q-F-E-Q-L-V-K-L-H-E-E-R-A-K-K-L-CONH<sub>2</sub>

H2: Ac-L-E-E-L-W-K-K-G-E-E-L-A-K-K-L-Q-E-A-L-E-K-G-K-K-L-A-K(BrAc)-CONH<sub>2</sub>

T: cyclo-(C(Ac<sub>m</sub>)-A-C(Trt)-P-G-C(Ac<sub>m</sub>)-A-C(Trt)-P-G)

The correct synthesis and high purity of the protein was confirmed by electrospray MS. The pheophorbids were obtained from chlorophyll *a* by standard procedures. Iron complexes were prepared by direct metallation using the acetate method. Additional binding energy of the iron pyropheophorbid *a* (Fe-PPheid) as compared to chlorophyll is expected from the coordination of the iron by two His and by electrostatic interaction of the free carboxylic group of the propionate side chain with Arg<sup>5</sup> and Arg<sup>25</sup> respectively, of H1.

The Fe-PPheid was dissolved in DMSO and an approx. two-fold molar excess was added to an anaerobic solution of 10  $\mu$ M peptide to avoid aggregation. The mixture was stirred under Ar for 0.5 h at room temperature and the excess Fe-PPheid was removed by two passages through a PD10 column (Pharmacia).

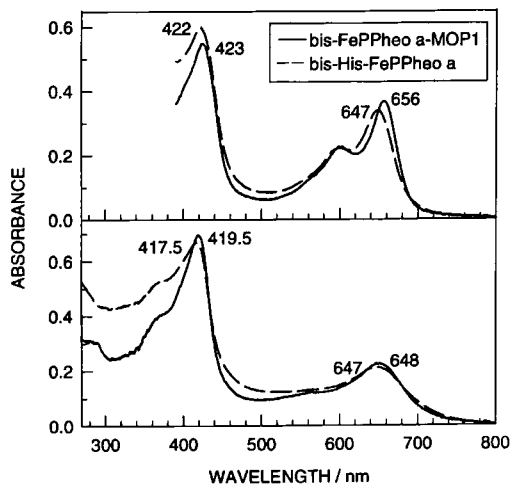


Fig.1. Absorbance spectrum of Fe-pyropheophorbide *a* bound to the modular protein MOP1 (full line) and dissolved in the presence of His (broken line). Top, reduced; bottom, oxidized.

The stable ligation of Fe-PPheid *a* was verified by passage through a 300 nm gelfiltration column. The spectrum of the reduced complex with Fe(II) shows a protein induced shift in the absorbance maximum from 647 to 656 nm if compared to that in the presence of His. Above is the spectrum of Fe(III)-PPheid *a* after oxidation. This molecule is a step towards a light harvesting module. The distance of the Ppheid *a* groups is well suited for energy transfer. It will also allow modification of the residues in contact with chlorophyll for increased binding stability and tight packing.

## References

1. Choma, C.T., Lear, J.D., Nelson, M.J., Dutton, P.L., Robertson, D.E. and DeGrado, W.F., *J. Am. Chem. Soc.*, 116 (1994) 856.
2. Mutter, M., Altmann, K.-H., Hersperger, R., Koziej, P., Nebel, K., Tuchscherer, G. and Vuilleumier, S., *Helv. Chim. Acta*, 71 (1988) 835.
3. McDermott, G., Prince, S.M., Freer, A.A., Hawthornthwaite-Lawless, A.M., Papiz, M.Z., Cogdell, R.J. and Isaacs, N.W., *Nature*, 374 (1995) 517.
4. Rau, H. and Haehnel, W., *Ber. Bunsenges. Phys. Chem.*, 100 (1996) 2052.

# Synthesis of semicaged ruthenium(II) complexes of a branched peptide containing three bipyridine ligands

Barney M. Bishop, Matthew C. Foster, Richard W. Vachet  
and Bruce W. Erickson

Department of Chemistry, University of North Carolina at Chapel Hill,  
Chapel Hill, NC 27599, USA

Some caged and semicaged complexes of ruthenium(II) have long-lived metal-to-ligand charge-transfer states [1, 2]. In addition, such semicaged complexes should be less susceptible to photoinduced dissociation of the ligand. We have described the synthesis of 4'-aminomethyl-2,2'-bipyridine-4-carboxylic acid (Abc), an amino acid that allows the 2,2'-bipyridine (bpy) ring system to be incorporated into the main chain of a peptide [3]. This paper describes the use of Abc in the engineering of the branched peptide, **ama**, which contains three bpy groups for coordination of a ruthenium(II) ion (Fig. 1).

## Results and Discussion

Apopeptide **ama** has two bpy groups in the Abc residues present in the peptide main chain and a third bpy group in the Mbc (4'-methyl-2,2'-bipyridine-4-carboxylic acid) group present in the branch. This branched peptide was designed to form facially bridged Ru<sup>II</sup> complexes but not meridionally bridged complexes. The only stereogenic center in apopeptide **ama** is the  $\alpha$ -carbon atom of the branching L-ornithine residue. Holo peptide Ru<sup>II</sup>(**ama**) contains the Ru<sup>II</sup> atom as a second stereogenic center, which can have either the  $\Lambda$  or  $\Delta$  geometry. Thus Ru<sup>II</sup>(**ama**) can exist as either the ( $\Lambda$ ,L) or the ( $\Delta$ ,L) diastereomer.

The acetylated peptide amide **ama** was assembled by manual solid-phase synthesis using a combination of Fmoc and Boc-amino acids. Metallopeptide Ru<sup>II</sup>(**ama**) was formed by reaction of **ama** with RuCl<sub>2</sub>(DMSO)<sub>4</sub> (Fig. 2). RP-HPLC indicated that the product mixture contained four Ru<sup>II</sup>/peptide complexes in nearly equal amounts. These four com-

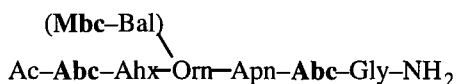


Fig. 1. Structure of the branched apopeptide **ama**, where **Abc** is 4'-aminomethyl-2,2'-bipyridine-4-carboxylic acid, **Ahx** is 6-aminohexanoic acid, **Apn** is 5-aminopentanoic acid, **Bal** is 3-aminopropanoic acid, and **Mbc** is 4'-methyl-2,2'-bipyridine-4-carboxylic acid.

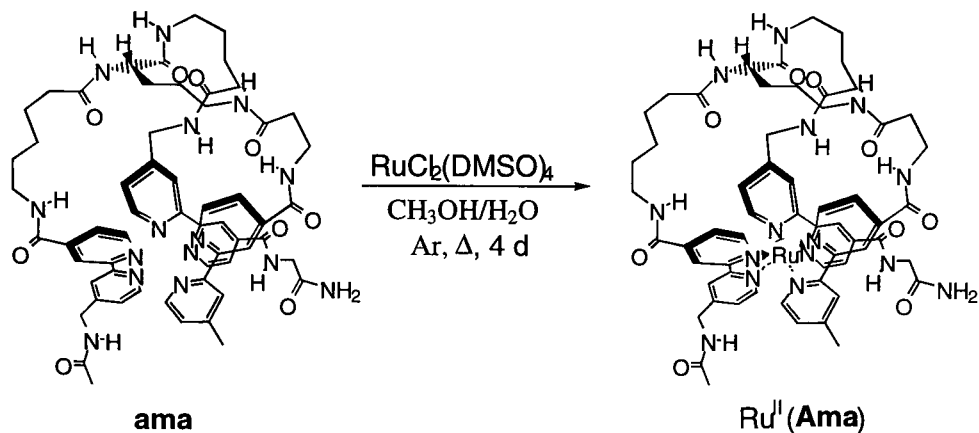


Fig. 2. Synthesis of the semi-caged metallopeptide  $\text{Ru}^{\text{II}}(\text{ama})$ . The (*out*, $\Delta$ ,L) isomer is shown.

pounds were separated by HPLC and were shown to be monomeric isomers of  $\text{Ru}^{\text{II}}(\text{ama})$  based on the distribution of masses observed by fourier-transform ion cyclotron resonance mass spectrometry. By CD spectroscopy,  $\text{Ru}^{\text{II}}(\text{ama})$  isomers 1 and 4 (in order of HPLC elution time) were determined to be ( $\Lambda$ ,L) diastereomers and isomers 2 and 3 to be ( $\Delta$ ,L) diastereomers. By  $^1\text{H-NMR}$ , isomers 1 and 2 were found to be a related pair of ( $\Lambda$ ,L)/( $\Delta$ ,L) diastereomers and isomers 4 and 3 were a different related pair of ( $\Lambda$ ,L)/( $\Delta$ ,L) diastereomers. These  $\text{Ru}^{\text{II}}(\text{ama})$  isomers were stable at  $90^\circ\text{C}$  but were partially interconverted by prolonged exposure to intense near-UV light.

Since the semicaged complex  $\text{Ru}^{\text{II}}(\text{ama})$  can only exist as a facially bridged complex, the existence of two pairs of ( $\Lambda$ ,L)/( $\Delta$ ,L) diastereomers must be due to different orientations of the branching ornithine residue, which can exist in either the *in* or *out* geometry. The *in* isomers have the ornithine  $\alpha$ -hydrogen atom pointing into the semicage towards the  $\text{Ru}^{\text{II}}$  atom. In contrast, the *out* isomers have this  $\alpha$ -hydrogen atom pointing outwards from the semicage away from the  $\text{Ru}^{\text{II}}$  atom (see Fig. 2). Thus isomers 1 and 2 of  $\text{Ru}^{\text{II}}(\text{ama})$  are either the (*in*, $\Lambda$ ,L)/(*in*, $\Delta$ ,L) pair or the (*out*, $\Lambda$ ,L)/(*out*, $\Delta$ ,L) pair, respectively, and isomers 4 and 3 are the other stereoisomeric pair, respectively. Which pair is which is not yet known.

## References

1. DeCola, L., Belser, P and von Zelewsky, A., J. Chem. Soc., (1988) 1057.
2. Fitzgerald, M.C., Larson, S.L. and Beeston, R.F., Inorg. Chem., 28 (1989) 4187.
3. Bishop, B.M., Ray, G.T., Mullis, B.H., McCafferty, D.G., Lim, A. and Erickson, B.W., In Kaumaya, P.T. and Hodges, R.S. (Eds.), Peptides: Chemistry, Structure and Biology, Kingswinford, England, 1995, p. 105.

# Design of new tentoxin analogues: Study of the ATP-synthase catalytic mechanism

Florine Cavelier,<sup>a</sup> Christine Enjalbal,<sup>a</sup> Jérôme Santolini,<sup>b</sup> Francis Haraux,<sup>b</sup> Claude Sigalat,<sup>b</sup> Jean Verducci<sup>a</sup> and François André<sup>b</sup>

<sup>1</sup> LAPP, ESA 5075 CNRS, Université Montpellier II, 34095 Montpellier cedex 5, France;

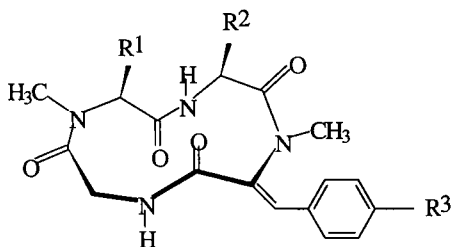
<sup>2</sup> Section de Bioénergétique, DBCM, CEA-SACLAY, 91191 Gif-sur-Yvette cedex, France

Tentoxin is a natural cyclotetrapeptide produced by several phytopathogenic fungi of the *Alternaria* family [1]. As a non host-specific toxin, it causes chlorosis in the seedlings of some higher plants, in particular in dicotyledone plants. Some cereals however are not sensitive [2]. This species-specificity raised the possibility of using tentoxin as a potential biogenic selective herbicide [3]. Very little is known about the modes of action of this phytotoxin. On the molecular level, it is now well-established that tentoxin binds specifically to the soluble CF<sub>1</sub> part of the chloroplast ATP-synthase [4]. For sensitive plants, tentoxin *in vitro* inhibits CF<sub>1</sub> ATPase activity at low concentration (below 10<sup>-8</sup> M) but starts to stimulate this activity at high concentration (above 10<sup>-6</sup> M). By the use of new synthetic analogues of tentoxin, we are investigating the molecular basis of this dual phenomenon and examining the mechanistic implications in the H<sup>+</sup> F<sub>1</sub>-ATPase machinery.

## Results and Discussion

On the basis of our NMR analysis of tentoxin structure in water [5], we first designed a close synthetic analogue (MeSer<sup>1</sup>-TTX) which proved to exhibit the same inhibitory power as tentoxin but was deprived of significant stimulatory activity [6]. This demonstrated that the two bioactivities could be uncoupled using judicious synthetic analogues. With <sup>14</sup>C-labelled tentoxin, we also demonstrated the existence of two distinct binding sites [7]. For

R <sup>1</sup>	R <sup>2</sup>	R <sup>3</sup>	
CH <sub>3</sub>	CH <sub>2</sub> -CH(CH <sub>3</sub> ) <sub>2</sub>	H	Tentoxin
H	CH <sub>2</sub> -CH(CH <sub>3</sub> ) <sub>2</sub>	H	Sar <sup>1</sup> -Tentoxin
CH <sub>2</sub> -OBn	CH <sub>2</sub> -CH(CH <sub>3</sub> ) <sub>2</sub>	H	MeSer(Bn) <sup>1</sup> -Tentoxin
CH <sub>2</sub> -OH	CH <sub>2</sub> -CH(CH <sub>3</sub> ) <sub>2</sub>	H	MeSer <sup>1</sup> -Tentoxin
CH <sub>2</sub> -CO <sub>2</sub> tBu	CH <sub>2</sub> -CH(CH <sub>3</sub> ) <sub>2</sub>	H	MeGlu(tBu) <sup>1</sup> -Tentoxin
CH <sub>2</sub> -CO <sub>2</sub> H	CH <sub>2</sub> -CH(CH <sub>3</sub> ) <sub>2</sub>	H	MeGlu <sup>1</sup> -Tentoxin
CH <sub>3</sub>	(CH <sub>2</sub> ) <sub>4</sub> -NHZ	H	MeLys(Z) <sup>2</sup> -Tentoxin
CH <sub>3</sub>	(CH <sub>2</sub> ) <sub>4</sub> -NH <sub>2</sub>	H	MeLys <sup>2</sup> -Tentoxin
CH <sub>3</sub>	CH <sub>2</sub> -CH(CH <sub>3</sub> ) <sub>2</sub>	OMe	MeTyr(Me) <sup>3</sup> -Tentoxin
CH <sub>3</sub>	CH <sub>2</sub> -CH(CH <sub>3</sub> ) <sub>2</sub>	OH	MeTyr <sup>3</sup> -Tentoxin



a careful investigation of the role of these two sites, we designed a whole set of analogues in which chemical modifications are located on the side chains of residues 1, 2 and 3 : The

two N-methylations, the cyclic backbone conformation *cis-trans-cis-trans*, and the  $\alpha,\beta$ -dehydro amino acid, were preserved. This work exploits a recent strategy developed in the laboratory for preparing cyclic tetrapeptides of this family [8]. The effects of tentoxin derivatives on the ATPase activity of the isolated CF<sub>1</sub> are summarized in Table 1. The table also includes our activity measurement of Sar<sup>1</sup>-TTX (MeAla<sup>1</sup> replaced by MeGly<sup>1</sup>), an analogue that has previously been described [9] and that we resynthesized for its ability to bind to the second site with a better affinity than the natural toxin.

*Table 1. Effect of tentoxin (TTX) and derivatives on the activity of CF<sub>1</sub>-ATPase. The reactivation effect is expressed in percentage of the activity of the control enzyme (without toxin).*

	natural TTX	Sar <sup>1</sup>	MeSer <sup>1</sup>	MeSer( MeGlu <sup>1</sup> Bn) <sup>1</sup>	MeGlu (OtBu) <sup>1</sup>	Lys <sup>2</sup>	Lys(Z) <sup>2</sup>	Me $\Delta$ Tyr <sup>3</sup>	Me $\Delta$ Tyr (Me) <sup>3</sup>	
IC <sub>50</sub> ( $\mu$ M)	0.04	0.07	0.04	0.5	5	2	4	1	0.04	0.05
Stimulation level (%)	220	240	30	0	0	0	0	40	75	290

In conclusion, all analogues proved to be efficient inhibitors, but at different concentrations (IC<sub>50</sub>). They also exhibited various responses concerning their ability to stimulate the enzyme at high concentrations. All the data could be fitted with a good approximation to a double-site model. The affinity constants derived from the two-sites model and from competition experiments between active and non-activaty analogues will help us to characterize the topology, the role, and the functional relationship between the two binding sites.

### Acknowledgements

This work was supported by a contract ACC-SV5 (interface Chimie-Biologie) from the Ministère de l'Enseignement Supérieur et de la Recherche, No. 9505221 (F. André).

### References

1. Fulton, N.D., Bollenbacher, K. and Templeton, G. E., *Phytopathol.*, 55(1965)49.
2. Durbin, R.D. and Uchytel, T.F., *Phytopathol.*, 67(1977)602.
3. Lax, A.R., Shepherd, H.S. and Edwards, J.V., *Weed Technol.*, 2(1988)540.
4. Steele, J.A., Uchytel, T.F., Durbin, R.D., Bhatnagar, P. and Rich, D.H., *Proc. Natl. Acad. Sci. U.S.A.*, 73(1976)2245.
5. Pinet, E., Neumann J.-M., Dahse, I., Girault, G. and André, F., *Biopolymers*, 36(1995)135.
6. Pinet, E., Cavelier, F., Verducci, J., Girault, G., Dubart, L., Haraux, F., Sigalat, C. and André, F., *Biochemistry*, 35(1996)12804.
7. Pinet, E., Gomis, J.-M., Girault, G., Cavelier, F., Verducci, J. and André, F., *FEBS Lett.*, 395 (1996)217.
8. Cavelier, F. and Verducci, J., *Tetrahedron Lett.*, 36(1995)4425.
9. Rich, D.H., Bhatnagar, P.K., Bernatowicz, M.S., In Siemion, I.Z, Kupryszewski, G. (Eds.), *Peptides 1978*, Wroclaw University Press, Poland, 1979, p.349.

# Investigation of conformational properties of calcium-binding peptides in the cell adhesion molecules

Wei Yang<sup>a</sup> and Jenny J. Yang<sup>b</sup>

<sup>a</sup>Department of Biology, <sup>b</sup>Department of Chemistry,  
Georgia State University, Atlanta, GA 30302, USA

Cadherins are calcium-dependent surface molecules that are fundamental to controlling the development and maintenance of tissues. It has been reported that single amino acid substitutions in the putative Ca(II) binding "motif B" of the N-terminal domain (D135A and D135K) abolish the adhesion function of cadherin. In order to establish the relative importance of the calcium ligand in determining the coordination geometry and affinity of metal binding and unravel calcium function of cadherin in cell adhesion, we have synthesized two peptide analogs with altered calcium binding ligands encompassing motif B (residues from 129 to 145)[1]. Peptide 129-145 corresponds to the native calcium binding sequence. A potentially stronger calcium binding motif is constructed using Asp to replace Ala at position 133 (peptide 129-145/A133D). The modified peptide contains ligands that are the same as those of the calcium binding loop of  $\alpha$ -lactalbumin. Here we focus on the conformational and ion binding properties of these peptides using CD, fluorescence and high resolution NMR.

P129-145 from E-cadherin	AC-MKVSATDADDDVNTYNA-NH <sub>2</sub>
P129-145/A133D	AC-MKVS <del>D</del> TADDDVNTYNA-NH <sub>2</sub>
Human $\alpha$ -lactalbumin (78-94):	DKFLDDDDITDDIMCAKK

## Results and Discussion

The conformational properties of peptides P129-145 and P129-145/A133D have been examined by far uv CD. These peptides have little regular secondary structure at 25 °C (10 mM Tris, 1mM EGTA, pH 7.5). When pH values are lower than 4, the ellipticity at 222 nm for both peptides increased slightly, suggesting an increase of helical conformation at lower pH. The addition of KCl up to a concentration of 200 mM had no observable effect on the conformation of the peptides. The addition of organic solvents, such as methanol, trifluoroethanol (TFE) and 1,1,1,3,3,3-hexafluoro-2-propanol changed the conformation of both peptides with the increase of negative molar ellipticity at 222 nm and a decrease of the signal at 198 nm. However, the helical structure induced (from 8% in water to 19% in 80% TFE) was relatively small, which is in agreement with the low intrinsic helical propensities of both sequences. At pH 7.5, essentially no concentration dependence was observed at 198 nm over the concentration range from 5 to 100  $\mu$ M for both peptides both in water and 50% methanol.

The calcium binding abilities of both peptides were examined in aqueous solution and organic solvents. In 10 mM Tris at pH 7.5, no detectable change of the CD and fluorescence spectra of either peptide was observed upon addition of calcium. However,

the addition of calcium resulted in a change of chemical shifts of both peptides in 1D and 2D DPGTOCSY spectra (Fig 1). Calcium had a bigger effect on P129-145/A133D than on P129-145. In 50% methanol, the addition of Ca(II) resulted in significant changes in the far UV CD spectra of the native and modified peptides. These results clearly suggest that the conformation of both peptides is switched by Ca(II). We have been able to measure the Ca(II) binding constant of peptide analogs by monitoring ellipticity at 198 nm as a function of Ca(II) concentration. The Ca(II) affinity of the modified peptide is increased compared with that of native peptide about 5-fold ( $K_d = 0.50$  mM for P129-145 and  $K_d = 0.1$  for P129-145/A133D). In this preliminary work, we have demonstrated that a better Ca(II) binding motif can be designed based on the high affinity structure of a calcium binding protein such as  $\alpha$ -lactalbumin. Further conformational studies on these peptide analogs by NMR and fluorescence will provide us with detailed information about the role of Ca(II) in cadherins.

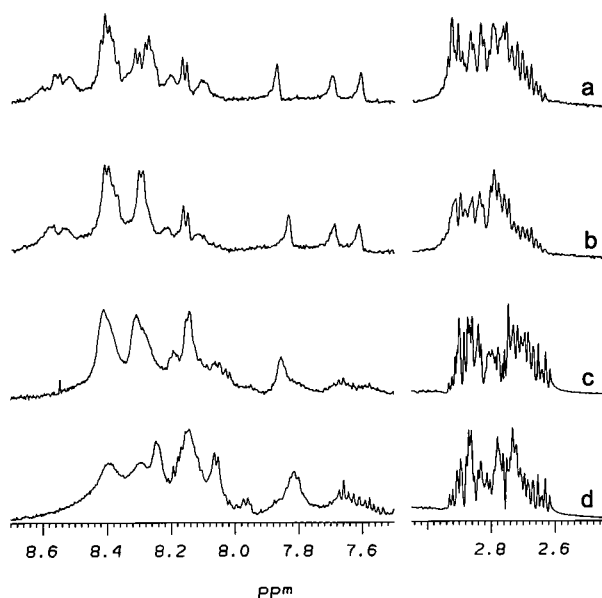


Fig.1. 1D  $^1\text{H}$  NMR spectra of peptide P129-145 in the absence (a) and presence of excess calcium (5 mM  $\text{CaCl}_2$ ) (b), and of peptide P129-145/A133D in the absence (c) and presence of excess calcium (5 mM  $\text{CaCl}_2$ ) (d). Spectra were recorded in 10 mM Tris, 25 °C at pH 7.5 using 500 MHz and 600 MHz NMR.

## References

1. Ozawa, M., Engel, J. and Kemler, R. Cell, 63 (1990) 1033.

# End capping and helix stabilization in short peptides

**Hemender K. Reddy and Krishnan P. Nambiar**

*Department of Chemistry, University of California, Davis, CA 95616, USA*

Designing peptides and proteins that fold into predetermined secondary structures is a challenging biochemical problem [1].  $\alpha$ -Helix, which is a landmark protein secondary structure, has attracted considerable attention in recent years. Several laboratories have been investigating the parameters that influence helix stability [2]. We and others have recently shown that amino acids with side chains capable of hydrogen bonding with the free NH groups at the amino terminus and the free carbonyls at the carboxy terminus have a stabilizing effect on the helical structure of short peptides [2-7]. In order to test the efficacy of various functional groups in amino end capping, we synthesized a series of molecules containing different functional groups capable of hydrogen bonding with free NH groups and incorporated them at the amino terminus of a 15-residue alanine rich peptide. The end capped peptides show high helical content in aqueous solution.

## Results and Discussion

In an earlier report, we had shown that sulfur groups at various oxidation states serve as good amino end capping residues for helix stabilization [8]. The high helicity observed in a short model peptide (X-HN-Ala<sub>4</sub>-Glu-Ala<sub>3</sub>-Lys-Ala<sub>4</sub>-Tyr-Arg-CONH<sub>2</sub>), prompted us to investigate the amino end capping propensities of various common functional groups. Different molecules containing various functionalities were synthesized and incorporated at the amino terminus of the 15-residue model peptide. The end capped peptides show relatively high helicity in aqueous solution.

The potential  $\alpha$ -helix inducing effect of various residues such as acetate, carboxylate, phosphonate, sulfonate and nitrate capable of amino end capping was determined by synthesizing peptides **1-8**. The peptides were synthesized as their carboxamides using PAL resin on a Milligen/Biosearch 9050 peptide synthesizer and Fmoc chemistry and BOP / HOBT activation. The peptides were purified using a reversed phase C<sub>18</sub> HPLC and their primary structure confirmed by quantitative amino acid analysis and mass spectrometry. The peptide concentrations were determined by measuring the absorbance of tyrosine residues at 275 nm at 25 °C in 6M guanidine.HCl. The helix content was measured using a 10  $\mu$ M solution of each peptide by CD at 0 °C in 10 mM phosphate buffer at pH 7. Helical content is taken directly proportional to the mean residue ellipticity at 222 nm  $[\theta]_{222}$  100 % helicity was estimated using the formula  $^{helix}[\theta]_{222} = -40,000 \times [1 - (2.5/n)]$  where n = number of amino acid residues [9].  $\alpha$ -Helicity was independent of peptide concentration in the range of 10-200  $\mu$ M. Table 1 shows the  $\alpha$ -helical content of the peptides. The trend in  $\alpha$ -helix inducing ability was found to be sulfonate > carboxylate > Phosphonate > nitro > acetyl. Our data clearly demonstrate the feasibility of designing

novel molecules which when incorporated into peptides at helical termini can induce helical folding and stabilize folded structures via end capping.

Table 1.  $\alpha$ -Helical content of peptides 1-8

Peptide	X	$-\theta]_{222}^a$ deg.cm <sup>2</sup> .dmol <sup>-1</sup>	Helicity (%) <sup>b</sup>
1	H	5800	17
2	CH <sub>3</sub> CO-	10700	32
3	H <sub>2</sub> O <sub>3</sub> P-CH <sub>2</sub> -CO-	14000	42
4	H <sub>2</sub> O <sub>3</sub> P-CH <sub>2</sub> -CH <sub>2</sub> -CO-	17800	54
5	O <sub>2</sub> N-CH <sub>2</sub> -CH <sub>2</sub> -CO-	13800	41
6	O <sub>2</sub> N-(o)-C <sub>6</sub> H <sub>4</sub> -CO-	3500	11
7	HO-CO-CH <sub>2</sub> -CH <sub>2</sub> -CO-	21100	63
8	HO-SO <sub>2</sub> -CH <sub>2</sub> -CH <sub>2</sub> -CO-	24400	73

<sup>a</sup>Mean residue ellipticity  $[\theta]_{222}$  was determined from the CD spectra of 10  $\mu$ M solution of peptides in 10 mM phosphate buffer at pH 7. <sup>b</sup>Percentage helicity was calculated as  $100 \times ([\theta]_{222} / [\theta]_{222}^{\max})$ .  $[\theta]_{222}^{\max} = -40,000 [1 - (2.5/n)]$ , where  $n=15$ .

## Acknowledgement

This research was supported by a grant from National Institutes of health (GM 39822).

## References

1. Creighton, T. E. Proteins: Structures and Molecular Properties, 2nd Ed.; W. H. Freeman and Co., New York, 1993.
2. Forood, B., Feliciano, E. J. and Nambiar, K. P., Proc. Natl. Acad. Sci. USA, 90 (1993) 838 and references cited therein.
3. Bruch, M. D.; Dhingra, M. M.; Gierasch, L. M. Proteins: Struct. Funct. Genet., 10 (1991) 130.
4. Lyu, P. C.; Wemmer, D. E.; Zhou, H. X.; Pinker, R. J.; Kallenbach, N. R. Biochemistry, 32 (1993) 421.
5. Chakrabarty, A.; Doig, A. J.; Baldwin, R. L. Proc. Natl. Acad. Sci. USA, 90 (1993) 11332.
6. Yumoto, N.; Murase, S.; Hattori, T.; Yamamoto, H.; Tatsu, Y.; Yoshikawa, S. Biochem. Biophys. Res. Commun., 196 (1993) 1490.
7. Kemp, D. S., Boyd, J. G. and Muendel, C. C. Nature, 352 (1991) 451.
8. Forood, B.; Reddy, H. K. and Nambiar, K. P., J. Am. Chem. Soc., 116 (1994) 6935.
9. Scholtz, J. M.; Qian, H.; York, E. J., Stewart, J. M.; Baldwin, R. L. Biopolymers, 31 (1991) 1463.

# Novel $\alpha,\alpha$ -disubstituted amino acids for peptide secondary structure control

Christopher L. Wysong, Muna K. Thalji,  
Thad A. Labbe and Robert P. Hammer

Department of Chemistry, Louisiana State University, Baton Rouge, LA 70803, USA

We are interested in water-soluble peptides containing a high percentage of  $\alpha,\alpha$ -disubstituted amino acids ( $\alpha\alpha$ AAs) for both their bioactivity and for their use as molecular design tools. It is known that peptides possessing a high percentage of  $\alpha\alpha$ AAs are potential antimicrobial agents [1]. We envision the lysine-like 4-aminopiperidine-4-carboxylic acid (Api) as a prototypical polar  $\alpha\alpha$ AA [2]. To study the effects of chirality on peptide secondary structure we have developed a novel, chiral  $\alpha\alpha$ AA, 1-amino-3-methylcyclohexane carboxylic acid, H-Ach<sup>3Me</sup>-OH. Using straightforward synthetic methods, we obtain both the “like” (*l*) and “unlike” (*u*) pairs of diastereomerically pure Fmoc-Ach<sup>3Me</sup>-OH in good overall yields (~60% for 3 or 4 steps).

## Results and Discussion

We have recently reported the synthesis of a protected trifunctional  $\alpha\alpha$ AA Fmoc-Api(Boc)-OH [2], which is suitable for use in Fmoc/*t*Bu SPPS strategies. Three-dimensional orthogonal SPPS with Api in which the endocyclic nitrogen of Api can be used as starting point for building the peptide backbone requires that the acid-labile Boc group be replaced with the acid-stable Alloc protecting group. Using the Alloc group rather than the Boc group allows for selective deprotection of the endocyclic nitrogen. Subsequent reactions can be performed on the ring nitrogen without cleaving the peptide from the resin or causing premature cleavage of the N-terminal Fmoc group of the peptide. The Fmoc-Api(Alloc)-OH derivative was synthesized from Fmoc-Api(Boc)-OH as shown in Fig. 1.

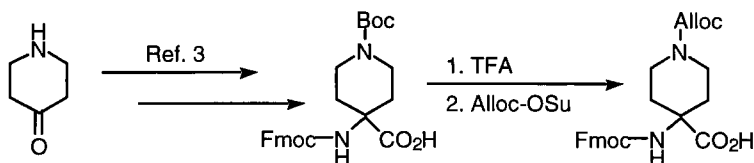


Fig. 1. Synthesis of Fmoc-Api(Alloc)-OH.

Another aspect of our research focuses on cyclic, chiral  $\alpha\alpha$ AAs as controlling factors of peptide secondary structure. In general, synthesis of enantiopure  $\alpha\alpha$ AAs (e.g.,  $\alpha$ MeVal,

$\alpha$ MePhe) is time consuming and involves alkylation of expensive chiral template anions [3]. An alternative strategy uses enantiopure alkylating agents as in the preparation of cyclic BINAP-based  $\alpha\alpha$ AA [4]. In our approach, chiral substituted cyclohexanones provide rapid access to chiral cyclic  $\alpha\alpha$ AAs via Strecker-like chemistry. Thus, Bücherer-Bergs reaction [5] (Fig. 2) of 3-methylcyclohexanone produces the (*l*)-isomers (1*R*,3*R* and 1*S*,3*S*) of the spirohydantoin, which is then converted to Fmoc-(*l*)-Ach<sup>3Me</sup>-OH by basic hydrolysis and protection with Fmoc-OSu.

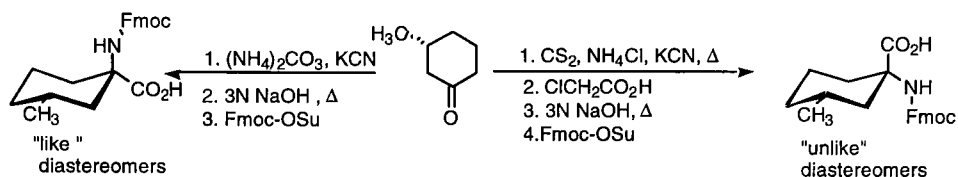


Fig. 2. Synthesis of "like" and "unlike" diastereomers of 1-amino-3-methylcyclohexane carboxylic acid.

When using pure (*R*)-3-methylcyclohexanone as the starting material, the (*S,S*)-isomer is formed in >95% enantiomeric excess as determined by RP-HPLC of the Fmoc-protected (*R*)-phenylethylamide derivative. Alternatively, Carrington modification of the Bücherer-Bergs reaction [5] produces the opposite relative stereochemistry at the  $\alpha$ -carbon, giving the (*u*)-spirodithiohydantoin (1*S*,3*R* and 1*S*,3*R*). The dithiohydantoin is first converted to the (*u*)-spirohydantoin by desulfurization with chloroacetic acid and then transformed to the Fmoc-(*u*)-Ach<sup>3Me</sup>-OH as before.

In conclusion, we have successfully synthesized two new polar  $\alpha,\alpha$ -disubstituted amino acids that are suitable for peptide synthesis. These amino acids are useful additions to the arsenal of peptide chemists, for controlling secondary structure and as tools for molecular design of water-soluble, peptide-based structures. A new approach to chiral and highly enantiomerically enriched  $\alpha\alpha$ AAs has been developed starting from unsymmetrically substituted cyclohexanones.

## References

1. Yokum, T.S., Elzer, P.H., McLaughlin, M.L., *J. Med. Chem.*, 39(1996) 3603.
2. Wirth, T., *Angew. Chem. Int. Ed. Eng.*, 36(1997) 225.
3. Wysong, C.L., Yokum, T.S., Morales, G.A., Gundry, R.L., McLaughlin, M.L., Hammer, R.P., *J. Org. Chem.*, 61(1996) 7650.
4. Mazaleyrat, J.-P., Gaucher, A., Wakselman, M., Tchertanov, L., Guilhem, J., *Tetrahedron Lett.*, 37(1996) 2971.
5. Carrington, H.C., *J. Chem. Soc.*, (1947) 681.

# Design of antimicrobial peptides based on sequence analogy and amphipathicity

**A. Tossi, C. Tarantino, N. Mitaritonna, G. Rocco and D. Romeo**

*Department of Biochemistry, Biophysics and Macromolecular Chemistry, University of Trieste, Trieste I-34127, Italy*

Peptide-based host defense can be considered a pervasive and evolutionarily ancient mechanism of immunity. Antimicrobial peptides have been isolated from all animals and plants in which they have been sought, and so far several hundred different sequences have been characterized in higher organisms [1]. Antimicrobial peptides differ markedly in length, sequence and structure, but share two common traits, in that they are generally polycationic and their active structures are normally amphipathic. A currently accepted classification divides them into two broad classes, cyclic peptides (with one or more S-S bridges) and linear peptides. The most abundant type of linear peptide has amphipathic  $\alpha$ -helical domains. They tend to be short (< 40 residues), easily accessible to solid phase synthesis, and have structures that are well defined and easily characterized.

## Results and discussion

Attempts to obtain artificial antimicrobial peptides of this type have essentially followed three methodologies: modification of natural peptides; *ex novo* design of peptides based purely on physical-chemical properties such as amphipathicity; and synthesis of peptides based on conformationally constrained combinatorial libraries [2,3].

We have developed an alternative method for the *ex novo* design of  $\alpha$ -helical antimicrobial peptides which is based on the comparison of sequences from naturally occurring peptides with  $\alpha$ -helical domains and extracting sequence patterns which are favoured by this type of peptide. These patterns were then used to construct peptides with an elevated helix-forming potential, in such a way as to maintain high amphipathicity (Table 1). Other potentially important features, such as cationicity and hydrophobicity, were also considered. Determination of the most frequent types of amino acids over 20 positions for 85 different sequences allowed the design of a first peptide. The design of three further peptides was based on the comparison of eight sequences from  $\alpha$ -helical peptides derived from the mammalian Cathelicidin family of precursors [4,5]. The four peptides were synthesized in the solid state using Fmoc chemistry, with cycles aimed at maximizing the yield. After purification and mass determination, CD analysis showed that they undergo a transition from random coil in aqueous solutions to an  $\alpha$ -helical conformation on addition of TFE, confirming the amphipathic nature of the helices. The peptides displayed a potent antimicrobial activity against selected Gram-positive and Gram-negative bacteria, including some antibiotic resistant strains, and fungi (Table 1). Permeabilization of both the outer and cytoplasmic membranes of *E. coli* by selected

peptides was found to be quite rapid at concentrations close to the MIC value, and a dramatic drop in colony forming units (CFU) was observed after 5 min in time-killing experiments. At comparable concentrations, permeabilization of the cytoplasmic membrane of *S. aureus*, was instead initially quite slow, gathering speed only after about 45 min, which corresponds to the time required for significant inactivation in time-killing studies.

*Table 1. Sequence, amphipathicity and antibacterial activity of synthetic peptides.*

Peptide	Sequence	$\mu\text{H}(\delta)^a$	<i>E.c</i> <sup>b</sup>	<i>S. t</i>	MIC ( $\mu\text{M}$ )				
					<i>P. m</i>	<i>S. a</i>	<i>B. m</i>	<i>A. n</i>	
PGAa	GILSKLKGKALKKAAKHAACA-NH <sub>2</sub>	3.7 (98°)	8	8	>32	8	4	16	
PGG	GLLRRLRKKIGEIFKKYK-OH	4.2 (96°)	2	1	nd	4	4	nd	
PGYa	GLLRRLRDFLKKIGEFKKIGY-NH <sub>2</sub>	4.5 (100°)	4	4	>32	4	1	8	
PGP	GRFRRLGRKFKKLFKKYGP-OH	4.1 (102°)	4	8	nd	8	8	nd	

<sup>a</sup> Maximum mean hydrophobic moment (not normalized), calculated over the entire sequence, corresponding to the side chain projection angle  $\delta$  (shown in parentheses).

<sup>b</sup> *E.c*, *S. t*, *P. m*, *S. a*, *B. m*, *A. n* refer to *E. coli*, *S. typhimurium*, *P. mirabilis*, *S. aureus*, *B. megaterium* and *A. niger*, respectively.

The cytotoxic activity of the peptides was determined on normal and transformed cell lines, and was found to be generally low at values corresponding to the MIC. Marked cytotoxicity was observed only at over 100  $\mu\text{M}$ .

In conclusion, we have shown that it is possible to obtain quite potent artificial antimicrobial agents by comparing the sequences of naturally occurring peptides and abstracting significant patterns that are to be included in relatively short sequences. The results of biological activity studies, carried out with the designed peptides, are in line with a currently accepted model for their mechanism of action [6] involving permeabilization of the cytoplasmic membrane. Furthermore, both membrane permeabilization and bacteriocidal activity are slower against Gram-positive than Gram-negative bacteria. This is possibly due to the presence of a thick, multilayer peptidoglycan layer and of teichoic and teicuronic acids in the former, which may act to slow down the approach to the cytoplasmic membrane.

## References

- 1 Sequences available in the AMSDB database at: <http://www.univ.trieste.it/~nirdbbcm/antimic.html>.
- 2 Maloy, W., and Kari, U., *Biopolymers*, 37(1995)105.
- 3 Blondelle, S.E., and Houghten, R.A., *Trends Biotechnol.*, 14(1996)60.
- 4 Zanetti, M., Gennaro, R., and Romeo, D., *FEBS Lett.*, 374(1995)1.
- 5 Storici, P., Tossi, A., Lenarcic, B., and Romeo, D., *Eur. J. Biochem.*, 238(1996)769.
- 6 Nicholas P., and Mor A., *Annu. Rev. Microbiol.*, 49(1995)277.

# Synthesis and structural characterization of the ligand binding site of macrophage scavenger receptor

Hironobu Hojo,<sup>a</sup> Yoshiko Akamatsu,<sup>a</sup> Yu Nakamura,<sup>b</sup> Shunji Miki,<sup>c</sup>  
Kiyoshi Yamauchi<sup>a</sup> and Masayoshi Kinoshita<sup>a</sup>

<sup>a</sup>Department of Bioapplied Chemistry, Faculty of Engineering, Osaka City University, Sugimoto 3, Sumiyoshi-Ku, Osaka 558, Japan, <sup>b</sup>Department of Neuropsychiatry, Osaka University Medical School, 2-2 Yamadaoka, Suita, Osaka, 565, Japan, <sup>c</sup>Nissei Hospital, 6-3-8 Itachibori, Nishi-Ku, Osaka 550, Japan.

The macrophage scavenger receptor (SR) mediates the endocytosis of modified LDLs. These ligands, when incorporated in excess, promote the conversion of macrophages into foam cells, which may result in arterial sclerosis. The modified LDL-binding site in human SR is located in the collagen-like domain (HSR(323-341): Ala-Gly-Arg-Pro-Gly-Asn-Ser-Gly-Pro-Lys-Gly-Gln-Lys-Gly-Glu-Lys-Gly-Ser-Gly) [1]. In the present study, a new synthetic strategy for trimeric peptides was developed and applied to the syntheses of HSR(323-341) models (Fig. 1). The effect of spacer (X) on the structure was characterized by CD.

## Results and Discussion

The method developed here enables the crosslinking of peptide chains one by one at their *N*-termini to generate trimeric peptides. To accomplish this strategy, two peptides were prepared by the solid-phase method: a peptide which has a glutamic acid  $\alpha$ -thioester at its *N*-terminus (**xa**,  $x=1-4$ ) and the same peptide without the glutamic acid (**xb**). The synthetic procedure for peptides **xa** is shown in Fig. 2a. Peptides **xb** were prepared as **xa** except that Fmoc group was introduced instead of Fmoc-Glu-SCH<sub>2</sub>CH<sub>2</sub>COOEt and removed after the introduction of Boc groups. Crosslinking was achieved by the activation of the thioester group (Fig. 2b) [2]. Peptides **xa** and **xb** were dissolved in DMSO in the presence of HOSu and silver ions were added. The coupling reaction proceeded without serious side reactions to give dimers **xc**. After Fmoc group was removed, **xc** was crosslinked with **xa**. The reaction for peptides **2** and **3** proceeded at room temperature. In contrast, heating to 90°C was required to initiate the condensation for peptides **1** and **4**. This fact might show that peptides form triple-helix like structure in DMSO and that the spacer of peptides **1** and **4** can not provide enough length to connect peptide chains. After the removal of protecting

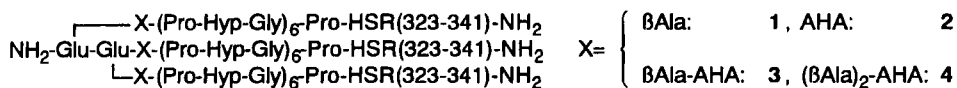


Fig. 1. Structure of triple helical peptide prepared.

groups, the crude product was purified by GFC and HPLC to give peptides **1-4**. Mass and amino acid analyses confirmed that highly pure peptides were obtained. The yield of peptides **1, 2, 3, 4** were 10%, 20%, 20%, 2% based on dimers **xb** ( $x=1-4$ ), respectively.

CD spectra show that the peptides **1-4** are at the triple helical state at 10°C and at the random state at 75°C (Fig. 3). At 10°C  $[\theta]_{224}$  is higher in peptides **2** and **3** than **1** and **4**. In contrast,  $[\theta]_{224}$  of all peptides are comparable at 75°C. This fact may indicate that peptides **2** and **3** have higher helix contents than **1** and **4** at 10°C. Thus, it is suggested that AHA or  $\beta$ Ala-AHA as spacers are the practical option for ease of preparation of trimers and of the helix content of the trimers. A modified LDL binding experiment is under study.

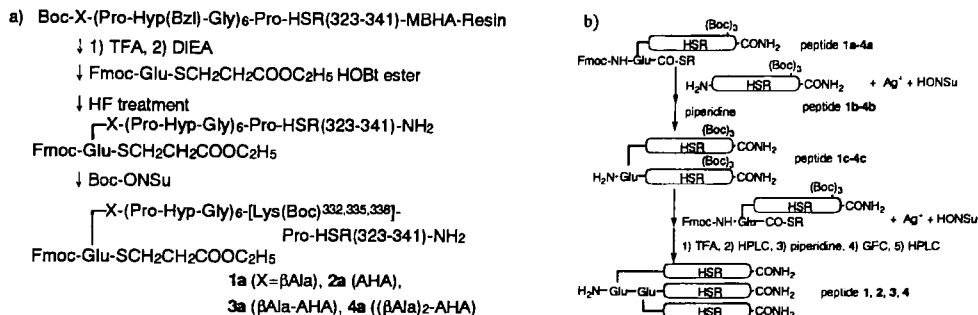


Fig. 2. Preparation of peptides. a) Synthetic route for peptides **1a-4a**. b) Synthetic route for trimeric peptides.

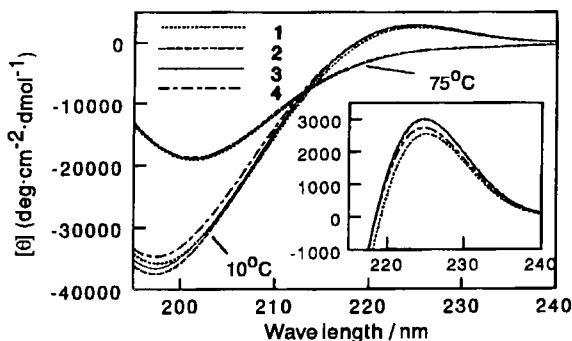


Fig. 3. CD spectra of peptides.

## References

1. Brown, M.S. and Goldstein, J.L., *Annu. Rev. Biochem.*, 52 (1983) 223.
2. Hojo, H., Yoshimura, S., Go, M. and Aimoto, S., *Bull. Chem. Soc. Jpn.*, 68 (1995) 330.

# Enantiomeric structural libraries of unnatural peptides which bind DNA and alter enzymatic activity

L. M. Martin, B-H. Hu and C. Li

Department of Biomedical Sciences, College of Pharmacy, University of Rhode Island,  
Kingston, RI 02881-0809, USA

The intent of this study was to explore comprehensively the conformational possibilities of a set of DNA-binding peptides containing C-terminal amides (Fig. 1). First, potential peptide conformations were computer generated to determine possible low-energy solution conformations and DNA-binding modes. Second, solid-phase peptide synthesis was used to produce an enantiomeric tetrapeptide library [1] comprised of unnatural amino acids. The solution properties of all 16 possible tetrapeptides were determined by RP-HPLC (Fig. 2a). All of the tetrapeptide amides generated in the library were found to bind to DNA, and their DNA-binding affinities were compared by a novel approach to affinity capillary electrophoretic analysis(ACE) (Fig. 2b).

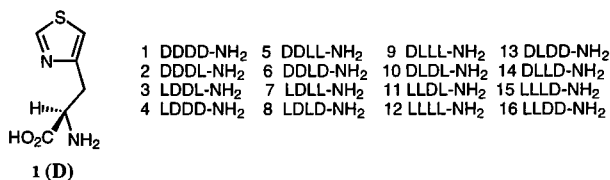


Fig. 1. D: D-(3)-(4-thiazolyl) alanine.

L: L-(3)-(4-thiazolyl) alanine.

## Results and Discussion

A peptide library of sixteen individual tetrapeptide amides was constructed using the unnatural amino acids D-3-(4-thiazolyl)alanine **1** and L- 3-(4-thiazolyl)alanine **2** (obtained from Synthetech, Inc., Albany, OR, USA) on a simultaneous multiple peptide synthesizer. Peptide syntheses were carried out using a MBHA resin and the BOC strategy. BOC deprotection and amino acid coupling reactions were monitored by the ninhydrin reaction. HF cleavage of the product peptides from the solid support was performed without adding any scavenger. The peptide products were analyzed by RP-HPLC and CZE (15 mM Tris, 10 mM MgCl<sub>2</sub>, 1 mM DTT, 30 mM KCl pH 7.85 at 20°), and identified by <sup>1</sup>H-NMR analysis. The crude products were homogeneous by both HPLC and CE (not shown), and were used in binding and topoisomerase I inhibition studies without further purification. Topoisomerase I inhibition assays (50 mM Tris, 0.1 mM EDTA, 1 mM DTT, 50 mM NaCl pH 7.5 at 37°) were performed using pBR322 supercoiled ds DNA (2.8 x 10<sup>3</sup> kD, 4,363 bp) after preincubation with the peptide drug, in duplicate. Digests were run at 37° for 30 minutes and the products analyzed by agarose gel electrophoresis (1% agarose, 89 mM Tris-borate, 2.5 mM EDTA, pH 8.2) and stained with ethidium bromide (0.05% for 45 minutes) [2]. The effects from the order of enantiomers in the tetrapeptide upon the overall hydrophobicity (as measured by HPLC [3]) of the peptide was striking (Fig. 2a). Molecular modeling, with MMII energy minimization using the CACHE system (Oxford Molecular Group), indicates that each peptide has different types of low-energy

conformations available to it, depending upon the ability of the backbone carbonyl to interact with the thiazole ring, and this conformational heterogeneity may explain the RP-HPLC results.

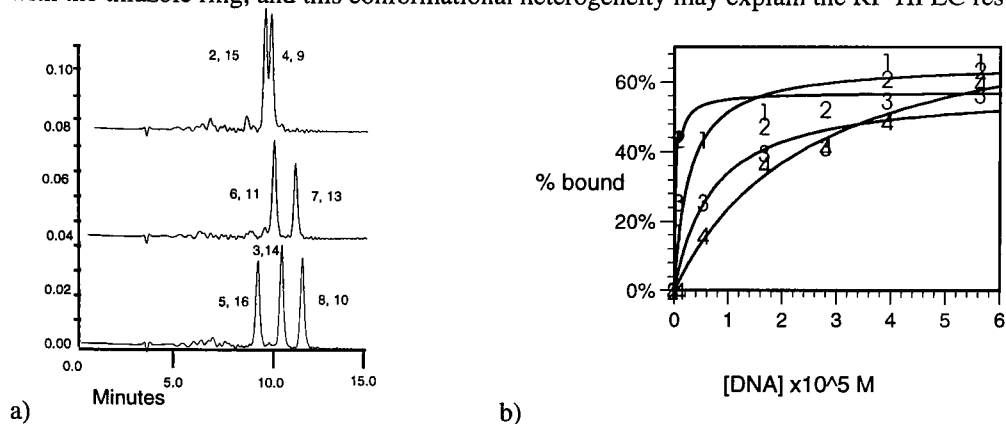


Fig. 2. a) RP-HPLC traces at 220 nm showing differential hydrophobicities of peptides in the libraries. b) Results of binding experiments using affinity capillary electrophoresis of the peptide-DNA complex.

Both the HPLC conformational and the CE / topo I bioassay results highlight the role of a single amino acid in determining the overall conformation of the peptide. Our study offers a systematic look at the interplay between chirality of the monomers and helix nucleation. Although all of the designed peptides bind to double-stranded DNA, as determined by ACE, they exhibited diverse double-stranded DNA-binding affinities. The DNA unwinding enzyme, topoisomerase I, was inhibited by some of the peptides and studies are ongoing to determine the structure-activity profiles of the peptides. Because drug inhibition of topo I activity has been correlated with antineoplastic activity *in vivo*, so the ability to control topo I activity in the peptide design process may lead to a better understanding of the mechanism of topo I inhibition [4]. Only the peptides with a single enantiomeric amino acid in the second position (peptides 7 and 13) consistently inhibited topoisomerase cleavage of the test DNA. With regard to topo I inhibition there seems to be no preference for one enantiomeric peptide over the other, indicating that diastereomeric interactions between the peptide and DNA did not affect topoisomerase inhibition in this library. Conformational space may be experimentally mapped using combinatorial techniques and readily correlated with the results of biological activity measurements. A small library was used to efficiently probe one aspect of peptide-DNA interaction and forces such as those arising from hydrogen-bonding and shape complementarity could be assessed. Ongoing efforts are aimed at improving the binding constants of the peptides to DNA, and exploring other constrained amino acid side chains with different topologies.

## References

1. Houghten, R. A., Proc. Natl. Acad. Sci. U.S.A., 82 (1985) 5131.
2. Rodriguez-Campos, A., Azorin, F. and Portugal, J., Biochem., 35 (1996) 11177.
3. Guo, D., Mant, C. T., Taneja, A. K., Parker, J. M. R. and Hodges, R. S., J. Chrom., 359 (1986) 499.
4. Chen, A. Y. and Liu, L. F., Ann. Rev. Pharmacol. Toxicol., 34 (1994) 191.

# Interplay of hydrophobicity and electrostatics in peptide-bilayer interactions

Li-Ping Liu and Charles M. Deber

*Division of Biochemistry Research, Hospital for Sick Children, Toronto, Ontario M5G 1X8; and  
Department of Biochemistry, University of Toronto, Toronto, Ontario M5S 1A8, Canada*

In previous studies, we established a 'threshold hydrophobicity' that dictates the interaction of peptides with membranes [1,2]. Based on this 'threshold hydrophobicity' hypothesis, membrane-interactive sequences can be divided into two groups: (1) intrinsically hydrophobic; and (2) hydrophobic/hydrophilic. The first group, which possesses a generally non-polar primary sequence of segmental hydrophobicity above the 'threshold value,' can insert into membranes spontaneously from an aqueous phase. The second group, whose segmental hydrophobicity is below the 'threshold hydrophobicity' because it contains some relatively polar side chains, can nevertheless interact with membranes efficiently if facilitated by intermediate assistance through electrostatic binding to oppositely-charged lipid head groups [2]. In this work, we describe two peptides that have similar structural features but differ from each other in hydrophobicity [1]. Their interactions with negatively-charged phospholipid vesicles are evaluated quantitatively and the salt effects on these interactions are examined.

## Results and Discussion

The 'X' residues in the 'host-guest' peptide model Lys-Lys-Ala-Ala-Ala-X-Ala-Ala-Ala-Ala-Ala-X-Ala-Ala-Trp-Ala-Ala-X-Ala-Ala-Ala-Lys-Lys-Lys-Lys-amide were replaced by Met and Gln, respectively. These substitutions were chosen because Met and Gln have similar side chain steric requirements, and both have a positive tendency to form  $\alpha$ -helix in aqueous environments [3]. This helix forming tendency is crucial as we employ  $\alpha$ -helical content to monitor their conformations in water as well as in contact with lipids.

In aqueous buffer, both Met and Gln peptides form partially  $\alpha$ -helical conformations (Fig. 1a). Upon titrating the peptides with negatively-charged dimyristoyl-phosphatidylglycerol (DMPG) vesicles, their helical content increased with the addition of lipid and subsequently reached a maximum level when the lipid/peptide ratio was 100/1 (Met peptide) and 150/1 (Gln peptide), respectively (Fig. 1b). Based on the titration experiments, the interaction of the peptides with vesicles can be evaluated quantitatively by an apparent binding constant ( $K_{app}$ ), which represents the affinity of the peptide to the lipid vesicles.  $K_{app} = C_b / (C_1 \times C_f)$ , where  $C_b$  is the lipid-associated peptide concentration,  $C_1$  is the lipid concentration [for small unilamellar lipid vesicles (SUVs), only the outer leaflet (~60% of total lipid) is involved in peptide binding], and  $C_f$  is the unbound peptide concentration [4]. In the present systems, the estimated apparent binding constants of Met and Gln peptides are  $3 \times 10^4$  and  $1 \times 10^4$  M<sup>-1</sup>, respectively. Values of  $K_{app}$  can be converted

into the free energy of binding according to  $\Delta G = -RT\ln K_{app}$ , from which  $\Delta G = -6.10$  kcal/mol for Met peptide, and  $-5.45$  kcal/mol for the Gln peptide.

These calculation indicate that the binding affinities of the two peptides to DMPG vesicles are very similar. This result can be attributed, in principle, to the availability to both peptides of strong electrostatic interactions between the Lys residues and the negatively-charged lipid head groups. However, a more physically meaningful analysis separates the electrostatic interaction from the hydrophobic penetration. As it is known that adding concentrated salt to lipid vesicles will screen electrostatic contributions, this method can be used to 'separate' the two types of interactions. When we examined a sample containing  $20 \mu\text{M}$  peptide,  $4 \text{ mM}$  vesicles +  $400 \text{ mM}$  NaCl, the interaction between the Gln peptide with DMPG vesicles was dramatically diminished, as judged by the observation that its  $\alpha$ -helical content remained identical to that in aqueous buffer (Fig. 1c). In contrast, upon vesicle addition the  $\alpha$ -helical content of the Met peptide increased as much as in  $10 \text{ mM}$  NaCl, demonstrating that hydrophobicity is the major driving force for the Met peptide penetration into vesicles. The present study supports the proposition that their abilities to insert into membranes are likely governed by distinct mechanisms.

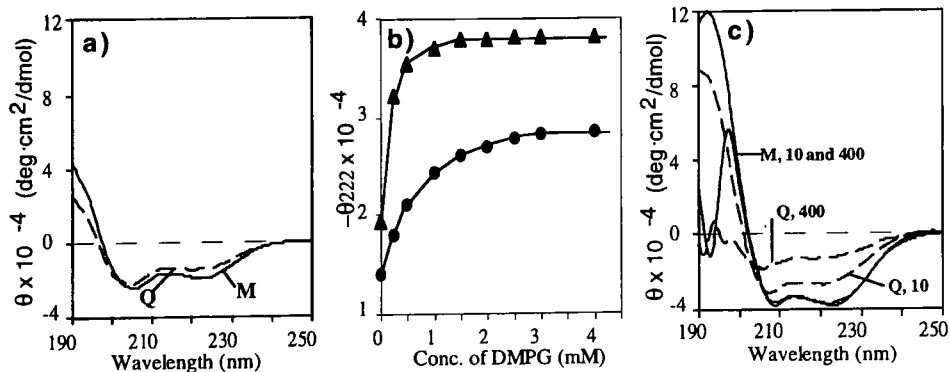


Fig. 1. (a) CD spectra of model peptides (see text) in  $10 \text{ mM}$  Tris-HCl,  $10 \text{ mM}$  NaCl buffer ( $\text{pH} = 7.0$ ). Peptide concentration =  $20 \mu\text{M}$ . (b) Increment of molar ellipticity ( $222 \text{ nm}$ ) of Met (▲) and Gln (●) peptides on addition of DMPG SUVs. (c) CD spectra of Met (solid lines) and Gln (dashed lines) peptides in DMPG SUVs in  $10 \text{ mM}$  NaCl or  $400 \text{ mM}$  NaCl.

## References

1. Liu, L.-P., Li, S.-C., Goto, N.K. and Deber, C.M., *Biopolymers*, 39(1996)465.
2. Liu, L.-P. and Deber, C.M., *Biochemistry*, 26(1997)5476.
3. Chou, P.Y. and Fasman, G.D., *Annu. Rev. Biochem.*, 47(1978)251.
4. Ben-Tal, N., Ben-Shaul, A., Nicholls, A. and Honig, B., *Biophys. J.*, 70(1996)1803.

## **An investigation of position 3 in arginine vasopressin (AVP)**

**M. Manning,<sup>a</sup> S. Stoev,<sup>a</sup> L. L. Cheng,<sup>a</sup> A. Olma,<sup>a</sup> W. A. Klis,<sup>a</sup>  
W. H. Sawyer,<sup>b</sup> N. C. Wo<sup>c</sup> and W. Y. Chan<sup>c</sup>**

<sup>a</sup>*Dept. of Biochemistry and Molecular Biol, Medical College of Ohio, Toledo, OH 43699, USA*

<sup>b</sup>*Dept. of Pharmacology, Columbia University, New York, NY 10032, USA*

<sup>c</sup>*Dept. of Pharmacology, Cornell University Medical College, New York, NY 10021, USA*

Based on studies on lysine vasopressin (LVP) (peptides A-C, Table 1) [1] and on a recent study on AVP (peptide D, Table 1) [2], position three in AVP has long been considered intolerant of change. Consequently, position three in AVP has been largely unexplored. Our interest in investigating this position was sparked by our recent findings that position three in the non-selective AVP V<sub>2</sub>/V<sub>1a</sub> antagonist d(CH<sub>2</sub>)<sub>5</sub>[D-Tyr(Et)<sup>2</sup>]VAVP surprisingly tolerates a broad spectrum of structural change with retention of moderate to full antidiuretic (V<sub>2</sub>-receptor) antagonism[3]. We now report the synthesis and preliminary pharmacological properties of 12 new AVP position 3 analogs (Table1).

### **Results and Discussion**

The antidiuretic potencies of peptides 1-6 (Table 1) range from 0.46 to 20.3 units/mg as opposed to 323 units/mg for AVP. Similarly, these 6 peptides have vasopressor (V<sub>1a</sub> receptor) potencies ranging from 0.003 to 8.99 units/mg compared to 396 units/mg for AVP, confirming earlier findings that position 3 in AVP, like LVP, is intolerant to modifications with polar, aromatic and conformationally restricted amino acids [1,2]. In striking contrast, as the antidiuretic data for peptides 8-12 clearly indicate, position 3 in AVP is highly tolerant to structural changes with a broad range of aliphatic amino acids. Thus, peptides 8-12 exhibit antidiuretic potencies ranging from 86.7 to 249 units/mg. The Leu<sup>3</sup> and Nle<sup>3</sup> analogs (peptides 8 and 9) are in fact equipotent with AVT (231 units/mg) as antidiuretic agonists. However, while peptides 1-12 are significantly less potent than AVT as oxytocic agonists, peptides 7, 8 and 11 are more potent than AVP. With diminished vasopressor potencies, peptides 8-12 also exhibit significant enhancements in antidiuretic/vasopressor selectivity relative to AVP. The high antidiuretic potency of peptide 7 (379±14 units/mg) confirms the early promise of the thienylalanine<sup>3</sup> [Thi<sup>3</sup>] modification in V<sub>2</sub> agonist design [4].

### **Conclusion**

The findings on peptides 7-12 provide useful clues for the design of potent and selective AVP V<sub>2</sub> agonists and also show that further study of position 3 in AVP agonists is well warranted.

Table 1. Some Pharmacological Properties of Position 3 Modified Analogs of AVP.

No.	Peptide	Antidiuretic Act. U/mg	Vasopressor Act. U/mg	Oxytocic Act. U/mg
	AVP <sup>a</sup>	323±16	396±6	13.9±0.5
	AVT ([Ile <sup>3</sup> ]AVP) <sup>b</sup>	231±30	160±4	127±9
	LVP ([Lys <sup>8</sup> ]VP) <sup>a</sup>	~260	285±21	5±0.5
	LVT([Ile <sup>3</sup> ,Lys <sup>8</sup> ]VP) <sup>b</sup>	25±3	133±13	80±10
A	[Ser <sup>3</sup> ]LVP <sup>b</sup>	~0.02	<0.01	<0.01
1	[Ser <sup>3</sup> ]AVP <sup>c</sup>	3.23±0.39	0.38±0.01	0.02±0.003.
B	[Trp <sup>3</sup> ]LVP <sup>b</sup>	-	~0.07	<0.01
2	[Trp <sup>3</sup> ]AVP <sup>c</sup>	1.60±0.18	0.31±0.01	~0.01
C	[Tyr <sup>3</sup> ]LVP <sup>b</sup>	0.18±0.08	1.6±0.2	~0.01
3	[Tyr <sup>3</sup> ]AVP <sup>a,c</sup>	20.3±2.2	4.93±0.20	0.026±0.003
4	[2-Nal <sup>3</sup> ]AVP <sup>c,d</sup>	1.53±0.25	3.60±0.21	0.31±0.002
5	[Atc <sup>3</sup> ]AVP <sup>c</sup>	12.7±1.2	8.99±0.44	0.11±0.004
D	[Tic <sup>3</sup> ]AVP <sup>e</sup>	0.91±0.08	0.25±0.03	~0.022
6	[Pro <sup>3</sup> ]AVP <sup>c</sup>	0.46±0.03	<0.003	<0.005
E	[Thi <sup>3</sup> ]LVP <sup>f</sup>	332±32	243±5	19.0±0.5
7	[Thi <sup>3</sup> ]AVP <sup>c</sup>	379±14	360±9	36.2±1.9
8	[Leu <sup>3</sup> ]AVP <sup>c</sup>	229±19	21.4±0.6	2.1±0.2
9	[Nle <sup>3</sup> ]AVP <sup>c</sup>	249±28	84.6±4.3	4.72±0.16
10	[Val <sup>3</sup> ]AVP <sup>c</sup>	114±9	45.0±2.0	11.3±1.6
11	[Nva <sup>3</sup> ]AVP <sup>c</sup>	134±5.	31.2±0.9	28.4±0.2
12	[Abu <sup>3</sup> ]AVP <sup>c</sup>	86.7±2.5	4.29±0.13	0.45±0.03

<sup>a</sup>Ref. 2; <sup>b</sup>Ref. 1; <sup>c</sup>This publication; <sup>d</sup>Reported in ref. 5 as a weak V<sub>2</sub> agonist; <sup>e</sup>Ref. 2; <sup>f</sup>Ref. 4.

### Acknowledgements

We thank Ms. Suzanne Payne for her expert help in the preparation of this manuscript and NIH grants GM-25280 and DK-01940.

### References

1. Jost, K., Lebl, M. and Brtnik, F., CRC Handbook of Neurohypophyseal Hormone Analogs. CRC Press, Inc. 1987, Vol. II, Part 2.
2. Manning, M., Cheng, L.L., Stoev, S., Bankowski, K., Przybylski, J., Klis, W.H., Sawyer, W.H., Wo, N.C. and Chan, W.Y., J. Peptide Sci., 1 (1995) 66
3. Manning, M., Cheng, L.L., Stoev, S., Klis, W.A., Nawrocka, E., Olma, A., Sawyer, W.H., Wo, and Chan, W.Y., J. Peptide Science, 3 (1997) 31.
4. Smith, C.W., Ferger, M.F. and Chan, W.Y., J. Med. Chem., 18 (1975) 822
5. Lammek, B., Czaja, M., Derdowska, I., Rekowski, P., Trzeciak, H.I., Sikora, P., Szkrobka, W., Stojko, R. and Kupryszewski, G., J. Peptide Res., 49 (1997) 261.

# Design and expression of recombinant Rop protein analogs which have metal binding ability

**Takahisa Nakai, Osamu Odawara, Takemune Yasuda and Nobutaka Tani**

*Takasago Research Laboratories, Research Institute, KANEKA Corporation, 1-8 Miyamae-machi, Takasago-cho, Takasago, Hyogo 676 Japan*

We have investigated a possibility of carbon dioxide fixation using materialized peptides. The basic idea is that metal molecules with photo-catalytic activity could be arranged on a peptide matrix by means of the regular three-dimensional structure of  $\alpha$ -helical peptides. According to this idea, we selected the 63 amino acid Rop (Repressor Of Primer) protein[1, 2], which forms a dimer consisting of a four  $\alpha$ -helical bundle, as a peptide template to introduce a functional group for metal binding. Here, we present the design and data on the expression and purification of the Rop protein analogs.

## Results and Discussion

The iminodiacetic acid moiety[3] was designed as a functional group to charge with a metal ion having coordination number four. This functional group is introduced into a peptide by the chemical modification of lysine (Lys) residues using  $\text{ICH}_2\text{COOH}$  or *N,N*-dicarboxymethyl-glycine. The native Rop protein has only three Lys residues which have no regular arrangement in their side chain geometry. In order to make the metal molecules line up on the  $\alpha$ -helices of the Rop protein, we introduced several amino acid mutations by which Lys residues are periodically arranged on the  $\alpha$ -helices, and designed two models, ROP-K6 (Fig. 1) and ROP-K10. Two genes encoding the ROP-K6 and ROP-K10 proteins were designed and synthesized to construct the expression vectors, pUROP-K6 and pUROP-K10. *Escherichia coli* B strain BL21 was transformed with pUROP plasmids. The transformant of pUROP-K6 produced a protein of the expected molecular weight. However, that of pUROP-K10 did not give rise to a protein (Fig. 2).

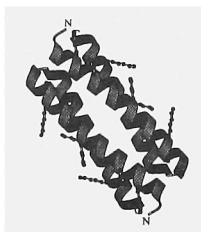


*Fig. 1. A schematic drawing of the model of the ROP-K6 protein. The Lys residues are displayed as ball-and-stick models. The display was generated by the program MOLSCRIPT [4].*

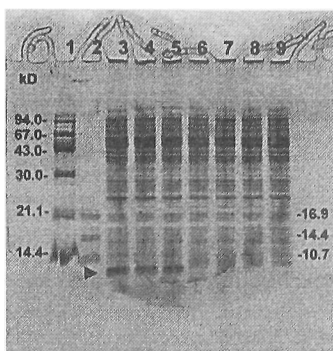


Fig. 2. SDS-PAGE of proteins expressed in recombinant strains of *E. coli* BL21. Lanes 3-5, pUROP-K6; 6-8, pUROP-K10; 9, pUCNT. The molecular weights of standard proteins are shown in lanes 1 and 2.

The purification procedure was developed for the ROP-K6 protein. A large scale (24 l) culture of the recombinant strain of *E. coli* was grown in LB medium plus ampicillin at 37 °C for 20 hr. Recombinant ROP-K6 protein was purified to apparent homogeneity in three steps, (1) incubating 65 °C for 10 min; (2) DEAE-Sepharose; (3) Reversed-phase HPLC, from a crude, soluble fraction obtained after sonication. The ROP-K6 protein was identified by determining the N-terminal amino acid sequence and a time of flight (TOF) mass spectrometry. Purity was checked by SDS-PAGE. The final yield of the purified ROP-K6 protein, from 24 l of bacterial culture, was ~ 160 mg.

## Conclusion

We have designed two Rop protein analogs as a peptide template for testing metal binding ability. The recombinant ROP-K6 product was expressed in *E. coli* B strain BL21 and purified from a cell extract in three steps.

## Acknowledgment

This work was supported in part by The New Energy and Industrial Technology Development Organization (NEDO).

## References

1. Banner, D. W., Cesareni, G. and Tsernoglou, D., *J. Mol. Biol.*, 170(1983)1059.
2. Banner, D. W., Kokkinidis, M. and Tsernoglou, D., *J. Mol. Biol.*, 196(1987)657.
3. Hochuli, E., *Pure & Appli. Chem.*, 64(1992)169.
4. Kraulis, P. J., *J. Appli. Crystallogr.*, 24(1991)945.

# Combination of $\alpha$ -helix peptides with intercalator anthracene for reporting peptide-DNA interactions

**Tsuyoshi Takahashi, Akihiko Ueno and Hisakazu Mihara**  
*Department of Bioengineering, Faculty of Bioscience and Biotechnology,  
Tokyo Institute of Technology, Nagatsuta, Yokohama 226, Japan*

Reporting and sensing DNA recognition are in great demand for elucidating peptide-DNA interactions and developing the sensor devices of DNA manipulations as well as designing therapeutical and diagnostic chemicals [1]. To design sensitive reporter molecules for DNA interaction, we have synthesized  $\alpha$ -helix peptides combined with an artificial intercalator, anthracene, and examined peptide-DNA interactions using anthracene UV, fluorescence and CD properties.

## Results and Discussion

A cationic 16-mer peptide was designed to take an amphiphilic  $\alpha$ -helix structure upon binding to DNA (Fig. 1A). A pair of anthracene (Ant) groups were selectively introduced on the side chains of Lys residues at the 6th and 9th (Ant6,9) or 6th and 10th (Ant6,10) positions to examine how the side-chain chromophores behave *via* DNA binding. The C-terminal Cys residue was employed for future use on a material surface. The peptides were synthesized by the Fmoc solid-phase method with the use of selective protecting groups.

The Ant-peptides were in a random structure in a buffer (pH 7.4) with 40 mM NaCl, whereas an  $\alpha$ -helix structure seemed to be induced *via* binding to calf thymus DNA fragments (Fig. 1B). An increase in ellipticity at 222 nm was observed by the addition of DNA and the extent of increase of Ant6,9 was larger than that of Ant6,10. Furthermore, upon the binding to DNA, CD spectra based on the excitation coupling were remarkably observed at the Ant-region (254 nm). These results revealed that the two Ant groups were fixed to orient in a chiral sense, that is, Ant6,9 showed a left-handed arrangement of the Ant groups, whereas Ant6,10 showed a right-handed one [2]. As a result of the DNA interaction, these chiral signals also indicate  $\alpha$ -helix formation of the peptides. In trifluoroethanol, both peptides took on an  $\alpha$ -helix structure and showed the same sense in the excitation couplings as that bound to DNA. Each sense of the chromophore orientation was dependent on the positions at which the Ant groups were introduced. The peptide with one Ant group (Ant6) did not show strong CD at the Ant region. In the UV measurements, the absorbance of Ant groups was decreased and shifted to a longer wavelength by the addition of DNA. The binding of peptides with DNA was estimated by the site exclusion equation of McGhee and Von Hippel [3]. Both peptides showed binding constants of a  $\mu$ M order: Ant6,9;  $1.3 \times 10^6 \text{ M}^{-1}$  ( $n=4.5$ ), Ant6,10;  $2.4 \times 10^5$

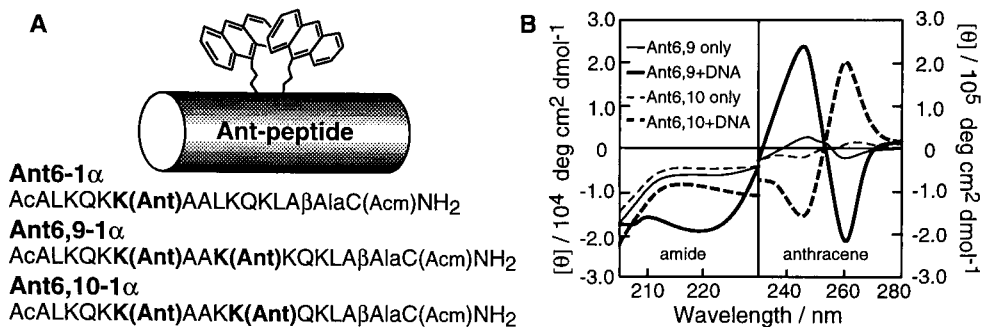


Fig. 1. Structure (A) and CD spectra (B) of Ant-peptides with (135  $\mu$ M) or without ct-DNA. [Peptide]=4.8  $\mu$ M at 25 C.

$M^{-1}$  ( $n=4.0$ ) ( $n$  is the number of base pairs per a binding site). Ant6,9 binds to DNA 5 times more strongly than Ant6,10, although the  $n$  values are almost the same ( $\sim 4$ ). The peptide with a left-handed chiral sense of the chromophore orientation may be a better binder to DNA than that with a right-handed one. As a reference, Ant6 bound to DNA at a binding constant of  $6.4 \times 10^4 M^{-1}$  ( $n=2.8$ ). An increase in number of the Ant-chromophores enhanced the DNA binding ability of the peptide.

On analyzing the CD data by using the number of base pairs per a binding site,  $n$ , the binding constants for titration curves at 222 nm and 245-261 nm were almost comparable to those analyzed by the UV measurements. These results suggest that the peptides fold in an  $\alpha$ -helix structure, the chromophores at the side chains being fixed in a coincidental manner as they are deployed.

The fluorescence intensity of Ant groups was increased by the addition of DNA. The binding constants from these data were also comparable to those obtained from the CD and UV measurements. The Ant groups may bind to a groove at the DNA concentration, when these chromophores are fixed to orient on the  $\alpha$ -helix. The fluorescence intensity of Ant6 was also increased by the addition of DNA.

In conclusion, a new type of peptidyl molecule which bound to DNA was designed and synthesized. In the peptides, anthracene chromophores were fixed to arrange *via* binding to DNA so as to interact with each other at the ground state. This property was utilized to characterize the peptide-DNA binding. The reporting function of chromophores on the  $\alpha$ -helix structure may be applicable to design a sensor device using photo-activity or electro-functions.

## References

1. Douglas, S.J. and Dale, L.B., In Atwood, J.L., Davies, J.E.D. and Vogtle, F. (Eds.), *Comprehensive Supramolecular Chemistry*, Vol 4, Pergamon, UK, 1996, p. 73.
2. Harada, N. and Nakanishi, K., *Acc. Chem. Res.*, 5 (1972) 257.
3. Mcghee, J.D. and Hippel, H.V., *J. Mol. Biol.*, 86 (1974) 469.

## Macroitorials: Concept and synthetic examples using PTH (1-34)

Wanli Ma,<sup>a</sup> Jeffrey A. Dodge,<sup>b</sup> and Arno F. Spatola<sup>a</sup>

<sup>a</sup>Department of Chemistry, University of Louisville, Louisville, KY 40292; <sup>b</sup>Lilly Research Laboratories, Indianapolis, IN 46285, USA

Macroitorials are synthetic peptides that contain a macrocyclic core and two or more appendages. By consolidating a relatively rigid component with diversity in the side arms, the advantages of combinatorial chemistry may be used to probe a given volume of conformational space.

As an initial foray into this new class of molecules, several analogs of parathyroid hormone (PTH 1-34) were synthesized by solid phase methods using orthogonal (Boc and Fmoc) protection. These individual molecules were characterized by amino acid analysis, positive and negative modes of electrospray mass spectrometry, and by PTH binding and functional assay (in progress). Specific sequences are given in Table 1.

Table 1. Structure and physical properties of macroitorials related to PTH; General structure R-X-A-cyclo(Glu-Pro-Ala-Lys)-B-NH<sub>2</sub>

Compound	N-terminal R-X-	HPLC (k')	MW Calc.	MW Found
1	R = H; X = Ala	12.04	2603.8	2603.4
2	R = Ac; X = Ala	12.74	2645.8	2645.7
3	R = H; X = Ser	12.06	2619.8	2619.7
4	R = Ac; X = Ser	12.47	2661.8	2662.1

A = -Val-Ser-Glu-Ile-Gln-Sar-Sar-

B = -Sar-Sar-Arg-Lys-Lys-Leu-Gln-Asp-Val-His-Asn-Phe-

As a more general proof-of-concept, a series of macroitorials were prepared with the following structures:



where G = Gly

X = Glu, His, Phe

Y = Val, Leu, Arg

A series of cyclic tetrapeptides with two N- and C-terminal extensions (7- and 8-mers) was prepared. A total of 6 variable positions and 3 amino acids per position (X and Y) were incorporated in a positional scan mode. X and Y were selected to mimic possible key residues of PTH(1-34) using putative N- and C-terminal binding and message domains [1]. Glycine residues were used as spacer elements.

No significant biological activity was found in the library mixtures; but in this case the selection of amino acid variables was severely limited to assist in mixture characterization. A more serious problem is the inclusion of large numbers of flexible glycine residues at intervening positions. This flexibility was shown to be a significant deterrent to bioactivity in other work from our laboratory [2], undoubtedly due to the much greater array of conformational possibilities and subsequently lower concentration of any given potential pharmacophore.

Molecular modeling comparisons of the library products with intact PTH(1-34) demonstrated reasonable structural similarity, depending on the conformational tendencies selected. More rigid spacer elements would reduce flexibility but simultaneously limit the conformational space being sampled. Future synthetic efforts will focus on discovering the optimal compromise within these limits.

### **Acknowledgements**

Supported by NIH GM33376 and Lilly Research Laboratories.

### **References**

1. Chorev, M. and Rosenblatt, M., In Bilezikian, J.P., Levine, M.A. and Marcus, R. (Eds.), *The Parathyroids*, Raven Press, New York, 1994, pp. 139-156.
2. Wiegandt Long, D.L. and Spatola, A.F. 15<sup>th</sup> American Peptide Symposium, 1997, poster.

# Metal ion-induced folding of a *de novo* designed coiled-coil

W. D. Kohn, C. M. Kay and R. S. Hodges

Department of Biochemistry and the Protein Engineering Network of Centres of Excellence,  
University of Alberta, Edmonton, Alberta, T6G 2H7, Canada

Recently, we have designed environmentally sensitive coiled-coils, which can be induced to fold by changes in salt and pH conditions [1,2]. Subsequently, we have engaged in design of sequences that undergo a random coil to coiled-coil transition upon specific metal ion-binding. Our approach is to destabilize the coiled-coil so that it is prevented from folding under benign pH 7 conditions by incorporation of interhelical ionic repulsions involving residues at the e and g heptad positions. Bridging of a metal ion between residues which repel one another and destabilize the apo-peptide will promote folding. A successful design requires both enough destabilization of the apo-peptide that it is completely or nearly completely random coil and a high metal-binding affinity. To accomplish this goal, the unusual amino acid  $\gamma$ -carboxyglutamic acid (Gla) has been employed (Fig 1A). Here we report on the design of a 35-residue disulfide bridged dimer which undergoes an almost complete random coil to coiled-coil transition upon high affinity binding of  $\text{La}^{3+}$ .

## Results and Discussion

The sequence of the designed metal-binding peptide  $\text{Gla}_2\text{Nx}$  (Fig. 1B) is based on our

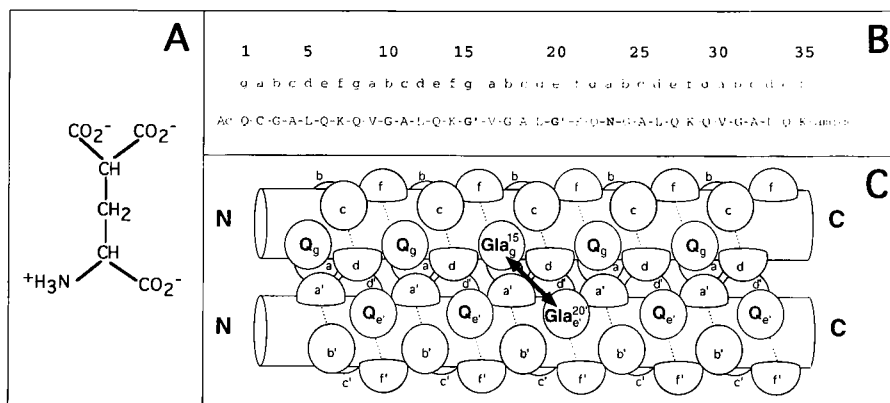


Fig. 1. A, Structure of  $\gamma$ -carboxyglutamic acid (Gla). B, Sequence of the metal-binding coiled-coil  $\text{Gla}_2\text{Nx}$ . Substitutions of Gla (denoted G<sup>1</sup>) for Gln at positions 15 and 20 and Asn for Val at position 23, which distinguish  $\text{Gla}_2\text{Nx}$  from  $\text{Nx}$ , are highlighted in bold type. C, Helical rod diagram representing a side view of the  $\text{Gla}_2\text{Nx}$  coiled-coil.

"native" coiled-coil Nx, which has a  $\Delta G_u$  of 5 kcal/mol and was used as a control in previous studies [2,3].  $\text{Gla}_2\text{Nx}$  is destabilized relative to Nx by the substitution of Asn for Val at the hydrophobic position 23 and by Gla substitutions for Gln at positions 15 and 20. These Gla residues form destabilizing interhelical  $i$  to  $i+5$  (g-e') repulsions [3]. The circular dichroism spectrum of Nx (Fig. 2A) is indicative of a highly helical structure, the spectrum of apo- $\text{Gla}_2\text{Nx}$  is essentially that of a random coil peptide. The molar ellipticity at 222 nm ( $\theta_{222}$  value) is a good measure of helical content.  $\theta_{222}$  for  $\text{Gla}_2\text{Nx}$  is -2,500 compared with -35,200 for Nx. Addition of the helix-inducing solvent trifluoroethanol (50% v:v) causes a large increase in the  $\theta_{222}$  value for  $\text{Gla}_2\text{Nx}$  to -20,900 (59% of the  $\theta_{222}$  value for Nx). Addition of 5 mM  $\text{LaCl}_3$  causes a much larger induction of helical structure in  $\text{Gla}_2\text{Nx}$ , resulting in a  $\theta_{222}$  value of -33. Titration of  $\text{Gla}_2\text{Nx}$  with  $\text{LaCl}_3$  (Fig. 2B) illustrates tight binding. From the initial slope, the stoichiometry is two  $\text{La}^{3+}$  ions per peptide dimer. This result fits with the prediction that one  $\text{La}^{3+}$  ion will be coordinated between Gla residues at positions 15 and 20' and another will be coordinated between Gla residues at 15' and 20 (Fig. 1C). Each metal ion is complexed by four carboxylate groups (up to eight oxygen atoms in the coordination sphere). The data fit a model with two independent binding sites and  $K_D$  of  $0.6 \pm 0.3 \mu\text{M}$ . It was found that  $\text{Ca}^{2+}$  also induced significant helical structure in  $\text{Gla}_2\text{Nx}$  but displayed a very weak binding affinity ( $K_D \sim 18 \text{ mM}$ ). Thus,  $\text{Gla}_2\text{Nx}$  can be specifically induced to fold by a trivalent metal ion.

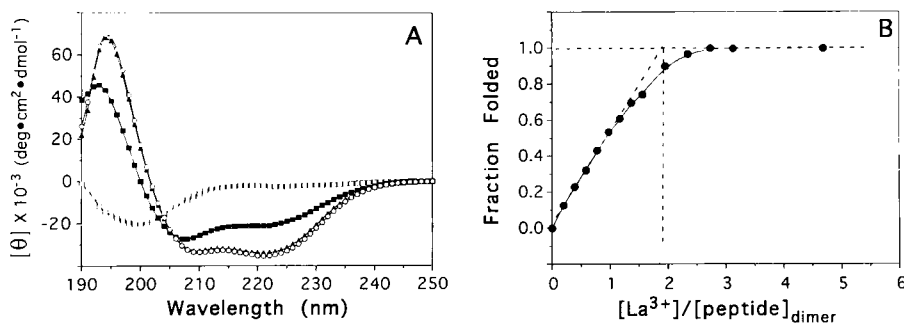


Fig. 2. A, Circular dichroism (CD) spectra of Nx (open circles) and  $\text{Gla}_2\text{Nx}$  (open squares), in 25 mM MOPS, 25 mM KCl buffer, pH 7 at 20°C. Also shown are spectra of  $\text{Gla}_2\text{Nx}$  under the same conditions plus either 50% trifluoroethanol (v:v) (closed squares) or 5 mM  $\text{LaCl}_3$  (closed triangles). B,  $\text{LaCl}_3$  titration of  $\text{Gla}_2\text{Nx}$  as monitored by CD.

## References

1. Zhou, N.E., Kay, C.M. and Hodges, R.S., J. Mol. Biol., 237 (1994) 500.
2. Kohn, W.D., Monera, O.D., Kay, C.M. and Hodges, R.S., J. Biol. Chem., 270 (1995) 25495.
3. Kohn, W.D., Kay, C.M. and Hodges, R.S., Protein Science, 4 (1995) 237.

# $\alpha$ to $\beta$ transitions of peptides caused by hydrophobic defects

Yuta Takahashi, Akihiko Ueno and Hisakazu Mihara

Department of Bioengineering, Faculty of Bioscience and Biotechnology,  
Tokyo Institute of Technology, Nagatsuta, Yokohama 226, Japan

An improved understanding of protein misfolding and off-pathway aggregation [1] is critical to the study of proteins related to amyloid pathogens such as Alzheimer's [2] and prion diseases [3,4], as well as to the clarification of protein folding pathway. In the prion proteins the  $\alpha$ -helix-rich form is transformed to the scrapie isoform with a higher  $\beta$ -sheet content, which initiates fibril formation. In general, hydrophobic clustering seems to be an important feature for peptide transformation. In this study, we applied the concept of hydrophobic defect to design and synthesize a peptide capable of performing an  $\alpha$ -to- $\beta$  structural transition (Fig. 1A).

## Results and Discussion

A two- $\alpha$ -helix peptide was designed as a simplified leucine zipper model, and each N-terminus was modified with an adamantane group (Ad-2 $\alpha$ ) as a hydrophobic defect (Fig. 1B). CD studies revealed that Ad-2 $\alpha$  initially formed an  $\alpha$ -helical structure, but the conformation gradually changed to a  $\beta$ -structure in a neutral aqueous solution after 4 h at 25 °C (Fig. 1C). Gel-filtration analysis indicated that the peptide was in a monomeric 2 $\alpha$ -helix structure at first, and formed aggregates coinciding with the  $\alpha$ -to- $\beta$  transition. The acetylated-2 $\alpha$  (C<sub>2</sub>-2 $\alpha$ ) lacking the hydrophobic defect formed an  $\alpha$ -helical structure, but failed in the transition. One segmental peptide (Ad-1 $\alpha$ ) was in an almost random structure and did not show a transformation. These results suggested that both the hydrophobic defect and the initial  $\alpha$ -helix structure were essential for transformation. Denaturation

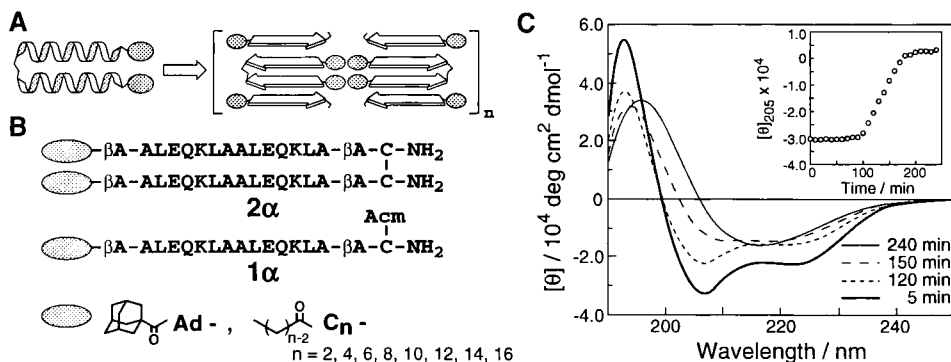


Fig. 1.  $\alpha$ -To- $\beta$  structural transition of the peptides containing hydrophobic defects. (A) Schematic representation of the  $\alpha$ -to- $\beta$  transition. (B) Amino acid sequences of the peptides and hydrophobic groups at N-termini. (C) CD spectral changes and time course of  $[\theta]_{205}$  (inset) of Ad-2 $\alpha$ .  
Table 1. Summary of conformational properties of the peptides with aliphatic chains.

Peptide	Initial state in a neutral aqueous solution			$\alpha \rightarrow \beta$ Transition <sup>b</sup>
	Oligomerization <sup>a</sup>	$-\langle \theta \rangle_{222} / \text{deg cm}^2 \text{ dmol}^{-1}$	$-\Delta G_{\text{H}_2\text{O}} / \text{kcal mol}^{-1}$	
C <sub>2</sub> -2 $\alpha$	1 mer	15 800	0.45	$\alpha$
C <sub>4</sub> -2 $\alpha$	1 mer	15 500	0.86	$\alpha \rightarrow \beta^*$ 14 h
C <sub>6</sub> -2 $\alpha$	1 mer	16 200	1.09	$\alpha \rightarrow \beta^*$ 8 h
C <sub>8</sub> -2 $\alpha$	1 mer	21 000	0.76	$\alpha \rightarrow \beta$ 4 h
C <sub>10</sub> -2 $\alpha$	1-3 mer	25 000	1.74	$\alpha \rightarrow \beta$ 14 h
C <sub>12</sub> -2 $\alpha$	3 mer	25 300	2.88	$\alpha$
C <sub>14</sub> -2 $\alpha$	3 mer	25 600	2.87	$\alpha$
C <sub>16</sub> -2 $\alpha$	3 mer	26 000	2.46	$\alpha$

<sup>a</sup> determined by size exclusion chromatography. <sup>b</sup>  $\alpha$  means that a peptide stays in  $\alpha$ -helix.  $\alpha \rightarrow \beta$  and  $\alpha \rightarrow \beta^*$  denote an almost complete and an incomplete  $\alpha$ -to- $\beta$  transitions, respectively, occurred within indicated periods.

experiments using guanidine hydrochloride revealed that both the  $\alpha$ -helix and  $\beta$ -structure did not possess high stability ( $-\Delta G_{\text{H}_2\text{O}}$  were 1.0 and 2.5 kcal mol<sup>-1</sup>, respectively). The low stabilities in both structures and their small difference seemed to provide the peptide with the ability to undergo a slow transition.  $\beta$ -Cyclodextrin ( $\beta\text{CDx}$ ), which has a high affinity for capturing the adamantane group in the cavity, inhibited the transition of Ad-2 $\alpha$  in a concentration-dependent manner. The addition of 10 equiv. of  $\beta\text{CDx}$  completely inhibited the transition.

To clarify the effects of hydrophobic groups on the  $\alpha$ -to- $\beta$  transition, aliphatic acyl groups with a range of chain lengths (C<sub>2</sub> - C<sub>16</sub>) were attached to the 2 $\alpha$ - and 1 $\alpha$ -peptides (Fig. 1B). It became clear that there was an optimum hydrophobicity for the transitions, and the transitional properties of the peptides seemed to be dependent on the initial  $\alpha$ -helix states (Table 1). The octanoyl-group was most effective for the transition of the 2 $\alpha$ -peptide. The peptides with longer acyl chains (C<sub>12</sub>-, C<sub>14</sub>-, C<sub>16</sub>-2 $\alpha$ ) had a more stable  $\alpha$ -helix structure due to the formation of oligomers, and did not transform. The 1 $\alpha$ -peptides capable of forming  $\alpha$ -helix (C<sub>12</sub>-, C<sub>14</sub>-, C<sub>16</sub>-1 $\alpha$ ) also transformed to a  $\beta$ -structure. The 1 $\alpha$ -peptides with shorter chains were in a random coil and did not transform. These results confirmed that the appropriate hydrophobic defects in  $\alpha$ -helix peptides with low stability are responsible for the  $\alpha$ -to- $\beta$  transitions.

## References

1. Taubes, G., *Science*, 271 (1996) 1492.
2. Selkoe, D. J., *Trends Neurosci.*, 16 (1993) 403
3. Prusiner, S. B., *Science*, 252, (1991) 1515.
4. Harrison, P. M., Bamborough, P., Daggett, V., Prusiner, S. B., Cohen, F. E., *Curr. Opin. Struct. Biol.*, 7 (1997) 53.

# A natural motif approach to protein folding and design [1]

Daniel J. Butcher,<sup>a</sup> M. Anna Kowalska,<sup>b</sup> Song Li,<sup>a</sup> Zhaowen Luo,<sup>a</sup> Simei Shan,<sup>a</sup> Zhixian Lu,<sup>a</sup> Stefan Niewiarowski<sup>b</sup> and Ziwei Huang<sup>a</sup>,

<sup>a</sup> Kimmel Cancer Institute, Jefferson Medical College, Thomas Jefferson University, Philadelphia, PA 19107, USA; <sup>b</sup> Dept. of Physiology, Temple University School of Medicine, Philadelphia, PA 19140, USA

The design of smaller functional mimics of large proteins has long been an important challenge. In this study we use the natural leucine zipper as a structural template to design a 31-residue peptide analog that mimics the function of the larger platelet factor 4 (PF4) protein. The heparin binding activity of PF4 has been introduced into an unrelated leucine zipper sequence only by virtue of incorporating four lysines of PF4. Circular dichroism and binding experiments have shown that the designed leucine zipper peptide adopts a stable helical conformation and shows significant PF4-like heparin binding activity. These results strongly suggest that the lysine residues play an important role in the binding of PF4 to heparin. The *de novo* generation of the PF4 function in a designed leucine zipper peptide demonstrates that the leucine zipper motif is a useful scaffold for the design of functional peptides and proteins.

## Results and Discussion

The heparin binding activity of the designed leucine zipper peptide PF4<sub>zip</sub> was measured by retention on a heparin-agarose column in the presence of increasing NaCl concentrations. Fig. 1 shows that the designed leucine zipper peptide strongly binds heparin like the native PF4 protein. In contrast, no heparin binding activity is observed in the control native leucine zipper peptide GCN4<sub>zip</sub> which contains an identical amino acid sequence except for the three modified lysine residues. These results demonstrate that the remarkable heparin binding activity of the designed leucine zipper peptide is specifically due to the introduction of the lysine residues. Further *in vitro* functional assay studies have shown that the designed leucine zipper peptide also reverses heparin anticoagulation, as determined by the activated partial thromboplastin time (APTT), while the control leucine zipper peptide does not have such activity (data not shown).

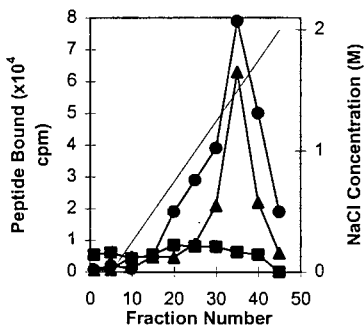


Fig. 1. Heparin binding of the PF4<sub>zip</sub> (●) as compared to the control GCN4<sub>zip</sub> (■) as well as native PF4 (▲)

In order to determine the structural basis for the observed heparin binding activity of the designed leucine zipper peptide, we have carried out circular dichroism (CD) experiments to investigate the solution conformation of this peptide. The CD spectrum of this peptide (Fig. 2) indicates that the peptide adopts a highly helical conformation in aqueous solution. In addition, the peptide displays a two-state melting profile which is typical for a fully folded native protein (data not shown). The  $T_m$  for GCN4<sub>zip</sub> is 55°C and 42°C for PF4<sub>zip</sub>. These results demonstrate that the

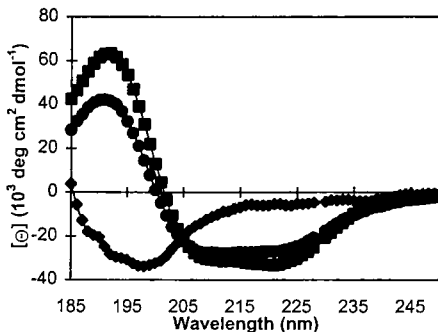


Fig. 2. CD Spectra of PF4<sub>zip</sub> (●) as compared to GCN4<sub>zip</sub> (■) and PF4<sub>58-70</sub> (◆).

designed leucine zipper peptide maintains a native-like helical conformation of the leucine zipper template. In addition, to further investigate the importance of this helical conformation for heparin binding activity, we studied the solution conformation of a peptide comprising the C-terminal helix of PF4 (PF4<sub>58-70</sub>). Although this peptide contains the binding domain of PF4 with the four lysines proposed as heparin binding sites, the peptide has very low binding affinity for heparin. CD spectrum of the peptide shows that it displays a random coil conformation. This explains the loss of binding activity of the peptide and confirms the importance of the helical conformation as a framework for presenting the heparin binding lysine side chains.

## Conclusion

The results of this study demonstrate the feasibility of our method in utilizing leucine zipper motifs as templates to design novel biological properties. The designed leucine zipper peptide adopts a stable conformation and possesses significant PF4-like heparin binding activity. This study suggests that the diverse structural motifs that nature has provided us can be exploited to design new functional peptides and proteins.

## Acknowledgements

These studies were supported in part by grants from the National Institutes of Health, the American Cancer Society, the National Multiple Sclerosis Society and the Sidney Kimmel Foundation for Cancer Research. We would like to thank members of our laboratories and our collaborators for their contribution and helpful discussion. Z.H. is the recipient of the Kimmel Scholar Award in cancer research.

## References

1. Butcher, D.J., Kowalska, M.A., Li, S., Luo, Z., Shan, S., Lu, Z., Niewiarowski, S., Huang, Z., FEBS Letters, 409 (1997) 183

# Engineering of a cationic coiled-coil protein bearing RGD-like ligands on proline-II helical spacers

Harold D. Graham, Jr., Deborah M. John and Bruce W. Erickson

Department of Chemistry, University of North Carolina at Chapel Hill,  
Chapel Hill, NC 27599, USA

A RAMP is a receptor-adhesive modular protein (RAMP) which is designed to bind to two (or more) receptors on the surface of the same cell at the same time [1, 2]. Arg-Gly-Asp (RGD) is a peptide ligand present in some extracellular matrix proteins that binds to certain members of the integrin family of cell-surface receptors. JUDY and JUDF are RGD-like peptides containing 4-amidinobenzoic acid (J) and  $\beta$ -alanine (U) that bind tighter than RGD to these integrins [3, 4]. We have engineered **JUDY-Procoil**, a 90-residue dimeric RAMP containing two JUDY ligands that are each attached to an  $\alpha$ -helical coiled coil by two flexible linkers and a rigid proline-II helical spacer (Fig. 1).

## Results and Discussion

The designed amino-acid sequence of the disulfide-linked dimeric protein JUDY-Procoil is:

```
JUDYXPPPPPPPXLKKLKKKLKKLKKKLKKLKKLKKLKKLKX-
NH2
      . . . . . |
JUDYXPPPPPPPXLKKLKKKLKKLKKKLKKLKKLKKLKKLKX-
NH2
```

where the linker is 6-aminohexanoic acid (X), the diamonds (•) indicate hydrophobic interactions, and the vertical bar (|) is the disulfide bridge between the C-terminal cysteine residues. Each chain of this RAMP contains JUDY as the N-terminal ligand, octaproline

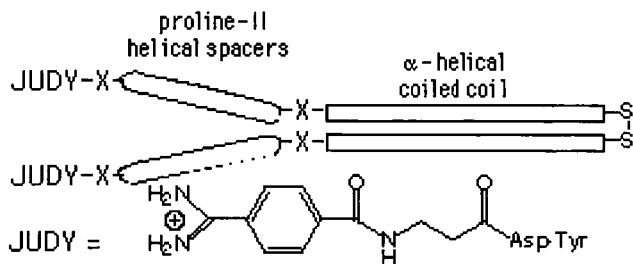


Fig. 1. Modular structure of receptor-adhesive modular protein JUDY-Procoil.

as the spacer, and a highly cationic  $\alpha$  helix. The  $P_8$  spacer should fold into a proline-II helix about 25 Å long. The four-heptad repeat (LKKLKKK)<sub>4</sub> should fold into an  $\alpha$  helix about 42 Å long. The flexible linkers X are each about 5 Å long when extended. The 45-residue monomer should oxidize to form a dimer (Fig. 1). The JUDY ligands could be as much as 65 Å apart and might bind to two integrins. The highly cationic parallel  $\alpha$ -helical coiled coil should have many positive charges on its 40 exterior lysine residues.

We have designed, synthesized, and characterized JUDY-Procoil. The 45-residue monomer was assembled by automated solid-phase synthesis and manual capping with J, purified by RP-HPLC, and air oxidized to afford the 90-residue dimer, which was also purified by RP-HPLC on butyl-silica. ESI mass spectrometry indicated that 80% of the dimer had the J cap on both chains and 20% had it on only one chain. The CD spectrum of a proline-II helix exhibits a strong negative band at 205 nm and a weak positive band at 226 nm; that of an  $\alpha$  helix shows strong negative bands at 208 nm and 222 nm. The CD spectrum of JUDY-Procoil (Fig. 2, left) suggests the presence of both helical types. Reduction of the disulfide bond with dithiothreitol (DTT) abolishes the  $\alpha$ -helical structure while maintaining the proline-II helix (center). Subtracting the latter spectrum from the former reveals the  $\alpha$ -helical coiled coil ( $[\theta]_{222}/[\theta]_{208} = 0.98$ ) that was lost on reduction (right). Thus formation of the disulfide bond induces folding of the cationic coiled coil.

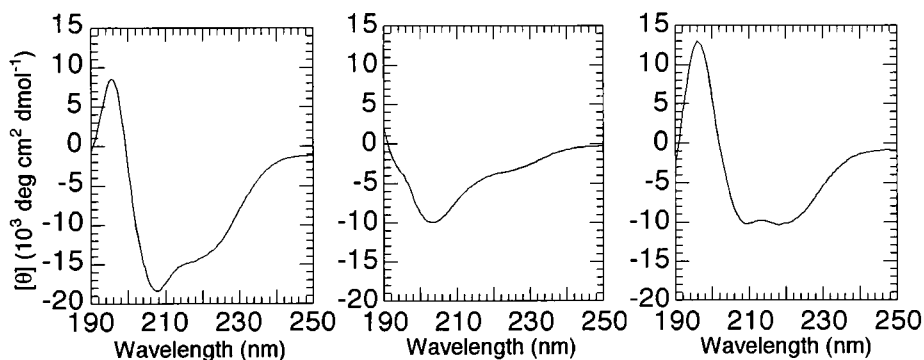


Fig. 2. CD spectra of 0.021 M JUDY-Procoil in 0.05 M phosphate (pH 7.0) and 0.05 M KCl at 25 °C without DTT (left) and with DTT (center) and their difference spectrum (right).

## References

1. Slate, C.A., Weninger, S.C., Church, F.C. and Erickson, B.W., *Int. J. Peptide Prot. Res.*, 45 (1995) 290.
2. McCafferty, D.G., Slate, C.A., Nakhle, B.M., Graham, H.D., Austell, T.L., Vachet, R.W., Mullis, B.H. and Erickson B.W., *Tetrahedron*, 51 (1995) 9859.
3. Alig, L., Edenhofer, A., Hadvary, P., Hurzeler, M., Knopp, D., Muller, M., Steiner, B., Trzeciak, A. and Weller, T., *J. Med. Chem.*, 35 (1992) 4393.
4. Ojima, I., Chakravarty, S. and Dong, Q., *Bioorg. Med. Chem.*, 3 (1995) 337.

# Conformational comparison of peptide templates and their folding enhancements on TASP

Zhenwei Miao,<sup>a</sup> Guangzhong Tu,<sup>b</sup> Xiaojie Xu,<sup>a</sup> Riqing Zhang<sup>b</sup>  
and Youqi Tang<sup>a</sup>

<sup>a</sup>Department of Chemistry, Peking University, Beijing 100871, China

<sup>b</sup>Department of Biology Science and Technology, Tsinghua University, Beijing 100084, China

To avoid the problem of protein folding, Mutter [1] has developed a method called template-assembled synthetic protein (TASP) in which a template molecule is introduced to help the synthetic protein fold into its desired tertiary structure. This strategy has diverse applications in protein *de novo* design [2]. In the present contribution, we focus on how the templates influence TASP folding. Two cyclic peptide templates, C<sub>12</sub>, C<sub>12</sub> and two linear templates, L<sub>10</sub>, L<sub>12</sub>, were thus designed to incorporate two *de novo* designed  $\alpha$ -helical peptide segments, H<sub>12</sub> and H<sub>16</sub>. The conformations of the so obtained four helical bundles were characterized by circular dichroism(CD).

C <sub>10</sub>	cyclo(Lys-Pro-Gly-Lys-Gly) <sub>2</sub>	L <sub>10</sub>	Ac-(Lys-Pro-Gly-Lys-Gly) <sub>2</sub> -Me
C <sub>12</sub>	cyclo(Phe-Lys-Pro-Gly-Lys-Gly) <sub>2</sub>	L <sub>12</sub>	Ac-(Phe-Lys-Pro-Gly-Lys-Gly) <sub>2</sub> -Me
H <sub>12</sub>	Ac-A-E-E-L-L-K-K-L-E-E-L-G-OH	H <sub>16</sub>	Ac-A-(E-E-L-L-K-K-L) <sub>2</sub> -G-OH

## Results and Discussion

All of the peptides were synthesized via fragment condensation of solution method and purified by HPLC. The C<sub>10</sub> and C<sub>12</sub> templates were prepared from cyclic dimerization of their pentapeptide and hexapeptide precursors [3]. Four helical bundles, C<sub>58</sub>, L<sub>58</sub>, C<sub>60</sub>, L<sub>60</sub>, C<sub>76</sub> and L<sub>76</sub>, were obtained by selective connection of the C-terminal carboxyl groups of H<sub>12</sub> or H<sub>16</sub> with the  $\epsilon$ -amino groups of the templates, respectively. For example, C<sub>60</sub> = C<sub>12</sub>+4H<sub>12</sub> and L<sub>60</sub>=L<sub>12</sub>+4H<sub>12</sub>.

Circular dichroism(CD) studies demonstrate that the conformations of the cyclic peptide templates are similar to that of the corresponding linear templates, but the cyclic peptides have more stable conformations in polar solvents due to their backbone constraints [4]. The solution structures of C<sub>10</sub> and C<sub>12</sub> were further determined by 2D-NMR techniques. C<sub>12</sub> has a 'double-V' like conformation in DMSO-d<sub>6</sub> and its four lysine side-chains locate the same endo-face of the 'double-V' [5]. C<sub>10</sub> has a boat like conformation in DMSO-d<sub>6</sub>, and its lysine side-chains are placed in the same exo-face of the 'boat bottom'. Such a conformation of either C<sub>10</sub> or C<sub>12</sub> is advantageous to the folding of TASPs, for its side chains position the same face of the templates. This prediction was confirmed through CD studying of the single  $\alpha$ -helical segment and the TASPs in aqueous solution. From Fig. 1, it can be found that H<sub>12</sub> exists in a random coil structure, L<sub>60</sub> and L<sub>58</sub> have only 35-45%

$\alpha$ -helix content, but  $C_{60}$  and  $C_{58}$  have much greater (70%)  $\alpha$ -helical structure. This shows that cyclic templates enhance the helical structures of the TASPs to a much greater extent than the linear templates, although the latter are also beneficial to TASP folding. However, the difference between cyclic and linear templates in their folding enhancements on TASPs is very small when a longer helix segment,  $H_{16}$ , was linked. As shown in Fig. 2,  $H_{16}$  has only 45%  $\alpha$ -helix content, while  $L_{76}$  and  $C_{76}$  have about 90%  $\alpha$ -helix content. The hydrophobic interactions among the long helical segments compensate for the disadvantageous flexibility of the linear template backbone.

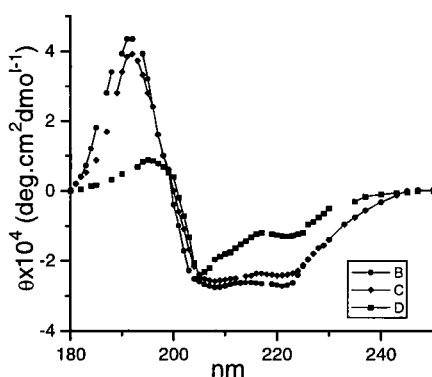
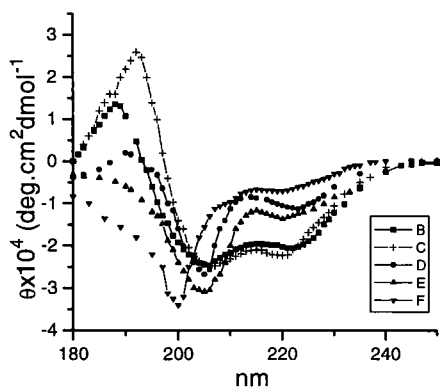


Fig. 1. CD spectra of  $C_{58}$ (B),  $C_{60}$ (C),  $L_{58}$ (D),  $L_{60}$ (E) and  $H_{12}$ (F) in neutral aqueous solution. Fig. 2. CD spectra of  $C_{76}$ (B),  $L_{76}$ (C) and  $H_{16}$ (D) in neutral aqueous solution.

## Conclusion

The tertiary folding of a TASP is dependent on both the conformation of the template and the secondary potential of the peptide segment.

## References

1. Mutter, M. and Vuilleumier, S., *Angew. Chem. Int. Ed. Engl.*, 28(1989) 535
2. Tuchscherer, G. and Mutter, M., *J. Peptide Science*, 1(1995) 3
3. Jiang, Y. Miao, Z. W. and Xu, X. J., *Peptides: Biology and Chemistry*(Proceedings of the 1994 Chinese Peptide Symposium), ESCOM, Leiden, The Netherlands, 1995, p.56
4. Jiang, Y. Miao, Z. W., Xu, X. J. and Tang, Y. Q., *Acta Physico-chimica Sinica*, 12(1996) 91
5. Lai, L. H., Ma, L. B., Xu, X. J. and Tang, Y. Q., *Acta Chimica Sinica*, 52(1994) 1028

# Use of a potent and selective highly constrained peptide agonist to design *de novo* an equally potent and selective non-peptide mimetic for the $\delta$ -opioid receptor

Victor J. Hruby,<sup>a</sup> Subo Liao,<sup>a</sup> Mark D. Shenderovich,<sup>a</sup>  
Josue Alfaro-Lopez,<sup>a</sup> Keiko Hosohata,<sup>b</sup> Peg Davis,<sup>b</sup>  
Frank Porreca<sup>b</sup> and Henry I. Yamamura<sup>b</sup>

<sup>a</sup>Departments of Chemistry and <sup>b</sup>Pharmacology, The University of Arizona,  
Tucson, AZ 85721, USA

A major but elusive goal of peptidomimetic research is the translation of 3D pharmacophore information of a potent bioactive peptide to a small non-peptide molecule with the same agonist biological activities. Successfully bridging the design gap from peptide to non-peptide mimetic requires, clarification of the geometrical relationships of key pharmacophores. First we undertook a detailed development of a 3D peptide pharmacophore based on design, synthesis and comprehensive evaluation of conformational ( $\phi$ ,  $\Psi$ ) and topographical ( $\chi$ ) space. We have used a potent and highly  $\delta$  opioid receptor-selective analogue [(2S,3R)-TMT<sup>1</sup>]DPDPE to successfully design, *de novo*, a high affinity, highly selective  $\delta$ -opioid receptor ligand.

## Results and Discussion

The key pharmacophores for  $\delta$  opioid receptors include the phenol ring and  $\alpha$ -amino group of Tyr<sup>1</sup>, the phenyl ring of Phe<sup>4</sup>, and a sterically bulky lipophilic group in position 2. We examined the 3D relationships of these groups in the highly constrained  $\delta$  opioid peptide [(2S,3R)-TMT<sup>1</sup>]DPDPE using 2D NMR, detailed computer modeling and molecular

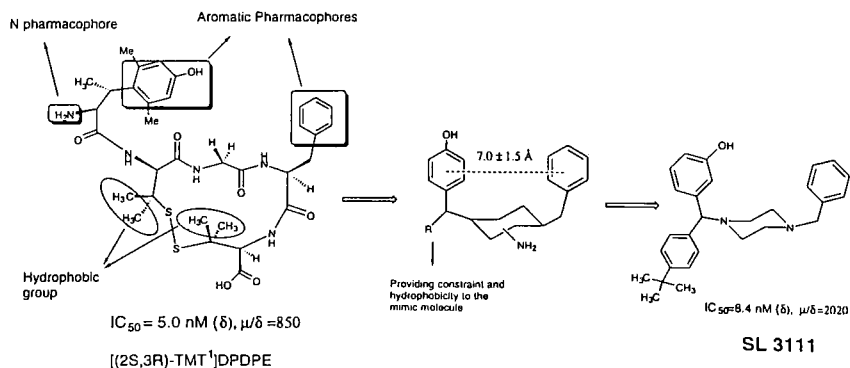


Fig. 1. Design of  $\delta$ -selective non-peptide mimetic from a potent and selective peptide lead.

*Table 1. Effect of the Mutation of Cloned Human  $\delta$ -Opioid Receptor on the Binding Affinity ( $IC_{50}$ , nM) of  $\delta$ -Selective Opioid Ligands*

Ligand	Wt	W284L	W284L/Wt
[Phe(p-Cl) <sup>4</sup> ]DPDPE	1.53 $\pm$ 0.26	1.55 $\pm$ 0.11	1.0
SL-3111	4.43 $\pm$ 0.49	17.1 $\pm$ 10.6	3.9
SNC-80	2.85 $\pm$ 0.26	49.1 $\pm$ 4.33	17.2

Wt: cloned human  $\delta$ -opioid receptor. W284L: mutated  $\delta$  receptor- Trp 284 to Leu.

dynamics[1]. The low energy conformations were compared with those of the potent through non-selective  $\delta$  non-peptide ligand SIOM ( $k_i=1.4$  nM at  $\delta$  and 10.6 nM at  $\mu$  receptors) [2]. These studies led to the pharmacophore shown in Figure 1 for [(2S,3R)TMT<sup>1</sup>]-DPDPE. Key topographical elements in the bioactive conformation were a distance between the aromatic rings of  $7.0 \pm 1.5 \text{ \AA}$ , a bulky hydrophobic group on the face opposite the aromatic pharmacophores, and the  $\alpha$ -amino group. Computer-assisted modeling for several non-peptide scaffolds led to six-membered ring templates (Figure 1). To simplify the synthetic requirements for testing the different structure requirements of the pharmacophore, a piperazine template was chosen. A variety of structures related the SL-3111 were synthesized. The binding affinities and  $\delta$  vs  $\mu$  opioid receptor selectivities were determined using the standard guinea pig brain membrane radioligand binding assays, with [<sup>3</sup>H]DAMGO ( $\mu$ -ligand) and [<sup>3</sup>H][Phe(p-Cl)<sup>4</sup>]DPDPE ( $\delta$ -ligand). The most potent and selective compound from the initially designed group was SL-3111 (Figure 1) which has an  $IC_{50}$  binding affinity of 8.4 nM at  $\delta$  receptors and a  $\delta$  vs  $\mu$  opioid binding selectivity of 2000. This is comparable or better than the peptide lead [(2S,3R)-TMT<sup>1</sup>]DPDPE ( $IC_{50}=5.0$  nM,  $\mu/\delta=850$ ). We next examined whether the non-peptide ligand mimics peptide or non-peptide ligands in its interactions with  $\delta$  receptors. Previously we had shown [3] that replacement of Trp<sup>284</sup> of the human  $\delta$  opioid receptor by a Leu residue lead to a  $\delta$  opioid receptor in which binding of  $\delta$  peptides e.g. [Phe(p-Cl)<sup>4</sup>]DPDPE was not affected, whereas non-peptide  $\delta$  selective agonist ligands e.g. SNC-80 [4] were greatly reduced. When SL-3111 was examined, its binding was very similar in both receptors (Table 1) as expected for a peptide mimetic. Several other tests of structure-activity similarities or differences of peptide vs non-peptide ligands are currently being examined.

## References

1. Qian, X., Shenderovich, M.D., Kövér, K.E., Davis, P., Horvath, R., Zalewska, T., Yamamura, H.I., Porreca, F. and Hruby, V.J., *J. Am. Chem. Soc.*, 118 (1996) 7280.
2. Portoghese, P.S., Moe, S.T. and Takamori, A.F., *J. Med. Chem.*, 36 (1993) 2572.
3. Xi, X., Knapp, R.J., Stropova, D., Varga, E., Wang, Y., Malatynska, E., Calderon, S., Rice, K., Rothman, R., Porreca, F., Hruby, V.J., Roeske, W.R. and Yamamura, H.I., *Analgesia 1* (1995) 539.
4. Calderon, S.N., Rothman, R.B., Porreca, F., Flippen-Anderson, J.L., McNutt, R.W., Xu, H., Smith, L.E. Bilsky, E.J., Davis, P. and Rice, K., *J. Med. Chem.* 37 (1994) 2125.

# Engineering of the deltoid protein: A model for the four corners of quadrin, a square octamer from the hepatitis delta antigen

Matthew J. Saderholm,<sup>a</sup> Gopal K. Balachandran,<sup>a</sup>  
Stanley M. Lemon<sup>b</sup> and Bruce W. Erickson<sup>a</sup>

<sup>a</sup>Department of Chemistry and <sup>b</sup>School of Medicine,  
University of North Carolina at Chapel Hill, Chapel Hill, NC 27599, USA

Hepatitis delta virus (HDV) is a small satellite virus of hepatitis B virus that can cause fatal liver disease in man [1]. HDV RNA encodes one known protein, hepatitis delta antigen (HDAg). Multimerization of HDAg is needed for replication and virion assembly. We have synthesized **quadrin**, a 50-residue peptide consisting of HDAg segment 12-60 plus a C-terminal tyrosine residue [2]. Quadrin forms a thermally stable  $\alpha$ -helical coiled-coil multimer that binds to antisera from patients infected with HDV [2].

The crystal structure of quadrin at 1.8 Å resolution reveals a 400-residue square octamer having  $D_4$  symmetry [3]. Each quadrin monomer contains a long five-turn A helix (HDAg residues 13-48) and a short B helix (HDAg residues 51-59). Each edge of the open square consists of one antiparallel  $\alpha$ -helical coiled-coil dimer (A/A interaction). Four quadrin dimers form a square octamer surrounding a 45 Å by 45 Å solvent-filled square hole. At each of the four corners of the quadrin octamer, two quadrin dimers form a right angle (AB/AB interaction). We modeled the quadrin corner with **deltoid**, a 51-residue peptide containing half of a quadrin dimer, and examined its ability to dimerize in solution.

## Results and Discussion

Deltoid monomer is a chimeric peptide containing sequentially the N terminus of one quadrin monomer (HDAg residues 12-28), the  $\alpha$ -hairpin loop of *Thermus thermophilus* serine tRNA synthase (residues 59-65), and the C terminus of another quadrin monomer

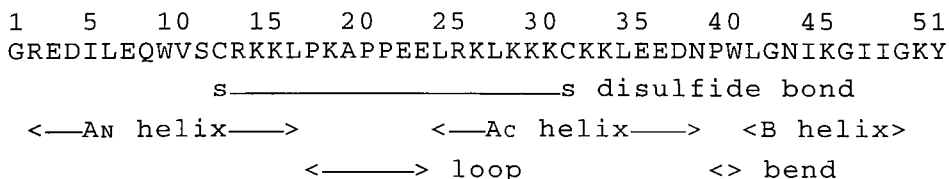
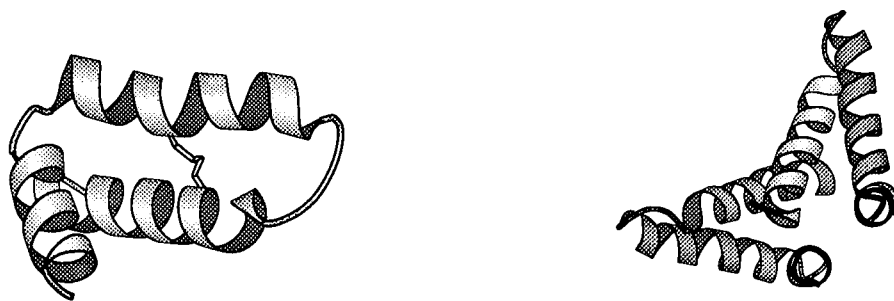


Fig. 1. Amino-acid sequence of the deltoid monomer and its major structural features.



*Fig. 2. Ribbon diagrams of the deltoid monomer (left) and the deltoid dimer (right).*

(HDAG residues 34-60 plus Tyr) (Fig. 1). Deltoid monomer was designed by homology modeling and molecular modeling to be a three-helical bundle in which  $\alpha$  helices AN and AC form an antiparallel coiled coil through hydrophobic interactions and helix B packs against the other two helices by hydrophobic contacts (Fig. 2). Deltoid has a disulfide bridge but reduced deltoid has two cysteine residues. Two deltoid monomers might form an isologous dimer through hydrophobic contacts of their AN and B helices (Fig. 2).

The reduced deltoid monomer was synthesized by the solid-phase method, purified by RP-HPLC, and air oxidized to the deltoid monomer, which was also purified by RP-HPLC. The molecular masses of the reduced deltoid chain (6046 Da) and the deltoid chain (6044 Da) were confirmed by ESI mass spectrometry. By ELISA studies, the deltoid protein bound as tight as quadrin octamer to polyclonal antibodies from a human patient with HDV and to a monoclonal antibody raised against the quadrin octamer. Thus HDAG, quadrin, and deltoid fold into conformationally similar structures.

By CD spectroscopy, reduced deltoid and deltoid each showed substantial  $\alpha$ -helical content and underwent reversible thermal unfolding. The melting temperature for reduced deltoid ( $\sim 60^\circ\text{C}$ ) was about  $35^\circ\text{C}$  lower than that for deltoid. By sedimentation equilibrium studies in the analytical ultracentrifuge, each protein underwent reversible dimerization at  $20^\circ\text{C}$ . The dissociation constant for the reduced deltoid dimer ( $\sim 60\ \mu\text{M}$ ) was only about half that of the deltoid dimer. Thus the disulfide bond of deltoid significantly stabilises it towards thermal unfolding but slightly destabilises the deltoid dimer in its equilibrium with deltoid monomer. Deltoid is a good model protein for studying the interactions involved in forming the corners of the quadrin octamer.

## References

1. Lai, M.C.C., *Annu. Rev. Biochem.*, 64 (1995) 259.
2. Rozzelle, J.E., Wang, J.G., Wagner, D.S., Erickson, B.W. and Lemon, S.M., *Proc. Natl. Acad. Sci. U.S.A.*, 92 (1995) 382.
3. Zuccolla, H.J., Lemon, S.E., Rozzelle, J.E., Erickson, B.W. and Hogle, J.M., submitted.

# Engineering of helical oligoproline redox assemblies that undergo photoinduced electron transfer

**Cheryl A. Slate, Durwin R. Striplin, Robert A. Binstead,  
Thomas J. Meyer and Bruce W. Erickson**

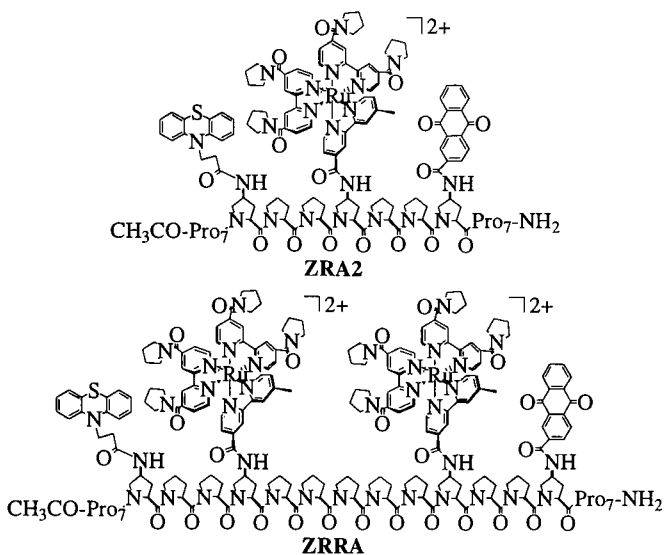
*Department of Chemistry, University of North Carolina at Chapel Hill,  
Chapel Hill, NC 27599, USA*

Engineering of a molecular system that efficiently mimics the redox-separated state (rss) of a photosynthetic reaction center is an unsolved problem of photophysics. The long-term goal is to construct light-harvesting arrays that function as photochemically and electrochemically coupled molecular reactors [1]. A short-term goal is to achieve efficient redox separation and light harvesting through photoinitiation of a series of intramolecular electron transfers. One design strategy is to use peptide secondary structure to control the orientation and spacing of the redox sites involved in the electron transfers.

Functionalized oligoprolines can form stable helical peptides. Using a modular synthetic strategy, McCafferty et al. [2] engineered the 13-residue redox triad ZRA, whose rss had a lifetime of 175 ns and a quantum yield of formation of ~50% per photon absorbed. We have engineered a longer oligoproline redox array with increased rss lifetime.

## Results and Discussion

We have designed, synthesized, and characterized oligoproline arrays containing the new redox chromophore  $\text{Ru}^{\text{II}}_{\text{p}_2\text{m}}$ , a derivative of tris(2,2'-bipyridine)ruthenium(II) with an aminocarbonyl group on five of its six pyridine rings. It contains two copies of the novel ligand p, 2,2'-bipyridine-4,4'-dicarboxylic acid bis(pyrrolidine amide), and one copy of ligand m, 4'-methyl-2,2'-bipyridine-4-carboxylic acid, which is bound to the 4-amino group of Boc-(2*S*,4*S*)-4-aminoproline (Boc-Pra). Solid-phase assembly using the new redox module Boc-Pra( $\text{Ru}^{\text{II}}_{\text{p}_2\text{m}}$ ), the electron-accepting anthraquinone module Boc-Pra(Anq), and the electron-donating phenothiazine module Boc-Pra(Ptz) afforded the 21-residue redox triad  $\text{CH}_3\text{CO-Pro}_7\text{-Pra(Ptz)-Pro}_2\text{-Pra(Ru}^{\text{II}}_{\text{p}_2\text{m}}\text{)-Pro}_2\text{-Pra(Anq)-Pro}_7\text{-NH}_2$  (ZRA2) as well as  $\text{CH}_3\text{CO-Pro}_7\text{-Pra(Ptz)-Pro}_2\text{-Pra(Ru}^{\text{II}}_{\text{p}_2\text{m}}\text{)-Pro}_5\text{-Pra(Ru}^{\text{II}}_{\text{p}_2\text{m}}\text{)-Pro}_2\text{-Pra(Anq)-Pro}_7\text{-NH}_2$  (ZRRRA), a 27-residue redox tetrad. These orange solids were analytically pure by HPLC and gave the expected molecular masses by ESI mass spectrometry (3629 Da for ZRA2, 5225 Da for ZRRRA). Circular dichroic studies of ZRA, which has only a Pro<sub>3</sub> segment at each terminus, showed that it forms a proline-II helix in water or CH<sub>3</sub>CN [2]. In contrast, the redox arrays ZRA2 and ZRRRA, which have a longer Pro<sub>7</sub> segment at each terminus, fold into a left-handed proline-II helix in water but into a right-handed proline-I helix in CH<sub>3</sub>CN.



Nanosecond laser-flash photolysis of ZRA2 and ZRRA in  $\text{CH}_3\text{CN}$  with absorbance monitoring showed characteristic transient absorption bands for the bipyridine radical anion at 375 nm,  $\text{Ptz}^{*\cdot+}$  at 520 nm, and  $\text{Anq}^{\cdot-}$  at 590 nm. Kinetic analysis revealed that the rss lifetime is the same for ZRA2 (170 ns) as for ZRA but is eleven times longer for ZRRA (2000 ns). Three lines of evidence indicate that electron transfer from the rss ( $\text{Ptz}^{*\cdot+} \dots \text{Anq}^{\cdot-}$ ) back to the ground state proceeds through the bonds of the oligoproline chain rather than through space. First, the through-space distance from  $\text{Ptz}^{*\cdot+}$  to  $\text{Anq}^{\cdot-}$  is  $\sim 18 \text{ \AA}$  for the proline-II helix of ZRA and only  $\sim 11 \text{ \AA}$  for the proline-I helix of ZRA2, but their rss lifetimes are the same. Second, although the through-space distance for back electron transfer is  $\sim 14 \text{ \AA}$  longer for the proline-II than for the proline-I helical form of ZRRA, their rss lifetimes are the same in  $\text{CH}_3\text{CN}$ . Third, the rss lifetime of the latter is only slightly longer at lower temperatures.

## References

1. Meyer, T.J., In Meyer, T.J. (Ed.) *Intramolecular Photochemical Electron and Energy Transfer*, Elsevier, 1991, p. 133.
2. McCafferty, D.G., Friesen, D.A., Danielson, E., Wall, C.G., Saderholm, M.J., Erickson, B.W. and Meyer, T.J., *Proc. Natl. Acad. Sci. USA*, 93 (1996) 8200.

# The use of 5-*tert*-butylproline to study nucleation of polyproline type I conformation.

Eric Beausoleil and William D. Lubell

*Département de chimie, Université de Montréal,*

*C. P. 6128, Succursale Centre Ville, Montréal, Québec, Canada H3C 3J7*

Prolyl amide geometry dictates two kinds of helical conformations in polyproline [1]. *N*-terminal amides to proline are all *cis*-isomers in type I polyproline (PPI), which is a right handed helix with an axial translation of 190 pm. Type II polyproline (PPII) is a left handed helix with an axial translation of 320 pm due to the prolyl amides existing as *trans*-isomers. Peptides adopting PPII conformations have been observed to bind to kinases, SH2 and SH3 domains, and MHC class II proteins by NMR spectroscopy and X-ray crystallography [2]. Because of conformational lability, PPI has been studied mostly in the solid state by X-ray diffraction and little is known about this peptide structure and its relevance in protein biology [1-3]. In order to better characterize the physical and biological properties of PPI, we are using the steric interactions of 5-alkylprolines to augment *cis*-isomer populations in polyproline helices. We report attempts to induce PPI geometry in water by incorporating 5-*tert*-butylproline (tBuPro) into polyproline hexamers as studied by NMR and CD spectroscopy.

## Results and Discussion

Ac-Pro-Pro-NH<sub>2</sub> (1)

Ac-Pro-Pro-Pro-Pro-Pro-tBuPro-NH<sub>2</sub> (4)

Ac-Pro-tBuPro-NH<sub>2</sub> (2)

Ac-Pro-Pro-tBuPro-Pro-Pro-tBuPro-NH<sub>2</sub> (5)

Ac-Pro-Pro-Pro-Pro-Pro-NH<sub>2</sub> (3)

Ac-Pro-tBuPro-Pro-tBuPro-Pro-tBuPro-NH<sub>2</sub> (6)

Proline oligomers 1-6 were prepared to examine both the local and global effects of tBuPro on polyproline conformation. Fmoc-Pro-tBuPro (7) was first synthesized from (2*S*,5*R*)-*N*-Boc-5-*tert*-butylproline methyl ester (8) [4]. Boc group removal with TFA in DCM, transesterification with allyl alcohol and *p*-TsOH in benzene, liberation of the amine with NaHCO<sub>3</sub>, coupling to Fmoc-Pro using BOP-Cl and DIPEA in DCM, and finally allyl ester removal with Pd(PPh<sub>3</sub>)<sub>4</sub> and *N*-methylaniline in THF/DMSO/HCl afforded 7 in 60% overall yield from 8. Proline oligomers 1-6 were synthesized on Rink MBHA resin (0.67 mmol/g) which was swollen in DCM for 20 min, and treated with 20% piperidine in DMF to effect Fmoc deprotection. Fmoc-Pro and 7 were introduced using TBTU and DIPEA in DMF. Final oligomers were *N*-acetylated with excess Ac<sub>2</sub>O and pyridine in DMF, cleaved with 95:5 TFA/H<sub>2</sub>O, and purified by semi-preparative HPLC on a RP-C18 column with a linear gradient of 0-50% CH<sub>3</sub>CN in H<sub>2</sub>O with 0.1% TFA.

Dipeptides 1 and 2 were examined by <sup>1</sup>H NMR spectroscopy in water to discern the influence of the *t*-butyl group on the prolyl amide equilibrium. The Pro-Pro amide of 1 was

primarily in the *trans*-isomer which displayed a strong NOE between H $\alpha$  of the *i* and H $\delta$  of the *i*+1 residues. The spectrum of **2** indicated a 37:63 ratio of *trans*- and *cis*-isomers as assigned based on NOEs between the Pro H $\alpha$  and tBuPro H $\delta$  for the *trans* and between the Pro H $\alpha$  and tBuPro H $\alpha$  for the *cis*-isomer.

Hexapeptide **3** was observed to adopt a PPII conformation by  $^1\text{H}$  and  $^{13}\text{C}$  NMR spectroscopy [3,5]. A strong NOE was apparent between the H $\alpha$  and H $\delta$  signals of **3**. The  $^1\text{H}$  spectrum of **4** depicted a PPII-like conformation in which a *cis*/*trans* amide equilibrium was present at the *N*-terminal to the tBuPro residue with a 61:39 ratio of *cis*- and *trans*-isomers. The *trans*-isomer of **4** exhibited NOE between the Pro H $\alpha$  and tBuPro H $\delta$ . The CD spectrum of **3** confirmed a PPII structure with a strong negative band at 203 nm and a weak positive band at 227 nm [1] (Fig.). The CD spectra for **4-6** deviated from PPII-like curves. The negative band diminished in intensity shifting to higher wavelength and the positive band disappeared as more tBuPro residues were introduced into the hexapeptide; however, PPI-like spectra were not observed in water.

In conclusion, tBuPro was readily introduced into polyproline oligomers. The *t*-butyl substituent augmented amide *cis*-isomer in dimer **2** and hexamer **4**; however, the conformation of **4** remained mostly PPII in water. As tBuPro content increased PPII geometry was disturbed, but PPI was not observed in water. Thus, tBuPro exerted mostly local effects on prolyl amide geometry and not global effects on polyproline helical conformation in water. Alternative solvents and tBuPro 5-position stereochemistry are now being examined because they may enhance nucleation of PPI geometry [1,3].

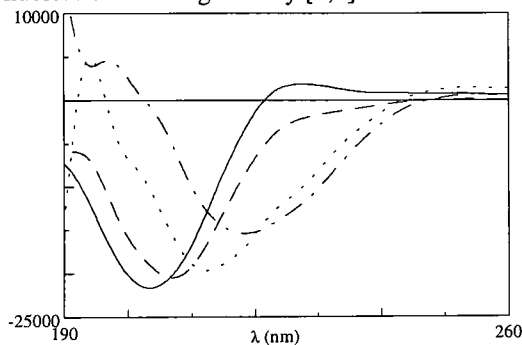


Fig.1. CD spectra of polyproline hexamers **3** (—), **4** (---), **5** (···) and **6** (-·-) in water.

## References

1. Rabanal, F., Ludevid, M. D., Pons, M. and Giral, E., *Biopolymers*, 33 (1993) 1019.
2. Siligardi, G. and Drake, A. F., *Biopolymers*, 37 (1995) 281.
3. Torchia, D. A. and Bovey, F. A., *Macromolecules*, 4 (1971) 246.
4. Beausoleil, E., L'Archevêque, B., Bélec, L., Atfani, M. and Lubell, W.D., *J. Org. Chem.*, 61 (1996) 9447.
5. McCafferty, D.G., Slate, C.A., Nakhle, B.M., Graham, H.D.Jr., Austell, T.L., Vachet, R.W., Mullis, B.H. and Erickson, B.W., *Tetrahedron*, 51 (1995) 9859.

# Structure-activity relationships in cyclic $\beta$ -sheet antibacterial peptides

Leslie H. Kondejewski,<sup>a</sup> Masood Jelokhani-Niaraki,<sup>a</sup> Robert E.W. Hancock<sup>b</sup> and Robert S. Hodges<sup>a</sup>

<sup>a</sup>*Protein Engineering Network of Centres of Excellence, University of Alberta, Edmonton, Alberta, T6G 2S2, Canada.* <sup>b</sup>*Canadian Bacterial Diseases Network, University of British Columbia, Vancouver, British Columbia, V6T 1Z3, Canada*

We have utilized the head-to-tail cyclic decapeptide gramicidin S (GS) as the basis for our design of novel antibacterial peptides. Results from our previous study [1] indicated that the disruption of  $\beta$ -sheet structure and amphipathicity in cyclic peptides related to GS appeared to be responsible for conferring a high degree of specificity for microorganisms over higher eukaryotic cells (a high therapeutic index). In the present study we test this hypothesis using GS14, a highly amphipathic  $\beta$ -sheet peptide which exhibits low antimicrobial activity and extremely high hemolytic activity. Fourteen diastereomers of GS14 were synthesized, each containing a single enantiomeric substitution, with the goal of disrupting the  $\beta$ -sheet conformation and amphipathicity of the molecule.

## Results and Discussion

GS14, cyclo(Val-Lys-Leu-Lys-Val-dTyr-Pro-Leu-Lys-Val-Lys-Leu-dTyr-Pro), and its fourteen diastereomers were synthesized, cyclized and isolated as reported previously [1]. Shown are the CD spectra of GS14 and a representative number of diastereomers under aqueous conditions (Fig. 1A). The CD spectrum of GS14 is typical of those seen for other cyclic  $\beta$ -sheet/ $\beta$ -turn peptides such as GS, and therefore contains  $\beta$ -sheet structure. The alternating hydrophobic-basic residue pattern therefore confers a high degree of amphipathicity to the molecule. GS14 diastereomers all exhibited CD spectra more typical of disordered structures, indicating that the  $\beta$ -sheet conformation was disrupted by the incorporation of the single enantiomeric substitutions.

GS14 and the diastereomers were resolved by reversed-phase HPLC, with all diastereomers eluting at shorter retention times compared to the parent molecule. GS14 and the present diastereomers all have the same intrinsic hydrophobicity, and any differences in retention time are due to their effective hydrophobicity which is related to the ability of the peptide to present a hydrophobic face to the HPLC matrix. Retention time on reversed-phase HPLC of the present analogs is therefore a measure of the ability of the peptide to achieve a  $\beta$ -sheet conformation and an amphipathic nature.

There was a clear relationship found between retention time on reversed-phase HPLC and hemolytic activity, with those analogs having the lowest retention times also showing the least hemolytic activity (data not shown). The antibacterial activity and therapeutic index of GS14 and the diastereomers against a representative microorganism is shown in Fig. 1B. GS14

exhibits low antibacterial activity coupled with extremely high hemolytic activity (a low therapeutic index), whereas the diastereomers exhibit a wide range of activities, with some analogs showing activities similar to GS14, and some exhibiting complete opposite activities resulting in very favourable therapeutic indices. As with hemolytic activity, there was a clear relationship between antibacterial activity and retention time on reversed-phase HPLC, indicating that the least amphipathic peptides possess the most desirable biological properties.

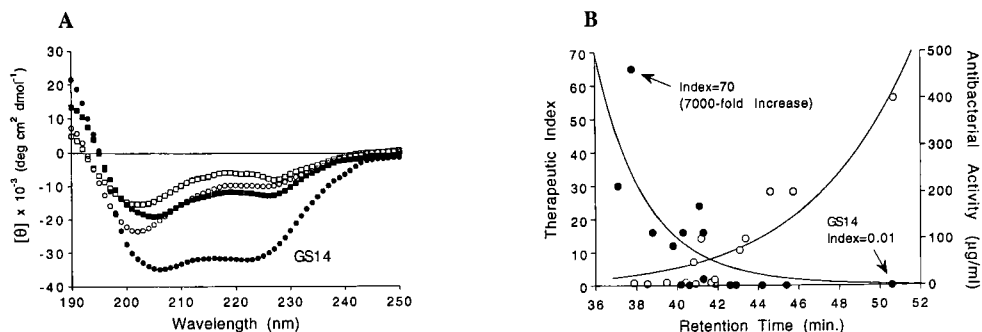


*Fig. 1. Structure and activity of GS14 and GS14 diastereomers. A) CD spectra of GS14 and representative analogs under aqueous conditions measured as reported previously [3,4]. B) Relationship between retention time, antibacterial activity (MIC, open circles) and therapeutic index (closed circles) of analogs against a *Pseudomonas aeruginosa* strain. The therapeutic index = hemolytic activity / antibacterial activity as described previously [4].*

## Conclusion

A definite structure-activity relationship exists in the present cyclic fourteen residue antimicrobial peptides based on GS. The disruption of the overall  $\beta$ -sheet/ $\beta$ -turn structure in GS14, and hence the amphipathic pattern of the molecule, appears to be the key to designing GS analogs with desirable biological properties.

## References

1. Kondejewski, L.H., Farmer, S.W., Wishart, D.S., Kay, C.M., Hancock, R.E.W., and Hodges, R. S., *J. Biol. Chem.*, 271 (1996) 25261.

# Chimeric TASP molecules as biosensors

Lukas Scheibler,<sup>a</sup> Pascal Dumy,<sup>a</sup> Mila Bontcheva,<sup>b</sup> Horst Vogel<sup>b</sup> and  
Manfred Mutter<sup>a</sup>

<sup>a</sup> *Institute of Organic Chemistry, University of Lausanne, CH-1015 Lausanne, Switzerland*

<sup>b</sup> *Swiss Federal Institute of Technology, EPFL, CH-1015 Lausanne, Switzerland*

Systems that integrate biological, chemical and physical units have great potential in biosensor technology. In particular, peptide and protein modules self-assembled on gold surfaces in combination with surface plasmon resonance spectroscopy (SPR) as surface-sensitive analytical technique proved to be a versatile approach for the development of new biosensors [1].

## Results and Discussion

Topological templates were previously introduced in protein *de novo* design for constructing tertiary folds, such as 4-helical bundles, termed Template Assembled Synthetic Proteins (TASP) [2,3]. For the construction of a potential biosensor based on the TASP concept, a cyclic decapeptide offering two regioselectively addressable faces is used as a template. One face is functionalized with four identical amphipathic helices while the other face carries two antigenic peptides. N-terminal cysteine residues on the helices allow for the immobilization on gold surfaces in a self-assembly process. The topological template acts as (a) a device for the induction of a 4 helix bundle and (b) linkage between the antigenic peptide and the module for immobilization on gold surfaces.

(Asn-Ala-Asn-Pro)<sub>3</sub> recognized by the monoclonal antibody E9 was chosen as biologically active peptide because of its relevance in the immune response against malaria parasites. The helix comprising 12 amino acids of the sequence Ac-Cys-Ala-Ser-Ala-Aib-Ser-Ser-Ala-Aib-Ser-Ala-Gly-OH is designed to span a monolayer formed by self-assembled 11-mercaptopundecanol. Aminoisobutyric acid residues (Aib) were incorporated for stabilizing the helix and the polar serine residues serve as the hydrophilic part of the resulting amphipathic helix.

After the formation of either pure self-assembled TASP or mixed TASP/11-mercaptopundecanol monolayers, the reversible binding of the monoclonal antibody E9 towards the functionalized surface was investigated by SPR spectroscopy. The results show that the assembled TASP present the antigenic peptide in a proper way, i.e. the antibody has free access to the binding site in harmony with the proposed structure (Fig. 1b). The binding constant of the antibody is  $K = 5 \times 10^7 \text{ M}^{-1}$ , which is about 100 times higher than that of the antibody/antigen complex in solution (Fig. 1a). Furthermore, the antibody could be displaced by washing the surface with a solution containing the free antigen (Asn-Ala-Asn-Pro)<sub>3</sub>.

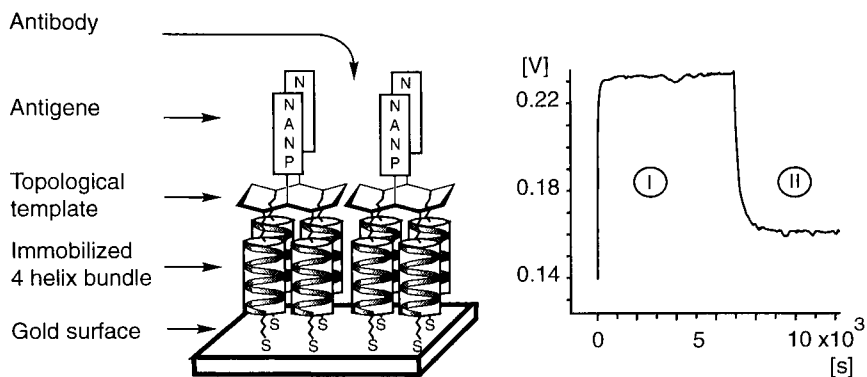


*Fig. 1. Left: Self-assembled TASP molecules on a gold surface. The topological template induces a 4-helix bundle and acts as linker between the helical bundle and the antibody recognition site. Right: SPR scan of the binding (a) and displacement (b) of the antibody to the self-assembled TASP monolayer.*

## Conclusion

A chimeric TASP molecule, consisting of a 4-helix bundle motif and an antibody recognition site, has been covalently attached to a gold surface. The reversible antibody binding to the self-assembled monolayer as monitored by surface plasmon resonance spectroscopy demonstrates the versatility of the TASP concept for the construction of biosensors.

## Acknowledgments

This work was supported by the Priority Programme Biotechnology of the Swiss National Science Foundation.

## References

1. Duschl, C., Sévin-Landais, A.F., Vogel, H., *Biophys. J.*, 70 (1996) 1985.
2. Mutter, M., *Trends Biochem. Sci.*, 13 (1988) 260.
3. Pawlak, M., Meseth, U., Dhanapal, B., Mutter, M., Vogel, H., *Protein Sci.*, 3 (1994) 1788.

# Topologies of consolidated ligands for the Src homology (SH)3 and SH2 domains of Abelson protein-tyrosine kinase

Qinghong Xu,<sup>a,b</sup> Jie Zheng,<sup>a</sup> George Barany<sup>b</sup> and David Cowburn<sup>a</sup>

<sup>a</sup>*The Rockefeller University, New York, NY 10021*

<sup>b</sup>*Department of Chemistry, University of Minnesota, Minneapolis, MN 55455, USA*

Src homology (SH)2 and SH3 domains are found in a variety of proteins involved in the control of cellular signalling and architecture [1,2]. The two domains are frequently found together in the same protein, for example in the Abelson kinase (Abl). SH2 domains recognize motifs that include key phosphotyrosine residues [3], while SH3 domains recognize sequences with multiple proline residues [4]. The interactions between these domains are poorly understood. Here, we describe an approach called "consolidated" ligands to probe structural and functional activities of multidomain proteins. These ligands, having multiple binding portions, may be expected to bind with high affinity and specificity when a linker between the two affine segments is of the correct orientation and length.

## Results and Discussion

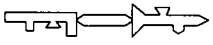
NMR studies on the Abl SH3 construct suggested that the Abl SH(32) dual domain is a monomer in solution, and that there is no interdomain interaction other than the covalent connection [5]. The topologies of these ligands for the Abl SH(32) dual domains are illustrated in Table 1, which also summarizes the binding affinities measured by quenching of intrinsic tryptophan fluorescence. The linkers here are comprised of moieties containing about 5-8 glycyls according to computer-based predictions.

All of the bivalent consolidated ligands in Table 1 were chemically synthesized by *N*<sup>α</sup>-9-fluorenylmethyloxycarbonyl (Fmoc) solid-phase chemistry. The syntheses of type A ligands were achieved by introducing a branching point at lysine through application of the 1-(4,4-dimethyl-2,6-dioxocyclohexylidene)ethyl (Dde) group which is removed under orthogonal conditions of hydrazinolysis [6,7]. Type B ligands were assembled by a novel strategy featuring acylation of G<sub>n</sub>-2BP-resin by glutaric anhydride, followed by coupling of the 3BP peptide fragment.

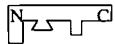
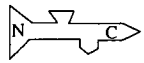
Affinities determined for all ligands (Table 1) showed that type A and type C ligands can bind to both SH2 and SH3 dual domains with high specificity and affinity. The values of ligands varied with linker lengths, an optimal length being about G<sub>6</sub> (type A ligand) or G<sub>7</sub> (type C ligand). An order of magnitude increase was observed comparing the most strongly bound single ligand (2BP, K<sub>d</sub> = 2,350 nM) [6], while type B and type D ligands only interfere with SH2 domains with low affinity. It is concluded that ligated Abl SH(32) can adopt multiple subdomain orientations. Detailed analysis by isothermal titration calorimetry (ITC) permits the estimation of the relative contribution of entropy and enthalpy to the binding energies. In conclusion, this approach of consolidated ligands can be used to identify the interfaces between domains for rational design of higher affinity

binding reagents, and to probe the relative rigidity between domains or the dynamics of interdomain motion.

Table 1. Affinities of ligands to Abl SH(32).

Ligand	Structure	Binding Subdomain	K <sub>d</sub> (nM)
A		SH2 + SH3	200-400
B		SH2	~20,000
C		SH2 + SH3	200-400
D		SH2	~20,000

		
2BP (PVY*ENV)	Linker (G <sub>n</sub> )	3BP (PPAYPPPVP)

## Acknowledgments

This work was supported by NIH Grants GM-42722 and GM-51628 (to G. B.), and GM-47021 (to D. C.). Q. X. is the C.H. Li Memorial Fund Fellow.

## References

1. Pawson, T., *Adv. Cancer Res.*, 64 (1994) 87.
2. Schlessinger, J. *Curr. Opin. Genetics & Development*, 4 (1994) 25.
3. Zhu, G., Decker, S.J., Maclean, D., McNamara, D.J., Singh, J. and Sawyer, T.K., *Oncogene*, 9 (1994) 1379.
4. Ren, R., Mayer, B.J., Cicchetti, P. and Baltimore, D., *Science*, 259 (1993) 1157.
5. Gosser, Y., Zheng, J., Overduin, M., Mayer, B.J. and Cowburn, D., *Structure*, 3 (1995) 1075.
6. Cowburn, D., Zheng, J., Xu, Q. and Barany, G., *J. Biol. Chem.*, 270(1995) 26738.
7. Xu, Q., Zheng, J., Cowburn, D. and Barany, G., *Letts. Pep. Sci.*, 3 (1996) 31.

# Toward design of a triple stranded antiparallel $\beta$ -sheet

**Heather L. Schenck and Samuel H. Gellman**

*Department of Chemistry, University of Wisconsin-Madison, Madison, WI 53706, USA*

A recent report from our laboratory demonstrated that a D-proline residue could induce  $\beta$ -hairpin formation in a 16-residue peptide in aqueous solution. The L-proline containing diastereomer displayed no  $\beta$ -hairpin structure [1]. This observation prompted us to try to generate a triple stranded  $\beta$ -sheet by incorporating two D-proline residues. Such a structure should be incrementally disruptable: replacement of either D-Pro with L-Pro should destroy one or the other of the hairpins. The use of chirality to alter structure is appealing because the peptides to be compared will be as similar as possible (diastereomers differing at one chiral center). In addition, any changes in stability of the remaining (D-Pro containing) hairpin in either L-Pro diastereomer may have implications for the energetics of  $\beta$ -sheet stabilization in proteins.

## Results and Discussion

Cooperative formation and stabilization of  $\alpha$ -helical structure is a well accepted fact in peptide and protein science [2]. Similar information on  $\beta$ -sheets has been heretofore unavailable, due to the intractable nature of  $\beta$ -sheets: peptidic models have been self-associating, precluding study of incremental steps in structure formation [3,4].

Recent approaches to intramolecular  $\beta$ -sheet design have used  $\beta$ -hairpins; evidence suggests that hairpins can exist as stable structures in aqueous solution, in the absence of obvious intermolecular interactions [5, 6, 7]. The next step in design of nonaggregating  $\beta$ -sheets is the design of additional linked strands. Such a structure could provide previously inaccessible information about cooperativity [8].

The use of D-Pro in the design of  $\beta$ -hairpins is predicated on two established facts in protein science. First, proline is known to induce formation of  $\beta$ -turns (the loop linking hairpin strands), although L-Pro generates type I and II turns, which are rare in two-residue-turn hairpins [9]. Second, the "mirror image" turns, types I' and II', promoted by D-Pro, are commonly found in hairpins of the type we wish to generate [10].

One of the most important considerations in such a design is the avoidance of aggregation. In order to obtain information about the formation and stability of a discrete secondary structure element (intramolecular  $\beta$ -sheet), intermolecular interactions must be prevented.  $\beta$ -sheets found in proteins are commonly amphiphilic, which allows one face of the sheet to pack against a hydrophobic protein surface while the other face is solvent-exposed. A design using this type of structure would be prone to self-association. Even distribution of polar and nonpolar residues on both faces of the designed sheet, as well as selection of residues with high propensities for  $\beta$ -sheet formation, is the approach we have

selected. Our design thus probes whether  $\beta$ -sheet secondary structure relies on an amphipathic pattern.

Further consideration in the design of a three strand  $\beta$ -sheet includes strategic placement of residues with sidechains that offer structural information. Our previous experience suggests that aromatic amino acids are particularly "communicative" with regard to structural information from NOE interactions.

The analysis of structure in our peptide series focuses largely on NMR characterization techniques. 2D NMR methods commonly used in the study of proteins are employed; COSY and TOCSY sequences provide intraresidue chemical shift information, and ROESY spectra offer sequence assignment and evaluations of proton-proton proximity.

Additional information available from NMR data is based on comparisons of experimental chemical shifts to tabulated random coil values from the literature [11]. In the case of  $H_{\alpha}$  protons, for example,  $\beta$ -structure is known to cause downfield shifting relative to random coil values.

## Conclusion

The peptides we are designing represent a new level of structure in synthetic  $\beta$ -sheet peptides, and may offer insights on possible cooperative aspects of  $\beta$ -sheet formation.

## References

1. Haque, T.S., Gellman, S.H., *J. Am. Chem. Soc.*, 119 (1997)2303.
2. Zimm, B.H., Bragg, J.K., *J. Chem. Phys.* 31(1959)526.
3. Osterman, D.G., Kaiser, E.T., *J. Cell. Biochem.* 29(1985)57.
4. Schenck, H.L., Dado, G.P., Gellman, S.H., *J. Am. Chem. Soc.* 118(1996)12487.
5. de Alba, E., Jiménez, M.A., Rico, M., *J. Am. Chem. Soc.* 119(1997)175.
6. Searle, M.S., Zerella, R., Williams, D.H., Packman, L.C., *Protein Engng* 9(1996)559.
7. Ramírez-Alvarado, M., Blanco, F.J., Serrano, L., *Nature Struct. Biol.* 3(1996)604.
8. Mattice, W.L., *Annu. Rev. Biophys. Biophys. Chem.* 18(1989)93.
9. Wilmot, C.M., Thornton, J.M., *J. Mol. Biol.* 203(1988)221.
10. Sibanda, B.L., Thornton, J.M., *Nature* 316(1985)170.
11. Wishart, D.S., Sykes, B.D., Richards, F.M., *J. Mol. Biol.* 222(1991)311, and references therein.

## Copper(II)-induced folding of betabellin 15D, a designed beta-sheet protein

Amareth Lim,<sup>a</sup> Mathias Kroll<sup>a</sup>, Yibing Yan<sup>a</sup>, Matthew J. Saderholm<sup>a</sup>,  
Alexander M. Makhov<sup>b</sup>, Jack D. Griffith<sup>b</sup> and Bruce W. Erickson<sup>a</sup>

<sup>a</sup>Department of Chemistry and <sup>b</sup>Lineberger Comprehensive Cancer Center,  
University of North Carolina at Chapel Hill, Chapel Hill, NC 27599, USA

The betabellin molecule is a designed 64-residue protein that can fold into a  $\beta$ -sandwich by isologous interaction of two 32-residue  $\beta$  sheets [1, 2]. When three pairs of D-amino acid residues are used at the four t and two r positions, which favors formation of three inverse-common (type-I')  $\beta$  turns [3], the peptide chain can fold into a 4-stranded antiparallel  $\beta$  sheet stabilized by as many as 18 interstrand hydrogen bonds (Fig. 1A). This  $\beta$  sheet is designed to have 12 polar residues protruding from one face and 12 nonpolar residues from the other so that two such  $\beta$  sheets can fold into a  $\beta$  sandwich through multiple hydrophobic interactions between their nonpolar faces [4]. In some cases, formation of  $\beta$  structure requires the presence of an intersheet disulfide bond [5].

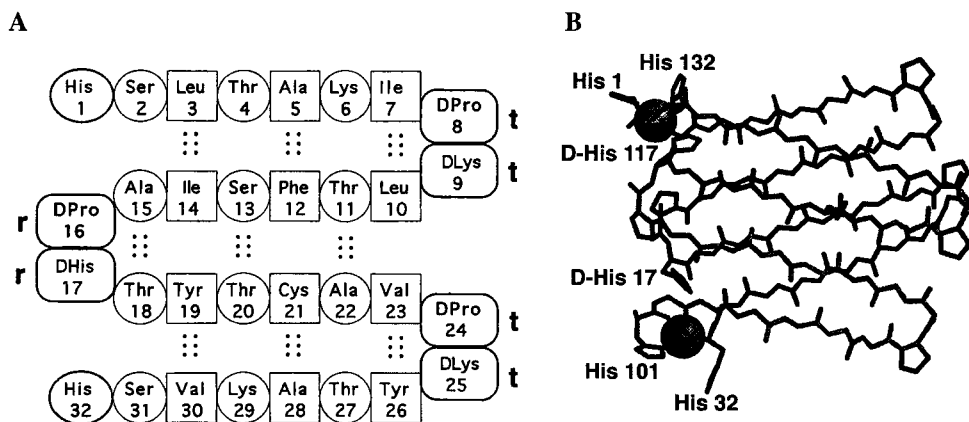


Fig. 1. A. Predicted  $\beta$ -sheet structure of one chain of betabellin 15D showing 18 interstrand  $C=O \cdots H-N$  hydrogen bonds ( $\cdots$ ) between pairs of polar residues (circled, side chains down) or nonpolar residues (boxed, side chains up). B. A computer-generated model of a molecule of betabellin 15D binding two  $Cu^{II}$  ions (spheres) through histidine residues.

## Results and Discussion

A molecule of betabellin 15D consists of two betabellin-15 chains covalently linked by a disulfide bond between their cysteine residues. The 32-residue chain (Fig. 1A) was assembled by solid-phase peptide synthesis, purified to homogeneity by reversed-phase HPLC, and air oxidized in 20% (CH<sub>3</sub>)<sub>2</sub>SO at 37 C to provide betabellin 15D. The molecular masses of the single chain (3512 Da) and the disulfide-linked two-chain molecule (7022 Da) were confirmed by electrospray-ionization mass spectrometry.

Circular dichroic studies showed that a solution of 40 μM betabellin 15D in 10 mM ammonium acetate without CuCl<sub>2</sub> did not exhibit β structure at pH 5.8, 6.4, or 6.7. Addition of one molecule of CuCl<sub>2</sub> per molecule of betabellin 15D, however, induced the formation of substantial β-sheet structure ( $[\theta] = -9500 \text{ deg cm}^2 \text{ dmol}^{-1}$  at 218 nm and pH 6.7). The Cu<sup>II</sup>/betabellin 15D complex showed more β structure at pH 6.7 than at pH 5.8 or 6.4, which is consistent with binding of Cu<sup>II</sup> to a neutral imidazole ring on the side chain of a histidine residue. When folded into a β sandwich, betabellin 15D has six histidine residues clustered at the rr end that can bind Cu<sup>II</sup> ions (Fig. 1B).

Electron microscopic studies showed that 40 μM betabellin 15D in 10 mM ammonium acetate at pH 6.7 without CuCl<sub>2</sub> did not form fibrils. But a solution of 36 μM betabellin 15D and 110 μM CuCl<sub>2</sub> in 10 mM ammonium acetate at pH 6.7 formed fibrils that were 35 ± 26 nm long (mean ± SD) but only 7 ± 2 nm wide. When folded into a β sandwich (Fig. 1B), betabellin 15D is about 3.3 nm wide, so an average fibril is about 100 molecules of betabellin 15D long and only two molecules wide. The structure of these Cu<sup>II</sup>/betabellin 15D fibrils is probably stabilized by many intermolecular β-sheet hydrogen bonds along its length (cross-β structure) and many intermolecular Cu<sup>II</sup>/histidine bonds across its width (metal-ligand structure).

## Acknowledgments

This work was supported by NIH research grants GM 42031 (to B.W.E.) and GM 31819 (to J.D.G.) from the U.S. Public Health Service.

## References

1. Richardson, J.S. and Richardson, D.C., In Oxender, D.L. and Fox, C.F. (Eds.) Protein Engineering, Liss, New York, 1987, p. 149.
2. Erickson, B.W., Daniels, S.B., Reddy, P.A., Higgins, M.L., Richardson, J.S. and Richardson, D.C., ICSU Short Rep., 8 (1988) 4.
3. Yan, Y., Tropsha, A., Hermans, J. and Erickson, B.W., Proc. Natl. Acad. Sci. USA, 90 (1993) 7898.
4. Wagner, D.S., Melton, L.G., Yan, Y., Erickson, B.W. and Andereg, R.J., Protein Sci., 3 (1994) 1305.
5. Yan, Y. and Erickson, B.W., Protein Sci., 3 (1994) 1069.

# Engineering of an iron(II)-braced tripod protein containing proline-II helical legs

Bassam M. Nakhle, Tracie L. Vestal, Matthew J. Saderholm  
and Bruce W. Erickson

Department of Chemistry, University of North Carolina at Chapel Hill,  
Chapel Hill, NC 27599, USA

Oligoproline assemblies bearing an electron donor, an electron acceptor, and a redox chromophore mimic photosynthetic reaction centers by converting light energy into chemical energy [1]. Controlling the distance between these redox modules is an important factor for the efficiency of energy conversion. Five or more contiguous proline residues form a stable rod-like helix [2] that can serve as a rigid molecular framework for linking the redox modules.

We have designed, synthesized, and characterized an iron(II)-braced tripod protein that contains a redox-active chromophore (Fig. 1). It consists of three copies of a rigid 10-residue leg peptide that is covalently linked through sulfide bonds to an N-terminal mesitylene apex and by amide bonds to an iron(II)tris(Mbc) brace, where Mbc-OH is 4'-methyl-2,2'-bipyridine-4-carboxylic acid. A  $C_3$  symmetry axis runs through the centers of the apex and the iron(II) atom of the brace.

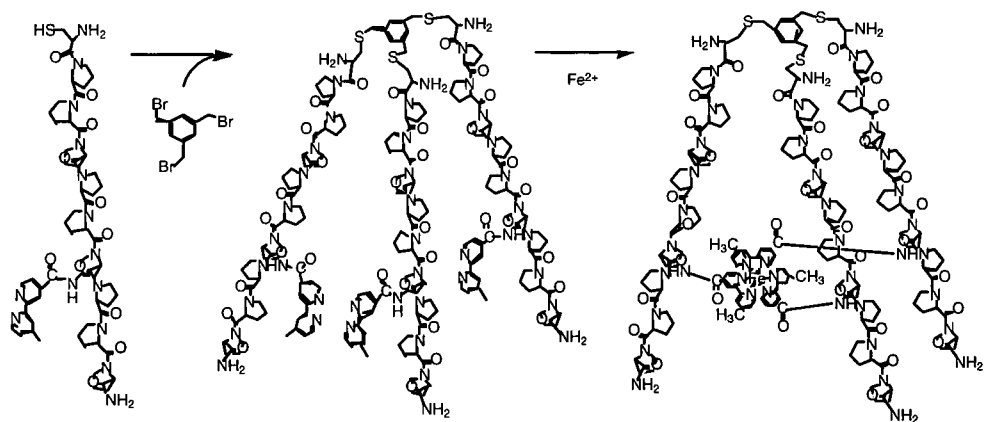


Fig. 1. Synthesis of an iron(II)-braced tripod protein. Three copies of the leg peptide (left) are S-alkylated by 1,3,5-tris(bromomethyl)benzene and the resulting unbraced tripod (center) is complexed with one  $Fe^{2+}$  ion to furnish the iron(II)-braced tripod (right).

## Results and Discussion

The leg peptide (H-Cys-Pro<sub>5</sub>-Pra(Mbc)-Pro<sub>3</sub>-NH<sub>2</sub>), where Pra is *cis*-4-amino-L-proline, was assembled by the solid-phase method using Boc chemistry and Boc-Pra(Mbc)-OH. The latter was made by coupling Mbc-OH to the 4-amino group of Boc-Pra-OCH<sub>3</sub> [3] using BOP, DMAP, HOBT and NMM and saponifying the methyl ester, Boc-Pra(Mbc)-OCH<sub>3</sub>.

The five modules of the tripod protein (3 legs, apex and brace) were assembled in two steps (Fig. 1). First, the thiol groups of three copies of the leg peptide were regiospecifically alkylated by 1,3,5-tris(bromomethyl)benzene to furnish the unbraced tripod protein. Second, the braced tripod was obtained by complexing one molecule of the unbraced tripod with one Fe<sup>2+</sup> ion from Fe(NH<sub>4</sub>)<sub>2</sub>(SO<sub>4</sub>)<sub>2</sub>·6H<sub>2</sub>O.

The expected molecular masses of the unbraced tripod (3730 Da) and the braced tripod (3786 Da) were confirmed by electrospray-ionization mass spectrometry. The iron(II)-braced tripod exhibited a metal-to-ligand charge transfer (MLCT) absorption band at 545 nm. Far-UV circular dichroic spectroscopy (CD) revealed that the leg peptide, the unbraced tripod, and the braced tripod each fold in aqueous solution into a proline-II helix, which showed a strong negative CD band at 205 nm and a weak positive band at 226 nm. Iron(II)tris(2,2'-bipyridine) complexes can exist in either the right-handed  $\Delta$  conformation or the left-handed  $\Lambda$  conformation. Based on its negative CD band at 310 nm, the braced tripod exists predominantly in the  $\Delta$  conformation [4].

In 20:1 (v/v) acetonitrile/water, the proline-II helical form of the unbraced tripod undergoes substantial isomerization into the proline-I helical form, as indicated by its strong negative CD band at 205 nm becoming a weaker negative band at 200 nm and its weak positive CD band at 226 nm becoming a much stronger positive band at 216 nm. In contrast, the braced tripod remains predominantly in the proline-II form, because of the shift of its weak positive CD band from 226 nm to 220 nm does not change its intensity.

## Acknowledgments

We thank Amareth Lim for recording the mass spectra and the U.S. Public Health Service for research grant GM 42031 from the National Institute of General Medical Sciences.

## References

1. McCafferty, D.G., Bishop, B.M., Wall, C.G., Hughes, S.G., Mecklenberg, S.L., Meyer, T.J. and Erickson, B. W., *Tetrahedron*, 51 (1995) 1093.
2. Deber, C.M., Bovey, F.A., Carver, J.P. and Blout, E.R., *J. Am. Chem. Soc.*, 92 (1970) 6191.
3. McCafferty, D.G., Slate, C.A., Nakhle, B.M., Graham, H.D., Austell, T.L., Vachet, R.W., Mullis, B.H. and Erickson, B.W., *Tetrahedron*, 51 (1995) 9859.
4. Mason, S.F., Peart, B.J. and Waddel, R.E., *J. Chem. Soc., Dalton Trans.*, (1973) 944.

# ***De novo* design and synthesis of a heme-binding four-helix TASP capable of light-induced electron transfer**

**Harald K. Rau, Niels de Jonge and Wolfgang Haehnel**

*Albert-Ludwigs-Universität Freiburg, Institut für Biologie II / Biochemie  
Schänzlestr. 1, D-79104 Freiburg, Germany*

Redox proteins are the largest group of known enzymes. They serve a wide range of functions including electron transport, light-induced charge separation, proton pumping and catalysis. Therefore, *de novo* design of redox proteins is an attractive approach for investigating the factors involved in electron transfer and to create proteins with new properties. The use of chemoselective ligation methods of unprotected peptide fragments in combination with the template assembled synthetic protein (TASP) concept [1] enables us to synthesize *de novo* designed redox proteins with high structural complexity and defined topology [2]. We present here the design and synthesis of a heme-binding antiparallel four-helix TASP with a covalently bound Ru(bipy)<sub>3</sub>-complex.

## **Results and Discussion**

Three different amphiphilic helices (H1-H3) were designed to form a water soluble antiparallel four-helix bundle protein, which was intended to bind one heme group in its hydrophobic interior using two histidine side chains of the helices H1 and H3 as ligands (Fig. 1). The sequence of the peptides was the following:

- H1: Mal-G-N-A-R-E-L-H-E-K-A-L-K-Q-L-E-E-L-F-K-K-W-amide  
H2: Ac-N-L-E-E-F-L-K-K-F-Q-E-A-L-E-K-A-Q-K-L-L-K(Mal)-amide  
H3: Mal-G-N-A-L-E-L-H-E-K-A-L-K-Q-L-E-C(Acm)-L-L-K-Q-L-amide

The peptides were synthesized by solid phase peptide synthesis. After modification of either the N-terminus of the peptides H1 and H3 or the ε-amino group of the C-terminal Lys of H2 with 3-maleimidopropionic acid (Mal) the peptides were cleaved from the resin and purified by RP-HPLC (Cys<sup>16</sup> of H3 was still Acm protected). The synthesis of the cyclic template (*cyclo*[C(Acm)-A-C(Trt)-P-G-C(Acm)-A-C(StBu)-P-G]) was carried out with modifications as described by Dumy et al. [3]. The TASP molecule MOP2 was obtained *via* thioether bond formation of the helical peptides to the orthogonally protected template.

The [Ru(4-bromomethyl,4'-methyl-2,2'-bipyridyl)(2,2'-bipyridyl)<sub>2</sub>]<sup>2+</sup>-complex was synthesized in a five step synthesis as described by Geren et al. [4]. It was coupled chemoselectively *via* a stable thioether group to Cys<sup>16</sup> (after Acm deprotection) in the hydrophilic face of the heme binding helix H3. Electrospray mass spectrometry confirmed the calculated molecular weight of the resulting peptide (Ru-MOP2) of 12,199 Da and showed the high purity of the peptide. One heme group was bound to the protein as judged by UV/Vis-spectroscopy. CD spectroscopy of heme-Ru-MOP2 showed the spectrum of a highly helical

protein with a mean residue molar ellipticity at 222 nm of  $[\theta]_{222} = -25,500 \text{ deg cm}^2 \text{ dmol}^{-1}$ . The CD-spectra of MOP2 and Ru-MOP2 were superimposable on the spectrum of heme-Ru-MOP2. Size exclusion chromatography revealed that the protein is monomeric in solution over

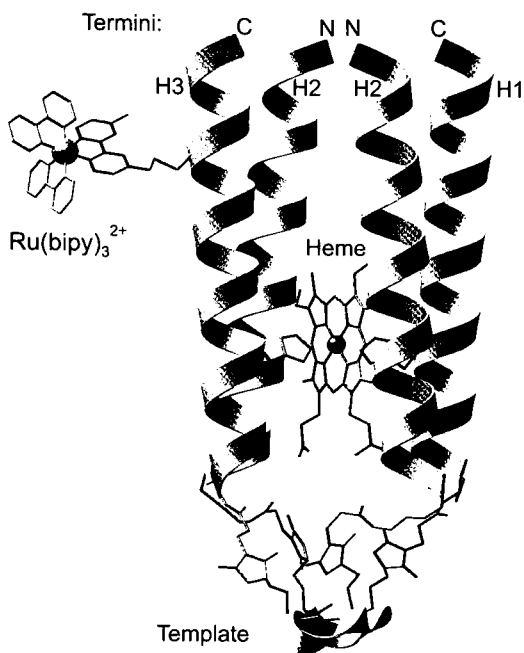


Fig. 1. Structural proposal of heme-Ru-MOP2.

## Acknowledgments

This work was supported by the BMBF and the Volkswagen Stiftung.

## References

1. Mutter, M., Altmann, E., Altmann, K.-H., Hersperger, R., Koziej, P., Nebel, K., Tuchscherer, G. and Vuilleumier, S., *Helv. Chim. Acta*, 71 (1988) 835
2. Rau, H. and Haehnel, W., *Ber. Bunsenges. Phys. Chem.*, 100 (1996) 2052
3. Dumy, P., Eggleston, I. M., Cervigni, S., Sila, U., Sun, X. and Mutter, M., *Tetrahedron Lett.*, 36 (1995) 1255
4. Geren, L., Hahm, S., Durham, B. and Millet, F., *Biochemistry*, 30 (1991) 9450
5. Santoro, M. M. and Bolen, D. W., *Biochemistry*, 27 (1988) 8063

a wide concentration range. An electrochemical midpoint potential of  $-170 \text{ mV}$  was found by redox potentiometry for the heme group in the heme-Ru-MOP2 molecule. The stability of heme-Ru-MOP2 was determined by following the molar ellipticity at 222 nm as a function of guanidinium chloride concentration. Using the two-state transition model of Santoro and Bolen [5] the free energy of unfolding in the absence of denaturant is  $35 \text{ kJ/mol}$  ( $m = -9.5 \text{ kJ M}^{-1} \text{ mol}^{-1}$ ). The rate of the aser-induced intramolecular electron transfer from the Ru-complex to the heme group was calculated to  $2.28 \times 10^6 \text{ s}^{-1}$  from the kinetic measurements of the luminescence lifetime of the Ru-complex in the presence and absence of heme.

## Inhibition of nitric oxide synthase with calmodulin binding peptides

Karen S. Gregson,<sup>a</sup> Michael A. Marletta<sup>a,b</sup> and Henry I. Mosberg<sup>a</sup>

<sup>a</sup>Interdepartmental Program in Medicinal Chemistry, <sup>b</sup>Department of Biological Chemistry, University of Michigan, Ann Arbor MI 48109, USA

The constitutive isoforms of nitric oxide synthase (nNOS and eNOS) are regulated by calmodulin, which adopts an active conformation upon binding calcium and binds to target proteins. The inducible isoform of NOS (iNOS) copurifies with calmodulin [1] and was reported not to require calcium for activation [2]. It has been shown that a peptide corresponding to the calmodulin binding region of iNOS (iP), shown below, completely inhibits the inducible isoform at a molar ratio of peptide to enzyme concentration of 12:1 [3]. A peptide from the calmodulin binding domain of nNOS (nP), shown below, was synthesized and completely inhibited nNOS at a molar ratio of peptide to enzyme concentration of 8:1. However, this peptide is unable to inhibit iNOS at molar ratios of peptide to enzyme concentrations up to 16:1. These results suggest that calmodulin interacts differently with the two NOS isoforms. These peptides are alpha helical and show 43% identity. There are, however, striking differences in charge and hydrophobicity in nine individual amino acid residues (shown in bold below) located at corresponding positions in the two peptides.

nP:           KRR**A**IGF**K**KL**A**E**A**V**K**FSA**K**LM**G**Q**A**MA**K**R**V**R  
iP:           RRR**E**IR**F**RV**L**V**K**V**V**F**F**AS**M**LM**R**K**V**MA**S**R**V**R

### Results and Discussion

It was observed that these nine dissimilar positions lie on one face of the alpha helix, as shown in Figure 1. In an effort to confer the inhibitory activity of iP to another peptide, eight residues were incorporated into the calmodulin binding domain of skeletal muscle light chain kinase, which binds to calmodulin but was previously shown to be unable to inhibit iNOS. The new composite peptide was truncated before the glutamic acid residue in order to maintain the positive charge on the amino terminus, a charge typical of peptides that bind tightly to calmodulin [4]. Sequences are shown below with changed and corresponding residues in bold. This new composite peptide is able to inhibit iNOS, unlike the peptide from MLCK, although at concentrations that are ten fold higher than the original iP peptide.

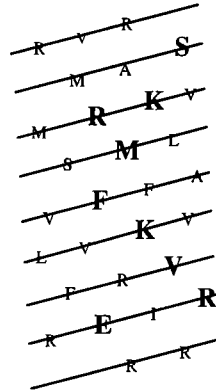


Fig. 1. One face of the alpha helix formed by the calmodulin binding domain of iNOS

iP: RRREI**R**FRVL**V**KV**V**FFAS**M**LM**R**KV**M**AS**R**VR  
 MLCK KR**R**W**K**KN**F**IA**V**SA**A**NR**F**K**I**SS**S**G**A**L  
 Composite RR**W**K**V**N**F**KA**V**FA**A**N**M**F**K**R**K**SS**S**S**A**L

## Conclusion

The residues responsible for the differential inhibition of the isoforms of NOS by calmodulin binding peptides have been isolated on the composite peptide. Future plans include the synthesis of shorter composite peptides.

## Acknowledgments

This work was supported by grants CA 50414 (MAM) and DA03910 (HIM) from the National Institutes of Health.

## References

1. Cho, H.J., et al. *J.Exp.Med.*, 176 (1992) 599.
2. Hevel, J.M., White, K.A. and Marletta, M.A., *J.Biol.Chem.*, 266 (1991) 22789.
3. Stevens-Truss, R. and Marletta, M., *Biochemistry*, 34 (1995) 15638.
4. Means, A.R. and Conn, P.M. (Eds.) *Methods in Enzymology*, Academic Press, Inc. 1987, p. 455.

# Improved peptides for holographic data storage

Palle H. Rasmussen, P. S. Ramanujam,<sup>a</sup> Søren Hvilsted and Rolf H. Berg

Condensed Matter Physics and Chemistry Department, <sup>a</sup>Optics and Fluid Dynamics  
Department, Risø National Laboratory, DK-4000 Roskilde, Denmark

There has been much interest in recent years in developing materials for erasable holographic data storage [1]. Although many promising organic and inorganic compounds and composites have been explored, at present there are none that meet all the prerequisites for the ideal material. We have recently reported that holographic gratings with large first-order diffraction efficiencies can be recorded and erased optically in thin films of a new class of azobenzene-containing peptides (DNO oligomers) [2]. The gratings also exhibit good thermal stability. This paper summarizes some of our efforts to modify the DNO structure so as to accelerate the recording speed.

## Results and Discussion

As reported elsewhere [3], it takes on the order of 5 minutes to obtain a diffraction efficiency of about 76% with an ornithine-based DNO dimer. For comparison, such diffraction efficiency can be obtained with photorefractive polymers within hundreds of milliseconds [4]. However, by systematically varying the DNO structure a notable decrease in recording time can be obtained. For example, with diaminobutyric acid-based DNO decamer **1** (Fig.1), a diffraction efficiency of 78% is reached in about 10

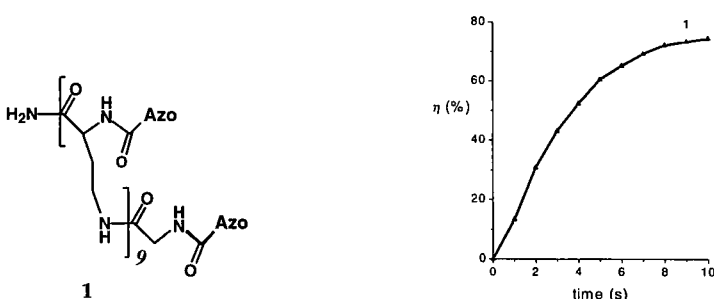


Fig. 1. First-order diffraction efficiency as a function of time, measured during grating formation in a thin film of a diaminobutyric acid-based DNO decamer (**1**). Azo =  $-\text{CH}_2-\text{O}-\text{C}_6\text{H}_4-\text{N}=\text{N}-\text{C}_6\text{H}_4-\text{CN}$ .

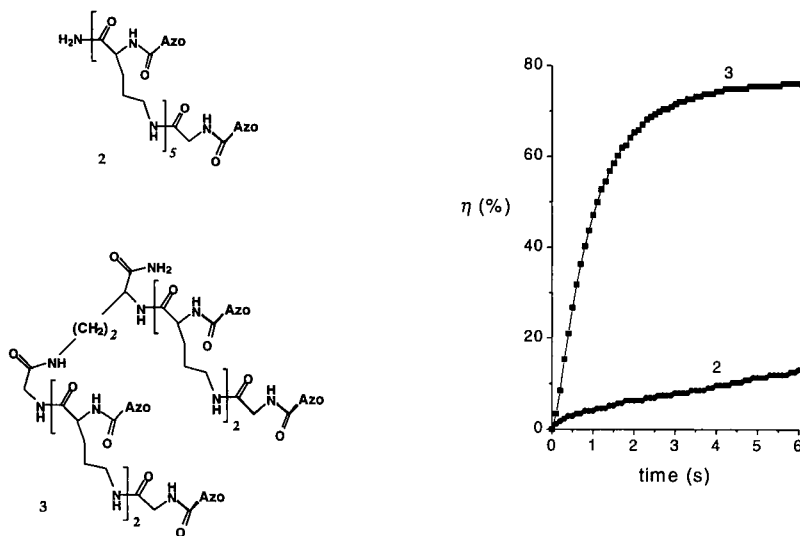


Fig. 2. First-order diffraction efficiencies as a function of time, measured during the grating formation in thin films of an ornithine-based DNO hexamer (2) and an ornithine-based DNO bis-trimer (3).

seconds [2]. Another remarkable example is shown in Fig. 2. Here the recording speed achieved with bis-trimer **3** is enhanced dramatically when compared with hexamer **2** made from the same number of ornithine backbone units and containing the same number of azobenzene chromophores. We ascribe the accelerated recording speed of **3** to an increased secondary structure stability by which the coordinated reorientation of the chromophores (which eventually orient themselves in a stationary orientation with the optical transition moment axis perpendicular to the polarization of the laser beam) has become more efficient.

**Acknowledgements** We thank Ms. Anne Bønke Nielsen for skilled technical assistance. This research is supported by The Danish Research Councils and The Danish Materials Technology Development Programme.

## References

1. Sincerbox, G. T., *Opt. Mater.*, 4 (1995) 370.
2. Berg, R. H., Hvilsted, S. and Ramanujam, P. S., *Nature*, 383 (1996) 505.
3. Berg, R. H., Rasmussen, P. H., Hvilsted, S. and Ramanujam, P. S. In Tam, J. P. and Kaumaya, P. T. P. (Eds.) *Proceedings of the 15th American Peptide Symposium*, ESCOM/Kluwer, Leiden, 1997.
4. Meerholz, K., Volodin, B. L., Sandalphon, Kippelen, B. and Peyghambarian, N., *Nature*, 371 (1994) 497.



**Session III**

**Peptide Mimetics**



# Structure-based *de novo* design and discovery of nonpeptide antagonists of the pp60<sup>Src</sup> (Src) SH2 domain

K. S. Para,<sup>a</sup> E. A. Lunney,<sup>a</sup> M. S. Plummer,<sup>a</sup> C. J. Stankovic,<sup>a</sup> A. Shahripour,<sup>a</sup> D. Holland,<sup>a</sup> J. R. Rubin,<sup>a</sup> Humblet,<sup>a</sup> J. Fergus,<sup>b</sup> J. Marks,<sup>b</sup> S. Hubbell,<sup>c</sup> R. Herrera,<sup>c</sup> A. R. Salties<sup>c</sup> and T. K. Sawyer<sup>a</sup>

<sup>a</sup>Department of Chemistry, <sup>b</sup>Department of Biochemistry, and the <sup>c</sup>Department of Cell Biology, Parke-Davis Pharmaceutical Research, Division of Warner Lambert Company  
2800 Plymouth Road, Ann Arbor, MI 48105, USA

The pp60<sup>Src</sup> (Src) is a nonreceptor tyrosine kinase which is known to interact with several key signalling proteins via sequence-specific phosphotyrosine (pTyr) mediated binding with its SH2 domain [1]. An X-ray crystal structure of Src SH2 complexed with phosphopeptide **1** (shown below) provided the first detailed molecular map of the family of SH2 domains with respect to their binding interactions with pTyr-containing ligands [2]. Two major binding pockets for pTyr and the P+3 Ile exist. Intermolecular H-bonding contacts to the P+1 Glu(NH) as well as two water mediated H-bonding contacts to the P+1 Glu(C=O) and the P+3 Ile(NH) are observed.

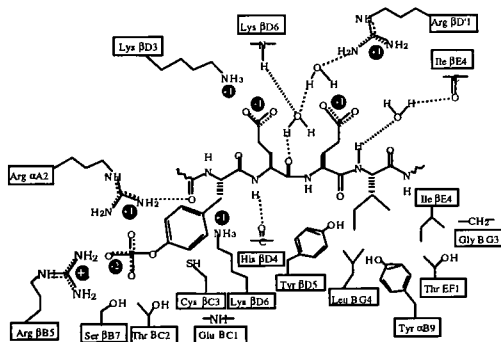
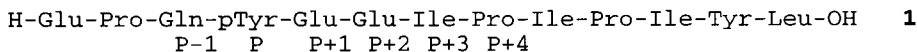


Fig. 1. Schematic illustration of intermolecular contacts of **1** and Src SH2 [2].

## Results and Discussion

As detailed below, our drug discovery strategy has focused on the *de novo* design of a novel series of achiral nonpeptides. It was based on a benzamide template (Fig. 2), and first tested by the nonpeptide **2**. Relative to the phosphopeptide **1**, the nonpeptide **2** does not possess any amino acid substructure. Furthermore, the benzamide CONH<sub>2</sub> moiety was designed to bind directly to the SH2 domain with intermolecular H-bonding with Ile $\delta$ D6(NH) and Lys $\delta$ B4(NH).

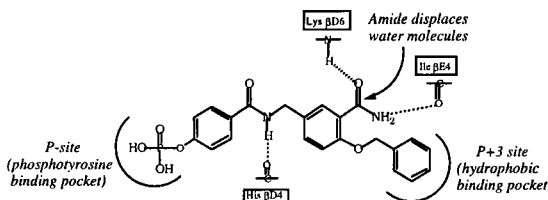


Fig. 2. *De novo* design of a novel nonpeptide ligand (**2**) for the Src SH2 domain.

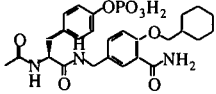
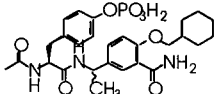
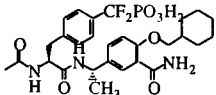
The structure-activity relationships of a series of analogs of nonpeptide **2** are summarized in Table 1, and results were obtained using a competitive binding assay as previously described [3]. In brief, these studies supported the design concept for the nonpeptide series with respect to the importance of the P-site phosphophenyl moiety, P+3 site hydrophobic group, and benzamide CONH<sub>2</sub> functionality. An X-ray structure of compound **3** complexed with the Src SH2 domain has been determined (Lunney *et al.*, unpublished data) and supported the *de novo* design strategy of the nonpeptide series.

Table 1. Binding Affinities of *De Novo* Designed Nonpeptide Analog.

Compound Number	Analog	IC <sub>50</sub> μM
2		9.7
3		6.6
4		6.5
5		5.6

Another series of nonpeptides was next advanced by systematic modifications at both the P-site and the P+1 site as summarized in Table 2. Substitution of pTyr at the P-site in nonpeptide **4** retained similar binding affinity as shown by the “hybrid” analog **6**. Relative to the “hybrid” pTyr-nonpeptide **6**, the effect of *alpha*-methyl substitution was quite significant as exemplified by compound **7** (IC<sub>50</sub> = 0.7 μM). Furthermore, replacement of pTyr in **7** by the nonhydrolyzable F<sub>2</sub>Pmp provided a potent analog **8** (IC<sub>50</sub> = 0.3 μM) which was considered a breakthrough lead compound of possible use in cellular studies. The “hybrid” analog **8** was further evaluated for specificity properties relative to the SH2 domains of Abl, PLC, Grb2 and Syp (Table 3) using methods previously described [4]. Indeed, the “hybrid” F<sub>2</sub>Pmp-nonpeptide **8** showed both high affinity and specificity for

Table 2. Binding Affinities of De Novo Designed Nonpeptide Analogs.

Compound Number	Analog	IC <sub>50</sub> μM
6		8.5
7		0.7
8		0.3

Src SH2, as compared to the reference pentapeptide Ac-F<sub>2</sub>Pmp-Glu-Glu-Ile-Glu-OH **9**. In summary, we have successfully advanced a novel series of nonpeptides to provide a lead compound suitable for cellular studies to examine the Src SH2 domain as a possible therapeutic target in cancer and/or osteoporosis drug discovery.

Table 3. SH2 Specificity of Compounds **8** and **9**.

Compound Number	Src	Abl	Syp(N)	PLCγ(C)	Grb2
8	1.9	9	>100	>100	>100
9	1.4	15.3	>100	>100	>100

## References

1. Courtneige, S.A., Fumagalli, S., Koegl, M., Superti-Furga, G. and Twamley Stein, G.M., *Development*, (1993) 57.
2. Waksman, G., Shoelson, S. E., Pant, N., Cowburn, D. and Kuriyan, J., *Cell*, 72(1993) 779.
3. Plummer, M. S., Lunney, E. A., Para, K. S., Prasad, J. V. N. V., Shahripour, A., Singh, J., Stankovic, C. J., Humblet, C., Fergus, J. H., Marks, J. S. and Sawyer, T. K., *Drug Design Disc.*, 13(1996) 75.
4. Stankovic, C. J., Plummer, M. S. and Sawyer, T. K. "Peptidomimetic Ligands for Src Homology-2 Domains"; A. Abell, Ed.; *Advances in Amino Acid Mimetics and Peptidomimetics*, JAI Press, *in press*.

# New RGD amphiphilic cyclic peptide and new RGD-mimetic constrained diketopiperazines

Jean-François Pons,<sup>a</sup> Mamadou Sow,<sup>a</sup> Frédéric Lamaty,<sup>a</sup> Jean-Luc Fauchère,<sup>b</sup> Annie Molla,<sup>c</sup> Philippe Viallefont<sup>a</sup> and René Lazaro<sup>a</sup>

<sup>a</sup> LAPP CNRS ESA 5075, Université Montpellier II, 34095, Montpellier,<sup>b</sup> Institut de Recherches Servier, 92150, Suresnes,<sup>c</sup> LEDAC CNRS UMR 5538, 38706, La Tronche, FRANCE

The search for peptide-based or peptidomimetic derivatives is an on-going challenge in obtaining new lead compounds with increased bioavailability and selectivity compared to the parent peptide. Unfortunately, in linear peptides the RGD sequence is poorly resistant to biodegradation and poorly selective, since it acts on at least seven of the twenty integrin receptors described up to now [1]. We have therefore introduced this sequence in a cyclic structure, cyclo[Deg-Arg-Gly-Asp-] bearing a diazaethyleneglycol derivative (Deg =  $\text{NHC}_2\text{H}_4\text{OC}_2\text{H}_4\text{NHCOC}_2\text{H}_4\text{CO}$ ).

Furthermore, assuming that increasing the rigidity would enhance bioavailability and selectivity, we have designed and prepared a series of diketopiperazines (DKPs) containing a bicyclic residue (Abo = (2S) 2-aza-bicyclo[2.2.2]-octan-3-carboxylic acid [2]) coupled to Asp, the latter supplying the essential  $\beta$ -carboxylic group. Amine or amine-like functions (guanidine, piperidine, benzamidine) supplying the necessary positive charge have been further grafted through different linkers to the DKP ring.

For biological screening, in addition to the well-known ADP-induced platelet (dog) aggregation assay, we have developed new tests using HEL cell adhesion that are more convenient tools for investigating the potency and selectivity of integrin antagonists. HEL cells from hematopoietic erythroblastic cell line [3] grown in suspension indeed become adherent in the presence of matrix proteins such as fibronectin or fibrinogen through their respective  $\alpha_5\beta_1$  or  $\alpha_{IIb}\beta_3$  receptors.

## Results and Discussion

*c(DegRGD)*; *DKP synthesis*: Trt-NHC<sub>2</sub>H<sub>4</sub>OC<sub>2</sub>H<sub>4</sub>NHCOC<sub>2</sub>H<sub>4</sub>COOH has been prepared in 4 steps (Yield: 70-90% / step), starting from available NH<sub>2</sub>C<sub>2</sub>H<sub>4</sub>OC<sub>2</sub>H<sub>4</sub>OH (H-A-OH): H-A-OH + Trt-Cl → Trt-A-OH + (PPh<sub>3</sub> / DEAD) + NHPht → Trt-A-NPht + (N<sub>2</sub>H<sub>4</sub>, EtOH, THF) → Trt-A-NH<sub>2</sub> + [(C<sub>2</sub>H<sub>4</sub>CO)<sub>2</sub>O, DMAP, TEA] → Trt-Deg-OH. The linear peptide precursor has been constructed in solution starting from BocGlyOBn with standard peptide activations and protections: BOP/DMF/DIEA for BocArg(NO<sub>2</sub>), TrtOeg and ZAsp(OBu<sup>t</sup>)OSu. The peptide cyclization has been performed at 4mM concentration in DMF using BOP / NaHCO<sub>3</sub> for coupling (40% yield, after HPLC purification [4]).

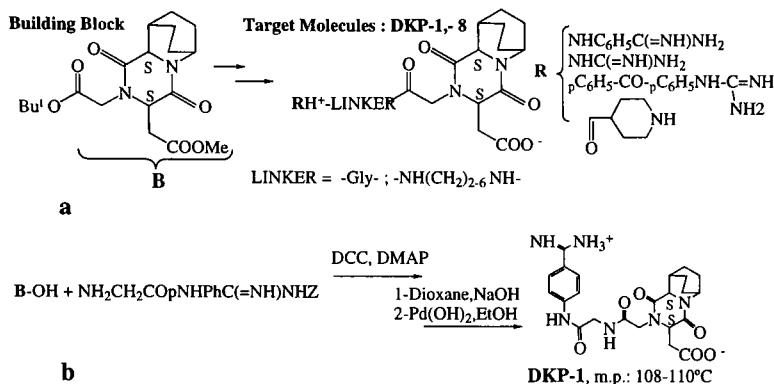


Fig 1. **a** : a general scheme of the new diketopiperazines (DKPs) ; **b** : DKP -1 synthesis.

The best way to prepare the functionalized DKP (B-OH) used as building block was by cyclizing HAsp(OMe)-AboOMe, (Yield: 75%, d.e.>95%) and by performing a smooth N-alkylation of the resulting DKP by HNa and BrCH<sub>2</sub>CO<sub>2</sub>Bu<sup>t</sup> in THF giving an 80% yield of DKP (B-OBu<sup>t</sup>). A monocrystal X-ray analysis has shown that the S,S configuration was maintained. As an example, DKP-1 synthesis is briefly depicted, in Fig.1b.

**Biological activity:** All DKPs except DKP-1 are inactive against ADP-induced platelet aggregation and in the HEL-cell adhesion assays. Inhibitory activities (IC<sub>50</sub> μM) of c(DegRGD) and DKP-1 for HEL cell binding to fibronectin, are respectively, 65 and >1000, to fibrinogen 14 and 27, and for the platelet aggregation assay 73 and 18 μM.

Whereas the cyclic peptide displays the same activity level in both assays, DKP-1 is active only on fibrinogen binding both in the HEL cell adhesion and platelet aggregation assays which involve the α<sub>IIb</sub>β<sub>3</sub> receptors and has no inhibitory action on HEL cell adhesion mediated by α<sub>5</sub>β<sub>1</sub> fibronectin binding. This selectivity may be related to the presence of a benzamidine instead of a guanidine [5] group and/or to the higher rigidity of the DKP-1 molecule as compared to the cyclic peptide.

## References

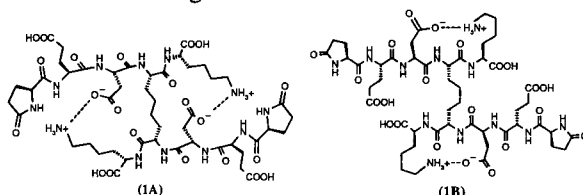
1. Hynes, R.O., Cell, 48 (1992) 545-549.
2. Vincent, M., Pascard, C., Cesario, M., Remond, G., Bouchet, J.-P., Charton, Y. and Laubie, M., Tetrahedron Lett., 33 (1992) 7369-7372.
3. Martin, P. and Papayannopoulou, T., Science, 216 (1982) 1233-1235.
4. All new compounds exhibit satisfactory <sup>1</sup>H-NMR (250 MHz) and (FAB) Mass spectra, HRMS.
5. Zablocki, J.A., Miyano, M., Garland, R.B., Pireh, D., Schretzman, L., Rao, S.N., Lindmark, R.J., Panzer-Knodle, S.G., Nicholson, N.S., Taite, B.B., Salyers, A.K., King, L.W., Campion, J.G. and Feigen, L.P., J. Med. Chem., 36 (1993) 1811-1819.

# A pharmacophore model of a hematoregulatory peptide, SK&F 107647 and design of peptidomimetic analogs

P. K. Bhatnagar,<sup>a</sup> E. K. Agner,<sup>c</sup> D. Alberts,<sup>a</sup> J. Briand,<sup>a</sup> J. F. Callahan,<sup>a</sup>  
A. S. Cuthbertson,<sup>c</sup> H. Fjordingstad,<sup>c</sup> D. Heerding,<sup>a</sup> J. Hiebl,<sup>d</sup> W. F.  
Huffman,<sup>a</sup> M. Husbyn,<sup>c</sup> A. G. King,<sup>b</sup> S. LoCastro,<sup>a</sup> D. Løvhaug,<sup>c</sup> L. M.  
Pelus,<sup>b</sup> G. Seibel<sup>a</sup> and J. S. Takata<sup>a</sup>

<sup>a</sup>Departments of Medicinal Chemistry and <sup>b</sup>Molecular Virology and Host Defense, SmithKline Beecham Pharmaceuticals, 709 Swedeland Road, P.O. Box 1539, King of Prussia, PA 19206, USA, <sup>c</sup>Nycomed Pharma As, Gaustadalléne 21, Oslo, Norway, <sup>d</sup>Hafslund Nycomed Pharma, St. Peter-Strasse 25, P.O. Box 120, A-2021 Linz, Austria

SK&F 107647 (**1**, (pGlu-Glu-Asp)<sub>2</sub>-Sub-(Lys)<sub>2</sub>)<sup>1</sup> induces a chemokine from murine and human stromal cells that synergizes with various hematopoietic growth factors and affects their ability to modulate hematopoiesis [1]. SK&F 107647 also enhances effector cell functions [2]. A molecular target for this peptide has not yet been identified. A proposed pharmacophore model of **1** [3], based on detailed SAR studies [4], has been utilized to design potent peptidomimetic analogs.



## Results and Discussion

Most structural modifications of **1** result in a loss of activity and only a few substitutions give either equipotent or more potent analogs. The SAR studies also show that the  $\beta$ -carboxylic group of Asp<sup>3</sup> and the  $\omega$ -amino group of Lys<sup>5</sup> are required for biological activity [4] suggesting that these functional groups either interact with a putative receptor or form intramolecular salt bridges. The observation that the biological activity is lost when Lys<sup>5</sup> is replaced by Orn ((pGlu-Glu-Asp)<sub>2</sub>-Sub-(Orn)<sub>2</sub>) but can be restored if Asp<sup>3</sup> is concomitantly replaced with Glu ((pGlu-Glu-Glu)<sub>2</sub>-Sub-(Orn)<sub>2</sub>), supports the concept of intramolecular salt bridges between the side chains of these two residues (**1A** and **1B**). These SAR studies have prompted us to propose a pharmacophore model in which the salt bridges, in conjunction with the diamino dicarboxylic acid at position 4, correctly present the pharmacophore elements (consisting of the two N-terminal residues) to the putative

<sup>1</sup> Sub= (2S,7S)-2,7-diaminosuberic acid

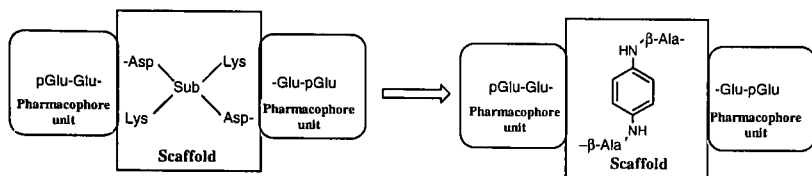
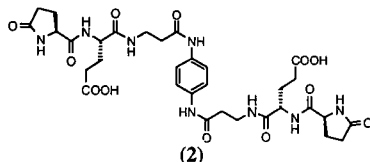
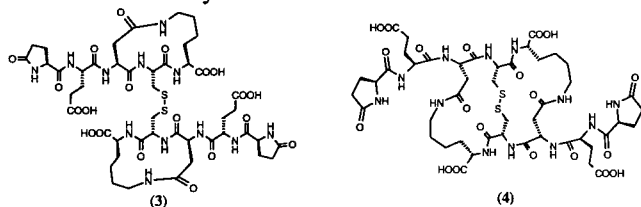


Fig. 1. Proposed pharmacophore model for SK&F 107647 and its peptidomimetic analogs.

receptor. If the model approximates the bioactive conformation then the three C-terminal residues, acting as scaffold, may be replaced with a simpler spacer (Fig. 1). After evaluating several spacers it was found that the entire scaffold can be substituted with a bis-( $\beta$ -Ala)-1,4-phenylenediamine unit. Attachment of the two N-terminal residues to this unit yields a peptidomimetic analog **2** that retains the entire spectrum of biological activities of **1**. Although all of the allowable structural modifications, such as replacement of pGlu<sup>1</sup> with picolinic acid or Pro, as well as Glu<sup>2</sup> with Asp or Ser, to the pharmacophore region of **1** are also accommodated in **2**, this class of compounds is somewhat less active than **1** (EC<sub>50</sub> of **2** and **1**: 684pM, 4pM [4]) indicating that bis-( $\beta$ -Ala)-1,4-phenylenediamine may not be an optimal spacer.



To better understand the role of the side chain functional groups in Asp<sup>3</sup> and Lys<sup>5</sup>, we attempted to constrain the side chains of residues three and five via amide bonds. The HPLC of the resulting product was too complex and it was not possible to distinguish between the interchain or intrachain lactams. Therefore, it was reasoned that if the Sub<sup>4</sup> was replaced with a cystine then the reduction of the disulfide bond would permit distinction between the intra- and interchain lactams. The unambiguous syntheses of cyclic peptides **3** and **4** were designed (data not shown) and reduction of the disulfide bonds in the final products was used to confirm structure. Since lactamization would be expected to reduce the size of the ring versus the corresponding salt bridge and since single methylene deletion in the Lys<sup>5</sup> side chain resulted in an inactive molecule, we were concerned that



both cyclic peptides **3** and **4** might be devoid of activity. Remarkably, both peptides **3** and **4** retained substantial biological activity when compared with **1**; in fact, **4** appeared to be more potent than **3**. These results can be rationalized if one assumes that the critical feature

for biological activity is the correct presentation of the two sets of pharmacophore elements (residues one and two). Exact mimicry of the conformation of the spacer units, as found for example in compound **1** may not be required. The previous results with Lys<sup>5</sup> methylene deletion could have resulted from competing salt bridge formation (e.g., between Lys<sup>5</sup> and Glu<sup>2</sup>) which may have placed the pharmacophore elements in an improper orientation. NMR studies to discern the conformation of cyclic peptides **3** and **4** are ongoing but preliminary molecular modeling studies suggest that either orientation of the peptide scaffold can be accommodated by the bis-( $\beta$ -Ala)-1,4-phenylenediamine spacer unit (Fig. 2) consistent with the biological results.

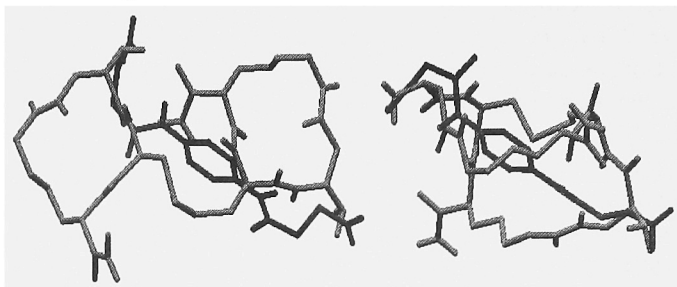


Fig. 2. Over lay of bis-( $\beta$ -Ala)-1,4-phenylenediamine spacer on a minimum energy conformation of the cyclic-tripeptide (Asp-Cys-Lys) unit of **2** and **3**.

## Conclusion

The synthesis of cyclic constrained peptide analogs has supported a proposed pharmacophore model of **1**. Though the utility of the model has been shown by the synthesis of potent peptidomimetic analogs, additional structural information is required to fully substantiate the model.

## References

1. King, A.G., Frey, C.L., Arbo, B., Scott, M., Johansen, K., Bhatnagar, P.K., Pelus, L.M., Blood, 86 (suppl. 1) (1995) 309.
2. DeMarsh, P. L., Socoloski, S. K., Frey, C. L., Koltin, Y., Actor, P., Bhatnagar, P. K., Petteway, S. R., Immunopharmacol., 27 (1994) 199.
3. Bhatnagar, P.K., Alberts, D., Callahan, J.F., Heerding, D., Huffman, W.F., King, A.G., LoCastro, S., Pelus, L.M., Takata, J.S., J. Am. Chem. Soc., 118 (1996) 12862.
4. Bhatnagar, P.K., Agner, E.K., Alberts, D., Arbo, B.E., Callahan, J.F., Cuthbertson, A.S., Engelsens, S.J., Fjordingstad, H., Hartmann, M., Heerding, D., Hiebl, J., Huffman, W.F., Husbyn, M., King, A.G., Kremminger, P., Kwon, C., LoCastro, S., Lovhaug, D., Pelus, L.M., Petteway, S., Takata, J.S., J. Med. Chem., 39 (1996) 3814.

# Design and synthesis of potent and selective peptidomimetic Vitronectin receptor antagonists

**Jochen Knolle,<sup>a</sup> Roland Baron,<sup>b</sup> Gerhard Breipohl,<sup>a</sup> Pierre Broto,<sup>b</sup>  
Tom Gadek,<sup>c</sup> Jean F. Gourvest,<sup>b</sup> Glenn R. Hammonds,<sup>c</sup> Anusch  
Peyman,<sup>a</sup> Karl H. Scheunemann,<sup>a</sup> Hans U. Stilz<sup>a</sup> and Volkmar Wehner<sup>a</sup>**  
*<sup>a</sup>HMR, Building G838, D-65926 Frankfurt am Main, Germany; <sup>b</sup>Roussel, 102 route de Noisy,  
93230 Romainville, France; <sup>c</sup>Genentech, Inc., 460 Point San Bruno Blv.,  
South San Francisco, CA 94080, USA*

In recent years integrin antagonists have been recognized as potential targets in the treatment of thrombotic disorders [1] bone and immune diseases [2], tissue repair [3], tumor invasion and angiogenesis [4]. In general, integrins bind to short peptide recognition motifs of their ligands. Several integrins share the RGD tripeptide as a common recognition motif [5]. Therapeutically applicable integrin antagonists therefore must be specific for their respective integrin, despite the common recognition motif. The discovery of potent, specific and orally available fibrinogen receptor antagonists by us and others has provided evidence that the discrimination between several integrins with a common recognition motif is achievable. To design specific and potent vitronectin receptor antagonists we took the same approach for the drug discovery process as for the fibrinogen receptor antagonist S 5740, which is currently in clinical development [6]. The procedure includes:

- 1) Optimization of distance between pharmacophoric groups
- 2) Optimization of ionic interactions and hydrophobic sites at pharmacophores
- 3) Search for hydrophobic sites at the vitronectin receptor
- 4) Optimization of central RGD mimetic-scaffold

## Results and Discussion

The initial lead compound V005 was found by screening our RGD mimetic library synthesized for the fibrinogen receptor antagonist project (Fig. 1). Further SAR studies led to V0223. This compound is already selective for the vitronectin receptor. The hydantoin scaffold as in V0223 and the tyrosine scaffold as in V0245 (another selective lead compound) served as templates for extended SAR studies. In our initial studies we determined that the optimal distance between the guanidine and the carboxylic acid in the mimetic is 2-3 Å shorter compared with the GP IIb/IIIa antagonists. In the next step we optimized the ionic interactions between the guanidine group and the receptor. Electron withdrawing groups diminished the activity. Cyclic guanidine derivatives improved the potency and the specificity for the vitronectin receptor. The incorporation of large

hydrophobic substituents at the C-terminus led to very potent and specific vitronectin antagonists. These antagonists were found to be highly active in various *in vivo* models of osteoporosis and angiogenesis.

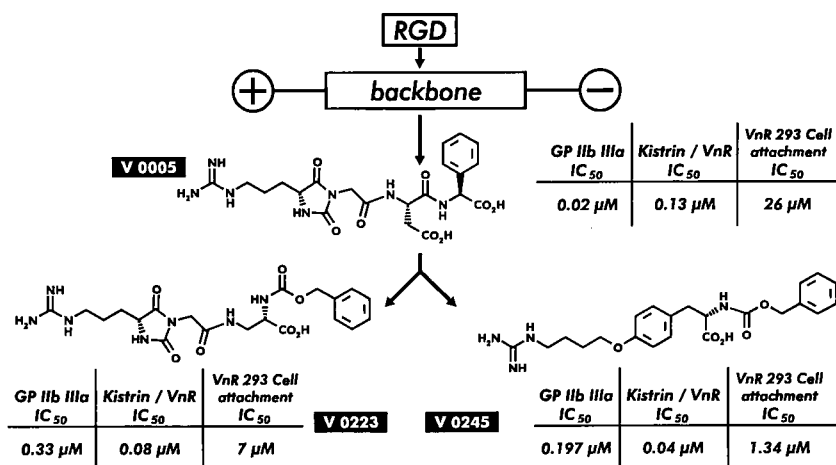


Fig. 1. Vitronectin receptor antagonist lead structures

## Conclusion

By systematic SAR based on our past experience with specific RGD mimetics for the fibrinogen receptor we were able to obtain potent and specific vitronectin receptor antagonists.

## References

- Lefkovits, J., Plow, E.F., Topol, E.J. and N. Engl., J. Med., 332 (1995) 1553.
- Engleman, V.W., Nickols, G.A., Ross, F.P., Horton, M.A., Griggs, D.W., Settle, S.L., Ruminski, P.G. and Teitelbaum, S.L., J. Clin. Invest., 99 (1997) 2284.
- Deluca, M., Pellegrini, G., Zambruno, G. and Marchisio, P.D., J. Dermatol., 21 (1994) 821.
- Brooks, P.C., Montgomery, A.M.P., Rosenfeld, M., Reisfeld, R.A., Hu, T., Klier, G. and Cheresch, D.A., Cell, 79 (1994) 1157.
- Hynes, R.O., Cell, 69 (1992) 11.
- Stilz, H.U., Jablonka, B., Just, M., Knolle, J., Paulus, E.F. and Zoller, G., J. Med. Chem., 39 (1996) 2118.

# Structure-based design of small molecule protein-tyrosine phosphatase inhibitors

Zhu-Jun Yao,<sup>a</sup> Bin Ye,<sup>a</sup> He Zhao,<sup>a</sup> Xinjian Yan,<sup>a</sup> Li Wu,<sup>b</sup>  
David Barford,<sup>c</sup> Shaomeng Wang,<sup>d</sup> Zhong-Yin Zhang<sup>b</sup>  
and Terrence R. Burke, Jr.<sup>a</sup>

<sup>a</sup>Laboratory of Medicinal Chemistry, DBS, NCI, NIH, Bethesda, MD 20892, USA.,

<sup>b</sup>Department of Molecular Pharmacology, Albert Einstein College of Medicine, Bronx, NY 10461, USA, <sup>c</sup>Laboratory of Molecular Biophysics, University of Oxford, Oxford, England, <sup>d</sup>Georgetown University Medical Center, Washington, DC 20007, USA

Protein-tyrosine phosphatases (PTPs) represent attractive targets for inhibitor development. Using the non-receptor PTP1B, we have employed an iterative process of inhibitor design and synthesis / biological evaluation / enzyme-ligand structure elucidation / redesign, to progress from peptide-based inhibitors toward potent small molecule analogues [1]. An example is our initial discovery that replacement of the phosphotyrosyl residue (pY, **1**) in the substrate peptide "D-A-D-E-pY-L" with the hydrolytically stable pY analogue, difluorophosphonomethyl phenylalanine (F<sub>2</sub>Pmp, **2**), resulted in extremely potent PTP1B inhibition (IC<sub>50</sub> = 100 nM) [2]. Our subsequent studies demonstrated that arylmethyl difluorophosphonates, lacking a peptide component, also retain moderate inhibitory potency [3]. While the simple phenyl difluorophosphonate **3** exhibited little affinity, addition of a second aryl ring significantly-enhanced potency (see naphthyl difluorophosphonate **4**, Table 1). Using the X-ray structure of a PTP1B-**4** complex, we designed analogue **5**, which doubled inhibitory potency by introducing a hydroxyl group to mimic an H<sub>2</sub>O molecule originally bound within the catalytic site [4]. In more recent work, we have extended our design rationale to take advantage of interactions outside the pY binding pocket. Some of these later analogues exhibit markedly enhanced inhibitory potencies.

## Results and Discussion

It had previously been shown for PTP1 (the rat homologue of human PTP1B) that acidic residues located proximal to the amino side of the pTyr residue are important for substrate recognition [5, 6]. The structural basis for the favorable effect of acidic residues was subsequently demonstrated using the X-ray structure of the PTP1B enzyme complexed with the peptide "D-A-D-E-pY-L" [7]. Here it was observed that the side chain carboxyls of acidic residues within the substrate could interact with Arg47, which was situated just outside the pTyr binding pocket (see Fig. 1A). Since we had shown by X-ray crystallography how the naphthyl difluorophosphonate compound **4** binds within the pTyr pocket, it was of interest to examine whether functionality could be appended onto **4** that would interact with this critical Arg47 residue. Analogue **6** was therefore designed as a new pTyr mimetic that provided a carboxyl group needed for attachment of the desired

acidic functionality. While the carboxyl group of **6** would not be expected to extend outside the pTyr pocket far enough to span the required distance to the Arg47, it was anticipated that additional functionality could be introduced which would extend the distance so as to allow interaction with Arg47. Simulations of molecular dynamics of one such analogue (**7**) indicated very favorable binding with the Arg47 guanidinium group (Fig. 1B). Because the exact binding of new inhibitors with the enzyme could not be predicted with certainty, the isomeric congener **8** was also designed to introduce variation in the orientation of the acidic side chain relative to the naphthyl ring.

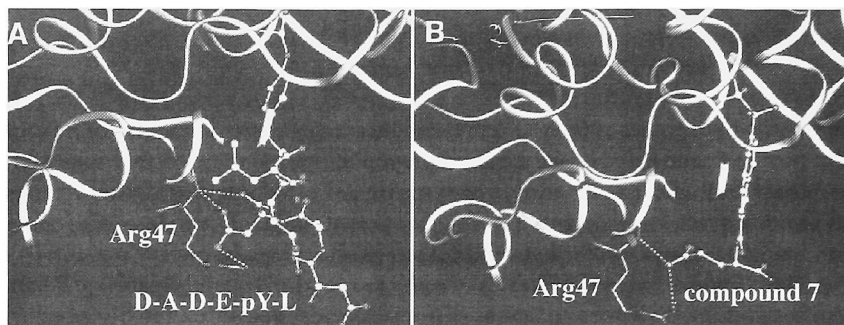


Fig. 1. Binding of ligands to PTP1B showing interaction of Arg47 with ligand acidic residues. (A) X-ray structure of bound peptide "D-A-D-E-pY-L" [7]. (B) Molecular dynamics simulation of mimetic **6**. Prior to simulation, the naphthyl difluorophosphonate moiety was first oriented in the pTyr binding pocket based on the X-ray structure of the PTP1B-**4** complex [4].

Analogues **6** - **8** were prepared and  $K_i$  values determined against PTP1B [8]. Relative to the parent naphthyl difluorophosphonate **4** ( $K_i = 180 \mu\text{M}$ ), a 15-fold enhancement in potency was observed for analogue **7** ( $K_i = 12 \mu\text{M}$ ). The isomeric compound **8** ( $K_i = 24 \mu\text{M}$ ), while being 2-fold less potent than **7**, also showed significantly increased binding affinity relative to parent **4**. The results with compound **7** are consistent with the molecular dynamics simulations which predicted a favorable interaction with the Arg47 residue. The lower potency of **8** may indicate less than optimal interaction with Arg47. Surprisingly, analogue **6**, whose carboxyl group could not bridge the distance to Arg47, also showed an 8-fold enhancement in potency ( $K_i = 22 \mu\text{M}$ ) relative to **4**. The basis for this unexpectedly potent binding of **6** has subsequently been elucidated from an X-ray crystal structure of the PTP1B-**6** complex, where it is seen that a hydrogen bonded  $\text{H}_2\text{O}$  molecule serves as a bridge between the ligand carboxyl and the enzyme [9]. Such a bridge may present interesting possibilities for inhibitor design. Precedents exist where incorporation of functionality onto an inhibitor that mimics critical  $\text{H}_2\text{O}$  molecules can result in significant increases in binding affinity. Our previous inhibitor **5** is one such example [4].

Table 1. Inhibition constants determined against PTP1B.

Compound	K <sub>i</sub> (μM)	Compound	K <sub>i</sub> (μM)
			>2000 <sup>a</sup>
1 pTyr X = O			180 <sup>b</sup>
2 F <sub>2</sub> Pmp X = CF <sub>2</sub>			90 <sup>b</sup>
			22 <sup>d</sup>
			12 <sup>d</sup>
			25 <sup>d</sup>

<sup>a</sup>Reference [8]. <sup>b</sup>Reference [4].

## Conclusion

Naphthyl difluorophosphonates **6** - **8** were prepared containing acidic functionality intended to interact outside the pTyr binding cavity. All of these analogues exhibited substantial increases in potency relative to the parent inhibitor **4**. While compounds **7** and **8** can conceivably interact with the Arg 47 residue, the simpler analogue **6** achieves enhanced potency through a water bridge between the carboxyl and the enzyme. This study demonstrates the utility of combining interactions both inside and outside the pTyr binding pocket for the preparation of potent small molecule inhibitors.

## References

- Burke T. R., Jr., Yao Z.-J., Smyth M. S. and Ye B., *Current Pharmaceutical Design*, 3 (1997) 291-304.
- Burke T. R., Jr., Kole H. K and Roller P. P., *Biochem. Biophys. Res. Commun.*, 204 (1994) 129-134.
- Kole H. K, Smyth M. S, Russ P. L and Burke, T. R. Jr., *Biochemical. J.*, 311 (1995) 1025-1031.
- Burke T. R., Jr., Ye B., Yan X. J., Wang S., Jia, Z. C., Chen L., Zhang Z. Y. and Barford D., *Biochemistry*, 35 (1996) 15989-15996.
- Zhang Z. Y., Thiemesefler A. M., Maclean D., Mcnamara D. J., Dobrusin E. M., Sawyer T. K. and Dixon J. E., *Proc. Natl. Acad. Sci. U.S.A.*, 90 (1993) 4446-4450.
- Zhang Z. Y., Maclean D., Mcnamara D. J., Sawyer T.K. and Dixon J. E., *Biochemistry*, 33 (1994) 2285-2290.
- Jia Z. C., Barford D., Flint A. J. and Tonks N. K., *Science*, 268 (1995) 1754-1758.
- Yao Z.-J., Ye B., Wu X., Wang S., Wu L., Zhang Z.-Y. and Burke, T. R., Jr., *J. Amer. Chem. Soc.* (in review).
- Burke, T. R., Jr. And Barford, D. (manuscript in preparation).

# Structure-activity relationships and spectroscopic insights into a series of retro-inverso tachykinin NK-1 receptor antagonists

A. Sisto,<sup>a</sup> R. Cirillo,<sup>b</sup> B. Conte,<sup>b</sup> C.I. Fincham,<sup>a</sup>  
E. Monteagudo,<sup>a</sup> E. Potier,<sup>a</sup> R. Terracciano,<sup>a</sup> F. Cavalieri,<sup>c</sup>  
M. Venanzi<sup>c</sup> and B. Pispisa<sup>c</sup>

<sup>a</sup>Chemistry and <sup>b</sup>Pharmacology Departments, Menarini Ricerche S.p.A., 00040 Pomezia (Rome), Italy and <sup>c</sup>Dipartimento di Scienze e Tecnologie Chimiche, Università di Roma "Tor Vergata", 00133 Roma, Italy

The introduction of some selected isosteric modifications to the C-terminal amide group in our cycloalkyl amino acid-based tachykinin NK-1 receptor antagonists resulted in the design and synthesis of MEN 10914 [1] bearing an N-methyl retro-amide group (Fig. 1), which had higher *in vitro* activity compared to the parent peptide MEN 10725 [2].

However, when MEN 10914 was tested in an *in vivo* animal model of neurogenic inflammation (plasma protein extravasation in guinea-pig bronchi after agonist challenge), the results were not in accordance with the expected antagonist activity. Nevertheless, the antagonist activity *in vitro* was interesting enough to select MEN 10914 as a suitable lead candidate for further chemical modifications. The rationale for planning these changes was derived from the hypothesis of the bioactive structure postulated for our series of cyclohexane-based antagonists [2].

## Results and Discussion

Our antagonists in methanol, but not in dioxane, show a UV absorption band at 285 nm not present in the sum spectrum of the two chromophores. The excited-state behavior parallels that in ground state, changing with the decrease in the solvent polarity (methanol versus dioxane): the fluorescence emission of the dipolar state at 340 nm disappears, while exciplex emission in the range 400-500 nm occurs.

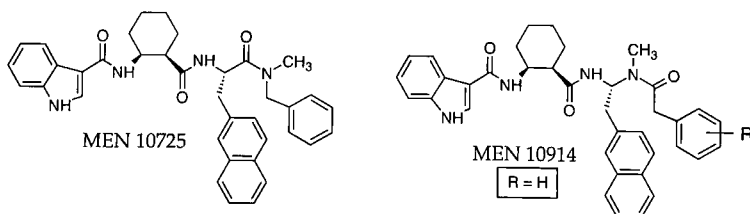


Fig. 1. Chemical structures of MEN 10725 and the retro-inverso modified analogue (MEN 10914 when R = H).

This behavior is thought to be due to an intramolecular indolyl-naphthyl charge-transfer complex that forms in different amounts, depending on the flexibility of the

Table 1: "In vitro" and "in vivo" antagonist activities.

Compounds	R	pKi	ED <sub>50</sub>
MEN 10914	H	8.0	> 1.0
MEN 11122	4-Cl	8.4	0.26
MEN 11318	4-OCH <sub>2</sub> CH <sub>3</sub>	7.7	> 3.0
MEN 11319	3-Cl	8.2	> 3.0
MEN 11339	3-NO <sub>2</sub>	7.7	N.T.
MEN 11366	3-NH <sub>2</sub>	8.3	> 1.0
MEN 11149	4-CH <sub>3</sub>	8.5	0.062

pKi: inhibition of binding of [<sup>3</sup>H] SP to human lymphoblastoma cell line IM9; ED<sub>50</sub>: i.v. dose in μmol/kg antagonizing [Sar<sup>9</sup>,Met(O<sub>2</sub>)<sup>11</sup>] SP-induced bronchoconstriction in guinea-pig (ED<sub>50</sub> were generated by the AUC values of at least three different doses).

scaffold [2,3]. The third aromatic moiety, not supposed to be involved in the charge-transfer complex (essential, in our hypothesis for interaction with the receptor) was selected as the target for the future changes to the chemical structure of MEN 10914. We systematically introduced a series of substituents onto the phenyl ring, selecting these by following stepwise the concept of the Topliss "decision tree" [4]. Using an iterative procedure first developed for optimizing of the biological activity of non-peptide compounds and selecting the aromatic ring from the previous spectroscopic studies, we were able to plan a series of modifications to the chemical structure of MEN 10914 [Table 1].

Preliminary NMR spectroscopy studies suggest that the overall structure in the series of retro-inverso analogues does not suffer any deep alteration by the introduction of the groups onto the third ring. It is conceivable that the activity of the analogues depends upon a local interaction of the modified aromatic ring with the corresponding part of the NK-1 receptor.

The selection of the substituent group was also guided by the results of *in vivo* tests. This approach resulted in the selective and orally effective compound MEN 11149.

## References

1. Fincham, C.I., Astolfi, M., Centini, F., Gröger, Lombardi, P., Madami, A., Manzini, S., Monteagudo, E.S., Parlani, M., Potier, E., Sisto, A. and Terracciano, R., 24th European Peptide Symposium, Edinburgh, Scotland, September 1996, poster n° 80.
2. Sisto, A., Bonelli, F., Centini, F., Fincham, C.I., Potier, E., Monteagudo, E., Lombardi, P., Arcamone, F., Goso, C., Manzini, S., Giolitti, A., Maggi, C. A., Venanzi, M. and Pispisa, B., *Biopolymers*, 36(1995) 511.
3. Pispisa, B., Cavaliere, F., Venanzi, M. and Sisto, A., *Biopolymers*, 40(1996) 529.
4. Topliss, J.G., *J. Med. Chem.*, 15(1972) 1006.

# Immunologically active mimetics of muramyl dipeptide

Danijel Kikelj,<sup>a</sup> Alenka Rutar,<sup>a</sup> Irena Merslavič,<sup>a</sup>  
Lučka Povšič<sup>b</sup> and Anton Štalc<sup>b</sup>

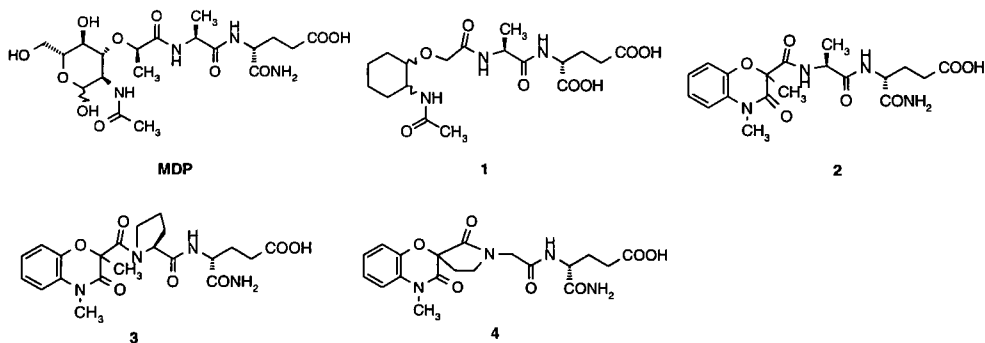
<sup>a</sup>University of Ljubljana, Faculty of Pharmacy, Aškerčeva 7, 1000 Ljubljana, Slovenia

<sup>b</sup>Lek d.d., Research and Development Division, Celovška 135, 1000 Ljubljana, Slovenia

N-acetylmuramyl-L-alanyl-D-isoglutamine (muramyl dipeptide, MDP) is the minimal immunologically active component of the bacterial cell wall peptidoglycan [1]. In last 20 years many research groups have been concerned with the synthesis and immunological studies of derivatives of this highly active glycopeptide in order to obtain molecules with improved and more defined pharmacological profiles. Although structure-activity relationships in MDP and its analogs have been well established, rational design of immunomodulators on the basis of MDP as a lead compound is impeded by the fact that the three-dimensional structure of the receptor binding site has not yet been determined. Therefore, systematic chemical modification of the molecule and development of more constrained analogs with reduced degrees of conformational freedom provide a good opportunity to define the bioactive conformation of MDP and analogs.

## Results and Discussion

In 1993, we showed, that carbocyclic *nor*-MDP analogs, e.g. **1**, retain the immunostimulant properties of MDP [2, 3]. Recently, we described novel immunologically-active conformationally constrained analog **2** in which the N-acetylmuramyl part of MDP was mimicked by 2-methyl-3-oxo-3,4-dihydro-2*H*-benzo[*b*][1,4]oxazine-2-carboxylic acid [4]. Thus, it has been shown for the first time that MDP analogs rigidified in the muramyl part of the molecule are active as immunostimulants [5]. Further conformational restriction in **2**,



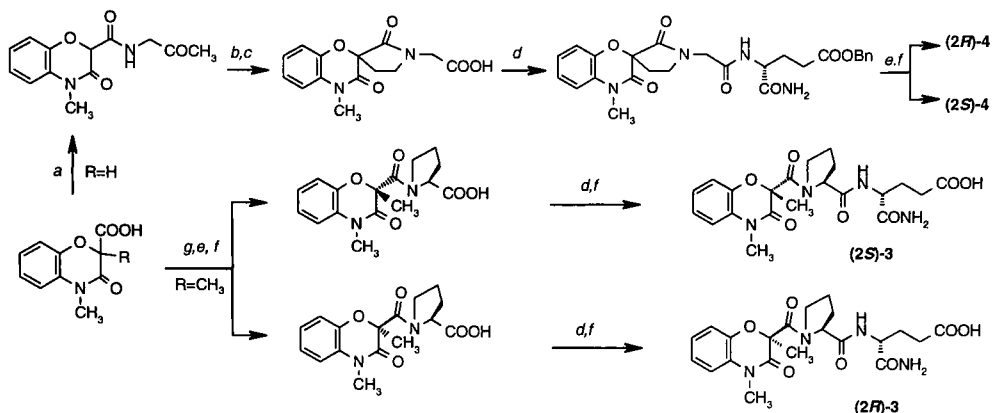


Fig. 1. Synthesis of compounds 3 and 4. a: Gly(OMe), DPPA, Et<sub>3</sub>N, DMF; b: NaH, Br(CH<sub>2</sub>)<sub>2</sub>Br, dioxane; c: NaOH, dioxane; d: D-Igln(OBn), DPPA, Et<sub>3</sub>N, DMF; e: chromatographic separation of diastereomers; f: H<sub>2</sub>, Pd/C, MeOH; g: L-Pro(OBn), DPPA, Et<sub>3</sub>N, DMF.

involving either the L-Ala-D-Igln chain alone or both the benzoxazinone moiety and the dipeptide part of 2 produced MDP mimetics 3 and 4 which were obtained as pure diastereomers. In the immunorestitution test in mice [6] and in the hemolytic plaque-forming cell assay [7] compounds 2, 3 and 4 displayed significant immunostimulating activity, comparable to that of MDP, romurtide [8] or azimexone [7]. The diastereomers of 2 and 3 differing in absolute configuration at C-2 of the morpholinone ring displayed different potencies in the immunological tests.

In conclusion, conformational restriction of carbocyclic MDP analog 2 in the dipeptide moiety furnished mimetics 3 and 4 which displayed significant immunostimulating activity. These novel MDP mimetics with stereoselective action may provide information concerning the putative receptor and the bioactive conformation of MDP analogs.

## References

1. Adam, A., Lederer, E., Med. Res. Rev., 4 (1984) 111.
2. Kikelj, D., Kidrič, J., Pristovšek, P. et al., Tetrahedron, 48 (1992) 5915.
3. Pečar, S., Kikelj, D., Urleb, U. et al., US Patent, 5,231,216 (1993).
4. Kikelj, D., Suhadolc, E., Rutar, A. et al., WO Patent Application, 94/24152 (1994).
5. Kikelj, D., Povšič, L., Štalc, A., Pristovšek, P., Kidrič, J., Med. Chem. Res., 6 (1996) 118.
6. Bicker, U., Ziegler, A. E., Hebold, G., J. Infect. Dis., 139 (1979) 389.
7. Jerne, N. K., Henry, C., Nordin, A. A., Transplant. Rev., 18 (1974) 130.
8. Azuma, I., Otani, T., Med. Res. Rev., 14 (1994) 401.

# Peptidomimetic tyrosine kinase inhibitors induce non apoptotic, Clarke-III type programmed cell death

György Kéri, László Ôrfi<sup>a</sup> Gergely Szántó, Judit Érchegyi, Ferenc Hollósy, Miklós Idei, Anikó Horváth, István Teplán, Aviv Gazit<sup>b</sup>, Zsolt Szegedi<sup>c</sup>, Béla Szende<sup>c</sup>

*Peptide Biochem Res Unit., Department of Medical Chemistry, <sup>a</sup>Institute of Pharmaceutical Chemistry, and <sup>b</sup>1st Institute of Pathology Semmelweis University of Medicine, Budapest, P.O.Box 260, Hungary-1444, <sup>c</sup>Department of Biological Chemistry, The Hebrew University of Jerusalem, Jerusalem, Israel-91904*

Tumor cells evolve negatively, with a switched off death program. In recent searches for signal transduction inhibitory compounds it has become clear that the inhibition of cell proliferation is not sufficient from a therapeutic point of view. Tumor cells have to be killed. Previously we have demonstrated a close correlation between tyrosine kinase inhibition and apoptosis [1]. In order to clarify the interrelationship of tyrosine kinase inhibition and apoptosis we synthesized a series of novel and also known peptidomimetic tyrosine kinase inhibitors and tested them for the induction of Programmed Cell Death (PCD). In our earlier work we have demonstrated that the well known tyrphostin AG213, which is an EGF-R selective tyrosine kinase inhibitor, induces non-apoptotic programmed cell death in tumor cells, which we characterized as Clarke III type programmed cell death. This type of PCD was previously described only in embryonic cells without a known trigger mechanism [2]. In the present work we have investigated the effect of a series of our peptidomimetic tyrosine kinase inhibitors on the induction of apoptosis and Clarke III type PCD in human colon tumor cells.

## Results and Discussion

We have developed a rationally designed library of peptidomimetic structures by combination and parallel processing of known elementary synthetic steps (diazocoupling, nucleophilic substitution, various condensation reactions, acylation, alkylation etc.,) The starting materials were various heterocyclic compounds or peptidomimetic oxanyl-hydrazide derivatives. The compounds were characterized by HPLC, NMR and MS as described previously [3]. The tyrosine kinase inhibitory activity of the compounds was tested on receptor tyrosine kinases as published earlier [2, 4].

We investigated the effect of various potent TK inhibitors on the induction of apoptosis and Clarke III type PCD. We have synthesized several potent TK inhibitor sub-families, such as styryl-quinazolines, imidazo-quinazolines, quinazolyl-propionic-anilides, oxazino-quinazolones, the benzoquinoxalines and the oxanyl-hydrazide derivatives having IC 50 values in the low micromolar range and certain selectivity for EGF or PDGF-RTK. We

also used several previously described tyrophostins [5] for our PCD inducing studies in the HT 29 human colon tumor cells.

Treatment of cultured tumor cells was performed 24 hours after plating. Samples were taken for cell count and cover slips for staining with hematoxylin and eosin 3, 24 and 48 hours after treatment. Cell viability was determined using methylene blue staining. Similarly, three cover slips per dose and time point were fixed in ethanol/acetic acid (3/1) and stained with hematoxylin and eosin. Acridin orange and Hoechst 33342 staining was also carried out and the cells were examined under a fluorescence microscope. The stained histological preparations were investigated for morphological signs of apoptosis or Clarke III type PCD, the number of such cells were counted, and the relevant PCD index was calculated. Immunohistochemical reaction using Apop-Tag kit was performed 24 hours after treatment.

After testing more than a hundred tyrosine kinase inhibitors and related structures we found that several of our potent inhibitors showed a strong apoptotic effect, causing more than 90% apoptotic cell death in the 100 $\mu$ M dose range. The apoptosis inducing effect correlated with the TK inhibitory activity, but not with the selectivity of the compounds. On the other hand, we found 5 compounds (4 tyrophostins and 1 oxanyl hydrazide derivative), more or less selective for the EGFR tyrosine kinases which induced the previously unknown Clarke III type programmed cell death. Tumor cells treated with these compounds showed homogenization of the nuclear chromatin and strong vacuolization of the cytoplasm after 24 and 48 hours. The reaction with Apop-Tag was negative in these cells. The induction of this non-apoptotic programmed cell death by certain peptidomimetic tyrosine kinase inhibitors raises the possibility for selective killing of tumor cells.

## Acknowledgments

This work was supported by a grant from the Hung. National Research Fund (OTKA7722)

## References

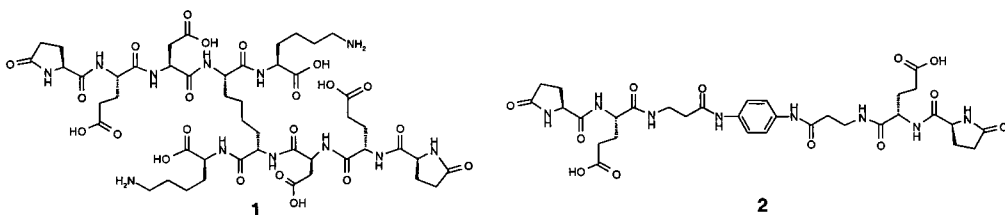
1. Kéri, Gy., Érchegeyi, J., Horváth, A., Mezô, I., Idei, M., Vántus, T., Balogh, A., Vadász, Zs., Bökönyi, Gy., Teplán, I., Csuka, O., Tejada, M., Gaál, D., Szegedi, Zs., Szende, B., Roze, C., Kalthoff H. and Ullrich, A., *Proc. Natl. Acad. Sci., USA*, 93 (1996) 12513
2. Szende, B., Kéri, Gy., Szegedi, Zs., Benedeczky, I., Csikós, A., Örfi, L. and Gazit, A., *Cell Biology International*, 19 (1995) 903.
3. Örfi, L., Kökösi J., Szász Gy., Kövesdi, I., Mák, M., Teplán, I. and Kéri Gy., *Bioorganic & Medicinal Chemistry*, 4 (1996) 547.
4. Strawn, L.M., McMahon, G., App, H., Schreck, R., Kuchler, W.R., Longhi, M.P., Hui, T.H., Tang, C., Levitzki, A., Gazit, A., Chen, I., Kéri, Gy., Örfi, L., Risau, W., Flamme, I., Ullrich, A., Hirth, K.P. and Shawver, L.K., *Cancer Research*, 56 (1996) 3540
5. Gazit, A., Yaish, P., Gillon, C. And Levitzki, A., *J. Med. Chem.*, 32 (1989) 2344.

# SAR of a series of related peptidomimetics derived from a novel hematoregulatory peptide, SK&F 107647

J. F. Callahan,<sup>a</sup> D. Alberts,<sup>a</sup> J. L. Burgess,<sup>a</sup> L. Chen,<sup>a</sup> D. Heerding,<sup>a</sup> W. F. Huffman,<sup>a</sup> A. G. King,<sup>b</sup> S. LoCastro,<sup>a</sup> L. M. Pelus<sup>b</sup> and P. K. Bhatnagar<sup>a</sup>

<sup>a</sup>Department of Medicinal Chemistry and <sup>b</sup>Department of Molecular Virology and Host Defense, SmithKline Beecham Pharmaceuticals, 709 Swedeland Rd., King of Prussia PA 19406, USA

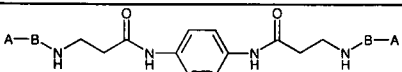
We have previously reported the hematopoietic activity of a novel peptide, SK&F 107647 (**1**) [1]. This peptide has been shown to induce from stromal cells a novel factor, designated hematopoietic synergistic factor (HSF), which directly enhances host effector cell function and synergizes endogenous growth factors, such as G-, M- and GM-CSF [2, 3]. An examination of the SAR of **1** allowed the formulation of a pharmacophore model in which the Asp and Lys residues of **1** interact with each other by forming either inter- or intra-chain salt bridges about the linking 2-(S),7-(S)-diaminosuberic acid (Sub) residue [1, 4]. This combination of the salt bridges and the Sub residue act as a scaffold which presents the residues, pGlu<sup>1</sup> and Glu<sup>2</sup> in the correct orientation [4]. These residues are responsible for the putative receptor interaction. As an initial validation of this hypothesis, this salt-bridge containing scaffold has been replaced by a much simpler structural template to give the peptidomimetic analog **2** which displayed significant hematopoietic activity [4].



## Results and Discussion

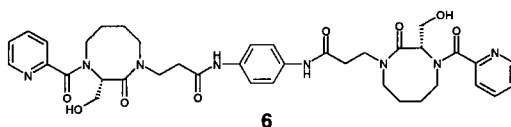
Once **2** was identified as a much simpler mimetic of the nonapeptide **1**, further work was initiated to ascertain the contribution of its side chains and backbone amide bonds to biological activity. First, substitutions were made of the p-Glu and Glu residues, which are proposed to interact with the putative receptor. The data show substitutions that were allowed in the peptide **1** were also accommodated in the peptidomimetic series (e.g., Table 1). These results confirm the assertion that the scaffold in the peptidomimetic **2** presents the first two sets of residues in a manner similar to the peptide **1**.

Table 1. HSF Activity of Peptidomimetic Analogs.

Compound			HSF Release <sup>1</sup> (units/mL)
	A	B	
<b>2</b>	pGlu	Glu	$2.0 \times 10^3$
<b>3</b>	Pic	Ser	$2.0 \times 10^3$
<b>4</b>	Pic	NMeSer	$1.7 \times 10^3$
<b>5</b>	Pro	Ser	$1.7 \times 10^3$

<sup>1</sup> All analogs tested at 1 ug/mL; HSF release for **1** =  $2.7 \times 10^4$  units/mL (same experiment).

After confirming the role of the side chains of A and B in peptidomimetic **3**, this analog was used to examine the effects of the backbone heteroatoms on biological activity. Replacement of the amide bonds between the  $\beta$ -Ala residue and aromatic ring with an alkyne, *trans*-olefin, ethylene group or N-methyl amide gave analogs that lost biological activity. Replacement of the Ser- $\beta$ -Ala amide bonds with either a *trans*-olefin, amino-methylene, N-methylamide or thioamide also gave analogs that lost biological activity. Again, loss of biological activity was found in mimetic **6** which constrained the pharmacophore elements of **3** by linking the Pic-Ser and Ser- $\beta$ -Ala amide nitrogens with a four methylene bridge. Although some of these mimetics may have different sets of low energy conformations available to them relative to the parent mimetic **3**, the data implies that the backbone amide bonds of these peptidomimetics may interact with the putative receptor.



## References

1. Bhatnagar, P. K., Agner, E. K., Alberts, D., Arbo, B. E., Callahan, J. F., Cuthbertson, A. S., Engelsen, S. J., Fjordingstad, H., Hartmann, M., Heering, D., Hiebl, J., Huffman, W. F., Hysben, M., King, A. G., Kremminger, P., Kwon, C., LoCastro, S., Lovhaug, D., Pelus, L. M., Petteway, S. and Takata, J. S., *J. Med. Chem.*, 39 (1996) 3814.
2. King, A.G., Frey, C.L., Arbo, B., Scott, M., Johansen, K., Bhatnagar, P.K. and Pelus, L.M., *Blood*, 86 suppl. 1 (1995) 309a.
3. King, A.G., Scott, R., Wu, D.W., Strickler, J., McNulty, D., Scott, M., Johansen, K., McDevitt, D., Bhatnagar, P.K., Balcerek, J. and Pelus, L.M., *Blood*, 86 suppl. 1 (1995) 310a.
4. Bhatnagar, P. K., Alberts, D., Callahan, J. F., Heering, D., Huffman, W. F., King, A. G., LoCastro, S., Pelus, L. M. and Takata, J. S., *J. Am. Chem. Soc.*, 118 (1996) 12862.

# Applications of tropane-based peptidomimetics

Philip E. Thompson, David L. Steer, Kerry A. Higgins,  
Marie-Isabel Aguilar and Milton T. W. Hearn

Centre for Bioprocess Technology, Department of Biochemistry and Molecular Biology,  
Monash University, Clayton 3168, Australia

The use of heterocyclic structures as peptidomimetics has attracted special attention with the increasing use of combinatorial chemistry and mass screening technologies. We have examined the tropane class of heterocyclics as it offers a semi-rigid template, with manipulable configurations that can be readily functionalized. Most importantly, a wealth of literature already exists which can be utilized in the synthesis of functionalized tropane-based Fmoc-protected amino acids for use in SPPS [1].

## Results and Discussion

The synthesis of N-protected nortropane amino acids has been successfully achieved by adaptation of literature approaches to native tropanes. Synthesis ultimately has depended upon N-demethylation and re-protection of the corresponding tropane derivative. In this way a range of variants have been accessed as shown in Fig. 1. In particular, we have found that ethyl chloroformate is a stable, inexpensive reagent for effecting N-demethylation. The resulting ethyl carbamate is relatively stable, yet can be effectively removed by treatment with TMSI (generated *in situ* from hexamethyldisilane and iodine) [2]. These protected amino acids have proven particularly amenable to inclusion in SPPS protocols affording high coupling efficiencies even when used as the limiting reagent.

Conformational analysis of model peptides using molecular dynamics has shown that incorporation of these tropane amino acids restricts the resultant peptide to a narrowed range of conformers. Analysis of the distance between the  $\alpha$ -carbons of residues adjacent to the tropanes in Ac-Lys-Xxx-Gly [3] shows the discrete conformations that isomeric tropane-containing peptides can adopt (Fig. 2)

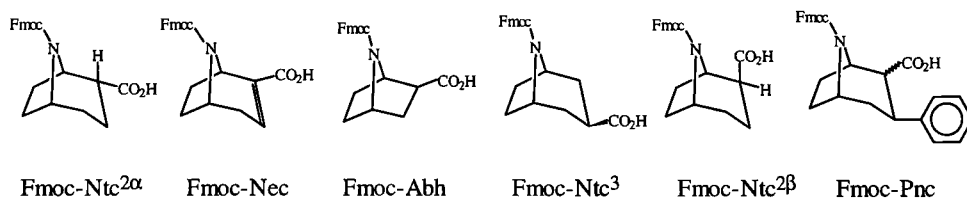


Fig. 1. Novel Fmoc-protected tropane amino acids.

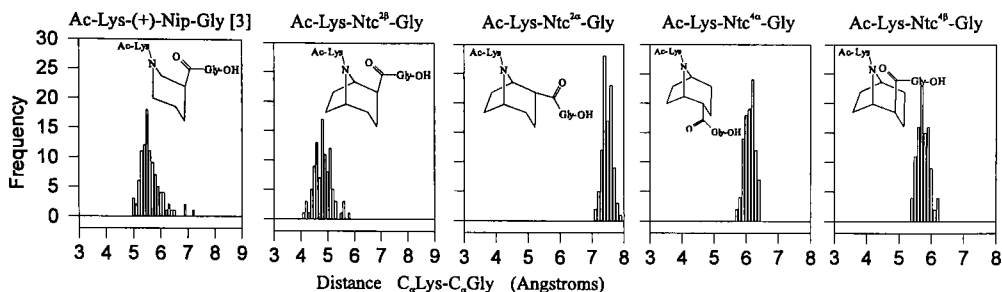


Fig. 2. 300K Molecular dynamic of Ac-Lys-Xxx-Gly peptides.

One of our first applications of tropane-based amino acid residues involves substitution into reported  $\gamma$ -chain and RGD-type GPIIb/IIIa antagonists.[3] Preliminary data shows the influence of these substitutions on inhibition of platelet aggregation, (Table 1) and the enhanced potency of the D-Lys substitution (5) and RGDS analog (6).

Table 1. Inhibition of thrombin induced washed platelet aggregation by tropane derivatives.

Sequence	% inhibition		
	20 $\mu$ m	100 $\mu$ m	500 $\mu$ m
1. Ac-Lys-( $\pm$ )-Nip- $\beta$ -Ala [3]	-	8	68
2. Ac-Lys-( $\pm$ )-Ntc <sup>2<math>\alpha</math></sup> - $\beta$ -Ala	-	5	19
3. Ac-Lys-( $\pm$ )-Nec- $\beta$ -Ala	-	-	-4
4. Ac-D-Lys-( $\pm$ )-Abh- $\beta$ -Ala	-	-	4
5. Ac-D-Lys-( $\pm$ )-Ntc <sup>2<math>\alpha</math></sup> - $\beta$ -Ala	-	26	68
6. Arg-( $\pm$ )-Ntc <sup>2<math>\alpha</math></sup> -Asp-Ser	38	68	70

For conclusion, the utilization of tropane-based amino acids is providing valuable structure-function data in our studies of bioactive peptides. Other applications that are being pursued include the synthesis of combinatorial libraries of oligotropanes, cyclic peptide libraries which incorporate tropanes as a conformational determinant, and non-amide peptidomimetics which utilize the tropane amino acids as a starting template.

## References

1. Thompson, P. E., Hearn, M. T. W., Tetrahedron Lett., in press.
2. Xu, R., Chu, G., Bai, D., Tetrahedron Lett., 37 (1996) 1463
3. Hoekstra, W. J., Beavers, M. P., Andrade-Gordon, P., Evangelisto, M. F., Keane, P. M., Tomko, K. A., Fan, F., Kloczewiak, M., Mayo, K. H., Durkin, K. A., Liotta, D. C., J. Med. Chem., 38 (1995) 1582.

# Structure-activity relationship studies of dialkylamine derivatives exhibiting wide spectrum antimicrobial activities

U.P. Kari, S.R. Maddukuri, M.T. MacDonald, L.M. Jones,  
D.L. MacDonald, and W.L. Maloy

*Magainin Pharmaceuticals Inc., Plymouth Meeting, PA 19462, USA*

Previously, we reported the design and the synthesis of amino acid and peptide conjugates of diaminoalkanes [1]. Now the synthesis and antibacterial activities of amino acid and peptide conjugates of dialkylamines will be discussed. The molecules in the present study are designed to have a positively charged guanidino group attached to two alkyl chains to provide optimal interaction with the bacterial membrane.

## Results and Discussion

The synthesis of the amino acid conjugates was carried out by condensing the amino blocked derivative with dialkylamine, removing the protecting group, and converting the resulting amine to either a nitroguanidino group or a guanidino group. The nitro group was then removed by hydrogenation to obtain the desired molecules. The dipeptide conjugates were prepared by coupling a protected arginine to the above deblocked amino acid conjugate followed by hydrogenolysis.

The antimicrobial activities against various organisms are reported in Table 1. In general, the conversion of the amino group to the guanidino function resulted in better activities (**cpds 1 and 2**). The length of the alkyl chain was varied (**cpds 4-6**) and it was observed that better activities were obtained when the chain length was between six and eight. The replacement of Phe with more hydrophobic amino acids, such as Trp (**cpd 7**),  $\beta$ -naphthylalanine (**cpd 8**) or cyclohexylalanine (**cpd 9**), resulted in the loss of activity against gram negative organisms. When Phe was substituted with the basic hydrophilic amino acid histidine (**cpd 10**), the activities were significantly improved. Substitution of Phe in the para-position of the aromatic ring with fluorine (**cpd 11**) or using its enantiomer (**cpd 3**) did not alter the antibacterial activities significantly; however, the addition of a p-NH<sub>2</sub> group produced improved activity against gram negative organisms (**cpd 12**). **Compounds 13-16**, which were made with non-alpha amino acids, also retained antimicrobial activity, with the analog having the shortest carbon chain (**cpd 16**) exhibiting the best activities. The dipeptide analogs (**cpds 17-19**) with the basic guanidino group in the amino acid side chain showed good antimicrobial activities. It is interesting to compare analogs 7 and 18. The dipeptide 18 exhibits activity against *E.coli* but not the other gram negative organism, *P.aeruginosa*. Thus, these analogs can delineate clear differences in the activities of the gram negative organisms. The hemolysis of red blood cells, which is considered a measure of selectivity for prokaryotic over eukaryotic cells, was carried out at various concentrations. Interestingly, there is no hemolysis at 10 $\mu$ g/ml, while at 100 $\mu$ g/ml concentrations the analogs were

significantly hemolytic (data not shown). The hemolytic activity likely results from a non-specific detergent effect at higher concentrations.

*Table 1. Antimicrobial Activities of the Dialkylamine Compounds.*

Cpd #	Compound Name	MIC ( $\mu\text{g/ml}$ )			
		S.aureus	E.coli	P.aeruginosa	C.albicans
1	Phe-dioctylamide	4	256	256	256
2	Amidino-Phe-dioctylamide	1.0	16	128	1
3	Amidino-D-Phe-dioctylamide	2	64	256	2
4	Amidino-Phe-didecylamide	128	256	256	64
5	Amidino-Phe-dihexylamide	0.5	16	32	8
6	Amidino-Phe-dipentylamide	4	64	128	64
7	Amidino-Trp-dioctylamide	8	256	256	16
8	Amidino- $\beta$ -Nal-dioctylamide	4	256	256	4
9	Amidino-Cha-dioctylamide	2	>256	>256	2
10	Amidino-His-dioctylamide	1	4	8	1
11	Amidino-p-F-Phe-dioctylamide	2	64	128	2
12	Amidino-p-NH <sub>2</sub> -Phe-dioctylamide	1	4	32	0.5
13	p-Guanidino methyl-benzoyl-dioctylamide	1	4	64	0.5
14	$\delta$ -Guanidino-valeryl-dioctylamide	2	8	256	1
15	$\gamma$ -Guanidino-butyryl-dioctylamide	0.5	4	32	0.25
16	$\beta$ -Guanidino-propionyl-dioctyl amide	0.5	4	16	1.0
17	Arg-Phe-dioctylamide	4	4	16	16
18	Arg-Trp-dioctylamide	2	4	256	16
19	Arg-His-dioctylamide	4	8	16	8

## References

1. Maddukuri, S.R., Hendi, M.S., Frauncis, J.P., Jones, L.M., MacDonald, D.L., Maloy, W.L. and Kari, U.P., 14th American Peptide Symposium, Columbus, OH., 1995, Abs# P657.

# Identification of prototype peptidomimetic agonists at the human melanocortin receptors, MC1R and MC4R

Carrie Haskell-Luevano,<sup>a</sup> Tomi K. Sawyer,<sup>b</sup> Mac E. Hadley,<sup>c</sup>

Victor J. Hruby,<sup>c</sup> and Ira Gantz<sup>a</sup>

<sup>a</sup>University of Michigan Medical Center, Ann Arbor, MI 48109, <sup>b</sup>Parke-Davis Pharmaceutical Research, Ann Arbor, MI 48105, and <sup>c</sup>University of Arizona, Tucson, AZ 85721, USA

The melanotropin peptides include  $\alpha$ -,  $\beta$ -,  $\gamma$ -melanocyte stimulating hormones (MSH) and adrenocorticotropin (ACTH). All of these hormones are derived by posttranslational processing of the pro-opiomelanocortin (POMC) gene transcript, and all possess a central His-Phe-Arg-Trp "message" sequence. Studies using frog and lizard skin bioassays have identified Ac-His-Phe-Arg-Trp-NH<sub>2</sub> as the minimal synthetic fragment to elicit a melanotropic response. Relative to  $\alpha$ -MSH, Ac-His-Phe-Arg-Trp-NH<sub>2</sub> was 400,000-fold less potent in the frog skin bioassay [1], and approximately 7,000-fold less potent in the lizard skin bioassay [2], and neither  $\alpha$ -MSH or this tetrapeptide possessed prolonged (residual) melanotropic activity in either assay. Truncation studies [3] of the highly potent, enzymatically stable, and prolonged acting agonist Ac-Ser-Tyr-Ser-Nle<sup>4</sup>-Glu-His-Dphe<sup>7</sup>-Arg-Trp-Gly-Lys-Pro-Val-NH<sub>2</sub> (NDP-MSH), identified the prolonged acting tripeptide Ac-DPhe-Arg-Trp-NH<sub>2</sub> (**1**) as the minimally active NDP-MSH fragment. Further stereochemical modifications of this tripeptide resulted in tripeptides with increased potencies of 5- to 20-fold in the frog skin bioassay simply by changing the chirality at positions 8 and 9 respectively. Five human melanocortin receptor subtypes (hMC1R - hMC5R) have been cloned and characterized [4-9]. All these receptors respond to all of the melanotropin peptides with the exception of the hMC2R, which only responds to ACTH, and thus has been deleted from this study. The goal of this study was to examine stereochemically modified tripeptides and tetrapeptides on the human melanocortin receptors to determine selectivity, functional properties (i.e. agonism), and to correlate with recent frog skin melanocortin studies [3]. Such information is expected to provide a basis for future structure-based design studies that are focused on the discovery of MSH peptidomimetic agonists.

## Results and Discussion

Table 1 summarizes the binding affinities and signal transduction efficacy (intracellular cAMP accumulation) of stereochemically modified tri- and tetrapeptides. The  $\alpha$ -MSH and NDP-MSH tridecapeptides have been included for reference. Intracellular cAMP accumulation bioassays were only performed on analogues which possessed greater than 50% competitive displacement of [<sup>125</sup>I] NDP-MSH at 10  $\mu$ M.  $\alpha$ -MSH possessed binding IC<sub>50</sub>s of 5.97 nM and 38.7 nM at the hMC1R and hMC4R, respectively. NDP-MSH possessed IC<sub>50</sub>s of 0.51 nM and 1.16 nM at the hMC1R and hMC4R, respectively. Tetrapeptide **1** possessed binding affinities of 0.6  $\mu$ M at the hMC1R and 1.1  $\mu$ M at the hMC4R and were 1,200- and 990-fold less potent than NDP-MSH, respectively. This

peptide, at a 10  $\mu\text{M}$  concentration, was unable to competitively displace [ $^{125}\text{I}$ ] NDP-MSH at either the hMC3R or the hMC5R. Analogue 2 was the only other tetrapeptide that was

Table 1. Binding  $\text{IC}_{50}$  and cAMP  $\text{EC}_{50}$  results on the human MC1R and MC4R.

Peptide	hMC1R		hMC4R	
	$\text{IC}_{50}$ ( $\mu\text{M}$ )	$\text{EC}_{50}$ ( $\mu\text{M}$ )	$\text{IC}_{50}$ ( $\mu\text{M}$ )	$\text{EC}_{50}$ ( $\mu\text{M}$ )
1 Ac-His-DPhe-Arg-Trp-NH <sub>2</sub>	0.62±0.04	0.23±0.09	1.15±0.21	0.79±0.44
2 Ac-His-Phe-Arg-DTrp-NH <sub>2</sub>	6.35±0.62	1.43±0.21	>10	
3 Ac-DPhe-Arg-Trp-NH <sub>2</sub>	>10		2.08±0.44	40%
4 Ac-DPhe-Arg-DTrp-NH <sub>2</sub>	>10		9.16±0.77	50%

able to competitively displace [ $^{125}\text{I}$ ] NDP-MSH in a dose-response manner at the hMC1R and resulted in 6  $\mu\text{M}$  binding affinity. The tripeptides examined in this study were only able to generate dose-response competitive binding curves at the hMC4R. Analogue 3 resulted in a 1.8-fold decreased potency compared with analogue 1. Of particular note, however, is that analogue 1 was able to generate the maximum intracellular cAMP accumulation observed for NDP-MSH, but the tripeptide 3 resulted in only 40 % generation of maximal cAMP at 10  $\mu\text{M}$  concentration. Analogue 4 resulted in a 9  $\mu\text{M}$  binding affinity but was only able to generate 50% maximal cAMP accumulation at 10  $\mu\text{M}$  concentration.

## References

1. Hruby, V. J., Wilkes, B. C., Hadley, M. E., Al-Obeidi, F., Sawyer, T. K., Staples, D. J., DeVaux, A., Dym, O., Castrucci, A. M., Hintz, M. F., Riehm, J. P., Rao, K. R., *J. Med. Chem.*, 30 (1987) 2126.
2. Castrucci, A. M., Hadley, M. E., Sawyer, T. K., Wilkes, B. C., Al-Obeidi, F., Staples, D. J., DeVaux, A. E., Dym, O., Hintz, M. F., Riehm, J., Rao, K. R., Hruby, V. J., *Gen. Comp. Endocrinol.*, 73 (1989) 157.
3. Haskell-Luevano, C., Sawyer, T. K., Hendrata, S., North, C., Panahinia, L., Stum, M., Staples, D. J., Castrucci, A. M., Hadley, M. E., Hruby, V. J., *Peptides*, 17 (1996) 995.
4. Chhajlani, V., Wikberg, J. E. S., *FEBS Lett.*, 309 (1992) 417.
5. Mountjoy, K. G., Robbins, L. S., Mortrud, M. T., Cone, R. D., *Science*, 257 (1992) 1248.
6. Gantz, I., Konda, Y., Tashiro, T., Shimoto, Y., Miwa, H., Munzert, G., Watson, S. J., DelValle, J., Yamada, T., *J. Biol. Chem.*, 268 (1993) 8246.
7. Roselli-Rehffuss, L., Mountjoy, K. G., Robbins, L. S., Mortrud, M. T., Low, M. J., Tatro, J. B., Entwistle, M. L., Simerly, R. B., Cone, R. D., *Proc. Natl. Acad. Sci.*, 90 (1993) 8856.
8. Gantz, I., Miwa, H., Konda, Y., Shimoto, Y., Tashiro, T., Watson, S. J., DelValle, J., Yamada, T., *J. Biol. Chem.*, 268 (1993) 15174.
9. Chhajlani, V., Muceniece, R., Wikberg, J. E. S., *Biochem. Biophys. Res. Commun.*, 195 (1993) 866.

# Cyclic Somatostatins containing $\alpha$ -benzyl-o-AMPA as a cis peptide bond mimic

Dirk Tourwé, Valerie Brex, Jo Van Betsbrugge and Patricia Verheyden  
Department of Organic Chemistry, Vrije Universiteit Brussel, Pleinlaan 2, 1050 Brussels, Belgium

We have used  $\alpha$ -benzyl-o-aminomethylphenylacetic acid ( $\alpha$ -Bn-o-AMPA) as a cis peptide bond mimic replacing Phe<sup>11</sup>-Pro<sup>6</sup> in the cyclic somatostatin analogue c(Pro<sup>6</sup>-Phe<sup>7</sup>-D-Trp<sup>8</sup>-Lys<sup>9</sup>-Thr<sup>10</sup>) [1]. The N-Me analogue **1a** (Fig. 1) displays high inhibition of GH release ( $IC_{50}$ = 0.2 nM) activity. The synthesis of racemic  $\alpha$ -Bn-o-AMPA has been performed [2] and resulted in two epimeric analogues **1b** and **1c** having different affinities for the SSTR2 receptor. The configuration of the chiral center was assigned tentatively.

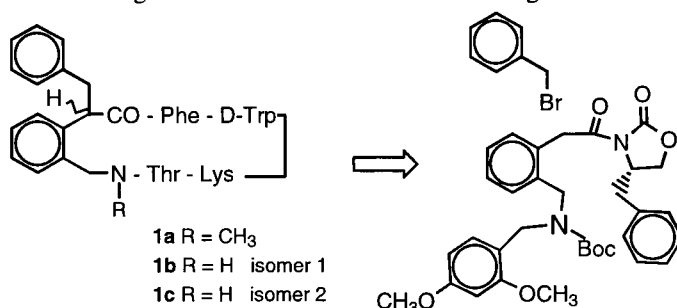


Fig. 1. Cyclic somatostatin analogues and retrosynthetic analysis.

## Results and Discussion

In order to assign an absolute configuration in **1b** and **1c**, the peptide bond mimic  $\alpha$ -Bn-o-AMPA was prepared by asymmetric synthesis using 4-(*R*)-benzyl-2-oxazolidinone as a chiral auxiliary [3]. The  $\alpha$ -(*R*)-Bn-o-AMPA was obtained in > 95% yield as determined by NMR spectroscopy. Double nitrogen protection is needed to avoid intramolecular lactam formation. After cleavage of the chiral auxiliary, solid phase peptide synthesis and HF cleavage, HPLC analysis indicated a 90 to 10 proportion of the two epimeric peptides. Further cyclization and deprotection revealed that isomer one **1b**, having a  $K_i$  of 33 nM for the SSTR2 receptor, has the (*R*) configuration of the mimic, and the isomer two **1c** with a  $K_i$  of 5.12 nM therefore has the (*S*) configuration. The previously reported tentative assignment has to be corrected [2]. The solution conformation of both isomers was studied by <sup>1</sup>H NMR in both DMSO-*d*<sub>6</sub> and CD<sub>3</sub>OH solution. In DMSO, both isomers adopt a  $\beta$  II' conformation over the tetrapeptide part. In isomer 1 an equilibrium between a  $\delta$ -turn and a  $\beta$  VI turn is observed over the o-AMPA part, whereas for isomer 2 no turn type could be

defined for this area. The study in CD<sub>3</sub>OH allowed us to observe more NOE cross peaks at 300 K, which can be used as constraints in molecular dynamics experiments. For both isomers the low energy conformers are superimposed in Fig.2, showing a well conserved  $\beta$  II' turn, but a less defined or more flexible spacer part. Goodman proposed a folded bioactive conformation [4] for cyclic somatostatin analogues. Overlap studies of the conformations shown in Fig.2, fitting the tetrapeptide backbone with the folded or the flat structures proposed by Goodman, revealed that for the less potent (*R*) isomer **1b** the benzyl sidechain of *o*-AMPA can overlap with the Phe<sup>11</sup> sidechain in both structures. For the more potent (*S*) isomer **1c**, these aromatic sidechains overlap when fitting the folded model, but not when fitting the flat model.

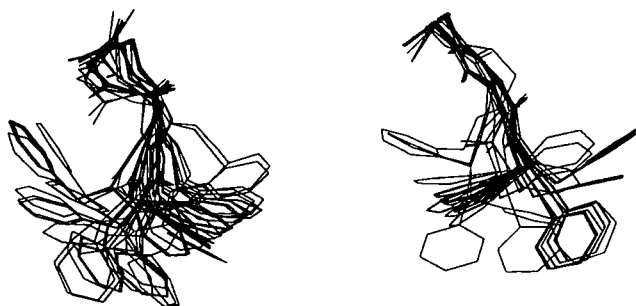


Fig.2. Superposition of low energy conformations for **1b** (left) and **1c** (right). For clarity, only the benzyl sidechain of  $\alpha$ -Bn-*o*-AMPA is displayed.

## Conclusion

Asymmetric synthesis of  $\alpha$ -(*R*)-benzyl-*o*-AMPA using the Evans chiral auxiliary allowed the assignment of the configuration of **1b** and **1c**. Conformational analysis by <sup>1</sup>H NMR and molecular dynamics shows a better fit of the more potent (*S*) isomer **1c** with the flat model proposed by Goodman, which is in agreement with a model proposed by Weber [5].

## References

1. Tourwé, D., *Lett. Pept. Sci.*, 2 (1995) 182.
2. Brex, V., Misicka, A., Verheyden, P., Tourwé, D. and Van Binst, G., *Lett. Pept. Sci.*, 2 (1995) 165.
3. Evans, D.A., Ennis, M.D. and Mathre, D.J., *J. Am. Chem. Soc.*, 104 (1982) 1737.
4. Huang, Z., He, Y.-B., Raynor, K., Tallent, M., Reisine, T. and Goodman, M., *J. Am. Chem. Soc.*, 114 (1992) 9390.
5. Veber, D.F., In Smith, J.A. and Rivier, J.E. (Eds), *Peptides: Chemistry and Biology (Proceedings of the Twelfth American Peptide Symposium)*, ESCOM, Leiden, The Netherlands, 1992, p. 3.

# Alpha-helix nucleation between peptides using a covalent hydrogen bond mimic

Elena Z. Dovalsantos, Edelmira Cabezas and  
Arnold C. Satterthwait

Department of Molecular Biology, The Scripps Research Institute,  
La Jolla, CA 92037, USA

Constraining peptides to the conformations they occupy in native proteins provides a means for converting biologically inactive peptides to bioactive peptides. We have shown that a peptide can be induced to form a full length  $\alpha$ -helix in water by attaching its carboxyl terminus to an  $\alpha$ -helix nucleation site (NucSite) [1]. A NucSite constitutes one turn of an  $\alpha$ -helix stabilized by a covalent hydrogen bond mimic. In the initial NucSite, a hydrazone link was used to replace a hydrogen bond formed between a main-chain amide proton on one amino acid and an amide carbonyl oxygen of a second amino acid.

In this work, we extend the utility of the NucSite by adding an  $\alpha$ -amino group to the linker that allows its insertion between two peptides. In this case, the hydrazone link replaces a hydrogen bond that forms between the side chain of asparagine and the main chain amide proton of an ( $i, i+3$ ) amino acid (Fig. 1). This design satisfies complex steric and stereochemical demands by building on a natural mechanism for  $\alpha$ -helix nucleation used in proteins [2].

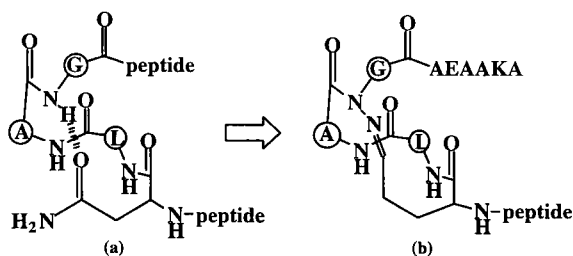
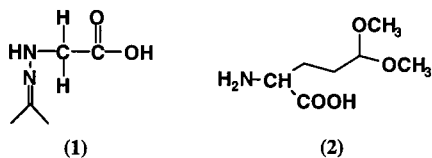


Fig. 1 (a) One turn of an  $\alpha$ -helix showing how the side chain of asparagine stabilizes  $\alpha$ -helix formation by hydrogen bonding to a main chain amide proton; (b) replacing the side chain hydrogen bond with a covalent mimic allows subsequent extension from the N-terminus.

## Results and Discussion

The new NucSite is synthesized on solid supports using Fmoc chemistry and two linkers, Z and J'. Z (**1**) was synthesized as previously described and protected with Fmoc-chloride to give Fmoc-Z [3]. J' (**2**) was synthesized by chemically transforming the side chain of L-glutamic acid to the dimethyl acetal via an alcohol and aldehyde.



The Fmoc protected residues Z, Ala-Cl or Pro-Cl, Leu, and J' were sequentially added to the solid support [3]. Cyclization was rapid when catalyzed by one equivalent of HCl in 10% TFE/DCM. The NucSite was synthesized either separately and then appended to a peptide (AEAAKA) on solid support or each residue of the NucSite was added sequentially to the peptide on a resin, then cyclized and cleaved.

The ability of the modified NucSite to initiate  $\alpha$ -helix formation in the appended peptide in 10% D<sub>2</sub>O/H<sub>2</sub>O at room temperature was evaluated by comparison of the amide -NH regions of NMR spectra and by following criteria established in previous work [1]. To simplify the NMR spectra, the second site for peptide attachment was capped by acetylation. The following observations and conclusions support  $\alpha$ -helix formation: (a) coupling constants for the hydrazone proton (HC=N) undergo a change characteristic of that observed for  $\alpha$ -helix nucleation; (b) the expected terminal carboxamide-NH signal moves upfield, consistent with hydrogen bonding in a full length  $\alpha$ -helix; (c) signals for the amide protons spread out with several signals moving up field indicating a better defined environment and hydrogen bonding throughout the length of the peptide; and (d) substitution of Pro for Ala in the NucSite accentuates the prior changes by inducing greater  $\alpha$ -helicity in the appended peptide.

These results provide clear evidence that the NucSite, modified for N-terminal extension, retains its ability to induce  $\alpha$ -helix formation in an added peptide. Insertion of the mimic into peptides during solid phase synthesis greatly simplifies the syntheses of NucSites and lays the ground work for the insertion of hydrogen bond mimics into supersecondary structures and synthetic proteins.

## References

1. Cabezas, E., Chiang, L.-C. and Satterthwait, A.C. In Hodges, R.S. and Smith, J.A. (Eds.) Peptides: Chemistry, Structure and Biology, Proceedings of the 11th American Peptide Symposium, ESCOM, Leiden, The Netherlands, 1994, p.287.
2. Richardson, J.S. and Richardson, D.C., *Science*, 240,(1988)1648.
3. Chiang, L.-C. et al., In Hodges, R.S. and Smith, J.A. (Eds.) Peptides: Chemistry, Structure and Biology, Proceedings of the 11th American Peptide Symposium, ESCOM, Leiden, The Netherlands, 1994, p.278.

# Development of inhibitors of MAdCAM-1/ $\alpha_4\beta_7$ interactions

**H.N. Shroff, C.F. Schwender, A.D. Baxter,<sup>a</sup> N. Hone,<sup>a</sup> N.A. Cochran,  
D.L. Gallant, M.J. Briskin**

*LeukoSite, Inc., 215 First Street, Cambridge, MA 02142, USA*

*<sup>a</sup>Oxford Diversity Limited, 57 Milton Park, Abingdon, Oxon OX 144RS, UK*

Inflammation is characterized by infiltration of affected tissue by leukocytes such as lymphocytes, lymphoblasts and mononuclear phagocytes. Leukocytes preferentially migrate to various tissues during both normal and inflammatory cell processes that result from a series of adhesive and activating events involving multiple receptor-ligand interactions. MAdCAM-1 (Mucosal Addressin Cell Adhesion Molecule-1) is an immunoglobulin superfamily adhesion molecule for lymphocytes expressed in the gastrointestinal tract endothelium that specifically binds to the lymphocyte  $\alpha_4\beta_7$  integrin and participates in the homing of these cells to mucosal sites [1,2].

Previously we reported that the sequence LDT from the CD loop of the murine MAdCAM-1 is an important recognition motif for murine MAdCAM-1/ $\alpha_4\beta_7$  interactions [3]. We wish to report further studies which support LDT as a binding motif required for human MAdCAM-1/ $\alpha_4\beta_7$  interactions. A peptide based structure activity study was carried out leading to a number of potent and selective human MAdCAM-1 inhibitors.

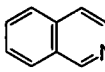
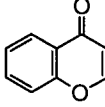
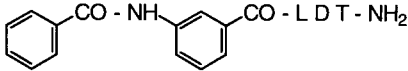
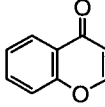
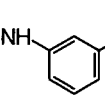
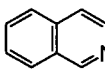
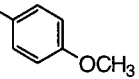
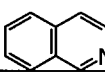
## Results and Discussion

Although cyclization of LDT did not improve potency more than 5 fold, modification of the N-terminal amine and the C-terminal carboxamide improved inhibitor potency up to 250 fold when subjected to MAdCAM-1/ $\alpha_4\beta_7$  mediated cell adhesion assays.

Acylation of N-terminal amine of LDT with a variety of aryl and heterocyclic groups enhanced the potency significantly. The addition of a spacer such as aminobenzoyl and amino methylbenzoyl groups made these peptides even more potent inhibitors. Finally, modification of the C-terminal carboxamide with a variety of aryl and heterocyclic groups gave highly potent, selective and more bioavailable human MAdCAM-1/ $\alpha_4\beta_7$  inhibitors. Some of the examples of modified LDT peptides are listed in Table 1.

Cell adhesion assays involving RPMI 8866 cells activated with  $MnCl_2$  and soluble human MAdCAM-1 produced in a baculovirus expression system were used in a 96 well format. [4].  $IC_{50}$  values (the concentration of inhibitor required to prevent 50% of cells from adhering to MAdCAM-1 plates) are reported as an average of multiple determinations. The compounds were also tested in fibronectin/K562 binding assay as described by Pytela [5]. None of the compounds inhibited binding of K562 cells to fibronectin.

Table 1. Inhibition of human MAdCAM-1/ $\alpha_4\beta_7$  binding by small peptides.

Peptides	IC50 ( $\mu\text{M}$ )
Ac - L D T - NH <sub>2</sub>	250
Ac - C L D T C - NH <sub>2</sub> 	45
 CO - L D T - NH <sub>2</sub>	4
 CO - L D T - NH <sub>2</sub>	1.7
 CO - L D T - NH <sub>2</sub>	1.6
 CO - NH -  CO - L D T - NH <sub>2</sub>	2.4
 CO - L D T - NH -  OCH <sub>3</sub>	1
 CO - L D T - NH - 	1

Based on these studies it appears possible that highly potent, selective and bioavailable peptidomimetic inhibitors of human MAdCAM-1/ $\alpha_4\beta_7$  mediated leukocyte adhesion may be found.

## References

1. Butcher, E. C., *Cell*, 67 (1991) 1033.
2. Springer, T. A., *Cell*, 76 (1994) 301.
3. Shroff, H. N., Schwender, C. F., Dottavio, D., Yang, L. L. and Briskin, M. J., *Bioorganic & Medicinal Chemistry Letters*, 6 (1996) 2495.
4. Briskin, M. J., Rott, L. and Butcher, E. C., *J. Immunol.*, 156 (1996) 719.
5. Pytela, R., Pierschbacher, M. D. and Ruoslahti, E., *Cell*, 40 (1985) 191.

# Synthesis of cyclic RGD-tetra-peptoids and optimization of the submonomer solid phase coupling protocol

J. S. Schmitt,<sup>a</sup> S. L. Goodman,<sup>b</sup> A. Jonczyk<sup>b</sup> and Horst Kessler<sup>a</sup>

<sup>a</sup>Institut für Organische Chemie und Biochemie, Technische Universität München, Lichtenbergstr. 4, D-85747 Garching, Germany; <sup>b</sup>Merck KGaA, Frankfurter Str. 250, D-64271 Darmstadt, Germany

In the past few years the cyclic pentapeptide *cyclo*(-Arg-Gly-Asp-D-Phe-Val-), a highly active and selective antagonist against the  $\alpha_v\beta_3$ -integrin, has been observed to prevent angiogenesis and to induce apoptosis, which may open new pathways of cancer therapy [1, 2]. Efforts to optimize this lead structure with respect to metabolic stability and pharmacokinetics led us to the concept of *peptoids*, a new class of synthetic polymers [3, 4]. In this context we designed the target cyclic peptoids **5** - **8** as retrosequences of the lead peptide. Since the tertiary amide bonds in peptoids reveal more flexibility than the parent peptide, the more constrained tetrameric cyclic peptoids were synthesized omitting valine as a variable position that is not involved in binding to the receptor.

## Results and Discussion

For solid phase synthesis of the linear peptoids **1** and **2**, submonomeric strategy [5] and standard Fmoc-monomer SPS were combined. The submonomeric coupling protocol of bromoacetic acid was optimized for a rapid and quantitative reaction using bromoacetic acid anhydride, which can be readily prepared in situ by combining bromoacetic acid bromide and excess bromoacetic acid (Fig. 1). Cyclization of the tetrapeptoid at RT exclusively led to cyclodimerization, whereas at higher temperatures the desired protected

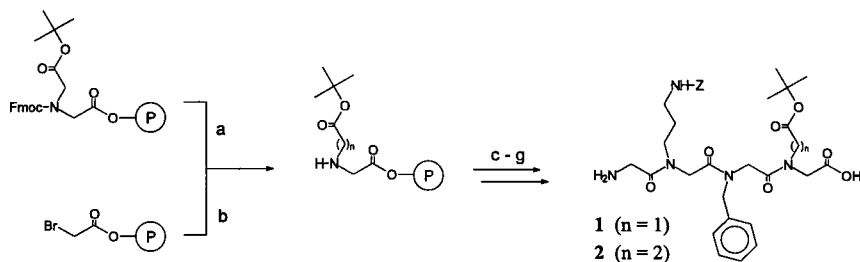


Fig. 1. a) 5 eq.  $H_2N-(CH_2)_2-COObu$ , 6.5 eq. DIEA, NMP, 45°C, 18 h; b) 20% piperidine/DMF; c) 8 eq. bromoacetic acid anhydride, 20 eq. DIEA,  $CH_2Cl_2$ , 10 min; d) 30 eq. benzylamine, NMP, 4 h; subsequently c); e) 5 eq.  $H_2N-(CH_2)_3-NH-Z$ , 5 eq. DIEA, NMP, 4 h; f) 2 eq. Fmoc-Gly-OH, 2 eq. PyBrOP, 5 eq. DIEA,  $CH_2Cl_2$ , 1.5 h; subsequently b); g) AcOH/TFE/ $CH_2Cl_2$  1/1/3, 1 h.

tetracycles were obtained. Partial deprotection of Norn(Z) and subsequent guanylation of the side chain amino functional group yielded the Narg containing cycles (Fig. 2, Table 1). Compounds **5-8** were tested against the isolated  $\alpha_{IIb}\beta_3$ - and  $\alpha_v\beta_3$ -integrin receptors and showed no inhibitory capacity.

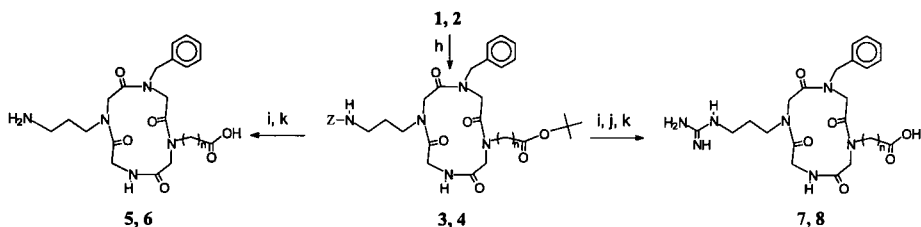


Fig. 2. h.) 3 eq. DPPA, 5 eq. NaHCO<sub>3</sub>, DMF, 50°C, 4 h; i.) H<sub>2</sub> (1 atm), 5% Pd/C, MeOH, 1 h; j.) 3 eq. 1H-pyrazole-1-carboxamide hydrochloride, 6 eq. DIEA, MeOH/H<sub>2</sub>O 9/1, 45°C, 3 h (repeat once); k.) TFA, 1 h. DPPA = Diphenylphosphoryl azide.

Table 1. Yields of linear and cyclic peptoids and characterization by mass spectrometry.

product	yield [%]	FAB-MS (M+H <sup>+</sup> )	product	yield [%]	FAB-MS (M+H <sup>+</sup> )
1 H-Gly-Norn(Z)-Nphe-Nasp(t-Bu)-OH	86	-	2 H-Gly-Norn(Z)-Nphe-Nglu(t-Bu)-OH	85	-
3 c(-Nphe-Nasp(t-Bu)-Gly-Norn(Z)-)	10 <sup>a</sup>	624	4 c(-Nphe-Nglu(t-Bu)-Gly-Norn(Z)-)	21 <sup>a</sup>	-
5 c(-Nphe-Nasp-Gly-Norn-)	40 <sup>a</sup>	434	6 c(-Nphe-Nglu-Gly-Norn-)	23 <sup>a</sup>	448
7 c(-Nphe-Nasp-Gly-Narg-)	21 <sup>a</sup>	476	8 c(-Nphe-Nglu-Gly-Narg-)	60 <sup>a</sup>	490

<sup>a</sup> Yield after RP-HPLC purification, respectively.

## References

- Haubner, R., Finsinger, D., Kessler, H., *Angew. Chem.*, in press (July 1997).
- Friedlander, M., Brooks, P. C., Schaffer, R. W., Kincaid, C. M., Varner, J. A., Cheresch, D. A., *Science*, 270(1995)1500.
- Simon, R. J., Kania, R. S., Zuckermann, R. N., Huebner, V. D., Jewell, D. A., Banville, S., Ng, S., Wang, L., Rosenberg, S., Marlowe, C. K., Spellmeyer, D. C., Tan R., Frankel A. D., Santi, D. V., Cohen F. E., Bartlett, P. A., *Proc. Natl. Acad. Sci.*, 89(1992)9367.
- Kessler, H., *Angew. Chem.*, 105(1993)572; *Angew. Chem. Int. Ed. Engl.*, 32(1993)543.
- Zuckermann, R. N., Kerr, J. M., Kent, S. B. H., Moos, W. H., *J. Am. Chem. Soc.*, 114(1992)10646.

# Reduced amide bond pseudopeptides induce antibodies against native proteins of *Plasmodium falciparum*

**José Manuel Lozano, Fabiola Espejo, Diana Diaz, Fanny Guzmán, Julio C. Calvo, Luz M. Salazar and Manuel Elkin Patarroyo**

*Instituto de Inmunología, Hospital San Juan de Dios, Universidad Nacional de Colombia, Ave. 1 No. 10-01, Santafé de Bogotá, D. C., Colombia*

The malaria peptide coded 1513 whose primary structure is NH<sub>2</sub>-GYSLFQKEKMVL-NEGTSGTA-NH<sub>2</sub> was designed from the amino acid sequence of *Plasmodium falciparum* protein MSP-1. The primary sequence of the binding motif KeKMVL of 1513 to RBCs is also contained in the structure of the SPf-66 synthetic malaria vaccine[1].

In order to explore the immunogenicity of 1513 peptide analogues containing reduced amide bonds, a set of peptide mimetics was synthesized and biochemically characterized. The analogues were synthesized by systematically replacing one CO-NH peptide bond at a time by a reduced amide CH<sub>2</sub>-NH isostere according to the Coy strategy [2].

To determine the bidimensional structure of each 1513 analogue <sup>1</sup>H-NMR studies were performed in a mixture of H<sub>2</sub>O/D<sub>2</sub>O in a ratio 90/10 as well as in aqueous 30% TFE. NMR analysis performed for the Pse-437 analogue containing the Ψ[CH<sub>2</sub>-NH] bond between Val<sub>11</sub> and Leu<sub>12</sub> showed features of secondary structure not yet detected for the parent non modified 1513 peptide. The recorded Pse-437 NMR data were processed for molecular modeling on an Indigo-II computer provided with a graphic package from Biosym/MSI. In the present work we propose a preliminary tridimensional molecular model for Pse-437.

Polyclonal antibodies were obtained after immunization of BALB/c mice and New Zealand rabbits with oxidized pseudopeptide analogues of 1513 containing a cysteine residue at the N and C termini. Monoclonal antibodies to Pse-437 were obtained by standard cellular fusion of mice spleen cells to X-63Ag8 myeloma cells [3]. Seven immunoglobulin producing hybridomas to Pse-437 showed strong reactivity by ELISA and Western blot against *Plasmodium falciparum* protein MSP-1 as well as against the SPf-66 vaccine. Each reactive hybrid cell was cloned to obtain cross-reacting mAbs to 195 kDa, and 83 kDa proteins and SPf-66.

We propose these second generation novel peptides as possible tools for the development of chemically synthesized *Plasmodium falciparum* malaria vaccines.

## Results and Discussion

MALDI-TOF mass spectrometry analyses were performed to identify the five reduced amide containing analogues of 1513. A normal single [M] peak corresponding to the molecular weight of each pseudo-peptide was observed for Pse-437 and Pse-439 and an additional peak of increased height [M-18] observed for Pse-440, Pse-441 and Pse-442

analogues. We propose that a glutamimide ring is formed [4] when the  $\Psi[\text{CH}_2\text{-NH}]$  bond approaches the N-terminal of the 1513 analogues.

A careful analysis of the mass spectrometry data shows the strong tendency for the glutamimide ring formation on the Pse-441 and Pse-442 analogues may be due to the introduction of the  $\Psi[\text{CH}_2\text{-NH}]$  isostere bond between the Glu<sub>8</sub>-Lys<sub>9</sub> and Lys<sub>7</sub>-Glu<sub>8</sub>, respectively, which is absent on the non modified parent 1513 peptide.

According to the 2D-NMR experiments, an  $\alpha$ -helix is formed between Tyr<sub>2</sub>-Phe<sub>5</sub>, Phe<sub>5</sub>-Glu<sub>8</sub> and Ser<sub>3</sub>-Phe<sub>5</sub> since  $d\alpha(\text{Ni}+1)$ ,  $d\alpha(\text{N})$ ,  $d\alpha(\text{iNi}+2)$ ,  $d\text{N}(\text{iNi}+2)$ ,  $d\alpha(\text{iNi}+1)$  and  $d\alpha(\text{iNi}+4)$  interactions and conectivities are observed. According to the proposed molecular structure, the motif Val<sub>11</sub>- $\Psi[\text{CH}_2\text{-NH}]$ -Leu<sub>12</sub> form a hydrogen bond network producing the subsequent structure stabilization on the Pse-437.

A set of mAbs was induced to Pse-437 1513 analogue that recognizes *Plasmodium falciparum* proteins as well as the SPf-66 malaria vaccine (data not shown).

## References

1. Urquiza, M., Rodriguez, L., Suarez, J., Guzmán, F., Ocampo, M., Curtidor, H., Segura, C., Trujillo, M. and Patarroyo, M.E., *Parasite Immunology*, 18 (1996) 505.
2. Sasaki, Y., Murphy, W. and Coy, D., *J. Med. Chem.*, 30 (1987) 1162.
3. Lambros, C. and Vandenberg, J.P., *J. Parasitol.*, 65 (1979) 418.
4. Calvo, J. C., Guzmán, F., Torres, E., Alba, M. P. and Patarroyo, M. E., *These Proceedings*.

# Inhibition of *Ras* farnesyl transferase by histidine-(N-benzylglycinamide) type molecules

**Kevon R. Shuler, Daniele M. Leonard, Dennis J. McNamara, Jeffrey D. Scholten, Judith S. Sebolt-Leopold, Annette M. Doherty**

*Parke-Davis Pharmaceutical Research, Division of Warner-Lambert Co.,  
2800 Plymouth Rd., Ann Arbor, MI 48105, USA*

Ras proteins undergo farnesylation at the cysteine residue in the conserved C-terminal "CAAX" motif, where A is an aliphatic amino acid and X is Glu, Met, Ser, Cys, or Ala [1], in the presence of farnesyltransferase (FTase). Farnesylation of the ras protein allows its localization onto the cell membrane, leading to biological functioning. The mutant forms of *ras* p21, which are also farnesylated, are associated with 20% of all human cancers, and in greater than 50% of pancreatic and colon tumors [2]. Inhibition of ras farnesylation by FTase may represent a potential therapeutic target in cancer treatment.

Through high volume screening of our compound library with rat brain FTase, a potent selective pentapeptide FTase inhibitor PD083176, Cbz-His-Tyr-(OBzl)-Ser-(OBzl)-Trp-DAla-NH<sub>2</sub>, was identified [3]. Systematic truncation of the pentapeptide to a tripeptide, followed by substitution of the Ser(OBzl) moiety by an O-benzylethyl-amide group and transposition of the benzyloxybenzyl group from the  $\alpha$ -C to the adjacent nitrogen led to the modified dipeptide PD152440 [4]. The C-terminus was then modified further. In particular, substitutions with phenethylamine resulted in PD161956, **1**, which was shown to inhibit farnesylation of H-ras (transformed NIH 3T3 cells) at a concentration of 100 nM (Table 1) [5,6]. Structure-activity relationships were carried out at the C-terminus of the PD161956 series following the Topliss tree approach on the phenyl ring in addition to other structural modifications at this position.

## Results and Discussion

Substitution of O-benzyl-phenethylamine by phenethylamine at the C-terminus led to a potent and selective ras FTase inhibitor: PD161956, **1** (Fig. 1). The optimal length of the methylene spacer was found to be two. The results of the Topliss tree approach showed that substitution at the ortho position with the halogens F, **3**, and Cl, **2**, was tolerated, giving cellular activity similar to the parent compound (100 and 200 nM). These compounds were also selective for FTase (Table 1). Replacement of the phenyl ring with a series of heterocycles led to compounds less active than PD161956, with the exception of the 2-pyridyl analogue, **4**, which had similar cellular activity to the parent compound (200 nM).



# Synthesis of dipeptide secondary structure mimetics

Masakatsu Eguchi,<sup>a,b</sup> Hwa-Ok Kim,<sup>a</sup> Benjamin S. Gardner,<sup>a</sup>  
P. Douglas Boatman,<sup>a</sup> Min S. Lee,<sup>a,b</sup>  
Hiroshi Nakanishi<sup>a,b</sup> and Michael Kahn<sup>a,b</sup>

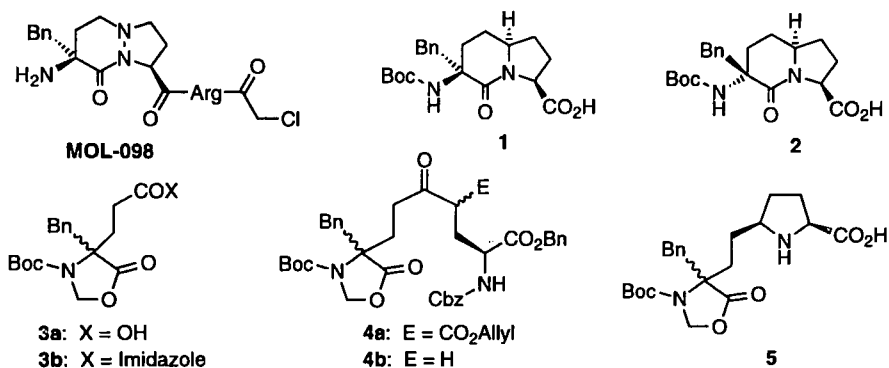
<sup>a</sup>Molecumetics Ltd., 2023 120th Ave. N.E., Suite 400, Bellevue, WA 98005, USA and <sup>b</sup>Department of Pathobiology, University of Washington, Seattle, WA, 98195, USA

Secondary structures in proteins and peptides play an important role in biological recognition systems. In principle, conformationally restricted mimetics of such bioactive local structures can enhance the activity of bioactive molecules.

Our previous studies [1] showed that a 3-benzyl 6,5-bicyclic dipeptide mimetic for D-Phe-Pro coupled with an Arg moiety (MOL-098) afforded effective thrombin inhibitory activity (IC<sub>50</sub> = 1.2 nM). X-ray co-crystal structural analysis of MOL-098 with human  $\alpha\alpha$ -thrombin revealed that the potent inhibitory activity was due to the extended strand structure of MOL-098 interacting with the  $\beta$ -sheet backbone structure of the thrombin active site, and the benzyl group at the P3 position of the inhibitor interacting favorably through a hydrophobic aromatic interaction with Trp<sup>215</sup> of thrombin. In this study, we have designed a conformationally constrained analogue of the 3-benzyl 6,5-bicyclic dipeptide, (3*R* and 3*S*, 6*S*, 9*S*)-3-(*t*-butyloxycarbonyl)amino-3-benzyl-1-aza[4.3.0]nonan-2-one-9-carboxylic acid (**1**, **2**), and developed efficient syntheses of these templates.

## Results and Discussion

We have completed the synthesis of **1** and **2** in 36% overall yield from commercially available Boc-Glu and Z-Glu-OBn. A crossed Claisen condensation, reductive amination, and base-promoted lactam cyclization were employed as the key steps of the multi-gram scale synthesis. Treatment of Boc-Glu with paraformaldehyde and a catalytic amount of *p*-toluenesulfonic acid in refluxing DCE gave the corresponding oxazolidinone in 78% yield. The benzyl derivative **3a** was synthesized in 98% yield via generation of the enolate with 2 equivalents of LHMDS in anhydrous THF, followed by the addition of benzyl bromide. Allyl esterification of Cbz-Glu-OBn was carried out by reacting the cesium salt of the carboxylic acid with allyl bromide in DMF to afford the corresponding allyl ester in quantitative yield. A crossed Claisen condensation was performed by the generation of Cbz-Glu(OAllyl)-OBn  $\gamma$ -enolate [**2**] with 3 equivalents of LHMDS in THF at -78 °C followed by a reaction with *N*-acyl imidazole derivative **3b** generated *in situ* from **3a** with 1,1'-carbonyldiimidazole in THF. The resulting allylic  $\beta$ -keto ester **4a** was obtained in 69% yield. Palladium-catalyzed decarboxylation of **4a** using Tsuji's procedure [3] provided **4b** in 81% yield. Hydrogenation of **4b** in ethanol at 320 psi with a mixture of platinum oxide and palladium-carbon catalysts proceeded with the removal of the Cbz group, imine formation, and reduction of the imine to



yield the  $\delta$ -substituted proline **5** in 91% yield. Only the *cis* isomer was observed due to hydrogenation proceeding from the less sterically hindered face of the imine. Base-promoted lactam cyclization was performed with 1N sodium hydroxide in methanol produced a mixture of **1** and **2** in a 1 : 1 ratio in 92% yield. The complete diastereomeric separation of **1** and **2** was carried out by flash column chromatography (silica-gel, 170 g per 1 g of the product, ethyl acetate / methanol / AcOH, 300 / 2 / 1). The stereochemistry of the bicyclic templates, **1** and **2**, was assigned by analysis of the 500 MHz ROESY experiment at -20 °C.

Templates **1** and **2** were coupled with Arg(Mtr)-  $\alpha$ -ketobenzothiazole [4], followed by removal of the Boc and Mtr groups to provide the electrophilic thrombin inhibitors. Excellent inhibitory activity ( $K_i = 85$  pM) was observed for the inhibitor derived from **1**. The other isomer from **2** had a  $K_i$  value of 10 nM.

## Acknowledgments

We thank Professor G. Stork (Columbia University) for stimulating discussion.

## References

1. Eguchi, M., Boatman P. D., Ogbu C. O., Nakanishi, H., Bolong, C., Lee, M. S., Kahn, M., "Dipeptide Mimetics for Thrombin Substrates and Inhibitors", 212th American Chemical Society National Meeting (Orlando), 1996.
2. Bosco, M. D., Johnstone, A. N. C., Bazza, G., Lopatriello, S., North, M., *Tetrahedron*, 51 (1995) 8545.
3. Tsuji, J., Nisar, M., Shimizu, I., *J. Org. Chem.*, 50 (1985) 3416.
4. Edwards, P. D., Wolanin, D. J., Andisk, D. W., Davis, M. W., *J. Med. Chem.*, 38 (1995) 76.

# Design and synthesis of nanomolar $\delta$ -opioid selective non-peptide mimetic agonists based on peptide leads

Subo Liao,<sup>a</sup> Mark D. Shenderovich,<sup>a</sup> Josue Alfaro-Lopez,<sup>a</sup> Dagmar Stropova,<sup>b</sup> Keiko Hosohata,<sup>b</sup> Peg Davis,<sup>b</sup> Kevin A. Jernigan,<sup>a</sup> Frank Porreca,<sup>b</sup> Henry I. Yamamura<sup>b</sup> and Victor J. Hruby<sup>a</sup>

<sup>a</sup>Departments of Chemistry and <sup>b</sup>Pharmacology, The University of Arizona, Tucson, AZ 85721, USA

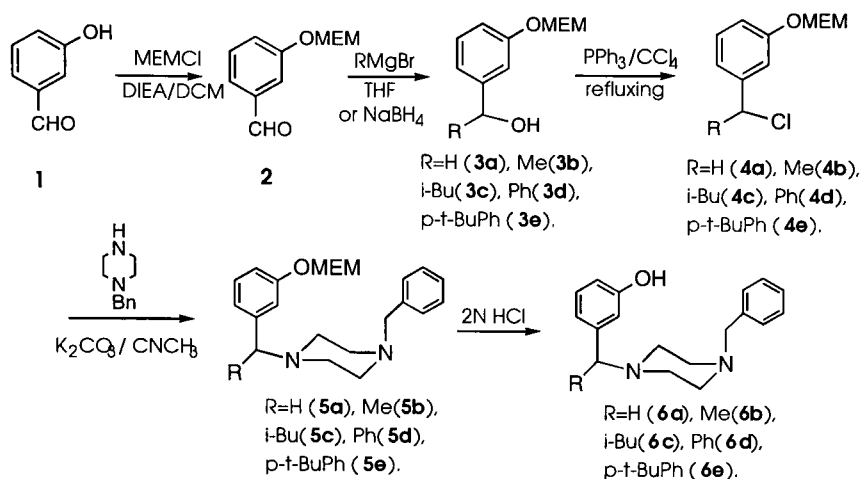
Based on the proposed bioactive conformation of a highly conformationally constrained  $\delta$ -selective opioid peptide lead, [(2S,3R)-TMT<sup>1</sup>]DPDPE and the SAR of  $\delta$ -selective opioid peptide ligands[1-4], we have designed and synthesized a series of non-peptide mimetics using a piperazine ring as template.

## Results and Discussion

The synthesis of designed non-peptide mimetics began with commercially available 3-hydroxybenzaldehyde **1** as shown in Scheme 1. The free hydroxyl group was protected as a methoxyethoxymethyl ether **2** which was reacted with various Grignard reagents or reduced by sodium boron hydride to form the secondary and primary alcohols **3**, respectively. The intermediate **3** was converted into chloride **4** in the presence of triphenylphosphine and tetrachloromethane. The chloride **4** was then reacted with 1-benzylpiperazine to form intermediate **5** whose hydroxyl protection were removed with 2N hydrochloric acid to provide the desired products **6** as hydrochloride acid salts.

The binding assay results of the synthesized non-peptide mimetics against radio labeled highly selective opioid ligands are listed in the Table 1. As shown, the hydrophobicity of the R group has a dramatic effect on the binding and selectivity of the non-peptide ligand **6** to the  $\delta$ -opioid receptor. Analogue **6e** (SL 3111) with a very hydrophobic *para*-t-butylphenyl substituent showed the highest binding affinity (IC<sub>50</sub>=8.4 nM) with over 2000 fold greater selectivity for the  $\delta$ -opioid receptor than for the  $\mu$  receptor. This exceeds the selectivity of the peptide lead [(2S,3R)TMT<sup>1</sup>]DPDPE for the  $\delta$ -opioid receptor. Although a further *in vitro* bioassay on **6e** (SL 3111) indicates that its *in vitro* bioactivity with an IC<sub>50</sub> =85 nM at MVD ( $\delta$ ), and its selectivity ( $\mu/\delta = 460$ ) are lower than expected. This may be due to the racemic materials examined. Alternatively, the ligand does not have all the proper pharmacophores to interact with the  $\delta$ -opioid receptor. Nonetheless, SL-3111 is a novel  $\delta$ -opioid selective non-peptide lead that indeed mimics the peptide ligand. Further modification on this non-peptide lead is currently underway in our laboratory.

Scheme 1



In conclusion, a series of  $\delta$ -selective opioid non-peptide mimetics based on a piperazine template have been synthesized. A hydrophobic group was found to be crucial for these ligands to have high binding affinity and selectivity for the  $\delta$ -opioid receptor.

Table 1. The Binding Affinity of  $\delta$ -Selective Opioid Peptide Ligands.

Compound	Binding data $\text{IC}_{50}$ (nM) $\pm$ SEM [ $^3\text{H}$ ]DAMGO ( $\mu$ )	[ $^3\text{H}$ ]P-CIDPDPE( $\delta$ )	Selectivity ( $\mu/\delta$ )
[(2S,3R)TMT $^1$ ]DPDPE $^3$	43000 $\pm$ 820	5.0 $\pm$ 0.1	860
6a (R= H)	8100 $\pm$ 790	6400 $\pm$ 3200	1
6b (R= Me)	780 $\pm$ 72	610 $\pm$ 306	1.3
6c (R=i-Bu)	2100 $\pm$ 600	420 $\pm$ 38	5.0
6d (R=Ph) (SL-3088)	495 $\pm$ 52	34 $\pm$ 17	15
6e (R=t-BuPh) (SL-3111)	18000 $\pm$ 3000	8.4 $\pm$ 1.6	2100

## References

- Lomize, A.L., Pogozeva, I.D., Mosberg, H.I., Biopolymers, 38 (1996), 221.
- Qian, X., Shenderovich, M.D., Kövér, K.E., Davis, P., Horváth, R., Zalewska, T., Yamamura, H.I., Porreca, F. and Hruby, V.J. J. Am. Chem Soc., 118 (1996), 7280.
- Qian, X., Liao, S., Stropova, D., Yamamura, H.I. and Hruby, V.J. Regulatory Peptides, 65 (1996), 79.
- Shenderovich, M.D., Qian, X., Kövér, K.E. and Hruby, V.J., 14th American Peptide Symposium, Poster 475. Ohio, Columbus, 1995.

# Development of the new potent non-peptide GpIIb/IIIa antagonist NSL-95301 by utilizing combinatorial idea

**Yoshio Hayashi, Takeo Harada, Jun Katada, Akira Tachiki, Kiyoko Iijima, Tohru Asari, Isao Uno and Iwao Ojima<sup>a</sup>**

*Life Science Research Center, Advanced Technology Research Laboratories, Nippon Steel Corporation, 3-35-1 Ida, Nakahara-ku, Kawasaki 211, Japan. <sup>a</sup>Department of Chemistry, State University of New York at Stony Brook, NY 11794-3400, USA*

Undesired platelet aggregation and subsequent thrombosis are suspected to play an important role in various vasoocclusive diseases such as unstable angina and stroke [1]. Effective drugs to prevent such irregular platelet aggregation are in serious demand. The fibrinogen receptor, GpIIb/IIIa, has been one of the major targets for antagonist development as a promising new class of anti-thrombotic agents, because fibrinogen binding to GpIIb/IIIa is considered a final common pathway of platelet aggregation through the cross-linking of adjacent platelets [2]. In this binding process, it is known that the RGD sequence(s) in fibrinogen is responsible for the recognition of GpIIb/IIIa. The guanidino group of the Arg residue and the  $\beta$ -carboxylic acid of the Asp residue are the essential functionalities in this recognition [3]. Therefore, most of the GpIIb/IIIa antagonists have initially been designed to reproduce the three-dimensional configuration of these residues, especially the distance between both functional groups [4]. Here, we report the synthesis of a new RGD-based non-peptide GpIIb/IIIa antagonist utilizing the combinatorial chemistry.

## Results and Discussion

It has been suggested from molecular modeling studies of small RGD peptides that the distance between the guanidino group of Arg residue and the  $\beta$ -carboxylic acid of the Asp residue is a very important factor and should be within the 13~16 Å to show GpIIb/IIIa antagonist activity [5]. Therefore, we can design antagonist molecules only by arranging the appropriate basic and acidic moieties to reside within 13~16 Å and by stabilizing the molecule to this conformation. Such molecular design is attainable by utilizing a simplified combinatorial strategy with limited diversity of unit compounds.

Here, a three component combinatorial strategy, in which molecules were constructed from N-terminal, spacer and C-terminal units, was adopted. To adjust the distance between both terminals and to reduce conformational flexibility, a ring structure was employed in both the N-terminal (benzoic acid derivatives) and C-terminal units (piperidine derivatives) as shown in Fig. 1. All the compounds were synthesized by manual Fmoc-based SPPS using Wang resin. After loading each C-terminal unit onto the resin, it was divided into three portions for the assembly of the next spacer units and then for the next N-terminal assembly. Each compound was cleaved from the resin by TFA in the presence of thioanisole and m-cresol, and purified by reverse-phase HPLC.

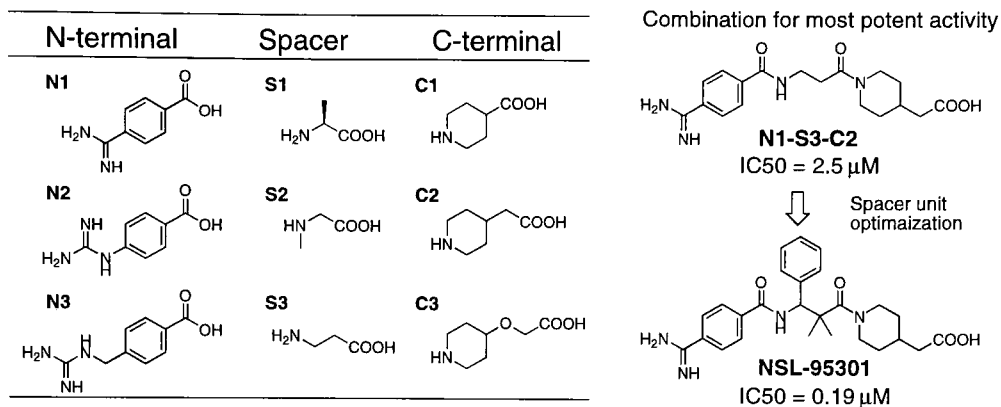


Fig. 1. Three component combinatorial strategy and discovery of NSL-95301.

In a screening assay for collagen-induced human platelet aggregation, the combination of 4-amidinobenzoic acid, 3-aminopropionic acid, and piperidine-4-acetic acid, i.e., [N1-S3-C2], showed the highest inhibitory activity. Thus, this was chosen as the lead compound for further optimization of the spacer unit. Various kinds of  $\beta$  and/or  $\gamma$  substituted 3-aminopropionic acid derivatives were adopted for the spacer unit.

From this modification, NSL-95301, whose spacer unit is 3-amino-3-phenyl-2,2-dimethylpropionic acid, showed the best inhibitory activity for collagen-induced platelet aggregation. NSL-95301 also inhibited *in vitro* platelet aggregation induced by several agonists at submicromolar concentrations and showed a plasma half-life of 90 min ( $T_{1/2\beta}$ , 1 mg/kg i.v.) in guinea pigs. The enantiomers of NSL-95301 were separated by chiral HPLC. This resolution revealed that (+)-NSL-95301 was an active enantiomer with an  $IC_{50}$  value of 92 nM, which is 300 times more potent than that of the (-)-enantiomer.

A molecular modeling study revealed that NSL-95301 exhibited a rigid cup-shaped conformation with the distance of about 14.2 Å between the amidino and the  $\beta$ -carboxyl groups. It is suggested that the steric repulsion resulting from the side chains at  $\alpha$ - and  $\beta$ -position fixes this molecule to such an active conformation.

In conclusion, by applying the idea of combinatorial chemistry, the highly potent fibrinogen receptor antagonist NSL-95301 was developed.

## References

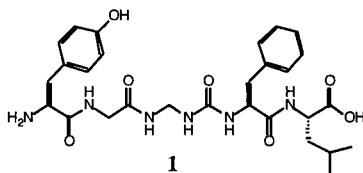
- Falk, E., *Circulation*, 71 (1985) 699.
- Phillips, D.R., Charo, I.F., Parise, L.V. and Fitzgerald, L.A., *Blood*, 71 (1988) 831.
- Ruoslahti, E. and Pierschbacher, M.D., *Science*, 238 (1987) 491.
- Samanen, J., *Annu. Rept. Med. Chem.*, 31 (1996) 91.
- Peishoff, C.E., Ali, F.E., Bean, J.W., Calvo, R., D'Ambrosio, C.A., Eggleston, D.S., Hwang, S.M., Kline, T.P., Koster, P.F., Nichols, A., Powers, D., Romoff, T., Samanen, J.M., Stadel, J., Vasko, J.A. and Kopple, K.D., *J. Med. Chem.*, 35 (1992) 3962.

# A flexible strategy for the incorporation of ureas into peptide linkages

J.A. Kowalski and M.A. Lipton

*Department of Chemistry, Purdue University, West Lafayette, IN 47906-1393, USA*

A class of peptidomimetics, which we have termed ureidopeptides, involves replacement of an amide bond linkage with a urea linkage (denoted as  $\psi$ [NHCONH]). Although a few examples of this type of amide bond replacement exist in the literature [1, 2], to date it has been underutilized as a peptidomimetic. A novel methodology for the synthesis of ureidopeptides involves bistrifluoroacetoxyiodobenzene (PIFA)-promoted Hofmann rearrangement of L-amino acid amides, followed by nucleophilic attack of an amine on the isocyanate intermediate. Ureidopeptides are afforded in good yield (80-95%) from a variety of N-protected amino acid amides using this novel methodology. In addition, the reaction proceeds well in a variety of solvents (THF,  $\text{CH}_2\text{Cl}_2$ ,  $\text{CH}_3\text{CN}$ , DMA) and without racemization. The methodology was tested by synthesizing a novel [Leu<sup>5</sup>]enkephalin analog, H-YGG $\psi$ [NHCONH]FL-OH (**1**), in which the ACE-labile Gly<sup>3</sup>-Phe<sup>4</sup> bond [3] was replaced with the urea linkage. The proteolytic stability of the analog was also studied.



## Results and Discussion

Synthesis of **1** involved the Hofmann rearrangement of a Z-protected tripeptide amide, followed by nucleophilic addition of a dipeptide amine (Fig. 1). Peptides **2** and H-FL-OBzl were synthesized using standard Boc-based solution methods (HBTU, HOBt, DIEA,  $\text{CH}_2\text{Cl}_2$ ) and were both obtained in 86% overall yield. PIFA-promoted Hofmann rearrangement of **2**, followed by addition of H-FL-OBzl afforded the fully protected analog **3** in 30% yield. The low yield in this step is thought to be the result of deprotection of the Tyr Bzl-protecting group during the reaction. Benzyl ethers are known to be oxidatively cleaved by PIFA [4]. Investigation is underway in order to find a more suitable protecting group. The synthesis was completed by hydrogenolysis of all three protecting groups to afford **1** in 79% yield after RPHPLC purification.

**1** and [Leu<sup>5</sup>]enkephalin were then subjected to reaction with ACE, in order to demonstrate the proteolytic stability imparted to **1** by replacement of the susceptible bond with a urea linkage. The reactions were monitored by RPHPLC (Fig. 2).

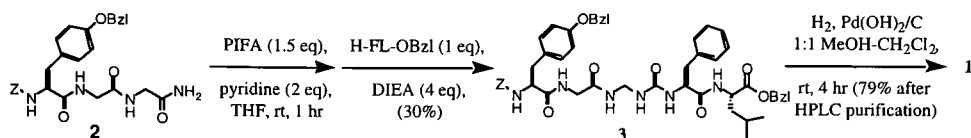


Fig. 1. Synthesis of **1**.

**1** and [Leu<sup>5</sup>]enkephalin were then subjected to reaction with ACE, in order to demonstrate the proteolytic stability imparted to **1** by replacement of the susceptible bond with a urea linkage. The reactions were monitored by RPHPLC (Fig. 2).

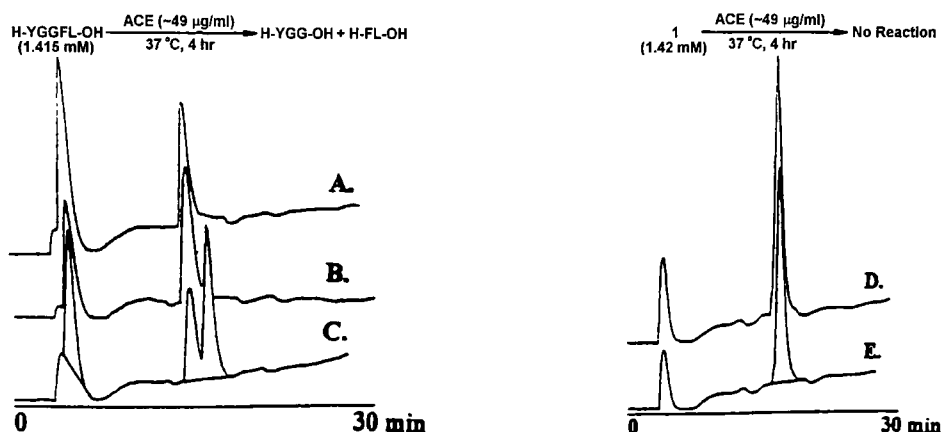


Fig. 2. RP-HPLC analysis of the reaction of ACE with [Leu<sup>5</sup>]enkephalin and **1** (*C*<sub>8</sub> Vydac analytical column, gradient of 5% to 95% CH<sub>3</sub>CN-H<sub>2</sub>O with 0.1% TFA, 1.2 mL/min, 214 nm). (A) reaction of ACE with [Leu<sup>5</sup>]enkephalin, (B) co-injection with authentic H-FL-OH, and (C) co-injection of reaction with control (no ACE). (D) reaction of ACE with **1** and (E) co-injection with control (no ACE).

In the presence of ACE, [Leu<sup>5</sup>]enkephalin is cleaved into tri- and di-peptide fragments. The presence of the dipeptide fragment, H-FL-OH, was also confirmed by FABMS. Under identical reaction conditions with ACE, **1** remained intact, as confirmed by FABMS. Currently, studies are underway to demonstrate that **1** is a substrate for ACE and to determine its biological activity.

## References

1. Kawasaki, K., Maeda, M., Watanabe, J. and Kaneto, H., *Chem. Pharm. Bull.*, 36 (1988) 1766.
2. Ancans, J., Makarova, N. A. and Cipens, G., *Bioorg. Khim.*, 7 (1981) 336.
3. Erdős, E. G., Johnson, A. R. and Boyden, N. T., *Biochem. Pharm.*, 27 (1978) 843.
4. Spyroudis, S., and Varvoglis, A., *J. C. S. Chem. Comm.*, (1979) 615.



**Session IV**

**Synthetic Methods**

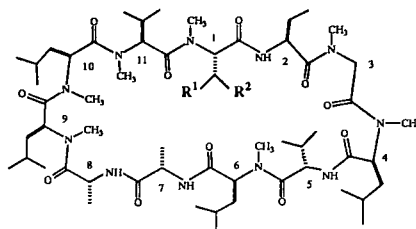


# On-resin N-methylation circumvents a deletion peptide formed during the synthesis of cyclosporin analogs

Prakash Raman, Yvonne M. Angell, George R. Flentke  
and Daniel H. Rich

Department of Chemistry and School of Pharmacy, University of Wisconsin-Madison,  
425 N. Charter Street, Madison, WI 53706, USA

Synthesis of Cyclosporin A [CsA, cyclo(-MeBmt<sup>1</sup>-Abu<sup>2</sup>-Sar<sup>3</sup>-MeLeu<sup>4</sup>-Val<sup>5</sup>-MeLeu<sup>6</sup>-Ala<sup>7</sup>-D-Ala<sup>8</sup>-MeLeu<sup>9</sup>-MeLeu<sup>10</sup>-MeVal<sup>11</sup>-)] where MeBmt = (4R)-4-[(2'E)-butenyl]-4,N-dimethyl-(L)-threonine; Sandimmune<sup>®</sup>, **1**] has been carried out only in solution [1] even though solid phase methods offer many distinct advantages [2]. The seven sterically hindered N-methyl amino acids give rise to difficult peptide couplings, although the simple analog [MeLeu<sup>1</sup>]CsA (**2**) was synthesized using a combination of solid-phase and solution-phase methods [3]. Here we show that the difficult coupling between the MeVal residue in the 11-position and the 1-position residue can be overcome to form [MeSer(OBzl)<sup>1</sup>]CsA (**3**) and [MeThr(OBzl)<sup>1</sup>]CsA (**4**), analogs of CsA with a β-oxygen functionality as in MeBmt (Fig. 1).



- 1: CsA , R<sup>1</sup> = OH; R<sup>2</sup> = CH(CH<sub>3</sub>)CH<sub>2</sub>CH=CHCH<sub>3</sub>
- 2: [MeLeu<sup>1</sup>]CsA, R<sup>1</sup> = H; R<sup>2</sup> = CH(CH<sub>3</sub>)<sub>2</sub>
- 3: [MeSer(OBzl)<sup>1</sup>]CsA : R<sup>1</sup> = OBzl; R<sup>2</sup> = H
- 4: [MeThr(OBzl)<sup>1</sup>]CsA : R<sup>1</sup> = OBzl; R<sup>2</sup> = CH<sub>3</sub>

Fig. 1. Structures of CsA analogs.

## Results and Discussion

Detailed procedures for the synthesis of linear undecapeptide precursors as well as a novel on-resin cyclization method for the synthesis of a number of CsA analogs using solid phase techniques will be reported elsewhere [3,4]. During the course of these studies, we encountered a problematic coupling between MeVal<sup>11</sup> and MeSer(OBzl) and MeThr(OBzl) as the 1-position residues. Coupling of Fmoc-MeSer(OBzl)-OH and Fmoc-MeThr(OBzl)-OH with the hexapeptide H-Abu-Sar-MeLeu-Val-MeLeu-Ala-HAL-PEG-PS

synthesized on a Millipore 9050 Plus Synthesizer proceeded in nearly quantitative yield. However, the DPCDI/HOAt/DMF double coupling strategy for the coupling of Fmoc-MeVal-OH onto the heptapeptide resin containing the  $\beta$ -substituted 1-position residue, which had proven successful in the synthesis of [MeLeu<sup>1</sup>]CsA, gave only a 70% yield for the MeSer(OBzl)-heptapeptide resin and only 50% for the MeThr(OBzl)-heptapeptide resin.

When we switched the solvent to NMP and raised the temperature to 60°C [5], coupling of Fmoc-MeVal-OH proceeded quantitatively onto the Fmoc-MeSer(OBzl)-heptapeptide resin. Under these same conditions, the coupling of Fmoc-MeVal-OH onto the Fmoc-MeThr(OBzl)-heptapeptide resin increased to only 70%. Use of hydrogen bonding solvents such as TFE and HFIP had little or no effect on the coupling yield. Surprisingly, upon cleavage of the linear undecapeptide from the resin and cyclization, we obtained substantial amounts of the cyclic decapeptide in which the MeVal<sup>11</sup> residue was missing, despite capping with N-acetyl imidazole at each step. Washes with the chaotropic agent KSCN [6] did not improve the coupling yield but did enable capping with N-acetyl imidazole after the coupling of Fmoc-MeVal-OH, thereby avoiding the formation of the deletion peptide. Using these optimized conditions, the linear undecapeptide precursors for [MeSer(OBzl)<sup>1</sup>]CsA (3) and [MeThr(OBzl)<sup>1</sup>]CsA (4) were synthesized smoothly using NMP at 60°C for the coupling of the last four amino acid residues beginning with MeVal<sup>11</sup>. Cleavage from the resin and cyclization in solution using (PrPO<sub>2</sub>)<sub>3</sub> and DMAP in CH<sub>2</sub>Cl<sub>2</sub> led to the successful synthesis of [MeSer(OBzl)<sup>1</sup>]CsA (3) and [MeThr(OBzl)<sup>1</sup>]CsA (4) in excellent overall yields (5-16%).

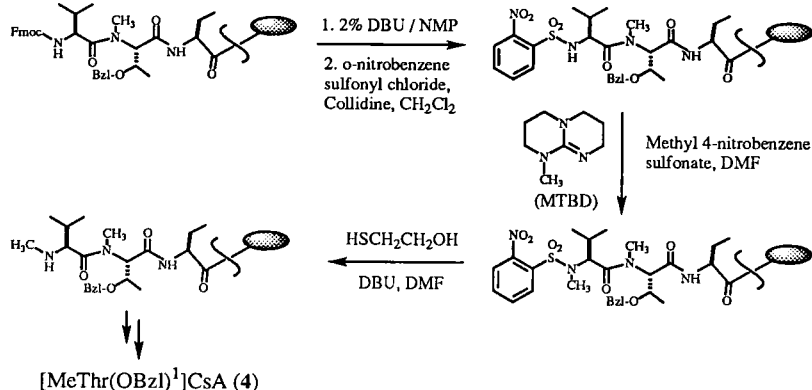


Fig. 2. Synthesis of [MeThr(OBzl)<sup>1</sup>]CsA (4) via on-resin N-methylation.

We then decided to investigate other methods to see if we could improve the coupling yield for Fmoc-MeVal-OH onto MeThr(OBzl)-heptapeptide resin. A possible solution would be to couple Fmoc-Val-OH instead of Fmoc-MeVal-OH in the 11-position followed by site-selective N-methylation [7]. MeThr(OBzl)-heptapeptide resin was synthesized using the standard protocol starting with Fmoc-Ala-HMPB-PEG-PS. The coupling of Fmoc-Val-OH proceeded quantitatively using NMP at 60°C, to give Fmoc-

Val-MeThr(OBzl)-heptapeptide resin. The Fmoc group was cleaved using 2% DBU in NMP, followed by sulfonylation with o-nitrophenylsulfonyl chloride. Deprotonation with the hindered base MTBD and treatment with the methylating agent methyl p-nitrobenzenesulfonate gave the N-methyl sulfonamide. Cleavage of the sulfonamide group with 2-mercaptoethanol and DBU proceeded smoothly to give the N-methylated Val-octapeptide resin (Fig. 2). The resin was then reintroduced in the synthesizer and synthesis of the linear undecapeptide was completed using NMP at 60°C for the remaining couplings. Cleavage from the resin followed by cyclization using  $(\text{PrPO}_2)_3$  / DMAP gave the desired [MeThr(OBzl)<sup>1</sup>]CsA (**4**) analog in 9% overall yield after chromatography. Even though the overall yield did not improve significantly, no deletion peptides were observed, leading to much easier purification.

### Acknowledgement

Financial support from the National Institutes of Health (AR 32007) is gratefully acknowledged.

### References

1. (a) Wenger, R.M., *Helv. Chim. Acta*, 67 (1984) 502 and references therein. (b) Colucci, W.J., Tung, R.D., Petri, J.A. and Rich, D.H., *J. Org. Chem.*, 55 (1990) 2895.
2. (a) Merrifield, R.B., *J. Am. Chem. Soc.*, 85 (1963) 2149. (b) Merrifield, R.B., *Science*, 232 (1986) 341. (c) Fields, G.B. and Noble, R.L., *Int. J. Peptide Protein Res.*, 35 (1990) 161.
3. Angell, Y.M., Thomas, T.L., Flentke, G.R. and Rich, D.H., *J. Am. Chem. Soc.*, 117 (1995) 7279.
4. Raman, P., Angell, Y.M., Flentke, G.R. and Rich, D.H., submitted to *J. Am. Chem. Soc.* for publication.
5. Tam, J.P. and Lu, Y.-A., *J. Am. Chem. Soc.*, 117 (1995) 12058.
6. Pugh, K.C., York, E.H. and Stewart, J.M., *Int. J. Peptide Protein Res.*, 40 (1992) 208.
7. Miller, S.C. and Scanlan, T.S., *J. Am. Chem. Soc.*, 119 (1997) 2301.

# Synthetic approaches to elucidate roles of disulfide bridges in peptides and proteins

George Barany

*Department of Chemistry and Department of Laboratory Medicine and Pathology,  
University of Minnesota, Minneapolis, Minnesota 55455, USA*

The pairing of cysteine residues to form disulfide bridges represents the only way that nature establishes covalent crosslinks bringing together in three dimensions portions of linear polypeptide chains that are apart in the linear sequence. As a consequence, conformations of peptides and proteins can be “locked” and both their stabilities and biological activities are affected. Disulfide bridges can also be harnessed in creative ways for *de novo* design studies. Finally, an active research question is to understand the roles of disulfide bridges in the folding process; the answer may be different for protein sequences able to readily access their final stable packed conformations *versus* peptide molecules that are generally quite conformationally flexible until covalent crosslinks are introduced.

In order to develop a better understanding of the relative importance of disulfides, our laboratory continues to develop methods for the reliable assembly of cystine-containing peptides and small proteins, and for the construction of the required bridges [1]. We also consider a variety of analogous structures, including those in which disulfides are replaced by trisulfides, in which disulfides have been intentional mispaired, and in which paired half-cysteines have been replaced by paired  $\alpha$ -amino-*n*-butyric acid isosteres. These approaches are applied to a range of target molecules, including oxytocin and deamino-oxytocin (9 residues, disulfide bridge between residues 1 and 6), somatostatin (14 residues, disulfide bridge between residues 3 and 14),  $\alpha$ -conotoxin SI (13 residues, disulfide bridges between residues 2 and 7; 3 and 13), apamin (18 residues, disulfide bridges between residues 1 and 11; 3 and 15), and bovine pancreatic trypsin inhibitor (BPTI, 58 residues, disulfide bridges between residues 5 and 55; 14 and 38; and 30 and 51). This article surveys our most recent progress both on synthetic aspects and on conformational/biological consequences, some of which is detailed further in the Proceedings of this Symposium [2]. We report new cysteine protecting groups and racemization-free anchoring and coupling procedures, a reusable polymeric reagent to mediate intramolecular disulfide formation, and studies which compare solution and on-resin regioselective schemes for disulfide bridge formation.

## Results and Discussion

In our work, peptide chain elongation occurs by 9-fluorenylmethyloxycarbonyl (Fmoc) stepwise solid-phase synthesis, with Cys protection provided by *S*-acetamidomethyl (Acm), *S*-triphenylmethyl (Trt), *S*-2,4,6-trimethoxybenzyl (Tmob), or *S*-9*H*-xanthen-9-yl (Xan) [1,3]. Cys residues may be exposed to base, with *possible* abstraction of the  $\alpha$ -proton, at various stages of the synthetic process. While the risk of racemization of *C*-terminal Cys

anchored as an *ester* has been appreciated for some time, it has been recognized just recently that racemization of *N,S*-protected derivatives of Cys residues during their incorporation into *internal amide* linkages can also be a serious concern [2a,4]. The problem is a function of activation/coupling protocols, particularly with certain newly popularized phosphonium and aminium salts that are applied in the presence of tertiary amine bases. Fortunately, “safe” conditions have been developed by switching to weaker auxiliary bases and less polar solvents, and by addressing preactivation issues. In addition, we confirm that pentafluorophenyl esters can be used without racemization. Once incorporated, Cys retains its optical purity through many cycles of further chain growth.

Racemization of *C*-terminal Cys is prevented by a novel side-chain anchoring strategy [2f,5] that combines our recently reported *S*-Xan protection [3] and xanthenyl (XAL) handle for anchoring amides [6]. In addition, this approach circumvents formation of 3-(1-piperidinyl)alanine by-products, a recently described side reaction involving base-catalyzed  $\beta$ -elimination at *C*-terminal anchored Cys [7]. Detachment of completed peptides anchored through the Cys side-chain can be carried out under mild conditions, with possible retention of protecting groups on other side-chains, either by acidolysis or by application of oxidative reagents [in this latter case, requiring a downstream Cys(Xan) and resulting in *direct* disulfide formation].

Regioselective construction of multiple disulfides in the conotoxin family [2e] updates earlier precedents [8] and assumes that the placement of orthogonally removable *S*-protecting groups during the linear chain assembly will govern the eventual alignment of bridges. In the newer studies, *S*-Xan was used along with *S*-Acm, the order of loop formation differed from earlier work, and the unnatural “discrete” and “nested” isomers were accessed for the first time. The best yields and purities, with minimal scrambling, were observed when both disulfide-forming steps were carried out in solution. In preliminary bioassays, mispaired regioisomers showed negligible activity.

Efficient formation of intramolecular disulfide bridges in peptides can be mediated by a novel family of polymer-bound reagents in which 5,5'-dithiobis(2-nitrobenzoic acid) (Ellman's reagent) is bound through *two* sites to PEG-PS or other supports [1b,2b]. This approach brings a mild oxidizing reagent into a milieu that is compatible with peptides, facilitates the desired cyclization step through *pseudo-dilution*, and allows isolation of the oxidized product in solution by simple filtration. We have shown the beneficial effect of a lysine spacer, and devised ways to recycle the polymeric reagent as well as to recover peptide that remains covalently adsorbed. Oxidations of a number of peptide substrates were found to proceed with good rates and yields over the pH range 2.7 - 6.6; for tetrathiol substrates (conotoxin, apamin), partial regioselectivity was observed insofar as the major products had the naturally occurring disulfide arrays.

A recent area of interest to us and others relates to trisulfide variants of peptides and proteins [9]. Taking advantage of a facile directed displacement reaction involving the novel *S*-(*N*-methyl-*N*-phenylcarbamoyl)disulfanyl (Snm) protecting/activating group, we devised efficient syntheses of the trisulfide analogues of oxytocin and deamino-oxytocin. These novel peptides interacted with the oxytocin receptor and were observed to have

unusual *protracted* action [9]. Our chemistry was extended to prove the putative trisulfide structure of a low-level by-product from an industrial preparation of the somatostatin analogue lanreotide [2c]. On the basis of receptor binding assays, we conclude that the trisulfide offers considerable *selectivity* between the hSSTR2 and hSSTR5 receptors.

Over the past few years, we have explored the roles of disulfide bridges in the small protein BPTI by chemical synthesis of analogues which replace some or all of the paired Cys by Abu isosteres [2d,10]. Additional analogues replace selected Cys or Tyr residues with Ala. In these ways, we have obtained partially unfolded species which are characterized by an array of biophysical techniques; in particular sequential assignments and dynamics studies are made possible by heteronuclear NMR-experiments that follow site-specific incorporation of stable isotope labels. We conclude that the presence of *native* disulfide(s) leads to a decrease in the *entropy* of the extended (unfolded) species, and allows the rapid, cooperative formation of an ensemble of fluctuating structures with a common stable hydrophobic core.

## References

1. (a) Andreu, D., Albericio, F., Solé, N.A., Ferrer, M., and Barany, G. In Pennington, M.W. and Dunn, B.M. (Eds.) *Methods in Molecular Biology*, Vol. 35: Peptide Synthesis Protocols, Humana Press, Totowa, N.J., 1994, p. 91. (b) Barany, G. and Chen, L. In Epton, R. (Ed.) *Innovation and Perspectives in Solid Phase Synthesis & Combinatorial Chemical Libraries: Biomedical & Biological Applications*, 1996, Mayflower Scientific Ltd., Kingswinford, England, 1996, p. 181. (c) Annis, I., Hargittai, B., and Barany, G., In Fields, G.B. (Ed.) *Methods in Enzymology*, Academic, Orlando, 1997, vol. 289, in press.
2. All in this volume: (a) Angell, Y., Han, Y., Albericio, F., and Barany, G. (b) Annis, I. and Barany, G. (c) Chen, L., Skinner, S.R., Gordon, T.D., Taylor, J.E., Barany, G., and Morgan, B.A. (d) Gross, C.M., Woodward, C., and Barany, G. (e) Hargittai, B. and Barany, G. (f) Hargittai, B., Han, Y., Kates, S.A., and Barany, G.
3. Han, Y. and Barany, G., *J. Org. Chem.*, 62 (1997) 3841, and references therein.
4. Han, Y., Albericio, F., and Barany, G., *J. Org. Chem.*, 62 (1997) 4307, and references therein.
5. Han, Y., Vágner, J., and Barany, G. In Epton, R. (Ed.) *Innovation and Perspectives in Solid Phase Synthesis & Combinatorial Chemical Libraries: Biomedical & Biological Applications*, 1996, Mayflower Scientific Ltd., Kingswinford, England, 1996, p. 385.
6. Han, Y., Bontems, S.L., Hegyes, P., Munson, M., Minor, C.A., Kates, S.A., Albericio, F., and Barany, G., *J. Org. Chem.*, 61 (1996) 6326.
7. Lukszo, J., Patterson, D., Albericio, F., Kates, S.A., *Lett. Pept. Science*, 3 (1996) 157.
8. Munson, M.C. and Barany, G., *J. Am. Chem. Soc.*, 115 (1993) 10203.
9. Chen, L., Zouliková, I., Slaninová, J., and Barany, G. *J. Med. Chem.*, 40 (1997) 864, and references therein.
10. (a) Ferrer, M., Woodward, C., and Barany, G., *Int. J. Pept. Prot. Res.*, 40 (1992) 194 (b) Ferrer, M., Barany, G., and Woodward, C., *Nature Struct. Biol.*, 2 (1995) 211. (c) Barbar, E., Gross, C.M., Woodward, C., and Barany, G., In Fields, G.B. (Ed.) *Methods in Enzymology*, Academic, Orlando, 1997, vol. 289, in press.

# Synthesis of cyclopsychotride by orthogonal ligation using unprotected peptide precursor

Yi-An Lu and James P. Tam

Department of Microbiology and Immunology, Vanderbilt University, A5119 MCN, Nashville, TN 37232, USA

A new method for orthogonal cyclization [1] without protection or activation steps has been developed for the synthesis of Cyclopsychotride (CPT), a 31-residue, end-to-end cyclic peptide with three disulfide bonds (Fig. 1). This method uses a "triangulation strategy". First, intramolecular transthioesterification by the nucleophilic thiol at the  $\alpha$ -amine terminus with the  $\alpha$ -thioester forms the end-to-end thiolactone. A subsequent ring contraction through S- to N- acyl migration angles back to the intended course of forming the end-to-end amide bond (Fig. 2).



Fig. 1. Amino acid sequences of kalata B1, Circulin B and CPT. Bold amino acids indicate conserved residues.

## Results and Discussion

CPT [2] isolated from the tropical plant *Psychotria longipes* is among the largest cyclic peptides found in nature. It exhibits inhibition of neurotensin receptor binding. The disulfide bond connectivity of CPT is not known but based on sequence homology and cysteinyl placements, this peptide belongs to the Kalata family of cyclic peptides with a cysteine-knot motif. The solution structure of Kalata B1 has been determined and its disulfide connectivity is 1-4, 2-5, and 3-6 (Fig. 1).

CPT was synthesized as a linear unprotected precursor peptide containing an N<sup>α</sup>-cysteine and C<sup>α</sup>-thioester by solid-phase synthesis on Boc-Gly-SCH<sub>2</sub>CH<sub>2</sub>CO-methylbenzhydryl-amine (MBHA) resin [3]. The least hindered site for cyclization between Gly-31 and Cys-1 was chosen as the respective C<sup>α</sup>- and N<sup>α</sup>-terminal residues. To confirm the disulfide connectivity, we used a two-step disulfide bond forming strategy [4] which employed two sets of thiol protecting groups for cysteine. Based on the cysteinyl alignment with Kalata, acetamidomethyl (Acm) for Cys 3 and Cys 6 and methylbenzyl (MBzl) for

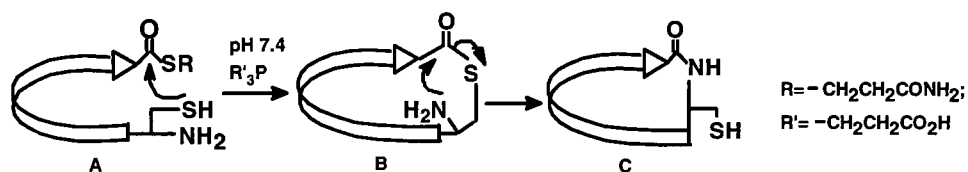


Fig. 2. Cyclization of an unprotected peptide precursor (A) derived from solid-phase synthesis through intramolecular transthioesterification to form a thiolactone (B) and then an S, N-acyl migration to form an end-to-end peptide (C).

the other four Cys were used. The unprotected peptide thioester ( $[M+H]^+$ ,  $m/z$  3486.7 found, 3485.07 calcd.) was cleaved from the resin by HF and allowed to refold and cyclize in descending concentrations of an 8M urea solution containing 0.1M Tris HCl, pH 7.4 and a 10 fold excess of water-soluble Tris (2-carboxyethyl) phosphine to prevent polymeric disulfide formation. Disulfide formation was achieved by DMSO to give three disulfide isomers ( $[M+H]^+$ ,  $m/z$  3376 found, 3376.04 calcd.). The disulfide connectivities of each isomer were determined by partial acid hydrolysis [5]. The expected disulfide isomer of Cys-1,4; 2,5 was obtained in 30% yield. The third disulfide was formed by I<sub>2</sub>/MeOH to give CPT ( $[M+H]^+$ ,  $m/z$  3232.2 found, 3230.89 calcd.). The synthetic material was identical to naturally isolated CPT both chemically and biochemically. These results support the conclusion that CPT has a disulfide connectivity similar to Kalata B1 and that the orthogonal ligation to form a cyclic peptide is a convenient and efficient method which could be achieved essentially under one-pot reaction from the crude peptide after peptide cleavage from the resin.

### Acknowledgment

We thank Dr. Witherup for supplying the native Cyclopsychotride. This work was supported by US PHS grants CA36544 and AI 37965.

### References

1. Zhang, L., Tam, J. P., *J. Am. Chem. Soc.*, 119 (1997) 2363.
2. Witherup, K.M., Bogusky, M.J., Anderson, P.S., Ramjit, H., Ransom, R.W., Wood, T., Sardana, M., *J. Natural Products*, 57 (1994) 1619.
3. Hojo, H., Aimoto, S., *Bell. Chem. Soc. Jpn.*, 64 (1991) 111.
4. Yang, Y., Sweeney, W.V., Schneider, K., Chait, B.T., Tam, J.P., *Protein Science*, 3 (1994) 1267.
5. Zhou, Z., Smith, D. L., *J. Protein Chemistry*, 9 (1990) 523.

# Methionine as the ligation site in the orthogonal ligation of unprotected peptides

Qitao Yu and James P. Tam

Department of Microbiology and Immunology, Vanderbilt University, A5119-MCN, Nashville, TN 37232-2363, USA

Novel approaches to blockwise ligation for peptide synthesis using unprotected peptide segments have received recent attention because of their potential accessibility to diverse groups of macromolecules which were previously difficult to obtain through conventional approaches using protecting group schemes. Among these methods, the orthogonal ligation of two unprotected peptides segments provided approaches for amide formation [1-3]. One such strategy is based on Wieland's transthioesterification [4] and acyl transfer concepts proposed by Kemp et al [5]. In this paper, we describe the orthogonal ligation of an unprotected homocysteiny peptide mediated through transthioesterification and S,N-acyltransfer with a peptide thioester followed by subsequent S-methylation to give Met at the ligation site (Fig. 1).

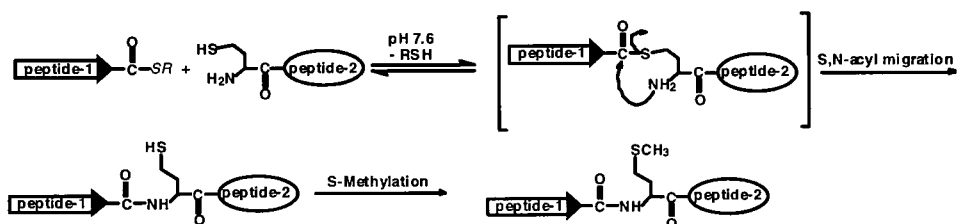


Fig. 1. Synthetic scheme of orthogonal ligation with Met at the ligation site.

Furthermore, we have also extended this method to the synthesis of cyclic peptides from homocysteiny peptide thioesters (Fig. 2).



Fig. 2. Scheme of cyclization from a linear  $N^{\alpha}$ -homocysteiny peptide thioester to form a cyclic peptide.

## Results and Discussion

The intermolecular transthioesterification scheme of the orthogonal ligation method, which results in Met at the ligation site, requires the synthesis of two unprotected peptide building blocks, one bearing a thioester at the  $\alpha$ -COOH terminus and another an  $\alpha$ -homocysteine at the amino terminus. The synthesis of these two building blocks was accomplished by

conventional solid phase synthesis. Peptide building blocks ranging from 4 to 17 amino acid residues were used for transthoesterification to yield peptides of 10 to 34 residues. Some of these peptides were derived from PTH (parathyroid hormone) and contained both Lys and His, which are useful for determining the regioselectivity of the transthoesterification and S-methylation. Transesterification was performed at pH 7.6 in phosphate buffer in a highly reductive environment containing a 3-fold excess of water soluble R<sub>3</sub>P, tris(carboxyethyl)phosphine (TCEP) to prevent disulfide formation and to accelerate the desired reaction. The ligation reaction usually occurred cleanly and efficiently in yields ranging from 79 to 97%. Intramolecular transesterification occurred between the C-terminal homocysteine and N-terminal thioester of the linear N<sup>α</sup>-homocysteinyl peptide thioester precursor. The selective S-methylation of homocysteinyl peptides was performed at room temperature using a large excess of methyl *p*-nitrobenzenesulfonate as methylating reagent [6]. The model peptide, human PTH fragment 1-34 prepared with our orthogonal ligation-S-methylation method, was identical to the standard sample obtained from the commercial source and gave correct molecular weight by MS measurement.

## Conclusion

Our results show that blockwise orthogonal ligation of unprotected peptides can be carried out at methionine site. This adds to the repertoire of ligation sites of cysteine, histidine, glycine and thiaproline. Both the transthoesterification and S-methylation proceed with high efficiency and regioselectivity. In the synthesis of PTH fragment 1-34, the side chain functional groups of Lys and Arg, as well as the imidazole ring of His, do not interfere with this orthogonal ligation scheme.

## References

1. Liu, C.F. and Tam, J. P. Proc. Natl. Acad. Sci. U.S.A., 91 (1994) 6584.
2. Dawson, P.E., Muir, T.W., Clark-Lewis, I. and Kent, S.B.H. Science, 266 (1994) 776.
3. Tam, J.P., Lu, Y.-A., Liu, C.F. and Shao, J. Proc. Natl. Acad. Sci. U.S.A., 92 (1995) 12485.
4. Wieland, T., Bokelmann, E., Bauer, L., Lang, H.U., Lau, H.H. and Schafer, W. Liebigs Ann. Chem., 583 (1953) 129.
5. Kemp, D.S. Biopolymers, 20 (1981) 1793.
6. Henrikson, R.L. J. Biol. Chem., 246 (1971) 4090.

# Low scale multiple array synthesis and DNA hybridization of peptide nucleic acids

**Ralf Hoffmann, Hildegund C.J. Ertl, Anne Marie Pease, Zhenning He,  
Giovanni Rovera and Laszlo Otvos, Jr.**

*The Wistar Institute, Philadelphia, PA 19104, USA*

Although PNA, a new class of DNA and RNA mimics, were originally developed to improve the antisense and antigene technology for treatment of diseases at the level of gene expression [1], the attractive features of PNA recently opened up a wide range of new applications [2]. We hypothesized that the synthetic ease associated with the preparation of medium-sized PNA together with the outstanding selectivity of PNA to hybridize with complementary DNA in solution would allow the development of a convenient and reliable system for the diagnosis of genetic diseases or the detection of infectious agents. Our goal is to apply the high density DNA arrays currently used for mutational screening [3] to PNA. At the first attempt, we have synthesized a set of model PNA sequences on cellulose membranes. We varied the length of the PNA from 8 to 12 residues, and introduced frameshift and point mutations. Subsequently we hybridized the paper-bound PNA array with a corresponding fluorescein-labeled 20-mer oligonucleotide or a 600 base pair rabies glycoprotein DNA.

## Results and Discussion

The PNA oligomers were assembled according to conventional solid-phase peptide synthesis protocols by using Fmoc-protected base analogs (PerSeptive Biosystems) and HATU activation. Completion of coupling steps was followed by staining the paper with bromophenol blue. For quality control, some spots were derivatized with a TFA-cleavable linker, and the cleaved and deprotected PNA was subjected to reversed-phase HPLC and MALDI-mass spectroscopy. The analytical methods detected remarkably pure products regardless of whether they were made manually or by an Abimed 422 robotic arm. As many as 260 PNA sequences could be assembled on a single 9 x 13 cm cellulose sheet.

The deprotected PNA attached to the paper was placed in a resealable plastic bag and 150,000 lux units of purified DNA were added in 10 mM Tris buffer containing EDTA. After incubation the paper was washed and the DNA bound to the PNA spots was measured on a fluoroi-mager. During these conditions, the rabies DNA bound stronger to the 10-mer PNA than to the 8-mer, but further increase in PNA size did not improve binding.

Subsequent experiments were based on the best binder 3' catctccctt 5' sequence. A frameshift in mid-chain position (3' catctccctt 5') completely eliminated the ability of PNA to hybridize with the rabies glycoprotein oligonucleotide. To study the effect of point mutations, two analogs were synthesized. Both mutations considerably reduced DNA-binding. Because the same rabies DNA probe hybridized with various efficiency to PNA from other sections of the glycoprotein, we are trying to set conditions that will make the

PNA-DNA binding less sequence-dependent. Our preliminary results indicate that extreme (either high or low) pH is advantageous to reach this goal.

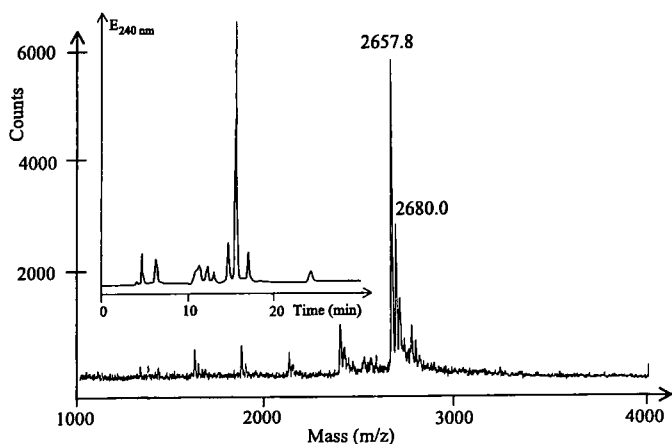


Fig 1. Representative reversed-phase HPLC profile and MALDI-mass spectrum of the PNA 3' catctccctt 5' synthesized on an amino-derivatized cellulose membrane.

Table 1. Single base mutations reduce the binding of the PNA array to the corresponding rabies DNA sequence. The numbers represent fluorescent counts on the PNA spots.

PNA	Origin	Prehybridization	2 hour incubation	16 hour incubation
catctccctt	rabies G	876	14697	24561
catcaccctt	5t → a	939	8050	13142
catctcactt	7c → a	945	4717	3616
accacctcgt	control	1241	2241	not tested

## References

1. Nielsen, P.E., Egholm, M., Berg, R.H. and Buchardt, O., *Science*, 254 (1991) 1497.
2. Hyrup, B. and Nielsen, P.E., *Bioorg. Med. Chem.*, 4 (1996) 5.
3. Matson, R.S., Rampal, J., Pentoney, S.L., Anderson, P.D. and Coassin, P., *Anal. Biochem.*, 224 (1995) 110.

# Intramolecular orthogonal ligation for the synthesis of cyclic peptides

Chuan-Fa Liu,<sup>a</sup> Chang Rao and James P. Tam

*Department of Microbiology and Immunology, Vanderbilt University, A 5119 MCN, Nashville, TN 37323-2363, USA, <sup>a</sup>Current address: Amgen Boulder Inc., 3200 Walnut St., AC-5A, Boulder, CO 80301, USA*

Cyclic peptides are of great interest therapeutically and chemically. With a designed structural rigidity, these molecules often possess enhanced biological potency and selectivity, and are metabolically more stable than their linear counterparts. However, the synthesis of cyclic peptides, especially those with head-to-tail lactam linkages, remains challenging. A significant recent advance in synthetic peptide and protein chemistry is the development of novel convergent approaches to aqueous-phase peptide/protein synthesis using unprotected segments as building blocks [1-5]. A key element of those methods is to introduce two special functional groups with complementary reactivity onto the respective C- and N- termini of two unprotected peptides. The specific capture reaction between these two groups brings the two termini together, leading to spontaneous formation of a peptide bond through an entropy-driven acyl transfer. Forming a peptide bond in this way is also referred to as orthogonal ligation, because it permits specific peptide bond formation in the presence of many other functionalities. With demonstrated utility in protein synthesis, these methods hold equal promise for the synthesis of cyclic peptides [6]. In this case, the two reactive groups are placed at the C- and N- termini of the same unprotected peptide molecule, and their reaction leads to forming a lactam linkage through the same mechanism.

## Results and Discussion

We recently reported on a new orthogonal ligation method that utilizes a peptide thiocarboxylic acid to capture an N-Cys(Npys)-peptide [5]. The net result is the formation of an Xxx-Cys bond at the ligation site. The general procedure for cyclic peptide synthesis with this method involves the use of t-Boc chemistry on a benzhydryl thioester resin, **1**. Boc-Cys(Npys) is incorporated at the last step of solid phase synthesis. HF treatment releases the CO-SH, **2**, that captures the N-terminal cysteinyl Npys-sulfur group to form an acyl-disulfide, **3**, which in turn rearranges to an amide bond, **4**. Thiolytic reduction of the reaction mixture gives the desired cyclic peptide, **5**.

A 10-aa cyclic peptide of the sequence cyclo(-Cys-Gly-Arg-Phe-Glu-Gly-Pro-Lys-Leu-Ala) was first prepared by using this method. We found the entire synthesis to be a simple procedure. In fact, the cyclic product was formed during HF work-up and a single preparative HPLC step was sufficient to purify the product to homogeneity. It was observed that the thiolcarboxylic capture step was already accomplished by the time of

ether precipitation, since the ether phase from washing the cleaved resin and crude peptide precipitates was yellow and contained free Npys-H, as revealed by HPLC analysis. The low pKa value of the thiolcarboxylic group was responsible for this unusual nucleophilicity under acidic conditions.

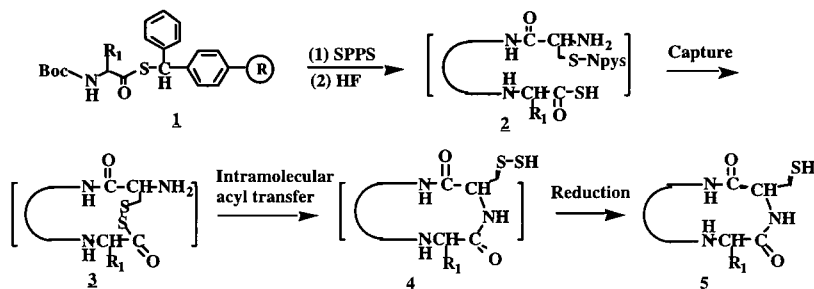


Fig. 1. General scheme for cyclic peptide synthesis.

It was actually impossible to isolate the intermediate linear peptide thiolcarboxylic acid with an Npys-Cys residue in its sequence. The subsequent acyl transfer reaction from an acyl disulfide to an amide occurred when the crude peptide was extracted with a buffered solution (pH 5-6) containing 20% acetonitrile. Since the S-SH group generated from the acyl transfer step is both a reductant and an oxidant, it was unstable and underwent a series of oxidation/reduction reactions to generate various products that were all reducible to the desired cyclic peptide. Therefore, after incubation for 30 min, the peptide extract was treated by reduction with dithiothreitol (DTT) or tricarboxyethylphosphine (TCEP) before being applied to HPLC purification. The purified product was analyzed by MALDI-TOF MS and had a  $[M+H]^+$  of 1059.8 (Theo. 1060). Tryptic digestion produced the fragment H-Leu-Ala-Cys-Gly-Arg-OH, confirming the formation of the Ala-Cys linkage. The overall yield on the basis of the starting resin substitution was about 20%. A number of other cyclic peptides were also prepared in good yield. The cysteinyl thiol group in these cyclic peptides is also a ligation site. We have exploited Michael addition of a thiol to the double bond of an acrylic moiety for chemoselective peptide ligation. Using this method, a symmetric peptide dendrimer was prepared by assembling four copies of a cysteinyl cyclic peptide derived from the V3 loop of the gp 120 protein of HIV-1(III-B strain) onto pentaerythritol tetraacrylate (PETA) (C.F. Liu and J.P. Tam, manuscript in press).

In conclusion, intramolecular orthogonal ligation provides a convenient approach to synthesizing cyclic peptides from totally unprotected linear precursors.

## References

1. Kemp, D.S., *Biopolymers*, 20 (1981) 1793.
2. Liu, C.F. and Tam, J.P. *J. Am. Chem. Soc.*, 116 (1994) 4149.
3. Dawson, P.E., Muir, T.W., Clark-Lewis, I. and Kent, S.B.H. *Science*, 266 (1994) 776.
4. Tam, J.P., Lu, Y.-A., Liu, C.F. and Shao, J. *Proc. Natl. Acad. Sci. U.S.A.*, 92 (1995) 12485.
5. Liu, C.F., Rao, C. and Tam, J.P. *Tetrahedron Lett.*, 37 (1996) 307.
6. Zhang, L. and Tam, J.P. *J. Am. Chem. Soc.*, 119 (1997) 2363.

# A new approach to phosphono-peptide analogs

Maria de Fatima Fernandez, Joseph C. Kappel and  
Robert P. Hammer

Department of Chemistry, Louisiana State University, Baton Rouge, LA 70803, USA

Phosphono-peptide analogs **1** (Fig. 1) in which an amide bond is replaced with a phosphonate ester or phosphonamide linkage are highly effective inhibitors of proteases [1] and synthetases [2] and are widely employed as haptens for catalytic antibody generation [3]. While simple phosphonates and phosphonamides (**1**, A, W = H; R<sup>1</sup>, R<sup>2</sup> = alkyl or aryl) can be prepared easily via nucleophilic addition to phosphonochloridates **2**, the additional functionality (A = PhthN, BocNH, FmocNH, CbzNH; W = CO<sub>2</sub>R or CONHR) and α-carbon branching (R<sup>1</sup>, R<sup>2</sup> ≠ H) present in the amino acid or peptide coupling partners result in moderate to poor yields for most phosphono-peptides. For example, a phosphonate ester analog of cyclohexylglycine-Trp (**1**, X = O, R = *p*-nitrobenzyl, A = FmocNH, R<sup>1</sup> = cyclohexyl, R<sup>2</sup> = 3-indolylmethyl, W = CONH<sub>2</sub>) could be prepared in 40% yield, but the corresponding phosphonamide (X = NH) could not be prepared at all [3]. Although advances in the phosphoryl chloride method for preparation of both phosphonate ester [4] and amide [5,6] peptide analogs have been made, further improvements are needed.

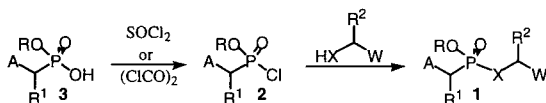


Fig. 1. Traditional phosphorus(V) approach to phosphono-peptides.

## Results and Discussion

We are developing a new general approach to phosphonate derivatives using nucleophilic addition to much more reactive P(III) intermediates [7]. Hydrogen-phosphinate esters **4** are non-oxidatively activated *in situ* to phosphonochloridites **5**, which are subsequently reacted rapidly with a heteroatom nucleophile (X = O, NR, S). The resultant P(III) intermediate **6** is then oxidized/sulfurized to provide the phosphonate product.

Using hydrogen-phosphinate amino acid esters having a range of urethane and phosphorus ester protection (Table 1), a variety of phosphosphoramidate dipeptides have been prepared according to Fig. 3 using a slight modification of published protocol [8]. All products were purified to homogeneity by silica gel chromatography and characterized by FAB-MS, <sup>31</sup>P NMR and <sup>1</sup>H NMR.

NMR analysis of crude reaction mixtures at all stages of the process (activation, coupling, oxidation) show very clean chemistry (>80% purity) of the phosphorus-

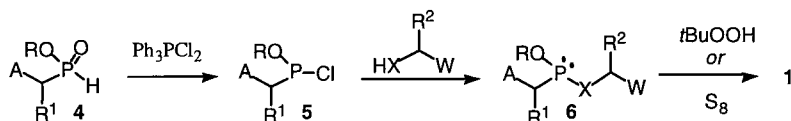


Fig. 2. Phosphorus(III) approach to phosphonopeptides.

containing products, indicating the compatibility of the methodology with standard protection strategies. The moderate isolated yields of phosphonopeptides **9** are mostly due

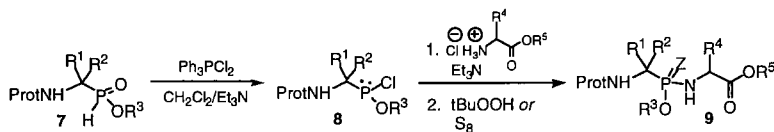


Fig. 3. Phosphonamide dipeptide synthesis from H-phosphinate amino acids.

to loss during purification (difficulties separating away  $\text{Ph}_3\text{P}=\text{O}$  coproduct). The very sterically hindered phosphonamides **9c** and **9d** derived from an  $\alpha,\alpha$ -disubstituted phosphinate amino acid indicate the great potential of this approach for preparation of phosphonate peptide analogs not available by current P(V) methodology.

Table 1. Yield and  $^{31}\text{P}$  NMR of phosphonamide dipeptides **9** prepared from amino acids **7**.

	Prot	R <sup>1</sup>	R <sup>2</sup>	R <sup>3</sup>	R <sup>4</sup>	R <sup>5</sup>	Z	$^{31}\text{P}$ ( $\delta$ )	yield (%)
a	Boc	iPr	H	tBu	H	Et	S	71.0, 71.2	40
b	Fmoc	Bn	H	Bn	H	Et	O	28.0, 29.3	20
c	Fmoc	CH <sub>3</sub>	CH <sub>3</sub>	Bn	H	Et	O	28.2	50
d	Fmoc	CH <sub>3</sub>	CH <sub>3</sub>	Bn	H	Et	S	92.7	40
e	Cbz	Bn	H	Allyl	iBu	CH <sub>3</sub>	O	25.3-27.1	56
f	Cbz	Bn	H	Allyl	iBu	CH <sub>3</sub>	S	82.8-85.8	20

In conclusion, phosphonodipeptides with allyl ester protection at phosphorus (Table 1, entries e and f) have been treated with catalytic Pd(0) to generate the corresponding phosphonamidate dipeptides, which are being evaluated as zinc protease inhibitors.

## References

- Kaplan, A.P., Bartlett, P.A., *Biochemistry*, 30 (1991) 8165.
- Kwon, D.S., Lin C.H., Chen, S.J., Coward, J.K., Walsh, C.T., Bollinger, J.M., *J. Biol. Chem.*, 272 (1997) 2429.
- Smith, A.B., III, Taylor, C.M., Benkovic, S.J., Hirschmann, R., *Tetrahedron Lett.*, 35 (1994) 6853.
- Campagne, J.M., Coste, J., Jouin, P., *J. Org. Chem.*, 60 (1995) 5214.
- Musiol, H.-J., Grams, F., Rudolph-Böhner, S., Moroder, L., *J. Org. Chem.*, 59 (1994) 6144.
- Malachowski, W.P., Coward, J.K., *J. Org. Chem.*, 59 (1994) 7616.
- Fernandez, M.d.F., Vlaar C.P., Fan, H., Liu Y.H., Fronczek F.R., Hammer R.P., *J. Org. Chem.*, 60 (1995) 7390.

# Protected amino acid chlorides: Coupling reagents suitable for the most highly hindered systems

Michael Beyermann,<sup>a</sup> Dumitru Ionescu,<sup>b</sup> Petra Henklein,<sup>a</sup> Ayman El-Faham,<sup>b</sup> Holger Wenschuh,<sup>c</sup> Michael Bienert<sup>a</sup> and Louis A. Carpino<sup>b</sup>

<sup>a</sup> *Forschungsinstitut für Molekulare Pharmakologie, D-10315 Berlin, Germany,* <sup>b</sup> *University of Massachusetts, Amherst, MA 01003, U.S.A., and* <sup>c</sup> *MPI für Infektionsbiologie, D-10117 Berlin, Germany*

The most highly hindered systems with respect to peptide bond formation are encountered when the  $\alpha$ -amino acid units to be coupled are C( $\alpha$ )-dialkylated and/or N( $\alpha$ )-alkylated. As model compounds to investigate the applicability of amino acid halides for such highly hindered systems, we studied coupling reactions between  $\alpha$ -aminoisobutyric acid (Aib) and/or N-methyl- $\alpha$ -aminoisobutyric acid (MeAib).

## Results and Discussion

Fmoc amino acid fluorides have proven to be generally useful for peptide synthesis, even in the case of hindered systems such as those incorporating adjacent Aib residues. In such cases, Fmoc-Aib-F has been shown to be more efficient than the corresponding acid chloride (Fig. 1) because the urethane-protected amino acid chloride is converted much more readily than the acid fluoride to the corresponding oxazolone. On the other hand Fmoc-amino acid fluorides appear to have reached their limits in attempted applications to very highly hindered substrates, e.g. the coupling of Fmoc-protected proteinogenic amino acids to MeAib substrates. The corresponding amino acid chlorides, although long disregarded due to deficiencies associated with available protocols, can, in fact, overcome these limitations. In the presence of bis(trimethylsilyl)-acetamide (BSA), urethane-protected amino acid chlorides provide for a far more efficient process than the corresponding fluorides (Fig. 1).

By switching to other forms of N( $\alpha$ )-protection that are more compatible with the acid chloride functionality such as N-arenesulfonyl protectants for which the already high reactivity of the acid chloride unit is increased by inductive effects, it is possible to couple Aib to MeAib units within a few minutes. Indeed it is even possible to couple MeAib to MeAib, a reaction never achieved previously. Because of its facile removal the Pbf group was used as N( $\alpha$ )-protectant. Thus, Pbf-MeAib-Cl (1 eq.) was coupled to MeAib-OMe•HCl (2 eq.) in toluene in the presence of DIEA (2 eq.) and BSA (1 eq.) within 2-3 h in a 70% yield. The structure of the resulting dipeptide (Pbf-MeAib-MeAib-OMe), purified by preparative HPLC, was confirmed by NMR analysis, mass spectrometry, and CHN analysis. Removal of the Pbf-group by means of 10% dimethylsulfide in trifluoroacetic acid (v/v) for 1 h at ambient temperature yielded the desired dipeptide, MeAib-MeAib-OMe, in a yield of 87%.

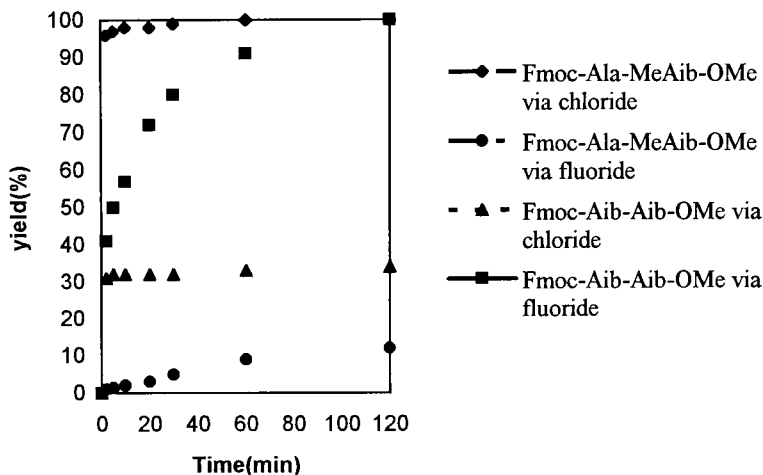


Fig. 1. Coupling efficiency of Fmoc amino acid chlorides versus the corresponding fluorides in DCM; (a)  $Fmoc\text{-Aib-X/Aib-OMe} \bullet HCl/DIEA = (1.25/1/2)$ , and (b)  $Fmoc\text{-Ala-X/MeAibOMe} \bullet HCl/BSA = (1.25/1/2.2)$ .

## Conclusion

These results demonstrate that acid chloride activation is highly suited for the coupling of very hindered systems. Similar results have recently been described by others [1,2]. The N-sulfonyl protectants which prevent decomposition of the highly activated acid chlorides provide for coupling of even the most hindered systems. Although suitable in the case of amino acids not bearing functional side chains, the Pbf residue would not be compatible with peptide synthesis protocols involving t-butyl and related side chain protection. For such systems, a more easily deblocked temporary sulfonyl-type N( $\alpha$ )-protectant must be developed.

## Acknowledgments

The authors thank the Deutsche Forschungsgemeinschaft (Be 1432/2-2) and the U.S. National Institutes of Health and the National Science Foundation for financial support.

## References

1. Meldal, M., Schulze, P. and Müller, R., *Tetrahedron Lett.*, 38 (1997) 443.
2. Konopelski, J.P., Filonova, L.K. and Olmstead, M.M., *J. Am. Chem. Soc.*, 119 (1997) 4305.

# Stereoselective synthesis of highly topographically constrained $\beta$ -isopropyl substituted aromatic amino acids

Yinglin Han, Jun Lin, Subo Liao, Wei Qiu,  
Chaozhong Cai and Victor J. Hruby

*Department of Chemistry, The University of Arizona, Tucson, Arizona 85721, USA*

The introduction of topographically constrained unusual amino acids into biologically active peptides is one of the most powerful approaches for examining the topographical pharmacophore requirements of peptide bioactivities [1]. Recently, the asymmetric synthesis of  $\alpha$ -amino acids has become an area of substantial activity. Many procedures described in the literature make use of a suitable chiral auxiliary to generate stereoselectivity at the  $\alpha$ -position. We have designed and synthesized several  $\beta$ -branched amino acid analogues of phenylalanine, tyrosine and other aromatic amino acids [2] and utilized them in the design of several biologically active peptides [3]. These studies have shown that utilizing such topographically constrained analogues can lead to dramatic changes in potency and receptor selectivity, and have provided valuable insights into how these amino acid residues in the peptide interact with their receptors [4]. The key reactions in our synthetic strategy are the asymmetric Michael-like addition utilizing copper complexes, and direct electrophilic azidation with trisyl azide or bromination with NBS. Our recent studies have been directed to the extension of this methodology to the preparation of  $\beta$ -isopropyltyrosine and  $\beta$ -isopropyl-2',6'-dimethyltyrosine on a large scale. These are the most highly topographically constrained novel amino acids that have been to date.

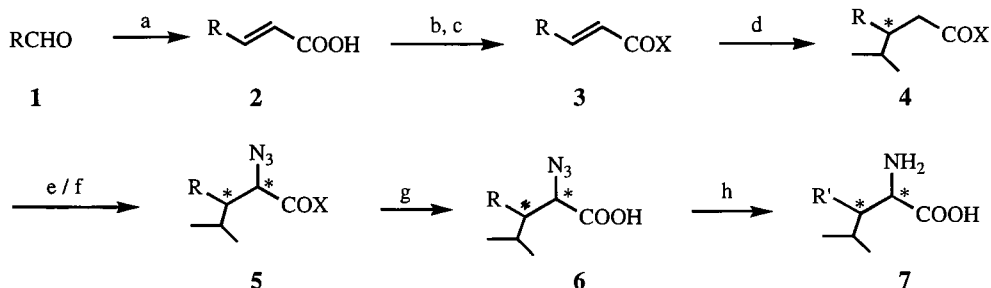
## Results and Discussions

Our synthetic route is shown in Scheme 1. (2*E*)-5-Methyl-2-hexanoic acid (**2a**) was prepared in 94% yield as described in the literature with modifications. **2a** was treated with trimethylacetyl chloride to give the corresponding mixed anhydride which was directly coupled with (4*R* or 4*S*)-4-phenyloxazolidinone to afford the corresponding unsaturated N-acyloxazolidinones **3a** and **3b** following procedures recently developed in our laboratory.

Using a similar methodology, the unsaturated N-acyloxazolidinones **3c** and **3d** were prepared from 2',6'-dimethylanisaldehyde in 84% and 87% yields, respectively.

The stereoselective Michael addition of organometallic reagents to  $\alpha,\beta$ -unsaturated acyl derivatives that contain a chiral auxiliary is one of the most reliable methods for synthesizing optically pure  $\beta$ -branched carbonyl derivatives. We have developed an efficient procedure to prepare these important intermediates via asymmetric Michael addition using optically pure 4-phenyloxazolidinone as an auxiliary [2]. However, in our initial attempts to synthesize the much more sterically-hindered  $\beta$ -isopropyl aromatic amino acids, the addition of isopropylmagnesium bromide to **3d** did not work well using

the previously developed reaction conditions. Instead, we had to apply a chiral resolution method to synthesize the desired optically pure intermediates of  $\beta$ -phenyl isohexanoic acid derivatives [5].



**1-3:** R = *iso*-C<sub>3</sub>H<sub>7</sub>, 4-CH<sub>3</sub>O-2,6-(CH<sub>3</sub>)<sub>2</sub>C<sub>6</sub>H<sub>2</sub>; **4-6:** R = *iso*-C<sub>3</sub>H<sub>7</sub>, *p*-CH<sub>3</sub>OC<sub>6</sub>H<sub>4</sub>, 4-CH<sub>3</sub>O-2,6-(CH<sub>3</sub>)<sub>2</sub>C<sub>6</sub>H<sub>2</sub>; **7:** R' = *p*-CH<sub>3</sub>OC<sub>6</sub>H<sub>4</sub>, 4-CH<sub>3</sub>O-2,6-(CH<sub>3</sub>)<sub>2</sub>C<sub>6</sub>H<sub>2</sub>, *p*-HOC<sub>6</sub>H<sub>4</sub>, 4-HO-2,6-(CH<sub>3</sub>)<sub>2</sub>C<sub>6</sub>H<sub>2</sub>  
X=(4*R* or 4*S*)-4-phenyloxazolidinone.

*Scheme 1.* (a) malonic acid, pyridine, piperidine; (b) trimethylacetyl chloride, triethylamine, THF; (c) lithium (4*R* or *S*)-4-phenyloxazolidinone; (d) Grignard reagent, CuBr•S(CH<sub>3</sub>)<sub>2</sub>, THF; (e) KHMDS, trisylazide, THF; (f) Bu<sub>3</sub>BOTf, NBS in CH<sub>2</sub>Cl<sub>2</sub> and then TMGA; (g) LiOH, CH<sub>3</sub>OH-H<sub>2</sub>O; (h) H<sub>2</sub>, Pd-C, EtOH-HCl; (j) trifluoromethane sulfonic acid, TFA, thioanisole.

Recently, we have re-examined the asymmetric Michael reaction in order to develop a general approach for the asymmetric syntheses of highly hindered  $\beta$ -isopropyl aromatic amino acids. We found that the addition worked very well with modifications such as not using dimethylsulfide as co-solvent and using a catalytic amount of copper complex, even when the highly sterically hindered 2',6'-dimethylphenyl magnesium bromide was also employed. The addition of 4-methoxyphenylmagnesium bromide or 2',6'-dimethyl-4-methoxy-phenylmagnesium bromide to N-acyloxazolidinones **3a** or **3b** gave the corresponding desired compounds **4a-d** with 85-95% yields and high selectivities. No diastereoisomers were found from <sup>1</sup>H-NMR. The addition of isopropylmagnesium bromide to N-acyloxazolidinones **3c** or **3d** also proceeded well with high yields (90-95%). However, a mixture of diastereoisomers was obtained. Various modifications of the reaction conditions to improve the stereoselectivity failed. Nonetheless, the predominant isomer could be easily obtained in diastereomerically pure form by fractional crystallization from ethyl acetate-hexane.

The amount of the copper catalyst has a great effect on the reaction. A highly polar by-product was formed without using the copper complex. Only catalytic amounts (0.3 eq.) of the copper complex are needed when the benzyl ring has no methoxy group. Introduction of the azido group to **3a-f** was achieved either directly by stereoselective electrophilic azidation [6] or indirectly by stereoselective bromination [6] and subsequent replacement of the bromide with nucleophilic tetramethylguanidium azide [7]. When we first tried direct azidation using the reaction conditions developed in our group we found that the reaction did not work well. A large amount of the starting material was recovered. Various

modifications of the reaction conditions were made and we finally found that the reaction time before quenching with acetic acid has a great effect. Usually more than 10 minutes are needed before the azidation reactions are completed. Thus, when N-acyloxazolidinones were successively treated with potassium bis(trimethylsilyl)amide (KHMDs) at  $-78^{\circ}\text{C}$  for 30 min and then with trisylazide for 15 min, azido acid derivatives were obtained in high yields (80-90%) and very high stereoselectivities ( $de > 95\%$ ). An X-ray crystal structure of (2*R*,3*S*)-azido oxazolidinone derivative **5c** was obtained to confirm the suggested absolute stereochemistry. The same results were obtained with electrophilic stereoselective bromination. Usually, a longer reaction time was needed for complete conversion. No stereoisomers were found from  $^1\text{H-NMR}$ .

The azido acids were obtained by catalyzed hydrolysis of the corresponding azido acid oxazolidinone derivatives with simultaneous recovery of the chiral auxiliary according to published procedures[2]. In all cases, no epimerization at the  $\alpha$ -carbon was detected.

Free amino acids were obtained by hydrogenolysis of the resulting azido acids in mixed solvents of acetic acid and water (50/50, w/w) or better, in ethanol containing 2 equivalents of hydrochloric acid to yield the hydrochloride salts of the phenol-protected tyrosine derivatives. Higher hydrogen pressures (50-70 psi) and longer reaction times were employed. The methoxy protecting group of the amino acids was removed either by trifluoromethane sulfonic acid and thioanisole in trifluoroacetic acid at low temperature or by sodium iodide in 47% hydrobromic acid at  $90\text{--}95^{\circ}\text{C}$ . No racemization was found in either case. Free amino acids were obtained by using ion-exchange chromatography. It is very important to note that before loading the ion-exchange resin, the crude amino acids should be extracted two times with hexane to remove water insoluble organic impurities.

Using the same methodology, all four isomers of  $\beta$ -isopropyltyrosine were obtained in 35-40% total yield and high diastereoselectivities.

## References

1. Hruby, V.J., *Life Sciences*, 31 (1982) 189.
2. (a) Dharanipragada, R. *et al.*, *Tetrahedron*, 48 (1992) 4733; (b) Nicolas, E. *et al.*, *J. Org. Chem.*, 58 (1993) 766; (c) Nicolas, E. *et al.*, *J. Org. Chem.*, 58 (1993) 7565; (d) Jiao, D. *et al.*, *Tetrahedron*, 49 (1993) 3511; (e) Li, G. *et al.*, *J. Chem. Soc. Perkin Trans. 1*, (1994) 3057; (f) Qian, X. *et al.*, *Tetrahedron*, 51 (1995) 1033; (g) Li, G. *et al.*, *Tetrahedron Lett.*, 34 (1993) 2561; (h) Li, G. *et al.*, *Tetrahedron Lett.*, 35 (1994) 2301; (i) Kazmierski, W.M. and Hruby, V.J., *Tetrahedron Lett.*, 32 (1994) 5769; (j) Boteju, L.W. *et al.*, *Tetrahedron Lett.*, 33 (1992) 7491.
3. (a) Shenderovich, M.D. *et al.*, *Biopolymers*, 38 (1996) 141; (b) Haskell-Luevano, C. *et al.*, *J. Med. Chem.*, 38 (1995) 4720; (c) Azizeh, B.Y. *et al.*, *J. Med. Chem.*, 39 (1996) 2449.
4. (a) Hruby, V.J., *Biopolymers*, 33 (1993) 1073; (b) Toniolo, C., *Int. J. Pep. Protein Res.*, 35 (1990) 287; (c) Hruby, V.J. *et al.*, *Biochem. J.*, 268 (1990) 249.
5. Liao, S. and Hruby, V.J., *Tetrahedron. Lett.*, 37 (1996) 1563.
6. (a) Evans, D.A. and Weber, A.E., *J. Am. Chem. Soc.*, 108 (1986) 6757. (b) Evans, D.A. *et al.*, *J. Am. Chem. Soc.*, 112 (1990) 4011.
7. Papa, A. J., *J. Org. Chem.*, 31 (1966) 1426.

# Development of a new class of protecting groups for use in solid phase peptide synthesis

Amelie H. Karlström and Anders E. Undén

Department of Neurochemistry and Neurotoxicology, Stockholm University,  
S - 106 91 Stockholm, Sweden

The selection of protecting groups for trifunctional amino acids in peptide synthesis is an important issue since a number of side reactions are highly dependent on how the side chain is protected. We have investigated the concept of using flexible, sterically hindered alkyl protecting groups as a new class of protecting groups that minimize side reactions related to nucleophile lability. This type of protection has been introduced for aspartic acid [1-3], histidine [4], tryptophan [5] and tyrosine [6] (Fig. 1) and it has been shown that these protecting groups suppress common side reactions such as aspartimide formation and premature cleavage by nucleophiles.

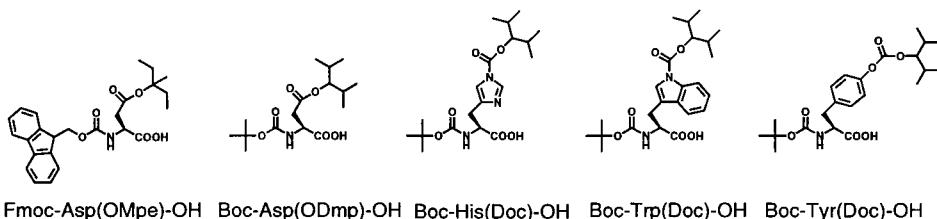


Fig. 1. New amino acid derivatives.

A serious side reaction which occurs in Boc chemistry is the alkylation of the amino acid side chains of Cys, Tyr, Met and Trp by carbocations generated by acidolytic cleavage of the benzylic protecting groups. The addition of scavengers suppresses this side reaction, but does not always provide sufficient protection. In the present study we have investigated the alkylation of cysteine residues by carbocations generated by cleavage of different types of protecting groups. To see if the extent of this side reaction is affected by the choice of side chain protecting groups, three different protecting groups for aspartic acid were used as sources for carbocations, the *tert*-benzyl (Bzl) ester, the *tert*-cyclohexyl (cHex) ester and the *tert*-2,4-dimethyl-3-pentyl (Dmp) ester, and the alkylation of cysteine residues in model peptides was studied.

## Results and Discussion

The model peptide Asp(OR)-Cys(MeBzl)-Asp(OR)-Pro-Phe(NO<sub>2</sub>)-NH<sub>2</sub>, where R=Bzl, cHex or Dmp, was synthesized on MBHA resin by standard Boc chemistry using TBTU/HOBt/DIEA in DMF for coupling and 50% TFA-DCM with 2% N-acetylcysteine

for deprotection of the Boc group. Boc-Asp(ODmp)-OH was synthesized as previously described [3]. 10 mg peptide resin was treated with 2 ml liquid HF with 10% (v/v) *p*-cresol-*p*-thiocresol at 0°C for 1h. After work-up the crude peptide was reduced by DTT in  $\text{NH}_4\text{HCO}_3$ . The peptides were subsequently analyzed by reversed phase HPLC on a  $\text{C}_{18}$  column at 280 nm and by plasma desorption mass spectrometry to determine the relative amounts of alkylated peptide using the different protecting groups and cleavage conditions.

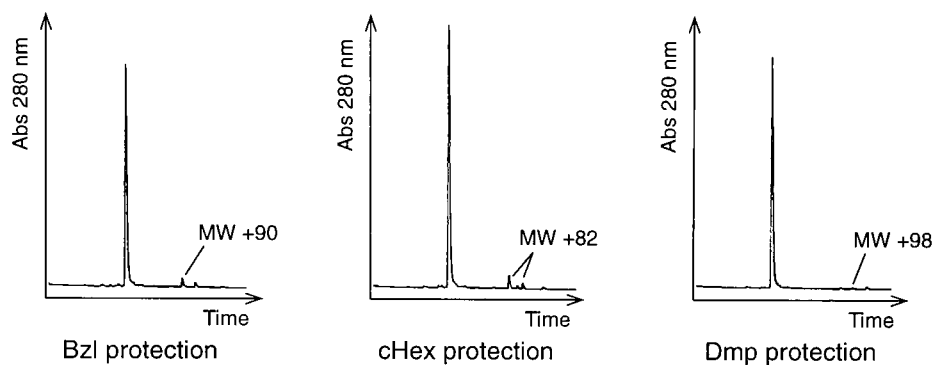


Fig. 2. HPLC elution profiles of the peptide  $\text{DCDPF}(\text{NO}_2)\text{-NH}_2$  synthesized with Boc-Asp(OBzl)-OH, Boc-Asp(OcHex)-OH or Boc-Asp(ODmp)-OH.

The HPLC elution profiles of the peptides synthesized with different aspartyl protecting groups showed one major peak (Fig. 2), which by mass spectrometry was identified as the correct product (MW= 639). In addition to this peak, the major by-product in the peptide synthesized with Asp(OBzl) had a mass difference of +90, which corresponds to the peptide alkylated by a benzyl cation. In the peptide synthesized with Asp(OcHex) the major by-products formed had mass differences of +82, which correspond to the peptide alkylated by a cyclohexyl cation. Two peaks with this molecular weight were found and a plausible explanation is that the cyclohexyl cation rearranges to the 1-methyl-1-cyclopentyl cation [7] which can alkylate the peptide and give the same mass difference. In the peptide synthesized with Asp(ODmp), only small peaks in addition to the correct product were found in the HPLC elution profile. Mass spectrometry analysis showed that one peak had a mass difference of +98 which corresponds to the peptide alkylated by a 2,4-dimethylpent-3-yl cation. The relative amounts of by-products formed when using the different aspartyl protecting groups are shown in Table 1.

All peptides contained a peak eluting late in the HPLC chromatogram which had a mass difference of +104. This corresponds to a peptide in which Cys(4-MeBzl) has not been completely deprotected. Since this by-product was found in all peptides its occurrence is probably independent of the choice of aspartyl protecting group.

Table 1. Alkylation of the model peptide Asp(OR)-Cys(4-MeBzl)-Asp(OR)-Pro-Phe(NO<sub>2</sub>)-NH<sub>2</sub>, where R = Bzl, cHex and Dmp, by cations generated by cleavage of the aspartyl protecting groups.

Asp protecting group	Alkylation
Bzl	4.5 %
cHex	3.5 %
Dmp	<0.5 %

## Conclusion

It was concluded that under the cleavage conditions used, the cations generated by cleavage of the Bzl and the cHex protecting groups were able to alkylate the peptide DCDPF(NO<sub>2</sub>)-NH<sub>2</sub>, whereas cations generated by cleavage of the Dmp protecting group were less reactive and caused significantly less alkylation.

It must be emphasized that the branched alkyl protecting groups have in several respects proven to be superior to the protecting groups commonly used in Boc synthesis of peptides, which is an additional advantage. The Doc/Dmp protecting groups are extremely resistant to nucleophiles and therefore reduce side reactions such as aspartimide formation and premature cleavage of protecting groups during synthesis. They can be used in connection with orthogonal base/nucleophile-cleavable protecting groups that can be selectively removed in the presence of the Doc/Dmp groups. In contrast to the commonly used protecting groups for His and Trp, which have to be removed in a separate deprotection step, they are all cleaved by anhydrous acid along with other protecting groups used, and as shown in this study they also reduce the level of alkylation.

## References

1. Karlström, A. and Undén, A. *Tetrahedron Lett.*, 36 (1995) 3909.
2. Karlström, A. and Undén, A. *Tetrahedron Lett.*, 37 (1996) 4243.
3. Karlström, A. and Undén, A. *Int. J. Peptide Prot. Res.*, 48 (1996) 305.
4. Karlström, A. and Undén, A. *J. Chem. Soc., Chem. Commun.*, (1996) 959.
5. Karlström, A. and Undén, A. *J. Chem. Soc., Chem. Commun.*, (1996) 1471.
6. Rosenthal, K., Karlström, A. and Undén, A. *Tetrahedron Lett.*, 38 (1997) 1075.
7. Olah, G. A. *Angew. Chem. Internat. Ed.*, 12 (1973) 173.

# Sequential orthogonal ligation for the synthesis of $\beta$ defensin

**Christophe Hennard and James P. Tam**

*Department of Microbiology and Immunology, Vanderbilt University, A 5119 MCN  
Nashville, TN, 37232, USA*

Orthogonal ligation involves amide bond formation by a specific  $\alpha$ -amine in the presence of other amines on unprotected peptides [1-3]. An example is thioester ligation in which a weakly activated thioester on the C-terminus of the first segment is captured by the thiol nucleophile on the side chain of the  $\alpha$ -Cys of the second segment [3]. The transient formation of the thioester is followed by spontaneous intramolecular acyl migration forming the peptide bond. So far, this strategy without any protecting group is limited to the ligation of two segments since the peptide bearing the thioester is prone to cyclization if a free N-terminal cysteine is present [2]. To allow sequential orthogonal ligations, the N-terminal cysteine of the thioester segment needs to be protected. This protecting group should be compatible with Boc chemistry, which is the favored method for preparing thioester peptides. Furthermore, this protecting group should be removable under mild aqueous conditions to be compatible with the characteristics of the unprotected peptide. We have designed a thiazolidine-based phenacyl protecting group for the N-terminal cysteine that fulfills these requirements. Here we demonstrate sequential orthogonal ligation through a three-segment sequential thioester ligation of a human  $\beta$ -defensin.

## Results and Discussion

Human  $\beta$ -defensin is a 36-residue peptide containing 6 cysteines with 3 disulfide bonds. The sequence, D-H-Y-N-C<sup>1</sup>-V-S-S-G-G-Q-C<sup>2</sup>-L-Y-S-A-C<sup>3</sup>-P-I-F-T-K-I-Q-G-T-C<sup>2</sup>-Y-R-G-K-A-K-C<sup>1</sup>-C<sup>3</sup>-K, was synthesized through the successive thioester ligation of three segments as shown in Fig. 1 and 1, 2 and 3 of Cys represent the disulfide bond forming cysteine pairs while the amino acids shown in bold face are the chosen ligation sites. Each segment was synthesized on solid support using Boc chemistry. The thiazolidine protecting group of the middle segment (Mopt-C-P-I-F-T-K-I-Q-G-T-thioester) was formed by condensing the purified unprotected  $\alpha$ -Cys peptide with 4-monomethoxy phenacyl aldehyde in an aqueous solution containing 60% CH<sub>3</sub>CN. After 2 hr, the excess aldehyde was extracted by CH<sub>2</sub>Cl<sub>2</sub> and the middle segment was used for the ligation with the C-terminal segment (C-Y-R-G-K-A-K-C-C-K) at pH 7.4 without further purification. After ligation of the M+C segments, the medium was acidified to pH 4 with acetate buffer and the Mopt was removed by irradiation with a mercury lamp at 10 °C for 1 hr [4] in the presence of 10 mg/ml of 1,2-aminothiol as scavenger. Deprotection can be performed with zinc in acetic acid [5]. After purification by HPLC the deprotected M+C segment was ligated with the N-terminal segment (D-H-Y-N-C-V-S-S-G-G-Q-C-L-Y-S-A-thioester)

and after oxidation with DMSO yielded human  $\beta$ -defensin. In conclusion, our strategy for sequential orthogonal ligation is efficient and holds promise for the synthesis of proteins.

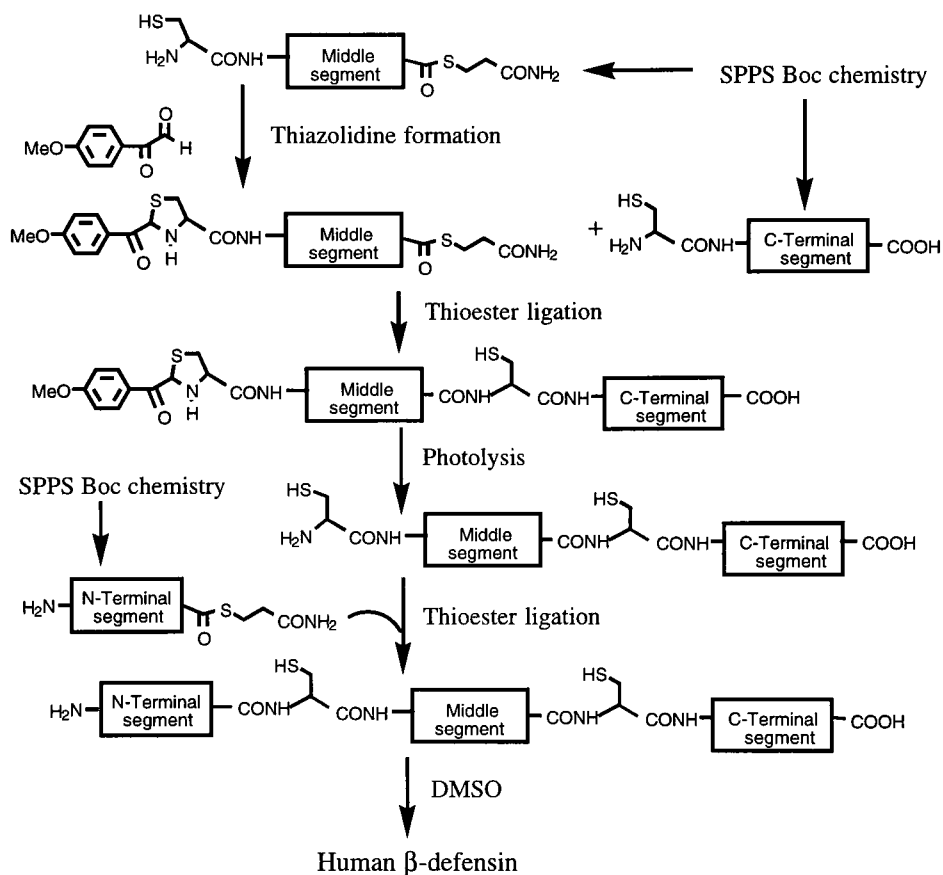


Fig. 1. Schematic representation of the sequential three-segment ligation of human  $\beta$ -defensin.

## References

1. Liu, C.F. and Tam, J.P., *J. Am. Chem. Soc.*, 116 (1994) 4149.
2. Zhang, L. and Tam, J.P., *J. Am. Chem. Soc.*, 119 (1997) 2363.
3. Tam, J.P., Lu, Y.A., Liu, C.F. and Shao, J., *Proc. Natl. Acad. Sci.*, 92 (1995) 12485.
4. Sheehan, J.C. and Umezawa, K. *J. Org. Chem.*, 38 (1973) 3771.
5. Hendrickson, J.B. and Kandall, C. *Tetrahedron Lett.*, (1970) 343.

# A facile metal ion-assisted amidation on solid supports

Kalle Kaljuste and James P. Tam

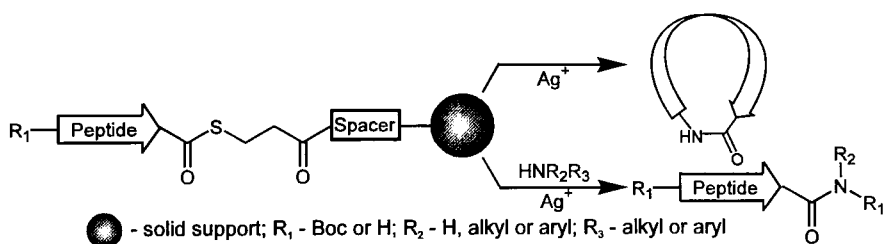
Department of Microbiology and Immunology, Vanderbilt University, A5119, MCN,  
Nashville TN, 37232, USA

Peptides with C- $\alpha$  thioesters have been used for the synthesis of proteins, cyclic peptides and peptide dendrimers in aqueous solution [1-3]. We have found that the peptide-thioesters are useful and facile for generating carboxamides and cyclic peptides in solid phase. The method is based on metal ion-assisted intra- or intermolecular aminolysis of thioester, involving complexation of thiophilic metal ions with the amine nitrogen and the sulfur of thioester, followed by an *S-N* acyl migration [4].

## Results and Discussion

Peptides were synthesized either on nondetachable aminomethyl or a detachable *p*-methylbenzhydrylamine resin carrying the thioester linker, HS-(CH<sub>2</sub>)<sub>2</sub>-CO-Nle (Scheme 1). The norleucine served as a spacer and as an internal standard for amino acid analysis. Protected peptides were C-terminally amidated and simultaneously cleaved from the resin by treatment with an excess of amine and silver trifluoroacetate in CH<sub>2</sub>Cl<sub>2</sub> alone or in a mixture of CH<sub>2</sub>Cl<sub>2</sub> and DMSO. The silver ions were precipitated by addition of NaCl solution, and the mixture was further purified by HPLC. The on-resin amidation proceeded quickly, and most of the reactions were complete in 1h with high yield (Table 1) and purity (Fig. 1A). This method has special value for the preparation of peptide amides of weak and sterically hindered amines which are difficult to achieve by other methods.

Similarly, cyclization of peptides on solid support was conducted as described above. After the removal of the *N*-terminal protecting group, silver trifluoroacetate in CH<sub>2</sub>Cl<sub>2</sub> was

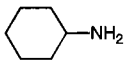
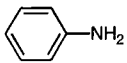
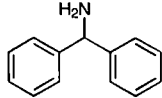
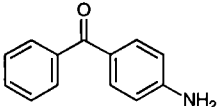
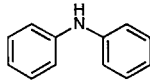
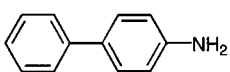


Scheme 1. The synthesis of C-terminally amidated peptides and cyclic peptides on thioester resin.

added and then diisopropylethylamine was added to neutralize the reaction medium (Scheme 1). The silver ions were precipitated by addition of NaCl solution, and cleaved peptides were purified by HPLC. A sample chromatogram for the hexapeptide *c*(Gly-Thr(Bzl)-Phe-Leu-Tyr(2,6-dichloro-Bzl)-Ala) is shown in Fig. 1B. Similar to the amidation

reactions, end-to-tail cyclization on a thioester resin proceeded quickly. This cyclization is simple to perform as well as efficient largely because of the dual entropic and enthalpic activation by the  $\text{Ag}^+$  ions without risk of polymerization.

Table 1. The cleavage yields of thioester resin with various amines.

Amine	% peptide cleaved	Amine	% peptide cleaved
	92		96
	91		91
	98		95

The cleavage yields are given for the peptide-resin Boc-Gly-Leu-Phe-COS-( $\text{CH}_2$ )<sub>2</sub>CO-Nle-aminomethyl resin. 0.5 M of amine solution in  $\text{CH}_2\text{Cl}_2$  was mixed with 3 equivalents of  $\text{CF}_3\text{COOAg}$  dissolved in 10 ml toluene; this mixture was added to 10 mg of resin and shaken for 1 hr.

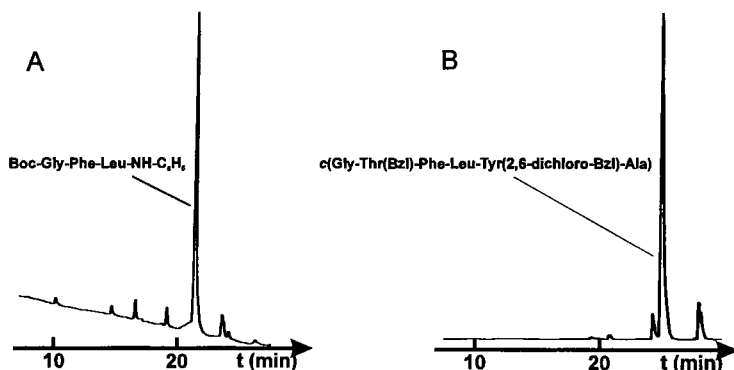


Figure 1. HPLC elution profile of (A) crude peptide Boc-Gly-Phe-Leu-NH- $\text{C}_6\text{H}_5$  and (B) crude *c*(Gly-Thr(Bzl)-Phe-Leu-Tyr(2,6-ClBzl)-Ala) after  $\text{Ag}^+$  ion-mediated reactions.

## References

1. Tam, J. P., Lu, Y.-A., Liu, C.-F. and Shao, J., Proc. Natl. Acad. Sci. USA, 92 (1995) 12485.
2. Dawson, P. E., Muir, T. W., Clark-Lewis, I. and Kent, S. B. H., Science, 266 (1994) 776.
3. Zhang, L. and Tam, J. P., J. Am. Chem. Soc., 119 (1997) 2363.
4. Schwyzer, R. and Hürlimann, Ch., Helv., 35 (1954) 155.

# Sequence assisted peptide synthesis (SAPS): A structural evaluation of the technology

B. Due Larsen,<sup>a</sup> A. Holm,<sup>a</sup> D. H. Christensen<sup>b</sup>  
and O. Faurskov Nielsen<sup>b</sup>

<sup>a</sup>Research Center for Medical Biotechnology, Chemistry Department, The Royal Veterinary and Agricultural University, Thorvaldsensvej 40, DK-1871 Frederiksberg C, <sup>b</sup>Department of Chemistry, Laboratory of Chemical Physics, University of Copenhagen, The H. C. Ørsted institute, Universitetsparken 5, DK-2100, Copenhagen, Denmark

Since the introduction of solid-phase peptide synthesis by Merrifield in 1963 [1] certain problems have been recognized. Among these problems are "incomplete Fmoc-deprotection" in the synthesis of difficult sequences [2, 3]. In a previous report [4] we presented a new concept - Sequence Assisted Peptide Synthesis (SAPS) - for the synthesis of difficult sequences. The SAPS technology has proven to be very effective in synthesizing a number of difficult sequences, resulting in crude products of high purity [unpublished data]. In this report we present results from a structural investigation of the SAPS approach using NIR-FT Raman spectroscopy.

## Results and Discussion

The SAPS technology is based on incorporation of a short peptide sequence (pre-sequence) between the polymeric support and the target peptide. Recently we have investigated the synthesis of H-Ala<sub>n</sub>-Lys-(Lys)<sub>m</sub>-OH using the SAPS approach [6] and only the target peptide could be detected with m = 2, 5 and n = 10 and m = 5 and n = 20 [4].

To investigate the structural influence of the pre-sequence Lys<sub>m</sub> on the target peptide, H-Ala<sub>10</sub>-Lys-(Lys)<sub>m</sub>-OH with m = 5, we used NIR-FT Raman spectroscopy in a stepwise manner by recording the NIR-FT Raman spectra at every coupling and deprotection step during the chain assembly. The resin-bound peptides were synthesized on a PepSyn Gel resin (1 mmol/g) with a HMPA linker using the Fmoc-strategy. Raman spectroscopy was performed as earlier described [3]. The results clearly show a different structural course in comparison to earlier studies of alanine peptides without a pre-sequence [3]. Previously it was concluded that the Fmoc-protected alanine peptides with m = 0 and n = 3 - 10 were adopting a  $\beta$ -sheet structure and it was observed that the Fmoc-group supported  $\beta$ -sheet formation. The corresponding deprotected peptide showed a tendency to switch conformation towards random coil. The structural assignment was based on Raman bands located in the structure sensitive amide-I (1600-1700 cm<sup>-1</sup>) and the amide-III (1230-1300 cm<sup>-1</sup>) regions [3].

Amide-I bands for H-Ala<sub>n</sub>-Lys<sub>6</sub>-OH with n = 1 - 10 are observed at 1668 cm<sup>-1</sup> and the

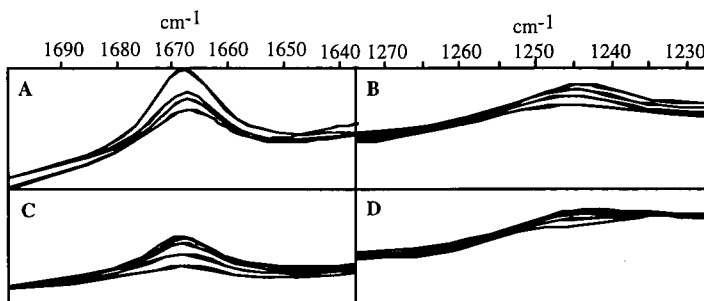


Fig. 1. NIR-FT Raman spectra Amide-I (A), Amide-III (B) of  $H\text{-Ala}_n\text{-Lys}_6\text{-OR}$  with  $n = 1, 3, 5, 7, 10$  curves from bottom to top at  $1670\text{ cm}^{-1}$  and  $1240\text{ cm}^{-1}$  respectively; Amide-I (C), Amide-III (D) of  $\text{Fmoc-Ala}_n\text{-Lys}_6\text{-OR}$  with  $n = 1, 3, 5, 7, 10$  curves from bottom to top at  $1670\text{ cm}^{-1}$  and  $1240\text{ cm}^{-1}$  respectively.

amide-III bands at  $1245\text{ cm}^{-1}$  (Fig. 1). The same bands are observed for the corresponding Fmoc-protected sequences. These bands can definitely be assigned to a random coil structure [5]. The structural observations - using the SAPS approach - agree with previously obtained chemical results where neither deletion nor Fmoc-protected peptides could be detected in the synthesis of the alanine peptides  $H\text{-Ala}_n\text{-Lys}_6\text{-OH}$  with  $n = 10$  and  $20$  [4].

## Conclusion

Using NIR-FT Raman spectroscopy, we have shown that the pre-sequence  $(\text{Lys})_m$  induces a random coil structure in the resin-bound alanine peptide and thereby prevents the formation of the undesirable  $\beta$ -sheet structure.

## References

1. Merrifield, R. B., *J. Am. Chem. Soc.*, 85 (1963) 2149.
2. Larsen, B. D., and Holm, A., *Int. J. Peptide & Protein Res.*, 43 (1994) 1.
3. Due Larsen, B., Christensen, D. H., Holm, A., Zillmer, R., and Faurskov Nielsen, O. *J. Am. Chem. Soc.*, 115 (1994) 6247.
4. Due Larsen, B.; and Holm, A. *Peptides: Proceeding of the 24th European Peptide Symposium 1996*, in press.
5. Tu, A. T., *Raman Spectroscopy in Biology: Principles and Applications*; John Wiley and Sons; New York 1982; p. 1.

# The design of congener breaking sets to determine the function of amino acid residues in biologically active peptides

James A. Burton, Timothy B. Frigo<sup>a</sup> and Bore G. Raju<sup>b</sup>

*RSP Amino Acid Analogues, Inc., 50 Moraine Street, Boston MA 02130, <sup>a</sup>Advanced Magnetics, Cambridge MA 02136, <sup>b</sup>Boston University Medical Center, Boston MA 02118, USA*

A major focus of modern drug discovery is to rationalize the methods used in the process. Older intuitive methods are being replaced by systematic techniques such as rational drug design, QSAR, and combinatorial chemistry. The evident power of the first two techniques has not been fully realized for the conversion of peptide lead sequences into drugs because of two related problems: the flexible nature of peptides and a lack of amino acid analogues. The lack of conformational constraints means that replacing amino acid residues in a peptide chain may greatly alter conformation of the peptide. In turn this may make it impossible to correlate structure with activity. This perception has discouraged the labor-intensive effort needed to develop new amino acid analogues that could be used in rational or quantitative methods of drug design. Clearly it is not reasonable to go to the trouble of synthesizing, resolving, and derivatizing new amino acid analogues for synthesis without an underlying paradigm to help select compounds that are likely to be useful.

## Results and Discussion

One approach to the problem of selecting amino acids for synthesis is to choose families of amino acid analogues that have the same effect on the conformation of a model peptide. This tends to weaken the perception that different solution conformations make it impossible to do systematic structure-activity relationships with peptides.

One efficient way to evaluate the effect of various analogues on peptide conformation is with a Difference Minimum Energy Ramachandran Plot (DMER-Plot). In the studies reported here, Ramachandran Plots were calculated using an MM3 forcefield for the tripeptide Ala-Phe-Ala. The  $\phi$ - $\psi$  angles are those associated with the phenylalanine residue. Unlike most Ramachandran Plots in which all rotatable angles except for the  $\phi$ - $\psi$  angles of interest are fixed, the calculations discussed here involved a global search for the minimum energy conformation of the tripeptide at each  $\phi$ - $\psi$  pair. The resulting plot is called a Minimum Energy Ramachandran Plot (MER-Plot). The underlying assumption is that this conformation will eventually be realized by the peptide in solution.

Subtracting the MER Plots for various tripeptides in which the central phenylalanine residue is replaced with homologues allows the rapid identification of amino acid families that have the same effect on the conformation of the model tripeptide. We have found that while the energies of the MER plots for Ala-Phe-Ala and Ala-Phe(4-Cl)-Ala vary over approximately 20,000 cal/mol the DMER plots vary over less than 100 cal/mol. This is taken to indicate that the *p*-substituent does not greatly affect the solution conformation of

the model tripeptide. For screening purposes DMER-Plots are constructed for all *p*-substituted phenylalanine residues that may be used in peptide design.

Once a set of amino acids that have similar effects on solution conformation are defined, these can be further examined for appropriateness in peptide design. The physical properties that are widely agreed to correlate with activity are lipophilicity, size, hydrogen bond donor and acceptor abilities, charge, parachor and electron distribution. Two criteria are used to select the analogues synthesized. First, the physical properties that may be correlated with biological activity should exhibit a reasonable range of values. *p*-Substituted phenylalanine analogues which have log P values that range over 3-order of magnitude were chosen.

The second criterion for choice of phenylalanine analogues is to avoid co-linearity between properties. For example, size and lipophilicity are frequently highly correlated. A series of analogues in which these properties vary to the same degree in the same direction are not useful in deciding which variable is correlated with activity. It is important to choose analogues in which these, and other parameters, are separable. For example, Phe(4-Et) and Phe(4-CH<sub>2</sub>OH) have similar sizes but markedly different lipophilicities. If a peptide containing the latter analogue has about the same biologic activity as the former this indicates that lipophilicity will not be correlated with activity at this position.

Using the above approach sets or kits of amino acids each centered around one of the coded amino acids can be developed to help in peptide drug design.

## Conclusion

Sets of amino acid analogues based on each of the coded amino acids have been developed for the design of peptide based drugs. DMER plots were used to identify amino acid analogues that affect the conformation of a model peptide in the same way as each of the coded amino acids. Further criteria such as the range of physical properties and lack of co-linearity are then used to refine the set of amino acid analogues.

# Application of different coupling and deprotection conditions in the synthesis of “difficult sequences”

M. Villain,<sup>a</sup> P. L. Jackson,<sup>b</sup> N. R. Krishna<sup>b</sup> and J. E. Blalock<sup>a</sup>

<sup>a</sup>*Dept. Physiology and Biophysics,* <sup>b</sup>*Dept. Biochemistry & Mol. Genetics, University of Alabama at Birmingham, Birmingham, Al, 35294, USA*

The term “difficult sequences” is used for peptide sequences characterized by a high tendency to form secondary structure (e.g.  $\alpha$ -helix or  $\beta$ -sheets) or to aggregate during SPPS. The associated shrinking of the resin support during chemical synthesis can lead to poor coupling and slow deprotection in the growing peptide chain. Use of a mixture of dipolar aprotic solvents (Magic Mixture) and high temperature reduces this problem [1]. In continuous flow SPPS, use of polyethylene glycol resin can partially overcome this problem, although the use of the Magic Mixture is not easily applicable to automated systems. The synthesis of the trans-membrane fragment 361-402 of a rat brain Na<sup>+</sup> channel represents an interesting model for this analysis because our first synthesis attempt was unsuccessful. Therefore we monitored the deprotection of Leu<sup>392</sup> (the first poorly deprotected residue) with different solvent mixtures to optimize synthesis. Combinations of DMF, NMP, DCM, and Triton X 100 were used with either piperidine or 1,8-diazabicyclo[5,4,0]undec-7-ene (DBU) [2] as the deprotecting agent. The ratio between deprotected peptide/Fmoc-peptide in each condition gave us the optimal solvent mixture. Differences in deprotection efficiency between the same deprotecting agent in different mixtures were used as an index of the ability of that mixture to swell the resin and eliminate inter-chain interactions. We proposed that the solvent combination determined for the leucine step could be optimal for the coupling of the entire synthesis. To test this hypothesis, peptide synthesis was performed using as coupling solvent DMF/NMP 1:1, 1% Triton X 100, the HOAt activating agent, coupling time two hours and deprotection with 1% DBU in the same mixture. The final 41 amino acid product contained 45% of the full length 361-402 rat brain Na<sup>+</sup> channel compared to 10% for the 24 amino acid truncated sequence in the first attempt.

## Results and Discussion

In a first attempt, a 24 amino acid peptide was synthesized using a PEGA-PS resin with a substitution of 0.2 mmol/g in a 0.2 mmol scale. The solvent used was DMF, 20% piperidine for the deprotection, and OPfp/HOBt as coupling amino acid with one hour recycling. UV monitoring indicated poor deprotection starting at Leu<sup>392</sup> (70%) that remained low up to residue 24. The correct sequence was identified by TOF-MALDI mass spectrometry after HPLC purification and represented only 10% of the crude product.

For the new synthesis procedure we started with the same resin and stopped without deprotection at Leu<sup>392</sup>. The resin was then washed with DCM and dried. Ten mg of the resin were suspended in different mixtures of DMF, NMP, DCM, and Triton X 100 and then packed

in glass pipettes stoppered with glass wool . One hundred  $\mu$ l of the corresponding solvent mixture with 20% piperidine or 1% DBU was applied to the column and then the column was washed with DMF, DCM and dried. The resin was cleaved for 2 hour with TFA (reagent K) and cold ether precipitated. The lyophilized product was analyzed by RP-HPLC at 220 nm. The amount of deprotection for each solvent was calculated from the ratio of peak area of deprotected peptide/Fmoc-peptide. As expected, DBU was the better deprotecting agent, with the ratios for all the different mixtures ranging from 1.7 to 10.1. Piperidine was less active, ranging from 0.18 to 0.53. The solvent mixture that gave the best deprotection was DMF/NMP1:1, 1% Triton X 100 with both piperidine and DBU. DCM seems to have a negative effect that is more marked when used with Triton X 100. The synthesis proceeded using DMF for the washing steps. Before the acylation steps the solvent was changed with DMF/NMP/Triton X 100 and the OPFP amino acids were activated with HOAt in the same solvent mixture. Recycling was carried out for 2 hours. Every 10 residues 10 mg of resin was cleaved and analyzed by HPLC and mass spectrometry. The yields of the correct products ranged from 70 to 50% of the crude product measured as area of the correct peak by RP-HPLC. The final product was confirmed by mass spectrometry and amino acid analysis.

*Table 1. Ratio Deprotected peptide/Fmoc-Peptide in different solvent conditions.*

Solvent	20% Piperidine	1% DBU
DMF	0.325	4.16
1:1 DMF/NMP	0.510	7.65
1:1 DMF/NMP 1% Triton X100	0.529	10.11
1:1:1 DMF/NMP/DCM	0.201	1.83
1:1:1 DMF/NMP/DCM 1% Triton X100	0.185	1.67

The method presented here provides a semi-empirical approach for determining optimal synthesis conditions of difficult sequences. This approach should have general application and in fact we have used it successfully for the synthesis of other potentially difficult sequences. The changes from a normal synthesis scheme are minimal, and it is suitable for automatization.

### Acknowledgment

Supported in part by: NIH grants MH52527 and NS29719 (J.E. Blalock), NCI grant CA-13148 and NSF grant MCB-9630775 (N.R. Krishna).

### References

- Zhang, L, Goldammer, C., Henkel, B., Zuhl, F., Panhaus, G. Jung, G. and Bayer, E., In Epton, R., (Ed.) *Innovation and Perspective in Solid Phase Synthesis, Peptides, Proteins and Nucleic Acid*, Mayflower Worldwide Ltd. Birmingham, 1994, p. 711.
- Wade, J.D., Bedford, J., Sheppard, R.C. and Tregear, G.W., *Peptide Research*, 4 (1991) 191.

# An artificial receptor for a tri(histidine) ligand

Sanku Mallik, Suguang Sun, Jennifer Saltmarsh and Ipsita Mallik

Department of Chemistry, University of North Dakota, Box: 9024, Grand Forks, ND 58202, USA

We are interested in the recognition of histidine containing peptides and proteins by multiple transition metal ion based receptors [1,2]. The imidazole moiety of the amino acid histidine binds to various transition metal ions (e.g.,  $\text{Cu}^{2+}$ ,  $\text{Ni}^{2+}$ ,  $\text{Co}^{2+}$ ,  $\text{Hg}^{2+}$ ,  $\text{Zn}^{2+}$  etc.) with good affinities. We are using these metal ion to histidine interactions as the basis of the recognition process.

## Results and Discussion

As a model system, we have designed the ligand **L** (Fig. 1) to position three histidines  $\sim 12$  Å apart. The design was carried out by the molecular modeling software "insight II" and "discover" (BioSymb Technologies/MSI Inc., Version 95.0). The structures were energy minimized in the gas phase using the consistent valence force field (cvff). A complementary receptor **R** (Fig. 1) was then designed (using the same software) to position three transition metal ions  $\sim 12$  Å apart. The mono-histidine **C** was used as a control for the recognition studies.

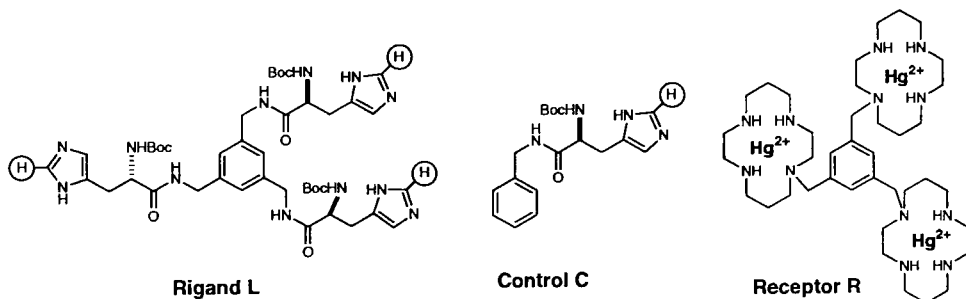


Fig. 1. Structures of the tris(histidine) ligand **L**, its receptor **R** and the control **C** used for the binding studies. Chemical shifts of the hydrogens monitored in the titration studies are circled.

Recognition studies were conducted in a highly polar organic solvent, *dms* $\text{-}d_6$ , and were followed by  $^1\text{H}$  NMR spectroscopy. The C-2-H of the imidazole moieties (indicated in Fig. 1) were found to be shifted down-field (by about 0.9 ppm) upon complexation with the  $\text{Hg}^{2+}$  ions of the receptor **R** (10 mM in **R**). The control **C** was in fast-exchange with the receptor and only an average signal was observed (for the bound and free forms) in the titration experiments. This peak was followed as a function of the concentration of added **C** (3-50 mM). Non-linear regression analysis of the binding data [3,4] (Sigma Plot, Jandel Scientific) provided the value for the binding constant,  $K_{\text{RC}} = 1.3 \times 10^4 \text{ M}^{-1}$  (10% error).

Similar titration experiments (10 mM in **R**, 3-40 mM in **L**) showed that **R** interacts differently with its ligand **L** compared to the control **C**. **L** was found to be in slow-exchange with **R**. Two different C-2-H signals were observed for the free ( $\delta = 7.55$  ppm) and bound ( $\delta = 8.43$  ppm) ligand. The amount of free **L** (measured by the integration of the bound and free peaks) was very small with up to 1:1 stoichiometry and then increased rapidly. The aromatic hydrogens of **L** were found to be shifted up-field (by about 0.5 ppm) in the presence of the receptor **R**. These observations indicated that **R** is forming a 1:1 complex with its ligand **L** and the two benzene rings of the receptor and the ligand are stacking.

Due to inherent errors in the integration of very small peaks in  $^1\text{H}$  NMR spectra, only a lower limit of the binding constant between **R** and **L** ( $K_{\text{RL}}$ ) can be determined (i.e.,  $K_{\text{RL}} > 10^5 \text{ M}^{-1}$ ). When a 1:1 complex of **R** and **L** (10 mM) was titrated with **C** (3-50 mM), **C** was unable to displace **L** to any measurable concentration (followed by  $^1\text{H}$  NMR). In the competition experiment, C-2-H signals for bound **L** remained unaffected while the C-2-H peak for free **C** increased steadily. Analysis of the competition experiment data (Fig. 2) [1] indicated that **R** is favoring **L** over **C** by a factor of at least 20.

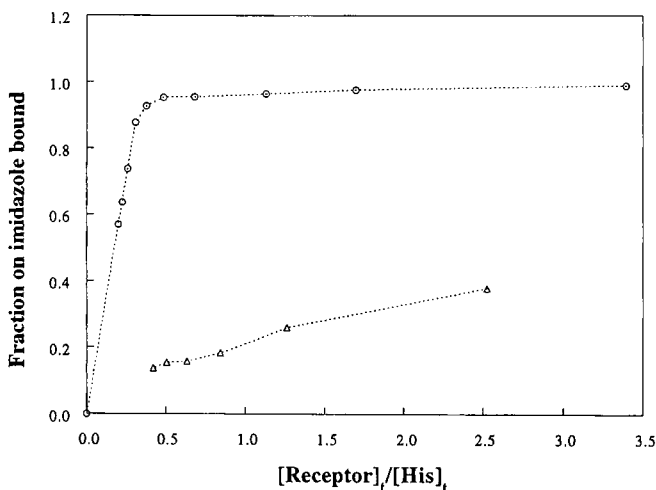


Fig. 2. Fraction of bound **C** ( $\Delta$ ) in the competition experiments. The corresponding fraction bound in the titration expts for **C** ( $O$ ) are also plotted.

## References

1. Mallik, S., Johnson, R. D. and Arnold, F. H., *J. Am. Chem. Soc.*, 116 (1994) 8902.
2. Mallik, S. and Mallik, I., *Synlett*, (1996) 734.
3. Wang, Z. -X., Ravi Kumar, N. and Srivastava, D. K., *Anal. Biochem.*, 206 (1992) 376.
4. Deans, R., Cooke, G. and Rotello, V. M., *J. Org. Chem.*, 62 (1997) 836.

# Comparative studies of racemization during peptide synthesis

Todd T. Romoff,<sup>a</sup> Thuy-Anh Tran<sup>b</sup> and Murray Goodman<sup>b</sup>

<sup>a</sup>Affymax Research Institute, 3410 Central Expressway, Santa Clara, CA 95051, USA

<sup>b</sup>Department of Chemistry and Biochemistry 0343, University of California, San Diego, La Jolla, CA, 92093, USA

We have developed a simple protocol for measuring the intrinsic rates of racemization of N-protected amino acid intermediates using urethane-protected N-carboxyanhydrides (UNCAs) [1] as unique model reactants. Under typical conditions for peptide synthesis, the influences of the amino acid side chain, solvent, and added tertiary amine were probed for their contributions to the rate of racemization. In addition, *isolated* activated intermediates (OAt and OBt esters) normally generated *in situ* via “onium-type” activating reagents were synthesized, and a comparative study of the intrinsic tendencies toward epimerization was carried out.

## Results and Discussion

The general protocol (Fig. 1) relies on the quantitative separation of enantiomeric N<sub>α</sub>-protected N-benzyl amino amides by chiral HPLC (Chiralcel OD, hexane/isopropanol).

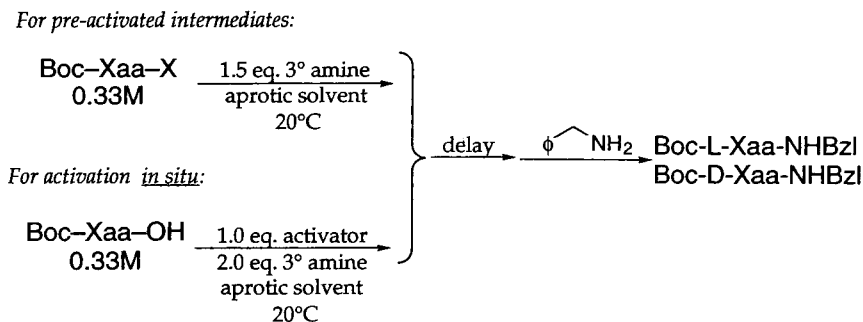


Fig. 1. The general protocol for determining rates of racemization.

The half-life for racemization ( $t_{1/2}^R$ ) is calculated from the delay time (the time during which only epimerization can occur) and the molar ratio of L:D enantiomers following instantaneous quenching of the activated intermediates with benzylamine [2]. The UNCA is particularly well suited for this study, because its planar ring structure allows epimerization only by direct abstraction of the  $\alpha$ -proton and not by any other mechanism

Table 1. Effect of the side chain, solvent and tertiary amine on the racemization rate of activated amino acid intermediates.

Activated Amino Acid	Solvent	Tertiary Amine	Half-Life ( $t_{1/2}^R$ )
Boc-Phe-NCA	toluene	TEA	16 min
Boc-Phe-NCA	toluene	DIEA	4.6 hr
Boc-Phe-NCA	toluene	4-methylmorpholine	240 hr
Boc-Ser(OBzl)-NCA	toluene	DIEA	42 min
Boc-Ser(OBzl)-NCA	toluene	4-methylmorpholine	130 min
Boc-Ser(OBzl)-NCA	DCM	4-methylmorpholine	23 min
Boc-Ser(OBzl)-NCA	DMF	4-methylmorpholine	13 min
Boc-Asp(OBzl)-NCA	toluene	TEA	6.0 min
Boc-Val-NCA	toluene	TEA	150 hr
Boc-Cys(4MB)-NCA	THF	DIEA	27 min
Boc-Cys(4MB)-OBt	THF	DIEA	510 min
Boc-Cys(4MB)-OAt	THF	DIEA	197 min
Boc-Cys(4MB)-OAt	DCM	DIEA	12 min
Boc-Cys(4MB)-F	THF	DIEA	26 hr

(e.g. 5(4*H*)-oxazolone formation [3]). For comparison, isolated OBt and OAt esters and acyl fluorides were subjected to the general protocol. The effect of varying reaction conditions on the rate of racemization of amino acid intermediates is shown in Table 1.

## Conclusion

The results from the experiments with UNCAs unequivocally establish factors that control epimerization. The rate of racemization is decreased by carrying out reactions in nonpolar solvents such as toluene and THF, and by employing weak hindered bases such as *N*-alkylmorpholines. Amino acids that have electron-withdrawing groups at the  $\beta$ -position (Cys, Ser, Asp, etc.) are particularly susceptible to epimerization and require prudent choices of reagents. These trends among the factors (tertiary amine structure, side chain structure, solvent) influencing the rate of racemization of UNCAs are observed under the conditions of *in situ* activation using "onium-type" activating agents, and are consistent with trends found in classical studies in the literature. Our protocol can be used to measure the rate of racemization for any type of activation under all reaction conditions.

## References

1. Fuller, W.D., Goodman, M., Naidler, F. and Zhu, Y.-F., *Biopolymers (Peptide Science)*, 40 (1996) 183.
2. Eliel, E.L., Wilen, S.H. and Mander, L.N., *Stereochemistry of Organic Compounds*, John Wiley & Sons, New York, 1994, ch. 7.
3. Goodman, M., & Glaser, A. in Weinstein, B. and Lande, S., (Eds.), *Peptides, (Proceedings of the First American Peptide Symposium)* Marcel Dekker, New York, 1970, p. 267.

# A novel approach for SPPS of compounds with an amidino group in the C-terminal residue using trityl resins

Torsten Steinmetzer,<sup>a</sup> Andrea Schweinitz,<sup>a</sup> Lydia Seyfarth,<sup>a</sup>  
Siegmond Reißmann<sup>a</sup> and Jörg Stürzebecher<sup>b</sup>

<sup>a</sup>Institute of Biochemistry & Biophysics and <sup>b</sup>Centre for Vascular Biology and Medicine,  
Friedrich-Schiller-University, Philosophenweg 12, D-07743 Jena, Germany

A large number of active biological compounds, e.g. protease inhibitors or hormone agonists and antagonists, contain an amidino group in their C-terminal residue. Many of them do not have an  $\alpha$ -carboxyl or other suitable group to achieve anchoring to a support for use in SPPS. To our knowledge, such compounds have been synthesized exclusively by solution synthesis. Therefore, we investigated the possibility of attaching amidines to trityl resins for use in SPPS. Several compounds of the general structure arylsulfonyl-aa-DL-3-amidinophenylalanyl-methylester were synthesized and analyzed as factor X<sub>a</sub> inhibitors (Fig. 1).

## Results and Discussion

The starting material Fmoc-DL-Phe(3-Am)-Ome **4** was synthesized as described in Fig. 1.

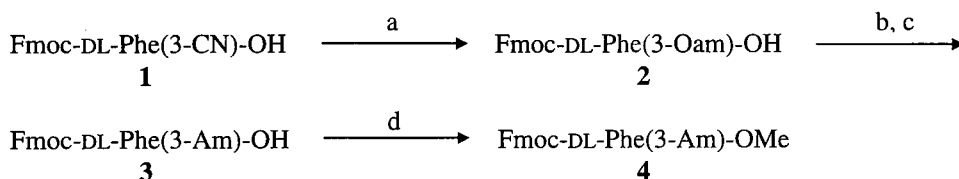


Fig. 1. Synthesis of Fmoc-DL-Phe(3-Am)-OME. a)  $\text{NH}_2\text{-OH}$  / DIEA, RT, 24 h in ethanol, b) acetic anhydride in AcOH, c)  $\text{H}_2$  / Pd in AcOH containing HCl, RT, 5 h, d)  $\text{SOCl}_2$  in methanol, RT, 12 h, (Oam = hydroxyamidino, Am = amidino).

Compound **4** was attached to 4 different trityl resins (2-chlorotrityl-, trityl-, 4-methyltrityl- and 4-methoxytrityl chloride resin). In general, 1.5 equivalents of **4** and a 6-fold excess of DIEA in dry DCM (5 h, RT) compared to the trityl groups resulted in a similar resin loading between 0.20 and 0.35 mmol/g determined by UV-absorption at 301 nm after Fmoc cleavage. In contrast, there were large differences in the rate of product cleavage. The release of **4** from the different resins with 95% TFA/H<sub>2</sub>O was measured spectrophotometrically at 300 nm ( $\epsilon \sim 4650 \text{ M}^{-1} \text{ cm}^{-1}$ , Fig. 2).

As seen in Fig. 2, only the release of **4** from the Mmt resin is fast enough to be of interest for the synthesis of C-terminal amidines in SPPS. The cleavage follows a pseudo

first order reaction with an approximate half-life time of  $\sim 6.5$  hours at  $35^\circ\text{C}$ .

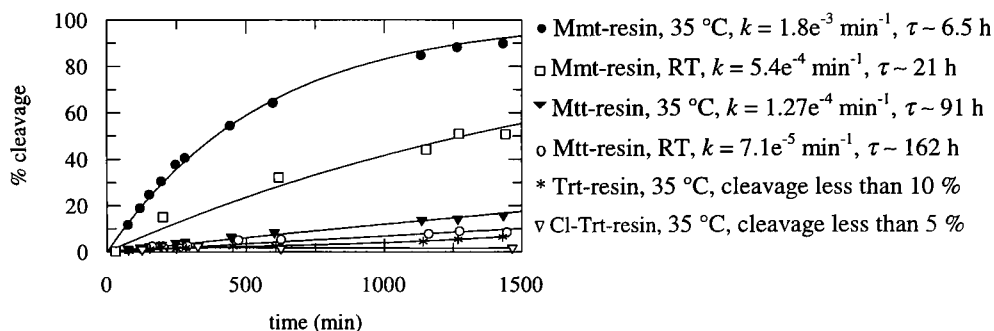


Fig. 2. Time dependence of the release from Fmoc-DL-Phe(3-Am)-OMe from different trityl resins. Mmt = 4-methoxytrityl, Mtt = 4-methyltrityl, Trt = trityl, Cl-Trt = 2-Cl-trityl.

First attempts to synthesize compounds of the general structure arylsulfonyl-aa-DL-3-Phe(3-Am)-OMe starting from Fmoc-DL-Phe(3-Am[4-Mmt resin])-OMe resulted quantitatively in a hydrophobic side product, which was identified by MS to be the double acylated product, e.g.  $\beta$ -Nas-Pro-DL-Phe(3-Am[ $\beta$ -Nas-Pro])-OMe. Therefore, after attachment of **4** to the 4-Mmt resin the support was treated with 4,4'-dimethoxytrityl chloride / DIEA in DCM for one hour to achieve full protection of the amidino group. This resin was used to synthesize the inhibitors listed in Table 1. After a two step cleavage procedure with TFA/H<sub>2</sub>O/triisopropylsilane 92/4/4 (5 min to remove the 4,4'-dimethoxytrityl group followed by 24 h) nearly pure products could be isolated.

Table 1. Structure activity relationship against factor X<sub>a</sub>, trypsin and thrombin.

No.	Structure <sup>a, b, c</sup>	Inhibition constants K <sub>i</sub> (μM)			
		X <sub>a</sub> bovine	X <sub>a</sub> human	trypsin	thrombin
1	$\beta$ -Nas-Gly-DL-Phe(3-Am)-OMe	0.44	1.1	5.2	1.9
2	$\beta$ -Nas-Pro-DL-Phe(3-Am)-OMe	1.6	4.0	2.0	1.3
3	$\beta$ -Nas-Lys-DL-Phe(3-Am)-OMe	21	32	10.7	9.0
4	$\beta$ -Nas-Glu-DL-Phe(3-Am)-OMe	3.6	8.5	21	32
5	Mtr-Gly-DL-Phe(3-Am)-OMe	1.6	3.8	3.71	0.42
6	Tbp-Gly-DL-Phe(3-Am)-OMe	0.38	0.7	4.28	1.43
7	Tips-Gly-DL-Phe(3-Am)-OMe	3.8	7.0	3.42	0.95

<sup>a</sup>Nas=naphthylsulfonyl, <sup>b</sup>Tbp=4-tert butylphenylsulfonyl, <sup>c</sup>Tips = 2,4,6-triisopropylphenylsulfonyl

This series of inhibitors showed moderate activity and weak selectivity against factor X<sub>a</sub> in comparison to trypsin and thrombin. However, this synthesis procedure may be useful for further development of inhibitors with C-terminal amidino groups.

# Mild methods for the synthesis of peptide aldehydes directly from thioester resin

Aleksandra Wyslouch-Cieszynska and James P. Tam

Department of Microbiology and Immunology, Vanderbilt University, A 5119 MCN, Nashville, TN 37232-2363, USA

Peptide aldehydes are useful enzyme inhibitors, synthons for peptide mimetics and peptide-derived biologically active heterocyclic molecules [1]. They are also versatile building blocks in orthogonal coupling methods of peptide synthesis [2]. Although solution synthesis of N-protected  $\alpha$ -amino aldehydes has been well developed, only a few methods exist for their solid phase synthesis [3,4]. Thus, a facile and general method of on-resin generation of peptide aldehydes is still highly desirable. The formation of thioesters is a known method of activating an acyl moiety. In particular, peptide thioesters undergo different nucleophilic substitutions in solution including amidation, transthioesterification and hydride reduction to peptide aldehydes [5,6,7]. Furthermore, thioesters have been shown to be stable linkers in solid phase peptide synthesis [8]. Here, we describe three new methods leading directly from peptide thioester resin to peptide aldehydes or their masked acetal forms under mild reaction conditions (fig. 1). A simple tripeptide, BocPheValAla, was used as a model for optimizing the reaction conditions. Several longer peptide aldehydes were also prepared.

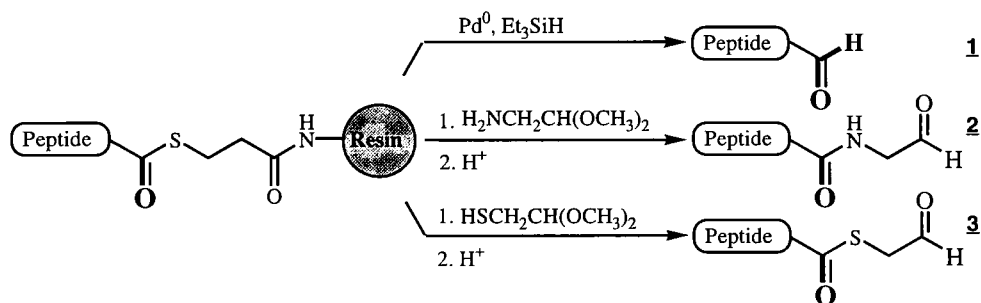


Fig. 1. Three different methods to generate peptide aldehydes directly from thioester resin.

## Results and Discussion

Peptides were synthesized using t-Boc chemistry on MBHA or TentaGel resins containing thiopropionic acid as a detachable linker. Similar results can also be obtained using a nondetachable linker anchored on the aminomethyl resin.

1. **Pd<sup>0</sup> catalyzed on-resin reduction.** Treatment of N-protected peptide thioester with Pd<sup>0</sup> and Et<sub>3</sub>SiH gives the cleaved C-terminal peptide aldehyde **1**. The reaction was performed under N<sub>2</sub> in THF or DCM using 20-30 fold excess of Et<sub>3</sub>SiH in 4°C to avoid aldehyde racemization. The catalyst was obtained by *in situ* reduction of Pd(OAc)<sub>2</sub>. The yield ranged from 80-89%.

2. **On-resin C<sup>α</sup>-amidation with a masked glycinal.** To obtain an acetal masked form of a peptide elongated with glycinal residue at the C-terminus **2**, we used silver-ion assisted amidation using a 10 fold excess of aminoacetaldehyde dimethyl acetal in DCM and a solution of CF<sub>3</sub>COOAg in toluene. After evaporating the reaction mixture, the conversion of peptide acetal to its aldehyde form was easily performed by treatment with TFA in water, in 0°C with an overall yield of more than 90%.

3. **On-resin thiol-thioester exchange.** Treatment of peptide thioester resin with dimethyl acetal of thioacetaldehyde in the presence of trialkylphosphine in a mixture of DCM and DMF was followed by a thiol-thioester exchange. This reaction provides an interesting C-terminal glycinal peptide derivative with the last amide bond substituted with a thioester **3**. Such derivatives may be useful for orthogonal ligation strategies and as bifunctional reagents, specifically, cross-linking the thiol and amine groups at close proximity. The excess of highly boiling thioacetal and phosphine was removed by HPLC (yields = 40-50%).

## Conclusions

We show that thioester resin linkages are a source for peptide aldehydes under very mild conditions. Changing the nature of nucleophile used for cleavage of the peptide, three different derivatives containing a C-terminal aldehyde moiety can be obtained from a single batch of peptide thioester resin. Thus, the on-resin synthesis of peptide aldehydes provides the possibility of obtaining longer peptide aldehydes not accessible from natural sources or by molecular biology techniques (i.e. mimetics of ubiquitin aldehyde) and enables the preparation of libraries of small heterocycles.

## References

1. Golebiowski, A. Jurczak, J., Chem. Rev., (1989) 149.
2. Liu, C-F., Tam, J.P. J. Am. Chem. Soc., 116 (1994) 4149.
3. Fehrentz, J.-A., Paris, M., Heitz, A., Velek, J., Liu, C-F., Winternitz, F., Martinez, J., Tetrahedron Lett., 36 (1995) 7871.
4. Murphy, A.M., Dagnino, R., Vallar, P.L., Trippe, A.J., Sherman, S.L., Lumpkin, R.H., Tamura, S.Z., Webb, T.R., J. Am. Chem. Soc., 114 (1992) 3156.
5. Kaljuste K., Tam J.P. Proceedings of the 15th American Peptide Symposium, Kluwer Academic Publishers, 1997.
6. Tam, J.P., Lu Y.-A., Liu, C-F., Shao, J., Proc. Natl. Acad. Sci. USA, 92 (1995) 12485.
7. Fukayama, T., Shao Cheng, L., Leping, L., J. Am. Chem. Soc., 112 (1990) 1050.
8. Hojo, H. and Aimoto, S., Bull. Chem. Soc. Jpn., 64 (1991) 111; Blake, J. and Li, C.H., Proc. Natl. Acad. Sci. USA, 78 (1993) 4055.

# Synthesis of cyclic ureas and cyclic thioureas from acyl dipeptides

Adel Nefzi, Marc A. Giulianotti, Edward Brehm, Christa C. Schoner,  
Vince T. Hamashin and Richard A. Houghten

Torrey Pines Institute for Molecular Studies, 3550 General Atomics Ct.,  
San Diego, CA 92121, USA

Peptides can be used for the synthesis of a wide range of heterocyclic compounds. The ready availability of a diverse range of protected amino acids and the strength of solid phase peptide synthesis facilitates such transformations. The use of the "libraries from libraries" concept [1] enables peptide combinatorial libraries to be transformed into heterocyclic combinatorial libraries [2]. The current status of heterocyclic combinatorial libraries has recently been reviewed [3]. We describe here the design and the solid phase synthesis of cyclic ureas and cyclic thioureas derived from dipeptides.

## Results and Discussion

Employing a selective N-alkylation of the amide-linked resin-bound N-tritylated amino acid [2], and reduction of the amide groups of acylated dipeptides **1** [4], the cyclization reactions to obtain the five member ring ureas **2a** and thioureas **2b** were performed using carbonyldiimidazole and thiocarbonyldiimidazole. The cyclization step has also been successfully carried out using triphosgene and thiophosgene (Fig. 1).

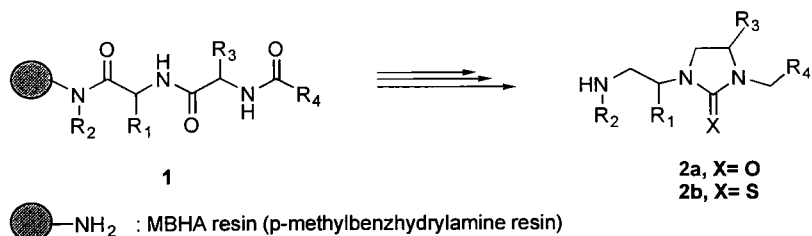


Fig. 1. Reaction scheme for the synthesis of cyclic ureas and cyclic thioureas from acyl dipeptides.

In Fig. 2 we show the HPLC-MS of the cyclic urea derived from the reduced dipeptide H<sub>2</sub>N-Val-Phe-NH-Bzl acylated with phenyl acetic acid (expected mass = 455). Using the

synthetic methods described above, we have prepared four separate combinatorial libraries ( $R_2 = \text{Me, Bzl}$ ;  $X = \text{O, S}$ ), each containing 118,400 cyclic ureas or cyclic thioureas [2].

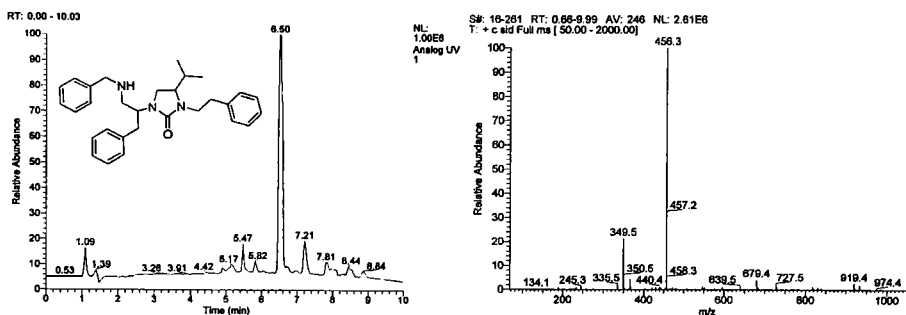


Fig. 2. HPLC-MS of the cyclic urea derived from the reduced dipeptide  $H_2N\text{-Val-Phe-N-Bzl}$  acylated with phenyl acetic acid.

## Conclusion

Amino acids and small peptides are versatile precursors for the solid phase synthesis of heterocyclic combinatorial libraries. We have prepared a range of different heterocyclic combinatorial libraries from peptides, including cyclic ureas and cyclic thioureas.

## Acknowledgments

This work was funded by National Science Foundation Grant No. CHE-9520142 and by Trega Biosciences, Inc. of San Diego, California.

## References

1. Ostresh, J.M., Husar, G.M., Blondelle, S.E., Dörner, B., Weber, P.A. and Houghten, R.A., Proc. Natl. Acad. Sci. U.S.A., 91 (1994) 11138.
2. Nefzi, A., Ostresh, J. M., Meyer, J.-P. and Houghten, R.A., Tetrahedron Lett., 38 (1997) 931.
3. Nefzi, A., Ostresh, J.M. and Houghten, R.A., Chemical Reviews., 97 (1997) 449.
4. Cuervo, J.H., Weitzl, F., Ostresh, J.M., Hamashin, V.T., Hannah, A.L. and Houghten, R.A., In Maia, H.L.S. (Ed.), Peptides 1994 (Proceedings of the 23rd European Peptide Symposium), ESCOM, Leiden, The Netherlands, 1995, p.465.

# Tri-*t*-butyl-DTPA: A versatile synthon for the preparation of DTPA-containing peptides by solid phase

Ananth Srinivasan and Michelle A. Schmidt

Mallinckrodt Inc., 675 McDonnell Blvd., Hazelwood, MO 63042, USA

Diethylenetriaminepentaacetic acid (DTPA), a chelator of In-111, is routinely conjugated to receptor-targeted peptides [1,2] for diagnostic nuclear medicine applications. For example, In-111-DTPA-Octreotide ("Octreoscan", Fig. 1) is currently used for the visualization of neuroendocrine tumors using  $\gamma$ -scintigraphy. In this case, conjugation of DTPA at the N-terminus of Octreotide maintains tumor targeting. DTPA also imparts favorable solubility properties and renal clearance properties. DTPA-peptides can be easily labeled with In-111 in high specific activity, and the In-DTPA-chelates are metabolically stable.

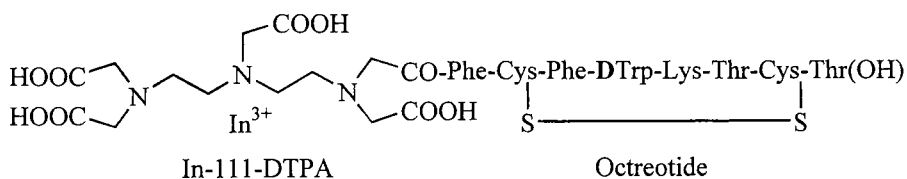


Fig. 1. Structure of In-111-DTPA-Octreotide.

## Results and Discussion

DTPA is often introduced at the N-terminal position of the peptides by the reaction of the bireactive reagent, DTPA-bis anhydride. This approach generally results in the formation of the bis-adduct as the major product in which two peptide units are attached to the DTPA moiety [3]. Hence, a monoreactive agent capable of producing a monoadduct devoid of any side products is necessary. While our work was in progress, Arano and co-workers published the synthesis of a monoreactive DTPA derivative, tetra-*t*-butyl-DTPA [4].

Tri-*t*-butyl-DTPA (Fig. 2) was prepared by a modification of the procedure of Williams and Rapoport [5] and can be used in an automated synthesizer. Upon activation, tri-*t*-butyl-DTPA presumably forms an anhydride which reacts with amines to form the corresponding amides. Upon cleavage and deprotection, the peptides were isolated devoid of any dimeric products. The utility of this versatile synthon is illustrated by the examples shown below (Table 1).

Compounds **1-3** were synthesized by placing tri-*t*-butyl-DTPA in the appropriate location in the automated synthesizer. Incorporation of *p*-Alloc-Aphe in the peptide chain, followed by removal of the Alloc-protecting group with Pd(0), and reaction with tri-*t*-butyl-DTPA anhydride afforded compound **4**. Diaminoethane-trityl resin was used to prepare the

protected des-DTPA peptide, the precursor to **5**. Reaction with tri-*t*-butyl-DTPA anhydride followed by deprotection gave **5**. Tri-*t*-butyl-DTPA anhydride was prepared by the reaction of tri-*t*-butyl-DTPA with DCC in DMF. DTPA-Octreotide was synthesized using Threoninol-Rink resin [6].

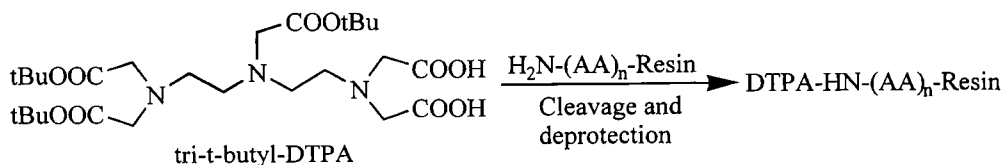


Fig. 2. General scheme for the synthesis of DTPA-containing peptides by SPPS.

Table 1. Examples of DTPA-containing peptides synthesized by Fmoc SPPS using the tri-*t*-butyl-DTPA synthon

PEPTIDE	m/z (M+H) <sup>+</sup>
DTPA-Arg-Pro-Lys-Pro-Gln-Gln-Phe-Phe-Gly-Leu-Met-NH <sub>2</sub> , <b>1</b>	1783.2
DTPA-Asp-Tyr-Met-Gly-Trp-Met-Asp-Phe-NH <sub>2</sub> , <b>2</b>	1438.8
DTPA-Asp-Tyr-Nle-Gly-Trp-Nle-Asp-Phe-NH <sub>2</sub> , <b>3</b>	1402.8
Asp-Tyr-Nle-Gly-Trp-Nle-Asp-Aphe( <i>p</i> -NH-DTPA)-NH <sub>2</sub> , <b>4</b>	1417.7
Asp-Tyr-Nle-Gly-Trp-Nle-Asp-Phe-NH-(CH <sub>2</sub> ) <sub>2</sub> -NH-DTPA, <b>5</b>	1481.4
DTPA-Octreotide (for structure see Fig. 1) [6]	1394.7

## Conclusion

Tri-*t*-butyl-DTPA can be efficiently used in an automated synthesizer for SPPS and in solution phase for the synthesis of DTPA-containing peptides devoid of dimeric products. Examples of N-terminal DTPA-peptides and peptides containing DTPA at other locations, through the use of orthogonal protecting groups, were prepared.

## References

- Bakker, W. H. *et al.*, *Life Sciences*, 49 (1991) 1583.
- Fischman, A. J., Babich, J. W. and Strauss, H. W., *J. Nucl. Med.*, 34 (1993) 2253.
- Bard, D. R., Knight, C. G. and Page-Thomas, D. P., *Brit. J. Cancer*, 62 (1990) 919.
- Arano, Y. *et al.*, *J. Med. Chem.*, 39 (1996) 3451.
- Williams, M. A. and Rapoport, H., *J. Org. Chem.*, 58 (1993) 1151.
- Schmidt, M. A., Wilhelm, R. R. and Srinivasan, A., "Solid Phase Synthesis of Peptide Alcohols Using Rink Acid Resin," 15<sup>th</sup> APS Meeting, Nashville, TN, 1996.

# Intramolecular migration of the $\beta$ -Dde protecting group of diaminopropionyl to the $\alpha$ -position during Fmoc solid phase synthesis

Ananth Srinivasan, R. Randy Wilhelm and Michelle A. Schmidt

*Mallinckrodt Inc., 675 McDonnell Blvd., Hazelwood, MO 63042. USA*

The utility of Dde (1-(4,4-dimethyl-2,6-dioxocyclo-hexylidene)-ethyl) protecting group has been illustrated by the orthogonal protection [1] of the  $\epsilon$ -amine of lysine in the synthesis of branched peptides and unsymmetrically functionalized polyamines [2]. However, Jung and co-workers observed migration of the  $\epsilon$ -Dde protecting group to other lysines during Fmoc removal with piperidine (Fig. 1) [3].

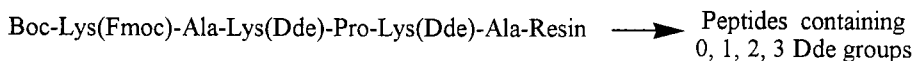


*Fig. 1. Migration of Dde protecting group in peptides containing multiple lysines.*

## Results and Discussion

We were interested in the use of  $\alpha,\beta$ -diaminopropionic acid as a possible candidate for the isosteric replacement of aspartic acid because it would provide a site for incorporation of a metal chelating moiety such as diethylenetriaminepentaacetic acid. In the following CCK<sup>26-33</sup> analog, we chose to incorporate Fmoc-Dpr( $\beta$ -Dde) in the place of Asp<sup>32</sup>. At the end of the solid phase synthesis, the resin was treated with 2% hydrazine/DMF followed by the incorporation of tri-*t*-butyl-DTPA anhydride [4]. After cleavage and deprotection, two isomeric peptides were obtained. The above results, combined with the observation of Jung and co-workers, suggested the possibility of formation of isomeric peptides due to Dde migration (Fig. 2).

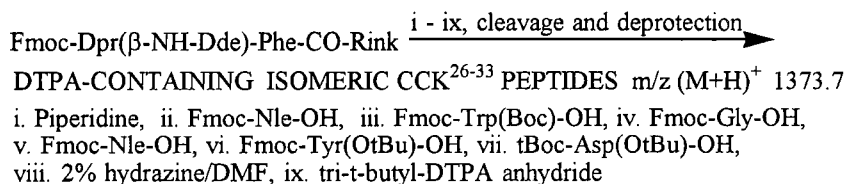


*Fig. 2. Formation of DTPA-containing isomeric CCK<sup>26-33</sup> analogs.*

We chose the model peptide, Asp-Trp-Dpr-Ser-Phe-NH<sub>2</sub>, to study in detail the migration of the Dde protecting group. Compound **1**, upon completion of the synthesis followed by deprotection (step iv), gave a mixture of Dde-containing peptides, **4** and **5**. Initial treatment with 2% N<sub>2</sub>H<sub>4</sub>/DMF followed by deprotection (step v) yielded a mixture of **2** and **3** (Fig. 3). Peptides **2-5** were identified by LC mass spectral analysis of the mixture. Peptides **2** and **3** were individually prepared by SPPS by employing Fmoc-Dpr(β-Boc)-OH and Boc-Dpr(β-Fmoc)-OH, respectively for comparison by HPLC.

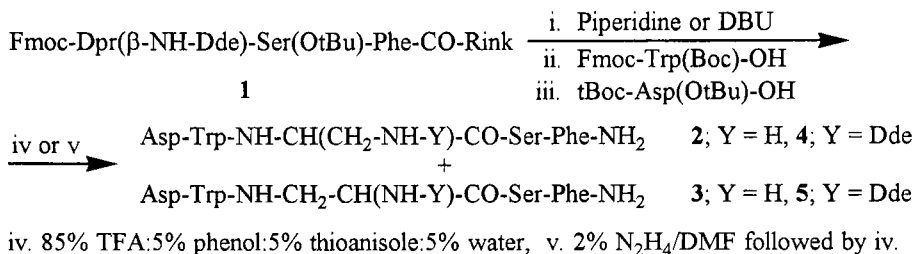


Fig. 3. Migration of Dde protecting group during Fmoc SPPS.

The migration is independent of the nature of the base (piperidine or DBU) employed for Fmoc removal from Dpr. As a mechanism, we propose a nucleophilic addition of the α-amino group of the Dpr (after the Fmoc-removal) to the α,β-unsaturated carbonyl to give the imidazoline intermediate. The retro-Michael addition ultimately results in the formation of isomeric Dpr-containing peptides. We verified this phenomenon with at least three other sequences incorporating Fmoc-Dpr(β-Dde)-OH.

## Conclusion

The above observations demonstrate the limitations of Dde as an orthogonal protecting group in Fmoc-based SPPS. In particular, the intramolecular migration of Dde in diaminopropionic acid is facile in the presence of base.

## References

1. Bycroft, B. W. *et al.*, Chem. Comm., (1993) 778.
2. Byk, G., Frederic, M. and Scherman, D., Tetrahedron Lett., 38 (1997) 3219.
3. Jung, G. *et al.*, "A Side Reaction of Dde Protecting Group: Migration to Unprotected Lysine", Abstract No. 399, 24<sup>th</sup> EPS Meeting, Edinburgh, Scotland, 1996.
4. Srinivasan, A. and Schmidt, M. A., "Tri-t-butyl DTPA: A Versatile Synthone for the Preparation of DTPA-containing Peptide by Solid Phase", 15<sup>th</sup> American Peptide Symposium, Nashville, TN, 1997.

# Intentional syntheses of disulfide-mispaired isomers of $\alpha$ -conotoxin SI and SIA

Balazs Hargittai and George Barany

Department of Chemistry, University of Minnesota, Minneapolis, Minnesota 55455, USA

A significant research goal of our laboratory is to devise orthogonal chemistries for the regioselective formation of multiple disulfide bonds in peptides [1-2]. The present investigations center on several solution, solid-phase, and mixed solid/solution phase routes for the syntheses of the snail-derived tridecapeptide amides,  $\alpha$ -conotoxin SI and  $\alpha$ -conotoxin SIA, and their disulfide-mispaired isomers. These molecules contain cysteine in the 2, 3, 7, and 13 positions, and only one of the three possible regioisomers is found in nature (Fig. 1).

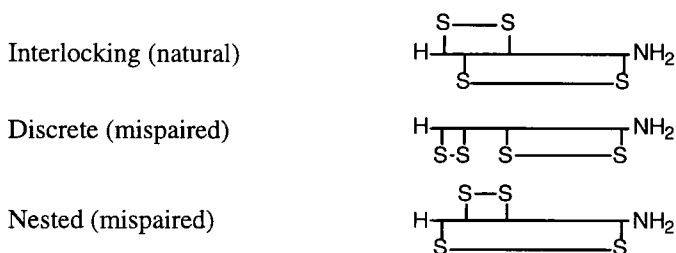


Fig. 1. Disulfide arrays in regioisomers of  $\alpha$ -conotoxins.

## Results and Discussion

The protection strategies chosen involved the base-labile Fmoc  $N^\alpha$ -amino protecting group, acidolyzable trityl and *tert*-butyl type side-chain protecting groups, and the acidolyzable tris(alkoxy)benzylamide (PAL) anchoring linkage. Side-chain protection of cysteine was provided by suitable pairwise combinations of the *S*-xanthenyl (Xan) and *S*-acetamidomethyl (Acm) protecting groups. For all syntheses in this work, the *C*-terminal Cys<sup>13</sup> and its intended partner were protected with *S*-Xan; selective acidolytic deprotections gave the corresponding bis(thiols) and subsequent oxidation allowed the “large loop” disulfide bridges to be formed first. In a second stage, the “small loop” disulfide bridges were formed by orthogonal oxidation of *S*-Acm groups on the remaining two Cys residues.

The linear precursors were converted to disulfide-bridged forms by three different strategies. The highest overall yields were obtained when both disulfides were formed in solution. Thus, acidolytic cleavage/deprotections of the peptide-resins were achieved by Reagent K (TFA-phenol-water-thioanisole-1,2-ethanedithiol = 82.5:5:5:5:2.5), which gave the corresponding peptide amides, with the *S*-Xan protecting groups removed but the *S*-

Acm groups still intact. Oxidation with DMSO (1% v/v) in pH 7.5 phosphate buffer gave the first disulfide, and oxidation with I<sub>2</sub>, Tl(Tfa)<sub>3</sub>, or DMSO/Me<sub>3</sub>SiCl mixtures converted the S-Acm pairs and gave the second disulfide. Alternatively, the S-Xan protecting groups were removed selectively by treatment of the peptide-resins with Reagent X (TFA-CH<sub>2</sub>Cl<sub>2</sub>-triethylsilane = 2:97:1), while retaining the peptide on the support for on-resin oxidation mediated by Et<sub>3</sub>N in NMP, or by aqueous K<sub>3</sub>Fe(CN)<sub>6</sub>. At this point, the pairwise S-Acm oxidation could be carried out in either of two ways: (i) another on-resin oxidation, using I<sub>2</sub> or Tl(tfa)<sub>3</sub>, followed by final cleavage with Reagent B (TFA-phenol-water-triethylsilane = 88:5:5:2), or (ii) cleavage of the peptide from the support with Reagent B, followed by solution oxidation of S-Acm as already described. Control experiments with pure two-disulfide regioisomers showed that neither the acid nor the oxidative reagents used in these studies affected or scrambled the disulfide bonds once they were formed.

Syntheses of the “nested” regioisomers proved to be much more difficult than syntheses of the “discrete” regioisomers. When both disulfides were created in solution, the isomers predicted from the protection schemes were in all cases the predominant product (usually 75-97%), and the overall yields were also relatively the highest (43-54% for “discrete”; 17-24% for “nested”). However, when both disulfides were formed by on-resin oxidation procedures, overall yields were low (3-9%) and the “natural” isomer was a dominant product obtained *irrespective* of the protection scheme. The strategies involving on-resin formation of the first disulfide, followed by release from the support and formation of the second disulfide in solution, gave intermediate yields with the intended regioisomer usually predominant [exception was formation of “discrete” isomer in some experiments directed at “nested”]. In terms of reagents, iodine oxidation at the second step was preferred for maximal purities and yields, whereas DMSO/Me<sub>3</sub>SiCl or Tl(tfa)<sub>3</sub> led to more by-products with scrambling of bridges.

Most of these studies were carried out on 4 μmol scales. The best procedures were repeated on 30 μmol scales, following which preparative HPLC purifications provided isolated yields of 17% for “nested” conotoxin SI, 6% for “nested” conotoxin SIA, 21% for “discrete” conotoxin SI, and 43% for “discrete” conotoxin SIA regioisomers.

## Conclusion

A number of disulfide bridge-forming chemistries have been tested with the goal of creating peptides with disulfide arrays that are not found in nature. For the conotoxin model, “discrete” isomers have proven to be more readily synthesized than “nested” isomers.

## References

1. Munson, M.C. and Barany, G., J. Am. Chem. Soc., 115 (1993) 10203.
2. Annis, I., Hargittai, B. and Barany, G., In Fields, G.B. (Ed.) Methods in Enzymology, Academic, Orlando, 1997, vol. 289, in press.

# S-Xanthenyl side-chain anchoring for solid-phase synthesis of cysteine-containing peptides

Balazs Hargittai,<sup>a</sup> Yongxin Han,<sup>a</sup> Steven A. Kates<sup>b</sup>  
and George Baranya<sup>a</sup>

<sup>a</sup>Department of Chemistry, University of Minnesota, Minneapolis, MN 55455, USA

<sup>b</sup>PerSeptive Biosystems, Framingham, MA 10701, USA

Many naturally occurring peptides contain a cysteine residue at the C-terminal, and this terminus is also of interest as an attachment point for generation of antibodies. Anchoring of *S*-protected C-terminal cysteine as an ester in Fmoc solid-phase synthesis has attendant risks of racemization [1]. As chain elongation proceeds, a serious side reaction can occur that involves  $\beta$ -elimination of protected sulfur and addition of piperidine across the ensuing dehydroalanine intermediate to produce 3-(1-piperidinyl)alanine by-products [2]. We recently reported initial studies on a novel side-chain anchoring strategy in which an *S*-xanthenyl handle derivative of cysteine, with Fmoc for  $N^{\alpha}$ -protection and *tert*-butyl for  $C^{\alpha}$ -protection (structure **1a** in Fig. 1), was used to attach the C-terminal cysteine [3]. This approach uses key intermediates that are common to our previously reported XAL handles [4], and builds on our experience with *S*-xanthenyl-type protection for cysteine [5]. Importantly, it was shown by modified assays with Marfey's reagent that racemization of the C-terminal cysteine did not occur in Fmoc synthesis with this strategy [3]. The present article illustrates further the scope of side-chain anchoring, and reports the new allyl derivative **1b** which we hope to apply later for orthogonal syntheses of bicyclic peptides.

## Results and Discussion

Preparation of preformed handle derivative **1a** was outlined previously [3]; preparation of **1b** was achieved in overall 69% yield following the same steps except that introduction of the allyl ester onto bis(Fmoc)-cysteine was accomplished by a method using  $\text{Me}_3\text{SiCl}$  as catalyst with a mixture of allyl alcohol and dry  $\text{CH}_2\text{Cl}_2$  [6].

Handle **1a** coupled smoothly onto amino-containing PEG-PS supports, and was the starting point for further peptide chain elongation by stepwise Fmoc chemistry (Fig. 2).

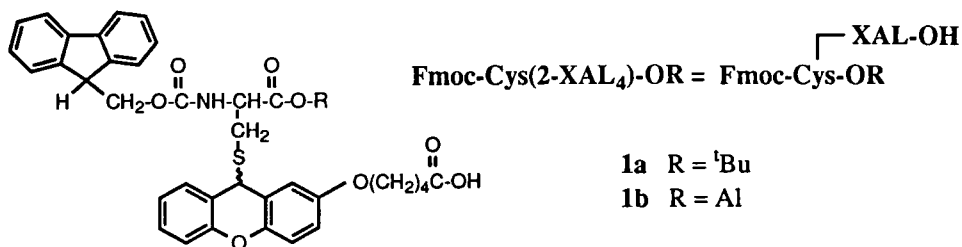


Fig. 1. Preformed handle derivatives for side-chain anchoring of cysteine.

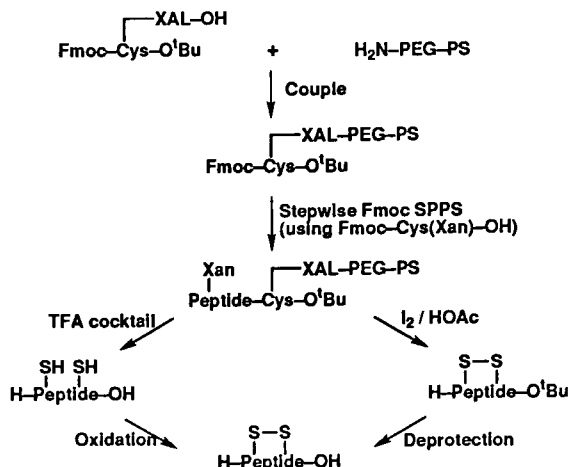


Fig. 2. Side-chain anchoring strategy for solid-phase synthesis of disulfide-bridged peptides.

The  $\beta$ -elimination side reaction mentioned earlier [2] is circumvented by side-chain anchoring, since any occurrence would be accompanied by loss of chains from the support and the resultant solubilized undesired by-products would not contaminate the desired peptide which is retained until the end of the synthesis.

Detachment of completed peptides anchored through the cysteine side-chain can be carried out under mild conditions either by acidolysis or by application of oxidative reagents (Fig. 2). Acid/scavenger cocktails with dilute TFA cleave the XAL anchor in high yield and expose the free cysteine thiol while *tert*-butyl type protecting groups on other side-chains remain stable; alternatively, the common cocktails with higher TFA concentration promote full cleavage/deprotection. The presence of silane scavengers ensures quantitative formation of reduced cysteine(s). At any stage, standard oxidation protocols can be applied in solution (Fig. 2, left side). Further options involve *concurrent* cleavage/oxidation, without affecting other side-chain protecting groups, by use of iodine in acetic acid (Fig. 2, right side). This route permits *direct* disulfide formation. A final deprotection step follows in solution.

## References

1. Andreu, D., Albericio, F., Solé, N.A., Ferrer, M. and Barany, G. In Pennington, M.W. and Dunn, B.M. (Eds.) *Methods in Molecular Biology*, Vol. 35: Peptide Synthesis Protocols, Humana Press, Totowa, N.J., 1994, p. 91.
2. Lukszo, J., Patterson, D., Albericio, F. and Kates, S.A., *Lett. Pept. Science*, 3 (1996) 157.
3. Han, Y., Vágner, J. and Barany, G. In Epton, R. (Ed.) *Innovation and Perspectives in Solid Phase Synthesis & Combinatorial Chemical Libraries: Biomedical & Biological Applications*, 1996, Mayflower Scientific Ltd., Kingswinford, England, 1996, p. 385.
4. Han, Y., Bontems, S.L., Hegyes, P., Munson, M., Minor, C.A., Kates, S.A., Albericio, F. and Barany, G., *J. Org. Chem.*, 61 (1996) 6326.
5. Han, Y. and Barany, G., *J. Org. Chem.*, 62 (1997) 3841.
6. Belshaw, P.J., Mzengeza, S. and Lajoie, G.A. *Synth. Commun.*, 20 (1990) 3157.

# Isolation, characterization, and synthesis of a trisulfide related to the somatostatin analog lanreotide.

Lin Chen,<sup>a</sup> Steven R. Skinner,<sup>b</sup> Thomas D. Gordon,<sup>b</sup> John E. Taylor,<sup>b</sup>  
George Barany<sup>a</sup> and Barry A. Morgan<sup>b</sup>

<sup>a</sup>University of Minnesota, Dept. of Chemistry, Minneapolis, MN 55455, USA, and <sup>b</sup>Biomeasure Inc., Milford, MA 01757, USA

Lanreotide [1] is a cyclic octapeptide with somatostatin agonist activity, and is currently approved for the treatment of acromegaly. Several minor impurities generated during the synthesis were characterized as an adjunct to process validation studies. One such impurity, present at <0.1% in the synthetic sample, was isolated to 70% purity and characterized by mass spectroscopy, NMR, and elemental analysis. This analysis led to the conclusion that the impurity was the corresponding trisulfide, in which the disulfide bond between the two cysteine residues in Lanreotide had in some way been converted to a trisulfide. To confirm this conclusion, it was desirable to prepare the trisulfide material by unambiguous synthesis.

## Results and Discussion

New approaches developed recently in one of our laboratories [2] for the preparation of novel peptide trisulfides were applied and extended, with the goal of confirming the identity of the putative lanreotide trisulfide. Thus, a directed reaction of a nucleophilic  $\beta$ -thiol from an internal cysteine residue onto an *S*-[(*N*-methyl-*N*-phenylcarbonyl)disulfanyl] (Ssnm) protected cysteine residue was envisaged to form the key trisulfide linkage. The protected dipeptidyl building block *N* <sup>$\alpha$</sup> -*tert*-butyloxycarbonyl-D-3-(2'-naphthyl)alanine-Cys(Ssnm)-OH was prepared in 59% yield starting with Boc-D-3-(2'-naphthyl)alanine (Boc-D-Nal-OH), which was converted to its *N*-hydroxysuccinimido ester, coupled with *S*-acetamidomethyl-L-cysteine hydrochloride (HCl•Cys(Acm)-OH), and transformed further with (chlorocarbonyl)disulfanyl chloride and *N*-methylaniline. Next, starting with Fmoc-PAL-PEG-PS, the sequence Boc-D-Nal-Cys(Ssnm)-Tyr(*t*Bu)-D-Trp-Lys(Boc)-Val-Cys(Tmob)-Thr(*t*Bu)-PAL-PEG-PS was assembled manually by stepwise solid-phase synthesis, with the *N*-terminal protected dipeptide added in a single step. Fmoc removal was carried out with piperidine-DMF (1:4) and the couplings were mediated by DIPCDI/HOBt. Tmob alkylation was suppressed to the greatest extent (<10%) with the thioanisole-containing cocktail TFA-thioanisole-phenol-*i*Pr<sub>3</sub>SiH-H<sub>2</sub>O (84:4:4:4:4), which was also preferred because the ratio of desired trisulfide:disulfide was ~ 2-3:1. It should be emphasized that no special steps were required to induce trisulfide formation; the cyclization occurred during the standard procedure of cleavage and workup.

Isolation of the pure trisulfide peptide required two consecutive preparative HPLC runs. During the first run, trisulfide and contaminant disulfide merged in a single peak,

whereas in the second run, baseline separation of the disulfide and trisulfide was accomplished. The pure Lanreotide trisulfide was isolated with ~17% overall yield, based on the initial loading of Fmoc-PAL-PEG-PS resin.

Characterization by electrospray MS indicated that the synthetic preparation displayed the expected mass of  $m/z$  1128, or 32 higher than Lanreotide. In addition, the synthetic preparation was run on analytical HPLC along with the material from the side-cut isolate. The pure synthetic trisulfide (>98%) co-injected with the material isolated from manufactured Lanreotide. It was therefore concluded that the isolated material was identical with the material obtained by targeted synthesis, and that the original characterization of the isolated material as a trisulfide was correct.

The availability of pure trisulfide from directed synthesis allowed measurement of biological potency in terms of affinity at the various human somatostatin receptor subtypes hSSTR1-5. Clonal cell lines expressing these receptors were obtained by transfection into CHO-K1 cells [3]. Receptor binding assays were run using [ $^{125}$ I-Tyr $^{11}$ ]SRIF-14 as radioligand, except for the hSSTR-2 assay when [ $^{125}$ I]MK-678 was employed. The data ( $K_i$ , nM) are shown in the following table:

	hSSTR1	hSSTR2	hSSTR3	hSSTR4	hSSTR5
Lanreotide	1214± 81	0.75±0.10	97.8±14.5	1826± 264	12.7± 7.5
Trisulfide	4641 (n=1)	0.84± 0.22	498 (n=1)	>5000	114± 10

The trisulfide is similar in profile to Lanreotide in terms of potency, the only significant difference being at hSSTR5. Thus the trisulfide is significantly more selective for the hSSTR2 compared to hSSTR5, with a  $K_i$  ratio hSSTR5/hSSTR2 of approximately 140-fold. The corresponding ratio for Lanreotide is 17. Other structural modifications which lead to increased hSSTR5/2 selectivity have recently been described [4].

In conclusion, the side-product isolated from lanreotide crude product has been confirmed to be the corresponding trisulfide by unambiguous synthesis. The authentic trisulfide has an affinity profile similar to Lanreotide at human somatostatin receptor-subtypes, but is more selective towards the hSSTR2 sub-type due to a decreased  $K_i$  at the hSSTR5.

## References

1. Johnson, M.R., Chowdrey, H.S., Thomas, F., Grint, C. and Lightman, S.L., *Eur. J. Endocrinology*, 130 (1995) 229.
2. Chen, L., Zouliková, I., Slaninová, J. and Barany, G., *J. Med. Chem.* 40 (1997) 864. see also: Mott, A.W. and Barany, G. *Synthesis*, (1984) 657; Mott, A.W., Słomczynska, U. and Barany, G. in *Forum Peptides Le Cap d'Agde 1984* (Castro, B., Martinez, J. Eds.), Les Impressions Dohr: Nancy, France, 1986, p. 321.
3. Ausabel, F.M., Brent, R., Kingston, R.E., Moore, D.D., Seidman, J.D., Smith, J.A. and Struhl, K., *Current Protocols In Molecular Biology*, John Wiley & Sons, 1987.
4. Moreau, J.-P., Kim, S., Dong, J.Z., Ignatiou, F., Jackson, S., Moreau, S.C., Morgan, B.A., Touraud, F., Taylor, J.E., Tissier, B., Pellet, M., Murphy, W. and Davis, T., *Metabolism*, 45S1 (1996) 24.

# Novel safety-catch protecting groups and handles cleavable by intramolecular cyclization

Chongxi Yu and George Barany

Department of Chemistry, University of Minnesota, Minneapolis, MN 55455, USA

The design, synthesis, and evaluation of libraries of small molecules are currently a major frontier in organic chemistry. One important aspect of achieving facile synthesis of these libraries is the development of protecting groups and handles that are stable to specific reaction conditions, yet orthogonally cleavable under other, preferably mild, conditions. To this end, we have prepared a variety of *S*-protected/linked  $\omega$ -mercaptoalkyl esters. Cleavage of the protecting group off sulfur is followed by intramolecular cyclization that furnishes a free carboxyl group. The original inspiration for this work comes from Ho and Wong [1], who reported cleavage of  $\omega$ -chloroalkyl by displacement with sulfides. Additionally, disulfide-containing linkers have been described for peptide and DNA synthesis; reduction of the disulfide triggers a similar cleavage mechanism.

## Results and Discussion

To demonstrate the principle, we carried out protection and deprotection of Boc-Phe-OH as outlined in Fig. 1. The appropriate esters were formed by DCC/DMAP-mediated coupling. Removal of *S*-triphenylmethyl (Trt) or *S*-9*H*-xanthen-9-yl (Xan) protection was carried out *selectively* (i.e., in the presence of the Boc group) with dilute trifluoroacetic acid (TFA) in the presence of silane scavengers for 2 h. The media was then made slightly basic (pH ~ 9 for aliquot spotted on wet litmus paper) by addition of the tertiary amine DIEA, and ester cleavage via intramolecular cyclization was complete in 5 h. The best yields required the presence of the reducing agent dithiothreitol (DTT); in its absence some of the  $\omega$ -mercaptoalkyl intermediates formed stable disulfide dimers.

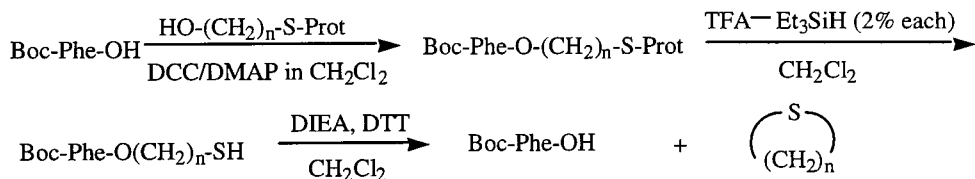


Fig. 1. Protection and safety-catch deprotection of Boc-Phe-OH. Chemistry demonstrated for Prot = Trt and Xan, and for  $n = 2$  or 4.

The chemistry of Fig. 1 was readily melded with that of our recently reported xanthenyl (XAL) handles for anchoring amides and thiols [2]. The handle intermediate 5-[(9-hydroxyxanthen-2-yl)oxyvaleric acid] [2] was treated with  $\beta$ -mercaptoethanol under acidic conditions, and the resulting product was coupled onto amino functionalized PEG-

PS. After chain assembly by standard methods gave the protected peptide-resin shown in Fig. 2, cleavage at the site shown by the horizontal dotted line was accomplished with TFA-Et<sub>3</sub>SiH-CH<sub>2</sub>Cl<sub>2</sub> (1:1:48) (80% yield in 1 h, 90% in 2 h at 25°C). The cleavage mixture was then made basic with DIEA to effect cyclization. In this way, the model peptide Fmoc-Lys(Boc)-Gly-Glu(OtBu)-Ala-OH was obtained in >85% purity.

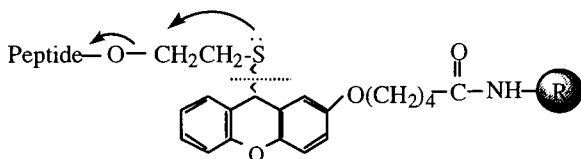


Fig. 2. A novel acidolyzable handle for preparation of protected peptide acids.

Further directions to apply the principles of this work for the preparation of orthogonally cleavable handles are illustrated in Fig. 3. The three-membered ring of commercially available 1-aziridineethanol is opened with thiol derivatives corresponding to known *S*-protecting groups, e.g., with triphenylmethanethiol (Trt-SH) or *p*-methoxybenzylmercaptan (Mob-SH). Straightforward transformations and chain assemblies set the stage for cleavage at the vertical dotted line; for Prot = Trt by using TFA-Et<sub>3</sub>SiH-CH<sub>2</sub>Cl<sub>2</sub> (5:2:93) for 3 x 1 h, and for Prot = Mob with mercury (II) trifluoroacetate (2 equiv) in 80% aqueous HOAc for 10 h, followed by on-resin treatment with β-mercaptoethanol to remove mercury. In both cases, cyclizations to form the six-membered ring and simultaneously effect release of the protected peptide from the support were carried out in a milieu of DMF or acetonitrile. For optimal cleavages, it was necessary to apply elevated temperatures and add sodium borohydride (20 equiv) as a reducing agent [yields: 40% in 12 h at 25 °C, 80% in 2 h at 50 °C, 85% in 1 h at 70 °C]. Without borohydride or use of DTT, the process was not effective. The final purity of model peptide Fmoc-Lys(Boc)-Gly-Glu(OtBu)-Ala-OH was >95%.

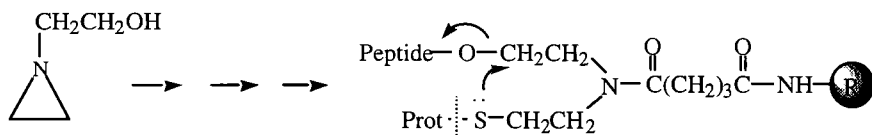


Fig. 3. Novel orthogonally cleavable safety-catch handles for preparation of protected peptide acids. Chemistry demonstrated for Prot = Trt and Mob.

## References

1. Ho, T.-L and Wong, C.M., *Synth. Commun.*, 4 (1974) 307.
2. Han, Y., Bontems, S.L., Hegyes, P., Munson, M., Minor, C.A., Kates, S.A., Albericio, F. and Barany, G., *J. Org. Chem.*, 61 (1996) 6326.

# Synthesis of conformationally constrained peptides using the Heck reaction

David E. Wright

*R.W. Johnson Pharmaceutical Research Institute, San Diego, CA 92121, USA*

Conformational constraint designed into the synthesis of peptides has led to mimetics with increased potency and receptor selectivity. One avenue of conformational constraint is the synthesis of cyclic peptides. Cyclization is usually brought about through amide bond formation using lysine and glutamic acid or aspartic acid side chains as well as disulfide bond formation using cysteine or cysteine derivatives. A number of enkephalin derivatives have been synthesized using these cyclization approaches. The Heck reaction, which is a carbon-carbon bond formation reaction, recently has been shown to be applicable to synthesis on solid supports [1-4]. In the present study the Heck reaction was used to develop cyclic peptides. In this approach cyclization was carried out using a *p*-iodophenylalanine residue and an alkene group. Since numerous cyclic derivatives of opiate peptides have been synthesized using amide bond cyclization and disulfide bond formation, the Heck reaction was used to synthesize new cyclic opiate peptides.

## Results and Discussion

When applied to the synthesis of new cyclic peptide derivatives, the Heck reaction is useful for the formation of carbon-carbon bonds. The Heck reaction provides a more stable bond than the usual cyclization methods of disulfide and amide bond formation. Peptide cyclization can be carried out both in solution and on the solid support.

The optimal conditions for carrying out the cyclization on the solid support are as follows: Peptide-resin (0.015 mmoles), tris(2-tolyl) phosphine (0.01 mmole), tetrabutylammonium trifluoromethanesulfonate (0.015 mmoles) were placed in 0.85 ml dimethylformamide/0.1 ml water/0.05 ml triethylamine. The mixture was bubbled with argon after which Palladium(II) acetate (0.05 mmoles) was added. The reaction was stirred overnight at 60°. The mixture was filtered, and the resin was washed with dimethylformamide, ethanol, methylene chloride, ethanol, and water. The peptide was cleaved from the resin using trifluoroacetic acid/water (9:1). The resulting cleaved peptide was analyzed by mass spectroscopy and HPLC. The cyclization was done on three different resins: Rink-amide resin (0.50 mmoles/g), high load PEG-resin (0.38 mmoles/g) and PEG-resin (0.16 mmoles/g). With all three resins no starting material was seen after the reaction had taken place. Both the Rink-amide and high load PEG-resins gave about 25% desired product. The Rink-amide resin appeared to produce more polymer peaks than the high load PGR-resin, whose major side product was the cyclic dimer. The standard PEG-resin gave the best result with 60% of the desired product being obtained with and the

blance being mainly dimer. Thus even though the reaction can take place using all three resins, a lower substitution is preferred to minimize polymerization and dimer formation.

Similar reaction conditions are used to for the solution cyclization and are as follows: peptide (0.01 mmoles), tris(2-tolyl) phosphine (0.01 mmole), tetrabutylammonium trifluoromethanesulfonate (0.01 mmoles) were placed in 4.4 ml dimethylformamide/0.5 ml water/0.1 ml triethylamine. The mixture was bubbled with argon after which Palladium(II) acetate (0.05 mmoles) was added. The reaction was stirred overnight at 60°. The mixture was concentrated to dryness by lyophilization. The resulting cleaved peptide was analyzed by mass spectroscopy and HPLC. The above reaction conditions give about 60% desired product with the major side product again being the cyclic dimer. If the reaction is run using less solvent more dimer and polymer are obtained.

Cyclization of three opiate peptides was performed according to the reaction conditions listed above. They were allylacetyl-Tyr-Tic-Phe-Phe(I)-amide, Tyr-DL-vinylglycine-Gly-Phe(I)-Leu-amide, and Tyr-D-allylglycine-Gly-Phe(I)-Leu-amide. For the first two peptides the reaction went well with no starting material remaining whether the reaction was run in solution or on the solid support. However, when allylglycine was substituted for vinylglycine, no reaction took place. It would appear that vinylglycine is not activated enough for the reaction to occur even when using reaction conditions for nonactivated alkenes [5]. The reaction also can be analyzed by UV spectroscopy since the starting material, desired cyclic product and side reaction cyclic dimer have different characteristic spectra.

## Conclusion

The Heck reaction can be used for making new cyclic peptides and mimetics both on the solid support and in solution. Using the Heck reaction with regard to peptides opens up new opportunities for peptide design since the reaction forms a carbon-carbon bond rather than reaction the usual amide or disulfide bond. Conditions have been determined to favor the formation of the desired product. Side reactions such as dimerization and polymerization were found to be common but could be minimized by using the proper resin for solid support cyclization or correct reaction volume for solution cyclization. This peptide cyclization procedure can be done with alkynes as well as alkenes and could be used in a combinatorial setting as well.

## References

1. Yu, K.-L., Deshpande, M.S. and Vyas, D.M., *Tetrahedron Lett.*, 35 (1994) 8919.
2. Hiroshige, M., Hauske, J.R. and Zhou, P., *Tetrahedron Lett.*, 36 (1995) 4567.
3. Yun, W. and Mohan R., *Tetrahedron Lett.*, 37 (1996) 7189.
4. Pop, I.E., Dhalluin, C.F., Deprez, B.P., Melnyk, P.C., Lippens, G.M. and Tartar, A.L., *Tetrahedron*, 52 (1996) 12209.
5. Crisp, G.T. and Gebauer, M.G., *Tetrahedron*, 52 (1996) 124651.

# A facile synthesis of 3-substituted pipercolic acids

**Gergely M. Makara and Garland R. Marshall**

*Department of Molecular Biology and Pharmacology, School of Medicine, Washington University  
at St. Louis, St. Louis, MO 63110, USA*

Pipercolic acid, the next higher homolog of proline, has generated considerable attention as a proline analog. Not only can the compound serve as an analog of proline, but it has utility in the area of constrained amino acids. Substitution of the six-membered ring by any sidechain moiety found in natural amino acids yields a constrained, chimeric amino acid. By holding the sidechain and the backbone in a limited number of conformations, active analogs of biologically active peptides containing this unusual amino acid can provide valuable insights into the conformational requirements of ligand binding [1]. Computational studies indicate that pipercolic acid shows a similar, if not higher, propensity to occupy the *i*+2 position in reverse turns compared to proline (Y. Takeuchi, G.R. Marshall unpublished). Thus, incorporation at appropriate positions of carefully designed pipercolic acid analogs as peptide building blocks can trigger the formation of turns while retaining the sidechain functionality for important molecular recognition.

Several routes have recently been published for the synthesis of pipercolic acid and its derivatives [2]. However, no methods for the synthesis of 3-analogs having polar functionality and appropriate protection for solid phase peptide synthesis have been reported.

## Results and Discussion

The synthesis of the protected 3-hydroxy and 3-mercapto analogs was envisioned as depicted in Fig. 1 starting from the commercially available 3-hydroxypyridinecarboxylic acid. The free hydroxyl group of **4** was to be masked as a benzylether to give a key intermediate of the desired BocPip(OBz). However, this functionality proved to be extremely labile and gave the 2,3-dehydroanalogs as side products. All attempts to circumvent this undesired elimination were fruitless and, thus, an alternate route had to be sought to achieve a suitably protected 3-OH analogue. This involved the use of the Fmoc strategy. An approximately 50-50% mixture of *cis* and *trans* **5** was isolated indicating an elimination-addition mechanism instead of  $S_{N2}$ -substitution, which is consistent with the ease of elimination of 3-OR moieties observed throughout these syntheses. The two pairs of diastereomers of **5** were conveniently separated by flash chromatography.

Major goals in the synthesis of the 3-carboxyl analog were to distinguish between the 2- and 3- positions and to achieve stereoselectivity to reduce the number of isomer products (Fig. 2.). We took advantage of the selective ring opening of quinolinic anhydride during alcoholysis to give monoester **10**, which can be reduced to the corresponding *cis* piperidine derivative **11**. An appropriately selected sequence of reactions provided the

suitably protected **15** in 56% overall yield from **10**. One can easily envision the easy access of other carboxylic acid derivatives starting from **12**. The mesylate of **4** could also likely serve as an excellent intermediate for the synthesis of other 3-position analogs.

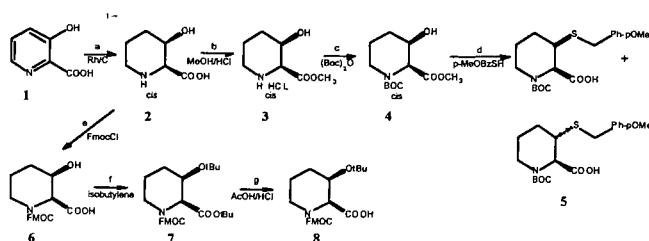


Fig. 1

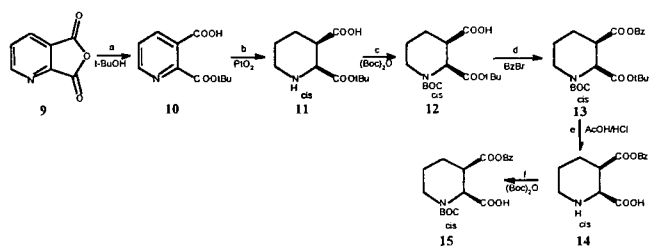


Fig. 2.

The stereochemistry of compounds **5**, **8** and **15** was established by  $^1\text{H}$  NMR. Proton NMR and molecular modeling showed that the Boc protected piperidic acids can exist only in a conformation in which the 2-COOH is axial due to steric interference with the bulky vicinal groups. This effect can account for the ease of coupling observed in SPPS (TBTU, HOBt/DIEA). Incorporation of **15** into Asp-Tyr(OSO<sub>3</sub>H)-Nle-Gly-Trp-Nle-Asp-Phe-NH<sub>2</sub> (CCKA inhibitor) peptide sequence revealed an important side reaction resulting in further constrained piperidine-2,3-dicarboximide peptides.

## References

1. a, Kaczmarek, K., Li, K.-M., Skeeane, R., Dooley, D., Humblet, C., Lunney, E., Marshall, G.R., In Hodges, R. and Smith, J.A., (Eds) Peptides: Proceedings of the 13th American Peptide Symposium, ESCOM Leiden, 1994, p. 687. b, Olma, A., Nikiforovich, G.V., Nock, B. and Marshall, G.R., In Hodges, R. and Smith, J.A., (Eds) Peptides: Chemistry, Structure and Biology, ESCOM Leiden, 1994, p. 684.
2. For example, see a, Fernandez-Garcia, C. and McKerverve, M.A., Tetrahedron: Asymmetry, 6 (1995) 2905. b, Angle, S.R. and Arnaiz, D.O., Tetrahedron Lett., 30 (1989) 515. c, Adams, D.R., Bailey, P.D., Collier, I.D., Heffernan, J.D. and Stokes, S. J., Chem. Soc. Chem. Commun., (1996) 349. c, Shuman, R.T., Ornstein, P.L., Paschal, J.W. and Gesellchen, P.D., J. Org. Chem., 55 (1990) 738. d, Bailey, P.D., Londebrought, D.J., Hancox, T.C., Heffernan, J.D. and Holmes, A.B., J. Chem. Soc. Chem. Commun., (1994) 2543.

# Rapid thioester couplings mediated by new uronium salts

Hartmut Echner and Wolfgang Voelter

Abteilung für Physikalische Biochemie des Physiologisch-chemischen Instituts der Universität  
Tübingen, Hoppe-Seyler-Str. 4, D-72076 Tübingen, Germany

Two of the most popular reagents in SPSS are tetramethyluronium salts like 2-(1H benzotriazolyl-1-yl)-1,1,3,3-tetramethyluronium hexafluorophosphate (HBTU) [1] and phosphonium salts like benzotriazolyl-1-yl-oxy-tris(dimethylamino)phosphonium hexafluorophosphate (BOP) [2]. These compounds are able to form *in situ* O-benzotriazolyl active esters as acylating species.

However, until now, no reports describe the use of thioesters for the coupling steps in SPSS. Only few reports exist on thioester couplings in classical peptide synthesis. For example, Farrington [3] and Kenner [4] described 4-nitrophenylthioester to be 16-fold faster in coupling with amines than standard 4-nitro-phenylesters. Also, S-(2-benzothiazolyl)-thioesters were described as reacting very rapidly with amines [5]. We therefore combined the well-known fast coupling uronium salts and different arylmercaptanes to achieve several new *in situ* acylating reagents based on preformed thioesters as highly active intermediates. The general formula is:

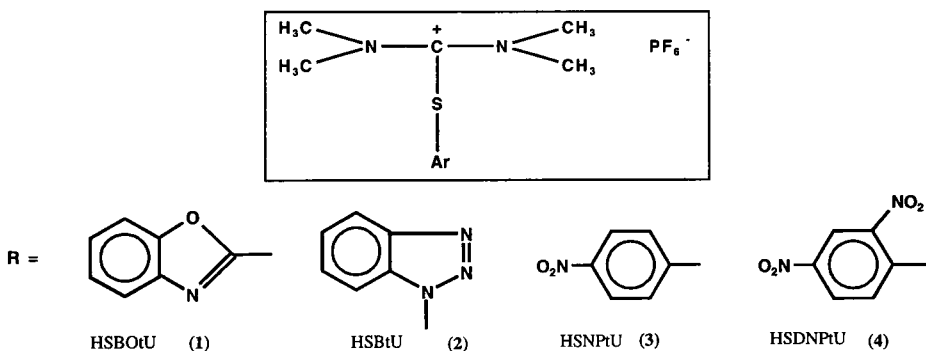


Fig. 1. S-aryl-uronium salts: 2-(2-mercaptobenzoxazol-2-yl)-1,1,3,3-tetramethyluronium-hexafluorophosphate (1), 2-(1-mercaptobenzotriazol-1-yl)-1,1,3,3-tetramethyluronium-hexafluorophosphate (2), 2-(1-mercapto-4-nitrophenyl-1-yl)-1,1,3,3-tetramethyluronium-hexafluorophosphate (3), 2-(1-mercapto-2,4-dinitrophenyl-1-yl)-1,1,3,3-tetramethyluronium-hexafluorophosphate (4).

## Results and Discussion

1,1,3,3-tetramethyl-2-chlorouroniumchloride was synthesized similar to the procedure of Knorr [6]. 2-Mercaptobenzoxazole was commercially available, 1-mercapto-benzotriazole

was synthesized from 1-hydroxybenzotriazole by conversion with 3N HBr/HAc into 1-bromobenzotriazole and afterwards with 1 eq. NaHS into the product. 4-Nitro-1-mercapto-benzene and 2,4-dinitro-1-mercapto-benzene were prepared according to the procedure of Takahashi [7] from p-nitro-chlorobenzene and 2,4-dinitro-chlorobenzene, respectively, by addition of a solution of 2 eq. NaSH in 90 % ethanol. Addition of 1 mol potassium hydroxide to a hot saturated ethanolic solution of the aryl mercaptanes lead to the potassium salts of the S-aryl compounds. Syntheses of the S-aryl-1,1,3,3-tetra-methyluronium compounds were accomplished by reaction of the potassium mercaptides with 1 eq. of tetra-methyl-2-chlorouroniumchlorid and potassium hexafluorophosphate under slight cooling. The products were recrystallized from dichloromethane/ether, yielding 20,33 g (1) ( $C_{12}H_{16}N_3OSPF_6 = 379,3$ ), 33,7 g (2) ( $C_{11}H_{16}N_5SPF_6 = 395,3$ ), 25 g (3) ( $C_{11}H_{16}N_5SPF_6 = 395,3$ ) and 23 g (4) ( $C_{11}H_{15}N_4O_4SPF_6 = 540,4$ ).

To test the usefulness of our new compounds for SPPS we synthesized the following opioid peptides using Fmoc/tBu strategy, with an automatic ECOSYN P synthesizer (Eppendorf Biotronik, Maintal, Germany):

- 1) orphanin FQ: (FGGFTGARKSARKLANQ), on [5-[4-(Fmoc-amino)-methyl]-3,5-dimethoxy-phenoxy] valeric acid coupled to aminomethyl-PEG-resin (Rapp-Polymere, Tübingen, Germany). Activating agent: HSBtU / acylation time: 10 min.
- 2) dynorphin A: (YGGFLRRIRPKLKWDNQ), on 2-Chlorotriylchloride-polystyrene resin (Barlos-resin) loaded with Fmoc-Gln(Trt)-OH. Activating agent: HSBotU / acylation time: 10 min.
- 3)  $\alpha$ -endorphin: (YGGFMTSEKSQTPLVT), on Fmoc-Thr(tBu)-TentaGel S-PHB-resin (Wang-resin), (Rapp-Polymere, Tübingen, Germany). Activating agent: HSNPtU / acylation time: 15 min.
- 4) dynorphin B: (YGGFLRRQFKVVT), on Fmoc-Thr(tBu)-Tentagel-S-PHB-resin (Wang-resin), (Rapp-Polymere, Tübingen, Germany). Activating agent: HSDNPtU / acylation time: 5 min.

All opioid peptides were cleaved from the resin, following standard procedures, lyophilized and purified using RP-HPLC. The structures were reconfirmed by laser-desorption-mass-spectroscopy.

## References

1. Dourtoglou, V., Ziegler, J. C. and Gross, B., *Tetrahedron Lett.*, (1978) 1269.
2. Castro, B., Evin, G., Selve, C. and Seyer, R., *Synthesis*, (1977) 413.
3. Farrington, J. A., *J. Chem. Soc.*, (1957) 1407.
4. Kenner, G. W., Thomson, P. J. and Turner, J. M., *J. Chem. Soc.*, (1958) 4148.
5. Ueda, M., Seki, K. and Imai, Y., *Synthesis*, (1981) 991.
6. Knorr, R., Trzeciak, A., Bannwarth, W. and Gillesen, D., *Tetrahedron Lett.*, 30 (1989) 1927.
7. Takahashi, J., *J. Pharm. Soc. Jpn.*, 55 (1935) 875.

# Chemical synthesis, purification and characterization of a 107 residue fragment of the prion protein

Haydn L. Ball,<sup>a</sup> Michael A. Baldwin,<sup>a</sup> Tatiana Bekker,<sup>a</sup> Paolo Mascagni,<sup>b</sup>  
David King<sup>c</sup> and Stanley B. Prusiner<sup>a,d</sup>

<sup>a</sup>Department of Neurology and <sup>d</sup>Department of Biochemistry & Biophysics, University of California, San Francisco, CA 94143, <sup>b</sup>Italfarmaco Cinisello Balsamo 20092, Milan, Italy and <sup>c</sup>HHMI, University of California, Berkeley, CA 94720, USA

The prion protein (PrP) in its mature form is a 209 residue glycolipid anchored sialoglycoprotein that is implicated in the development of scrapie in sheep, bovine spongiform encephalopathy and Creutzfeld-Jacob disease in humans. Cellular PrP is ubiquitous in neurons where it normally exists as a benign cellular form (PrP<sup>C</sup>), but may be transformed into a pathogenic isoform (PrP<sup>Sc</sup>), either spontaneously due to pathogenic mutations or by interacting with an infectious particle comprised perhaps entirely of PrP<sup>Sc</sup>. As a result of unfavorable physical properties, large quantities of PrP are difficult to obtain from natural sources. We describe the chemical synthesis of a 107 residue chimeric mouse/hamster/mouse protein from PrP (MH2M 107) using an optimized stepwise solid-phase peptide synthesis approach. It appears that a similar entity in N2a cells can undergo conversion to PrP<sup>Sc</sup> [1]. We report the synthesis, purification, refolding and characterization of the MH2M 107 protein.

## Results and Discussion

Initially, MH2M 107 was synthesized using a highly efficient t-Boc chemical protocol [2]. An aliquot of peptidyl-resin was removed half way through the synthesis and cleaved with hydrogen fluoride. The RP-HPLC chromatogram of the crude product showed a complicated mixture of products consisting mainly of deletion sequences. These were believed to have been due to secondary structure of the growing resin bound peptide. The addition of 20% trifluoroethanol to the coupling solvent overcame most of these problems by reducing intermolecular interactions. Unfortunately extending the synthesis to give the full-length protein resulted in a highly contaminated cleavage product. Extensive analysis by RP-HPLC and mass spectrometry allowed the identification of "difficult" couplings. Despite use of various strategies we were unable to obtain a sufficiently pure product for the 107-mer using t-Boc chemistry. We then investigated the alternative Fmoc chemical approach. A highly optimized protocol was used involving DCC/HOBt activation and extended deprotection and coupling times. Removal of side-chain protecting groups and cleavage of protein from the resin was achieved using a 6 hr treatment with Reagent K [3]. Analysis of the crude product by RP-HPLC (Fig. 1A) and ESI-MS (Fig. 1B) showed a highly homogeneous product with virtually no deletion sequences. Purified protein was readily obtained by semi-preparative RP-HPLC at 50°C, which reduced interaction between protein chains resulting in higher yields. Natural PrP possesses an intramolecular disulfide bridge which is present in both

PrP<sup>C</sup> and PrP<sup>Sc</sup> [4]. Attempts to oxidize the Cys residues at basic pH failed due to lack of solubility and so lower pH solutions were investigated. Success was achieved by dissolving the protein at 0.5mg/ml in water, pH 3.5. Disulfide bond formation was monitored and confirmed by RP-HPLC as indicated by the appearance of an earlier eluting peak and ESI-MS (-2 Da) and shown to be complete after 3 day. The oxidized MH2M 107 was purified on RP media at elevated temperature. The overall yield from 120mg of crude protein for the two RP purification steps and Cys oxidation was 8.7mg (7.3%). RP-HPLC (Fig. 1C) and ESI-MS (Fig. 1D) showed that the correct protein had been obtained.

Secondary structural analysis by circular dichroism showed that before Cys oxidation MH2M 107 adopted a  $\beta$ -sheet conformation. However, after refolding the protein became predominantly  $\alpha$ -helical, reflecting the behavior of a 142-residue recombinant PrP protein. MH2M 107 with mutations predicted to increase the  $\beta$ -sheet character is being assayed for prion infectivity in laboratory rodents.

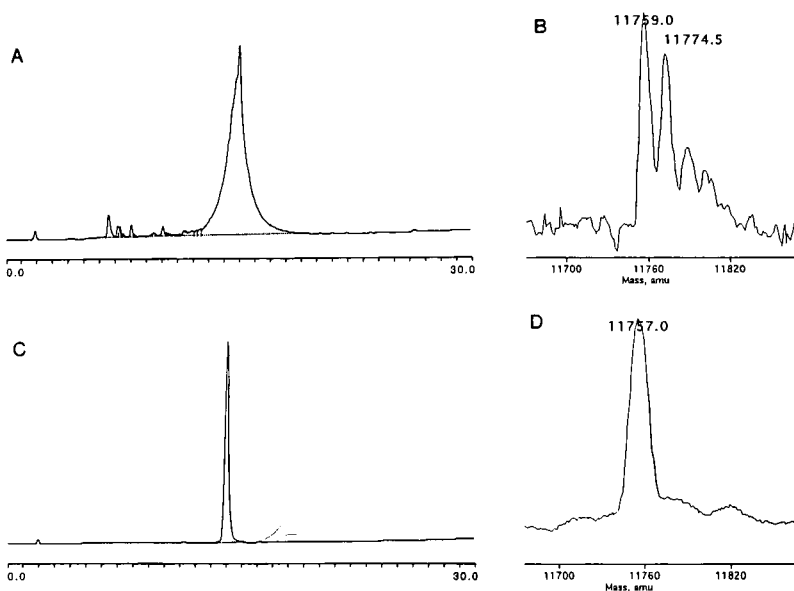


Fig.1. Analysis of MH2M 107 synthesized using Fmoc chemistry. (A) RP-HPLC and (B) ESI-MS of crude MH2M 107, showing Met[O] impurities. (C) RP-HPLC and (D) ESI-MS of pure, refolded and Cys oxidized MH2M 107. Calculated mass 11758.

## References

1. Muramoto, T., Scott, M., Cohen, F.E. and Prusiner, S.B., Proc. Natl. Acad. Sci. USA, 93 (1996) 15457.
2. Ball, H.L. and Mascagni, P., Int. J. Pep. Protein Res., 48 (1996) 31.
3. King, D., Fields, C. and Fields, G., Int. J. Pep. Protein Res., 36 (1990) 255.
4. Turk, E., Teplow, D.B., Hood, L.E. and Prusiner, S.B., Eur. J. Biochem., 176 (1988) 21.

# Problems encountered with the synthesis of a glycosylated hydroxylysine derivative suitable for Fmoc-solid phase peptide synthesis

**Henriette A. Remmer and Gregg B. Fields**

*Biomedical Engineering Center and Department of Laboratory Medicine and Pathology,  
University of Minnesota, Minneapolis, MN 55455, USA*

Hydroxylysine (Hyl) is the glycosylation site within type IV collagen tumor cell recognition sequences  $\alpha 1(\text{IV})$  531-543 and  $\alpha 1(\text{IV})$ 1263-1277 as well as type II collagen T-cell recognition sites. In order to investigate the role of glycosylation in tumor cell interaction with type IV collagen, it is desirable to synthesize peptide models of cell adhesion sites that incorporate Hyl(2-O- $\alpha$ -D-glucopyranosyl)- $\beta$ -D-galactopyranoside. Some protected Hyl derivatives have been synthesized in non-glycosylated [1-3] and glycosylated [4] forms but are not suitable for Fmoc-SPPS. The synthesis of Fmoc-Hyl(N $\epsilon$ -Boc,O $\delta$ -TBDMS)-OH was reported in a poster abstract [5], but a detailed description of the synthesis has not appeared.

## Results and Discussion

Starting from pure L-Hyl, we have been developing a solution synthesis of a fully protected N $\alpha$ -Fmoc-Hyl derivative which will then be glycosylated. Three synthetic strategies compatible with Fmoc chemistry have been investigated based on the use of Boc, Cbz or Alloc for N $\epsilon$ -protection (Fig. 1, pathways A, B, C; Cbz can be cleaved with TFA/thioanisole [6]). In the Boc approach (Fig. 1, A) reaction 3A was performed using supersaturated EDTA at pH 9 and 7. The subsequent Fmoc acylation did not yield the expected product **IV-A** [Fmoc-Hyl(Boc)-OH, MW: 485 amu]. FAB-MS showed an [M+H]<sup>+</sup> peak of 607 amu and a peak at 485 amu. By <sup>1</sup>H-NMR spectroscopy, no Boc signal was found and integration data proved the presence of two Fmoc groups. The mass of 607 amu corresponds to Fmoc-Hyl(Fmoc)-OH. Due to the missing Boc signal in the <sup>1</sup>H-NMR, the peak at 485 amu in the FAB-MS can be unambiguously assigned to the glycerine matrix. We believed that the Boc group was removed during disruption of the Cu-complex with EDTA. This side reaction did not occur when fresh EDTA was used. In the Cbz approach (Fig. 1, B) H-Hyl(Cbz)-OH was poorly soluble in commonly used organic solvents and reactions 4,5,6 B could hardly be performed. The Alloc-approach (Fig. 1, C) was successfully applied to yield **IV-C**, as revealed by ES-MS and <sup>1</sup>H-NMR. This Fmoc-Hyl(Alloc)-OH could not be extracted into organic solvents for purification and/or crystallization. We expect that  $\delta$ -hydroxy protection and esterification (reactions 5C and 6C) would render the molecule more hydrophobic and thus relatively easy to purify. These reactions are currently under investigation.

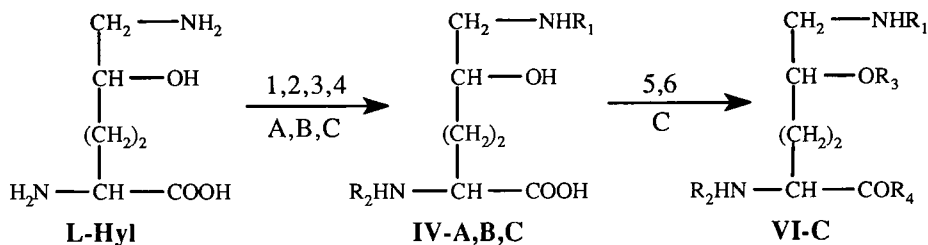


Fig. 1. Synthesis of a fully protected Fmoc-Hyl derivative. PROTECTING SCHEMES: pathway A:  $R_1=\text{Boc}$ ,  $R_2=\text{Fmoc}$ ; pathway B:  $R_1=\text{Cbz}$ ,  $R_2=\text{Trt}$ ; pathway C:  $R_1=\text{Aloc}$ ,  $R_2=\text{Fmoc}$ ,  $R_3=\text{Trt}$ ,  $R_4=\text{OPfp}$  or  $\text{GlyOPfp}$ . REACTIONS: 1 A,B,C:  $\text{CuSO}_4/\text{NaOH}$ ,  $30^\circ\text{C}$ , 15 min; 2A:  $\text{Boc-ON}/\text{Et}_3\text{N}$  in dioxane/water, RT, 2 h; 2B:  $\text{Cbz-Cl}$ ,  $0^\circ\text{C}$ , 2 h; 2C:  $\text{Aloc-Cl}$ ,  $0^\circ\text{C}$ , 2 h; 3A: supersaturated  $\text{EDTA}/\text{NaHCO}_3$ , RT, pH 9, 2 h, pH 7, 12 h; 3B,C:  $\text{KCN}$ , RT, 1 h; 4A,C:  $\text{FmocOSu}/\text{NaHCO}_3$  in DME/water, RT, 15 h; 5C:  $\text{Trt-Cl}$  in chloroform/acetonitrile, RT, 2 h; 6C:  $\text{Pfp-OH}/\text{DCCI}$  ( $0^\circ\text{C}$ , 1 h) or  $\text{GlyOPfp}/\text{DIC}/\text{HOBT}$  (RT, 1 h) in DME.

## Conclusion

The results show that synthesis scheme C (Fig. 1) using Ne-Aloc protection is the pathway of choice to obtain a fully protected Hyl derivative as a building block for Fmoc-SPPS. Fmoc-Hyl(Ne-Aloc)-OH can be obtained in four steps. Ne-Boc protection seems to be another feasible approach when avoiding EDTA disruption of the Cu-complex. Comparing the protection schemes of the Boc and Aloc approaches, the latter is preferable because of its orthogonality, which allows for selective deblocking of the  $\delta$ -hydroxy function and facile introduction of the glycosyl moiety.  $\delta$ -Hydroxy and  $\alpha$ -carboxy protection as well as glycosylation are now under investigation.

## Acknowledgements

This work is supported by NIH and Biostratum, Inc. We gratefully acknowledge K. J. Jensen for informative discussions and Degussa for supplying pure L-Hyl.

## References

- Zahn, H. and Umlauf, E., Hoppe Seyler's Z. Physiol. Chem., 297 (1954) 127.
- Zahn, H. and Zuern, L., Liebigs Ann. Chem., 613 (1958) 76.
- Schnabel, E., Liebigs Ann. Chem., 667 (1963) 179.
- Koeners, H.J., Schattenkerk, C., Verhoeven, J.J., and v. Boom, H.J., Tetrahedron, 37 (1981) 1763.
- Penke, B., Zsigo, J., and Spiess, J., Poster P-335, 11th APS, La Jolla, CA, 1989.
- Kiso, Y., Ukawa, K. and Akita, T., J. Chem. Soc. Chem. Comm., (1980) 101.

# Efficient assembly of stable site-directed fluorescence labeled peptides

Holger Wenschuh,<sup>a</sup> Ulrich Schaible,<sup>a</sup> Stephanie Lamer,<sup>a</sup>  
Michael Bienert<sup>b</sup> and Eberhard Krause<sup>b</sup>

<sup>a</sup> Max-Planck-Institut für Infektionsbiologie, Monbijoustr. 2, D-10117 Berlin, Germany,

<sup>b</sup> Forschungsinstitut für Molekulare Pharmakologie, Alfred-Kowalke Str. 4.,  
D-10315 Berlin, Germany

The most commonly used derivatives for studying the interaction of fluorescence-labeled proteins and peptides with living cells [1] are isothiocyanates such as fluorescein isothiocyanate (FITC). However, major problems arise from the relatively low reactivity of the isothiocyanates and the low stability of the thioureas formed [2]. Activated esters of 5(6)-carboxyfluorescein (e.g. the N-hydroxysuccinimide ester) have been shown to be highly reactive and to generate stable amide bonds [3,4]. In general, these active esters can react with various amino functions. Previous receptor binding studies with different site-specific fluorescent analogs of glucagon [5] inspired the present work on the synthesis of peptides bearing stable fluorescent labels introduced at selected amino functions.

## Results and Discussion

Substance P (RPKPQQFFGLM-NH<sub>2</sub>) was chosen as model peptide to examine selective incorporation of 5(6)-carboxyfluorescein-N-hydroxysuccinimide ester (FLUOS) at various pH levels and amounts of active ester used. Reactivity toward the  $\alpha$ - and  $\epsilon$ -amino functions was examined in borate buffer adjusted to pH values of 7.0, 7.5, 8.0, 8.5, 9.0, 9.5, and 10.0 using 1 eq. of FLUOS (Fig. 1A). The effect of the molar ratio of FLUOS/Substance P was studied at pH 8.5 (borate buffer, 10% DMF) followed by stepwise changes from 0.75 to 2.0 eq. FLUOS (Fig. 1B). Optimized conditions (pH 9.0, 0.9 eq. FLUOS) were applied to verify the found effect on the 41 amino acid-containing h-CRF molecule yielding a stable product with >80% of the N <sup>$\epsilon$</sup> -labeled product. In a second approach solid phase methodology was evaluated for the synthesis of both N-terminally or side chain-labeled species. Substance P was assembled via the Fmoc-strategy on a Tenta-Gel resin. The Mtt-group was chosen to protect the amino function of Lys<sup>3</sup> allowing its selective removal in the presence of other side chain protecting groups for which 95% TFA is required for deprotection [6].

After the synthesis, amino functions subject to modification were deprotected in separate batches using either 25% piperidine/DMF for 15 min (N-terminal amino group) or 1% TFA, 5% TIPS, DCM for 45 min (Lys<sup>3</sup> amino group). After fluorescence labeling with FLUOS, the Fmoc-group of the side chain modified peptide was removed and peptide resin cleavages were carried out along with deprotection of the remaining side chain protecting groups. The selectively labeled crude peptides were obtained in HPLC purities of >70%.

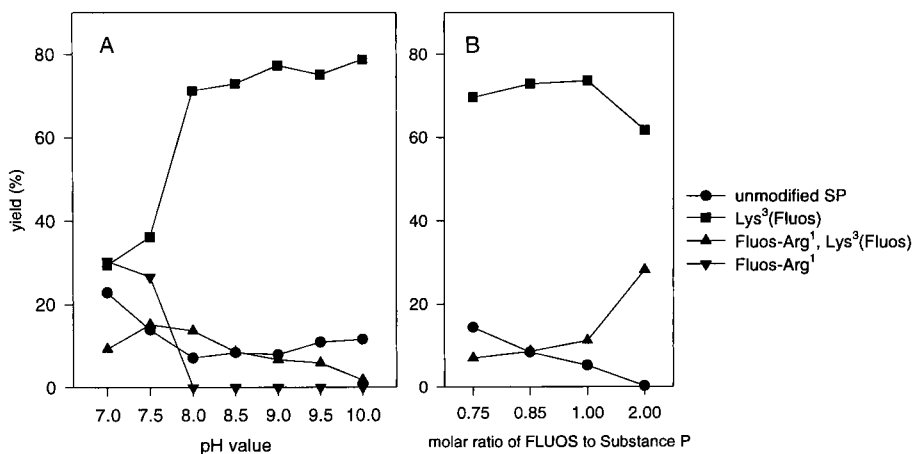


Fig. 1. Influence of (A) pH and (B) molar ratio of FLUOS/peptide for the acylation of Substance P amino functions.

The stably modified peptides could be purified by preparative HPLC. Labeling position was confirmed by MALDI-MS Post Source Decay (PSD) analysis. The general applicability of the SPS method was confirmed by its application to the synthesis of an MHC class I restricted antigenic peptide (GYKDGNEYI) from listeriolysin selectively labeled either at the N-terminus or the Lys side chain.

## References

1. Maxfield, F.R., In Wang, Y.-L., Taylor, D.L. (Eds.) *Methods in Cell Biology*, Academic Press, Inc., San Diego, 1989, 29, p.13.
2. Rypacek, F., Drobnik, J. and Katal, J., *Anal. Biochem.*, 104 (1980)141.
3. Vigers, G.P.A., Coue, M. and McIntosh, J., *J. Cell Biol.*, 107 (1988) 1011.
4. Tota, M.R., Daniel, S., Sirotna, A., Mazina, K.E., Fong, T.M., Longmore, J. and Strader, C.D., *Biochemistry*, 33 (1994) 13079.
5. Unson, C.G., Fleischer, M. and Merrifield, R.B., In Smith, J.A. and Rivier, J.E. (Eds.) *Peptides, Chemistry & Biology*, ESCOM Leiden, 1992, p. 400.
6. Barlos, K., Gatos, D., Chatzi, O., Koutsogianni, S. and Schäfer, W., In Schneider C.H., Eberle, A.N. (Eds.) *Peptides 1992*, ESCOM, Leiden, 1993, p. 283.

# Solid phase synthesis of lanthionine peptides

J. P. Mayer, J. Zhang, S. Gröger and C. F. Liu

*Amgen Boulder Inc., 3200 Walnut St., Boulder, CO 80301, USA*

Recently, the monosulfide cystine analog, lanthionine, that is found in a number of peptide antibiotics [1,2] and natural product enzyme inhibitors [3], has been utilized as a constraining residue in several enkephalin-related opioid compounds [4]. The thioether linkage of lanthionine approximates the constraint of a disulfide bridge but lacks the instability of the latter under physiological as well as chemical conditions. Despite the utility of this residue and the versatile methodologies developed by Goodman et al. [4-6], the synthesis of lanthionine-containing peptidomimetics remains a challenge. The present strategy involves a reaction between a  $\beta$ -bromo-alanine obtained by on-resin bromination of an unprotected serine residue and a cysteine thiol group. This new all solid-phase approach is demonstrated for H[D-Ala<sub>L</sub><sup>2</sup>, L-Ala<sub>L</sub><sup>5</sup>] enkephalin **1**.

## Results and Discussion

The analog H[D-Ala<sub>L</sub><sup>2</sup>, L-Ala<sub>L</sub><sup>5</sup>] enkephalin **1** was synthesized from its linear D-serine containing precursor in 25% yield based on the initial loading of Rink resin and the HPLC purity and weight of the final material (Fig. 1). The crude peptide was shown to be homogeneous by HPLC and the purified material was extensively characterized. Amino acid analysis, electrospray mass spectrometry, and <sup>1</sup>H-NMR data all correlated closely with published data [4]. Attempts to synthesize H[L-Ala<sub>L</sub><sup>2</sup>, L-Ala<sub>L</sub><sup>5</sup>] enkephalin from the L-serine-containing precursor yielded material in approximately the same yield and was found surprisingly to be indistinguishable from the D-serine derived material by HPLC analysis and <sup>1</sup>H-NMR. Since the cyclization does not proceed with retention of configuration at the  $\alpha$  carbon, this suggests that one or possibly both precursors cyclize via the dehydroalanine intermediate to give **1**, consistent with the previous finding that only a single isomer, [D-Ala<sub>L</sub><sup>2</sup>, L-Ala<sub>L</sub><sup>5</sup>] EA, for steric reasons, forms from the dehydroalanine precursor [4]. In order to clarify this we assessed the chiral integrity of the  $\alpha$  carbon of the  $\beta$ -bromoalanine prior to the cyclization step by converting the D-serine and L-serine derived brominated intermediates to their corresponding phenylcysteine products with thiophenol. The cleaved peptides were shown to be distinct by C-18 HPLC analysis demonstrating that the  $\beta$  elimination to the dehydroalanine (the "Goodman intermediate") occurs during the cyclization step, possibly because direct bromine displacement is unfavored for steric reasons. Although our results do not definitively elucidate the mechanism of cyclization, the demonstration that the serine to bromoalanine conversion proceeds efficiently and without racemization suggests that this methodology may be applicable to lanthionine formation in less sterically hindered peptides.

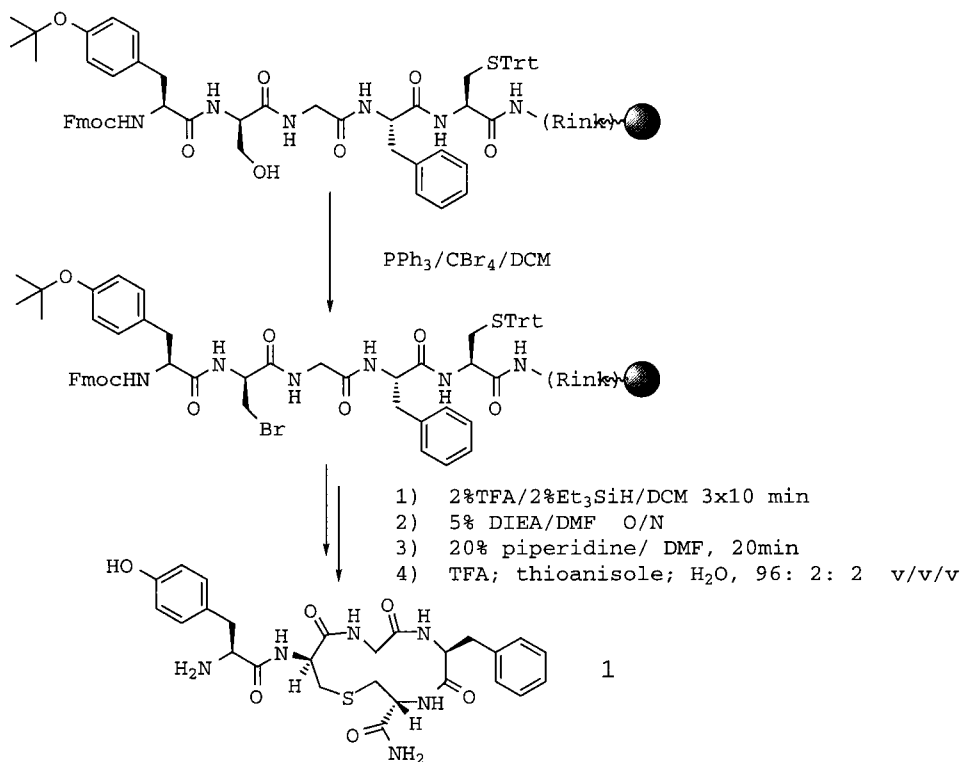


Fig. 1. Solid phase synthesis of  $H[D-Ala^2, L-Ala^5]$  enkephalin I.

## References

1. Sahl, H. G., Jack, R.W. and Bierbaum, G. Eur. J. Biochem., 230 (1995) 827.
2. Jack, R.W., and Sahl, H.G. Trends Biotechnol., 13 (1995) 269.
3. Wakimiya, T., Ueki, Y., Shiba, T., Kido, Y. and Motoki, Y. Tetrahedron Lett., 26 (1985) 665.
4. Polinsky, A., Cooney, M. G., Toy-Palmer, A., Ösapay, G. and Goodman, M., J. Med. Chem., 35 (1992) 4185.
5. Shao, H., Wang, S. H. H., Lee, C. W., Ösapay, G. and Goodman, M., J. Org. Chem., 60 (1995) 2956.
6. Ösapay, G., Zhu, Q., Shao, H., Chadha, R. K. and Goodman, M., Int. J. Peptide Prot. Res., 46 (1995) 290.

# Synthesis of $\beta$ -methyl aspartic acids

Guoxia Han, Andrew Burritt, Jung-Mo Ahn and Victor J. Hruby

Department of Chemistry, University of Arizona, Tucson, AZ 85721, USA

The incorporation of topographically constrained amino acids has proven to be useful in the design of bioactive peptides, providing ligands with both improved potency and receptor selectivity. Several potent  $\alpha$ -melanocyte-stimulating hormone ( $\alpha$ -MSH) agonists [1] and antagonists [2] with aspartic acid at position 5 have been developed in the past decades. However, there is a need to develop more constrained  $\alpha$ -MSH analogues that will provide both high potency and selectivity for only one of the melanocortin receptors (MC1R, MC3R, MC4R, and MC5R). One way to design such analogues is to incorporate  $\beta$ -substituted aspartic acids in position 5. We are exploring two simple synthetic approaches to the preparation of these types of amino acid derivatives with easy protection and deprotection of all the functional groups, which will provide more easy access to these compounds than previously reported approaches [3, 4].

## Results and Discussion

As shown in Fig. 1, all of the functional groups in *L*-aspartic acid are fully protected in the

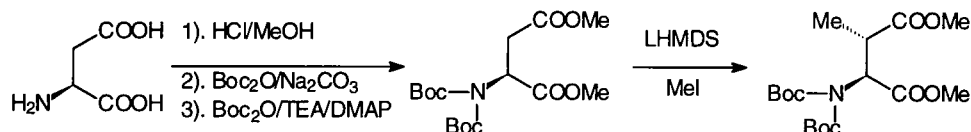


Fig. 1. Synthesis of  $\beta$ -methyl aspartic acid via bis-Boc protection.

first step. The acid groups are protected by esterification with methanol. This is accomplished by bubbling dry HCl gas into a methanol solution of aspartic acid, followed by protection of the  $\alpha$ -amino group with two Boc groups. The first Boc group was introduced by a widely used method [5]. However, the same approach did not work for the second Boc group which was successfully introduced by using triethylamine (TEA) with a catalytic amount (10%) of *p*-dimethylaminopyridine (DMAP) in ethyl acetate. Computer modeling has shown one side of the  $\beta$ -position is hindered by one of the Boc groups, suggesting that good stereoselectivity could be achieved when alkylation occurs at the  $\beta$ -position. Although this alkylation step gave almost exclusively one diastereomer (>98% d.e.), the yield was poor due to side reactions.

Our second approach to the synthesis of  $\beta$ -methyl aspartic acids is shown in Fig. 2. In this case, all the functional groups in *L*-aspartic acid are protected by benzyl groups. Refluxing a mixture of aspartic acid and benzyl bromide (excess) in an aqueous potassium carbonate and sodium hydroxide solution afforded the fully benzyl-protected aspartic acid

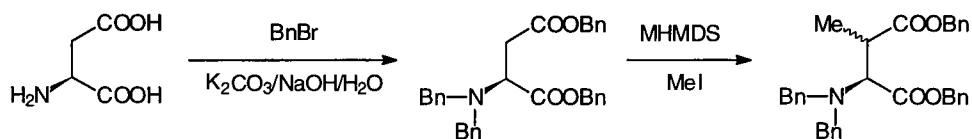


Fig. 2. Synthesis of  $\beta$ -methyl aspartic acid via bis-benzyl protection.

derivative. No epimerization was found in this process. Methylation of the  $\beta$ -position was achieved by treatment with methyl iodide and one of the bases shown in Table 1. Isolated yields varied from 50% to 80%. Thus far we have not found suitable conditions for the separation of the  $\beta$ -methyl diastereoisomers by flash chromatography. However, they can be separated by reverse phase HPLC which also was used to determine the d.e. of the alkylation.

Table 1. Alkylation results of bis-Bn protected aspartic acid derivative.

Reaction	MHMDS	Temperature (°C)	Time (hrs)	d.e (R:S)
A	LHMDS	-78	2	3.0 : 1.0
B	LHMDS	-30	2	2.1 : 1.0
C	NaHMDS	-78	8	1.8 : 2.0
D	KHMDS	-78	8*	1.0 : 1.1

Note\*: 70% conversion

Further research is needed to improve the selectivity of the alkylation step using our second approach. We are currently investigating the diastereoselectivity by varying the reaction temperature, base, solvent and alkyl reagent as well as exploring the synthesis with a variety of functional nucleophiles.

## Acknowledgements

This research is supported by grants from the USPHS and NIDA.

## References

- Al-Obeidi, F., Hadley, M.E., Pettitt, B.M. and Hruby, V.J., *J. Am. Chem. Soc.*, 111 (1989) 3413.
- Hruby, V.J., Lu, D., Sharma, S.D., de L. Castrucci, A., Kesterson, R.A., Al-Obeidi, F.A., Hadley, M.E. and Cone, R.D., *J. Med. Chem.*, 38 (1995) 3454.
- Dunn, P.J., Haner, R. and Rapoport, H., *J. Org. Chem.*, 55 (1990) 5017.
- Humphrey, J.M., Bridges, R.J., Hart, J.A. and Chamberlin, A.R., *J. Org. Chem.*, 59 (1994), 2467.
- Bodanszky, M., and Bodanszky, A. (Eds.), *The Practice of Peptide Synthesis*, 2nd Ed., Springer-Verlag, 1994, p. 9.

# Total solid-phase synthesis of human cholecystokinin (CCK)-39

K. Kitagawa,<sup>a</sup> C. Aida,<sup>a</sup> H. Fujiwara,<sup>a</sup>  
T. Yagami<sup>b</sup> and S. Futaki,<sup>c</sup>

<sup>a</sup> Niigata College of Pharmacy, Niigata 950-21, Japan; <sup>b</sup> National Institute of Health Sciences, Tokyo 158, Japan; <sup>c</sup> Institute for Medicinal Resources, The University of Tokushima, Tokushima 770, Japan

To date many synthetic methods for the peptide containing tyrosine *O*-sulfate [Tyr(SO<sub>3</sub>H)] have been reported including the solid-phase approach; however, a general and convenient synthetic method has not yet been established. Recent advances in Fmoc-SPPS using the solid-phase method have made the direct synthesis of the sulfated peptide possible. When Fmoc-strategy is adopted, conditions for the final cleavage/deprotection with acidic reagents becomes crucial. During the course of our efforts to find a general synthetic method for the Tyr(SO<sub>3</sub>H)-containing peptides, 90% aqueous TFA at *low temperature* proved effective in minimizing the deterioration of Tyr(SO<sub>3</sub>H) [1]. Based on this finding, we have recently established a facile solid-phase method for the preparation of Tyr(SO<sub>3</sub>H)-containing peptide and have shown that this methodology could be applied to the preparation of fairly large sulfated peptides [2].

CCK is known to have several molecular forms, but the significance of the presence of such molecular diversity and physiological roles, especially of its large molecular forms, are still unclear. In order to extend our methodology and to evaluate the biological activity of the large molecular form peptide of CCK, we have undertaken total solid-phase synthesis of human CCK-39.

## Results and Discussion

The synthetic route to CCK-39 is shown in Fig. 1. The C-terminal dipeptide amide, Fmoc-Asp-Phe-NH<sub>2</sub>, was first linked to a 2-chlorotrityl (Clt)-resin [3] through the side-chain carboxyl group of Asp, then each Fmoc-amino acid including Fmoc-Tyr(SO<sub>3</sub>Na)-OH was introduced stepwise to the peptide-chain. In order to carry out the synthesis with a minimum of protecting groups, Asn and Gln residues were introduced by Fmoc-Asn/Gln-OPfp in the presence of HOObt. The guanidino function of four Arg residues was protected with the Pbf group [4], which was the most sensitive to our deprotection conditions (90% aq. TFA at 4°C) among the various guanidino protecting groups. The *Bu<sup>t</sup>/Boc* protecting groups were used for the amino acids requiring the side-chain protecting group including His, which was introduced with a form of His(Boc). After the construction of the full-length peptide-chain on the resin, the resin-bound peptide was subjected to a *two-step cleavage/deprotection*; first with a mixture of AcOH-CF<sub>3</sub>CH<sub>2</sub>OH-CH<sub>2</sub>Cl<sub>2</sub> (1:1:3 v/v, 25°C, 30 min) for *cleavage*, followed with 90% aq. TFA (4°C, 15 h) for *deprotection*. The first mild acid treatment could detach the protected peptide from the Clt-resin nearly quantitatively without affecting the sulfate. The second acid treatment at

low temperature could deprotect the protecting groups including four Pbf groups on the Arg residues with minimum damage on the sulfate despite the prolonged acid treatment. Although the crude peptide thus obtained showed a fairly complicated HPLC elution profile, a highly homogeneous product was obtained after one-step HPLC purification. The main peak in HPLC proved to be an objective CCK-39; the amino acid analysis of this product agreed well with the theoretical value, and the intactness of the sulfate was directly established with MALDI-MS. Although the yield from the cleavage/deprotection step was not excellent (8%) due to the presence of highly oxidation-sensitive Met residues, the yield is judged to be acceptable for synthesizing *sulfated peptide colse to 40-residue*. Thus CCK-39 was synthesized by our newly developed solid-phase approach in a quite facile manner.

The insulinotropic effect of the synthetic human CCK-39 was examined using rat isolated pancreatic islets at high glucose concentration (11.1 mM). Synthetic human CCK-39 increased insulin release in a dose-dependent manner and, at the dose of  $10^{-8}$  or  $10^{-9}$  M, the relative molar potency of CCK-39 was comparable to that of CCK-8 and CCK-33.

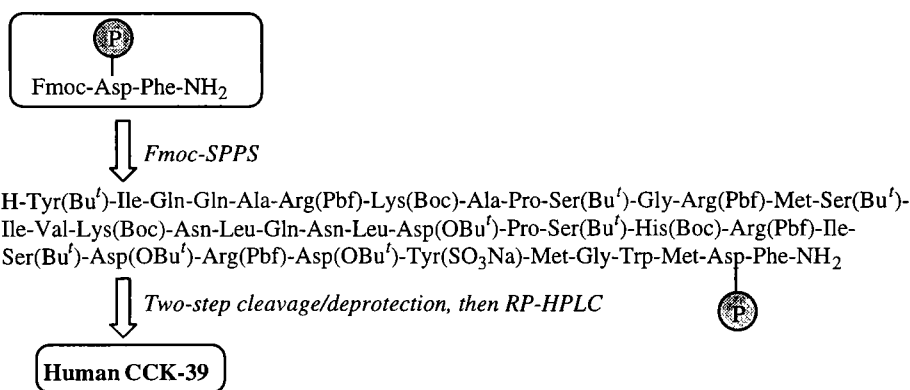


Fig.1. Synthetic outline for human CCK-39.

## References

1. Yagami, T., Shiwa, S., Futaki, S. and Kitagawa, K., *Chem. Pharm. Bull.*, 41 (1993) 376.
2. Kitagawa, K., Aida, C., Fujiwara, H., Yagami, T. and Futaki, S., *Tetrahedron Lett.*, 39 (1997) 599.
3. Barlos, K., Gatos, D., Kallitsis, K., Papaphoutiu, P., Sotiriou, P., Wenqing, Y. and Schafer, W., *Tetrahedron Lett.*, 30 (1989) 3943.
4. Carpino, L. A., Shroff, H., Triolo, S. A., Mansour, E-S. M. E., Wenschuh, H. and Albericio, F., *Tetrahedron Lett.*, 34 (1993) 6661.

# Studies on synthesis of peptides with C-terminal glutamine para-nitroanilide

**Lili Guo, Dongxia Wang, Patrick J. Edwards, Navayath Shobana and Roger W. Roeske**

*Department of Biochemistry and Molecular Biology, Indiana University School of Medicine, 635 Barnhill Drive, Indianapolis, Indiana 46202-5122, USA.*

Para-nitroanilides (pNA) of amino acids and peptides are useful chromogenic substrates for the determination of the activity of proteases. Synthesis of these compounds is complicated by the weak nucleophilicity of p-nitroaniline. Many coupling reagents have been tried, with limited success, but the mixed anhydride of Boc amino acids with pivaloyl chloride [1], and the reaction with POCl<sub>3</sub> [2] have given good yields in most cases. We report here attempts to use HBTU and HATU, two potent coupling agents, in the synthesis of Boc-Gln-pNA and Fmoc-Glu(OtBu)-pNA.

There is no general method for the solid phase synthesis of peptide-pNA. Voyer *et al.* [3] attempted aminolysis with pNA's of a peptide linked to an oxime resin and obtained a yield of 30% for the cleavage step. We describe a method that is potentially useful for the solid phase synthesis of pNA's of peptides having a C-terminal Glu, Gln, Asp or Asn residue.

## Results and Discussion

Attempts to couple Boc-Gln with pNA using HATU or HBTU did not succeed. The main product (yield 44%) of the reaction is Boc-glutarimide identified by elemental analysis, mass spectrum and NMR (Table 1). Boc-Gln-pNA was formed in only 6% yield. We found that one equivalent of base (DIEA) gave a cleaner reaction mixture than two equivalents of base. The attempt to react Fmoc-Glu(OtBu) with pNA by HATU also did not succeed; only a trace amount of Fmoc-Glu(OtBu)-pNA was formed.

However, with the phosphorazo-method [4], Fmoc-Glu(OtBu) was converted by PCl<sub>3</sub> to Fmoc-Glu(OtBu)-pNA in 90% yield. After allowing PCl<sub>3</sub> (1.0 eq.) and pNA (2 eq.) to react in pyridine at room temperature for 1 hour, Fmoc-Glu(OtBu) (1.0 eq.) was added. The reaction was stirred at 40° C for 3 hours. After appropriate workup, the crude product was purified by flash chromatography on silica gel.

The compound was treated with TFA to remove the t-butyl ester, and linked to a Rink Amide MBHA resin. Using Fmoc t-butyl chemistry, the sequence Asp-Ser-Arg-Glu-Thr-Leu-Phe-Glu(Rink Amide MBHA resin)-pNA was assembled on an ABI 431A automatic synthesizer on a 0.1 mmole scale using a 10-fold excess of Fmoc amino acids with HBTU/HOBt-mediated coupling. After treatment with TFA, the resin gave the desired product, 95% pure by HPLC, in a yield of 47%. The compound was identified by its mass spectrum.

In contrast to the report that the p-nitroanilide bond in Fmoc-Glu-pNA is not stable in 20% piperidine in NMP (a loss of 4-nitroaniline in 1h) [5], we found that the p-nitroanilide bonds in Fmoc-Glu(OtBu)-pNA, Fmoc-Glu-pNA and Boc-Gln-pNA are stable in 20% piperidine in DMF; even after 24 hrs treatment, no p-nitroaniline was found on TLC.

Table 1. Properties of the products of the reaction of Boc-Gln with pNA by HATU or HBTU coupling method.

Products	Elemental analysis			Mass spectra Calculated (Found, M+H <sup>+</sup> )	NMR
	Calculated (found)				
	C	H	N		
Boc-Gln-pNA	52.45	6.05	15.30	366.4	1.45 (s, 9H, Boc)
	(52.48)	(6.07)	(15.30)	(367.7)	2.04 (m, 2H, β-CH <sub>2</sub> )
					2.34 (m, 2H, γ-CH <sub>2</sub> )
					4.28 (s, 1H, α-CH)
					6.52 [m, 2H, Gln(CONH <sub>2</sub> )]
					7.85/7.88-8.14/8.17 (dd, 4H, arom pNA)
Boc-glutarimide	52.62	7.07	12.28	228.2	1.46 (s, 9H, Boc)
	(52.37)	(7.13)	(12.07)	(229.2)	1.88 (m, 2H, β-CH <sub>2</sub> )
					2.69 (m, 2H, γ-CH <sub>2</sub> )
					4.30 (m, 1H, α-CH)
					5.36 (s, 1H, NH-Gln)
					8.15 (s, 1H, imide-NH)

## Conclusion

If Glu or Gln and presumably, Asp or Asn are located at or near the C-terminus of a peptide pNA, the above procedure should allow synthesis by the solid phase method. After this work was completed, a similar result was reported by A. Kaspari *et al* [5].

In addition, we found that PCl<sub>3</sub> method can be used to synthesize Fmoc-Glu(OtBu)-pNA and this may be extended to the coupling of all other Fmoc-amino acid with pNA.

## References

1. Noda, K., Oda, M., Sato, M. and Yoshida, N., *Int. J. Peptide Protein Res.*, 36 (1990) 197.
2. Rijkers, D.T.S., Adams, H.P.H.M., Hemker, H. C. and Tesser, G.I., *Tetrahedron*, 51 (1995) 11235.
3. Voyer, N., Lavoie, A., Pinette, M. and Bernier, J., *Tetrahedron Lett.*, 35 (1994) 355.
4. Goldschmidt, S. and Rosculet, G., *Chem. Ber.*, 93 (1960) 2387.
5. Kaspari, A., Schierhorn, A. and Schutkowski, M., *Int. J. Peptide Protein Res.*, 48 (1996) 486.

# Solid phase synthesis of peptide nucleic acid-peptide conjugates

**Lynn Mayfield, Revathi Katipally, Carla Simmons and David R. Corey**

*Howard Hughes Medical Institute, Department of Pharmacology, University of Texas,  
Southwestern Medical Center at Dallas, Dallas, TX 75235, USA*

Peptide nucleic acids (PNAs) are analogs of DNA in which the phosphodiester backbone has been replaced by 2-aminoethyl glycine units with the nucleobases attached through methylene carbonyl linkages to the glycine amino group. PNAs hybridize to complementary DNA and RNA with higher affinity and stability than analogous DNA oligomers. They are not substrates for endogenous proteases or nucleases, and have the remarkable ability to perform strand invasion at target sequences within duplex DNA. While their application for experiments *in vitro* is becoming increasingly broad [1], they lack membrane permeability, and their potential for regulating cellular processes is unknown. We describe here the synthesis of PNA-peptide conjugates, consisting of PNAs targeting to the RNA active site of telomerase and peptides derived from the third helix of Antennapedia homeodomain, one of which is known to enter cells [2]. PNA-peptide chimera can be efficiently synthesized with the PNA at either the C or the N-terminus and can be labeled with fluorescein or rhodamine. PNA-peptide chimera containing full length peptides accumulate within cells, while those containing truncated peptides do not.

## Results and Discussion

PNA-peptide chimera were synthesized with either the peptide or the PNA in the C-terminal position by solid phase coupling rather than conjugation of the peptide and PNA by disulfide exchange, thus reducing purification steps and increasing yield. PNAs are synthesized manually for economy and better control over coupling chemistry [3]. After completion of the initial synthesis, a small aliquot was deprotected, cleaved from the resin, and characterized by MALDI-TOF mass spectroscopy. Once the quality of the synthesis was confirmed, the fully protected peptide or PNA was extended by automated synthesis or manual synthesis respectively. Although Boc synthesis of PNA typically results in a better yield with fewer side products, Fmoc synthesis was necessary when PNA was added to the N-terminus of a peptide previously prepared by Fmoc chemistry. PNAs or PNA-peptide hybrids were purified by reverse phase HPLC using 0.1% TFA in acetonitrile as the mobile phase.

PNAs were labeled with either fluorescein maleimide, through a cysteine, or rhodamine (carboxytetramethylrhodamine from Molecular Probes). Since rhodamine proved to be stable to TFA or TFMSA cleavage conditions, it was coupled directly to the N-terminus of the protected conjugate. Coupling was usually complete in twenty minutes, but was sometimes left overnight. Excess rhodamine was washed away with DMF or NMP.

*Table 1. PNA-peptide conjugates.*


---

Import peptide-fully complementary PNA (conjugate 1)
NH <sub>2</sub> -GlyGlyArgGlnIleLysIleTrpPheGlnAsnArgArgMetLysTrpLysLys-GGGTTAGACAA-Lys
Truncated (control) peptide-fully complementary PNA (conjugate 2)
NH <sub>2</sub> -GlyGlyLysIleTrpPheGlnAsnArgArgMetLysTrpLysLysGluAsn-GGGTTAGACAA-Lys
Fully complementary PNA-import peptide (conjugate 3)
NH <sub>2</sub> -GGGTTAGACAA-GlyGlyGlyArgGlnIleLysIleTrpPheGlnAsnArgArgMetLysTrpLysLys
Fully complementary PNA-truncated (control) peptide (conjugate 4)
NH <sub>2</sub> -GGGTTAGACAA-GlyGlyGlyLysIleTrpPheGlnAsnArgArgMetLysTrpLysLysGluAsn

---

A peptide was chosen as a carrier domain for delivery of PNAs into cells because several different peptide sequences have been shown to promote the cellular uptake of attached molecules. A 16 amino acid peptide sequence derived from the third helix of Antennapedia homeodomain has been shown to deliver peptides, proteins, and oligonucleotides into cells [2]. The PNA domain was designed to be complementary to the RNA template of human telomerase. We observed that PNA-peptide chimera containing full length peptide in either orientation (conjugates 1 and 3) are able to cross cell membranes in culture. Chimera containing truncated peptides (conjugates 2 and 4) or fluorescently labeled PNAs lacking any peptide were not taken up by cells.

## Conclusion

Our data show that PNA-peptide hybrids can be taken up by cells. Uptake is independent of the relative orientation of the PNA and the peptide, and occurs quickly. Somewhat surprisingly, given that hybrid synthesis requires 25-30 coupling steps, the hybrids can be made rapidly and in good yield, and the modular nature of our synthesis helps ensure good quality of the final product.

## References

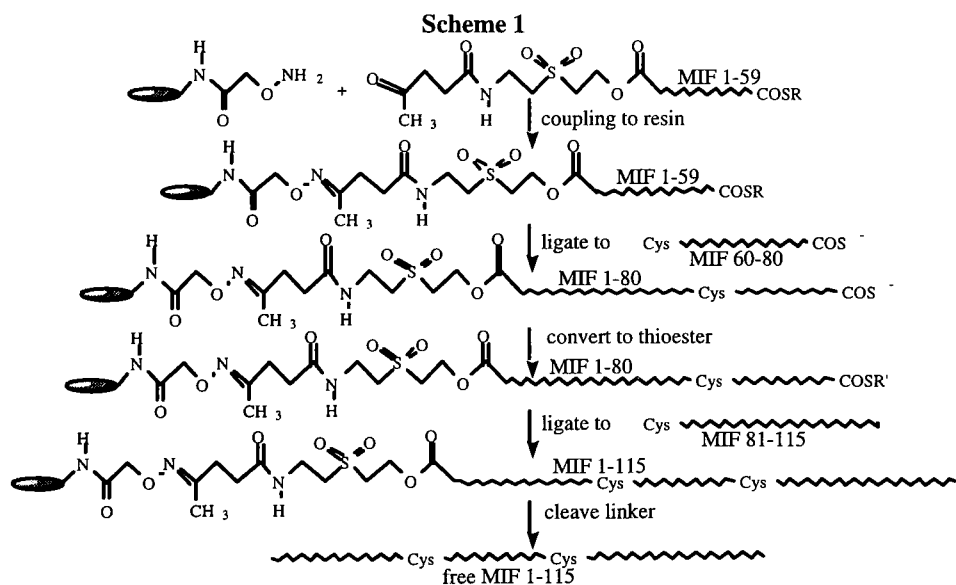
1. Corey, D.R., (1997) Trends in Biotechnology, in press.
2. Prochaintz, A. *Curr., Op. Neurobiology* ,8 (1996) 629.
3. Norton, J.C., Waggenpack, J.H., Varnum, E. and Corey, D.R., *Bioorg. Med. Chem.*, 3 (1995) 437.

# Solid phase protein synthesis by chemical ligation of unprotected peptide segments in aqueous solution

Lynne E. Canne, Darren A. Thompson, Reyna J. Simon and  
Stephen B. H. Kent

Gryphon Sciences, 250 E. Grand Ave., Suite 90, So. San Francisco, CA 94080, USA

Sequential ligations of three or more free peptide segments in solution typically require temporary protection of one of the functionalities of the difunctional middle segments and a purification step (e.g. HPLC) after each ligation [1]. We have developed a solid phase ligation technique based on principles originally enunciated by Merrifield [2]. Our approach avoids the need for multiple purifications of intermediate ligation products in solution and uses fully unprotected peptide segments. The strategy, as outlined in Scheme 1, employs: (i) ligations in an N- to C-terminal direction, (ii) modification of the N-terminal peptide segment with a cleavable linker functionalized with a group capable of chemoselective reaction with the solid support [3], and (iii) sequential native chemical ligations of unprotected peptide segments in aqueous solution [4]. This technique was applied to the synthesis of a lymphokine protein, Macrophage Migration Inhibitory Factor (MIF).



## Results and Discussion

Peptide segments corresponding to the amino acid sequence of MIF were synthesized using *in situ* neutralization/HBTU activation protocols for Boc chemistry [5]. The three unprotected peptide segments were ligated as outlined in Scheme 1. The final product, full length MIF 1-115 as cleaved from the solid support, is shown in Fig 1. The advantages of solid phase protein synthesis are numerous and include: (i) purification of resin-bound intermediates by simple filtration and washing; (ii) faster overall synthesis of the final product because no time-consuming intermediate purifications are necessary; (iii) higher reaction rates from higher concentrations of reactants; (iv) solubility problems are overcome by attachment of the growing peptide to solid support; (v) much larger peptides and proteins can be made than presently attainable by more conventional methods; (vi) easy scale up due to high resin loadings; (vii) automation possible because of the repetitive nature of the operations; and (viii) completed full length peptide is totally unprotected and requires only cleavage from the solid support. We expect solid phase protein synthesis by the chemical ligation of unprotected peptide segments in aqueous solution to be of major utility in the future and to have a high impact on the world of synthetic protein chemistry, bringing within our grasp previously unattainable protein targets.

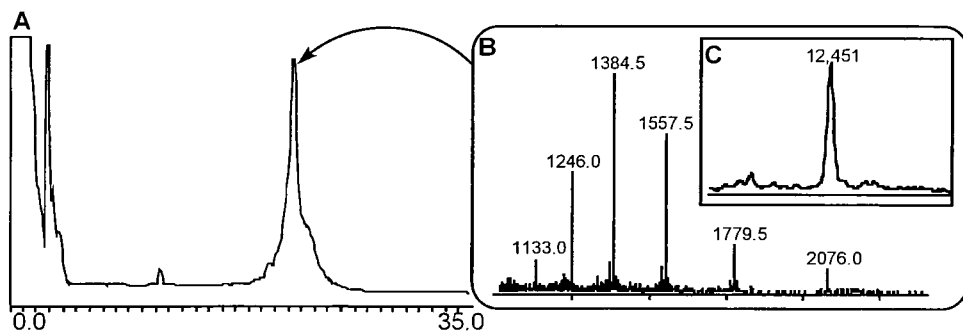


Fig. 1. (A) Analytical HPLC of crude MIF 1-115 after cleavage from the solid support. (B) Electro-spray MS of the HPLC-purified peak showing the distribution of protonation states. (C) Hypermass reconstruction of the raw MS data to a single charge state. Full length MIF 1-115 had an observed mass of  $12451 \pm 1$  Da (expected mass 12450 Da).

## References

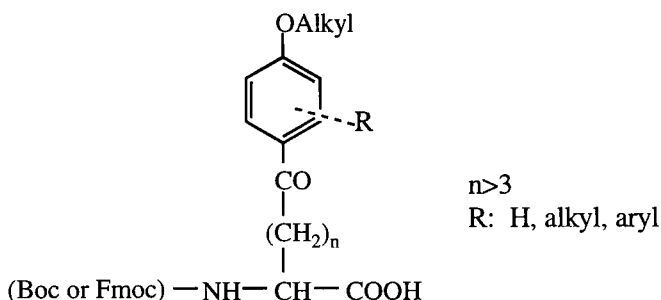
1. Figliozzi, G.M., *et al.*, Abstracts of Posters, 24th Symposium of the European Peptide Society; Edinburgh, Scotland; The European Peptide Society and The Royal Society of Chemistry: London, England, 1996, P.202.
2. Merrifield, R.B., *J. Am. Chem. Soc.*, 85 (1963) 2149.
3. Canne, L.C., Winston, R.L. and Kent, S.B.H., *Tetrahedron Lett.*, 38 (1997) 3361.
4. Dawson, P.E.; Muir, T.W.; Clark-Lewis, I. and Kent, S.B.H., *Science*, 266 (1994) 776.
5. Schnölzer, M., *et al.*, *Int. J. Pept. Protein Res.*, 40 (1992) 180.

# Amino acids with alkyloxyaryl-keto function in their side chains

Maria A. Bednarek

Department of Medicinal Chemistry, Merck Research Laboratories, Rahway, NJ 07065, USA

Formation of ketones has been repeatedly observed when peptides with glutamyl residues were cleaved from the polymeric support with liquid HF in the presence of anisole as scavenger [1,2]. We noted [3] that under similar conditions, the carboxyl group of C-terminal  $\omega$ -amino acids, with at least four carbon atoms between the amino and the carboxyl group, is also completely converted into ketone derivatives. In the present study we exploited this reaction for the facile preparation of amino acids with alkyloxyaryl-keto side chain function.



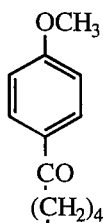
## Results and Discussion

D,L- $\alpha$ -Aminopimelic acid was treated with liquid HF in the presence of a compound susceptible to electrophilic substitution, such as anisole, 2-methoxybiphenyl, 3-methylanisole or butyl phenyl ether. After one hour at 0° C, HF was removed by evaporation, the residue triturated with ether, the precipitate filtered and dried. In each case, the product of the reaction,  $\omega$ -keto- $\alpha$ -amino acid, was secured in excellent yield. Its purity was tested by RP-HPLC, <sup>1</sup>H NMR, mass spectrometry and elemental analysis. The novel keto-amino acids were converted into the  $\alpha$ -N-Boc- or  $\alpha$ -N-Fmoc- derivatives and subsequently, smoothly incorporated into model peptides by conventional coupling methods, on 431A ABI peptide synthesizer, e.g.

Formation of cyclic Schiff bases or lactams, during coupling or deprotection steps, was not observed. Neither ions 18 Da smaller than expected nor ions corresponding to truncated fragments of the peptides could be detected in the mass spectra of the final crude products.

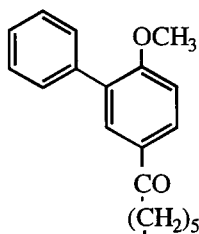
Also, an alternative route for preparation of Fmoc-protected  $\omega$ -(alkyloxyaryl)-keto- $\alpha$ -amino acids was explored. First, D,L- $\alpha$ -aminopimelic acid, or L- $\alpha$ -aminosuberic acid, was converted into the Fmoc-derivative, by reaction with Fmoc-OSu, and then treated with

liquid HF (0°C, 1 hr) in the presence of selected alkyloxyaryl compounds. Once again, Fmoc-protected ω-(alkyloxyaryl)-keto-α-amino acids were secured in excellent yields.



D,L-NH<sub>2</sub>-CH-CO-L-Lys-L-Lys-L-Val-amide

(Fmoc synthesis)



Gly-Ala-NH-CH-CO-Arg-His-Arg-Lys-Val-amide

(Boc synthesis)

## References

1. Sano, S. and Kawanishi, S., *Biochem. Bioph. Res. Commun.*, 51 (1973) 46.
2. Feinberg, R.S. and Merrifield R.B., *J. Am. Chem. Soc.*, 97 (1975) 3485.
3. Bednarek M.A., Springer J.P., Cunningham B.R., Bernick A.M. and Bodanszky M., *Int. J. Pept. Prot. Res.*, 42 (1993) 10.



starting oxazolidinone and formation of the resin-bound Asn amide. Amide **8** was obtained in a crude mass yield of 80% in a purity of > 90% as measured by percent area (%Area) at 230 nM via RP-HPLC.

An array synthesis of 12 different Asn, Asp, and Gln amides was produced using primary amines, and we observed complete conversion, based on the absence of any absorption at  $1800\text{ cm}^{-1}$ . All new compounds were analyzed and characterized by HPLC, mass spectroscopy, and  $^1\text{H}$  and  $^{13}\text{C}$  NMR spectroscopy. This chemistry also works using 4-7 immobilized on pins ( $1.2\text{ }\mu\text{mol/crown}$ ).

In conclusion, the oxazolidinone protection scheme is suitable for side-chain immobilization of Asp and Glu and for "activation" of the  $\alpha$ -carboxylic acid. The polymer bound oxazolidinones underwent ring opening reactions with a wide range of primary aliphatic and benzylic amines to give Asn, Asp, and Gln amides in high yield and high purity. We further established single bead FT-IR microspectroscopy for monitoring oxazolidinone carbonyl IR band at  $1800\text{ cm}^{-1}$ .

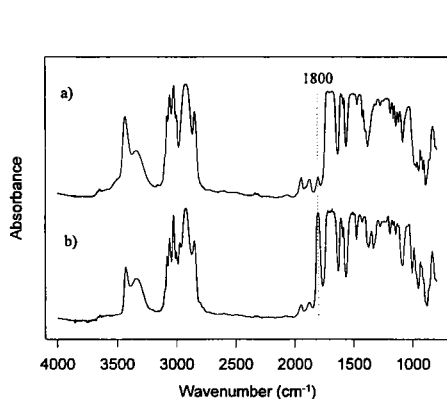


Fig. 1. FT-IR spectra taken from (a) Knorr-Fmoc resin and (b) after Fmoc-deprotection and coupling of oxazolidinone.

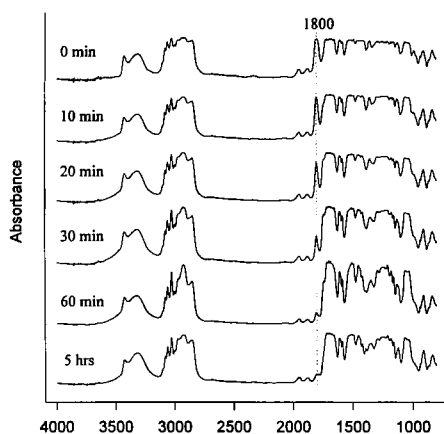


Fig. 2. Single bead IR at various times after initiation of ring-opening reaction depicted in scheme 1.

## References

1. Marti, R.E., Yan, B. and Jarosinski, M.A., *J. Org. Chem.*, 62 (1997) in press.
2. Williams, R. M., Glinka, T., Kwast, E., Coffman, H. and Stille, J.K., *J. Am. Chem. Soc.*, 112 (1990) 808.
3. Lee, K.-I., Kim, J.H., Ko, K.Y. and Kim, W.-J. *Synthesis*, (1991) 935.
4. Yan, B., Kumaravel, G., Anjaria, H., Wu, A., Petter, R.C., Jewell, C.F. and Wareing, J.R., *J. Org. Chem.*, 60 (1995) 5736.
5. Yan, B. and Kumaravel, G., *Tetrahedron*, 52 (1996) 843.
6. Yan, B., Fell, J.B. and Kumaravel, G., *J. Org. Chem.*, 61 (1996) 7467.
7. Scholtz, J.M. and Bartlett, P.A., *Synthesis*, (1989) 542.
8. Carpino, L.A., *J. Am. Chem. Soc.*, 115 (1993) 4397.

# Synthesis and applications of a bis-sulfonyl handle for solid-phase synthesis of peptides

Marta Planas,<sup>a,b</sup> Susumu Funakoshi,<sup>c,\*</sup> Eduard Bardajía<sup>a</sup> and Fernando Albericio<sup>d</sup>

<sup>a</sup>Faculty of Sciences, University of Girona, 17071 Girona, Spain

<sup>b</sup>Department of Chemistry, University of Minnesota, Minneapolis, MN 55455, USA

<sup>c</sup>Faculty of Pharmaceutical Sciences, Kyoto University, Kyoto 606, Japan

<sup>d</sup>Department of Organic Chemistry, University of Barcelona, 08028 Barcelona, Spain

Convergent solid-phase peptide synthesis is one of the most attractive strategies for the synthesis of large peptides or small proteins. Up to now, several handles have been developed for anchoring and selectively removing the peptides from the polymer support with the protecting groups intact. Photo labile [1], fluoride labile [2] or Pd(0) [3] cleavable handles have been designed to suit either Boc or Fmoc chemistries. The use of hypersensitive acid-labile [4] or of nucleophile- and base-labile [5] handles allow only the preparation of Fmoc/*t*-butyl or of Boc/Bzl protected peptides respectively.

We report here the synthesis and development of a new handle, *N*-{2-[4-(hydroxyethylsulfonyl)benzenesulfonyl]ethyl}succinamic acid (EBEL) **1** labile to bases through a  $\beta$ -elimination process. This handle is based into alkyl/arylsulfonyl ethoxycarbonyl groups used for temporary *N* <sup>$\alpha$</sup> -protection [6].

## Results and Discussion

*N*-{2-[4-(hydroxyethylsulfonyl)benzenesulfonyl]ethyl}succinamic acid **1** was synthesized in four steps from commercially available 2-(4-chlorophenylthio)ethanol (Fig. 1) in an overall yield of 43% after purification.

The EBEL handle (5 equiv.) was attached to an amino functionalized PEG-PS resin (0.28 mmol/g) containing NLeu as internal reference with DIPCDI and HOBT using DMF as solvent. A qualitative ninhydrin test was used to ascertain the completion of the coupling. The *C*-terminal Boc-amino acid (5 equiv.) was anchored to the hydroxyethyl group of the EBEL-resin using DIPCDI and HOBT in the presence of catalytic amount of DMAP in DMF. Peptides were then built up by a Boc/Bzl strategy following standard protocols used in our laboratories.

Boc-Leu-OH and Boc-Phe-OH were stepwise attached to the handle-resin and the resultant dipeptide used as a model to evaluate the stability of the linkage towards DMF and DIEA. Amino acid analysis of both the acid hydrolysates of the resin before and after the cleavage showed that the EBEL-resin is stable to DMF (24h at 25° C) and that the low loss observed upon treatment with DIEA-DMF (1:19) (<7% loss after 2h at 25° C) does not prevent its use on SPPS using a Boc/Bzl strategy.

---

\* Deceased.

A kinetic study of the cleavage of a rather hindered amino acid [Boc-Tyr(BrZ)-OH] was performed in order to establish the lability of EBEL-resin. These experiments showed that a 35 min. treatment with piperidine-DMF (1:19) was sufficient to cleave the model amino acid from the resin. However, to cleave protected peptides longer times and more concentrated piperidine solutions [2-4 hours, piperidine-DMF/CH<sub>2</sub>Cl<sub>2</sub> (2:8, v/v)] were needed.

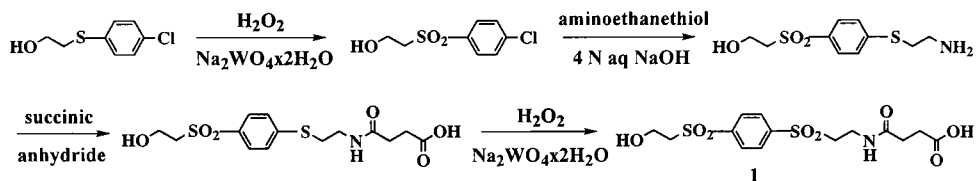


Fig. 1. Synthesis of the EBEL handle.

The usefulness of the new handle was demonstrated by the synthesis of Boc-Leu-enkephalin, Boc-Ala-Arg(Tos)-Lys(CIz)-Leu-Ala-Asn-Gln-OH and Boc-Phe-Gly-Gly-Phe-Thr(Bzl)-Gly-Ala-Arg(Tos)-Lys(CIz)-Ser(Bzl)-OH. Those peptides were successfully cleaved with piperidine [piperidine-DMF/CH<sub>2</sub>Cl<sub>2</sub> (2:8, v/v), 2-4 hours].

In summary, the new handle *N*-{2-[4-(hydroxyethylsulfonyl)benzenesulfonyl]ethyl}succinamic acid is easily synthesized and can be used with any amino-functionalized resin. The anchor has proved to be stable throughout SPPS approach following a standard Boc/Bzl strategy, even to the neutralization step with tertiary amines such as DIEA.

## References

1. Kneib-Cordonier, N., Albericio, F. and Barany, G., *Int. J. Peptide Protein Res.*, 35 (1990) 527, and references cited therein.
2. Mullen, D.G. and Barany, G., *J. Org. Chem.*, 53 (1988) 5240, and references cited therein.
3. Lloyd-Williams, P., Merzouk, A., Guibé, F., Albericio, F. and Giralt, E., *Tetrahedron Lett.*, 35 (1994) 4437, and references cited therein.
4. Albericio, F. and Barany, G., *Tetrahedron Lett.*, 32 (1991) 1015, and references cited therein.
5. Rabanal, F., Giralt, E. and Albericio, F., *Tetrahedron*, 51 (1995) 1449, and references cited therein.
6. a) Verhart, C.G.J. and Tesser, G.I., *Recl. Trav. Chim. Pays-Bas*, 107 (1988) 621.  
b) Funakoshi, S., Fukuda, H. and Fujii, N., *Proc. Natl. Acad. Sci. USA*, 88 (1991) 6981.  
c) García-Echeverría, C., *Chem. Comm.*, (1995) 779.

# Side reactions during synthesis of p-benzoylphenylalanine scanned analogs of the yeast tridecapeptide pheromone

Michael Breslav,<sup>a,b</sup> Boris Arshava,<sup>a</sup> Jeffrey M. Becker<sup>c</sup> and Fred Naider<sup>a</sup>

<sup>a</sup>Department of Chemistry, College of Staten Island, City University of New York, Staten Island, NY 10314; <sup>b</sup>R.W. Johnson Pharmaceutical Research Institute, Spring House, PA 19477;

<sup>c</sup>Departments of Microbiology and Biochemistry, Cellular and Molecular Biology, University of Tennessee, Knoxville, TN 37996, USA

p-Benzoylphenylalanine (Bpa) is an unnatural amino acid which has been used for the UV initiated cross-linking of Bpa-containing biologically active peptides with binding sites of receptors and enzymes. One of the problems associated with this field of research is to insert Bpa in the peptide molecule without compromising biological activity. In order to find the most active Bpa-containing analogs of the  $\alpha$ -factor from *Saccharomyces cerevisiae* we synthesized a Bpa-scanned series of an analog (WHWLQLRPGQP-Nle-Y) of this tridecapeptide. We prepared 10 analogs using automated Fmoc-based SPPS on a Wang resin followed by cleavage from the resin using the conventional 95% TFA/2.5% water/2.5% 1,2-ethanedithiol (EDT) cocktail [1].

## Results and Discussion

Major impurities caused by the reaction between the diaryl ketone side chain of Bpa and the EDT scavenger under the described cleavage conditions were observed in the crude products recovered for the 10 Bpa-containing peptides [1]. Efforts to reverse the reaction and regenerate Bpa from its dithioketal derivative were subsequently initiated (Fig. 1).

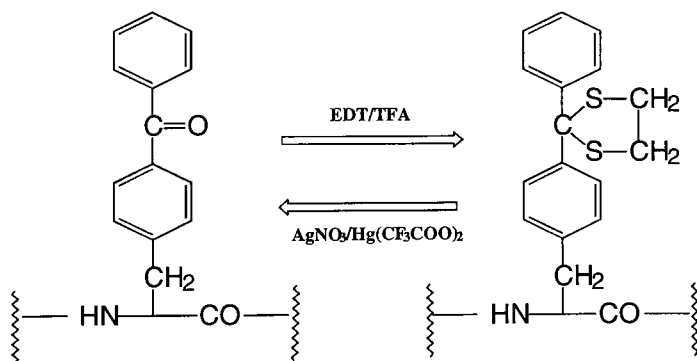


Fig. 1. Reversible transformation of Bpa to and from its dithioketal derivative.

Previous attempts to reverse dithioketal formation have utilized mercury salts or dimethylsulfoxide at high temperature [2,3]. Using dimethylsulfoxide under published conditions we observed the complete decomposition of the Bpa-containing  $\alpha$ -factor analogs. Accordingly, dithioketals of a model tripeptide (Ac-Ala-Bpa-Leu-OH) or of one of the  $\alpha$ -factor analogs were dissolved in a 50% water/acetonitrile mixture at a concentration of 0.5 - 2.0 mg/ml, mercury (II) trifluoroacetate was added to the reaction mixture and the progress of the reverse transformation of the Bpa(dithioketal) to Bpa was monitored using HPLC. Regeneration of the Bpa function in [Ac-Ala-Bpa(dithioketal)-Leu-OH] proceeded rapidly under these conditions. In contrast, we noted in the case of several Bpa-containing  $\alpha$ -factor analogs that there was significant degradation of the peptide, thus leading us to explore other conditions for regeneration of this photosensitive moiety.

With silver nitrate as the reagent we observed a slow but highly specific regeneration of the Bpa functionality from its dithioketal derivative. A large molar excess of this metal salt over the peptide was required for complete reaction. However, in contrast to  $\text{Hg}(\text{CF}_3\text{COOH})_2$ , in no case using silver nitrate did we observe side reactions with the  $\alpha$ -factor analogs. We found that the use of the mercury salt calls for an accurate salt-to-peptide ratio which is hard to maintain because of the uncertain residual amounts of TFA, water and other solvents in peptides after HPLC purification. Transformation was only ~75% when a supposedly equimolecular amount of  $\text{Hg}(\text{CF}_3\text{COOH})_2$  was weighed and added to the reaction medium, and a 1.5 molar excess of this salt was necessary for 100% conversion. Since excess  $\text{Hg}(\text{CF}_3\text{COOH})_2$  may cause modification of amino acids with sensitive side chain groups such as tryptophan, the silver nitrate method may prove advantageous. In addition, this method avoids the problem of disposal of mercury ions in the waste solvents.

To summarize, unintended reaction of the Bpa with dithioketals may be avoided by excluding conventional EDT from the cleavage cocktail or substitution of EDT with dithiothreitol, which does not react with Bpa [1]. However, if desired, dithioketal formation may be used for temporary protection of the light sensitive Bpa function followed by the regeneration with  $\text{Hg}(\text{CF}_3\text{COOH})_2$  or  $\text{AgNO}_3$ .

## Acknowledgments

These studies have been supported by NIH grants GM22086 and GM22087. One of us acknowledges the excellent scientific support of RWJPRI management.

## References:

1. Breslav, M., Becker, J. and Naidler, F., *Tetrahedron Lett.*, 38 (1997) 2219.
2. Srinivasa Rao, H., Chandrasekharam, M., Ila, H. and Junjappa, H., *Tetrahedron Lett.*, 33 (1992) 8163.
3. Seebach, D., *Synthesis*, 1 (1969) 17.

# Diaminopimelate-containing isopeptides are cleavable by leucine aminopeptidase and metalloproteinases in tumors

Yoshimitsu Yamazaki, Michael Savva and Michael Mokotoff

Department of Pharmaceutical Sciences, School of Pharmacy, University of Pittsburgh,  
Pittsburgh, PA 15261, USA

In this study we describe a method for designing prodrugs of biologically active peptides. It involves blocking the side-chain functionality of a specific amino acid residue essential for its biological activity with a protective group that can later be removed enzymatically. Although a few studies have been done on the enzymatic deprotection of side-chain functional groups, little has been reported regarding *in vivo* enzymatic deprotection for purposes of drug activation. Mezoë et al. [1] has reported that a tuftsin (Thr-Lys-Pro-Arg) derivative acylated by Thr at the  $\epsilon$ -amino group of Lys, Lys(Thr)-Pro-Arg, was hydrolyzed at the isopeptide Lys(Thr) linkage by leucine aminopeptidase (LAP), but that the reaction rate was very slow. The  $\epsilon$ -amino group of Lys is a good modification site because this amino acid appears in many biologically active peptides, generally has some role in biological activity, and thus could afford a temporarily inactivated derivative when modified. It also can easily be modified by acylation to form a chemically stable isopeptide linkage, whereas side-chain acylation of amino acid residues Arg, Ser, Tyr and Cys give labile isopeptide linkages, and Lys isopeptide linkages can be deblocked by LAP with wide substrate specificity [2]. Aminopeptidase N, similar in activity to LAP, was reported to be rich in human melanoma cells [3], suggesting that this enzyme could be used for tumor-specific drug activation.

Protease cleavage of isopeptides branching at the Lys  $\epsilon$ -amino group has been found to be slow compared with linear peptides. We postulate that the slow rate is due to the lack of an amide or carboxyl group  $\alpha$  to the Lys  $\epsilon$ -nitrogen cleavage site, and thus the isopeptide bond is amide-like, whereas by substituting 2,6-diaminopimelic acid (Dpm) for Lys, the corresponding isopeptide bond is more peptide-like. Many synthetic peptides containing the Dpm residue have been prepared, but the enzymatic cleavage of an isopeptide bond from Dpm has not been reported in the literature. Therefore, this study was initiated to compare the ability of proteases to cleave isopeptide bonds in both Lys- and Dpm-containing peptides.

## Results and Discussion

We prepared (2S,6S)-Z-Dpm(Z)(OMe) by protease-mediated hydrolysis of (R,R/S,S)-Z-Dpm(Z)(OMe)-OMe and then converted it to (2S,6S)-Dpm(Z)(OMe) via  $\text{PCl}_5$  to an NCA intermediate and hydrolysis. Protection of the free amino group with Boc, ammonolysis of the Me ester, hydrogenolysis of the Z group, and protection with Fmoc gave (2S,6S)-Boc-Dpm(Fmoc)(NH<sub>2</sub>) (**1**). Using **1** and SPPS, we prepared Ac-Gly-(2S,6S)-Dpm(Leu)(NH<sub>2</sub>)-

Ala (**2**), Ac-Gly-(2S,6S)-Dpm(Ac-Gly-Pro-Gln-Gly-Leu)(NH<sub>2</sub>)-Ala (**3**) and Ac-Gly-(2S,6S)-Dpm(NH<sub>2</sub>)-Ala (**6**) and the Lys peptides Ac-Gly-Lys(Leu)-Ala (**4**), Ac-Gly-Lys(Ac-Gly-Pro-Gln-Gly-Leu)-Ala (**5**) and Ac-Gly-Lys-Ala (**7**).

Enzymatic and kinetic studies showed that the Leu moiety in **2** was hydrolyzed 68-fold and >1000-fold more rapidly than it was from **4** by microsomal LAP and cytosol LAP, respectively, via comparison of their *V<sub>max</sub>* values. The rate of formation of Leu from **2** was also faster than the formation of Leu from Leu-NH<sub>2</sub> by both LAP's. The enzymatic cleavage of Leu from **2** was also greater than from **4** when incubated with homogenates of various tissues from C57Bl/6 mice implanted with C3 sarcomas. The tumor homogenate was better able to cleave Leu from **2** than from **4** by a factor of about 8-9, was higher than those of lung, muscle and blood, but about equal to that of liver and intestine. In an attempt to suppress isopeptide cleavage in tissues other than tumor we prepared peptides **3** & **5** because it is known that Ac-Gly-Pro-Gln-Gly-Leu is a substrate for matrix metalloproteinases (MMPs) and is preferably cleaved between the Gly-Leu bond [4]. Because malignant tumors are usually rich in MMPs [5], we expected that isopeptides protected by this sequence would, after cleavage of Ac-Gly-Pro-Gln-Gly, leave Leu remaining which would then be cleaved by LAP. In fact, isopeptides **3** & **5** were enzymatically cleaved by tissue homogenates to Leu, Ac-Gly-Pro-Gln-Gly and the parent peptides **6** & **7**. The rate of liberation of Leu was again faster from **3** than from **5**.

## Conclusion

The synthesis of (2S,6S)-Boc-Dpm(Fmoc)(NH<sub>2</sub>), a blocked carboxamide analog of Lys, which has potential use in the preparation of isopeptides with enhanced enzymatic side-chain cleavage, was accomplished. The entire penta-isopeptide side-chain of **3** & **5** was presumably cleaved by the cooperative action of LAP and MMP present in C3 sarcoma tissue and occurred more efficiently with Dpm-isopeptide **3** than with Lys-isopeptide **5**. These studies suggest that Dpm-containing isopeptides may be for the design of peptide prodrugs useful for targeting protease-rich tumors.

## References

1. Mezoe, G., Szekerke, M., Sarmay, G. and Gergely, J., *Peptides*, 11 (1990) 405.
2. Plessing, A., Siebert, G., Wissler, J.H., Puigserver, A.J. and Pfaender, P., *Hoppe-Seyler's Z. Physiol. Chem.*, 363 (1982) 279.
3. Menrad, A., Speicher, D., Wacker, J. and Herlyn, M., *Cancer Res.*, 53 (1993) 1450.
4. Netzel-Arnet, S., Sang, Q.-X., Moore, W.G.I., Navre, M., Birkedal-Hansen, H. and Van Wart, H.E., *Biochemistry*, 32 (1993) 6427.
5. MacDougall, J.R. and Matrisian, L.M., *Cancer Metastasis Rev.*, 14 (1995) 351.

# Synthesis and optical properties of cyclic bis-cysteinyl-peptides and their linear precursors with a built-in light-switch

Michaela Schenk,<sup>a</sup> Sabine Rudolph-Böhner,<sup>a</sup> Josef Wachtveitl,<sup>b</sup> Thomas Nägele,<sup>b</sup> Dieter Oesterhelt<sup>a</sup> and Luis Moroder<sup>a</sup>

<sup>a</sup> Max-Planck-Institut für Biochemie, 82152 Martinsried, Germany; <sup>b</sup> Institut für Medizinische Optik, LMU, 80797 München, Germany.

The redox potentials of active-site fragments of thiol-protein oxidoreductases depend strongly the intervening dipeptide sequence of the Cys-X-Y-Cys motif and the preferred conformation of the disulfide-bridged loops [1]. Strong effects on the redox properties are, therefore, to be expected from the restriction of the conformational space of such bis-cysteinyl-peptides via backbone cyclization. Further modulation of the conformational and, correspondingly, the redox properties of the cyclic bis-cysteinyl-peptides were envisaged by incorporation of photoresponsive moieties into the peptide backbone, e.g. of an azobenzene group capable of significant light-induced configurational changes (size of the molecule in *trans* 9.0 Å and in *cis* 5.5 Å).

## Results and Discussion

Unlike the azobenzene derivative reported by Ulysse *et al.* [2] we selected (4-amino)phenylazobenzoic acid (APB) as the light-switchable pseudo-amino acid where the absence of spacers for both the amino and carboxyl function should guarantee a maximum of impact of the photomodulated azobenzene configuration on peptide conformation. This azobenzene derivative is characterized by extremely poor nucleophilicity of the amino group which, however, could be exploited for its C-terminal extension to the pseudo-dipeptide derivative without additional N-protection. The amino group of the resulting H-APB-Ala-OtBu then proved to be sufficiently nucleophilic to allow, after silylation, for its acylation via the fluoride procedure. Upon C-terminal deprotection, the intermediate **1** (Fig. 1) was used as synthon in the subsequent steps of peptide synthesis to produce the linear nonapeptide derivative H-Phe-APB-Ala-Cys(StBu)-Ala-Thr(tBu)-Cys(StBu)-Asp(OtBu)-Gly-OH.

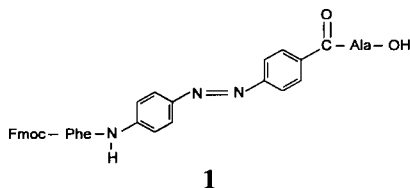


Fig. 1. *N*- and *C*-derivatized (4-amino)phenylazobenzoic acid (APB) as synthon for incorporation into peptide sequences.

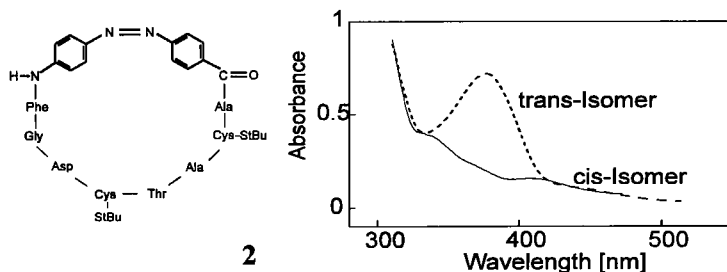


Fig. 2. Structure of the thiol-protected monocyclic peptide **2** corresponding to the active-site sequence 134-141 of thioredoxin reductase bridged by the light-switch APB; UV spectra of the thermally stable *trans*- and *cis*-isomers, fully interconvertible by irradiation at 370 and 430 nm, respectively.

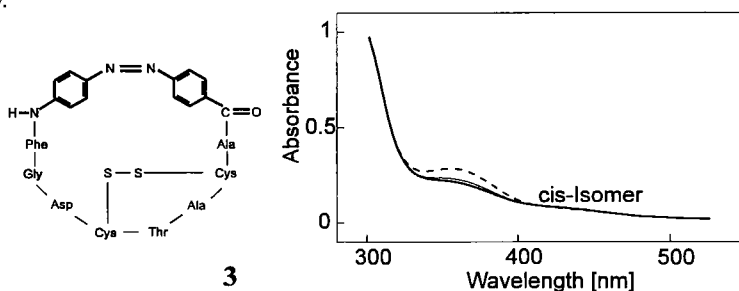


Fig. 3. Structure of the disulfide-bridged bicyclic peptide and the related UV spectra of the *cis*-isomer prior to and upon irradiation at 430 nm.

The azobenzene moiety of the linear peptide is essentially in *trans*-configuration, and its light-induced *trans*→*cis* isomerization was found to be fast, fully reversible and without effect on the cyclization step to the monocyclic compound **2** (Fig. 2). Conversely, the monocyclic thiol-protected peptide **2** behaves as bistable system, fully interconvertible upon irradiation, but characterized by extremely slow thermal relaxation. Finally, phosphine-mediated cysteine deprotection and air oxidation leads to quantitative conversion of the monocyclic peptide **2** to the bicyclic peptide **3** with the azobenzene moiety in exclusively *cis*-configuration (Fig. 3). In the bicyclic form the system is virtually non-responsive to irradiation, confirming a maximum of rigidity as required for efficient photomodulation of the redox potentials of the systems *cis*-**2**→*cis*-**3** and *trans*-**2**→*cis*-**3**.

## References

1. Moroder, L., Besse, D., Musiol, H.-J., Rudolph-Böhner, S. and Siedler, F., *Biopolymers Peptide Sci.*, 40 (1996) 207.
2. Ulysse, L., Cubillos, J. and Chmielewski, J. *Am. Chem. Soc.*, 117 (1995) 8466.

# Cyclodextrin as carrier of bioactive peptides

Norbert Schaschke,<sup>a</sup> Stella Fiori,<sup>a</sup> Daniel Fourmy<sup>b</sup> and Luis Moroder<sup>a</sup>

<sup>a</sup>Max-Planck-Institut für Biochemie, 82152 Martinsried, Germany; <sup>b</sup>INSERM U151, CHU Rangueil, 31054 Toulouse Cedex 04, France

We have recently elaborated the chemistry of mono-functionalization of  $\beta$ -cyclodextrin with linear and flexible carboxyalkyl spacers for the synthesis of peptide conjugates [1]. Covalent grafting of the calpain inhibitor I, Leu-Leu-Nle-H, to the cyclomaltoheptaose, in addition to enhancing the solubility of the peptide aldehyde, was found to lower only negligibly its inhibitory power. Mapping the ligand binding sites of the CCK-B/gastrin receptor by the use of lipo-gastrin peptides, mutagenesis data and molecular modelling led to a hormone binding model consisting of insertion of the C-terminal tetrapeptide amide of gastrin, i.e. the message part of the hormone, into the helix bundle with the residual N-terminal extension interacting mainly with the extracellular portion of the receptor at the water/lipid interphase [2]. According to this binding model, covalent linkage of the tetragastrin moiety to  $\beta$ -cyclodextrin via a sufficiently large spacer was expected to allow for binding to the receptor with minimal effects on affinity.

## Results and Discussion

Adopting a succinyl group as C4 spacer, both the tetra- and heptagastrin peptide were linked to  $\beta$ -cyclodextrin to produce the conjugates **1** and **2** (Fig. 1). The intra-peptide and inter-peptide/carbohydrate NOEs of [Nle<sup>15</sup>]-HG-[14-17]/ $\beta$ -cyclodextrin in aqueous

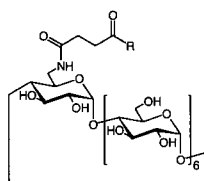


Fig. 1. Gastrin/ $\beta$ -cyclodextrin conjugates: **1**,  $R = \text{Trp-Nle-Asp-Phe-NH}_2$ , **2**,  $R = \text{Ala-Tyr-Gly-Trp-Nle-Asp-Phe-NH}_2$ .

solution are strongly supportive of a bended conformation of the peptide moiety with significant interactions of the aromatic side chains of Trp and Phe with the carrier molecule in a host/guest-type complexation. This is further supported by the CD spectra of the conjugate in the far uv region but particularly in the near uv region where the sharp  $L_b$  bands of Trp (at 282 and 289 nm) and the well resolved vibronic structure of the phenyl  $L_b$  transitions indicate rigidity of the two aromatic groups. Conversely, both the NOESY

Table 1. Binding affinities of gastrin/ $\beta$ -cyclodextrin conjugates to the CCK-B/gastrin receptor expressed in COS7 cells.

Gastrin/ $\beta$ -Cyclodextrin Conjugate	IC <sub>50</sub> [nM]
H-Trp-Met-Asp-Phe-NH <sub>2</sub>	12.0
$\beta$ -CD-NH-CO-(CH <sub>2</sub> ) <sub>2</sub> -CO-Trp-Nle-Asp-Phe-NH <sub>2</sub> (1)	18.0
Pyr-Ala-Tyr-Gly-Trp-Nle-Asp-Phe-NH <sub>2</sub>	3.2
$\beta$ -CD-NH-CO-(CH <sub>2</sub> ) <sub>2</sub> -CO-Ala-Tyr-Gly-Trp-Nle-Asp-Phe-NH <sub>2</sub> (2)	8.0

spectrum of [Nle<sup>15</sup>]-HG-[11-17]/ $\beta$ -cyclodextrin and its CD spectra in the near and far uv indicate a large degree of flexibility of the peptide chain in this conjugate which apparently is no longer interacting with the hydrophobic cavity of the cyclomaltoheptaose. It is well known that the K<sub>d</sub> values of inclusion complexes of  $\beta$ -cyclodextrin with hydrophobic compounds are in the mmolar range whereas ligand/receptor complexes are generally characterized by nmolar K<sub>d</sub> values. Correspondingly, complexation of receptor ligands to cyclodextrin is not expected to affect their binding affinities. In fact, the IC<sub>50</sub> values of the gastrin-peptide/ $\beta$ -cyclodextrin conjugates **1** and **2** for the CCK-B/gastrin receptor were comparable to those of the parent tetra- and heptagastrin, as shown in Table 1. In both cases the affinity is lowered by a factor of about 2, independently of whether host/guest-type complexation is taking place. These results support the proposed binding mode of gastrin to the receptor with insertion of solely the C-terminus into the helix bundle since the cyclomaltoheptaose moiety with its highly hydrophilic outer surface and considerable size can hardly insert itself into more hydrophobic interiors of the receptor. In the parent gastrin peptide on the other hand the N-terminal extension of the heptagastrin consists of the characteristic pentaglutamic acid sequence which in the conjugates could be mimicked by the  $\beta$ -cyclodextrin moiety at least in terms of hydrophilicity. However, a related effect on the IC<sub>50</sub>, i.e. an enhanced binding affinity as observed upon elongation of the heptagastrin with the [Glu]<sub>5</sub> sequence, could not be observed. In contrast to previous results obtained with the enkephalin conjugate DPDPE/ $\beta$ -cyclodextrin [3], their receptor binding affinities were largely retained upon linkage of the gastrin peptides to  $\beta$ -cyclodextrin. Moreover, in the case of the tetragastrin compound **1**, all the beneficial effects of this type of drug carrier system can be envisaged in addition to full water solubility.

## References

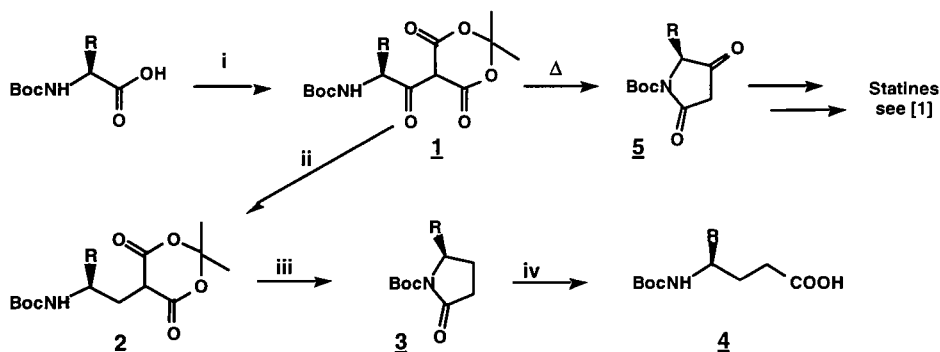
- Schaschke, N., Musiol, H.-J., Assfalg-Machleidt, I., Machleidt, W., Rudolph-Böhner, S. and Moroder, L., *FEBS Lett.*, 391 (1996) 297.
- Lutz, J., Romano-Götsch, R., Escrieut, Ch., Fourmy, D., Mathä, B., Müller, G., Kessler, H. and Moroder, L., *Biopolymers*, 41 (1997) 799.
- Hristova-Kazmierski, M.K., Horan, P., Davis, P., Yamamura, H.I., Kramer, T., Horvath, R., Kazmierski, W.M., Porreca, F. and Hruby, V.J., *Bioorg. Med. Chem. Lett.*, 3 (1993) 831.

## Facile stereoselective synthesis of $\gamma$ -amino acids from the corresponding $\alpha$ -amino acids

Pavel Majer, Martin Smrcina, Eva Majerová, Tatiana A. Guerassina and Michael A. Eissenstat

Structural Biochemistry Program, SAIC, National Cancer Institute, Frederick Research and Development Center, Frederick MD, 21702-1201, USA

Recently, while synthesizing 3-hydroxy-4-t-butoxycarbonylamino-5-phenyl pentanoic acid using a modification of the described procedure [1], we consistently observed a side product after sodium acetoxyborohydride mediated reduction of tetramic acid **5**. Analysis of the NMR spectra of the side product revealed the presence of three carbonyls and the acetonide moiety. It was thus assigned structure **2** ( $R = \text{benzyl}$ ), resulting from complete reduction of exocyclic carbonyl of **1**. Unreacted **1** present in crude **5** apparently underwent reduction of its ketone functionality, followed by dehydration to unsaturated ester which was further reduced to **2** (Scheme 1). A literature search revealed that the analogous reduction of acyl derivatives of Meldrum's acid and barbituric acid have been described [2], but its synthetic potential has been virtually unexplored.



Scheme 1.  $R = \text{benzyl}$  (Phe),  $i$ -propyl (Val),  $i$ -butyl (Leu), benzyloxymethyl (Ser(Bzl)), benzylthiomethyl (Cys(Bzl)), benzyloxycarbonylmethyl (Asp(Bzl)).

i) Meldrum's acid, DCC, DMAP,  $\text{CH}_2\text{Cl}_2$ ,  $0^\circ\text{C}$ , 12h; ii) toluene, reflux, 3h; iii)  $\text{NaBH}_4$ , AcOH,  $\text{CH}_2\text{Cl}_2$ ,  $-5^\circ\text{C}$ , 8h; iv) NaOH, acetone, water, 0.5h.

Decarboxylative ring closure of compound **2** forms the N-Boc-5-substituted pyrrolidinone, precursor of the corresponding  $\gamma$ -substituted,  $\gamma$ -amino acid **4**. These functionalities are found in natural compounds [3],  $\gamma$ -Amino acids have been used for peptide modification [4], possess various biological activities [5], and could also serve as building blocks for combinatorial chemistry.

## Results and Discussion

In our method (Scheme 1) the N-t-butoxycarbonyl (Boc) protected amino acid is coupled with Meldrum's acid at 0°C in dichloromethane using dicyclohexyl carbodiimide (DCC) and 4-dimethylaminopyridine (DMAP) for activation. The precipitated dicyclohexyl urea is filtered off and DMAP removed by bisulfate extraction. The CH<sub>2</sub>Cl<sub>2</sub> solution is dried with MgSO<sub>4</sub> and used directly for the sodium acetoxyborohydride reduction which gives **2**, typically in 60 to 90% overall yield. The intermediates **2** are stable and easy to purify. The decarboxylative ring closure of **2** proceeds smoothly and gives the 5-substituted pyrrolidinones **3** in high yields and sufficient purity to be used for the next step. The final basic hydrolysis gives the N-Boc- $\gamma$ -amino acids **4** in almost quantitative yield. The convenience of the present method is best shown by its comparison with the published procedure based on alkylation of diethylmalonate [6]. Our method is shorter, directly yields the N-Boc protected  $\gamma$ -amino acid in 40 to 60 % overall yield, and because the reaction conditions in all steps are mild, is compatible with most common side chain protecting groups and sensitive functionalities.

Stereoselectivity of the present method was proven by comparison of  $[\alpha]_D$  with literature values where were available and by synthesis of separable diastereoisomeric derivatives.

## Conclusion

We have developed a short stereospecific and general method of conversion of  $\alpha$ -amino acids to corresponding  $\gamma$ -amino acids.

## References

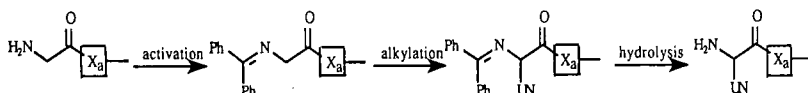
1. Jouin, P., Castro, B., Nisato and D., *J. Chem. Soc. Perkin Trans. I*, (1987) 1177.
2. a) Nutaitis, C.F., Schultz, R.A., Obaza, J. and Smith, F.X., *J. Org. Chem.*, 45 (1980) 4606.  
b) Obaza, J. and Smith, F.X., *Synth.Comm.*, 12 (1982) 19.  
c) Rosowsky, A., Forsch, R., Uren, J., Wick, M., Kumar, A. and Freisheim, J., *J. Med. Chem.*, 26 (1983) 1719.
3. Ackermann, J., Matthes, M. and Tamm, C., *Helv. Chim. Acta*, 73 (1990) 122.
4. Rajashekhar, B. and Kaiser, E.T., *J. Biol. Chem.*, 261 (1986) 13617.
5. a) Killinger, S., Blume, G.L., Bohart, L., Bested, A., Dias, L.S., Cooper, B., Allan, R.D. and Balcar, V.J., *Neurosci. Lett.*, 216 (1996) 101.  
b) Wilk, S. and Thurston L.S., *Neuropeptides*, 16 (1990) 163.  
c) Silverman, R.B. and Levy, M.A., *J. Biol. Chem.*, 256 (1981) 11565.
6. Tseng, C.C., Terashima, S. and Yamada, S., *Chem. Pharm. Bull.*, 25 (1977) 29.

# Unnatural peptide synthesis (UPS): A positional scan study

Peteris Romanovskis,<sup>a</sup> David Mendel,<sup>c</sup> Martin J. O'Donnell,<sup>b</sup> William C. Scott,<sup>c</sup> Arno F. Spatola<sup>a</sup> and Changyou Zhou<sup>b</sup>

<sup>a</sup> Department of Chemistry, University of Louisville, Louisville, KY 40292 USA; <sup>b</sup> Department of Chemistry, Indiana University-Purdue University Indianapolis, Indianapolis, IN 46202, USA; <sup>c</sup> Lilly Research Laboratories, Indianapolis, IN 46285 USA

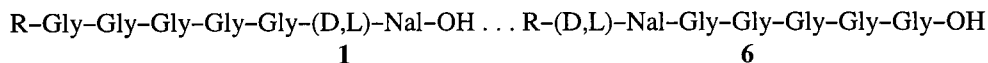
Unnatural peptide synthesis (UPS) is a method for introducing novel side chains during solid phase amino acid and peptide synthesis [1]. The technique involves activation of the N-terminal residue of the resin-bound substrate as a Schiff base (imine) followed by  $\alpha$ -carbon alkylation of this residue and then hydrolysis of the alkylated product.



Alkylation is accomplished at room temperature in the presence of the alkyl halide by using the strong, non-ionic phosphazene-type base, BEMP (Schwesinger base) (2).

## Results and Discussion

The scope of UPS has been explored further through the solid-phase synthesis of a series of model peptides including sequential isomers of hexaglycine 1-6 (R = quinaldoyl), in which the 2-naphthylmethyl (Nal) side chain is introduced by UPS on each one of the glycine residues.



Following cleavage of the products from the resin, the resulting hexapeptides were analyzed by LC-MS. LC-MS analysis results demonstrated that the further the Schiff base-activated glycine residue in the peptide chain is from the peptide-resin attachment point, the more likely formation of di-alkyl (and even tri-alkyl) by-products (Fig. 1).

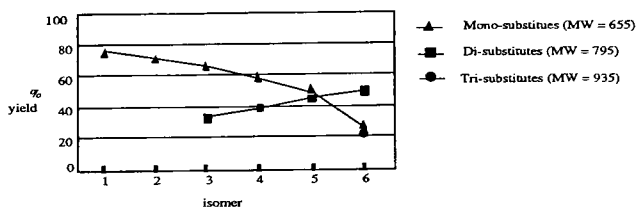
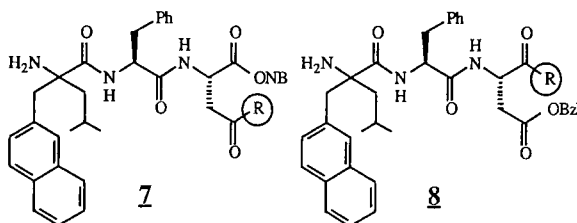


Fig. 1. Percentage of the mono-, di-, and tri-naphthylmethyl derivatives in the crude products of sequential isomers 1-6.

No special attempts were made to optimize the UPS conditions undertaken in this work. To the contrary, the hexaglycine model and the stoichiometries of the alkylating agent and Schwesinger base (4-times excess as opposed to only 2-times excess in the original method) amplify the occurrence of potential side products.

From these data it is apparent that the presence of increasing numbers of base-labile amide hydrogens leads to undesired oligo-N-alkylation, at least with the sterically accessible glycylic residues.



The use of UPS to prepare more sterically demanding resin-bound peptides has also been studied. Resin-bound tripeptide H-Leu-Phe-Asp- (attached either through  $\beta$ -Asp or the  $\alpha$ -COOH group), when activated by forming aldimine with 3,4-dichlorobenzaldehyde, submitted to alkylation (with 2-(bromomethyl)naphthalene in the presence of BEMP), hydrolyzed (with 1N HCl in THF), followed by deprotection and cleavage from the resin gave a good yield of the desired H-(D,L)-(Nal)Leu-Phe-Asp-OH (62% for 7 and 78% for 8, respectively).

Remarkably, in both of the latter cases, the presence of di-naphthylmethyl derivatives in the crude products was less than 5% as evidenced by LC-MS.

From an analysis of reaction by-products from our studies, we observed:

- rapid transesterification of the Asp  $\alpha$ -ONB ester by primary or secondary alcohols in the presence of small quantities of BEMP; the results indicate the sensitivity of the -ONB ester to the UPS conditions;
- incomplete Asp side chain deprotection by HF when the latter had been blocked as its -OBzl ester. This may be a function of partial steric hindrance.

From these results we conclude that with adequate precautions, the synthesis of at least some longer chain  $\alpha,\alpha$ -dialkylated peptides using the solid phase approach should be practical.

## Acknowledgements

Supported by NIH GM 33376 and by Lilly Research Laboratories.

## References

1. O'Donnell, M.J.; Zhou, C.; Scott, W.L. *J. Am. Chem.Soc.*, 118 (1996) 6070.
2. Schwesinger, R.; Schlemper, H.; Hasenfratz, C.; Willaredt, J.; Dambacher, T.; Breuer, T.; Ottaway, C. Fletschinger, M.; Boele, J.; Fritz, H.; Putzas, D.; Rotter, H.W.; Bordwell, F.G.; Satish, A.V.; Ji, G.-Z.; Peters, E.-M.; Peters, K.; von Schnering, H.G.; Walz, L. *Liebigs Ann.*, (1996) 1055.

# Preparation of peptide thioester segments using Fmoc-solid-phase peptide synthesis and application of the thioester ligation strategy to the construction of TASP molecules

Shiroh Futaki,<sup>a</sup> Koji Sogawa,<sup>a</sup> Masayuki Fukuda,<sup>a</sup> Mineo Niwa<sup>a</sup>  
and Hironobu Hojo<sup>b</sup>

*a*Institute for Medicinal Resources, The University of Tokushima, Tokushima 770, Japan

*b*Department of Bioapplied Chemistry, Faculty of Engineering, Osaka City University, Sumiyoshi-ku, Osaka 558, Japan

The distinctive feature of peptide synthesis using a partially protected S-alkyl thioester [1] is its feasibility in obtaining highly homogenous peptides and proteins. Direct preparation of the S-alkyl thioester by the Fmoc method is, however, difficult because the thioester is sensitive to piperidine. Here we report our new approach to prepare S-alkyl thioester segments with the aid of Fmoc-SPPS. Application of the thioester method to the preparation of a TASP molecule [2] composed of helices corresponding to a transmembrane segment of the calcium channel is also reported.

## Results and Discussion

The protected peptide fragment corresponding to one of the transmembrane segments (S4 in repeat IV) of rabbit skeletal muscle calcium channel [3] was prepared by Fmoc-SPPS on 2-chlorotrityl resin followed by detachment from the resin with AcOH-TFE-DCM (1:1:8) at r. t. for 1 h (Fig. 1). Coupling of the fragment with HS-(CH<sub>2</sub>)<sub>2</sub>-COOEt (20 eq) was then conducted in DMF using water soluble carbodiimide (WSCDI, 10 eq) (4°C, 12 h). Treatment of the protected thioester segment with 95% aqueous TFA (r. t., 2 h) followed by purification by HPLC afforded the desired segment **1** in a 20% yield. Another peptide segment corresponding to an alamethicin analog, Ac- Leu- Pro- Leu- Ala- Leu- Ala- Gln- Leu- Val- Leu- Gly- Leu- Leu- Pro- Val- Leu- Leu- Glu- Gln- Phe- Gly- S- (CH<sub>2</sub>)<sub>2</sub>-COOEt, was similarly prepared in good yield (59%).

In order to examine the applicability of the thioester method to the construction of TASP molecules, the above-obtained thioester segment **1** (12 eq) was introduced onto a Mutter-type template, Ac-Lys-Ala-Lys-Pro-Gly-Lys-Ala-Lys-Gly-NH<sub>2</sub>, in the presence of HOBt (36 eq), AgNO<sub>3</sub> (24 eq) and diisopropylethylamine (36 eq) in DMSO at 37°C for 48 h (Fig. 2). After DMSO was removed by evaporation, the sample was treated with 1M (CH<sub>3</sub>)<sub>3</sub>SiBr-thioanisole in TFA in the presence of *m*-cresol and ethanedithiol to remove the remaining Cl-Z group followed by the purification on HPLC to afford the desired four-helix-bundle protein **2** in a 19% yield (for the two steps).

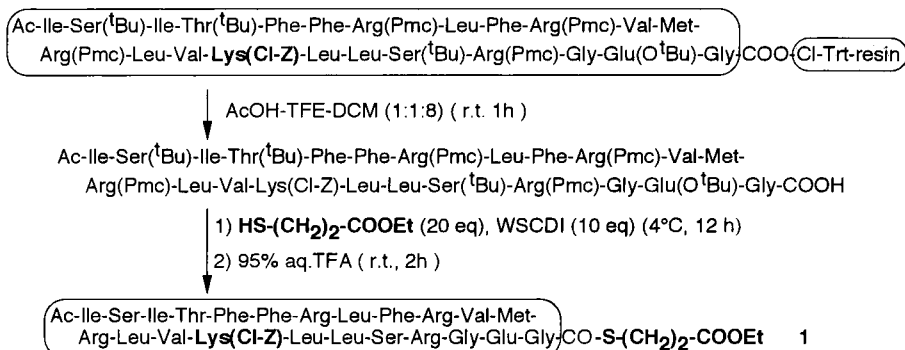


Fig. 1. Preparation of a peptide thioester segment **1** corresponding to a transmembrane sequence of the calcium channel (S4 in repeat IV).

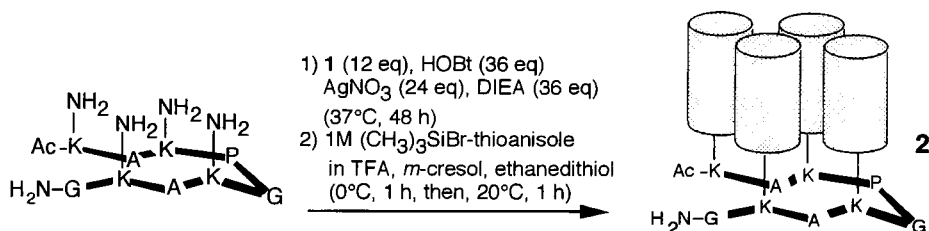


Fig. 2. Construction of a TASP molecule using a partially protected peptide thioester segment **1**.

In conclusion, we have developed a new approach to prepare the S-alkyl thioester of partially protected peptide segments using Fmoc-SPPS. Also, our results should open the way for the construction of TASP molecules using peptide thioesters. The ion channel activity of **2** is under investigation in our laboratory.

## References

1. Hojo, H. and Aimoto, S., *Bull. Chem. Soc. Jpn.*, 68 (1995) 330, and other referenced cited therein.
2. Mutter, M. *Angew. Chem., Int. Ed. Engl.*, 24 (1985) 639.
3. Tanabe, T., Takeshima, H., Mikami, A., Flockerzi, V., Takahashi, H., Kangawa, K., Kojima, M., Matsuo, H., Hirose, T. and Numa, S. *Nature*, 328 (1987) 313.

# Racemization induced by excess base during activation with uronium salts

**Jo-Ann Jablonski, Russel Shpritzer and Stephen P. Powers**

*Immologic Pharmaceutical Corporation, Waltham, MA 02154, USA*

Uronium salts have gained wide acceptance in SPPS as reagents which rapidly activate amino acids in polar solvents with low racemization and side reactions [1]. However, more recent publications have drawn attention to the susceptibility to racemization of some residues in the presence of the excess organic base customarily used with uronium salts [2]. We investigated the ability of excess base to promote racemization during pre-activation of Boc-protected amino acids with TBTU in DMF with or without HOBt. The extent of racemization was measured by hydrolysis of the activated amino acids and derivatization with Marfey's reagent. The effectiveness of pre-activation using one or two equivalents of base was compared by coupling to Val-PAM-resin, an amino component of recognized steric hindrance.

## Results and Discussion

Racemization was examined under three pre-activation conditions:

- a) To 0.6 M TBTU in DMF were added amino acid, then DIEA (molar ratio of 1:1:2).
- b) To 0.6 M amino acid in DMF were added HOBt, DIEA, then TBTU (molar ratio of 1:1:2:1).
- c) To 0.6 M amino acid in DMF were added DIEA, then TBTU (molar ratio of 1:1:1).

Aliquots were taken at the time points indicated in Fig. 1, and the active ester was separated using a C18 Sep Pak, eluted using acetonitrile/water, solvents removed by vacuum centrifugation and the Boc group removed by treatment with 6N HCl/dioxane 1:1 (a treatment which left the side-chain protection intact). Solvents were removed again and the amino acid derivatized with Marfey's reagent. The percentage of D-amino acid derivative was determined by HPLC. Control samples subjected only to removal of the Boc group showed levels of D-amino acid of approximately 0.2%.

For Boc-Asp(OcHex)-OH and Boc-Phe-OH racemization increased with time. When only one equivalent of base was used and when neutralization of the amino acid was performed before addition of the activating agent the rate of racemization was reduced.

The coupling efficiencies to Val-PAM-resin were compared for methods a and c. Pre-activation was performed for two minutes, and a three-fold excess of activated amino acid was added to a sample of the resin. Aliquots of resin were removed over the time course shown in Fig. 2. The degree of coupling was assessed using the quantitative ninhydrin test

[3]. Coupling efficiency was as good or better when one equivalent of base was used as when two equivalents of base were used.

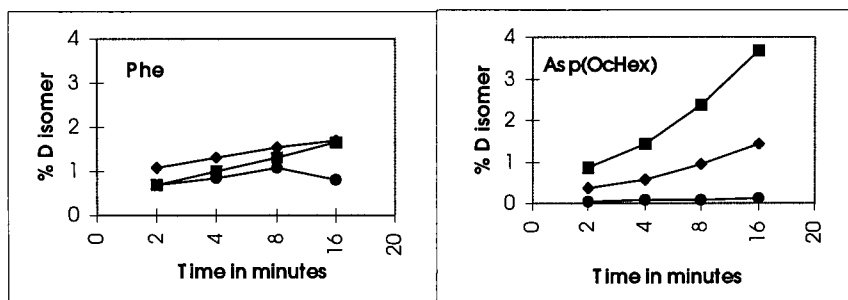


Fig. 1. Comparison of activation methods a (■), b (◆) and c (●) showing the % D isomer formed as a function of time.

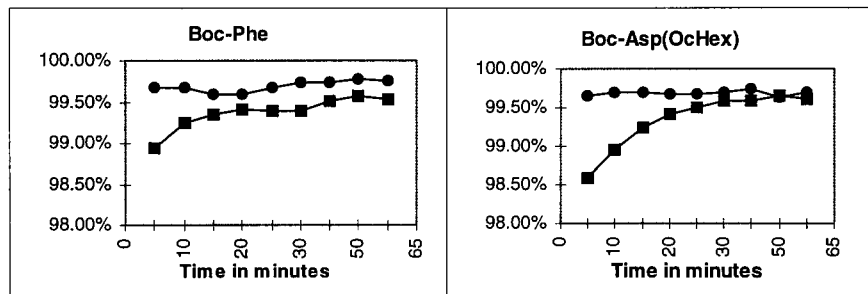


Fig. 2. Coupling efficiencies to Val-PAM resin using a 3-fold excess of amino acid pre-activated for 2 min using method a (■) or method c (●).

In the cases studied, mixing one equivalent of base with the amino acid component followed by addition of TBTU provided superior results in minimizing racemization and increasing coupling efficiency.

## References

- 1 Fields, C.G., Lloyd, D.H., Macdonald, R.L., Otteson, K.M. and Noble, R.L., Peptide Research, 4 (1991) 95.
- 2 Romoff, T.R. and Goodman, M., J. Peptide Res., 49 (1997) 281.
- 3 Sarin, V.K., Kent, S.B.H., Tam, J.P. and Merrifield, R.B., Analytical Biochem., 117 (1981) 147.

# Synthesis and characterization of a novel tryptophan derivative

Ted J. Gauthier, Bo Liu, Guillermo A. Morales and  
Mark L. McLaughlin

*Department of Chemistry, Louisiana State University, Baton Rouge, LA 70803, USA*

Fluorescence spectroscopy is uniquely capable of reporting structure and dynamics under conditions ranging from dilute solutions to intact cells. Tryptophan has been widely used to detect protein structures and dynamics [1]. However, tryptophan can have as many as six conformers, each of which is significant. As a result, each ground state tryptophan conformation can exhibit a distinct fluorescence lifetime [2]. This characteristic makes it possible, although challenging, to deduce structural information of tryptophan-containing peptides and proteins. Here, we report the synthesis and characterization of a novel tryptophan derivative specifically designed to limit its conformational flexibility. As a result, we are able to isolate and study just two of the six possible conformers.

## Results and Discussion

In order for tryptophan to be used more effectively as a conformational probe, the relationship between the fluorescence lifetimes and the six ground states must be determined. Ideally, we need to isolate each conformation and to study its fluorescence characteristics alone. We have synthesized a constrained tryptophan derivative which places the amino and carboxylate groups in fixed locations. This derivative mimics two of the six tryptophan conformers by judiciously fusing a six-membered ring to the  $\alpha$  and  $\beta$  carbons. The six-membered ring has two possible conformations about the  $C^\alpha$ - $C^\beta$  bond that can interconvert via a ring flip. However, a single  $C^\alpha$ - $C^\beta$  bond conformation is dictated by equatorial placement of the sterically bulky 3-indolyl substituent on the six-membered ring. Six-membered annulation and replacement of the  $\beta(S)$  hydrogen atom favors the  $C^\beta$ - $C^\gamma$  torsion angle of  $+90^\circ$ . This  $C^\beta$ - $C^\gamma$  torsion angle preference is due to van der Waals repulsion of the indole H4 with the axial hydrogen atom on C3 of the six-membered ring. Thus, the six-membered ring constrains both the  $C^\alpha$ - $C^\gamma$  and  $C^\beta$ - $C^\gamma$  torsion angles in tryptophan-like conformational geometries.

The synthesis of the target molecule begins with the formation of ketone **1** as reported by Freter [3]. Ketone **1** is converted to **2** via electrophilic aromatic substitution followed by hydantion formation via the Bücherer-Bergs synthesis [4]. The target molecule, **3**, is obtained by hydrolysis of **2** under strong alkaline conditions, high temperature and pressure (Fig.1).

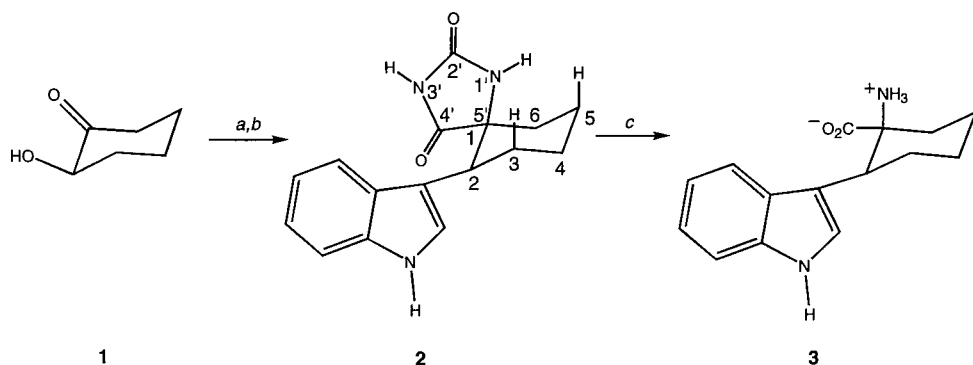


Fig. 1. Synthesis of tryptophan derivative. (a) Indole, HOAc,  $H_3PO_4$ ; (b) KCN,  $(NH_4)_2CO_3$ ; (c)  $Ba(OH)_2$ .

Edward and Jitrangri have studied the stereochemistry of the Bücherer-Bergs reaction [5]. They report that a Bücherer-Bergs reaction using 4-*tert*-butylcyclohexanone gives primarily one isomeric hydantoin, designated  $\alpha$ , and a trace of the other isomer,  $\beta$ . In our lab, chromatography shows that only one isomer is present. nOe difference spectroscopy and X-ray crystallography of the hydantoin indicates that only the  $\alpha$  isomer is obtained. A strong nOe is observed between the N1' proton ( $\delta=8.5$  ppm) and the C3 and C5 axial protons ( $\delta=1.99-1.42$  ppm) but no nOe is observed between the N1' proton and the C2 proton ( $\delta=3.36-3.20$  ppm). Because the  $\beta$  isomer would show an nOe between the N1' proton and the C6 and C2 axial protons, which was not observed the  $\alpha$  isomer is, therefore, the sole product of the Bücherer-Bergs reaction. NOESY experiments confirm that the  $C^\beta-C^\gamma = -90^\circ$  conformer is much more prevalent than the  $C^\beta-C^\gamma = +90^\circ$  conformer. A much stronger nOe is observed between the C2 proton with the C4' proton than with the C2' proton.

## Acknowledgment

We gratefully acknowledge support from NIH grant GM42101.

## References

1. Beecham, J.M. and Brand, L., *Ann. Rev. Biochem.*, 54 (1985) 43.
2. McLaughlin, M.L. and Barkley, M.D., *Meth. Enzymology*, (1997).
3. Freter, K., *Liebigs Ann. Chem.*, (1978) 1357.
4. Bücherer, H.T. and Lieb, V.A., *J. Prakt. Chem.*, 141 (1934) 5.
5. Edward, J.T. and Jitrangri, C., *Can. J. Chem.*, 53 (1975) 3339.

# On resin preparation of C-terminal peptide amides, analogs of the nematode neuropeptide PF1, SDPNFLRF-NH<sub>2</sub>, by application of a cysteine-specific precursor cleavage

Teresa M. Kubiak, Alan R. Friedman and Martha J. Larsen

*Pharmacia & Upjohn, Inc., Kalamazoo, MI 49001, USA*

Described in this report is a solid-phase variant of a procedure previously reported for the modification of recombinant proteins in solution to yield C-terminal amides [1, 2]. The hallmark of this method is a site-specific cleavage at the amino side of the peptide bond of an S-cyanylated cysteine residue located in the peptide chain [3]. This reaction, when carried out under mild aqueous alkaline conditions, affords two products, a peptide with a C-terminal carboxyl group, and a peptide with a 2-iminothiazolidine-4-carbonyl residue at the N-terminus [3]. In a similar way, C-terminal primary or secondary amides can be generated *via* a short-time exposure of the S-cyanylated peptide to moderate concentrations of aqueous ammonia or dilute amines, respectively [1, 2].

We adapted these methods to the on-resin preparation of C-terminal amides. In this approach, the cyanylation reaction and subsequent treatment with the amine are carried out on a side-chain deprotected, resin-bound, cysteine-containing precursor peptide (Scheme 1). The application of TentaGel-S-NH<sub>2</sub> resin is essential since it accommodates peptide synthesis and side-chain deprotection in pure organic solvents as well as the subsequent S-cyanylation and aminolysis under aqueous conditions.

## Results and Discussion

The cysteine-containing resin-bound precursors, SDPNFLRCGG-Resin, FLRC-Resin or FLRFCGG-Resin, were prepared starting with the attachment of Fmoc-Cys(tBu) either directly or through a Gly-Gly spacer to TentaGel-S-NH<sub>2</sub> resin (Advanced ChemTech), after which the main steps were as follows: (i) peptide synthesis via Fmoc chemistry, (ii) Fmoc removal with 20% piperidine in DMF and side chain deprotection with Reagent K, followed by a series of sequential washes with DCM, ACN and 0.1M AcOH; (iii) a 15-20 min. on-resin S-cyanylation reaction with 0.05-0.15 M 1-cyano-4-(dimethylamino)-pyridinium tetrafluoroborate (CDAP) in aqueous 0.1 M AcOH (3-5 fold molar excess) followed by a series of washes with 0.1 M AcOH and water; (iv) a 30 to 60 minute treatment of the S-cyanylated resin-bound peptide with 0.2 M-0.4 M amine (phenethylamine or methylamine) in 30% aqueous acetonitrile (ca. 10-20 molar excess). The latter step resulted in the cleavage and release from the resin of the C-terminally amidated peptides SDPNFLR-NH-(CH<sub>2</sub>)<sub>2</sub>-C<sub>6</sub>H<sub>5</sub>, FLR-NH-(CH<sub>2</sub>)<sub>2</sub>-C<sub>6</sub>H<sub>5</sub> or FLRF-NH-CH<sub>3</sub>, respectively. Following dilution with excess 0.2% TFA, the reaction products were either lyophilized or directly purified by HPLC on a semi-preparative Vydac C<sub>18</sub> column (0.1% TFA/ACN systems) and lyophilized. While the aminolysis reaction was quantitative under the conditions employed, the cyanylation reaction

was incomplete with a 3-molar excess of CDAP. A significant improvement was achieved with the 5 molar excess CDAP which corresponded to ca. 30% overall yields of the HPLC purified amidated peptides.

The biological activity of PF1 includes its ability to cause muscle relaxation in muscle preparations from a porcine gut-living nematode (*A. suum*) [4]. The C-terminal modifications reported here for PF1 and its fragments led to the loss of this muscle-relaxing.

In summary, the presented procedures for on-resin cyanylation and aminolysis are fast and simple and can effectively afford a variety C-terminal primary or secondary amides.

## References

1. Koyama, N., Kuriyama, M., Amano, N. and Nishimura, N., *J. Biotechnol.*, 32 (1994) 273.
2. Nakagawa, S., Tamakashi, Y., Hamana, T., Kawase, M., Taketomi, S., Ishibashi, Y., Nishimura, Nishimura, O. and Fukuda, T., *J. Am. Chem. Soc.*, 116 (1994) 5513.
3. Stark, G.R., *Methods Enzymol.*, 47 (1977) 129.
4. Maule, A.G., Geary, T.G., Bowman, J.W., Marks, N.J., Blair, K.L., Halton, D.W., Shaw, C. and Thompson, D.P., *Invertebrate Neurosci.*, 1 (1995) 255.

# Synthesis of a series of “cationic”, orthogonally protected, $\alpha,\alpha$ -disubstituted amino acids

T. S. Yokum, M. G. Bursavich, S. A. Piha-Paul, D. A. Hall  
and M. L. McLaughlin

*Department of Chemistry, Louisiana State University, Baton Rouge, LA 70803, USA*

$\alpha,\alpha$ -Disubstituted amino acids ( $\alpha,\alpha$ AAs) are important tools in the design of peptides because of their ability to promote specific secondary structures [1]. Aib ( $\alpha$ -amino isobutyric acid) and Aib-like residues (where the side chains are not extremely bulky) have been incorporated into peptides to form  $\alpha$ - and  $3_{10}$ -helices [2]. The helix type formed depends upon the design of the peptide and the placement and percentage of  $\alpha,\alpha$ AAs. Unfortunately, the majority of  $\alpha,\alpha$ AAs that have been incorporated have been hydrophobic, which has limited the characterization of the resulting peptides to organic media. Polar  $\alpha,\alpha$ AAs are required to synthesize highly helical, water soluble peptides that contain high percentages of  $\alpha,\alpha$ AAs. These peptides allow the study of the solvent effects on the  $3_{10}$ / $\alpha$ -helix equilibrium, stability of the  $3_{10}$ -helix in aqueous media, and the design of short antimicrobial peptides. To date, there have been few reports in the literature of polar  $\alpha,\alpha$ AAs that promote helicity and are suitable for incorporation into peptides via solid-phase peptide synthesis (SPPS) [3]. We report the synthesis of a series of “cationic”  $\alpha,\alpha$ AAs that may be readily incorporated into peptides via SPPS (Fig. 1).

## Results and Discussion

A six-membered ring was used as the backbone for these amino acids because of the helix promoting effects shown by six-membered cyclic  $\alpha,\alpha$ AAs [3]. The synthesis of the polar  $\alpha,\alpha$ AAs begins with a reductive amination using  $\text{NaBH}(\text{OAc})_3$  and the amine on 1,4-cyclohexanedione monoethylene ketal, **1** [4]. The ketone functionality is unmasked by refluxing with 10% TFA. The side chain nitrogen is protected using  $(\text{Boc})_2\text{-O}$  and DMAP to yield **2A-D**. The hydantoin is formed using a traditional Bücherer-Bergs synthesis followed by the activation of the hydantoin nitrogens with  $(\text{Boc})_2\text{-O}$  and DMAP to yield **3A-D**. This activation of the hydantoin allows a mild hydrolysis to occur without removal of the side chain Boc protecting group. If normal hydantoin cleavage techniques were employed (i.e. pressure and high temperature with strong base) the side chain protecting group would be cleaved and selective protection of the  $\alpha$ -nitrogen over the side chain nitrogen would be difficult. Thus, the bis-Boc hydantoin is treated with 1N LiOH to yield the free amino acids, **4A-D** [5]. The free amino acids are treated with DIEA and TMS-Cl followed by the addition of solid Fmoc-Cl. After aqueous workup, the orthogonally protected amino acids **5A-D** are obtained [6]. This is a general method for the synthesis of polar  $\alpha,\alpha$ AAs.

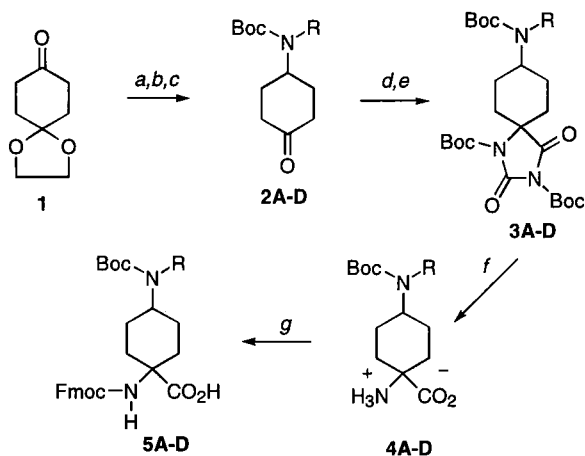


Fig. 1. Synthesis of amino acids 5A-D (A, R=ethyl; B, R=butyl; C, R=benzyl, D, R=2-naphthyl methyl) (a)  $H_2NR$ ,  $NaBH(OAc)_3$ ,  $HOAc$ ; (b) 10% TFA; (c)  $(Boc)_2-O$ , DMAP; (d)  $KCN$ ,  $(NH_4)_2CO_3$ ; (e)  $(Boc)_2-O$ , DMAP; (f)  $LiOH$ ; (g) 1. DIEA, TMS-Cl, 2. Fmoc-Cl, 3.  $H^+$ .

## Acknowledgments

We gratefully acknowledge support from: Howard Hughes Medical Institute for S.A.P. and M.G.B., NSF REU for D.A.H., and the United States Public Health Service via grant number NIH (GM42101).

## References

1. (a) Balaram, P., *Curr. Opin. Struct. Biol.*, 2 (1992) 845. (b) Toniolo, C. and Benedetti, E., *Trends Biochem. Sci.*, 16 (1991) 350.
2. (a) Yokum, T.S., Gauthier, T.J., Hammer, R.P. and McLaughlin, M.L., *J. Am. Chem. Soc.*, 119 (1997) 1167. (b) Karle, I.L., Flippen-Anderson, J.L., Gurunath, R. and Balaram, P., *Protein Science*, 3 (1994) 1555. (c) Basu, G. and Kuki, A., *Biopolymers*, 33 (1993) 995.
3. Wysong, C.L., Yokum, T.S., Morales, G.A., Gundry, R.L., McLaughlin, M.L. and Hammer, R.P., *J. Org. Chem.*, 61 (1996) 7650.
4. Abdel-Magid, A.F., Maryanoff, C.A. and Carson, K.G., *Tetrahedron Lett.*, 31 (1990) 5595.
5. Kubik, S.; Meissner, R.S. and Rebek, J., *Tetrahedron Lett.*, 35 (1994) 6635.
6. Bolin, D.R., Sytwu, I.-L., Humiec, F. and Meienhofer, J., *Int. J. Pept. Protein Res.*, (1989) 353.

# Synthesis of N<sup>α</sup>-*t*-Boc-benz[*f*]tryptophan: an intrinsic/extrinsic fluorescent probe

T.S. Yokum, P.K. Tungaturthi, and M.L. McLaughlin

*Department of Chemistry, Louisiana State University, Baton Rouge, LA 70803, USA*

The development of amino acid based fluorescent probes of peptide structure and dynamics is a long term goal of our group. Peptide hormones are flexible molecules in solution that adopt a unique conformation upon receptor binding. Fluorescence spectroscopy possesses the potential to determine peptide hormone structure while in the receptor site. This information can be used for the rational design of peptide hormone agonists and antagonists. Tryptophan is an excellent intrinsic fluorescent probe for the determination of peptide conformation. Unfortunately, upon peptide binding to receptors, tryptophan can suffer spectral overlap with other tryptophans and other fluorophores present in the protein receptor. To overcome this issue, we have designed an intrinsic red shifted fluorescent probe which closely mimics the structure of tryptophan. We report the synthesis of N<sup>α</sup>-*t*-Boc-benz[*f*]tryptophan, **6**, an amino acid based intrinsic fluorescent probe suitably protected for incorporation via solid-phase peptide synthesis (SPPS) (Fig. 1).

## Results and Discussion

Benz[*f*]tryptophan best mimics the structure of tryptophan and least perturbs peptide structure compared to other benzannulated derivatives, benz[*g*]tryptophan and benz[*e*]tryptophan. The natural electronic effects of the naphthalene moiety allow an easier route to benz[*g*]tryptophan and benz[*e*]tryptophan via their benzannulated indoles. The routes utilizing the indole intermediates for the synthesis of benz[*f*]tryptophan are not practical because of the low benz[*f*]indole yields obtained [1]. Our synthesis begins by refluxing allyl bromide with 3-bromo-2-amino naphthalene, **1**, and Na<sub>2</sub>CO<sub>3</sub> in DMF [2,3]. The indoline backbone is formed by treating the diallyl compound with *t*-butyllithium at -78 °C and allowing it to warm to room temperature [2]. The solution is immediately recooled, DMF is added, and warmed to room temperature to yield the aldehyde, **2** [3]. The aldehyde is converted to the corresponding hydantoin, **3**, via a modified Bucherer-Bergs synthesis [4]. The next obvious step is to remove the allyl group and oxidize to the indole, but after the removal of the allyl group, the resulting molecule is sparingly soluble in organic media. To overcome this problem and to allow the mild hydrolysis of the hydantoin, we protect the hydantoin nitrogens with Boc by treating the hydantoin, **3**, with (Boc)<sub>2</sub>-O and DMAP to yield **4** [4]. The allyl protecting group is now removed by treating the bis-Boc hydantoin with Pd<sup>0</sup> and thiosalicylic acid to give the free indoline [5]. The air sensitive indoline is immediately oxidized to the indole, **5**, using DDQ. The

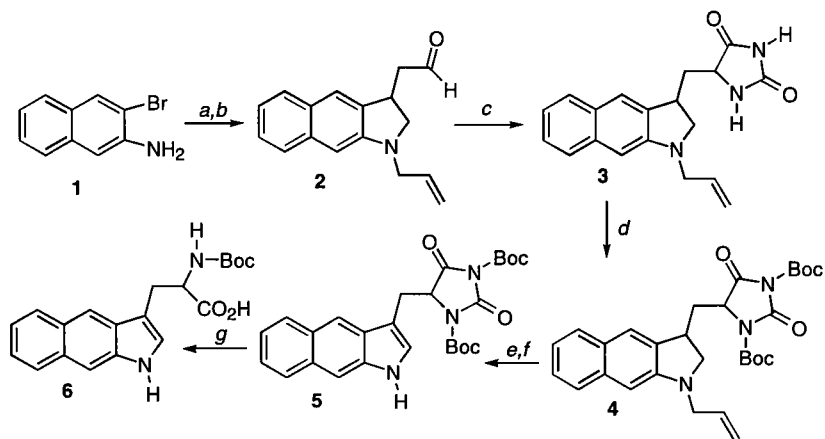


Fig 1. Synthesis of  $N^{\alpha}$ -*t*-Boc-benz[*f*]tryptophan. (a) allyl bromide,  $\text{Na}_2\text{CO}_3$ ; (b) 1. *t*-butyllithium, 2. DMF; (c) KCN,  $(\text{NH}_4)_2\text{CO}_3$ ; (d)  $(\text{Boc})_2\text{-O}$ , DMAP; (e)  $\text{Pd}^0$ , thiosalicylic acid; (f) DDQ; (g) LiOH.

indole hydantoin is treated with 1N LiOH to give  $N^{\alpha}$ -*t*-Boc-Benz[*f*]tryptophan, **6** [4,6]. We expected to obtain the free amino acid upon hydrolysis of the bis-Boc indole hydantoin based on previous results [4,6]. However, only  $\alpha,\alpha$ -disubstituted hydantoin have been hydrolyzed using this method while our bis-Boc indole hydantoin is only monosubstituted on the  $\alpha$ -carbon.

Preliminary experiments have shown this chromophore is an excellent red-shifted fluorescent probe with simpler fluorescence decay behavior than the parent indole chromophore.

## Acknowledgments

We gratefully acknowledge support from the United States Public Health Service via grant number NIH (GM42101).

## References

- Morales, G.A. Louisiana State University, Ph.D. Dissertation, 1995.
- Zhang, D., Liebeskind, L.S., *J. Org. Chem.*, 61 (1996) 2594-2595.
- Bailey, W.F., Jiang, X.L., *J. Org. Chem.*, 61 (1996) 2596-2597.
- Wysong, C.L., Yokum, T.S., Morales, G.A., Gundry, R.L., McLaughlin, M.L., Hammer, R.P., *J. Org. Chem.* 61 (1996) 7650-7651.
- Lemaire-Audoire, S., Savignac, M., Genêt, J.P., Bernard, J.M., *Tetrahedron Lett.*, 36 (1995) 1267-1270.
- Kubik, S., Meissner, R.S., Rebek, J., *Tetrahedron Lett.*, 35 (1994) 6635-6638.

# Synthesis of HIV-1 protease analog by ligation of bromoacetyl and mercaptoethylamide peptide prepared using disulfide linkage to solid-support

Yoshiaki Kiso,<sup>a</sup> Tooru Kimura,<sup>a</sup> Yoichi Fujiwara,<sup>a</sup> Naoki Nishizawa,<sup>a</sup>  
Hikaru Matsumoto,<sup>a</sup> Masamichi Kishida,<sup>a</sup> Kenichi Akaji<sup>a</sup>  
and Haruo Takaku<sup>b</sup>

<sup>a</sup>Department of Medicinal Chemistry, Kyoto Pharmaceutical University, Yamashina-Ku, Kyoto 607, Japan, <sup>b</sup>Bioscience Research Laboratories, Japan Energy Co., Todashi, Saitama 335, Japan

The chemical ligation strategy which is based on chemoselective reactions of special functions on unprotected peptide segments is often employed for the synthesis of large peptides [1]. Englebretsen *et al.* reported a synthesis of HIV-1 protease analog employing thioether forming ligation which is a reaction of peptide-mercaptoethylamide with bromoacetyl-segment [2]. In the synthesis, they prepared the mercaptoamide-segment using a thiol-releasing resin by acid treatment. However this strategy sometimes caused trouble due to the released thiol group. In order to obtain the thiol-segment without difficulty, we employed a new strategy using a multi-detachable linker to avoid contact of thiol with strong acids.

## Results and Discussion

In order to prepare the mercaptoamide-peptide, we investigated various linkages releasing the thiol function by acid treatment, which contained substituted benzyl thioethers [3]. However large peptide segments could not be obtained in good purity using these linkages.

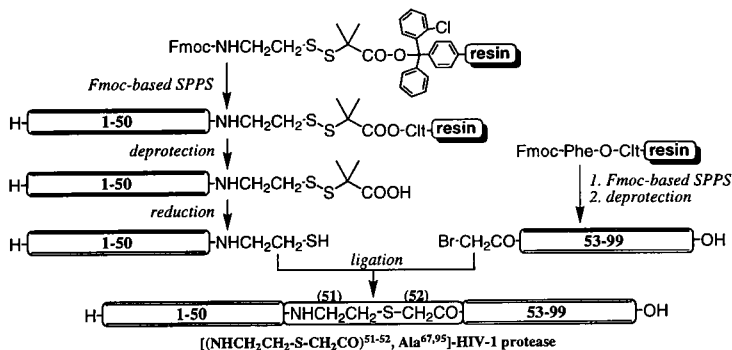


Fig. 1. Synthetic scheme for HIV-1 protease analog using thioether forming ligation.

Because we suspected that the results were due to the thiol involving side-reactions, we attempted to protect the thiol group during the acid treatment. An aminoethyldithio-2-isobutyric acid (AEDI), which can connect the mercaptoamide-peptide to the solid support by disulfide bond [4], is stable under the conditions during SPPS and acid treatment. We introduced AEDI on an acid-labile resin and used it as a multi-detachable linker. In this strategy, the peptide containing a masked thiol moiety was cleaved from the resin by acid-deprotection, and then the thiol was generated by reduction. We applied it to the synthesis of HIV-1 protease analog (Fig. 1).

A mercaptoethylamide-peptide segment, HIV-1 protease (1-50)-NHCH<sub>2</sub>CH<sub>2</sub>SH, was prepared starting from an Fmoc-AEDI-O-Clt-resin (Clt-resin = 2-chlorotriptyl-resin). SPPS was performed with a ABI 431A synthesizer with standard DCC-HOBt protocol, and then the peptide segment containing the linker moiety was cleaved by HF-dimethyl sulfide-*m*-cresol (3:6:1) (0°C, 1h). The cleavage result was treated with dithiothreitol (DTT) in 6M guanidine•HCl (pH 8) and gave the desired product in good purity. Purification by RP-HPLC gave a homogeneous product in 29.9% overall yield, which was characterized by amino acid analysis of the hydrolyzate and MALDI-TOF MS.

Another segment, BrCH<sub>2</sub>CO-[Ala<sup>67,95</sup>]-HIV-1 protease (52-99), was also prepared by the usual SPPS, deprotection by HF-*m*-cresol and purification on RP-HPLC (8.0%).

The ligation of the above two segments was carried out in 6M guanidine•HBr, 200mM Tris buffer (pH 8.5) at r.t. for 5 h with vigorous stirring. The product was purified on Hiload 16/60 superdex 75 pg in 8 M urea and then gel-filtered to remove urea. The desired product, [NHCH<sub>2</sub>CH<sub>2</sub>SCH<sub>2</sub>CO<sup>51-52</sup>, Ala<sup>67,95</sup>]-HIV-1 protease was obtained in 50% yield and characterized by MALDI-TOF MS (*m/z*: 10759.2±0.1%, calcd:10758.6).

After folding, the synthetic protease analog possessed enzymatic activity, although it showed minor differences to recognize substrates. The synthetic protease had comparable enzymatic activity to the wild type enzyme against a substrate, H-Lys-Ala-Arg-Val-Tyr\*Phe(NO<sub>2</sub>)-Gln-Ala-Nle-NH<sub>2</sub>. The K<sub>m</sub> values of the synthetic protease and wild type were 12.8μM and 26.8μM, respectively. On the other hand, the protease analog had larger K<sub>m</sub> (>30mM) than the wild type protease (21.4mM) against H-Ser-Gln-Asn-Tyr\*Pro-Ile-Val-OH. The non-peptide region at the flap of synthetic protease may affect substrate recognition.

## References

1. Schnölzer, M. and Kent, S.B.H., *Science*, 256 (1992) 221; Canna, L.E., Amare, A.R.F., Burley, S.K. and Kent, S.B.H., *J. Am. Chem. Soc.*, 117 (1995) 2998; Dawson, P.E., Muir, T.W. and Clark-Lewis, I. and Kent, S.B.H., *Science*, 266 (1994) 776.
2. Englebretsen, D.R., Garnham, B.G., Bergman, D.A. and Alewood, P.F., *Tetrahedron Lett.*, 36 (1996) 8871.
3. Fujiwara, T., Nishizawa, N., Kimura, T., Akaji, K. and Kiso, Y., In Nishi, N. (Ed.), *Peptide Chemistry 1995 (Proceeding of the 33rd Symposium of Peptide Chemistry)*, Protein Res. Found., Osaka, Japan, 1996, p.53.
4. Méry, J., Brugidou, J. and Derancourt, J., *Pept. Res.*, 5 (1992) 233; Méry, J., Granier, C., Juin, M. and Brugidou, J., *Int. J. Peptide Protein Res.*, 42 (1993) 44.

# An efficient preparation of the potent and selective pseudopeptide thrombin inhibitor, Inogatran

Wayne L. Cody,<sup>a</sup> John X. He,<sup>a</sup> Patrice Prévaille,<sup>b</sup> Micheline Tarazi,<sup>b</sup>  
M. Arshad Siddiqui<sup>b</sup> and Annette M. Doherty<sup>a</sup>

Departments of Chemistry, <sup>a</sup>Parke-Davis Pharmaceutical Research, Division of Warner-Lambert Co., 2800 Plymouth Road., Ann Arbor, MI, 48105, U.S.A.

<sup>b</sup>BioChem Therapeutic, Inc., 275 Armand-Frappier Boulevard, Laval, Québec, Canada, H7V 4A7

Thrombin is a trypsin-like serine protease that plays a major role in blood coagulation. In particular, thrombin is responsible for conversion of the soluble plasma protein fibrinogen to the insoluble fibrin by cleavage of the Arg<sup>16</sup>-Gly<sup>17</sup> amide bond, leading to clot formation. As with other serine proteases, thrombin utilizes a catalytic triad of amino acids (Ser<sup>195</sup>, His<sup>57</sup> and Asp<sup>102</sup>) to initiate this conversion. Currently, potent small molecule and specific inhibitors of thrombin are of significant pharmaceutical interest. Several common problems have been encountered in the development of these small molecule inhibitors; a) lack of selectivity for thrombin over other trypsin-like enzymes, b) low oral bioavailability, c) short duration of action, d) rapid clearance and e) increased bleeding times [1,2].

Recently, Inogatran (**1**), a pseudopeptide, has been reported to be an effective, noncovalently bound, direct and selective inhibitor of thrombin in several *in vitro* and *in vivo* models ( $K_i = 15$  nM for thrombin, 45 nM for trypsin) [3-8]. Inogatran inhibits arterial thrombosis more effectively than acetylsalicylic acid or heparin in a closed-chest porcine model [7] and moderately increases bleeding times at high doses [8]. Also, Inogatran has significant oral bioavailability in rats (32-51%) and dogs (34-44%) [4-6]. Herein, we report an efficient and convergent chemical synthesis of **1** that is amenable to the preparation of multiple gram quantities.

## Results and Discussion

The synthesis of **1** was achieved by a convergent strategy in which the molecule was divided into two components (**A** and **B**) (Fig. 1). Component **A** was prepared in five steps (29% overall) starting from L-phenylalanine. L-Phenylalanine was converted to its t-butyl ester with isobutylene (72%), hydrogenated to cyclohexylalanine (75%) and alkylated with benzyl-2-bromoacetate (62%). The resulting secondary amine was protected with the benzyloxycarbonyl group (86%) and the carboxylate liberated by treatment with HCl to yield Component **A** (>99%). Component **B** was prepared in four steps (61% overall) from Boc-1,3-diaminopropane. The free amine of Boc-1,3-diamino-propane was guanylated with bis-Z-1*H*-pyrazole-carboximidine (75%), Boc deprotected with HCl and coupled to N<sup>α</sup>-Boc-pipecolic acid with BOP reagent (85% for both steps). The product was Boc depro-

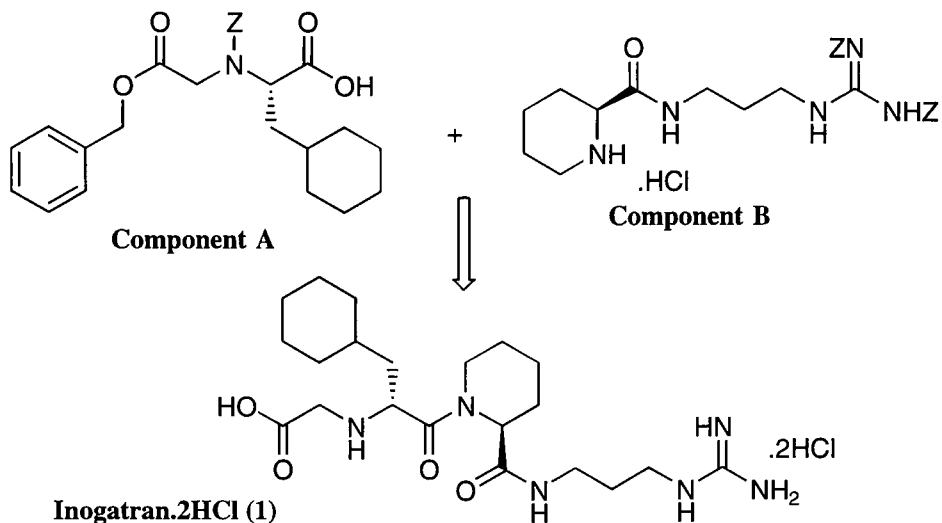


Fig. 1. Synthetic strategy utilized for the preparation of Inogatran (1).

protected once more (95%) to yield Compound **B**. Several conditions were explored to couple Compound **A** and **B**. HATU proved to be the optimum coupling reagent, providing fully protected Inogatran (56%) which, upon hydrogenolysis, conversion to the HCl salt, and lyophilization, provided **1** (100% for both steps) without the need for purification (>98% pure by RPHPLC). This synthetic sample has a  $K_i$  of 3.0 nM for thrombin which compares favorably with the values reported in the literature [3-8].

## References

1. Tapparelli, C., Metternich, R., Ehrhardt, C. and Cook, N.G., *Trends Pharmacol. Sci.*, 14 (1993) 366.
2. Edmunds, J.J., Rapundalo, S.T. and Siddiqui, M.A., *Ann. Rep. Med. Chem.*, 31 (1996) 51.
3. Teger-Nilsson, A.C.E. and Bylund, R.E., *World Patent Appl.* 93 11152 (1993).
4. Eriksson, U.G., Renberg, L., Vedin, C. and Strimfors M., *Thromb. Haemostasis*, 73 (1995) 1318.
5. Gustafsson, D., Elg, M., Lenfors, S., Borjesson, I., Teger-Nilsson, A.C., *Thromb. Haemostasis*, 73 (1995) 1319.
6. Teger-Nilsson, A.C., Gyzander, E., Andersson, S., Englund, M., Mattsson, C., Ulvinge, J.C. and Gustafsson, D., *Thromb. Haemostasis*, 73 (1995) 1325.
7. Uriuda, Y., Wang, Q.D., Grip, L., Rydén L., Sjöquist, P.O. and Mattsson, C., *Cardiovasc. Res.* 32 (1996) 320.
8. Gustafsson, D., Elg, M., Lenfors, S., Börjesson, I., Teger-Nilsson, A.C., *Blood Coagul. Fibrin.*, 7 (1996) 69.

# Application of novel organophosphorus compounds as coupling reagents for the syntheses of bioactive peptides

Yun-hua Ye, Chong-xu Fan, De-yi Zhang, Hai-bo Xie,  
Xiao-lin Hao and Gui-ling Tian

Department of Chemistry, Peking University, Beijing, 100871, China

We have developed the syntheses of four organophosphorus compounds (Fig. 1.): DEPBO, DOPBO, DOPBT and DEPBT [1] which can be used as novel coupling reagents in peptide synthesis. We have synthesized a number of bioactive peptides such as analogues of delta sleep inducing peptide, a group of  $\gamma$ -glutamyl oligopeptides isolated from *Panax ginseng* and a cyclic heptapeptide isolated from *Caryophyllaceae* by using these organophosphorus compounds as coupling reagents in both solution and solid phase peptide syntheses. Among the four compounds, DEPBT affords the best results. DEPBT is much better than the others as far as racemization is concerned, and is also especially useful in the cyclization of linear peptides.

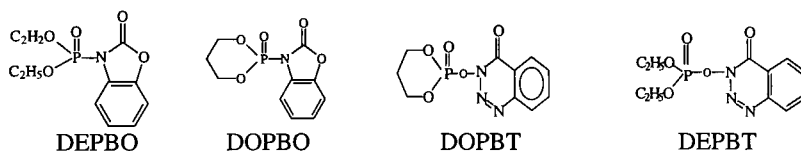


Fig. 1. The structures of four organophosphorus compounds.

## Results and Discussion

All of these organophosphorus compounds are stable colourless crystals which can be easily prepared in large quantity. The physical properties of the protected peptides synthesized by DEPBO, DOPBO, DOPBT, DEPBT are in agreement with those peptides prepared by other methods. During the coupling reaction, the hydroxy group in the amino component does not need to be protected, and the dehydration of Asn, which is caused by DCC or EDC, was not observed (Table 1 and Table 2). The racemization caused by these organophosphorus compounds is much less than that from BOP and DCC. Among them, the best result was obtained from DEPBT in which racemization was less than 1% as detected by the Young test [2], while 18.4% and 36.8% D-isomers were formed by BOP and DCC (without HOBT), respectively.

Table 1. The physical constants of oligopeptides synthesized by DEPBO and DEPBT.

Peptide	DEPBO			DEPBT		
	Yield(%)	m.p.(°C)	$[\alpha]_D^{20}$ (c,Sol.)	Yield(%)	m.p.(°C)	$[\alpha]_D^{20}$ (c,Sol.)
Z-AlaSerOMe	85	135-136	-15.7°(1,MeOH)	66	137-138	-20.0°(1,MeOH)
Z-AlaPheOMe	82	98-99.5	-7.3°(1,EtOH)	94	101-102	-11.5°(1,EtOH)
Z-AlaTyrOMe	80	118-120	-11°(2,DMF)			
Z-AsnPheOMe				73	199-201	-3.0°(1,DMF)
Boc-LeuGlyOEt	72	86-88	-19.4°(1,EtOH)			
Boc-IleTyrOMe				91	144-146	-17°(1, EtOH)
Boc-TrpLys(Z)GlyOMe				82	150-151	+28.7°(1,MeOH)

Table 2. The physical constants of oligopeptides synthesized by DOPBO and DOPBT.

Peptide	DOPBO			DOPBT		
	Yield(%)	m.p.(°C)	$[\alpha]_D^{20}$ (c,Sol.)	Yield(%)	m.p.(°C)	$[\alpha]_D^{20}$ (c,Sol.)
Z-AlaTyrOMe	90	125-126	-6.4°(1,MeOH)	79	122-124	-6.0°(1,MeOH)
Boc-AlaPheOMe	84	88-89	-20.2°(1,MeOH)	72	84-87	
Z-MetGlyOEt	81	90-92	-18.5°(1,EtOH)	67	92-94	-19.0°(1,EtOH)
Z-AlaPheOMe	83	101-103	-12.7°(1,EtOH)	72	97-100	
Z-AsnPheOMe	76	199-200	-5.1°(1,DMF)	58	195-198	-4.3°(1,DMF)
Z-AlaGlyOEt	72	101-102	-24.0°(1,EtOH)	66	100-101	-22.1°(1,EtOH)
Z-AlaSerOMe	68	137-138	-20.0°(1,MeOH)	53	137-139	-19.5°(1,MeOH)
Boc-TrpGlyOEt	73	118-121	-14.7°(1,EtOH)	50	116-119	-12.7°(1,EtOH)

DEPBT has been used successfully in the cyclization of linear peptides such as cyclo(GlyTyrGlyGlyProPhePro) in dilute solution ( $10^{-3}$  mol/L) for 24h with 61% yield.

#### Acknowledgments.

The authors would like to thank the National Natural Science Foundation of China and Doctoral Program Foundation of Institute of Higher Education for the financial support.

#### References

1. Fan, C.-X., Hao, X.-L. and Ye, Y.-H., Synthetic Communication, 26(1996)1455.
2. Williams, W. and Young G.-T., J. Chem. Soc., (1963)881.

# Minimization of cysteine racemization during stepwise solid-phase peptide synthesis

Yvonne M. Angell,<sup>a</sup> Yongxin Han,<sup>a</sup> Fernando Albericio,<sup>b</sup>  
and George Baranya<sup>a</sup>

<sup>a</sup>Department of Chemistry, University of Minnesota, Minneapolis, MN 55455, USA

<sup>b</sup>Department of Organic Chemistry, University of Barcelona, 08028-Barcelona, Spain

Upon their incorporation into internal amide linkages, racemization of *N,S*-protected derivatives of cysteine residues can be a serious concern in Fmoc stepwise solid-phase synthesis. We have recently reported a systematic study of this problem, as a function of coupling conditions and  $\beta$ -thiol protecting groups, i.e., *S*-acetamidomethyl (Acm), *S*-triphenylmethyl (Trt), *S*-2,4,6-trimethoxybenzyl (Tmob), and *S*-9*H*-xanthen-9-yl (Xan) [1]. A convenient and quantitative model system assay involving HPLC resolution of H-Gly-L-Cys-Phe-NH<sub>2</sub> from H-Gly-D-Cys-Phe-NH<sub>2</sub> was developed to monitor this problem. We now report an extension of the earlier racemization studies to include a variety of hindered bases, as well as additional coupling reagents.

## Results and Discussion

Many of the recently popularized *in situ* coupling reagents such as BOP/HOBt, HBTU/HOBt, or HATU/HOAt, when used with DMF as solvent in the presence of a tertiary amine base, e.g., NMM or DIEA, along with a 5-min preactivation time, were found to give 5 - 33% levels of cysteine racemization, which are unacceptable. By using a less polar solvent combination during coupling, e.g., CH<sub>2</sub>Cl<sub>2</sub>-DMF (1:1), avoiding the preactivation step with *in situ* protocols, and/or using a weaker or more hindered base, for example collidine, we were able to reduce racemization to acceptable levels of < 0.2 % [1].

Carpino and coworkers have shown that whereas DIEA and NMM promote considerable racemization during segment condensation [2], a series of more highly hindered bases, e.g., collidine, lutidine, TEMP, OHA, DB[DMAP] (structures shown in Fig. 1) permit reduced racemization levels [3]. For the present studies, we applied some of these unique bases (Fig. 1) to our model assay system in order to evaluate the ability of each to allow cysteine incorporation with minimal racemization.

In one set of experiments, we used (BOP or HBTU)/HOBt/base (4:4:4) in CH<sub>2</sub>Cl<sub>2</sub>-DMF (1:1), without preactivation, conditions known to be "safe" [1] when the base is TMP. In successive experiments, we replaced TMP with one of the following bases: pempidine, OHA, TEMP, DB[DMAP], lutidine, or acridine. Excellent results were obtained under these conditions. All bases tested allowed efficient coupling of Fmoc-Cys(Trt)-OH (60 - 90 min coupling time), with the exception of acridine, which

required double coupling for complete reaction. Racemization was not detected with the first four of these bases, and was 0.2 - 0.4 % with lutidine or acridine.

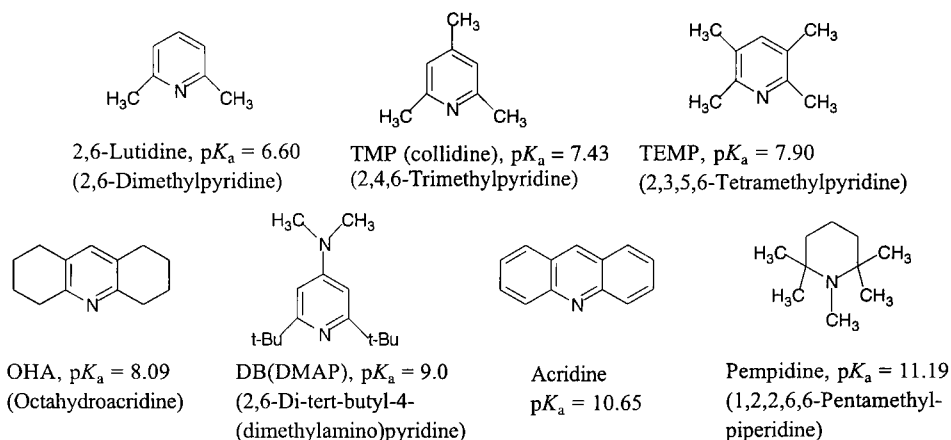


*Fig. 1. Hindered tertiary amines proposed to minimize racemization during segment condensation [3], applied to cysteine racemization studies in the present work.*

A second set of experiments used two coupling reagents, PyBOP and PyAOP, that were not tested previously with our model system. Racemization was not detected under these conditions: PyBOP/HOBt/TMP or PyAOP/HOAt/TMP (4:4:4) without preactivation in  $\text{CH}_2\text{Cl}_2$ -DMF (1:1). However omission of the coupling additives HOBt and HOAt, respectively, did result in 3 - 4 % racemization with these reagents. In conclusion, a set of "safe" conditions has been found for racemization-free cysteine coupling. Several highly hindered bases have been shown to be useful for prevention of cysteine racemization. Less polar solvents [e.g.,  $\text{CH}_2\text{Cl}_2$ -DMF (1:1) vs. neat DMF] also aid in reducing racemization. Use of additives such as, HOAt and HOBt, with PyAOP and PyBOP, respectively reduces racemization.

## Acknowledgements

We appreciate Professor L.A. Carpino's generous gift of TEMP, OHA, and DB[DMAP], and thank NIH: GM 18341 (Y.M.A. postdoctoral fellowship), GM 43552 (G.B) and GM 51628 (G.B) for support.

## References

1. Han, Y., Albericio, F., Barany, G., *J. Org. Chem.*, 62(1997)3841.
2. Carpino, L.A., El-Faham, A., *J. Org. Chem.*, 59(1994)695.
3. Carpino, L.A., Ionescu, D., El-Faham, A., *J. Org. Chem.*, 61(1996)2460.

# Solid phase synthesis of *N*-methyl amino acids: Application of the Fukuyama amine synthesis

Lihu Yang and Kuenley Chiu

Modular Synthesis, Department of Medicinal Chemistry  
Merck Research Laboratories, PO Box 2000, Rahway, NJ 07065, USA

The incorporation of *N*-methyl amino acids into biologically active peptides has been widely used to study conformation and biological activity, and to improve oral activity and duration of action. *N*-methylated peptides are normally synthesized by incorporation of protected *N*-methylated amino acids. Existing methods for the synthesis of *N*-methyl amino acids or their *N*-protected forms require strong basic, acidic or reducing conditions, which exclude their use in some sensitive systems, such as tryptophan and Boc orthogonally protected lysine analogs. Herein we report the solid phase synthesis of *N*-methyl amino acids and their *N*-Fmoc analogs by applying Fukuyama amine synthesis [1]. This methodology has very general applications and can be used for the preparation of a variety of amino acid derivatives (Fig. 1).

## Results and Discussion

We investigated the scope of the reaction by using amino acids preloaded on 2-Cl-trityl resin, since it has been widely used for fully protected peptide fragment synthesis. After some experimentation, the best sulfonylation results were obtained by using 2-nitrobenzenesulfonyl chloride (2-NBSCl, 4 equivalents) and *N,N*-diisopropylethylamine (DIEA, 6 equivalents) in THF/DCM. The reaction was monitored by the Kaiser ninhydrin test and generally went to completion in less than three hours. DMAP can be added to accelerate the reaction. Methylation of the resulting sulfonamide was carried out with methanol under Mitsunobu conditions [2]. It should be noted that replacing methanol with other alcohols produced *N*-alkyl amino acid derivatives, providing an

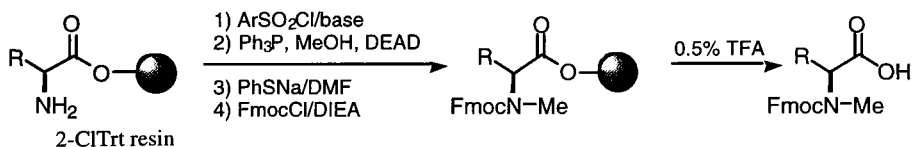


Fig. 1. Synthesis of Fmoc *N*-methyl amino acids.

Table 1. Analytical data for the Fmoc-N-Me amino acids and retention time comparison with Fmoc-amino acids.

entry	amino acids	Fmoc-AA	FmocN-Me AA		
		Rt (min.)	Rt (min.)	purity <sup>†</sup>	yield <sup>†</sup>
1	Val	7.32	8.58	96	95%
2	Trp	8.20	8.60	88	100%
3	Trp(Boc)	12.31	13.11	96	98%
4	Lys(Boc)	8.58	9.45	90	100%
5	Ser( <sup>t</sup> Bu)	8.49	9.39	98	100%
6	Asp( <sup>t</sup> Bu)	8.51	9.38	90	96%

<sup>†</sup>: Purity & crude yield after cleavage. Analysis was performed using a Partisil ODS-3 RAC II column (100x4.6 mm, 5 μm) eluting with a linear gradient of 40-80% acetonitrile in water containing 0.1% TFA as buffer over 15 minutes at 1 mL/min. The HPLC is equipped with a PDA detector and the results are plotted at 278 nm with band width of 8 nm.

alternative to reductive alkylation [2]. Direct alkylation with methyl iodide (4 equiv.) and fine K<sub>2</sub>CO<sub>3</sub> powder (10 equiv.) also gave good results (DMF, 6 h). Removal of the sulfonyl protecting group was accomplished using the commercially available thiophenol sodium salt (or lithium salt) in DMF (0.5 M, 1h, twice). The Fmoc protecting group was introduced by treatment with DIEA (6 equiv.) and FmocCl (4 equiv.) in DCM for 2 hours. The intermediates or final N-Fmoc N-methylated amino acids were cleaved from the resin under the usual acidic conditions (0.5% TFA/DCM). The purities of the Fmoc protected amino acids were quite good (generally >90%, see Table 1). If necessary, reverse phase HPLC purification will yield pure products.

## Conclusion

In summary, Fukuyama amine synthesis is a reliable method for the conversion of amino acids to their N-methylated forms on solid phase in high yield and purity. The procedure is especially valuable for the preparation of N-methylated amino acids that are difficult to synthesize by conventional methods. In addition, this methodology can be easily adapted for the preparation of other N-alkyl amino acids providing a good alternative to reductive alkylation.

## References

1. Fukuyama, T.; Jow, C.-K.; Cheung, M. *Tetrahedron Lett.*, 36 (1995) 6373.
2. Papaioannou, D.; Athanassopoulos, D.; Magafa, V.; Karamanos, N.; Stavropoulos, G.; Napoli, A.; Sindona, G.; Aksnes, D. W.; Francis, G. W. *Acta Chem. Scand.*, 48 (1994) 324.

# Novel solid-phase reagents for facile formation of intramolecular disulfide bonds in peptides under mild conditions

Ioana Annis and George Barany

Department of Chemistry, University of Minnesota, Minneapolis, Minnesota 55455, USA

Disulfide bridges are important structural motifs in many peptides and proteins. The controlled formation of intramolecular disulfide bridges in peptides, while avoiding unwanted oligomerization by-products, is a significant challenge. We have developed a family of novel solid-phase reagents which efficiently form disulfide bonds in peptides over a wide pH range under mild conditions.

## Results and Discussion

Ellman's reagent, 5,5'-dithiobis(2-nitrobenzoic acid) (**1**), was developed in the context of an assay for measuring free thiol concentrations under physiological conditions. When bound through two sites to a solid support (PEG-PS, aminated Sephadex, controlled-pore glass), the reagent mediates the formation of disulfide bonds in a variety of peptides.

The preparations of solid-phase bound Ellman's reagents are outlined in Fig. 1. Ellman's reagent **1** was reduced to **2**, and the aromatic thiol was protected with the xanthenyl group to give **3**. Derivative **3** was coupled to both the  $\alpha$ - and the  $\epsilon$ -amino groups of a lysine spacer, which made it possible to carry out subsequent on-resin deprotection/oxidation of intermediate **4** to completion. Earlier attempts to form **5** without lysine resulted in up to 20% of reduced Ellman's reagent bound to the solid-phase, due to site isolation. Oxidation

Table 1. Effect of pH on rates and yields of oxidation of peptide substrates by resin-bound Ellman's reagent **5**.<sup>a</sup>

Substrate	pH 2.7		pH 6.6	
	t <sub>1/2</sub> (min)	% yield	t <sub>1/2</sub> (min.)	% yield
Somatostatin	50	25	5	62
Conotoxin (SH 2&7)	240	65	4	92
Conotoxin (SH 3&7)	330	70	3.5	90
Conotoxin (SH 3&13)	390	65	2.2	88
Conotoxin (4 SH)	54	64 <sup>b</sup>	3	78 <sup>b</sup>
Apamin (4 SH)	240	71 <sup>b</sup>	3	75 <sup>b</sup>

<sup>a</sup> All reactions were monitored by HPLC. Reagent **5** was derived from PEG-PS with 0.21 mmol/g loading, and used in 15-fold excess. Initial concentrations of peptides were 1 mg/mL.

<sup>b</sup> Yield of correctly paired regioisomer. Depending on the pH, a further 19-27% mispaired isomers were formed for apamin, and a further 15-22% for conotoxin SI.

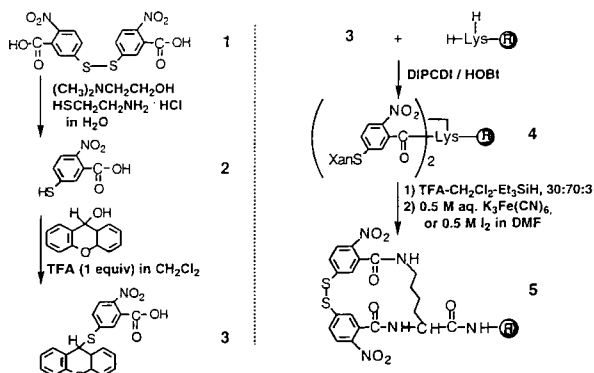


Fig. 1. A general scheme for preparation of solid-phase bound Ellman's reagents.

with **5** was tested on the reduced linear precursors of somatostatin (14 residues, disulfide bridge between residues 3 and 14),  $\alpha$ -conotoxin SI (13 residues, disulfide bridges between residues 2 and 7; 3 and 13), and apamin (18 residues, disulfide bridges between residues 1 and 11; 3 and 15). As further controls, differentially protected derivatives were prepared [conotoxin (SH 2&7), conotoxin (SH 3&7), conotoxin (SH 3&13)] and used to investigate selective formation of predetermined (single) bridges denoted by the numbers. Kinetics were determined as a function of pH value, solid support loading, and excess oxidizing reagent (Table 1, and unpublished studies from our laboratory). The reagent **5** allowed successful formation of disulfide bonds in the substrates tested, even at quite acidic pH values. From pH 2.7 to 5.0, a plot of reaction rate versus hydrogen ion concentration was linear. Upon completion of incubation and simple filtration, the major product in solution was the desired oxidized product, but some peptide remained covalently bound to the solid support through two disulfide bonds. The support-bound by-products were easily converted to soluble, reduced peptide by treatment with dithiothreitol. Following such reduction, reagent **5** was regenerated by repeating the last step in Fig. 1. Solid support loadings also affected the oxidation reactions using **5**. Higher loadings resulted in slower rates and more support-bound by-product, and therefore lower yields. As another factor, a direct linear dependence was observed of the reaction rate as a function of an excess of oxidizing reagent **5**. In the cases of conotoxin SI and apamin, which have four thiols to be oxidized, the correctly paired regioisomers were the main products, but mispaired regioisomers were also detected. Improved selectivities were observed at higher pH values. In summary, we have proposed and demonstrated novel solid-phase oxidizing reagents. Particular advantages of our approach include fast reaction times under mild conditions over a wide range of pH values, from 2.7 to 6.6; facile purification of disulfide-containing products; and the specificity and reusability of the reagents.

# Fmoc-2-aminopalmitic acid for the synthesis of lipopeptides with an hydrophobic chain on a C-C bond

**Anna M. Papini, Silvia Mazzucco, Elena Nardi, Mario Chelli,  
Mauro Ginanneschi and Gianfranco Rapi**

*Dipartimento di Chimica Organica "Ugo Schiff" and Centro C.N.R. di Studio sulla Chimica e la Struttura dei Composti Eterociclici e loro Applicazioni, Università di Firenze, Via Gino Capponi 9, I-50121 Firenze, Italy*

Lipopeptides have been demonstrated to have immunoadjuvant properties both *in vitro* and *in vivo*. They can play an important role in the regulation of cellular functions, such as the antigen processing pathway, by anchoring the lipophilic moiety to the cellular membrane. An interesting goal is the use of lipopeptides to induce the proliferation of T cell clones to develop synthetic vaccines and to study immunological disorders of autoimmune diseases such as multiple sclerosis (MS).

In the natural post-translational processes, palmitoylation of a cysteinyl residue *via* a thioester or a thioether bond is one of the most common modifications of the C-terminal part of a protein that doesn't require a consensus sequence.

It was previously reported that a single modification on the C-terminal position of peptides derived from HIV-1 env sequences by N<sup>ε</sup>-palmitoyl-L-lysine amide allowed the induction of a relevant CTL response [1].

The palmitoyl moiety can also be introduced in a peptide sequence on the N-terminal side either directly by SPPS, by using the pentafluorophenyl ester of palmitic acid, or by appending an N<sup>ε</sup>-palmitoyl-L-lysyl residue to the sequence.

## Results and Discussion

With the aim of introducing a lipophilic moiety directly in the peptide sequence by continuous flow SPPS following the Fmoc/*t*-Bu strategy, we recently synthesized the racemic mixture of Fmoc-2-aminopalmitic acid (Fmoc-Apalm-OH). Because H-Apalm-OH [2] is poorly soluble in the reaction media usually employed for the Fmoc protection of the amino function, it was necessary to prepare the *p*-toluenesulfonate salt of its benzyl ester by Dean-Stark apparatus (70% yield). This salt was allowed to react with Fmoc-OSu in benzene (84% yield). After controlled catalytic hydrogenation (Pd/C 10%) in 5% ethanolic AcOH, Fmoc-Apalm-OH was obtained as a racemic mixture in 80% yield.

By using this derivative, we synthesized the peptide H-Apalm-h-MBP(83-99) (H-Apalm-Glu-Asn-Pro-Val-Val-His-Phe-Phe-Lys-Asn-Ile-Val-Thr-Pro-Arg-Thr-Pro-OH) by SPPS. The two diastereomeric peptides were separated by RPHPLC and characterized by ESMS and aminoacid analysis. These peptides, tested for the proliferation of human CD4+ T cell clones from MS patients, showed different behaviors. Only one of them gave a noteworthy reproducible response, in respect to the wild type peptide. In order to identify the enantiomer

responsible for the biological activity, we attempted to obtain the pure enantiomers of Fmoc-Apalm-OH.

The reaction of Fmoc-Apalm-OH with *S*(-)-*sec*-phenethyl alcohol, DCC, DMAP/DMAP·TFA in dry DCM gave two diastereomeric esters that were partially resolved by fractional crystallization from petroleum ether (80:20 ratio between the diastereomers, as detected by HPLC on silica). The resolution procedure was also performed by crystallization of the diastereomeric salts of Fmoc-Apalm-OH with *R*(-)-2-amine-1-benzyloxybutane [3], but this led to a less satisfactory enantiomeric excess. The complete resolution of Fmoc-Apalm-OH can be achieved by separation of its diastereomeric esters with *S*(-)-*sec*-phenethyl alcohol by semipreparative HPLC followed by catalytic hydrogenation.

We are trying to obtain single crystals from the two diastereomeric esters in order to determine the absolute configuration of the asymmetric carbon of 2-aminopalmitic acid by X-ray analysis.

## Conclusion

The new lipophilic building-block Fmoc-Ampa-OH can be a useful tool for synthesizing peptides in which the hydrophobic chain is present as a side-chain linked with a C-C bond in any part of the peptide backbone.

## Acknowledgments

This research was supported by "1st Project on Multiple Sclerosis", Istituto Superiore di Sanità, Ministero della Sanità, Italy.

We thank Dr. B. Mazzanti, Dr. M. Vergelli and Dr. L. Massacesi (Dipartimento di Scienze Neurologiche e Psichiatriche, Università di Firenze, Italy) for the preliminary proliferative study of CD4+ T cell line to the two diastereomeric peptides.

## References

1. Deprez, B., Sauzet, J.-P., Boutillon, C., Martinon, F., Tartar, A., Sergheraert, C., Guillet, J.-G., Gomard, E. and Gras-Masse, H., *Vaccine*, 14 (1996) 375.
2. Gibbons, W.A., Hughes, R.A., Charalambous, M., Christodoulou, M., Szeto, A., Aulabaugh, A.E., Mascagni, P. and Toth, I., *Liebigs, Ann. Chem.* (1990) 1175.
3. Touet, J., Faveriel, L. and Brown, E., *Tetrahedron* 51 (1995) 1709.

## **Session V**

# **Structure, Folding and Conformational Analysis**



# Folding of a predominantly $\beta$ -sheet protein with a central cavity

P.L. Clark,<sup>a,b</sup> M. Sukumar,<sup>a</sup> Z.P. Liu,<sup>b</sup> J. Rizo,<sup>b</sup> B.F. Weston,<sup>a</sup>  
K.S. Rotondi<sup>a</sup> and L.M. Gierasch<sup>a</sup>

<sup>a</sup>*Department of Chemistry, University of Massachusetts, Amherst, MA 01003, USA*

<sup>b</sup>*University of Texas Southwestern Medical Center, Dallas, TX 75235, USA*

While we have known for many years that an amino acid sequence is sufficient to direct the folding of a protein to its native structure [1], the mechanism by which the sequence guides the process of folding is still not well understood. Particularly lacking are principles by which  $\beta$  structure forms. Cellular retinoic acid binding protein I (CRABPI) serves as an apt model for detailed study of the folding of a predominantly  $\beta$ -sheet protein with a simple topology, no cofactors or disulfides, and reversible unfolding-refolding behavior. The structure of CRABPI is composed of a short helix-turn-helix and a ten-stranded compressed  $\beta$ -barrel which surrounds a central cavity (Fig. 1) [2,3]. Analysis of the kinetics of CRABPI refolding by stopped-flow fluorescence (SF-Flu) of wild-type and single-Trp variants, stopped-flow circular dichroism (SF-CD), hydrogen exchange, and probing of ligand binding has provided a description of the stages in its folding pathway. These results are complemented by study of peptide fragments corresponding to regions in the sequence of CRABPI, which enable an assessment of the importance of local conformational propensities in guiding folding.

## Results and Discussion

CRABPI contains three tryptophan residues, at positions 7, 87 and 109. SF-Flu during folding shows that the protein folds with four kinetic phases (see Table 1), with the process initiated via global hydrophobic collapse, indicated by an increase in fluorescence intensity

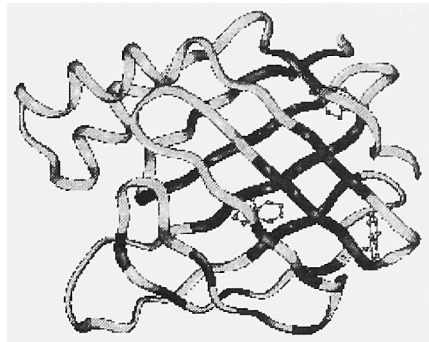


*Fig. 1. Ribbon diagram of the crystal structure of CRABPI [2]. Amino acid residues with amide protons observed in the quenched-flow experiments are shown as darkened sections of ribbon; the locations of the three tryptophan sidechains are drawn as ball-and-stick representations.*

and the blue-shift of the emission spectrum [4]. SF-Flu of the folding of single-Trp CRABPI variants demonstrates that 70% of the Trp7 environment evolves on a 100-200 ms time scale (including the docking of the N-

and C-termini), the quenching of Trp109 fluorescence by the guanidino group of Arg111 (a specific native state tertiary interaction) occurs on a 1 s time scale, and the presence of a slow folding phase attributable to proline isomerization.

Quenched-flow NMR experiments show the development of stable hydrogen bonds during folding [5]: all observable amide protons in the  $\beta$ -clamshell are protected from hydrogen exchange with similar phases; 80% of protection occurs on a 1 s time scale, with 20% in a longer 15 s phase. These phases correlate well with the SF-Flu phase corresponding to the development of a specific tertiary environment involving Trp109, and with proline isomerization, and indicate that hydrogen bond formation occurs relatively late in the folding process.

We also determined when the central cavity of CRABPI is formed, using a fluorescent dye, ANS, that binds specifically to the cavity [5]. Adding the dye after specified folding intervals clearly shows that the binding cavity emerges on a 100 ms time scale—coincident with the time scale observed for the docking of the N- and C-termini. Therefore, the surrounding  $\beta$ -clamshell structure develops without the assistance of a hydrogen bonding network, but rather via specific sidechain interactions.

Two peptide fragments of CRABPI have been studied in an effort to dissect sequence contributions to the kinetic folding events. A peptide corresponding to the helix-turn-helix region of CRABPI (residues 10 to 32, peptide H-Sm-H) retains local sequence-driven conformational tendencies [6]. Embedded in the sequence of H-Sm-H is a motif found in many proteins and associated with helix termination and folding back of one secondary structural unit on another—the so-called Schellman motif [7]. NMR data in aqueous solution clearly show that H-Sm-H spends a significant proportion of time in a native-like conformation with a key local hydrophobic interaction between Leu19 and Val24 stabilizing the helix-helix arrangement. The Gly residue at position 23 is also critical to the local influence on folding.

Table 1. Summary of the kinetic pathway for CRABPI folding.

Kinetic Phase	Folding Events	Methods
Burst (<10 ms)	Hydrophobic Collapse	Fluorescence
	Secondary Structure (excess helix?)	ANS Binding (non-specific) CD
Fast (100-200 ms)	Cavity Formation	ANS Binding
	Docking of N- and C-termini	Fluorescence
Medium (1 s)	Hydrogen Bonding Network	Quenched-Flow NMR
	Specific Tertiary Interactions	Fluorescence CD
Slow (~20 s)	Proline <i>cis-trans</i> isomerization	Fluorescence
		CD
		Quenched-Flow NMR

We have recently begun to explore the importance of the turn regions in CRABPI in specifying the architecture of the  $\beta$  sheets. Strikingly, NMR data shows that a peptide corresponding to residues 72 to 82 has a highly populated native-like turn conformation in aqueous solution. NOEs are consistent with distances calculated for the native protein; the temperature coefficient of the Arg79 NH is significantly lower than those for adjacent NHs, as expected for the native turn; and all NH- $\alpha$ H coupling constants are as expected for the native  $\phi$  angles. This turn is stabilized in the protein by favorable side chain interactions between Arg79/Asp77, Lys80/Glu74 and Arg82/Glu72.

## Conclusion

We find that CRABPI folding is characterized by several kinetic events (Table 1): Early events (<10 ms) lead to a hydrophobically collapsed state with considerable structure. This state of the protein rearranges on a 100 to 200 ms time scale to adopt a structure with native-like topology including the central ligand-binding cavity and close approach of the N- and C-termini. Yet only on a 1 s time scale are the stable native hydrogen bonds in the  $\beta$  sheets formed, along with the specific tertiary packing of all side chains. We conclude that the topology of the  $\beta$  sheets in CRABPI is guided by incipient native side chain interactions; stable hydrogen bonding and presumably, solvent exclusion, occur only during the final stage of folding. Peptide fragments show that there are regions of CRABPI in which local sequence strongly directs the adoption of native-like conformation, even without the context of the entire protein. These regions may reflect initiation sites for the folding pathway.

## Acknowledgments

This research was supported by a grant from the NIH (GM27616).

## References

1. Anfinsen, C.B., *Science*, 181(1973)223.
2. Kleywegt, G.J. *et al.*, *Structure*, 2(1994)1241.
3. Thompson, J.R., Bratt, J.M. and Banaszak, L.J., *J. Mol. Biol.*, 252(1995)433.
4. Clark, P.L., Liu, Z.P., Zhang, J. and Gierasch, L.M., *Protein Science* 5(1996)1108.
5. Clark, P.L., Liu, Z.P., Rizo, J. and Gierasch, L.M., submitted.
6. Sukumar, M. and Gierasch, L.M., *Folding & Design*, in press.
7. Schellman, C., In Jaenicke, R. (Ed.) *Protein Folding*, Elsevier, North-Holland, New York, (1980) 52.

# Insights into the molecular mechanisms of protein folding and misfolding

**Sheena E. Radford**

*Department of Biochemistry and Molecular Biology, University of Leeds, Leeds LS2 9JT, UK*

The field of protein folding commenced more than twenty five years ago with Chris Anfinsen's Nobel prize winning discovery that protein folding is a spontaneous process [1]. Since then, new and exciting methods have been developed to try to delineate the mechanisms by which proteins fold, the steps taken, the structure and roles of partially folded states, and the nature of the transition states that separate them. Ingenious methods involving hydrogen exchange labeling and detection of protected amides by  $^1\text{H}$  NMR [2], and later by electrospray mass spectrometry [3], provided the first insights into the structure of partially folded states, their stability and the kinetics of their formation. In addition, the stopped flow methods of circular dichroism to detect nascent secondary structure and fluorescence to detect hydrophobic collapse have shed light on the nature of events in the first few msec of folding (see [4] for a review). Most recently, the very early stages of folding occurring on  $\mu\text{sec}$  and  $\text{nsec}$  time scales are being revealed using novel methods that include very rapid mixing or temperature jump experiments [5]. We have been using a number of different biophysical methods to determine, in as much detail as possible, how one protein, hen lysozyme, folds [6]. We have shown that the protein folds along parallel pathways and that the major folding route involves an intermediate partially folded state in which only one domain composed of purely  $\alpha$ -helices (the  $\alpha$ -domain) is folded [7]. For all of these experiments, conditions have to be found (11-fold dilution of the protein denatured in 6M guanidinium chloride sodium acetate buffer, pH5.2, 20°C), under which protein folding is a unimolecular event, and any intermolecular processes involving transient or irreversible protein association or aggregation are avoided. *In vivo*, folding conditions cannot be so strictly controlled, and a new and exciting field of protein misfolding, highlighted by the role of protein aggregation in Alzheimer's disease and the transmissible spongiform encephalopathies, is now at the forefront of research.

## Results and Discussion

Hydrogen exchange labeling studies monitored by  $^1\text{H}$  NMR have demonstrated that formation of the  $\beta$ -domain is the rate limiting step in lysozyme folding [7]. In order to probe the nature of this step, we have studied the folding of a three disulphide lysozyme derivative in which one of the four native disulphide bonds (Cys6-Cys127) has been reduced and the resulting cysteine residues carboxymethylated [8]. This species retains the native fold, but is significantly destabilized relative to its four disulphide counterpart [9]. Reduction of the disulphide bond was shown to destabilize the  $\alpha$ -domain intermediate to such an extent that it is no longer populated during folding. Despite this, the rate of folding

of the  $\beta$ -domain is unaffected, suggesting that folding this domain is an independent and intrinsically slow process. More recent experiments, in which the  $\alpha$ -domain is destabilized by refolding lysozyme at high temperature (50°C), are in agreement with these results (Matagne, Radford and Donson, unpublished).

Our interest in the folding of the  $\beta$ -domain of lysozyme was heightened by the discovery that mutations in this domain in human lysozyme (replacement of Ile for Thr at position 56, or Asp for His at position 67) result in the deposition of lysozyme in amyloid fibrils [10, 11]. Our knowledge of the folding characteristics of lysozyme provided us with a unique opportunity to try to gain new insights into the mechanisms of fibril formation at the molecular level [11]. Using a combination of methods we demonstrated that the amyloidogenic lysozyme variants are less stable than the wild-type protein (by about 12°C at pH7), and that they unfold non-cooperatively via a partially folded state resembling a typical 'molten globule' state. In addition, the recombinant form of the variant proteins form fibrils *in vitro* by extended incubation at pH 7, 37°C. Fibrillogenesis involved structural conversion of the mainly helical structure of the native fold to a typical amyloid cross  $\beta$ -fold. Taken together, the data suggest that a reduction in the cooperativity between the two domains caused by the mutations is responsible for the unique amyloidogenic properties of the variant forms.

To investigate further the folding and aggregation of the  $\beta$ -domain we have synthesized this region of hen lysozyme as two short synthetic peptides (corresponding to residues 41-60 and 61-84 in native lysozyme) [12, 13]. Peptide 41-60 encompasses the  $\beta$ -sheet in native lysozyme, including the site of one of the amyloidogenic mutations. The peptide forms  $\beta$ -sheet structure at low pH in a concentration dependent manner [12]. At very high concentrations (~10mg/ml) the peptide forms a solid gel-like material which also is formed of antiparallel  $\beta$ -sheets and, excitingly, appears to be fibrillar in nature [14]. This and other peptides taken from naturally occurring proteins or designed *de novo* to self assemble are being actively studied at the Center for Self Organizing Molecular Systems in Leeds. A simple 11-residue peptide was designed and found to assemble spontaneously into the desired structure. The  $\beta$ -sheet tapes are much simpler than fibrils from intact proteins, some of the tapes are a single molecule in thickness, whilst others stack back-to-back. Molecular self assembly of the peptides to polymeric  $\beta$ -sheet tapes provides a powerful system to investigate the molecular nature of the self assembly and structural nature of the polymers. In addition, we hope that a molecular understanding of the assembly process of these simple systems will provide inspiration for new therapies for amyloid diseases, as well as proving novel routes to the production of new materials.

## Acknowledgements

Much of the work described was performed at the Oxford Centre for Molecular Sciences (OCMS). I would like to acknowledge the enormous role that Chris Dobson, Carol Robinson, Maureen Pitkeathley and Margaret Sunde at the OCMS played in this work, and our collaborators, Mark Pepys and his group at the Royal Postgraduate Medical School,

Hammersmith Hospital (London), for introducing us to the exciting field of amyloidosis. I also thank my new research group in Leeds for their hard work and, in particular, the contributions of Nevil Boden, Amalia Aggeli, Mark Bell and Andrew Strong on the structural nature of peptide gels. There are many others, too many to mention here individually, who have also contributed to the work described. I hope that all of these appear in the reference list, if they are not listed here. Finally, I thank the EPSRC, BBSRC, MRC, the Wellcome Trust and the Royal Society for supporting this work.

## References

1. Anfinsen, C. B. *Science*, 181 (1973) 223.
2. Englander, S. W. and Mayne, L. *Annu. Rev. Biophys. Biomol. Struct.*, 21 (1992) 243.
3. Miranker, A., Robinson, C. V., Radford, S. E. and Dobson, C. M., *FASEB J*, 10 (1996) 1.
4. Evans, P. A. and Radford, S. E. *Current Opinion in Structural Biology*, 4 (1994) 100.
5. Wolynes, P. G., Luthey-Schulten, Z. and Onuchic, J. N. *Chemistry and Biology*, 3 (1996) 425.
6. Radford, S. E. and Dobson, C. M., *Proc. Roy. Soc. London B*, 348 (1995) 17.
7. Radford, S. E., Dobson, C. M. and Evans, P. A. *Nature*, 358 (1992) 302.
8. Eyles, S. J., Robinson, C. V., Radford, S. E. and Dobson, C. M. *Biochemistry*, 33 (1994) 1534.
9. Cooper, A., Eyles, S. J., Radford, S. E. and Dobson, C. M. *J. Mol. Biol.*, 225 (1992) 939.
10. Pepys, M. B., Hawkins, P. N., Booth, D. R., Vigushin, D. M., Tennent, G. A., Soutar, A. K., Totty, N., Nguyen, O., Blake, C. C. F., Terry, C. J., Feast, T. G., Zalin, A. M. and Hsuan, J. J., *Nature*, 362 (1993) 553.
11. Booth, D., Sunde, M., Bellotti, V., Robinson, C. V., Hutchinson, P., Fraser, W., Hawkins, P. E., Dobson, C. M., Radford, S. E., Blake, C. C. F. and Pepys, M. P., *Nature*, 385 (1997) 787.
12. Yang, J. J., Pitkeathly, M. and Radford, S. E., *Biochemistry*, 33 (1994) 7345.
13. Yang, J. J., Buck, M., Pitkeathly, M., Kotik, M., Haynie, D. T., Dobson, C. M. and Radford, S. E., *J. Mol. Biol.*, 252 (1995) 483.
14. Aggeli, A., Bell, M., Boden, N., Keen, J., Knowles, P.F., McLeish, T.C.B., Pitkeathly, M. and Radford, S.E. *Nature*, 386 (1997) 259.

# Prediction of protein transmembrane segments using a hydrophobicity scale derived from hydrophobic peptides

Li-Ping Liu, Chen Wang and Charles M. Deber

*Division of Biochemistry Research, Hospital for Sick Children, Toronto M5G 1X8; and  
Department of Biochemistry, University of Toronto, Toronto M5S 1A8, Ontario, Canada*

Hydrophobicity analyses have been used extensively in algorithms to predict membrane-spanning segments of proteins; several hydrophobic scales for amino acid residues have been proposed to facilitate these studies [for a review, see ref. 1]. However, significant differences exist among these scales due to their varying methods of determination, and/or the peptides used as the experimental basis for construction of the scale. Previous studies have suggested that the interaction between a peptide's hydrophobic face with the hydrophobic stationary phase of a reversed-phase high performance liquid chromatography (RP-HPLC) column is a reasonable mimic for the interaction of a peptide with a membrane-mimetic environment [2]. Accordingly, through evaluating the retention time behavior of model hydrophobic peptides in RP-HPLC experiments, we developed a new hydrophobicity scale [3], and in the present work compare it with two other commonly-used hydrophobicity scales [4,5]. We find that our HPLC-based scale - derived specifically from properties of hydrophobic peptides - may have some advantage over the Kyte-Doolittle (KD) and Engelman-Steitz-Goldman (GES) scales in predicting protein transmembrane (TM) segments.

## Results and Discussion

*De novo* designed peptides with typical sequence Lys-Lys-Ala-Ala-Ala-X-Ala-Ala-Ala-Ala-Ala-X-Ala-Ala-Trp-Ala-Ala-X-Ala-Ala-Ala-Lys-Lys-Lys-Lys-amide were synthesized by Fmoc solid phase chemistry [6], where X residues were substituted with each of the 20 commonly-occurring amino acids. An uninterrupted 19-amino acid hydrophobic core was employed to mimic membrane-interactive TM  $\alpha$ -helices. Since the distribution of three 'X' residues is angularly and longitudinally symmetric, amphipathic bias is minimized when 'X' is defined by any charged or polar residues.

Peptide retention times were recorded on a reversed-phase Primesphere C4 column (250 x 4.6 mm, 10  $\mu$ m, 300 Å) using a linear AB gradient (2% B/min) elution at a flow rate of 1 ml/min, where eluent A is 0.1% TFA/dd water, and B is 0.1% TFA/acetonitrile (Table 1). Despite the obvious differences between the two sets of model peptides in length (25 residues vs. 18 residues) intrinsic character (non-amphipathic vs. Amphipathic) number of guest residues per peptide (3 vs. 1) and the differing chromatographic conditions, comparison of the retention times of the present peptide series with the 'AX9 peptides' of Sereda *et al.* (typical sequence: Ac-Glu-Ala-Glu-Lys-Ala-Ala-Lys-Glu-X-Glu-Lys-Ala-Ala-Lys-Glu-Ala-Glu-Lys-amide) [7] gave an excellent correlation ( $r = 0.97$ ). This result

may relate to the comparable helical 'face' (clusters of Ala residues + one guest residue) presented by each set of peptides to the stationary phase of the HPLC column. These findings provide evidence that the retention times can reflect the intrinsic hydrophobic character of the substituted 'X' residues remarkably well.

If we assume that the retention time of a peptide is directly related to the summed hydrophobicity/hydrophilicity of the amino acids, the measured retention times of each peptide can be converted to a relative hydrophobicity scale for the corresponding substituted 'X' residues. For data analysis, we set  $H = 10 \times \Delta t_{R_{X-Lys}} / \Delta t_{R_{Phe-Lys}} - 5.00$ , where  $H$  = amino acid residue hydrophobicity,  $\Delta t_{R_{X-Lys}}$  is the retention time difference (min.) between the 'X' peptide and the 'Lys' peptide, and  $\Delta t_{R_{Phe-Lys}}$  is the retention time difference between 'Phe' peptide and the most hydrophobic 'Lys' peptide [3]. Through this calculation, Phe is assigned a value of +5, while the most hydrophilic, Lys is assigned a value of -5. The resulting values are listed in Table 1.

The advantages of this HPLC-derived scale are as follows: (1) the scale is based on a set of transmembrane  $\alpha$ -helical peptides [8]; and (2) the measured retention times arise from a combination of the hydrophobicity and helicity of peptides upon interaction with the hydrophobic stationary surface of the column. These factors should produce a scale which

*Table 1. Retention times and hydrophobicity scale of model peptides (adapted from [3]).*

Residue	Retention time of corresponding peptide (min)	Hydrophobicity
Phe	22.58	5.00
Trp	22.49	4.88
Leu	22.40	4.76
Ile	22.13	4.41
Met	21.23	3.23
Val	21.07	3.02
Cys <sup>a</sup>	21.82	2.49
Tyr	20.28	2.00
Ala	18.88	0.17
Thr	17.92	-1.08
Glu	17.60	-1.49
Asp	16.84	-2.49
Gln	16.64	-2.75
Arg	16.63	-2.77
Ser	16.57	-2.84
Gly	16.22	-3.31
Asn	15.85	-3.79
His	15.21	-4.63
Pro	14.98	-4.92
Lys	14.92	-5.00

<sup>a</sup>To avoid the complexity of synthesizing a multiple Cys-containing peptide, only the middle 'X' residue was substituted by Cys, and the other two 'X' residues were replaced by Leu.

Table 2. TM helices in the photosynthetic reaction center (*R. viridis*) obtained by x-ray crystallography and by prediction using the hydrophathy scale from the present work.

L chain	M chain	H chain	Over-	Under-	Accuracy (%)
				prediction	prediction
<b>X-ray crystallography [9]</b>					
33-63 (21)	52-76 (25)	12-35 (24)			
84-111(28)	111-137 (27)				
116-139 (24)	143-166 (24)				
171-198 (28)	198-223 (26)				
226-249 (24)	260-284 (25)				
<b>hydrophathy scale prediction (17 residue window)</b>					
22-51(30)	55-80 (26)	10-32 (23)	34	31	76
81-109 (29)	110-135 (26)				
115-140 (26)	141-166 (26)				
176-194 (19)	201-223 (23)				
224-250 (27)	258-290 (33)				

will reflect closely the extant interactions between TM segments with membranes. Using this scale (Table 1), we attempted predictions of the TM helices in the photosynthetic reaction center - one of the very few membrane proteins studied by crystallography [9]. The segments identified as TM helices by the X-ray determination and those identified by the scale are given in Table 2. Using the method proposed by Ponnuswamy & Gromiha for assessing the accuracy of a theoretical prediction [10], the present scale correctly predicts 76% of TM residues. Similar predictive analyses gave an accuracy of 73% for the GES scale [5], and 45% for the KD scale [4]. A more definitive evaluation of the new scale awaits extension of these analyses to a broader sample of crystallized membrane proteins.

## References

1. Nakai, K., Kidera, A. and Kanehisa, M., *Prot. Engineering*, 2(1988)93.
2. Aguilar, M.-I., Hodder, A.N. and Hearn, M.T.W., *J. Chromatogr.*, 327(1985)115.
3. Liu, L.-P., Wang, C., Goto, N.K., Reithmeier, R.A.F. and Deber, C.M. (1997), submitted.
4. Kyte, J. and Doolittle, R.F., *J. Mol. Biol.*, 157(1982)105.
5. Engelman, D.M., Steitz, T.A. and Goldman, A., *Ann. Rev. Biophys. Biophys. Chem.*, 15(1982)321.
6. Atherton, E. and Sheppard, R.C., In Rickwood, D. and Hames, B.D. (Eds.), *Solid Phase Peptide Synthesis, A Practical Approach*, IRL Press, Oxford, U.K., 1990; p. 131.
7. Sereda, T.J., Mant, C.T., Sönnichsen, F.D. and Hodges, R.S., *J. Chromatogr. A*, 676(1994)139.
8. Liu, L.-P. and Deber, C.M., *Biochemistry*, 26(1997)5476.
9. Deisenhofer, J. Epp, O., Miki, K., Huber, R. and Michel, H., *Nature*, 318(1985)618.
10. Ponnuswamy, P.K. and Gromiha, M., *Int. J. Peptide Prot. Res.*, 42(1993)326.

# Structure, function, and modeling of human endothelin and its precursor polypeptide, BigET: Targets for rational drug design

**B.A. Wallace<sup>a</sup> and R.W. Janes<sup>b</sup>**

<sup>a</sup>*Dept. of Crystallography, Birkbeck College, Univ. of London, London WC1E 7HX, UK*

<sup>b</sup>*School of Biol. Sci., Queen Mary and Westfield College, Univ. of London, London E1 4NS, UK*

We have determined the crystal structure of human endothelin-1 (ET) [1], the most potent naturally-occurring vasoconstrictor. This 21-amino acid polypeptide has two disulfides which link residues 1 and 15, and 3 and 11, respectively. It consists of a short N-terminal  $\beta$ -strand followed by a hydrogen-bonded loop connected to a long irregular helix that extends to the C-terminus of the molecule (Fig. 1a). Comparisons of the X-ray structure, with the various and diverse NMR structures reported for the polypeptide indicate that the most significant differences are in those regions that are important for receptor binding and specificity, namely the central loop and the C-terminal helix [2].

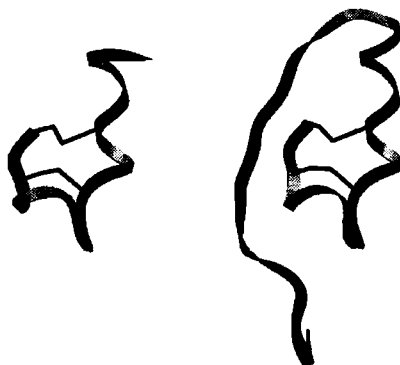


*Fig.1 Structures of ET and its precursor, BigET. A) Crystal structure of human ET-1 [1]; B) Molecular model of human BigET [10]. Both molecules are shown as ribbon diagrams in the same orientation, with the N-terminus being located to the left in the figure of ET.*

## **G-Protein Coupled Receptors and the Endothelin Crystal Structure**

One concern for either an NMR or X-ray structure of a relatively small polypeptide that may be flexible in solution or influenced by packing in a crystal, is whether the structure is related to the conformation that binds the target receptor *in vivo*. In this case, correlations between the structure and binding activity data for a number of ET analogues strongly support the crystal structure as being the biologically relevant form with respect to G-protein coupled receptor binding [3]. For example, alanine scan studies showed a functional periodicity of 3 or 4 residues in the C-terminus [4], indicative of a helically

repeating structure, as found in the X-ray but not the NMR structures. Furthermore, mapping of all the residues important for binding places them on a single face of the crystal structure [3]. No such clustering of sites (nor any sensible pattern) emerges from any of the NMR structures. Another test as to whether a structure is related to the biologically-active conformation is if two molecules which bind to the same site but which are chemically unrelated can be overlaid in three dimensions in a manner that places important functional groups in coincident positions. BQ123, a cyclic peptide containing D- and L-amino acids and a conformationally-restricted proline, is a competitive antagonist of ET. Although chemically very different, it shows remarkable overlap with residues 17 to 21 of the C-terminus of ET as found in the crystal structure, especially in its aromatic and carboxyl side chains [5]. No such overlaps could be made with any of the NMR structures. Thus it appears that, unlike any of the NMR structures, the X-ray structure is relevant to receptor-binding conformation. As a consequence, this structure provides an experimental basis for the rational drug design of new endothelin receptor antagonists.

### **A Model for the Structure of the Endothelin Precursor BigET**

ET is synthesized as a prepropolypeptide of 212 amino acids, which is subjected to a series of processing steps to produce the mature and active 21 amino acid ET molecule. The immediate precursor to ET, a 38 amino acid polypeptide designated BigET, appears to have no receptor-binding activity. The final processing step is the C-terminal cleavage of 17 amino acids at an unusual Trp-Val bond by the Endothelin Converting Enzyme (ECE) [6]. A three-dimensional structure of BigET would provide important information for rational drug design of inhibitors for the final step in the processing pathway. NMR studies of BigET have shown that the C-terminal extension is floppy and thus they have been unable to define the nature of the structure in the region of the cleaved bond and beyond [7,8]. A recent development has been the production of crystals of BigET (Cronin & Wallace, unpublished data), but the X-ray structure is unlikely to be available for some time. Hence, there is now a need for a testable model structure which can be used as a framework for design studies. Any correct model must satisfy the following biophysical criteria: 1) The NMR spectra of the common parts of BigET and ET are indistinguishable, thus indicating at least residues 1 to 18, and possibly residues 1 to 21, are in identical conformations [7,8]; 2) The 3-dimensional structure of ET has been defined by X-ray crystallography [1]; and 3) Circular dichroism spectroscopic studies indicate that the additional residues in the C-terminal extension adopt specific conformations [9]. Not unexpectedly, given the small size of the polypeptide, homology modeling studies did not produce any structures consistent with all of the above criteria (Peto, Janes, & Wallace, unpublished results). However, modeling using a threader algorithm on the proET molecule, followed by extracting the BigET fragment from that structure, produced a model that met all the criteria [10] (Fig. 1b). Its first 20 amino acids have the same conformations as they do in ET, and the C-terminal extension has the following notable features: residues 26 to 29 form a two-stranded  $\beta$ -sheet with residues 1 to 5 of the N-

terminus, the irregular helix which begins at residue 9 is extended to residue 23 (residues 21-23 being in a standard alpha helix conformation) and there is a hydrogen-bonded  $\beta$ -turn between the carbonyl group of residue 35 and the amino group of residue 38.

### **Endothelin Converting Enzymes and the BigET Model Structure**

Again, it is important to examine the relevance of the BigET structure to the conformation which is active *in vivo*, in this case, that which binds to proteases. Biochemical criteria can be used to test the BigET model structure. The BigET Trp<sup>21</sup>-Val<sup>22</sup> bond is cleaved by ECE; in the model structure, this bond is surface accessible, as it must be. Furthermore, the reduced susceptibilities to other proteases at other sites in BigET relative to the equivalent sites in ET [11] are correlated with sites of reduced surface accessibility in the model. Hence, all the currently available biophysical and biochemical evidence suggests this model structure is consistent with the type of structure cleaved by ECE. Since BigET itself does not exhibit vasoactivity, molecules which mimic its structure and are capable of binding to and inhibiting ECE could prove to be beneficial therapeutics in that they would prevent formation of the active mature ET molecule. Thus, the BigET model structure may provide a useful template on which inhibitor drugs for the endothelin converting enzyme could be designed.

In summary, the structures of ET and its precursor polypeptide BigET provide important new information for the rational design of antagonists of the ET<sub>A</sub> receptor and inhibitors of the ECE protease, respectively.

### **Acknowledgements**

The authors thank R. Corder, H. Peto, S. Krystek, and C. Peishoff for helpful discussions. This work was supported by British Heart Foundation Grant 95009 (to B.A.W.).

### **References**

1. Janes, R.W., Peapus, D.H., and Wallace, B.A., *Nature Struct. Biol.*, 1(1994) 311.
2. Wallace, B.A., Janes, R.W., Bassolino, D.A., and Krystek, S.R., *Prot. Sci.*, 4(1995) 75.
3. Wallace, B.A. and Janes, R.W., *J. Cardiovascular Pharm.*, 25(1995) s350.
4. Tam, J.P., Liu, W., Zhang J.-W., Galantino, M., Bertolero, F., Cristiani, C., Vaghi, F., and de Castiglione, R., *Peptides*, 15(1994) 703.
5. Peishoff, C.E., Janes, R.W., and Wallace, B.A., *FEBS Lett.*, 374(1995) 379.
6. Turner, A.J. and Murphy, L.J., *Biochemical Pharmacology*, 51(1995) 91.
7. Donlan, M.L., Brown, F.K., and Jeffs, P.W., *J. Biomol. NMR*, 2(1992) 407.
8. Inooka, H., Endo, S., Kikuchi, T., Wakimasu, M., Mizuta, E., and Fujino, M., *Pept. Chem.*, 28(1990) 409.
9. Wallace, B.A. and Corder, R., *J. Peptide Res.*, 49(1997) 331.
10. Peto, H., Corder, R., Janes, R.W., and Wallace, B.A., *FEBS Lett.*, 394(1996) 191.
11. Corder, R., *Biochemical Pharmacology*, 51(1996) 259.

## 3D modeling for TM receptors: Problems and perspectives

Gregory V. Nikiforovich,<sup>a</sup> Stan Galaktionov,<sup>a</sup> Vladimir M. Tseitin,<sup>a</sup>  
David R. Lewis,<sup>a</sup> Mark D. Shenderovich<sup>b</sup> and Garland R. Marshall<sup>a</sup>

<sup>a</sup>Center for Molecular Design, Washington University, Box 8036, St. Louis, MO 63110, USA;

<sup>b</sup>Department of Chemistry, University of Arizona, Tucson, AZ 85721, USA

Developing 3D models of transmembrane G-protein coupled receptors (TM GPCRs) starting from their amino acid sequences is one of the most challenging tasks facing computational biophysics. Some 3D information on TM proteins is known *a priori*. TM segments (presumably helical) are immobilized in the lipid environment. Also, protein fragments at the outer surface of the membrane would certainly not interact with fragments inside the cell. Therefore to attempt building 3D models of TM receptors several independent steps: are necessary (i) locate possible TM helical fragments in the GPCR sequence; (ii) build 3D structures for these helices; (iii) arrange isolated helices across membrane; (iv) calculate all pairwise helix-helix interactions; (v) assemble helical bundle(s), (vi) restore interhelical loops and N- and C-termini, and, (vii) refine the entire 3D structure(s). Most of these steps are either already developed as computer algorithms and are validated, or are at the implementation stage. Recent progress is briefly reported in this study.

### Results and Discussion

**Predicting Breaks in TM Helices.** We have developed a novel energy-based procedure for locating the ends of TM helical fragments. We have utilized the postulate that a peptide chain can "enter" an  $\alpha$ -helix at the N-end and "exit" from it at the C-end without steric hindrance by using only a limited number of backbone conformers for the terminal residues (e.g., [1]). Comparing conformational energy of the regular helical conformation for the peptide fragment,  $E(\alpha)$ , and the energies of the same fragment in conformations sterically allowing "entries to" or "exits from" a helical segment,  $E_i$ , we can obtain the minimal value out of  $E_i - E(\alpha)$  values,  $\Delta_k$ . The lesser is  $\Delta_k$ , the greater the tendency for the helix to be disrupted at the  $k$ -th residue in the amino acid sequence. Sliding the fragment "window" by one residue at a time along the sequence, we obtain several  $\Delta_k$  values; the smallest ones represent potential "signals" to disrupt the helix.

Validation of our procedure was performed by predicting possible breaks in 17 long helices belonging to 6 soluble globular proteins of known X-ray structures, namely 6adh, 2lzm, 1gpd, 3grs, 1mba and 1ccp. Energy calculations for each peptide fragment were performed as described earlier [2] employing the ECEPP/2 force field. Out of 17 cases, signals corresponding to the predicted N-terminal "breaks" coincided with the actual N-termini in 8 cases, and differed by one position in 7 cases, the maximal difference being

two positions. Out of 16 cases of C-terminal predictions, 13 C-terminal signals are located exactly at the actual C-termini or within one position of them, and in only 3 cases the differences are of two or three positions. The procedure was applied also to 17 transmembrane helices (10 helices of the photosynthetic reaction center (PRC) [3] and to 7 of bacteriorhodopsin (BR) [4]) In all cases but two, the N-terminal residues were marked by a signal located either at the same position, or shifted by just one position. This is also true for all C-terminal residues. Although these results show that our procedure is quite accurate, it produces multiple choices for possible "entries" and "exits" for each given helix.

**3D Structures of Isolated Helices.** Energy calculations performed employing the ECEPP force field for TM helices in the PRC L-subunit have yielded conformers with the following rms values for C $\beta$ -atoms in comparison with the X-ray structures: 0.84 Å for LA helix, 0.49 Å for LB, 2.9 Å for LC (LC helix contains 3 prolines), 0.93 Å for LD, and 1.2 Å for LE. The same calculations performed for BR helices produced the rms values of 0.85 Å for BR1, 1.95 Å for BR2, 2.34 Å for BR3, 0.63 Å for BR4, 0.57 Å for BR5, 1.34 Å for BR6, and 1.10 Å for BR7. These results strongly suggest that the backbone structures calculated for isolated helices would be almost the same in helical bundle(s). In other words, we can pack isolated helices consisting of the "hard cores" (backbones) and the "soft shells" (side chains).

**Predictions of Intramembrane Regions in TM Helices.** We have developed a computational procedure to place an isolated TM helical segment into the system of the double phase boundary (water/octanol/water) of a given thickness (for details see *Tseitlin V.M., Nikiforovich G.V., these Proceedings*). The procedure has been applied to predict intramembrane regions of the TM helices of the PRC L-subunit. The best prediction was obtained assuming a membrane thickness of *ca.* 24 Å; the intramembrane boundaries of helical fragments have been predicted with an average accuracy of 1.8 residues. The same values were 3.3 residues for the PRC M-subunit, and 1.5 for BR.

**Pairwise Packing of Helices.** We have developed an algorithm that calculates total conformational energy for two helices. The energy depends on the dihedral angles of the side chains for both helices (again, the backbones are kept frozen), and on the six additional "global" parameters describing relative movements of helices as rigid bodies. The calculation protocol consists of the initial scanning of the dihedral angles in side chains of both helices, minimization of energy with respect to these angles and to the six "global" parameters, then to renewed scanning of side chains in the newly found local minimum followed by new minimization, and so on. Energy calculations are performed systematically, starting in each "cube" in the six-dimensional space of the "global" parameters selected to completely cover the six-dimensional space available for each pair of helices. Some initial results show that the procedure reproduces the X-ray complex of the PRC helices LA/LB with the rms value of 1.6 Å when energy minimization was started from the experimental dihedral angle values and the experimental "global" parameters. We have also performed a limited number of calculations to find possible LA/LB complexes

starting from the calculated 3D structures for isolated LA and LB helices, and from various sets of "global" parameters. So far, our best results yield the rms value of 3.2 Å.

**Assembling Helical Bundle.** The above approach deals with a pair of helices. To assemble a bundle out of these pairs, we have developed a special algorithm employing the results of the previously described "pairwise" interactions. For each complex formed by a pair of helices (**a,b**), these results include the value of energy,  $E_{ab}$ , as well as the coordinates of the complex. Each sterically allowed ternary complex (**a,b,c**) can be revealed by manipulations with three (0,1)-matrices, namely  $Q_{ab}^{bc}$ ,  $Q_{bc}^{ca}$  and  $Q_{ac}^{ab}$ , containing information on pairs (**a,b**), (**a,c**) and (**b,c**). The elements  $\{d_{ij}\}$  of a matrix  $D = Q_{ab}^{bc}Q_{bc}^{ca}$  would be the numbers of the sterically allowed triplets (**a,b,c**) in which the pair (**a, b**) forms the binary complex of type *i* and the pair (**a,c**) of type *j*. Also, for each element  $\{d_{ij}\}$ , the element  $\{e_{ij}\}$  of the matrix of energies, *E*, would be determined, where  $e_{ij} = E_{ab}^i + E_{ac}^j + E_{bc}^{ij}_{\min}$ , the  $E_{bc}^{ij}_{\min}$  being the lowest energy for every  $d_{ij}$  complex of the type (**b,c**). Then, the matrices *D* and *E* could be used for further extending the ternary complex (**a,b,c**) by adding the fourth helix, **d**, which forms binary complexes with helices **a** and **c**, etc. Although the algorithm cannot exclude combinatorial problems completely, it reduces them to manipulations with (0,1)-matrices that can be performed very rapidly.

**Restoring Interhelical Loops.** We have developed a procedure to build loops in proteins based on the residue-residue contact matrix approach (for partial details of the approach see Galaktionov S., Nikiforovich G.V., Marshall G.R., *these Proceedings*). For this particular problem, we assumed that the contact matrix is composed of two main parts, one that is constant (the core part) and the variable or loop parts. After predicting the variable part of the matrix, the three-dimensional structures for loops are reconstructed at the level of  $C^\alpha$ -atoms, and then are restored at all-atomic resolution structure with subsequent refinement using the ECEPP force field. The procedure was used for loop restoration in five globular proteins of known X-ray structure, namely 4cpv, 1bp2, 351c, 3c2c and 3icb featuring two loops each ranging from 9 to 28 residues; the rms values between predicted and experimental spatial positions of  $C^\alpha$ -atoms were from 3.1 to 4.9 Å. Several 3D structures for loops 50-64 and 89-102 in 4cpv and for loops 16-25 and 55-63 in 3icb have been restored at all-atom resolution yielding conformers with the rms values from 1.6 to 2.9 Å [5].

## References

1. Efimov, A. V., *Molekuliarnaia Biologia* (in Russian), 20 (1986) 250.
2. Nikiforovich, G. V., *Int. J. Peptide Protein Res.*, 44 (1994) 513.
3. Deisenhofer, J., Epp, O., Sinning, I. and Michel, H., *J. Mol. Biol.*, 246 (1995) 429.
4. Henderson, R., Baldwin, J. M., Ceska, T. A., Zemlin, F., Beckmann, E. and Downing, K. H., *J. Mol. Biol.*, 23 (1990) 899.
5. Galaktionov, S., Shenderovich, M.D., Nikiforovich, G.V. and Marshall, G.R. In *Peptides - 1996. Proceedings of the 24th European Peptide Symposium, Edinburgh, 1996*, in press.

# Multicyclic side-chain bridged peptides designed for $\alpha$ -helix stabilization

John W. Taylor, Guihua Guo and Chongxi Yu

Department of Chemistry, Rutgers University, Piscataway, NJ 08855 USA

Our laboratory has used a series of model peptides, as well as peptide segments from native protein structures, to investigate and develop side-chain to side-chain links as conformational constraints favoring  $\alpha$ -helix formation in short monomeric peptides. Lys<sup>i</sup>, Asp<sup>i+4</sup> and Asp<sup>i</sup>, Lys<sup>i+4</sup> side-chain linkages are known to stabilize  $\alpha$ -helical structure [1]. In addition, helix stabilizing side-chain linkages for residue pairs separated by two turns of  $\alpha$  helix have also been developed. One such bridge that we reported recently consists of a 4-(aminomethyl)-phenylacetic acid residue (AMPA) linking the side chains of a 2,3-diaminopropionic acid residue (Dap) in position *i* and an Asp in position *i*+7 [2]. Our model peptide studies have now been extended (a) to investigate the importance of the intervening *i*+1, *i*+2 and *i*+3 residues in determining helix stabilization by the Lys<sup>i</sup>, Asp<sup>i+4</sup> lactam bridges, and (b) to test the helix stabilizing effects of combining the *i*, *i*+4 bridges and the *i*, *i*+7 bridges to create different bicyclic structures.

## Results and Discussion

We are interested in using peptides as models to investigate the protein folding and lipid binding properties of transmembrane proteins. To this end, we have studied the following peptide analogues of the second transmembrane helix (TMH2) proposed for the  $\delta$ -opioid receptor [3]:

- TMH2: Acetyl- $[\delta$ -receptor residues 81-108]-NH<sub>2</sub>  
A<sub>3</sub>-TMH2: Acetyl-(cyclo<sup>1-5</sup>)[Lys-Ala<sub>3</sub>-Asp-( $\delta$ -receptor residues 81-108)]-NH<sub>2</sub>  
R<sub>3</sub>-TMH2: Acetyl-(cyclo<sup>1-5</sup>)[Lys-Arg<sub>3</sub>-Asp-( $\delta$ -receptor residues 81-108)]-NH<sub>2</sub>  
S<sub>3</sub>-TMH2: Acetyl-(cyclo<sup>1-5</sup>)[Lys-Ser<sub>3</sub>-Asp-( $\delta$ -receptor residues 81-108)]-NH<sub>2</sub>

Table 1. Mean residue ellipticities of peptides measured at 25 °C in different solvents.

Peptide	Solvent	$[\theta]_{192}$	$[\theta]_{208}$	$[\theta]_{222}$
TMH2	20% HFIP in H <sub>2</sub> O	25,000	-10,000	-9,800
A <sub>3</sub> -TMH2	20% HFIP in H <sub>2</sub> O	59,700	-24,800	-24,300
R <sub>3</sub> -TMH2	20% HFIP in H <sub>2</sub> O	41,800	-19,100	-17,700
S <sub>3</sub> -TMH2	20% HFIP in H <sub>2</sub> O	31,400	-15,000	-14,500
biAMPA-9	100% H <sub>2</sub> O	2,100	2,300	12,100
biAMPA-14	100% H <sub>2</sub> O	46,400	-12,500	-12,100
KD/AMPA-9	100% H <sub>2</sub> O	7,700	-4,500	-1,200
KD/AMPA-14	100% H <sub>2</sub> O	42,400	-11,500	-15,100

These TMH2 peptides were designed to investigate the helix stabilizing effects of various Lys<sup>i</sup>, Asp<sup>i+4</sup> lactam-bridged pentapeptides as N-terminal extensions to transmembrane helical segments of the human  $\delta$ -opioid receptor. By measuring the CD spectra of the TMH2 analogs in 20% aqueous hexafluoroisopropanol (HFIP), we have shown (Table 1) that the helix stabilizing effects of the residues Xxx in the Lys<sup>i</sup>, Asp<sup>i+4</sup>-bridged N-terminal extensions, cyclo<sup>1-5</sup>[Lys-Xxx<sub>3</sub>-Asp]- are ordered Ala > Arg > Ser > no bridged extension. Therefore, within this limited series, the helix stabilizing effects of the intervening i+1, i+2 and i+3 residues in a Lys<sup>i</sup>, Asp<sup>i+4</sup> lactam-bridged peptide follow the order of helix forming propensities established previously for individual residues in linear peptides [4].

In a separate study, we have also extended our earlier studies of model dicyclic and bicyclic 14-residue peptides by combining the best helix stabilizing i, i+4 and i, i+7 side-chain bridges within the same peptides to create new bicyclic structures. These new model peptide structures are shown below (Z = Dap[AMPA]):

biAMPA-9: H-(cyclo<sup>1-8, 2-9</sup>)[Z-Z-K-L-K-E-L-D-D]-OH

biAMPA-14: H-(cyclo<sup>3-10, 7-14</sup>)[K-L-Z-E-L-K-Z-K-L-D-E-L-K-D]-OH

KD/AMPA-9: H-(cyclo<sup>1-5, 2-9</sup>)[K-Z-K-L-D-E-L-K-D]-OH

KD/AMPA-14: H-(cyclo<sup>3-10, 7-14</sup>)[K-L-Z-K-L-K-Q-D-L-D-E-L-K-Q]-OH

The CD spectra of these four peptides were measured at 25 °C in aqueous phosphate buffer, pH 7.0 (Table 1). These spectra indicated that both of the bicyclic 14-residue peptides, biAMPA-14 and KD/AMPA-14, had high helix contents. Furthermore, these helical structures were very resistant to thermal denaturation over the temperature range from 0 °C to 80 °C. In contrast, both of the 9-residue bicyclic peptides gave CD spectra indicating that no  $\alpha$ -helical structure was present at any temperature within this range.

## Conclusion

These results demonstrate (a) that the intervening residues between side-chain linked Lys<sup>i</sup> and Asp<sup>i+4</sup> residues determine, in part, the helix stabilizing effects of these bridges, and (b) that helix stabilizing side-chain linkages placed in overlapping positions in the linear amino-acid sequence of a peptide can be used to generate highly rigid  $\alpha$ -helical structures.

## References

1. Fry, D. C., Madison, V. S., Greeley, D. N., Felix, A. M., Heimer, E.P., Frohman, L., Campbell, R.M., Mowles, T.F., Toome, V., and Wegrzynski, B.B., *Biopolymers*, 32 (1992) 649.
2. Yu, C., and Taylor, J. W., *Tet. Lett.*, 37 (1996) 1731.
3. Evans, C. J., Keith, D. E., Morrison, H., Magendzo, K, and Edwards, R. H., *Science*, 258 (1992) 1952.
4. O'Neil, K. T., and DeGrado, W. F., *Science*, 250 (1990) 646.

# Natural selection with self replicating peptides

S.Q. Yao, I. Ghosh and J.A. Chmielewski

Department of Chemistry, Purdue University, West Lafayette, IN 47907, USA

The self-replicating capabilities of DNA have played a penultimate role in the widespread emergence of biotechnology strategies. The ability to produce useful quantities of DNA from a limited pool of molecules has revolutionized fields as diverse as criminology and genetic medicine. DNA is unique in its self-replication, and species which rely on DNA for replication of self can adapt to environmental changes through natural selection. There are recent examples of designed molecular systems capable of self-replication, including nucleotide-based oligomers, [1,2,3] adenine-Kemp's triacid conjugates [4], peptides [5] and micelles [6]. The production of a single self-replicating molecule from a large molecular pool, a form of *in vitro* natural selection, has been a more elusive target. Recent work of Lee *et al* demonstrated that peptides from the GCN4 leucine zipper domain self-replicate in an autocatalytic cycle [5]. We sought peptidic self-replicating systems that would be sensitive to environmental conditions and reproduce only under extreme conditions. We now disclose a system composed that displays the properties of natural selection via autocatalysis and cross-catalysis in an environmentally-dependent manner.

## Results and Discussion

We designed peptides E1E2 and K1K2 (Fig. 1) based on the peptides of Zhou *et al* (EE, KK) [7]. E1E2 was designed to form a coiled-coil under acidic conditions due to protonation of Glu side-chains at the *e* and *g* positions of the helical heptad repeats, whereas K1K2 was designed to form a coiled-coil at neutral pH only upon addition of helix-stabilizing salts, such as NaClO<sub>4</sub>. Under physiological conditions, however, the negatively-charged side-chains of Glu should destabilize the coiled-coil of E1E2, as should the protonated side-chains of K1K2, leading to a random coil conformation in both cases.

E1	Ac-ELYALEKELGALEKELA-COSR
E2	H-CLEKELGALEKELYALEK-NH <sub>2</sub>
E1E2	Ac-ELYALEKELGALEKELACLEKELGALEKELYALEK-NH <sub>2</sub>
K1	Ac-KLYALKEKLGALKEKLA-COSR
K2	H-CLKEKLGALKEKLYALKE-NH <sub>2</sub>
K1K2	Ac-KLYALKEKLGALKEKLACLKEKLGALKEKLYALKE-NH <sub>2</sub>
E1K2	Ac-ELYALEKELGALEKELACLKEKLGALKEKLYALKE-NH <sub>2</sub>
K1E2	Ac-KLYALKEKLGALKEKLACLKEKELGALEKELYALEK-NH <sub>2</sub>

Fig. 1. Sequences of the peptide fragments and potential products.

Two fragments each of E1E2 and K1K2 (Fig. 1), the electrophilic thioester-containing fragments E1 and K1, and the nucleophilic fragments E2 and K2, that contain free cysteine at their N-termini, were designed based on the thioester-promoted, peptide-bond formation strategy.[8] We predicted that under acidic conditions the coupling between E1 and E2 to form E1E2 should proceed via an autocatalytic pathway, whereby the coupled product, E1E2, would act as a template to organize the two subunits and accelerate their condensation. This should lead to enhanced E1E2 production from a mixture of the four peptide fragments. At neutral pH the organized structure of E1E2 and K1K2 should be lessened, and a mixture of the four potential products would result. Addition of 2M NaClO<sub>4</sub>, however, should enhance the coiled-coil of K1K2 and its templating ability, leading to enhanced production of K1K2 within the peptide mixture.

Circular dichroism spectroscopy (CD) was used to assess the helical content of the designed peptides by measuring their ellipticity at 222 nm. It was found that E1E2 adopted a helical conformation in a pH-dependent manner; the helical content reached a maximum of 90% at pH 4.0, presumably due to formation of a coiled-coil dimer in which the Glu residues are protonated. K1K2 adopted a helical conformation in a NaClO<sub>4</sub> concentration-dependent manner, with a maximum helicity of 90% reached at 2M NaClO<sub>4</sub>, presumably due to shielding of the positively-charged lysine side-chains, resulting in a stabilized coiled-coil.

To demonstrate that autocatalysis could be controlled by environmental modifications, the thiol-capture reaction with was performed with a mixture of E1, E2, K1 and K2 at pH 4.0 and at 7.5. At pH 4.0 the exclusive (>95%) product formed was E1E2 (Fig. 2). A decrease in E1E2 product formation was observed at pH 7.5, confirming the lack of autocatalysis upon deprotonation of the Glu residues and uncoiling of E1E2 (Fig. 2). The high rate of E1E2 formation at pH 4.0 as compared to pH 7.5 is most likely due to the autocatalytic nature of the reaction at pH 4.0 due to templating of the peptide fragments by E1E2. Addition of E1E2 to the pH 4.0 reaction mixture was shown to increase product formation (data not shown).

When the thiol-capture reaction was performed at pH 7.5 with 2 M NaClO<sub>4</sub>, K1K2 was the dominant product formed (Fig. 2) as was predicted by the circular dichroism studies, although the other three possible products were formed in significant quantities as well. The E1E2 peptide was also used in the mixed peptide reaction to further enhance the production of K1K2. K1K2 production was examined with 100 μM E1E2 at pH 7.5 with 2 M NaClO<sub>4</sub> (Fig. 2). Under these reaction conditions K1K2 production was significantly enhanced relative to the other products to greater than 80% of the reaction mixture.

In conclusion we have demonstrated that a peptide system may be designed in which both autocatalysis and cross-catalysis have occurred. Product distributions may be controlled by reaction conditions such as low pH and high salt., such that very high selectivity can occur under specific conditions. As such this system could be said to possess the attributes of both self-replication and natural selection.

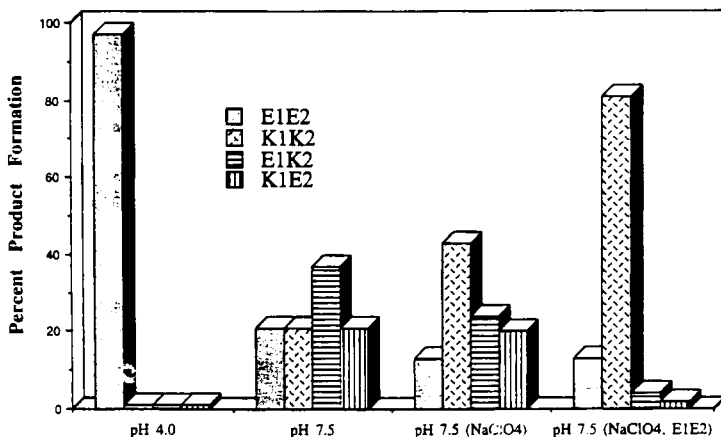


Fig. 2. Product formation with reaction conditions.

## References

- (a) von Kiedrowski, G.; Wlotzka, B.; Helbing, J.; Matzen, M.; Jordan, S. *Angew. Chem. Int. Ed. Eng.*, 30 (1991) 8839. (b) Sievers, D.; von Kiedrowski, G. *Nature*, 369 (1994) 221. (c) Achilles, T.; von Kiedrowski, G. *Angew. Chem. Int. Ed. Eng.*, 32 (1993) 1198. (d) von Kiedrowski, G. *Bioorg. Chem. Front.*, 3 (1993) 113.
- (a) Zielinski, W. S.; Orgel, L. E. *Nature*, 327 (1987) 346. (b) Orgel, L. E. *Nature*, 358 (1992) 203. (c) For a review, see: Orgel, L. E. *Acc. Chem. Res.*, 28 (1995) 109.
- Li, T.; Nicolaou, K. C. *Nature*, 369 (1994) 218.
- (a) Tjivikua, T.; Ballester, P.; Rebek, J. Jr. *J. Am. Chem. Soc.*, 112 (1990) 1249. (b) Nowick, J. S.; Feng, Q.; Tjivikua, T.; Ballester, P.; Rebek, J. Jr. *J. Am. Chem. Soc.*, 113 (1991) 8831. (c) Wintner, E. A.; Conn, M. M.; Rebek, J. Jr. *J. Am. Chem. Soc.*, 116 (1994) 8877.
- Lee, D. H.; Granja, J. R.; Martinez, J. A.; Severin, K.; Ghadiri, M. R. *Nature*, 382 (1996) 525.
- Bachmann, P. A.; Luisi, P. L.; Lang, J. *Nature*, 357 (1992) 57.
- (a) Zhao, N. E.; Kay, C. M.; Hodges, R. S. *J. Mol. Biol.*, 237 (1994) 500. (b) Kohn, W. D.; Monerra, O. S.; Kay, C. M.; Hodges, R. S. *J. Biol. Chem.*, 270 (1995) 25495. (c) Chao, H.; Houston, M. E. Jr.; Grothe, S.; Kay, C. M.; O'Connor-McCourt, M.; Irvin, R. T.; Hodges, R. S. *Biochemistry*, 35 (1996) 12175.
- (a) Dawson, P. E.; Muir, T. W.; Clark-Lewis, I.; Kent, S. B. H. *Science*, 266 (1994) 776. (b) Canne, L. E.; Bark, S. J.; Kent, S. B. H. *J. Am. Chem. Soc.*, 118 (1996) 5891. (c) Zhang, L.; Tam, J., *J. Am. Chem. Soc.*, 119 (1997) 2363.

# Exploring the foldability and function of insulin by combinatorial peptide chemistry

Ming Zhao, Satoe H. Nakagawa, Qingxin Hua and Michael A. Weiss

*Departments of Biochemistry & Molecular Biology and Chemistry, The University of Chicago,  
Chicago, IL 60637, USA*

Insulin, an ancestral and highly conserved motif of protein structure, provides a well-characterized model for the study of protein folding. Native disulfide pairing (A6-A11, A7-B7 and A20-B19; Fig. 1) is directed by sequences in the A- and B domains [1]. The isolated chains may, therefore, be regarded as peptide models of proinsulin-folding intermediates [2]. In previous studies of insulin and homologous proteins we and others have sought to define sequence determinants of protein foldability [3], the pathway of protein folding [4, 5], and the structures of protein-folding intermediates [6, 7]. Given that disulfide bridges are thought to *reflect* rather than *direct* nascent interactions in the folding chain, which contacts are most critical to specify disulfide pairing?. Conversely, in a rugged free-energy surface how are non-native pairing schemes (and other off-pathway kinetic traps; [8, 9]) avoided?.

In this paper we describe a synthetic approach to define the structural and functional roles of individual amino acids. This approach employs combinatorial peptide chemistry to compare the effect of L- and D-amino acid substitutions on insulin "foldability." A novel *in vitro* selection has been designed based on chain combination [10]; mass spectrometry is used to distinguish between "allowed" and "disallowed" B-chain sequences [11]. This method in principle allows systematic analysis of the mechanism of chain combination and is applied below to invariant sequence features of the B-chain: positions B8 and B24. Motivation is in each case based on crystal structures of the native state [12]. Gly<sup>B8</sup> exhibits an unusual structural transition involving its backbone dihedral angles in the two crystallographic states (T and R; see Nakagawa *et al.* in the volume). Although Phe<sup>B24</sup> adjoins the A20-B19 disulfide bridge in the hydrophobic core, paradoxical enhancement of bioactivity is observed on its substitution by D-amino acids.

## Results and Discussion

Modified insulin B chains were synthesized by SPPS using Fmoc chemistry. Four series of B-chain libraries were prepared with 17 (or 18) L- (or D-) amino acids at positions 8 and 24, respectively, by using a simple process of dividing, coupling and recombining the peptide resins to ensure the equimolarity of individual insulin B-chain analogs within the peptide pool. That the expected range of amino acids was incorporated in each B-chain library was verified by MALDI-TOF mass spectrometry. The individual libraries were each combined with the native A-chain (in an S-sulfonate form) [4], and the chain combination reaction was monitored by MS.

To our surprise, the B8 L-amino acid library yielded only a trace amount of insulins as detected by MS. The D-amino acid library by contrast resulted in native foldability (Fig. 2).

After chain combination the B8 D-library was subjected to gel filtration and RP-HPLC purification. All expected D-amino acid substitutions were detected by MS. Among these substitutions polar side chains at position 8 (such as D-Lys and D-Arg) gave a better yield in chain combination than non-polar or aromatic side chains (such as D-Ala and D-Trp). The purified D-amino acid insulin analogs or partially resolved HPLC fractions were assayed *in vitro* for their ability to interact with insulin receptors of human placental membranes. All samples exhibit very low affinity (< 0.5% of that of insulin, data not shown). Attempts to enhance the yield of L-amino acid analogs by manipulation of chain-combination conditions failed. In particular, use of prolonged reaction times resulted in a

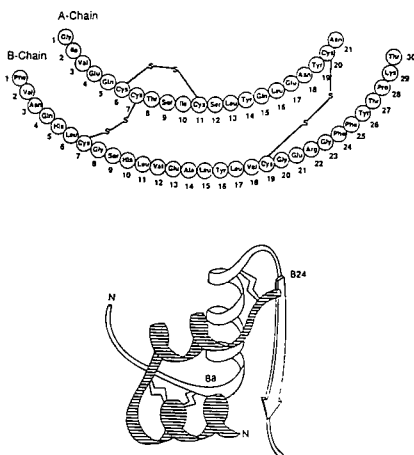


Fig. 1. Human insulin primary structure (top) and the ribbon model of insulin crystallographic T-state structure (bottom, the A chain is striped).

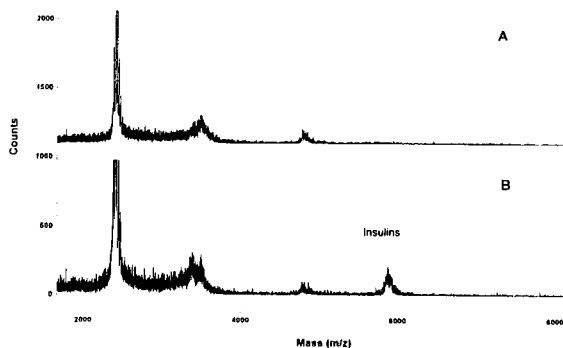


Fig. 2. MALDI-TOF spectra of the chain-combination reactions (24 hr, 4 °C) of L-B8 library (A) and D-B8 library (B).

considerable increase in the amounts of both insulins and A- and B-chain. polymer mixtures This observation was verified by conventional synthesis of L-Ala and D-Ala insulin B-chain analogs: the respective efficiencies of chain combination in each case mirrored those of the parent D- and L-amino acid libraries. These results have structural implications. Since the invariant residue Gly<sup>B8</sup> adopts the dihedral angles of a D-amino acid in the T-state and of an L-amino acid in the R-state, we speculate that the structural features of the T-state are more relevant to folding than are those of the R-state. We propose in particular that this B8  $\phi$  dihedral angle is critical in allowing or hindering formation of the A7-B7 disulfide bridge on the surface of the protein. The B24 libraries gave a distinct pattern of results. B-chain analogs with an L-amino acid at position B24 offered a significantly better yield in chain combination than those with a D-amino acid. However, the overall yields were in each case significantly lower than that characteristic of native insulin-chain combinations [4, 11]. Further, large differences were observed in the relative yield of distinct L-amino acids. These observations suggest that an L-amino acid (rather than a D-amino acid) is required at position B24 for efficient insulin foldability and that the particular properties of the side chain are important. The environment of Phe<sup>B24</sup> is similar in both T and R states: the side chain anchors the B-chain  $\beta$ -turn (B20-B23) and  $\beta$ -strand (B24-B28) to the hydrophobic core. We propose that the presence of a nonpolar or aromatic side chain at position B24 facilitates initial hydrophobic collapse of this part of the hydrophobic core, in turn directing the pairing of the A20-B19 disulfide bridge.

## References

1. Tang, J.G. and Tsou, C.L., *Biochem. J.*, 268 (1990) 429.
2. Oas, T.G. and Kim, P.S., *Nature*, 336 (1988) 42.
3. Hu, S.Q., Burke, G.T., Schwartz, G.P., Ferderigos, N., Ross, J.B.A. and Katsyannis, P.G., *Biochemistry*, 32 (1992) 26314.
4. Hober, S., Forsberg, G., Palm, G., Hartmanis, M. and Nilsson, B., *Biochemistry*, 31 (1992) 1749.
5. Miller, J.A., Narhi, L.O., Hua, Q.X., Rosenfeld, R., Arakawa, T., Rohde, M., Prestrelski, S., Lauren, S., Stoney, K.S., Tsai, L. and Weiss, M.A., *Biochemistry*, 32 (1993) 5203.
6. Narhi, L.O., Hua, Q.X., Arakawa, T., Fox, M., Tsai, L., Rosenfeld, R., Holst, P., Miller, J.A. and Weiss, M.A., *Biochemistry*, 32 (1993) 5214.
7. Hua, Q.X., Hu, S.Q., Frank, B.H., Jia, W.H., Chu, Y.C., Wang, S.H., Burke, G.T., Katsyannis, P.G. and Weiss, M.A., *J. Mol. Biol.*, 264 (1996) 390.
8. Hua, Q.X., Gozani, S.N., Chance, R.E., Hoffmann, J.A., Frank, B.H. and Weiss, M.A., *Nature Struct. Biol.*, 2 (1995) 129.
9. Booth, D.R., Sunde, M., Bellotti, V., Robinson, C.V., Hutchinson, W.L., Fraser, P.E., Hawkins, P.N., Dobson, C.M., Radford, S.E., Blake, C.C. and Pepys, M.B., *Nature*, 385 (1997) 787.
10. Cosmatos, A., Ferderigos, N. and Katsyannis, P.G., *Int. J. Peptide Protein Res.*, 14 (1979) 457.
11. Muir, T.W., Dawson, P.E., Fitzgerald, M.C. and Kent, S.B., *Chem. Biol.*, 3 (1996) 817.
12. Adams, M.J., Blundell, T.L., Dodson, E.J., Dodson, G.G., Vijayan, M., Baker, E.N., Hardine, M.M., Hodgkin, D.C., Rimer, B. and Sheet, S., *Nature*, 224 (1996) 491.

# Characterization of Transforming Growth Factor Alpha binding to Epidermal Growth Factor receptor through NMR structure determination and NOE analysis methods

Campbell McInnes,<sup>a</sup> David. W. Hoyt,<sup>a</sup>  
Maureen O'Connor-McCourt<sup>b</sup> and Brian D. Sykes<sup>a</sup>

<sup>a</sup>*Protein Engineering Network of Centres of Excellence, University of Alberta, Edmonton, Alberta, T6G 2S2, Canada, and* <sup>b</sup>*Biotechnology Research Institute, Montreal, Quebec, H4P 2R2, Canada*

TGF is a small mitogenic protein with three disulfide loops and thus possesses significant secondary structure in solution. Binding of this ligand to the EGF receptor (EGFR) propagates biological responses including wound healing and embryogenesis [1,2]. Most significantly, however, it is understood to play a role in tumor proliferation [3,4]. Analysis of NOE and relaxation rate data from NMR experiments of TGF in complex with the extracellular domain of the EGFR has been undertaken and utilized to elucidate the residues and regions of the ligand that contribute to the receptor combining site [5,6]. These data indicate a multidomain binding model for TGF in which the A and C loops comprise the receptor binding interface and also suggest the regions of the ligand that are non-essential for complexation. In particular, the amino terminus of TGF was identified as remaining flexible in the receptor bound form and thus targeted for design of a reductant molecule. Using this information, a TGF analog has been synthesized in which the N-terminal seven residues were deleted. This polypeptide, which has been demonstrated to be active in an EGFR phosphorylation assay, has been characterized using NMR chemical shift differences and structure determination. It was shown to have a near native fold, although differences in the A and B loops are observed. The synthesis of an active reductant TGF suggests the feasibility of the design and synthesis of molecules which are further reduced in size but not in efficacy and may lead to progress in the development of agonists or antagonists.

## Results and Discussion

For the purpose of determining the contribution of the N-terminus of TGF to receptor binding and activity, the truncated protein Ac-TGF 8-50 was synthesized and purified prior to oxidation. Subsequent to oxidation, TGF 8-50 was repurified to give homogenous material of the correct molecular weight as determined by electrospray M.S. The biological activity of this mutant was performed by quantifying the extent of phosphorylation of the EGF receptor and comparing this with that of TGF. Using this assay, TGF 8-50 was shown to have activity approximately equal to that of the intact protein. For the purposes of characterization of the 3-D structure and determination of the contribution of the N-terminal tail to the global fold of TGF, 2-D TOCSY and NOESY spectra were acquired for the 43 residue polypeptide and chemical shift assignments were obtained. Comparison of

the resonance assignments with the native protein confirmed the presence of the correct fold of the three disulfides. It was observed, however, that there were significant differences between the H resonances of the deletion mutant and those of the intact molecule. A plot of for the protons of the two proteins is shown below (Fig. 1). It can be seen that the variation in the chemical shifts is greatest in the A loop i.e. the residues between 8 and 21, although changes are observed in the hinge region between the two subdomains. The individual residues that showed a  $\delta\Delta$  of greater than 0.1 ppm were C8, T13, Q14, F15, K29 and C32.

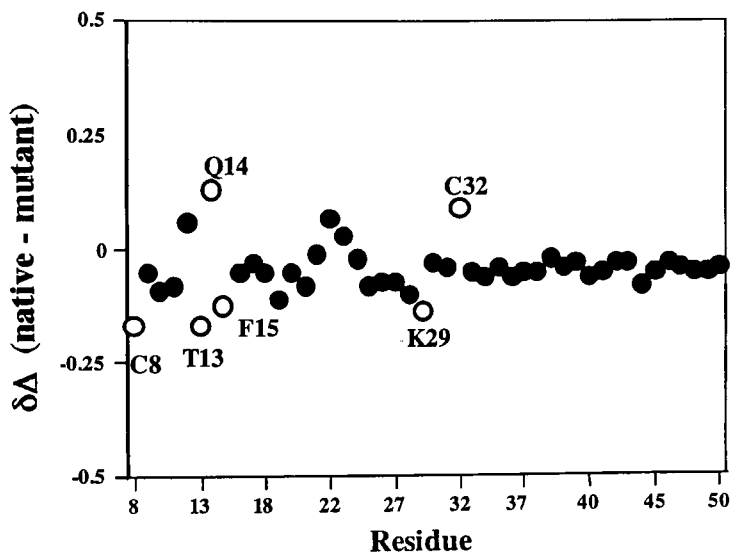
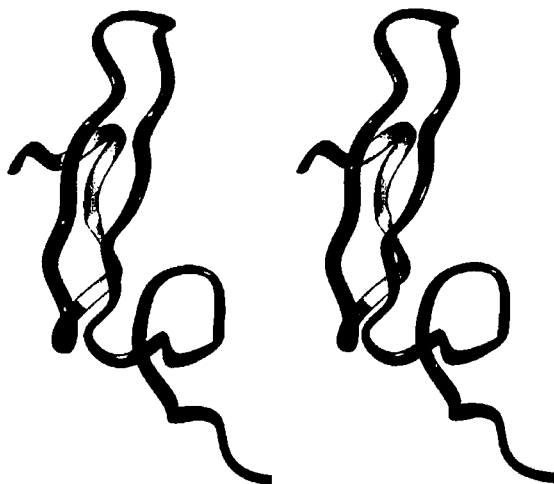


Fig. 1. Plot of  $\delta\Delta$  of -proton chemical shift differences between TGF and TG 8-50 at pH 6.0.

In order to calculate the solution structure of TGF 8-50, 407 NOE distance restraints were assigned from the NOESY spectrum of the  $D_2O$  and  $H_2O$  samples. These were used to calculate an ensemble of structures for the deletion analog using the simulated annealing-molecular dynamics program X-plor. The average structure is shown in a ribbon representation shown below (Fig. 2). The NMR structure reveals the differences between the TGF 8-50 and the native protein [7]. The A loop as suggested by the chemical shift variations of residues 8-21 loses the partial helix present in TGF. In addition, the C terminal subdomain has a different orientation from the wild type, being more perpendicular to the N-terminal subdomain. The conformational differences of TGF 8-50 and the near native activity suggest that it undergoes adaptation to the receptor binding pocket to adopt the structure of the native protein. TGF 8-50 was proposed based on the observation that the N-terminus of the protein remains flexible upon addition of the EGF receptor, as evidenced by the relaxation rate studies and that the N-terminal residues do not

lose any NOE's upon complexation. These data suggest that the flexibility of the tail residues do not contribute directly to receptor binding and thus are likely to be non-essential. Since the truncation analog has been demonstrated to be approximately as active as the wild type in the receptor phosphorylation assay, it is evident that this is true. Further TGF reductants may be possible, the study of which assist in the design of agonists/antagonists for this protein.



*Fig. 2. Stereoview of the NMR average structure of TGF 8-50.*

## References

1. Bennet, N. T., and Schultz, G. S., *Am. J. Surg.*, 165 (1993) 728-737
2. Bennet, N. T., and Schultz, G. S., *Am. J. Surg.*, 166 (1993) 75-81.
3. Derynck, R., Goeddel, D. V., Ullrich, A., Gutterman, J. U., Williams, R. D., Bringman, T. S., & Berger, W. H., *Cancer Res.*, 47 (1987) 707-712.
4. ten Dijke, P., & Iwata, K. K., *Bio/Technology*, 1 (1989) 793-798.
5. Hoyt, D. W., Harkins, R. N., Debanne, M. T., O'Connor-McCourt, M., and Sykes, B. D., *Biochemistry*, 33 (1994) 15283-15292.
6. McInnes, C., Hoyt, D. W., Harkins, Pagila, R. N., Debanne, M. T., O'Connor-McCourt, M., and Sykes, B. D., *J. Biol. Chem.*, 271 (1996) 32204-32211.
7. Moy, F. J., Li, Y.-C., Ravenbuehler, P., Winkler, M. E., Scheraga, H. A., & Montelione, G. T., *Biochemistry*, 32 (1993) 7334-7353.

## Vibrational and electronic circular dichroism study of 3<sub>10</sub>-helical stabilization in blocked ( $\alpha$ -Me)-Val peptides

Gorm Yoder,<sup>a</sup> T. A. Keiderling,<sup>a</sup> Alessandra Polese,<sup>b</sup> Fernando Formaggio,<sup>b</sup> Marco Crisma,<sup>b</sup> Claudio Toniolo,<sup>b</sup> Q. B. Broxterman<sup>c</sup> and Johan Kamphuis<sup>d</sup>

<sup>a</sup>Department of Chemistry, University of Illinois at Chicago, Chicago, IL 60607-7061, USA;

<sup>b</sup>Biopolymer Research Center, CNR, Department of Organic Chemistry, University of Padova, 35131 Padova, Italy; <sup>c</sup>DSM Research, Organic Chemistry and Biotechnology Section, 6160 MD Geleen, The Netherlands, <sup>d</sup>DSM Fine Chemicals, 6401 JH Heerlen, The Netherlands

Helical formation is a major factor in protein folding. While most helices in globular proteins are either  $\alpha$ -helical in conformation or distorted from that geometry, 3<sub>10</sub>-helices offer a major alternate form, yielding significant fractional contributions in a number of proteins. Furthermore, these "native" 3<sub>10</sub> helices are usually quite short, 1-2 turns, and often distorted. The determination of 3<sub>10</sub> helix formation for proteins in solution has long been a problem since many techniques give ambiguous results or are limited in their application. Recently, Toniolo et al. [1] proposed using the relative strengths of the  $n-\pi^*$  and  $\pi-\pi^*$  transitions as measured in electronic circular dichroism (ECD), in terms of  $R = \theta_{222}/\theta_{207}$ , to discriminate between peptides whose structures are primarily  $\alpha$ -helical ( $R \sim 1$ ) and 3<sub>10</sub>-helical ( $R \ll 1$ ). These R values were chosen based on measurements of the spectra of an unusually stable and well-formed 3<sub>10</sub>-helical octapeptide Ac-[L-( $\alpha$ -Me)Val]g-OtBu. ECD depends strongly on dipole coupling to sense stereochemistry and has an important length dependence. Its bandshapes are also susceptible to distortion due to electronic structure changes as might occur with  $\alpha$ -Me substitution and to overlap with unrelated transitions as often occurs with aromatic side chains. Since 3<sub>10</sub>-helices in proteins are often short and contain various residues, it is of interest to develop new tools for their detection. Vibrational CD (VCD) has been shown to be quite short range in sensitivity [2]. It develops a unique bandshape pattern for 3<sub>10</sub>-helices as compared to  $\alpha$ -helices [3], and is almost totally dependent on the relative orientation of the amides, which confers significant independence from the nature of the sidechain group or other perturbing effects such as solvation [4]. A comparison of ECD and VCD for  $\alpha$ -methylated oligopeptides of various lengths offers a basis for evaluating the reliability of such optical spectroscopic measures of 3<sub>10</sub> helix formation.

## Results and Discussion

Conformational variation in the homo-oligopeptide series Z-[L-( $\alpha$ -Me)-Val] $_n$ -OtBu ( $n=3$  to 8) and selected Ac-[L-( $\alpha$ -Me)-Val] $_n$ -OtBu oligomers ( $n=4, 6,$  and 8) was studied with ECD, VCD and Fourier transform IR (FTIR) spectra. This series was chosen as a test case due to its development of  $3_{10}$  helical conformational characteristics in very short oligopeptides and because of the regularity and closeness to ideal of the  $3_{10}$  helical torsional angles in the octamer as judged by its crystal structure [5]. VCD and FTIR data for the amide I and II bands of the former series were measured in  $\text{CDCl}_3$  and in TFE in what is the first VCD study of a complete homo-peptide series of  $\text{C}\alpha$ -methylated amino acids. The ECD spectra for both series were measured in TFE and HFIP over the 260-190 nm region. Octamer samples at various concentrations were studied with FTIR and ECD to probe the effect of peptide-peptide interactions on this structure.

The VCD spectra for these peptides with either blocking group confirm the  $3_{10}$  nature of the helices formed under these high concentration ( $\sim 0.5$  M in peptide), short path length conditions. For chain lengths as short as  $n=4$ , characteristic  $3_{10}$  helical VCD bandshapes were obtained, having a weak positive couplet for the amide I and a strong negative for the amide II. The Z blocked oligomers even gave similar results for  $n=3$ , while, for the Ac blocked peptides in TFE, generally weaker amide II VCD and broader VCD for  $n=4$  than for  $n=6,8$  were obtained. In general this pattern is consistent with previous spectroscopic and crystallographic characterizations of these oligomers [5]. FTIR data showed a steady decrease in amide I frequency and increase in amide II frequency with increasing peptide length. The VCD zero-crossings track this shift but maintain its band shape. This is a good example of the band shape being the primary diagnostic feature of VCD spectroscopy and the frequency, which can be affected by external perturbants, being relatively unimportant. The Z-blocked species have an extra urethane absorbance at  $\sim 1730$   $\text{cm}^{-1}$  which gives rise to little if any VCD since it is poorly coupled to the helical residues. These consistencies are effects of the VCD being dominated by amide-amide coupling and being relatively independent of other factors. The VCD observations confirm that the  $3_{10}$  helical conformation seen in the crystal structure is maintained in the high concentration solution.

ECD spectra measured for the Z series of peptides in TFE at  $\sim 0.1$  mM peptide concentration gave a somewhat different result from previous reports. The ECD bandshape for  $n=6$  is clearly less helical than for  $n=7$  or 8 and that for  $n=4$  is indicative of a coil form. However, the longer peptides had  $R \sim 0.8$ , somewhat higher than seen earlier [1,5]. Since the Z blocking group can interfere with the  $n\text{-}\pi^*$  ECD bands, the source of this discrepancy was in doubt. Remeasurement of the ECD for the Ac blocked peptides at  $\sim 1$  mM peptide indicated that the  $n=6,8$  bandshapes at high concentrations were similar and more closely resembled the proposed  $3_{10}$  helical form with  $R < 0.5$  and a weak 195 nm feature. This suggested the possibility of a concentration effect on the structure.

In TFE, as a function of decreasing concentration, the octamer has ECD spectra that progressively change from a bandshape similar to that associated with  $3_{10}$  helices [1] to one at lower concentrations that is more like that of an  $\alpha$ -helix due to a significant increase

in the intensity of both the 222 and 195 nm bands. While the two blocking groups give rise to somewhat differently shaped spectra, the general effect of concentration is seen with both. The relationships between the independent structural characterizations are important. The crystal structure is clearly  $3_{10}$  [5]; the VCD is  $3_{10}$ -like and was measured under very high concentration conditions to better mimic the crystal structure. Since the highest concentration ECD results have low R values, the VCD data provide a link to the structural data and support the proposal [1] that a low R value is indicative of  $3_{10}$  helical conformation. To confirm this link, the concentration dependence for the FTIR of the Z-octamer in  $\text{CDCl}_3$  showed no significant change in frequency or bands shape from 0.1 to 10 mM. In an independent test, we re-measured the ECD in HFIP over several days. Although initial spectra were  $3_{10}$ -like at high concentrations and  $\alpha$ -helical at low, gradually all spectra became similar with  $R \sim 1$ .

These results indicate a concentration induced shift in the  $3_{10}$ - to  $\alpha$ -helical equilibrium with  $3_{10}$ -helical stabilization by peptide-peptide interactions. The HFIP result implies that the solvent can also affect structural equilibrium with HFIP apparently better able to solvate the  $3_{10}$  aggregates. It is possible that, since they line up parallel to the helix axis, the side chains pack together much better in the  $3_{10}$  helical conformation. This conformation would favor that conformer in the crystal structure and at high concentration. Concentration induced helix stabilization has also been seen in previous VCD studies of  $(\text{LKKL})_n$  polymers and Ala rich helical peptides in water [6].

### Acknowledgment

This work was supported by a grant from the National Institutes of Health (GM30147).

### References

1. Toniolo, C., Polese, A., Formaggio, F., Crisma, M., Kamphuis, J., *J. Am. Chem. Soc.*, 18 (1996) 2744
2. Dukor, R. K. and Keiderling, T. A., *Biopolymers* 31 (1991) 1747. Freedman, T. B., Nafie, L. A., Keiderling, T. A., *Biopolymers (Peptide Science)*, 37 (1995) 265.
3. Yasui, S. C., Keiderling, T. A., Bonora, G. M., C. Toniolo, *Biopolymers*, 25 (1986) 79 . Yasui, S. C., Keiderling, T. A., Formaggio, F., Bonora, G. M., C. Toniolo, *J. Am. Chem. Soc.*, 108 (1986) 4988.
4. Keiderling, T. A., In G. D. Fasman (Ed.), "Circular Dichroism and the Conformational Analysis of Biomolecules" Plenum, New York (1996) p. 555
5. Polese, A., Formaggio, F., Crisma, M., Valle, G., Toniolo, C., Bonora, G. M., Broxterman, Q. B., Kamphuis, J., *Chem. Eur. J.*, 2 (1996) 1104.
6. Baumruk, V., Huo, D., Dukor, R. K., Keiderling, T. A., LeLeivre, D. and Brack, A., *Biopolymers*, 34 (1994) 1115. Yoder, G., Pancoska, P., Keiderling, T. A. (submitted).

# First peptide-based system of rigid donor, rigid acceptor, and rigid interchromophore spacer: A conformational and photophysical study

Claudio Toniolo,<sup>a</sup> Fernando Formaggio,<sup>a</sup> Marco Crisma,<sup>a</sup> Jean-Paul Mazaleyrat,<sup>b</sup> Michel Wakselman,<sup>b</sup> Clifford George,<sup>c</sup> Judith L. Flippen-Anderson,<sup>c</sup> Basilio Pispisa,<sup>d</sup> Mariano Venanzi<sup>d</sup> and Antonio Palleschi<sup>e</sup>

<sup>a</sup>Biopolymer Research Center, CNR, Department of Organic Chemistry, University of Padova, 35131 Padova, Italy; <sup>b</sup>SIRCOB, University of Versailles, F-78000 Versailles, France; <sup>c</sup>Laboratory for the Structure of Matter, Naval Research Laboratory, Washington, DC 20375, USA;

<sup>d</sup>Department of Chemical Sciences and Technologies, University of Rome, "Tor Vergata", 00133 Rome, Italy; <sup>e</sup>Department of Chemistry, University of Rome "La Sapienza", 00185 Rome, Italy

A proper understanding of the mechanisms of side-chain to side-chain interactions depends heavily upon the ability to design and build conformationally constrained structures whose intercomponent geometry is well defined. As appropriate templates, we chose to focus on structurally restricted  $3_{10}$ -helical peptides, which provide access to the investigation of through-space interactions between side chains of two  $\alpha$ -aminoacid residues incorporated at the  $i$  and  $i+3$  relative positions. By exploiting the conformationally restricted Aib residue and other helicogenic members of the  $C^{\alpha,\alpha}$ -disubstituted glycine family ( $Ac_6c$ ,  $Ac_7c$ , etc.) (Fig. 1) as the main building blocks [1, 2], it is possible to achieve stable  $3_{10}$ -helicity and excellent structural rigidity at very short peptide main-chain lengths.

In this communication we describe the results of our conformational and photophysical study of Boc-(S)-Bin-Ala-Aib-TOAC-(Ala)<sub>2</sub>-OtBu, the first peptide based on: (i) a *rigid*  $\alpha$ -aminoacid donor, (S)-Bin (Fig. 1), an optically pure, axially dissymmetric (atropoisomeric) 1,1'-binaphthyl-substituted Aib, which may also be considered a side-chain modified  $Ac_7c$  [3, 4]; (ii) a *rigid*  $\alpha$ -aminoacid acceptor, TOAC, an  $Ac_6c$  analog containing a stable nitroxide free radical [5]; (iii) a *rigid*  $3_{10}$ -helical interchromophore bridge. This N- and C-protected hexapeptide was synthesized by solution methods and fully characterized.

## Results and Discussion

The terminally-protected hexapeptide Boc-(S)-Bin-Ala-Aib-TOAC-(Ala)<sub>2</sub>-OtBu was synthesized by solution methods and fully characterized. Bin-Ala and TOAC-Ala peptide bond formation was achieved using the EDC/HOAt approach, while Ala-Aib and Aib-TOAC peptide bond formation was obtained *via* the symmetrical anhydride method. The -Ala-Aib-TOAC-Ala- sequence was built up using Fmoc N $^{\alpha}$ -protection.

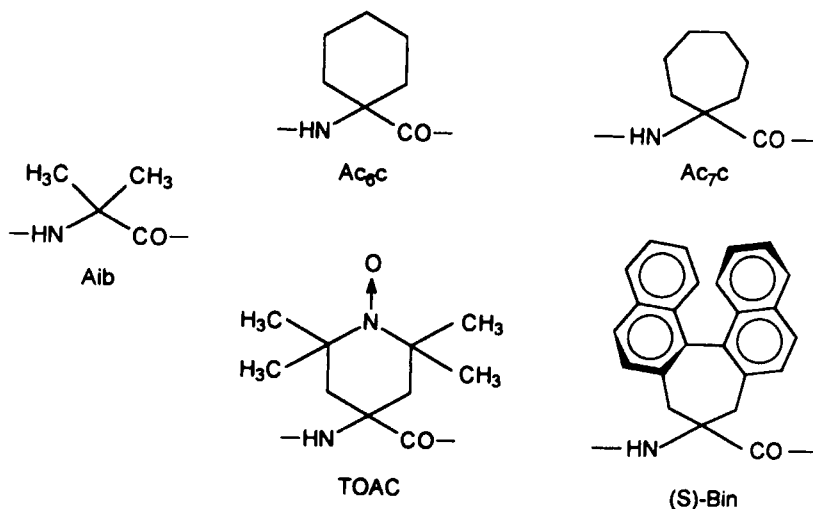


Fig. 1. Chemical structures of the five  $C^{\alpha,\alpha}$ -disubstituted glycines discussed in this work.

X-ray diffraction analysis of a crystal grown from acetone-light petroleum (by vapor diffusion) revealed the presence of two independent molecules (**A** and **B**) in the asymmetric unit. The conformational differences between molecules **A** and **B** are of minor significance. Figure 2 illustrates the 3D-structure of molecule **A**. The  $-(S)\text{-Bin}^1\text{-Ala-Aib-TOAC}^4-$  sequence is folded in a regular, *left-handed*  $3_{10}$ -helix, stabilized by three intramolecular  $1\leftarrow 4 \text{ C=O} \cdots \text{H-N}$  H-bonds. The  $\text{N}\rightarrow\text{O}$  bond of  $\text{TOAC}^4$  points towards the binaphthyl moiety of  $\text{Bin}^1$  after one complete turn of the ternary helix. The shortest intramolecular (nitroxide)  $\text{O} \cdots \text{C}$  (aromatic) distance is 4.8 Å. The angle between the direction of the  $\text{N-O}$  bond and the normal to the average plane of the closest naphthyl group is  $53^\circ$ . An FT-IR absorption study in the N-H stretching region in  $\text{CDCl}_3$  solution showed that two bands occur in the spectrum: (i) a weak band at  $3431 \text{ cm}^{-1}$ , associated with free, solvated NH groups, and (ii) an intense and broad band at lower wavenumbers (resolved into two components, with maxima at  $3341 \text{ cm}^{-1}$  and  $3312 \text{ cm}^{-1}$ , respectively), associated with intramolecularly H-bonded NH groups. These spectral features support the view that the hexapeptide is highly helical in solution.

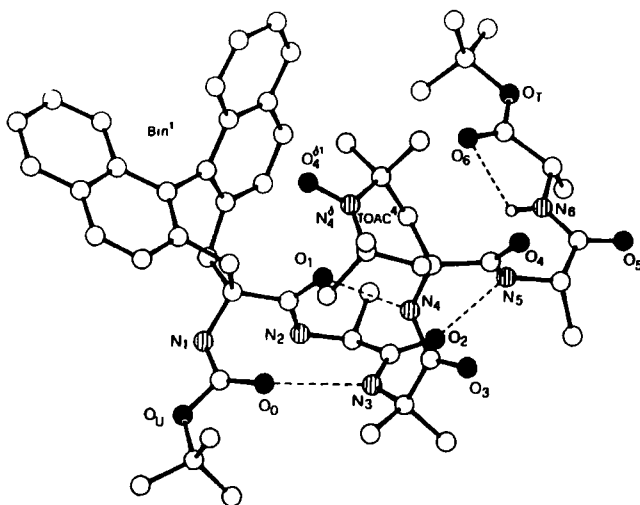


Fig. 2. X-Ray diffraction structure of one of the two independent molecules (A) in the asymmetric unit of Boc-(S)-Bin-Ala-Aib-TOAC-(Ala)<sub>2</sub>-OtBu.

The steady-state fluorescence spectrum of the hexapeptide ( $\lambda_{\text{ex}} = 305$  nm) shows a substantial quenching of binaphthyl singlet emission by TOAC. Fluorescence time decay measurements ( $\lambda_{\text{ex}} = 305$  nm,  $\lambda_{\text{em}} = 360$  nm) strongly suggest a bi-exponential decay. The shorter decay time ( $\tau_1$ ) ranges from 0.5 to 1.4 ns and the longer decay time ( $\tau_2$ ) from 3.1 to 4.5 ns, depending on the solvent medium. Both lifetimes may be interpreted as arising from a quenching process associated with an intramolecular electronic energy transfer from excited binaphthyl to TOAC, occurring within two rather rigid, left-handed  $3_{10}$ -helical conformers that exhibit a slightly different distance and relative orientation of the two photoprobes.

## References

1. Toniolo, C. and Benedetti, E., *Macromolecules*, 24 (1991) 4004.
2. Benedetti, E. and Toniolo, C., In Salamone, J.C. (Ed.), *Polymeric Materials Encyclopedia*, vol. 8P, CRC Press, Boca Raton, FL, 1996, p. 6472.
3. Mazaleyrat, J.P., Gaucher, A., Wakselman, M., Tchertanov, L. and Guilhem, J., *Tetrahedron Letters*, (1996) 2971.
4. Mazaleyrat, J.P., Gaucher, A., Wakselman, M., Toniolo, C., Crisma, M. and Formaggio, F., In Ramage, R. and Epton, R. (Eds.), *Peptides 1996*, Mayflower Worldwide, Kingswinford, England, 1997, in press.
5. Toniolo, C., Valente, E., Formaggio, F., Crisma, M., Piloni, G., Corvaja, C., Toffoletti, A., Martinez, G.V., Hanson, M.P., Millhauser, G.L., George, C. and Flippen-Anderson, J.L., *J. Pept. Sci.*, 1 (1995) 45.

# Correlation of kinetic data with crystallographic structures of Aspartic Proteinase

**Ben M. Dunn,<sup>a</sup> Kohei Oda,<sup>b</sup> Marina Bukhtiyarova,<sup>a</sup> Deepa Bhatt,<sup>a</sup> Chetana Rao-Naik,<sup>a</sup> W. Todd Lowther,<sup>a</sup> Paula E. Scarborough,<sup>a</sup> Brian M. Beyer,<sup>a</sup> Jennifer Westling,<sup>a</sup> John Kay,<sup>c</sup> Nora Cronin<sup>d</sup> and Tom Blundell<sup>d</sup>**

<sup>a</sup>University of Florida College of Medicine, Gainesville, FL, 32610-0245 USA, <sup>b</sup>Kyoto Institute of Technology, Kyoto, Japan, <sup>c</sup>College of Molecular and Medical Biosciences, University of Wales, College of Cardiff, Cardiff, Wales, UK, <sup>d</sup>Department of Biochemistry, University of Cambridge, Cambridge, UK.

The Aspartic Proteinase family of endopeptidases [E.C. 3.4.23.nn] includes members from various mammalian systems, yeast, bacteria, viruses and plants [1,2]. Because of this diversity, it is important to understand the functional relationships in the family. Consequences of this understanding would be the more precise design of organism-specific inhibitors as well as a greater understanding of enzymatic specificity in general.

Fortunately, significant efforts over the past twenty years have yielded the crystal structures of many members of the family [3], and the overall three-dimensional structures have been found to be remarkably similar, although not identical. Each enzyme contains two homologous domains comprised of two orthogonally-packed beta sheets, achieved by the retroviral members using two identical monomeric units. Located between the two domains is a deep and elongated active site cleft where substrate and inhibitor binding takes place. From the crystallography, we know that peptide ligand binding always takes place with an extended beta-strand conformation. This places as many as eight different amino acid side chains in unique positions, or sub-sites, along the cleft.

To study interactions within the active site, we have prepared sets of oligopeptide substrates of related structures [4]. By varying one residue at a time along the peptide, we can evaluate the resulting effects on catalytic cleavage by various members of the aspartic proteinase family. Maintaining the two residues at the cleavage point constant, and monitoring the efficiency of that cleavage, enables us to make the assumption that the flanking residues are occupying the same subsites in each case.

## Results and Discussion

Two series of chromogenic oligopeptide substrates have been used to obtain the kinetic parameters,  $k_{cat}$ ,  $K_m$ , and  $k_{cat}/K_m$ , of representative members of the Aspartic Proteinase family of enzymes: pig pepsin, human cathepsin D, human cathepsin E, *Rhizopus chinensis* pepsin, yeast proteinase A, and plasmepsin II of *Plasmodium falciparum*.

Critical features of the individual sub-sites of the active site cleft, such as hydrophobicity or the presence of a specific complementary side chain, are revealed in these analyses. In

particular, it has been found that pig pepsin can tolerate a Lys residue in the P2 position, while human cathepsin D [huCatD] (and many other aspartic proteinases) cannot. The S2 subsite of huCatD is comprised of mostly hydrophobic amino acids, and is dominated by two Met residues, 287 and 289 in the pepsin numbering system. Accordingly, hydrophobic amino acids in P2 for are required in order to create an effective substrate for huCatD.

The P2' position is also critical to determining an optimal match of substrate and enzyme, and in differentiating one aspartic proteinase from another. While long, positively charged amino acids such as Arg and Lys are acceptable in P2' for most enzymes we have studied, the negatively charged and short amino acids, Glu and, especially, Asp, in P2' produce peptides that are cleaved with very low values of the specificity constant,  $k_{cat}/K_m$ .

When the amino acids in positions such as P2 and P2' match the specificity of the enzyme under study, such as huCatD, the resulting value of  $k_{cat}/K_m$  falls in the range of  $1-10 \times 10^6 M^{-1} s^{-1}$ . This agreement of the maximum efficiency of these family members is consistent with the generally similar catalytic apparatus, primary specificity and overall three-dimensional structural similarity.

## Conclusion

Oligopeptide substrates may be used to determine specificity of proteolytic enzymes. This analysis generates informaton that can be of use in the design of selective inhibitors for therapeutic benefit. This work was supported by NIH grants DK 18865 and AI39211 to BMD.

## References

1. Dunn, B.M., (Ed.) Structure and Function of the Aspartic Proteinases: Genetics, Structures, and Mechanisms, Plenum, New York, 1991.
2. Takahashi, K., (Ed.) Aspartic Proteinases: Structure, Function, Biology, and Biomedical Implications), Plenum Press, New York, 1995.
3. Aguilar, C. F., Dhanaraj, V., Guruprasad, K., Dealwis, C., Badasso, M., Cooper, J. B., Wood, S. P., and Blundell, T. L., In Takahashi, K. (Ed.) Aspartic Proteinases: Structure, Function, Biology, and Biomedical Implications), Plenum Press, New York, 1995, p.155.
4. Dunn, B. M., Scarborough, P. E., Davenport, R., and Swietnicki, W. (1994) In Dunn, B. M. and Pennington, M. W. (Eds.), Peptide Analysis Protocols, Humana Press, Clifton, N.J., p.225.

# Structural characterization of two-stranded anti-parallel $\beta$ -sheet peptides designed for DNA major groove recognition

**Bing Y. Wu and Laurence H. Hurley**

*College of Pharmacy and Drug Dynamics Institute, The University of Texas at Austin,  
Austin, Texas 78712, USA.*

The design of sequence-specific DNA-binding ligands is important to the discovery of novel anticancer drugs [1,2]. However, past approaches have mainly focused on small molecules that bind into the DNA minor groove or between DNA base-pairs with low specificity and have severe side-effects[3]. In contrast, most gene regulatory proteins bind into the DNA major groove in a sequence-specific manner and usually recognize palindromic DNA sequences through a pair of  $\alpha$ -helices or a  $\beta$ -ribbon (a two-stranded anti-parallel  $\beta$ -sheet) [4]. A  $\beta$ -ribbon has a two-fold symmetry and twisted curvature complementary to that of the palindromic DNA. It is small in size and represents an ideal leading structure for the design of DNA-binding peptidomimetics. Here, we report our design and structural characterization of a series of two-stranded anti-parallel  $\beta$ -sheet peptides that structurally mimic the DNA-binding  $\beta$ -ribbon motif of a MetJ repressor dimer.

## Results and Discussion

We took an incremental approach to design a series of three anti-parallel  $\beta$ -sheet peptides based on the  $\beta$ -ribbon motif of a MetJ dimer[5] (Fig. 1A).  $\beta$ 7, a seven-residue peptide, was designed to mimic the  $\beta$ -strand (residues 22-28) of a MetJ repressor to form a  $\beta$ -ribbon as required for specific DNA binding. In order to increase DNA binding affinity by reducing entropy loss associated with peptide-DNA binding reactions, two strands of the seven-residue peptide were linked by a dipeptide, D-Phe-Pro, which is expected to form a unique type II' turn promoting the formation of the designed  $\beta$ -hairpin peptide,  $\beta$ 16. Finally, a cyclic  $\beta$ -ribbon,  $\beta$ 18, was designed in which two strands of the seven-residue peptide were linked at both ends by two type II' turns to further constrain the conformation of the peptide. Even the short seven-residue peptide  $\beta$ 7 forms a predominant  $\beta$ -sheet structure at concentrations above 125 $\mu$ M. The CD spectrum of the peptide shows a typical pattern of  $\beta$ -sheet conformation with a maximum of about 202nm and a minimum at around 221nm (Fig. 1B). Size-exclusion chromatography analysis of the  $\beta$ 7 gives an estimated molecular weight of 1929 and indicates a dimeric structure of the peptide, which is further confirmed by the presence of a molecular ion peak at 1687 in both FAB and ESI MS. Further supporting evidence for the native-like  $\beta$ -ribbon structure of the  $\beta$ 7 dimer come from structural studies of the  $\beta$ 16. A CD spectrum of the  $\beta$ 16 in aqueous solution again shows significant  $\beta$ -sheet structure formation (Figure 1B). The  $\beta$ 16 hairpin is monomeric in solution from micromoles to millimoles, as demonstrated by the concentration-independent

CD spectra and the chemical shifts of its amide proton resonance 2D NMR studies of the  $\beta 16$  in a mixed solvent of methanol and water (1/1, v/v) reveal three long-range  $\text{d}\alpha\alpha(i, i+j)$  NOE cross-peaks ( $\text{K}^2/\text{S}^{15}$ ,  $\text{S}^6/\text{K}^{11}$ , and  $\text{T}^4/\text{T}^{13}$ ), which are characteristic of the  $\beta$ -

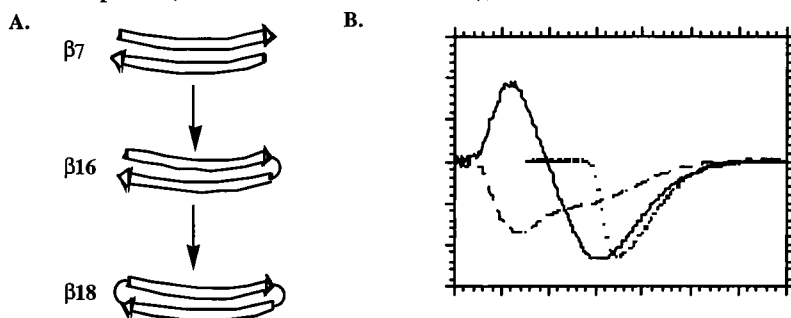


Fig 1. A. an incremental approach for the peptide design. Peptide sequences:  $\beta 7$ ,  $\text{Ac-K}^1\text{KITV}^5\text{SI-NHCH}_3$ ;  $\beta 16$ ,  $\text{Ac-K}^1\text{KITV}^5\text{SIFPK}^{10}\text{KITVS}^{15}\text{I-NHCH}_3$ ;  $\beta 18$ ,  $\text{cyclo-(K}^1\text{KITV}^5\text{SIFPK}^{10}\text{KITVS}^{15}\text{IFP)}$ . F, D-phenylalanine. B. CD spectra of  $\beta 7$ (—),  $\beta 16$ (----), and  $\beta 18$ (.....) in 10mM  $\text{NaH}_2\text{PO}_4$  and 100mM NaCl, pH 7.0, at 25°C.

hairpin structure. A deuterium-hydrogen exchange experiment shows that six amide protons of  $\text{I}^3$ ,  $\text{V}^5$  and  $\text{I}^7$  in one  $\beta$ -strand, and  $\text{K}^{10}$ ,  $\text{I}^{12}$ ,  $\text{V}^{14}$  in the second  $\beta$ -strand are well protected. A CD spectrum of the cyclic  $\beta 18$  shows a unique pattern (Fig. 1B), indicating special structure formation of the peptide. 2D NMR structural analyses of the cyclic  $\beta 18$  show a complete network of long-range NOE interactions characteristic of the cyclic  $\beta$ -ribbon. A deuterium-hydrogen exchange experiment revealed four pairs of slow-exchanging amide protons, that is,  $\text{K}^1/\text{K}^{10}$ ,  $\text{I}^3/\text{I}^{12}$ ,  $\text{V}^5/\text{V}^{14}$  and  $\text{I}^7/\text{I}^{16}$ , which suggest the formation of all eight intramolecular hydrogen-bonds in the cyclic peptide.

By taking an incremental approach, we have designed three anti-parallel  $\beta$ -sheet peptides of well-defined  $\beta$ -sheet conformations. Two linear peptides fold autonomously into  $\beta$ -sheet structures and provide us unprecedented opportunity to study the mechanism of  $\beta$ -sheet formation in peptides as well as in the early step of protein folding. These peptides structurally mimic the  $\beta$ -ribbon motif of the MetJ dimer and could serve as leading structures for the further design of the DNA major groove-binding peptidomimetics.

## References

1. Henderson, D., and Hurley, L.H. *Nature Medicine*, 1(1995) 525.
2. Gottesfeld, J., Neely, L., Trauger, J.W., Baird, E.E., and Dervan, P.B. *Nature*, 387(1997) 202.
3. Neidle, S., and Waring, M. (Eds.) *Molecular Aspects of Anticancer Drug-DNA Interactions*, CRC Press Inc., Boca Raton, 1993.
4. Pabo, C.O., and Sauer, R.T. *Ann. Rev. Biochem.*, 61(1992) 1053.
5. Somers, W.S., and Phillips, S.E.V. *Nature*, 359(1992) 387.

## Conformation and activity of antimicrobial peptides related to PGLa.

Jack Blazyk,<sup>a</sup> Janet Hammer,<sup>a</sup> Amy E. Kearns,<sup>a</sup>  
U. Prasad Kari<sup>b</sup> and W. Lee Maloy<sup>b</sup>

<sup>a</sup>Department of Chemistry, College of Osteopathic Medicine, Ohio University, Athens, OH 45701, U.S.A. <sup>b</sup>Magainin Pharmaceuticals, Inc., Plymouth Meeting, PA 19462, USA

Frog skin is a particularly rich source of host defense peptides, including magainins and PGLa [1]. These cationic peptides, which kill bacteria by permeabilizing their plasma membrane, do not appear to harm mammalian cells at antimicrobial concentrations. Although magainins and PGLa show broad antimicrobial activity, relatively high concentrations are required to kill most target organisms. It is possible to enhance antimicrobial activity while maintaining desired selectivity (i.e., inability to lyse red blood cells) through simple modifications of the native peptides. MSI-95, which was derived from PGLa by substituting G1K, M2L, and A8K, contains three heptamers of sequence KXXXXXX, where X represents a nonpolar residue. MSI-103, a trimeric repeat of the second heptamer segment of MSI-95, has the same antimicrobial activity as its parent. Here, we compare the conformation and activity of MSI-103 with two related peptides. MSI-144 is derived from MSI-103 by substituting the three glycines with lysine. MSI-1425 is similar to MSI-103 in that it contains six lysines, but the positions of three of the lysines are shifted, resulting in a significantly lower hydrophobic moment ( $\mu$ ), if the peptides adopt a helical structure.

	1	5	10	15	20																	
PGLa	G	M	A	S	K	A	G	A	I	A	G	K	I	A	K	V	A	L	K	A	L	-NH <sub>2</sub>
MSI-95	K	L	A	S	K	A	G	K	I	A	G	K	I	A	K	V	A	L	K	A	L	-NH <sub>2</sub>
MSI-103	K	I	A	G	K	I	A	K	I	A	G	K	I	A	K	I	A	G	K	I	A	-NH <sub>2</sub>
MSI-144	K	I	A	K	K	I	A	K	I	A	K	K	I	A	K	I	A	K	K	I	A	-NH <sub>2</sub>
MSI-1425	K	L	A	G	L	A	K	K	L	A	G	L	A	K	K	L	A	G	L	A	K	-NH <sub>2</sub>

### Results and Discussion

Several models have been proposed for transmembrane pores formed by magainin 2 amide in lipid bilayers [2,3]. These models require that the peptides adopt an  $\alpha$ -helical conformation. We previously demonstrated by FTIR and NMR spectroscopy that magainin 2 amide contains a mixture of both alpha-helical and beta-sheet secondary structure when bound to lipids [4]. Here, the model peptides described above possess substantially more antimicrobial activity, and only slightly higher hemolytic activity, compared to PGLa.

Peptide	<i>E. coli</i>	MIC (g/ $\mu$ mL)		% Hemolysis (500 g/ $\mu$ mL)
		<i>S. aureus</i>	<i>P. aeruginosa</i>	
PGLa	32	32	128	1
MSI-103	4	8	32	9
MSI-144	4	8	16	8
MSI-1425	8	16	128	9

In order to determine whether conformational differences exist among these peptides, we compared the amide I bands in the infrared spectrum. The amide I band is sensitive to secondary structure, and can be resolved to reveal the membrane-bound conformation of the peptides [4].

Peptide	Charge	H	$\mu$	Conformation (%)	
				$\alpha$ -Helix	$\beta$ -sheet
PGLa	+5	0.04	0.26	74	26
MSI-103	+7	-0.01	0.40	83	17
MSI-144	+10	-0.19	0.51	86	14
MSI-1425	+7	-0.07	0.25	60	40

The three model peptides are more cationic and less hydrophobic than PGLa. These results show that MSI-103 and MSI-144 are more helical than PGLa; however, MSI-1425 contains a substantially greater amount of beta-sheet structure compared to the other peptides. MSI-1425 shows good activity against *E. coli* and *S. aureus*, in spite of its relatively low hydrophobic moment and helical content.

In conclusion, these results demonstrate that antimicrobial activity does not require complete helical structure of bound peptides. Our data suggest that even peptides which cannot form a helix with a very large hydrophobic moment can be effective antimicrobial agents.

## References

1. Maloy, W.L. and Kari, U.P., *Biopolymers*, 37 (1995) 105.
2. Matsuzaki, K., Murase, O., Fujii, N. and Miyajima, K., *Biochemistry*, 35 (1996) 11361.
3. Ludtke, S.J., He, K., Heller, W.T., Harroun, T.A., Yang, L. and Huang, H.W., *Biochemistry*, 35 (1996) 13723.
4. Hirsh, D.J., Hammer, J., Maloy, W.L., Blazyk, J. and Schaefer, J., *Biochemistry*, 35 (1996) 12733.

# Structure-activity studies on a circular protein domain.

**Julio A. Camarero, Joanna Pavel and Tom W. Muir**

*Synthetic Protein Chemistry Laboratory, The Rockefeller University,  
1230 York Ave., New York, NY10021*

Cyclization of a polypeptide sequence offers an interesting method for studying the contributions of the N- and C-termini of a protein to folding and structural stability. Although backbone (head-to-tail) cyclization is commonly used to constrain the structure of small peptides, very little is known about the effect of this modification on the structural and function properties of a protein. Indeed, the small number of protein cyclization studies performed to date have all relied on the use of limited techniques such as random chemical crosslinking [1]. Here we describe the application of an intramolecular native chemical ligation strategy to the synthesis of a circular protein domain possessing a functional, native-like fold. In addition, we demonstrate that this synthetic strategy can be performed both in solution and directly from a solid support.

## Results and Discussion

Our initial protein cyclization studies have focussed on the 48 residue WW domain from the human Yes-kinase Associated Protein (YAP) [2]. This system was chosen because of the proximity of the N- and C-termini within the native protein fold [3], a feature which, in principle, allows the relationship between folding and chemical reaction rate to be explored. Two related synthetic pathways were successfully applied to the synthesis of the circular YAP WW domain (Fig. 1). The first of these extends the solution-based chemoselective cyclization approach previously applied to the synthesis of small cyclic peptides [4,5]. Key to this strategy was the generation of linear polypeptide precursor **1** which contains both the necessary groups for native chemical ligation [6]. Simply dissolving unprotected polypeptide **1** in phosphate buffer at pH 7.5 gave a single ligation product in quantitative yield. This ligation product was characterized as being the desired cyclomeric WW domain **2** using a combination of electrospray mass spectrometry, tryptic digestion and Edman sequencing. Moreover, the rate of cyclization was found to be related to the folded state of the protein since inclusion of 6 M Gdm-HCl in the ligation buffer significantly slowed down the reaction ( $\tau_{1/2}$  [0 M Gdm-HCl] = ~20 sec. vs  $\tau_{1/2}$  [6 M Gdm-HCl] = ~150 sec.). This rate-enhancement on going from unfolding to folding conditions can be understood in terms of the juxtaposition of the N- and C-termini within the native fold of the protein, i.e., folding assists the cyclization reaction by elevating the local concentration of the reactive groups.

A simplified synthetic route to circular WW domain **2** was developed which involves solely solid-phase transformations (Fig. 1). Key to this approach was the generation of a fully unprotected polypeptide tethered to a macroporous PEGA support through an alkyl  $\alpha$ -thioester linkage. Swelling these beads in the appropriate ligation buffer is enough to initiate the intramolecular ligation reaction leading to displacement of the newly cyclized polypeptide from the support. Note, commercially available aminomethyl PEGA resin can

be readily converted into the 3-mercaptopropionamide-PEGA (HS-PEGA) resin simply using solid-phase chemistries. Subsequent chain assembly using Boc-SPPS gives the immobilized polypeptide that can then be globally deprotected, *without cleavage from the support*, by treatment with HF. Importantly, this solid-phase ligation approach does not require the isolation and purification of any intermediates and is thus significantly more convenient than the previous solution-based synthetic route.

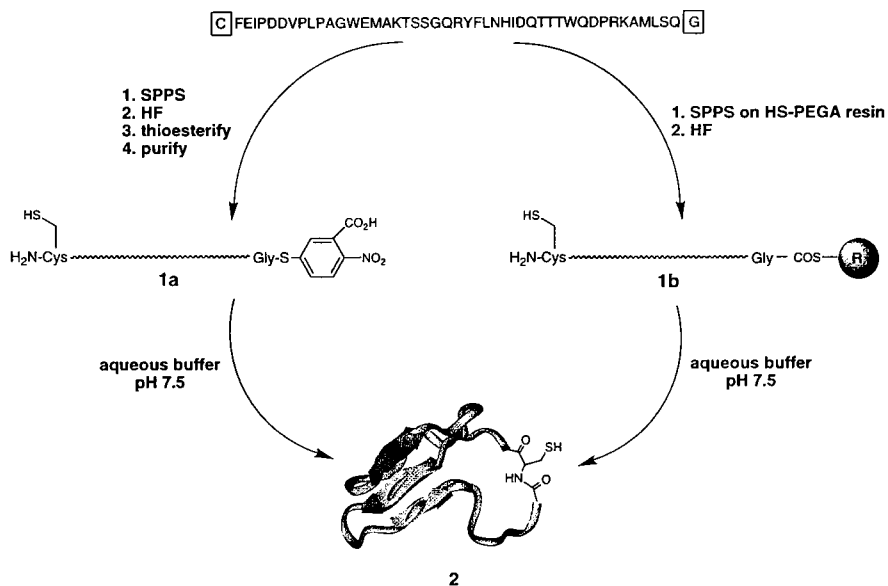


Fig. 1. Synthesis of a circular WW domain in solution and on solid-phase.

The effect of backbone cyclization on the structure and function of the YAP WW domain was investigated by multidimensional NMR spectroscopy and ligand-binding measurements, respectively. Two-dimensional  $^1\text{H}$  NMR studies revealed that, as expected, cyclization of the protein domain had no effect on the global fold of the protein. Chemical shift deviations for the mainchain protons were uniformly less than 0.05 ppm between the linear and circular versions of the protein. Consistent with the structural data, the circular WW domain was found to bind its cognate proline-rich ligand at least as tightly as the linear protein ( $K_d[\text{linear}] = 50 \pm 4$  mM,  $K_d[\text{cyclic}] = 35 \pm 4$  mM).

## References

1. Goldenburg, D.P. and Creighton, T.E. *J. Mol. Biol.*, 179, (1984) 527.
2. Chen, H.I. and Sudol, M. *Proc. Natl. Acad. Sci. USA* 92 (1995) 7819.
3. Macias, M.J. et al *Nature* 382 (1996) 646.
4. Camarero, J.A. and Muir, T.W. *J. Chem. Soc. Chem. Comm.* (1997) in press.
5. Zhang, L. and Tam, J.P. *J. Am. Chem. Soc.* 119 (1997) 2363.
6. Dawson, P.E., Muir, T.W. Clark-Lewis, I. and Kent, S.B.H. *Science* 266 (1994), 776.

# Folding and aggregation in mixed dimers of gramicidin D

William L. Duax, Brian M. Burkhart, David A. Langs,  
and Walter A. Pangborn

*Hauptman-Woodward Medical Research Institute, Inc.,  
73 High Street, Buffalo, New York 14203-1196, USA*

Gramicidin destroys gram-positive bacteria by forming channels in membranes that are specific for monovalent cations. The antibiotic consists of alternating D- and L-amino acids in the sequence, HCO-L-Val<sub>1</sub>-Gly<sub>2</sub>-L-Ala<sub>3</sub>-D-Leu<sub>4</sub>-L-Ala<sub>5</sub>-D-Val<sub>6</sub>-L-Val<sub>7</sub>-D-Val<sub>8</sub>-L-Trp<sub>9</sub>-D-Leu<sub>10</sub>-L-Trp<sub>11</sub>-D-Leu<sub>12</sub>-L-Trp<sub>13</sub>-D-Leu<sub>14</sub>-L-Trp<sub>15</sub>-NHCH<sub>2</sub>CH<sub>2</sub>OH. Naturally occurring gramicidin D is a mixture of six isoforms differing in amino acid composition at position 1, Val<sub>1</sub>(Vg)/Ile<sub>1</sub>(Ig), and position 11, Trp<sub>11</sub>(gA)/Phe<sub>11</sub>(gB)/Tyr<sub>11</sub>(gC). Electrophysiological measurements indicate that several types of channels having different conductance levels, channel accumulation and duration of channel opening are observed for homo- and heterodimers of natural and synthetic gramicidins and their mixtures. The Trp residues at the four sites (9, 11, 13, and 15) differ significantly with respect to their effect upon lipid association, ion coordination, and transport. Studies of naturally occurring and synthetic isomers indicate that amino acid variation at position 11, in particular, has significant effects on channel opening, duration, and transport properties.

## Results and Discussion

An antiparallel  $\beta$ -helix conformation has been found in crystals of uncomplexed gramicidin, obtained from methanol [1], ethanol [2], and n-propanol. Highly specific solvent effects result in cocrystallization of gA homodimers and gA/gC heterodimers from methanol and ethanol solutions and gA homodimers and VgA/IgA mixtures from n-propanol solution.

The  $\chi$ ,  $\phi$  values for the fifteen residues in the three dimers (a total of 90 residues) are plotted in Fig. 1a and compared with the distribution observed in the Protein Data Bank [3]. When the  $\chi_1$  and  $\chi_2$  values for the Trp residues are examined, (Fig.1b) the conformational trends of the amino acid side chains at position 11 emerge. In the plot, 24/29 residues have  $\chi_1$  values of  $\sim 180^\circ$ . The Trp 9, 13, and 15 residues in the ethanol and n-propanol structures have conformations with  $\chi_1 = -165 \pm 13^\circ$  and  $\chi_2 = -90 \pm 18^\circ$ . Variation of the  $\chi_1$  and  $\chi_2$  values in this subset is highly correlated. None of the Trp11 residues fall in this region of conformational space. The nine Trp<sub>11</sub> conformations are in less favored regions and four of them are among the five having  $\chi_1$  values closer to  $\pm 90^\circ$  than  $180^\circ$ . In one of these unusual conformations [ $\chi_1, \chi_2 = -60^\circ, -60^\circ$ ] the indole ring lies so close to the gramicidin backbone that several contacts of less than van der Waals distance are made between the ring and the carbonyl group of Leu 10. There is <sup>13</sup>C NMR evidence that this

which a Tyr replaces a Trp may have a sufficient increase in stability such that the formation of heterodimer  $\beta$ -ribbons is favored.

If Trp<sub>11</sub> takes up a conformation [ $\chi_1, \chi_2 = -60^\circ, -60^\circ$ ] that shields the carbonyl oxygen of Leu<sub>10</sub> and contributes to its enhanced electronegativity it could account for evidence that there is an ion binding site inside the channel near that position [4,5].

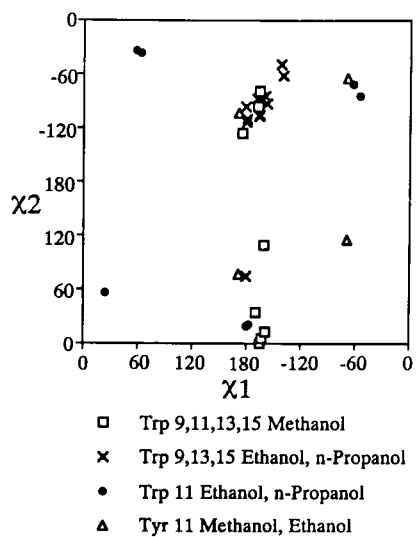
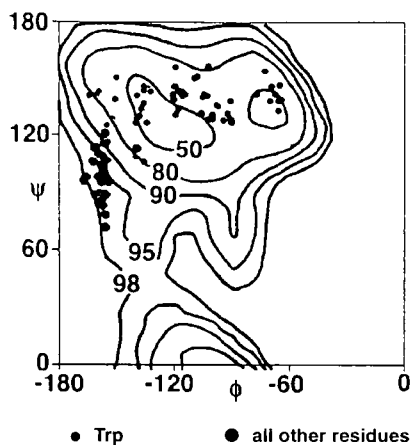
The Tyr on gC may be critically important to stabilization of the antiparallel  $\beta$ -ribbon and its conversion to the  $\alpha$ -helix to create a template for formation of homodimers of gA *via* specific end-to-end hydrogen bonds. The hydrophilicity of the Tyr residue in the heterodimer may prevent its facile entry into the membrane, whereas the homodimer of gA assembled on the template may more readily insert into membranes where it may undergo conformational change to an open pore reportedly found in crystals of the Cs<sup>+</sup> complex [7], the head-to-head single helical dimer postulated to be the more active channel form [8], or a tetramer that has also been suggested to be a channel forming species [9].

In addition to stabilizing the antiparallel  $\beta$ -ribbon the Tyr residue plays a critical role in determining the aggregation of dimers in the two crystal forms. In crystals obtained from ethanol a hydrogen bonded network consisting of Tyr<sub>11</sub>, two ethanols, and a water molecule link adjacent chains of dimers into infinite ladders that are arranged in a herringbone fashion [2]. In the methanol form the more polar solvent produced a crystal form having well defined solvent layers alternating with layers of gramicidin chains [1]. The Tyr residues are embedded in the solvent layer orienting the amphiphilic gramicidin chains with their more polar faces to the solvent layer.

The fact that a minor component in a heterogeneous mixture appears to have a profound effect on peptide folding and aggregation has potential applications to other systems in which anomalous behavior is exhibited by aggregation of apparently homogenous materials, such as the enigmatic behavior of the prion, responsible for bovine spongiform encephalitis and ovine scrapie, as well as the human equivalents kuru, Creutzfeldt-Jakob Disease, and Gerstmann-Straussler Syndrome. These diseases have been linked to a template-driven protein conformational change requiring the presence of small amounts of PrP<sup>Sc</sup>, a conformational mutant of a naturally occurring protein PrP<sup>C</sup>, that form heterodimers as a part of the disease process.

## References

1. Langs, D.A., Smith, G.D. and Courseille, C., Proc. Natl. Acad. Sci.-USA, 88(1991)5345 .
2. Langs, D.A., Science , 241(1988) 188.
3. Kleywegt, G.J. and Jones, T.A., Structure, (1996)1395.
4. Smith, R., Thomas, D.E., Atkins, A.R., Separovic, F. and Cornell, B.A., Biochem., Biophys, Acta., 1026 (1990) 1026.
5. Woolf, T.B. and Roux, B., Biophys.J., 72 (1997) 1930.
6. Chou, P.U.Y. and Fasman, G.D., Adv. Enzymol., 47 (1978) 45.
7. Wallance, B.A. and Ravikumar, K., Science, 241 (1988) 182.
8. Urry, D. Proc. Natl. Acad. Sci. USA, 68 (1971) 672.
9. Stark, G., Strassle, M. and Takacz, Z., J. Membrane Biol. 89 (1986) 23.



# RS-66271, a clinical candidate derived from parathyroid hormone related protein: The role of enhanced amphiphilic helicity

Maria Pellegrini,<sup>a</sup> Alessandro Bisello,<sup>b</sup> Michael Rosenblatt,<sup>b</sup> Michael Chorev<sup>b</sup> and Dale F. Mierke<sup>a</sup>

<sup>a</sup>Chemistry Department, Clark University, 950 Main Street, Worcester, MA 01610. <sup>b</sup>Division of Bone & Mineral Metabolism, Beth Israel Deaconess Medical Center, 330 Brookline Avenue, Boston, MA, 02215, USA

Parathyroid hormone (PTH) and parathyroid hormone related protein (PTHrP) bind to and activate a common receptor, the PTH/PTHrP receptor [1-4], that belongs to a subclass of a family of G-protein coupled receptors. The N-terminal portions of both hormones (fragments 1-34) constitute functionally active domains, retaining high binding affinity and PTH-like bone-related activities [5-7]. In most *in vitro* PTH/PTHrP receptor-related assays, the pharmacological profiles of PTH and PTHrP are nearly identical [1]. Comparable binding to the same receptor despite limited sequence homology (only 11 amino acids, of which 8 are located in the sequence 1-13) strongly suggests that both hormones present similar bioactive conformations (associated with recognition, binding, and activation) to the PTH/PTHrP receptor.

From truncation studies of PTH and PTHrP, the principal binding domain has been assigned to residues 25-34 [2]. When sequence 20-31 of hPTHrP(1-34) is folded into an  $\alpha$ -helix, it shows a well-defined hydrophobic face that is very similar to that produced when PTH is folded into an  $\alpha$ -helix; the only common feature of the opposite face of the helix is the predominance of polar residues.

The peptide RS-66271 incorporates the sequence of hPTHrP-(1-34)NH<sub>2</sub> in which the amino acids 22-31 have been substituted by the sequence E<sup>22</sup>-L-L-E-K-L-L-E-K-L, designed to model a perfect amphiphilic  $\alpha$ -helix (MAP, model amphipathic  $\alpha$ -helix peptide, Krstenansky *et al.* [3]). If this region in the receptor-bound conformation of active PTHrP is  $\alpha$ -helical, then incorporation of MAP should enhance the binding affinity to the PTH/PTHrP receptor. Of course, this conclusion presupposes that MAP will be helical within the PTHrP sequence. *In vitro*, RS-66271 displays a 10-fold lower affinity for the rat osteosarcoma-like cell line expressing PTH/PTHrP receptor than the parent analog hPTHrP-(1-34)NH<sub>2</sub>. In the same cell line RS-66271 is 6-fold less potent than the parent compound in stimulating adenylyl cyclase. This low *in vitro* activity is not in accord with the high *in vivo* anabolic activity in bone reported for RS-66271 [3], which suggests its potential use as a therapeutic agent in the treatment of osteoporosis. Here we describe the conformational study of RS-66271 in aqueous solution by CD and NMR spectroscopy.

## Results and Discussion

The pattern of NOEs observed for residues 1-15 is consistent with the "random coil" conformation (only structurally trivial, sequential and intraresidue NOEs were observed). In contrast, the NMR study provides strong evidence for an  $\alpha$ -helix beginning with residue 16 or 17 and extending to residue 30. Because of the degeneracy of the  $H_{\alpha}$ ,  $H_{\beta}$  and, to a lesser extent, amide protons (HN) in this region, many of the characteristic NOEs for an  $\alpha$ -helix (i.e.,  $H_{\alpha}(i)$ -HN(i+3),  $H_{\alpha}(i)$ -HN(i+4),  $H_{\alpha}(i)$ - $H_{\beta}(i+3)$ ) severely overlap with intraresidue and sequential NOEs. Nevertheless, the helix is well-characterized by the combination of NOEs, temperature coefficients, and chemical shifts (shown in Fig. 1).

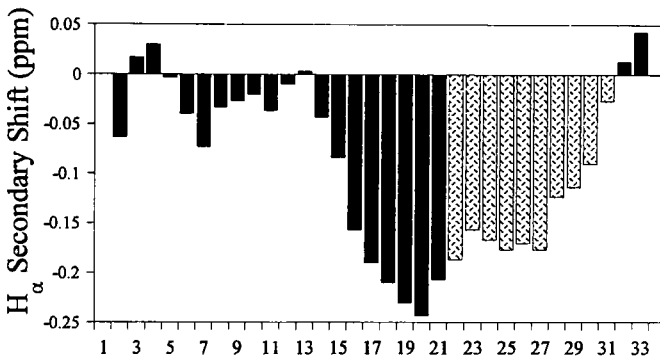


Fig. 1.  $H_{\alpha}$  secondary shifts of RS-66271 in water solution.

The NMR study of the peptide in aqueous solution in the presence of dodecylphosphocholine micelles provided a sufficient number of distance constraints despite serious overlapping. The results of distance geometry and calculation of molecular dynamics indicate the presence of  $\alpha$ -helix around residue 9 and residues 23-30. From CD studies the global  $\alpha$ -helix content is slightly higher than in water.

## References

1. Broadus, A. E.; Stewart, A. F. *The Parathyroids: Basic and Clinical Concepts*; Raven Press: New York, (1994).
2. Rosenblatt, M.; Callahan, E. N.; Mahaffey, J. E.; Pont, A.; Potts, J. T., Jr. *J. Biol. Chem.*, 252 (1977) 5847.
3. Krstenansky, J. L.; Ho, T. L.; Avnur, Z.; Leaffer, D.; Caulfield, J. P.; Vickery, B. H. In 23rd European peptide Symposium.

# Identification of a minimal peptide sequence of islet amyloid polypeptide (IAPP) with amyloidogenic and cytotoxic properties

Aphrodite Kapurniotu,<sup>a</sup> Jürgen Bernhagen,<sup>b</sup> Wolfgang Fischle,<sup>a</sup> Saul Teichberg,<sup>c</sup> Wolfgang Voelter<sup>a</sup> and Richard Bucala<sup>d</sup>

*<sup>a</sup>Physiologisch-chemisches Institut, Hoppe-Seylerstr. 4, D-72076 Tübingen, Germany; <sup>b</sup>Universität Stuttgart, Fraunhofer Institut, Nobelstr. 12, D-70569 Stuttgart, Germany; <sup>c</sup>North Shore University Hospital, 300 Community Drive, Manhasset, NY 11030, USA; <sup>d</sup>The Picower Institute for Medical Research, 350 Community Drive, Manhasset, NY 11030, USA*

The formation and cytotoxicity of pancreatic islet amyloid is strongly associated with  $\beta$ -cell damage and the progression and pathology of type II diabetes [1]. Islet amyloid is formed by the aggregation of islet amyloid polypeptide (IAPP or amylin), which is a peptide of 37 amino acid residues [1]. Soluble IAPP functions as an insulin counter-regulatory hormone. However, fibrillar aggregates have been found to be toxic to pancreatic  $\beta$ -cells [1]. We showed recently that hIAPP (human IAPP) aggregation proceeds via the formation of a dimeric, antiparallel  $\beta$ -sheet-containing conformational intermediate [2]. hIAPP aggregation is related to the region spanning residues 20 to 29 [3]. hIAPP(20-29) forms fibrils with the peptide chains arranged in an antiparallel  $\beta$ -sheet conformation and to date is known as the shortest amyloidogenic sequence of hIAPP [3].

Identification of a shorter, required minimal sequence of hIAPP that is sufficient for  $\beta$ -sheet formation, fibril formation and cytotoxicity might assist in designing inhibitors of pancreatic amyloidosis. To localize this sequence, we synthesized the following hIAPP fragments, based on their predicted  $\beta$ -sheet forming propensities: GAIL or hIAPP(24-27), FGAIL or hIAPP(23-27), and NFGAIL or hIAPP(22-27). Amyloid-related and cytotoxic properties of these peptides were then studied and compared to longer sequences, such as hIAPP(20-27), hIAPP(22-29) and hIAPP(20-29).

## Results and Discussion

According to secondary structure predictions, FGAIL is the shortest sequence of hIAPP that is still sufficient for  $\beta$ -sheet formation. In fact, electron microscopy revealed that supersaturated solutions of FGAIL formed long unbranched fibrils and fibril bundles (Fig. 1). Fibrils stained with Congo red and exhibited gold/green birefringence under polarized light, a feature that is characteristic for amyloid structures. Moreover, the main absorption band of FGAIL fibrils detected by FT-IR spectroscopy was at  $1633\text{ cm}^{-1}$ , suggesting that FGAIL was predominantly in a  $\beta$ -sheet conformation. These findings are in good agreement with a structural model of hIAPP(20-29) fibrils that indicates that FGAIL participates in formation of an intermolecular, antiparallel  $\beta$ -sheet [3]. By contrast, no fibril

formation could be detected for the tetrapeptide fragment GAIL. Consistent with this finding, mainly random coil structure was detected by FT-IR in aged GAIL solutions. Thus, GAIL alone is not sufficient for  $\beta$ -sheet and fibril formation. By contrast, supersaturated solutions of the hexapeptide NFGAIL formed fibrils that were birefringent by Congo red staining under polarized light. However, FT-IR spectroscopy of the fibrils showed them to contain significant amounts of random coil and turns in addition to the  $\beta$ -sheet structure.



Fig. 1. Electron micrograph of FGAIL fibrils (magnification: 19095x; 0.8 cm represents 400 nm).

Aggregation kinetics of the fragments revealed that aggregation and fibril formation *in vitro* proceeds by a nucleation-dependent polymerization mechanism. hIAPP(20-29) exhibited the lowest kinetic and thermodynamic solubility followed by hIAPP(22-29), hIAPP(20-27), NFGAIL, and FGAIL. Of note, NFGAIL and FGAIL show considerably higher kinetic solubility than hIAPP.

Finally, cytotoxicity of the hIAPP fragments towards the pancreatic cell line RIN5fm was studied. Only the fibrillar aggregates of FGAIL and NFGAIL were cytotoxic ( $EC_{50}$  1.8  $\mu$ M), whereas their soluble forms did not affect cell viability. Interestingly, the penta- and hexapeptide fibrils exhibited the same cytotoxicity as hIAPP(20-29), further adding to the significance of the FGAIL motif for amyloidogenicity and cytotoxicity.

## Conclusion

Our data strongly indicate that the pentapeptide sequence FGAIL is the minimal sequence of hIAPP that is still sufficient for  $\beta$ -sheet formation, aggregation, amyloid formation, and cytotoxicity. Therefore, FGAIL may provide a template for the design of inhibitors of hIAPP aggregation and pancreatic amyloid formation. FGAIL and FGAIL-derived compounds may therefore be potential therapeutics for the treatment of type II diabetes.

## References

1. Lorenzo, A., Razzaboni, B., Weir, G. C. and Yankner, B., *Nature*, 368(1994)756.
2. Kapurniotu A., Bernhagen J., Greenfield N., Voelter W. and Bucala R., *In*Peptides1996 Proceedings of the Twenty-Forth European Peptide Symposium, 1996, in press.

# Substrate specificity and mechanism of activation of hepatitis C virus protease

Elisabetta Bianchi, Andrea Urbani, Raffaele De Francesco  
Christian Steinkühler and Antonello Pessi

*Istituto di Ricerche di Biologia Molecolare P. Angeletti (IRBM)  
00040 Pomezia (Rome), Italy*

Hepatitis C Virus (HCV) infection is a major health problem for which no therapy or vaccine is yet available. Currently, the most promising target for an antiviral drug is the virally-encoded serine protease NS3. This protease is necessary for maturation of the nonstructural portion of the HCV polyprotein, performing cleavages at the NS3/NS4A, NS4A/NS4B, NS4B/NS5A and NS5A/NS5B junctions [1,2]. *In vivo* as well as *in vitro* NS3 must be activated by complex formation with another viral protein, NS4A. As a necessary step for the development of protease inhibitors, we have studied in detail the biochemistry of the enzyme using a recombinant protease domain and a synthetic peptide corresponding to the central 14-amino acid sequence of the protein (Pep4A, GSVVIVGRILSGR) which efficiently mimics the properties of full-length NS4 [1].

## Results and Discussion

Examination of NS3 substrate specificity of the NS4A/NS4B cleavage site (DEMEECASHL, cleavage between Cys and Ala) [2] indicated to us that the P-region of the substrate is the main determinant of ground-state binding whereas the P' region is crucial for catalytic efficiency. Further insight was gained by inverse alanine scanning of a "minimalist" substrate, a polyalanine containing only the consensus P6, P1, P3 and P1' residues (Peptide 2 in Table 1). This peptide is cleaved 70-85-fold less efficiently than the parent substrate (Peptide 1). Reintroduction of residues P5 (Peptide 3) or P4' (Peptide 4) has little effect on activity; simultaneous reintroduction of P5 and P4', however, restores activity to about 30% of the original value (Peptide 5).

Table 1. Inverse alanine scanning of NS4A/4B substrate Ac-DEMEECASHLPYK-NH<sub>2</sub>

Peptide	kcat/Km (M <sup>-1</sup> s <sup>-1</sup> , NS3)	kcat/Km (M <sup>-1</sup> s <sup>-1</sup> , NS3+ Pep4A)
1. Ac-DEMEECASHLPYK-NH <sub>2</sub>	104	1460
2. Ac-DAAEACAAAAPYK-NH <sub>2</sub>	1.2	21
3. Ac-DEAEACAAAAPYK-NH <sub>2</sub>	2.7	48
4. Ac-DAAEACAAALPYK-NH <sub>2</sub>	2.3	56
5. Ac-DEAEACAAALPYK-NH <sub>2</sub>	242	492

These findings confirm the view that substrate cleavage is modulated by several small contributions from both the P and the P' regions. The effect of the NS4A cofactor on substrate cleavage is to increase the kcat while leaving Km essentially unaffected. This is

particularly evident in the NS5A/5B cleavage site: for the peptide substrate Ac-EDVVCCSMSY-NH<sub>2</sub>, K<sub>m</sub> in the presence of Pep4A goes from 206 μM to 168 μM while k<sub>cat</sub> goes from 0.5 to 2.6 min<sup>-1</sup>. It is noteworthy that a decapeptide chimera encompassing the P-region of the NS4A/4B cleavage site and the P' region of the NS5A/5B cleavage site (Ac DEMEECSMSY-NH<sub>2</sub>) shows a turnover 10-fold higher than NS4A/4B (A. Urbani *et al.*, unpublished results).

We then studied NS3/NS4A interaction by CD. While addition of Pep4A to the enzyme had no apparent effect on secondary structure, we observed a large change in the near-UV region (see Fig. 1); this effect was confirmed by monitoring tryptophan fluorescence. The complex forms with a 1:1 stoichiometry and an apparent K<sub>d</sub> of 6.8 μM. Kinetic analysis shows a very slow on-rate (k<sub>on</sub>=390 M<sup>-1</sup>s<sup>-1</sup>) with a complex half-life of 3.5 min.

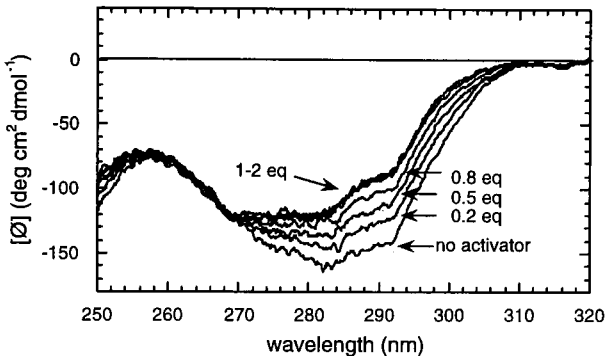


Fig 1. Pep4A-induced conformational change of NS3 as detected by near-UV CD in 50% glycerol, 2% CHAPS, 3mM DTT, phosphate buffer 50mM, pH 7.5, using 60 μM NS3 and increasing amounts of Pep4A (60-120 μM).

Our results are surprising in view of the recently published structure of the NS3/Pep4A complex, showing an extensive network of contacts with a total 2400 Å<sup>2</sup> of buried surface area [3]. The low K<sub>d</sub> observed in solution is also at variance with the stability of the complex between full-length NS3 and full-length NS4, as judged by *in vitro* translation experiments, where no evidence for dissociation was found for up to 6h (De Francesco *et al.*, unpublished). Our working hypothesis is now that other regions of the full-length NS3 or NS4 must contribute to complex stability. We have therefore synthesised full-length NS4A and spectroscopic experiments are in progress.

## References

1. Steinkühler, C, Urbani, A., Tomei, L., La Monica, N., Failla, C., Sardana, M., Bianchi, E., Pessi, A. and De Francesco, R., *J. Virology*, 70(1996) 6694.
2. Urbani, A., Bianchi, E., Narjes, F., Tramontano, A., De Francesco, R., Steinkühler, C. and Pessi, A., *J. Biol. Chem.*, 272(1997) 9204.
3. Kim, J.L., Morgenstern, K.A., Lin, C., Fox, T., Dwyer, M.D., Landro, J.A., Chambers, S.P., Markland, W, *et al.* and Thompson, J.A., *Cell*, 87(1996) 343.

# The allosteric-type mechanism of tetanus toxin metalloprotease activity determines its substrate specificity

**Fabrice Cornille, Loïc Martin, Christine Lenoir, Didier Cussac, Bernard P. Roques and Marie-Claude Fournié-Zaluski**

*Département de Pharmacochimie Moléculaire et Structurale, U266 INSERM - URA D1500 CNRS, Faculté de Pharmacie, Université René Descartes, 75006 Paris, France.*

Tetanus toxin (TeNT) is produced by the anaerobic bacillus *Clostridium tetani* and causes the paralytic tetanus syndromes by blocking neurotransmitter release at central synapses. The light chain of tetanus neurotoxin (TeNT-L chain) has been shown to be endowed with a highly selective zinc endopeptidase activity which is directed towards the single Gln76-Phe77 bond of synaptobrevin[1], a Vesicle-Associated Membrane Protein (VAMP) critically involved in neuro-exocytosis [2].

In previous reports, truncations at the NH<sub>2</sub>- and COOH-termini of synaptobrevin have shown that residues located in the sequences 27-49 and 82-93 of synaptobrevin were required for hydrolysis by TeNT, suggesting a role in the mechanism of substrate hydrolysis for residues distal from the cleavage site [3]. Three reasons could account for these results: i) the NH<sub>2</sub>- and COOH-terminal domains may induce a cleavable conformation of synaptobrevin at the Gln76-Phe77 bond; ii) the binding of the NH<sub>2</sub>- and COOH-terminal domains of synaptobrevin could ensure Michaelis complex formation; iii) the binding of the NH<sub>2</sub>- and COOH-terminal domains of synaptobrevin to TeNT could promote a proteolytic conformation of the toxin. In order to clarify these issues, various peptides corresponding to the synaptobrevin (S) acidic domain S1 (for S 27-55) and basic domain S2 (for S 82-93) (Fig.1) have been synthesized and their influence on purified TeNT L chain cleavage of synaptobrevin fragments lacking these sequences was studied.

## Results and Discussion

We show here that the cleavage of synaptobrevin fragment S 50-93 (respectively S 32-81), which is too short to be efficiently cleaved by TeNT, can be recovered by addition of 1 mM S1 (respectively 1mM S2) while the same concentrations of S1 or S2 do not affect the cleavage rate of S 32-93 . We also show that the coaddition of 1mM S1 and 1 mM S2 is required to recover the cleavage of S 56-81 by TeNT L chain .

Real time surface plasmon resonance experiments demonstrated that the presence of S2 is required for the binding of TeNT L chain to peptides S1 (data not shown).

Altogether these results show clearly that synaptobrevin cleavage is dependent on the double interaction of well-defined NH<sub>2</sub>- and COOH-terminal synaptobrevin domains S1 and S2, with complementary exosites present on TeNT. Furthermore the influence of S1 and S2 on the kinetic constants of the enzymatic reaction favours the idea that this mechanism could fit with the allosteric model of enzyme functioning [4]. This allosteric-type binding promotes the enzymatic activity of TeNT via a probable conformational

change which has not yet been investigated. This cooperative mechanism of enzymatic activity, not previously described for zinc peptidases, can be extended to other clostridial neurotoxins and could likely account for their high substrate specificity.

Hydrolysis of Synaptobrevin fragments by TeNT				Cleavage rate (pmoles.min <sup>-1</sup> .μg <sup>-1</sup> )
		32 LQQTQAQVDEVVDIMRVNVDKVLERDQKLSLDDRADALQAGASQFETSAAKLRKRYWVKNL 93	TeNT Cleavage	
A	27	S1 55 + S 32-93		102 ± 5
		S 32-93	+ 82 S2 93 AKLRKRYWVKNL	105 ± 5
				103 ± 5
B	27	S1 55 + S 50-93		1.5 ± 0.5
		S 50-93	+ 82 S2 93 AKLRKRYWVKNL	52 ± 2
				1.5 ± 0.5
C	27	S1 55 + S 32-81		< 0.1
		S 32-81	+ 82 S2 93 AKLRKRYWVKNL	15 ± 0.5
				< 0.1
D	27	S1 55 + S 56-81		< 0.1
		S 56-81	+ 82 S2 93 AKLRKRYWVKNL	< 0.1
		S 56-81	+ 82 S2 93 AKLRKRYWVKNL	12 ± 0.5

Fig. 1.  $10^{-4}M$  of peptide substrate ( $10^{-3}M$  in the case of S 56-81) were incubated in presence or in absence of 1 mM S<sub>1</sub> or/and 1mM S<sub>2</sub> in a total volume of 100 μl of 20 mM Hepes pH 7.4 with 1 μg of TeNT L chain at 37 °C. The reaction was stopped by addition of 50 μl of HCl 0.2 N. The released metabolites S 77-93 or S 77-81 were quantified by RP-HPLC in isocratic conditions.

## References

1. Schiavo, G., Benfenati, F., Poulain, B., Rossetto, O., Polverino de laureto, P., Dasgupta, B., and Montecucco, C., Nature, 359(1992)832.
2. Cornille, F., Deloye, F, Fournié-Zaluski, M.C., Roques, B.P., and Poulain, B., J. Biol. Chem., 270(1995)16826.
3. Yamasaki, S., Baumeister, A., Binz, T., Blasi, J., Link, E., Cornille, F., Roques, B.P., Fykse, E.M., Südhof, T.C., Jahn, R., and Niemann, H., J. Biol. Chem., 269(1994)12764.
4. Monod, J., Wyman, J., and Changeux, J.P., J. Mol. Biol., 12(1965)88.

# Structure activity studies of macrophage migration inhibitory factor show a functional role for cysteine residues

Jürgen Bernhagen,<sup>a</sup> Robert Kleemann,<sup>a</sup> Aphrodite Kapurniotu,<sup>b</sup>  
Richard Bucala<sup>c</sup> and Herwig Brunner<sup>a</sup>

<sup>a</sup>Universität Stuttgart, Fraunhofer Institut, Nobelstr. 12, D-70569 Stuttgart, Germany;

<sup>b</sup>Physiologisch-chemisches Institut, Hoppe-Seylerstr. 4, D-72076 Tübingen, Germany; <sup>c</sup>The Picower Institute for Medical Research, 350 Community Drive, Manhasset, NY 11030, USA

The classical T cell-derived factor, macrophage migration inhibitory factor (MIF), has re-emerged recently as a critical mediator of the host immune and stress response [1, 2]. MIF was found to be a multifunctional cytokine that participates in the regulation of several diseases including septic shock, and delayed-type hypersensitivity reactions [2]. The immunological functions of MIF include the modulation of the host macrophage, T cell, and B cell responses [2]. MIF is characterized by a number of unusual features that are not commonly seen in cytokines. For example, regulated secretion of MIF by the pituitary suggests that MIF can serve as a hormone. Other features include the counter-regulation of glucocorticoid action by MIF and the reported enzymatic functions [2]. The latter findings have opened a new dimension into our understanding of how this peptide mediator may function.

MIF is a 115 residue polypeptide that forms a homotrimer with 6  $\alpha$ -helices surrounding 3  $\beta$ -sheets. These 3  $\beta$ -sheets wrap around to form a solvent-accessible channel [3]. Although architectural similarities to a known enzyme have been found, the x-ray structure of MIF has not given conclusive evidence about the molecular mode of action of MIF. One structural feature of MIF is a conserved C-X-X-C motif that has been suggested to form an intramolecular disulfide bridge. However, no disulfides were found by x-ray analysis of recombinant protein. To confirm the existence and functional relevance of the proposed disulfide motif, we performed detailed structure activity studies of human MIF using thiol-alkylated and site-directed mutagenized protein.

## Results and Discussion

Isosteric mutants C57S and C57S/C60S were generated by PCR-based site-directed mutagenesis and expressed in *E. coli*. Mutant C57S was purified to homogeneity by ion exchange and C8-RP chromatography in high yield and was found to behave like wildtype MIF (wtMIF). However, C57S/C60S exhibited entirely different properties. In contrast to C57S and wtMIF, C57S/C60S was found to be contained within inclusion bodies. Gel chromatography and C8-RP chromatography were used for purification. In addition, wtMIF was reduced and/or alkylated to block cysteine residues, and all proteins then were employed in structure activity analyses. CD spectroscopy confirmed

Table 1. Conformational stabilities of MIF and cysteine-modified MIF. Stabilities were determined by GdnHCl-induced unfolding as described previously [4].

MIF type	Midpoint of unfolding [M, GdnHCl]	Free energy at zero conc. denaturant ( $\Delta G^{\circ}_{N-E}$ )
<i>Human MIF</i>	1.8	2.73
<i>Reduced human MIF</i>	1.25	2.44
<i>Mutant C57S</i>	1.3	1.92

that wtMIF and the mutants showed an overall structural similarity. This was verified further by analysis of the spectra using various deconvolution methods. However, GdnHCl-induced unfolding of wtMIF in comparison to mutant C57S and reduced MIF revealed a stabilizing effect of the putative disulfide bridge (Table 1). Similar observations were made when C60S was compared to wtMIF under solubility-enhancing conditions, i.e. in 0.8% hexafluoroisopropanol. These data indicated that MIF may be stabilized by an intramolecular disulfide between Cys-residues 57 and 60. Next, functional studies were performed and the observed effects for wtMIF compared with those of alkylated wtMIF and the cysteine mutants. Enzymatic redox activity was studied in a hydroxyethylidisulfide transhydrogenase assay. In this test, wtMIF exhibits a specific activity of 180 mU. We were surprised to find that MIF that had been alkylated under oxidizing conditions was twice as active as wtMIF. By contrast, when the alkylation was performed under reducing conditions, the resulting protein was completely inactive, suggesting that a disulfide bridge comprises the active center which participates in the transhydrogenase reaction. Further adding to this notion was the finding that C57S exhibited a markedly reduced biological activity in this test system.

In conclusion, our data strongly support the concept that the enzymatic redox activity of MIF is cysteine-dependent. Moreover, we conclude that a redox active disulfide bridge may form between Cys-residues 57 and 60 and that this structural feature is responsible for the above effect. These findings give important insights into the molecular mode of action of MIF.

## References

- Bernhagen, J., Calandra, T., Mitchell, R. A., Martin, S. B., Tracey, K. J., Voelter, W., Manogue, K. R., Cerami, A., & Bucala, R., *Nature (London)*, 365 (1993) 756.
- Bernhagen, J., Calandra, T., and Bucala, R., *J. Mol. Med.*, (1997) in press.
- Sun, H.-w., Bernhagen, J., Bucala, R., & Lolis, E., *PNAS, USA*, 93 (1996) 5191.
- Bernhagen, J., Mitchell, R. A., Calandra, T., Voelter, W., Cerami, A., & Bucala, R., *Biochemistry*, 33 (1994) 14144.

# Secondary and tertiary fold of the human parathyroid hormone 1-34 in different environments as a pathway to bioactive conformation

**Maria Pellegrini,<sup>a</sup> Stefano Maretto,<sup>a</sup> Miriam Royo,<sup>b</sup> Michael Rosenblatt,<sup>b</sup> Michael Chorev<sup>b</sup> and Dale F. Mierke.<sup>a</sup>**

<sup>a</sup>*Chemistry Department, Clark University, 950 Main Street, Worcester, MA 01610.* <sup>b</sup>*Division of Bone & Mineral Metabolism, Beth Israel Deaconess Medical Center, 330 Brookline Avenue, Boston, MA, 02215, USA*

The N-terminal portion of human parathyroid hormone (fragment 1-34) constitutes the functionally active domain, retaining high binding affinity and most of the biological functions of the full-length molecule. The large number of studies on the solution conformation of hPTH(1-34) agree on a mainly disordered structure in water compared to a high percent of  $\alpha$ -helix with trifluoroethanol. The present study details the conformation of hPTH(1-34)-NH<sub>2</sub>, investigated by CD and NMR spectroscopy in different environments and under varying experimental conditions. The structures obtained in benign aqueous solution, in near physiological conditions (H<sub>2</sub>O/buffer/salts), and in the presence of membrane mimetics have been refined by distance geometry (DG) and extensive molecular dynamics (MD) calculations (with explicit solvent simulation). The high resolution structures allow for comparison of the effect of the environment in enhancing the presence of secondary structure (i.e.,  $\alpha$ -helical domains) and in favoring tertiary interactions, as observed for hPTH(1-37) [1]. In particular, interaction with micelles may approximate the situation of the peptide approaching the membrane-bound G-protein-coupled receptor [2].

## Results and Discussion

The NMR and CD studies were performed on aqueous solutions of hPTH(1-34) in three different conditions: a) pH = 4 in benign water solution, b) 50 mM phosphate buffer/270 mM NaCl at pH = 6, c) 200 mM dodecylphosphocholine (d<sub>38</sub>). The CD spectra indicate an increasing content of  $\alpha$ -helical structure going from the first to the last listed condition

The NMR studies confirmed the presence of  $\alpha$ -helix in different proportions. Fig. 1 shows the fingerprint region of NOESY spectra for two of the studies. The shift of the resonances of H $\alpha$  protons toward typical values for residues in  $\alpha$ -helix and the abundance of cross-peaks indicative of secondary structures are easily observed. The structure calculations with a home written distance geometry program revealed a high degree of disorder for the peptide in condition a). Irregular helical loops are present between residues 23-29 and around residue 8. The helix loops proved to be stable in the presence of a full forcefield during 200 ps of restrained molecular dynamics in the presence of the solvent.

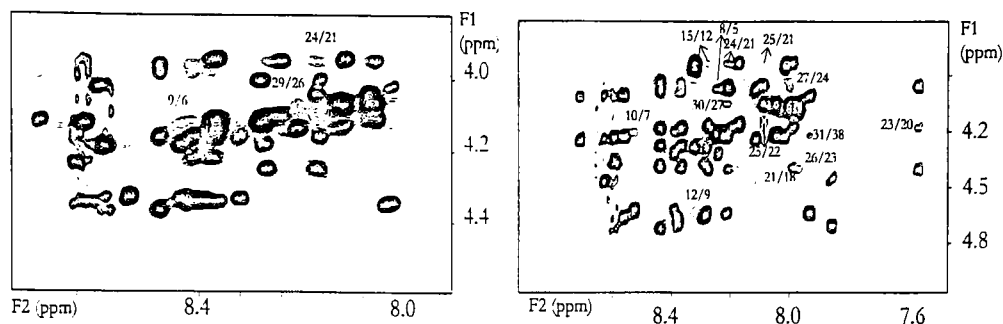


Fig. 1. Fingerprint region of NOESY spectra of hPTH(1-34) in the conditions *b* (left) and *c* (right).

The same calculation procedure (DG/MD) applied to the peptide in condition *b*) produced a more ordered structure especially in the region of the C-terminal helix. The utilization of the ensemble calculations approach [3] identified the C-terminal region as in equilibrium between an extended and an  $\alpha$ -helical conformation. Medium range NOEs observed between Leu<sup>15</sup> and Trp<sup>23</sup> are compatible both with a U-shaped tertiary fold and with a more extended structure.

The study in the presence of DPC micelles produced the most converging ensemble of structures with  $\alpha$ -helices in 5-9 and 21-33.

## Conclusion

The tendency of the peptide to fold into  $\alpha$ -helix in two segments is therefore clear from the three studies. The DPC micelles seem to favor greatly this secondary structure, indicating that the interaction of the peptide at the membrane interface where the receptor is embedded may play a major role in inducing the bioactive conformation.

## References

1. Marx, U. C.; Austermann, S.; Bayer, P.; Adermann, K.; Ejchart, A.; Sticht, H.; Walter, S.; Schmid, F. X.; Jaenicke, R.; Forssmann, W. G.; Rösch, P. *J. Biol. Chem.* ,270 (1995) 1519.
2. Moroder, L.; Romano, R.; Guba, W.; Mierke, D. F.; Kessler, H.; Delporte, C.; Winand, J.; Christophe, J. *Biochemistry* ,32 (1993) 13551.
3. Mierke, D. F.; Geyer, A.; Kessler, H. *Int. J. Pept. Protein res.*, 44 (1994) 325.

# Three-dimensional models of $\delta$ opioid pharmacophore: Molecular modeling and QSAR study of peptide and non-peptide ligands

Mark D. Shenderovich, Subo Liao, Xinhua Qian, Victor J. Hruby

Department of Chemistry, University of Arizona, Tucson, AZ 85721, USA

Selective agonists of the opioid  $\delta$  receptor have potential clinical advantages as analgesics that cause minimal side effects. The conformationally constrained peptide [*cyclo*(D-Pen<sup>2</sup>, D-Pen<sup>5</sup>)]enkephalin is known as a highly potent and selective  $\delta$  receptor agonist. Recently, we designed DPDPE analogs with topographically constrained  $\beta$ -methyl-2',6'-dimethyltyrosine (TMT) residues in position 1 [1]. Four stereoisomers of TMT prefer different side-chain rotamers, and only the (2S,3R)-isomer of [TMT<sup>1</sup>]DPDPE showed high potency and enhanced selectivity for the  $\delta$  receptor. Here we present comparative molecular modeling and QSAR study of [TMT<sup>1</sup>]DPDPE analogs and high-affinity non-peptide  $\delta$  receptor ligands aimed at the development of a three-dimensional (3D) model for the  $\delta$  receptor pharmacophore.

## Results and Discussion

3D structures of the non-peptide  $\delta$  opioid agonists 7-spiroindanyloxomorphone (SIOM) [2] and TAN-67 [3], and a partial agonist oxomorphindole (OMI) [4] were determined by molecular modeling with the MM3 force field. A good spatial overlap was found for pharmacophore groups including the basic nitrogen, hydroxyl and two aromatic rings of SIOM, TAN-67 and OMI (Fig. 1A) which allowed us to suggest that these non-peptide ligands may interact with the same binding site of the  $\delta$  receptor. Based on this overlap we proposed a tentative 3D pharmacophore model for  $\delta$  opioid agonists with distances of  $7.0 \pm 1.5$  Å between two aromatic rings and of  $8.3 \pm 1.5$  Å between nitrogen and the phenyl ring.

The highly potent (2S,3R)-stereoisomer of [TMT<sup>1</sup>]DPDPE, which shares the global backbone constraints of DPDPE with strong preferences for the *trans* rotamer ( $\chi^1 \approx 180^\circ$ ) of the aromatic side chain in position 1, is an excellent peptide template for the  $\delta$  opioid 3D pharmacophore. Molecular dynamics (MD) simulations at 300 K with the AMBER force field and a continuum hydration model were performed for the (2S,3R)-isomer and for a less potent (2S,3S)-isomer of [TMT<sup>1</sup>]DPDPE. Four 100 ps MD trajectories were collected for each analog starting from X-ray structures of DPDPE and [L-Ala<sup>3</sup>]DPDPE [5,6], and from two models of DPDPE bioactive conformations proposed in the literature [7,8] with the most populated TMT<sup>1</sup> rotamers. Low-energy conformations obtained from MD trajectories were filtered by the non-peptide pharmacophore query and then directly superposed with SIOM, OMI and TAN-67. The two conformations that showed the best overlap with the non-peptide pharmacophore (RMS deviations  $\leq 1.0$  Å for N, O atoms and

centers of two aromatic rings) were selected as putative biologically active conformations of [(2*S*,3*R*)-TMT<sup>1</sup>]DPDPE. Both conformations have similar backbone structure, *trans* rotamers of TMT<sup>1</sup>, and differ by *gauche* (-) and *gauche* (+) rotamers of Phe<sup>4</sup> (Fig. 1B). They are reasonably close to the X-ray structure of the active [*L*-Ala<sup>3</sup>]-DPDPE analog, but differ significantly from the X-ray structure of DPDPE itself. The proposed 3D models were used for rational design of new non-peptide  $\delta$  receptor ligands.

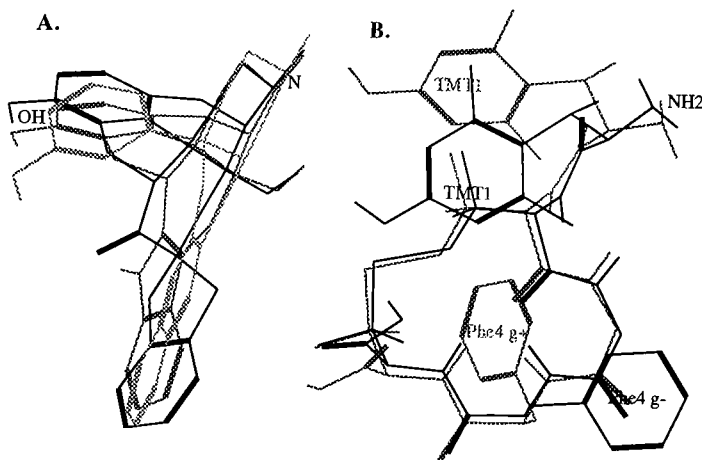


Fig. 1. A. Superposition of the  $\delta$  opioid pharmacophore of SIOM (black), OMI (dark) and TAN-67 (grey). B. Superposition of two putative biologically active conformations of [(2*S*,3*R*)-TMT<sup>1</sup>]DPDPE.

## References

1. Qian, X., Shenderovich, M.D., Kövér, K.E., Davis, P., Horváth, R., Zalewska, T., Yamamura, H.I., Porreca, F. and Hruby, V.J., *J. Am. Chem. Soc.*, 118 (1996) 7280.
2. Portoghese, P.S., Moe, S.T. and Takemori, A.E., *J. Med. Chem.*, 36 (1993) 2572.
3. Nagase, H., Wakita, H., Kawai, K., Endoh, T., Matura, H., Tanaka, C. and Takezawa, Y., *Jpn. J. Pharmacol.*, 64, Supl. I (1994) 35.
4. Portoghese, P.S., Larson, D.L., Sultana, M. and Takemori, A.E., *J. Med. Chem.*, 35 (1992) 4325.
5. Flippen-Anderson, J.L., Hruby, V.J., Collins, N., George, C. and Cudney, B., *J. Am. Chem. Soc.*, 116 (1994) 7523.
6. Collins, N., Flippen-Anderson, J.L., Haaseth, R.C., Deschamps, J.D., George, C., Kövér, K. and Hruby, V.J., *J. Am. Chem. Soc.*, 118 (1996) 2143.
7. Nikiforovich, G.V., Hruby, V.J., Prakash, O. and Gehrig, C., *Biopolymers*, 31 (1991) 941.
8. Chew, C., Villar, H.O. and Loew, G.H. *Biopolymers*, 33 (1993) 647.

This work was supported by grant DA 06284 from the National Institute of Drug Abuse.

# A chromophoric study of zinc coordination and conformer selectivity of the human insulin hexamer in solution

Mark L. Brader

Lilly Research Laboratories, Eli Lilly and Company, Indianapolis, IN 46285, USA

The respective pharmacological characteristics of the therapeutic insulin preparations Humulin<sup>®</sup> R (regular) Humulin<sup>®</sup> U (ultralente), and Humulin<sup>®</sup> N (Neutral Protamine Hagedorn) are based on the formulated stability of specific coordinate and conformational states of the zinc insulin hexamer that possess distinct physicochemical characteristics. The innovation of therapeutically improved insulin preparations requires a detailed understanding of how formulation excipients and solution conditions influence the structure and dynamics of the zinc hexamer.

Early x-ray crystallographic studies established that the zinc insulin hexamer exists as an oblate spheroidal assembly comprising three asymmetric dimers arrayed about a three-fold crystallographic axis of symmetry [1-3]. Current understanding of the conformational behavior of the hexamer is based on a three-state allosteric system where the T<sub>3</sub>R<sub>3</sub> state is an intermediate in the T<sub>6</sub>-to-R<sub>6</sub> phenolic-binding transition [4-9]. Because the solution coordination chemistry of the d<sup>10</sup> Zn(II) ion plays a central role in the pharmacological and physiological properties of the hexamer, the aim of this work was to identify a spectroscopic approach to probing both the zinc coordination and the conformer selectivity of the hexamer in solution.

## Results and Discussion

The compound 2-(1-(2-hydroxy-5-sulphophenyl)-3-phenyl-5-formazan) (zincon) (Fig. 1)

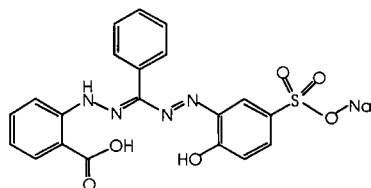


Fig. 1. Structure of zincon, monosodium salt.

forms a colored complex with the T-state zinc-insulin hexamer, possessing absorption band maxima at 630 nm, 540 nm, and 479 nm. The formation of a hexamer-bound zinc-zincon chromophore is indicated by the induced circular dichroism which resolves these transitions into components with extrema at 422 nm (+), 540 nm (-), and 645 nm (+). This

induced CD is attributed to excitonic coupling of the zinc transition dipole moments oriented within the asymmetric field of the hexamer, thus indicating intimate chromophoric contact between the zinc ligand and the insulin subunits. Zinc is a relatively bulky, achiral, multidentate ligand that has been used as a chelometric indicator for zinc [10]. It is inferred that zinc coordinates to the T-state zinc by replacing the coordinated water molecules. The distinctive UV-visible absorption spectrum and induced CD thus provide a useful T-state-specific signature of the zinc center.

## Conclusion

These results establish that the zinc-zinc-hexamer complex gives rise to an optically active chromophore that is sensitive to the extrachromophoric environment of the His<sup>B10</sup> sites. This technique provides a novel approach to probing the zinc site and the effects of ligand-binding in solution, thereby facilitating new insight into the zinc coordination, allostery, and kinetics of the phenolic-binding T<sub>6</sub>-to-R<sub>6</sub> transition.

## References

1. Adams, M. J., Baker, E. N., Blundell, T. L., Harding, M. M., Dodson, E. J., Hodgkin, D.C., Dodson, G. G., Rimmer, B., Vijayan, M. and Sheat, S. *Nature*, 224 (1969) 491.
2. Baker, E. N., Blundell, T. L., Cutfield, J. F., Cutfield, S. M., Dodson, E. J., Dodson, G. G., Hodgkin, D. M. C., Hubbard, R. E., Isaacs, N. W., Reynolds, C. D., Sakabe, K., Sakabe, N. and Vijayan, N. M. *Philos. Trans. R. Soc. Lond.*, B319 (1988) 369.
3. Peking Insulin Structure Group. *Peking Rev.*, 40 (1971) 11.
4. Smith, G. D., Swenson, D. C., Dodson, E. J., Dodson, G. G. and Reynolds, C. D. *Proc. Natl. Acad. Sci. U.S.A.*, 81 (1984) 7093.
5. Derewenda, U., Derewenda, Z., Dodson, E. J., Dodson, G. G., Reynolds, C. D., Smith, G. D., Sparks, C. and Swenson, D. *Nature*, 338 (1989) 594.
6. Whittingham, J. L., Chaudhuri, S., Dodson, E. J., Moody, P. C. E. and Dodson, G. G. *Biochemistry*, 34 (1995) 15553.
7. Jacoby, E., Kruger, P., Karatas, Y. and Wollmer, A. *Biol. Chem. Hoppe-Seyler*, 374 (1993) 877.
8. Brzovic, P. S., Choi, W. E., Borchardt, D., Kaarsholm, N. C. and Dunn, M. F. *Biochemistry* 33 (1994) 13057.
9. Birnbaum, D. T., Dodd, S. W., Saxberg, B. E. H., Varshavsky, A. D. and Beals, J. M. *Biochemistry*, 35 (1996) 5366.
10. Rush, R. M. and Yoe, J. H. *Anal. Chem.*, 26 (1954) 1345.

# Amide NH shift gradients: Quantitating peptide structure/disorder transitions

Jonathan W. Neidigh, Scott M. Harris, Hui Tong, Gregory M. Lee,  
Zhihong Liu and Niels H. Andersen

*Department of Chemistry, University of Washington, Seattle WA 98195, USA*

Many authors have used temperature gradient information in attempts to assess NH exposure in peptides and proteins. We recently established [1] that the common practice of correlating the  $\Delta\delta_{\text{NH}}/\Delta T$  value with NH sequestration from solvent has zero predictive validity for peptides which have even a modest degree of conformational averaging.

## Results and Discussion

For peptides, temperature-induced changes in conformer populations completely dominate the dependence of  $\delta_{\text{NH}}$  upon temperature. As a result, partially structured peptides can display a wide range of shift gradients ( $-35$  to  $+15$  ppb/ $^{\circ}$ ). For peptides, and some regions in proteins, rather than being a guide to NH hydrogen-bonding status or exposure,  $\Delta\delta_{\text{NH}}/\Delta T$  values are an exquisitely sensitive probe of both the  $\Delta G$  and degree of cooperativity of conformational transitions. For peptides, the occurrence of large shift deviations *and* abnormal gradients are diagnostic for partial structuring at lower temperatures which becomes increasingly randomized upon warming. Peptides that favor a single conformer at low temperatures can be recognized using a plot of the NH shift deviation versus  $\Delta\delta_{\text{NH}}/\Delta T$ . A good correlation coefficient ( $R \geq 0.80$ ) for NH-CSD and  $\Delta\delta/\Delta T$  values indicates that essentially all of the NH shift deviation from reference values is due to the concerted formation of a single structured state upon cooling. The correlation observed for a  $\beta$ -hairpin forming sequence [2] from the B1 domain of protein G is illustrative (Fig. 1).

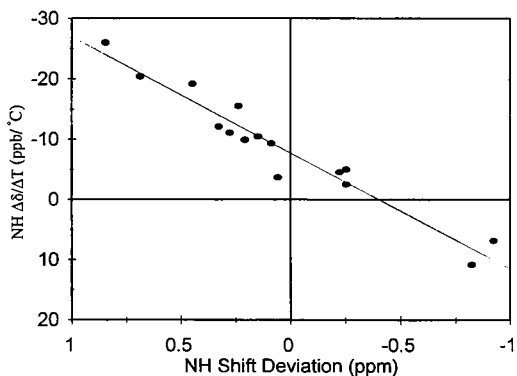


Fig. 1. The NH  $\Delta\delta/\Delta T$  and CSD correlation plot for Protein G, B1 domain fragment (41-56).

Many peptides with distinct low-temperature structure preferences display nearly linear plots of  $\delta_{\text{NH}}$  versus  $T$ . This can be rationalized within the context of our model only by assuming that structure loss is linear with temperature,  $f_{\text{S}}(T) = f_{\text{S}}^* + k\Delta T$  ( $f_{\text{S}}^*$  is the mole fraction of the structured state at the low temperature limit of the experiment,  $T^*$ ). In

order to derive explicit expressions for NH shift gradients and the slope and intercept of our  $\Delta\delta_{\text{NH}}/\Delta T$  versus HN-CSD plots, we assumed linear structure loss upon warming and define “ $\Delta\text{grad}$ ” as the difference between the intrinsic gradient of the structured and coil states,  $\Delta\text{grad} = (\Delta\delta/\Delta T)_{\text{S}} - (\Delta\delta/\Delta T)_{\text{rc}}$ , for each NH ( $\langle\Delta\text{grad}\rangle$  is the average).

$\partial\delta_{\text{NH}}/\partial T = [(\Delta\delta/\Delta T)_{\text{rc}} + f_{\text{S}}^* \cdot (\Delta\text{grad})] + 2k\Delta T(\Delta\text{grad}) + k(\text{CSD})_{\text{S}}$  where

the slope of the plot is given by  $m = k \cdot (f_{\text{S}}^*)^{-1}$ , the intercept is given by

$$(\Delta\delta/\Delta T)_{\text{CSD}=0} = (\Delta\delta/\Delta T)_{\text{rc}} + f_{\text{S}}^* \cdot [1 + 2m(T^{\text{m}} - T^*)] \cdot \langle\Delta\text{grad}\rangle,$$

where  $T^{\text{m}}$  is the midpoint of the temperature range examined in the CSD- $\Delta\delta/\Delta T$  plot.

For peptides that have been implicated as folding determinants, our studies indicate that structure loss is associated with a significant positive  $\Delta C_{\text{p}}$  value. Assuming that the value of  $\Delta S^0$  at the entropic convergence temperature should be at least  $17 \text{ JK}^{-1}$ /residue, a nearly linear dependence of  $\delta_{\text{NH}}$  upon temperature requires a positive  $\Delta C_{\text{p}}$  with a value at least 1.2 times  $\Delta S^0$ . Thus it appears that cooperative secondary structure formation for sequence fragments of proteins that have evolved to fold efficiently is the result of hydrophobic forces associated with intermediate range ordering rather than strictly local  $\phi/\psi$  preferences. In all likelihood, short peptide sequences (8 - 16 residues) have no meaningful secondary structure preferences in water except when an ordered state is favored by differential solvation effects.

## Conclusion

If this model is correct, the formation of secondary structure prior to molten globule formation in a protein folding pathway would be consistent with the demonstrated importance of the hydrophobic effect in the earliest stages of protein folding. This provides new support for NMR studies of sequence fragment conformational preferences as a tool for understanding the earliest stages of protein folding. The NH gradient/shift-deviation plot should prove very useful in such studies.

## Acknowledgement

This study is supported by an ACS-PRF grant (32244-AC).

## References

1. Andersen, N. H., Neidigh, J. W., Harris, S. M., Lee, G. L., Liu, Z. and Tong, H., J. Am. Chem. Soc., in press.
2. Blanco F. J. and Serrano, L. Eur. J. Chem., 230 (1995) 634.

# Predicting the conductance properties of ion channel structural models using the HOLE program

Oliver S. Smart

*Department of Crystallography, Birkbeck College, London WC1E 7HX, UK; from Sept. 1<sup>st</sup> 1997:  
School of Biochemistry, The University of Birmingham, Edgbaston, Birmingham B15 2TT, U.*

Ion channels are an important class of membrane proteins. Because of the difficulty of experimentally determining the three-dimensional structures of integral membrane proteins it is often necessary to resort to modeling techniques [1]. The aim of this work is to aid the validation of such model structures by producing an easy-to-use, rapid and accurate method of predicting the conductance for any given ion channel model [2]. The method is also useful in understanding normal behavior for experimental channel structures.

## Results and Discussion

The procedure adapts the HOLE method [3] which was developed to analyse the pore dimensions of ion channel models and has gained wide-spread acceptance. HOLE uses Monte Carlo Simulated Annealing to find the best route for a sphere with a variable radius to squeeze through the channel. The central pore of the channel, as delimited by HOLE, is treated as an ohmic conductor, enabling an immediate calculation of resistance or conductance. In practice it is found necessary to reduce the conductivity of the permeating ion solution by an empirical correction factor [2]. This factor (which is normally around five) reflects the fact that ions within a channel have their motions more restricted than in bulk solution.

The prediction routine was tested on all channel forming proteins and peptides for which both an experimental structure and conductance measurements are available [2]. Overall predictions were within an average factor of 1.62 of the true value and the predictive  $r^2$  was 0.90 (six systems tested, none in training set) [2]. The routine is already in use as an aid to modelling studies [1].

In addition to predicting the absolute conductance of a channel structure the routine can be modified to calculate the expected result on conductance of adding non-electrolyte polymers [2]. Such experiments have been interpreted in terms of a radius profile for a channel [4]. Encouraging preliminary results have been obtained in comparing the experimental profile and that expected from the X-ray structure for the cholera toxin B-subunit [2,4].

Future work aims to improve the method by detailed patch clamping measurements on channels of known structure. Empirical correction factors may be superseded by data derived from Molecular Dynamics simulation procedures.

## Conclusion

By systematically linking the three-dimensional structure of ion channels with conductance properties useful insights can be obtained. The HOLE program includes facilities needed to carry out all calculations described here and is available free to workers at non-profit organisations. Please address requests for the program by using the form on the world wide web - <http://www.cryst.bbk.ac.uk/~ubcg8ab/hole/top.html> or by e-mail to [o.smart@mail.cryst.bbk.ac.uk](mailto:o.smart@mail.cryst.bbk.ac.uk).

## Acknowledgement

Support by the Wellcome Trust by the provision of a Career Development Fellowship (042889) is gratefully acknowledged. Thanks to Dr Mark Sansom and group for encouragement and discussions.

## References

1. Breed, J., Biggin, P. C., Kerr, I. D., Smart, O. S. and Sansom, M. S. P., *Biochim. Biophys. Acta*, 1325 (1997) 235.
2. Smart, O. S., Breed, J., Smith, G. R. and Sansom, M. S. P., *Biophys. J.*, 72 (1997) 1109.
3. Smart, O. S., Goodfellow, J. M., and Wallace, B. A., *Biophys. J.*, 65 (1993) 2455.
4. Krasilnikov, O. V., Muratkhodjaev, J. N. , Voronov, S. E. and Yezepchuk, Y. V. *Biochim. Biophys. Acta.*, 1067 (1991) 166.

# Molecular dynamics simulation of epidermal growth factors in aqueous solution.

**Charles R. Watts, Sándor Lovas and Richard F. Murphy**  
*Department of Biomedical Sciences, Creighton University School of Medicine,  
 2500 California Plaza, Omaha, NE, 68178, USA*

The conserved six Cys residues of murine EGF (mEGF), human EGF (hEGF) and human TGF- $\alpha$  (hTGF- $\alpha$ ) form three disulfide bonds that divide the structures into three loops: the A-loop (Cys<sup>6</sup> to Cys<sup>20</sup>), B-loop (Cys<sup>14</sup> to Cys<sup>31</sup>), and C-loop (Cys<sup>33</sup> to Cys<sup>42</sup>). Residues 1 to 31 and 33 to 53, respectively, define the N-terminal and C-terminal domains with a hinge residue at position 32. MD simulations *in vacuo* have indicated differences in the degree of movement at the hinge residue between the three peptides and the importance of weakly polar interactions between aromatic residues in stabilizing peptide conformation [1]. The AMBER 4.1 force-field [2] was used here in 1.5 ns MD simulations to study the conformational features of TIP3P solvated mEGF, hEGF and hTGF- $\alpha$ .

## Results and Discussion

The total energy of the system for each peptide equilibrated rapidly within approximately 100 ps and remained stable throughout the trajectory. Analysis of backbone RMSD indicates that the most stable regions of mEGF are the N-terminus and C-loop while the most stable regions of hEGF and hTGF- $\alpha$  are the A- and B-loops. Secondary structure analysis reveals that the B-loop regions of mEGF and hEGF differ significantly from that of hTGF- $\alpha$ . The B-loop region of mEGF and hEGF consists of a shortened two strand antiparallel  $\beta$ -sheet from residues 20 to

*Table 1. Intra- and inter-loop  $\pi$ - $\pi$  and N- $\pi$  interactions for the trajectories of mEGF, hEGF and hTGF- $\alpha$ .*

	mEGF	hEGF	hTGF- $\alpha$
Intra-loop	Tyr <sup>10</sup> to Tyr <sup>13</sup> His <sup>22</sup> to Tyr <sup>29</sup> Trp <sup>49</sup> to Trp <sup>50</sup>	His <sup>10</sup> to Tyr <sup>13</sup> Tyr <sup>22</sup> to Tyr <sup>29</sup>	His <sup>4</sup> to Phe <sup>5</sup> His <sup>12</sup> to Phe <sup>15</sup> His <sup>35</sup> to Tyr <sup>38</sup>
Inter-loop	Tyr <sup>10</sup> to Tyr <sup>29</sup> Tyr <sup>13</sup> to Arg <sup>41</sup> Tyr <sup>37</sup> to Arg <sup>45</sup> Tyr <sup>37</sup> to Arg <sup>48</sup>	His <sup>10</sup> to Tyr <sup>22</sup> His <sup>10</sup> to Tyr <sup>29</sup> Tyr <sup>13</sup> to Tyr <sup>29</sup>	Phe <sup>5</sup> to Arg <sup>22</sup> His <sup>12</sup> to Phe <sup>23</sup> Phe <sup>15</sup> to Arg <sup>42</sup> Phe <sup>17</sup> to Arg <sup>42</sup> His <sup>18</sup> to Tyr <sup>38</sup>

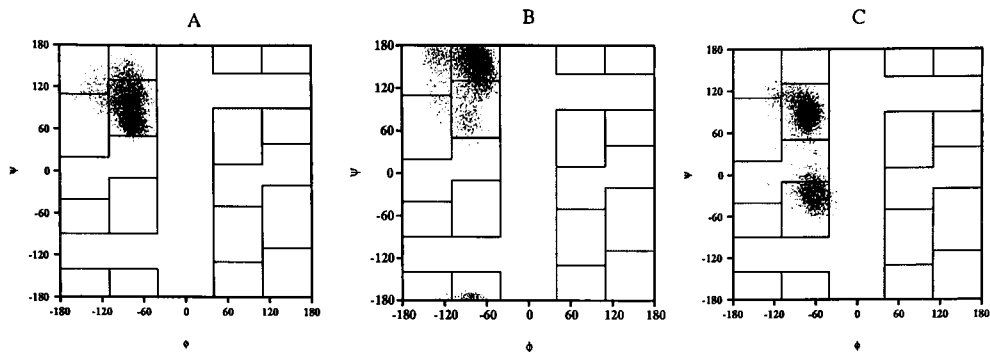


Fig 1. Ramachandran plot of the hinge residue overlaid on the energetically favorable regions of phase space as determined by Scheraga and coworkers for (A) mEGF, (B) hEGF and (C) hTGF- $\alpha$  [4].

21 and residues 30 to 31. The strands are connected by either a  $\beta$ -turn from residues 23 to 26 or a  $3_{10}$ -helix from residues 23 to 25 and a  $\beta$ -turn from residues 26 to 29. The B-loop of hTGF- $\alpha$  maintains a conformation that closely resembles the NMR structure [3]. The flexibility of the hinge residue is greater in hTGF- $\alpha$  than hEGF and mEGF (Fig 1).  $\phi, \psi$  Dihedrals of hTGF- $\alpha$  form two separate populations corresponding to either  $C_7^{eq}$  or  $\alpha$ -helical conformation while those of mEGF correspond to a  $C_7^{eq}$  conformation and hEGF to a region of contiguity [4]. Several weakly polar  $\pi$ - $\pi$  and N- $\pi$  interactions (Table 1) between the aromatic residues may play an important role in stabilizing the structures of each peptide [5,6]. Intra-loop interactions, Try<sup>10</sup> to Tyr<sup>13</sup> in mEGF, His<sup>10</sup> to Tyr<sup>13</sup> in hEGF and His<sup>12</sup> to Phe<sup>15</sup> in hTGF- $\alpha$ , stabilize the  $\alpha$ -helix in the A-loop of each peptide. Inter-loop interactions, Tyr<sup>10</sup> to Tyr<sup>29</sup> in mEGF, His<sup>10</sup> to Tyr<sup>22</sup> and His<sup>10</sup> to Tyr<sup>29</sup> in hEGF and His<sup>12</sup> to Phe<sup>23</sup> in hTGF- $\alpha$ , stabilize the interface of the A- and B-loops. Weakly polar interactions are especially important in facilitating the flexibility of the hinge in hTGF- $\alpha$ . The Phe<sup>15</sup> to Arg<sup>42</sup> and Phe<sup>17</sup> to Arg<sup>42</sup> interactions anchor the C-loop to the N-terminal domain stabilizing the peptide in both conformations.

Domain movement, facilitated by N- $\pi$  interactions, was observed only in the simulation of hTGF- $\alpha$  and could account for its different receptor binding properties.

## References

1. Lovas, S. and Murphy, R. F. J. Mol. Struct. (THEOCHEM) in press (1997).
2. Cornell, W. D., Cieplak, P., Bayly, C. I., Gould, I. R., Merz, K. M., Jr., Ferguson, D. M., Spellmeyer, D. C., Fox, T., Caldwell, J. W., and Kollman, P. A. J. Am. Chem. Soc., 117 (1995) 5179.
3. Kohda, D. and Inagaki, F. Biochem., 31 (1992) 677.
4. Zimmerman, S. S., Pottle, M. S., Némethy, G., and Scheraga, H. A. Macromolecules, 10 (1977) .
5. Burley, C. A. and Petsko, G. A. Science, 229 (1985) 23.
6. Watts, C. R., Tessmer, M. R., and Kallick, D. A. Lett. Pept. Sci., 2 (1995) 59.

# Engineering of snake venom cardiotoxin by computer modeling and chemical synthesis approach

Shui-Tein Chen,<sup>a</sup> Chi-Yue Wu<sup>a</sup> and Kung-Tsung Wang<sup>a,b</sup>

<sup>a</sup>Institute of Biological Chemistry, Academia Sinica, Taiwan. <sup>b</sup>Department of Chemistry, National Taiwan University, Taiwan.

Recently, polypeptides containing 60-80 amino-acid residues have been successfully synthesized in our laboratory by solid-phase peptide synthesizer with satisfying yields in about 10 days. The success of this methodology gives us a strong encouragement to try to synthesize cardiotoxins (CTXs) and their analogues to elucidate their structure and function relationships. CTX's are a group of basic proteins containing 60-63 amino acids and 4 disulfide bonds. First, we have developed a chemical synthesis methodology to successfully produce fully active CTX II (*Naja Naja Atra*) [1]. Second, we have used the above method to engineer the *N*-terminal residue of CTX II (*Naja Naja Atra*) and to study the effects of *N*-terminal substitutions on its structure and biological function [2]. Third, we have designed a disulfide-bond free CTX (calciumtoxin) in which the disulfide bonds in native CTX are replaced with two calcium coordination sites by computer modeling. The designed calciumtoxin presents a novel conformation and has biological activities of antigenicity and cytotoxicity similar to those of the native CTX in the presence of calcium ion [3].

## Results and Discussion

The complete sequence of CTX II is chemically synthesized by an automatic peptide synthesizer. After completion of peptide-chain elongation, the crude sample of reduced CTX is obtained from the peptide-resins, purified by RP-HPLC, air-oxidized, and repurified by RP-HPLC. The overall yield of synthetic CTX II is 3.9 mg (3.9%). Physicochemical characterization of synthetic CTX II is carried out by amino acid analysis, mass spectroscopy, capillary electrophoresis, peptide mapping, circular dichroism spectroscopy, and lethal toxicity [1]. The results indicate that the synthetic CTX possesses the same physicochemical properties as those of natural CTX II. Therefore, this synthesis method provides a direct and rapid route to obtain other snake toxins and their analogues for studying the structure/function relationship of CTXs.

To study the role of the *N*-terminal L-leucine residue in CTX II (*Naja naja atra*), this residue is systematically replaced with D-leucine (CTXII-L1-D-L) and glycine (CTXII-L1G) by the above established chemical synthesis method. Both CTX analogues are characterized by amino acid analysis, mass spectrometry and peptide mapping [2]. Structurally, changing the *N*-terminal L-Leu by D-Leu or Gly causes a drastic alteration in the entire CTX II structure as detected by circular dichroism [2], 1-anilino-naphthalene-8-sulfonate (ANS) fluorescence assay (Fig. 1). Functionally, both analogues still retained substantial biological activity of native CTX II [2]. These results indicate that both the chirality and the side-chain of the *N*-terminal leucine residue of CTX II are important elements in maintaining the whole CTX II structure.

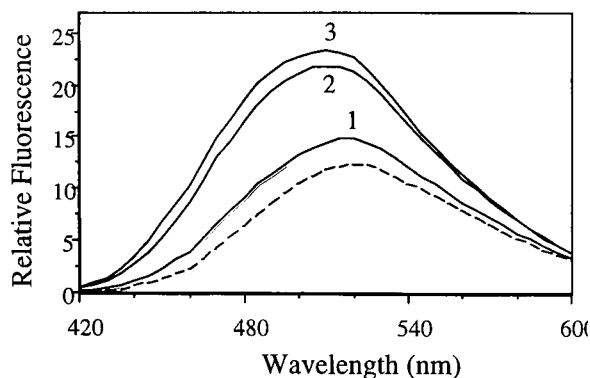


Fig. 1. Fluorescence spectra of ANS in the presence of various CTX samples. Curves: (1) CTX II, (2) CTXII-L1-D-L and (3) CTXL1G. The dotted line shows the fluorescence of ANS in the absence of sample.

The designed calciumtoxin by computer modeling utilizes two calcium coordination sites instead of disulfide bridges to stabilize the conformation. The coordination sites are introduced at the cleft of three  $\beta$ -sheet strands by replacing the residues of Leu-1, Leu-26, Ser-28, Leu-48, and Ser-55 with Glu and using their  $\gamma$ -carboxyl groups as chelaters. The residues of Cys at positions 3, 14, 21, 38, 42, 53, 54, and 59 of the four disulfide bridges were changed with Gly to remove all the disulfide bonds. Circular dichroism spectra showed that the synthesized peptide has a conformation similar to that of the native cardiotoxin of a defined structure only in calcium ion solution [3]. Immunoprecipitation assay, using the anti-cardiotoxin V, shows that in the presence of calcium ion calciumtoxin presents the same cross reaction as that of native cardiotoxin [3]. Hemolysis assay in the presence of calcium ion (150-250 mmol) and phospholipase A2 showed that the peptide had 65-70% as much cytolytic activity as the native toxin [3].

### Acknowledgments

Support for this research provided by Academia Sinica and the National Science Council, Taipei, Taiwan, is gratefully acknowledged.

### References

1. Wu, C.Y., Chen, S.T., Ho, C.L., and Wang, K.T. J. Chin. Chem. Soc., 43 (1996) 67.
2. Wu, C.Y., Chen, W.C., Ho, C.L., Chen, S.T. and Wang, K.T. Biochem. Biophys. Res. Commun., 233 (1997) 713.
3. Chen, S.T., Yang, M.T., Wu, S.Y. and Wang, K.T. J. Chin. Chem. Soc., (1997) in press.

# In search of the earliest events of hCG folding: Structural studies of the 60-87 peptide fragment

S. Sherman,<sup>a</sup> L. Kirnarsky,<sup>a</sup> O. Prakash,<sup>b</sup> H. M. Rogers,<sup>b</sup> R.A.G.D. Silva,<sup>c</sup> T.A. Keiderling,<sup>c</sup> D.D. Smith,<sup>d</sup> A.M. Hanly,<sup>d</sup> F. Perini<sup>a</sup> and R.W. Ruddon<sup>a</sup>

<sup>a</sup>*Eppley Cancer Institute, University of Nebraska Medical Center, Omaha, NE 68198, USA*

<sup>b</sup>*Department of Biochemistry, Kansas State University, Manhattan, KS 66506, USA*

<sup>c</sup>*Department of Chemistry, University of Illinois at Chicago, Chicago, IL 60607, USA*

<sup>d</sup>*Department of Biomedical Sciences, Creighton University, Omaha, NE 68178, USA*

X-ray analysis [1, 2] shows that the mature, fully folded  $\beta$ -subunit of human chorionic gonadotropin (hCG $\beta$ ) contains three hairpin-like fragments. Two of them (H1- $\beta$  and H3- $\beta$ ) are formed from antiparallel  $\beta$ -structures, while H2- $\beta$  is formed by polyproline-II-rich structural motifs. To better understand the earliest events of 28-residue peptide with a sequence corresponding to the 60-87 fragment of H3- $\beta$  was synthesized. The temperature, concentration, and environmental dependence of the conformational preferences of the peptide were studied by analysis of NMR, electronic CD (ECD) and vibrational CD (VCD), and Fourier transform infrared spectra (FTIR).

## Results and Discussion

The peptide RDVRFESIRLPGSPRGVNPVVSVAVALS (hCG $\beta$ <sub>60-87</sub>, S72) was synthesized on an Applied Biosystems 430A synthesizer using Merrifield's solid phase peptide synthesis methodology. Boc-amino acid derivatives were coupled to MBHA resin as their preformed hydroxybenzotriazole active esters in N-methylpyrrolidinone. The peptide was cleaved from the resin by the low-high TFMSA method and purified by RP-HPLC.

ECD spectra of the sample with both the 0.01 and 0.1 mg/ml concentrations showed that a majority of the amino acid residues within the peptide adopt an extended random coil conformation in a mixture of double distilled water (ddH<sub>2</sub>O) with 0, 10, or 20% TFE. The ECD spectrum in 30% TFE suggests the presence of a significant fraction of fully formed  $\alpha$ -helix conformation. There is little change in the ECD spectra from 30 to 50% TFE.

NMR data were acquired at 30°C in pure H<sub>2</sub>O and in a mixture of H<sub>2</sub>O with 30% TFE. Sequence-specific proton resonance assignments were established from phase sensitive, two-dimensional NOESY experiments. Proton resonance assignments were confirmed by a comparison of cross peaks in a NOESY spectrum with those of a total correlation (TOCSY) spectrum acquired for the peptides under similar experimental conditions. A total of 512 increments of 4K data points were recorded for double quantum filtered correlation spectroscopy (DQF-COSY) experiments. All data sets were collected in a hypercomplex phase sensitive mode. Inter- and intra-residue NOE intensities were measured in 100, 200, and 400 ms mixing time NOESY experiments.

The NMR data were used to retrieve conformational constraints for structure calculations. Newly developed programs and procedures [4] were applied to narrow the torsional angle constraints and to increase a number of stereospecific assignments. These data were used in NMR structure calculations by the DIANA program [5]. The DIANA structures were energy minimized using the NMR distance constraints and an AMBER force field implemented in the SYBYL 6.3 software package (Kollman all-atom parameters and Kollman atomic charges). The results of this structural interpretation of the NMR data suggest that, in H<sub>2</sub>O, most of the amino acid residues within the peptide adopt extended conformations corresponding to  $\beta$ -strand and polyproline II conformations, while in 30% TFE, eight C-terminal residues of the peptide adopt an  $\alpha$ -helix-like conformation.

FTIR and VCD were done at higher concentration of the sample (50 mg/ml). The spectra showed that in pure D<sub>2</sub>O, as well as in 30% and 50% TFE-OD, extended conformations (such as random coil and  $\beta$ -structures) dominate the spectra. According to both VCD and FTIR data, the highest percentage of  $\beta$ -structure is achievable in pure D<sub>2</sub>O in which the VCD signal is twice as large as in 30% TFE-OD. When TFE-OD is added, the growth of the helical component would serve to cancel the sheet/coil contribution to the spectrum, making it weaker and leading to the negative VCD band at 1665 cm<sup>-1</sup>. Again, there is little change in the VCD spectra when going from 30% TFE-OD to 50% TFE-OD.

## Conclusion

The results of our structural analysis of the peptide are consistent with a hypothesis that a turn in positions 72-76 observed in the crystal structure of the fully folded protein may be formed during the earliest stages of the folding, while formation of H3- $\beta$  may occur after a hydrophobic collapse, when the hydrophobic core of hCG $\beta$  is formed.

## Acknowledgments

This work was supported by National Cancer Institute grant CA32949 (to R.W.R.). The Molecular Modeling Core Facility of the UNMC Eppley Cancer Center was used in these studies. The facility is partially supported by Cancer Center Support Grant CA36727 from the National Cancer Institute.

## References

1. Laphorn, A.J., Harris, D.C., Littlejohn, A., Lustbader, J.W., Canfield, R.E., Machin, K.J., Morgan, F.J. and Isaacs, N.W. *Nature*, 369 (1994) 455.
2. Wu, H., Lustbader, J.W., Liu, Y., Canfield, R.E. and Hendrickson, W.A. *Structure*, 2 (1994) 545.
3. Ruddon, R.W., Sherman, S.A., and Bedows, E., *Protein Science*, 5 (1996) 1443.
4. Kirnarsky, L., Shats, O., and Sherman, S., *THEOCHEM*, in press.
5. Güntert, P. and Wüthrich, K., *J. Biomol. NMR* 1 (1991) 447.

# Synthetic peptides from putative amphipathic $\beta$ strand sequences of apolipoprotein B-100 associate with lipid in the $\beta$ strand conformation

Vinod K. Mishra,<sup>a</sup> Manjula Chaddha,<sup>a</sup> G. M. Anantharamaiah,<sup>a</sup>  
Mayakonda N. Palgunachari,<sup>a</sup> Krishnan K. Chittur,<sup>b</sup> Sissel Lund-Katz,<sup>c</sup>  
Michael C. Phillips<sup>c</sup> and Jere P. Segrest<sup>a</sup>

<sup>a</sup>Atherosclerosis Research Unit, UAB Medical Center, Birmingham, AL 35294; <sup>b</sup>Chemical and Materials Engineering Department, UAH, Huntsville, AL 35899; and <sup>c</sup>Department of Biochemistry, Allegheny University of the Health Sciences, Philadelphia, PA 19129, USA

Human apolipoprotein B-100 (apoB) is a nonexchangeable glycoprotein with 4536 amino acid residues. It is the only protein present in low density lipoprotein (LDL). The direct correlation between LDL concentrations in plasma and atherosclerosis makes structure-function studies on apoB physiologically relevant. Analysis of the potential amphipathic lipid-associating domains in apoB, using the program LOCATE, revealed a pentapartite structure consisting of three amphipathic  $\alpha$  helical domains alternating with two amphipathic  $\beta$  strand domains: NH<sub>2</sub>- $\alpha_1$ - $\beta_1$ - $\alpha_2$ - $\beta_2$ - $\alpha_3$ -COOH [1]. Although we previously suggested that amphipathic  $\beta$  strands in apoB are involved in lipid association [1], direct experimental evidence was lacking until now. Here we report the conformation and lipid affinity of two peptides, Ac-TFTLSCDGLRHKF-NH<sub>2</sub> (apoB:1390-1403, I) and Ac-EGNLKVRFPRLRLTGKIDF-NH<sub>2</sub> (apoB:3026-3043, II) from the  $\beta_1$  and  $\beta_2$  regions of apoB, respectively.

## Results and Discussion

The partition coefficients (expressed as natural log,  $\ln K_p$ ) of I and II into palmitoylcholine (POPC) multilamellar vesicles (MLV), using ultracentrifugation method [2], are 3.0 and 3.7, respectively. Fourier-transform infrared (FTIR) spectroscopy indicated that both peptides adopt predominantly  $\beta$  strand conformation in phosphate buffer saline (PBS; pH 7.4), and that this conformation is further stabilized in the presence of POPC MLV. Fig.1 shows the amide I' region of the FTIR spectra of II in PBS (Fig.1, left) as well as in the presence of POPC MLV (Fig.1, right). Disappearance of the 1637 cm<sup>-1</sup> band and a substantial increase in the 1627 cm<sup>-1</sup> band compared to the spectrum in PBS is consistent with the further stabilization of  $\beta$  strand conformation in the presence of POPC, presumably resulting from additional stronger H-bonding interactions (Fig.1).

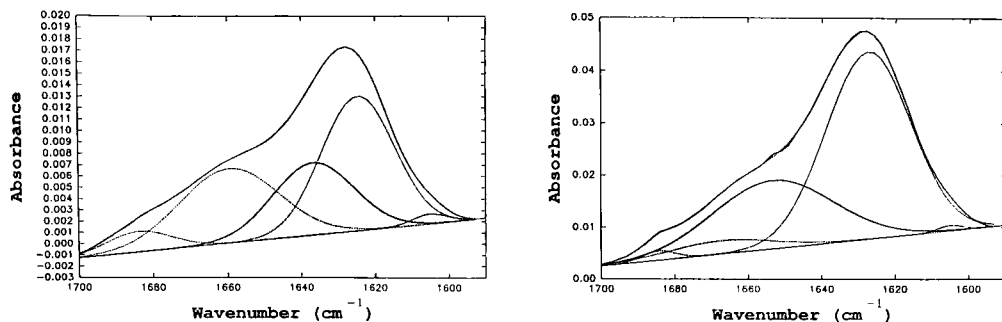


Fig. 1. Amide I' region of the FTIR spectra of II in PBS (left) and in the presence of POPC MLV (lipid to peptide ratio 2:1, w/w) (right). Spectra were recorded at room temperature using Digilab FTS-60A spectrometer at a resolution of 4 cm<sup>-1</sup>. Deconvolution was used to determine the number of bands in the amide I' envelope and curve-fitting was used to determine the secondary structure.

### Acknowledgments

This research is supported in part by NIH grant HL-34343.

### References

1. Segrest, J. P., Jones, M. K., Mishra, V. K., Anantharamaiah, G. M. and Garber, D. W., *Arterioscler. Throm.*, 14 (1994) 1674.
2. Spuhler, P., Anantharamaiah, G. M., Segrest, J. P. and Seelig, J., *J. Biol. Chem.*, 269 (1994) 23904.

# Proline puckering and cis-trans isomerization of proline-containing peptides

Young Kee Kang, Seong Jun Han and Jong Suk Jhon

Department of Chemistry, Chungbuk National University  
Cheongju, Chungbuk 361-763, Korea

Because of the conformational restriction in the pyrrolidine ring, the Pro residue has a relatively high intrinsic probability of having the cis peptide bond preceding the proline as compared with other amino acids [1,2]. The pyrrolidine ring may adopt two distinct down- and up-puckered conformations that are almost equally favorable [3]. Only a few studies have been performed for the ring puckering of cis- and trans-proline residues by analysis of X-ray crystal structures of peptides and proteins [4], by conformational energy calculations on proline-containing peptides [5,6], and by *ab initio* molecular orbital calculations on the proline dipeptide [7].

## Results and Discussion

All conformational energy calculations were carried out on terminally blocked Ac-X-Pro-NHMe dipeptides and Ac-X-Pro-Y-NHMe tripeptides using the ECEPP/3 force field [8]. For dipeptides, X included five types from all twenty amino acids, whereas for tripeptides one representative residue was chosen for each type of X and Y residue. A quasi-Newtonian algorithm SUMSL [9] was used for energy minimization. All torsion angles of each peptide were allowed to move during minimization. All minima of the Ac-X-NHMe with the relative energy  $\Delta E < 5$  (or 3) kcal/mol [10] and all minimum-energy conformations of Ac-Pro-NHMe [8] were combined to generate starting conformations for minimization.

The statistical populations of Ac-X-Pro-NHMe with cis- and trans-imide bonds depending on its down- and up-puckerings are shown in Table 1. The calculated overall preference is trans-down > trans-up > cis-down > cis-up. The higher populations of trans-down conformations may be ascribed to the significant contribution of the conformation tCd, which is the lowest energy conformation of Ac-Pro-NHMe [8]. The relative abundance of trans-down conformations appears to be overestimated, compared to that obtained from the analysis of X-ray structures of proteins, since the average abundance ratio of down:up for trans imides is calculated to be 78:19, whereas the corresponding ratio for proteins is 41:50 [4]. This overestimation can be attributed to the contribution of low energy conformations tAd and tFd [8], since our recent *ab initio* HF/6-31G calculations on Ac-Pro-NHMe indicate that these two conformations are not local minima at high levels of basis sets [7]. The lowest cis population is found for aromatic residues, whereas they are most abundant in protein X-ray structures.

Table 1. Statistical populations of Ac-X-Pro-NHMe (%)

X	trans-down	trans-up	cis-down	cis-up	PDB cis% <sup>a</sup>
aliphatic	68.5	29.3	2.1	0.2	4.1, 3.4
nonpolar	73.4	21.3	5.0	0.3	5.7, 4.9
aromatic	90.8	8.2	1.0	0.1	9.4, 7.7
polar	76.6	20.7	2.5	0.2	6.3, 6.2
charged	80.8	16.7	2.4	0.2	5.3, 4.8
PDB analysis <sup>b</sup>	40.8	50.0	8.2	1.0	

<sup>a</sup> Taken from refs. 1 and 2. <sup>b</sup> Taken from ref. 4.

This disparity may be interpreted as the weak aromatic-proline interactions for isolated dipeptides. From the analysis of secondary structures for the proline in Ac-X-trans-Pro-NHMe, the average  $\alpha\%$  and  $\beta\%$  populations are calculated to be 46% and 54%, respectively, which are in good agreement with the values obtained from X-ray structures of proteins [2,4] in spite of some overestimation for down-puckered conformations, as discussed above. In particular, the higher abundance of  $\beta$ -sheets relative to  $\alpha$ -helices for aromatic residues is promising, which may indicate that the bulkier side chains of X residues force the conformation of the Pro residue to be more extended.

Although there is some decrease in the population of trans-down conformers, the relative preference for puckering and imide isomerization for tripeptides is similar to that for dipeptides. The relative  $\alpha\%$  population for prolines in tripeptides is increased compared to that of dipeptides.

## References

1. Stewart, D.E., Sarkar, A. and Wampler, J.E., *J. Mol. Biol.*, 214 (1990) 253.
2. MacArthur, M.W. and Thornton, J.M., *J. Mol. Biol.*, 218 (1991) 397.
3. Momany, F.A., McGuire, R.F., Burgess, A.W. and Scheraga, H.A., *J. Phys. Chem.*, 79 (1975) 2361.
4. Milner-White, E.J., Bell, L.H. and MacCallum, P.H., *J. Mol. Biol.*, 228 (1992) 725.
5. Tanaka, S. and Scheraga, H.A., *Macromolecules*, 7 (1974) 698.
6. Schmidt, J.M., Brüscheiler, R., Ernst, R.R., Dunbrack, R.L., Jr., Joseph, D. and Karplus, M., *J. Am. Chem. Soc.*, 115 (1993) 8747.
7. Kang, Y.K., *J. Phys. Chem.*, 100 (1996) 11589.
8. Némethy, G., Gibson, K.D., Palmer, K.A., Yoon, C.N., Paterlini, G., Zagari, A., Rumsey, S. and Scheraga, H.A., *J. Phys. Chem.*, 96 (1992) 6472.
9. Gay, D.M., *ACM Trans. Math. Software*, 9 (1983) 503.
10. Vásques, M., Némethy, G. and Scheraga, H.A., *Macromolecules*, 16 (1983) 1043.

# Retention of a *cis*-proline rotamer in a small fragment of RNase A containing a non-natural proline analog - an NMR study

Yue-Jin Li, Cathy C. Lester, David M. Rothwarf, Jin-Lin Peng,  
Theodore W. Thannhauser, Lianshan Zhang,<sup>a</sup> James P. Tam<sup>a</sup>  
and Harold A. Scheraga

*Baker Laboratory of Chemistry, Cornell University, Ithaca, New York 14853-1301, U. S. A.*

*<sup>a</sup>Department of Microbiology and Immunology, Vanderbilt University, A 5119 MCN, Nashville, Tennessee 37232, USA*

Protein-folding studies are often complicated by proline isomerization processes which lead to the formation of non-intrinsic intermediates and slow down the folding processes [1,2]. It is of interest to design a protein in which the native *cis* conformation of an X-Pro peptide bond can remain even when the protein is unfolded. This would eliminate proline isomerization and significantly simplify protein folding studies. Native ribonuclease A (RNase A) has two prolines (Pro<sup>93</sup> and Pro<sup>114</sup>) in *cis* conformation and two others (Pro<sup>42</sup> and Pro<sup>117</sup>) in *trans* conformation. In this study, an analog tripeptide corresponding to the sequence Tyr<sup>92</sup>-Pro<sup>93</sup>-Asn<sup>94</sup> of RNase A was synthesized with proline replaced by a non-natural amino acid, 5, 5-dimethylproline (dmPro). The bulky methyl groups were introduced to retard the proline isomerization process. NMR techniques were used to characterize the solution conformation of the peptide.

## Results and Discussion

Conformationally constrained dimethylproline was synthesized using the method described by Magaard *et al.* [3]. L-Dimethylproline was separated from D-dimethylproline by crystallization with D-tartaric acid, and its purity was checked by a BGIT (2,3,4,6-tetra-O-benzoyl-beta-D-glucopyranosyl isothiocyanate) assay [4]. The tripeptide Tyr-dmPro-Asn was synthesized by a solution procedure using Boc-chemistry. A variety of coupling reagents were used to facilitate the formation of the Tyr-dmPro peptide bond that was impeded by the bulky dimethyl group. Satisfactory yields, 65% and 75%, were obtained by using Bis(2-oxo-3-oxazolidinyl)phosphinic chloride (BOP-Cl) [5] and tetramethylfluoroformamidinium hexafluorophosphate (TFFH) [6], respectively, as coupling reagents. Purification was carried out on a YMC C<sub>18</sub> column, and characterization by MALDI-MS, amino acid analysis and NMR techniques.

The 500 MHz NOESY experiment was carried out in D<sub>2</sub>O at 25 °C, pH 7.28, with a mixing time of 250 ms. A strong NOE between the  $\alpha$ -protons of tyrosine and dimethylproline and the absence of NOEs between the  $\alpha$ -proton of tyrosine and the  $\epsilon$ -protons of dimethylproline (Fig. 1a), together with the assignment of all chemical shifts

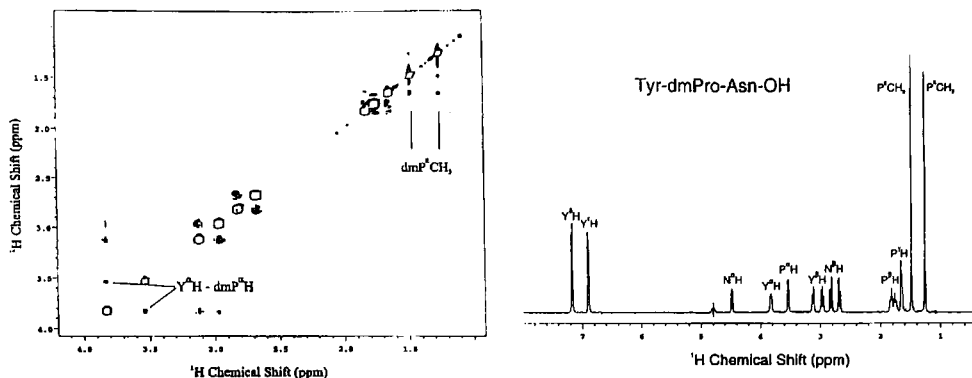


Fig. 1. 500 MHz NOESY spectra of Tyr-dmPro-Asn-OH in  $\text{D}_2\text{O}$  at pH 7.28 and 25  $^{\circ}\text{C}$ . (a) Expanded area of the NOESY spectrum recorded on a Varian Unity 500. The cross peaks between the Tyr  $\text{C}'\text{H}$  and dmPro  $\text{C}'\text{H}$  are labeled; (b) Assignment of all  ${}^1\text{H}$  chemical shifts.

and the ratios of intensities (Fig. 1b), led to the unambiguous conclusion that the Tyr-dmPro peptide bond was locked in a homogeneous *cis* rotamer.

## Conclusion

X-Pro peptide bonds in an unfolded protein can be locked in a *cis*-conformation by replacing proline by dimethylproline. This provides a powerful tool to assess the impact of proline *cis/trans* isomerization on protein folding pathways by selectively eliminating some proline isomerization processes, and will prove useful in both disulfide-intact and disulfide-coupled protein-folding studies.

## Acknowledgment

This work was supported by NIH grant GM-24893.

## References

1. Nall, B. T., in *Mechanisms of Protein Folding*, Pain, R. (Ed), Oxford University Press, New York, 1994, p. 80.
2. Houry, W. and Scheraga, H. A., *Biochemistry*, 35(1996)11719.
3. Magaard, V. M., Sanchez, R. M., Bean, J. and Moore, M. L., *Tetrahedron Lett.*, 34(1993)381.
4. Lobell, M. and Schneider, M. P., *J. Chromatography*, 633(1993)287.
5. Tung, R. D. and Rich, D. H., *J. Am. Chem. Soc.*, 107 (1985) 4342.
6. Carpino, L. A. and El-Faham, A., *J. Am. Chem. Soc.*, 117(1995)5401.

# Phosphorylation alters the three dimensional structure of the carboxyl terminal of bovine rhodopsin

**Arlene D. Albert,<sup>a</sup> Philip L. Yeagle,<sup>a</sup> James L. Alderfer,<sup>b</sup> Marc Dorey,<sup>a</sup>  
Todd Vogt,<sup>a</sup> Nilaya Bhawasar,<sup>a</sup> Paul A. Hargrave,<sup>c</sup>  
J. Hugh McDowell<sup>c</sup> and Anatol Arendt<sup>c</sup>**

*<sup>a</sup>Department of Biochemistry, SUNY at Buffalo, Buffalo, NY 14214, USA. <sup>b</sup>Biophysics Department, Roswell Park Cancer Institute, Buffalo, NY 14263, USA; <sup>c</sup>Department of Ophthalmology, University of Florida, Gainesville, FL 32610, USA*

Rod cells desensitize in response to high light levels. One mechanism of desensitization is phosphorylation of rhodopsin by rhodopsin kinase followed by arrestin binding [1]. Work in progress is providing three dimensional structural information for rhodopsin. We have determined the structure of the cytoplasmic surface of this receptor to moderately high resolution [2-5], and others [6] have determined a low resolution structure for the transmembrane helices.

Phosphorylation of rhodopsin occurs on the carboxyl terminal domain of the receptor [7]. Phosphorylation may change the conformation of the protein as well as add negative charge. We used the techniques of structural biology to determine whether phosphorylation alters the structure of the rhodopsin carboxyl terminal. We show that a peptide with 19 residues (from the carboxyl terminal) retained the structural characteristics of the parent 43 amino acid peptide and could be used to determine the effects of phosphorylation.

## Results and Discussion

The experimental plan was to solve the structures of the carboxyl terminal domain of rhodopsin in the presence and absence of phosphorylation to determine whether there is a conformation change induced by phosphorylation. Because of technical difficulties in synthesizing the phosphorylated peptides, it was necessary to explore whether a shorter peptide would carry the structural features of the parent. Therefore we determined the structures of peptides with 19, 25, 33 and 43 residues (from the carboxyl terminal of rhodopsin) to determine the shortest peptide that could be used that retained the structural features of the parent.

Unphosphorylated peptides were synthesized using Fmoc-Ala-Pam resin and the standard DCC/HOBt protocol. Cleavage from the resin and deprotection employed 95% trifluoroacetic acid/5% H<sub>2</sub>O for 90 min. Phosphopeptides were made on Boc-Ala-Pam resin using Boc-O-(diphenylphosphono)-serine and -threonine by the DCC/HOBt protocol. Cleavage and deblocking were performed in a single step using catalytic hydrogenolysis in the presence of palladium and platinum with anhydrous trifluoroacetic acid as solvent [8]. The structure of the 19mer and 25mer were determined in solution by NMR. Both contain

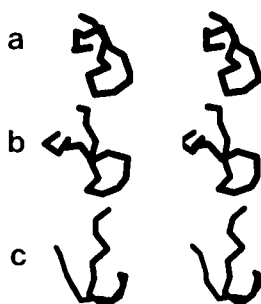


*Fig. 1. NMR-derived solution structures (ensemble average) of the carboxyl terminal of rhodopsin. A. 19 most C-terminal amino acids of a 43mer representing the carboxyl terminal of rhodopsin [4]. B. 19mer without phosphorylation as described in the text. C. 19mer with one serine phosphorylated, as described in the text.*

a  $\beta$ -turn with a short stretch of antiparallel  $\beta$ -sheet. These same structural features are found in the larger 33mer [2] and 43mer [4]. This structure appears to be locally stabilized as is typical of structures containing  $\beta$ -turns [9].

The structure of the 19mer + 1 phosphate (Ser 9 in the peptide, corresponding to Ser338) was determined by standard multidimensional NMR techniques. The results are shown in Fig. 1. A conformational difference is observed between the two peptides, although a turn is defined in all these peptides.

Phosphorylation changes both conformation and overall charge on this portion of rhodopsin, and both may play a role in promoting the binding of arrestin which in turn inhibits the activation of transducin by photoactivated rhodopsin. Whether this apparent conformational change persists with higher levels of phosphorylation is under investigation.

## References

1. Palczewski, K., *Protein Science*, 3 (1994) 1355.
2. Yeagle, P.L., Alderfer, J.L. and Albert, A.D., *Nature Struct. Biol.*, 2 (1995) 832.
3. Yeagle, P.L., Alderfer, J.L. and Albert, A.D., *Biochemistry*, 34 (1995) 14621.
4. Yeagle, P.L., Alderfer, J.L. and Albert, A.D., *Molecular Vision*, 2 (1996) <http://www.emory.edu/molvis/v2/yeagle>.
5. Yeagle, P.L., Alderfer, J.L. and Albert, A.D., *Biochemistry*, 36 (1997) 3864.
6. Schertler, G.R.X., Villa, C. and Henderson, R., *Nature*, 362 (1993) 770.
7. Zhao, X., Palczewski, K. and Ohguro, H., *Biophys. Chem.*, 56 (1995) 183.
8. Arendt, A., McDowell, J.H., Abdulaeva, G. and Hargrave, P.A., *Protein and Peptide Letters*, 3 (1996) 361.
9. Yang, A.-S., Hitz, B. and Honig, B., *J. Mol. Biol.*, 259 (1996) 873.

# Conformational calculations restrained by NMR and fluorescence data on functionalized Aib-based peptides

Basilio Pispisa,<sup>a</sup> Maria E. Amato,<sup>b</sup> Antonio Palleschi,<sup>c</sup>  
Mariano Venanzi,<sup>a</sup> Giancarlo Zanotti<sup>d</sup> and Anna L. Segre<sup>e</sup>

<sup>a</sup>Dipartimento di Scienze e Tecnologie Chimiche, Università di Roma Tor Vergata, 00133 Roma, <sup>b</sup>Dipartimento di Scienze Chimiche, Università di Catania, 95125 Catania, <sup>c</sup>Dipartimento di Chimica, Università di Roma La Sapienza, 00185 Roma, <sup>d</sup>Centro di Chimica del Farmaco del C.N.R., 00185 Roma, e C.N.R. Area della Ricerca di Roma, 00016 Monterotondo (Roma), Italy

Despite the idea that peptides shorter than 10-12 amino acids are generally devoid of structure and assume random conformations [1], we have recently shown that linear peptides formed by 6-10 amino acids, of the general formula Boc-(Leu)<sub>2</sub>-Lys(P)-(AA)<sub>n</sub>-(Leu)<sub>2</sub>-Lys(N)-OtBu, where n = 0-4, N = naphthalene, P = protoporphyrin IX and AA = Ala or Aib, are able to attain ordered structures in methanol or water/methanol (75/25, v/v) solution. By combining fluorescence with both IR and CD spectra results we were able to prove that the backbone chain of P(Ala)<sub>n</sub>N peptides populates  $\alpha$ -helical conformations, the size of  $\alpha$ -helices increasing with the length of the backbone, while that of P(Aib)<sub>n</sub>N attains  $3_{10}$ -helical structures [2,3].

To ascertain whether the high helix propensity of Aib holds even in destructuring solvents, such as DMSO, we thoroughly investigated the structural features of P(Aib)<sub>2</sub>N and (Aib)<sub>2</sub>N octapeptides in this solvent. <sup>1</sup>H-NMR and fluorescence results suggest the presence of two families of structures, both characterized by locally ordered arrangements, reminiscent of  $\beta$ -turn features. Only the combination of NMR coupling constants and NOE connectivities data with time resolved fluorescence results made it possible to build up the whole molecular structure.

## Results and Discussion

Both intra- and inter-residue NOE's cross-peaks involving backbone atoms were evidenced in the NOESY spectra, but the absence of NH-NH cross-peaks strongly suggests the lack of ordered conformations, either  $\alpha$ -helix or  $3_{10}$ -helix. In addition, the coupling constants for NH-C $\alpha$ H(i,i) of P(Aib)<sub>2</sub>N, by analysis of the line splitting in the 1-D spectra of non-overlapped signals, are around 8-9 Hz, which are inconsistent with  $\alpha$ -helical conformation but are similar to those of  $\beta$ -sheet structures (<sup>3</sup>J<sub>NH-C $\alpha$ H(i,i)</sub>  $\approx$  9.0 Hz). These results, together with other NOE evidence, support the idea that P(Aib)<sub>2</sub>N is somewhat structured in DMSO.

The steady-state fluorescence spectra of P(Aib)<sub>2</sub>N ( $\lambda_{ex}$  = 280 nm) show a substantial quenching of N singlet emission by the bound protoporphyrin in methanol and water/methanol 75/25 (v,v), but not in DMSO. In all cases, the efficiency of the quenching process, E<sub>N</sub>, parallels the efficiency of the fluorescence rise in P, E<sub>P</sub>, thus indicating that

the energy lost in the deactivation of the excited naphthyl chromophore is nearly completely transferred to the porphyrin group. This indicates that the N\* quenching chiefly occurs by intramolecular  ${}^1\text{N}^* \rightarrow \text{P}$  energy transfer. The modest N quenching observed in DMSO is suggestive of a rather large interchromophoric center-to-center distance or a mutual orientation of the probes approaching  $90^\circ$ , provided that the donor and acceptor molecules do not rotate fast enough to randomize their orientation during the donor lifetime [3]. This latter idea is supported by fluorescence time decay experiments of excited naphthalene in the same solvents. The curves were well fitted by a two-component exponential decay, the shorter decay time ( $\cong 3$  ns) being assigned to the energy transfer process,  ${}^1\text{N}^* \rightarrow \text{P}$  [2], while the longer decay time ( $\tau_2 \cong 45$  ns, in both methanol and water/methanol 75/25) is assigned to a minor exciplex decay. By contrast,  $\tau_2 \cong 38$  ns in DMSO, being similar to that observed for the unperturbed N\* decay ( $\tau_0 = 36 \pm 0.9$  ns). This suggests that the latter lifetime can be assigned to the natural N\* decay, which is suggestive of a poor interaction, and hence a large separation distance between N and P groups. Alternatively, even though the probes are close to each other, this result may be due to a perpendicular mutual orientation of the probes, which, according to Förster mechanism, prevents energy transfer to occur if they are frozen on the time scale of the donor lifetime [3]. Both long range NOE contacts and  $J_{\text{NH}}$  values were used as restraints, together with both the interprobe distance, R, and orientation parameter  $\kappa^2 = \cos^2\theta(3\cos^2\gamma + 1)$ , which describes a particular relative orientation between the probes [3], as obtained by fluorescence decay experiments. Energy minimization in terms of the internal rotation angles was carried out making use of the Karplus-Pardi expression, while  $R_m$  and  $\kappa_m^2$  values were employed for optimizing the agreement between experimental and calculated energy transfer efficiency of the *m*th conformer. From the results it appears that the molecules fold around the Aib residues, assuming a  $\beta$ -turn-like arrangement, which is stabilized by short range interactions within the backbone chain, as well as between the backbone and protoporphyrin group. The structural features of the other (unfolded) part of the molecules depend on whether the naphthyl moiety is close to protoporphyrin or far away from it, the average center-to-center distance changing from about 9 to 19 Å, respectively. In the former case, the chromophores are frozen in a perpendicular orientation, which prevents energy transfer to occur despite their proximity. In the latter case, the naphthyl moiety is freely rotating, thus being able to assume an average isotropic orientation with respect to the P group, the characteristic time for the internal rotation of naphthalene being shorter than that of the transfer process.

## References

1. Houston, M. E. Jr, Gannon, C. L., Kay, C. M. and Hodges, R. S., *J. Pept. Sci.*, 1 (1995) 274.
2. Pispisa, B., Venanzi, M., Palleschi, A. and Zanotti, G., *Biopolymers*, 36 (1994) 497.
3. Pispisa, B., Palleschi, A., Venanzi, M. and Zanotti, G., *J. Phys. Chem.*, 100 (1996) 6835, and references therein.

# Long-distance REDOR NMR measurements for determination of secondary structure and conformational heterogeneity in peptides

Boris Arshava,<sup>a</sup> Michael Breslav,<sup>a</sup> Octavian Antohi,<sup>a</sup> Ruth E. Stark,<sup>a</sup> Joel R. Garbow,<sup>b</sup> Jeffrey M. Becker<sup>c</sup> and Fred Naider<sup>a</sup>

<sup>a</sup>College of Staten Island, CUNY, Staten Island, NY 10314, <sup>b</sup>Monsanto Company, St. Louis, MO 63167, and <sup>c</sup>University of Tennessee, Knoxville, TN 37996, USA

High-resolution NMR spectroscopy of liquids has become a standard method for conformational studies in biochemistry. This method provides information on the secondary and tertiary structure of macromolecules and on intermolecular interactions such as ligand - receptor binding. These determinations are based mainly on interatomic distance measurements by quantitative analysis of NOESY spectra and, to a lesser degree, on torsion angle measurements based on homo- or heteronuclear scalar coupling constants. As with liquids, internuclear distances in solids are reflected in dipole-dipole coupling constants between the nuclear magnetic dipoles. Rotational-echo double resonance (REDOR) spectroscopy has been employed to determine heteronuclear dipole-dipole coupling constants [1,2] and to study internuclear distances in peptides, proteins and bound ligands.

An important target for the REDOR experiment is an amorphous solid. For biologically important amorphous solids that cannot be obtained in crystalline form, NMR spectroscopy is the only method for direct investigation of conformation at the atomic level. In the present study we examine the <sup>13</sup>C - <sup>15</sup>N REDOR of selectively labeled  $\alpha$ -factor peptide hormone in lyophilized powders. In order to understand the contribution of natural-abundance nuclei to the REDOR data at long evolution times, we have used a three-body calculation [3,4] and assumed a spherical distance distribution for natural abundance corrections. In addition we have evaluated the REDOR results in terms of a superposition of different distances with appropriate weighting factors. These approaches allow us to fit the experimental data on the  $\alpha$ -factor to a high degree of accuracy and to conclude that this peptide has a tendency to be bent in a lyophilized powder.

## Results and Discussion

Peptides investigated in this study were prepared by solid-phase synthetic methods and are selectively <sup>13</sup>C,<sup>15</sup>N-labeled analogs of the *Saccharomyces cerevisiae*  $\alpha$ -factor (WHWLQLKPGQPNleY) or melanostatin (PLG-NH<sub>2</sub>). The  $\alpha$ -factor was studied as an amorphous lyophilate, and melanostatin was examined in both crystalline and amorphous forms. Using a slightly modified three-body theory we were able to evaluate the contribution of natural abundance nuclei to the REDOR data. In these calculations we placed the labeled nuclei at specific distances and calculated the effects of background nuclei spherically distributed within shells of different radii. As expected, the contribution

of the naturally abundant atoms to the REDOR evolution curves ( $\Delta S/S_0$  versus  $\lambda$ ) depended on the size of the sphere, the distance between the labeled centers and the identity of the observed nucleus. For molecules of the size that we investigated, naturally abundant nuclei as far as 10 Å from the observed nucleus were found to contribute significantly to the REDOR peak amplitudes. We also observed that the influence of the natural-abundance correction on the data was dependent on the distance between the two labeled centers. A corrected  $\Delta S/S_0$  versus  $\lambda$  curve for labeled centers separated by 2 Å was almost identical to the uncorrected curve. As the internuclear distance increased to 8 Å, the deviations became quite significant when  $^{15}\text{N}$  was the observed nucleus but remained much smaller for  $^{13}\text{C}$  REDOR spectra. Using these natural-abundance corrections we determined that atoms separated by more than 5 Å can be identified using  $^{13}\text{C}$ -detected REDOR experiments.

To examine how the presence of conformational heterogeneity in a sample can affect REDOR results, we calculated  $\Delta S/S_0$  versus  $\lambda$  curves that would result from heteronuclear interactions of  $^{15}\text{N}$  and  $^{13}\text{C}$  labels having several distance distributions that differed significantly in their width and dispersity. Applying our natural-abundance correction to the REDOR data, the fit of the theoretical  $\Delta S/S_0$  curves with the experimental data was quite good. Our simulations showed that the presence of any conformational heterogeneity in a sample influences the shape of the  $\Delta S/S_0$  curve and leads to a monotonic upward trend in the apparent REDOR distance with increasing evolution time. This upward distance trend caused by the presence of more than one conformation in the sample closely resembles the observed experimental curves for the  $\alpha$ -factor lyophilates. Using the above approaches we ascertained that nuclei placed at residues 4 and 13 in the  $\alpha$ -factor peptide were separated by less than 7 Å.

## Conclusion

REDOR analysis may be used to study the conformational heterogeneity of amorphous peptides. In the case of  $\alpha$ -factor such investigations provided evidence that this linear peptide exists as a distribution of structures in a lyophilized solid and that the pheromone likely assumes a bend in the center of the molecule. Thus, the lyophilate of  $\alpha$ -factor maintains aspects of the solution conformation of this peptide.

## References

1. Gullion, T. and Schaefer, J., *J. Magn. Reson.*, 81 (1989) 196.
2. Gullion, T. and Schaefer, J., *Adv. Magn. Reson.*, 13 (1989) 57.
3. McDowell, L., Klug, C., Beusen, D., and Schaefer, J., *Biochemistry*, 35 (1996) 5395.
4. Naito, A. Nishimura, K., Tuzi, S., and Saito, H., *Chem. Phys. Lett.*, 229 (1994) 506.

# Interpretation of the fluorescence decay characteristics of cyclic $\beta$ -casomorphin analogs based on theoretically calculated ensembles of their low energy conformers

B. C. Wilkes,<sup>a</sup> B. Zelent,<sup>b</sup> H. Malak,<sup>b</sup> R. Schmidt<sup>a</sup> and P.W. Schiller<sup>a</sup>

<sup>a</sup>Clinical Research Institute of Montreal, Montreal, Que., Canada H2W 1R7; <sup>b</sup>Center of Fluorescence Spectroscopy, University of Maryland Medical School; Baltimore, MD 21201, USA

Cyclic  $\beta$ -casomorphin analogs described by the general formula H-Tyr-c[-D-Xxx-Yyy-D-Pro-Gly-] (Xxx = Orn, Lys; Yyy = Phe, Trp, 1-naphthylalanine (1-Nal), 2-Nal) have been shown to have high affinity for  $\mu$  opioid receptors and somewhat lower but still considerable  $\delta$  opioid receptor affinity [1]. Among various prepared analogs of this type, H-Tyr-c[-D-Orn-1-Nal-D-Pro-Gly-] was an agonist at both the  $\mu$  and the  $\delta$  receptor, whereas H-Tyr-c[-D-Orn-2-Nal-D-Pro-Gly-] turned out to be a novel prototype of a mixed  $\mu$  agonist/ $\delta$  antagonist. Opioid compounds with mixed  $\mu$  agonist/ $\delta$  antagonist properties are known to have potential as analgesics with low propensity for producing tolerance and dependence [2]. Since the Nal<sup>3</sup>-analogs contain a fluorescent naphthyl moiety, they are amenable to conformational analysis by fluorescence spectroscopic techniques. Here, we describe the results of fluorescence decay measurements and fluorescence quantum yield determinations that were undertaken in conjunction with a theoretical conformational analysis in an effort to elucidate distinct conformational features of the 1-Nal<sup>3</sup>- and 2-Nal<sup>3</sup>- $\beta$ -casomorphin analogs described above.

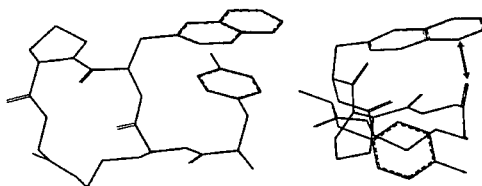


Fig. 1. Low energy conformers of H-Tyr-c[-D-Orn-2-Nal-D-Pro-Gly-] with extended Nal<sup>3</sup> side chain (left) and with the Nal<sup>3</sup> side chain in proximity of the Gly<sup>5</sup> carbonyl group (right).

## Results and Discussion

Naphthylalanine fluorescence decay measurements were performed in aqueous solution (Tris buffer, pH 7.5, 20°C) at low concentration ( $1 \times 10^{-5}$ M). Analysis of the fluorescence decay resulted in a single fluorescence decay time both for the reference compound N-acetyl-1-naphthylalanineamide (Ac-1-Nal-NH<sub>2</sub>) ( $\tau = 30.6$  ns) and for the cyclic peptide H-Tyr-c[-D-Orn-1-Nal-D-Pro-Gly-] ( $\tau = 31.3$  ns), indicating that the naphthyl

moiety in the peptide is fairly exposed to the aqueous environment. In the case of the 2-Nal-containing peptide, a two-component analysis produced the best fit with the fluorescence decay curve. The major component with an amplitude factor ( $\alpha$ ) of 0.95 was characterized by a decay time ( $\tau_1 = 30.2$  ns) similar to that of the corresponding reference compound N-Ac-2-Nal-NH<sub>2</sub> ( $\tau = 34.0$  ns), reflecting again a mostly aqueous environment of the fluorophore. The minor component ( $\alpha = 0.05$ ) with a much shorter decay time ( $\tau_2 = 6.9$  ns) indicated the existence of a small fraction of conformers in which drastic intramolecular quenching of the naphthyl fluorescence occurs. This was confirmed by steady-state fluorescence measurements which resulted in a lower quantum yield for H-Tyr-c[-D-Orn-2-Nal-D-Pro-Gly-] ( $\phi = 0.070$ ) as compared to H-Tyr-c[-D-Orn-1-Nal-D-Pro-Gly-] ( $\phi = 0.128$ ).

A molecular mechanics study (systematic grid search) resulted in 15 and 19 low energy conformations (< 3kcal/mol above the lowest energy conformation) for H-Tyr-c[-D-Orn-1-Nal-D-Pro-Gly-] and H-Tyr-c[-D-Orn-2-Nal-D-Pro-Gly-], respectively. In all low energy conformers of either peptide, one face of the naphthyl moiety was exposed at the surface of the molecule. This result is in agreement with the fluorescence data indicating a predominantly aqueous environment of the fluorophore in both peptides. However, the combined accessible surface area of the naphthyl moiety in the 2-Nal-containing peptide was found to be considerably larger than that of the naphthyl group in the 1-Nal-containing peptide. Two low energy structures of the 2-Nal peptide are shown in Fig. 1. Whereas the 1-Nal side chain is not located close to a carbonyl group in any of the low-energy conformers of H-Tyr-c[-D-Orn-1-Nal-D-Pro-Gly-], the 2-Nal side chain in the third-lowest energy conformer of H-Tyr-c[-D-Orn-2-Nal-D-Pro-Gly-] (Fig. 1, right panel) is folded over the peptide ring with the naphthyl moiety being in close proximity to and on top of the Gly carbonyl group. Since the carbonyl group is a strong fluorescence quencher, this conformer may represent the structure which gives rise to the short fluorescence decay time (minor component) observed with the 2-Nal peptide. Interestingly, this conformer showed excellent spatial overlap of its N-terminal amino group, phenol ring and naphthyl moiety with the corresponding pharmacophoric moieties in the non-peptide  $\delta$  antagonist naltrindole, thus providing a structural explanation for the  $\delta$  antagonist properties of H-Tyr-c[-D-Orn-2-Nal-D-Pro-Gly-].

## References

1. Schmidt, R., Vogel, D., Mrestani-Klaus, C., Brandt, W., Neubert, K., Chung, N.N., Lemieux, C. and Schiller, P.W., *J. Med. Chem.* 37 (1994) 1136.
2. Schiller, P.W., Weltrowska, G., Schmidt, R., Nguyen, T.M.-D., Berezowska, I., Lemieux, C., Chung, N.N., Carpenter, K.A. and Wilkes, B.C., *Analgesia*, 1 (1995) 703.

# Synthesis of the putative sixth transmembrane helix of the neurokinin-1 receptor and its structural analysis in phospholipid bilayer vesicles

**Chinchi C. Chen and Garland R. Marshall**

*Department of Molecular Biology and Pharmacology, Washington University, St. Louis, MO 63110, USA*

The neurokinin-1 (NK-1) receptor belongs to the class of seven transmembrane G-protein coupled receptors (7TM receptors). Ligand recognition and signal transduction in 7TM receptors are central themes in molecular pharmacology. Due to the physical nature of these proteins, direct methods for structural analysis [1], e.g. X-ray crystallography and multi-dimensional NMR, have so far yielded little information. Here we describe a strategy to circumvent some of these difficulties and produce structural information on 7TM receptors.

## Results and Discussion

Our general strategy was to synthesize transmembrane (TM) segments in which aromatic amino acid residues were replaced by their fluorinated analogs and to monitor their behavior in phospholipid membranes when embedded in phospholipid vesicles by <sup>19</sup>F NMR studies.

The 34-residue peptide KRKVVKMMIVVSTFAISWLPFHIFLLPYINPE, corresponding to the putative sixth transmembrane helix (TM6, residues 242-275) of the NK-1 receptor, was selected as a model TM segment. Synthesis was carried out manually on MBHA resin using Fmoc solid phase chemistry and TBTU/HOBt as coupling reagents. The four phenylalanine and one tryptophan residues were replaced with their monofluorinated analogs. The most effective method for peptide-resin cleavage and sidechain deprotection used a HF, EMS, and anisole cocktail in a ratio of 8:1:1. The crude peptide was then dissolved in AcOH/ACN/H<sub>2</sub>O (1:2:7, v/v), and purified by reverse phase HPLC. Four major peaks were observed on the HPLC profile (Fig. 1a), all of which corresponded to the desired product as identified by electrospray mass spectrometry. We hypothesized that the four peaks represented various conformers/aggregates of the peptide. Using MeOH/H<sub>2</sub>O (1:1, v/v) and 6 M GdnHCl solvent systems, which disrupt the secondary or tertiary structure of peptides to various extents, the HPLC profiles of the crude peptide (Fig. 1b & 1c), were reduced to only one predominant peak representing the desired product. The retention times of the most prominent peak observed in the AcOH/ACN/H<sub>2</sub>O, MeOH/H<sub>2</sub>O, and 6M GdnHCl solvent systems were at 48.95, 48.97 and 52.26 minutes, respectively. These differences in retention times could be attributed to changes in the hydrophobic surface of the peptide indicating that the conformation of the peptide was dependent on the particular solvent system. Based on HPLC analysis, greater than 30% of the crude cleavage mixture was the desired peptide when the MeOH/H<sub>2</sub>O dissolving system was applied.

$^1\text{H}$  NMR of the phospholipid bilayer vesicles made from egg yolk lecithin and  $^{19}\text{F}$  NMR of these vesicles containing fluorinated amino acid analogs were performed. Four probes, gadolinium, lanthanum, ferriocyanide and TEMPO were investigated. Gadolinium was most effective in signal line broadening and differentiation between internal and external surfaces of the vesicle. The resulting spectra implicated a through-space (dipolar or pseudocontact) interaction rather than transmission of electronic spin density through bonds (a contact shift).  $^{19}\text{F}$  NMR was performed in presence or absence of gadolinium on vesicles containing HPLC-purified TM6. As shown in figures 2a and 2b, the peak representing tryptophan disappeared and the phenylalanine peaks were broadened in presence of gadolinium. Disappearance of the tryptophan signal indicated that the tryptophan was exposed to water toward the outer surface of the vesicle. This is consistent with the current model for 7TM receptors [2]. Although the four labeled p-F-phenylalanines could not be assigned because of overlap, their line broadening in the presence of gadolinium indicated the effectiveness of this probe for lipid bilayer embedded peptides. Based on the above results, we propose that the relative broadenings observed can be quantitatively correlated to distances in the form of  $\langle r^{-6} \rangle$  [3]. Thus, the spatial relationships of the labeled amino acid residues can be readily calculated.

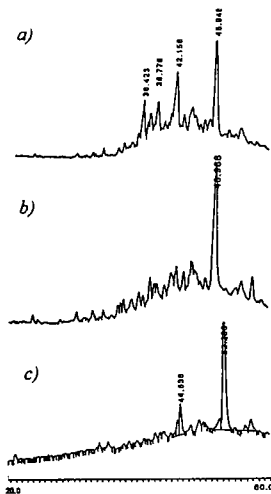


Fig. 1. HPLC profiles of crude TM6 when dissolved in a) AcOH/ACN/H<sub>2</sub>O (1:2:7, v/v) b) MeOH/H<sub>2</sub>O (1:1, v/v) c) 6M GdnHCl.

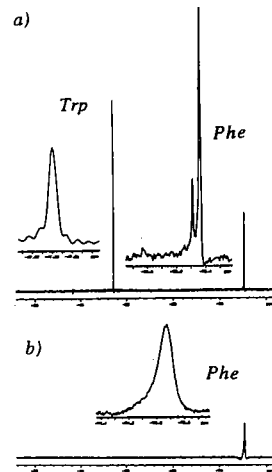


Fig. 2.  $^{19}\text{F}$  NMR spectra of the 2.5 mg/ml phospholipid vesicle containing the 0.5mM fluorine labeled TM6 in a) absence or b) presence (2.5 mM) of  $\text{Gd}^{3+}$

**References**

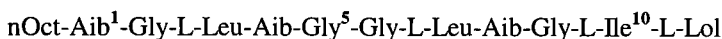
1. Nakanishi, S. *Ann. Rev. Neurosci.*, 14 (1991) 123.
2. Strader, C. D., Fong, T. M., Tota, M. R., Underwood, D., and Dixon, R. A. F., *Annu. Rev. Biochem.*, 33 (1994) 101.
3. Solomon, I. *Phys. Rev.*, 99 (1955) 559.

# Distinguishing $\alpha/3_{10}$ -helices in a lipopeptaibol antibiotic using the amino acid TOAC and ESR

Vania Monaco,<sup>a</sup> Claudio Toniolo,<sup>a</sup> Fernando Formaggio,<sup>a</sup> Marco Crisma<sup>a</sup>, Paul Hanson,<sup>b</sup> Glenn L. Millhauser,<sup>b</sup> Clifford George,<sup>c</sup> Judith L. Flippen-Anderson,<sup>c</sup> Sylvie Rebuffat<sup>d</sup> and Bernard Bodo<sup>d</sup>

<sup>a</sup>Biopolymer Research Center, CNR, Department of Organic Chemistry, University of Padova, 35131 Padova, Italy <sup>b</sup>Department of Chemistry and Biochemistry; University of California, Santa Cruz, CA 95064, USA <sup>c</sup>Laboratory for the Structure of Matter, Naval Research Laboratory, Washington, DC 20375, USA <sup>d</sup>Laboratoire de Chimie, Muséum National d' Histoire Naturelle, 75231 Paris 05, France

*Trichogin GA IV* is a terminally-blocked, membrane-modifying lipopeptaibol of fungal origin [1], characterized by: (i) Ten  $\alpha$ -aminoacids, one  $\beta$ -aminoalcohol (leucinol) at the C-terminus, and one *n*-octanoyl chain at the N-terminus, (ii) Three Aib residues at positions 1, 4, and 8, (iii) A mixed  $3_{10}/\alpha$ -helical structure (a  $3_{10}$ -helix near the N-terminus and an  $\alpha$ -helix in the central part) [2]. (iv) Amphiphilic properties: all of the hydrophobic groups (*n*-octanoyl, and Leu, Ile, and Lol side chains) are positioned on one helix face, while the four Gly residues comprise the hydrophilic face. The primary structure of trichogin GA IV is as follows:



We have also shown that the [L-Leu-OMe<sup>11</sup>] trichogin GA IV analog has almost identical conformational and membrane modifying properties as the natural lipopeptaibol [3]. To determine the structure of trichogin GA IV in solution, we have recently synthesized by solution methods and fully characterized three analogs, each with a double Aib  $\rightarrow$  TOAC replacement. Like Aib, TOAC is a strong  $3_{10}/\alpha$ -helical former, but it also contains a stable nitroxide free radical which may be exploited as a useful ESR probe [4]. In the TOAC(1,4) analog the double replacement is located in the  $3_{10}$ -helical region, whereas in the TOAC(4,8) analog it is positioned in the  $\alpha$ -helix region. The two TOAC residues in the TOAC(1,8) analog are separated by approximately two turns of helix.

## Results and Discussion

In the X-ray diffraction structure of the [Fmoc<sup>0</sup>, TOAC<sup>4,8</sup>, L-Leu-OMe<sup>11</sup>] trichogin GA IV analog [this work] the  $3_{10}$ -helix at the N-terminus (residues 1-4) is more regular than in the natural lipopeptaibol [2]. The central 4-8 sequence is folded in a classical  $\alpha$ -helix in both peptides. Therefore, TOAC may replace Aib at positions 1, 4, and 8 in the sequence

without significantly disturbing the overall peptide secondary structure. The nitroxide groups of the two TOAC residues are  $\sim 6 \text{ \AA}$  apart.

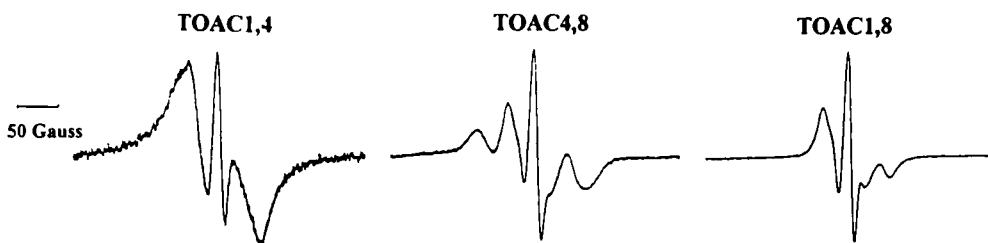


Fig. 1. ESR spectra of the *n*-octanoylated TOAC(1,4), TOAC(4,8), and TOAC (1,8) trichogin GA IV analogs in MeOH solution at 200 K. Peptide concentration: 1 mM. Scanwidth: 250 G.

From the relative strengths of the dipolar coupling interaction in the ESR spectra of the three doubly substituted analogs in MeOH solution at 200 K (Fig. 1) it may be concluded that the distances between the TOAC spin labels are  $d_{1,8} \gg d_{1,4} > d_{4,8}$ . In unilamellar vesicle experiments we found that the peptides are immobilized into the lipid bilayer and the rank order of distances between the TOAC spin labels is the same as that found in MeOH solution. In summary, the results of our ESR study support the view that the same mixed  $3_{10}/\alpha$ -helical structure, found in the crystal state for trichogin GA IV and its double TOAC analog, is largely preserved in solution and in a membrane-like environment. Under the latter experimental conditions all of the three *n*-octanoylated analogs are active in inducing membrane permeability.

## References

1. Auvin-Guette, C., Rebuffat, S., Prigent, Y. and Bodo B., *J. Am. Chem. Soc.*, 118 (1992) 2170.
2. Toniolo, C., Peggion, C., Crisma, M., Formaggio, F., Shui, X. and Eggleston, D.S., *Nature: Struct. Biol.*, 1 (1994) 908.
3. Toniolo, C., Crisma, M., Formaggio, F., Peggion, C., Monaco, V., Goulard, C., Rebuffat, S. and Bodo, B., *J. Am. Chem. Soc.*, 118 (1996) 4952.
4. Toniolo, C., Valente, E., Formaggio, F., Crisma, M., Pilloni, G., Corvaja, C., Toffoletti, A., Martinez, G.V., Hanson, M.P., Millhauser, G.L., George, C. and Flippen-Anderson, J.L., *J. Pept. Sci.*, 1 (1995) 45.

# 3D structure of the anti-AChR Fv antibody fragment complexed to the [Ala<sup>76</sup>]MIR antigen: A homology and molecular modelling approach

Piotr Orlewski,<sup>a</sup> Jens Kleinjung,<sup>a</sup> Avgi Mamalaki,<sup>b</sup> Christos Liolitsas,<sup>b</sup>  
Socrates J. Tzartos,<sup>b</sup> Vassilios Tsikaris,<sup>c</sup> Maria Sakarellos-Daitsiotis,<sup>c</sup>  
Constantinos Sakarellos<sup>c</sup> and Manh-Thong Cung<sup>a</sup>

<sup>a</sup>CNRS-URA 494, ENSIC-INPL, B.P. 451, F-54001, Nancy, France.

<sup>b</sup>Hellenic Pasteur Institute, 127 Vassilissis Sofias Avenue, GR-11521, Athens, Greece.

<sup>c</sup>Department of Chemistry, University of Ioannina, GR-54110, Ioannina, Greece.

*Myasthenia gravis* is a neuromuscular autoimmune disease induced by autoantibodies raised against the acetylcholine receptor (AChR) which consists of five subunits  $\alpha_2\beta\gamma\delta$ . The AChR epitope involved in the binding of mAbs, called 'main immunogenic region' (MIR), has been localized between residues 67-76 of the AChR  $\alpha$ -subunit. We used high field NMR spectroscopy to elucidate the solution structure of the antibody-bound peptide. Homology modelling and molecular docking led to a complex stabilized by some highly favorable intermolecular contacts.

## Results and Discussion

A modified MIR sequence of *Torpedo* electric organ, the decapeptide W<sup>67</sup>NPADYG-GIA<sup>76</sup>, was synthesized by solid phase synthesis. Alanine scan of the MIR sequence revealed in earlier investigations a threefold higher binding potency of the [Ala<sup>76</sup>]MIR compared to the native sequence [1]. A recombinant antibody fragment of the rat anti-MIR mAb198 was cloned by polymerase chain reaction and expressed as the soluble scFv fragment (scFv198) in *E. coli*. This fragment was capable of blocking the AChR in human cell cultures against the action of the intact mAb198 or Abs from human sera [2]. The construction of the scFv198 was based on two reference molecules of which structures were derived from crystallized complexes. The reference Abs IgM [3] and D1.3 [4] were chosen because of their sequence similarity to scFv. The canonical CDRs H1, H2, L1, and L2 were superimposed with those of the reference structures. Loop H3 was aligned with the sequence H3 of mAb Kol2fb4. The structure of CDR L3 was generated *de novo* and optimized. Superimposition of the constructed active site of the scFv fragment with the active site of the IgM yielded a RMS value of 1.45 Å for the L1, L2, and L3 loops and a RMS value of 0.85 Å for the H1 and H2 loops.

The structure elucidation of the [Ala<sup>76</sup>]MIR decapeptide complexed to the anti-MIR mAb in solution (molar ratio 50/1) was performed using transferred NOE experiments. Analysis of the spectra led to a well defined solution structure.

Molecular docking was initialized by a parallel and independent fit onto both structures, i.e. the modelled binding site of the antibody and the [Ala<sup>76</sup>]MIR decapeptide

derived from NMR experiments. The complex starting conformation was deduced from a crystallized myohemerythrin-Ab complex [5]. An energy minimization of both, the peptide and the CDR side chains (elimination of atom overlaps), led to a refined complex structure. In the [Ala<sup>76</sup>]MIR-scFv198 complex, the antigen backbone fits perfectly the channel formed by the CDRs (Fig. 1A). The most important contacts are formed between the Y<sup>72</sup> aromatic ring of [Ala<sup>76</sup>]MIR and the aromatic side chains of the H2, H3, and L3 CDRs. The tyrosine is surrounded by four aromatic residues and one arginyl residue (Fig. 1B). Residues H2-W<sup>52</sup>, H3-F<sup>100d</sup>, and L3-Y<sup>95</sup> give raise to a  $\pi$ - $\pi$  interaction system. In addition, the arginyl H2-R<sup>50</sup> side chain points perpendicularly towards the Y<sup>72</sup> ring, thus generating an additional  $\pi$ - $\pi$  energy contribution.

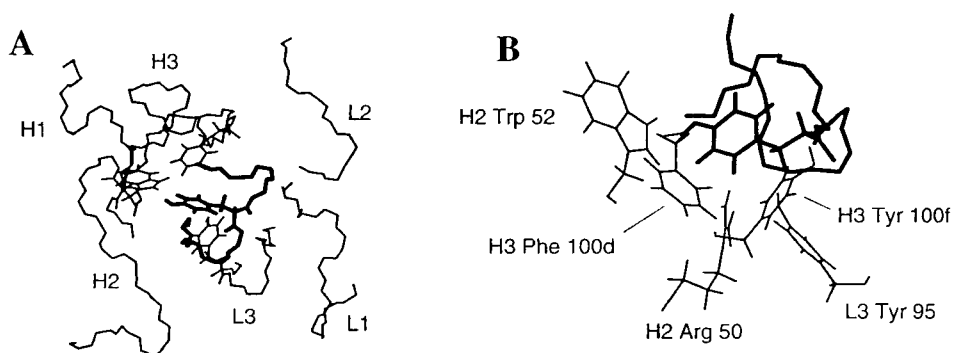


Fig. 1. Views of the [A<sup>76</sup>]MIR-scFv198 complex obtained after docking optimization. (A) The main chain traces of the 6 CDRs are shown as thin lines. (B) The central ligand [A<sup>76</sup>]MIR-Y<sup>72</sup> side chain is located in the cage of aromatic antibody groups.

## Acknowledgments

This work was supported by grants from CEC (Contract No ERBCHRXCT: 940547), AFM, CNRS and GSRT.

## References

1. Papadouli, I., Potamianos, S., Hadjidakis, I., Bairaktari, E., Tsikaris, V., Sakarellos, C., Cung, M.T., Marraud, M., Tzartos, S.J., *Biochem. J.*, 269 (1990) 239.
2. Mamalaki, A., Trakas, N., Tzartos, S.J., *Eur. J. Immunol.*, 23 (1993) 1839.
3. Fan, Z.C., Shan, L., Guddat, L.W., He, X.M., Gray, W.R., Raison, R.L., Edmundson, A.B., *J.Mol.Biol.*, 228 (1992) 188.
4. Fischmann, T.O., Bentley, G.A., Bhat, T.N., Boulot, G., Mariuzza, R.A., Phillips, S.E.V., Tello, D., Poljak, R.J., *J.Biol.Chem.*, 266 (1991) 1291
5. Stanfield, R.L., Fieser, T.M., Learner, R.A., Wilson, I.A., *Science*, 248 (1990) 712.

# Parathyroid hormone-related protein derived mono- and bicyclic agonists and antagonists: A conformational comparison

Stefano Maretto,<sup>a</sup> Elisabetta Schievano,<sup>a</sup> Evaristo Peggion,<sup>a</sup> Stefano Mammi,<sup>a</sup> Alessandro Bisello,<sup>b</sup> Michael Chorev,<sup>b</sup> Michael Rosenblatt<sup>b</sup> and Dale F. Mierke<sup>c,d</sup>

<sup>a</sup>Department of Organic Chemistry, University of Padova, Biopolymer Research Center, Via Marzolo 1, Padova, Italy, <sup>b</sup>Division of Bone and Mineral Metabolism, Harvard-Thorndike and Charles A. Dana Laboratories, Department of Medicine, Beth Israel Deaconess Medical Center, 330 Brookline Ave., Boston, MA 02215, U.S.A., <sup>c</sup>Gustaf H. Carlson School of Chemistry, Clark University, 950 Main Street, Worcester, MA, 01610, U.S.A., <sup>d</sup>Department of Pharmacology and Molecular Toxicology, University of Massachusetts, Medical School, 55 Lake Ave. North, Worcester, MA 01655, USA

To incorporate more conformational constraint into the peptide hormone parathyroid hormone-related protein, PTHrP, we initiated a program of incorporating (i)-to (ix4) side chain lactam bridge cyclization into the N-terminal 1-34 fully active fragment of PTHrP [1-3]. This modification has been previously shown to stabilize  $\alpha$ -helical conformations, a secondary structural element that has been proposed to be very important for the biological activity of parathyroid hormone and PTHrP. In this communication, the conformational results of lactam cyclization between Lys<sup>13</sup>-Asp<sup>17</sup>, Lys<sup>26</sup>-Asp<sup>30</sup>, and a bicyclic analog containing both of these lactams are presented. These modifications have been incorporated in both agonist peptide series, containing the full 1-34 sequence, and the truncated antagonist series, containing residues 7-34 of the PTHrP sequence.

## Results and Discussion

The results from the spectroscopic characterization including circular dichroism and nuclear magnetic resonance, clearly indicated a high  $\alpha$ -helix content for all members of this series of peptides. Interestingly, there does not seem to be a general synergy between the helix-inducing capacity of the mid-sequence (Lys<sup>13</sup>-Asp<sup>17</sup>) and the C-terminal (Lys<sup>26</sup>-Asp<sup>30</sup>) lactams, that is, the bicyclic analog does not display additional helicity in comparison to the two mono-lactam containing analogs. The conformational features of the peptides were refined by extensive computer simulations including metric matrix distance geometry calculations followed by molecular dynamics simulations using explicit solvent. The results from these studies illustrate striking similarities for the agonists and antagonists containing the same modification. As an example, the agonist PTHrP(1-34)-NH<sub>2</sub> and antagonist PTHrP(7-34)-NH<sub>2</sub> containing the mid-sequence and C-terminal lactams are shown superimposed in Fig. 1. In this figure the heavy atoms of residues 22-32 have been superimposed. Similar results are obtained with the comparison of the other pairs of similarly modified agonists and antagonists.

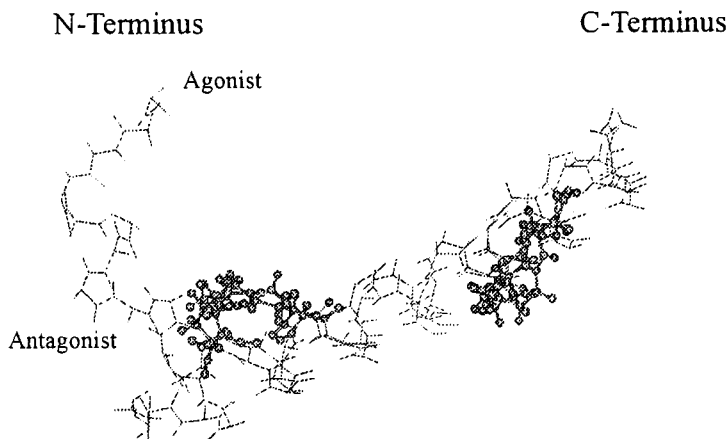


Fig. 1. Superposition of the bicyclic,  $\text{Lys}^{13}\text{-Asp}^{17}$ ,  $\text{Lys}^{26}\text{-Asp}^{30}$ , lactam containing PTHrP agonist PTHrP(1-34)- $\text{NH}_2$  and antagonist PTHrP(7-34)- $\text{NH}_2$ .

The lactam modified analogs have been shown to display similar binding properties and relative biological properties (agonist and antagonist). The mid-sequence lactam-containing analogs and the bicyclic analogs display high binding affinities and are highly potent while the analogs containing the C-terminal lactams display poor receptor binding [2]. Given these biological activities, the similarity between the conformational features of the agonists and antagonists is not surprising. The results indicate that the C-terminal lactam is not well tolerated when used alone. However, coupling with the mid-sequence lactam overcomes the deleterious effect of the C-terminal lactam and restores activity. Further efforts to explore this phenomenon and identify the source (dynamics or conformation or a combination of the two) are currently underway.

### Acknowledgment

This research was supported, in part, by the National Institutes of Health by Grants RO1-DK47940 (M.R.) and GM54082 (D.F.M.).

### References

1. Maretto, S., Mammi, S., Bissacco, E., Peggion, E., Bisello, A., Rosenblatt, M., Chorev, M. and Mierke, D. F., *Biochemistry*, 36 (1997) 3300.
2. Bisello, A., Nakamoto, C., Rosenblatt, M. and Chorev, M., *Biochemistry*, 36 (1997) 3293.
3. Mierke, D. F., Maretto, S., Schievano, E., Bisello, A., Mammi, S., Rosenblatt, M., Peggion, E. and Chorev, M., *Biochemistry*, in press.

# The NMR structure of a cyclic V3 loop peptide that binds tightly to a monoclonal antibody that potently neutralizes HIV-1

Edelmira Cabezas and Arnold C. Satterthwait,

*Department of Molecular Biology, The Scripps Research Institute,  
La Jolla, CA 92037, USA*

Cyclic[JHIGPGR(Aib)FGGZ]G-NH<sub>2</sub> was selected as the best binder to Mab 58.2 from a series of constrained peptides corresponding to the tip of the V3 loop on gp120 of HIV-1 [1]. The cyclic peptide binds about 256-fold better than the corresponding linear peptide, acetyl-GHIGPGRAFGGGG-NH<sub>2</sub>. Substitution of Aib for Ala improves the affinity of both peptides for Mab 58.2 about 2-4 fold. Mab 58.2 is the most potent neutralizer of primary HIV-1 isolates among several thousand Mabs evaluated by White-Scharf et al. [2] at the Repligen Corporation. Alanine scanning indicates that Mab 58.2 binds GPGRAF as a core epitope [2]. Enhanced affinity of the cyclic peptide for Mab 58.2 suggests that it adapts a conformation in water that mimics the conformation on antibody HIV-1. Since conformational mimicry can be critical for effective synthetic peptide vaccines [3], we compared solution structures of the linear and cyclic peptides using NMR spectroscopy.

## Results and Discussion

Signal assignments, temperature coefficients and NOEs were obtained from 1D and 2D P.E. COSY, TOCSY and ROESY spectra of 20 mM peptides at 21°C in 10% D<sub>2</sub>O/H<sub>2</sub>O on a 500 MHz Bruker NMR spectrometer. A FG/F(D-Ala) substitution was made for the NMR study and has little effect on affinity. Deuterated analogs of the cyclic peptide were used to isolate overlapping signals. The linear peptide showed evidence for Type I and/or Type II turns at GPGR as indicated by weak Pro<sup>δ</sup>-Gly<sup>N</sup> (i, i + 1) and Pro<sup>α</sup>-Arg<sup>N</sup> (i, i + 2) NOEs and a strong Pro<sup>α</sup>-Gly<sup>N</sup> (i, i + 1) NOE. Data for the cyclic peptide indicates a slight increase in the turn population at GPGR with a shift towards the Type I turn. Thus an Arg<sup>N</sup>-Gly<sup>N</sup> (i, i + 1) NOE is isolated, the Pro<sup>α</sup>Gly<sup>N</sup> (i, i + 1) decreases and the Arg<sup>N</sup> temperature coefficient is reduced. The Pro<sup>α</sup>-Arg<sup>N</sup> (i, i + 2) NOE is lost, possibly as a consequence of an increased distance for the Type I turn.

An Arg<sup>α</sup>-Phe<sup>N</sup> (i, i + 2) indicates that a second turn is formed at R(Aib)F in the cyclic peptide. This turn(s) is well populated. Signals for the two Aib β-methyl groups separate indicating a better defined environment while coupling constants and NOE's indicate that rotation about the Phe χ angle is restricted. However, medium NOEs from the Phe NH to both Aib methyl groups suggest that AibF forms more than one type of turn. The turn(s) at R(Aib)F could be part of a reverse turn(s) at GR(Aib)F and/or R(Aib)F(D-Ala). Observation of a lowered temperature coefficient for D-Ala<sup>N</sup> and not Phe<sup>N</sup>, supports the formation of a reverse turn(s) at R(Aib)F(D-Ala).

The NMR data suggest that cyclization of the linear peptide stabilizes two or more reverse turns that may exist in separate conformers and/or concurrently in the same conformer. While both turns are highly populated in the cyclic peptide, they are very likely in dynamic equilibria with disordered forms. Sequential reverse turns are frequently found in complex loops on protein surfaces [5]. The appearance of two or more turns in the V3 cyclic peptide and a *P. falciparum* malaria cyclic peptide [4], show that medium sized cyclic peptides can provide platforms for complex loop structures in water.

The formation of two or more reverse turns in the cyclic V3 peptide but not the linear peptide provides a basis for its enhanced affinity for Mab 58.2. Ghiara et al. [6] have reported that another neutralizing Mab 59.1 binds linear V3 peptides in multiple turn conformations. It thus remains likely that multiple turns constitute recognition elements at the "tip" of the HIV-1 V3 loop and can account for the neutralization properties of these Mabs. Further, it emphasizes the probable importance of multiple turns for HIV-1 vaccine design.

### Acknowledgements

This research was supported by NIH AI37512. This is publication 11040-MB from The Scripps Research Institute.

### References

1. Cabezas, E. and Satterthwait, A.C., In Kaumaya, P.T.P. and Hodges, R.S. (Eds.), Peptides: Chemistry, Structure and Biology, Proceedings of the Fourteenth American Peptide Symposium, Mayflower Scientific, Ltd., 1996, p.800
2. White-Scharf, M.E., Potts, B.J., Smith, M., Sokolowski, K.A., Rusche, J.R. and Silver, S., Virology, 192 (1993) 197.
3. Satterthwait, A.C., Cabezas, E., Calvo, J.C., Wu, J.X., Wang, P.L., Chen, S.Q., Kaslow, D.C., Livnah, O. and Stura, E.A. In Kaumaya, P.T.P. and Hodges, R.S. (Eds.), Peptides: Chemistry, Structure and Biology, Proceedings of the Fourteenth American Peptide Symposium, Mayflower Scientific, Ltd., 1996, p.772
4. Wilmot, C.M. and Thornton, J.M., Prot. Eng., 3 (1990) 479.
5. Cabezas, E. and Satterthwait, A.C., In Kaumaya, P.T.P. and Hodges, R.S. (Eds.), Peptides: Chemistry, Structure and Biology, Proceedings of the Fourteenth American Peptide Symposium, Mayflower Scientific, Ltd., 1996, p.734
6. Ghiara, J.B., Stura, E.A., Stanfield, R.L., Profy, A.T. and Wilson, I.A., Science, 264 (1994) 82; Ghiara, J.B., Ferguson, D.C., Satterthwait, A.C., Dyson, H.J. and Wilson, I. A., J. Mol. Biol., 266 (1997) 1.



generated (W-O1, W-O2 and W-O3). These peptides were shown to contain two disulfide bonds and their pairings were determined as shown in Table 1. W-O3 contains the native disulfide bonds. An intermediate (W-I) was rapidly formed reaching a maximum concentration after about 3 hrs and then gradually disappeared.

Table 1. Arrangement of the disulfide bridges in the oxidized peptides.

Peptides	W-O1 / M-O1	W-O2 / M-O2	W-O3 / M-O3
Disulfide bonds	183-219 , 200-227	183-200 , 219-227	183-227 , 200-219

The same conditions of oxidation and analysis were applied to the PM mutant. The oxidation was complete after 165 hrs (Fig. 2B). Two major peaks were obtained (M-O1 and M-O2) (Table 1). Only a trace amount of M-O3 with the native cysteine pairing could be detected. Two intermediates (M-I1 and M-I2) were formed reaching a maximum concentration at about 23 hrs.

Our results show that the mutated peptide does not follow the same mechanism of folding as the wild peptide, that its kinetic of oxidation is much slower and a very small amount of the loop with the native disulfide bonds is obtained.

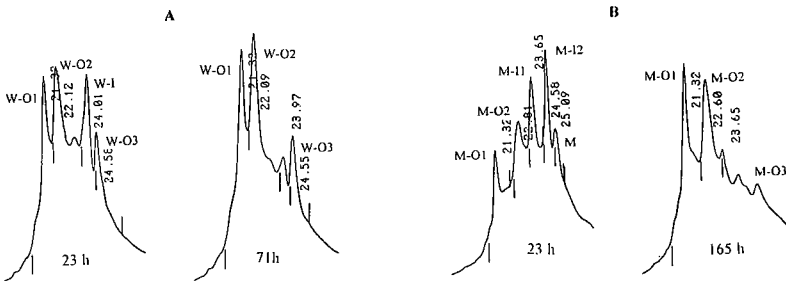


Fig. 2. HPLC analysis of the folding reaction. PLP (181-230) (A) and mutant (P215S) (B).

## Conclusion

We have shown that the PM mutation affects the folding of the loop 4 of PLP *in vitro* indicating that the inability of the extracellular domain of PLP to fold *in vivo* may contribute to the molecular defects responsible for Pelizaeus-Merzbacher disease.

## References

1. Hodes, M.E., Pratt, V.M. and Dlouhy, S.R., *Dev. Neurosci.*, 15 (1993) 383.
2. Lees, M.B., Brostoff, S.W., In Morell, P. (Ed), *Myelin*, Plenum Press, New York, 1984, p. 197.
3. Weimbs, T., Stoffel, W., *Biochem.*, 31 (1992) 12289.

# An improved template for the initiation of peptide helices

Evan T. Powers, Peter Renold, Sherri Oslick and D. S. Kemp

Department of Chemistry, Massachusetts Institute of Technology, Cambridge, MA 02139, USA

The N-terminal reporting conformational template AcHel<sub>1</sub> (1) has proven valuable in the study of peptide helicity [1], but its reporting feature, the *cis* / *trans* equilibrium of the acetyl group interferes with its ability to initiate helices. Replacing the acetyl with a sulfamate (N-SO<sub>3</sub><sup>-</sup>) yields the new template SO<sub>3</sub>Hel<sub>1</sub> (2) (Fig. 1). This modified template does not have an analogous conformational equilibrium that can hinder its helix initiating ability.

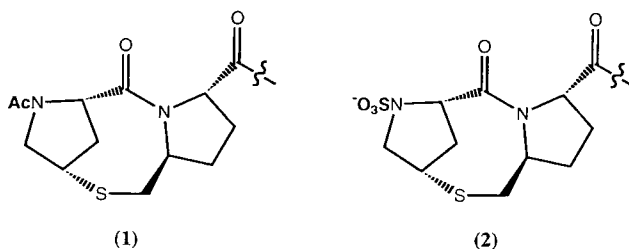


Fig. 1. N-terminal helix inducing templates AcHel<sub>1</sub> (1) and SO<sub>3</sub>Hel<sub>1</sub> (2).

## Results and Discussion

SO<sub>3</sub>Hel<sub>1</sub>-peptide conjugates are prepared by synthesizing a peptide terminating in BocHel<sub>1</sub> by standard Fmoc SPPS. BocHel<sub>1</sub>OH can be prepared by a modification of AcHel<sub>1</sub>'s synthesis ([2] and P. Renold, unpublished). The template-peptide conjugate is deprotected and cleaved from the resin by TFA to yield HHel<sub>1</sub>-peptide, in which the template has a free amine. This is sulfamated by dissolving the peptide to 5mM in 10% aq. NaHCO<sub>3</sub> and treating it with a large excess of SO<sub>3</sub>-pyridine (>100 eq.) for 12h at 25°C [3]. These conditions tolerate all side chains except those of Lys, His, and Tyr. SO<sub>3</sub>Hel<sub>1</sub>-peptide conjugates are stable for months in water solution at pH 3 to 7.

The CD spectra of HHel<sub>1</sub>, AcHel<sub>1</sub> and SO<sub>3</sub>Hel<sub>1</sub> as conjugates of Ala<sub>6</sub>-NH<sub>2</sub> are shown in Fig. 2. Judging by the per residue molar ellipticity at 222nm ([Θ]<sub>222</sub>), one can see that SO<sub>3</sub>Hel<sub>1</sub>Ala<sub>6</sub>-NH<sub>2</sub> is substantially more helical than AcHel<sub>1</sub>Ala<sub>6</sub>-NH<sub>2</sub> ([Θ]<sub>222</sub> = -10,200 vs. -7,150 deg cm<sup>2</sup> / dmol), and that HHel<sub>1</sub>Ala<sub>6</sub>-NH<sub>2</sub> is not helical at all. These CD data can also provide a rough estimate for σ, the Zimm-Bragg helix initiation parameter [4]. Assuming that the helix propagation constant for Ala, s<sub>Ala</sub>, is 1.02 [1] and that [Θ]<sub>222</sub> for the 100% helical peptide is -30,000 deg cm<sup>2</sup> / dmol [5], the calculated σ is probably in the range of 0.5 to 0.8 with the best fit being at σ = 0.6. This is about two orders of magnitude larger than the values reported for natural amino acids [6].

$\text{SO}_3\text{Hel}_1$  is a potent helix initiator, but is only available by total synthesis.  $\text{SO}_3\text{ProAla}$  is a much simpler analog that can adopt a conformation analogous to that of  $\text{SO}_3\text{Hel}_1$ .  $\text{SO}_3\text{Hel}_1$  and  $\text{SO}_3\text{ProAla}$  were compared by CD spectroscopy as conjugates of the peptide SELSRL- $\text{NH}_2$ , a sequence from the gut hormone secretin (Fig. 3). The spectra show that the unsulfamated control peptide, H-ProAlaSELSRL- $\text{NH}_2$  is a random coil, that  $\text{SO}_3\text{Hel}_1\text{SELSRL-}\text{NH}_2$  is fairly helical, and that  $\text{SO}_3\text{ProAlaSELSRL-}\text{NH}_2$  is markedly shifted away from a random coil and toward a helical conformation. While it is much too early to conclude that  $\text{SO}_3\text{ProAla}$  induces helicity by adopting the conformation of  $\text{SO}_3\text{Hel}_1$ , it is clear that sulfamation affects the structure of the peptide.

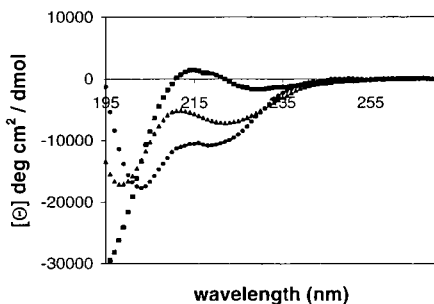


Fig. 2. CD spectra of  $\text{HHel}_1\text{Ala}_6\text{-NH}_2$  (squares),  $\text{AcHel}_1\text{Ala}_6\text{-NH}_2$  (triangles), and  $\text{SO}_3\text{Hel}_1\text{Ala}_6\text{-NH}_2$  (circles). Spectra were corrected for contributions due to the templates [5].

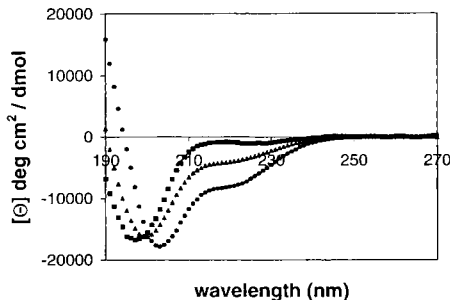


Fig. 3. CD spectra of  $\text{H-ProAlaSELSRL-NH}_2$  (squares),  $\text{SO}_3\text{ProAlaSELSRL-NH}_2$  (triangles), and  $\text{SO}_3\text{Hel}_1\text{SELSRL-NH}_2$  (circles).

## References

1. Kemp, D.S., Oslick, S. L., Allen, T. J., J. Am. Chem. Soc., 118 (1996) 4249.
2. McClure, K., Renold, P., Kemp, D. S., J. Org. Chem., 60 (1995) 454.
3. Baumgarten, P, Marggraff, I., Dammann, E., Hoppe-Seyler's Z. Physiol. Chem., 209 (1932) 145.
4. Zimm, B. H., Bragg, J. K., J. Chem. Phys. ,31 (1959) 526.
5. Oslick, S. L., Thesis, Massachusetts Institute of Technology, 1996.
6. Wojcik, J., Altmann, K.-H., Scheraga, H. A., Biopolymers, 30 (1990) 121.

## Conformational studies of PTH/PTHrP hybrids

Stefano Mammi,<sup>a</sup> Lara Pauletto,<sup>a</sup> Evaristo Peggion,<sup>a</sup> Vered Behar,<sup>b</sup>  
Michael Rosenblatt<sup>b</sup> and Michael Chorev<sup>b</sup>

<sup>a</sup>Department of Organic Chemistry, Biopolymer Research Center University of Padua, Via Marzolo 1, 35131 Padua, Italy. <sup>b</sup>Beth Israel Deaconess Medical Center, Harvard Medical School, 330 Brooklyne Ave., Boston, MA 02215, USA

The very low sequence homology in the 1-34 fragments of parathyroid hormone (PTH) and PTH-related protein (PTHrP) and the fact that they act on the same receptor by assuming a putative common bioactive conformation make these two peptides an ideal target for studies on segmental and point-mutated hybrid peptides. Recently, receptor binding studies of PTH/PTHrP (1-34) hybrids revealed that the 1-14 segment of PTHrP is incompatible with the 15-34 segment of PTH [1,2]. The incompatible sites were identified at position 5 [1,2] and in the triad of residues 19-21 [1]. Therefore, Gardella and coworkers [1] concluded that interactions between the two portions (1-14 and 15-34) of the agonist are essential for PTH-like activity.

In an attempt to gain insight regarding the structural elements responsible for biological activity, we have studied the PTH/PTHrP hybrids **I** [Glu<sup>22</sup>]hPTHrP(1-34)NH<sub>2</sub> and **II** [Glu<sup>19,22</sup>,Val<sup>21</sup>]hPTHrP(1-34)-NH<sub>2</sub>. In these hybrids the residues Arg<sup>19</sup>, Arg<sup>21</sup> and Phe<sup>22</sup> of the native PTHrP sequence were replaced by the corresponding residues Glu<sup>19</sup>, Val<sup>21</sup> and Glu<sup>22</sup> of the PTH sequence. *In vitro* studies revealed that hybrid **I** binds strongly to human osteosarcoma Saos-2/B10 cells, while hybrid **II** exhibits receptor affinity and bioactivity lower by 3 orders of magnitude. The conformational preference of the hybrids was studied by CD in different solvent systems including water and TFE as a helix-inducing solvent. The structural details of hybrid **I** in 1:1 water-TFE were elucidated by 2D-NMR spectroscopy and computer simulations.

### Results and Discussion

The CD spectra of hybrid **I** in aqueous solution are typical of a random structure with a small amount of  $\alpha$ -helix (10%). This figure is independent upon peptide concentration in the range  $1 \times 10^{-3}$ – $1 \times 10^{-5}$  M, and also pH-independent in the range 3.2–8.9. Upon addition of TFE to the solvent mixture there is an increase in helix content which reaches 80% in 1:1 (v/v) TFE/H<sub>2</sub>O (Fig. 1). In this solvent mixture the CD pattern is insensitive to a change in the apparent pH from 2.5 to 8.9. The CD properties of hybrid **II** under identical experimental conditions were very much the same as those of hybrid **I**. Hybrid **I** was further characterized by 2D-NMR and Distance Geometry calculations. Interresidue NOEs allowed the determination of secondary structure elements. At pH 2.5 two helical segments were identified, located in the sequences 4-10 and 18-34, connected by a type **I**  $\beta$ -turn. In all experimental conditions we were unable to identify long range NOE cross peaks indicative of interactions between the two N-terminal and C-terminal helices. Thus, in this

solvent system the proposed U-shaped bioactive structure was not identified. The general conformational features of the hybrid  $[Glu^{22}]hPTHrP(1-34)NH_2$  include two helical domains at both termini connected by a flexible region. This structure is very similar to those of the 1-34 fragments of PTH and PTHrP [3] and of the segmental hybrids PTHrP(1-27)- $[Tyr^{34}]bPTH(28-34)NH_2$  and PTHrP(1-18)- $[Nal^{23}, Tyr^{34}]bPTH(19-34)NH_2$  [4] studied in the same solvent system. The first hybrid is as active as hybrid I and 3 orders of magnitude more active than the second hybrid. These findings do not provide a conformational basis for understanding the different biological activities. One possibility is that, in this solvent system, the common conformation observed for highly and poorly bioactive analogues may not correspond to the bioactive conformation, and that this solvent system does not mimic correctly the receptor environment. Another possible explanation might involve ligand-receptor interactions. Namely, the conformation assumed in this solvent system is of biological relevance, but the presentation of different side-chain functionalities in the different ligands does not meet the essential requirements for interaction with the receptor.

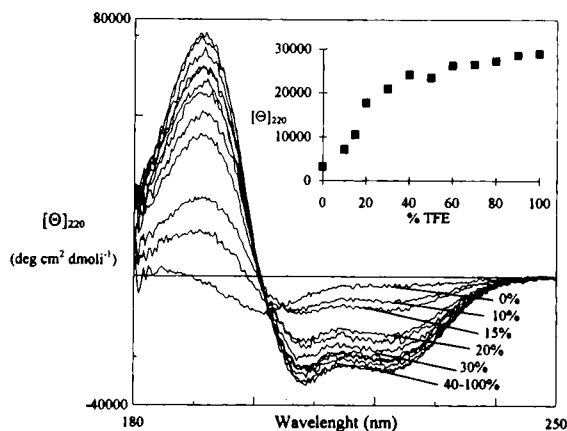


Fig. 1. CD spectra of  $10.4 \mu M [Glu^{22}]hPTHrP(1-34)NH_2$  in  $H_2O/TFE$  at various percentages (v/v) of TFE (indicated). In the insert, variation of molar ellipticity at 220 nm vs. TFE content.

## References

1. Gardella, T.J., Luck, M.D., Wilson, A.K., Keutmann H.T., Nussbaum, S.R., Potts, J.T. Jr, and Kronenberg, H.M., *J. Biol. Chem.*, 270 (1995) 6584
2. Behar, V., Nakamoto, C., Greenberg, Z., Bisello, A., Suva, L.J., Rosenblatt, M., and Chorev, M., *Endocrinology*, 137 (1996) 4217.
3. Strikland, L.A., Bozzato, R.P., and Kronis, K.A., *Biochemistry*, 32 (1993) 6050 and references therein.
4. Garbin, E., Mammi, S., Peggion, E., Behar, V., Rosenblatt, M., and Chorev, M., in *Peptides 1996*, (Proceedings of the 24th European Peptide Symposium) R. Ramage (Eds), in press.

# Synthesis and conformational analysis of C- and N-glycopeptides

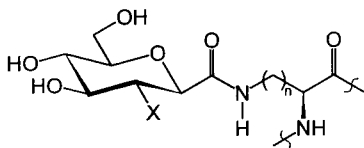
Fred Burkhart, Gerhard Hessler and Horst Kessler

Institut für Organische Chemie und Biochemie der Technischen Universität München,  
Lichtenbergstr. 4, D-85747 Garching, Germany

In most natural and synthetic glycopeptides the carbohydrate moiety is *N*-glycosidically linked to asparagine or *O*-glycosidically linked to hydroxy-containing amino acids. Unnatural and more stable linkages between carbohydrates and peptides are important for understanding the mutual interactions between both moieties and to improve the pharmacokinetic properties of peptides. Herein we present the synthesis of the *C*-glycopeptides 1-3, possessing a reversed amide bond as isosteric replacement of the *N*-glycosidic linkage. The structures are compared with their corresponding *N*-glycopeptides 4-6 to determine the influence of the glycosidic linkage and the sugar moiety on the peptide backbone.



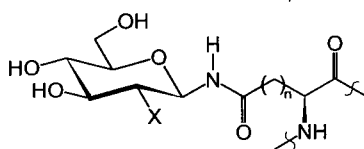
Gaa:



1: X = NHAc; n = 1

2: X = NHAc; n = 2

3: X = OH; n = 1



4: X = NHAc; n = 1

5: X = NHAc; n = 2

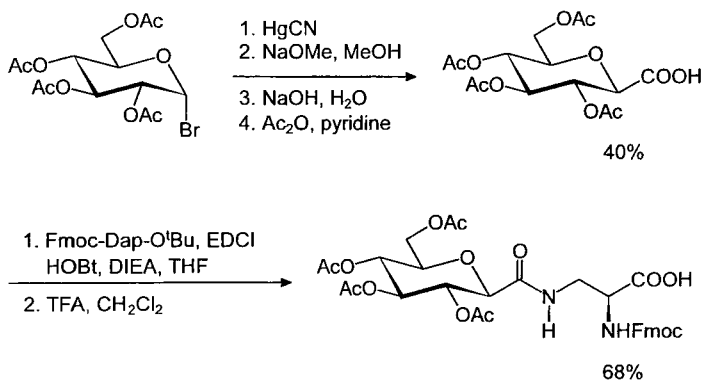
6: X = OH; n = 1

## Results and Discussion

*N*-glycopeptide 5 [1] and *C*-glycopeptide 1 [2] have already been published. All peptides were prepared by SPPS using Fmoc protected amino acids. The *N*-glycosylated amino acids have been synthesized according to described procedures [3].

The *C*-glycosylated amino acid building block for the synthesis of peptide 3 was prepared as outlined in Scheme 1 [4]. Peptide 2 was prepared by the subsequent glycosylation of the corresponding cyclopeptide with glutamine in position 4 which was built up by standard SPPS.

The structure of *C*-glycopeptide 1 shows a backfolding of the sugar residue over the peptide backbone with hydrogen bonds between the acetyl group of the glucosamine and Phe<sup>5</sup>NH and Phe<sup>6</sup>NH.



Scheme 1

The corresponding *N*-glycopeptide **4** also shows an interaction of the acetyl group with the peptide backbone, but only with Gaa<sup>4</sup>NH (Fig.1). In the other *C*- and *N*-glycopeptides no evidence for an interaction of the sugar residue with the peptide backbone was found. All peptides show a  $\beta$ II' turn with DPro<sup>1</sup> in the *i* + 1 position and a  $\beta$ I/ $\beta$ II-turn equilibrium with the glycosylated amino acid in the *i* + 1 position.

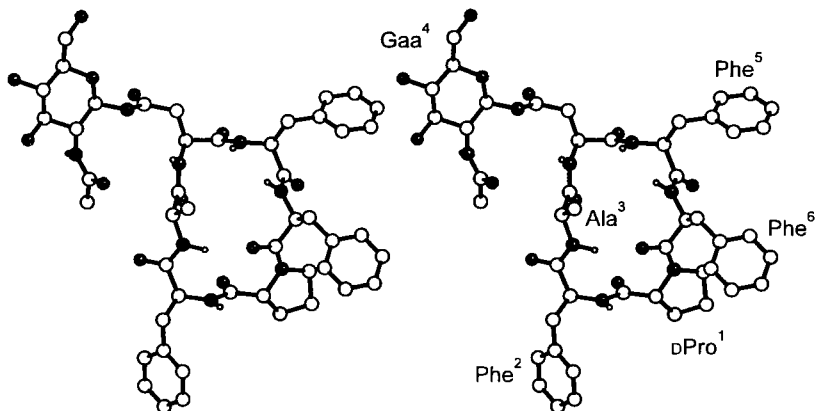


Fig.1. The structure of **4** determined by NMR techniques, distance geometry and restraint molecular dynamic calculations[5].

## References

1. Kessler, H., Matter, H., Gemmecker, G., Kling, A., Kottenhahn, M., J. Am. Chem. Soc., 113 (1991) 7550.
2. Hoffmann, M., Burkhardt, F., Hessler, G., Kessler, H., Helv. Chim. Acta, 79 (1996) 1519.
3. Paulsen, H., Peters, S., Bielfeldt, T., New Compr. Biochem. 29a (1995) 87.
4. Fuchs, E. F., Lehmann, J., Chem. Ber., 108 (1975) 2254.
5. Kessler, H., Seip, S., In Croasmun, W. R., Carlson, R. M. K. (Eds.), Two-Dimensional NMR Spectroscopy, VCH, Weinheim, 1994, p. 619.

## Lactam cyclization [*i* to (*i*+4)] for nucleation / stabilization of $\alpha$ -helices?

Gal Bitan,<sup>a,b</sup> Maria Pellegrini,<sup>a</sup> Michael Chorev<sup>b</sup> and Dale F. Mierke<sup>a</sup>

<sup>a</sup>Chemistry Department, Clark University, Worcester, MA 01610, USA and <sup>b</sup>Division of Bone and Mineral Metabolism, Beth-Israel Deaconess Medical Center, Boston, MA 02215, USA

The *i* to *i*+4 side-chain to side-chain lactam-type cyclization is a widely used modification for stabilization of proven or putative  $\alpha$ -helix secondary structures in peptides. Numerous structure-function studies have addressed the effects of ring-size, bond location, and bond direction in bioactive or model cyclic peptides containing this and similar modifications. Here we examine the effect of *i* to *i*+4 lactam-type cyclization through three forms of a model undecapeptide derived from the parathyroid hormone related protein (PTHrP): the linear sequence Ac-[PTHrP(10-20)]-NH<sub>2</sub>, the corresponding linear peptide in which the side-chain of Lys<sup>13</sup> is acetylated and Asp<sup>17</sup> is substituted by Asn, and a cyclic analog containing lactam-type cyclization between Lys<sup>13</sup> and Asp<sup>17</sup>. Lactam cyclization between Lys<sup>13</sup> and Asp<sup>17</sup> of PTHrP(1-34) has been shown to increase affinity towards the PTH/PTHrP receptor [1,2], as well as to induce helicity in solutions containing detergents [3] or TFE [4]. Unfortunately, in the NMR study of cyclo(13,17)-PTHrP(1-34) the conformation of the ring portion could not be analyzed in detail due to severe peak overlap [4]. Nevertheless, this study indicated some distortion away from a perfect  $\alpha$ -helix which could be attributed to the lactam ring. The current study was designed to address three questions: 1) In the absence of other driving forces, such as interactions with other parts of the full length molecule, or with membrane mimetics/detergents, or with the  $\alpha$ -helix inducing solvent TFE, will the lactam ring between positions 13 and 17 be sufficient to induce a helical conformation; 2) if a helical structure is formed under these conditions, how close is it to an ideal  $\alpha$ -helix; 3) can salt-bridges induce/stabilize the putative  $\alpha$ -helical conformation in comparison to the corresponding lactam-type cyclization.

### Results and Discussion

**NMR.** Only a small number of NOEs were observed for the linear analogs. The cyclic analog showed many structural NOEs, but not necessarily NOEs characteristic of an  $\alpha$ -helix. The high-field shift of the  $\alpha$ -protons observed in the central portion of the cyclic peptide is, however, in line with a helical structure. The corresponding  $\alpha$ -protons of the linear analogs do not show this shift.

**Computer simulations.** Distance geometry calculations have been performed for the three model peptides. In general the linear analogs show little order and appear to be conformationally free. The order parameter of the dihedral angles  $\Phi$  and  $\Psi$  indicates relatively high order for the ring portion of the cyclic model peptide and lower order in the corresponding portion of the linear analogs. Another indication is given by the average rmsd values calculated for the backbone atoms from the C $^{\alpha}$  of Lys<sup>13</sup> to the C $^{\alpha}$  of Asp<sup>17</sup>,

which are 0.75, 1.36 and 1.12 for the cyclic, linear free and linear blocked analogs, respectively.

Two families of structures were found for the cyclic analog. The major family is characterized by a distorted type III  $\beta$  turn about Ser<sup>14</sup>. The minor family has somewhat lower energy and shows nucleation of a helical conformation (one loop of a helix) with irregular dihedral angles between Ser<sup>14</sup> and Asp<sup>17</sup> (Fig. 1). Further molecular dynamics refinement of two low-energy structures, representative of the major and minor families of conformations of the model cyclic peptide, was performed in water. The overall conformation of the major family representative structure changed very little and maintained the distorted type III  $\beta$  turn about Ser<sup>14</sup>. On the other hand, the structure taken from the minor family folded into a helix spanning from Ser<sup>14</sup> to the C-terminus. The dihedral angles of this helix deviate from an ideal  $\alpha$ -helix, and some of them are more in line with a  $3_{10}$  helix.



Fig 1. Superposition of 51 structures of the major family (left) and 7 structures of the minor family (right) of the cyclic model peptide. The side-chains of Lys<sup>13</sup> and Asp<sup>17</sup> are shown in grey.

## Conclusion

1. In the absence of other driving forces lactam-type cyclization of model peptides with the general formula Ac-[PTHrP(10-20)]-NH<sub>2</sub> enables folding into a helix, but is not sufficient to induce this secondary structure. The helical conformation is probably not the major conformer in aqueous solution.
2. The helix formed is not an ideal  $\alpha$ -helix, but shows some distortion of the dihedral angles, presumably induced by the lactam ring.
3. The putative salt-bridge between Lys<sup>13</sup> and Asp<sup>17</sup> has little effect on the conformation of the peptide in aqueous solution, as both linear analogs, with free or blocked side-chains, were to be found similarly unstructured.

## References

1. Chorev, M., Roubini, E., McKee, R.L., Gibbons, S.W., Goldman, M.E., Caulfield, M.P., and Rosenblatt, M. *Biochemistry*, 30 (1991) 5968.
2. Bisselo, A., Nakamoto, A., Rosenblatt, M. and Chorev, M. *Biochemistry* 36 (1997) 3293.
3. Chorev, M., Epand, R.F., Rosenblatt, M., Caulfield, M.P. and Epand, R.E. *Int. J. Pept. Protein Res.*, 42 (1993) 342.
4. Maretto, S., Mammi, S., Bissacco, E., Peggion, E., Bisselo, A., Rosenblatt, M., Chorev, M. and Mierke, D.F. *Biochemistry*, 36 (1997) 3300.

# Molecular modeling and design of metal binding template assembled synthetic proteins (TASP)

**Gregory V. Nikiforovich,<sup>a</sup> Christian Lehmann<sup>b</sup> and Manfred Mutter<sup>b</sup>**

<sup>a</sup>Center for Molecular Design, Washington University, Box 8036, St. Louis, MO 63110, USA and

<sup>b</sup>University of Lausanne, BCH-Dorigny, CH-1015 Lausanne, Switzerland

This study presents further developments in the design of protein mimetics with potential metal binding properties. Extensive molecular modeling of the two-loop TASP constructed by condensation of two identical HAGHG fragments on the K<sup>3</sup>, K<sup>10</sup> and K<sup>5</sup>, K<sup>8</sup> side chains of the *cyclo*(PGKAKPGKAK) decamer template (RAFT, [1]) was performed employing various force fields and protocols. The results are compared to the available NMR data [2] and are to design rigidified analogs of RAFT. Possible metal binding properties of the TASP in question are discussed.

## Results and Discussion

Conformational calculations employing the ECEPP/2 force field were performed for all possible combinations of conformations corresponding to local minima for all residues in the PGAAAPGAAA decapeptide (13,824,000 conformers) that would allow proper closing of the cycle by geometrical considerations (9,778 conformers). After energy minimization, 55 low-energy conformers of backbone ( $\Delta E < 10$  kcal/mol) were found. The Nle side chains then were placed at the positions of the Lys residues (since those chains are not charged in TASPs), and energy minimization was repeated with the dielectric constant  $\epsilon = 2.0$  (the standard ECEPP value), and  $\epsilon = 45.0$  (the macroscopic value for DMSO), yielding 10 low-energy RAFT conformers, and 15, respectively.

Four out of ten low-energy RAFT conformers represent various types of "rectangular" conformation with two  $\beta$ -turns centered at the Pro-Gly fragments, and with the spatial arrangement of all Lys side chains "at the same side" of the RAFT backbone plane. A conformer of the same type was deduced earlier from the NMR data obtained in DMSO [2]. However, to satisfy all measured NMR parameters one needs consider the conformational equilibrium among several low-energy RAFT conformers. Independent energy calculations performed by stochastic conformational sampling with the MAB force field [3] found two families of low-energy conformation of RAFT of the same "rectangular" type, one more extended, and one more folded at the Lys-Ala-Lys fragments. Both limiting structures conform to the NMR data; the extended antiparallel  $\beta$ -sheet structure is obtained when additional transannular H-bonds are accepted.

Energy calculations employing the ECEPP/2 force field were also used to explore the possibilities of rigidifying the discussed "template" RAFT backbone. Substitutions of both Gly's by D-Ala's or Aib's did not limit the diversity of RAFT low-energy conformers, but when Gly's were replaced by D-Pro's, the scope of possible conformers was reduced to

those geometrically close to the desirable "template" conformer. This "template" conformer is also stabilized in the *bicyclo*(PGK(CKPGKC)K) compound, which was confirmed independently by calculations employing the ECEPP/2 and MAB force fields.

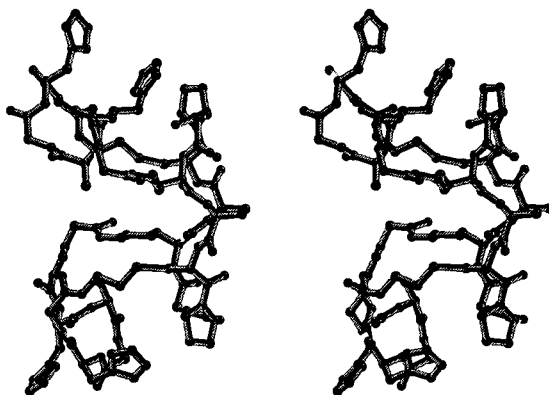


Fig. 1. Stereoview of the lowest-energy TASP conformer resulting from build-up procedure in the ECEPP/2 force field. All hydrogens are omitted.

The low-energy conformers for the entire TASP molecule were found by build-up procedure employing the ECEPP/2 force field for a single lowest-energy RAFT conformer. 391 low-energy conformers of each HAGHG fragment were combined with optimized rotamers of Lys side chains and oxime linkers allowing cycle closures. Totally, 1,886 conformers of the entire TASP molecule were selected for energy calculations. Out of the the resulting 8 low-energy conformers ( $\Delta E < 12$  kcal/mol), was found suitable to chelate a metal ion by all four imidazole rings of the His residues simultaneously in the same construct. The typical low-energy TASP conformer in depicted in Fig. 1. However, low-energy conformers of the depicted type still have an inherent propensity to dispose side chains into entropically favorable orientations for metal binding. Thereby, stoichiometries of 1.0 as well as 2.0 may be expected for complexation. In conclusion, we have demonstrated possibilities of detailed and extensive molecular modeling of TASP constitutions optimized for metal binding.

## References

1. Mutter, M., Dumy, P., Garrouste, P., Lehmann, C., Mathieu, M., Peggion, C., Peluso, S., Razaname, A. and Tuchscherer, G., *Angew. Chem. Int. Ed. Engl.*, 35 (1996) 1481.
2. Dumy, P., Eggleston, I.M., Esposito, G., Nicula, S. and Mutter, M., *Biopolymers* 39 (1996) 297.
3. Gerber, P.R., Müller, K., *J. Comp.-Aid. Drug Design*, 9 (1995) 251.

# Syntheses, conformational analysis and the bioactivities of the lanthionine analogs of a cell adhesion modulator

Haitao Li, Xiaohui Jiang and Murray Goodman

Department of Chemistry & Biochemistry, University of California at San Diego, La Jolla, CA 92093-0343, USA

Cell adhesion plays an important role in many biological processes, such as wound healing, immunity and inflammation. The proteins that mediate the adhesion processes are integrins. Finding an integrin antagonist or agonist is of great interest since either could have potential therapeutic value [1-2]. A lead integrin modulator, 1-FCA-Arg-c[Cys-Asp-Thz-Cys]-OH, a disulfide containing derivative, acts as an antagonist to VLA-4 which is an  $\alpha_4\beta_1$  integrin. We have developed the syntheses of lanthionine peptides that are conformationally more constrained and more stable towards enzymatic degradation than the parent disulfide peptides [3]. In order to study the structure-activity relationship and to improve stability and potency, we synthesized two lanthionine analogs of the parent disulfide molecule (Fig. 1).

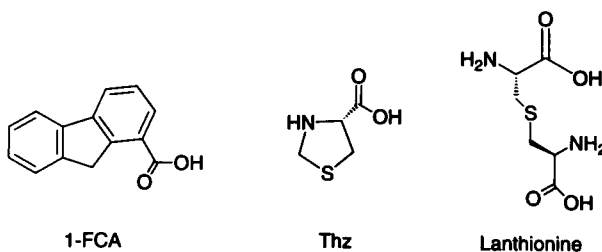


Fig. 1. The structures of 1-FCA, Thz and Lanthionine.

## Results and Discussion

The chemistry leading to the target molecule is presented in Fig 2. The lanthionine analogs (compounds, 1 and 2) have been tested as antagonists to VLA-4 (Table 1).

Table 1. Potencies of the parent compound and its lanthionine analogs as antagonists to VLA-4.

Parent compound	Compound 1	Compound 2
2.7nM	209nM	557nM

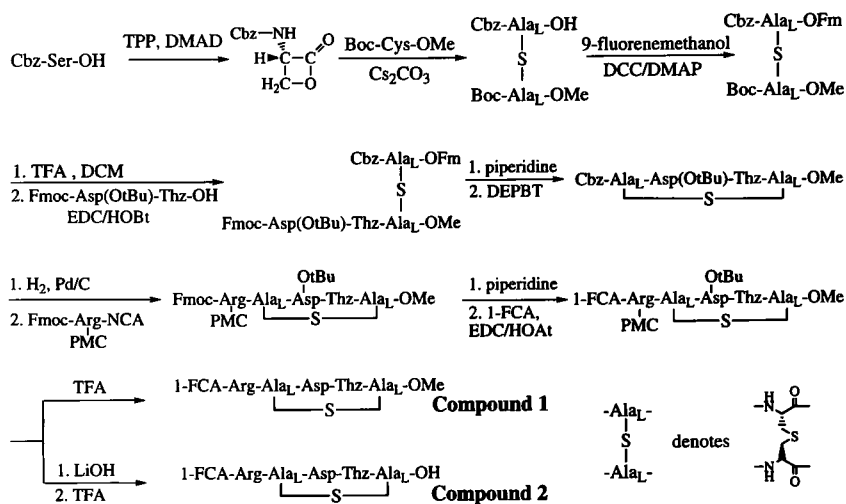


Fig. 2. The syntheses of the lanthionine analogs of a cell adhesion modulator.

From NMR and conformational studies, we observe that the overall topologies of the parent peptide and its lanthionine analogs are very similar. Particularly, the peptide bond between Asp<sup>3</sup> and Thz<sup>4</sup> exists only in the *cis* conformation in all three compounds. Compound 1 and the parent compound have similar conformations except for the C-terminus. The parent compound and compound 2 have differences arising from the psi angle of Thz<sup>4</sup>. From the NOE patterns, we determined that the C-terminal carboxylate and the amide bond between residues 4 and 5 have opposite orientations in the parent compound from that in compound 2. The parent compound and both lanthionine analogs showed no affinities to the other integrin receptors. Although the potency for compound 1 and 2 is diminished, the parent disulfide and the lanthionine analogs exhibit the same selectivity toward the  $\alpha_4\beta_1$  (VLA-4) integrin.

## References

1. Stuiiver, I., O'Toole, TE., Stem Cells, 13 (1995) 250
2. Nowlin, DM., Gorcsan, F., Moscinski, M., Chiang, SL., Lobl, TJ. And Cardarelli, PM., J. Biol. Chem., 268 (1993) 20352
3. Shao, H., Wang, S., Lee, C.W., Osapay, G. and Goodman, M., J. Org. Chem., 60 (1995) 2956

# Utilization of a reporting conformational template in probing the Phe-His interaction in the short alanine-rich peptide helices

Kwok Yin Tsang and Daniel S. Kemp

*Department of Chemistry, Massachusetts Institute of Technology, Cambridge, MA 02139, USA*

When N-terminally linked to polypeptides, a reporting conformational template (Ac-Hel<sub>1</sub>) derived from Ac-Pro-Pro initiates  $\alpha$ -helices and allows measurement of their helicity [1-5]. Located at the N-terminus, Ac-Hel<sub>1</sub> is least sensitive to energetic effects that arise locally at or near the C-terminus. Other reporting functions that reflect local helicity and that could be placed at arbitrary sites within the peptide chain would complement the Ac-Hel<sub>1</sub> and significantly extend its resolving power for detecting local energetic effects. Baldwin et al. have previously reported a Phe-His (*i, i + 4*) helical stabilization that results from an interaction between the aromatic side chains of Phe and His [6]. Through 1D and 2D <sup>1</sup>H NMR studies of templated peptide conjugates containing Phe and His, we report herein that the Phe-His (*i, i + 4*) helical stabilization is attributed to a Dougherty-type cation- $\pi$  interaction [7]. The temperature-dependent chemical shift differences between helical and non-helical states of the His imidazole 2-proton ( $\Delta_{\text{His-2}}$ ) are shown to reflect the local helicity within the Phe-His (*i, i + 4*) loop.

## Results and Discussion

Analysis of a locally energy-minimized -A<sub>4</sub>FA<sub>3</sub>HA<sub>4</sub>- helical model revealed that the Phe-His (*i, i + 4*) interaction is ascribed to a cation- $\pi$  interaction [7] with two sets of protons that likely render the NOE signals in a 2D NMR experiment, namely His-H<sub>2</sub>-Phe meta proton and His-H<sub>4 $\alpha$</sub> (*i-3*) -proton interactions. This model has been validated experimentally by a ROESY spectrum of Ac-Hel<sub>1</sub>-A<sub>4</sub>FA<sub>3</sub>HA<sub>4</sub>KANH<sub>2</sub> which shows all characteristic NOE crosspeaks. In water, the <sup>1</sup>H NMR spectra of templated peptide conjugates show two sets of resonances that correspond to the slowly equilibrating non-helical c-state and helical t-state. Through study of Ac-Hel<sub>1</sub>-A<sub>(5-m)</sub>FA<sub>m</sub>HA<sub>2</sub>NH<sub>2</sub>(*m*=0-3) from 2 to 60°C, we have observed that both the ratio of t-state to c-state (*t/c* ratio) and  $\Delta_{\text{His-2}}$  show a large temperature dependence when *m*=3, presumably due to the Phe-His (*i, i + 4*) interaction that locates the His-H<sub>2</sub> in the shielding zone of the Phe aromatic ring (Fig. 1a). For *m*≠3, the <sup>1</sup>H NMR chemical shift of the His-H<sub>2</sub> in the t- and c-states are nearly identical (Fig. 1b). This result implies that the simple relationship  $\Delta_{\text{His-2}} = \Delta_{\infty} - \alpha \Delta_{\infty} (c/t)$  must hold where  $\Delta_{\infty}$  is the limiting value for a 100% helical peptide. Fig. 2 validates the above equation by showing the excellent linear correlation between  $\Delta_{\text{His-2}}$  and inverse *t/c* ratio.

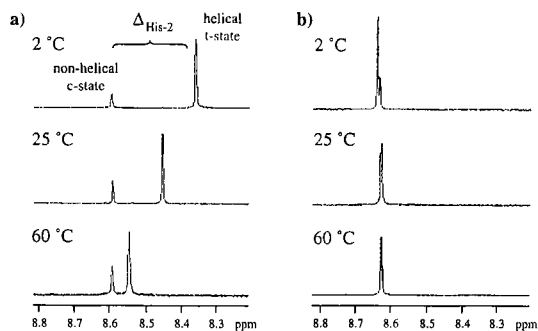


Fig. 1.  $^1\text{H}$  NMR spectra of  $\text{Ac-Hel}_1\text{-A}_{(5-m)}\text{FA}_m\text{HA}_2\text{NH}_2$  showing  $\text{His-H}_2$  resonances at 2, 25, and  $60^\circ\text{C}$ , respectively. a)  $m=3$ , b)  $m\neq 3$ .

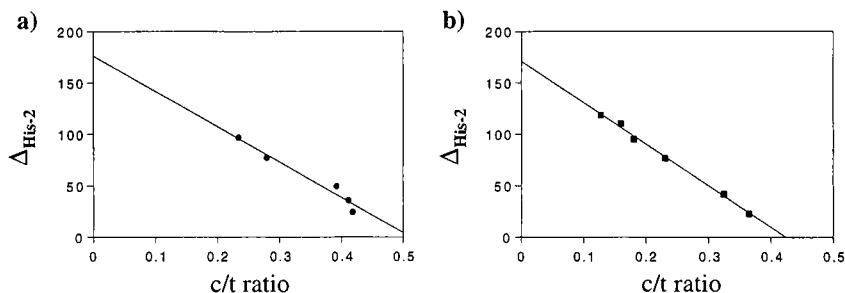


Fig. 2. The plots of  $\Delta_{\text{His-2}}$  vs  $c/t$ . a)  $\text{Ac-Hel}_1\text{-A}_3\text{FA}_3\text{HA}_2\text{NH}_2$ , b)  $\text{Ac-Hel}_1\text{-A}_4\text{FA}_3\text{HA}_2\text{NH}_2$

## Conclusion

$\Delta_{\text{His-2}}$  provides a direct measure of the helical structure in the C-terminal region, and the fractional helical structure that extends from the His residue to the C-terminus equals the simple ratio of  $\Delta_{\text{His-2}}$  to  $\Delta_{\infty}$ .

## References

1. Kemp, D.S., Allen, T.J., Oslick, S., *J. Am. Chem. Soc.*, 117 (1995) 6641.
2. Kemp, D.S., Allen, T.J., Oslick, S., Boyd, J.G., *J. Am. Chem. Soc.*, 118 (1996) 4240.
3. Kemp, D.S., Oslick, S., Allen, T.J., *J. Am. Chem. Soc.*, 118 (1996) 4249.
4. Groebke, K., Renold, P., Tsang, K.Y., Allen, T.J., McClure, K., Kemp, D.S., *Proc. Natl. Acad. Sci. USA*, 93 (1996) 2025.
5. Renold, P., Tsang, K.Y., Shimizu, L.S., Kemp, D.S., *J. Am. Chem. Soc.*, 118 (1996) 12234.
6. Armstrong, K.M., Fairman, R., Baldwin, R.L., *J. Mol. Biol.*, 230 (1993) 284.
7. Mecozzi, S., West, A.P., Dougherty, D.A., *Proc. Natl. Acad. Sci. USA*, 93 (1996) 10566.

# Structure-Activity Studies on the Abl-SH2 Domain

**Maria Pietanza and Tom Muir**

*Synthetic Protein Chemistry Laboratory, The Rockefeller University,  
1230 York Ave., New York, NY 10021, USA*

The cellular signaling protein, c-Abl, is one of the few non-receptor protein tyrosine kinases directly linked to human malignancies. The transforming activity of c-Abl is tightly controlled *in vivo* and is regulated by molecular interactions involving its Src Homology 2 (SH2) and Src Homology 3 (SH3) domains. It has been demonstrated that the SH3 domain suppresses the transforming activity of c-Abl, whereas the SH2 domain is absolutely required for the transforming activity of the activated form of this proto-oncogene [1]. These studies have also shown that altering the length of the linker region between the SH2 and SH3 domains, although a subtle change, causes the activity of the protein to be modified [1]. Since this linker region is of known importance in kinase activity, we are interested in systematically varying its length and studying the effect on structure and function. In order to accomplish this, it is necessary that we first identify precisely where in the primary sequence of c-Abl the SH3 domain ends and the SH2 domain begins. Previous work in our lab indicated that the SH3 sequence must be extended to at least Val-119 on the C-terminal side, in order for the domain to retain native structure and function. Here we use a chemical ligation strategy to define the minimum N-terminal boundary of the c-Abl SH2 domain.

## Results and Discussion

Based on multidimensional NMR studies [2] as well as sequence alignment analysis, it seemed likely that the minimum N-terminus of the protein lay somewhere in the region Asn120 - Trp127. We have previously demonstrated synthetic access to c-Abl SH2 (comprising residues 120-220) using a strategy which involved the native chemical ligation of two ~50 residue unprotected polypeptide fragments [3]. The present work took advantage of the modularity of this synthetic approach and involved the preparation of an N-terminally truncated set of protein sequences. Chemical ligation of a ladder of N-terminal peptide fragments (each one residue longer than the other) to a C-terminal fragment of fixed length, allowed the generation of the desired truncated array of protein domains with a minimum amount of synthetic effort. Note, the entire family of N-terminal peptides was obtained from a single synthesis by removing aliquots of the peptide-resin at appropriate points in the chain assembly. Following the ligation reaction, each protein was purified by preparative HPLC, folded by controlled dialysis from denaturant and characterized by electrospray mass spectrometry.

The effect on structure and function of systematically truncating the N-terminus of the domain was evaluated. A fluorescence-based assay was used to study the ligand binding affinity of each of the nine synthetic domains (Fig. 1a). Constructs Asn120 through Glu123

have dissociation constants ( $K_D$ ) similar to that previously reported for the recombinant protein ( $K_D = 2.5 \pm 0.3 \mu\text{M}$  [4]). Truncation beyond Glu123 leads to a rapid loss of function until by Ser126 no specific affinity for ligand can be detected using this assay. Each of the nine constructs was also studied by circular dichroism (CD) spectroscopy in order to determine the effect of systematic N-terminal truncation on overall secondary structure content (Fig 1b). Consistent with the biochemical data, truncation beyond Glu123 leads to a clear structural transition in which the protein goes from a native folded state to a misfolded state (although not entirely unstructured) with lower  $\alpha$ -helical content.

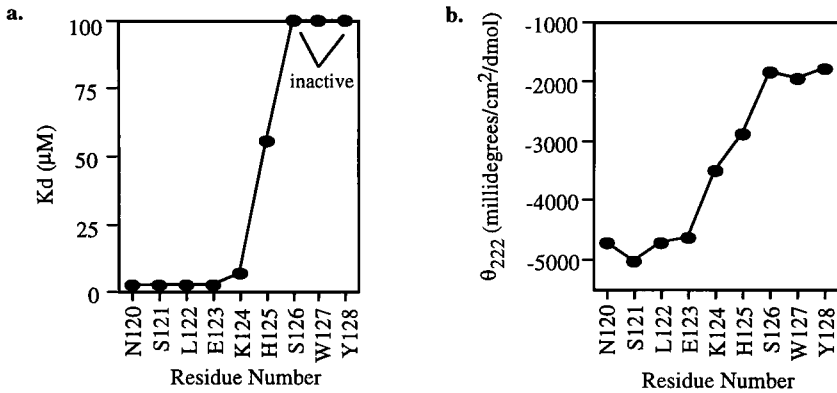


Fig.1. Effect of systematic N-terminal truncation on (a) Function and (b) Structure.

## Conclusion

We have demonstrated that native chemical ligation can be used to systematically probe the relationship between the primary amino acid sequence, structure and function of the c-Abl SH2 domain. Our results indicate that c-Abl SH2 cannot be N-terminally truncated beyond Glu123 without global changes in structure and function. This information is now being integrated into studies involving modifying the linker region between the SH3 and SH2 domains of the c-Abl protein.

## References

1. Mayer, B.J. and Baltimore, D., Mol. Cell Biol., 14 (1994) 2883.
2. Overduin, M., Rios, C.B., Mayer, B.J., Baltimore, D. and Cowburn, D., Cell 70 (1992) 697.
3. Pietanza, M.C. and Muir, T.W., 24th EPS, Edinburgh, (1996) in press.
4. Gossler, Y.Q. Zheng, J., Overduin, M., Mayer, B.J. and Cowburn, D., Structure 3 (1995) 1075.

# Design and use of amphiphilic peptides in liposomes as pH-triggered releasing agents

M. L. Brickner, C. Yusuf, K. M. Vogel, and J. A. Chmielewski

*Department of Chemistry, Purdue University, West Lafayette, IN 47907, USA*

Cell-specific targeting and delivery of drugs is an important clinical goal. The use of liposomes to conceal and deliver drugs to cells has received much attention [1]. One such method is folate receptor-mediated endocytosis which exploits the recognition of folic acid by a cell surface receptor. This method delivers liposomes conjugated to folate into the cytoplasm of cells [2]. Although drugs may be delivered into the cells *via* liposomes, they can remain trapped within the endosomal compartment. The endosome has a lower pH than the rest of the cytoplasm. This change in pH could be used as a triggering event for the release of the liposomal contents. Thus, there has been a great deal of work on pH sensitive liposomes [3]. In this study, we instead utilize a pH sensitive peptide encapsulated within the liposomes which undergoes a conformational switch to an  $\alpha$ -helix at endosomal pH from random coils at physiological pH. This would enable them to insert into the lipid bilayer and act as releasing agents from the endosome.

## Results and Discussion

The peptide sequences (Fig. 1) composed of Glu, Ala and Leu residues were designed to form amphiphilic  $\alpha$ -helices under mildly acidic conditions, to allow interaction with and insertion into the lipid bilayer structure. The peptides were synthesized using solid phase methodology [4] and Fmoc strategy [5].

Peptide EALA1  
Peptide EALA1s

AALAEALAEALAEALAEALAEALAAAAGGC(Acm)  
Ac-ALAEALAEALAEALA-NH<sub>2</sub>

*Fig. 1. Sequences of designed peptides.*

The pH-based peptide conformational switch was analyzed by CD spectroscopy. The peptides showed a pH-dependent helical content; EALA1 went from having 11% helical content at pH 7.4 to 37% at pH 5.0 (Table 1). EALA1s switched from 10% helical content at pH 7.4 to 16% at pH 5.0. These results are encouraging since the endosomal pH is about 5.5 [6], which is in the most helical range for the peptides. Incorporation of these peptides into phosphatidyl choline (PC) liposomes along with a fluorescent dye has enabled us to follow the pH-dependent release of the dye due to the conformational switching of the peptides. This release was quantitated using an assay in which the fluorescent dye calcein, which self-quenches at high concentration inside the liposomes [7], was coencapsulated with each peptide in PC liposomes. Aliquots of the liposomes were equilibrated for 8 hrs at

pH 7.4, 6.0, and 5.0 ( $\mu=0.5M$ ). All solutions were brought up to pH 8.0 to cancel the pH dependence of calcein's fluorescence, and the fluorescence of calcein released was measured at 520nm ( $\lambda_{ex} = 470$  nm). The percent of calcein released was determined by: % release =  $[(flu_{XL} - flu_{BG}) / (flu_{XLmax} - flu_{BGmax})] \times 100$ ; where  $flu_{XL}$  was the fluorescence of control or peptide-containing liposomes,  $flu_{XLmax}$  was the fluorescence of maximum release of the calcein which was induced by the addition of Triton X-100<sub>(reduced)</sub> detergent, and  $flu_{BG}$  was the fluorescence of liposomes prepared without dye or peptide. At pH 5.0, the liposomes encapsulating EALA1s released 19% greater than the control liposomes, and the EALA1 liposomes 33% (Table 1). At pH 7.4, these values were only 5% and 6% respectively. The pH dependent release of calcein follows that of the helical contents for these peptides, indicating that a helical conformation is needed in order for insertion into the lipid bilayer to trigger the release of the dye.

*Table 1. Comparison of pH dependence of helical contents and release data for peptides.*

pH	Helical Content <u>EALA1</u>	Helical Content <u>EALA1s</u>	% Release <u>EALA1</u>	% Release <u>EALA1s</u>
7.4	11%	10%	6%	5%
6.0	38%	10%	6%	13%
5.0	37%	16%	33%	19%

Liposomes were also made containing folate conjugated through a polyethylene glycol linkage to PC lipid [2] which coencapsulated the peptides and propidium iodide. These liposomes were added to a monolayer of KB cells cultured under folate deficient conditions. After 24 hours, the cells were suspended in media at  $1 \times 10^6$  cells/ml and then analyzed by flow cytometry. The fluorescence of the PI in 10,000 single cells per sample was measured after excitation at 488 nm using a 550 nm dichroic long pass filter. The cells treated with liposomes encapsulating the peptides showed higher fluorescence than the control liposomes due increase in quantum yield of PI upon binding to DNA in the cell following release from the endosome. The EALA1s liposomes showed an average increase of 1.13 fold from the control fluorescence, and the EALA1 showed a 1.19 increase. Thus, these peptides are able to switch to an  $\alpha$ -helical conformation at low pH and trigger the release of the contents of liposomes.

## References

1. Lasic, D. D., and Martin, F. J., 'Stealth Liposomes,' CRC Press, 1995.
2. Lee, R. J. and Low, P. S., J. Biol. Chem., 269 (1994) 3198.
3. Chu, C. J., and Szoka, F. C., J. Liposomes Res., 4 (1994) 361.
4. Merrifield, R. B., J. Am. Chem. Soc. 85 (1963) 2149.
5. Atherton, E. and Sheppard, R. C., In Gross, E. And Meienhofer, J. (Eds.), 'The Peptides,' Academic Press, New York, 1987, p. 1.
6. Tycko, B., Keith, C. H., and Maxfield, F. R., Cell 28 (1982) 643.
7. Chen, R. F., Knutson, J. R., Anal. Biochem. 172 (1988) 61.

# NMR structure determination and DNA binding properties of GCN4 peptidomimetics designed for $\alpha$ -helix initiation and stabilization

Min Zhang, Bingyuan Wu, Jean Baum and John Taylor  
*Department of Chemistry, Rutgers University, Piscataway, NJ 08855, USA*

GCN4 is a eukaryotic transcription regulating protein in the basic-leucine zipper (b-zip) family. Like all members of this family, it binds to DNA as a dimer. The two basic regions in the dimer constitute its entire DNA recognition surface. These peptide segments are disordered in aqueous solution, but fold into an  $\alpha$ -helical conformation upon specific DNA binding [1]. We have previously shown that the monomeric GCN4 basic-region peptide (yeast GCN4 residues 226-254) binds specifically to duplex DNA containing its recognition half-site, and that stabilization of its helical conformation increases its affinity for this DNA site [2]. We are now engaged in the development of small  $\alpha$ -helical peptidomimetics for specific DNA binding, based on the minimal recognition surface of the GCN4 basic region found within residues 234-243: -Arg-Asn-Xxx-Xxx-Ala-Ala-Xxx-Xxx-Ser-Arg-.

## Results and Discussion

Recently, we described the NMR structure determination [3] of a protected, bicyclic, side-chain lactam-bridged hexapeptide, Boc-(cyclo<sup>1-5,2-6</sup>)[Lys-Lys-Ala-Ala-Asp-Asp]-OPac. This peptide was  $\alpha$ -helical in 50% TFE, and appeared suitable as a central building block for the development of our DNA binding peptidomimetics. To investigate this possibility, we have now extended this peptide by two unconstrained residues in both the N-terminal and C-terminal directions. The resulting bicyclic decapeptide, GCN4bM1 (Fig. 1), contains all of the essential DNA recognition elements of the GCN4 basic region structure, and is constrained centrally by two overlapping Lys<sup>i</sup>, Asp<sup>i+4</sup> side-chain lactam bridges. In this extended peptide, these bridges link the side chains of residues 3 and 7 and residues 4 and 8.

Conformational analysis of GCN4bM1 by NMR was performed in aqueous solution. The assignment of the proton spectra was achieved using the 1-D proton spectrum, and the 2-D NOESY and TOCSY spectra. Most of the NOE correlations expected for  $\alpha$ -helix, such as  $N_i - N_{i+1}$ ,  $\alpha_i - N_{i+3}$  and  $\alpha_i - \beta_{i+3}$ , were observed (Fig. 1). In total, 143 distance constraints were determined from the NOESY spectrum at -5 °C and were used in restricted molecular dynamics simulations. These simulations resulted in a converged family of six conformers that were  $\alpha$ -helical throughout their structures. Therefore, the central bicyclic  $\alpha$ -helical hexapeptide structure in GCN4bM1 can propagate the  $\alpha$ -helical conformation in peptide extensions in both directions in aqueous solution. A comparison of our NMR structures.

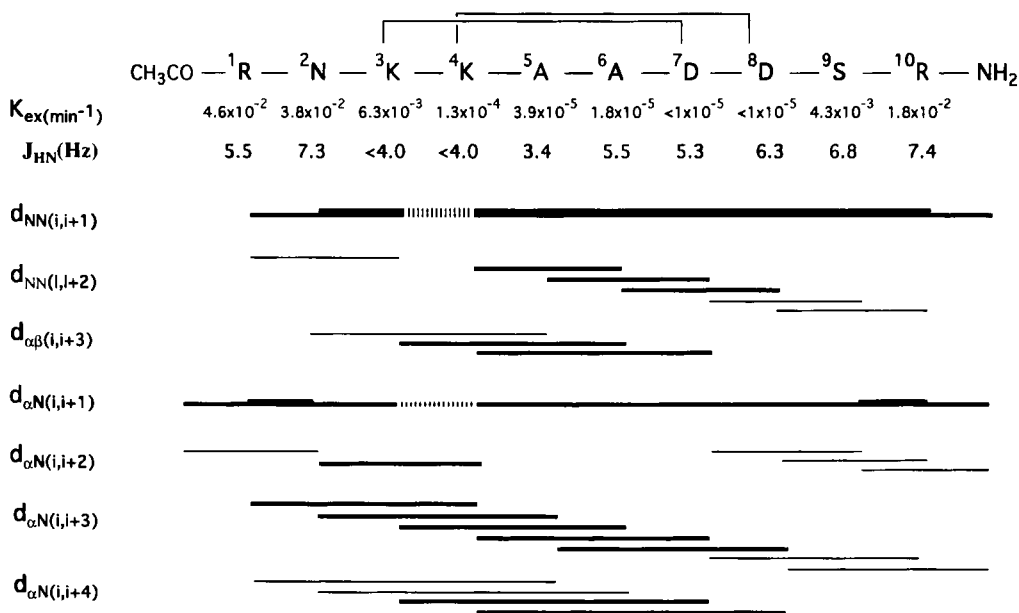


Fig. 1. NMR data for GCN4bM1 in 90%  $\text{H}_2\text{O}/\text{D}_2\text{O}$ ,  $\text{pH}=3.0$ . NOEs were measured at  $-5^\circ\text{C}$ . The thickness of the lines indicates relative intensities of the NOEs. Coupling constants and amide exchange rates ( $K_{\text{ex}}$ ) were measured at  $5^\circ\text{C}$ .

for GCN4bM1 with the crystal structure of the specific GCN4-DNA complex indicates that this  $\alpha$ -helical peptidomimetic is fully compatible with the required DNA binding conformation.

## Conclusion

Two overlapping  $\text{Lys}^i$ ,  $\text{Asp}^{i+4}$  side-chain lactam bridges in the central region of a peptidomimetic can initiate and stabilize  $\alpha$ -helix in small peptides. In the bicyclic decapeptide, GCN4bM1, this provides a useful model for studying specific DNA recognition by small peptidomimetic molecules.

## References

1. Talanian, R. V.; McKnight, C. J.; Kim, P. S., *Science*, 249 (1990) 769.
2. Wu, B., Taylor, J. W., In Hodges, R. S. and Smith, J. A. (Eds), *Peptides: Chemistry, Structure and Biology* (Proceedings of the Thirteenth American Peptide Symposium), ESCOM, Leiden, The Netherlands, 1994, p. 265.
3. Bracken, C., Gulyas, J., Taylor, J. W., Baum, J., *J. Am. Chem. Soc.*, 115 (1994) 6431.

# Synthesis and conformational analysis of axinastatin 5 and derivatives

Oliver Mechnich,<sup>a</sup> Gerhard Hessler,<sup>a</sup> Michael Bernd,<sup>b</sup>  
Bernhard Kutscher<sup>b</sup> and Horst Kessler<sup>a</sup>

<sup>a</sup>Institut für Organische Chemie und Biochemie, Technische Universität München,  
Lichtenbergstr.4, D-85747 Garching, Germany

<sup>b</sup>ASTA Medica AG, Weissmüllerstrasse 45, D-60314 Frankfurt am Main, Germany

The cyclic octapeptide *Axinastatin 5* (**1**) (cyclo(-Tyr<sup>1</sup>-Val<sup>2</sup>-Pro<sup>3</sup>-Leu<sup>4</sup>-Ile<sup>5</sup>-Leu<sup>6</sup>-Pro<sup>7</sup>-Pro<sup>8</sup>-)), recently isolated by Pettit and coworkers in 10<sup>-7</sup> % yield from the marine sponge *Axinella cf. Carteri*, was found to be a cancer cell growth inhibitor. Its GI<sub>50</sub> values were 0.3 to 3.3 µg/mL against selected human cancer cell lines [1]. In the course of our investigations of peptidic anticancer agents [2], *Axinastatin 5* (**1**) was synthesized to verify the proposed primary structure of the isolated compound and to provide sufficient amounts of the biologically active compound for structural and pharmaceutical investigations. A comparison with *didemnin B* [3], *bouvardin* [4] and other Tyr(Me) containing active compounds led us to investigate the biological effect of a modification of the Tyr side chain as methylether (**2**) and t-butylether (**3**).

## Results and Discussion

**Synthesis** - As described previously for the synthesis of *Axinastatin 5* (**1**) [5], the derivatives (**2**) and (**3**) were synthesized by cyclization of linear, side chain protected peptide building blocks. The linear peptides were synthesized by solid-phase synthesis, while tyrosine was used as t-butylether for (**1**) and (**3**), methylether for (**2**). We compared the <sup>1</sup>H- and <sup>13</sup>C-NMR chemical shifts of synthetic *Axinastatin 5* (**1**) with the natural product in CD<sub>3</sub>CN and found the compounds to be identical. ✓

**NMR Studies and Conformational Analysis** - The structure of *Axinastatin 5* in DMSO (Fig. 1) is characterized by a distorted βII-turn with Pro<sup>3</sup> in the *i+1* position and a βVI(a)-turn about Pro<sup>7</sup> and Pro<sup>8</sup> with a cis amide bond between these residues. Two bifurcated hydrogen bond motifs between Leu<sup>6</sup>CO, Tyr<sup>1</sup>NH (32%), Val<sup>2</sup>NH (100%) and Val<sup>2</sup>CO, Ile<sup>5</sup>NH (46%), Leu<sup>6</sup>NH (98%), respectively, result in a pseudo-β-strand overall conformation. An additional H-bond between Pro<sup>3</sup>CO and Ile<sup>5</sup>NH, consistent with a γ-turn about Leu<sup>4</sup>, is present during 94% of the simulation and results in the twisted βII-turn about Pro<sup>3</sup> and Leu<sup>4</sup>. As expected from the NMR data, the DG calculations for *Axinastatin 5* (Tyr(Me)) (**2**) and *Axinastatin 5* (Tyr(t-Bu)) (**3**) result in a backbone conformation similar to *Axinastatin 5* (**1**) (Fig. 1).

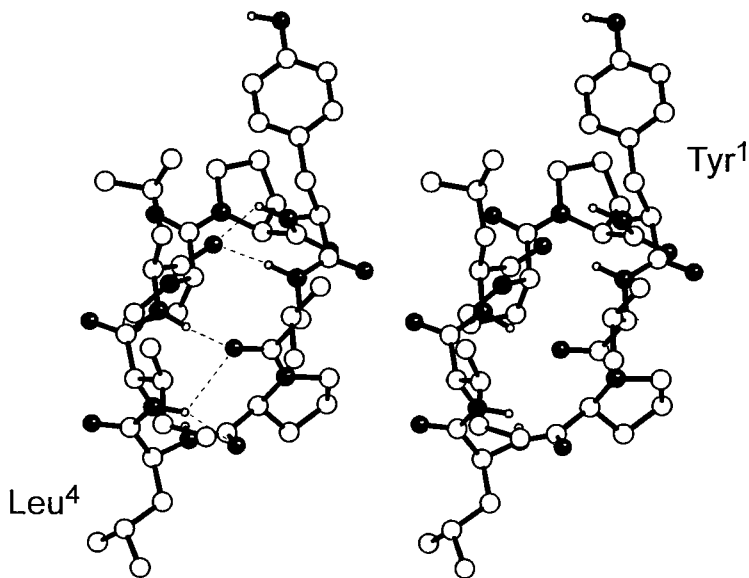


Fig. 1. Conformation of Axinastatin 5 (**1**) in DMSO obtained by averaging over the last 50 ps of the rMD trajectory and subsequent energy-minimization for 300 steps steepest descent.

**Biological Tests** - Synthetic Axinastatin 5 (**1**), and derivatives (**2**) and (**3**) were tested for inhibition of tumor cell growth in different human cancer cell lines (Table 1). For concentrations up to 31.6  $\mu\text{g/mL}$  no significant inhibition of cancer cell growth was found for synthetic Axinastatin 5 (**1**), indicating a lower activity of the natural product than initially assumed. As we have already found for Axinastatin 2, 3 and 4 [5], Axinastatin 5 also seems to be accompanied by highly active byproducts, such as the sponge halichondrins and halistatins. However, the modified peptides (**2**) and (**3**) show increasing activity with the change from Tyr(Me) to Tyr(t-Bu). A structural comparison with active compounds containing side chain alkylated tyrosines is in progress.

## References

1. Pettit, G. R., Gao, F., Schmidt, J. M., Chapuis, J., *Bioorg. Med. Chem. Lett.*, 4 (1994) 2935.
2. Konat, R. K., Mathä, B., Winkler, J., Kessler, H., *Liebigs Ann. Chem.* (1995) 765; Konat, R. K., Mierke, D. F., Kessler, H., Kutscher, B., Bernd, M., Voegeli, R., *Helv. Chim. Acta* 76 (1993) 1649; Mechnich, O., Kessler, H., *Lett. Pept. Sci.*, 4 (1997) 21.
3. Rinehart Jr., K. L., Gloer, J. B., Hughes Jr., R. G., Renis, H. R., McGovren, J. P., Swynenberg, E. B., Stringfellow, D. A., Kuentzel, S. L., Li, L. H., *Science*, 212 (1981) 933.
4. Boger, D. L., Patane, M. A., Jin, Q., Kitos, P. A., *Bioorg. Med. Chem.*, 2 (1994) 85.
5. Mechnich, O., Kessler, H., *Tetrahedron Lett.* 37 (1996) 5355; Mechnich, O., Hessler, G., Kessler, H., Bernd, M., Kutscher, B., *Helv. Chim. Acta*, (1997), in press.

# On the energetics of the heterodimerization of the Max and c-Myc leucine zippers

**P. Lavigne, L. H. Kondejewski, M. E. Houston Jr.,  
R. S. Hodges and C. M. Kay**

*Department of Biochemistry and the Protein Engineering Network of Centres of Excellence,  
University of Alberta, Edmonton, Alberta, Canada T6G 2S2*

The oncoprotein c-Myc (a member of the basic region-Helix-Loop-Helix-Leucine Zipper family of transcription factors) must heterodimerize with the b-HLH-LZ Max protein to bind DNA and activate transcription [1]. Max is also known to heterodimerize with proteins from the b-HLH-LZ Mad family. Max-Mad heterodimers are proposed to repress transcription [1]. It has been shown that the LZ domains of the c-Myc and Max proteins specifically form a heterodimeric LZ at room temperature and neutral pH [2,3]. This indicates that the LZ domains of the c-Myc and Max proteins play an important role in the heterodimerization of the corresponding gene products *in vivo* [2,3]. The solution structure of the c-Myc-Max heterodimeric LZ was solved and shown to be a parallel and two-stranded  $\alpha$ -helical coiled-coil [4]. The existence of a buried salt bridge that was proposed to play a crucial role in the heterodimerization specificity was also observed [2,4]. In order to gain more insights into the energetics of heterodimerization, the stability of the disulfide linked c-Myc and Max homodimeric LZs and the c-Myc-Max heterodimeric LZ have been studied by temperature induced denaturation monitored by CD spectroscopy at pH 7.0.

## Results and Discussion

Shown in Fig 1A and 1B are the fitted temperature denaturation curves for the Max homodimeric LZ and the c-Myc-Max heterodimeric LZ. It has been demonstrated that the c-Myc homodimeric LZ does not homodimerize [2,5]. The denaturation curves have been fitted assuming a two-state transition and that the temperature dependence of Gibbs free energy of unfolding ( $\Delta G^u$ ) is described by the Gibbs-Helmholtz equation [2]. We present in Fig.1C the corresponding stability curves ( $\Delta G^u(T)$ ) for the Max homodimeric LZ and the c-Myc-Max heterodimeric LZ. The c-Myc-Max heterodimeric LZ is more stable than the Max homodimeric LZ at 25°C (2.4 vs 0.9 kcal/mol) in accordance with the highly specific heterodimerization previously observed at this temperature [2]. On the other hand, the Max homodimeric LZ and the c-Myc-Max heterodimeric LZ have inherent low stabilities, both having  $T_{mS}$  of approximately 37°C. It is to be expected that heterodimerization will be less specific at 37°C compared to room temperature. Nonetheless, even if the Max homodimeric LZ and the c-Myc-Max, heterodimeric LZ have low stabilities, taking into account that the c-Myc LZ does not homodimerize folded c-Myc-Max heterodimeric LZ will always be preferred over the folded Max homodimer in a concentration dependent

manner (mass action). It is thought that apart from heterodimerization of the HLH-LZ domains (thermodynamic control) that the regulation (activation *vs* repression) of transcription in this family relies on the level of expression of the *mad* and *myc* genes [1]. In that regard, the low intrinsic stabilities for the Max homodimeric and the c-Myc-Max heterodimeric LZs are likely to be an advantage for the reassortment of the complete gene products *in vivo*. Indeed, if the Max homodimeric and the c-Myc-Max heterodimeric LZs were highly stable, they would only allow for low populations of dissociated monomers and impede reassortment through mass action dictated by the level of expression of the different transcription factors of this family.

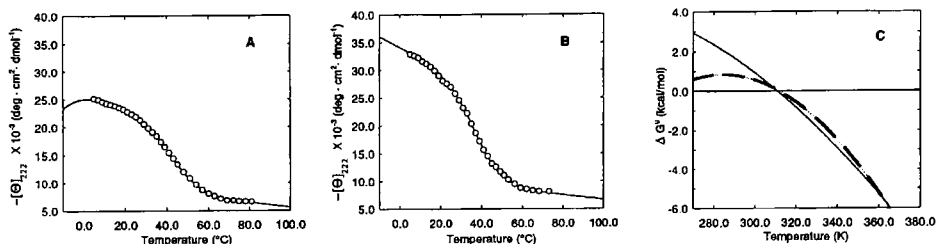


Fig. 1. Temperature induced denaturation of the Max homodimeric LZ (A) and the c-Myc-Max heterodimeric LZ (B) at pH 7.0 (50mM potassium phosphate buffer containing 50 mM KCl). The molar ellipticity at 222 nm was monitored. The LZs were cross-linked by air oxidation of a N-terminal Cys-Gly-Gly linker (2). (C) - The free energy of unfolding ( $\Delta G^0$ ) obtained from the non-linear least squares fitting for the Max homodimeric LZ (broken line) and the c-Myc-Max heterodimeric LZ (solid line).

## References

1. Littlewood, T. D. and Evans, G. I. *Protein Profile*, 1 (1994) 639.
2. Lavigne, P., Kondejewski, L.H., Houston, M.E. Jr., Sönnichsen, F.D., Lix, B., Sykes, B.D., Hodges, R.S. and Kay, C.M., *J. Mol. Biol.*, 254 (1995) 505.
3. Muhle-Goll, C., Nilges, N. and Pastore, A. *Biochemistry*, 34 (1995) 13554.
4. Lavigne, P., Crump, M.P., Gagné, S.M., Hodges, R.S., Kay, C.M. and Sykes, B.D. submitted.
5. Muhle-Goll, C., Gibson, T., Schuck, P., Nalis, D., Nilges, N. and Pastore, A. *Biochemistry*, 33 (1994) 11296.

# Synthesis and conformational analysis of cyclic hexapeptides related to somatostatin incorporating novel peptoid residues

Thuy-Anh Tran, Ralph-Heiko Mattern and Murray Goodman

Department of Chemistry and Biochemistry, University of California at San Diego,  
La Jolla, CA 92093, USA

Since the discovery of the highly potent somatostatin analog c-[Phe<sup>11</sup>-Pro<sup>6</sup>-Phe<sup>7</sup>-D-Trp<sup>8</sup>-Lys<sup>9</sup>-Thr<sup>10</sup>] **I** by Veber and coworkers [1], numerous cyclic hexapeptides related to somatostatin have been studied. We report the synthesis, bioactivity data and conformational analysis of potent analogs of **I** containing novel peptoid residues. Incorporation of *N*-benzyl glycine (Nphe, **II**), *N*-(*S*)- $\alpha$ -methylbenzyl glycine [(*S*)- $\beta$ -MeNphe, **III**], and *N*-(*R*)- $\alpha$ -methylbenzyl glycine [(*R*)- $\beta$ -MeNphe, **IV**] into position 6 of **I** led to the analogs c-[Phe<sup>11</sup>-Nxaa<sup>6</sup>-Phe<sup>7</sup>-D-Trp<sup>8</sup>-Lys<sup>9</sup>-Thr<sup>10</sup>] (**II-IV**).

## Results and Discussion

The synthesis of the peptoid residues was achieved by alkylation of the appropriate amines with ethyl bromoacetate. The linear hexapeptides were synthesized in solution via fragment condensation. DPPA mediated cyclization and deprotection led to the cyclic peptides **II-IV** in good overall yields.

These compounds show two set of signals in <sup>1</sup>H NMR corresponding to *cis* and *trans* isomers of the peptide bond between Phe<sup>11</sup> and the peptoid residue. The results of <sup>1</sup>H NMR studies and molecular modeling suggest that the *cis* isomers, which we believe to be the bioactive structures, adopt conformations similar to those observed for compound **I**. The conformational search for the *cis* isomers resulted in “folded” and “flat” conformations [2] which are consistent with the NMR data.

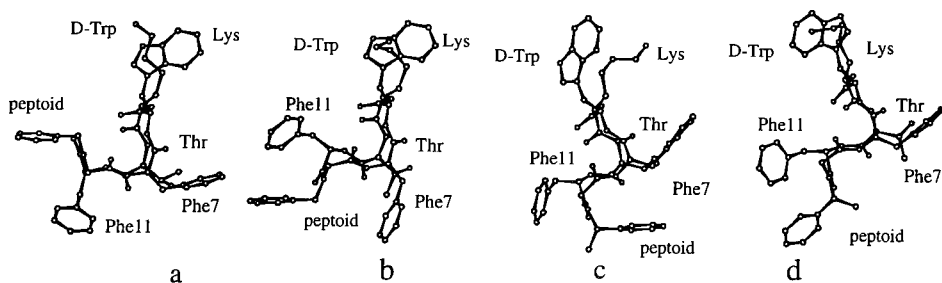


Fig. 1. Structures (a) and (b) show the two “folded” conformations observed for compound **II** and minimum-energy “folded” conformations (c) of compound **III** and (d) of compound **IV**.

Both conformations contain a type II'  $\beta$ -turn with D-Trp in the  $i+1$  position and a type VI  $\beta$ -turn spanning residues 11 and 6. The Nphe analog **II** shows more flexibility in the bridging region than compounds **III** and **IV** and adopts at least two "folded" conformations with considerable differences in the overall topology of the bridging region (Fig.1). The main conformational difference between compounds **III** and **IV** is the orientation of the rigid peptoid side chain relative to the Phe<sup>11</sup> side chain. In compound **IV** and in the conformation (**b**) of compound **II**, these two side chains are in close proximity while in compound **III** the peptoid side chain is orientated towards Phe<sup>7</sup> (Fig. 1).

Compound **II** and especially compound **IV** are SSTR2 selective with decreased binding activities to the SSTR5 compared to compound **I** while compound **III** shows reduced binding potencies to both SSTR2 and SSTR5 receptors. According to our model, the close spatial proximity of the aromatic side chains in positions 6 and 11 is responsible for the selectivity to the SSTR2 receptor of compounds **II** and **IV** compared to compound **III**. The results of the *in vivo* assays in rats suggest that the peptoid analogs inhibit specifically the release of growth hormone and have a much lower effect on insulin inhibition compared to sandostatin and RC-160.

## Conclusion

The incorporation of peptoid residues containing aromatic side chains led to potent cyclic hexapeptide analogs of somatostatin which exhibit selective binding to the isolated SSTR2. These analogs also inhibit the release of growth hormone selectively. Based on our studies we believe that the additional aromatic side chain of the peptoid residues and its specific orientation are responsible for the enhanced selectivity in the inhibition of growth hormone release. These results will have important applications for the design of more selective analogs of somatostatin.

## Acknowledgments

We would like to thank Dr. Michel Afargan at Peptor, Inc. for carrying out the *in vivo* studies and Drs. Barry Morgan and John Taylor at Biomeasure for the binding studies to the isolated receptors. R.M. gratefully acknowledges a DFG postdoctoral fellowship and an APS travel grant.

## References

1. Veber, D.F, Freidinger, R.M., Perlow, D.S., Palaveda, W.J., Holly, F.R.W., Strachan, G., Nutt, R.F., Arison, B.J, C., Homnick, W.C., Randall, M.S., Glitzer, R., Saperstein, R., Hirschmann, R., Nature 292 (1981) 55.
2. Huang, Z., He, Y.-B., Raynor, K., Tallent, M., Reisine, T., Goodman, M., J. Am. Chem. Soc. 114 (1992) 9390

# The importance of residue B8 in insulin activity, structure and folding

Satoe H. Nakagawa, Ming Zhao, Qingxin Hua and Michael A. Weiss

*Departments of Biochemistry & Molecular Biology and Chemistry, The University of Chicago, Chicago, IL 60637, USA*

Insulin provides a model for the study of protein folding and conformational change. The sequences of the insulin A- and B chains contain sufficient information to direct native disulfide pairing. Residue Gly<sup>B8</sup>, invariant among members of the insulin superfamily, is located at the junction of an invariant  $\alpha$ -helix (B9-B19) and a segment of variable conformation (B1-B8) [1]. This latter segment undergoes the T (extended)  $\rightarrow$  R (helical) transition in insulin hexamers. Whereas in the R-state [2] the mainchain dihedral angles are those of an L-amino acid, in the T-state Gly<sup>B8</sup> lies in the D-region of the Ramachandran plot. This study describes the effect of D-alanine and L-alanine substitutions at position B8 on insulin bioactivity, foldability and the T  $\rightarrow$  R conformational transition. The experimental design also employs a monomeric insulin analog, [Asp<sup>B10</sup>, Pro<sup>B28</sup>, Lys<sup>B29</sup>]insulin (DKP-insulin), as a template for mutagenesis [3].

## Results and Discussion

We designed and synthesized four insulin analogs, [D-Ala<sup>B8</sup>]-, [D-Ala<sup>B8</sup>]-DKP-, [Ala<sup>B8</sup>]- and [Ala<sup>B8</sup>]-DKP human insulin by solid-phase peptide synthesis of modified insulin B chains and chain combination of the B chains with the native insulin A chain [4]. DKP insulin analogs are monomeric and hence facilitate NMR structural study in solution. Insulin analogs were purified by a combination of gel-filtration and reversed-phase HPLC and characterized by peptide mapping following *Staphylococcus aureus* V8 protease digestion and MALDI-TOF mass spectrometry. It was found that the [D-Ala<sup>B8</sup>]- and [D-Ala<sup>B8</sup>]-DKP B chains gave excellent chain combination yields of the insulins (>20%) whereas yields of both [Ala<sup>B8</sup>]- and [Ala<sup>B8</sup>]-DKP insulins were very low (< 3%) under standard conditions [4]. Synthetic insulin analogs were studied with respect to their abilities to interact with the insulin receptors on human placental membranes. The following receptor binding potencies relative to human insulin were obtained: [Ala<sup>B8</sup>] insulin, 1.0% (reported 3% in ref.[5]); [Ala<sup>B8</sup>]-DKP insulin, 3.2%; [D-Ala<sup>B8</sup>] insulin, 0.12%; and [D-Ala<sup>B8</sup>]-DKP insulin, 0.16%. The structures of both [Ala<sup>B8</sup>]- and [D-Ala<sup>B8</sup>]-DKP insulins were examined by <sup>1</sup>H-NMR (Fig. 1). The ability of the [D-Ala<sup>B8</sup>]- and [Ala<sup>B8</sup>] insulins to undergo the T  $\rightarrow$  R conformational transition was evaluated by visible absorption spectroscopy. Co<sup>2+</sup> coordination changes characteristic of the R-state were in each case observed in the presence of phenol and SCN<sup>-</sup>. Our results demonstrate that a representative D-amino acid confers native foldability but markedly impairs receptor binding. By contrast substitution by an L-amino acid, associated with low but significant receptor-binding activity, blocks chain combination.

We conclude that flexibility at position B8 is important in the specification of disulfide pairing and may also enable the hormone to achieve a bioactive conformation on binding to the receptor. Conservation of glycine in the B-chain with variable D- or L-region dihedral angles suggests that this residue provides a "pivot points" in protein folding and bioactivity.

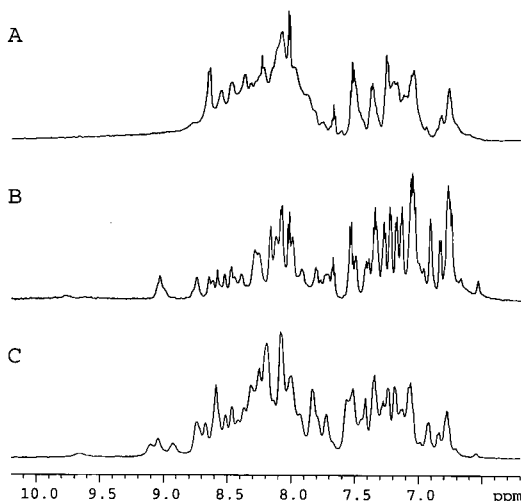


Fig. 1.  $^1\text{H-NMR}$  spectra of [Ala<sup>B8</sup>, Asp<sup>B10</sup>, Lys<sup>B28</sup>, Pro<sup>B29</sup>]-insulin (A), [D-Ala<sup>B8</sup>, Asp<sup>B10</sup>, Lys<sup>B28</sup>, Pro<sup>B29</sup>]-insulin (B) and [Asp<sup>B10</sup>, Lys<sup>B28</sup>, Pro<sup>B29</sup>]-insulin (C, DKP-insulin).

## References

1. Baker, E.N., Blundell, T.L., Cutfield, J.F., Cutfield, S.M., Dodson, E.J., Dodson, G.G., Hodgkin, D.M.C., Hubbard, R.E., Isaacs, N.W., Reynolds, C.D., Sakabe, K., Sakabe, N. and Vijayan, N.M., *Philos. Trans. R. Soc. Lond. [Biol.]*, 319 (1988) 369.
2. Derewenda, U., Derewenda, Z., Dodson, E.J., Dodson, G.G., Reynolds, C., Smith, G.D., Sparks, C. and Swenson, D., *Nature*, 338 (1989) 589.
3. Shoelson, S.E., Lu, Z.-X., Parlautan, L., Lynch, C.S. and Weiss, M.A., *Biochemistry*, 31 (1992) 1757.
4. Chance, R.E., Hoffman, J.A., Kroef, E.P., Johnson, M.G., Schirmer, E.W., Bromer, W.W., Ross, M.J. and Wetzel, R., In Rich, D.H. and Gross, E. (Eds.) *Peptides: Synthesis, Structure and Function* (Proc. 7th Amer. Pept. Symp.), Pierce Chem. Co., Rockford, IL, 1981, p. 721.
5. Kristensen, C., Kjeldsen, T., Wiberg, F.C., Schaffer, L., Hach, M., Havelund, S., Bass, J., Steiner, D.F. and Andersen, A.S., *J. Biol. Chem.*, 272 (1997) 12978.

# Opioidmimetic peptides containing $\alpha$ -aminoisobutyric acid

Sharon D. Bryant,<sup>a</sup> Remo Guerrini,<sup>b</sup> Severo Salvadori,<sup>b</sup> Clementina Bianchi,<sup>b</sup> Roberto Tomatis,<sup>b</sup> Martti Attila<sup>c</sup> and Lawrence H. Lazarus<sup>a</sup>

<sup>a</sup>National Institute of Environmental Health Sciences, R. T. P., NC 27709; <sup>b</sup>University of Ferrara, I-44100 Ferrara, Italy, <sup>c</sup>University of Helsinki, Helsinki, Finland FIN-00014

The design of highly selective peptides using the amphibian skin peptide deltorphin C (H-Tyr-D-Ala-Phe-Asp-Val-Val-Gly-NH<sub>2</sub>) provides a scaffold for probing opioid structure activity relationships since it exhibits high affinity and selectivity for  $\delta$  opioid receptors [1]. An  $\alpha,\alpha$ -dialkylated residue,  $\alpha$ -aminoisobutyric acid (Aib), is known to stabilize helices in peptides with 7 to 20 residues [2-4]. Aib could conceivably replace D-Ala<sup>2</sup> in deltorphin C because the symmetric carbon affords an equal possibility for L- or D-configurations<sup>2</sup> and Aib adopts ( $\phi$ ,  $\psi$ ) values that overlap those of D-Ala in the Ramachandran map [2,3]. The  $\alpha,\alpha$ -dimethyl groups of Aib might further offset the hydrophobicity of the phenyl side-chain of Phe<sup>3</sup> since the converse was observed when L-Phe replaced Aib residues in Aib-rich peptides [4]. It is feasible that Aib can substitute for the critical residues in the N-terminal region of deltorphin C without adversely affecting the physicochemical requirements for receptor recognition and at the same time induce conformational changes that influence receptor interaction. Here we explore Aib substitutions for D-Ala<sup>2</sup>, Phe<sup>3</sup>, and Asp<sup>4</sup> of deltorphin C and report its effect on  $\delta$  opioid receptor binding properties, biological activity and ligand conformation

## Results and Discussion

Substitutions by Aib for D-Ala<sup>2</sup> (2) or Phe<sup>3</sup> (3), or both (5), exhibited high  $\delta$  receptor affinity ( $K_i\delta = 0.12$  to 3.6 nM) and 5- to 9-fold greater selectivity ( $K_i\mu/K_i\delta = 5,000$  to 8,500) than the parent compound (1). This is the first definitive demonstration that the D-chirality of alanine and the aromaticity of phenylalanine are replaceable by an achiral  $\alpha,\alpha$ -dialkylated residue without a loss of binding affinity. Replacement of the anionic residue Asp<sup>4</sup> by Aib (4) resulted in high affinity for both  $\delta$  and  $\mu$  receptors (Table 1) underscoring the repulsive effect of a negative charge at  $\mu$  receptor sites. Individual substitutions of D-Ala and Phe were not detrimental to opioid binding; however, simultaneous substitution (5) of these residues resulted in decreased  $\delta$  affinity suggesting a conformational change. Molecular dynamics conformational analyses showed that Aib residues caused distinct changes in deltorphin C secondary structure when substituted for D-Ala<sup>2</sup> or Asp<sup>4</sup> and, simultaneously, for D-Ala<sup>2</sup> and Phe<sup>3</sup> but not when substituted for Phe<sup>3</sup>. Disparities between binding data and functional bioassays of [Aib<sup>3</sup>]deltorphin C indicated that Phe<sup>3</sup> was required for bioactivity in mouse vas deferens but not for interaction with  $\delta$  opioid receptors in rat brain membranes.

Table 1. Receptor binding profiles of delorphan C analogous containing  $\alpha$ -aminoisobutyric acid  $K_i$  and  $IC_{50}$  values for mouse vas deferens (MVD) and guinea pig ileum (GPI) are  $nM$ .

Peptide	$K_i\delta$	$K_i\mu$	$K_i\mu/K_i\delta$	$IC_{50}$	
				MVD	GPI
1 Tyr-D-Ala-Phe-Asp-Val-Val-Gly-NH <sub>2</sub>	0.15	147	980	0.46	420
2 Tyr-Aib-Phe-Asp-Val-Val-Gly-NH <sub>2</sub>	0.12	1,015	8,460	1.44	>10 $\mu M$
3 Tyr-D-Ala-Aib-Asp-Val-Val-Gly-NH <sub>2</sub>	0.80	4,544	5,680	57.3	>10 $\mu M$
4 Tyr-D-Ala-Phe-Aib-Val-Val-Gly-NH <sub>2</sub>	0.20	0.43	2.2	0.36	4.5
5 Tyr-Aib-Aib-Asp-Val-Val-Gly-NH <sub>2</sub>	3.62	15,200	4,200	70	>10 $\mu M$

## Conclusion

The aliphatic properties of Aib in deltorphin C derivatives may provide greater compatibility with a lipophilic binding site consisting of residues with hydrophobic or aromatic side chains [5]. Although the location and 3-dimensional arrangement of the  $\delta$  opioid receptor binding site is not known, site-directed mutagenesis of  $\delta$  receptors indicated that the opioid ligand enters a transmembrane channel to interact with regions of the receptor embedded in the membrane lipid bilayer [6,7]. Ligands adopting  $\alpha$ -helical or well ordered structures might be compatible with this region. Structure inducing amino acids such as Aib are useful for exploring the role of conformation in opioid receptor binding and activation.

## References

1. (a) Toniolo, C., Bonora, G.M., Bavoso, A., Benedetti, E., di Blasio, B., Pavone, V., Pedone, C. Erspamer, V. *Int. J. Dev. Neurosci.*, 10 (1992) 3.
2. Biopolymers 22 (1983) 205. (b) Karle, I.L., Balam, P. *Biochemistry*, 29 (1990) 6747. Di Blasio, B., Pavone, V., Lombardi, A., Pedone, C., Benedetti, E. *Biopolymers*, 33 (1993) 1037.
3. Basu, G., Bagchi, K., Kuki, A. *Biopolymers*, 31 (1991) 1763.
4. Befort, K., Tabbara, L., Kling, D., Maigret, B., Kieffer, B. *J. Biol. Chem.*, 271 (1996) 10161.
5. Valiquette, M., Vu, H.K., Yue, S.Y., Wahlestedt, C., Walker, P. *J. Biol. Chem.*, 271 (1996) 18789.
6. Surratt, C.K., Johnson, P.S., Moriwaki, A., Seidleck, B.K., Blaschak, C.J., Wang, J.B., Uhl, G.R. *J. Biol. Chem.*, 269 (1994) 20548.

# Circular dichroism study of the interaction of synthetic J protein of bacteriophage $\phi$ K with single-stranded DNA

Shin Ono,<sup>a</sup> Takayuki Okada,<sup>a</sup> Saburo Aimoto,<sup>b</sup> Ken-Ichi Kodaira,<sup>a</sup> Takayoshi Fujii,<sup>a</sup> Choichiro Shimasaki,<sup>a</sup> and Toshiaki Yoshimura<sup>a</sup>

<sup>a</sup>Chemical and Biochemical Engineering, Faculty of Engineering, Toyama University, Gofuku 3190, Toyama 930, Japan; <sup>b</sup>Institute for Protein Research, Osaka University, Suita, Osaka 565, Japan

Small icosahedral bacteriophages  $\phi$ K,  $\alpha$ 3, G4, and  $\phi$ X174 contain highly basic small, J proteins, which are 24-37 amino acids long [1-4]. These J proteins have been shown to be essential for DNA packaging into the phage capsids [5-8]. However, no detailed information on the mode of interaction of the J proteins with DNA has been obtained. Using a gel retardation assay, Kodaira et al. Recently showed that a synthetic  $\phi$ K J protein (SynJ, KKARRSPRRKGARLWYVGGGSQF, 23 amino acids long) bound tightly to the circular single-stranded DNA (ss-DNA) of  $\phi$ K phage to form a compact complex in 50 mM Tris-HCl (pH 7.3) [1]. We also reported that SynJ binds cooperatively to ss-DNA. in the same buffer containing 200 mM NaCl based on the results of circular dichroism (CD) and fluorescence methods [9]. In this work, we examined the CD spectral change of the SynJ/ss-DNA complex in 50 mM Tris-HCl (pH 7.3) at various NaCl concentrations (0, 0.2, and 1 M) to investigate the salt effect on the interaction of the SynJ with the ss-DNA,

## Results and Discussion

Upon addition of small amounts of the SynJ to the ss-DNA in 50 mM Tris-HCl (pH 7.3) at various NaCl concentrations (0, 0.2, and 1 M), changes were seen in the CD spectra in the range of 220-320 nm. The CD changes at each maximum observed for the buffer titrations in at 0, 0.2, and 1 M NaCl were plotted as a function of  $1/R$  ( $R = [\text{Nucleotide}]/[\text{SynJ}]$ ) in Figs. 1A, 1B, and 1C, respectively, because the spectra changes for the maximum at around 277 nm seem to result from structural changes in the DNA.

It was found that there are three states in SynJ/ss-DNA complex formation in the buffer containing 0.2 M NaCl, i.e. an initial state ( $1/R$  0-0.07) showing relatively small change, a middle state ( $1/R$  0.07-0.11) showing drastic change, and last state (beyond  $1/R$  0.11) without change (Fig. 1B). This suggests that the SynJ interacts with the ss-DNA to form a complex cooperatively in this conditions (0.2 M NaCl). Under high salt conditions, the CD value was decreased steadily with increasing  $1/R$  value (Fig. 1C), indicating that no significant structural change for the SynJ/ss-DNA complex took place. On the other hand, a complicated spectral change was observed under low salt conditions (Fig. 1A). The maximum (274 nm) and minimum (249 nm) observed for the free ss-DNA became more negative and positive with increasing  $1/R$  value and consequently an inversion of these CD bands appeared in the range of  $1/R$  0.052-0.079 (data not shown).

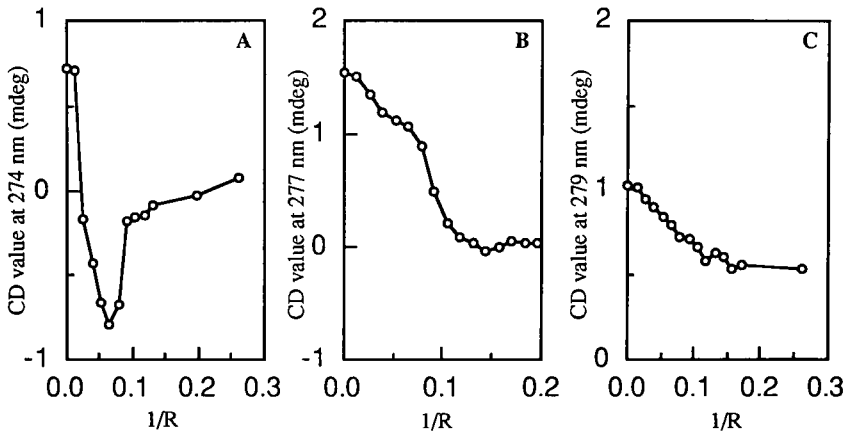


Fig. 1. CD changes accompanied by the titration of the ss-DNA with the SynJ in 50 mM Tris-HCl (pH 7.3) as a function of 1/R ratio ( $[SynJ]/[Nucleotide]$ ). The NaCl concentrations were 0 (A), 0.2 (B), and 1 M (C).

These results indicate that the SynJ interaction with the ss-DNA depends on the salt concentration and imply that the interaction between the SynJ and the ss-DNA electrostatics. Also, cooperative SynJ/ss-DNA complex formation was observed in the buffer containing 0.2 M NaCl. A fluorescence titration experiment under the same conditions showed that a hydrophobic interaction may also cause the cooperative complex formation [9]. In conclusion, the J protein can interact with DNA cooperatively by both electrostatic and hydrophobic interactions *in vitro*. However, it is still unknown how the J protein contributes to the packaging of viral DNA. Further study using the SynJ should be performed

## References

1. Kodaira, K.-I., Oki, M., Kakikawa, M., Kimoto, H. and Taketo, A., *J. Biochem.*, 119 (1996)1062.
2. Kodaira, K.-I. and Taketo, A., *Mol. Gen. Genet.*, 195 (1984) 541.
3. Godson, G.N., Barrell, B.G., Staden, R. and Fiddes, J.C., *Nature*, 276 (1978) 236.
4. Sanger, F., Coulson, A.R., Fiedmann, T., Air, G.M., Barrell, B.G., Brown, N.L., Fiddes, J.C., Hutchison, C.A., Slocombe, P.M. and Smith, M., *J. Mol. Biol.*, 125 (1978) 225.
5. Aoyama, A., Hamatake and Hayashi, M., *Proc. Natl. Acad. Sci. USA*, 78 (1981) 7285.
6. Fane, B.A., Head, S. and Hayashi, M., *J. Bacter.*, 174 (1992)2717.
7. Ilag, L.L., Tuech, J.K., Beisner, L.A., Sumrada, R.A. and Incardona, N.L., *J. Mol. Biol.*, 229 (1993) 671.
8. Hamatake, R.K., Aoyama, A. and Hayashi, M., *J. Mol.*, 54(1985)345.
9. Ono, S., Okada, T., Aimoto, S., Fujii, T., Morita, H., Shimasaki, C. and Yoshimura, T., *Chem. Lett.*, (1996) 1063.

# V3 loop of HIV gp120 protein: Molecular modeling of 3D structures interacting with cell proteins

**Stan Galaktionov, Gregory V. Nikiforovich and Garland R. Marshall**

*Center for Molecular Design, Washington University, Box 8036, St. Louis, MO 63110, USA*

The hypervariable V3 loop of gp120 is one of the principal components of interaction between gp120 and the target cell proteins, CD4 and HIV co-receptors. V3 loops of different HIV strains are 30-40-membered peptides cyclized by the disulfide bridge connecting the ends. The data on the binding of gp120 with mutations in the V3 loop to various cell proteins can be used to determine the possible "interacting" conformations of the V3 loop, which presumably should be common for all mutants displaying high levels of binding to target proteins.

## Results and Discussion

This study employed the residue-residue contact matrix algorithm [1] for elucidating a set of sterically consistent  $C^\alpha$ -traces for "potent analogs" of the V3 loop. Possible 3D shapes of different molecules then were compared in searching for geometrical similarity. As an example, we predicted sterically consistent  $C^\alpha$ -traces for the V3 loops of two SIV mutants, (CRRPGNKTVLPVTIMSGLVFHSQPINDRPKQAWC) for *mac251* and (CRRPGNKTVLPVTRIHGGPFRAQPINDRPKQAWC) for M4A [2]. Both possess the same high specific binding to CD4.  $C^\alpha$ -traces for their more distant homolog, HXB2, (CTRPNNNTRKRIRIQRGPGRAFVTIGKIGNMRQAHC) have also been calculated.

The procedure starts with predictions of secondary structure using the methods implemented in SYBYL 5.5 as well as the procedure available at the PHD mail server [3]. The consensus location of secondary structure was used for prediction of a coordination number vector [4]. These data were used for reconstruction of contact matrices [1]. The multiple criteria for optimal organization of the intraglobular contact network were formulated in terms of the relationship of a contact matrix with its powers and eigensystems and used in an iterative procedure over the set of spatially consistent matrices.  $C^\alpha$ -traces were restored on the basis of the contact matrix. The initial reconstruction of 3D structure employed elements of distance geometry. A refinement procedure corrected chosen intraglobular distances and removed stressed contacts.

Four different methods for secondary structure prediction positioned a  $\beta$ -strand between residues 10 and 18 in all three molecules, although in M4A and HXB2 it is significantly shorter. In HXB2, there is another  $\beta$ -strand consensus region, at residues 20-25. The presence of these strands as well as the end-to-end disulfide bond considerably limit the flexibility of the molecule. Various protocols for matrix prediction which proved to be effective in calculation of contact matrices for 1CRN and 1NXB were used for

calculation of contact matrices. They produced essentially the same type of contact matrices for *mac251*. Reconstruction of space structures corresponding to this matrix resulted in five distinct 3D structures. All of them are more or less similar in the central part of the molecule and differ in the packing of the terminal parts. For M4A, two different types of matrix were predicted. For the first matrix type, resembling that of *mac251*, a single 3D structure was found. On the basis of the contact matrix of the second type, five different structures were generated. In most structures of *mac251* and M4A, the fragment 20-25 is extended. Finally, for HXB2, four different structures were found.

Most NMR data on the whole V3 loops in solution (see [5] and references therein) and on the reduced linear peptide 6-29 bound to an anti-gp120 antibody [6] as well as X-ray data on the central decapeptide [7] reveal the turn at position 17-20. It is present in all predicted structures. In the most of these structures, the turn at position 3-6 suggested by [5] is also recognizable. The set of residue-residue contacts between regions 9-14 and 21-25 discovered by most NMR studies is also present in the calculated structures.

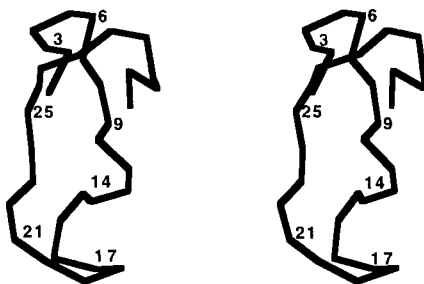


Fig. 1. Stereoview of the  $C^{\alpha}$ -trace common for both sets of calculated conformations for *mac251* and M4A ( $rms=2.8 \text{ \AA}$ ).

Comparison of  $C^{\alpha}$ -traces for *mac251* and for M4A revealed two very similar structure types (Fig. 1). These structures can serve as an initial template in a search for the V3 loop conformer interacting with CD4.

## References

- Galaktionov, S. G., Marshall, G.R., Proc 27th Int. Conf. Syst. Sci., 5 (1994) 326.
- Javaherian, K., Zuchowski, L., Clark, F., AIDS Res. Human Retrovir., 11 (1995)1104
- Rost, B., Sander, C., Schneider, R., CABIOS, 10 (1994) 53.
- Rodionov, M.A., Galaktionov, S.G., Mol. Biol., 26 (1992) 777.
- Vranken, W.F., Budesinsky, M.,Martins, J.C., Fant, F., Boulez, K., Gras-Masse, H., Borremans, F.A.M., Eur. J. Biochem., 236 (1996) 100.
- Zvi, A., Feigelson, D.J., Hayek, Y., Anglister, J., Biochemistry, in press.
- Ghiara, J.B., Stura, E.A., Stanfield, R.L., Profy, A.T., Wilson. I.A., Science, 264 (1994) 82.

# Conformational studies of a D-Trp<sup>12</sup>-substituted PTHrP-derived antagonist containing lactam-bridged side-chains

Stefano Maretto,<sup>a</sup> Elisabetta Schievano,<sup>a</sup> Stefano Mammi,<sup>a</sup> Alessandro Bisello,<sup>b</sup> Chizu Nakamoto,<sup>b</sup> Michael Rosenblatt,<sup>b</sup> Michael Chorev<sup>b</sup> and Evaristo Peggion<sup>a</sup>

<sup>a</sup>Department of Organic Chemistry, Biopolymer Research Center, University of Padua, Via Marzolo 1, 35131 Padua, Italy. <sup>b</sup>Beth Israel Deaconess Medical Center, Harvard Medical School, 330 Brookline Ave., Boston, MA 02215, USA

The N-terminal fragments 1-34 of both parathyroid hormone (PTH) and PTH-related protein (PTHrP), despite very low sequence homology, are equipotent and each retains all the calciotropic activity of the respective intact parent hormone [1]. In addition, truncation of the first 6 N-terminal residues generates PTH(7-34), a pure weak PTH/PTHrP receptor antagonist, and PTHrP(7-34), a weak partial agonist. We have previously studied the conformation of the highly potent pure PTH antagonist, [Leu<sup>11</sup>,D-Trp<sup>12</sup>]PTHrP(7-34)-NH<sub>2</sub> [2], and the weak partial agonist, [Lys<sup>26</sup>—Asp<sup>30</sup>]PTHrP(7-34)NH<sub>2</sub> [3,4]. In 50% TFE, CD, NMR and restrained molecular dynamics gave evidence of a long helix in their sequences 15-32 and 13-34, respectively. To assess the importance of this structural motif, we synthesized and studied an analogue containing both D-Trp<sup>12</sup> substitution and lactam-type cyclization: [Leu<sup>11</sup>, D-Trp<sup>12</sup>, Lys<sup>26</sup>—Asp<sup>30</sup>]PTHrP(7-34)-NH<sub>2</sub>. The conformational properties of this analog, which is a potent antagonist, were studied by CD, NMR and distance geometry calculations.

## Results and Discussion

In water (concentration  $2.8 \times 10^{-5}$  M), the CD spectrum of this PTHrP analogue is pH-independent in the range 3.8-7.4 and indicates the presence of a mixture of  $\alpha$ -helix and random coil with a helix content of ~30%. This behavior is quite different from that observed for the corresponding linear sequence, which was found in an almost completely random structure at neutral pH [2]. The helix content increases upon addition of TFE in the solvent mixture and saturation is reached at 30% TFE. Under these conditions the helix content is ~88%, higher than that of both the corresponding linear sequence and the 26 to 30 lactam lacking D-Trp<sup>12</sup> substitution [2,4]. All spectra fit a well-defined isodichroic point typical of coil-helix equilibrium. Thus, these results indicate that this analogue has a higher propensity to fold into the  $\alpha$ -helical structure than the linear peptide without the side-chain constraint. The conformational details of the peptide in 1:1 TFE-*d*<sub>3</sub>/H<sub>2</sub>O were further investigated by 2D-NMR. From all NOESY connectivities relevant for the determination of secondary structure elements, we identified a helical segment spanning the sequence from D-Trp<sup>12</sup> to Thr<sup>33</sup>. A structural refinement carried out by distance geometry

calculations yielded a structure comprising a long helical stretch spanning the sequence from *D*-Trp<sup>12</sup> to Thr<sup>33</sup> with a small bend around Arg<sup>21</sup> (Fig. 1). The structural motif of the corresponding linear analogue [Leu<sup>11</sup>, *D*-Trp<sup>12</sup>]PTHrP(7-34)-NH<sub>2</sub> is characterized by a slightly shorter  $\alpha$ -helical segment spanning the sequence Ile<sup>15</sup>-Ala<sup>34</sup> and by a loop similar to a  $\beta$ -turn located in the sequence Leu<sup>11</sup>-Ser<sup>14</sup>. The linear analogue [Leu<sup>11</sup>, *D*-Trp<sup>12</sup>]PTHrP(7-34)-NH<sub>2</sub> exhibits very potent antagonistic activity and very good receptor affinity [5]. The corresponding lactam constrained analogue of the present study also exhibits good antagonistic activity, but its binding affinity to the receptor is lower by one order of magnitude than that of the linear peptide. The lactamization between Lys<sup>26</sup>-Asp<sup>30</sup> in the agonist PTHrP(1-34) and in the antagonist PTHrP(7-34) also decreases receptor affinity. It was suggested that the amphipathic helical motif localized in the sequence 25-34 is of significance for receptor binding and may play an important role in the interaction with cellular lipid membranes. The reduced affinity for the receptor of analogues containing a Lys<sup>26</sup>-to-Asp<sup>30</sup> lactam bridge replacing His<sup>26</sup> and Glu<sup>30</sup> could be due either to elimination of charges essential for receptor binding and/or to an alteration of the amphipathic profile of the helical segment comprising the principal binding domain.

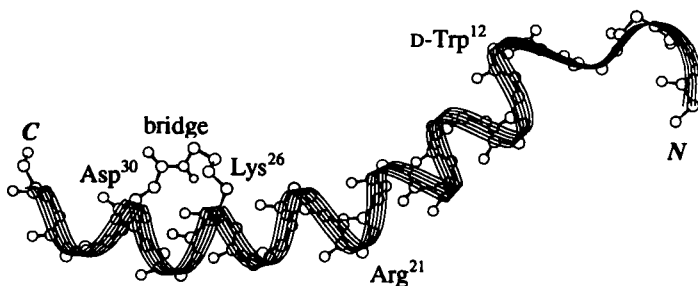


Fig. 1. Backbone representation of the best Distance Geometry structure. The lactam bridge is detailed at the C-terminal portion of the sequence.

## References

1. Chorev, M., and Rosenblatt, M., In Bilezikian, J. P., Levine, M. A., and Marcus, R. (Eds.), "Parathyroids. Basic and Clinical Concepts", Raven Press, New York, 1994, 139.
2. Chorev, M., Behar, V., Yang, Q., Rosenblatt, M., Mammi, S., Maretto, S., Pellegrini, M., Peggion, E., Biopolymers, 36 (1995) 485.
3. Bisello, A., Nokamoto, C., Rosenblatt, M., and Chorev, M., Biochemistry, 36 (1997) 3293
4. Maretto, S., Mammi, S., Bissacco, E., Peggion, E., Bisello, A., Rosenblatt, M., Chorev, M., and Mierke, D.F., Biochemistry, 36 (1997) 3300
5. Roubini, E., Doung, L.T., Gibbons, S.W., Leu, C.T., Caulfield, M.P., Chorev, M., and Rosenblatt, M., Biochemistry, 31 (1992) 4026.

# Cold denaturation studies of (LKELPEKL)<sub>n</sub> peptide using vibrational circular dichroism and FTIR

R. A. G. D. Silva,<sup>a</sup> Vladimir Baumruk,<sup>a</sup> Petr Pancoska,<sup>a</sup>

T. A. Keiderling,<sup>a</sup> Eric Lacassie<sup>b</sup> and Yves Trudelle<sup>b</sup>

<sup>a</sup>*Department of Chemistry, University of Illinois at Chicago, Chicago, IL 60607-7061, USA;*

<sup>b</sup>*Center de Biophysique Moleculaire, CNRS, 45071 Orleans Cedex 2, France*

While thermal denaturation of proteins is normally studied as a function of increasing temperature, several examples exist of cold denaturation of globular proteins. Recently, data for some model peptide systems have been reported which provide evidence for cold denaturation in simple systems which are highly helical at room temperature [1-3]. As opposed to many high temperature thermally denatured states, such cold denaturation is often a more gentle process that avoids aggregation and results in a reversible transition which is better suited for thermodynamic study of the basic coil-helix transition and is more relevant to protein folding studies now of wide spread interest.

Here we report Fourier transform infrared (FTIR) and vibrational circular dichroism (VCD) spectra of four related sequential polypeptides; which can be conveniently viewed as (XKELXEKL)<sub>n</sub> where X=P or L. That polymer based on a repeating octomer containing with two prolines, one every four residues, (PKELPEKL)<sub>n</sub>, will be denoted (P<sub>2</sub>)<sub>n</sub>; that without any prolines, (LKELLEKL)<sub>n</sub>, is denoted as (P<sub>0</sub>)<sub>n</sub>; and the other two with a proline present every eight residues, (LKELPEKL)<sub>n</sub> and (PKELLEKL)<sub>n</sub>, are denoted as (P<sub>1</sub>)<sub>n</sub> and (P'<sub>1</sub>)<sub>n</sub>, respectively. Of these, (P<sub>1</sub>)<sub>n</sub> exhibits cold denaturation behaviour in dilute aqueous solution as detected with electronic CD (ECD) [1].

All four polypeptides were pre-exchanged with D<sub>2</sub>O and then redissolved in D<sub>2</sub>O at concentrations of 50-60mg/ml. The samples were measured in a cell (Graseby Specac) equipped with CaF<sub>2</sub> windows and either 25 or 50μ path spacers. Temperature controlled FTIR and VCD studies of the (P<sub>1</sub>)<sub>n</sub> polypeptide in a 0.1M deuterated phosphate buffer (pD=7) at 20mg/ml were carried out over 5°C to 60°C using a laboratory constructed variable temperature cell controlled with a heating/cooling bath (Neslab). Temperature controlled ECD spectra of (P<sub>1</sub>)<sub>n</sub> polymer at 0.1mg/ml were also recorded in 5°C to 60°C temperature range using a Jasco J-600 spectrometer for comparison with earlier results [1]. The temperature dependent VCD and ECD spectra were quantitatively analyzed with our protein based factor analysis/restricted multiple regression (FA/RMR) method using twenty three proteins in the training set [4].

The VCD spectra of (P<sub>0</sub>)<sub>n</sub> and (P'<sub>1</sub>)<sub>n</sub> both show characteristic bandshapes of an α-helix while that for (P<sub>2</sub>)<sub>n</sub> shows a typical random coil signature (Fig. 1 left). By contrast, the room temperature VCD spectrum of (P<sub>1</sub>)<sub>n</sub> has a mixed helix/coil type bandshape. The observed temperature controlled VCD spectra of (P<sub>1</sub>)<sub>n</sub> shows the same type of cold denaturation behaviour (Fig. 1 right) for this peptide, even though the concentration is two hundred times higher than used for ECD studies [1]. However, the transition seems complete by 25°C under the VCD conditions and the final state is significantly more mixed in structure than reported in the ECD study. Our measurements of the ECD temperature

variation agree with the earlier results. FA/RMR analysis of both the VCD and ECD temperature dependent spectra indicate an increase in the helical content with increase in temperature, but the quantitative values are somewhat at variance. Presumably this reflects difference insensitivity of both techniques. The high temperature (ECD) value helix is in good agreement with published analysis [1] using a different model. However ECD based  $\beta$ -sheet estimates in our calculations were much higher than expected while the VCD estimates, which are more reliable for  $\beta$ -sheet [4], were near zero. The low temperature form appears to have much less helix. The most interesting aspect of this data is the difference in behaviour for  $(P_1)_n$  and  $(P'_1)_n$ . Adding proline residues is expected to disrupt helices so the general trend of  $(P_0)_n$ ,  $(P_1)_n$  to  $(P_2)_n$  is expected, but the positional dependence that leaves  $(P'_1)_n$  highly helical is surprising.

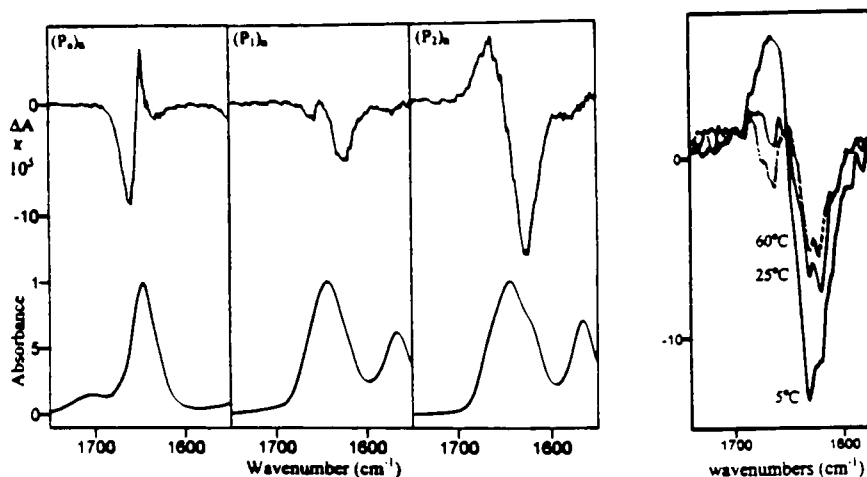


Fig. 1. (left) Normalized VCD (top) and FTIR (bottom) spectra of  $(P_0)_n$ ,  $(P_1)_n$  and  $(P_2)_n$  in  $D_2O$ . (right) Temperature-dependent VCD spectra of  $(P_1)_n$  in  $D_2O$  at ( $pD=7$ ).

## References

1. Lacassie, E., Delmas, A., Meunier, C., Sy, D. and Trudelle, Y., *Int. J. Peptide Protein Res.*, 48 (1996) 249.
2. Anderson, N.H., Cort, J.R., Liu, Z., Sjoberg, S.J. and Tong, H., *J. Am. Chem. Soc.*, 118 (1996) 10309.
3. Kitakuni, E., Kuroda, Y., Oobatake, M., Tanaka, T. and Nakamura, H., *Protein Science*, 39 (1994) 831.
4. Pancoska, P., Bitto, E., Janota, V., Urbanova, M., Gupta, V. and Keiderling, T.A., *Protein Science*, 4 (1995) 1384.

# Solution structure of human salivary statherin

**Tarikere L. Gururaja, Gowda A. Naganagowda and Michael J. Levine**

*Research Center in Oral Biology, School of Dental Medicine, State University of  
New York at Buffalo, Buffalo, NY 14214, USA*

Human statherin is a low molecular weight ( $M_r$  5380 Da, 43 aa residues) phosphoprotein secreted by salivary glands that is important in the maintenance of oral health [1,2]. While numerous reports are available on structure-function analyses of statherin and its fragments [2-4], little is known on the three-dimensional structure of the intact molecule in the solution state. Our recent study on this important phosphoprotein procured by solid-phase synthesis clearly indicated that synthetic statherin was identical to the native molecule [5], thus enabling us to proceed with solution state structural investigations.

## Results and Discussion

The solution structure of statherin was determined by 1D and 2D NMR spectroscopy using Varian Unity Inova 500 MHz spectrometer. The complete assignment of  $^1\text{H}$  resonances to individual residues was accomplished by combined analysis of 2D phase sensitive DQF-COSY, single as well as double relayed COSY, TOCSY and NOESY spectra. Delineation of the backbone conformation was performed utilizing the  $\phi$  values deduced from the coupling constant ( $J_{\text{NH-C}\alpha\text{H}}$ ) values, temperature coefficients of NH chemical shifts, hydrogen-deuterium exchange rates of amide resonances and the set of NOE connectivities. Figure 1 depicts the NH region of non-proline residues of statherin which are labelled based on the results obtained from a series of 2D experiments performed in aqueous environment (pH 4.5). When the spectrum was recorded in 50% trifluoroethanol (TFE- $d_3$ ) which is known to stabilize helical structures in aqueous solutions, residues comprising Ser<sup>2</sup>-Tyr<sup>16</sup> and Gln<sup>37</sup>-Phe<sup>43</sup> showed strong NH-NH (i, i+1) and fewer (i, i+2) cross peaks characteristic of helical structures at both N- and C-termini. In addition, CD studies, deuterium exchange and low temperature coefficients of the amide resonances further supported this observation. Although, it appears that the middle portion of statherin has a polyproline type extended structure due to high proline content, our NMR experiments did not yield any significant structural constraints for this region.

Previously, CD studies of statherin carried out in our laboratory in the presence of  $\text{Ca}^{2+}$  ions indicated that calcium ions have minimal influence on statherin secondary structure [4]. To substantiate this observation,  $^{31}\text{P}$  spectrum of statherin was recorded in water and showed a sharp  $^{31}\text{P}$  signal (Fig. 1a) having a linewidth of 10 Hz. This indicates that the two phosphate groups are chemically equivalent due to N-terminal flexibility. However Elgavish *et al.*, [6] found an identical but a broad  $^{31}\text{P}$  resonance of 300 Hz linewidth in the presence of excess calcium ions. In the present study, the intensity of the  $^{31}\text{P}$  signal was reduced exponentially upon  $\text{Ca}^{2+}$  addition and completely disappeared at high  $\text{Ca}^{2+}$  concentration (20 mM, Fig. 1b). This  $^{31}\text{P}$  signal loss may be attributed to: 1)

possible chelation of the two phosphate groups retarding their local motion, and 2) increased  $^{31}\text{P}$  relaxation rate as a result of the quadrupolar nature of the vicinal  $\text{Ca}^{2+}$  nucleus. On the other hand, titration with TFE (50%, v/v) resolved the  $^{31}\text{P}$  signal into two sharp signals (Fig. 1c) of equal intensity and no effect of  $\text{Ca}^{2+}$  ions was noticed on these two  $^{31}\text{P}$  signals. This clearly indicates a solvent-dependent conformational transition for the N-terminal domain of statherin from flexible to an ordered structure, which agrees well with our CD results. The separation of the  $^{31}\text{P}$  signal is due to the helical structure which makes the two phosphate groups non-equivalent. Although the effect of  $\text{Ca}^{2+}$  ions was negligible in non-aqueous conditions, there is indeed a significant effect of  $\text{Ca}^{2+}$  ions in water especially on the statherin N-terminal domain.

## Conclusion

Our NMR and CD results suggest that in aqueous phase statherin adopts largely a disordered structure and exhibits marked interaction with  $\text{Ca}^{2+}$  ions in the N-terminal domain.

Statherin = DS<sup>\*</sup>S<sup>\*</sup>E EKFLRRIGRFGYGYGPYQPVPEQLYPQYPQYQYQYTF; S<sup>\*</sup>-phosphorylated

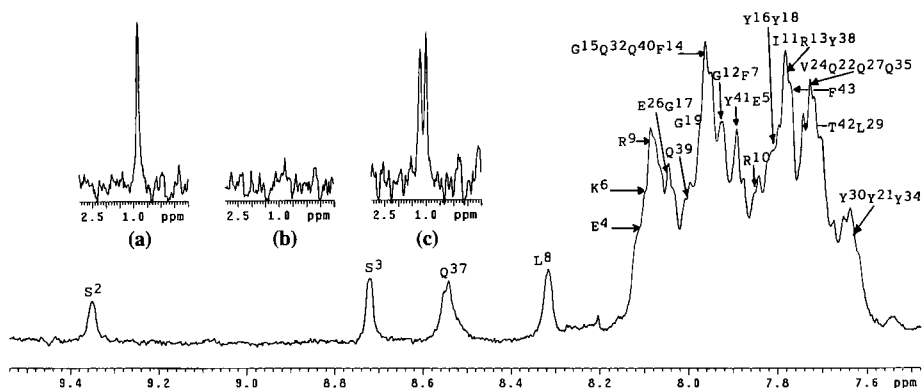


Fig. 1. Amide signals of non-proline residues and  $^{31}\text{P}$  NMR spectra (a-c) of statherin.

## References

1. Hay, D.I. and Moreno, E.C., In Tenovou, J.O. (Ed.), Human Saliva: Clinical Chemistry and Microbiology, Vol. 1, CRC Press, Boca Raton, 1989, p.131.
2. Raj, P.A., Johnsson, M., Levine, M.J. and Nancollas, G.H., J. Biol. Chem., 267 (1992) 5968.
3. Schwartz, S.S., Hay, D.I. and Schuleckebier, S.K., Calcif. Tissue Int., 50 (1992) 511.
4. Ramasubbu, N., Thomas, L.M., Bhandary, K.K. and Levine, M.J., Crit. Rev. Oral Biol. Med., 4 (1993) 363.
5. Gururaja, T.L. and Levine, M.J., Peptide Res., 9 (1996) 283.
6. Elgavish, G.A., Hay, D.I. and Schlesinger, D.H., Int. J. Peptide Protein Res., 23 (1984) 230.

# Interaction of melittin with a phospholipid monolayer modified silica support

**Tzong-Hsien Lee,<sup>a</sup> Hans-Jürgen Wirth,<sup>a</sup> Patrick Perlmutter<sup>b</sup> and Marie-Isabel Aguilar<sup>a</sup>**

*<sup>a</sup>Department of Biochemistry and Molecular Biology, <sup>b</sup>Department of Chemistry, Monash University, Clayton, Vic 3168, Australia*

The interaction between peptides and membranes plays a central role in mediating cellular processes. In order to understand these interactive processes at the molecular level, the structural changes and dynamic behavior of peptides can be investigated with natural and membrane model systems via various spectroscopic techniques [1]. The interaction of melittin with membranes is known to involve a coil-helix transition [2-4]. However, the influence of membranes on the thermodynamics and kinetics of this lipid-induced coil-helix transition has yet to be properly characterized. In the present study, a membrane model was synthesized by covalently immobilizing phosphatidylcholine (PC) onto an activated surface of porous silica particles. The structural properties and dynamic behavior of melittin were examined with this membrane model system at various methanol concentrations and at different temperatures.

## Results and Discussion

Retention plots were derived from the elution profiles (Fig. 1) and were used to probe the structural behavior of melittin upon interaction with phospholipids. Linear retention plots were observed for small molecules without secondary structure. However, significant deviation from the linearity of the retention plots was observed for melittin. As melittin is known to exist as an extended coil in aqueous solution and as an  $\alpha$ -helix either in methanol solution or bound to lipid micelles/vesicles, the non-linear behavior is consistent with changes in helical content during interaction with the PC ligands [5,6]. The dynamic behavior of melittin was also studied by measuring the changes in bandwidth of the elution peaks. Small molecules exhibited small uniform changes in the dependence of bandwidth on operating temperature and methanol content. However, large variations in bandwidth were observed for melittin. While asymmetric peak shapes and split peaks were observed for melittin, gaussian peak shapes were seen for the small molecules (Fig. 1). The multiple peaks coalesced at temperatures above 35°C, which indicates that the rate of coil-helix transition increases at higher temperature.

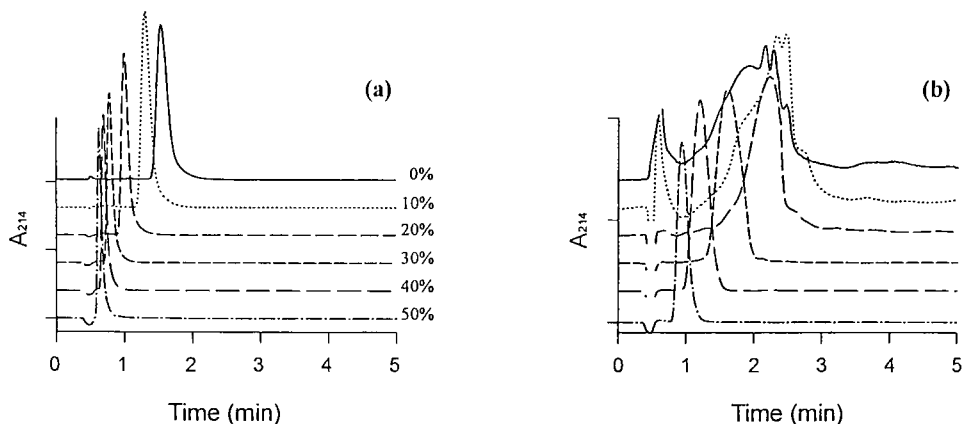


Fig.1. The elution profiles for (a) *N*-acetyl-*L*-tryptophanamide and (b) melittin at 35°C and different methanol content using PC-immobilized ZORBAX-300 column (4cm×4.6mm I.D.).

## Conclusion

In the present study, a novel membrane model was synthesized by immobilizing phosphatidylcholine onto an activated silica surface. The conformational properties and dynamic behavior of melittin were investigated with the immobilized lipid monolayer using HPLC techniques. Conformational heterogeneity of melittin upon interaction with the lipid monolayer was shown by the presence of multiple peaks in the chromatograms. Based on these experimental results, this silica-based phospholipid monolayer provides a stable and sensitive system for exploring the effects of environmental factors on peptide-lipid interactions.

## Acknowledgments

The financial support of the Australian Research Council is gratefully acknowledged.

## References

1. Parola, A.H., In Shinitzky, M. (Eds) *Biomembranes: Physical Aspects*. VCH. Balaban Publishers, 1993, p. 159.
2. Lauterwein, J., Brown, L.R. & Wüthrich, K., *Biochim. Biophys. Acta.* 622 (1980) 219.
3. Brown, L.R., Braun, W., Kumar, A. & Wüthrich, K. *Biophys. J.*, 37 (1982) 319.
4. Bazzo, R., Tappin, M.J., Pastore, A., Harvey, T.S., Carver, J.A. & Campbell, I.D., *Eur. J. Biochem.*, 173 (1988) 139.
5. Sui, S-F., Wu, H., Guo, Y. & Chen, K-S, *J. Biochem.* ,116 (1994) 482.
6. Weaver, A.J., Kemple, M.D., Brauner, J.W., Menddelsohn, R. & Prendergast, F.G *Biochemistry* ,31 (1992) 1301.

# Prediction of intramembrane regions in transmembrane helices

Vladimir M. Tseitin and Gregory V. Nikiforovich

*Center for Molecular Design, Washington University, Box 8036, St. Louis, MO 63110, USA*

A computational procedure has been developed to place a transmembrane (TM) helical segment into a triple phase system, namely "water/octanol/water". The system crudely mimics the actual situation for the TM helical fragment immersed in a membrane environment. The procedure moves the segment through this system step-by-step along an axis perpendicular to the boundary surface. At each step, energy of solvation is estimated for several possible tilts (up to 40°) and rotations (up to 180°) of the segment, as well as for various spatial arrangements of the side chains. The backbone conformation of the segment is considered to be "frozen" in the conformer obtained by energy minimization of the isolated segment employing the ECEPP/2 force field. Solvation energy is calculated according to the protocol described in [1] and with experimental parameters for the water/octanol system deduced in [2]. As a result, the procedure obtains estimates of the "energetic cost" for transfer of the helical fragment from one side of the membrane to another. The lowest estimates can indicate boundaries of the intramembrane helical segment.

## Results and Discussion

The procedure has been applied to predict the intramembrane regions of the transmembrane helices in the L- and M-subunits of the photosynthetic reaction center from *Rhodospseudomonas viridis* (PRC) [3] and bacteriorhodopsin (BR) [4]. Using membrane thickness as a parameter for the **L-subunit** of PRC, calculations were performed for several membrane thicknesses from 16 Å to 30 Å. The best prediction was obtained assuming a membrane thickness of 24 Å (Table 1); the intramembrane boundaries of helical fragments have been predicted with an average accuracy of 1.8 residues. The transmembrane arrangements of each fragment were determined mostly by distribution of hydrophobicity for amino acid residues within the helices. The position of the first helix was determined by two relatively hydrophilic residues, Tyr52 and Ser54 at its C-terminal part; the position of the second by Glu69, Arg90, Arg96, Lys97, Glu91 and Glu93; the third helix was positioned by Arg135; the fourth helix by Ser176, Ser177, Ser197 and Asn200; and the fifth helix by Ser228 and Arg231 at its N-terminus. The predictions for the **M-subunit** (Table 2) were obtained with the best average accuracy of 3.3 residues, the membrane thickness being 24 Å. In this case no hydrophilic residue influenced the position of the first helix; the position of the second one was influenced mainly by Asp109, Ser133 and Arg134; the third by Asn147 and Thr164; the fourth helix by Ser203 and Arg226; and the fifth helix by Arg265 in its N-terminal part.

Table 1. Intramembrane fragments (N- to C-end residues) for TM helices of the PRC L-subunit.

Membrane thickness, Å	L1	L2	L3	L4	L5
16.0	37 - 50	86 - 99	128 - 134	181 - 196	231 - 244
22.0	35 - 54	82 - 99	118 - 139	180 - 200	235 - 254
24.0	33 - 54	81 - 102	114 - 137	180 - 196	229 - 249
26.0	30 - 53	81 - 99	114 - 139	174 - 196	226 - 248
30.0	29 - 54	82 - 101	112 - 140	172 - 198	226 - 252
Experiment	33 - 53	84 - 104	116 - 138	171 - 196	229 - 249

Table 2. Intramembrane fragments (N- to C-end residues) for TM helices of the PRC M-subunit.

	M1	M2	M3	M4	M5
22.0	54 - 75	110 - 131	145 - 166	207 - 225	263 - 282
24.0	49 - 68	111 - 132	144 - 163	203 - 225	260 - 282
26.0	49 - 71	109 - 131	143 - 165	201 - 223	261 - 280
Experiment	48 - 67	118 - 137	141 - 157	198 - 220	262 - 281

Table 3. Intramembrane fragments (N- to C-end residues) for TM helices of BR.

Membrane thickness, Å	BR1	BR2	BR3	BR4	BR5	BR6	BR7
22.0	9 - 30	40 - 61	80 - 101	109 - 128	135 - 153	168 - 192	205 - 224
24.0	10 - 31	44 - 63	83 - 101	106 - 127	134 - 155	167 - 189	204 - 225
26.0	9 - 31	41 - 63	83 - 103	107 - 130	137 - 157	169 - 192	203 - 227
Experiment	10 - 31	42 - 62	80 - 100	- 122	137 - 156	168 - 189	204 - 225

An average accuracy of the results for BR (Table 3) was within 1.5 residues, although the fourth helix did not reach the membrane surface at the N-terminus [4]. The best prediction in this case was also obtained for a membrane thickness *ca.* 24 Å. Comparison with experimental data shows that the tilts of helices predicted by our procedures were mostly overestimated. However, the directions of the predicted tilts were correct, since a tilt is determined mainly by solvation energy of hydrophobic and hydrophilic residues. Therefore, a helix tilts in the way that the hydrophobic residues immerse their side chains into the membrane and the most hydrophilic atomic groups are exposed to water. This consideration can explain an overtilt of the isolated TM helix, which would not occur in the case of a helical bundle. The results of this study could be used to determine suitable "starting points" for more general procedure of helix packing.

## References

1. Hopfinger, A.J. and Battershell, R.D., *J. Med. Chem.*, 19 (1976) 569.
2. Hodes, Z.I., Nemethy, G. and Scheraga, H.A., *Biopolymers*, 18 (1979) 1565.
3. Deisenhofer, J., Epp, O., Sinning, I. and Michel, H., *J. Mol. Biol.*, 246 (1995) 429.
4. Henderson, R., Baldwin, J.M., Ceska, T.A., Zemlin, F., Beckmann, E. and Downing, K. H. J. *Mol. Biol.*, 23 (1990) 899

# Synthesis of gramicidin analogs with conformationally constrained dipeptides

Wei-Jun Zhang, Jeff Kao, Eduardo Groissman and Garland R. Marshall

*Departments of Molecular Biology and Pharmacology, of Chemistry and of Molecular Microbiology, Washington University, St. Louis, MO 63110, USA*

Gramicidin (D-Phe-Pro-Val-Orn-Leu)<sub>2</sub> is a cyclic decapeptide possessing antimicrobial activity. Its 3D structure is supposed to be an antiparallel strand stabilized by the two  $\beta$ -II' type turns formed by the two D-Phe-Pro segments [1]. Kelly and co-workers [2] have replaced one of the D-Phe-Pro fragments by the  $\beta$ -hairpin-nucleating 4-(2-aminoethyl)-6-dibenzofuranpropionic acid (DBZ) and omitted the other thus creating the linear peptide Val-Orn-Leu-DBZ-Val-Orn-Leu-NH<sub>2</sub> with retention of antimicrobial activity. Independently, energy calculations performed by Chalmers, Takeuchi and Marshall suggested that incorporation of the D(L)Pro-L(D)NMeAA (where AA is any amino acid residue and the two residues are hetrochiral, either LD or DL pairs) and D(L)Pro-L(D)Pro fragments into a peptide sequence would be a synthetically simpler way to induce a reverse turn [3]. This study present the results of such an incorporation into the gramicidin sequence.

## Results and Discussion

We have synthesized several linear peptides of the general sequence Val-Orn-Leu-X-Y-Val-Orn-Leu-NH<sub>2</sub>, where X-Y were D-Pro-L-Pro, L-Pro-D-Pro, D-Pro-L-NMePhe, L-Pro-D-NMePhe, D-Pro-L-Pip and L-Pro-D-Pip. Synthesis of these turn mimetic peptides presented some difficulties in coupling due to steric hinderance. They were successfully prepared using the Fmoc amino acid fluoride method or HATU coupling with the acid fluoride method which gave superior results. Formation of the Leu-X-Y-Val amide bonds was followed by a chloranil and acetoaldehyde test in DMF. This method was found to give an intense color only for secondary amines and was used to determine the completeness of coupling to these N-dialkyl amino acids. The color was the same (deep blue) using *p*-chloranil, but varied significantly using *o*-chloranil depending on the secondary amine (strong coffee color for Pro, deep purple red for Pip, and yellow for NMePhe).

The proton NMR spectra were obtained for Val-Orn-Leu-D-Pro-L-Pro-Val-Orn-Leu-NH<sub>2</sub> in both water and DMSO and for Val-Orn-Leu-D-Pro-L-NMePhe-Val-Orn-Leu-NH<sub>2</sub> in DMSO. All NMR measurements employed a Varian Unity Plus 500 or Varian Unity 600 spectrometer. NOESY and TOCSY spectra of these peptides were acquired and cross peak assignment completed. The spectra for the Val-Orn-Leu-D-Pro-L-Pro-Val-Orn-Leu-NH<sub>2</sub> in water were typical for an unordered conformation, whereas the same spectra in DMSO were more suitable for structural interpretation. One hundred possible 3D structures for Val-Orn-Leu-D-Pro-L-Pro-Val-Orn-Leu-NH<sub>2</sub> were generated from the NMR data in DMSO using the Tinker program [4] employing distance geometry techniques.

Some were further subjected to energy minimization by the SYBYL program which did not change their geometrical shapes to a significant extent.

The expected turns (or, more precisely, reverse turns) at the D-Pro-L-Pro fragment were present in all 100 generated conformers of Val-Orn-Leu-D-Pro-L-Pro-Val-Orn-Leu-NH<sub>2</sub>. However, only two conformers out of 100 could be regarded as more or less regular  $\beta$ -hairpin structures implying that chain reversal was not sufficient to stabilize the hairpin conformation in DMSO. All other conformers displayed significant conformational mobility of the N- and C-terminal Val-Orn-Leu tripeptide segments. The obvious conclusion is that the D-Pro-L-Pro fragment (and, perhaps, most of the other fragments considered in this study) are good enhancers of the central peptide chain-reversal, but may not be suitable for full induction of the  $\beta$ -hairpin structure in this particular sequence in DMSO and presumably in water. Accordingly, if the  $\beta$ -hairpin structure of this linear gramicidin sequence, is crucial for displaying antimicrobial activity our peptides may show diminished activity in comparison with Val-Orn-Leu-DBZ-Val-Orn-Leu-NH<sub>2</sub>. Indeed, the compounds were found inactive in "Minimal Inhibitory Concentration" assays against the strain of *E. coli* used by Kelly et al. although cyclic gramicidin S itself was a potent antimicrobial. These are preliminary results, however, and the compounds need to be directly compared with Val-Orn-Leu-DBZ-Val-Orn-Leu-NH<sub>2</sub>.

### Acknowledgments

This work was supported by the NIH Grant GM53630.. The authors are grateful to Prof. Gregory V. Nikiforovich for helpful discussions.

### References

1. Schmidt, G. M., Hodgkin, D. C., Oughton, B. M., *Biochem. J.*, 65 (1957) 744
2. Tsang, K. Y., Diaz, Gracian N Kelly, *J. Am. Chem. Soc.*, 116 (1994) 3985.
3. Y. Takevch, G. R. Marshall. *J. Am. Chem. Soc.*, in press.
4. Ponder, J.W., Richards, F. M. *J.Comput.Chem.*, 8 (1987) 1016.

# Conformational studies of rat brain sodium ion channel segment IS4 in different media

Zhenwei Miao,<sup>a</sup> Yun Jiang,<sup>a</sup> Saburo Aimoto,<sup>b</sup> Xiaojie Xu<sup>a</sup> and Youqi Tang<sup>a</sup>

<sup>a</sup>Department of Chemistry, Peking University, Beijing 100871, China; <sup>b</sup>Institute for Protein Research, Osaka University, Osaka 565, Japan

IS4 is the fourth of six transmembrane segments within the first domain of the rat brain sodium ion channel [1, 2]. It consists of 22 amino acid residues, the sequence of which is SALRTRVLRALKTISVIPGLK, with regular alternations of one positively charged and two hydrophobic residues. This segment is highly homologous with other sodium ion channels of different species [1, 2]. It is thus believed that IS4 plays an important role in channel opening and closing. There have been two main models proposed to explain the mechanism of action of IS4. One is the “sliding helix” model [1, 3], and the other is the “conformational change” model [4, 5]. However, the mechanism by which of IS4 regulates ionic conductance is still unclear. It is thus of great significance to elucidate the conformational properties of IS4 in different media. For this purpose, we have synthesized the IS4 peptide and characterized it under various conditions.

## Results and Discussion

The IS4 peptide was synthesized by solid phase method using Boc/Bzl chemistry on MBHA resin. Circular dichroism (CD) studies demonstrated that IS4 exhibits distinct conformations in different media (Fig. 1). In neutral aqueous buffers IS4 exists mostly in random coil structure, but in organic solvents IS4 becomes ordered. IS4 exhibits highly  $\alpha$ -helical conformation in ethanol, 1-propanol, n-butanol and trifluoroethanol, but  $\beta$ -sheet in methanol. The amount of  $\beta$ -sheet structure induced by methanol and  $\alpha$ -helix structure induced by ethanol increase dramatically as the concentrations of methanol and ethanol change from 25% to 100% (Fig. 2). In contrast, the amount of  $\alpha$ -helix structure induced by n-propanol increases only slightly, and in TFE remains almost the same. Moreover, the  $\alpha$ -helix content of IS4 in n-butanol, TFE and aqueous SDS are constant. This means that the conformations of IS4 these hydrophobic media are very similar.

Two-dimensional <sup>1</sup>H NMR techniques were also employed to determine the structure of IS4 in 90% TFE aqueous solution. Proton resonance assignments were obtained using 2D DQF-COSY, TCOSY and NOESY techniques. The cross-peak volumes in NOESY spectra were used for calculating the structure of IS4. These data, combined with the  $\Phi$  angle constraints deduced from <sup>3</sup>J<sub>H<sub>N</sub> $\alpha$  coupling constants, gave rise to a set of 10 structures with the program DIANA. The results, refined by unrestrained energy minimization, indicate that the conformation of IS4 in 90% CF<sub>3</sub>CD<sub>2</sub>OH aqueous solution is  $\alpha$ -helix from Leu<sup>3</sup> to Ile<sup>15</sup>.</sub>

Similarly, the conformation of IS4 in DMSO-d<sub>6</sub> was also determined by 2D-NMR techniques [6], and was found to be a random coil structure rather than  $\alpha$ -helix.

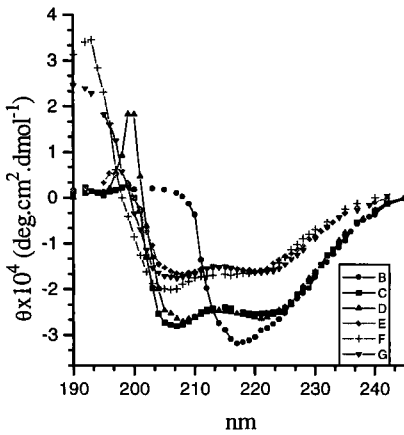


Fig. 1. CD spectra of IS4 in methanol(B), ethanol(C), 1-propanol(D), 1-butanol(E), TFE(F) and SDS(G) solution(SDS:IS4=100).

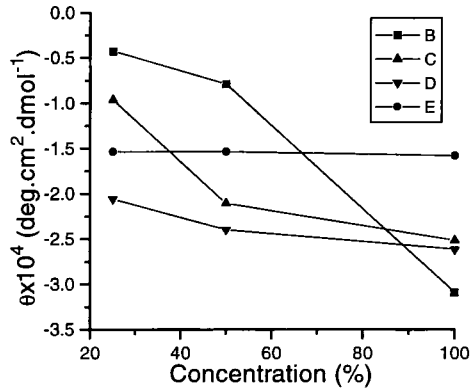


Fig. 2.  $\theta$  value changes with concentrations of ethanol(C), 1-propanol(D), and TFE(E), at 222 nm, but methanol(B) at 216 nm.

## Conclusion

According to the results of CD and 2D-NMR studies, the structure of IS4 is sensitive to its environment, undergoing conformational transition from random coil to  $\alpha$ -helix or  $\beta$ -sheet. This property may be related to its functional behavior in ion channel regulation.

## References

1. Catterall, W.A., *Science*, 242 (1988) 50.
2. Betz, H., *Biochemistry*, 29 (1990) 3591.
3. Guy, H.R. and Seetharamulo, P., *Proc. Natl. Acad. Sci. USA*, 83 (1986) 508.
4. Kosower, E.M., *FEBS Lett.*, 234 (1985) 1982.
5. Guy, H.R. and Conti, F., *TINS*, 13 (1990) 201.

# Identification of a novel human CD8 surface region involved in MHC class I binding

Song Li, Swati Choksi, Simei Shan, Jimin Gao,  
Robert Korngold, and Ziwei Huang

*Kimmel Cancer Institute, Jefferson Medical College, Thomas Jefferson University, Philadelphia, PA 19107, USA*

Human CD8 (hCD8) is a glycoprotein expressed on the surface of T cells that has specificity for antigens presented by major histocompatibility complex (MHC) class I proteins. hCD8 functions as a co-receptor with the T-cell antigen receptor (TCR) by binding to the MHC class I molecule on the antigen-presenting cell, thereby increasing the avidity of the TCR for its ligand. In this study, we have utilized an approach combining molecular modeling, synthetic peptide mapping, and hCD8-MHC class I binding assay to probe precise surface regions of hCD8 involved in MHC class I binding. These experiments have led to the identification of the DE loop of hCD8 protein that is implicated in the hCD8 interaction with MHC class I molecules. Synthetic conformationally restricted peptide analogs derived from the hCD8 DE loop have been shown to specifically inhibit hCD8-MHC class I binding. To further define the functional role of each residue of the DE loop, DE loop peptide analogs containing a series of alanine substitutions were synthesized and tested. These studies provide information about the structure-function relationship between the surface structural feature of the CD8 DE loop and CD8 mediated immunological function.

## Results and Discussion

Using peptide mapping and theoretical analysis methods similar to those used in recent 7CD4 studies [1-4], we have synthesized potent CD8 peptide inhibitors derived from the DE loop region of the CD8 protein as a surface functional epitope that may be important for the interaction between CD8 and MHC class I [5]. A conformationally restricted peptide, which was designed to mimic the surface shape and composition of the DE loop region of CD8, was able to specifically inhibit CD8-MHC class I binding in a cell adhesion assay and block human CD8-mediated T cell cytolytic responses *in vitro* (Fig. 1). A series of alanine substitution experiments were carried out for the peptide, and the results suggested an interesting structure-function relationship between the precise surface structure of the CD8 DE loop and CD8-dependent biological function. These results have revealed an important new functional site on the CD8 protein surface as a target for drug design.

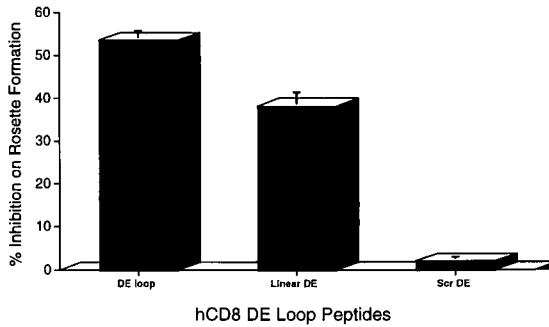


Fig. 1. Inhibitory effect of the synthetic peptide analogs derived from the hCD8 DE loop on hCD8-MHC class I binding as measured by the rosette formation. The sequences of the synthesized peptides are as follows: DE loop: CKRLGDTFVC, Linear DE: KRLGDTFV, Scrambled DE: CVGTFRKDLG.

## Conclusion

A conformationally restricted peptide, which was designed to mimic the surface shape and composition of the DE loop region of CD8, was able to specifically inhibit CD8-MHC class I binding in a cell adhesion assay and block human CD8-mediated T cell cytolytic responses *in vitro*. The experimental results of the peptide mapping and alanine substitution have revealed an important new functional site on the CD8 protein surface as a target for drug design.

## Acknowledgments

These studies were supported in part by grants from the National Institutes of Health, the American Cancer Society, the National Multiple Sclerosis Society and the Sidney Kimmel Foundation for Cancer Research. We would like to thank members of our laboratories and our collaborators for their contribution and helpful discussion. Z.H. is the recipient of the Kimmel Scholar Award in cancer research.

## References

1. Satoh, T., Li, S., Friedman, T.M., Wiaderkiewicz, R., Korngold, R. and Huang, Z. *Biochem. Biophys. Res. Commun.*, 225 (1996) 438
2. Satoh, T., Aramini, J.M., Li, S., Friedman, T.M., Gao, J., Edling, A., Townsend, R., Germann, M.W., Korngold, R. and Huang, Z. *J. Biol. Chem.*, 272 (1997) 12175.
3. Li, S., Gao, J., Satoh, T., Friedman, T., Edling, A., Koch, U., Choksi, S., Han, X., Korngold, R. and Huang, Z. *Proc. Natl. Acad. Sci. USA*, 94 (1997) 73.
4. Huang, Z., Li, S. and Korngold, R. *Med. Chem. Res.*, 7 (1997) 137.
5. Li, S., Choksi, S., Shan, S., Gao, J., Korngold, R., and Huang, Z. (1997) manuscript submitted.

# Surveying the protein folding landscape: equilibrium models for partially folded intermediates of bovine pancreatic trypsin inhibitor (BPTI)

Christopher M. Gross<sup>a,b</sup>, Clare Woodward<sup>b</sup> and George Baranya

<sup>a</sup>Department of Chemistry, University of Minnesota, Minneapolis, MN 55455, USA; <sup>b</sup>Department of Biochemistry, University of Minnesota, St. Paul, MN 55108, USA

Despite considerable advances over the past several years, the problem of protein folding remains perplexing. The “new view” of protein folding, championed by Chan and Dill, proposes that proteins fold along many pathways with the number of conformations diminishing as the protein collapses [1]. This is opposed to the previously favored frame-work hypothesis, which postulates a single pathway involving early formation of nascent secondary structure [2]. Equilibrium partially folded species are thought to resemble transient intermediates that exist in the first few milliseconds of folding [3]. Previous work from our laboratory has demonstrated that the BPTI analogue termed [14-38]<sub>Abu</sub>, which retains one disulfide bond between residues 14 and 38 and replaces other paired cysteines with pairs of the non-natural amino acid  $\alpha$ -amino-*n*-butyric acid (Abu), has the characteristics of a partially folded molten globule with a native-like hydrophobic core and multiple conformations in the outer regions [4,5]. We have now synthesized the related BPTI variants [30-51]<sub>Abu</sub> and [14-38]<sub>Ala</sub>. Biophysical criteria indicate that removal of four methyl groups from [14-38]<sub>Abu</sub> is sufficient to destabilize the partially folded state so that the protein no longer favors formation of the native-like, antiparallel  $\beta$ -sheet core. In contrast, the structure analogue [30-51]<sub>Abu</sub> is quite different from that reported in the literature for other analogues of [30-51] [6,7].

## Results and Discussion

Most studies of single disulfide mutants of BPTI utilize recombinant expression systems substituting either alanine [6] or serine [7] for reduced cysteine. Our work is predicated on total chemical synthesis, and allows the incorporation of Abu, which in our judgment is a superior cysteine isostere [4] (Fig. 1).

At 3° C and pH 6.3, [14-38]<sub>Ala</sub> shows negligible molar ellipticity at 220 nm, as well

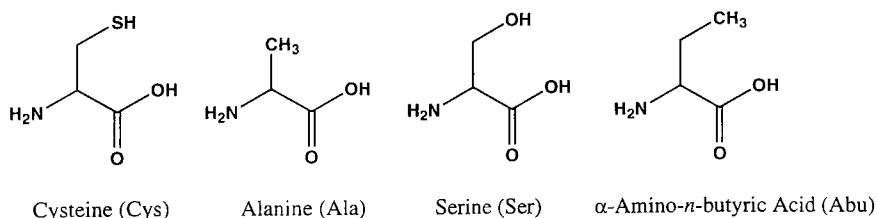


Fig. 1. Reduced cysteine replacements.

as an NMR spectrum lacking downfield dispersion of the amide protons. The structure present in [14-38]<sub>Abu</sub> is notably absent in [14-38]<sub>Ala</sub>. As reported previously, the  $T_m$  of [14-38]<sub>Abu</sub> is approximately 19 °C [4,8]. Taken together, the extra non-polar heavy atoms present in [14-38]<sub>Abu</sub> contribute considerably to its partially folded state. We anticipated that [30-51]<sub>Abu</sub> should be *stabilized* versus the analogs of [30-51] reported in the literature, i.e., [30-51]<sub>Ser</sub> with a  $T_m$  = 15 °C [7] and [30-51]<sub>Ala</sub> with a  $T_m$  of 35 °C [6]. Consistent with this, preliminary results indicate that [30-51]<sub>Abu</sub> denatures only at 4 M guanidine hydrochloride, and temperature-induced unfolding is clearly non-cooperative in the range 3-45 °C. The circular dichroism spectrum of [30-51]<sub>Abu</sub> has less molar ellipticity at 220 nm than [14-38]<sub>Abu</sub> (Fig. 2). However, from the trough above 200 nm, we conclude that [30-51]<sub>Abu</sub> has more structure than [R]<sub>Abu</sub> (Fig. 2) as well as some previously reported tyrosine to alanine mutants of [14-38]<sub>Abu</sub> [9] in random coil conformation.

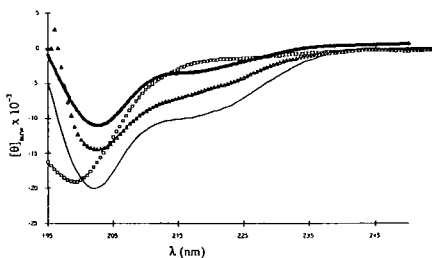


Fig. 2. Circular dichroism spectra of BPTI analogues at 3° C, pH 6.3. Thin line wt-BPTI, open triangles [14-38]<sub>Abu</sub>, open squares [R]<sub>Abu</sub>, thick line [30-51]<sub>Abu</sub>.

## Conclusion

Seemingly minor changes in amino acid sequence often lead to rather large protein conformational and/or stability changes. As such, the rules of protein folding are subtle and models for studying folding must perturb the protein as little as possible. The role of cysteine crosslinks in securing proteins, largely by destabilizing the denatured state, is well appreciated. The present studies point also to cysteine acting as a hydrophobic residue.

## References

1. Chan, S., Dill, K., Nature Struct. Biol., 4 (1997) 10.
2. Udgaonkar, J., Baldwin, R., Nature 335 (1988), 694.
3. Redfield, C., Smith, A., Dobson, C., Nature Struct. Biol., 1 (1994) 23.
4. Ferrer, M., Barany, G., Woodward, C., Nature Struct. Biol., 2 (1995) 211.
5. Barbar, E., Barany, G., Woodward, C. Biochemistry, 34 (1995) 11423.
6. Staley, J. P., Kim, P. S., Protein Sci., 3 (1994) 1822.
7. van Mierlo, C. P., Darby, N. J., Neuhaus, D., Creighton, T., J. Mol. Biol., 222 (1991) 353.
8. Barbar, E., LiCata, V., Barany, G., Woodward, C., Biophysical Chemistry, 64 (1997) 45.
9. Barbar, E., Barany, G., Woodward, C., Folding & Design, 1 (1995) 65.

# Structure activity studies of normal and retro pig cecropin- melittin hybrids

Padmaja Juvvadi, Satyanarayana Vunnam, Barney Yoo,  
and R. B. Merrifield

The Rockefeller University, 1230 York Ave, New York, NY 10021, USA

Antimicrobial peptides show significant diversity in sequence and structure but may be grouped into cecropins, melittins, magainins, cryptidins, defensins, proline-arginine rich peptides and others [1]. It has been found that certain synthetic hybrid peptides containing sequences from different antibacterial peptides were more active than the parent molecules [2]. Using the solid-phase technique we have synthesized various chimeric analogs of cecropin P1 (CP1) [3] and melittin (M) [4], to improve antibacterial activity and widen the spectrum of susceptible microbial species. The normal and retro sequences of the hybrids were synthesized to explore the effect of sequence, helix dipole, charge and amphipathicity on their antibacterial activity and channel forming ability.

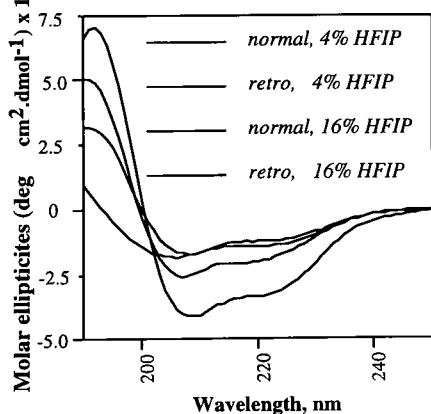
## Results and Discussion

Hybrids of CP1 and M [SWLSKTAKKIGAVLKV, CP1(1-9)M(2-8) (1), SWLSKTAKKGIGAVLKV, CP1(1-9)M(1-8) (2), and SWLSKTAKKLIGAVLKVL, CP1(1-10)M(2-9) (3)] amides were found to be active against Gram-negative *Escherichia coli* and also Gram-positive *Streptococcus pyogenes* (Table 1). The other bacterial strains, *Pseudomonas aeruginosa*, *Staphylococcus aureus*, and *Bacillus subtilis*, were found to be resistant to 1 and 2. However, analog 3 was also active against these three test bacteria. Acetylation of the amine resulted in lowered activity indicating the importance of the presence of free amine.

Retro analogs of 16-18 residue hybrids of CP1 and melittin showed lowered activity against all five bacteria tested. These results suggest that both sequence and helix dipole are important structural features for the activity of CP1-M hybrids.

The CD spectra of normal and retro sequences of all the synthesized CP1 - melittin hybrids revealed a random conformation in phosphate buffer at pH 7.2. The ellipticities of normal and retro peptides are not the differ, having the same amino acid composition because the sequences are inverted (Fig. 1). The retro peptide showed low  $\alpha$ -helical structure at the lower concentrations of HFIP, but as the HFIP concentration was increased, the retro analog had approximately the same  $\alpha$ -helicity as the normal peptide (Table 1). At a higher concentration

Fig. 1 : CD Spectra of normal and retro CP1(1-10)M(2-9)NH<sub>2</sub>



of HFIP (16-20%) the retro sequence showed higher helical content than its normal sequence. Acetylation of the N-terminus of the 16-18 residue normal and retro hybrid peptides reduced the net charge from +5 to +4 but had only a small effect on their secondary structure. Retro-CP1(1-10)M(2-9) amide showed higher helicity and is also more active compared to the other retro analogs synthesized.

Table 1. Lethal concentrations (mM), % of  $\alpha$ -helix and retention times for CP1-M hybrids.<sup>a</sup>

Peptide amide	Size	Escherichia coli	Streptococcus pyogenes	HFIP		Retention Time (min.)
				8%	20%	
CP1(1-9)M(2-8)	16	3.1	0.89	17	44	15.2
Retro-CP1(1-9)M(2-8)	16	64.8	8.9	12	61	10.7
CP1(1-9)M(1-8)	17	12	7.6	0	28	17.5
Retro-CP1(1-9)M(1-8)	17	>350	>350	0	35	8.4
CP1(1-10)M(2-9)	18	3.1	0.2	42	44	28.1
Retro-CP1(1-10)M(2-9)	18	4.6	5.0	46	75	17.2

<sup>a</sup>Lethal concentrations calculated from inhibition zones on agarose plates,  $\alpha$ -helices obtained from CD measurements and retention times from reverse phase HPLC

The retention times (RT) of normal and the retro sequences of the 16-18 residue peptides were obtained by reverse-phase analytical HPLC. It is interesting to note that these sequences with the same amino acid composition and relative hydrophobic contribution have different RT. This may be due to the conformational constraints in the retro sequence as compared to the normal peptide, which is probably due to the inverted helix dipole when viewed as the normal sequence. In all cases peptides with a normal sequence eluted later than the corresponding retro sequences (Table 1).

CP1-M hybrids produced ion-channels in artificial bilayers formed in hexadecane but not in bilayers formed in decane.  $\alpha$ -Helical 16-18 mers should span a distance of 24-27 Å (1.5 Å/residue) and are of a length appropriate to form channels in the bilayer formed in hexadecane but not in decane. We believe that these hybrid analogs first bind electrostatically to the phospholipid bilayer followed by a rearrangement to form an amphipathic helical conformation that leads to ion-channels or pores. A similar mechanism was earlier described for cecropins [2] and melittin [5]. The passage of ions would lower the proton gradient, destroy the membrane potential, thus stopping cellular metabolism, followed by cell death.

## References

1. Boman, H. G., Ann. Rev. Immunol., 13, (1995) 61.
2. Andreu, D., Ubach, J., Boman, A., B. Wahlin, B., Wade, D., Merrifield, R. B. and Boman, H. G., FEBS Lett., 296 (1992) 190.
3. Lee, J. Y., Boman, A., Chuanxin, S., Andersson, M., Jornvall, H., Mutt, V. and Boman, H. G., Proc. Natl. Acad. Sci. USA., 86 (1989) 9159.
4. Terwilliger, T. C. and Eisenberg, D., J. Biol. Chem., 257 (1982) 6016.
5. Juvvadi, P., Vunnam, S. and Merrifield, R. B., J. Am. Chem. Soc., 118 (1996) 8989.

**Session VI**

**Receptor-Ligand Interactions**



# A peptide mimetic of erythropoietin: Critical residues and description of a minimal functional epitope

**Dana L. Johnson,<sup>a</sup> Francis X. Farrell,<sup>a</sup> Frank J. McMahon,<sup>a</sup> Jennifer Tullai,<sup>a</sup> Francis P. Barbone,<sup>a</sup> Steven A. Middleton,<sup>a</sup> Kenway Hoey,<sup>b</sup> Oded Livnah,<sup>c</sup> Nicholas C. Wrighton,<sup>d</sup> William J. Dower,<sup>d</sup> Linda S. Mulcahy,<sup>a</sup> Enrico A. Stura,<sup>c</sup> Ian A. Wilson<sup>c</sup> and Linda K. Jolliffe<sup>a</sup>**

*<sup>a</sup>The R. W. Johnson Pharmaceutical Research Inst., Drug Discovery Research, 1000 Route 202 Box 300, Raritan, NJ, and <sup>b</sup>3535 General Atomic Court, San Diego, CA, <sup>c</sup>The Scripps Research Inst., Department of Molecular Biology and the Skaggs Inst. of Chemical Biology, 10550 N. Torrey Pines Road, La Jolla, CA, <sup>d</sup>Affymax Research Inst., 4001 Miranda Ave, Palo Alto, CA*

We have recently discovered a series of peptides which serve as erythropoietin (EPO) receptor agonists [1]. Further, the x-ray crystal structure of a member of this series (EMP1) complexed with the extracellular ligand binding domain of the erythropoietin receptor (erythropoietin binding protein; EBP) has been described [2]. Their ~2 kDa molecular weight makes these peptides significantly smaller than EPO and the sequences of these peptides are unrelated to the primary sequence of EPO. A significant feature of the peptide-receptor interaction is the ability of the mimetic peptide to promote both the crystallographic and solution phase dimerization of the EBP [2]. This family of EPO mimetic peptides is characterized by a conserved motif of xxxYxCxxGPxTWxCxPxxx, in which the cysteine residues are oxidized to form a disulfide bond and the indicated residues appear exclusively or at high frequency. Structurally, the -GPxTW- region forms a slightly distorted type 1  $\beta$ -turn and is primarily involved in peptide-receptor contacts. The Tyr<sup>4</sup> side-chain hydroxyl makes the only sidechain hydrogen bond from the peptide to the receptor [2].

## Results and Discussion

The original phage selection process and subsequent sequence analysis produced almost 80 distinct sequences with the EPOR binding [1]. Several positions within the 20 amino acid sequence were found to appear exclusively or at high frequency as indicated above. These conserved positions were replaced with Ala to determine the effect on both binding and mimetic activity in vitro. These substitutions were made within a single peptide sequence, EMP1, and the data are presented in Table 1. We employed a cell free binding assay format to measure the ability of the parent peptide or variants to compete for [<sup>125</sup>I]EPO binding to immobilized EBP [3] and EMP1 demonstrates an IC<sub>50</sub> of 5  $\mu$ M. The ability of the peptide variants to support cellular proliferation as an indicator of receptor activation was studied in an EPO-responsive cell line that expresses the recombinant human EPO receptor. Results from proliferation assays were standardized to the number of counts observed at the 50% maximal value obtained with EPO to calculate an EPO ED<sub>50</sub>

(Effective Dose 50% stimulation) value. The data were recorded as their measured ED<sub>50</sub>, if a peptide displayed adequate potential to reach the 50% maximum response level of EPO or >10  $\mu$ M (the highest concentration tested), if the peptide retained some activity but did not reach the 50% level. Peptides which did not induce levels of radioactivity greater than the EPO free control were scored as inactive. The data are reported as EPO ED<sub>50</sub> values since the more traditional value of half-maximal activity of each individual peptide could not be determined since peptide solubility or residual DMSO concentrations preclude determination of a plateau from which half-maximal activity can be estimated.

Most of the Ala substitutions of conserved residues decreased the relative binding affinity. Trp<sup>13</sup> substitution (EMP13) had the most significant effect, resulting in almost undetectable binding and a complete loss of mimetic activity. Ala substitution of Tyr<sup>4</sup>, Gly<sup>9</sup> or Thr<sup>12</sup> each resulted in significant relative binding losses and a concomitant loss of mimetic action. Unexpectedly, Ala substitution of Pro<sup>10</sup> (EMP10) had no effect on relative binding or mimetic activity suggesting that an acceptable  $\beta$ -turn structure can still be achieved. Substitution of Pro<sup>17</sup> (EMP15) resulted in a 100-fold loss of mimetic activity. The relative binding of this peptide was also significantly altered and was limited by decreased peptide solubility. This Pro is not as conserved as other positions in the phage selected sequences [1] and the reason for the importance of the residue is unclear. The two aromatic residues at positions Tyr<sup>4</sup> and Trp<sup>13</sup> appear to play important roles in both EPO receptor binding ability and EPO mimetic properties of EMP1. To investigate this further, Tyr<sup>4</sup> or Trp<sup>13</sup> was replaced with Phe. Restoration of aromaticity at position 4 (EMP8) resulted in the recovery of some binding activity (12-fold less than EMP1) and mimetic activity. Restoration of aromaticity at Trp<sup>13</sup> (EMP14) resulted in recovery of activity to a level similar to EMP1. The data indicate that aromatic residues at these positions are important for EMP1 agonist activity.

We next sought to determine the minimal active structure within the EMP1 sequence by truncating residues of the peptide outside the disulfide-bond. Deletion of the two C-terminal Gly (EMP16) resulted in a sequence with improved proliferative properties, while deletion of only the N-terminal Gly (EMP17) had a net negative effect. Deletion of the four N- and C-terminal Gly had a net negative impact on both binding and bioactivity (EMP18). Further truncation down to a sequence with two residues on either side of the cysteines (EMP19), demonstrated very poor activity. This loss of activity could be partially restored by deletion of the C-terminal Pro of EMP19 to obtain EMP20. This peptide sequence represents the minimal active structure that we have identified to date. Deletion of the C-terminal Lys (EMP21) resulted in a peptide whose activity measurements were limited by poor solubility properties. Within the context of the EMP20 sequence, which retained binding and proliferative potential, deletion of the Tyr (EMP24) resulted in an inactive peptide with retained binding activity.

Table 1. EMP-1 Based Substitution and Truncation Peptides

Sequence No.	Sequence	Binding IC <sub>50</sub> (μM)	Relative Binding‡	EPO ED <sub>50</sub> (μM)
EMP1	GGTYSCHFGPLTWVCKPQGG	5	1	0.1
EMP6	GGT <u>A</u> SCHFGPLTWVCKPQGG	120	24	IA <sup>1</sup>
EMP8	GGT <u>E</u> SCHFGPLTWVCKPQGG	60	12	>10
EMP9	GGTYSCHF <u>A</u> PLTWVCKPQGG	80	16	IA
EMP10	GGTYSCHFG <u>A</u> LTWVCKPQGG	10	2	0.3
EMP12	GGTYSCHFGPL <u>A</u> WVCKPQGG	90	18	IA
EMP13	GGTYSCHFGPLT <u>A</u> VCKPQGG	>500	>100	IA
EMP14	GGTYSCHFGPLT <u>F</u> VCKPQGG	30	6	0.1
EMP15	GGTYSCHFGPLTWVCK <u>A</u> QGG	>100*	>20*	10
EMP16	GGTYSCHFGPLTWVCKP <u>Q</u>	8	1.6	0.011
EMP17	TYSCHFGPLTWVCKPQGG	40	8	0.3
EMP18	TYSCHFGPLTWVCKP <u>Q</u>	30	6	1
EMP19	YSCHFGPLTWVCKP	45	9	>10
EMP20	YSCHFGPLTWVCK	70	14	8
EMP21	YSCHFGPLTWV <u>C</u>	>250*	>50*	IA
EMP24	SCHFGPLTWVCK	90	18	IA

Binding relative to EMP-1; <sup>1</sup>IA= inactive; \*Solubility limited ‡

These findings are in agreement with the X-ray crystal structure of the EMP1-EBP complex in which hydrophobic interactions play a critical role in the assembly of two mimetic peptides and two receptor subunits [2]. This information should prove useful in the reduction of the mimetic peptide into a small molecule with EPO-mimetic activity.

### Acknowledgments

This work supported in part by NIH Grant GM49497 (I.A.W.) and the Rueff-Wormser Scholarship Fund (O.L.)

### References

1. Wrighton, N.C., Farrell, F.X., Chang, R., Kashyap, A. K., Barbone, F.P., Mulcahy, L.S., Johnson, D.L., Barrett, R.W., Jolliffe, L.K., and Dower, W.J., *Science* 273 (1996) 458.
2. Livnah, O., Stura, E.A., Johnson, D.L., Middleton, S.A., Mulcahy, L.S., Wrighton, N.C., Dower, W.J., Jolliffe, L.K., and Wilson, I.A., *Science* 273 (1996) 464.
3. Johnson, D.L., Middleton, S.A., McMahon, F., Barbone, F.P., Kroon, D., Tsao, E., Lee, W.H., Mulcahy, L.S. and Jolliffe, L.K., *Protein Expression and Purification* 7 (1996) 104.

# Structure of rhodopsin-bound C-terminal $\alpha$ -peptide of transducin

Oleg Kisselev,<sup>a</sup> Yang C. Fann,<sup>b</sup> N. Gautam<sup>a</sup>  
and Garland R. Marshall<sup>b,c</sup>

*<sup>a</sup>Departments of Anesthesiology and of <sup>b</sup>Molecular Biology and Pharmacology and the <sup>c</sup>Center for Molecular Design, Washington University Medical School, St. Louis, MO 63110, USA*

Determination of the receptor-bound conformation of bioactive peptides as a prelude to peptidomimetic design has been a long-term goal of many investigators. One indirect approach has been to incorporate covalent constraints into peptides to limit their conformations and help resolve this issue. An experimental paradigm for the direct determination of the conformation of peptides when bound to G-protein coupled receptors (GPCRs) would be welcome. A significant problem facing such an experimental approach is the limitation of receptor availability. Visual signals in retinal rod cells are triggered by the interaction of photoexcited rhodopsin (Rh\*) with the heterotrimeric GTP-binding protein transducin (Gt). This G-protein coupled receptor has been well characterized with regard to the light-activation and is readily available in quantities sufficient for biophysical studies from bovine retina. The GTP-bound form of activated Gt differs markedly from the inactive GDP-bound state (1-4). Molecular details of the mechanism by which Rh\* recognizes Gt and catalyzes nucleotide exchange remain obscure. Several domains on the  $\alpha$ -, and  $\beta\gamma$ -subunits of Gt contribute to its rhodopsin-binding site and an eleven-residue segment, IKENLKDCGLF, at the carboxyl terminus of the  $\alpha$ -subunit, Gt $\alpha$ (340-350), has been shown to play a major role in receptor recognition and nucleotide exchange (5-7). This C-terminal segment of Gt $\alpha$  is disordered in all X-ray structures of G<sub>t</sub> (1-4). Transferred nuclear Overhauser effect (TRNOE) spectroscopy was used to elucidate the structure of the Gt $\alpha$ (340-350) peptide when bound to Rh\*. Despite the fact that this peptide binds to the intracellular face of rhodopsin rather than to the external face as do peptide ligands for other GPCRs, the success of this approach provides a model for the direct experimental determination of the GPCR-bound conformation of peptide ligands.

## Results and Discussion

In the dark-adapted state, only two medium-range NOE interactions were observed in the sample of Gt $\alpha$ (340-350) with rhodopsin. Exposure to 495 nM light produced a remarkable increase to 98 from 2 in the number of medium and longer-range interactions observed indicative of a discrete conformation in the Rh\*-bound state to give a total of 103 additional NOE cross-peaks (Fig. 1). These additional NOE cross-peaks relax in parallel to the decay of the light-activated form of rhodopsin, metarhodopsin II (MII) thought to bind and activate Gt. This argues for specific binding of Gt $\alpha$ (340-350) to Rh\* and parallels the ability of Gt to form a transient high-affinity complex with Rh\* (8). The paucity of

medium to long-range NOEs in the dark-adapted spectra indicates minimal, if any, binding of Gt $\alpha$ (340-350) to dark-adapted rhodopsin.

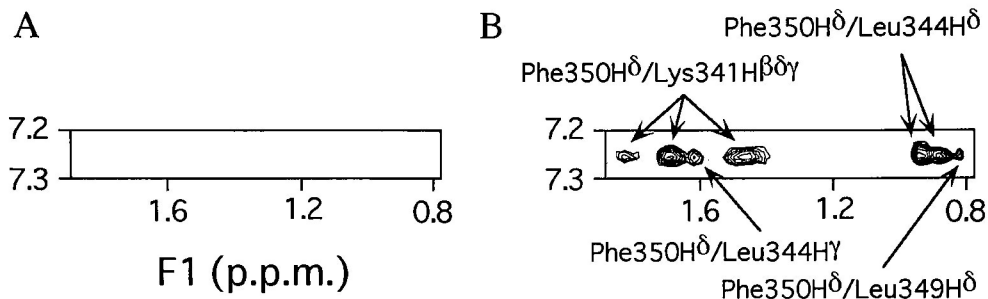


Fig. 1. Cross-peaks in the aromatic-aliphatic region showing interactions between F350 aromatic protons and sidechain protons of L349, L344, and K341 from the NOESY spectra of Gt $\alpha$ (340-350) in the presence of the dark-adapted (left panel) and photoexcited rhodopsin (right panel).

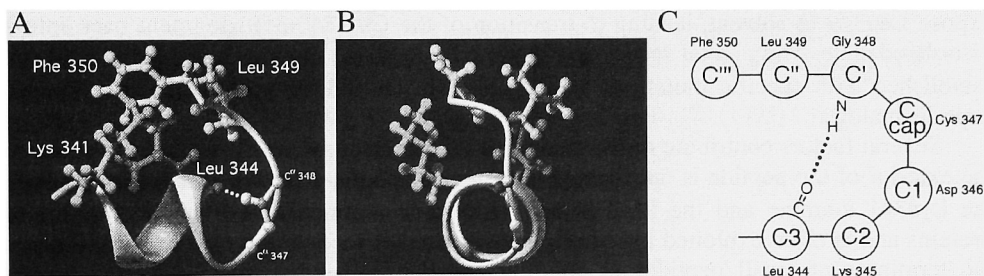


Fig. 2. Two orthogonal views of Rh\*-bound conformation of Gt $\alpha$ (340-350) IKENLKDCGLF as determined by TRNOESY. A = front, B = end view, C = scheme of the C-cap motif.

Independent computations of the NMR structure of Gt $\alpha$ (340-350) bound to Rh\* gave 20 structures with a high degree of convergence ( $0.30 \pm 0.12$  Å r.m.s.d. for C $\alpha$ s) for the bound state of Gt $\alpha$ (340-350) with a helical turn in the middle of the undecapeptide followed by an open reverse turn (Fig. 2). The Rh\*-bound structure of Gt $\alpha$ (340-350) is characterized by multiple strong peaks in the TRNOE spectra between the Phe350 aromatic ring and the sidechains of Leu349, Leu344 and Lys341 (Fig. 1) of Leu344 and the amide hydrogen of Gly348 which additionally stabilizes the reverse turn. The helical turn involving Glu342, Asn343, Leu344, Lys345, and Asp346 is supported by 48 medium- and long-range NOEs, and two main-chain hydrogen bonds between Lys341-Lys345 and Glu342-Asp346. The NOE cross-peak between the amide protons of Lys345 and Asn343,

(NH<sub>i,i+2</sub>) agrees with the presence of a helical turn. Gly348 is highly conserved in G-proteins of Gt and Gi families and appears invariant at position 348 in twenty four Gt $\alpha$ (340-350) peptide analogs selected for rhodopsin binding (9) consistent with the  $\phi/\psi$  torsional angles of Rh\*-bound Gt $\alpha$ (340-350). Expression of heterotrimeric G<sub>t</sub> mutants with substitutions of Gly348 by Ala or Pro (6, 7) in the  $\alpha$ -subunit severely impairs interaction with rhodopsin. Based on earlier NMR studies, Gly348 was suggested to be part of a type II  $\beta$ -turn at the C-terminus of the  $\alpha$ -subunit (10) which our results do not support. Comparison of the Rh\*-bound structure of Gt $\alpha$ (340-350) with known types of helix-terminating motifs revealed a high degree of similarity with the  $\alpha_L$  type of helix capping characterized by a hydrogen bond between the amide hydrogen at C' and carbonyl oxygen at C3 (5 $\rightarrow$ 1 type). When docked to the GDP-liganded crystal structure of Gt, the NMR structure of Gt $\alpha$ (340-350) provides a perfect continuation of the C-terminal helix  $\alpha_5$ , Gt $\alpha$ (325-340), terminated by the C-cap and hydrophobic cluster. The hydrophobic patch (Lys341/Leu344/Leu349/Phe350) points in the direction where rhodopsin would be found in a putative ternary complex with transducin. Hydrophobic shielding of this motif from water clearly requires a specific binding site on Rh\*. Light-induced exposure of a potential complementary binding site on the second (CD) and third (EF) intracellular loops (11) is consistent with the movement of transmembrane helices C and F recently shown to be required for light activation (12-13). Dissociation from the receptor would be expected to expose Leu349 to solvent, leading to transition of the Gt $\alpha$ (340-350) segment back into a disordered state. The pivotal roles of Leu344 and Leu349 in rhodopsin binding have been established with specific mutations at these sites in Gt and by studies of Gt $\alpha$ (340-350) peptide analogs.

Several factors contribute to the credibility of our results. The hydrophobic cluster on the exterior of the peptide is unexpected in water; the cation-aromatic interaction between the Lys341  $\epsilon$ -amine and the Phe350 phenyl ring is commonly seen in the interior of proteins and is often exploited in specific ligand-receptor recognition (14). Helical turns at the terminals of small peptides in solution are also somewhat unusual. Also, similar TRNOE experiments on an analog of Gt $\alpha$ (340-350) with an affinity approximately 100-fold greater show diminished NOE peaks in accord with the requirements for an appropriate exchange rate in ligand-receptor complexes. TRNOE experiments can produce artifacts due to spin diffusion via receptor protons and solids CPMAS NMR experiments of specifically labelled analogs of Gt $\alpha$ (340-350) are in progress to confirm and refine the Rh\*-bound conformation.

Our results provide direct evidence for the reversible ordering of the C-terminal eleven-residue segment of Gt $\alpha$  induced by Rh\*. The C-terminus of G $\gamma$  is also known (15-17) to interact with Rh\* and the combination of interactions could impact the interface between Gt $\alpha$  and Gt $\beta\gamma$ . If structurally coupled to the conformation of the nucleotide binding site, Rh\* catalyzed C-capping of Gt $\alpha$ (340-350) could trigger GDP release and subsequent GTP binding resulting in second messenger production. We believe that the strategy demonstrated for determination of the conformation of the undecapeptide Gt $\alpha$ (340-350) to the intracellular loops of the activated G-protein coupled receptor Rh\*

could be easily adapted to determining the receptor-bound conformation of many of the biologically active peptides binding to the extracellular loops of these receptors.

## References

1. J. P. Noel, H. E. Hamm, P. B. Sigler, *Nature*, 366 (1993) 654.
2. D. G. Lambright, J. P. Noel, H. E. Hamm, P. B. Sigler, *Nature*, 369 (1994) 621.
3. J. Sondek, D. G. Lambright, J. P. Noel, H. E. Hamm, P. B. Sigler, *Nature*, 372 (1994) 276.
4. D. G. Lambright, *et al.*, *Nature*, 379 (1996) 311
5. H. E. Hamm, *et al.*, *Science*, 241 (1988). 832
6. P. D. Garcia, R. Onrust, S. M. Bell, T. P. Sakmar, H. R. Bourne, *EMBO Journal*, 14 (1995). 4460
7. S. Osawa, E. R. Weiss, *J. Biol. Chem.*, 270 (1995) 31052.
8. F. Bornancin, C. Pfister, M. Chabre, *Eur. J. Biochem.* 184 (1989) 687.
9. E. L. Martin, S. Rens-Domiano, P. J. Schatz, H. E. Hamm, *J. Biol. Chem.*, 271 (1996) 361.
10. E. A. Dratz, *et al.*, *Nature*, 363 (1993) 276.
11. S. Acharya, Y. Saad, S. S. Karnik, *J. Biol. Chem.*, 272 (1997) 6519.
12. D. L. Farrens, C. Altenbach, K. Yang, W. L. Hubbell, H. G. Khorana, *Science* 274 (1996) 768.
13. S. P. Sheikh, T. A. Zvyaga, O. Lichtarge, T. P. Sakmar, H. R. Bourne, *Nature*, 383 (1996) 347.
14. D. A. Dougherty, *Science*, 271 (1996).
15. O. G. Kisselev, M. V. Ermolaeva, N. Gautam, *J. Biol. Chem.*, 269 (1994) 21399.
16. O. Kisselev, A. Pronin, M. Ermolaeva, N. Gautam, *Proc. Natl. Acad. Sci. USA*, 92 (1995) 9102.
17. O. G. Kisselev, M. V. Ermolaeva, N. Gautam, *J. Biol. Chem.*, 270 (1995) 25356.

# Molecular dissection of the GABA<sub>A</sub> receptor: The N-terminal domain of the $\gamma_2$ subunit is essential for benzodiazepine binding and subunit assembly

Andrew J. Boileau, Amy Kucken, Amy R. Evers and Cynthia Czajkowski  
*Department of Neurophysiology, University of Wisconsin-Madison, Madison, WI 53706, USA*

The GABA<sub>A</sub> receptor is the major inhibitory neurotransmitter receptor in the mammalian brain. This receptor is a member of the ligand-gated ion channel superfamily, which includes receptors for acetylcholine, glycine, and serotonin. It is a macromolecular protein comprised of an integral chloride-selective channel with specific binding sites for GABA<sub>A</sub>, benzodiazepines (BZDs), barbiturates, steroids and picrotoxin [1,2]. Although GABA receptor  $\alpha$  subunits are important for BZD binding and GABA-current potentiation by BZDs, the presence of a  $\gamma$  subunit is required for high affinity binding [3]. In order to determine which portions of the  $\gamma_2$  subunit confer BZD binding and potentiation, we generated chimeric protein combinations of rat  $\gamma_2$  and  $\alpha_1$  subunits, and expressed them, one at a time, with wild type  $\alpha_1$  and  $\beta_2$  subunits in HEK 293 cells and *Xenopus* oocytes. Chimeras containing appropriate regions of  $\gamma_2$  should bind BZDs, whereas others (e.g. those with insufficient or inappropriate  $\gamma$ ) and the  $\alpha_1\beta_2$  combination alone should not. In this study, we show that a chimeric subunit with  $\gamma_2$  sequence in the first 161 amino acid residues and an  $\alpha_1$  sequence in the rest efficiently substitutes for a wild-type  $\gamma_2$  subunit in assembling functional cell surface GABA<sub>A</sub> receptors that bind BZD's. Thus, the extracellular 161 amino acid residues of the  $\gamma_2$  subunit is sufficient for BZD binding and  $\gamma_2$  subunit assembly.

## Results and Discussion

Chimeric subunits containing 5'  $\gamma_2$  and 3'  $\alpha_1$  sequences (Fig. 1) were generated by a modification of a published protocol for random chimera production [4]. In order to determine whether the chimeric subunits contained appropriate  $\gamma_2$  domains for BZD binding, they were individually expressed with wild-type  $\alpha_1$  and  $\beta_2$  subunits in HEK 293 cells and the binding of [<sup>3</sup>H]flunitrazepam was measured. Only two chimeras,  $\gamma_161$  and  $\gamma_167$ ; which contain the N-terminal 161 and 167 amino acid residues of the  $\gamma_2$  sequence respectively, specifically bound [<sup>3</sup>H]flunitrazepam. The affinities of  $\alpha_1\beta_2\gamma_2$ ,  $\alpha_1\beta_2\gamma_161$  and  $\alpha_1\beta_2\gamma_167$  receptors for [<sup>3</sup>H]flunitrazepam (BZD agonist) and Ro15-1788 (BZD antagonist) were measured by radioligand saturation and competition binding experiments to determine if  $\gamma_161$  and  $\gamma_167$  containing receptors were altered in their ability to bind different classes of BZD's. Results from saturation binding experiments demonstrated that  $\alpha_1\beta_2\gamma_161$  and  $\alpha_1\beta_2\gamma_167$  receptors have an affinity ( $K_D$ ) for [<sup>3</sup>H]flunitrazepam similar to  $\alpha_1\beta_2\gamma_2$  receptors with  $K_D$ 's of 13.3 nM, 11.3 nM and 9.9 nM, respectively (Fig.1).

Competition binding experiments using RO15-1788 showed no significant differences in the  $K_1$ 's for this compound (Fig. 1). The above results demonstrate that the N-terminal 161 amino acid residues of  $\gamma_2$  not only contains the necessary information for correct assembly with  $\alpha_1$  and  $\beta_2$  subunits but in addition is sufficient for BZD binding. Thus, the  $\gamma_2$  determinants of BZD selectivity lie in the major extracellular portion of the subunit from the amino terminus to the conserved cyc-cys loop.

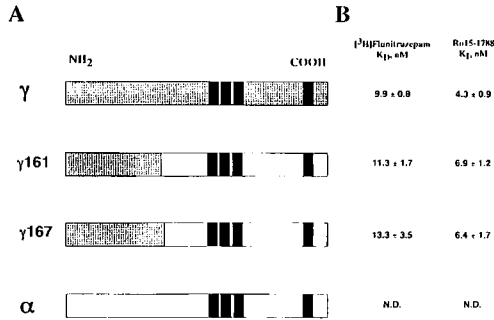


Fig. 1. Chimeric receptor subunits and their affinities for [ $^3$ H]flunitrazepam and Ro15-4513. (A) Schematic representation of the sequence encoding the rat  $\alpha_1$  and  $\gamma_2$  subunits and two chimeric subunits of the GABA<sub>A</sub> receptor. Shaded segments represent  $\gamma_2$  sequences, and unshaded segments represent  $\alpha_1$  sequences. The solid segments represent putative transmembrane domains. Chimeras are named as follows. The first symbol is the subunit from which the amino-terminal sequence is taken, the following number is the position of the chimera junction. (B) The affinity ( $K_D$  or  $K_1$ ) of a BZD agonist, [ $^3$ H]flunitrazepam, and a BZD antagonist, Ro15-1788, for GABA<sub>A</sub> receptors assembled from a wild-type  $\gamma_2$  or chimeric subunit with wild-type  $\alpha_1$  and  $\beta_2$  subunits. The numbers are the  $K_D$  or  $K_1$  means in nM, with the SEM derived from at least three experiments. N.D. Specific binding of [ $^3$ H]flunitrazepam was not detectable in receptors assembled from wild-type  $\alpha_1$  and  $\beta_2$  subunits.

To test the allosteric coupling between the BZD and GABA binding sites, GABA potentiation of [ $^3$ H]flunitrazepam binding was measured in membranes prepared from HEK 293 cells expressing  $\alpha_1\beta_2\gamma_2$ ,  $\alpha_1\beta_2\gamma_{161}$  and  $\alpha_1\beta_2\gamma_{167}$  receptors. Surprisingly, the ability of GABA to potentiate the binding of [ $^3$ H]flunitrazepam was significantly decreased in chimera-containing receptors (Fig. 2A). Chimeric receptors had a similar affinity for GABA as wild-type receptors. Thus, a decrease in GABA binding affinity was not responsible for the observed decrease in GABA potentiation.

The chimeric subunits were also co-expressed with wild-type  $\alpha_1$  and  $\beta_2$  cRNA in *Xenopus* oocytes and the ability of the BZD, diazepam, to potentiate GABA-mediated chloride current was measured. While the chimera-containing receptors displayed some diazepam potentiation of the GABA response, maximal potentiation was decreased approximately 85% as compared to  $\alpha_1\beta_2\gamma_2$  receptors (Fig. 2B). The results demonstrate that although the N-terminal 161 amino acid residues of the  $\gamma_2$  subunit is sufficient for high affinity BZD binding, it not sufficient for efficient allosteric coupling of the GABA and

BZD binding sites. Additional  $\gamma_2$  amino acid residues, C-terminal to the first 167 residues, are required.

Thus, by using these  $\gamma/\alpha$  chimeras, we have potentially separated two different functional regions of the  $\gamma_2$  subunit, a BZD binding domain and an allosteric coupling domain. Additional chimeric subunits constructed from smaller areas of the  $\gamma_2$  subunit will yield more information about the residues important for BZD binding, and further electrophysiological experiments may suggest a mechanism by which binding influences GABA-mediated ion flux. The chimeric subunits described in this report may be especially informative in this regard.

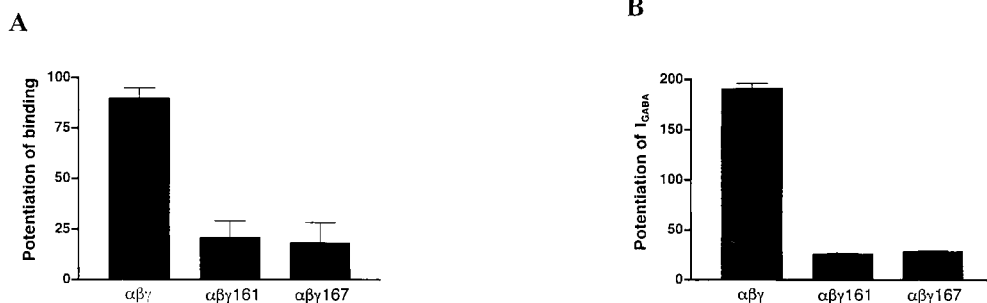


**Fig. 2.** The GABA and BZD binding sites are allosterically uncoupled in chimera-containing receptors. (A) GABA potentiation of [ $^3$ H]flunitrazepam binding by  $\alpha_1\beta_2\gamma_2$ ,  $\alpha_1\beta_2\gamma_2 161$  and  $\alpha_1\beta_2\gamma_2 167$  receptors expressed in HEK 293 cells. The bars represent the mean potentiation of 3nM [ $^3$ H]flunitrazepam binding by 3  $\mu$ M GABA  $\pm$  S.E.M. of at least three independent experiments. Potentiation was calculated as [(specific dpm +GABA)/(specific dpm - GABA)-1]  $\times$  100. (B) Diazepam potentiation of the GABA-mediated chloride current by  $\alpha_1\beta_2\gamma_2$ ,  $\alpha_1\beta_2\gamma_2 161$  and  $\alpha_1\beta_2\gamma_2 167$  receptor expressed in *Xenopus* oocytes. Standard two-electrode voltage clamp recording was used. Diazepam potentiation was recorded at approx. EC<sub>20</sub> for GABA. Dose-response curves for diazepam potentiation of the GABA response were measured. The bars represent the maximal potentiation of the GABA-gated current by diazepam  $\pm$  S.E.M. and were derived from a standard non-linear curve-fitting analysis of the dose-response data. Data are derived from experiments in > 4 oocytes from > 2 injected batches.

## References

1. Sieghart, W., *Pharmacological Reviews*, 47 (1995) 182.
2. Stephenson, F. A., *Biochem. J.*, 310 (1995) 1.
3. Pritchett, D. B., Sontheimer, H., Shivers, B., Ymer, S., Kettenmann, H., Schofield, P. R., and Seeburg, P. H., *Nature*, 338 (1989) 582.
4. Moore, K.R. and Blakely, R. D., *Biotechniques*, 17 (1994) 130.

# Glucagon receptor structure and function: Probing the putative hormone binding site with receptor chimeras

**Cecilia G. Unson, Aaron M. Cypess, Cui-Rong Wu, Connie P. Cheung  
and R. B. Merrifield**

*The Rockefeller University, 1230 York Avenue, New York, N. Y. 10021, USA*

Glucagon is a 29-residue peptide hormone that is secreted by pancreatic A cells and plays a central role in the maintenance of normal blood glucose levels. Its primary target organ is the liver where high affinity binding to specific receptors on the surface of the hepatocytes sets in motion a series of biochemical events that ultimately result within minutes in increased glucose output. The mechanism by which the recognition signal is transmitted by the receptor across the membrane, where intracellular domains activate G protein-coupled effectors inside the cell to generate the glucagon effect, is unknown.

The glucagon receptor belongs to a unique group within the superfamily of G protein-coupled receptors, which includes receptors for related peptide hormones glucagon-like peptide-1 (GLP-1), secretin, and other moderate-sized peptides (Fig. 1). While extensive structural information is available for GPCRs that bind small ligands, much less is known about the ligand binding and signaling characteristics of the glucagon receptor family.

Using site-directed mutagenesis we showed that a conserved Asp<sup>64</sup> at the N terminus is absolutely required for binding [1]. We further demonstrated using truncation mutants that the intracellular C-terminal tail was not necessary for binding and activity, while the N terminus, the transmembrane helices, and the extracellular intrahelical loops were important not only for ligand recognition but also for proper cellular transport to the plasma membrane surface [2]. Tentative structural models based on these initial findings portray the hormone binding site of the glucagon receptor as a discontinuous domain consisting of contributions from the long N-terminal extension, the extracellular loops, and some residues at the membrane interface of the transmembrane helices. Unraveling the chemical nature of this cavity and the interactions between ligand and receptor that dictate binding affinity and selectivity are crucial for the design of pharmacologically relevant glucagon antagonists.

Mutagenesis studies using glucagon/GLP-1 receptor chimeras have implicated the membrane proximal region residues 80-142 and the first extracellular loop as regions required for high affinity glucagon binding [3]. In recent studies we also demonstrated that peptide anti-glucagon receptor antibodies effectively competed for glucagon binding sites and inhibited subsequent hormone-dependent stimulation of adenylyl cyclase [4]. The DK-12 antiserum was generated against a peptide consisting of residues 126-137 from the membrane proximal portion of the N-terminal tail and the KD-14 antiserum was directed against a peptide representing residues 206-219 from the first extracellular loop. The antibodies behaved like glucagon antagonists and suggested that these epitopes might comprise part of the receptor binding pocket. It is likely that these sites also contain determinants of binding specificity that enable the receptor to discriminate among

glucagon's closest relatives, GLP-1 and secretin. To investigate this possibility, receptor chimeras were constructed wherein residues 126-137 and residues 206-219 of the glucagon receptor were each replaced with the analogous segments from the rat GLP-1 and secretin receptors. In a double mutant chimera, both sequences 126-137 and 206-219 were substituted with the corresponding residues of the GLP-1 receptor. Each receptor mutant was assessed for proper transport to the cell surface, glucagon binding, and adenylyl cyclase activation (Table 1).

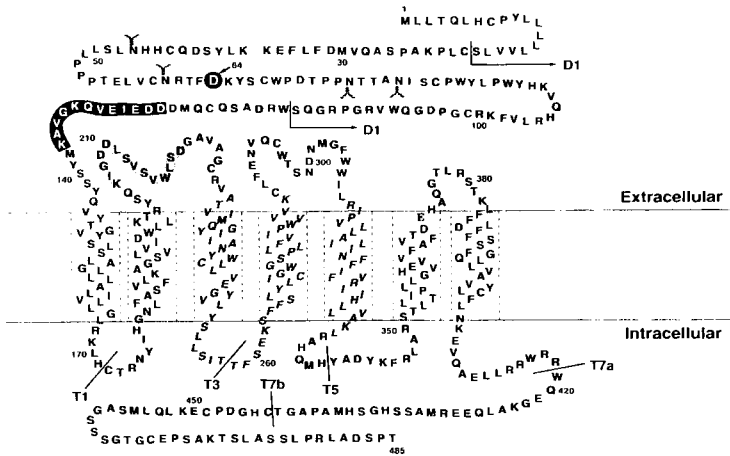


*Fig. 1. Schematic representation of the rat glucagon receptor. D1 mutant contained a deletion from the N-terminal tail indicated by arrows. Mutants T1, T3, T5, T7a, and T7b were truncated as shown. Antibodies generated against peptides in the boxed areas inhibited glucagon binding. In receptor chimeras, these regions were replaced with the analogous sequences from the GLP-1 and secretin receptors.*

## Results and Discussion

Mutant receptor chimeras were prepared by restriction fragment replacement "cassette mutagenesis" using a synthetic rat glucagon receptor gene, and expressed following transient transfection in COS-1 cells [1]. Endo H susceptibility analysis on immunoblots, of membranes from transfected cells showed that the mutant receptors were normally expressed on the plasma membrane surface [2]. The IC<sub>50</sub> for competitive binding (31.6 nM) and the EC<sub>50</sub> for glucagon-stimulated adenylyl cyclase activity (3.2 nM) of the wild type receptor were consistent with reported values. In general, there was good correlation for all the mutant receptors between the relative affinity (%) of ligand binding and the relative potency (%) of adenylyl cyclase stimulation, suggesting that the effect of the mutation on binding is functionally linked to activation. A decrease in binding affinity resulted in a decrease in the relative ability to activate cyclase.

Table 1. Receptor binding and adenylyl cyclase activity of rat glucagon receptor chimeras.

Glucagon receptor mutants	Receptor binding			Adenylyl cyclase activity		
	IC50 (nM)	Relative affinity %	Fold decrease	EC50 (nM)	Relative potency %	Fold decrease
GlucR (w.t.)	31.6	100.0		3.2	100.0	
secDK (126-137)	316.2	10.0	10.0	20.4	15.5	6.4
glpDK (126-137)	100.0	31.6	3.1	18.0	17.7	5.6
secloop (206-219)	≥1000	≤1.0	≥100	≥1000	≤1	≥100
glploop (206-219)	447.0	7.0	14.2	39.0	8.1	12.3
dblglp (126-137)(206-219)	≥1000	≤1.0	≥100	251.0	1.3	80.0

Replacement of the DK (peptide 126-137) region of the glucagon receptor with the analogous residues of the GLP-1 receptor in the mutant chimera *glpDK* led to a 3-fold decrease in binding affinity and a 5-fold decrease in activation. The corresponding change with secretin receptor residues in the mutant chimera *secDK* resulted in a tenfold decrease in binding affinity and a sixfold decrease in adenylyl cyclase activity (Table 1). In contrast, the *glploop* chimera lost greater than 90% of affinity and potency and the *secloop* displayed a hundredfold loss of function. Substitution of both the 126-137 and 206-219 segments with the residues from the GLP-1 receptor in the double mutant chimera, *dblglp*, resulted in greater than a hundredfold loss of binding and efficacy of activation.

These results indicate that residues 126-137 of the N-terminal tail and residues 206-219 of the first extracellular loop are indeed components of the glucagon binding pocket. The combined replacement of both regions led to a greater loss of function than either single modification, suggesting a cooperative effect. Mutation of the 206-219 segment in the first extracellular loop region (*glploop* and *secloop*) had a more profound effect on both binding and activity than the replacement of the 126-137 (*glpDK* and *secDK*) sequence in the membrane proximal part of the N-terminal tail. The first extracellular loop thus contains specific determinants of ligand binding. Close inspection of the loop sequence reveals unique charged residues that may interact directly with glucagon. The data further confirm a common structural motif in these regions recognized by glucagon and GLP-1 but these features are not contained in the analogous sequence of the secretin receptor.

U. S. PHS Grant DK 24039.

## References

1. Carruthers, C. J. L., Unson, C. G., Kim, H. N., and Sakmar, T. P., *J. Biol. Chem.*, 269 (1994) 29321
2. Unson, C. G., Cypess, A. M., Kim, H. N., Goldsmith, P. K., Carruthers, C. J. L., Merrifield, R., and Sakmar, T. S. *J. Biol. Chem.*, 270 (1995) 27720.
3. Buggy, J. J., Livingston, J. N., Rabin, J. N., and Yoo-Warren, H., *J. Biol. Chem.*, 270 (1995) 7474.
4. Unson, C. G., Cypess, A. M., Wu, C.-R., Goldsmith, P. K., Merrifield, R. B., Sakmar, T. S., *Proc. Natl. Acad. Sci. USA*, 93 (1996) 310.

# A new class of dipeptide derivatives that are potent and selective $\delta$ opioid agonists

P. W. Schiller, G. Weltrowska, I. Berezowska, C. Lemieux  
N. N. Chung, K. A. Carpenter and B. C. Wilkes

*Clinical Research Institute of Montreal, Montreal, Que., Canada H2W 1R7*

The development of  $\delta$  opioid agonists looks promising because there is evidence to indicate that, in comparison with currently used opiates of the  $\mu$  type, they may produce less physical dependence, no respiratory depression, and almost no adverse gastrointestinal effects [1]. Recently, we discovered that the  $\delta$  antagonist versus  $\delta$  agonist behavior of a series of dipeptide derivatives of the formula H-Tyr-Tic-NH-(CH<sub>2</sub>)<sub>n</sub>-Ph (Ph = phenyl) depended on the number of methylene groups contained in the C-terminal phenylalkyl substituent [2]. Analogs with n = 1 or 3 were  $\delta$  antagonists, whereas the compound with n = 2 was a moderately potent and somewhat selective  $\delta$  agonist (Table 1). In an effort to increase the  $\delta$  agonist potency and  $\delta$  receptor selectivity of H-Tyr-Tic-NH-(CH<sub>2</sub>)<sub>2</sub>-Ph, structural modifications of the C-terminal phenylethyl group were performed by introduction of an additional substituent in one of two different positions or by incorporation of conformational constraints. Furthermore, two different tyrosine derivatives were substituted for Tyr<sup>1</sup> in two of the compounds. The dipeptide derivatives were synthesized in solution using the mixed anhydride method. *In vitro* opioid activities of the resulting compounds were determined in the  $\mu$  receptor-representative guinea pig ileum (GPI) assay and in the  $\delta$  receptor-representative mouse vas deferens (MVD) assay, and their  $\mu$  and  $\delta$  receptor affinities were measured in binding assays based on displacement of  $\mu$ - and  $\delta$ -selective radioligands from rat brain membrane binding sites.

## Results and Discussion

Replacement of the Tyr<sup>1</sup> residue in the parent compound with 2',6'-dimethyltyrosine (Dmt) produced a compound, H-Dmt-Tic-NH-(CH<sub>2</sub>)<sub>2</sub>-Ph, showing  $\delta$  receptor affinity in the picomolar range and partial agonism (maximal inhibition of electrically evoked contractions = 70%) in the MVD assay (Table 1). Substitution of a chloro-, bromo- or methyl group in *ortho*-position of the phenyl ring in the C-terminal phenylethyl moiety resulted in analogs with increased  $\delta$  agonist potency and improved  $\delta$  receptor selectivity. The best compound in this series was H-Tyr-Tic-NH-(CH<sub>2</sub>)<sub>2</sub>-Ph(*o*-Cl) which showed an IC<sub>50</sub> value of 8.77 nM in the MVD assay, weak partial agonism in the GPI assay, and good  $\delta$  receptor selectivity ( $K_1^\mu/K_1^\delta = 68$ ) in the rat brain membrane binding assays.

A second series of analogs was obtained by introducing various substituents at the

Table 1. *In vitro* opioid activities of dipeptide  $\delta$  opioid agonists.

Compound	MVD assay	Opioid receptor binding <sup>a</sup>		
	IC50[nM]	K <sub>i</sub> <sup><math>\mu</math></sup> [nM]	K <sub>i</sub> <sup><math>\delta</math></sup> [nM]	K <sub>i</sub> <sup><math>\mu</math></sup> /K <sub>i</sub> <sup><math>\delta</math></sup>
H-Tyr-Tic-NH-(CH <sub>2</sub> ) <sub>2</sub> -Ph	82.0	69.1	5.22	13.2
H-Dmt-Tic-NH-(CH <sub>2</sub> ) <sub>2</sub> -Ph	2.3 (IC35) <sup>b</sup>	1.59	0.0577	27.6
H-Tyr-Tic-NH-(CH <sub>2</sub> ) <sub>2</sub> -Ph( <i>o</i> -Cl)	8.77	96.9	1.43	67.8
H-Tyr-Tic-NH-(CH <sub>2</sub> ) <sub>2</sub> -Ph( <i>o</i> -Br)	13.9	23.3	1.24	18.8
H-Tyr-Tic-NH-(CH <sub>2</sub> ) <sub>2</sub> -Ph( <i>o</i> -CH <sub>3</sub> )	10.1	38.7	1.75	22.1
H-Tyr-Tic-NH-CH <sub>2</sub> -CH(Ph) <sub>2</sub>	3.77	28.8	0.981	29.4
Tyr(NMe)-Tic-NH-CH <sub>2</sub> -CH(Ph) <sub>2</sub>	0.261	12.7	0.581	21.9
H-Dmt-Tic-NH-CH <sub>2</sub> -CH(Ph) <sub>2</sub>	0.726	1.62	0.693	2.34
H-Tyr-Tic-NH-CH <sub>2</sub> -CH(Ph)Me (S)	21.4	82.3	6.31	13.0
H-Tyr-Tic-NH-CH <sub>2</sub> -CH(Ph)Me (R)	26.0	51.3	3.67	14.0
H-Tyr-Tic-NH-CH <sub>2</sub> -CH(Ph)COOEt (I)	1.28	886	0.569	1560
H-Tyr-Tic-NH-CH <sub>2</sub> -CH(Ph)COOEt (II)	8.64	153	3.03	50.5
H-Tyr-Tic-NH-CH <sub>2</sub> -CH(Ph)CONH <sub>2</sub> (I)	34.0	73.7	21.5	3.43
H-Tyr-Tic-NH-CH <sub>2</sub> -CH(Ph)CONH <sub>2</sub> (II)	P.A. <sup>b</sup>	191	22.8	8.38
H-Tyr-Tic-2-S-At	38.1	55.8	4.55	12.3
H-Tyr-Tic-2-R-At	36.3	26.3	1.72	15.3
H-Tyr-Tic-NH-Pcp ( <i>trans</i> , I)	P.A. <sup>b</sup>	38.0	4.13	9.20
H-Tyr-Tic-NH-Pcp ( <i>trans</i> , II)	7.31	11.5	1.36	8.46

<sup>a</sup>Displacement of [<sup>3</sup>H]DAMGO ( $\mu$ -selective) and [<sup>3</sup>H]DSLET ( $\delta$ -selective) from rat brain membrane binding sites. <sup>b</sup>Partial agonist.

$\beta$ -carbon of the C-terminal phenylethylamine moiety. Introduction of a second phenyl group at this position led to a compound, H-Tyr-Tic-NH-CH<sub>2</sub>-CH(Ph)<sub>2</sub>, which compared with the parent peptide was a 20 times more potent  $\delta$  agonist with 2-fold improved  $\delta$  selectivity. Methylation of the N-terminal amino group in the latter peptide produced a compound, Tyr(NMe)-Tic-NH-CH<sub>2</sub>-CH(Ph)<sub>2</sub>, with subnanomolar  $\delta$  agonist potency and still considerable  $\delta$  selectivity. The corresponding Dmt<sup>1</sup>-analog was a similarly potent, but non-selective  $\delta$  agonist. Both isomers of an analog containing a methyl substituent at the  $\beta$ -carbon of the phenylethyl group displayed only moderate  $\delta$  agonist potency and  $\delta$  selectivity. On the other hand, one of the isomers (I) of H-Tyr-Tic-NH-CH<sub>2</sub>-CH(Ph)COOEt turned out to be a superior  $\delta$  agonist, showing excellent  $\delta$  agonist potency (IC50 = 1.58 nM) in the MVD assay, subnanomolar  $\delta$  receptor affinity (K<sub>i</sub> <sup>$\delta$</sup>  = 0.569 nM) and extraordinary  $\delta$  selectivity (K<sub>i</sub> <sup>$\mu$</sup> /K<sub>i</sub> <sup>$\delta$</sup>  = 1560). One of the two isomers of a corresponding analog containing a -CONH<sub>2</sub> substituent at the  $\beta$ -carbon was a relatively weak  $\delta$  agonist and the other was a partial  $\delta$  agonist.

Conformational constraints were introduced by replacing the phenylethyl moiety with a tetralinyl- or a *trans*-2-phenylcyclopropyl (Pcp) group. Both isomers of the aminotetralin (At) analog showed higher  $\delta$  agonist potency and higher  $\delta$  receptor affinity than the parent compound (Table 1). One of the isomers (II) of the *trans*-Pcp-containing dipeptide analog displayed high  $\delta$  agonist potency and high  $\delta$  receptor selectivity, whereas the other was a partial  $\delta$  agonist.

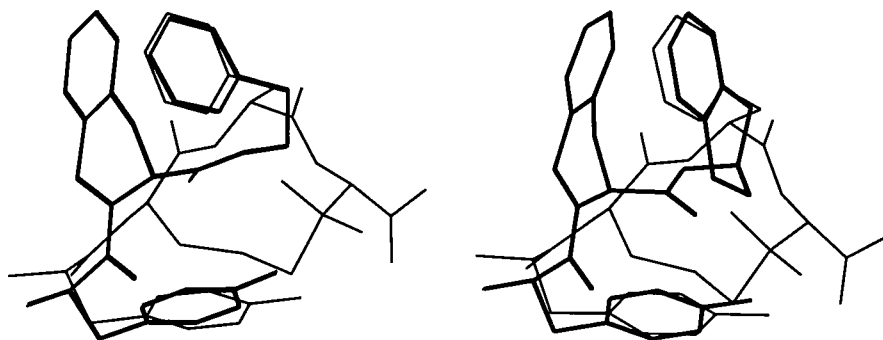


Fig. 1. Spatial overlap of the proposed bioactive conformation of JOM-13 with low energy conformers of H-Tyr-Tic-NH-(CH<sub>2</sub>)<sub>2</sub>-Ph (left) and H-Tyr-Tic-R-At (right).

Recently, a convincing model of the receptor-bound conformation of the selective  $\delta$  opioid agonist H-Tyr-c[D-Cys-Phe-D-Pen]OH (JOM-13) has been proposed [3]. A molecular mechanics study performed with H-Tyr-Tic-NH-(CH<sub>2</sub>)<sub>2</sub>-Ph resulted in several low energy conformers. One of these, with an energy 0.75 kcal/mol higher than the lowest energy structure, showed excellent spatial overlap of its N-terminal amino group, phenol ring and C-terminal phenyl group with the corresponding pharmacophoric moieties in the proposed bioactive conformation of JOM-13 (Fig. 1, left panel). An excellent fit with this model was also observed with a low energy conformer of the conformationally constrained  $\delta$  agonist H-Tyr-Tic-R-At (Fig. 1, right panel). It can therefore be concluded that the low energy conformers of the two dipeptides depicted in Fig.1. represent a plausible candidate structure of the receptor-bound conformation of this class of  $\delta$  agonists.

In conclusion, a new class of potent and selective  $\delta$  agonists was developed. Because of their low molecular weight and lipophilic character, these compounds may cross the blood-brain barrier and have potential as centrally acting analgesics.

### Acknowledgments

This work was supported by grants from the MRCC (MT-10131) and NIDA (DA-04443).

### References

1. Bilsky, E.J., Calderon, S.N., Wang, T., Bernstein, R.N., Davis, P., Hruby, V.J., McNutt, R.W., Rothman, R.B., Rice, K.C. and Porreca, F., *J. Pharmacol. Exp. Ther.*, 273(1995)359.
2. Schiller, P.W., Weltrowska, G., Nguyen, T.M.-D., Lemieux, C. and Chung, N.N., In Maia, H.L.S. (Ed.), *Peptides 1994 (Proceedings of the Twenty-Third European Peptide Symposium)*, ESCOM, Leiden, The Netherlands, 1995, p. 632.
3. Lomize, A.L., Pogozeva, I.D. and Mosberg, H.I., *Biopolymers*, 38(1996)221.

## Discovery of small non-peptidic CD4 inhibitors as novel immunotherapeutics

**Song Li, Jimin Gao, Takashi Satoh, Thea M. Friedman,  
Andrea E. Edling, Ute Koch, Swati Choksi, Xiaobing Han,  
Robert Korngold and Ziwei Huang**

*Kimmel Cancer Institute, Jefferson Medical College, Thomas Jefferson University, Philadelphia,  
PA 19107, USA*

The interaction between CD4 and major histocompatibility complex (MHC) class II proteins is critical for the activation of CD4<sup>+</sup> T cells which are involved in transplantation reactions and a number of autoimmune diseases. In this study, we have identified a CD4 surface pocket as a functional epitope implicated in CD4-MHC class II interaction and T cell activation. A computer-based strategy has been utilized to screen ~150,000 non-peptidic organic compounds in a molecular database and identify a group of compounds as ligands of the proposed CD4 surface pocket. These small organic compounds have been shown to specifically block stable CD4-MHC class II binding, and exhibit significant inhibition of immune responses in animal models of autoimmune disease and allograft transplant rejection, suggesting their potential as novel immunosuppressants. This structure-based computer screening approach may have general implications for studying many immunoglobulin-like structures and interactions that share similar structural features. Furthermore, the results from this study have demonstrated that the rational design of small non-peptidic inhibitors of large protein-protein interfaces may indeed be an achievable goal.

### Results and Discussion

We applied the computational screening approach to search ~150,000 non-peptidic organic compounds in a chemical database for potential ligands of the CD4 D1 domain surface pocket implicated in MHC class II binding and T cell activation. This led to the discovery of several novel inhibitors of CD4 function, with the structure of the two most potent compounds and the binding of one of these organic inhibitors, TJU104 to the CD4 D1 surface pocket is shown in Fig. 1. These compounds were shown to be non-toxic to the cells of the lymphoid system *in vivo* and appeared to be specific for their target CD4 protein. More importantly, they displayed significant *in vivo* immunosuppressive activity of CD4<sup>+</sup> T cell-mediated responses in murine models of experimental allergic encephalomyelitis and skin allograft rejection. These results demonstrated that the computer screening of chemical databases may represent an effective approach to discover small molecular inhibitors with therapeutic potential.

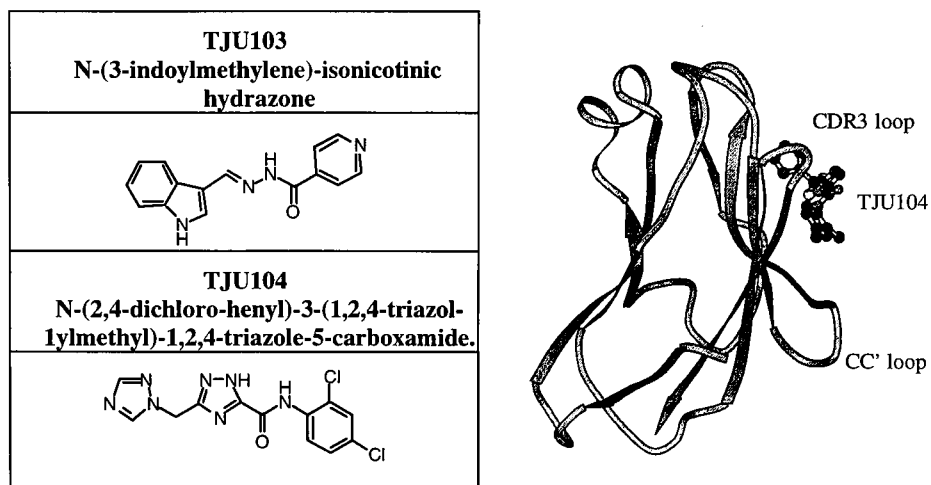


*Fig. 1. Two representative non-peptidic organic inhibitors of CD4 discovered by using the computer screening approach (left). The binding of an organic inhibitor TJU104 to the CD4 D1 surface pocket (right).*

The small non-peptidic organic inhibitors identified here may have important implications for the development of a new generation of non-toxic and orally available immunosuppressants for the treatment of autoimmune diseases and transplantation reactions. Current therapeutic strategies for these immunopathological conditions include the use of monoclonal antibodies (mAbs) such as anti-CD4 mAb to block inflammatory T cell activation. However, the inherent immunogenicity of xenogeneic mAbs have reduced their value as an effective treatment. In comparison with mAbs, small molecular inhibitors are likely to be less immunogenic. Also, unlike peptide-based therapeutics that are generally unstable and therefore not orally available, non-peptidic organic structures are normally more stable and also more amenable for modifications using standard medicinal chemistry techniques to improve potency and oral activity. For these reasons, the group of organic compounds with diverse and distinctive non-peptidic structures identified here may represent promising leads for the development of new immunosuppressive agents.

This study may provide a paradigm for the inhibitor design of many Ig-related protein structures and interactions. As members of the immunoglobulin superfamily (IgSF) may have a conserved backbone folding pattern, it is likely that this generic structure provides some common scaffolds for efficient protein-protein interactions. It is interesting to note that similar structural themes may be involved in a diversity of molecular interactions and biological functions of IgSF proteins. Therefore, it is possible that the computer screening approach developed from this study of the CD4 protein may also be applicable to the design of small non-peptidic inhibitors of other IgSF molecular interactions.

## Conclusion

We have tested the hypothesis that non-peptidic organic inhibitors targeting a small functionally important surface epitope could be sufficient for the effective blockade of a protein-protein interaction with a large interface. Employing theoretical analysis of protein structure and subsequent synthetic peptide mapping approaches, we have identified a surface pocket on the CD4 D1 domain as a critical functional epitope, involved either directly or indirectly in stable CD4-MHC class II interaction and T cell activation. A computer-based database screening strategy has been employed to identify a diverse group of novel non-peptidic organic ligands of this CD4 surface pocket that specifically block CD4-MHC class II cell adhesion and exhibit significant immunosuppressive activity in animal models of autoimmune disease and transplant rejection. This computer screening approach should have general implications for studying many Ig-related molecules that utilize similar surface structural features for diverse intermolecular binding and biological functions. Finally, the results from this study have demonstrated that the structure-based, computer-assisted design of small non-peptidic inhibitors of large protein-protein interfaces may indeed be an achievable goal.

## Acknowledgments

These studies were supported in part by grants from the National Institutes of Health, the American Cancer Society, the National Multiple Sclerosis Society and the Sidney Kimmel Foundation for Cancer Research. We would like to thank members of our laboratories and our collaborators for their contribution and helpful discussion. Z.H. is the recipient of the Kimmel Scholar Award in cancer research.

## References

1. Satoh, T., Li, S., Friedman, T.M., Wiaderkiewicz, R., Korngold, R., Huand, Z., *Biochem. Biophys. Res. Commun.*, 224 (1996) 438.
2. Satoh, T., Aramini, J.M., Li, S., Friedman, T.M., Gao, J., Edling, A., Townsend, R., Germann, M.W., Korngold, R., Huang, Z., *J. Biol. Chem.*, 272 (1997) 12175.
3. Li, S., Gao, J., Satoh, T., Friedman, T.M., Edling, A., Korngold, R., Huang, Z., Koch, U., Choksi, S., Han, X. *Proc. natl. Acad. Sci. USA*, 94 (1997) 73.
4. Huang, Z., Li, S., Korngold, R., *Med. Chem. Res.*, (1997) in press.

# Biochemistry and biology of phospholipase C- $\gamma$ 1

Graham Carpenter, Qun-sheng Ji, and Debra Horstman

Department of Biochemistry, Vanderbilt University School of Medicine,  
Nashville, TN 37232-0146, USA

Growth factor polypeptides bind to specific cell surface receptors and thereby activate intracellular tyrosine kinases. This activation is the initial intracellular step in the complex process of signal transduction that ultimately stimulates cell proliferation. Among the known substrates of these tyrosine kinases is phospholipase C- $\gamma$ 1 (PLC- $\gamma$ 1), an enzyme that, when activated, catalyzes the hydrolysis of phosphatidylinositol 4,5-bisphosphate (PIP<sub>2</sub>) to produce two second messenger molecules: diacylglycerol, which activates protein kinase C, and inositol 1,4,5-trisphosphate, which regulates the level of intracellular, free Ca<sup>2+</sup> (1).

A schematic representation of PLC- $\gamma$ 1 based on primary structure appears in Fig. 1. The regions denoted X and Y are associated in the folded enzyme so as to constitute the active site and are conserved in all members of the PLC- $\beta$ , PLC- $\delta$  and PLC- $\gamma$  families (1). PLC- $\gamma$ 1 and - $\gamma$ 2 are unique among PLC isoforms as they possess regulatory motifs, designated SH2 and SH3. SH2 domains are known to mediate association with other proteins that contain phosphotyrosine, while SH3 motifs facilitate association with proteins that contain proline-rich sequences (2). Activation of PLC- $\gamma$ 1 is mediated by its tyrosine phosphorylation at three known sites (1).

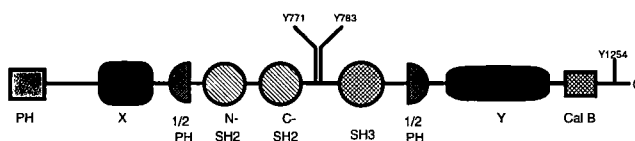


Fig. 1. Schematic representation of sequence motifs in the PLC- $\gamma$ 1 primary structure. PH, pleckstrin homology domain; SH, src homology domain; Cal B, calcium phospholipid binding domain; X and Y, catalytic subdomains; Y numbered, sites of tyrosine phosphorylation.

## Results and Discussion

Recently, a crystallographic study of PLC- $\delta$ 1 has illuminated how the X and Y subdomains cooperate in the folded enzyme to constitute an active site for PIP<sub>2</sub> hydrolysis (3). Also, biochemical studies have demonstrated that X and Y domains remain tightly associated when the polypeptide chain between them is hydrolyzed by proteases (4,5). We have assessed the capacity of X and Y domains to self-associate by using baculovirus to express individual polypeptides in insect cells. Cells were infected with virus encoding PLC- $\gamma$ 1 holoenzyme or co-infected with separate viruses containing information for X or Y domains (6). Co-precipitation studies showed that when expressed together in the same cell, X and Y polypeptides formed an association complex with a high degree of efficiency. However,

attempts to induce association of the two polypeptides *in vitro* has, so far, been unsuccessful.

We next determined whether the X:Y complex constituted from individual X and Y polypeptides in insect cells was biochemically active, as measured by its capacity to hydrolyze PIP<sub>2</sub> *in vitro*. The specific enzyme activity of the X:Y complex was, surprisingly, much higher than that of the recombinant PLC- $\gamma$ 1 holoenzyme. At high and low substrate concentrations, respectively, the X:Y complex was 20- to 100-fold more active than the recombinant holoenzyme. These data indicated that the X:Y complex, which represents a deletion of the -SH2-SH2-SH3- sequences present in the holoenzyme, is an activated form of PLC- $\gamma$ 1.

These results have allowed construction of a model of PLC- $\gamma$ 1 to account for regulation of the basal level of enzyme activity, as well as incorporating the tyrosine phosphorylation events known to produce the activated form of the enzyme (Fig. 2). Within the tertiary structure of PLC- $\gamma$ 1, the central SH region of the holoenzyme is proposed to interact with and/or occlude the active site X:Y region. Whether the physical relationship of the SH region with the X:Y region within the protein is direct or indirect is unknown. Nevertheless, the model proposes that, in its non-tyrosine phosphorylated state, PLC- $\gamma$ 1 activity is repressed by an intramolecular mechanism. This model would allow activation of PLC- $\gamma$ 1 by derepression or modulation of the relationship between the SH region and the catalytic site.

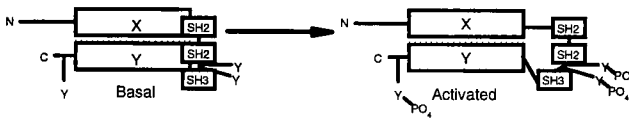


Fig. 2. Model for the intramolecular regulation of PLC- $\gamma$ 1 activity by tyrosine phosphorylation.

Known mechanisms for the activation of PLC- $\gamma$ 1 would support or at least be in agreement with the model described above. Phosphorylation of Tyr 783, located between the SH2 and SH3 domains (Fig. 1), is essential for PLC- $\gamma$ 1 activation by tyrosine phosphorylation in intact cells (7). V8 protease treatment of PLC- $\gamma$ 1 *in vitro* produces cleavage between the SH3 and Y domains and also activates the enzyme (5). Lastly, deletion of the SH region, as described above, activates the enzyme. Hence, modulations of the physical structure of the SH region are, in most known cases, activating events. Unknown, however, are the exact element(s) or sequence(s) in the SH region that have a function/physical relationship to the X:Y catalytic domain.

The biologic significance of PLC- $\gamma$ 1 has remained ill-defined by studies performed with cultured cells, in the sense that there is evidence that PLC- $\gamma$ 1 is essential for mitogenic signal transduction and evidence that this protein is not essential for growth factor-induced responses (1). To resolve this issue we have used homologous recombination to target and disrupt the *Plcg1* gene in mice (8). The targeted mutation is actually a genomic deletion that removes exons encoding all of the X domain and both SH2 domains. Transmission of this mutation in mice in its heterozygous (*Plcg1*<sup>+/−</sup>) form has no influence on development, growth, or other observable functions of the animals. Hence, loss of one *Plcg1* allele is not deleterious. However, when both functional copies of this allele are disrupted (*Plcg1*<sup>−/−</sup>), the

effect is severe as embryos do not survive beyond 9.0 days gestation. Therefore, the partial loss of PLC- $\gamma$ 1 can be tolerated, but the complete absence of this protein cannot.

These results indicate that in the intact organism, PLC- $\gamma$ 1 is essential for growth and development. The loss of PLC- $\gamma$ 1 is not compensated for by other signaling pathways that emanate from growth factor receptor tyrosine kinases. Nor can the loss of this enzyme be compensated by other *Plc* genes, which encode nine additional PLC isozymes. Interestingly, viable cells can be cultured from *Plcg1*<sup>-/-</sup> embryos and these cells are immortal under cell culture conditions.

### Acknowledgements

The authors appreciate the efforts of Suzanne Carpenter in the preparation of figures and the manuscripts. Funding from a National Cancer Institute grant CA43720 is acknowledged.

### References

1. Kamat, A. and Carpenter, G., Cytokine & Growth Factor Reviews (in press).
2. Cohen, G.B., Ren, R., and Baltimore, D., Cell 80 (1995) 237.
3. Essen, L.-O., Perisic, O., Cheung, R., Katan, M., and Williams, R.L., Nature 380 (1996) 595.
4. Cifuentes, M.E., Honkanen, L., Rebecchi, M.J., J. Biol. Chem., 268 (1993) 11586.
5. Fernald, A.W., Jones, G.W., and Carpenter, G., Biochem. J., 302 (1994) 503.
6. Horstman, D.A., DeStefano, K., and Carpenter, G., Proc. Natl. Acad. Sci. USA, 93 (1996) 7518.
7. Kim, H.K., Kim, J.W., Zilberstein, A., Margolis, B., Kim, J.G., Schlessinger, J., Rhee, S.G., Cell 54 (1991) 435.
8. Ji, Q.-S., Winnier, G.E., Niswender, K.D., Horstman, D., Wisdom, R., Magnuson, M.A., and Carpenter, G., Proc. Natl. Acad. Sci., 94 (1997) 2999.

# Tumor cell interactions with type IV collagen: Synthetic peptide dissection of post-adhesion signal transduction mechanisms

**Janelle L. Lauer and Gregg B. Fields**

*Department of Laboratory Medicine & Pathology and The Biomedical Engineering Center,  
University of Minnesota, Minneapolis, MN 55455 USA*

Tumor cell interactions with the extracellular matrix (ECM) are mediated by a great variety of cell surface molecules. The best characterized receptors are integrins, which are heterodimeric proteins composed of one  $\alpha$  and one  $\beta$  subunit. During the invasion process, tumor cell integrins interact with basement membrane (type IV) collagen. The collagen-binding integrins include  $\alpha1\beta1$ ,  $\alpha2\beta1$ , and  $\alpha3\beta1$  [1]. In addition to promoting adhesion, integrins provide a linkage between the ligand and intracellular proteins. The role of adhesion in signal transduction and subsequent cellular behaviors is of great interest. Integrin-mediated binding to collagen results in the Tyr phosphorylation of a ~125 kDa kinase that is found at focal adhesions (focal adhesion kinase, or p125<sup>FAK</sup>) [2]. Each of the collagen-binding integrins has been implicated in signal transduction events [3-7]. We can use isolated collagen sites for dissecting integrin mediated post-adhesion events. A peptide incorporating the  $\alpha1(IV)531-543$  sequence promotes adhesion and migration of numerous cell types [8, 9]. It was also shown that human melanoma and ovarian carcinoma cells bound equally well to the single-stranded (SSP) and triple-helical forms (THP) of this peptide [9], indicating that its cellular recognition is conformation independent. Recently, we correlated cell adhesion to the  $\alpha1(IV)531-543$  sequence to cell binding via the  $\alpha3\beta1$  integrin of human melanoma cells [10]. In the present study, we have examined the induction of melanoma cell signal transduction by the  $\alpha1(IV)531-543$  sequence. We have also studied the effects of secondary structure on signaling activities.

## Results and Discussion

Signal transduction events, specifically p125<sup>FAK</sup> Tyr phosphorylation, were examined for melanoma cell binding to type IV collagen. Following 30 min of adhesion to type IV collagen, immunoprecipitation and immunoblotting analysis identified pp125<sup>FAK</sup> as one of the proteins phosphorylated on Tyr residues. Although three integrins can bind type IV collagen, our interest was whether or not the  $\alpha3\beta1$  integrin induces p125<sup>FAK</sup> Tyr phosphorylation, because the  $\alpha1(IV)531-543$  sequence used in this study is known to be bound specifically by this integrin. In response to  $\alpha3$  monoclonal antibody binding and subsequent cross-linking by a secondary antibody, p125<sup>FAK</sup> Tyr phosphorylation peaked at 2 min, and declined back to baseline after 5 min.

We examined the capability of the  $\alpha3\beta1$  integrin binding sequence  $\alpha1(IV)531-543$  to induce p125<sup>FAK</sup> phosphorylation utilizing a solution-phase binding procedure. The  $\alpha1(IV)531-543$  sequence was used in either the SSP or THP form to determine the importance of secondary structure on signaling events. At a concentration of 2  $\mu$ M, the

$\alpha 1(\text{IV})531-543$  SSP did not induce any detectable phosphorylation. When the concentration of the peptide was increased to  $10 \mu\text{M}$ , phosphorylation of  $\text{p}125^{\text{FAK}}$  was induced at 10 min, and reached maximum levels at 30 min following binding. Induction at 30 min was 2.3 times that of the control. The  $\alpha 1(\text{IV})531-543$  THP produced higher levels of  $\text{p}125^{\text{FAK}}$  phosphorylation compared with the SSP at both  $2 \mu\text{M}$  and  $10 \mu\text{M}$  (5.7 times that of the control). The phosphorylation peaked at 20 min rather than 30 min as seen with the SSP. Although cellular recognition of the  $\alpha 1(\text{IV})531-543$  sequence was independent of substrate conformation, it appears that the intensity of signaling induced by this peptide is enhanced by triple-helical conformation. The overall implications of this data are (i) interaction of the  $\alpha 3\beta 1$  integrin with type IV collagen may play a role in post-adhesion tumor cell activities and (ii) ligand secondary, tertiary, and quaternary structure could modulate integrin-mediated signal transduction.

The  $\alpha 1\beta 1$  and  $\alpha 2\beta 1$  integrins serve as primary receptors for cell binding to type IV collagen [11, 12], while the  $\alpha 3\beta 1$  integrin mediates only low affinity binding but has been implicated in cell migration of type IV collagen [13]. Although  $\alpha 3\beta 1$  binding to a type IV collagen model sequence induces signal transduction events, the ultimate role of this integrin is not clear. We believe that binding to type IV collagen is initiated via the  $\alpha 1\beta 1$  and  $\alpha 2\beta 1$  integrins and then  $\alpha 3\beta 1$  integrin is recruited to sites on the substrate including  $\alpha 1(\text{IV})531-543$ . This model is consistent with that of DiPersio et al. [14], who demonstrated that the  $\alpha 3\beta 1$  integrin is localized to focal contacts following cell adhesion to type IV collagen, but does not initiate cell adhesion to this ligand. The primary role of the  $\alpha 3\beta 1$  integrin could then be in initiating post-adhesion signal transduction events.

Melanoma cells bind to a single-stranded and triple-helical peptide models of the  $\alpha 1(\text{IV})531-543$  sequence via the  $\alpha 3\beta 1$  integrin [9, 10]. Post-adhesion events induced by integrin binding to the  $\alpha 1(\text{IV})531-543$  sequence were evaluated. Single-stranded and triple-helical peptide models of  $\alpha 1(\text{IV})531-543$  induced Tyr phosphorylation of intracellular proteins. Immunoprecipitation analysis identified one of these proteins as  $\text{p}125^{\text{FAK}}$ . The effects of triple-helicity on shortening the time of  $\text{p}125^{\text{FAK}}$  phosphorylation indicate that, although  $\alpha 3\beta 1$  integrin binding to  $\alpha 1(\text{IV})531-543$  appears to be independent of substrate conformation [9], signaling via this receptor is influenced by substrate conformation. It is possible that this sequence of events represents a regulatory mechanism whereby cell binding to a triple-helical substrate, such as the intact basement membrane, induces phosphorylation of  $\text{p}125^{\text{FAK}}$  and the corresponding signaling cascade (Fig. 1). This activity is then followed by cellular production of growth factors, protease activators, and/or proteases which bring about degradation of the basement membrane and loss of cellular contact with the triple-helical substrate. Contact with the newly unwound substrate caused a downregulation of the signaling cascade, decreased production of cellular factors causing basement membrane destruction, and increased cell motility. This model of collagen structural modulation of signal transduction is consistent with the data presented here, and from other laboratories.

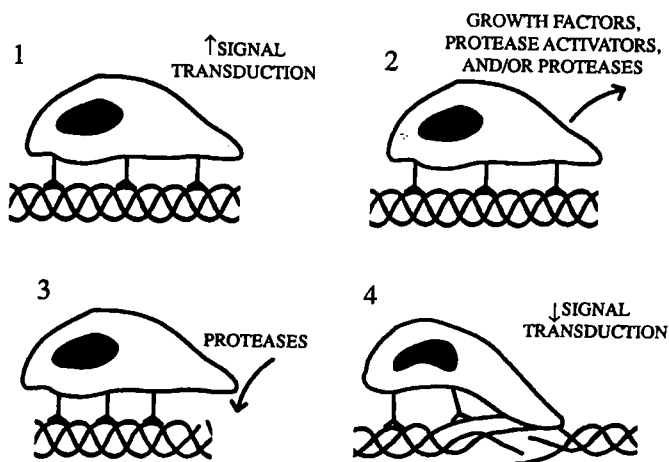


Fig. 1. Collagen structural modulation of tumor cell behavior.

## References

1. Kuhn, K., *Matrix Biol.*, 14 (1994) 439.
2. Richardson, A. and J.T. Parsons, *BioEssays*, 17 (1995) 229.
3. Kapron-Bras, C., L. Ritz-Gibbon, P. Jeevaratnam, J. Wilkins, and S. Dedhar, *J. Biol. Chem.*, 268 (1993) 20701.
4. Polanowska-Grabowska, R., M. Geanacopoulos, and A.R.L. Gear, *Biochem. J.*, 296 (1993) 543.
5. Defilippi, P.B., C., G. Volpe, G. Romano, M. Venturino, L. Silengo, and G. Tarone, *Cell Adhesion Commun.*, 2 (1994) 75.
6. Fujii, C., S. Yanagi, K. Sada, K. Nagai, T. Taniguchi, and H. Yamamura, *Eur. J. Biochem.*, 226 (1994) 243.
7. Bozzo, C., P. Defilippi, L. Silengo, and G. Tarone, *Exp. Cell Res.*, 214 (1994) 3138. Wilke, M.S. and L.T. Furcht, *J. Invest. Dermatol.*, 95 (1990) 264.
9. Miles, A.J., A.P.N. Skubitz, L.T. Furcht, and G.B. Fields, *J. Biol. Chem.*, 269 (1994) 30939.
10. Miles, A.J., J.R. Knutson, A.P.N. Skubitz, L.T. Furcht, J.B. McCarthy, and G.B. Fields, *J. Biol. Chem.*, 270 (1995) 29047.
11. Staatz, W.D., S.M. Rajpara, E.A. Wayner, W.G. Carter, and S.A. Santoro, *J. Cell. Biol.*, 108 (1989) 1917.
12. Eble, J., R. Golbik, K. Mann, and K. Kuhn, *EMBO J.*, 12 (1993) 4795.
13. Yoshinaga, I.G., J. Vink, S.K. Dekker, M.C.J. Mihm, and H.R. Byers, *Melanoma Res.*, 3 (1993) 435.
14. DiPersio, C.M., S. Shah, and R.O. Hynes, *J. Cell. Sci.*, 108 (1995) 2321.

# Somatostatin receptor antagonists based on a mixed neuromedin B antagonist/somatostatin agonist

David H. Coy,<sup>a</sup> Rahul Jain,<sup>a</sup> William A. Murphy,<sup>a</sup> Wojciech J. Rossowski,<sup>a</sup> Joseph Fuselier<sup>a</sup> and John E. Taylor<sup>b</sup>

<sup>a</sup>Peptide Research Laboratories, Department of Medicine, Tulane University Medical Center, New Orleans, LA 70112 and <sup>b</sup>Biomeasure, Inc., Milford, MA 01757, USA

This laboratory has had a long-standing interest in the design of somatostatin (SRIF) receptor antagonists which we have felt would be very useful tools for elucidating the many physiological functions of SRIF. They may also have therapeutic implications, particularly for the stimulation of GH levels in elderly patients with high SRIF tone by blocking the inhibitory actions of endogenous SRIF on GH release. A number of years ago we reported [1] the discovery of several short peptide analogs with apparent inhibitory effects on SRIF in several *in vivo* assay systems. However, we have subsequently been unable to demonstrate that these previous analogs have significant binding affinity for any of the 5 individual SRIF receptor subtypes. Thus, we were intrigued by the recent report [2] by Bass et al. [2] on the discovery of SRIF octapeptide antagonists containing D-Cys rather than L-Cys in position 2 which displayed high affinity binding for cells transfected with human type 2 and type 5 receptors.

We have reported [3] previously that *D-Nal-Cys-Tyr-D-Trp-Lys-Val-Cys-Nal-NH<sub>2</sub>* is a NMB antagonist with a  $K_i$  of 47 nM and a somatostatin (SRIF) agonist with a  $K_i$  of 10.6 nM for the transfected human type 2 SRIF receptor and had its D-Cys<sup>2</sup> analog on file. This analog was devoid of SRIF agonist activity and turned out to be a SRIF receptor antagonist at both rat and human type 2 SRIF receptors. It was used as the basis for the design of a number of analogs with increased antagonist potencies.

## Results and Discussion

The primary assay for the testing of new SRIF antagonists employed monolayer cultures of dispersed rat pituitary cells stimulated to secrete GH by addition of GRH(1-29)NH<sub>2</sub>, a process largely under the control of SRIF type 2 receptors in the rat [4]. The ability of new analogs to block the inhibitory effects of SRIF-14 in this system at various doses allowed IC<sub>50</sub> values versus 1 nM SRIF-14 to be calculated. They are shown in Table 1. Additionally, key analogs were examined at various concentrations for their abilities to displace <sup>125</sup>I-labeled SRIF-14 from CHO cells stably transfected with SRIF type 2 and type 5 receptors, thus allowing  $K_d$  values to be calculated. Several of the analogs shown to be antagonists were also tested for their abilities to block the inhibitory effects of SRIF-14 on pentagastrin-stimulated gastric acid release after infusions in conscious rats which is a process also mediated by type 2 receptors [5]. Analog 2 was able to weakly block SRIF GH-release inhibiting effects on rat pituitary cells with an IC<sub>50</sub> of 1.36 mM and bind to

human 2 and 5 receptors with a  $K_i$  of 68 nM and 1.06 mM, respectively, compared to the reported analog 1 [2] which had a rat  $IC_{50}$  of 50 nM. It bound to type 2 and type 5 receptors with a  $K_i$  of 23 and 101 nM, respectively. Thus, in our hands this type of analog has generally high specificity for the human type 2 receptor and analog 2 was not as potent as previously reported [2]. The effects of various combinations of L- and D-Nal at the N- and C-termini were investigated next. It appeared that L-L combinations gave the highest potencies (see analog 4, Table 1). This is a major SAR difference from somatostatin agonists, which prefer 1 a D-amino acid in position 1. Also, acetylation of the amino terminus had little effect on potency but seriously decreased solubility (analog 7). To search for increased solubility, other amino acids were substituted in the 3 position and it was discovered that Pal actually increased both solubility and potency from 35 to 15 nM (analog 9). Combinations of other aromatic amino acids were then examined at both termini and the best combinations were found in analogs 13-15 which had further improved  $IC_{50}$ s in the 2.5 nM region.

Table 1. Antagonist inhibition of SRIF-14(1 nM) inhibition of GH release from rat pituitary cells.

	$IC_{50}$ (nM)
1 Nfa-D-Cys-Tyr- D-Trp-Lys-Val-Cys-Tyr-NH <sub>2</sub>	50
2 D-Nal-D-Cys-Tyr-D-Trp-Lys-Val-Cys-Nal-NH <sub>2</sub>	1360
3 D-Nal-D-Cys-Tyr-D-Trp-Lys-Thr-Cys-Nal-NH <sub>2</sub>	>10000
4 Nal-D-Cys-Tyr-D-Trp-Lys-Val-Cys-Nal-NH <sub>2</sub>	35
5 D-Nal-D-Cys-Tyr-D-Trp-Lys-Val-Cys-D-Nal-NH <sub>2</sub>	380
6 Nal-D-Cys-Tyr-D-Trp-Lys-Val-Cys-D-Nal-NH <sub>2</sub>	280
7 Ac-Nal-D-Cys-Tyr-D-Trp-Lys-Val-Cys-Nal-NH <sub>2</sub>	57
8 Nal-D-Cys-His-D-Trp-Lys-Val-Cys-Nal-NH <sub>2</sub>	53
9 Nal-D-Cys-Pal-D-Trp-Lys-Val-Cys-Nal-NH <sub>2</sub>	15
10 Nal-D-Cys-Bta-D-Trp-Lys-Val-Cys-Nal-NH <sub>2</sub>	230
11 Pfa-D-Cys-Pal-D-Trp-Lys-Val-Cys-Pfa-NH <sub>2</sub>	820
12 Fpa-D-Cys-Pal-D-Trp-Lys-Val-Cys-Fpa-NH <sub>2</sub>	56
13 Cpa-D-Cys-Pal-D-Trp-Lys-Val-Cys-Cpa-NH <sub>2</sub>	2.4
14 Bpa-D-Cys-Pal-D-Trp-Lys-Val-Cys-Bpa-NH <sub>2</sub>	2.6
15 Cpa-D-Cys-Pal-D-Trp-Lys-Val-Cys-Nal-NH <sub>2</sub>	2.6
16 Nal-D-Cys-Pal-D-Trp-Lys-Gly-Cys-Nal-NH <sub>2</sub>	1500
17 Nal-D-Cys-Pal-D-Trp-Lys-Ala-Cys-Nal-NH <sub>2</sub>	420
18 Nal-D-Cys-Pal-D-Trp-Lys-Leu-Cys-Nal-NH <sub>2</sub>	52
19 Nal-D-Cys-Pal-D-Trp-Lys-Ile-Cys-Nal-NH <sub>2</sub>	120

Nfa, 4-NO<sub>2</sub>-Phe; Nal,  $\beta$ -(2-naphthyl)-Ala; Pal, 3-(2-pyridyl)-Ala; Bpa, 4-phenyl-Phe; Bta,  $\beta$ -(2-benzothienyl)-Ala; Pfa, pentafluoro-Phe; Cpa, 4-Cl-Phe; Fpa, 4-F-Phe.

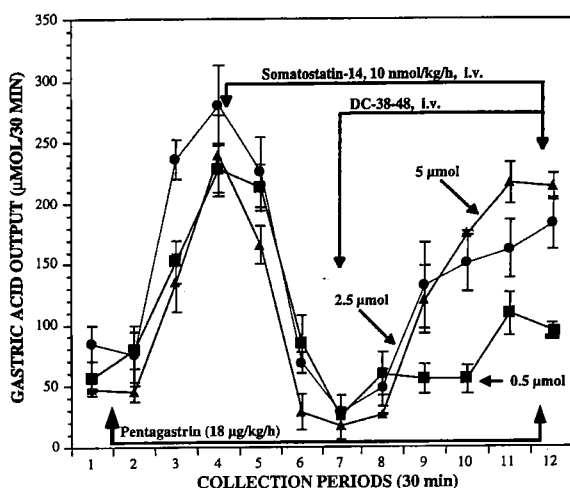


Fig 1. Inhibitory effects of  $Nal-D-Cys-Pal-D-Trp-Lys-Val-Cys-Nal-NH_2$  on SRIF inhibition of pentagastrin-stimulated gastric acid release in conscious rat.

In another study, SARs in position 6 (Val) were investigated (analogs 16-19). Substitution of this position with Thr results in loss of potency (analog 3), another major departure from the somatostatin agonists, which often prefer Thr in this position. Hydrophobic, branched amino acids appeared essential for high affinity with Val being the best choice.

Several of these antagonists have been tested for their ability to block *in vivo* actions of SRIF-14 in rats. One of these experiments is shown in Fig. 1 in which DC-38-48 (analog 9) inhibited the inhibitory effects of SRIF-14 on gastrin stimulated gastric acid release using an infusion protocol to minimize pharmacokinetic differences between peptides. This analog completely blocked the effects of SRIF-14 infused at 10 nmoles/kg/h at a dose of 500 nmoles/kg/h. Its  $IC_{50}$  calculated from these data was 87 nM against 1 nM SRIF-14 which compares reasonably well with the *in vitro*  $IC_{50}$  of 15 nM. Other analogs examined in this bioassay generally displayed *in vivo* potencies commensurate with the *in vitro* data.

## Conclusion

High potencies in this type of type 2 receptor specific SRIF antagonist reside in the use of optimized aromatic amino acid structures in position 1 and 8. We initially suspected that the ability of these side chains to form pi-pi complexes might offer an explanation for these results. However, molecular modeling studies in progress on these octapeptides, the agonist versions of which are quite well understood, suggests little possibility that this occurs. Indeed, the D-Cys<sup>2</sup> residue appears to force rotation of the position 1 side chains so that they protrude in the opposite direction to agonist side-chains with the remainder of the molecule being little changed. This may be the reason for their antagonist properties.

Several of the reported structures have inhibitory potencies which should make them suitable tools for examining the endogenous functions of SRIF at its type 2 receptors.

## References

1. Fries, J.L., Murphy, W.A., Sueiraz-Diaz, J. and Coy, D.H., *Peptides*, 3 (1982) 811.
2. Bass, R.T., Buckwalter, B.L., Patel, B.P., Pausch, M.H., Price, L.A., Strnad, J. and Hadcock, J.R., *Mol. Pharmacol.*, 50 (1996) 709.
3. Orbuch, M., Taylor, J.E., Coy, D.H., Mrozinski, J.E., Mantey, S., Battey, J.F., Moreau, J-P. and Jensen, R.T., *Mol. Pharmacol.*, 44 (1993) 841.
4. Raynor, K., Murphy, W.A., Coy, D.H., Taylor, J.E., Moreau, J-P., Yasuda, K., Bell, G.I. and Reisine, T., *Mol. Pharmacol.*, 43 (1993) 838.
5. Rossowski, W.J., Gu, Z.F., Akarca, U.S., Jensen, R.T. and Coy, D.H., *Peptides*, 15 (1994) 1421.

# The origin of specificity in the opioid receptor family

Irina D. Pogozheva, Andrei L. Lomize and Henry I. Mosberg

*College of Pharmacy, University of Michigan, Ann Arbor, MI 48109, USA*

The  $\delta$ ,  $\mu$ , and  $\kappa$  opioid receptors belong to the superfamily of seven-helical G-protein coupled receptors (GPCR). The common “average” model of the transmembrane domain of GPCRs has recently been calculated using the distance geometry algorithm with hydrogen bonds formed by intramembrane polar side chains in various proteins from the family collectively applied as distance constraints [1]. The models of 28 different GPCRs (bovine rhodopsin, 1bok PDB file; human  $\delta$ ,  $\mu$  and  $\kappa$  opioid receptors, etc.) were calculated in a similar manner using H-bonds of each specific receptor and the “average” model to restrain spatial positions of the helices. The receptor models are consistent with experimental data and are complementary to their natural and synthetic ligands [1].

## Results and Discussion

The structures of  $\delta$ ,  $\mu$ , and  $\kappa$  opioid receptors, calculated solely from the H-bonding constraints, have binding cavities complementary to different opioid ligands, such as the  $\delta$  agonist Tyr-c[D-Cys-Phe-D-Pen]OH (JOM-13) and  $\delta$  antagonists Tyr-Tic-Phe-Phe-OH (TIPP) and naltrindole (NTI),  $\mu$ -agonists (-)-morphine, Tyr-c[D-Cys- $\Delta^E$ Phe-D-Pen]NH<sub>2</sub> (JH-42),  $\mu$ -antagonist D-Phe-c[Cys-Tyr-D-Trp-Orn-Thr-Pen]Thr-NH<sub>2</sub> (CTOP),  $\kappa$ -antagonist norbinaltorphimine (norBNI), and many others. The rigid nonpeptide and constrained peptide ligands demonstrate precise geometrical fits to the receptor binding sites and form characteristic H-bonds and hydrophobic contacts with receptor sidechains. The binding pocket consists of a deeper “conserved region”, identical in  $\delta$ ,  $\mu$  and  $\kappa$  opioid receptors (Gln<sup>105</sup>, Tyr<sup>109</sup>, Cys<sup>121</sup>, Val<sup>124</sup>, Asp<sup>128</sup>, Tyr<sup>129</sup>, Met<sup>132</sup>, Cys<sup>198</sup>, Lys<sup>214</sup>, Ile<sup>215</sup>, Phe<sup>218</sup>, Trp<sup>274</sup>, Ile<sup>277</sup>, His<sup>278</sup>, Cys<sup>303</sup>, Ile<sup>304</sup> and Tyr<sup>308</sup> residues using the  $\delta$ -receptor numbering) and a “variable region”, composed of 19 residues near the extracellular surface, which differs in  $\delta$ ,  $\mu$ , and  $\kappa$  subtypes and which is responsible for subtype specificity of various ligands (Fig. 1). The conserved residues in the bottom of the pocket interact with the tyramine part of alkaloids or Tyr<sup>1</sup> of opioid peptides (with ligand N+ and OH groups forming H-bonds with Asp<sup>128</sup> and His<sup>278</sup>, respectively), while the center of the pocket is occupied by the tripeptide cycle of JOM-13, Tic<sup>2</sup> of TIPP, or ring systems of alkaloids, oriented perpendicularly to the tyramine part. Side-chains of Phe<sup>3</sup> residues and COO<sup>-</sup> termini of JOM-13 and TIPP occupy spatially identical sites formed by a number of conserved and variable residues, that correlate with their similar structure-activity relationships. The spatial positions of functionally equivalent N+ and OH groups vary by 0.5-2.5 Å depending on the ligand. Incorporation of a bulky group near the N-terminus of the ligand, between helices III and VI or VII (cyclopropylmethyl of NTI and norBNI, or

the more deeply embedded Tyr<sup>1</sup> of TIPP and D-Phe<sup>1</sup> of CTOP) probably leads to the functional antagonism displayed by these ligands.

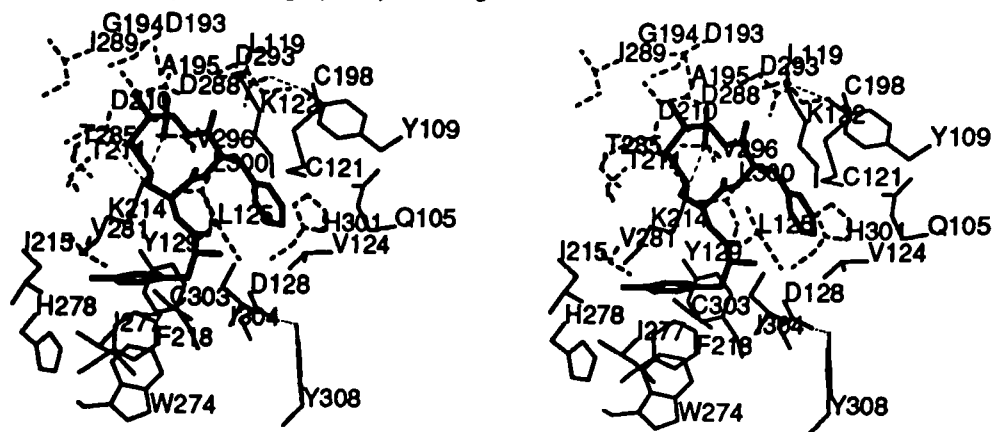


Fig. 1. JOM-13 (thick line) inside the binding pocket of  $\delta$ -opioid receptor (stereoview). The solid line denotes conserved residues within the opioid receptor family while the dashed line indicates variable residues.

The origin of receptor selectivity of many different opioid ligands can be deduced by docking these ligands with the models of the  $\delta$ ,  $\mu$  and  $\kappa$  receptors. For example, JOM-13 ( $K_i^\delta=0.74$  nM,  $K_i^\mu=51.5$  nM), and its  $\Delta^Z$ -Phe<sup>3</sup> analog fit well to the binding pocket of  $\delta$  receptor (Fig. 2), providing, in addition to the tyramine binding site, packing of the ligand Phe<sup>3</sup> side-chain in *gauche* conformation and a favorable electrostatic interaction between the terminal COO<sup>-</sup> group of JOM-13 with Lys<sup>214</sup>. However, the replacement of Leu<sup>300</sup> in helix VII of the  $\delta$  receptor by Trp in the  $\mu$  receptor causes a shift of the tripeptide cycle of JOM-13 or its analogue JH-42 (Fig. 2). This slightly changes the spatial positions of Tyr<sup>1</sup> (allowed by the replacement of Thr<sup>211</sup> in the  $\delta$  receptor by Asn in the  $\mu$ ) and leads to the repositioning of the Phe<sup>3</sup> ring and shifts the peptide terminal COO<sup>-</sup> group toward the Glu sidechain in helix V (Asp<sup>210</sup> in the  $\delta$  receptor). The necessary reorientation of the Phe<sup>3</sup> side chain from  $\chi^1=-60^\circ$  to  $\chi^1=180^\circ$  is facilitated by the replacement of Leu<sup>119</sup> and Asp<sup>293</sup> in the  $\delta$  receptor by Ile and Thr, respectively, in the  $\mu$ -receptor. This explains the observation that a *trans* orientation of the Phe<sup>3</sup> sidechain (as in  $\Delta^E$ -Phe<sup>3</sup> of JH-42,) and an amidated C-terminus are preferred for binding to  $\mu$  receptors [2], as seen for JH-42 ( $K_i^\delta=195$  nM,  $K_i^\mu=7.92$  nM).

Small morphine-like compounds have only a few "selective interactions". An interaction of the aromatic rings of morphine and Trp<sup>318</sup> in helix VII (Leu<sup>300</sup> in  $\delta$  and Tyr<sup>312</sup> in  $\kappa$  receptor) and formation of an H-bond between the 6 $\alpha$ -OH of (-)-morphine with Asn<sup>230</sup> in helix V of the  $\mu$  receptor (Thr<sup>211</sup> in  $\delta$ -receptor and Leu<sup>224</sup> in  $\kappa$ -receptor) modestly increase  $\mu$  binding relative to  $\delta$  and  $\kappa$  binding. Larger ligands have many "selective interactions" with the receptors. For example, D-Phe<sup>1</sup> and Tyr<sup>3</sup> of CTOP interact with the

Trp<sup>318</sup> sidechain in helix VI of the  $\mu$ -receptor, Orn<sup>5</sup> forms an ionic pair with Glu<sup>310</sup> (Arg<sup>291</sup> in the  $\delta$  and His<sup>304</sup> in the  $\kappa$  receptor), and the C-terminal group of Thr<sup>8</sup> in CTOP can H-bond with the polar sidechains of Ser<sup>214</sup>, Gln<sup>314</sup> and Thr<sup>315</sup> (Ala<sup>195</sup>, Val<sup>296</sup> and Val<sup>297</sup> in the  $\delta$  receptor and Val<sup>207</sup>, Val<sup>308</sup>, Leu<sup>309</sup> in the  $\kappa$  receptor).

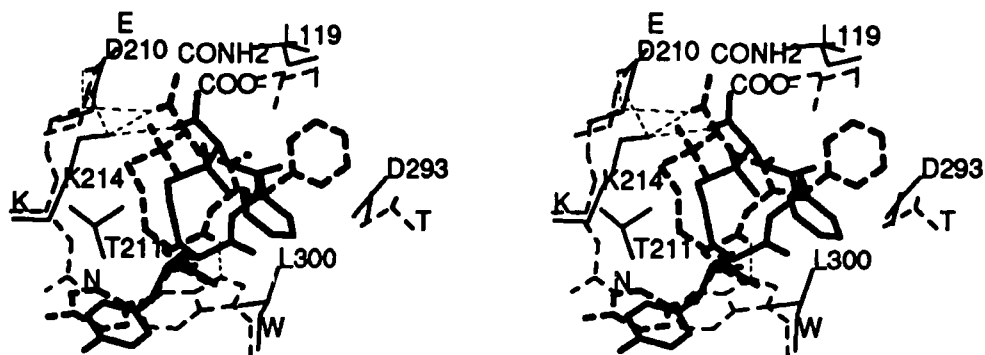


Fig. 2. Superposition of the binding pockets of the  $\delta$  (solid line) and  $\mu$  (dashed line) opioid receptors with their selective ligands JOM-13 and JH-42, respectively. Only variable side chains of the receptors, responsible for ligand selectivity are shown (thin line).

The set of residues participating in the binding pocket includes several residues which have been identified as functionally important by mutagenesis of opioid receptors (Asp<sup>128</sup>, Tyr<sup>129</sup>, Phe<sup>218</sup>, Trp<sup>274</sup>, His<sup>278</sup>, Tyr<sup>308</sup>) [3]. However, some structurally important residues that are remote from the binding pocket, such as Asp<sup>95</sup>, Trp<sup>173</sup> and Ser<sup>177</sup> but participate in the formation of interhelical H-bonds in the model (Asp<sup>95</sup>-Asn<sup>314</sup>, Asn<sup>90</sup>-Trp<sup>173</sup> and Thr<sup>134</sup>-Ser<sup>177</sup>), have also been shown to affect ligand binding [3].

## Acknowledgments

Financial support from the NIH (DA03910, DA09989 and DA00118) and from the University of Michigan College of Pharmacy Upjohn Research Award are gratefully acknowledged.

## References

1. Pogozheva, I.D., Lomize, A.L. and Mosberg H.I., *Biophys. J.*, 70 (1997) 1963.
2. Mosberg, H.I., Dua, R. K., Pogozheva, I. D. and Lomize, A. L., *Biopolymers.*, 39 (1996) 287.
3. Opioid receptor point mutation database (<http://www.opioid.umn.edu/ptmut.html>).

# Mapping of the interleukin-10/interleukin-10 receptor combining site using structurally different peptide scans

**Ulrich Reineke, Robert Sabat, Hans-Dieter Volk,  
and Jens Schneider-Mergener**

*Institut für Medizinische Immunologie, Universitätsklinikum Charité, Humboldt-Universität zu  
Berlin, Schumannstr. 20-21, 10098 Berlin, Germany*

The interaction of interleukin-10 (IL-10) with the specific interleukin-10 receptor (IL-10R) is similar to many other biological recognition processes mediated via discontinuous protein-protein combining sites. Many approaches for the investigation of the molecular basis of such binding events have been described. Recently, the mapping of non-linear antibody epitopes [1, 2] as well as the IL-6/IL-6R-interaction [3] using ligand sequence-derived scans of overlapping peptides synthesized by spot synthesis [4] was developed. This approach was restricted to the mapping of linear epitopes due to the fact that the affinity of separated parts of discontinuous epitopes to their respective binding partners is too low. Only the complete and correctly folded discontinuous binding site enables high affinity binding. Here we describe strategies for the mapping of the putative IL-10/IL-10R combining site: (1) The detection of low affinity protein-peptide interactions and (2) the use of overlapping peptide scans with peptides of different length.

## Results and Discussion

We probed two IL-10-derived scans of overlapping peptides (15mers, 14 amino acids overlapping and 6mers, 5 amino acids overlapping) synthesized by spot synthesis on continuous cellulose membrane supports with the soluble part of the IL-10R. For analysis, peptide-bound IL-10R was electrotransferred onto polyvinylene difluoride membranes in three subsequent steps (Fig. 1) and detected using anti-IL-10R sera and a peroxidase-labelled secondary antibody in combination with a chemiluminescence detection system. The blotting technique was applied to prevent the washing away of IL-10R, which is peptide-complexed with very low affinities during incubation with the detection antibodies. Taking all blot membranes into consideration, peptides covering three binding regions were identified (Fig. 2). Peptides of region A could only be detected using the 6mer peptide scan whereas peptides derived from region B only bound IL-10R as 15mers. Spots from both regions were visible only in the first blot. On the other hand region C was detected utilizing both the first blot of the IL-10R incubated membrane of 6meric and the third blot of the 15meric peptides. The finding that the spot pattern varied in the three subsequent blots could be due to different peptide-IL-10R affinities. The rationale for using peptides of different length was that only a few amino acids of a binding region are in contact with the binding partner, whereas the other amino acids are usually buried in the protein. These residues can be accessible for the binding partner when synthesized in the form of overlapping linear peptides and influence especially low affinity interactions in an

unpredictable manner. The portion of residues in contact with the binding partner in a mode similar to the protein-protein complex can vary using peptides of different length.

The data obtained by the peptide scanning approach are essentially consistent with a computer-derived model of the IL-10/IL-10R complex [5] which is based on the crystal structure of the IFN $\gamma$ /INF $\gamma$ R complex. Furthermore, the prediction of the IL-10R combining site was supported by the epitope mapping of the two IL-10-neutralizing monoclonal antibodies CB/RS/3 and CB/RS/10 (Fig. 2). In conclusion, this approach should be generally applicable for the mapping of discontinuous protein-protein contact sites.

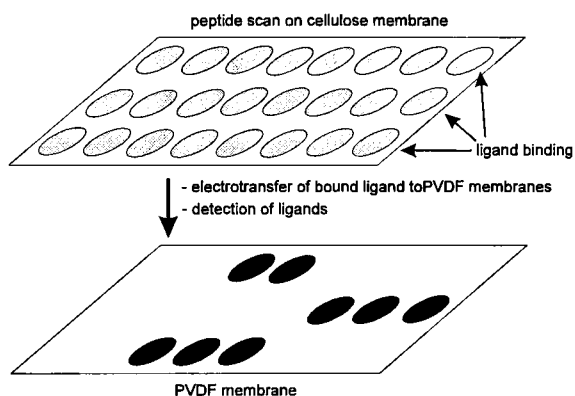


Fig. 1. (left) Schematic illustration of high sensitivity mapping of protein-protein contact sites.

Fig. 2. (below) Sequence of interleukin-10. Peptides which bound the interleukin-10 receptor are underlined. Residues which are in contact with the interleukin-10 receptor in the complex model are bold marked. Epitopes of monoclonal antibodies CB/RS/3 and CB/RS/10 are displayed.



## References

1. Reineke, U., Sabat, R., Kramer, A., Stigler, R.-D., Michel, T., Volk, H.-D. and Schneider-Mergener, J., Mol. Div., 1 (1995) 141.
2. Gao, B. and Esnouf, P., J. Immunol., 157 (1996) 183.
3. Weiergräber, O., Schneider-Mergener, J., Grötzinger, J., Wollmer, A., Küster, A., Exner, M. and Heinrich, P. C., FEBS Lett., 379 (1996) 122.
4. Frank, R., Tetrahedron, 48 (1992) 9217.
5. Zdanov, A., Schalk-Hihi, C. and Wlodawer, A., Prot. Sci., 5 (1996) 1955.

# Design and synthesis of specific proline-rich peptides with high affinity for Grb2

**Didier Cussac, Fabrice Cornille, Gilles Tiraboschi, Christine Lenoir,  
Bernard Roques and Christiane Garbay**

*Unité de Pharmacochimie Moléculaire et Structurale, U266 INSERM - URA D 1500 CNRS,  
Université René Descartes, 4, avenue de l'Observatoire, 75270 Paris Cedex 06, France*

Grb2 is a small adaptor protein involved in the ras signalling pathway and is composed of one SH2 domain surrounded by two SH3 domains [1]. Grb2 couples receptor tyrosine kinase activation to the ras signalling pathway, by an interaction of its SH2 domain with phospho-tyrosine motifs of receptors and by interaction of its SH3 domains to proline-rich motifs of Sos, the exchange factor of ras. In order to block ras activation in tumor cells and provide potential antiproliferative drugs, we have designed dimeric proline-rich peptides.

## Results and discussion

"Peptidimers" made of two proline-rich sequences connected by different sized spacers have been designed using molecular modeling based on the crystal structure [2] of Grb2 and the results of NMR studies on its N-SH3 domain complexed with the proline-rich peptide VPPVPPRRR (V10R) derived from Sos [3]. The complex was built using one monomer of the dimeric crystal structure of Grb2. The two proline-rich motifs were docked on the hydrophobic recognition platform of each SH3 domain as determined by NMR data. In order to adopt the orientation required for interacting with their recognition sites, VPPVPPRRR peptides needed to be connected by their C-terminal part. This was achieved by solid phase peptide synthesis, using the two amino groups of a lysine already coupled to the resin, to bind subsequently step by step each amino acid of the two proline-rich sequences through Fmoc chemistry. After deprotection and cleavage from the resin, peptides dimers were obtained (i.e:  $4 \rightarrow \text{H}_2\text{N-VPPVPPRRR-(N}^\alpha\text{)K(N}^\epsilon\text{)-RRRPPVPPV-NH}_2$  referred as V10R-K-(V10R)).

Using a fluorescence assay [4], we found that the affinity of the peptidimers for Grb2 is  $10^2$  and  $10^3$  higher than their affinity for the N and C-terminal SH3 domains, respectively (Table 1). These results show that both proline-rich regions of the peptidimers interact with Grb2 leading to derivatives which exhibit the highest affinity so far described for Grb2 SH3 domains. The specificity of the interaction was checked using control peptides where the second proline-rich motif was deleted or replaced by a peptide devoid of the consensus PXXPXR motif recognized by SH3 domains (data not shown). These compounds displayed affinities for Grb2 lying in the same range as that of V10R **1**. Reduction of the connecting chain length of the peptidimers (compounds **3** and **4**) did not change their affinity for Grb2 (Table 1). Only a lysine between the two proline-rich peptides is sufficient to generate good affinity, in agreement with molecular modeling. Moreover, this result

supports the fact that both SH3 domains of Grb2 are close together in the solution structure.

*Table 1: Affinities of peptidimers for Grb2 and its N- and C-terminal SH3 domains.*

	Complete Grb2	N-terminal SH3	C-terminal SH3
Peptides	Kd ( $\mu$ M)	Kd ( $\mu$ M)	Kd ( $\mu$ M)
V10R : <b>1</b>	18 $\pm$ 2	2.6 $\pm$ 0.2	40 $\pm$ 5
V10R-Aha-K-(Aha-V10R): <b>2</b>	0.05 $\pm$ 0.005	2.2 $\pm$ 0.2	40 $\pm$ 5
V10R-Aha-K-(V10R): <b>3</b>	0.04 $\pm$ 0.005	2.2 $\pm$ 0.2	ND
V10R-K-(V10R) : <b>4</b>	0.04 $\pm$ 0.005	2.2 $\pm$ 0.2	ND

V10R = VPPPVPPRRR ; Aha = H<sub>2</sub>N-(CH<sub>2</sub>)<sub>5</sub>-COOH; ND = not determined

In order to evaluate directly the effect of the peptidimers on Grb2-Sos interaction, increasing concentrations of **4** were added to an ER22 cell extract and the Grb2-Sos complex, which was trapped on a phosphotyrosine peptide previously coupled to Sepharose beads, was subsequently analyzed with anti-Grb2 and anti-Sos antibodies. A concentration of only 50 nM of **4** is able to totally inhibit the Grb2-Sos complex formation, while 5  $\mu$ M of the monomer **1** is necessary to observe the same effect (not shown).

These results suggest that peptidimers may provide potential inhibitors of cell proliferation mediated by the constitutively activated ras pathway involving Grb2 -Sos complex formation.

## References

1. Chardin, P., Cussac, D., Maignan, S., Ducruix, A., FEBS Lett., 369 (1995) 47.
2. Maignan, S., Guilloteau, J.P., Fromage, N., Arnoux, B., Becquart, J., Ducruix, A., Science, 268 (1995) 291.
3. Goudreau, N., Cornille, F., Duchesne, M., Parker, F., Tocqué, B., Garbay, C., Roques, B.P., Nature Struct. Biol., 1 (1994), 898.
4. Cussac, D., Frech, M., Chardin, P., EMBO J., 13(17) (1994) 4011-4021.

# **N-terminal myristoylation of HBV Pre-S1 domain affects folding and receptor recognition**

**Menotti Ruvo, Sandro De Falco, Antonio Verdoliva,  
Angela Scarallo and Giorgio Fassina**

*TECHNOGEN S.C.P.a. Parco Scientifico, 81015 Piana di Monte Verna (CE), Italy*

PreS1(1-119) is the proline rich N-terminus portion of the large (L) protein, one of the three proteins that compose the envelope of Hepatitis B Virus (HBV) [1]. PreS1 seems to be directly involved in receptor recognition and consequently to be responsible for viral infectivity. Several studies have suggested a prominent role for residues 21-47 in receptor binding [2,3]. Further investigations have also shown that myristoylation on the Gly<sup>2</sup> residue of this protein is essential for virion assembly and for viral infectivity [4,5,6]. A complete and detailed characterization of PreS1 structural requirements needed for HBV interaction with cellular receptors has been hampered by the lack of an adequate source of isolated viral protein domains. In this study, we have produced by stepwise solid phase chemical synthesis the PreS1 region of the HBV surface antigen, adw2 subtype, PreS1(1-119) and its myristoylated form, Myr-PreS1(2-119), in order to establish the influence of the myristoyl group on folding and its importance in receptor binding.

## **Results and Discussion**

Pre-S1(1-119) and Myr-Pre-S1(2-119) were prepared by single step solid phase synthesis. During chain assembly (Fmoc/DCC/HOBtO, resin aliquots were removed to progressively increase the amino-acid:resin ratio and to prevent clogging of the reaction vessel caused by the increase in resin volume. Synthesis progression was checked monitoring Fmoc deprotection and by cleaving small aliquots of resin after each set of ten couplings in order to evaluate the quality of the corresponding peptide fragments. All intermediates were highly homogeneous and data obtained by amino acid analysis and molecular weight determination were in good agreement with the expected values. After coupling of the Gly<sup>2</sup> residue, the resin was acetylated and then treated with piperdine. PreS(1-119) was obtained by coupling Fmoc-Met-OH to the resin, while the myristylated protein was obtained by attaching the myristic acid via HBTU/HOBt/DIEA-mediated coupling. Given the high homogeneity of the crude products, as shown in Fig. 1, a single chromatographic step (semi-preparativ RP-HPLC) was sufficient to purify both proteins. Protein purity and identity were confirmed by HPLC analysis, TOF-MALDI mass spectrometry, and trypsin digestion. CD measurements performed in aqueous buffers and in the presence of 50% TFE (v/v) showed the presence of a significant content of ordered structure in the myristylated derivative. In a receptor binding assay performed using plasma membranes (PM) prepared from the hepatocyte carcinoma cell line HepG2 [7], Pre-S1(1-119) showed reduced receptor recognition compared to its homologue bearing the fatty acid on the N-terminus,

suggesting that the main role of N-terminal myristoylation is to induce conformational transitions important for receptor binding.

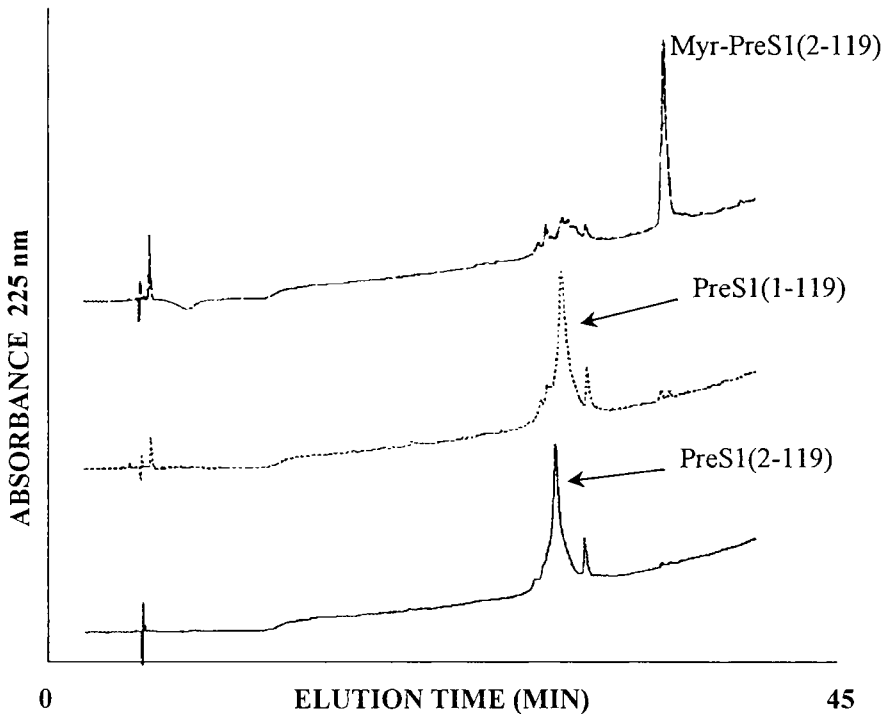


Fig. 1. HPLC analysis of crude PreS1(2-119), PreS1(1-119) and Myr-PreS1(2-119). Column: RP-18 Jupiter 250X4.6mm ID. Flow: 1.0 mL.min,  $\lambda=225$  nm; gradient: from 5% 50 60% of  $\text{CH}_3\text{CN}$ , 0, 1% TFA in 40 minutes.

## References

1. Tiollais, P., Poucel, C. and Dejean, A., *Nature*, 317 (1985) 489-495.
2. Neurath, A.R., Kent, S.B.H., Strick, N. and Parker D., *Cell*, 46 (1986) 429-436.
3. Pontisso, P., Ruvoletto, M.G., Tribelli, C., Gerlich, W.H., Ruol A. and Alberti, A., *J. Gen. Virol.*, 73 (1992) 2041-2045.
4. Gripon, P., Le Seyec, J., Rumin, S. and Guguen-Gillouzo, C., *Virology*, 213 (1996) 292-299.
5. Bruss, V., Haglestein, J., Gerhardt, E. and Galle, P.R., *Virology*, 218 (1996) 396-399.
6. Macrae, D.R., Bruss, V. and Ganem D., *Virology*, 181 (1991) 359-363.
7. Neurath, A.R. and Kent, S.B.H., *Adv. Virus. Res.*, 34 (1988) 65-142.

# High affinity IgE-receptor- $\alpha$ -subunit-derived peptides as antagonists of human IgE binding

Waleed Danho, Raymond Makofske, Joseph Swistok, Michael Mallamaci, Mignon Nettleton, Vincent Madison, David Greeley, David Fry and Jarema Kochan

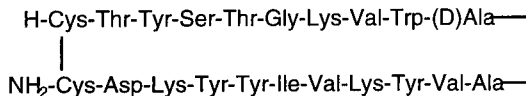
Roche Research Center, Hoffmann-La Roche Inc., Nutley, NJ 07110, USA

Immediate hypersensitivity is mediated by IgE binding and cross-linking of high affinity receptors for IgE (Fc $\epsilon$ RI) on basophils and mast cells. *In vitro* and *in vivo* studies demonstrate that preventing either IgE binding or receptor crosslinking by addition of neutralizing Abs inhibits antigen-specific allergic responses. The goal of our project is to identify a novel agent that competes for or displaces the binding of IgE to its high affinity receptor, and is therapeutically effective in the management of IgE-mediated diseases. The high affinity receptor for IgE is a tetrameric structure consisting of  $\alpha$ ,  $\beta$ , and  $\gamma$  subunits. The extracellular portion of the  $\alpha$  subunit is capable of binding IgE with high affinity in the absence of the other two subunits.

## Results and Discussion

Site-directed mutagenesis of the IgE Fc $\epsilon$ RI $\alpha$  subunit (Fc $\epsilon$ RI $\alpha$ ) was used to characterize the amino acid residues which are important for human IgE binding. From single-site mutations to alanine, nine amino acid residues were identified in domain 2 [Val<sup>140</sup>, Val<sup>143</sup>, Tyr<sup>145</sup>, Tyr<sup>146</sup>, Lys<sup>147</sup>, Asp<sup>148</sup>, Tyr<sup>174</sup>, Gly<sup>178</sup>, Val<sup>180</sup>] as essential for IgE binding. In domain 1, twelve additional residues were identified as being important for binding. A structural model of the two Ig-like domains of Fc $\epsilon$ RI $\alpha$  indicates that the binding epitopes in domain 2 would form a contiguous three-dimensional patch on the receptor surface.

A series of overlapping linear peptides and cyclic peptides were designed to present the binding residues in a manner similar to that in the structural model of the receptor. The most potent cyclic peptide (Ro 25-7162) with an IC<sub>50</sub> of 40 $\mu$ M was shown to completely inhibit IgE binding in a competitive manner and showed selectivity since it demonstrated no activity in the IL-1 or IL-2 binding assay at concentration up to 1 mM.



Ro 25-7162

Ro 25-7162 connects strand F (173-181) and C (140-148) of the second domain of the receptor. In order to verify Ro 25-7162 as a lead, the synthesis and biological evaluation of

the Ala, and Lys analogs were carried out (Table 1). The residues, Gly<sup>178</sup>, Val<sup>180</sup>, Val<sup>140</sup>, Val<sup>143</sup>, and Asp<sup>148</sup> were identified as a subset of the critical residues involved in the binding between IgE-Fc and FcεRIα. Substitution of Asp<sup>148</sup>, by Lys in Ro 25-7162 resulted in an inactive peptide confirming the critical role of this residue. Val<sup>140</sup> and Val<sup>143</sup> were also shown to play critical roles since substitution by Ala also gave inactive peptides. Substitution of Gly<sup>178</sup> and Val<sup>180</sup> by Ala yielded active peptides. These changes are not sufficient to inactivate the peptide even though they do inactivate the FcεRIα. Gly<sup>178</sup> may play a critical role in packing the protein chains.

The loss of activity upon substitution of Ala for Val<sup>140</sup> and Val<sup>143</sup> is evidence that Ro 25-7162 mimics receptor protein binding.

Table 1. SAR Studies of Ro 25-7162

Ro Number	Substitution	IC <sub>50</sub> μM
25-7162		40
25-8688	Lys <sup>148</sup>	inactive
25-8689	Ala <sup>140</sup> , Ala <sup>143</sup>	inactive
25-8690	Ala <sup>178</sup> , Ala <sup>180</sup>	40
25-8694	Val <sup>178</sup>	40
25-9735	Tyr(2,6-DichloroBzl) <sup>175</sup> , Tyr(2,6-DichloroBzl) <sup>146</sup>	100
25-9165	Des 177-181, 140-144	inactive
25-9166	Des 173-177, 144-148	inactive
25-8619	Des Thr <sup>173</sup>	inactive
25-8617	Des Thr <sup>173</sup> , Tyr <sup>174</sup>	inactive
25-8754	Fmoc-Des-Thr <sup>173</sup> , Tyr <sup>174</sup> , Tyr <sup>175</sup>	inactive

The solution conformation of Ro 25-7162 in DMSO was studied by <sup>1</sup>H-NMR and NOE constrained molecular dynamics. This large cyclic peptide has local segments which were well ordered, but overall the peptide is very flexible. Therefore, three different strategies were pursued for stabilizing the β-strand conformation for compounds related to Ro 25-7162. The first is the synthesis of bicyclic analogs, the second is the synthesis of cyclic analogs of one central disulfide and one lactam link, and the third is the synthesis of homo- and heterodimers of (140-148) and (173-181). Based on these strategies a new series of peptides were synthesized and assayed. Ro 25-9612, a homodimer consisting of residues (140-148), was able to inhibit IgE binding with an IC<sub>50</sub> of 30 μM in a competitive manner. Its mode of action appears to involve binding to the IgE-Fc and blocking the binding site for FcεRIα. Shortened analogs of Ro 25-9612 were prepared and analyzed. Ro 25-9960, which was shorter by one amino acid in each chain (sequence 141-148), exhibited an IC<sub>50</sub> of 2 μM. In conclusion, we succeeded in minimizing the protein/protein interaction to a small peptide/protein interaction. The next challenge will be to develop a peptide-mimetic based on the peptide information obtained.

# Highly potent human parathyroid hormone analogs

Jesse Z. Dong,<sup>a</sup> Chizu Nakamoto,<sup>b</sup> Michael Chorev,<sup>b</sup> Barry A. Morgan,<sup>a</sup>  
Michael Rosenblatt<sup>b</sup> and Jacques-Pierre Moreau<sup>a</sup>

<sup>a</sup>Biomeasure Incorporated, 27 Maple Street, Milford, Massachusetts 01757, USA,

<sup>b</sup>Beth Israel Deaconess Medical Center, Harvard Medical School,  
330 Brookline Ave., Boston, Massachusetts 02215, USA

There is growing evidence showing that intermittent administration of human parathyroid hormone, hPTH(1-84), or its N-terminal fragment hPTH(1-34) can effectively build bone in animals and humans [1]. In an effort to develop a novel bone anabolic agent for the treatment of osteoporosis, we are involved in a search for more potent hPTH(1-34) analogs.

NMR studies have indicated that in aqueous solution the major conformational features of hPTH(1-34) include two amphiphilic  $\alpha$ -helices located at the N- and C-termini connected by a defined reverse turn region [2,3]. Our research was mainly focused on modification of residues in the hydrophobic face of the N-terminal amphiphilic  $\alpha$ -helix, in the reverse turn and at the beginning of the C-terminal  $\alpha$ -helix.

## Results and Discussion

PTH(1-34) analogs were synthesized using the rapid Boc-chemistry SPPS strategy developed by Schnolzer et al. [4] and assayed for the stimulation of cAMP production in human osteosarcoma cells [5].

It is known that the amphiphilic  $\alpha$ -helix has membrane searching and binding properties [6], and the concept that membranes catalyze agonist-receptor interactions has been suggested [7]. In addition, there is evidence implicating a possible interaction of the N-terminus of PTH with the transmembrane region of the PTH receptor [8]. From these considerations, we hypothesized that the two amphiphilic  $\alpha$ -helices of PTH, especially the one at the N-terminal, could have a membrane associating function which promotes efficient hormone-receptor interactions, and could also prevent PTH from fast proteolysis and excretion. Based on this hypothesis, hPTH(1-34) analogs bearing cyclohexylalanine (Cha) in the hydrophobic face (positions 7 and 11) of the N-terminal amphiphilic  $\alpha$ -helix were designed. The bulky side-chain of Cha increases the size and the hydrophobicity of the hydrophobic face, improving membrane affinity of the peptide. These analogs (peptides 1-3) were 1.7 to 6.7-fold more active than the parent peptide, hPTH(1-34), in stimulating cAMP production (Table 1).

Because the C-terminal  $\alpha$ -helix could be a critical conformational requirement for PTH-receptor interactions, and a more stable  $\alpha$ -helix could have a higher lipid membrane

Table 1: Biological activity in production of cAMP in human osteosarcoma cells.

Peptide	cAMP(EC <sub>50</sub> )(nM)	Relative Activity to hPTH(1-34)	Sequences
1	2.3	1.7	[Cha <sup>7</sup> ]hPTH(1-34)NH <sub>2</sub>
2	2.0	2.0	[Cha <sup>11</sup> ]hPTH(1-34)NH <sub>2</sub>
3	0.6	6.7	[Cha <sup>7,11</sup> ]hPTH(1-34)NH <sub>2</sub>
4	0.7	5.7	[Aib <sup>16</sup> ]hPTH(1-34)NH <sub>2</sub>
5	0.6	6.7	[Aib <sup>19</sup> ]hPTH(1-34)NH <sub>2</sub>
6	0.6	6.7	[Aib <sup>16,19</sup> ]hPTH(1-34)NH <sub>2</sub>
7	3.0	1.3	[Aib <sup>17</sup> ]hPTH(1-34)NH <sub>2</sub>
8	1.1	3.6	[Cha <sup>7,11</sup> ,Aib <sup>6</sup> ]hPTH(1-34)NH <sub>2</sub>
9	0.5	8.5	[Cha <sup>7,11</sup> ,Aib <sup>19</sup> ]hPTH(1-34)NH <sub>2</sub>
10	1.3	3.1	[Cha <sup>15</sup> ]hPTH(1-34)NH <sub>2</sub>
11	1.4	2.9	[Cha <sup>7,11,15</sup> ]hPTH(1-34)NH <sub>2</sub>

affinity, we designed another series of analogs in which  $\alpha$ -aminoisobutyric acid (Aib) was substituted for the residues at positions 16, 17 or 19 near the end of C-terminal  $\alpha$ -helix with the goal of stabilizing this helix[9]. The resulting analogs (peptides #4-#7) were 1.3 to 6.7-fold more potent than hPTH(1-34).

Combining modifications of Cha<sup>7,11</sup> and Aib<sup>19</sup> yielded the most potent of our analogs (peptide 9, EC<sub>50</sub>= 0.5nM). However, [Cha<sup>7,11</sup>,Aib<sup>16</sup>]hPTH(1-34)NH<sub>2</sub> hybrid did not improve the activity, indicating that these modifications are not necessarily additive.

In another class of analogs, the leucine 15 residue in the putative reverse turn region of the molecule was replaced with Cha with the intention of creating favorable hydrophobic interaction with the tryptophan 23 residue, and thereby stabilizing this reverse turn. These analogs (peptides 10 and 11) were also more active than hPTH(1-34) in stimulating cAMP production.

In conclusion, several novel hPTH(1-34) analogs have been designed and synthesized. The structure-activity relationship data reported here are consistent with our hypothesis that membrane binding of PTH plays a role in the process of PTH-receptor interactions.

## References

- Whitfield, J.F. and Morley, P., *TiPS*, 16 (1995) 382.
- Barden, J.A. and Kemp, B.E., *Biochemistry*, 32 (1993) 7126.
- Marx, U.C. et al., *J. Biol. Chem.*, 270 (1995) 15194.
- Schnolzer, M. et al., *Int. J. Peptide Protein Res.*, 40 (1992) 180.
- Pines, M. et al., *Endocrinology*, 135 (1994) 1713.
- Eisenberg, D., *Ann. Rev. Biochem.*, 53 (1984) 595.
- Schwyzler, R., *Natural Products and Biological Activities*, Tokio Press and Elsevier: Tokio, (1986) 197.
- Gardella, T.J. et al., *Endocrinology*, 135 (1994) 1186.
- Aleman, C., *Biopolymers*, 34 (1994) 841.

# Monitoring binding interactions of peptide-peptide, peptide-protein, ligand-protein and substrate-enzyme by NILIA-CD spectroscopy

**Giuliano Siligardi and Rohanah Hussain**

*EPSRC National Chiroptical Spectroscopy Centre, King's College London,  
Department of Pharmacy, Manresa Road, London SW3 6LX, UK*

In protein-ligand complexes, aromatic *aa* residues, which are commonly found at the interface between the protein (receptor, catalytic site) and the ligand (peptide, substrate, cofactor, inhibitor, metal ion, drug), provide excellent *in situ* molecular probes. CD associated with aromatic residues can be successfully used to monitor *in vitro* ligand binding and enzymatic reactions. The binding constant can be determined analyzing the CD data at a single wavelength by non-linear regression to the general equilibrium reaction in which the CD intensity is proportional to the concentration of each species. The negative solutions of the quadratic equation derived from the binding of the ligand to a single site can be used to fit the CD data. Here we present several binding interactions studied in solution by NILIA-CD spectroscopy.

## Results and Discussion

The titration of CDR-derived tumor imaging EPPT1 (YCAREPPTTRTFAYWG) with deglycosylated mucin-derived PDTRP (YVTSAPDTRPAGST) did not induce significant backbone conformational changes. Binding, however, was revealed by the CD changes in the aromatic side-chain region between the observed and calculated EPPT1-PDTRP [1:5] spectra [1].

Binding of PR proline rich peptide (PPRPLPVAPGSSKT) to fyn-SH3 domain was clearly determined by the CD changes in the Trp aromatic side-chain of the SH3 domain upon addition of proline rich but aromatic free PR peptide. The CD intensities at 293nm were used to calculate  $K_d=28\mu\text{M}$ . This was in agreement with the  $K_d=50\mu\text{M}$  calculated from NMR data but was achieved much more rapidly [2].

Drug screening of non-chiral ligands to proteins is readily achieved in solution by CD spectroscopy. Only the bound species show induced CD that is unambiguously indicative of drug-binding. Subtraction of HSA contribution from the CD spectrum of HSA-diclofenac (DC) complex revealed a positive-negative-positive CD profile that was assigned to three diclofenac bound species. The addition of caprylic acid (CA) to the HSA-DC complex showed CD changes that were indicative of competitive binding. In the 330-250nm region, CA is transparent and therefore the observed CD profile derives only from the bound species of DC to HSA. The bound species of DC were reduced from three to two and to one by a molar excess of caprylic acid.

The reconstitution of Cytochrome b<sub>5</sub> from apo-Cyt b<sub>5</sub> and heme was monitored by CD. The heme has no intrinsic CD *per se* but upon binding to the apo-Cyt b<sub>5</sub> an induced CD is observed for the heme Soret band at 420nm. CD intensities at 420nm were used to calculate a K<sub>d</sub>=16nM for the reconstituted Cyt b<sub>5</sub> (Siligardi, Hussain, Whitford, Newbold, personal communication).

The binding of a monoclonal antibody MAb (150KDa) to an antigenic protein Ag (120KDa) was detected in both backbone and aromatic side-chain regions. The backbone secondary structure and the local tertiary structure of the aromatic side-chains of MAb and/or Ag were affected on binding. An apparent dissociation constant K<sub>d</sub>=50nM was obtained in both regions with the CD data analyzed at 216nm and 275nm, respectively (R. Hussain, R. Verma and G. Siligardi, personal communication).

Reconstitution of porphobilinogen (PBG) deaminase from apo-enzyme with PBG and preuro-porphyrinogen substrates was monitored in both backbone and aromatic regions [3]. The holo-enzyme contains a covalently linked dipyrromethane cofactor that derives from of PBG as two rings. In the enzyme, reconstitution from apo-enzyme and PBG was only partial compared to the full activity of the holo-enzyme. The correct folding with 70% of enzyme activity was achieved using the product of the enzyme reaction, the linear tetrapyrrole preuroporphyrinogen, rather than the PBG substrate.

## Conclusion

NILIA-CD is the technique of choice to monitor qualitatively and quantitatively enzymatic reactions, enzyme reconstitution, ligand competitions and binding interactions. NILIA-CD defines and provides the means of investigating these systems very quickly. Information on conformational changes can be rapidly elucidated for further studies using high resolution techniques.

Unlike ELISA, BIAcore and IAsys biosensor techniques, neither the protein nor the ligand needs to be immobilized. In NILIA-CD the risk of masking the binding site due to immobilization is therefore avoided, resulting in direct detection of binding in solution.

## References

1. Hussain, R., Courtenay-Luck, N.S. and Siligardi, G., Biomed. Peptides, Proteins and Nucleic Acids, in press.
2. Renzoni, D.A., Pugh, D.J.R., Siligardi, G., Das, P., Morton, C.J., Rossi, C., Waterfield, M.D., Campbell, I.D. and Ladbury, J.E., Biochemistry, 35(1996)15646.
3. Awans, S., Siligardi, G., Shoolingin-Jordan, P.M. and Warren, M.J., Biochemistry, in press.

# Peptide libraries with free carboxy-terminus used to characterize epitopes recognized by PDZ domains

Ulrich Hoffmüller,<sup>a</sup> Rudolf Volkmer-Engert,<sup>a</sup> Mark Kelly,<sup>b</sup>  
Hartmut Oschkinat,<sup>c</sup> and Jens Schneider-Mergener<sup>a</sup>

<sup>a</sup>*Institut für Medizinische Immunologie, Universitätsklinikum Charité, Humboldt-Universität zu Berlin, Schumannstr. 20-21, 10098 Berlin, Germany,* <sup>b</sup>*European Molecular Biology Laboratory, Meyerhofstr. 1, 69117 Heidelberg, Germany;* <sup>c</sup>*Forschungsinstitut Für Molekulare Pharmakologie, Alfred-Kowalke-Str. 4, 10315 Berlin, Germany*

PDZ domains are protein modules found in various cell junction associated proteins [1]. They mediate protein-protein interactions by recognizing linear epitopes at the C-terminus of their ligands. Determination of the specificity of the interaction and subsequent identification of new binding partners would provide detailed insights into their biological functions. Conventional solid phase-bound peptide libraries, usually powerful tools to study protein-peptide interactions, are not applicable in this case since a free C-terminus is essential for the interaction.

Therefore, we synthesized peptides on continuous cellulose membrane bearing a free C-terminus to study the binding specificity of PDZ domains. This was achieved by cyclizing the peptide and subsequent linearization next to the C-terminal residue (Fig. 1A) [2]. This demands (i) stable anchoring, (ii) cyclization of the peptide, (iii) and an orthogonally cleavable linker. To allow screening of large amounts of different peptides, this approach was combined with peptide spot synthesis on continuous cellulose membrane [3]. To demonstrate the applicability of this method, the binding of a PDZ domain to different peptide analogs was tested.

## Results and Discussion

The preparation of peptides with free C-termini schematically shown in Fig. 1A. The synthesis is performed on cellulose membranes carrying a stable anchor (amino-2-hydroxy-propyl-ether [4]). (i) Coupling of Fmoc-Glu(TMSE)-OH (TMSE: trimethylsilylethyl) activated with TBTU / DIEA. (ii) The HMB linker is coupled after Fmoc-deprotection. (iii) The first Fmoc-amino acid is attached via an ester bond by activating with DIC / NMI (1-methyl imidazole). (iv) Subsequent couplings as described for conventional spot synthesis [3, 5]. (v) The TMSE protecting group is selectively cleaved with tetrabutyl ammonium fluoride. Subsequently, the construct is head-to-side-chain cyclized using PyBOP / NMM activation [6]. (vi) After side chain deprotection, the ester bond between the peptide and HMB is hydrolyzed by treating the membrane with a saturated Li<sub>2</sub>CO<sub>3</sub> solution.

Using this protocol, a substitutional analysis of the epitope peptide N<sub>6</sub>Y<sub>5</sub>K<sub>4</sub>Q<sub>3</sub>T<sub>2</sub>S<sub>1</sub>V<sub>0</sub> of the PSD95 PDZ2 domain was synthesized. Binding of a peroxidase-conjugated PDZ2-GST fusion protein was visualized using a chemiluminescence detection system

(Fig. 1B). This experiment identifies V<sub>0</sub> and T<sub>-2</sub> as key residues, which can not be substituted without loss of binding. K<sub>-4</sub> can only be replaced by R, showing that a basic residue is required at the -4 position. Interestingly, some substitutions show a significant increase in binding, e.g. the substitution of Q<sub>-3</sub> by E which also reportedly occurs in natural binding partners of the PDZ2 domain.

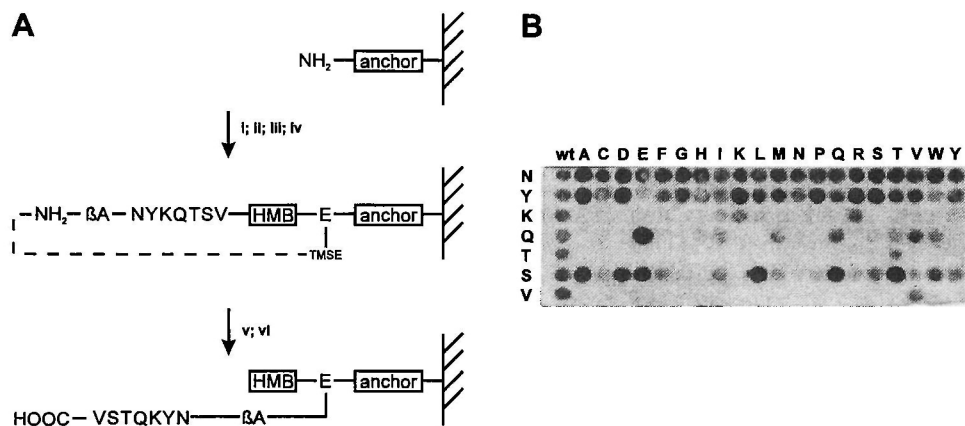


*Fig. 1. (A) Synthesis of cellulose bound peptides with a free C-terminus (dashed line: cyclization, βA: β-alanine). (B) Substitutional analysis of the PDZ domain epitope NYKQTSV prepared by spot synthesis. All spots in the left column (wt) are identical wild type epitope peptides. Each position of the epitope is substituted by all 20 amino acids (rows).*

## References

1. Saras, J. and Heldin, C., *TIBS*, 21 (1996) 455.
2. Kania, R.S., Zuckermann, R.N. and Marlowe, C.K., *J. Am. Chem. Soc.*, 116 (1994) 8835.
3. Frank, R., *Tetrahedron Lett.*, 48 (1992) 9217.
4. Volkmer-Engert, R., Hoffmann, B. and Schneider-Mergener, J., *Tetrahedron Lett.*, 38 (1997) 1029.
5. Kramer, A. and Schneider-Mergener, J., *Meth. Mol. Biol.*, 87 (1997) in press.
6. Winkler, D., Stigler, R.D., Hellwig, J., Hoffman, B. and Schneider-Mergener, J., In Kaumaya, P.T.P. and Hodges, R.S. (eds.) *Peptides: chemistry, structure, and biology.*, Proc. 14. Am. Peptide Symp., Mayflower Scientific Ltd., Kingswinford, UK, 1995, p. 315.

# Functional site studies with peptide segments of Cdk inhibitory proteins

Peter P. Roller,<sup>a</sup> Feng-Di T. Lung,<sup>a</sup> Masato Mutoh<sup>b</sup>  
and Patrick M. O'Connor<sup>b</sup>

<sup>a</sup>Laboratory of Medicinal Chemistry and <sup>b</sup>Laboratory of Molecular Pharmacology, Division of Basic Sciences, National Cancer Institute, NIH, Bethesda, MD 20892, USA

A number of intracellular proteins contribute to checkpoints for replication of the genetic material of the cell. One such family of proteins includes p21<sup>Cip1/Waf1</sup> and p27<sup>Kip1</sup> that function through the inhibition of cyclin-dependent kinases (Cdk's) [1]. Cdk/Cyclin complexes drive the cell cycle through G1/S and G2/M checkpoints, and these kinases phosphorylate Rb/transcription factor complexes in the gene activation step. P21, a 164 amino acid long protein, has broad specificity, inhibiting various Cdk/Cyclin complexes. In our previous study we synthesized p21 with overlapping peptide segments, and used these peptides to determine their Cdk binding and/or inhibitory function, their association with other proteins, and for determine local conformations [2]. These studies revealed that specific p21 N-terminal segments (17-26 and 58-77) bound, but did not inhibit Cdk2/Cyclin E complexes with histone H1 as substrate. Also, the C-terminal segment peptide (139-164) bound PCNA, a protein required for DNA polymerase function and thus for DNA replication. This report aims at identifying the Cdk/Cyclin kinase-inhibitory regions of p21 using the natural (*in vivo*) substrate, the retinoblastoma (Rb) protein, which is a negative regulator of the E2F transcription factors that facilitate cell cycle entry.

## Results and Discussion

A set of 10 overlapping synthetic peptides were synthesized with 4 amino acid overlaps spanning the p21 protein, using Fmoc chemistry based SPPS methodology. Peptides were evaluated using Cdk4/Cyclin D1 and Cdk2/Cyclin E kinase complexes in inhibitory assays, with recombinant Rb protein as substrate. Impressive kinase inhibitory activity was found for the C-terminal Peptide **10** (139-164) that inhibited the Cdk2/Cyclin E and Cdk4/Cyclin D1 complexes, with IC<sub>50</sub>'s of 7 and 16 μM, respectively. An N-terminal peptide, p21(15-40), inhibited these complexes with IC<sub>50</sub>'s in the range of 540-570 μM. Indeed, much of the earlier work has focussed on the well demonstrated Cdk inhibitory N-terminal 70 amino acid. region of p21 [3]. Our current findings and those of others [4,5] concerning the existence of two inhibitory domains p21 open up new avenues for investigation.

The X-ray structure of the N-terminal region of p27<sup>Kip1</sup> complexed with Cdk2/Cyclin A was disclosed recently [6]. This region is highly homologous to the N-terminal domain of p21. By analogy, the X-ray structure suggests that the principal interaction site containing the RRLF motif in p21 (amino acids 18-26) binds to the cyclin subunit, and an α-helical segment spans the Cdk2/Cyclin interphase. The inhibitor interacts extensively

with the  $\beta$ -sheet array of Cdk2, and a conserved  $3_{10}$ -helical segment (PKLYLP<sup>79</sup>) is bound in the ATP binding site (Fig. 1). As distinct from p27, the p21 C-terminal inhibitory domain also has a peptide motif that is predicted to be a cyclin binding motif (p21(155-160)) a segment (p21(147-151)) that may bind to the Cdk2 ATP binding region.

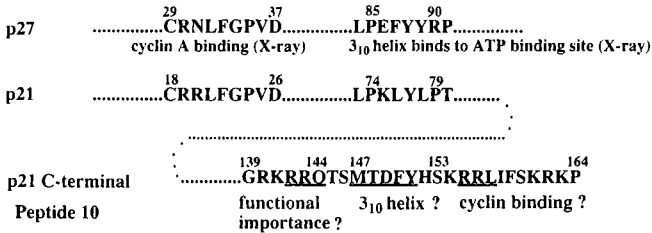


Fig. 1. The enigma of two homologous Cdk/Cyclin inhibitory sites in *p21<sup>Cip1/Waf1</sup>*. Comparison of conserved regions of p27, and the N- and C-terminal regions of p21.

In initial structure activity studies we evaluated a number of synthetic variants of Peptide 10. Among these were the alanine mutants, Peptide 10 (RRL<sup>157</sup>>AAA<sup>157</sup>) and Peptide 10 (RRQ<sup>144</sup>>AAA<sup>144</sup>), and a mutant in which the MTDFY<sup>151</sup> segment was replaced by GSGSG<sup>151</sup>. Kinase inhibitory assays revealed that, while all mutations decreased the inhibitory effect by 4 to 18 fold, Cdk2/Cyclin E inhibitory activity was affected most in the RRL and the RRQ mutants. Cdk4/Cyclin D1 inhibition was decreased most significantly in the MTDFY mutated peptide, but the other mutants were also affected. These latter results also highlight significant differences in the binding and inhibitory mode of the Cdk2 versus Cdk4 kinase complexes. Recent work by others [5], for example, indicate that a C-terminal peptide, p21(141-160), binds to both Cdk4 and also to Cyclin D1, whose X-ray structure [6] does not provide a model. Mechanistic interpretation of the dual inhibitory regions of p21 is not yet possible. However, the impressive kinase inhibitory activity of the p21 C-terminal region highlights a potentially important contributor to its biological function.

## References

1. Sherr, C.J. and Roberts, J.M., *Genes Devel.*, 9 (1995) 1149.
2. Chen, I.-T., Akamatsu, M., Smith, M.L., Lung, F.-D.T., Duba, D., Roller, P.P., Fornace, A.J., Jr. and O'Connor, P.M., *Oncogene*, 12 (1996) 595.
3. Nakanishi, M., Robetorye, R.S., Adami, G.R., Pereira-Smith, O.M. and Smith, J.R., *EMBO J.*, 14 (1995) 555.
4. Adams, P.D., Sellers, W.R., Sharma, S.K., Wu., A.D., Nalin, C.M. and Kaelin, W.G., Jr., *Molec. Cell. Biol.*, 16 (1996) 6623.
5. Ball, K.L., Lain, S., Fahraeus, R., Smythe, C. and Lane, D.P., *Current Biology*, 7 (1997) 71.
6. Russo, A.A., Jeffrey, P.D., Patten, A.K., Massague, J. and Pavletich, N.P., *Nature*, 382 (1996) 325.

# Expression of C5a receptors (CD 88) on human bronchial epithelial cells (HBEC): C5a-mediated release of IL-8 upon HBEC exposure to cigarette smoke

Anthony A. Floreani, Art J. Heires, Laurel Clark-Pierce, Lisbeth Welniak, Amanda Miller-Lindholm, Steven I. Rennard, Edward L. Morgan<sup>a</sup> and Sam D. Sanderson

Eppley Institute for Research in Cancer and Department of Internal Medicine, University of Nebraska Medical Center, 600 So. 42nd St., Omaha, NE 68198, USA, <sup>a</sup>Department of Immunology, Scripps Institute, 10666 North Torrey Pines Road, La Jolla, CA 92037, USA

The immunoinflammatory properties of human C5a anaphylatoxin are initiated upon its binding to the specific, high affinity C5a receptor (C5aR) expressed on the surface of the corresponding target cell. Traditionally, C5aR expression has been viewed as being limited to cells of myeloid origin [1]. However, cells of nonmyeloid origin have now been shown also to express C5aRs [1,2], raising interesting questions about the nature and role of the C5a-mediated response in these cells under normal and aberrant physiologic conditions.

In this study, we report that human bronchial epithelial cells (HBEC) constitutively express C5aRs and respond to C5a by releasing small but significant levels of interleukin-8 (IL-8). However, exposure of HBECs to cigarette smoke markedly enhances the C5a-mediated release of IL-8, a response effect that is abolished in the presence of an anti-human C5aR antibody (Ab).

## Results and Discussion

We have shown at the protein and mRNA levels that untreated (control) HBECs and HBECs treated with 5% cigarette smoke extract (CSE) for 1 hour express C5aRs [3]. For example, Western blot analysis of HBEC lysates with an anti-C5aR Ab revealed a 46 kDa band characteristic of the C5aR (Fig. 1). Also, C5aR-specific mRNA was detected by reverse transcriptase-polymerase chain reaction (RT-PCR) of RNA isolated from untreated and CSE-treated HBECs using primers designed to yield a 550 bp fragment of the human C5aR (Fig. 2).

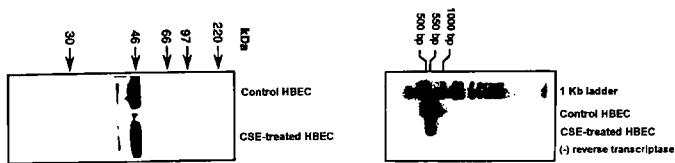


Fig.1 (left). Western blot analysis showing the binding of anti-C5aR Ab to lysates of control (untreated) HBECs and HBECs treated with 5% CSE for 1 hour.

Fig. 2 (right). RT-PCR/Southern analysis of RNA from control (untreated) HBECs and HBECs treated with 5% CSE for 1 hour.

Interestingly, despite the presence of C5aRs, untreated HBECs released only small, but statistically significant, amounts of IL-8 when challenged with 50 nM C5a (Fig.3). In contrast, HBECs treated with 5% CSE for 1 hour responded in a dose-dependent manner by releasing significantly higher levels of IL-8 than their untreated counterparts (Fig.3). Moreover, this C5a-mediated release of IL-8 from CSE-treated HBECs was abolished in the presence of the anti-human C5aR Ab (Fig. 4).

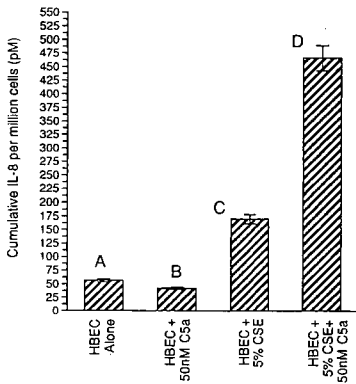


Fig. 3. Accumulation (18 hrs) of IL-8 released by HBECs under the following conditions: (A) HBECs in medium only, (B) HBECs + 50 nM C5a, (C) HBECs exposed to 5% CSE for 1 hour, and (D) HBECs exposed to 5% CSE for 1 hour + 50 nM C5a.

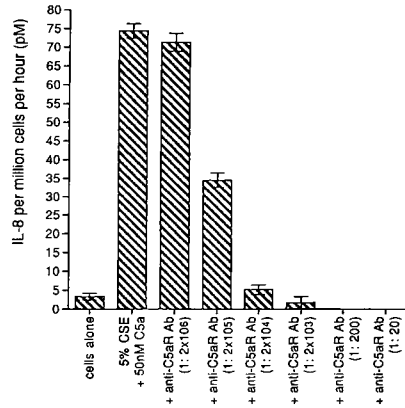


Fig. 4. HBECs treated with 5% CSE for 1 hour were incubated for 2 hours with varying dilutions of the anti-C5aR Ab (500 µg/ml). Ab-treated cells were then incubated for 18 hours in the presence of 50 nM C5a and IL-8 released into the medium measured with an IL-8-specific ELISA.

In conclusion, these (and other) results indicate that HBECs constitutively express the C5aR. Moreover, a priming step (HBEC exposure to an inflammatory stimulus) is required for the C5aR to respond maximally to C5a-mediated release of IL-8. These *in vitro* observations may be important in the lung *in vivo*, where the bronchial epithelium is one of the first tissue beds to encounter cigarette smoke. The ability of these epithelial cells to engage complement-derived C5a to release at least IL-8 may be one mechanism by which this tissue responds to the damage incurred by its exposure to cigarette smoke and other environmental irritants.

## References

1. Wetsel, R.A., *Curr. Opin. Immunol.*, 7 (1995) 48.
2. Haviland, D.L., McCoy, R.L., Whitehead, W.T., Akama, H., Molmenti, E.P., Brown, A., Haviland, J.C., Parks, W.C., Perlmutter, D.H. and Wetsel, R.A. J., *Immunol.*, 154 (1995) 1861.
3. Floreani, A.A., Heires, A.J., Welniak, L.A., Miller-Lindholm, A., Clark-Pierce, L., Rennard, S.I., Morgan, E.L. and Sanderson, S.D. *J. Exp. Med.*, submitted.

# Mapping and characterization of epitopes recognized by WW domains using cellulose-bound peptide libraries

Ulrich Hoffmüller,<sup>a</sup> Hartmut Oschkinat<sup>b</sup> and Jens Schneider-Mergener<sup>a</sup>

<sup>a</sup>Institut für Medizinische Immunologie, Universitätsklinikum Charité,

Humboldt-Universität zu Berlin, Schumannstr. 20-21, 10098 Berlin, Germany

<sup>b</sup>European Molecular Biology Laboratory, Meyerhofstr. 1, 69117 Heidelberg, Germany

WW domains are protein modules found in various proteins having structural, regulatory, and signalling functions [1]. They play a role in protein-protein-interactions similar to SH2 and SH3 domains and recognize proline-rich, linear peptide motifs. We prepared peptide libraries bound to continuous cellulose supports [2] to map and characterize linear binding determinants of the WW domain of YAP (Yes-associated protein) [1].

## Results and Discussion

Until now the epitopes of the YAP WW domain were estimated by sequence comparison of the two known putative ligands WBP-1 and WBP-2 [3]. To map the epitopes experimentally, peptide scans of WBP-1 and WBP-2, i.e. sets of overlapping peptides scanning the entire protein sequence, were synthesized using peptide spot synthesis on cellulose membranes [2, 4]. Binding of a peroxidase-conjugated WW-GST fusion protein was visualized using a chemiluminescence detection system (Fig. 1).

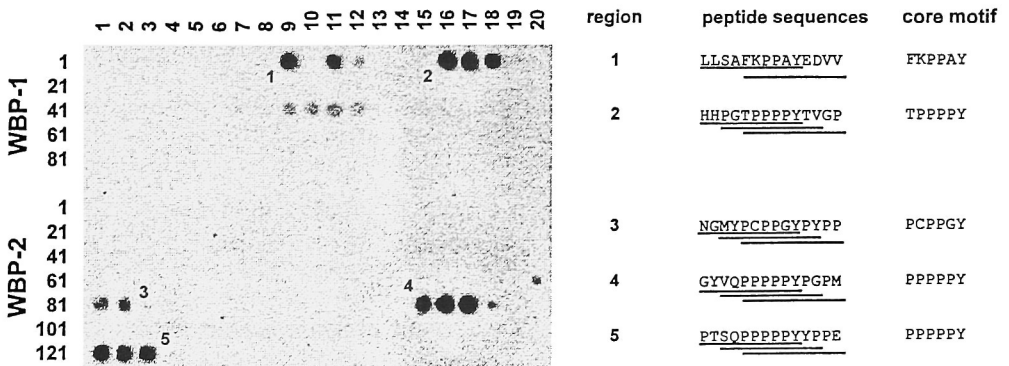


Fig. 1. Left: Peptide scans of WBP-1 and WBP-2. (10mer peptides, 8 overlapping residues) Right: Sequences of the binding peptides and their common motifs.

Five binding regions were identified, all containing the common motif PPXY. Regions 2, 4, and 5 were already presumed to be putative epitopes called PY motifs [3], whereas region 1 and 3 were so far unknown epitopes. Inverse PY motifs like YPPPP are not

bound. The region 2-derived peptide ligand GTPPPPYTVG was chosen for further characterization since the NMR structure of this peptide in complex with the WW domain has been determined [5]. A substitutional analysis and an epitope minimization of this sequence indicated that the proline residues at positions 4 and 5 and tyrosine 7 are key residues, i.e. substitutions at these positions lead to significant loss of binding (Fig. 2).

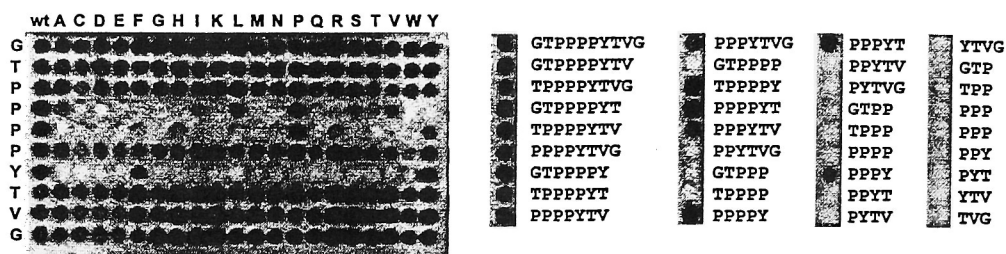


Fig. 2. Substitutional analysis (left) and epitope minimization (right) of the peptide GTPPPPYTVG. In the substitutional analysis all spots in the left column (wt) are identical wild type epitope peptides. Each position of the epitope is substituted by all 20 amino acids (rows).

The epitope minimization revealed that all peptides containing the PPPY motif are recognized. Even though the tetrapeptide PPPY is responsible for specificity, the flanking residues are required for high affinity binding.

## Acknowledgement

The authors wish to acknowledge similar experiments performed by Chen, H. I., Einbond, A., Kwak, S., Linn, H., Koepf, E., Peterson, S., Kelly, J. W., and Sudol, M., J. Biol. Chem. (1997) (in press).

## References

1. Sudol, M., Chen, H., Bougeret, C., Einbond, A., Bork, P., FEBS-Lett., 369 (1995) 67.
2. Kramer, A. and Schneider-Mergener, J., Meth. Mol. Biol., 87 (1997) in press.
3. Chen, H. I. and Sudol, M., Proc. Natl. Acad. Sci. USA, 92 (1995) 7819.
4. Frank, R., Tetrahedron Let., 48 (1992) 9217.
5. Macias, M., Hyvonen, M., Baraldi, E., Schultz, J., Sudol, M., Saraste, M. and Oschkinat, H., Nature, 6592 (1996) 646.

# Biological and physicochemical properties of urocortin

Andreas Rühmann, Ines Bonk,  
Andreas K. E. Köpke and Joachim Spiess

*Department of Molecular Neuroendocrinology, Max Planck Institute for Experimental Medicine  
Hermann-Rein-Str. 3, D 37075 Göttingen, Germany*

This paper describes the synthesis of 40 amino acid neuropeptide urocortin (Ucn), belonging to the peptide family of corticotropin-releasing factor (CRF) and investigates their binding affinity and biopotency in HEK 293 cells, permanently transfected with rat CRFR1 (rCRFR1).

## Results and Discussion

In competitive binding assays with [ $^{125}\text{I-Tyr}^0$ ]oCRF and membranes of HEK 293 cells, permanently transfected with rCRFR1 [1], only oCRF showed binding to a high ( $K_d = 2.2 \pm 0.4$  nM) and a low affinity site ( $K_d = 82 \pm 14$  nM) of the receptor (Table 1.). As expected, high affinity binding of oCRF to the receptor could be efficiently inhibited in the presence of 50  $\mu\text{M}$  GTP $\gamma$ S ( $K_d = 62 \pm 12$  nM). It is well known that guanine nucleotides do not significantly effect antagonist binding to their receptors. In agreement with these findings, binding of [D-Phe $^{12}$ ,Nle $^{21,38}$ ]h/rCRF-(12-41) and [D-Phe $^{11}$ ]rUcn-(11-40) to its receptor gave similar  $K_d$  values in the absence ( $K_d \sim 24$  nM) or presence ( $K_d \sim 15$  nM) of GTP $\gamma$ S. Surprisingly, rUcn did not exhibit typical binding characteristics expected for agonist binding to rCRFR1. Cells treated with GTP $\gamma$ S bound rUcn with a similar high affinity ( $K_d = 7.3 \pm 1.9$  nM) as non-treated cells ( $K_d = 1.3 \pm 0.2$  nM). Scatchard analysis indicated a significant shift from typical oCRF like two-site binding via UcnCRF and CRFUcn to rUcn, showing only one-site binding. GTP $\gamma$ S treatment of cells suppressed high affinity binding of oCRF, UcnCRF, CRFUcn and rUcn with  $K_d$  values of  $62 \pm 12$  nM,  $46 \pm 19$  nM,  $17 \pm 8.3$  nM and  $7.3 \pm 1.9$  nM, respectively. The peptide ligands were tested for their ability to stimulate cAMP production in HEK 293 cells, permanently transfected with rCRFR1. The agonists oCRF, CRFUcn and UcnCRF exhibited similar biopotency to cause cAMP accumulation in HEK 293 cells with  $\text{EC}_{50}$  values of  $0.45 \pm 0.17$ ,  $0.25 \pm 0.08$  and  $0.34 \pm 0.11$  nM, respectively. However, rUcn showed lower biopotency with an  $\text{EC}_{50}$  value of  $0.93 \pm 0.54$  nM (Table 1.). Furthermore, rUcn exhibited significantly higher  $\alpha$ -helicity in physiological buffer solutions than oCRF and showed longer retention times on  $\mu\text{C}18$  columns, due to an increase of lipophilicity,  $\alpha$ -helicity or amphiphilicity of this peptide when compared to oCRF (Table 2.). Two chimera (CRFUcn, UcnCRF) based on the amino acid sequence of oCRF and rUcn were used to investigate the different binding behavior of oCRF and rUcn in transfected HEK 293 cells. Interestingly, all four peptides (oCRF, rUcn, UcnCRF and CRFUcn) showed similar high affinity binding ( $K_d = 1.2 - 2.2$  nM) to the receptor.

Table 1. Binding constants ( $K_d$ , [nM]) found for different CRF analogs when bound in the absence or presence of GTP $\gamma$ S to recombinant rCRFR1. Biopotency ( $EC_{50}$  [nM]) of CRF analogs to stimulate intracellular cAMP in transfected HEK cells. Data are the mean ( $\pm$  SEM) from 4-7 exp.

peptides	$K_{d1}$ , [nM]	$K_{d2}$ , [nM]	$K_{dGTP\gamma S}$ , [nM]	$EC_{50}$ [nM]
oCRF	2.2 $\pm$ 0.4	82 $\pm$ 14	62 $\pm$ 12	0.45 $\pm$ 0.17
rUcn	1.3 $\pm$ 0.2	7.3 $\pm$ 1.9	0.93 $\pm$ 0.54	
UcnCRF	1.2 $\pm$ 0.4	64 $\pm$ 15	46 $\pm$ 19	0.34 $\pm$ 0.11
CRFUcn	2.1 $\pm$ 0.5	17 $\pm$ 8.3	0.25 $\pm$ 0.08	
[D-Phe <sup>12</sup> ,Nle <sup>21,38</sup> ]- h/rCRF-(12-41)	22 $\pm$ 4.2	14 $\pm$ 0.6		
[D-Phe <sup>11</sup> ]rUcn-(11-40)	25 $\pm$ 1.7	15 $\pm$ 1.0		

Table 2. Physicochemical characterization of CRF analogs.

peptides	RPHPLC CD cpep=20 $\mu$ M in 20 mM SPB, pH 6.5			
	Rt [min]	$\alpha$ -helix [%]	$\beta$ -sheet [%]	remain [%]
oCRF	25.9	24	29	47
rUcn	27.2	33	25	42
UcnCRF	26.8	25	31	44
CRFUcn	26.6	24	32	44
[D-Phe <sup>12</sup> ,Nle <sup>21,38</sup> ]- h/rCRF-(12-41)	24.4	26	31	43
[D-Phe <sup>11</sup> ]rUcn-(11-40)	24.5	21	37	42

oCRF SQEPPISLDLTFHLLREVLEMTKADQLAQQAHNSNRKLLDIA  
rUcn DDPPLSIDLTFHLLRTLLELARTQSQRERAEQNRIIFDSV  
UcnCRF DDPPLSIDLTFHLLRTLLELTKADQLAQQAHNSNRKLLDIA  
CRFUcn SQEPPISLDLTFHLLREVLELARTQSQRERAEQNRIIFDSV  
h/rCRF SEEPPISLDLTFHLLREVLEMARAEQLAQQAHNSNRKLM EII

rUcn is an atypical agonist (partially inverse agonist). It shows high affinity binding to G-protein coupled and uncoupled receptors. As a result rUcn exhibits decreased biopotency to stimulate cAMP production at low concentrations that can be expected *in vivo*. rUcn and CRFUcn show much higher binding affinity to rCRFR1 than [D-Phe<sup>11</sup>]rUcn-(11-40) indicating that the N-terminal half of the peptide induces a conformation in the C-terminal part of the peptide, necessary for high affinity binding to rCRFR1 and receptor activation. The differences in the amino acid sequence of oCRF 1-19 and rUcn 1-18 do not seem to play a major role for the rUcn C-terminal binding affinity.

## References

1. Rühmann, A., Köpke, A.K.E., Dautzenberg, F.M. and Spiess, J., Proc. Natl. Acad. Sci. USA, 93 (1996) 10609-10613.

# Towards a rational approach in the finding of potent peptide ligands for Grb2 SH2

C. García-Echeverría, B. Gay, P. Furet, J. Rahuel,  
H. Fretz, J. Schoepfer and G. Caravatti

*Oncology Research, Novartis Pharma Inc., CH-4002 Basel, Switzerland*

Intracellular signalling pathways that couple growth factor activation with cell control offer new target sites for pharmacological intervention in tumor therapy. This is the case for the growth factor receptor-bound protein 2 (Grb2), which links growth factor activated receptor tyrosine kinases to Sos, a guanine nucleotide exchange factor that upon receptor binding and translocation of the Grb2-Sos complex to the plasma membrane converts the inactive Ras-GDP to active Ras-GTP. Activated Ras triggers the MAP kinase cascade that is essential for cell growth and differentiation. The interaction between the activated tyrosine kinase receptor and Grb2 is mediated by the Src homology 2 (SH2) domain of the signaling protein. Agents that specifically disrupt this protein-protein interaction could potentially shut down the Ras pathway and present an intervention point for blocking human malignancy. Starting with the recognition motif of the SH2 domain of Grb2, we have initiated a medicinal chemistry program to identify agents that specifically disrupt the interaction between the activated EGF receptor and the SH2 domain of Grb2. In this communication, we report our initial efforts.

## Results and Discussion

Degenerate phosphotyrosyl peptide libraries have shown that the sequence specificities of SH2 domains for phosphotyrosyl peptides lie in the portion of the peptide immediately adjacent to the carboxy terminal of the phosphotyrosine residue [1]. For the SH2 domain of Grb2, the consensus sequence is Tyr(PO<sub>3</sub>H<sub>2</sub>)-Xxx-Asn-Yyy (Xxx= Val, Gln, Tyr, Ile and Yyy= Gln, Tyr, Phe) and the specificity determining residue is asparagine. Synthetic peptides derived from the Grb2-SH2 binding motif have inhibitory activities in the low  $\mu$ M range (e.g., H-Glu-Tyr(PO<sub>3</sub>H<sub>2</sub>)-Ile-Asn-NH<sub>2</sub>, IC<sub>50</sub>= 7.9  $\pm$  0.5  $\mu$ M; H-Tyr(PO<sub>3</sub>H<sub>2</sub>)-Ile-Asn-NH<sub>2</sub>, IC<sub>50</sub>= 56.9  $\pm$  6.8  $\mu$ M). Incorporation of the 2-amino-benzoic acid (Abz) to the N-terminus of the Xxx-Tyr(PO<sub>3</sub>H<sub>2</sub>)-Ile-Asn-NH<sub>2</sub> phosphopeptide produced a dramatic, unexpected boost in its binding affinity for Grb2-SH2 (e.g., Abz-Glu-Tyr(PO<sub>3</sub>H<sub>2</sub>)-Ile-Asn-NH<sub>2</sub>, IC<sub>50</sub>= 22  $\pm$  5 nM). In the absence of an X-ray structure of the Grb2-SH2 domain in complex with a phosphotyrosyl peptide, we used the 3D-structure of the ligated Lck SH2 domain [2] to derive a working hypothesis for the "anthranilic acid effect". An examination of the crystal structure of the Lck-SH2 domain in complex with a high affinity phosphotyrosine containing peptide indicates that the amino acids of the protein which interact with phosphotyrosine and the residues at positions -1 and +1 relative to this amino acid are highly conserved in the Grb2-SH2 domain. The high degree of homology between

the SH2 domains of Lck and Grb2 strongly argues in favor of a similar bound conformation for phosphotyrosine and the residue at position -1. Constructing the anthranilic acid moiety on the X-ray structure of the ligated Lck-SH2, followed by energy minimization, places the aromatic ring in an optimal position to make a favorable planar  $\pi$ - $\pi$  stacking interaction with the guanidinium moiety of Arg  $\alpha$ A2. In addition, the 2-amino functionality is within hydrogen bonding distance of one of the phosphotyrosine phosphate oxygen atoms. This model, which is in full agreement with the SAR data obtained from phosphopeptides appended at the *N*-terminus with a set of groups based on the anthranilic acid moiety (data not shown), was subsequently used to design the 3-amino-benzoyloxycarbonyl group to replace the Abz-Xxx moiety. This new *N*-terminal group mimics the interaction of the 2-aminobenzoyl group with the guanidinium moiety of Arg  $\alpha$ A2 but does not compromise the other interactions and the potency of the peptide inhibitors (e.g., 3-amino-Z-Tyr(PO<sub>3</sub>H<sub>2</sub>)-Ile-Asn-NH<sub>2</sub>, IC<sub>50</sub>= 65 ± 45 nM). With the X-ray structure of the ligated Grb2-SH2 in hand [3] and a strong CAMM support, we were able to improve the binding affinity of the 3-amino-Z containing peptides optimizing the interaction at the X<sub>+1</sub> position. In the X-ray structure of the ligated Grb-SH2, the residue at the X<sub>+1</sub> position adopts a helical left-handle conformation with its side chain interacting with Phe $\beta$ D5 and Gln $\beta$ D3; in addition, its C $\beta$  atom forms van der Waals interactions with TrpEF1, which closes the active site cleft with its side chain and forces the ligand to adopt a folded conformation. Based on this information, a series of  $\alpha,\alpha$ -disubstituted amino acids were selected and incorporated into the model sequence 3-amino-Z-Tyr(PO<sub>3</sub>H<sub>2</sub>)-Xxx-Asn-NH<sub>2</sub> (data not shown). Replacement of isoleucine by 1-amino-cyclohexyl-1-carboxylic acid (Ac<sub>6</sub>C) increased the activity of the original 3-mer peptide (3-amino-Z-Tyr(PO<sub>3</sub>H<sub>2</sub>)-Ac<sub>6</sub>C-Asn-NH<sub>2</sub>, IC<sub>50</sub>= 1.05 ± 0.21 nM) 65-fold. The increase in binding activity observed for the Ac<sub>6</sub>C containing peptide is presumably due to a local conformational effect; Ac<sub>6</sub>C should promote a conformation that favors the adoption of  $\beta$ -turn. In the isoleucine residue, the side chain of Ac<sub>6</sub>C can also establish hydrophobic contacts with Phe $\beta$ 5 and Gln  $\beta$ D3. Further details on the optimization of the above peptide will be reported in due course.

## References

1. Songyang, Z., Shoelson, S.E., McGlade, J. et al., *Mol. Cell. Biol.*, 72 (1994) 2777.
2. Eck, M.J., Schoelson, S.E. and Harrison, S.C., *Nature*, 362 (1993) 87.
3. Rahuel, J., Gay, B., Erdmann, D., Strauss, A., García-Echeverría, C., Furet, P., Caravatti, G., Fretz, H., Schoepfer, J. and Grütter, M.G., *Nat. Struct. Biol.*, 3 (1996) 586-589.

# Multivalent carbohydrate-linked peptides interfere with adherence of *Candida albicans* to asialo-GM<sub>1</sub> receptor: Toward the design of anti-adhesin therapeutics

C. M. Charles Yang, Wah Y. Wong, Ole Hindsgaul, Randall T. Irvin, and Robert S. Hodges

Protein Engineering Network Centres of Excellence, University of Alberta  
Edmonton, Alberta, T6G 2S2, Canada

Microbial adherence is the first important step in the initiation stage of infectious diseases. *Candida albicans* is an opportunistic fungal pathogen and employs surface adhesins to facilitate its adherence to host cells [1,2,3]. Previous studies showed that selectin-like fimbrial adhesins on *C. albicans* interacted with the glycosphingolipid receptor (asialo-GM<sub>1</sub>) via the carbohydrate  $\beta$ GalNAc(1-4) $\beta$ Gal sequence of the receptor, and this minimal carbohydrate receptor sequence was suggested to play a crucial role in fimbriae-mediated adhesion of *C. albicans* [4,6,7]. To elucidate the mechanism of cell adhesion mediated by multiple protein-carbohydrate interaction through selectin adhesins [5], we utilize multivalent template presentation systems to examine the interaction of the putative carbohydrate receptor sequence,  $\beta$ GalNAc(1-4) $\beta$ Gal, with *C. albicans* adhesins. The delineation of the multivalent nature of *C. albicans* adhesins is investigated using multivalent carbohydrate ligand systems to affect the binding of biotinylated *C. albicans* whole cells to immobilized asialo-GM<sub>1</sub> receptor.

## Results and Discussion

Multivalent carbohydrate-linked peptides (Fig. 1A) were prepared via conjugation of  $\beta$ GalNAc(1-4) $\beta$ Gal-linker to the cysteinyl thiol groups on synthetic peptides. The structures of the carbohydrate-linked peptides are: RCGnKKGnCR (R =  $\beta$ GalNAc(1-4) $\beta$ Gal-linker; DS1,  $n = 1$ ; DS4,  $n = 4$ ) and RCGnK(-KGnCR)-K(-KGnCR)GnCR (TS1,  $n = 1$ ; TS4,  $n = 4$ ).

ELISA showed that both two di-valent (DS1 and DS4) and two tetra-valent carbohydrate-linked peptides (TS1 and TS4) inhibited biotinylated *C. albicans* whole-cell binding to asialo-GM<sub>1</sub>. Maximum inhibition of 30-50% was reached at concentrations of 100~200  $\mu$ M. The maximum inhibition ability was in the order of TS1>DS1>TS4>DS4 (Fig. 1B), with  $I_{50} = 200$   $\mu$ M for TS1,  $I_{45} = 100$   $\mu$ M for DS1,  $I_{40} = 100$   $\mu$ M for TS4 and  $I_{40} = 200$   $\mu$ M for DS4. The carbohydrate-linked peptide TS1, with a shorter linker and four equivalents of disaccharide  $\beta$ GalNAc(1-4) $\beta$ Gal units, was shown to be the most effective inhibitor (Fig. 1B), indicating that the binding-site density on the *C. albicans* cell-surface adhesins is high. However, at low carbohydrate-linked peptide concentrations (< 50  $\mu$ M), all of them enhanced the whole-cell binding to asialo-GM<sub>1</sub> and the maximum enhancement was reached (~25% for TS4) at 10  $\mu$ M. This enhancement was in the order of TS4>DS4>TS1>DS1 and implicated that the long templates in DS4 and TS4 offered much more flexibility to the multivalent receptor analogues

so that each disaccharide unit was able to interact with adhesins on different cells. At low concentration range, non-covalently cross-linked cells through carbohydrate-adhesins binding, resulted in an increased effective adhesin concentration, which presumably account for the enhanced whole-cell binding to asialo-GM<sub>1</sub>.

All the results above demonstrated that multivalent  $\beta$ GalNAc(1-4) $\beta$ Gal-linked peptides and asialo-GM<sub>1</sub> competed with each other for binding to *C. albicans* adhesins. Using multivalent carbohydrate receptor analogues to block the attachment of microbial surface adhesins raises a potential for the development of anti-adhesin therapeutics. However, carbohydrate-carbohydrate and carbohydrate-protein interactions are only one part of the mechanisms by which *C. albicans* adhere to host cells, inhibitor design using the multivalency template is still a possible approach in the development of effective anti-adhesin therapeutics.

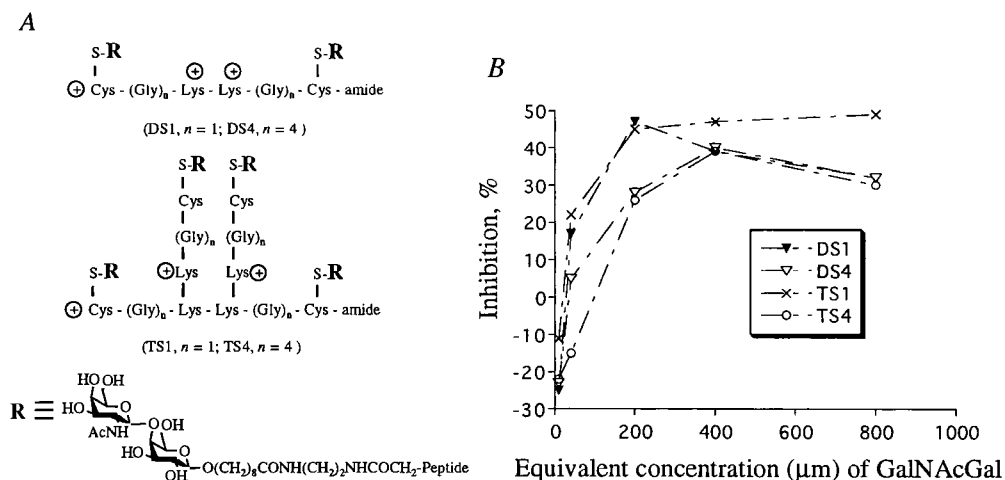


Fig. 1. (A) Structures of the carbohydrate-linked peptides and (B) their abilities to inhibit *C. albicans* whole-cell binding to asialo-GM<sub>1</sub>. Cells were pre-incubated with the carbohydrate-linked peptides.

## References

1. Beachey, E.H. J., *Infect. Dis.*, 143 (1981) 325-345.
2. Cutler, J.E., *Annu. Rev. Microbiol.*, 45 (1991) 187-218.
3. Karlsson, K.-A., *Rev. Biochem.*, 58 (1989) 309-350.
4. Krivan, H.C., Roberts, D.D. and Ginsbury, V., *Proc. Natl. Acad. Sci. USA*, 85 (1988) 6157-6161.
5. Lasky, L.A., *Science*, 258 (1992) 964-969.
6. Pendrak, M.L. and Klotz, S.A., *FEMS Microbiol. Lett.*, 129 (1995) 103-113.
7. Yu, L., Lee, K.K., Paranchych, W., Hodges, R.S. and Irvin, R., *Mol. Microbiol.*, 19 (1996) 1107-1116.

# Development of somatostatin agonists with high affinity and specificity for the human and rat type 5 receptor subtype

David H. Coy<sup>a</sup> and John E. Taylor<sup>b</sup>

<sup>a</sup>Peptide Research Laboratories, Department of Medicine, Tulane University Medical Center, New Orleans, LA 70112 and <sup>b</sup>Biomeasure, Inc., Milford, MA 01757, USA

There are currently 5 known human SRIF receptors. By employing cell systems transfected with these SRIF receptors the widely investigated cyclic SRIF octapeptide analogs were shown to have subnanomolar affinity for type 2 SRIF receptors, low affinity for type 3 receptors, and virtually no affinity for type 1 and 4 receptor subtypes. Other analogs have now been found with selectivity for some of the other receptors, particularly 3 and 5 [1,2]. In the present study, the additional complication of receptor affinity differences between species is examined.

## Results and Discussion

Cell membranes of the 5 transfected cell types (rat 2,3,5 and human 1,2,3,4,5) were obtained from homogenates of the corresponding CHO-K1 cells and analog  $K_i$ s were calculated from displacement studies using  $^{125}\text{I-Tyr}^{11}\text{-SRIF}$  (types 1,3,4,5) or  $^{125}\text{I-MK-678}$  (type 2). The structures of the analogs tested are given in Table 1 and their  $K_i$  values in Table 2.

Octapeptide analogs of the octreotide/lanreotide variety, including SMS-201-995 (octreotide), RC-160, and BIM-23014 (lanreotide) had little affinity for the type 1 and 4 subtypes in either species but bound very well and with good correlation to the type 2 receptors of both. The linear analog BIM-23052 (Table 1) had high affinity for type 5 and type 3 receptors in both species (Table 2). Therefore, although of value, this analog is of limited use in physiological experiments in rats since it cannot distinguish between receptor 5 and 3-mediated events in either species. The linear analog BIM-23056, previously reported [1] to be very type 3-specific and used in many investigations on the various physiological roles of SRIF receptors, unfortunately was found in this study to have low affinity for all rat and human receptors and thus does not appear to be useful for SRIF receptor selectivity investigations.

Extended ring, cyclic analogs [2] BIM-23268 and BIM-23313 had much higher specificity and very high affinity for the human type 5 over the other receptors and should be of potential clinical value. However, they had no specificity between rat 3 and 5 receptors and thus are not of value for distinguishing between rat type 3 and 5 receptor function. Conversely, BIM-23295 had good selectivity and high affinity for rat type 5 receptors and should be useful tool for basic animal studies. Unique among octapeptide analogs, BIM-23268 also exhibited good affinity for the human type 1 receptor ( $K_d$  12 nM) and may be a useful lead compound for type 1 receptor-specific ligand discovery.

In conclusion, the subtle effects of minor structural changes to analogs provide promising

leads for the development of compounds selective for each somatostatin receptor. Care must be taken, however, to evaluate analogs at the actual receptors of the species in which biological studies are to be conducted if meaningful attributions of receptor function are to be made.

Table 1. Amino acid sequences of SRIF analogs.

Peptide	Sequence
BIM-23014	D-Nal-c[Cys-Tyr-D-Trp-Lys-Val-Cys]-Thr-NH <sub>2</sub>
BIM-23052	D-Phe-Phe-Phe-D-Trp-Lys-Thr-Phe-Thr-NH <sub>2</sub>
BIM-23056	D-Phe-Phe-Tyr-D-Trp-Lys-Val-Phe-D-Nal-NH <sub>2</sub>
BIM-23268	c[Cys-Phe-Phe-D-Trp-Lys-Thr-Phe-Cys]-NH <sub>2</sub>
BIM-23295	c[Cys-Phe-Tyr-D-Trp-Lys-Thr-Phe-Cys]-NH <sub>2</sub>
BIM-23296	c[Cys-Phe-Nal-D-Trp-Lys-Thr-Phe-Cys]-NH <sub>2</sub>
BIM-23313	c[Cys-Phe-I-Tyr-D-Trp-Lys-Thr-Phe-Cys]-NH <sub>2</sub>
MK-678	c[D-Trp-Lys-Val-Phe-N-MeAla-Tyr]
SMS-201-995	D-Phe-c[Cys-Phe-D-Trp-Lys-Thr-Cys]-Thr-ol
RC-160	D-Phe-c[Cys-Tyr-D-Trp-Lys-Val-Cys]-Trp-NH <sub>2</sub>
L-362,855	c[Ahep-Phe-Trp-D-Trp-Lys-Thr-Phe]

Abbreviations: Abu,  $\alpha$ -aminobutyric acid; Nal,  $\beta$ -(2-naphthyl)-alanine; Ahep, 7-aminoheptanoic acid.

Table 2. Comparison of binding affinities of key cyclic octapeptides for 5 human and 3 rat SRIF receptors present on transfected CHO-1 cells<sup>a</sup>.

Peptide	K <sub>i</sub> (nM)				
	hSSTR1	hSSTR2 (r)	hSSTR3 (r)	hSSTR4	hSSTR5 (r)
BIM-23014	2414	0.75 (1.47)	12 (115)	1826	5.21 (23)
BIM-23023	6610	0.42 (0.57)	89 (92)	2700	4.18(14.0)
BIM-23052	97	11.9 (69.0)	5.58 (3.5)	126	1.22 (2.4)
BIM-23056	692	132 (3400)	177 (272)	174	12 (536)
BIM-23268	12.2	15.1 (101)	61.5 (4.1)	19.9	0.37 (3.4)
BIM-23295	86.8	6.19 (57.0)	318 (5.7)	3.36	0.34 (0.65)
BIM-23313	151	4.78 (45.0)	115 (11.2)	55.3	0.27 (9.9)
MK-678	>1000	0.13 (0.48)	88 (45.0)	>1000	15.5(72.0)
SMS-201-995	875	0.57 (2.0)	35 (14.0)	>1000	6.78(17.0)
RC-160	481	0.57 (0.85)	795 (87.0)	351	7.53 (6.8)
L-362,855	993	2.96 (12.0)	98 (33.0)	467	0.76 (51.0)
SRIF	2.25	0.23 (1.43)	1.43 (1.33)	1.76	1.41 (4.46)
SRIF-28	2.38	0.29 (1.78)	1.02 (0.81)	7.93	0.38 (1.02)

<sup>a</sup>Structures shown in Table 1; rat data shown in parentheses; nd, not done.

## References

1. Raynor, K., Murphy, W.A., Coy, D.H., Taylor, J.E., Moreau, J-P., Yasuda, K., Bell, G.I. and Reisine, T., *Mol. Pharmacol.*, 43 (1993) 838.
2. Coy, D.H. and Taylor, J.E., *Metabolism*, 34 (Suppl. 1) (1996) 21.

## Properties of GnRH conjugates *in vivo*

Imre Mezö,<sup>a</sup> B. Vincze,<sup>b</sup> G. Tóth,<sup>c</sup> J. Pató,<sup>d</sup> D. Gaál,<sup>b</sup> T. Kremmer,<sup>b</sup> A. Kálnay,<sup>b</sup> E. Gulyás,<sup>c</sup> I. Teplán,<sup>a</sup> F. Ötvös,<sup>e</sup> S. Lovas,<sup>e</sup> R.F. Murphy<sup>e</sup> and I. Pályi<sup>b</sup>

<sup>a</sup> Dept. Medical Chemistry, Semmelweis Univ. Medicine, Budapest, Hungary, <sup>b</sup> Nat. Inst. Oncology, Budapest, <sup>c</sup> Biol. Res. Center, Hung. Acad. Sci., Szeged, Hungary, <sup>d</sup> Central Res. Inst. Chemistry, Hung. Acad. Sci., Budapest, <sup>e</sup> Department of Biomedical Sciences, Creighton Univ., School of Medicine, Omaha, NE, USA.

The direct antitumor activity of GnRH-III *in vivo* is increased by conjugation to poly(N-vinylpyrrolidone-co-maleic acid) (P) (molecular weight *c.a.* 10,000) through a GFLG tetrapeptide spacer (X) [1]. To examine the biodistribution and clearance of the conjugates and components thereof, the following radiolabeled derivatives were prepared: carboxyl groups (2%) of P were coupled with <sup>125</sup>I-tyrosylamide before conjugation through (X) with GnRH-III [2] to form <sup>125</sup>I-tyrosylamide-P-X-GnRH-III, and [<sup>3</sup>H]GnRH-III [3] was conjugated with P-X to form P-X-[<sup>3</sup>H]GnRH-III. Compounds were injected *s.c.* into CBA/CA mice with MCF-7 human breast cancer xenografts.

### Results and Discussion

Radioactivity in blood peaked immediately after injection of [<sup>3</sup>H]GnRH-III and then cleared rapidly. Following injection of P-X-[<sup>3</sup>H]GnRH-III, however, blood radioactivity was only slightly elevated by the sixth hour and then decreased continuously. Radioactivity in liver and kidney similarly increased and decreased immediately after injection of [<sup>3</sup>H]GnRH-III but accumulated in the spleen after 6 hours. Following the injection of P-X-[<sup>3</sup>H]GnRH-III, radioactivity in the liver and spleen peaked at 6 hours and in the kidney at three hours and then decreased gradually. Accumulation of radioactivity in the kidney was 6 times higher following injection of the conjugate than of the free peptide.

Proportionately higher accumulation of radioactivity in xenografts was observed 24 hours after injection of <sup>125</sup>I-tyrosylamide-P-X-GnRH than of either [<sup>3</sup>H]GnRH-III or <sup>125</sup>I-tyrosylamide-P. The <sup>125</sup>I-tyrosylamide-P-X-GnRH-III conjugate may have had greater retention than the P-X-[<sup>3</sup>H]GnRH-III conjugate because of greater lipophilicity.

FPLC analysis (Fig.1.) of blood serum on Sephadex G25, 0.5, 3 and 24 hours after injection of P-X-[<sup>3</sup>H]GnRH-III, showed that no radioactivity was detected in fractions with molecular weight  $\leq 1,000$ , suggesting that catabolism does not release peptide from conjugates. Over 90 percent of the <sup>3</sup>H radioactivity was found in fractions with molecular weight  $\geq 5,000$ . Analysis of urine, however, showed that significant <sup>3</sup>H radioactivity was present after 3 hours in material with molecular weight  $\leq 1,000$ , presumably catabolite(s); little radioactivity was detected after 24 hours.

In general, the results show that, conjugation of GnRH-III with the copolymer favors tissue retention of intact bound peptide. Conjugation apparently affords protection from proteolytic degradation in blood circulation whereas the free peptide resembles polypeptide hormones of comparable size in that it is readily cleared. This may contribute to the superior antitumor effects of conjugates *in vivo*.

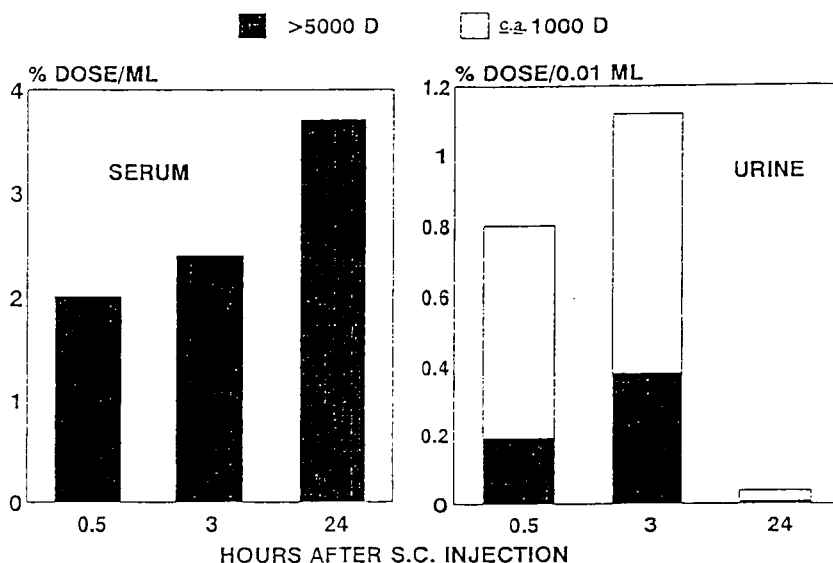


Fig. 1. FPLC analysis of P-X-[ $^3H$ ]GnRH-III metabolites in CBA/Ca mice.

### Acknowledgments

This work was supported by the OMFB (NO: 94-97-48-0735), OTKA T 016323 and US-Hungarian Science & Technology Joint Fund #455.

### References

1. Mezö, I., Seprödi, J., Vadász, Zs., Teplán, I., Vincze, B., Pályi, I., Kálnay, A., Turi, G., Móra, M., Pató, J., Tóth, G., Lovas, S. and Murphy, R.F., In Kaumaya, P.T.P. and Hodges, R.S., (Eds) Peptides: Chemistry, Structure and Biology, Mayflower Scientific Ltd., Kingswinford 1996 p. 239-240.
2. Sower, S.A., Chiang, Y-C., Lovas, S. and Conlon, J.M., *Endocrinology*, 132, (1993) 1125.
3. Mezö, I., Lovas, S., Pályi, I., Vincze, B., Kálnay, A., Turi, G., Vadász, Zs., Seprödi, J., Idei, M., Tóth, G., Gulyás, É., Ötvös, F., Mák, M., Horváth, J.E., Teplán, I. and Murphy, R.F., *J. Med. Chem.*, in press.

# Phospholipid vesicle binding by an amphiphilic $\beta$ -sheet structure from serum apolipoprotein B-100

Jinliang Lu and John W. Taylor

*Department of Chemistry, Rutgers University, Piscataway, NJ 08855., USA*

The serum apolipoproteins all contain within their structures amino-acid sequences with the potential to form amphiphilic  $\alpha$ -helices, often with cationic hydrophilic faces. The function of these structural domains in binding to the phospholipid surfaces of the serum lipoprotein particles has been thoroughly characterized. However, apolipoprotein B (apoB), the protein constituent of low-density lipoproteins (LDL), is unique amongst the serum apolipoproteins in that it contains proline-rich sequences that have the potential to form anionic amphiphilic  $\beta$ -sheets. These structures have also been proposed as lipid-binding domains [1]. We now report the first characterization of the phospholipid vesicle-binding properties of this anionic structural motif, and compare its apparent and intrinsic affinities for small, unilamellar vesicles with those of a model cationic amphiphilic  $\alpha$ -helical peptide, and a model cationic amphiphilic  $\beta$ -sheet peptide.

## Results and Discussion

We have used the weak Phe fluorescence of N $^{\alpha}$ -acetylated native apoB peptide amides, 20 and 40 residues in length that corresponds to one of the proline-rich apoB segments (apoB[2698-2717], and apoB[2678-2717], respectively) to investigate peptide binding to single-bilayer phospholipid vesicles. Different vesicle preparations consisted of egg lecithin phosphatidyl choline (PC) doped with varying molar percentages of the cationic lipid 1,2-dioleoyl-3-trimethylammonium-propane (TAP) or the anionic lipid 1-palmitoyl-2-oleoyl-sn-glycero-3-phosphoglycerol (PG), creating different net positive or negative surface charge densities. The binding isotherms obtained by titrating the anionic apoB peptides with increasing vesicle concentrations indicated a length requirement of 40 residues for saturable binding to neutral vesicles, and only a weak additional electrostatic attraction to the cationic vesicles. These binding curves were analyzed directly to obtain the apparent partition constants,  $K_p^*$ , shown in Table 1. Analysis of the binding to cationic vesicles according to Gouy-Chapman theory [2] gave an intrinsic partition constant,  $K_p$ , for the 40-mer of  $0.97 \times 10^3 \text{ M}^{-1}$ , which corresponded closely to the  $K_p^*$  value of  $1.1 \times 10^3 \text{ M}^{-1}$  obtained for neutral vesicles.

For comparison with the phospholipid binding properties of the apoB peptides, two cationic model peptides were also studied. The first was a Tyr<sup>22</sup>-substituted analogue of a previously described model amphiphilic  $\alpha$ -helical peptide designed to have its cationic side-chains segregated near the hydrophobic surface of the helical structure. Studies of the Tyr fluorescence upon addition of vesicles indicated that there was saturable binding of the 22-residue peptide to all types of vesicles. Analysis of the binding isotherms for this amphiphilic  $\alpha$ -helical peptide gave intrinsic partition constants ( $K_p = 2.8 \times 10^3$ -  $3.9 \times 10^3$

$M^{-1}$ ) that were similar to those obtained for the apoB-derived 40-mer. However, the  $\alpha$ -helical model peptide showed much stronger additional electrostatic attraction to the net negatively charged vesicle surfaces than the anionic apoB peptide showed for the net positively charged vesicle surfaces ( $K_p^*$  values in Table 1).

Table 1. Analysis of peptide lipid binding curves.

Peptide	Net Charge	Lipid Composition	Apparent Partition Constant, $K_p^*$ , $\times 10^{-3} (M^{-1})$	Intrinsic Partition Constant, $K_p$ , $\times 10^{-3} (M^{-1})$
Helical Model	+1	25% PG (-)	13.0	3.9
		10% PG (-)	5.1	2.8
		Neutral (PC)	2.3	-
$\beta$ -Sheet Model	+3	25% PG (-)	3.7	0.09
		10% PG (-)	1.0	0.18
Apo B 40-mer	-4	25% TAP (+)	2.2	-
		10% TAP (+)	3.7	0.97
		Neutral (PC)	1.1	-
Apo B 20-mer	-3	25% TAP(+)	1.6	-
		10% TAP (+)	2.1	-

The second model peptide studied for comparison was a cationic 20-residue model of the proposed amphiphilic  $\beta$ -sheet motif in apoB: Ac-Tyr-Leu-Lys-Val-Pro<sup>5</sup>-Lys-Leu-Asp-Val-Pro<sup>10</sup>-Lys-Leu-Lys-Val-Pro<sup>15</sup>-Lys-Leu-Asp-Val-Pro<sup>20</sup>-NH<sub>2</sub>. Tyr fluorescence of this peptide indicated a strong electrostatic attraction to anionic vesicles. However, an analysis of the binding isotherms according to Gouy-Chapman theory suggested that it had only a very weak intrinsic affinity for these vesicles ( $K_p = 0.1 \times 10^3 - 0.2 \times 10^3 M^{-1}$ ). Consistent with this analysis and the prior results for the apoB peptide of the same length, this cationic amphiphilic  $\beta$ -sheet model peptide did not bind to neutral vesicles.

Overall, these studies demonstrate for the first time that a proline-rich region of apoB can bind to electrically neutral phospholipid vesicles. This supports the phospholipid binding function in LDL that was originally proposed for these  $\beta$ -sheet structures [1].

## References

1. Knott, T.J., Pease, R.J., Powell, L.M., Wallis, S.C., Rall, Jr., S.C., Innerarity, T.L., Blackhart, B., Taylor, W.H., Marcel, Y., Milne, R., Johnson, D., Fuller, M., Lusic, A.J., McCarthy, B.J., Mahley, R. W., Levy-Wilson, B. and Scott, J., *Nature*, 323 (1986) 734.
2. McLaughlin, S., *Annu. Rev. Biophys. Biophys. Chem.*, 18 (1989) 113.

# Stability and binding of SH3 domain of Bruton's tyrosine kinase

**Jya-Wei Cheng, Himatkumar V. Patel,  
Shiou-Ru Tzeng and Chen-Yee Liao**

*Department of Life Sciences, National Tsing Hua University, Hsinchu 30043, Taiwan, R.O.C.*

The gene involved in X-linked agammaglobulinemia (XLA), an inherited immunodeficiency disease, has been found to code for a cytoplasmic protein tyrosine kinase (Bruton's tyrosine kinase, BTK) [1]. Patients suffering from XLA fail to mount an antibody response and consequently suffer from recurrent, sometimes lethal, bacterial infections. Like many other cytoplasmic tyrosine kinases, BTK contains an SH3 domain, a PH domain, an SH2 domain, and a catalytic tyrosine kinase domain [2-5]. The signal transduction pathways that regulate cell growth and differentiation are characterized by a cascade of specific protein-protein recognition events that occur intracellularly upon extracellular stimulation [2-5]. SH3 and SH2 domains are small protein modules that mediate protein-protein interactions in signaling pathways. It has been found that mutations or deletions within these domains result in X-linked agammaglobulinemia [6, 7]. SH3 domains form a compact  $\beta$  barrel structure composed of five to eight  $\beta$  strands [2-5, 8]. Structural and peptide-binding analyses of various SH3 domains show that proline-rich peptides containing the PXXP motif can bind to SH3 domains [2, 5]. The reductionistic approach of studying individual domains has been successful as well as informative [2, 5, 8]. Nonetheless, details of the interaction between the domains still remain unclear. Study of the interaction of inter- and intramolecular organization of the domains is thus a significant objective.

## Results and Discussion

A point mutation resulting in the deletion of 14 amino acids constituting the C-terminal of the BTK SH3 domain has been identified as a cause of XLA in a patient family [7]. We therefore studied the stability and ligand binding of a 58-residue peptide (aa 216-273) corresponding to the SH3 domain of BTK and a 44 residue peptide (216-259) lacking the C-terminal 14 aa residues of BTK SH3 domain (truncated SH3 domain). Studies on the latter peptide can shed light on the factor that causes XLA. We found that proline rich peptides (P1, P3) of the BTK TH domain bind to the BTK SH3 domain (Table 1). We also found that the truncated SH3 domain binds weakly to the BTK TH domain peptide (P3). Attachment of nonpeptidic molecules like fluorescein to the proline peptide (P4) enhances binding to the SH3 domain. Furthermore, the association of the truncated SH3 domain with proline rich peptide (P6) of p120<sup>cb1</sup> was weaker than with the intact SH3 domain. We have demonstrated earlier that the mutation (loss of the C-terminal 14 aa residues) results in transformation of the  $\beta$ -barrel structure of the SH3 domain to a random coil

conformation [9]. Herein we show that the mutation-truncation that causes XLA saps the SH3 domain of its ability to bind to its target, probably due to aberrant folding. This likely renders the kinase abnormal. The transformation of the  $\beta$ -barrel type structure to a random coil conformation in the truncated SH3 domain delineates unequivocally the importance of the C-terminal in maintaining the structural integrity of SH3 domains in general, and of BTK in particular. Furthermore, since deletion of the C-terminal 14 amino acid residues causes XLA, our result also indicate that improper folding and/or instability of the SH3 domain of BTK likely renders the kinase non-functional or diseased.

*Table 1. Interaction of SH3 domain (SH3-58) and truncated SH3 domain (SH3-44) of BTK with proline-rich peptides.*

No	peptide sequence	SH3-58 $K_d$ ( $\mu$ M)	SH3-44 $K_d$ ( $\mu$ M)
P1	TKKPLPPTPE	49.9	
P2	TKRALPPLPE	38.4	
P3	HRKTKKPLPPTYQ	14.9	76.5
P4	FITC-HRKTKKPLPPTYQ	3.1	
P5	AAPPLPPRKT	239	
P6	SLHKDKPLVPPYQ	34.5	112.2

In conclusion, we have shown that the BTK SH3 domain can bind to proline rich peptides of the BTK TH domain. Our results delineate the importance of the C-terminal in ligand binding of SH3 domains and also indicate that improper folding and altered binding behavior of the mutant BTK SH3 domain likely causes XLA.

## References

1. Vetrie, D., Vorechovsky, I., Sideras, P., Holland, J., Davies, A., Flinter, F., Hammarström, L., Kinnon, C., Levinsky, R., Bobrow, M., Smith, C. I. E. and Bentley, D. R., *Nature*, 361 (1993) 226.
2. Pawson, T., *Nature*, 373 (1995) 573.
3. Shokat, K. M., *Chemistry & Biology*, 2 (1995) 509.
4. Yu, H. and Schreiber, S. L., *Structural Biology*, 1 (1994) 417.
5. Cohen, G. B., Ren, R. and Baltimore, D., *Cell*, 80 (1995) 237.
6. Vihinen, M., Nilsson, L. and Smith, C. I. E., *Biochem. Biophys. Res. Comm.*, 205 (1994) 1270.
7. Zhu, Q., Zhang, M., Rawlings, D. J., Vihinen, M., Hagemann, T., Saffran, D. C., Kwan, S. P., Nilsson, L., Smith, C. I. E., Witte, O. N., Chen, S. H. and Ochs, H. D., *J. Exp. Med.*, 180 (1994) 461.
8. Kuriyan, J. and Cowburn, D., *Current Opinion in Structural Biology*, 3(1993)828.
9. Chen, Y.-J., Lin, S.-C., Tzeng, S.-R., Patel, H. V., Lyu, P.-C. and Cheng, J.-W., *Proteins*, 26(1996)465.

# The interaction between monoclonal antibody 4A5 and fibrinogen gamma chain peptides studied by nuclear magnetic resonance

Michael Blumenstein<sup>a</sup> and Gary R. Matsueda<sup>b</sup>

<sup>a</sup>*Department of Chemistry, Hunter College, New York, NY 10021, USA and* <sup>b</sup>*Bristol-Myers Squibb Pharmaceutical Research Institute, Princeton, NJ 08543, USA*

Fibrinogen  $\gamma$ 392-411, LTIGEGQQHHLGGAKQAGDV, is involved in the formation of fibrin clots [1] and interaction with the platelet integrin receptor [2]. Due to the physiological significance of this region, efforts have been made to determine its conformational properties [3-5]. We have previously observed [3] that the peptide corresponding to this sequence possesses a type II  $\beta$ -turn from Gln<sup>407</sup> to Asp<sup>410</sup>. The turn is retained when Gly<sup>409</sup> is replaced by D-Ala, but the population of the turn is greatly reduced when L-Ala is substituted into this position.

Monoclonal antibody 4A5 has a high affinity for both fibrinogen and the  $\gamma$ 392-411 segment [6]. The L-Ala substitution in residue 409 leads to decreased antibody affinity, while the D-Ala substitution leads to slightly increased affinity for 4A5, suggesting that the  $\beta$ -turn may serve as part of the antibody recognition motif [4]. We report here our initial studies in which NMR is used to directly monitor the interaction between  $\gamma$ 392-411 (and analogues) and monoclonal antibody 4A5, with the ultimate goal of elucidating the antibody-bound conformation of the peptides.

## Results and Discussion

The peptide LTIGEGQQHHL\*G\*G\*A\*KQ\*A\*G\*D\*V was enriched with <sup>15</sup>N in the backbone amide nitrogens of the designated (\*) residues. The peptide was complexed with the F<sub>ab</sub> fragment of 4A5 in a 1:1 ratio and the interaction was studied via two-dimensional NMR employing the <sup>1</sup>H-<sup>15</sup>N heteronuclear single quantum filtered (HSQC) experiment. Assignments were made by using several singly labeled peptides. While amide <sup>1</sup>H resonances of Leu<sup>402</sup> and Gly<sup>403</sup> shift downfield on complexation with antibody, all other amide <sup>1</sup>H resonances shift upfield in the presence of 4A5. All <sup>15</sup>N resonances other than that of Leu<sup>402</sup> display significant upfield shifts in the antibody-bound peptide, HSQC experiments were also performed with the <sup>15</sup>N enriched D-Ala<sup>409</sup> analog, which has a higher affinity for 4A5 than does native 392-411. The bound <sup>1</sup>H and <sup>15</sup>N shifts of the D-Ala analog were very similar to those observed for native 392-411, with differences being observed only in residue 409 and directly adjacent residues.

The observation of substantial <sup>1</sup>H and <sup>15</sup>N shifts throughout the 402-411 region of 392-411 upon antibody binding is an indication of a peptide-antibody interaction involving as many as ten peptide residues. Since there were only minor differences in bound shifts

between native 392-411 and the D-Ala<sup>409</sup> analog, these two peptides must bind in the same manner, and with identical conformations, to the antibody. The increased affinity for the D-Ala analog is likely due to favorable hydrophobic interactions of the D-Ala methyl group with antibody side chains.

The nature of the observed chemical shifts may have conformational significance. There is a correlation [7], albeit weak, of the shifts of amide protons with secondary structure, a series of upfield shifts being indicative of helical conformation. Thus, residues 404-411 may be in a helical conformation in the antibody-bound peptide. In previous work involving peptide-antibody interaction [8], a helical conformation was determined based on nuclear Overhauser (NOE) measurements, and this peptide also displayed a series of upfield amide <sup>1</sup>H shifts upon antibody binding. NMR studies [5] have indicated that a substantial portion of the 392-411 region is in a helical conformation when bound to the integrin receptor.

We intend to undertake NOE measurements of the peptide-4A5 complex in order to get a more rigorous determination of the conformation of the bound peptide. We will also employ the labeled L-Ala<sup>409</sup> analog to monitor the binding of this peptide, and will utilize peptides enriched with <sup>13</sup>C in the Ala and D-Ala side chains to elucidate the role of these moieties in peptide-antibody interaction.

## References

1. Budzynski, A.Z., *CRC Crit. Rev. Oncol./Hematol*, 6 (1986) 97.
2. Kloczewiak, M., Timmons, S., Lukas, T.J. and Hawiger, J., *Biochemistry*, 23 (1984) 1767.
3. Blumenstein, M., Matsueda, G.R., Timmons, S. and Hawiger, J., *Biochemistry*, 31 (1992) 10692.
4. Donahue, J.P., Patel, H., Anderson, W.F. and Hawiger, J., *Proc. Natl. Acad. Sci. USA*, 91 (1994) 12178.
5. Mayo, K.H., Fan, F., Beavers, M.P., Eckhardt, A., Keane, P., Hoekstra, W.J. and Andrade-Gordon, P., *Biochemistry*, 35 (1996) 4434.
6. Bernatowicz, M.S., Costello, C.E. and Matsueda, G.R., in Marshall, G.R. (Ed.) *Peptides, Chemistry and Biology; Proceedings of the 10<sup>th</sup> American Peptide Symposium*, ESCOM, Leiden, 1988, p. 187.
7. Wishart, D.S., Sykes, B.D. and Richards, F.M., *J. Mol. Biol.*, 222 (1991) 311.
8. Tsang, P., Rance, M., Fieser, T.M., Ostresh, J.M., Houghten, R.A., Lerner, R.A. and Wright, P.E., *Biochemistry*, 31 (1992) 3862.

# A potent synthetic dimeric peptide agonist of the erythropoietin receptor

Palaniappan Balasubramanian, Qun Yin, Surekha Podduturi,  
Nicholas C. Wrighton and William J. Dower

Affymax Research Institute, 4001 Miranda Avenue, Palo Alto, CA, USA

Erythropoietin (EPO) is a glycoprotein of molecular mass 34 kDa that stimulates the proliferation and differentiation of erythroid progenitor cells in the bone marrow [1]. Under normal circumstances it is produced at low levels in the adult kidney for maintenance of the red blood cell mass, but expression is increased in response to tissue hypoxia. It is used clinically to treat the anemia associated by anti-cancer and anti-HIV chemotherapy in addition to replacement therapy for EPO insufficiency resulting from renal disease. Using peptide phage display technology, we identified and developed a family of peptides that bind to and activate the EPO receptor [2]. The peptides were synthesized in the monomeric form, but were capable as acting as full EPO mimetics. Since the receptor is believed to be activated by homodimerization, we reasoned that the peptides might themselves undergo non-covalent dimerization in order to function as agonists. We therefore synthesized a covalent dimer of an EPO mimetic to test this hypothesis, with the assumption that covalent dimerization would lead to increased affinity for the EPOR and elevated biological activity. The details of the bioassay of the monomer (1) and dimer (2) will be published elsewhere [3]. In the current paper the synthetic procedure is discussed in detail.

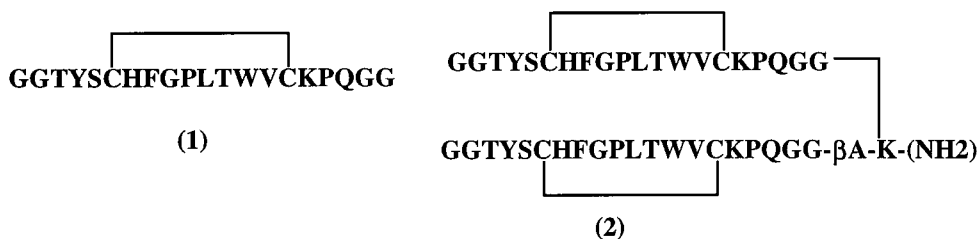


Fig. 1. Synthesis of a dimeric peptide agonist of the EPOR.

## Results and Discussion

The general scheme for the dimer synthesis is shown in Fig. 1. Peptide synthesis was carried out using Fmoc chemistry on acid-labile linker coupled to PEG-PS support. We used Lys at the C-terminal as a branch point. After coupling Fmoc-Lys(Alloc)-OH to the resin the Fmoc-β-Ala-OH was coupled to the α-NH<sub>2</sub> of the Lys. The β-alanine residue at this position produces a pseudo symmetrical branch for two chains. The Cys(Acm) was

coupled in the first chain. The Boc group at the N-terminus helped to prevent chain elongation during the second chain synthesis. After completion of the first chain, a small amount of the resin was cleaved, purified and confirmed by ESMS. The  $\epsilon$ -Alloc group was removed using Pd[P(C<sub>6</sub>H<sub>5</sub>)<sub>3</sub>]<sub>4</sub>, 4-methyl morpholine and chloroform[4]. A small amount of the resin was cleaved and purified and the structure was confirmed by ESMS. The second parallel chain was synthesized on the Lys  $\epsilon$ -NH<sub>2</sub> group. Fmoc-Cys(Trt)-OH was coupled in the second chain as orthogonal protection to the Cys(Acm) in the first chain. After synthesis was completed, the peptide was cleaved using TFA/scavenger. The crude peptide was purified by RHPLC and confirmed by ESMS. The first disulfide bond was formed by stirring with 20%DMSO/water overnight [5]. The peptide was further purified and confirmed by ESMS. The removal of Acm group and cyclization was accomplished by stirring with iodine/methanol for 24 hours [6]. The crude peptide was further purified and all fractions were checked by ESMS (Calculated 4367.0, Observed: 4366.6). The fractions with the correct mass value were pooled and lyophilized. The final yield was 5% based on the initial loading of the resin. This material was further used for the bioassay.

The dimer peptide was then subjected to assays to determine EPOR binding affinity and *in vitro* EPO biological potency [3]. Compared to the single chain disulfide molecule (1), which has an IC<sub>50</sub> of 200 nM in the immobilized PIG-tailed EPOR binding assay, the dimer analogue (3) exhibits a two log increase in affinity with an IC<sub>50</sub> of approximately 2 nM. In the FDCP-1/hEPOR cell proliferation assay, the dimer (2) showed an agonist potency that was one log higher than the monomer (1).

## References

1. Jelkmann, W., *Physiological Reviews*, 72 (1992) 449.
2. Wrighton, N.C., Farrell, F.X., Chang, R., Kashyap, A.K., Barbone, F.P., Mulcahy, L.S., Johnson, D.L., Barrett, R.W., Jolliffe, L.K. and Dower, W.J., *Science*, 273 (1996) 458.
3. Wrighton, N.C., Balasubramanian, P., Barbone, F.P., Kashyap, A.K., Farrell, F.X., Jolliffe, L.K., Barrett, R.W. and Dower, W.J., *Manuscript in preparation*.
4. Kates, S.A., Sole, N.A., Albericio, F., Barany, G., *Peptides: Design, Synthesis and Biological Activity*, Birkhauser, (1994) 39.
5. Tam, J.P., Wu, C-R., Liu, W. and Zhang, J-W., *J. Am. Chem. Soc.*, 113 (1991) 6657.
6. Kamar, B., Hartmann, A., Eisler, K., Riniker, B., Rink, H., Sieber, P. and Rittel, W., *Helv. Chem. Acta.*, 63 (1980) 899.

# **Binding studies of cytokines rhGM-CSF and rhIL-3 with a peptide fragment of hGM-CSF receptor $\alpha$ -chain by non-immobilised ligand interaction assay (NILIA) using circular dichroism (CD)**

**Rohanah Hussain,<sup>a</sup> Paolo Rovero,<sup>b</sup> Claudia Galoppini<sup>b</sup>  
and Giuliano Siligardi<sup>a</sup>**

<sup>a</sup>*EPSRC National Chiroptical Spectroscopy Service, King's College London,  
Department of Pharmacy, Manresa Road, London SW3 6LX, U.K.*

<sup>b</sup>*CNR-IMD, Lab Sintesi Peptidica, Via Svezia 2A, I-56124, Pisa, Italy*

Granulocyte-macrophage colony stimulating factor (GM-CSF) cytokine is essential for the proliferation and differentiation of blood myeloid progenitor cells and activation of several functions of macrophages, neutrophils, eosinophils and megakaryocytes [1-3]. Peptide P115 (Ac-KQPRTYQKLSYLDFQYQ-NH<sub>2</sub>) of hGM-CSF receptor  $\alpha$ -chain was found to interact with cytokine rhGM-CSF (14.6KDa) by ELISA and affinity chromatography [4]. Binding specificity of P115 to rhGM-CSF, related cytokine rhIL-3 and unrelated protein BSA were examined by NILIA-CD spectroscopy.

## **Results and Discussion**

Unambiguous evidence of binding hGM-CSF receptor  $\alpha$ -chain peptide P115 to cytokine rhGM-CSF was observed mainly in the spectral region characteristic of tryptophan aromatic side-chain and disulphide bond chromophores (290-320nm) ( $K_{dapp}=35\mu\text{M}$ ) by NILIA-CD spectroscopy. Only rhGM-CSF possesses two tryptophan residues and two disulphide bond chromophores (Fig. 1). Phe and Tyr residues are present in both rhGM-CSF and P115. The CD data at single wavelength (290nm and 310nm) were analysed by non-linear regression to the general equilibrium reaction in which the CD intensity is proportional to the concentration of each species. The negative solutions of the quadratic equation derived from the binding of the peptide ligand to a single cytokine site were used to fit the CD data.

P220 (Ac-YQDYKQQLYRTQKPFLS-NH<sub>2</sub>) a scrambled P115 sequence showed no CD changes in the 290-330nm region indicating no GM-CSF-P220 interaction occurring. IL-3 belongs to the same cytokine family as GM-CSF and shares the same receptor  $\beta$ -subunit as GM-CSF and IL-5. rhIL-3 (15KDa) showed no evidence of binding to P115 by NILIA-CD. No BSA-P115 interactions were present since no significant CD changes in the backbone and aromatic regions were observed. It is thus evident that non-specific binding of P115 to BSA was absent.

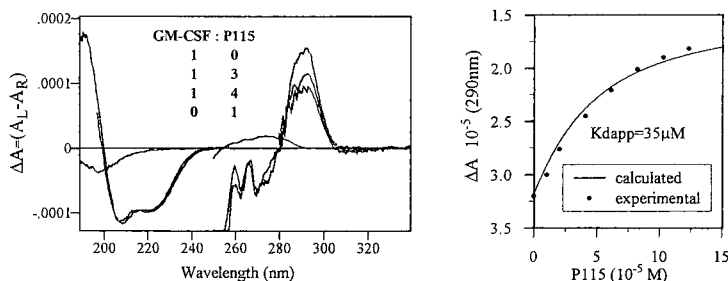


Fig. 1. CD spectra of rhGM-CSF:P115 mixture at various ratios. The  $\Delta A$  values at 290nm were used to calculate the apparent binding constant,  $K_{dapp}=35\mu M$ .

## Conclusion

NILIA-CD was successfully employed in monitoring, quantifying and discriminating the binding interaction of GM-CSFR $\alpha$  peptide P115 to cytokines rhGM-CSF, rhIL-3 and unrelated protein BSA. P220 as a negative control was also successfully monitored as a non-rhGM-CSF binding peptide by NILIA-CD. Trp/S-S regions of rhGM-CSF were identified as the residues involved in the binding interaction with P115. Since no significant CD changes were observed in the backbone region between the bound and free hGM-CSF, the binding area of hGM-CSF for P115 can thus be mapped using the crystal structure of hGM-CSF (1csg.pdb).

In NILIA-CD, no labelling of ligand/receptor, sandwich assay or immobilisation are required unlike ELISA, BIAcore and IAsys biosensor techniques. Added information on conformational changes due to binding interaction can also be elucidated by NILIA-CD. This is vital for further improvement in drug design/targeting. NILIA-CD, thus, provides an ideal technique for monitoring ligand receptors interactions in solution.

## Acknowledgements

We would like to thank Sandoz Pharma, Switzerland, for the generous supply of rhIL-3.

## References

1. Lopez, A.F., Williamson, D.J., Gamble, J.R., Begley, G., Harlam, J., Klebanoff, S., Waltersdorff, A., Wong, G.C., Clark, S.C. and Vadas M., J. Clin. Invest., 78(1986)1220.
2. Grabstein, K.H., Urdal, D.L., Tushinski, R.S., Mochizuki, D.Y., Price, V.L., Candrell, M.A., Gillis, S. and Conlon, P.J., Science, 265(1986)506.
3. Metcalf, D., Science, 254(1991)529.
4. Di Bartolo, V., Danè, A., Cassano, E., Viganò, S., Chiello, E., Verniani, D., Befly, P., Pegoraro, S., Hamdan, M., Rovero, P. and Revoltella, R.P., J. Rec. Signal Transds. Res., 16(1996)77.

# Synthesis, bioactivity, 2D NMR and ESR of Angiotension II and its spin labeled derivative

Xiaoyu Hu, Rui Wang, Xiaoxu Li and Jianheng Shen

*Department of Biology, State Key Laboratory of Applied Organic Chemistry,  
Lanzhou University, Lanzhou, Gansu 73000, China*

Angiotensin II (AngII) is an important constituent of the renin-angiotension system (RAS)[1]. The amino acid sequence of AngII is DRVYIHPF. AngII plays an important role both in maintenance of normal blood pressure and in the occurrence of hypertension. AngII binding receptor can induce many kinds of physiological effects. Spin labeling is an effective method that has greatly enhanced our knowledge of the structure, movement and interactions of biological molecules. For example, it has been used successfully in studying the interaction of antigen and antibody. Some stable free radical compounds are not only useful for obtaining information but are also functional [2].

we designed and synthesized AngII-R and studied AngII-R's ESR spectra before and after its binding to the AngII receptor. Interaction information of AngII and its receptor may produce different spectra as determined by ESR when AngII-R is not in a constrained state. Our purpose was to find an effective, simple method for studying the molecular environment of peptide and receptor interaction. The secondary structure of AngII in solution was indicated by 2DNMR study.

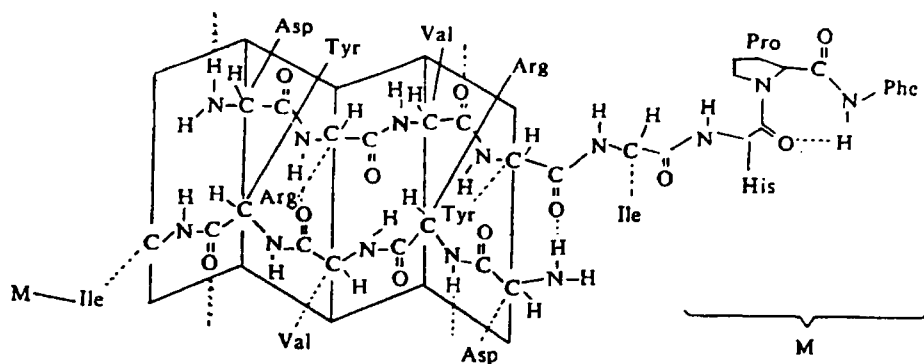
## Results and Discussion

The purity of AngII was 95% and that of AngII-R was 92%, which was determined by reverse phase HPLC, the data from amino acid analysis were in agreement with the theoretical values: FABMS:AngII=1046, AgII-R 1211. ESR spectrum of AngII-R showed three peaks of stable nitroxide free radicals and suggested successful labeling of AngII.

Our results show receptor biding assay,  $IC_{50}(\text{mol L}^{-1})$ : AngII  $1.4 \times 10^{-8}$ , AngII-R  $1.5 \times 10^{-8}$ . Action on blood vessel,  $EC_{50}(\text{mol L}^{-1})$ : AngII  $2 \times 10^{-8}$ , AngII-R  $6.7 \times 10^{-8}$ ,  $P < 0.05$ . Action on cholescyst,  $EC_{50}(\text{mol L}^{-1})$ : AngII  $2.7 \times 10^{-8}$ , AngII-R  $4.3 \times 10^{-7}$ ,  $P < 0.05$ . Action on blood pressure,  $ED_{50}(\mu\text{g/kg})$ : AngII 1.84, AngII-R 7.26,  $P < 0.01$ .

After binding reaction of AngII-R ( $10^{-2}\text{M}$ ) with the AngII receptor preparation (concentration of membrane protein: 20mg/mL), the AngII-R-receptor complex was obtained by centrifugation or by fast filtration and gave signals via ESR measurements. The existence of anisotropy in the spectrum suggested the constraint of AngII-R, and immobilization peaks revealed AngII R's tight binding to the receptor. The calculated  $\tau_c$  value of AngII-R is  $5.6 \times 10^{-11}\text{S}$ . The  $\tau_c$  value is estimated to be  $10^{-8}\text{S}$ , the intensively prolonged  $\tau_c$  value also reflects immobilization of R· group [3]. We also note that immobilization peaks come from bound AngII-R and the nonimmobilization peaks from unbound or absorbed AngII-R.

The secondary structure of AngII in solution was proposed by 2DNMR study. The N-terminal from Asp to Tyr should be in reversed  $\beta$ -sheet form and the C-terminal from Phe to His might form a ring with a hydrogen bond. The diagrammatic sketch is as follows:



## Conclusion

The bioassays studied *in vitro* and *in vivo* indicated that: 1) The affinity of AngII·R to AngII receptor was near to that of AngII. 2) In blood vessel contraction and blood pressure models, the decrease in activity of AngII·R is due to modification of the N-terminal of AngII. We suggest that the contribution of N-terminal activity is larger than that to binding ability. Immobilization signals suggest that R· to receptor indicates that since the labeling to AngII does not interfere with the AngII molecular system, it is a suitable paramagnetic label.

## Acknowledgement

The authors would like to thank Professor Du Li (Brigham Young University) and Professor Changlin Li and Jingfen Lu (Beijing Medical University) for their kind help. This work was supported by grants from the Fok Ying Tung (Hong Kong) Education Foundation, the national Natural Science foundation of China (No. 29502007) and the State Education Commission of China.

## References

1. Tom, J., Prog in Physio Sci., 10(1979) 85.
2. Sartz, H.M., Bolton, J.R., Borg, D.C., Biological applications of electron spin resonance. Wiley-Interscience Press, New York, 1972, p. 132.
3. Strayer, L., Griffith, O.H., Proc. Natl. Acad. Sci. USA., 54 (1965) 785.

# Structure-function studies on synthetic tetrapeptide analogs of AVP(4-8)

Ke-Yin Ma and Yu-Cang Du

*Shanghai Institute of Biochemistry, Chinese Academy of Sciences, Shanghai 200031, CHINA*

Tetrapeptide Asn-Leu-Pro-Arg (NLPR) has been reported as the shortest but most potent analog of arginine-vasopressin in learning and memory behavioral responses [1]. Similar to AVP<sub>4-8</sub>, NLPR markedly induced *in vivo* NGF gene expression in normal and memory-impaired rat brains following corresponding improvement in the acquisition and maintenance of behavioral (BD) [2]. Currently, more structure-function studies are being performed using tritium-labeled NLPR binding assay and 2D NMR assay in comparison with several synthetic analogs, such as NWPR, Ac-NLPR, Ac-NLPR(Tos)-NH<sub>2</sub>, ZNC(C-OMe)PR, and ZDC(C)PR.

## Results and Discussion

Characterization of NLPR binding site in brain membranes. At the optimum condition (pH 7.4 in the presence 5 mM NiCl<sub>2</sub>), NLPR binding on the hippocampal synaptosomal membranes was characterized as saturable, reversible and displaceable, and with high affinity. As shown in Fig. 1A, NLPR had two specific binding sites on hippocampal membranes with lower or higher affinities. Their dissociation constants and maximum bindings were found to be ( $K_D$ ) 2.62 and 0.19 nM, and ( $B_{max}$ ) 6,96 and 2.04 fmol/mg protein, respectively. This obviously differs from the binding character of AVP<sub>4-8</sub>, which showed only one binding site on the hippocampus with a  $K_D$  of 3.12 nM and  $M_{max}$ , 31 fmol/mg protein [3].

In the preparations of rat amygdala and anterior cortex, only one kind of [<sup>3</sup>H]NLPR binding site could be found. Scatchard plots presented in Fig. 1B and 1C illustrate the characteristic parameter:  $K_D$ , 0.75 nM and  $B_{max}$ , 10.2 fmol/mg protein for the amygdala and  $K_D$ , 1.6 nM and  $B_{max}$ , 11.2 fmol/mg protein for the anterior cortex, respectively.

Competition of NLPR binding site on amygdala membranes. As shown in Fig. 2, NLPR binding to amygdala membranes was potently competed by ZDC(C)PR, the most effective antagonist of AVP<sub>4-8</sub>, and NWPR, an aromatic analog of NLPR that is significantly displaced by an N-terminal blocked analog, Ac-NLPR but not by AVP. In view of the high structural similarity between AVP<sub>4-8</sub> and ZDC(C)PR, it seems likely that the NLPR receptor in rat amygdala may be the same as that of AVP<sub>4-8</sub> [3]. Unexpectedly, our preliminary data showed that the NLPR binding site could not be displaced by AVP<sub>4-8</sub>. Whether there is another receptor that differs from AVP-R or the AVP<sub>4-8</sub> receptor we have described as in rat brain remains to be explored.

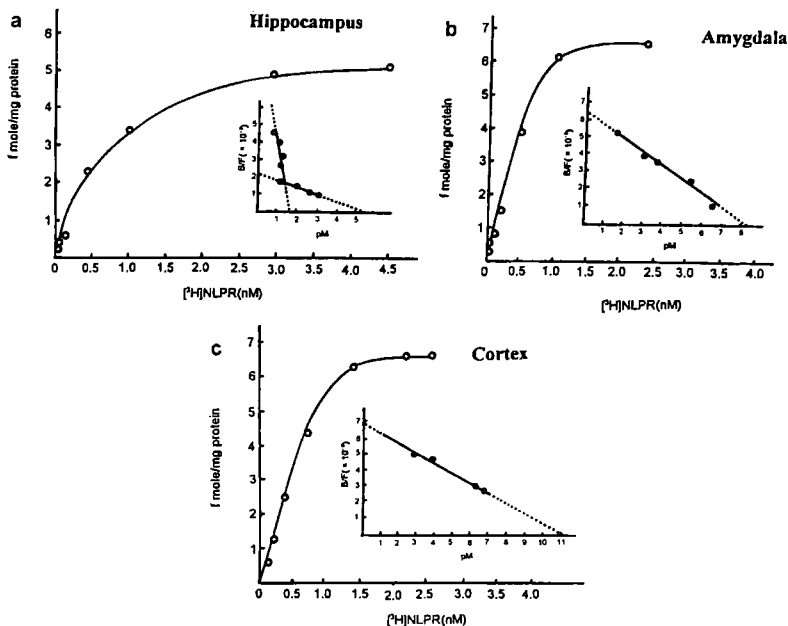


Fig. 1. Saturation plots of NLPR binding to hippocampal(a), amygdala(b) and anterior cortical(c) synaptosomal membranes.

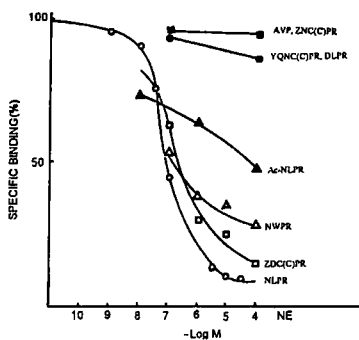


Fig. 2. Displacement of NLPR binding to amygdala membranes by its analogs.

NMR studies. In order to obtain more structural information, the NMR spectrum of four NLPR analogs has been studied. Data (Fig. 3) from NOESY experiments provided evidence for highly compact conformations of Ac-NLPR(3b), Ac-NLPR(Tos)-NH<sub>2</sub>(3c), ZDC(C)PR(3e) and Ome)PR(3d) and a relative loose structure of NLPR. The compactibility among them arose from the increasing hydrophobicity of their side chain [roughly, structure (e) > (c) ~ (b)~ (d) >> (a)]. In view of the behaviorally active conformation of AVP<sub>4-8</sub>, which is a

compact structure with relative plasticity, it is suggested that NLPR may have its own specific receptor. It may prefer a molecule with a looser conformation, and  $AVP_{4-8}(ZNC(C)PR)$  receptor may prefer a more or less rigid structure. Nevertheless, both of them differ greatly from AVP-R.

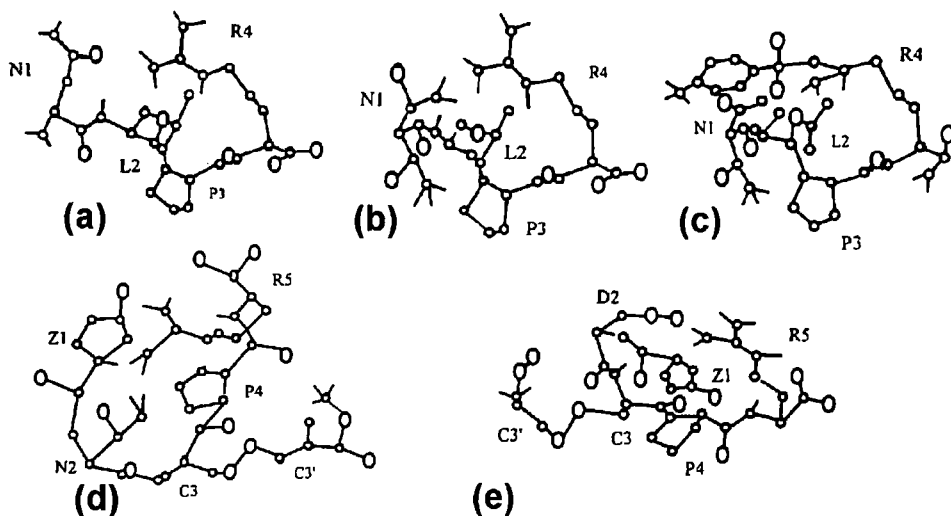


Fig. 3. Structure model of NLPR (a), Ac-NLPR (b), Ac-NLPR(Tos)-NH<sub>2</sub> (c), ZNC(C-OMe)PR (d) and ZDC(C)PR (e) deduced from NOE constraints. Protons with observed NOEs (<5Å).

## References

1. Du, Y.C., Zhou, A.W., Ma, K.Y., Jiang, X.M. and Wang, P.L., in "Peptide: Biology and Chemistry, Proceedings of the 1994 Chinese Peptide Symposium", (Eds. Gui-sheng Lu et al.) ESCOM, Leiden, 1994, p. 35.
2. Zhou, A.W., Guo, J. and Du, Y.C., Biomedical Peptides, Proteins and Nucleic Acids, 1(1995)57-58.
3. Du, Y.C., Wu, J.H., Jiang, X.M. and Gu, Y.J., Peptides, 15(1994) 1273-1279.

# Development of feeding and Y-1 NPY receptor antagonists

Z. Tao,<sup>a</sup> F. Peng,<sup>a</sup> S. Sheriff,<sup>a</sup> P. Eden,<sup>b</sup> J. Taylor,<sup>b</sup>  
W. T. Chance<sup>a</sup> and A. Balasubramaniam<sup>a</sup>

<sup>a</sup>*Surgery, University of Cincinnati, Cincinnati, OH 45267, USA &*

<sup>b</sup>*Biomeasure Inc., Milford, MA 01757, USA*

The potent orexigenic effect of neuropeptide Y (NPY) has inspired numerous investigators to develop appetite controlling drugs based on this peptide. NPY also exhibits a variety of other central and peripheral effects. These actions are mediated by a number of receptor subtypes including Y-1, Y-2, Y-3, Y-4 & Y-5 [1]. This observation suggests that NPY effects can be dissociated, and receptor selective analogs can be developed. Our efforts directed toward this goal have previously resulted in the development of Bis (31/31') {[Cys<sup>31</sup>, Trp<sup>32</sup>, Nva<sup>34</sup>] NPY(31-36)} (**T-190**) (IC<sub>50</sub> for Y-1 = 46±14 nM; Y-2 > 3000 nM) and [D-Trp<sup>32</sup>]NPY, which antagonized the effects of NPY on Y-1 cells [2] and rat hypothalamus [3], respectively. [D-Trp<sup>32</sup>]NPY also antagonized NPY-induced feeding in both rats [3] and mice [4]. However, other reports suggest that [D-Trp<sup>32</sup>]NPY is an inactive or a weak agonist. This disparity may be due to differences in the site of administration, concentration or both. Nevertheless, [D-Trp<sup>32</sup>]NPY has been shown to be a selective ligand to the recently cloned Y-5 receptors speculated to mediate NPY-induced feeding [5]. In a continuation of this work, we have now developed more potent and low molecular weight compounds that attenuated effects of NPY on Y-1 cells and feeding, respectively.

## Results and Discussion

Preliminary NMR investigations with **T-190** and the corresponding monomer suggested that these peptides may have predominantly  $\alpha$ -helical structures. These observations, and the finding that tandem peptides may exhibit increased  $\alpha$ -helicity, led us to synthesize **T-241**, [Trp-Arg-Nva-Arg-Tyr]<sub>2</sub>-NH<sub>2</sub>. **T-241** exhibited increased affinity to SK-N-MC cells (Y-1 receptors) (IC<sub>50</sub> = 9.68±0.95 nM), and hardly bound to Y-2 cells (IC<sub>50</sub> > 1000 nM). This peptide did not exhibit agonist activity in Y-1 cells, but potently (IC<sub>50</sub> = 1.74±1.06 nM) antagonized intracellular mobilization of calcium in HEL cells (Y1 receptor) induced by NPY (5 nM). Moreover, **T-241** had no effect on feeding. We also synthesized Cyclo(32/36)[Trp<sup>32</sup>, Nva<sup>34</sup>] NPY(32-36), **T-249**, containing i → i+4 cyclization believed to stabilize the helical structure. However, **T-249** exhibited poor affinity to both Y-1 and Y-2 receptors. This may be due to the absence of a C-terminal amide group which has been shown to be crucial for activity.

SAR studies with [D-Trp<sup>32</sup>]NPY led to the development of three lower molecular weight (<800) compounds. These compounds exhibited low affinity (IC<sub>50</sub> > 300  $\mu$ M) to Y-1 and Y-2 receptors. One of these compounds, **T-54**, when administered by the intrahypothalamic route, inhibited iht-NPY (1  $\mu$ g)-induced feeding in rats, in a dose-dependent manner. Experiments were also conducted in Schedule-Fed rats which exhibit increased hypothalamic NPY levels.

Again, iht-**T-54** (20 µg) significantly inhibited food intake compared to iht-artificial cerebrospinal fluid treated Schedule-fed rats. Moreover, the effect of **T-54** lasted for more than 24 hours.

Recently, we have also shown that hypothalamic nuclear extracts obtained from iht-NPY treated and fasted rats exhibited increased <sup>32</sup>P-cAMP responsive element (CRE) binding [6]. However, iht **T-54** (20 µg) significantly inhibited NPY and fasting induced elevation of <sup>32</sup>P-CRE binding. It therefore appears that **T-54** blocks NPY-induced feeding by inhibiting the signal transduction pathway of the intact hormone. However, at present, it is not clear whether this antagonism is physiological or competitive in nature because the effects of **T-54** on NPY receptors (Y-5 or those remaining to be cloned) mediating feeding have not been investigated.

In summary, we have developed a potent Y-1 receptor antagonist as well as a lower molecular weight compound which attenuated the food intake by Schedule-Fed and NPY-treated rats. The effects of these peptides on other NPY receptors, Y-3, Y4 and Y-5, remain to be determined.

### Acknowledgement

This work was supported in part by a grant from National Institutes of Health GM47122.

### References

1. Balasubramaniam, A., *Peptides*, 18 (1997) 445.
2. Balasubramaniam, A., Zhai, W., Sheriff, S., Tao, Z., Chance, W.T., Fischer, J.E., Eden, P. and Taylor, J., *J. Med. Chem.*, 39 (1996) 811.
3. Balasubramaniam, A., Sheriff, S., Johnson, M.E., Prabhakaran, M., Huang, S.-G., Fischer, J.E., and Chance, W.T., *J. Med. Chem.*, 37 (1994) 811.
4. Broqua, P., Wettstein, J.G., Rocher, M-N., Gauthier-Martin, B., Riviere, P.J.M., Junien, J-L., and Dahl, S. G., *Brain Res.*, 724 (1996) 25.
5. Gerald, C., Walker, M.W., Criscione, L., et al., *Nature*, 382 (1996) 168.
6. Sheriff, S., Chance, W.T., Fischer, J.E. and Balasubramaniam, A., *Mol. Pharmacol.*, 51 (1997) 597.

# Receptor 3D homology molecular modeling and *in vitro* mutagenesis identify putative melanocortin (hMC1R) agonist ligand-receptor interactions and a proposed mechanism for receptor activation

Carrie Haskell-Luevano, Ying-kui Yang, Chris Dickinson,  
and Ira Gantz

University of Michigan Medical Center, Ann Arbor, MI 48109, USA

The melanocortin receptor, MC1R [1,2], regulates mammalian pigmentation and coat color. We have developed a working 3D homology molecular model of the human MC1R [3] and tested specific proposed agonist ligand-receptor interactions (Fig. 1) by site directed mutagenesis. This study included single, double, triple, and quadruple mutations of the hydrophilic and hydrophobic binding pockets. Mutational analysis included both competitive binding and functional (cAMP) bioassays. The ligands analyzed on each of these mutations included the native hormones  $\alpha$ -MSH (Ac-SYSMEHFRWGKPV-NH<sub>2</sub>),  $\gamma$ -MSH (YVMGHFRWDRPG) and the superpotent synthetic ligands NDP-MSH ([Nle<sup>4</sup>, DPhe<sup>7</sup>]  $\alpha$ -MSH) and MTII (c[Asp<sup>5</sup>, DPhe<sup>7</sup>, Lys<sup>10</sup>]  $\alpha$ -MSH(4-10).

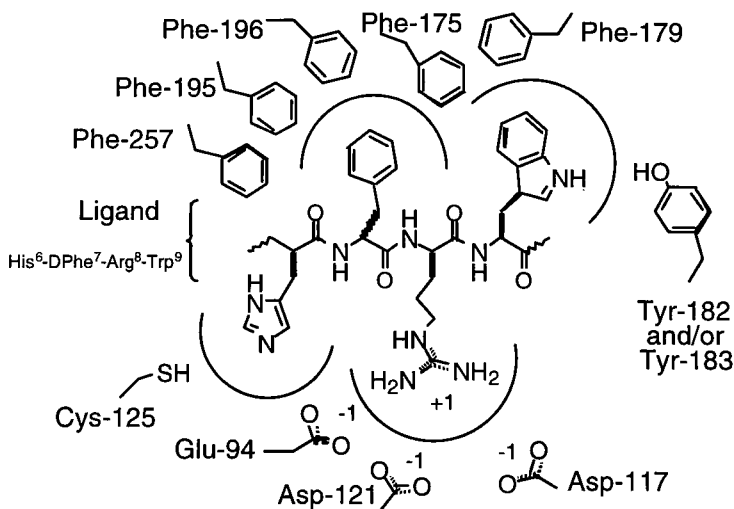


Fig. 1 Putative melanocortin core sequence (His-DPhe-Arg-Trp)-hMC1R interaction.

## Results and Discussion

Table 1 summarizes mutational results of the putative hydrophilic region of the hMC1R binding pocket. Interestingly, all these mutations result in a shift in potency order from MTII>NDP> $\alpha$ -MSH> $\gamma$ -MSH to NDP>MTII> $\alpha$ -MSH> $\gamma$ -MSH. Additionally,  $\gamma$ -MSH lost its ability to competitively displace [ $^{125}$ I] NDP-MSH in all these mutant receptors.

*Table 1. Binding IC<sub>50</sub> (nM) values of the melanocortin ligands on the mutant receptors.*

Mutant	$\alpha$ -MSH	NDP-MSH	MTII	$\gamma$ -MSH
hMC1R	2.58±0.33	0.67±0.09	0.24±0.02	11.5±0.76
E94A	268±13	2.15±0.46	15.5±3.3	>1000
D117A	125±9	5.20±0.35	42±3	>1000
D121A	235±9	7.10±0.80	86±15	>1000
D117A/D121A	176±11	9.20±2.50	97±32	>1000
E94A/	293±15	10.6±1.2	123±10	>1000
D117A/D121A				
D121K	>1000	31.2±1.8	>1000	>1000
D121N	>1000	27.5±3.8	>1000	>1000

*Table 2. Binding (B) and cAMP (C) fold difference from wild type values.*

Mutant	$\alpha$ -MSH		NDP-MSH		MTII		$\gamma$ -MSH	
	B	C	B	C	B	C	B	C
D117A	48	291	7.8	13	176	753	none	none
D121K	none	none	47	none	none	none	none	none
D121N	none	none	41	513	none	none	none	none
D117A/D121A	68	621	14	825	404	7215	none	none
E94A/	113	none	16	3258	512	none	none	none
D117A/D121A								

Comparison of the intracellular cAMP accumulation for the mutants correlated well with the binding IC<sub>50</sub> values with the exception of D117A, D121K, D121N, D117A/D121A, and E94A/D117A/D121A mutant receptors (Table 2). The difference is determined by comparing the mutant ligand values with the corresponding hMC1R wild type values. Mutations of the aromatic residues resulted in up to ca.10-fold differences (data not shown). These data strongly implicate the importance of these residues for signal transduction.

## References

1. Chhajlani, V., Wikberg, J. E. S., FEBS Lett., 309 (1992) 417.
2. Mountjoy, K. G., Robbins, L. S., Mortrud, M. T., Cone, R. D., Science, 257 (1992) 1248.
3. Haskell-Luevano, C., Sawyer, T.K., Trumpp-Kallmeyer, S., Bikker, J.A., Humblet, C., Gantz, I., Hruby, V.J., Drug Design & Disc., 14 (1996) 197.
4. Robbins, L.S., Nadeau, J.H., Johnson, K.R., Kelly, M.A., Roselli-Rehffuss, L., Baack, E., Mountjoy, K.G., Cone, R.D., Cell, 72 (1993) 827.

# Novel non-phosphorylated peptides binding to the Grb2-SH2 domain

Feng-Di T. Lung,<sup>a</sup> Lakshmi Sastry,<sup>b</sup> Shaomeng Wang,<sup>c</sup> Bih-Show Lou,<sup>d</sup> Joseph J. Barchi,<sup>a</sup> C. Richter King<sup>b</sup> and Peter P. Roller<sup>a</sup>

<sup>a</sup>Laboratory of Medicinal Chemistry, Division of Basic Sciences, National Cancer Institute, Bethesda, MD 20892, U.S.A.; <sup>b</sup>Lombardi Cancer Center and <sup>c</sup>Department of Neurology, Georgetown University Medical Center Washington, DC 20007, U.S.A. <sup>d</sup>Chang-Gung College of Medicine and Technology, Taiwan, R.O.C.

Grb2 is an intracellular adaptor protein that functions in transmitting growth factor (GF) signaling through its SH2 domain and two SH3 domains. The involvement of mutated erbB family of GF receptors is well documented in a number of cancers, and phosphorylated regions of such receptors interact with the Grb2-SH2 domain [1,2]. With the aim of developing antagonists to such interactions, a non-phosphorylated cyclic peptide with high affinity for the Grb2-SH2 domain was identified (**1**, Table 1), using phage library methods ( $IC_{50} = 10\text{-}25\ \mu\text{M}$ ) [3]. This lead peptide has 9 amino acid residues flanked by 2 terminal disulfide linked cysteines. **1** has been shown to competitively inhibit the binding of the open-chain pTyr peptide, **2**. These initial studies also showed that reduction of the disulfide link in **1** or replacement of the terminal cysteines with serines, producing open chain analogs **3** and **4**, abrogated Grb2 binding affinities. We report here our structure activity studies on this novel cyclic non-phosphorylated Grb2-SH2 domain binding peptide, **1**, with the aim of identifying the a.a.'s required for high binding affinity, and the development of redox stable thioether cyclized analogs that should be useful in *in cell* studies

## Results and Discussion

Alanine was substituted at positions 2 to 10 in the phage library based lead peptide, **1**, using Fmoc chemistry based SPPS on PAL amide resin, and using  $K_3Fe(CN)_6$  catalyzed disulfide bridge formation. Binding affinity studies, using surface plasmon resonance, demonstrated that all a.a. substituents, except Leu<sup>3</sup> and Gly<sup>8</sup>, are functionally important for high affinity binding to Grb2-SH2. The evidence for extensive interactions of a.a. residues with the SH2 domain binding site supports the initial results showing selectivity to Grb2-SH2, compared to Src-SH2 (unpublished results).

Several redox stable cyclic peptide analogs were prepared. Our design of a thioether analog, **5**, essentially similar in ring size to **1** (35 bonds in **1**, and 33 bonds in **5**), retained full binding affinity ( $IC_{50}=10\text{-}15\ \mu\text{M}$ ). Peptide **5** was prepared starting with the PAL resin-bound protected peptide, ELYENVGMYC, which was then N-terminally chloroacetylated [4]. After resin cleavage and deprotection, the peptide was cyclized to the thioether at pH 8 through intramolecular nucleophilic displacement of the chloro group by the cysteine SH. An N-terminally Gly extended analog **6**, was inactive in binding assays. Also, the amide backbone

cyclized peptide **7**, containing the 9 a.a.'s of **1**, was found to be inactive (27 membered ring).

Table 1. Binding affinity of various synthetic peptides to Grb2-SH2.

Peptide	Chemical structure	IC <sub>50</sub> (μM)	Peptide	Chemical structure	IC <sub>50</sub> (μM)
<b>1</b>	$\begin{array}{c} \text{C}^1\text{-E-L-Y}^4\text{-E-N}^6\text{-V-G-M-Y-C}^{11} \\ \text{CH}_2\text{-----S-----S-----CH}_2 \end{array}$	10-25	<b>5</b>	$\begin{array}{c} \text{O} \\ \parallel \\ \text{C}^1\text{-NH-E}^1\text{-L-Y-E-N-V-G-M-Y-C}^{10} \\ \text{CH}_2\text{-----S-----CH}_2 \end{array}$	10-15
<b>2</b>	D <sup>1</sup> -D-P-S-pY-V-N-V-Q <sup>9</sup>	2	<b>6</b>	$\begin{array}{c} \text{O} \\ \parallel \\ \text{C}^1\text{-NH-G}^1\text{-E-L-Y-E-N-V-G-M-Y-C}^{11} \\ \text{CH}_2\text{-----S-----CH}_2 \end{array}$	inactive <sup>c</sup>
<b>3</b>	C <sup>1</sup> -E-L-Y-E-N-V-G-M-Y-C <sup>11</sup>	inactive <sup>a</sup>	<b>7</b>	$\begin{array}{c} \text{O} \\ \parallel \\ \text{HN-E}^1\text{-L-Y-E-N-V-G-M-Y}^2\text{-C} \end{array}$	inactive <sup>c</sup>

<sup>a</sup>carried out in presence of DTT, IC<sub>50</sub> > 200 μM. <sup>b</sup>at 200 μM peptide concentration < 20% activity found.

<sup>c</sup>no activity observed at 200 μM.

Our results indicate that the cyclic structure and specific ring size are determining factors for retaining binding affinity. Initial NMR studies were confirmatory, showing that peptide **5** has a defined conformation in DMSO, with a β-type turn in the Y<sup>3</sup>-E-N-V<sup>6</sup> region, as shown by strong NH - - HN NOE between Asn<sup>5</sup> and Val<sup>6</sup>; and a low temperature-coefficient for the Val-NH proton exchange, indicating hydrogen bonding. Modeling studies, using Grb2-SH2 3D coordinates [2], predict that a cyclic peptide with such a turn can be accommodated in binding to the Grb2-SH2 domain.

The redox stable **5**, but not **1**, was effective in blocking Grb2 binding to activated phosphoprotein p185<sup>erbB2</sup> in cell homogenates, thus inhibiting downstream cellular signaling. **1** and **5** are the first peptides which clearly demonstrate significant SH2 domain binding properties in the absence of phosphate or phosphate-mimicking functionality.

## References

- 1 Zhou, S. and Cantley, L.C., Trends Biochem Sci., 20 (1995) 470.
- 2 Rahuel, J., Gay, B., Erdmann, D., Strauss, A., Garcia-Echeverria, C., Furet, P., Caravatti, G., Fretz H., Schoepfer, J. and Grutter, M.G., Nature Struct. Biology, 3 (1996) 586.
- 3 Oligino, L., Sastry, L., Lung, F.-D., Bigelow, J., Cao, T., Curran, M., Burke, T.R., Wang, S.-M Kragg, D., Roller, P.P. and King, C.R., J. Biol. Chem., in press.
- 4 Lindner, W. and Robey, F.A., Int. J. Peptide Protein Res., 30 (1987) 794.

# An endothelin-A / lutropin chimeric receptor exhibits ligand-mediated internalization in the absence of signaling

Neil Bhowmick, Prema Narayan and David Puett

*Department of Biochemistry and Molecular Biology, University of Georgia, Life Science Building, Athens, GA 30602-7229, USA*

Endothelin-1 (ET-1) is a 21 amino acid residue peptide that elicits potent contractile actions in vascular smooth muscle cells, and also has proliferative and cytokine activity [1,2]. These actions are initiated by its binding to the extracellular domain and within the pocket of the seven transmembrane helices of the endothelin-A receptor (ET<sub>A</sub>R), a member of the G protein-coupled receptor family (GPCR). Ligand binding results in the primary activation of G<sub>q</sub>, to give rise to an increase in intracellular concentrations of inositol 1,4,5-trisphosphate (IP<sub>3</sub>), 1,2-diacylglycerol, and calcium [3,4]. Another GPCR member, the lutropin receptor (LHR), was studied. It is involved in gonadal steroidogenesis and signals primarily by activating G<sub>s</sub>, thus stimulating the cAMP pathway, upon binding the glycoprotein hormone, human choriogonadotropin (hCG) [5]. The events regulating the subsequent internalization and possible recycling of the receptor-ligand complex are, however, poorly understood. In addressing the relationship of GPCR signal transduction and receptor internalization, we engineered a chimeric construct replacing the cytoplasmic tail of ET<sub>A</sub>R with that of LHR (E/L-R) that retained ET-1 binding similar to that of wild type ET<sub>A</sub>R, but exhibited no signaling by either IP<sub>3</sub> or cAMP pathways. Interestingly, ligand-mediated E/L-R internalization still occurred, although at a slower rate than with ET<sub>A</sub>R.

## Results and Discussion

We set out to elucidate the molecular determinants for ligand-mediated endocytosis of ET<sub>A</sub>R. Receptor cDNAs of wild type and chimeric E/L-R and L/E-R (LHR with a ET<sub>A</sub>R cytoplasmic tail) were expressed in HEK 293 cells for saturation binding studies with the respective radioiodinated ligands, [<sup>125</sup>I]hCG and [<sup>125</sup>I]ET-1, and exhibited similar binding affinities (Table 1). The lack of cell surface binding by L/E-R precluded further studies with this chimera. Equal numbers of cell surface ET<sub>A</sub>R and chimeric receptors (66,000 receptors/cell), expressed in clonal HEK 293 cells, yielded very different signaling characteristics. At a maximal concentration of 0.1 mM ET-1, HEK 293 cells expressing ET<sub>A</sub>R activated an 8-fold stimulation of IP<sub>3</sub> and a 2-fold increase of cAMP, whereas the E/L-R yielded no significant stimulation of IP<sub>3</sub> or cAMP above basal levels. The wild type LHR activated over a 100-fold stimulation of cAMP and negligible levels of IP<sub>3</sub> with a maximal dose of 1.3 mM hCG.

Next, the consequence of diminished signaling by the chimera on receptor endocytosis was studied using an adapted concanavalin A-mediated plasma membrane separation method [7]. Cells expressing the receptor constructs were pre-incubated with their respective radiolabeled ligand (0.1 nM [<sup>125</sup>I]ET-1 and 1.3 nM [<sup>125</sup>I]hCG) at 0°C. Subsequently, the cells

were washed and incubated at 37°C for 0-2 h in the absence of ligand such that the same amount of initial ligand was bound at all time points. Concanavalin A binding to intact cells enabled enhanced separation of plasma membrane (fractions 10-12) from intracellular membranes (fractions 2-4) by sucrose gradient centrifugation. Due to the tight receptor binding of peptide ligands such as ET-1, this method was employed rather than the common acid-wash procedure [8] in determining the rate of endocytosis. Rapid [<sup>125</sup>I]ET-1 internalization ( $t_{1/2} = 5$  min,  $k_e = 0.1 \text{ min}^{-1}$ ) was observed upon incubation with the ET<sub>A</sub>R clonal HEK 293 line at 37°C, while LHR and the chimera both exhibited similar  $k_e$ s ( $0.03 \text{ min}^{-1}$ ) and a  $t_{1/2} = 15$  min (Table 1).

*Table 1. The binding, signaling, and endocytic properties of receptor constructs.  $K_D$  was determined by saturation binding of [<sup>125</sup>I]ET-1 to ET<sub>A</sub>R and E/L-R, and [<sup>125</sup>I]hCG to LHR. IP<sub>3</sub> production in 5 s at 37°C and cAMP accumulation for 30 min at 37°C was measured in the presence of their respective ligands. ND denotes non-detectable or negligible signaling above basal level.*

Recept	Binding (KD)	Signaling		Endocytic Rate (Ke) [6]
		IP <sub>3</sub> (EC <sub>50</sub> )	cAMP(EC <sub>50</sub> )	
EA <sub>A</sub> R	0.1nM	1.3nM	9.4 nM	0.10 min <sup>-1</sup>
E/L-R	0.1nM	ND	ND	0.03 min <sup>-1</sup>
LHR	0.3nM	ND	0.1 nM	0.03 min <sup>-1</sup>

These results indicate that ET-1 is rapidly internalized by ET<sub>A</sub>R in the presence or absence of second messenger signaling. The ET<sub>A</sub>R cytoplasmic tail is important in IP<sub>3</sub> and cAMP induction but is not required for internalization. Since the ability of the LHR-cytoplasmic tail only retards ET<sub>A</sub>R endocytosis, it appears to have more of a modulatory role in ligand-mediated receptor endocytosis.

## References

1. Inoue, A., Yanagisawa, M., Kimura, S., Miyachi, Y., Goto, K., and Masaki, T., Proc. Natl. Sci. U.S.A., 86 (1989) 2863.
2. Miller, R.C., Pelton, J.T., and Huggins, J.P., Trends Pharmacol. Sci., 14 (1993) 54.
3. Inoue, A., Oike, M., Nakao, K., Kitamura, K., and Kuriyama, H., J. Physiol., 423 (1990) 171.
4. Vigne, P., Marsault, R., Breittmayer, J.P., and Frelin, C., Biochem. J., 266 (1990) 415.
5. Segaloff, D.L. and Ascoli, M., Endocrine Rev. 14 (1993) 324.
6. Wiley, H.S. and Cunningham, D.D., J. Biol. Chem., 257 (1982) 4222.
7. Kassis, S. and Sullivan, M., J. Cyclic Nucl. Prot. Phos. Res., 11 (1986) 35.
8. Wu-Wong, J.R., Chiou, W.J., Magnuson, S.R., and Opgenorth, T.J., J. Pharmacol. Exper. Ther., 274 (1995) 499.

# Examination of the role of TMH VII in subtype-selective ligand binding using semi-synthetic muscarinic receptors

Carol B. Fowler,<sup>a</sup> Harry LeVine<sup>b</sup> and Henry I. Mosberg<sup>a</sup>

<sup>a</sup>Interdepartmental Program in Medicinal Chemistry, University of Michigan, Ann Arbor, MI 48109, U.S.A. and <sup>b</sup>Neurological and Neurodegenerative Diseases, Parke-Davis Pharmaceutical Research, Warner-Lambert Company, Ann Arbor, MI 48105, USA

The human muscarinic (hm) receptors, which are members of the G protein-coupled receptor superfamily, consist of seven transmembrane helices (TMH I-VII) interconnected by intracellular and extracellular loops (Fig. 1a). Although ligand binding in the superfamily requires the presence of all seven transmembrane helices, it does not require their covalent interconnection. Proteolysis of the  $\beta$ -adrenergic receptor showed that the receptor fragments were able to catalyze agonist-stimulated binding of GTP $\gamma$ S [1]. In another study, biochemically truncated bacteriorhodopsin (TMH III-VII) was reconstituted in liposomes with two synthetic peptides to regenerate function [2]. The purpose of this research was to generate a semi-synthetic muscarinic receptor capable of binding ligand and to explore the role of TMH VII in subtype selective ligand binding [3] by combining a cloned truncated receptor of subtype 1 (hm1 trunc) with a synthetic peptide corresponding to either the TMH VII of hm1 or hm2 (Fig. 1b).

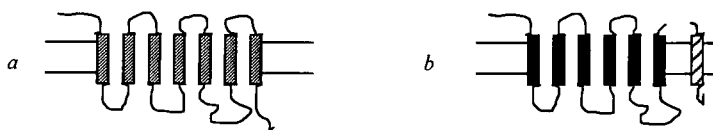


Fig. 1 Structure of the wildtype muscarinic receptor (a) and reconstituted receptor (b), which consists of a cloned and expressed receptor fragment (■) and synthetic transmembrane helix VII (▨).

## Results and Discussion

hm1 VII	PETLWELGYWLCYVNSTINPMCIALCNKAFRDTRF
hm2 VII	PNTVWTIGYWLCYINSTINPACYALCNATFFKKTFFK

Peptides corresponding to TMH VII of hm1 and hm2 were synthesized using Fmoc chemistry. After incorporation into liposomes from mixed soybean phospholipids [4], the membrane localization and conformation of the hm1 VII peptide were evaluated by fluorescence quenching and circular dichroism (CD). Quenching of the tryptophan fluorescence by 30 mole% (6-7 dibromo) phosphatidylcholine (PC) (Fig. 2a) suggested that

the peptide was incorporated into the bilayer. Negative CD bands at 220 and 210 nm indicated that the lipid-bound peptide had considerable alpha-helical content (Fig. 2b).

The gene fragments for the truncated m1 and wild type m1 receptors (Fig. 1) were generated by PCR and cloned into the pCDNA 3.1 His expression vector. Following transfection of the plasmids into human 293-T cells, stable transformants were selected with 3 mg/ml neomycin. The resulting clones were then grown in cell culture and the membranes isolated. Neither hm1 trunc alone nor hm1 trunc fused with blank liposomes showed ligand binding displaceable with atropine. Fusion of the truncated muscarinic receptor in membranes by two cycles of freeze-thawing with soybean lipid liposomes containing a 1000-fold molar excess of TMH VII peptide resulted in a receptor capable of displaceable ligand binding. Saturation ligand binding studies with  $^3\text{H-N}$ -methyl scopolamine ( $^3\text{H-NMS}$ ) indicated that hm1 trunc. reconstituted with hm1 VII had an apparent  $K_D$  approximately 10-fold greater than the m1 wild type (11 and 1 nM, respectively). Competition ligand binding assays with the m1-selective antagonist, pirenzepine, showed that the hm1 trunc + hm2 VII and the hm1 trunc + hm1 VII receptors had reduced affinity for pirenzepine ( $K_i = 5.5$  vs.  $0.83$   $\mu\text{M}$ , respectively), compared to m1 wild type (23 nM).

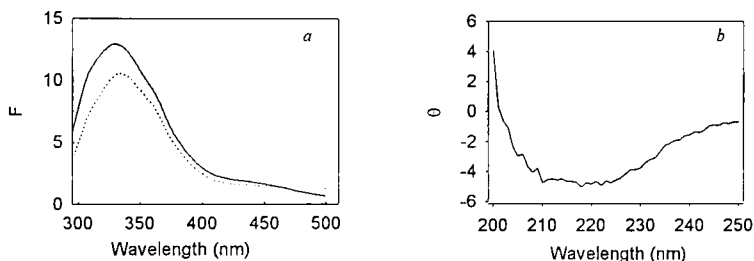


Fig. 2. Fluorescence quenching of hm1 VII in 30 % Br-PC vesicles (a) and CD spectra of hm1 VII in PC vesicles (b)

Preliminary results suggest that a truncated muscarinic receptor (TMH I-VI) can be reconstituted with a synthetic peptide corresponding to the TMH VII of either hm1 or hm2 to regenerate saturable specific muscarinic ligand binding. While the reconstituted receptors have lower affinity for both  $^3\text{H-NMS}$  and pirenzepine than wild type, the hm1 trunc + hm1 VII receptor appears to have a 6-fold-selectivity for pirenzepine over the hm1 trunc + hm2 VII reconstituted receptor.

## References

1. Rubenstein, R.C., Wong, S.K. and Ross, E.M., *J. Biol. Chem.*, 262 (1987) 16655.
2. Kahn, T. and Engelman, D., *Biochemistry*, 31 (1992) 6144.
3. Wess, J., Bonner, T.I. and Brann, M., *Mol. Pharmacol.*, 38 (1990) 872.
4. Tamm, L.K. and Tatulian, S.A., *Biochemistry*, 32 (1993) 7720.

# Modeling somatostatin receptor-ligand complexes

Xiaohui Jiang and Murray Goodman

*Department of Chemistry and Biochemistry, University of California at San Diego  
La Jolla, CA 92093, USA*

Somatostatin is a cyclic tetradecapeptide which was originally characterized as a physiological inhibitor of growth hormone [1]. In addition, somatostatin has effects on many other biological processes. The actions of somatostatin are mediated by specific receptors. To date, five somatostatin receptor subtypes (SSTR1-5) have been cloned [2]. Since somatostatin receptors are membrane-bound proteins, it is difficult to determine their structures by either x-ray or NMR. Meanwhile, empirical approaches and mutagenesis studies have been carried out to probe interactions between the somatostatin receptor and its ligands[3,4]. In the current study, we modeled somatostatin receptors (SSTR2 and SSTR5) by using rhodopsin as the template and docked somatostatin analogs into the binding site. Based on the interactions in the somatostatin receptor-ligand complexes, we designed and synthesized novel somatostatin analogs.

Somatostatin H-Ala-Gly-c[Cys-Lys-Asn-Phe-Phe-Trp-Lys-Thr-Phe-Ser-Cys]-OH  
L-363,301 c[Pro<sup>6</sup>-Phe<sup>7</sup>-D-Trp<sup>8</sup>-Lys<sup>9</sup>-Thr<sup>10</sup>-Phe<sup>11</sup>]

## Results and Discussion

As shown in the structure of SSTR2/L-363,301 complex (Fig. 1), the binding pocket of the receptor is located in the center pole surrounded by TM 3-7. L-363,301 was docked into the binding pocket in which D-Trp<sup>8</sup>-Lys<sup>9</sup> sits at the bottom. The bridge region of L-363,301 (Phe<sup>11</sup>-Pro<sup>6</sup>) interacts with extracellular loop 3 (ECL3) which is at the top of the binding pocket.

By examining our model of the somatostatin receptor-ligand complexes, we can identify the specific interactions between the residues in the receptor and the critical components in the ligands, such as the sidechains of Phe<sup>7</sup>, D-Trp<sup>8</sup>, Lys<sup>9</sup> and Phe<sup>11</sup>. In addition, we found that the electrostatic properties of ECL3 are very different in SSTR2 and SSTR5. In SSTR2, this loop is relatively neutral while in SSTR5 the loops is highly acidic. We envision that subtype selective somatostatin analogs can be obtained by modifying the corresponding residues in the ligands that interact with the binding pocket and ECL3. Based our model, we designed and synthesized analogs of L-363,301 (I) in which Pro<sup>6</sup> was replaced by peptoid residues such as N-benzyl glycine (II), N-(R)- $\alpha$ -methylbenzyl glycine (III) and N-(S)- $\alpha$ -methylbenzyl glycine (IV).

The parent compound (I) can bind to SSTR2 and SSTR5 with equal affinity at the nanomolar level. Compound (II) has 3-fold selectivity towards SSTR2. When chiral sidechains are introduced into the peptoid structure, compound (III) shows increased

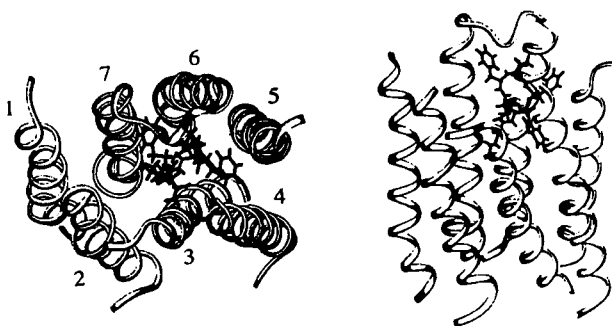


Fig. 1. The structure of SSTR2/L-363,301 complex.

binding affinity to SSTR2 one order of magnitude greater than compound (I) while compound (IV) shows reduced binding potencies to both SSTR2 and SSTR5.

## Conclusion

We modeled somatostatin receptor SSTR2 and SSTR5 by using rhodopsin as a template and docked somatostatin analog L-363,301 into the binding pocket. Based on our model of the receptor-ligand complex, we designed and synthesized peptoid-containing analogs that show SSTR2 selectivity compared to the parent compound. The approach which we presented is now being explored in our laboratories to develop more selective somatostatin analogs.

## Acknowledgement

We would like to thank Haitao Li and Thuy-Anh Tran at University of California, San Diego for their synthetic work and Drs Andy McCammon, Jim Briggs and Ralph Mattern at University of California, San Diego for many helpful discussions. We also wish to thank Drs. Barry Morgan and John Taylor at Biomeasure for the binding assays. This work was supported by NIH-DK15410.

## References

1. Brazeau, P., Vale, W., Burgus, R., *et al.*, Science, 129 (1972) 77-79.
2. Reisine, T. and Bell, G.I., Endocr. Rev., 16 (1995), 427-442.
3. Huang, Z., He, Y., Raynor, K., Tallent, M., Reisine, T. and Goodman, M., J. Am. Chem. Soc., 114 (1992) 9390-9401.
4. Kaupmann, K., Weber, H.P., Mattes, H. and Lubbert, H., EMBO Journal, 14 (1995) 727-35.



## **Session VII**

# **Neuro-, Endocrino-, and Bioactive Peptides**



# Solution synthesis and structure revision of dendrotoxin I

Hideki Nishio,<sup>a</sup> Tatsuya Inui,<sup>a</sup> Yuji Nishiuchi,<sup>a</sup> Edward G. Rowan,<sup>b</sup>  
Alan L. Harvey,<sup>b</sup> Terutoshi Kimura<sup>a</sup> and Shumpei Sakakibara<sup>a</sup>

<sup>a</sup>Peptide Institute, Inc., Protein Research Foundation, Minoh-shi, Osaka 562, Japan <sup>b</sup>Department of Physiology and Pharmacology, Strathclyde Institute for Drug Research, University of Strathclyde, Glasgow G1, UK

Dendrotoxin I (DTX-I) is a specific blocker of neuronal voltage-sensitive potassium channels consisting of 60 amino acid residues that was isolated from the venom of the black mamba *Dendroaspis polylepis polylepis* [1, 2]. Calcicludine (CaC), a peptide highly homologous to DTX-I, isolated from the venom of *Dendroaspis augusticeps* (the green mamba), has been shown to be a potent blocker of high-threshold calcium channels with a high affinity for L-type channels in cerebellar granule neurons [3]. Our recent study of CaC synthesis by the solution procedure demonstrated that the synthetic peptide is identical to natural CaC [4]. To elucidate the structure-activity relationships of these homologous peptides with different biological activities, we synthesized DTX-I according to the reported structure (PyrPLRKLCILHRNPGRCYQKIPAFYYNQKKKQCEGFTWSGCGG-NSNRFKTIIEECRRTCIRK) by the same procedure used for CaC synthesis and compared it with the natural product by HPLC as well as by measuring receptor binding.

## Results and Discussion

The protected peptide was assembled in solution from six segments as reported for the synthesis of CaC using our newly developed *N*<sup>im</sup>-cyclohexyloxycarbonyltryptophan compound Trp(Hoc) which is suitable for Boc strategy [4, 5]. The protected peptide was treated with HF/anisole (9/1) at -5°C for 1 h without addition of thiol to remove all but Ac<sub>m</sub> protecting groups. After purification by RP-HPLC, the resulting (6Ac<sub>m</sub>)-peptide was treated with Hg(Oac)<sub>2</sub>/2-mercaptoethanol to remove the remaining Ac<sub>m</sub> groups. The reduced peptide thus obtained was subjected to the oxidative folding reaction in the presence of reduced and oxidized glutathione (GSH/GSSG) and then purified by HPLC. Amino acid analysis and the molecular weight of the final product agreed well with theoretical values. The disulfide structure of the final product was confirmed to be the same as that of the reported structure [6]. When compared by HPLC with natural DTX-I, the synthetic product had different profiles on HPLC and CZE (Fig. 1). After DTT reduction followed by pyridylethylation and enzymatic digestion, the products were mapped on HPLC, and one fragment of our synthetic peptide was found to have a different retention time from the corresponding natural fragment. Determination of their structures showed that the Asn residue at position 12 in the synthetic product should be replaced by Asp, although the reported structure of DTX-I had been confirmed by NMR [7]. We thus resynthesized DTX-I with Asp instead of Asn at position 12 and found it to be identical with the natural product in all respects.

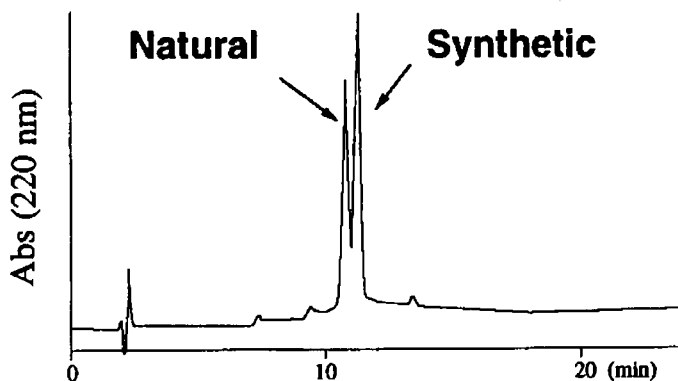


Fig. 1. Coinjection of the synthetic peptide and natural DTX- I on RP-HPLC.

Next, we measured the binding activity of both [Asn<sup>12</sup>]- and [Asp<sup>12</sup>]-DTX-I as well as natural DTX-I on the dendrotoxin receptor of rat brain synaptosomal membrane. The results demonstrated that [Asp<sup>12</sup>]-DTX-I has almost the same binding activity as that of natural DTX-I, while [Asn<sup>12</sup>]-DTX-I has slightly higher binding activity. In order to confirm the possibility of conversion of [Asn<sup>12</sup>]-DTX-I into [Asp<sup>12</sup>]-DTX-I, we examined the stability of both synthetic peptides on HPLC under the various conditions used for isolation and purification of natural DTX-I [1, 8]. The data demonstrated that both peptides were stable and no specific conversion had occurred. From these results, we concluded that the Asn residue at position 12 in the DTX-I molecule should be revised to Asp, although this amino acid substitution does not affect binding activity. We have also synthesized two chimeric peptides of DTX-I and CaC, DTX-I(1-29)/CaC(30-60) and CaC(1-29)/DTX-I(30-60), to help elucidate which part of the molecule is responsible for distinguishing between calcium and potassium channel blockers. The binding activity measurements of both chimeric peptides on the dendrotoxin receptor showed that the N-terminal half region of the DTX-I molecule is important for binding to its receptor.

## References

1. Strydom, D. J., *Nature, New Biol.*, 243 (1973) 88.
2. Rehm, H. and Lazdunsky, M., *Proc. Natl. Acad. Sci. USA*, 85 (1988) 4919.
3. Schweitz, H., Heurteaux, C., Bois, P., Moinier, D., Romey, G. and Lazdunski, M., *Proc. Natl. Acad. Sci. USA*, 91 (1994) 878.
4. Nishio, H., Nishiuchi, Y., Inui, T., Kimura, T. and Sakakibara, S., In N. Nishi (Ed.), *Peptide Chemistry 1995*, Protein Research Foundation, Osaka, 1996, p. 113.
5. Nishiuchi, Y., Nishio, H., Inui, T., Kimura, T. and Sakakibara, S., *Tetrahedron Letters*, 42 (1996) 7529.
6. Hollecker, M. and Creighton, T.E., *J. Mol. Biol.*, 168 (1983) 409.
7. Foray, M.-F., Lancelin, J.-M. and Marion, D., *Eur. J. Biochem.*, 211 (1993) 813.
8. Schweitz, H., Bidard, J.-N. and Lazdunski, M., *Toxicon*, 28 (1990) 847.

# Amphipathic $\alpha$ - and $3_{10}$ -helical peptides with *in vitro* and *in vivo* bioactivity

Mark L. McLaughlin,<sup>a</sup> T. Scott Yokum,<sup>a</sup> Ted J. Gauthier,<sup>a</sup>  
Robert P. Hammer<sup>a</sup> and Philip H. Elzer<sup>b</sup>

<sup>a</sup>Departments of Chemistry and <sup>b</sup>Veterinary Science, Louisiana State University,  
Baton Rouge, LA 70803, USA

Melittin, cecropins, and magainins are representatives of scores of natural peptide toxins and antimicrobial peptides that contain putative amphipathic  $\alpha$ -helical domains [1]. *De novo* peptides designed to form perfectly amphipathic  $\alpha$ -helices have the same or higher bioactivities as these natural peptides [2]. We discovered *de novo* peptide helicity correlates with cytotoxicity and that shorter peptides retained antimicrobial activity but have reduced cytotoxicity [3]. To retain helicity as peptide length was further reduced, we have replaced natural amino acids with  $\alpha,\alpha$ -disubstituted amino acids ( $\alpha\alpha$ AAs) to give peptides that contain 50-80%  $\alpha\alpha$ AAs [4]. We have tested these peptides *in vitro* against representative Gram negative and Gram positive bacteria and *in vitro* and *in vivo* against an intracellular pathogen, *Brucella abortus*. Interestingly, *B. abortus* is one a few Gram negative bacteria that are relatively resistant to the direct antimicrobial effects of this class of peptides [5]. Pi-10 and Ipi-10 show no MIC activity at 100  $\mu$ M peptide concentrations against *B. abortus*, yet show *in vivo* Brucella reductions in chronically infected Balb/C mice at lower whole animal peptide concentrations. *B. abortus* infects and replicates in host macrophages causing chronic infection in livestock and humans [6]. In animals, *Brucella* sp. causes abortion and infertility. In humans, *Brucella* sp. causes brucellosis or undulant fever with flu-like symptoms for up six months and is sometimes fatal. A 30-45 day antibiotic regimen reduces complications, but relapses can occur, symptoms of the disease persist, and there is no safe human vaccine. Brucella infection is slow to respond to treatment because intracellular Brucella are protected from effective antibiotic concentrations, the complement cascade, neutrophils, and brucella specific antibodies. There is clearly a need for more effective treatments to combat brucellosis and other diseases caused by intracellular pathogens. For instance, tuberculosis has a similar etiology and is the single most lethal infectious disease in man [7].

## Results and Discussion

These  $\alpha\alpha$ AA rich peptides have higher *in vitro* antimicrobial activity than *de novo* peptides composed of all natural amino acids of the same length, similar sequence, and hydrophobicity [4]. In order to prepare amphipathic peptides with 80%  $\alpha\alpha$ AA content, we have synthesized novel  $\alpha\alpha$ AAs that are lysine analogs [8]. 4-Aminopiperidine-4-carboxylic acid, Api, is one example used to prepare two sequence permutation isomers, Pi-10, H-Aib-Aib-Api-Lys-Aib-Aib-Api-Lys-Aib-Aib-NH<sub>2</sub>, and Ipi-10, H-Api-Aib-Aib-Lys-Aib-

Aib-Lys-Aib-Aib-Api-NH<sub>2</sub>, which form amphipathic  $\alpha$ - and  $3_{10}$ -helices in membrane mimetic media [9] but have significantly different bioactivities *in vitro* and *in vivo*. Pi-10 has MIC values of 7.7 and 123  $\mu$ M against *E. coli* and *S. aureus*, respectively. Of the score of peptides tested, Pi-10 has the best *in vivo* activity against *B. abortus* in Balb/C mice and the best *in vitro* selectivity for killing brucella infected murine macrophages (T.S. Yokum, R.P. Hammer, M.L. McLaughlin and P.H. Elzer, unpublished). Pi-10 reduces splenic brucellae loads by 90% in a single i.v. dose of 500  $\mu$ g/mouse and selectively kills *B. abortus* infected murine macrophages at higher rates than normal, non-infected murine macrophages.

In spite of reports in the literature suggesting that *de novo* amphipathic  $3_{10}$ -helical peptides are devoid of antimicrobial activity against representative Gram negative and Gram positive bacteria [10], we find that Ipi-10 has high antimicrobial activity against *E. coli* but no activity against *S. aureus* with MIC values of 4.0 and >256  $\mu$ M, respectively. Ipi-10 is also more toxic in mice than its  $\alpha$ -helical isomer, Pi-10, but retains modest antibrucella activity in mice reducing splenic brucella loads 55% in a single 500  $\mu$ g i.v. dose/mouse. Unfortunately, the mice were stressed at this dose.

Pi-10 is the most active example of several  $\alpha\alpha$ AA rich peptides that selectively lyse infected macrophages thus releasing the intracellular brucella that are killed *in vivo* by the immune response. Ipi-10 is the first example of a basic amphipathic  $3_{10}$ -helical peptide with MIC activity against *E. coli*. The  $3_{10}$ -helix is about 20-25% longer with a tighter helix than an  $\alpha$ -helical peptide of the same length. As a result,  $3_{10}$ -helical peptides may retain higher activity at shorter lengths than analogous  $\alpha$ -helical sequences.

## References

1. Maloy, W.L. and Kari, U.P., Biopolymers (Peptide Science), 37 (1995) 105.
2. Cornut, I., Buttner, K., Dasseux, J.-L. and Dufourcq, J., FEBS Lett., 349(1994) 29.
3. Javadpour, M.M., Juban, M.M., Lo, W.-C.J., Bishop, S.M., Alberty, J.B., Cowell, S.M., Becker, C.L. and McLaughlin, M.L., J. Med. Chem., 39 (1996) 3107.
4. Yokum, T.S., Elzer, P.H. and McLaughlin, M.L., J. Med. Chem., 39(1996) 3603.
5. Martinez de Tejada, G.T., Pizarro-Cerda, J., Moreno, E., Moriyon, I., Infect Immun. 63 (1995) 3054.
6. Dettleux, P.G., Deyoe, B.L. and Cheville, N.F., Infect. Immun., 58 (1990) 2320.
7. Bloom, B.R., Ed. Tuberculosis: Pathogenesis, Protection and Control. ASM Press, Washington, DC 1994.
8. Wysong, C.L., Yokum, T.S., Morales, G.A., Gundry, R.L., McLaughlin, M.L. and Hammer, R.P., J. Org. Chem., 61 (1996) 7650.
9. Yokum, T.S., Gauthier, T.J., Hammer, R.P. and McLaughlin, M.L. J., Am. Chem. Soc., 119 (1997) 1167.
10. Iwata, T., Lee, S., Oishi, O., Aoyagi, H., Ohno, M., Anzai, K., Kirino, Y., Sugihara, G. J., Biol. Chem., 269 (1994) 4928.

# **[D-Pen<sup>2,7</sup>]-human- $\alpha$ -calcitonin gene-related peptide: A novel CGRP antagonist**

**D. David Smith,<sup>a</sup> Shankar Saha,<sup>a</sup> David J. J. Waugh<sup>b</sup> and Peter W. Abel<sup>b</sup>**

<sup>a</sup>Department of Biomedical Sciences and <sup>b</sup>Department of Pharmacology, Creighton University, Omaha, NE 68178, USA

*Human- $\alpha$ -Calcitonin gene-related peptide (h- $\alpha$ -CGRP), the product of alternative splicing of the calcitonin gene, is a potent vasodilator of numerous blood vessels [1]. This peptide (Fig. 1) possesses a well-defined loop bridged by a disulfide bond between positions 2 and 7, and an  $\alpha$ -helix spanning positions 8 to 18 [2]. Previous structure-activity studies have shown that the disulfide bond is essential for binding to and activates of CGRP receptors in cardiac tissues [3]. To examine the effect of conformationally constraining the disulfide bridge we report the synthesis, binding and functional properties of CGRP analogues containing L/D-Pen residues in positions 2 and/or 7.*

## **Results and Discussion**

All analogues listed in Table 1 were synthesized by Merrifield's solid phase peptide synthesis methodology on an Applied Biosystems 430A peptide synthesizer. Boc-amino acid derivatives were coupled to MBHA resin using DIC and HOBt in NMP. Asn<sup>31</sup> and Gly<sup>21</sup> to Ala<sup>1</sup> were double coupled to maintain coupling yields >99%. Double coupling of Boc-D-Pen(MeOBzl)-OH to Val<sup>8</sup> of the growing peptide resin resulted in a poor yield of 78%. Attempts to optimize the coupling conditions led to the use of the BOP reagent, which improved the yield to 93% after a double coupling. Cleaved products were purified by RP-HPLC and had satisfactory amino acid compositions and mass determinations.

The binding affinity of each analogue was determined as its ability to inhibit <sup>125</sup>I-h- $\alpha$ -CGRP binding to membranes prepared from pig coronary arteries and functional experiments determined each analogue's ability to relax pig coronary arteries. h- $\alpha$ -CGRP caused relaxation of coronary arteries and bound to G-protein coupled and uncoupled states of the receptor. [Pen<sup>2</sup>]-h- $\alpha$ -CGRP was an equipotent full agonist with the same affinity as h- $\alpha$ -CGRP for the CGRP receptor. Changing the configuration of Pen<sup>2</sup> only caused minor reductions in potency and affinity. However, a Pen residue in position 7 resulted in significant reductions in potency and binding affinity. Furthermore, [D-Pen<sup>7</sup>]-h- $\alpha$ -CGRP, rather than showing any agonist effects but was a weak antagonist. Binding and functional properties of the disubstituted Pen analogues were consistent with those of the monosubstituted Pen analogues. All [D-Pen<sup>7</sup>]-containing analogues were antagonists of which [D-Pen<sup>2,7</sup>]-h- $\alpha$ -CGRP had the highest affinity.

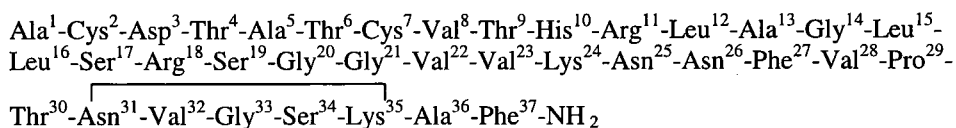


Fig. 1. Primary structure of human- $\alpha$ -calcitonin gene-related peptide.

Table 1. Potencies and binding affinities of Pen substituted h- $\alpha$ -CGRP analogues.

Analogue	Potency EC <sub>50</sub> (nM)	Binding Affinity K <sub>D</sub> (nM)	
h- $\alpha$ -CGRP	3.58 ± 0.49	0.18 ± 0.12	5.19 ± 1.6
h- $\alpha$ -CGRP (8-37)	212.05 ± 51.48 <sup>a</sup>	18.88 ± 6.6	
[Pen <sup>2</sup> ]-h- $\alpha$ -CGRP	7.64 ± 1.27	0.11 ± 0.08	4.89 ± 1.34
[Pen <sup>7</sup> ]-h- $\alpha$ -CGRP	296.15 ± 56.4	83.03 ± 10.88	
[D-Pen <sup>2</sup> ]-h- $\alpha$ -CGRP	30.91 ± 7.6	6.12 ± 1.28	
[D-Pen <sup>7</sup> ]-h- $\alpha$ -CGRP	2830 ± 1932 <sup>a</sup>	136.42 ± 10.86	
[Pen <sup>2,7</sup> ]-h- $\alpha$ -CGRP	>10,000	115.75 ± 15.7	
[D-Pen <sup>2,7</sup> ]-h- $\alpha$ -CGRP	629.5 ± 94.3 <sup>a</sup>	92.32 ± 2.1	
[Pen <sup>2</sup> , D-Pen <sup>7</sup> ]-h- $\alpha$ -CGRP	1224.6 ± 78.3 <sup>a</sup>	75.62 ± 19.8	
[D-Pen <sup>2</sup> , Pen <sup>7</sup> ]-h- $\alpha$ -CGRP	165.4 ± 56.2	50.05 ± 9.8	

<sup>a</sup>Antagonist K<sub>B</sub> values.

Substitution of Cys<sup>7</sup> for D-Pen abolishes agonist the effects of h- $\alpha$ -CGRP and produces an antagonist. The most potent antagonist, [D-Pen<sup>2,7</sup>]-h- $\alpha$ -CGRP, has an affinity for CGRP receptors similar to that of h- $\alpha$ -CGRP (8-37). NMR and CD studies of this conformationally constrained peptide should provide useful insights into the topographical and conformational properties of CGRP receptor antagonists.

## References

1. Poyner, D.R., *Pharmac. Ther.*, 56(1992) 23.
2. Breeze, A.L., Harvey, T.S., Bazzo, R., Campbell, I.D., *Biochemistry*, 30(1991) 575.
3. Dennis, T., Fournier, A., St Pierre, S., Quirion, R., *J. Pharmacol. Exp. Ther.*, 251(1989) 718.

## Improved parathyroid hormone analogue for the treatment of osteoporosis

**J.-R. Barbier, V. Ross, P. Morley, J.F. Whitfield and G.E. Willick**

*Institute for Biological Sciences, National Research Council, Ottawa, ON, CANADA, KIA 0R6*

Parathyroid hormone (PTH) and various analogues have been shown to be effective stimulators of bone synthesis [1]. The hormone stimulates both adenylyl cyclase (AC) and phosphatidylinositol-specific phospholipase-C $\beta$  (PI-PLC). PI-PLC activity requires only the 29-32 sequence. AC and full bone anabolic activities require only the 1-31 sequence, which also lacks PLC activity [2]. We have shown that residues 21-31 contain an amphiphilic  $\alpha$ -helix [3], and that this helix can be stabilized by forming lactams between the naturally occurring sequences Glu<sup>22</sup>..Lys<sup>26</sup> or Lys<sup>26</sup>..Asp<sup>30</sup> [4]. In this work, we have examined the secondary structure and bioactivities of lactams of hPTH(1-31)-NH<sub>2</sub> formed between Glu<sup>22</sup>..Lys<sup>26</sup>, Lys<sup>26</sup>..Asp<sup>30</sup>, and Lys<sup>27</sup>..Asp<sup>30</sup>.

### Results and Discussion

The absolute value of  $\theta_{222}$  is related to the amount of  $\alpha$ -helix in a peptide. Formation of both of the *i, i+4* lactams led to an increase in  $\alpha$ -helix, compared to either linear form, whereas the *i, i+3* lactam had diminished  $\alpha$ -helix (Table 1). The Glu<sup>22</sup>..Lys<sup>26</sup> lactam (**3**) had about 3x the AC activity of its linear parent sequence (**2**). However, both of the other lactams resulted in some diminishing of AC activity compared to the linear parent (Table 1).

Table 1 *Circular dichroism and adenylyl cyclase activities of hPTH analogues.*

Peptide	$-\theta_{222} \times 10^{-3}$ (deg.cm <sup>2</sup> .dmol <sup>-1</sup> ) <sup>a</sup>	AC (EC <sub>50</sub> ) (nM) <sup>b</sup>
(1) hPTH(1-31)NH <sub>2</sub>	7.55	19.9 ( $\pm$ 3.9)
(2) [Leu <sup>27</sup> ]hPTH(1-31)NH <sub>2</sub>	7.35	11.5 ( $\pm$ 5.2)
(3) [Leu <sup>27</sup> ]c(Glu <sup>22</sup> -Lys <sup>26</sup> )hPTH(1-31)NH <sub>2</sub>	10.88	3.3 ( $\pm$ 0.3)
(4) [Leu <sup>27</sup> ]c(Lys <sup>26</sup> -Asp <sup>30</sup> )hPTH(1-31)NH <sub>2</sub>	10.56	16.9 ( $\pm$ 3.3)
(5) c(Lys <sup>27</sup> -Asp <sup>30</sup> )hPTH(1-31)NH <sub>2</sub>	6.32	40.3 ( $\pm$ 2.3)

<sup>a</sup> CD in 25 mM sodium phosphate, pH 7.2, measured with JASCO J600 spectropolarimeter.

<sup>b</sup> Peptide concentration (EC<sub>50</sub>) inducing 50% of maximum observed production of [<sup>3</sup>H]-cAMP.

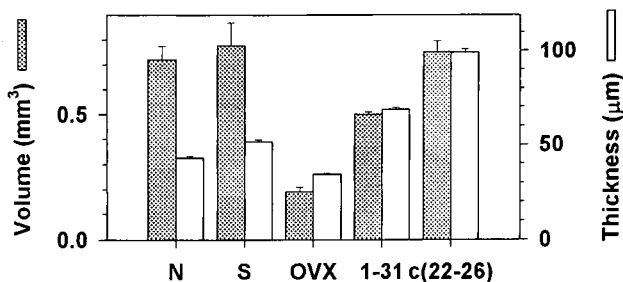


Fig. 1. Trabecular volumes and mean trabecular thicknesses of rat femurs treated with analogue 3.

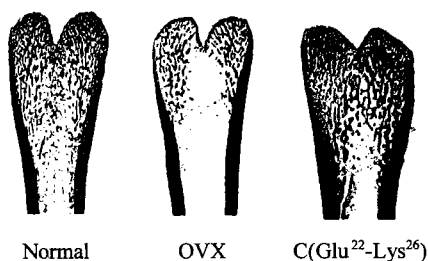


Fig. 2. Demineralized specimens of normal, OVX, lactam 3 treated distal femurs.

To test the anabolic activity of the analogues, rats were depleted of bone for 9 weeks after ovariectomy (OVX). Rats were injected subcutaneously daily (6 days/week) with 0.6nmol/100 g of peptide or vehicle (0.15 M NaCl, 0.001 N HCl, H<sub>2</sub>O). By 8 weeks after ovariectomy, there was severe depletion of femoral trabecular bone, as seen in metaphyseal mean trabecular volumes and thicknesses (Fig. 1) and decalcified sections (Fig. 2). HPTH(1-31)NH<sub>2</sub> (1) and its lactam analogues 3 and 4 were able to restore bone. Lactam 3 was the most effective of the 3 analogues and bone loss was restored fully by treatment with this analogue (see data in Fig 1 and 2).

## References

- Whitfield, J.F., Morley, P., Langille, R., Willick, G., (1997) In: Whitfield JF, Morley P (eds) Anabolic Treatments for Osteoporosis., CRC Press, Boca Raton, in press.
- Whitfield, J.F., Morley, P., Willick, G.E., Ross, V., Barbier, J.-R., Isaacs, R.J., and Ohannessian-Barry, L., *Calcif. Tissue Int.*, 58 (1996) 81.
- Neugebauer, W., Surewicz, W.K., Gordon, H.L., Somorjai, R.L., Sung, W. and Willick, G.E., *Biochemistry*, 31 (1992) 2056.
- Barbier, J.-R., Neugebauer, W., Morley, P., Ross, V., Soska, M., Whitfield, J.F. and Willick, G.E., *J. Med. Chem.*, 40 (1997) 1373-1380.
- Whitfield, J.F., Morley, P., Ross, V., Preston, E., Soska, M.; Barbier, J.R., Isaacs, R.J., MacLean, S.; Ohannessianbarry, L., Willick, G.E., *Calcif. Tissue Int.*, 60 (1997) 302-308.
- Whitfield, J.F., Morley, P., Willick, G., Langille, R., Ross, V., Maclean, S. and Barbier, J.-R. J., *Bone Miner. Res.*, (1997) in press.

# Multifunctional chimeric analogs of small peptide hormones: Agonists and receptor-selective antagonists

**John Howl and Mark Wheatley**

*School of Biochemistry, University of Birmingham, Edgbaston, Birmingham, B15 2TT, UK*

G-protein-coupled receptors (GPCRs) for the structurally diverse nonapeptide hormones vasopressin (AVP) and bradykinin (BK) regulate all major physiological systems and are important therapeutic targets. The strategy of synthesizing tandem-linked chimeric peptides to target GPCRs was largely pioneered by Ülo Langel and coworkers who derivatized N-terminal fragments of the neuropeptide galanin to produce galanin receptor antagonists and novel probes of signal transduction events [1,2]. This intriguing approach was further developed by studies in our laboratory in which we synthesized chimeric peptides to combine structural and functional motifs of AVP and BK in a single molecule [3]. The rationale behind these studies was to develop chimeric peptides (agonists and antagonists) capable of interacting with multiple pharmacologically distinct GPCRs and to investigate the potential of exploiting specific ligand:GPCR interactions for the selective delivery of bioactive moieties to appropriate cells and/or tissues.

## Results and Discussion

The well characterized structure:activity relationships of AVP and BK [4,5] can be utilized in the design of tandem-linked chimeric peptides which are pharmacologically selective. Single chain chimeric peptides including AVP(1-9)-BK(1-9) (H17) and AVP(1-9)- $\epsilon$ Ahx-BK(1-9) ( $\epsilon$ Ahx = aminohexanoic acid, H18) bind with high affinity to the bovine B<sub>2a</sub> bradykinin receptor (BKR [6]) and stimulate inositol phosphate production via B<sub>2</sub> BKRs expressed by NG115 401L cells [3]. These findings illustrate that chimeric peptides can activate GPCRs in a similar manner to monomeric agonists. Further studies revealed that peptides including [PhaaDTyr(Et)<sup>2</sup>Arg<sup>6</sup>]AVP(1-8)- $\epsilon$ Ahx-DArg<sup>0</sup>[Hyp<sup>3</sup>DPhe<sup>7</sup>Leu<sup>8</sup>]BK(1-9) (Phaa = phenylacetyl, H22), combining well characterized V<sub>1a</sub>-selective and B<sub>2a</sub>-selective sequences (Table 1), are mixed high affinity antagonists at both the rat V<sub>1a</sub> vasopressin receptor (VPR) and bovine B<sub>2a</sub> BKR [3]. Similar strategies are compatible with the synthesis of bioactive analogs of both AVP and BK derivatized with mastoparan, an active component of wasp venom, or the integrin-targeting function of fibronectin-related 'RGD' peptides. Significantly, chimeric hormone-mastoparan peptides are known to modulate the activity of several membrane-bound enzymes and exhibit biological actions different from those of their components and which may be independent of ligand:GPCR interaction [2,7]. These findings fuel additional interest in the application of chimeric peptides to address the molecular details of enzyme catalysis and signal transduction.

Table 1. Examples of tandem-linked chimeric peptides.

Peptide sequence	Binding affinity ( $k_d$ , mean $\pm$ SEM, nM)	
	V <sub>1a</sub> VPR	B <sub>2a</sub> BKR
AVP(1-9)-BK(1-9)	1,900 $\pm$ 400	52.1 $\pm$ 2.9
[PhaaDTyr(Et) <sup>2</sup> Arg <sup>6</sup> ]AVP(1-8)- $\epsilon$ Ahx-DArg <sup>0</sup> [Hyp <sup>3</sup> DPhe <sup>7</sup> Leu <sup>8</sup> ]BK(1-9)	0.31 $\pm$ 0.14	4.81 $\pm$ 2.13
[PhaaDTyr(Me) <sup>2</sup> Arg <sup>6</sup> Tyr <sup>9</sup> ]AVP(1-9)-mastoparan	3.76 $\pm$ 0.41	n.a
RGDF- $\epsilon$ Ahx-DArg <sup>0</sup> [Hyp <sup>3</sup> DPhe <sup>7</sup> Leu <sup>8</sup> ]BK(1-9)	n.a	12.8 $\pm$ 2.3

Homo-dimeric peptides, synthesized by crosslinking an amino-terminal extended BK analog and a V<sub>1a</sub>-selective antagonist, represent new classes of B<sub>2</sub> BKR agonist and V<sub>1a</sub>-selective VPR antagonist, respectively [3]. These findings are significant considering current models of peptide hormone:GPCR interaction which have specifically located GPCR-bound AVP and BK to a spatially confined hydrophobic domain of both the V<sub>1a</sub> VPR and B<sub>2</sub> BKR [8, 9]. We interpret our findings with chimeric and homo-dimeric peptides as evidence that analogs of AVP and BK interact with a peptide hormone binding site located at the molecular interface between the extracellular domains and more hydrophobic transmembrane helices of their respective GPCR [10].

We conclude that chimeric and homo-dimeric peptides, combining functional epitopes of AVP and BK, are novel tools for studying the biological activity of small peptide hormones and for probing the ligand binding site of GPCRs.

## References

1. Juréus, A. and Langel, Ü., *Acta. Chim. Slovenica.*, 43(1996) 51.
2. Langel, Ü., Pooga, M., Kairane, C., Zilmer, M. and Bartfai, T., *Regul. Pept.*, 62(1996) 47.
3. Howl, J., Langel, Ü., Hawtin, S.R., Valkna, A., Yarwood, N.J., Saar, K. and Wheatley, M., *FASEB J.*, 11(1997) in press.
4. Manning, M., Bankowski, K. and Sawyer, W.H., In Jard, S. and Jamison, R., (Eds), *Vasopressin*, Plenum, New York, 1987, p.335.
5. Regoli, D., Rhaleb, N.-E., Dion, S. and Drapeau, G., *Trends Pharmacol. Sci.*, 11(1990) 156.
6. Howl, J., Yarwood, N.J., Davies, A.R.L. and Wheatley, M., *Kidney Int.*, 50(1996) 586.
7. Mezna, M., Langel, Ü., Hällbrink, M., Wheatley, M., Michelangeli, F. and Howl, J., *Biochem. Soc. Trans.*, 25(1997) 450S.
8. Mouillac, B., Chini, B., Balstre, M.N., Trumppkallmeyer, S., Hoflak, J., Hibert, M., Jard, S. and Barberis, C., *J. Biol. Chem.*, 270(1995) 25711.
9. Kyle, D.J., Chakravarty, S., Sinsko, J.C. and Stormann, T.M., *J. Med. Chem.*, 37(1994) 1347.
10. Howl, J. and Wheatley, M., *Biochem. J.*, 317(1996) 577.

## Generation of New Dmt-Tic $\delta$ Opioid Antagonists: *N*-Alkylation

Lawrence H. Lazarus,<sup>a</sup> Severo Salvadori,<sup>b</sup> Gianfranco Balboni,<sup>b</sup> Remo Guerrini,<sup>b</sup> Clementina Bianchi,<sup>b</sup> Peter S. Cooper<sup>a</sup> and Sharon D. Bryant<sup>a</sup>

<sup>a</sup>NIEHS, Research Triangle Park, NC, 27707, U. S. A., <sup>b</sup>University of Ferrara, Ferrara 44100, Italy

To enhance  $\delta$  antagonist interaction at opioid receptors, new opioid antagonists were developed by substitution of 2',6'-dimethyl-L-tyrosine (Dmt) for Tyr<sup>1</sup> in Tyr-Tic peptides (DToH), in these peptides,  $K_{i\delta}$  and selectivity ( $K_{i\mu}/K_{i\delta}$ ) increased *ca.* 5 orders of magnitude and >1,000-fold, respectively [1]. The peptides were antagonists *in vitro* [1] and *in vivo* [2,3]. A limiting factor is the formation of a diketopiperazine during synthesis [4,5], nonetheless, *cyclo*(Dmt-Tic) exhibited activity with  $K_{i\delta}$  *ca.* 10 nM, weak selectivity and bioactivity [6] which implied the dimethyl groups enhanced activity compared to the inactive *cyclo*(Tyr-Tic) [7]. To prevent cyclization and augment hydrophobicity, DToH antagonists were *N*-alkylated to form secondary or tertiary amines, and the C-terminal free acid function was modified.

### Results and Discussion

*N*-Alkylation of DToH yielded high affinity  $\delta$  antagonists (Table 1). *N*Me- or *N,N*(Me)<sub>2</sub>-Tyr-Tic cognates elevated  $K_{i\delta}$  and  $K_{i\mu}$ , but were orders of magnitude less selective than DToH. *N*Me-DToH **1** and the amidated analogue **3** decreased  $K_{i\delta}$  *ca.* 10- and 17-fold, respectively, and lost selectivity through increased  $K_{i\mu}$  while  $\delta$  antagonism doubled relative to the title peptides. *N*Me-Dmt-Tic-Ala-OH (*N*Me-DTAOH) **4** had comparable activities. D-Dmt<sup>1</sup> analogues were generally detrimental; however, while **2** and **5** decreased  $K_{i\delta}$  by 100-200-fold to low nM values, **5** yielded  $\delta$  antagonism equal to **1**. A des-amino- $\alpha$ Me-Dmt<sup>1</sup> analogue was inactive. Dimethylated peptides **6-8** exhibited high  $K_{i\delta}$  and 10-fold increased antagonism, although  $K_{i\mu}/K_{i\delta}$  of **7** fell relative to **6**. These peptides (**6-8**) also exhibited weak  $\mu$  antagonism. Other *N*-alkylated derivatives of DToH (diethyl, piperidine, pyrrolidine, pyrrole) decreased  $K_{i\delta}$  to the 1-2 nM range and decreased selectivity accordingly. Increased  $K_{i\mu}$  of **3** and **7** reflected changes observed in amidated analogues [1]. Similarly, C-terminal modification (OMe, NH-NH<sub>2</sub>, NH-Me, NH-adamantane) greatly increased  $K_{i\mu}$ , such that adamantanyl amide with or without *N,N*-methylation exhibited both high  $K_{i\delta}$  and  $K_{i\mu}$  and was an agonist.

## Conclusion

*N*-Alkylation of DTOH and DTAOH forms secondary and tertiary *N*-terminal amines that maintained high  $K_i\delta$ ,  $\delta$  selectivity, and enhanced  $\delta$  antagonism. With increased hydrophobicity, they might act as probes to define the ligand-binding domain of  $\delta$  receptors and to expedite passage through the blood-brain barrier. As  $\delta$  antagonists they might have therapeutic applications to counter narcotic addiction, alcohol dependency, and to impair immune response.

Table 1. Activity of *N*-alkylated *Dmt-Tic*  $\delta$  antagonists.  $K_i$  and  $K_e$  values are nM for rat brain membranes and mouse *vas deferens* (MVD), while guinea-pig ileum (GPI)  $K_e$  and  $IC_{50}$  values are  $\mu$ M.

Cmpd	$K_i\delta$	$K_i\mu$	$K_i\mu/K_i\delta$	MVD (nM)		GPI ( $\mu$ M)		
				pA <sub>2</sub>	$K_e$	pA <sub>2</sub>	$K_e$	IC <sub>50</sub>
DTOH	0.022	3,320	150,800	8.20	5.7	-	-	>10
DTAOH	0.285	5,810	20,400	8.40	4.0	-	-	>10
1 NMe-DTOH	0.20	380	1,870	8.55	2.8	-	-	>10
2 NMe-D-DTOH	3.19	2,000	628	6.85	141	-	-	>10
3 NMe-DT-NH <sub>2</sub>	0.38	955	2,500	8.66	2.2	-	-	>10
4 NMe-DTAOH	0.14	5,850	43,000	8.85	1.4	-	-	>10
5 <i>N,N</i> (Me) <sub>2</sub> -D-DTOH	5.74	13,100	2,280	8.62	2.38	-	-	>10
6 <i>N,N</i> (Me) <sub>2</sub> -DTOH	0.12	2,440	20,640	9.54	0.28	4.85	14.1	-
7 <i>N,N</i> (Me) <sub>2</sub> -DT-NH <sub>2</sub>	0.31	511	1,655	9.91	0.12	6.27	0.54	-
8 <i>N,N</i> (Me) <sub>2</sub> -DTAOH	0.076	1,520	20,000	9.64	0.22	4.86	13.8	-

## References

1. Salvadori, S., Attila, M., Balboni, G., Bianchi, C., Bryant, S. D., Crescenzi, O., Guerrini, R., Picone, D., Tancredi, T., Temussi, P. A. and Lazarus, L. H., *Mol. Med.*, 1(1995)678.
2. Guerrini, R., Capasso, A., Sorrentino, L., Anacardio, Bryant, S. D., Lazarus, L. H., Attila, M. and Salvadori, S., *Eur. J. Pharmacol.*, 302(1996)37.
3. Capasso, A., Guerrini, R., Balboni, G., Sorrentino, L., Temussi, P. A., Lazarus, L. H., Bryant, S. D. and Salvadori, S., *Life Sci.*, 59(1996)PL 93.
4. Marsden, R. H., Nguyen, T. M.-D. and Schiller, P. W. *Int. J. Pept. Prot. Res.*, 41(1993)313.
5. Capasso, S., Sica, F., Mazzarella, L., Balboni, G., Guerrini, R. and Salvadori, S., *Int. J. Pept. Prot. Res.*, 45(1995)567.
6. Balboni, G., Guerrini, R., Salvadori, S., Tomatis, R., Bryant, S. D., Bianchi, C., Attila, M. and Lazarus, L. H., *Biol. Chem.*, 378(1997)19.
7. Bryant, S. D., Balboni, G., Guerrini, R., Salvadori, S., Tomatis, R. and Lazarus, L. H., *Biol. Chem.*, 378(1997)107.

# Novel D-amino acid hexapeptide calmodulin antagonists identified from synthetic combinatorial libraries

Sylvie E. Blondelle,<sup>a</sup> Ema Takahashi,<sup>a</sup> Ed Brehm,<sup>a</sup> Rosa Aligue,<sup>b</sup> Richard A. Houghten<sup>a</sup> and Enrique Pérez-Payá<sup>a,c</sup>

<sup>a</sup>Torrey Pines Institute for Molecular Studies, San Diego, CA 92121, USA, <sup>b</sup>Department Biologia Celular, Universitat Barcelona, E-08028 Barcelona, Spain, <sup>c</sup>Department Bioquímica i Biologia Molecular, Universitat Valencia, E-46100 Burjassot, Spain

Calmodulin (CaM), the major intracellular calcium receptor, is involved in many processes that are crucial to cellular viability. In particular, CaM is implicated in calcium-stimulated cell proliferation. CaM antagonists have been shown to have potential as antitumor agents, and as tools to help define the role of CaM in various biological processes. Using the synthetic combinatorial library approach [1,2], we have identified novel D-amino acid hexapeptides that exhibited 2- to 3-fold higher CaM inhibitory activity than known antagonists such as trifluoperazine and N-(4-aminobutyl)-5-chloro-2-naphthalenesulfonamide (W13) [3].

## Results and Discussion

The formation of a calcium-dependent complex between CaM and the antagonists was examined by gel electrophoresis. Binding of the antagonists to CaM was expected and found to result in a change in mobility as determined by an electrophoretic band shift assay. Thus, a small band shift for both Ac-lwrlw-NH<sub>2</sub> occurred only in the presence of calcium (Fig. 1).

In support of the above data, a slight conformational change was observed for CaM in the presence of Ac-lwrlw-NH<sub>2</sub>. In particular, a shift to lower wavelengths and variations in intensity were observed for the spectra in the far UV region of CaM in the presence of Ac-lwrlw-NH<sub>2</sub> (Fig. 2). Significant changes in the CD signal in the near UV region for both CaM and Ac-lwrlw-NH<sub>2</sub> were also observed. Due to its hydrophobic nature, Ac-lwrlw-NH<sub>2</sub> can be envisioned to adsorb the hydrophobic site of CaM that forms upon interactions with calcium, which would affect the orientation of the hydrophobic chromophores in CaM.

The formation of complexes between the antagonists and CaM was also supported by marked changes in fluorescence emission spectra, quantum yields, and anisotropy. Similar variations were seen for Ac-lwrlw-NH<sub>2</sub> and Ac-LWRILW-NH<sub>2</sub>, which confirms a lack of stereospecificity in the binding site of these peptides to CaM. Interestingly, the linear dimers formed through the tryptophan residues appeared to exhibit increased inhibitory activities (2- to 5-fold) relative to the monomer, while further polymerization led to a loss in activity.

The formation of antagonists/CaM complexes, as well as their *in vivo* activities, were evaluated. The ability of the newly identified CaM antagonists to inhibit CaM activity in cell proliferation *in vivo* was initially investigated using normal rat kidney cells (NRK cells). The effects of the identified D-amino acid hexapeptide antagonists, as well as of the corresponding L-amino acid hexapeptide counterparts, were analyzed from the DNA synthesis in NRK cells

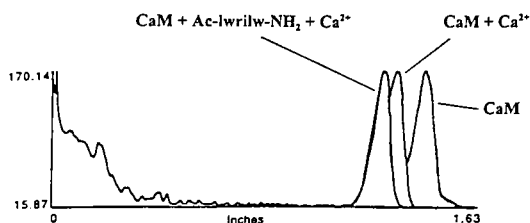


Fig. 1. Densitometric measurement of gel bands.

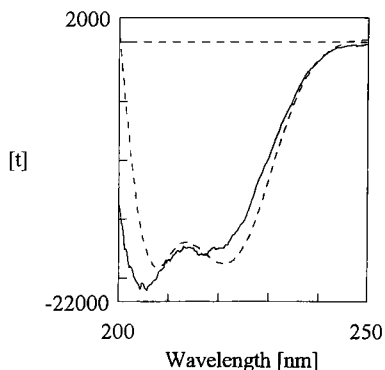


Fig. 2. CD spectra of CaM (—) in the presence or (---) absence of Ac-lwrlw-NH<sub>2</sub>.

activated to proliferate from quiescence [4]. The CaM hexapeptide antagonists showed potent *in vivo* activity, with the most active peptide, Ac-lwrlw-NH<sub>2</sub>, exhibiting 41% inhibition of DNA synthesis at 7.5 μM, while 30 μM of the known CaM antagonist W13 was necessary for the same level of inhibition. Similar activities were found for the D-amino acid hexpeptides and their L-counterparts. In contrast, the peptides did not exhibit any inhibitory effect on cell growth, as demonstrated by the lack of inhibition of (<sup>35</sup>S)-methionine incorporation. This indicates that the inhibition of CaM occurs rapidly following the addition of the inhibitory peptides. Furthermore, the inhibition of DNA synthesis was permanent in the case of Ac-lwrlw-NH<sub>2</sub> and W13, that the L-amino acid peptide Ac-LRWRLW-NH<sub>2</sub>, as expected, was not stable in the long run. Finally, similar efficacy was observed on the DNA synthesis in rat liver cells that were in the stage of partial hepatectomy. Thus, the intravenous injection of 1 mg of Ac-lwrlw-NH<sub>2</sub> in male Sprague-Dawley rats resulted in 50% inhibition of DNA synthesis. These *in vivo* results are encouraging for potential pharmacological use of compounds that are identified from synthetic combinatorial libraries using *in vitro* assays.

## References

1. Houghten RA, Pinilla C, Blondelle SE, Appel JR, Dooley CT, and Cuervo JH. *Nature*, 354 (1991) 84.
2. Pinilla, C., Appel, J.R., Blanc, P., and Houghten, R.A. *Biotechniques*, 13 (1992) 901.
3. Pérez-Payá, E., Takahashi, E., Mingarro, I., Houghten, R.A., and Blondelle, S.E. In Kaumaya, P.T.P. and Hodges, R.S. (Eds) *Peptides: Chemistry, Structure and Biology*. Proceedings of the 14th American Peptide Symposium, Mayflower Scientific Ltd, UK, 1996, p. 303.
4. López-Girona, A., Bosch, M., Bachs, O., and Agell, N. *Cell Calcium*, 18 (1995) 30.

# Pseudopeptides and cyclic peptides analogues of osteogenic growth peptide (OGP): Synthesis and biological evaluation

Yuchen Chen,<sup>a,b</sup> Itai Bab,<sup>a</sup> Andras Muhrad,<sup>a</sup> Arye Shteyer,<sup>a</sup> Marina Vidson<sup>a</sup>, Zvi Greenberg,<sup>a</sup> Dan Gazit<sup>a</sup> and Michael Chorev<sup>b</sup>

Faculties of Dental Medicine<sup>a</sup> and Medicine<sup>b</sup>, The Hebrew University of Jerusalem, Jerusalem 91120, Israel

Osteogenic growth peptide (OGP), ALKRQGR<sup>T</sup>LYGF<sup>G</sup>GG, is a 14-amino acid endogenous peptide corresponding to the C-terminal structure of histone H4 (89-102) [1]. OGP stimulates the proliferation and alkaline phosphatase activity of osteoblastic MC3T3 E1 and fibroblastic NIH 3T3 cells *in vitro*. *In vivo* OGP increases bone formation and trabecular bone density. Furthermore, OGP is a key factor in the mechanism of the systemic osteogenic reaction to bone marrow injury, and is thus considered a potential therapeutic agent for treating systemic skeletal defects including nonunion fracture, periodontal disease and osteoporosis [2]. OGP could be truncated considerably from the amino terminal without loss of activity. Full activity was obtained with only the C-terminal pentapeptide YGF<sup>G</sup>GG [3]. In an effort to further our understanding of the structure-anabolic activity relationship we performed a study in which systematic structural modifications were introduced. In this report, we describe the synthesis and biological evaluation of cyclic and partially nonpeptidic analogues of OGP. In the latter, individual amide bonds were replaced by isosteric peptide bond surrogates.

## Results and Discussion

The linear peptides described in this study were prepared by solid phase peptide synthesis methodology using Boc chemistry and a standard side chain protecting-group strategy. The cyclization of linear peptides was carried out (high dilution, 0 °C) with diphenyl phosphoryl azide as coupling agent. For the synthesis of the Asp and Aib containing cyclic peptides the Kaiser's oxime resin method was employed [4]. A linear peptide was assembled by solid phase synthesis (SPS). Cyclization was accompanied by concomitant removal of the peptide from resin. In general, the cyclic OGP analogues prepared on the oxime resin yielded crude products that were easily purified by RP-HPLC. The introduction of the  $\Psi(\text{CH}_2\text{NH})$  peptide bond isostere was accomplished by solid phase reductive alkylation of the N-terminal amino group of the resin-bound peptide with the corresponding Boc-protected  $\alpha$ -amino aldehyde in the presence of sodium cyanoborohydride ( $\text{NaBH}_3\text{CN}$ ) in DMF containing 1% AcOH [5].

*In vitro* proliferative activity of synthetic OGP analogues was measured in osteoblastic MC3T3 E1 and fibroblastic NIH 3T3 cells. The relative potencies of the proliferative activity of individual analogues were expressed as the mean of results (with respect to native OGP). 95% confidence limits are given in parentheses in Table 1, obtained in at least three independent experiments.

Table 1. Proliferative activity of selected synthetic OGP analogues.

	Analogue	Relative <i>in vitro</i> potency	
		MC3T3 E1 cells	NIH3T3 cells
1	OGP(1-14)	1.00 (standard)	1.00 (standard)
2	[desaminoTyr <sup>10</sup> ,Sar <sup>11</sup> ]OGP(10-14)	0.31(0.25-0.37)	0.39(0.26-0.52)
3	[desaminoTyr <sup>10</sup> ,Sar <sup>13</sup> ]OGP(10-14)	0.15(0.07-0.23)	0.11(0.05-0.17)
4	[desaminoTyr <sup>10</sup> ψ(CH <sub>2</sub> NH)Gly <sup>11</sup> ]OGP(10-14)	0.81(0.71-0.91)	0.79(0.67-0.91)
5	[desaminoTyr <sup>10</sup> ,Phe <sup>12</sup> ψ(CH <sub>2</sub> NH)Gly <sup>13</sup> ]OGP(10-14)	0.70(0.65-0.75)	0.88(0.76-1.00)
6	[desaminoTyr <sup>10</sup> ,Gly <sup>13</sup> Ψ(CH <sub>2</sub> CH <sub>2</sub> )Gly <sup>14</sup> ]OGP(10-14)	0.78(0.73-0.83)	0.88(0.79-0.97)
7	c(Tyr-Gly-Phe-Gly-Gly)	0.79(0.72-0.86)	1.12(1.06-1.17)
8	c(Tyr-Gly-Phe-Gly)	0.35(0.30-0.40)	0.43(0.40-0.46)
9	c(Gly-Gly-D-Phe-Gly-D-Tyr)	1.03(0.95-1.11)	1.16(1.10-1.22)
10	c(Gly-Tyr-Gly-Phe-Gly-Gly)	0.26(0.19-0.33)	0.20(0.17-0.23)
11	c(γAbu-Tyr-Gly-Phe-Gly-Asp)-OH	0.13(0.10-0.16)	0.07(0.03-0.11)

While the reduced backbone amide modification Ψ(CH<sub>2</sub>NH) was well tolerated, the N-methylation of amide bonds Ψ(CONMe) led to a significant loss of potency. Conformational constraint in the form of end-to-end cyclization generated cyclic pentapeptide c(YGFGG) and its retro-inverso isomer c(GGfGy) possessing enhanced activity. However, expansion or contraction of ring size led to a great loss of potency. Truncation, amide bond replacement by surrogate bonds and conformational constraint led to active OGP analogues which will be very instrumental in the future design of non-peptidic OGP-mimetic therapeutics.

## References

1. Bab, I., Gazit, D., Chorev, M., Muhlrads, A., Shteyer, A., Greenberg, Z., Namdar, M., Kahn, A., The EMBO Journal, 11(1992)1867.
2. Greenberg, Z., Chorev, M., Muhlrads, A., Shteyer, A., Namdar, M., Mansur, N., Bab, I., Biochim. Biophys. Acta, 1178(1993)273.
3. Bab, I., Greenberg, Z., Chorev, M., Shteyer, A., Namdar, M., Daphni, L., Gurevitch, O., Einhorn, T., Ashurst, D.E., Muhlrads, A., J. Bone and Miner. Res., 8(1993) (Supplement 1)S354.
4. DeGrado, W.F., Kaiser, E.T., J. Org. Chem., 45(1980)1295.
5. Sasaki, Y., Coy, D.H., Peptides, 8(1987)119.

# A cyclic heptapeptide mimics CD4 domain 1 CC' loop and inhibits CD4 biological function

**Takashi Satoh, James M. Aramini, Song Li, Thea M. Friedman, Jimin Gao, Andrea E. Edling, Robert Townsend, Ute Koch, Swati Choksi, Markus W. Germann, Robert Korngold, and Ziwei Huang**

*Kimmel Cancer Institute, Jefferson Medical College, Thomas Jefferson University, Philadelphia, PA 19107, USA*

The interaction between CD4 and major histocompatibility complex (MHC) class II proteins provide a critical co-receptor function for the activation of CD4<sup>+</sup> T cells implicated in the pathogenesis of a number of autoimmune diseases and transplantation responses. A small synthetic cyclic heptapeptide was designed and shown by high resolution NMR spectroscopy to closely mimic the CD4 domain 1 CC' surface loop [1-4]. This peptide effectively blocked stable CD4-MHC class II interaction, possessed significant immunosuppressive activity *in vitro* and *in vivo*, and strongly resisted proteolytic degradation. These results demonstrate the therapeutic potential of this peptide as a novel immunosuppressive agent, and suggest a general strategy of drug design by using small conformationally constrained peptide mimics of protein surface epitopes to inhibit protein interactions and biological functions.

## Results and Discussion

To search for potential CD4 functional epitopes that could be targeted for the design of new inhibitors, a computer analysis was conducted for the CD4 D1 domain in conjunction with synthetic peptide mapping. This led to the identification of a surface pocket potentially involved in the CD4-MHC class II interaction. This CD4 surface pocket is formed by the FG loop (also known as the third complementarity determining region or CDR3) and the CC' loop. While the CDR3 has long been proposed to be involved in MHC class II interaction and recent studies with peptide mimics have confirmed their involvement, our analysis suggested that the highly protruded CC' loop may also serve as a surface epitope critical for CD4 function.

Based on this finding, a cyclic peptide, cyclo (CNSNQIC), was designed as a CD4 D1 domain CC' loop mimic, incorporating a disulfide bridge to enhance the structural stability of the  $\beta$ -turn around NSNQ of the native CC' region. The high resolution NMR spectroscopic experiments confirmed that this peptide adopts conformations highly resembling a type I  $\beta$ -turn of the native CC' loop, as observed in the crystal structure of CD4 D1D2 domains. This synthetic peptide mimic of the CD4 CC' loop was shown to effectively inhibit CD4-MHC class II interaction, block CD4-dependent T cell response *in vitro*, and possess significant immunosuppressive activity *in vivo* in murine models of experimental allergic encephalomyelitis (EAE) for MS and of skin allograft transplantation. These findings suggested the therapeutic potential of this CD4 peptide inhibitor and demonstrated a general approach of bioactive peptide design by the

functional mimicry of protein surface epitopes to generate potential novel therapeutic agents.

## Conclusion

We have proposed the CC' loop as an important functional epitope on the CD4 surface for intermolecular binding, and found that small peptide mimics of this epitope are sufficient to interrupt a larger protein-protein interface. In particular, a synthetic cyclic heptapeptide (CNSNQIC) has been shown to closely mimic the CC' surface epitope, effectively block CD4-MHC class II-dependent cell rosetting, possess significant immunosuppressive activity *in vitro* and *in vivo*, and strongly resists proteolytic degradation. These findings have demonstrated a general approach of bioactive peptide design by the functional mimicry of protein surface epitopes to generate potential novel therapeutic agents.

## Acknowledgments

These studies were supported in part by grants from the National Institutes of Health, the American Cancer Society, the National Multiple Sclerosis Society and the Sidney Kimmel Foundation for Cancer Research. We would like to thank members of our laboratories and our collaborators for their contribution and helpful discussion. Z.H. is the recipient of the Kimmel Scholar Award in cancer research.

## References

1. Satoh, T., Li, S., Friedman, T.M., Wiaderkiewicz, R., Korngold, R. and Huang, Z. *Biochem. Biophys. Res. Commun.*, 224(1996)438.
2. Satoh, T., Aramini, J.M., Li, S., Friedman, T.M., Gao, J., Edling, A., Townsend, R., Germann, M.W., Korngold, R. and Huang, Z.J. *Biol. Chem.*, 272(1997)12175.
3. Li, S., Gao, J., Satoh, T., Friedman, T., Edling, A., Koch, U., Choksi, S., Han, X., Korngold, R. and Huang, Z., *Proc. Natl. Acad. Sci. USA*, 94(1997)73.
4. Huang, Z., Li, S. and Korngold, R. *Med. Chem.* : in press, (1997).

# Analogs of the main autophosphorylation site of pp60<sup>src</sup> PTK as substrates for Syk and Src PTKs

Paolo Ruzza,<sup>a</sup> Andrea Calderan,<sup>a</sup> Barbara Biondi,<sup>a</sup>

Arianna Donella-Deana,<sup>b</sup> Lorenzo A. Pinna<sup>b</sup> and Gianfranco Borin<sup>a</sup>

<sup>a</sup>C.N.R. Biopolymer Research Center, Department of Organic Chemistry, University of Padova, via Marzolo 1, 35131 Padova, ITALY <sup>b</sup>Department of Biological Chemistry, University of Padova, via Trieste 75, 35127 Padova, ITALY.

Protein tyrosine kinases (PTKs) catalyze the phosphorylation of proteins on specific tyrosine residues. This reaction enables the PTKs to control various cell functions such as signal transduction, differentiation and proliferation. An overactivation or mutation of protooncogenes encoding tyrosine protein kinases can result in cell transformation. To investigate the conformational requirements of *Syk*- and *Src*-substrates we synthesized different conformational constrained analogs of EDNEYTA, a heptapeptide sequence that represents the common major autophosphorylation site of *Src*-PTK family. As previously reported, end to end cyclization of EDNEYTA induces a rigid conformation with a decrease of biological activity compared to linear [1]. Another type of cyclization is the side-chain lactam-bridge, characterized by a covalent bond between the side-chain of Asp or Glu and the side-chain of Lys or Orn. To synthesize this kind of cyclic analogs, The Asn residue of EDNEYTA was replaced by Asp or Glu, whereas Orn or Lys were alternatively substituted for Thr or Ala. The obtained side-chain cyclic peptides (Table 1) displayed different sized rings. They were tested as substrates for different splenic tyrosine kinases, and the biological data were correlated with conformational analysis.

## Results and Discussion

The peptides were synthesized by classical solution synthetic methodologies using Z/tBu combined to Boc/OChx strategies with BOP mediated coupling in THF. Side-chain cyclizations were performed using the BOP method in diluted solutions. The peptides were purified and characterized as usual.

The conformational properties of the peptides were investigated by CD spectroscopy

Table 1. Sequences of synthetic peptides (bold characters indicate the position of lactam-bridges).

Peptide	Amino acid sequence
A	H-Glu-Asp-Asn-Glu-Tyr-Thr-Ala-OH
B	H-Glu-Asp-c( <b>Glu</b> -Glu-Tyr-Thr- <b>Lys</b> )-OH
C	H-Glu-Asp-c( <b>Asp</b> -Glu-Tyr-Thr- <b>Orn</b> )-OH
D	H-Glu-Asp-c( <b>Glu</b> -Glu-Tyr- <b>Lys</b> )-Ala-OH
E	H-Glu-Asp-c( <b>Asp</b> -Glu-Tyr- <b>Orn</b> )-Ala-OH

Table 2. Kinetic constants for *Syk* and *Fgr* with synthetic peptide substrates.

PEPTIDE	p38 <sup>syk</sup>			c-Fgr		
	V <sub>max</sub> (pmol·min <sup>-1</sup> )	K <sub>m</sub> (μM)	Efficiency	V <sub>max</sub> (pmol·min <sup>-1</sup> )	K <sub>m</sub> (μM)	Efficiency
<b>A</b>	54.9	67	0.82	31.7	150	0.21
<b>B</b>	74.6	96	0.78	5.9	232	0.02
<b>C</b>	45.0	204	0.22	16.9	333	0.05
<b>D</b>	40.0	641	0.06	19.0	769	0.02
<b>E</b>	52.6	208	0.25	41.7	204	0.20

in the far-UV region. In 5 mM Tris-HCl, pH 6.8, all peptides gave CD spectra typical of a predominantly random conformation (strong negative band below 200 nm). In 50% TFE, peptides existed as a mixture of conformers and their CD spectra reflect more than one prevailing secondary structure. Tyr fluorescence quantum yield experiments show similar value for all peptides, with the exception of peptide **C** which exhibited a half value of quantum yield. Tyr fluorescence anisotropy experiments showed very similar values for *i*, *i*+3 bridge peptides (**D** and **E**), with intermediate intensity between the value exhibited by the *i*, *i*+4 bridge peptide **C** and the very low value found for the *i*, *i*+4 bridge peptide **B**. These fluorescence results could be due to a different tyrosine topography in the two larger *i*, *i*+4 rings. The synthetic peptides have been assayed for their ability to serve as phosphoacceptor substrates for the non-receptor tyrosine kinase p38<sup>syk</sup>, a proteolytic hyperactive derivative of p72<sup>syk</sup>, and for the *Src*-like kinase *Fgr*. The data (Table 2) show that the introduction of different side-chain lactam-bridges to the peptide substrates affects differently the phosphorylation ability of the two kinases tested. In particular, *Fgr* perceived the different constraints as negative specificity determinants of the peptide substrates, which are phosphorylated by the enzyme with 4/10-fold lower efficiency than that shown with the linear sequence. The only exception is peptide **E** which can be good as a substrate for *Fgr* as the parent sequence in terms of both K<sub>m</sub> and V<sub>max</sub>. On the contrary the tyrosine kinase *Syk*, which also recognizes the side-chain lactam-bridges as negative specificity determinants, can phosphorylate the analog **B** with kinetic parameters similar to that shown by the native peptide. The phosphorylability of derivative **B** by *Syk* correlate with the conformational studies which suggesting a higher structural flexibility displayed by this analog.

## References

1. Ruzza, P., Calderan, A., Filippi, B., Biondi, B., Donella-Deana, A., Cesaro, L., Pinna, L.A. and Borin, G. *Int. J. Peptide Protein Res.*, 45 (1995) 529.

# Positively charged residues of glucagon: Role in glucagon action

**Cecilia G. Unson, Cui-Rong Wu, Connie P. Cheung  
and R. B. Merrifield**

*The Rockefeller University, 1230 York Ave., New York, New York 10021, USA*

Secreted by pancreatic A cells, the 29-residue peptide hormone glucagon is responsible together with insulin for maintaining normal levels of glucose critical to the survival of an organism. Glucagon activity is mediated by its receptor, which is a member of a unique class within the superfamily of G protein-coupled receptors. It includes receptors for the glucagon family of hormones, glucagon-like peptide 1 (GLP-1), secretin, and vasoactive intestinal peptide (VIP). Specific binding to its cell surface receptors constitutes the signal that is transmitted across the membrane to G protein-linked intracellular effectors that are ultimately responsible for glucose production. The glucagon binding cavity on the receptor is believed to involve contributions from the long amino terminal extension as well as the extracellular loops that connect the seven transmembrane helices. Information about the peptide ligand and receptor protein interactions that dictate the binding phenomenon is central to the design of glucagon antagonists that might be clinically relevant.

Extensive structure function studies of glucagon have afforded some insight into the understanding of its mechanism of action. The general picture that has emerged is that the active pharmacophore is dispersed throughout the glucagon molecule and that the intact hormone is necessary for the expression of full hormonal activity. Nevertheless, specific active site residues responsible for either high affinity binding or activation have been singled out. We have demonstrated that the negatively charged side chain of aspartic acid residues at positions 9, 15, and 21 play important roles in either the binding or activity function of the hormone [1, 2]. The N-terminal histidine, which is strictly conserved within the family, furnishes determinants of both hormone binding and activity [3]. One of the earliest pieces of information to come from site-directed mutagenesis of the glucagon receptor protein identified Asp<sup>64</sup> in the extracellular N-terminal tail to be absolutely required for the recognition function of the receptor, which suggests it may interact with a complementary positive charge on the hormone [4]. Based on these initial findings, we assessed the contribution of the positively charged groups at positions 12, 17, and 18 to receptor recognition and activation, which had not been clearly established.

## Results and Discussion

We performed alanine substitutions replacing Lys<sup>12</sup>, Arg<sup>17</sup>, and Arg<sup>18</sup> of glucagon to examine the effect of eliminating the positive charge at those sites on binding and adenylyl cyclase activity (Table 1). Ala<sup>12</sup> and Ala<sup>18</sup> glucagon amides lost 80% binding affinity for the glucagon receptor in rat liver membranes, and Ala<sup>17</sup> lost 60%. Ala<sup>12</sup> and Ala<sup>18</sup> were capable of a full agonist response with a slight decrease in potency. In contrast, Ala<sup>17</sup> was a weak partial agonist that stimulated adenylyl cyclase with a potency of less than 1%. Intere-

Table 1. Position 12, 17, and 18 replacement analogs of glucagon.

Analog of glucagon amide	Binding affinity, %	Adenylyl cyclase activity	
		Maximu Activity, %	Related potency, %
Glucagon amide	100	100	15
1. Ala <sup>12</sup>	17.3	60	15.8
2. Ala <sup>17</sup>	38	20	0.013
3. Ala <sup>18</sup>	13	94.4	70.8
4. Ala <sup>17</sup> Ala <sup>18</sup>	8	97	27.5
5. Ala <sup>12</sup> Ala <sup>17</sup> Ala <sup>18</sup>	0.08	62	1.3
6. Asp <sup>12</sup>	0.6	78.4	10
7. Asp <sup>17</sup>	1.4	82.4	4.4
8. Asp <sup>18</sup>	0.22	69.2	0.24
9. Asp <sup>17</sup> Asp <sup>18</sup>	na		

stingly, despite a 90% loss in affinity Ala<sup>17</sup>Ala<sup>18</sup> exhibited only a moderate attenuation of activity. Substitution of all three positions with alanines in Ala<sup>12,17,18</sup> glucagon amide induced an almost complete loss of binding and reduced the potency of activation to 1%. Aside from an alanine scan, the positive residues were each replaced with an aspartic acid. Asp<sup>12</sup>, Asp<sup>17</sup>, and Asp<sup>18</sup> glucagon amides displayed poor binding affinities and stimulated adenylyl cyclase activation with reduced potencies. Unlike Ala<sup>17</sup>Ala<sup>18</sup>, however, Asp<sup>17</sup>Asp<sup>18</sup> was rendered incapable of receptor recognition. In general, for all the peptide analogs, the effect of the substitution on binding was functionally linked to activation. These results indicate that except for His<sup>1</sup>, the other positively charged amino acids of glucagon are not crucial for the activation function. In addition, unlike positions 9 and 15 where the precise location of an aspartic acid residue is critical to hormone/receptor interaction, it appears that glucagon binding affinity is not regulated by the topographic location of a specific positive charge but by a net positive charge. A neutral molecule was well tolerated but a negatively charged molecule was not. An overall positively charged glucagon molecule most likely contributes to the stabilization of the binding interaction with the glucagon receptor.

## References

1. Unson, C. G., Macdonald, D., Ray, K., Durrah, T. L., and Merrifield, R. B., *J. Biol. Chem.*, 266 (1991) 2763.
2. Unson, C. G., Wu, C.-R., and R. B. Merrifield, *Biochemistry*, 33 (1994) 6884.
3. Unson, C. G., Macdonald, D., and Merrifield, R. B., *Arch. Biochem. Biophys.*, 300 (1993) 747.
4. Carruthers, C. J. L., Unson, C. G., Kim, H. N., and Sakmar, T. P., *J. Biol. Chem.*, 269 (1994) 29321.

# Synthesis and activity of proteolysis-resistant GLP-1 analogs

**D.L. Smiley, R.D. Stucky, V.J. Chen, D.B. Flora, A. Kriauciunas,  
B.M. Hine, J.A. Hoffmann, W.T. Johnson, R.A. Owens,  
F.E. Yakubu-Madus and R.D. DiMarchi**

*Lilly Research Laboratories, Indianapolis, IN 46285, USA*

Glucagon-Like Peptide-1 (GLP-1) is produced by intestinal L cells in response to a meal and has two active forms that result from post-translational processing of the pre-proglucagon gene product[1]. GLP-1(7-37)OH and GLP-1(7-36)NH<sub>2</sub> interact with a specific receptor on pancreatic islets to stimulate insulin secretion during periods of hyperglycemia[2]. Both native forms have been administered to human patients by intravenous or subcutaneous routes and are equally efficacious[3]. The biological half-life of these native forms is rendered extremely short due to proteolysis by a widely distributed mammalian enzyme, dipeptidyl peptidase-IV (DPP-IV)[4]. DPP-IV cleaves the N-terminal dipeptide to yield des(7-8) products that have reduced affinity for the GLP-1 receptor. Removal of the amino group from the N-terminal residue of peptide hormones is known to impede DPP-IV cleavage and provides a longer acting molecule [5]. In this study, des-amino His<sup>7</sup> GLP-1 (designated IP) was prepared by SPPS and evaluated for its ability to release insulin in an hyperglycemic clamped rat model. Additional analogs with histidine-like character at the N-terminus were prepared and their resistance to DPP-IV cleavage in serum was measured as well as their ability stimulate cAMP in a functional GLP-1 receptor assay.

## Results and Discussion

The IP analog demonstrated an enhanced ability to stimulate insulin secretion relative to native GLP-1 (7-37)-OH in a normal Sprague Dawley rat (Table 1). Removal of the N-

*Table 1. Hyperglycemic clamped rat study: AUC response to peptide.*

Peptide (1.0ng/kg,IV)	Plasma Insulin Response (ng/ml*min)	Glucose Infusion Rate Change (mg/kg)
Vehicle	-0.265±1.8	39.41±10.16
GLP-1(7-37)OH	16.67±3.97	130.74±28.64
IP	25.57±3.61	324.43±45.35

terminal amino group resulted, however, in a reduced potency in stimulating cAMP in CHO cells transfected with the GLP-1 receptor (Table 2). Thus it appears that the increase in insulin secretion and infused glucose is a result of increased serum half-life. When Arg was substituted for Lys<sup>26</sup> in the IP analog cAMP potency was unexpectedly restored. Similarly, a di-methyl substitution on the  $\alpha$ -carbon of the 4-imidazole acetyl derivative (DMIA analog)

surprisingly also restored full cAMP potency to the unmethylated (IA analog) and monomethylated (MIA analog) imidazole acetyl derivatives. The disappearance of the native GLP-1 or an analog with simultaneous appearance of any des(7-8) cleavage product was measured by HPLC. A qualitative + was assigned if the starting peak disappeared very slowly and no des(7-8) appeared (Table 2).

Table 2. cAMP stimulation and serum stability of N-terminally modified GLP-1 analogs.

Analog	GLP-1 backbone	cAMP %Rel.Potency	Serum Stability
DMIA	(7-37)OH	108.0±22.4	+
native	(7-37)OH	100.0*	-
IP	Arg <sup>26</sup> (7-37)OH	89.0±12.6	+
native	(7-36)NH <sub>2</sub>	88.4±29.4	-
IA	(7-36)NH <sub>2</sub>	24.2±9.8	+
MIA	(7-37)OH	23.4±3.9	not determined
IP	(7-37)OH	21.9±7.8	+

DMIA=  $\alpha, \alpha$ -dimethyl-4- imidazole acetyl, IP= 4-imidazole propionyl, MIA=  $\alpha$ -methyl-4-imidazole acetyl, IA= 4-imidazole acetyl, \*EC<sub>50</sub>=0.20±0.02 (n=26)

## Conclusion

This SAR indicates that DPP-IV is the major proteolytic enzyme in sera and that an N-terminal amino group is required for GLP-1 cleavage. Novel histidine GLP-1 mimetics have been identified that inhibit DPP-IV proteolysis and retain significant potency relative to the native hormone. One or more of the His<sup>7</sup> derivatives may provide a GLP-1 analog more ideally suited for pharmaceutical use.

## References

1. Fehmann, H. and Habener, J., Trends in Endo. and Metab., 3(1992)158.
2. Holst, J., Gastroenterology, 107(1994)1848.
3. Fehmann, H., Goke, R. and Goke, B., Mol. and Cell. Endo., 85(1992)C39
4. Mentlein, R., Gallwitz, B. and Schmidt, W., Eur.J.Bio., 214(1993)829.
5. Frohman, L., Downs, T., Heimer, E., and Felix, A, J.Clin.Invest. 83(1989)1533.

# Homo-oligomeric opioid analogues and incorporation of 4-*trans*-aminomethylcyclohexanecarboxylic acid (Amcca)

DeAnna L. Wiegandt Long,<sup>a</sup> Peg Davis,<sup>b</sup> Frank Porreca<sup>b</sup>  
and Arno F. Spatola<sup>a</sup>

<sup>a</sup>Department of Chemistry, University of Louisville, Louisville, KY 40292 USA

<sup>b</sup>Department of Pharmacology, University of Arizona, Tucson, AZ 85721 USA

Synthesis of peptides on a lysine or oligolysine core was introduced by Tam as a novel method for antigen amplification [1]. We have previously shown, this technique can be useful for probing dimer or higher homologs of peptides with single or multiple bioactive sequences (homo-oligomeric or hetero-oligomeric peptides) [2]. In this report we explore the effects of various spacer elements between a dermorphin/deltorphin N-terminal sequence (Tyr-D-Ala-Phe) and the lysine amine functions. The novel amino acid, 4-*trans*-aminomethylcyclohexanecarboxylic acid (Amcca), and Aib were introduced as constrained linkages.

## Results and Discussion

Peptides were synthesized by solid phase techniques on Merrifield resin using orthogonal (Boc and Fmoc) amine-protecting groups. The peptides were purified using reversed phase high performance liquid chromatography and were characterized by amino acid analysis and electrospray-mass spectrometry. The 10 sequences and their *in vitro* opioid potencies are reported in Table 1.

Table 1. *In vitro* opioid bioassay results.

Structure	IC <sub>50</sub> (nM)	
	GPI	MVD
1 [YaFG] <sub>2</sub> K-Aca-A	804 ± 159	1502 ± 411
2 [YaFG-Aib] <sub>2</sub> K-Aca-A	1183 ± 82	350.1 ± 69.1
3 [YaFG-Aca] <sub>2</sub> K-Aca-A	683.3 ± 81.4	2586 ± 674
4 [YaF-Amcca-G] <sub>2</sub> K-Aca-A	1544 ± 234	1896 ± 438
5 [YaF-Aib] <sub>2</sub> K-Aca-A	1418 ± 92	1196 ± 830
6 [YaFE-Amcca] <sub>2</sub> K-Aca-A	10,000	1070 ± 140
7 [YaFG-Amcca] <sub>2</sub> K-Aca-A	1720 ± 170	348 ± 87
8 [YaF-Aib-Amcca] <sub>2</sub> K-Aca-A	1280 ± 80	277 ± 62
9 [YaF-Aib-Amcca-Amcca] <sub>2</sub> K-Aca-A	377 ± 77	380 ± 9
10 [YaF-Aib-Amcca-Amcca-Amcca] <sub>2</sub> K-Aca-A	445 ± 35	479 ± 44

Aca = aminocaproic acid; Amcca = 4-*trans*-aminomethylcyclohexanecarboxylic acid;  
Assays: GPI = guinea pig ileum; MVD = mouse vas deferens.

The dimeric opioid analogs shared a common C-terminus composed of -Lys-Aca-Ala-OH. The amino caproic acid spacer was chosen to minimize possible interference between the polystyrene backbone of the resin and the branched lysine during synthesis. The N-terminal opioid sequence Tyr-D-Ala-Phe was connected to the lysine amines using a variety of spacers ranging from the flexible glycine residue in structure **1** to the rigid Aib link with compound **4**; however there was little difference in biological potency between these two extremes. An even more flexible choice, combining Gly with Aca (compound **3**), likewise failed to improve potency. Since hydrophobic collapse might be a factor explaining the unexpected potency drop with these dimeric opioids, additional analogs were prepared incorporating varying lengths of the relatively rigid spacer moiety, Amcca. Somewhat surprisingly the *in vitro* results again showed little potency differences among the members of this series. NMR evidence (NOESY studies) did not reveal any evidence of intramolecular interaction between the dimer arms. In summary, a series of dimeric opioid analogs with flexible and rigid spacer arms showed a relatively constant level of potency and selectivity using standard functional assays.

### Acknowledgements

This work was supported by NIH GM-33376.

### References

1. Tam, J.P., Proc. Natl. Acad. Sci. USA, 85 (1988) 5409.
2. Wiegandt Long, D., Ma, W., Spatola, A.F., In Kaumaya P.T.P. and Hodges, R.S. (Eds.), Peptides: Chemistry, Structure and Biology (Proceedings of the 14th American Peptide Symposium), Mayflower, England, 1996, p. 595.

# Replacements at positions 17, 18, and 21 of glucagon leads to formation of a new salt bridge and to an increase in binding affinities

Dev Trivedi,<sup>a</sup> Jung-Mo Ahn,<sup>a</sup> Ying Lin,<sup>a</sup> John L. Krstenansky,<sup>a</sup>  
Stephen K. Burley<sup>b</sup> and Victor J. Hruby<sup>a</sup>

<sup>a</sup>Department of Chemistry, University of Arizona, Tucson, AZ 85721, USA and

<sup>b</sup>Howard Hughes Medical Institute, The Rockefeller University, New York, NY 10021, USA

The x-ray structure of the crystalline form of glucagon formed under basic conditions [1] shows that the C-terminal region of the molecule has an  $\alpha$ -helical structure. Earlier [2], it was reported that [Lys<sup>17,18</sup>,Glu<sup>21</sup>]glucagon exhibits increased receptor binding and adenylate cyclase potency with correlates with enhanced  $\alpha$ -helical content for the glucagon molecule. We have obtained the x-ray crystal structure of this superagonist analogue and explored the possibility that a salt bridge formation between charged side chains in position 18 and 21 may explain its seven fold increase in binding affinity. Five glucagon analogues were synthesized by substituting the Arg<sup>17</sup> and Arg<sup>18</sup> residues in a step-wise manner to further examine the features necessary for the formation of a salt bridge and its influence on biological activity.

## Results and Discussion

In the x-ray crystal structures (Fig. 1), the difference between glucagon and the superagonist was the formation of a salt bridge between the  $\alpha$ -amino group of Lys<sup>18</sup> and the carboxyl of

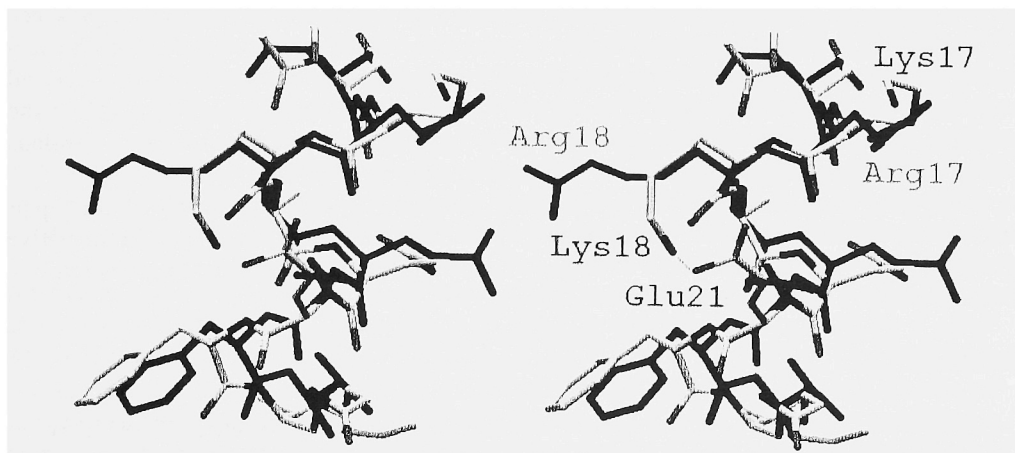


Fig. 1. Stereoview of superimposed fragments 16-23 of the crystal structures of glucagon (dark) and [Lys<sup>17,18</sup>,Glu<sup>21</sup>]glucagon (light).

Table 1. Biological activities of glucagon analogues.

Compound	Binding		Adenylate Cyclase	
	IC <sub>50</sub> (nM)	Relative Binding(%)	EC <sub>50</sub> (nM)	Maximum Stimulation(%)
1) Glucagon	1.5	100	5.6	100
2) [Lys <sup>17,18</sup> ,Glu <sup>21</sup> ]Glucagon	0.2	700	0.8	100
3) [Lys <sup>17</sup> ]Glucagon-NH <sub>2</sub>	0.7	220	2.2	100
4) [Lys <sup>18</sup> ]Glucagon-NH <sub>2</sub>	4.1	36	40.8	100
5) [Nle <sup>17</sup> ,Lys <sup>18</sup> ,Glu <sup>21</sup> ]Glucagon-NH <sub>2</sub>	1.0	150	1.7	100
6) [Orn <sup>17,18</sup> ,Glu <sup>21</sup> ]Glucagon-NH <sub>2</sub>	2.0	74	8.7	100
7) [D-Arg <sup>18</sup> ]Glucagon	25.0	6	158	78

(distance=2.4Å). We believe that this new salt bridge may stabilize the turn of an  $\alpha$ -helix at residues 18-21, which can explain the observed increase in a  $\alpha$ -helical content in the C-terminal region of the superagonist.

The binding affinities and adenylate cyclase activity of the glucagon analogues are summarized in Table 1. The ability to form a salt bridge between position 18 and 21 depends on the length and flexibility of the charged side chains in these positions and is evident from the binding affinity of analogues 2, 4, 5, and 6. The substitution for Arg<sup>17</sup> in analogues 3, 5, and 6 further decreases binding potency, which may suggest an independent role of the side chain in the position 17 for glucagon receptor interactions. For example, in analogues 3 and 5 where hydrophobic residues(Lys and Nle) are substituted for Arg<sup>17</sup>, it is observed that the binding affinity remains relatively high. This may imply that the presence of a hydrophobic pocket facilitates a better receptor fit. In analogue 7, where a D-amino acid is substituted, a big drop in binding potency is seen and this further supports the suggested requirement of a positive charge at position 18 for ligand binding to the receptor. All of the substitutions introduced do not seriously alter the amphipathic character of the C-terminus and allows these analogues to reach 78-100% stimulation of adenylate cyclase(Table 1).

The x-ray crystal structure of [Lys<sup>17,18</sup>,Glu<sup>21</sup>]glucagon suggests that the Lys<sup>18</sup>-Glu<sup>21</sup> pair is probably optimal for salt bridge formation, in contrast to the Arg<sup>18</sup>-Asp<sup>21</sup> pair in the native glucagon. The salt bridge is most likely the key feature responsible for the large increase in binding potency of the superagonist analogue.

## References

1. Sasaki, K., Dockerill, S., Admiak, D.A., Tickle, I.J. and Blundell, T., *Nature*, 257(1975)751.
2. Krestenansky, J.L., Zechel, C., Trivedi, D. and Hruby, V.J., *Int. J. Pep. Prot. Res.*, 20(1988)468.

# Design and synthesis of novel GnRH-endothelin chimeras

Dror Yahalom,<sup>a,b</sup> Yitzhak Koch,<sup>b</sup> Nurit Ben-Aroya<sup>b</sup> and Mati Fridkin<sup>a</sup>

<sup>a</sup>Departments of Organic Chemistry and Neurobiology, <sup>b</sup>Weizmann Institute of Science, Rehovot, 76100, Israel.

Gonadotropin releasing hormone (GnRH, pGlu-His-Trp-Ser-Tyr-Gly-Leu-Arg-Pro-Gly-NH<sub>2</sub>) is a decapeptide that regulates the reproductive system. Synthetic GnRH analogs may be used for contraception and for the treatment of various hormone-dependent diseases including prostate and breast cancers. In view of the significant clinical potential of GnRH analogs, the aim of our study was to design and synthesize GnRH-based chimeric peptides with augmented biopotency. Chimeric peptides which are composed of two different ligands for two distinct receptors may have the ability to bind these two receptors simultaneously. Cross-linking may enhance the binding affinity of each of the ligands in the chimera for its respective receptor. This model was previously suggested to account for the high affinity of chimeric peptides for both galanin and substance P receptors [1]. A VIP-neurotensin chimera was shown to be a potent VIP antagonist [2].

## Results and Discussion

We have used an antagonist of endothelin (ET) for these studies because pituitary gonadotropes express the ET<sub>A</sub> receptor [3]. The sequence of this antagonist {Ac-(D-Trp)-Leu-Asp-Ile-Ile-Trp, Ac-ETAnt} is derived from the C-terminus sequence of ET. Its IC<sub>50</sub> for ET<sub>A</sub> receptors is 130nM [4]. Since the free carboxylic moiety in the C-terminus of Ac-ETAnt is crucial for its binding to ET receptors, we have used its N-terminus for conjugation by utilizing the unacetylated peptide (ETAnt).

Two alternative approaches to combine EAnt with a GnRH analog were tested. The easiest synthetic procedure was to link EAnt via a spacer (ACA; aminocaproic acid) to the C-terminal residue of GnRH, resulting in a linear chimera (GnRH-Aca-EAnt). The second approach was based on various studies showing that position 6 of GnRH is tolerant to substitution by various D-amino acids and their bulky derivatives. We employed [D-Glu]<sup>6</sup>GnRH to construct [D-Glu-EAnt]<sup>6</sup>GnRH and two derivatives thereof containing a spacer between the two moieties: [D-Glu-ACA-EAnt]<sup>6</sup>GnRH and [D-Glu-Gly-Gly-Gly-EAnt]<sup>6</sup>GnRH. The conjugation of these chimeras was achieved using DCC/HOBT in solution. [D-Lys]<sup>6</sup>GnRH was conjugated to EAnt via a succinyl (Suc) spacer by a solid-phase condensation of soluble [D-Lys]<sup>6</sup>GnRH and Suc-EAnt-Wang-Resin. Cleavage from the resin resulted in the formation of [D-Lys-N<sup>ε</sup>-Suc-EAnt]<sup>6</sup>GnRH. The attempt to synthesize this chimera by condensation in solution has failed, probably due to unique steric hindrance of the free carboxyl moiety of the intermediate ([D-Lys-N<sup>ε</sup>-Suc]<sup>6</sup>GnRH). An alternative conjugation of EAnt to [D-Lys]<sup>6</sup>GnRH was achieved by reacting bromoacetyl AcBr]<sup>6</sup>GnRH) with Cys-EAnt to obtain [D-Lys-N<sup>ε</sup>-Ac-S-Cys-EAnt]<sup>6</sup>GnRH succinimide

Table 1. Binding affinities and *in vitro* activities of GnRh analogs.

Peptide	IC <sub>50</sub> (nM) <sup>a</sup>	ED <sub>50</sub> (nM) <sup>b</sup>
(D-Glu) <sup>6</sup> GnRH	2.5	0.5
(D-Glu-ETAnt) <sup>6</sup> GnRH	25	0.5
(D-Glu-Gly-Gly-Gly-ETAnt) <sup>6</sup> GnRH	40	0.5
(D-Glu-ACA-ETAnt) <sup>6</sup> GnRH	75	0.5
GnRH-Aca-ETAnt	-	-
(D-Lys) <sup>6</sup> GnRH	0.1	0.02
(D-Lys-N <sup>E</sup> -Suc-ETAnt) <sup>6</sup> GnRH	400	0.5
(D-Lys-N <sup>E</sup> -Ac-S-Cys-ETAnt) <sup>6</sup> GnRH	40	1.0

<sup>a</sup>IC<sub>50</sub> = the concentration required to displace 50% of <sup>125</sup>I-(D-Trp)<sup>6</sup>GnRH specific binding to rat pituitary homogenates. <sup>b</sup>ED<sub>50</sub> = the effective dose that gives 50% of maximal LH release from pituitaries of 12-day female rats *in vitro*.

ester with [D-Lys]<sup>6</sup>GnRH, and then condensing the resulting ([D-Lys-N<sup>E</sup>-Position 6 of (D-Glu)<sup>6</sup>GnRH is suitable for anchoring the hexapeptide ETAnt, without loss of binding affinity for the GnRH receptor or *in vitro* LH releasing activity (Table 1). Attachment of the same peptide (ETAnt) to the C-terminus of GnRH resulted in a linear chimera (GnRH-Aca-ETAnt) which does not bind the GnRH receptor and is devoid of any LH releasing activity (Table 1). This result is in agreement with previous reports demonstrating the importance of the GnRH C-terminus for receptor recognition. The introduction of small spacers between [D-Glu]<sup>6</sup>GnRH and ETAnt did not improve GnRH receptor affinity of the resulting chimeras. Chimeras based on [D-Lys]<sup>6</sup>GnRH, unlike those based on [D-Glu]<sup>6</sup>GnRH, exhibited extremely reduced binding affinity for the GnRH receptor in comparison with their congener GnRH analog (table 1). This low affinity may be explained by the masking of the D-Lys<sup>6</sup> side-chain or by conformational changes. All the chimeras as well as [D-Glu]<sup>6</sup>GnRH, but not [D-Lys]<sup>6</sup>GnRH, have demonstrated a discrepancy between their low GnRH binding affinity and their capacity to induce LH release (table 1). An explanation for our observations is yet to be found. Among all the above chimeras, only [D-Glu-ETAnt]<sup>6</sup>GnRH recognizes the ET<sub>A</sub> receptor (28% displacement of <sup>125</sup>ET-1 at 1μM, in comparison with 73% for Ac-ETAnt at the same concentration). Further studies are therefore required to test the potential application of the model of biceptor cross-linkers for the development of novel and potent GnRH analogs.

## References

1. Langel U., Land T., Bartfai T., *Int. J. Pept. Protein Res.*, 39 (1992) 516.
2. Gozes I., McCune S.K., Jacobson L., Warren D., Moody T.W., Fridkin M., Brenneman D.E., *J. Pharm. Exp. Ther.*, 257 (1991) 959.
3. Stojilkovic S.S., Balla T., Fukuda S., Cesnjaj M., Merelli F., Krsmanovic L.Z., Catt K.J., *Endocrinology*, 130 (1992) 465.
4. Doherty AM, Cody WL, DePue PL, et al, *J. Med. Chem.*, 36 (1993) 2585.

# Receptor specificity of [2,3-cyclopropane amino acids]-fMLP analogs

Hiroaki Kodama,<sup>a</sup> Eiichi Hirano,<sup>a</sup> Takahiro Yamaguchi,<sup>a</sup> Satoshi Osada,<sup>a</sup> Masaya Miyazaki,<sup>a</sup> Ichiro Fujita,<sup>b</sup> Sumio Miyazaki<sup>b</sup>  
and Michio Kondo<sup>a</sup>

<sup>a</sup>Department of Chemistry, Faculty of Science and Engineering, Saga University, Saga 840 and  
<sup>b</sup>Department of Pediatrics, Saga Medical School, Saga 849, Japan

Conformationally constrained 2,3-cyclopropane amino acids of bioactive peptides have been used to design receptor-specific and -selective compounds and to further clarify their structure-activity relationships [1]. We have synthesized chemotactic peptides, fMLP analogs containing optically active 2,3-cyclopropylphenylalanine,  $\nabla^E\text{Phe}^3\text{-fMLP}$  (Fig. 1) [2]. These results suggest that the  $\nabla^E\text{Phe}^3\text{-fMLP}$  analogs can discriminate between receptors of chemotaxis and superoxide production for human neutrophils. In the present study, to elucidate the role of fMLP analogs of cyclopropane amino acid in interactions with fMLP receptors, novel fMLP analogs containing 1-aminocyclopropane-1-carboxylic acid (Acc) (Fig. 1), Aib, D-Phe and L-Ala at the 3rd position were synthesized and examined for superoxide generation by human neutrophils.

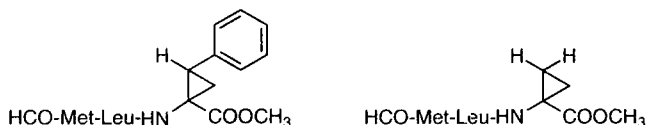


Fig. 1. Chemical structures of  $\nabla^E\text{Phe}^3\text{-fMLP}$  and  $\text{Acc}^3\text{-fMLP}$ .

## Results and Discussion

Peptide synthesis was carried out by solution method. Amino acid methyl ester was coupled with HCO-Met-Leu-OH by MA method. The structures of synthetic peptides were confirmed by <sup>1</sup>H-NMR. Biological activities of synthetic analogs were evaluated as the superoxide production by human neutrophils as previously described [3].

With the 1  $\mu\text{M}$  dose of Z-form analogs, (2S,3S)- and (2R,3R)- $\nabla^E\text{Phe}^3\text{-fMLP-OME}$  showed the same activity levels as fMLP and fMLP-OME. However, both  $\nabla^E\text{Phe}$  analogs, (2S,3R)- and (2R,3S)- $\nabla^E\text{Phe}^3\text{-fMLP-OME}$  were almost inactive for superoxide production. It was suggested that the receptors or receptor subtypes for superoxide production prefer the Z-configuration of the side-chain of Phe<sup>3</sup> residue with strict chiral selectivity. At the same concentration,  $\nabla^E\text{Phe}^3\text{-fMLP-OME}$  showed rapid cytoplasmic calcium mobilization (data not shown). From the results, two E-form analogs of Phe<sup>3</sup>-fMLP-OME could bind to some of the fMLP receptors but are not able to activate membrane-bound NADPH-oxidase complex. All the analogs containing Acc, Aib, D-Phe and L-Ala in position 3 were almost

inactive at 100 nM concentration and had significant activities at 1  $\mu$ M (56%, 24%, 69% and 31% activity against for optimal dose of fMLP (1  $\mu$ M), respectively). To investigate the effect of cytoplasmic calcium ion mobilized by  $\nabla^E$ Phe<sup>3</sup>-fMLP-OMe, synergistic effects of superoxide production were investigated. Five minutes after addition of fMLP analog (100 nM), which does not induce significant activity, the cells were activated by the stimulant fMLP (1  $\mu$ M). The response of superoxide production to an optimal dose of fMLP was enhanced more than 1.6 and 2.5 times after pretreatment with the  $\nabla^E$ Phe and Acc analogs, respectively (Fig. 2). This synergistic effect was also observed for the analog containing D-Phe residues. This phenomenon is known as priming of neutrophils; that is, after interaction with enhancing or priming agents, IFN- $\gamma$ , calcium ionophore and platelet-activating factor, the biological response in human neutrophils is not activated, but is enhanced upon subsequent stimulation with fMLP [4-6]. The molecular mechanism of this priming reaction is still unknown. Koenderman et al. [6] reported that multiple pathways, such as calcium-dependent and -independent routes, are involved in neutrophil priming. In our experiments, the priming caused by cyclopropane-fMLP analogs was maximal within 5 min. From the results, it can be concluded that these priming reactions, induced by  $\nabla^E$ Phe and Acc analogs, have calcium-dependent mechanisms.

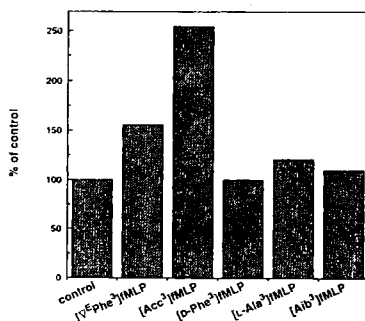


Fig. 2. Priming reaction of fMLP analogs for superoxide production.

## References

1. Stammer, C.H., Tetrahedron., 46 (1990) 2231; Kodama, H. and Shimohigashi, Y., J. Synth. Org. Chem, Jpn., 53 (1994) 180.
2. Miyazaki, M., Kodama, H., Fujita, I., Hamasaki, Y., Miyazaki, S. and Kondo, M., Peptide Chemistry, 1994 (1995) 293.
3. Miyazaki, M., Kodama, H., Fujita, I., Hamasaki, Y., Miyazaki, S. and Kondo, M., J. Biochem., 117 (1995) 489.
4. Nathan, C.F., Murray, H.W., Wiebe M.E. and Rubin, B.Y., J. Exp. Med., 158 (1983) 670.
5. Weisbart, R.H., Golde, D.W., Clark, S.C., Wong, G.G. and Gasson, C., Nature, 314 (1985) 361.
6. Koenderman, L., Yazdanbakhsh, M., Roos, D. and Verhoeven, A.J., J. Immunol., 142 (1989) 623.

# Synthesis of short analogs of neuropeptide Y specific for the Y2 receptor using the TASP concept

Eric Grouzmann,<sup>a</sup> Alain Razaname,<sup>b</sup> Gabriele Tuchscherer,<sup>b</sup> Maria Martire<sup>c</sup> and Manfred Mutter<sup>b</sup>

<sup>a</sup>Division of Hypertension, CHU Vaudois, CH-1011 Lausanne, Switzerland; <sup>b</sup>Institute of Organic Chemistry, University of Lausanne, CH-1015 Lausanne, Switzerland; <sup>c</sup>Institute of Pharmacology, Catholic University of S. Heart, I-00168 Rome, Italy

Neuropeptide Y (NPY) is a 36-amino acid peptide that exerts many biological effects [1]. Y2 receptors mediate the inhibition of catecholamine release [2]. Specific antagonists for the Y2 receptors have not yet been described. Based on the concept of template-assembled synthetic proteins (TASP), we have used a cyclic template molecule containing two  $\beta$ -turn mimetics [3] for covalent attachment of two, three or four copies of the C-terminal fragment RQRYNH<sub>2</sub> (NPY 33-36) resulting in TASP molecules of the type T<sub>4</sub>-n[NPY(33-36)] with n= 2, 3, 4 .

## Results and Discussion

Using the TASP concept, the C-terminal tetrapeptide of NPY (RQRY) was attached to the topological template c[Amn-K-G-K] via its N-terminal end applying oxime bond formation and orthogonal protection. TASP molecules exhibiting two, three or four copies of NPY(33-36) were prepared. Their chemical integrity was confirmed by HPLC and ES-MS. Receptor binding studies using SKN-MC and LN 319 cell lines reveal selective binding of the TASP molecules to the Y2 receptor, e.g. T<sub>4</sub>- 4[NPY(33-36)] binds to LN 319 cells with an IC<sub>50</sub> of 67.2 nM but only with low affinity to the Y1 receptor (IC<sub>50</sub>= 6.6 $\mu$ M) (Table 1). In contrast, the two constituent elements, i.e. the template molecule and the individual NPY(33-36) tetrapeptide, bound neither to Y1 nor to Y2 [4].

Table 1. Receptor binding of NPY and analogs to Y1 and Y2 receptors.

Peptide	IC50 (nM) Y1 receptor	IC50 (nM) Y2 receptor
1-36 NPY	0.5	0.085
13-36 NPY	1000	0.126
33-36 NPY	>10000	>10000
T <sub>4</sub> -[NPY(33-36)] <sub>2</sub>	>10000	680
T <sub>4</sub> -[NPY(33-36)] <sub>3</sub>	>10000	137.5
T <sub>4</sub> -[NPY(33-36)] <sub>4</sub>	6600	67.2
Template, T <sub>4</sub>	>10000	>10000

To assess whether these peptidomimetics have intrinsic agonist/antagonist activity we tested their ability to inhibit cAMP accumulation in a Y2 expressing cell line. All these TASP

molecules had no effect on forskolin-stimulated cAMP levels at concentrations up to 10  $\mu$ M. Confocal microscopy also was used to examine the NPY-induced increase in intracellular calcium in single LN 319 cells. Preincubation of the cells with T<sub>4</sub>-4[NPY(33-36)] at concentrations ranging from 0.1 nM to 10  $\mu$ M shifted the dose-response curve for free calcium mobilization induced by NPY to the right (Figure 1a). No intrinsic agonistic properties either of calcium or cAMP transduction systems were observed. Finally, we assessed the competitive antagonist properties of T<sub>4</sub>-4[NPY(33-36)] at presynaptic peptidergic Y<sub>2</sub> receptors by measuring the blockade of the inhibitory action of a Y<sub>2</sub> agonist on K<sup>+</sup>-induced <sup>3</sup>H-norepinephrine release from perfused rat hyperthalamic synaptosomes. The compound caused a right shift of the concentration-response curve of NPY13-36, a Y<sub>2</sub> agonist fragment, yielding a pA<sub>2</sub> of 8.48 (Figure 1b) and therefore, demonstrating that T<sub>4</sub>-4[NPY(33-36)] acts as a fully competitive antagonist.

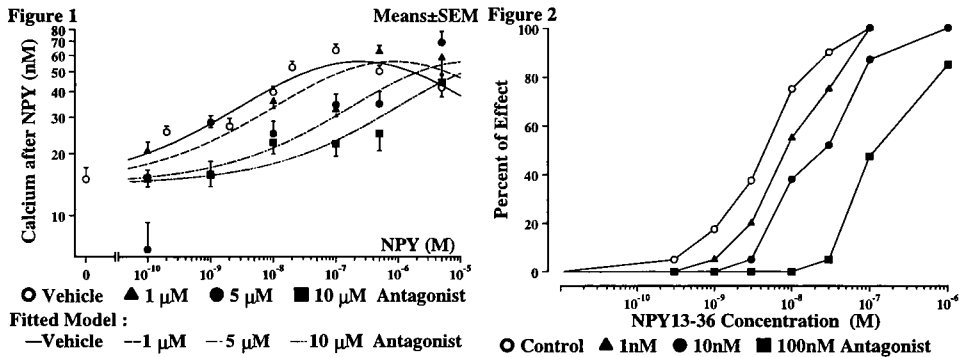


Fig. 1. (a) Geometric means of the calcium response to NPY in cells treated with T<sub>4</sub>-4 [NPY(33-36)]; (b) dose-response curve of the inhibitory effect of the NPY13-36 fragment on <sup>3</sup>H-norepinephrine release in rat hypothalamus in the presence of T<sub>4</sub>-4[NPY(33-36)].

In conclusion, by the covalent attachment of multiple copies of NPY(33-36) to a topological template, we obtained TASP molecules that specifically bind to the Y<sub>2</sub> receptor; consequently, the TASP concept should provide a valuable tool for studying receptor specificities and result in novel selective antagonists for NPY.

## References

1. Tuchscherer, G. and Mutter, M., *J. Pept. Science*, 1 (1994) 3.
2. Wahlestedt, C. and Reis, D.J., *Annu. Rev. Pharmacol. Toxicol.*, 32 (1993) 309.
3. Ernest, I., Kalvoda, J., Sigel, C., Rihs, G., Fritz, H., Blommers, M.J.J., Raschdorf F., Francotte, E. and Mutter, M., *Helv. Chim. Acta*, 1539 (1993) 1539.
4. Grouzmann, E., Martire, M., Razaname, A. and Mutter, M., *J. Biol. Chem.*, 272 (1997) 7699.

# Interaction with membranes of peptides related to the fusogenic region of PH-30 $\alpha$ , a sperm-egg fusion protein

Haruhiko Aoyagi,<sup>a</sup> Miyuki Kimura,<sup>a</sup> Takuro Niidome,<sup>a</sup>  
Tomomitsu Hatakeyama<sup>a</sup> and Hisakazu Mihara<sup>b</sup>

<sup>a</sup>*Faculty of Engineering, Nagasaki University, Nagasaki 852, Japan*

<sup>b</sup>*Faculty of Bioscience and Biotechnology, Tokyo Institute of Technology,  
Yokohama 226, Japan*

The peptide sequence of PH-30 $\alpha$ , a protein active in sperm-egg fusion, was deduced from its nucleotide sequence. Based on characteristics of virus fusion proteins a potential fusogenic region in PH-30 $\alpha$  was estimated to be residues 90-111 [1]. The presence of a Lys<sup>89</sup> residue and two Pro<sup>99</sup>-Pro<sup>100</sup> residues before and within the fusogenic peptide region attracts one's attention because fusogenic peptides have often been found to be cationic and Pro-Pro sequence may play varied roles in structure and/or activity. In order to investigate the property of the putative fusogenic region, we synthesized three related peptides: sperm fusion peptide (SFP)22 (residues 90-111), SFP23 (residues 89-111; Ac-KLIATGISSIPPIRALFAAIQIP-NH<sub>2</sub>) and SFP23AA in which the Pro-Pro sequence of SFP23 was replaced with Ala-Ala, their secondary structures and activities were examined against lipid membranes and blood cells [2].

## Results and Discussion

The peptide amides were prepared by stepwise elongation of Fmoc-amino acids on SAL-resin. CD measurement indicated that the structures of SFP22 and SFP23 were random in buffer solution (pH 7.4), while SFP23AA showed a  $\beta$ -structural spectrum. In TFE, all peptides showed some  $\alpha$ -helical content. In the presence of DPPC or DPPC/DPPG (3/1) SUV, SFP22 and SFP23 were predominant in  $\beta$ -structure, while SFP23AA gave an  $\alpha$ -helix-like CD curve. Similar CD curves were obtained for these peptides in the presence of DOPC or DOPC/DOPG (3/1) LUV. The FT-IR study showed that these peptides were rich in  $\beta$ -structure.  $\langle P_{\alpha} \rangle$  and  $\langle P_{\beta} \rangle$  values were calculated to be 1.02 and 1.08 for SFP22, 1.03 and 1.08 for SFP23, and 1.10 and 1.10 for SFP23AA, respectively. Therefore, it is essentially difficult for SFP22 and SFP23 to take on an  $\alpha$ -helical structure, while SFP23AA can adopt either an  $\alpha$ -helix or a  $\beta$ -structure according to its environment. In this connection, Muga et al. reported that a synthetic peptide which corresponds to 89-112 of PH-30 $\alpha$  took a  $\beta$ -structure upon interaction with lipid membranes [3].

The CF-leakage activities of the peptides were different in the presence of DOPC or DOPC/DOPG (3/1) vesicles. The membrane-perturbing activity of SFP23AA was 3-5 times higher than that of SFP23 at the peptide concentration of 1  $\mu$ M. SFP23 showed lower activity than SFP22, but the effect of Lys<sup>89</sup> was small. Comparison of the three peptides in

lysing human erythrocytes showed that none of the peptides had any appreciable activity, meaning that the membrane-perturbing action of the peptides was not strong enough to disturb biomembranes.

Fusogenic activities of the peptides were evaluated by intermixing measurement. FP23 was much more potent in fusogenic activity than SFP23AA in DOPC/DOPG (3/1) vesicles (Fig. 1). The fusogenic activity of SFP23AA was very weak, indicating that the presence

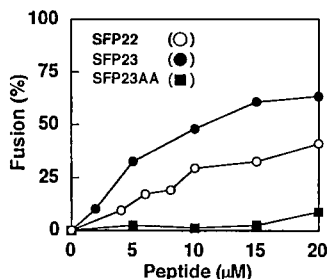


Fig. 1. Profiles of membrane-mixing of DOPC/DOPG (3/1) liposomes by peptides.

of the Pro-Pro sequence is very important for activity. The fact that SFP23 showed high fusogenic activity supports the speculation reported by Blobel et al. [1]. Removal of the Lys residue from SFP23 reduced the activity, indicating that the presence of Lys is favorable but not essential. Proline residues are often involved in biological activity in various kinds of peptides and proteins. For example, a pardaxin analog with Ala instead of Pro<sup>13</sup> had much less cytolytic activity than pardaxin despite the analog's higher indicating that the hinge structure formed by the Pro residue was essential for activity [4]. Together with this and other findings, it may be concluded that the Pro-Pro sequence plays a role in stabilizing the active secondary structure of the fusogenic region of PH-30α in membranes.

## References

1. Blobel, C. P., Wolfsberg, T. G., Turck, C. W., Myles, D. G., Primakoff, P. and White, J. M., *Nature*, 356 (1992) 248.
2. Niidome, T., Kimura, M., Chiba, T., Ohmori, N., Mihara, H. and Aoyagi, H., *J. Peptide Res.*, in press.
3. Muga, A., Neugebauer, W., Hiram, T. and Surewicz, W. K., *Biochemistry*, 33 (1994) 4444.
4. Shai, Y., Bach, D. and Yanovsky, A., *J. Biol. Chem.*, 265 (1990) 20202.

# Elucidation of the conformational features within a series of tetrapeptides which determine the selective recognition of $\mu$ versus $\delta$ opioid receptors

Jeffrey C. Ho, Carol A. Mousigian, Henry I. Mosberg

College of Pharmacy, University of Michigan, Ann Arbor, MI 48109 USA

We have previously described the cyclic  $\mu$  opioid receptor selective tetrapeptide Tyr-c[*D*-Cys-Phe-*D*-Pen]NH<sub>2</sub> (S-Et-S) (JOM-6) [1]. In the present study we report the development of a  $\mu$  receptor pharmacophore model using residue 1 and 3 JOM-6 analogs. The  $\mu$  opioid pharmacophore groups of JOM-6 (i.e., the phenol and N $\alpha$  group of Tyr<sup>1</sup> and the phenyl group of Phe<sup>3</sup>) lie outside the cyclic portion of the tetrapeptide and are conformationally labile. In contrast to the pharmacophore groups, the tripeptide cycle (a 13-membered ring) experiences only moderate flexibility by virtue of the ethylene dithioether cyclization. To reduce peptide flexibility several residue 1 and 3, and peptide cycle analogs of JOM-6 were prepared. The residue 1 and 3 analogs include: *trans*-3-(4'-hydroxyphenyl)proline (*t*-Hpp) and 2-amino-6-hydroxytetralin-2-carboxylic acid (Hat) in the place of Tyr<sup>1</sup>, and  $\Delta$ EPhe in the place of Phe<sup>3</sup>. The peptide cycle analogs incorporate disulfide (S-S) or ethyne dithioether (S-*cis*-HC=CH-S) bridges instead of an ethylene dithioether (S-Et-S) bridge. The low energy conformations of each of these analogs were generated using molecular mechanics and then compared to deduce the probable  $\mu$  receptor bound conformation of JOM-6 and its analogs.

## Results and Discussion

In comparison with the *t*-Hpp<sup>1</sup>, Hat<sup>1</sup>, and ethyne dithioether derivatives of JOM-6, all of which displayed high affinity ( $K_{j\mu} < 4$  nM) to  $\mu$  receptor sites, the fourth analog employed for this study, Tyr-c[*D*-Cys- $\Delta$ EPhe-*D*-Pen]NH<sub>2</sub>(S-S) (JH-42), displayed slightly reduced  $\mu$  affinity ( $K_{j\mu} = 8.74$  nM). After identifying all possible low energy conformations for each analog (with  $\Delta E < 4$  kcal/mol), the sets of conformations were overlaid to determine the probable  $\mu$  receptor bound geometry of these tetrapeptides. The receptor bound conformation of JOM-6 requires a  $\chi^1$  orientation of *trans* ( $\sim 180^\circ$ ) for the sidechains of both Tyr<sup>1</sup> and Phe<sup>3</sup>.

The  $\mu$  receptor bound conformation of JOM-6 was compared with the previously reported  $\delta$  receptor bound conformation of Tyr-c[*D*-Cys-Phe-*D*-Pen]OH(S-S) (JOM-13) [2,3] to delineate the conformational features which determine  $\mu$  versus  $\delta$  receptor selective binding (Fig. 1). Overlap is observed between the conformations of the Tyr<sup>1</sup>

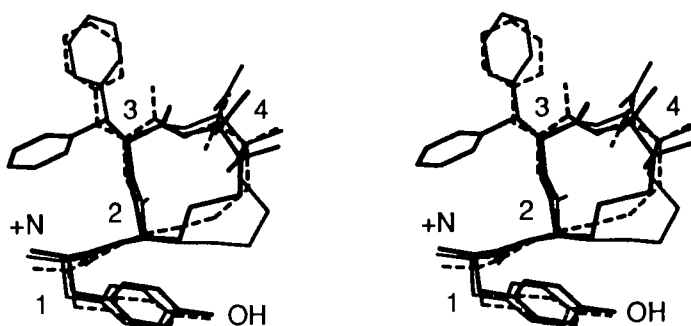


Fig. 1. Superposition (stereoview) of the  $\mu$  receptor bound conformations of JOM-6 (solid line) and the disulfide-containing tetrapeptide analog JH-42 (dashed line) and the  $\delta$  receptor bound conformation of JOM-13 (bold solid line). The C $\alpha$  atom of residue 3 and the functionally important N $\alpha$ , O $\eta$ , C $\eta$ , C $\epsilon$ 1, and C $\epsilon$ 2 atoms of Tyr<sup>1</sup> were used for the superposition.

residue as well as the mainchain atoms within the peptide cycles, including the C-terminal functional groups. The most apparent difference lies in the orientation of the aromatic ring of residue 3. Unlike the *trans* ( $\chi^1 \sim 180^\circ$ ) orientation required for residue 3 of the  $\mu$  bound geometry, the  $\delta$  bound geometry requires a *gauche*<sup>+</sup> ( $\chi^1 \sim -60^\circ$ ) orientation. By comparing the  $\mu$  and  $\delta$  pharmacophore models developed from the structurally similar JOM-6 and JOM-13 tetrapeptides, the conformational feature underlying  $\mu$  versus  $\delta$  receptor selectivity in this series appears to be the orientation of the aromatic ring of Phe<sup>3</sup>.

## Acknowledgments

This work was supported by the National Institute on Drug Abuse (DA03910). J.C.H. gratefully acknowledges the financial support of pre-doctoral fellowships from the American Foundation for Pharmaceutical Education and the Horace H. Rackham School of Graduate Studies, as well as a Training Grant from the National Institutes of Health (T32 GM0767).

## References

1. Mosberg, H. I., Omnaas, J. R., Medzihradsky, F., Smith, C. B., *Life Science*, 43 (1988) 1013-1020.
2. Mosberg, H. I., Lomize, A. L., Wang, C., Kroona, H., Heyl, D. L., Sobczyk-Kojiro, K., Ma, W., Mousigian, C., Porreca, F., *J. Med. Chem.*, 37 (1994) 4371-4383.
3. Mosberg, H. I., Omnaas, J. R., Lomize, A. L., Heyl, D. L., Nordan, I., Mousigian, C., Davis, P., Porreca, F., *J. Med. Chem.*, 37 (1994) 4384-4391.

## Structure activity relationships of NDF isoforms

**T. J. Zamborelli,<sup>a</sup> G. S. Elliot,<sup>b</sup> S. Hara,<sup>b</sup> D. L. Lacey,<sup>b</sup> D. M. Lenz,<sup>a</sup> N. Lu,<sup>b</sup> S. K. Pekar,<sup>b</sup> B. Ratzkin,<sup>b</sup> J. E. Tarpley,<sup>b</sup> J. S. Whoriskey,<sup>b</sup> S. K. Yoshinaga<sup>b</sup> and J. P. Mayer<sup>a</sup>**

<sup>a</sup>Amgen Inc., 3200 Walnut St. Boulder, CO 80301, USA; <sup>b</sup>Amgen Inc., 1840 DeHavilland Dr., Thousand Oaks CA 91320, USA

NDF (*neu* differentiation factor), also known as heregulin, was first isolated from rat fibroblasts and subsequently shown to stimulate the growth and development of mammary epithelial cells *in vitro* [1,2]. Structurally, the proteins share a heparin binding domain, an IgG domain and an EGF-like domain encompassing residues 177-228. Splicing within the C-terminal region of this domain gives rise to  $\alpha$  and  $\beta$  isoforms. To define the structure-activity relationships between the  $\alpha$  and  $\beta$  isoforms, we synthesized their respective EGF domains, named NDF<sub>e</sub> $\alpha$  and NDF<sub>e</sub> $\beta$ . The EGF domains of the  $\alpha$  and  $\beta$  isoforms are homologous in the 177-212 region but differ in the 213-228 region. To define the functional significance of this heterogeneity, two chimeric sequences, NDF<sub>e</sub> $\alpha/\beta$  and NDF<sub>e</sub> $\beta/\alpha$  were synthesized, in which the 222-228 tail regions were “swapped” between the native sequences. The four NDF<sub>e</sub> domain structures were evaluated in cellular and cell-free assays along with the full length NDF  $\alpha$  and  $\beta$  proteins.

### Results and Discussion

The EGF domains of the NDF  $\alpha$  and  $\beta$  isoforms (NDF<sub>e</sub> $\alpha$  and NDF<sub>e</sub> $\beta$ ) as well as the two hybrid sequences (NDF<sub>e</sub> $\alpha/\beta$  and NDF<sub>e</sub> $\beta/\alpha$ ) were synthesized by solid phase synthetic methodology using the Fmoc/*t*-Bu protocol [3,4]. The final materials were shown to be homogeneous by a number of analytical criteria including amino acid analysis, sequence analysis, mass determination and enzymatic fragmentation.

The NDF<sub>e</sub> $\alpha/\beta$  chimera induced morphological changes in the LIM 1215 (colonic epithelial) cell line and stimulated phosphorylation activity in contrast to the NDF<sub>e</sub> $\beta/\alpha$  chimera, which showed no activity. A quantitative profile of the proliferative activity effects for all NDF<sub>e</sub> minimal domains is summarized in Fig 1. It shows that the NDF<sub>e</sub> $\alpha/\beta$  chimeric structure is equipotent to the NDF<sub>e</sub> $\beta$  native sequence. These strongly suggest that the key structural determinant for NDF $\beta$  activity in the stimulation of colonic epithelium resides in the 7 C-terminal residues of the EGF domain.

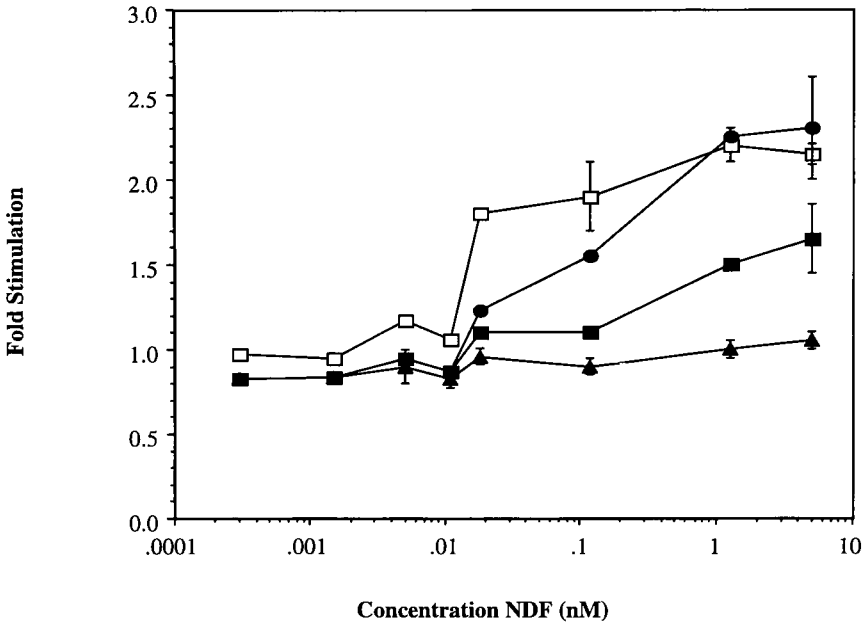


Fig. 1. Proliferative activity effects for all  $NDF_e$  minimal domains. (Solid squares -  $NDF_e\alpha$ , circles -  $NDF_e\beta$ , open squares -  $NDF_e\alpha/\beta$ , triangles -  $NDF_e\beta/\alpha$ ).

## References

1. Holmes, W.E., Sliwkowski, M.X., Akita, R.W., Henzel, W.J., Lee, J., Park, J.W., Yansura, D., Abadi, N., Raab, H., Lewis, G.D., Shepard, H.M., Kuang, W-J., Wood, W.I., Goeddel, D.V., Vandlen, R.L. *Science*, 256 (1992), 1205-1210.
2. Wen, D., Peles, E., Cupples, R., Suggs, S.V., Bacus, S.S., Luo, Y., Trail, G., Hu, S., Silbiger, S.M., Levy, R.B., Koski, R.A., Lu, H.S., and Yarden, Y., *Cell*, 69 (1992), 559-572.
3. Merrifield, R.B. *J. Am. Chem. Soc.*, 85 (1963), 2149-2154.
4. Atherton, E. and Sheppard, R.C. *Solid Phase Peptide Synthesis, A Practical Approach*. IRL Press, Oxford, 1989.

# Solid state conformation of constrained Somatostatin analogs with high potency and specificity for the $\mu$ -opioid receptor

Judith L. Flippen-Anderson,<sup>a</sup> Jeffrey R. Deschamps,<sup>b</sup> Christi Moore,<sup>a</sup> Clifford George,<sup>a</sup> Victor J. Hruba,<sup>b</sup> Wieslaw Kazmierski<sup>b</sup> and G. Gregg Bonner<sup>b</sup>

<sup>a</sup>Laboratory for the Structure of Matter, Naval Research Laboratory, Washington, D. C. 20375

<sup>b</sup>Department of Chemistry, University of Arizona, Tucson, AZ 85721, USA

Somatostatin (H-Ala-Gly-Cys-Lys-Asn-Phe-Phe-Trp-Lys-Thr-Phe-Thr-Ser-Cys-OH), an important regulatory hormone, is distributed throughout the central and peripheral nervous system. Residues 7-10 are essential for its activity and its potency can be increased by substitution of D-Trp for L-Trp in the 8th position. Somatostatin has also been shown to have some neurotransmitter-like properties. It binds weakly at opioid receptors and at high doses can cause an *in vivo* analgesic response in mice. These activities have led to research aimed at developing somatostatin-like analogs with potent and receptor-specific opioid activity and little or no somatostatin-like activity. This work has centered on the design and synthesis of a series of conformationally restricted cyclic octapeptides containing residues 7 - 10 of somatostatin. D-Trp was substituted for the L-Trp of the native hormone. The parent peptide of this series is CTP (D-Phe-Cys-Tyr-D-Trp-Lys-Thr-Pen-Thr-NH<sub>2</sub>), which was found to be a highly selective and potent antagonist for the  $\mu$  opioid receptor that is much longer acting than naloxone. Modifications of CTP have involved substitutions at positions 1 and/or 5. Substituting Arg or Orn for Lys gives CTAP and CTOP. Replacing residue 1 with D-Tic produces TCTAP and TCTOP respectively. CTAP and CTOP are the most potent  $\mu$  antagonists of the series, having an activity more than 10 times that of naloxone.

## Results and Discussion

NMR studies indicated that these compounds would form a type II'  $\beta$ -bend around D-Trp-R (R=Lys, Arg or Orn) and that both the peptide backbone and side chains would be conformationally flexible [1,2]. These conclusions are reinforced by solid state studies on Somatostatin analogs. An X-ray study has been done on the synthetic somatostatin analog octreotide [3], which differs from CTAP at residues 3,5 and 6 (Phe, Lys and Cys in octreotide and Tyr, Arg and Pen in CTAP). It crystallizes with three molecules in the asymmetric unit all of which show a type II'  $\beta$ -bend around residues 4 and 5 (D-Trp - Lys) but with two different conformations around the S-S bridge. Lys is gauche<sup>-</sup> and D-Trp is trans in all three molecules, yet they exhibit three distinct orientations which differ from one another. Crystallization conditions have been determined for both CTAP and TCTAP. The crystals are too small for analysis by traditional serial X-Ray diffractometers but TCAP has been collected using a CCD solid state optical detector coupled to a high energy rotating anode X-Ray source. TCTAP crystals surveyed to date have not scattered beyond

2Å resolution. A very thin CTAP crystal (0.3 x 0.2 x 0.015 mm) yielded data to ~1.5Å resolution. At this resolution the backbone flat  $\beta$ -bend of the peptide is clearly defined as the orientation of the Tyr and Phe side chains (Fig 1). Both the Arg and Trp residues appear to have multiple orientations and approximately 20% of the total scattering is due to disordered solvent molecules. This helps explain why these crystals diffract more like proteins than small amino acids. CTAP has a type II'  $\beta$ -bend around residues 4 and 5 (D-Trp - Arg) making it possible to derive three possible orientations for the D-Trp residue by doing backbone fits for residues 4 and 5 of CTAP with residues 4 and 5 of the three octreotide molecules. Initial least-squares refinement indicates that all three orientations would be allowable in the CTAP unit cell. Attempts continue to get better crystals of both compounds.

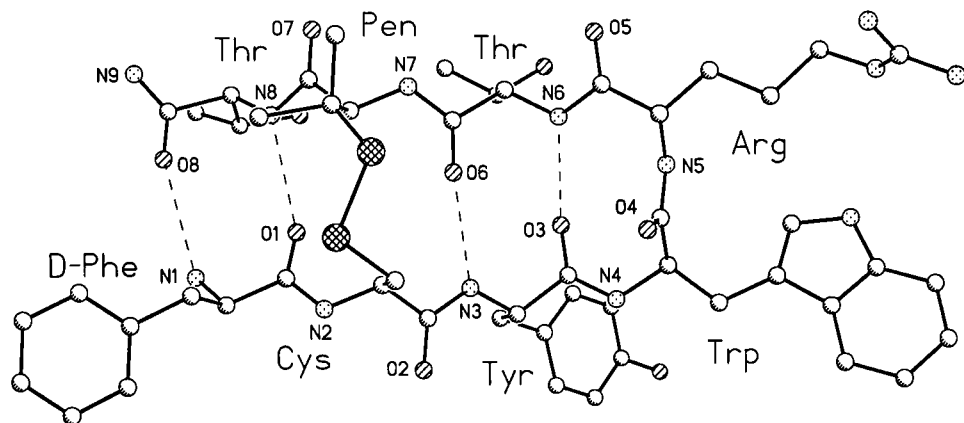


Fig. 1. Solid state conformation of CTAP indicating the four intramolecular hydrogen bonds. For clarity only 1 of the possible conformations for the D-Trp and Arg side-chains is shown.

## References

1. Veber, D. F. in Rich, D. F. and Gross, E. (Eds), Peptides: Synthesis, Structure, Function, Pierce Chemical Company, Rockford, IL, 1981, 3.
2. Pelton, J. T., Whalon, M., Cody, W. L. and Hruby, V. J., Int. J. Peptide Protein Res., 31 (1988) 109.
3. Pohl, E., Heine, A., Sheldrick, G., Dauter, Z., Wilson, K. S., Kallen, J., Huber, W., and Pfaffli, P. J., Acta Cryst, D51 (1995) 48.

## Design, synthesis and biological activity of cyclic GHRP-6 analogues

Kjeld Madsen,<sup>a</sup> Peter H. Andersen,<sup>b</sup> Birgit Sehested Hansen,<sup>a</sup>  
Nils Langeland Johansen<sup>a</sup> and Henning Thøgersen<sup>a</sup>

<sup>a</sup>Med Chem Research, Novo-Nordisk A/S, Novo Nordisk Park, DK-2760 Måløv, Denmark

<sup>b</sup>Receptor Technologies, DK-2600 Glostrup, Denmark

Growth Hormone (GH) secretion is normally stimulated by GHRH. In 1984 C.Y. Bowers and F.A. Momany synthesized the hexa-peptide Growth Hormone Releasing Peptide (GHRP-6) and discovered its ability to stimulate GH release in various species [1]. With the aim to identify the bioactive conformation of GHRP-6, a series of constrained monocyclic analogs were prepared. The cyclizations involved the termini and/or the side chains and, in some of the analogs, a reduced peptide bond was also introduced.

### Results and Discussion

As a part of a SAR study the four analogs 2, 3, 4, 5 were synthesized and tested to evaluate the importance of the positively charged functionalities in GHRP-6 for their ability to induce GH release *in vitro* from rat pituitary cells in primary culture [2] (Table 1).

Table 1. GH releasing potency and antagonism of peptides a rat pituitary cell assay.

No.	Sequence	EC <sub>50</sub> nM	IC <sub>50</sub> nM
1	H-His-D-Trp-Ala-Trp-D-Phe-Lys-NH <sub>2</sub>	1.7	
2	H-His-D-Trp-Ala-Trp-D-Phe-NH <sub>2</sub>	10	
3	H-D-Trp-Ala-Trp-D-Phe-Lys-NH <sub>2</sub>	25	
4	Acetyl-His-D-Trp-Ala-Trp-D-Phe-Lys-NH <sub>2</sub>	51	
5	Propionyl-D-Trp-Ala-Trp-D-Phe-NH-hexyl	10 <sup>4</sup>	
6	$\square$ -His-D-Trp-Ala-Trp-D-Phe-Lys $\square$	2000	
7	H-Glu-D-Trp-Ala-Trp-D-Phe-Lys-NH <sub>2</sub>	750	
8	$\square$ -His-D-Trp-Ala-Trp-D-Phe $\square$	> 10 <sup>5</sup>	115 ± 20
9	$\square$ -His-D-Trp-Ala-Trp-D-Phe-Ψ(CH <sub>2</sub> NH) $\square$	112	
10	$\square$ -His-D-Trp-Ala-Trp-D-Phe-Lys-Ψ(CH <sub>2</sub> NH) $\square$	> 10 <sup>4</sup>	
11	H-His-D-Trp-D-Orn-Trp-D-Phe-Lys-	400	
12	$\square$ -D-Trp-Ala-Trp-D-Phe-Ψ(CH <sub>2</sub> NH) $\square$	> 10 <sup>5</sup>	weak

The EC<sub>50</sub> values obtained indicate that the removal of one or two of the charges causes only a moderate decrease in potency whereas complete removal of the positive charges lead to complete loss of GH releasing activity. It seems that a positive charge in one terminal can compensate for the loss of positive charge in the opposite terminal. This indicates that the N- and C- termini are very close to each other in the bioactive conformation of GHRP-6 and suggests a possible  $\beta$ -turn in its central part.

This hypothesis prompted us to synthesize a series of cyclic analogs of GHRP-6 where at least one positive charge was retained (6, 7, 9, 10, 11, 12) (Table 2). In 9 and 10, one positive charge was introduced as an aminomethylene peptide bond replacement.

The only ~ 10 fold reduction in potency of 9 as compared to the linear analogue 2 clearly demonstrates that the N- and C- termini are close to each other in the bioactive conformation of GHRP-6. Furthermore, because the corresponding analogue 8 without an aminomethylene substitution is a very potent antagonist, we suggest that the positive charge is essential for agonist activity.

Table 2. Peptide synthesis.

No.	Resin bound intermediate used	Procedures
1	H-His(Trt)-D-Trp-Ala-Trp-D-Phe-Lys(Boc)-[Rink resin]	a,c
2	H-His(Trt)-D-Trp-Ala-Trp-D-Phe-[Rink resin]	a,c
3	H-D-Trp-Ala-Trp-D-Phe-Lys(Boc)-[Rink resin]	a,c
4	Acetyl-His(Trt)-D-Trp-Ala-Trp-D-Phe-Lys(Boc)-[Rink resin]	a,c
5	Propionyl-D-Trp-Ala-Trp-D-Phe-[Sasrin® resin]	a,j
6	Boc-Lys(Cl-Z)-His(Trt)-D-Trp-Ala-Trp-D-Phe-[Wang resin]	a,c,f,h
7	Boc-Glu(OFm)-D-Trp-Ala-Trp-D-Phe-Lys(Fmoc)-[MBHA resin]	b,h,g,d
8	H-Trp-D-Phe-His(Trt)-D-Trp-Ala-[Wang resin]	a,c,f
9	Boc-D-Phe- $\Psi$ (CH <sub>2</sub> NH)-His(Bom)-D-Trp(For)-Ala-Trp(For)-[PAM resin]	b,e,d,f,h
10	Boc-Lys(Cl-Z)- $\Psi$ (CH <sub>2</sub> NH)-His(Trt)-D-Trp-Ala-Trp-D-Phe-[Wang resin]	a,e,c,f,d
11	Fmoc-His(Trt)-D-Trp-D-Orn(Boc)-Trp-D-Phe-Lys(Dde)-[Wang resin]	a,c,f,i
12	Boc-D-Phe- $\Psi$ (CH <sub>2</sub> NH)-D-Trp-Ala-Trp-[Wang resin]	a,e,h,c,f

Procedures:

- |                                   |  |
|-----------------------------------|--|
| a. Fmoc SPPS.                     | f. Cycl. in dil. DMF solution using EDAC/HOBt. |
| b. Boc SPPS.                      | g. Cycl. on resin using HBTU.                  |
| c. TFA cleavage.                  | h. 20% piperidine in DMF.                      |
| d. HF cleavage.                   | i. 2% hydrazine hydrate in DMF.                |
| e. On resin reductive alkylation. | j. Aminolysis with neat hexylamine             |

## References

1. Bowers, C.Y., Momany, F.A., Reynolds, G.A. and Hong, A., *Endocrinology*, 114 (1984) 1537.
2. Heiman, M.L., Nekola, M.V., Murphy, W.A., Lance, V.A., Coy, D.H., *Endocrinology*, 116 (1985) 410.

# Systematic lactam scan of hGRF 1-29-NH<sub>2</sub> yields potent agonists and antagonists

L. Cervini, C. Donaldson, S. Koerber, W. Vale and J. Rivier

Clayton Foundation Laboratories for Peptide Biology, The Salk Institute,  
10010 N. Torrey Pines Rd., La Jolla, CA 92037, USA

A recent development in SAR studies complementary to the classic alanine and D-amino acid scans is the systematic lactam scan of a peptide. Such a scan is based on pioneering studies [1] where putative salt bridges were fused into conformationally constrained lactams by side-chain to side-chain amide formation. Typically, this approach has yielded potent analogs of peptides that assume a helical conformation in their bioactive state (GRF, CRF, PTH) [2-4]. In an earlier study, we found Glu and Lys to be the optimal bridgehead residues in an *i* - (*i* + 3) ring scaffold, since smaller lactam ring sizes (<18 atoms) led to molecules with diminished potency [5]. We hereby present a complete *i* - (*i* + 3) lactam scan of [MeTyr<sup>1</sup>, Ala<sup>15</sup>, Glu<sup>1</sup>, Lys<sup>i+3</sup>, Nle<sup>27</sup>]-hGRF(1-29)-NH<sub>2</sub>.

## Results and Discussion

Potencies for the 26 analogs in this series were compared to that of the agonist standard hGRF(1-40)-OH. Fourteen analogs had potencies < 25%; five were equipotent and seven had potencies 3-14 times greater than that of the standard (Fig. 1). Interestingly, the outcome was not entirely predictable from the results derived from the Ala- and D-series.

The most potent analogs were those with *i* - (*i* + 3) cycles between residues 4-7, 5-8, 9-12, 16-19, 21-24, 22-25 and 25-28. A circular dichroism experiment (CD) of the five C-

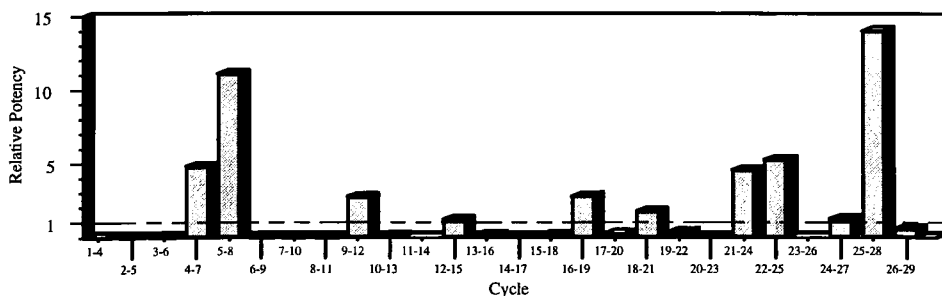


Fig. 1. Relative potencies of cyclic analogs of cyclo[*i*-(*i*+3)][MeTyr<sup>1</sup>, Ala<sup>15</sup>, Glu<sup>1</sup>, Lys<sup>i+3</sup>, Nle<sup>27</sup>]-hGRF(1-29)-NH<sub>2</sub>.

Table 1. Cyclic antagonists of hGRF<sub>1-29</sub>NH<sub>2</sub>. Potencies include 95% confidence limits.

[Substituted]-hGRF <sub>1-29</sub> NH <sub>2</sub>	Potency	I.A. (1 μM)
<b>1</b> [MeTyr <sup>1</sup> ,DArg <sup>2</sup> ,Cpa <sup>6</sup> ,Nle <sup>27</sup> ]-rGRF <sub>1-29</sub> NH <sub>2</sub> <b>standard</b>	1.00	
<b>2</b> c(22-25)[MeTyr <sup>1</sup> ,DArg <sup>2</sup> ,Cpa <sup>6</sup> ,Ala <sup>15</sup> ,Glu <sup>22</sup> ,Lys <sup>25</sup> ,Nle <sup>27</sup> ]	4.0 (2.4-6.9)	13%
<b>3</b> c(25-28)[MeTyr <sup>1</sup> ,DArg <sup>2</sup> ,Cpa <sup>6</sup> ,Ala <sup>15,22</sup> ,Glu <sup>25</sup> ,Nle <sup>27</sup> ,Lys <sup>28</sup> ]	4.3 (2.9-6.5)	11%
<b>4</b> c(25-29)[MeTyr <sup>1</sup> ,DArg <sup>2</sup> ,Cpa <sup>6</sup> ,Ala <sup>15,22</sup> ,DAsp <sup>25</sup> ,Nle <sup>27</sup> ,Orn <sup>29</sup> ]	1.9 (1.2-2.9)	15%

aqueous conditions although the possibility of facilitated helix formation in a membrane environment cannot be ruled out.

Three antagonists were designed by including point substitutions (Darg<sup>2</sup> and Cpa<sup>6</sup>) [6, 7] in representative, potent cyclic analogs of the lactam scan (Table 1). The i - (i + 4) analog **4** is half as potent as analogs **2** and **3** with smaller cycles, and all three bridging scaffolds yielded relatively more potent agonists than antagonists.

In conclusion, modifications that produce increased agonist potencies may also produce potent antagonists, albeit to a slightly lesser degree. These antagonists exemplify the application of SAR scan data to rationally design potent analogs and provide a useful tool for probing the structural requirements necessary for GRF receptor binding. Conformational restriction yields subtle effects in the peptide-receptor interaction, but bridging elements in a peptide.

## References

1. Felix, A. M., Heimer, E. P., Wang, C. T., Lambros, T. J., Fournier, A., Mowles, T. F., Maines, S., Campbell, R. M., Wegrzynski, B. B., Toome, V., Fry, D. and Madison, V. S., *Int. J. Pep. Prot. Res.*, 32 (1988) 441.
2. Fry, D. C., Madison, V. S., Greeley, D. N., Felix, A. M., Heimer, E. P., Frohman, L., Campbell, R. M., Mowles, T. F., Toome, B. and Wegrzynski, B. B., *Biopolymers*, 32 (1992) 649.
3. Romier, C., Bernassau, J.-M., Cambillau, C. and Darbon, H., *Prot. Eng.*, 6 (1993) 149.
4. Chorev, M., Behar, V., Yang, Q., Rosenblatt, M., Mammi, S., Maretto, S., Pellegrini, M. and Peggion, E., *Biopolymers*, 36 (1995) 485.
5. Cervini, L. A., Corrigan, A., Donaldson, C. J., Koerber, S. C., Vale, W. W. and Rivier, J. E., In R. S. Hodges and J. A. Smith (Eds.), *Peptides: Chemistry, Structure and Biology*, ESCOM Science Publishers B.V., Leiden, The Netherlands, 1994, p. 541-543.
6. Robberecht, P., Coy, D. H., Waelbroeck, M., Heiman, M. L., DeNeef, P., Camus, J. C. and Christophe, J., *Endocrinology*, 117 (1985) 1759.
7. Pandol, S. J., Dharmasathaphorn, K., Schoeffield, M. S., Vale, W. and Rivier, J., *Am. J. Physiol.* 250 (1986) G553.

# The interaction between gramicidin S and lipid bilayers: Evidence for cholesterol attenuation of phospholipid-peptide interactions

T.P.W. McMullen,<sup>a</sup> E.J. Prenner,<sup>a</sup> R.N.A.H. Lewis,<sup>a</sup> L.H.  
Kondejewski,<sup>a,b</sup> R.S. Hodges<sup>a,b</sup> and R.N. McElhaney<sup>a</sup>

*<sup>a</sup>Department of Biochemistry and <sup>b</sup>Protein Engineering Network of Centers of Excellence,  
University of Alberta, Edmonton, Alberta, Canada T6G 2H7*

The cyclic decapeptide gramicidin S (GS) is known to inhibit the growth of many bacteria and fungi. Currently available data suggest that GS is targeted against the structural integrity of cell membranes in general, without any requirements for specific interaction with membrane proteins. GS also exhibits significant hemolytic activity. This property is a major barrier against the therapeutic development of GS and its analogues as broad-spectrum antibiotics. Although GS seems generally to be targeted against cell membranes, there is also evidence that its effects vary markedly with membrane lipid composition. This observation, and the fact that mammalian and bacterial membranes differ markedly in their lipid composition and cholesterol content, suggest that the known differences between the hemolytic and antibiotic activities of GS may well be a function of the lipid composition of the cell membrane. We have, therefore, begun a study of the ways in which the interaction of GS with lipid bilayers is influenced by the lipid composition of the membrane target [1]. In this communication we present evidence that membrane cholesterol does affect GS-membrane interactions and that it can diminish the potentially membrane-disruptive effects of the peptide.

## Results and Discussion

The effects of GS on a range of cholesterol-free and cholesterol-containing model membranes were examined by a combination of calorimetric and spectroscopic techniques. Our calorimetric data indicate that GS does not significantly alter the gel/fluid phase transition temperature of dimyristoyl phosphatidylcholine (DMPC). In the presence of GS this lipid exhibits a broader transition centered near 24°C with a pronounced high temperature shoulder. The latter is correlated with a deeper penetration of the peptide into the fluid phases of the lipid. DMPC bilayers containing  $\cong 25$  mol% cholesterol exhibit very broad gel/fluid phase transitions centered near 29°C. Upon interaction with GS these shift to lower temperatures ( $\cong 24^\circ\text{C}$ ) and a relatively sharp low-temperature shoulder appears on the DSC thermograms. These results can be explained in terms of a greater penetration of the peptide into the more disordered gel phases of the cholesterol-containing membranes.

FTIR spectroscopic studies indicate that the gel/fluid phase transitions of all lipid membranes are accompanied by an increase in the frequencies of the amide I absorption bands of GS. Since this is not correlated with a change in peptide conformation, we

conclude that it is the result of a decrease in the polarity of the local environment of the peptide upon melting of the lipid hydrocarbon chains. When dispersed in cholesterol-free DMPC bilayers, GS exhibits amide I frequencies near 1638 and 1646  $\text{cm}^{-1}$  in the gel and fluid phases, respectively. Under comparable conditions GS dispersed in cholesterol-containing DMPC exhibits amide I frequencies near 1629 and 1642  $\text{cm}^{-1}$ , respectively. These results indicate that GS exists in a lower polarity environment when dispersed in cholesterol-containing DMPC bilayers and are consistent with GS penetrating less deeply into the cholesterol-containing lipid bilayers.

The effects of GS on cholesterol-free and cholesterol-containing dipalmiteladoyl phosphatidylethanolamine membranes were examined by  $^{31}\text{P}$ -NMR spectroscopy. When GS is dispersed in the cholesterol-free membranes (lipid:peptide  $\cong$  25:1), spectroscopic evidence for nonlamellar phase formation is observed near 55°C, some 30-35°C below the temperature at which it is normally observed in the absence of the peptide. In the presence of cholesterol, spectroscopic evidence for significant GS-induced nonlamellar phase formation is first observed at temperatures near 70°C, a temperature which is very close to the range at which these cholesterol-containing membranes spontaneously form nonlamellar phases. This result clearly shows that cholesterol significantly attenuates the capacity of GS to induce nonlamellar phase formation in these membranes.

Finally, the differential sensitivities of cholesterol-free and cholesterol-containing membranes to the membrane-disrupting activities of GS were evaluated by the release of entrapped calcein from 1-palmitoyl, 2-oleoyl phosphatidylcholine vesicles. We find that the sterol dramatically reduces the sensitivity to GS-induced calcein leakage. For example, at low vesicular lipid concentrations and lipid:GS ratios near 25:1, some 50% of the dye was released from cholesterol-free vesicles compared to 25% from the cholesterol-containing (25 mol%) vesicles. This result provides direct evidence that the potential membrane-disrupting activity of GS is markedly attenuated by the presence of membrane cholesterol. Unlike mammalian membranes, bacterial membranes are normally devoid of cholesterol. It may thus be possible to exploit this fact in the design of more therapeutically useful GS analogues.

## References

1. Kondejewski, L.H., Farmer, S.W., Wishart, D.S., Hancock, R.E.W. and Hodges, R.S., *Int. J. Peptide Protein Res.*, 47 (1996) 460.

# New synthetic peptides derived from human fibroblast growth factor-1: Search for agonists and inhibitors

S. Kiyota,<sup>a</sup> A.G. Gambarini,<sup>a</sup> W. Viviani,<sup>a</sup> S. Oyama,<sup>a</sup> B.D. Sykes<sup>b</sup> and M.T.M. Miranda<sup>a</sup>

<sup>a</sup>Departamento de Bioquímica, Universidade de São Paulo, CP 26077, CEP 05599-970, São Paulo, Brasil; <sup>b</sup>Department of Biochemistry, University of Alberta, T6G2R3, Edmonton, Canada

Expression of FGFs by several mammalian tissues is associated with many important physiopathological processes such as cell growth and division, angiogenesis, neuronal survival, wound repair and tumor development [1].

In our search for small agonists or inhibitors of human FGF-1, we studied the segment <sup>97</sup>YISKKHAEKNWFVGLKKNKNGSCKRGPRT<sup>132</sup> located in its C-terminal portion [2] which contains Site 2. This site has been implicated as determinant not only for receptor binding and dimerization, but also for the receptor subtype specificity [3]. The peptide Ac-WFVGLKKNKNGSCKRGPRT-NH<sub>2</sub> (I) was the best agonist obtained so far, although it was 10<sup>4</sup> fold less active than the native protein [4]. In this paper we describe its preferred conformation in solution as determined by <sup>1</sup>H-NMR analysis and the design, synthesis and mitogenic activity of the following new peptides: Ac-WFVGLKKNKNGSCKRGPRT-NH<sub>2</sub> (II) Ac-WFVGLPSKR-NH<sub>2</sub> (III) Ac-WFVGLPSKRGPRT-NH<sub>2</sub> (IV), Ac-SKKHAEKNWF-NH<sub>2</sub> (V) and c(1-5)[Ac-CKKHCEKNWF-NH<sub>2</sub>] (VI).

These peptides were designed based on the tridimensional structure of the native hFGF-1 [5] and on other data available in the literature. They were manually synthesized by the solid phase method using t-Boc strategy [6], purified by semi-preparative RP-HPLC and characterized by amino acid analysis and mass spectrometry. Cyclization of peptide VI was achieved by oxidation of the thiol groups of the cysteines with K<sub>3</sub>Fe(CN)<sub>6</sub> [7]. Mitogenic activity was determined by measuring tritiated thymidine incorporated into the DNA of Balb/c 3T3 fibroblasts. Cellular binding assays were determined by competition with <sup>125</sup>I-hFGF-1 as described [4].

## Results and Conclusion

<sup>1</sup>H-NMR analysis of peptide I implicated that this is largely in a random coil configuration which is in agreement with the theoretical analysis. Only minor conformations corresponding to  $\beta$ -structure were observed. From these data, we concluded that the low mitogenic activity of I is due to its great conformational flexibility in solution. It is conceivable that the stabilization of the  $\beta$ -structure, which we believe is the active conformation, may be induced by the receptor-ligand binding.

II - IV were designed to investigate the contribution of the two adjacent lysines (K<sup>6</sup> K<sup>7</sup>) and the segment KKNKNGS to the mitogenic activity of I as well as to test whether the function of the cluster K<sup>6</sup> K<sup>7</sup> could be mimicked by the cluster K<sup>12</sup> R<sup>13</sup>. As these peptides were essentially inactive, we concluded that: 1) the two adjacent lysines are critical for the mitogenic activity of peptide I; 2) the replacement of KKNKNGS by proline, as in III and IV, was inefficient probably because these peptides do not contain the pair of lysines. Besides,

it is possible that this segment has a structural function not mimicked by the Pro residue; 3) the deletion of *KKNGS* placed the cluster *K<sup>12</sup> R<sup>13</sup>* closer to the hydrophobic core *WF(V)*. As it did not lead to active peptides, it is possible that not only the orientation of the positive side-chain but also the structural features of lysine are required.

**V** and **VI** were synthesized to determine whether peptides containing a hydrophobic core and a cluster of positive charges, but not the same sequence as peptide **I**, would be mitogenically active. Peptide **VI** presented an  $ED_{50}$  of about 60  $\mu M$ , which is similar to that found for peptide **I**. In contrast, peptide **V** was inactive. The theoretical conformation analyses of these peptides showed that **V** is much more flexible than **VI**. Moreover, it became clear that the preferred theoretical conformation of peptide **VI** is similar to that assumed by the corresponding fragment in the native protein. These results led us to suggest that the structural constraint imposed was sufficient to place some specific amino acid side-chains, perhaps the two adjacent lysines, into the right position for an effective receptor binding. In this regard, **VI** could be seen as an analog of **I**, although equally potent.  $^1H$ -NMR analyses of peptide **V** and **VI** are now in progress.

Peptides **I** and **VI** competed with hFGF-1 for the cellular receptor ( $ID_{50}$  ~20-30  $\mu M$ ). However, we can not rule out the possibility that their mitogenic signal is being generated through their binding to other receptors besides FGFR.

## References

1. Yayon, A. and Klagsbrun, M., *Cancer Metastasis Rev.*, 9 (1990) 191.
2. Murzin, A. G., Lesk, A. M. and Chothia, C., *J. Mol. Biol.*, 223 (1992) 531.
3. Blaber, M., DiSalvo, J., and Thomas, K. A., *Biochemistry*, 35 (1996) 2986.
4. Oyama, S., Miranda, M. T. M, Toma, I., Viviani, W. and Gambarini, A. G., *Biochem. Mol. Biol. Int.*, 30 (1996) 1237.
5. Zhu, Z., Komiya, H., Chirino, A., Fahan, S., Fox, G. M., Arakawa, T., Hsu, B. T. and Rees, D. C., *Science*, 251 (1991) 23.
6. Stewart, J. M. and Young, J. D., "Solid Phase Peptide Synthesis", Pierce Chemical Company, 2nd ed., 1984.
7. Misicka, A. and Hruby, V.J., *Polish J. Chem.*, 68 (1994) 893.

# Rapid modular total chemical synthesis of chemokines based on genome sequence data

Michael A. Siani, Darren A. Thompson, Lynne E. Canne, Jill Wilken,  
Gianine M. Figliozzi, Stephen B. H. Kent and Reyna J. Simon

*Gryphon Sciences, 250 E. Grand Ave. Suite 90, South San Francisco, CA 94080, USA*

Chemokines are a potent class of small protein molecules that act as important biological effectors in inflammatory responses, AIDS and hematopoiesis [1]. Because of the size of the polypeptide chain (~70 amino acid residues) and the distinctive pattern of conserved Cys residues, more than 60 chemokine-related open reading frames have been identified in nucleic acid sequence data arising from the genome initiatives. Rapid production of chemokines is desired for efficient elucidation of the function of these new chemokine genes. Gryphon Sciences' chemical synthesis and ligation technologies provide rapid access to known and novel chemokines [2]. Synthesis, ligation and folding under normal circumstances for chemokine-sized proteins takes approximately three weeks and yields 50-100 milligrams of high purity proteins with full biological activity. Exodus [3], a novel chemokine whose sequence was discovered from genome data, has been synthesized via this method and is described herein.

## Results and Discussion

Exodus was synthesized in two segments using *in situ* neutralization/HBTU activation protocols for Boc chemistry [4]. The N-terminal segment was prepared on Glycine  $\alpha$ -thiocarboxylate resin [5]. The crude product from HF cleavage was first treated with 20% BME, 6M GuHCl, 0.1M phosphate, pH 7.5 for one hour to remove the DNP protecting groups from Histidine. After solvent exchange into 0.1M NaOAc, pH 4.0, the peptide was reacted with 50mM bromoacetic acid for 10 minutes to alkylate the C-terminal  $\alpha$ -thiocarboxylate. Subsequent C4-HPLC purification gave pure Exodus(1-35)-SCH<sub>2</sub>CO<sub>2</sub>H ready for ligation. The C-terminal segment was synthesized using the same Boc protocols on Methionine-PAM resin. Following HF cleavage and C4-HPLC purification, the segment was ready for ligation.

The peptide segments were dissolved in 6M GuHCl, 0.1M phosphate, pH 7.0 to a final concentration of approximately 4mM in each peptide. After mixing, 0.5% thiophenol was added to maintain a reducing environment and facilitate thioester exchange for a faster reaction. The progress of the reaction was monitored by C4-HPLC (Fig. 1) and the desired product was purified when the reaction was completed. Folding was accomplished by dissolving lyophilized peptide into 2M GuHCl, 0.1M Tris, pH 8.5 to a final concentration of 1mg/mL peptide with stirring. C4-HPLC and MS were used to identify the folded product by a decrease in HPLC retention time and a loss of 4 Da due to formation of two

disulfide bonds. Biological activity was determined by chemotaxis on normal human PBMCs [3].

Over 30 milligrams of folded active Exodus have been shipped to our collaborators. Chemical ligation of fully unprotected peptide segments has also been successful in the preparation of more than 30 chemokines representing 15 *different* native molecules and their analogues and has been useful for the synthesis of other protein systems [6].

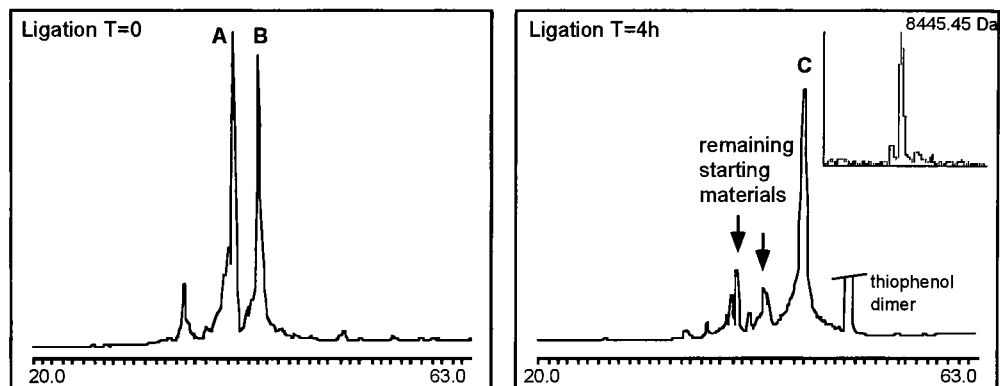


Fig. 1. The left panel shows the time = 0 HPLC trace for the Exodus ligation. Peaks A and B are the two starting materials, Exodus (1-35)-SCH<sub>2</sub>CO<sub>2</sub>H and Exodus(35-74), respectively. The right panel shows the progress of the ligation after 4 hours. C is the product. The inset gives the hypermass reconstruction of the raw MS data to a single charge state for C. Exodus(1-74) had an observed mass of 8445.45 Da (calculated mass 8446.99 Da).

## Acknowledgments

The authors thank Ronald Godiska and Patrick Gray from ICOS Corporation for a fruitful collaboration on Exodus and other chemokines.

## References

1. a) Clark-Lewis, I. et al. *J. Biol. Chem.* 269 (1994) 16075; b) Baggiolini, M. B. et al. *Cytokine* 3 (1991) 165; c) Sykes B. D. et al. *Science*, 264 (1994) 90.
2. Dawson, P. E., Muir, T. W., Clark-Lewis, I. and Kent, S. B. H. *Science* 266, (1992) 776.
3. Hromas, R. et al. *Blood*, 89 (1997) 3315.
4. Schnolzer M. et al. *Int. J. Pept. Protein Res.*, 40 (1992) 180.
5. Canne, L. M. et al. *Tetrahedron Lett.*, 36 (1995) 2998.
6. a) Figliozzi, G. M. et al. Abstracts of Posters, 24th Symposium of the European Society; Edinburgh, Scotland; The European Peptide Society and The Royal Society of Chemistry; London, England, 1996; poster 202; b) Lu, W. et al. *Biochemistry*, 36 (1997) 673, c) Muir, T. W. *Structure*, 3 (1995) 649.

# Synthesis and study of all-L and all-D normal and retro isomers of cecropin A-melittin hybrids and selective enzyme inactivation

Satyanarayana Vunnam, Padmaja Juvvadi, Kenneth S Rotondi  
and R. B. Merrifield

*The Rockefeller University, 1230 York Ave, New York, NY 10021, USA*

Two antimicrobial peptides, cecropin A [1] and melittin [2], possess high activity against both Gram-positive and Gram-negative bacteria. Melittin, however, has the very detrimental property of killing eukaryotic cells. To understand the structural requirements for the antimicrobial activity of chimeric analogs of cecropin A and melittin, we have synthesized normal, enantio, retro, and retroenantio hybrid analogs, and have related activity to their sequence, helix dipole (amide bond direction), chirality and end group charges. To compare the effect of the end groups, each of these analogs was synthesized both with an acid and an amide C-terminus and also with and without an N-acetyl N-terminus and tested against 5 strains of bacteria. The results are presented here.

## Results and Discussion

The observed activities of amide analogs of CA(1-13)M(1-13) against four of the test bacteria show that the essential structural features may be either sequence or helix dipole, but not both of these together nor chirality. *Bacillus subtilis* is more demanding and the required structural features for this organism were both sequence and helix dipole. The antibacterial activities for the eight analogs of CA(1-13)M(1-13)-OH showed that two bacterial strains, one Gram-negative, *Escherichia coli*, and one Gram-positive, *Streptococcus pyogenes*, responded in a way similar to that of their corresponding amide analogs. For *B. subtilis* the pattern for C-terminal acid analogs corresponds to the requirement of either sequence, or helix dipole. All-L CA(1-13)M(1-13)-OH and CA(1-7)M(2-9)-OH are less active than their D enantiomers against some of our test bacteria. This may be attributed to the role of proteolytic enzymes produced during the growth of the assay culture. Our earlier results with several cecropin-melittin hybrids showed that L and D isomers were equally active [3].

All-L CA(1-13)M(1-13) acid was 5 times and its retro isomer was 2 times less active than their corresponding all-D isomers against *Staphylococcus aureus*. The corresponding acetylated analogs behaved similarly, indicating that the charge on the N-terminal amine has little effect on the antibacterial activity of any of these derivatives. All-L CA(1-13)M(1-13)-OH was 9 times less active against *P. aeruginosa* and all-L retro acid was 2 times less active than their corresponding all-D enantiomers (Table 1). These results suggest that the L acid isomers are degraded during the antibacterial assay, while the all-L amides are resistant.

The retro and retroenantio analogs of CA(1-13)M(1-13) acid were as active as their normal and enantio analogs against all five test bacteria. The C-terminal amides showed similar activities. It is interesting to note that the negative end of the helix dipole of a normal

peptide points toward the carboxy terminus, whereas it points away in the case of the retro derivatives when they are inverted to give the same sequence as normal peptide.

The observed activities of CA(1-7)M(2-9) show that L and D enantiomers with C-terminal acids and amides were equally active against *E. coli*, *B. subtilis* and *S. pyogenes*. These data match the prediction for a requirement of either sequence or helix dipole but not both of these features at the same time. Different results were obtained against *P. aeruginosa* and *Staph. aureus*. All-L CA(1-7)M(2-9)-OH was, respectively fourteen times and five times less active than the all-D enantiomer against *Pseudomonas* and *Staphylococcus*. N<sup>α</sup>-acetyl derivatives showed similar differences. However, the corresponding L and D retro analogs differed only marginally. The L and D enantiomers of 15-residue hybrid analogs with C-terminal amides were equally active. Both sequence and helix dipole were found to be necessary structural features for their activity against *P. aeruginosa* and *Staph. aureus*. All 29 hybrid analogs reported here were found to be good antibacterial peptides. It should be mentioned that these analogs did not show any significant lysis of eukaryotic cells, such as sheep erythrocytes.

To demonstrate the probable effect of enzymes on the differences in the activities of L and D analogs, both the L and D peptides of CA(1-13)M(1-13)-OH and CA(1-7)M(2-9)-OH were treated with an extract of *Staph. aureus*. All-L peptides became 7 to 8 fold less active against *Staph. aureus*, while the all-D isomers were as active as the peptide without the enzyme treatment. Heat eliminated the effect of the extract.

These results clearly show that peptide chirality can affect antibacterial activity against some organisms. An active proteolytic enzyme produced by the organism during the assay would preferentially hydrolyse the all-L isomer and result in lowered antibacterial activity. The D enantiomers, however, are known to be resistant to enzyme degradation and were expected to retain their activity. We have earlier reported variable chiral effects for pig cecropin analogs and for proline-arginine rich PR-39 [4].

Table 1. Lethal and lysis concentrations ( $\mu\text{M}$ ) for CA(1-13)M(1-13)-NH<sub>2</sub>/OH analogs.

Organism	Normal		Enantio		Retro		Retroenantio	
	amide	acid	amide	acid	amide	acid	amide	acid
<i>E. coli</i>	0.7	0.7	0.8	0.8	3.8	3.0	2.4	2.3
<i>P. aeruginosa</i>	4.1	15	1.6	1.6	6.0	18	7.0	8.2
<i>Staph. aureus</i>	2.0	11	0.8	2.1	2.0	16	5.7	7.8
<i>Strep. pyogenes</i>	0.7	1.4	0.8	0.9	2.5	2.3	1.0	0.4
<i>B. subtilis</i>	0.9	1.7	1.1	0.9	37	1.7	27	1.2
Sheep red cells	320	139	430	246	100	170	100	65

The CD spectra of all-L and all-D normal and retro analogs of CA(1-13)M(1-13)-OH and CA(1-7)M(2-9)-OH revealed a random conformation in phosphate buffer at pH 7.2 and their  $\alpha$ -helical conformation increased as the concentration of HFIP was increased. Acetylated peptides showed higher helical contents than their unmodified hybrids.

## References

1. Hultmark, D., Steiner, H., Rasmuson, T. and Boman, H.G., *Eur. J. Biochem.*, 106 (1980) 7.
2. Habermann, E. and Jentsch, J., *Hoppe-Seylers Z. Physiol. Chem.*, 348 (1967) 37.
3. Wade, D., Boman, A., Wahlin, B., Drain, C. M., Andreu, D., Boman, H. G. and Merrifield, R. B., *Proc. Natl. Acad. Sci. U.S.A.*, 87 (1990) 4761.
4. Vunnam, S., Juvvadi, P. and Merrifield, R. B., *J. Peptide Res.*, 49 (1997) 59.

# Characterization of neurokinin receptor types and their intracellular signal transduction in C1300 cells

**Shigetomo Fukuhara, Hidehito Mukai and Eisuke Munekata**

*Institute of Applied Biochemistry, University of Tsukuba, Tsukuba, Ibaraki 305, Japan*

Neurokinin A and B (NKA, NKB) are a family of neuropeptides which interact with distinct cell surface receptors classified as NK<sub>1</sub>, NK<sub>2</sub> and NK<sub>3</sub> [1]. Recently, we found that murine neuroblastoma C1300 cells express endogenous neurokinin receptors [2,3]. Herein we characterized the neurokinin receptor types present in this cell line and investigated their intracellular signal transduction.

## Results and Discussion

Previously, we demonstrated that NKA and NKB induce an increase in the concentration of intracellular free Ca<sup>2+</sup> ([Ca<sup>2+</sup>]<sub>i</sub>), while Has a slight effect on Ca<sup>2+</sup> mobilization even at 10 μM [2], suggesting the existence of neurokinin receptors in C1300 cells. Therefore, RNA blot analysis was carried out to identify the types of neurokinin receptors in this line. NK<sub>2</sub> and NK<sub>3</sub> receptor mRNAs, but not NK<sub>1</sub> receptor mRNA, were expressed. To confirm the functional expression of NK<sub>2</sub> and NK<sub>3</sub> receptors, we examined whether [βAla<sup>8</sup>]NKA(4-10) and senktide, which are NK<sub>2</sub> and NK<sub>3</sub> receptor agonists, respectively, could induce the [Ca<sup>2+</sup>]<sub>i</sub> increases. [βAla<sup>8</sup>]NKA (4-10) at 10 μM slightly evoked a [Ca<sup>2+</sup>]<sub>i</sub> increase, and senktide concentration-dependently induced the Ca<sup>2+</sup> response, although its maximal response was about 10-fold less than that of NKA and NKB. In addition, we also examined the inhibitory effects of selective antagonists for NK<sub>2</sub> and NK<sub>3</sub> receptors on the [Ca<sup>2+</sup>]<sub>i</sub> increases in response to NKA and NKB. The [Ca<sup>2+</sup>]<sub>i</sub> increase induced by 0.33 μM NKA was completely inhibited by SR 48968, an NK<sub>2</sub> receptor antagonist, whereas the partial response to 0.33 μM NKB (about 8% of total response) was unaffected. The response to NKB resistant to SR 48968 was completely inhibited by SR 142801, an NK<sub>3</sub> receptor antagonist. In addition, Ca<sup>2+</sup> response to 0.33 μM senktide was inhibited by SR 142801 but not by SR 48968. These findings suggested that C1300 cells expressed functional NK<sub>2</sub> and NK<sub>3</sub> receptors (Fig. 1). However, because of the low potency of [βAla<sup>8</sup>]NKA (4-10) to increase [Ca<sup>2+</sup>]<sub>i</sub> NK<sub>2</sub> receptors present in C1300 cells might be different type from those characterized in other systems. It was also demonstrated that NK<sub>2</sub> and NK<sub>3</sub> receptors can be activated independently by 3.3 μM NKA in the presence of 1.0 μM SR 142801 or 1.0 μM senktide, respectively.

The signal transduction evoked by endogenous NK<sub>2</sub> and NK<sub>3</sub> receptors was investigated using this cell system. The independent activation of NK<sub>2</sub> and NK<sub>3</sub> receptors induced not only a [Ca<sup>2+</sup>]<sub>i</sub> increase, but also stimulated the formation of inositol trisphosphates (IP<sub>3</sub>), and of which were inhibited by U73122, a phospholipase C (PLC) inhibitor. In addition, NK<sub>2</sub> and NK<sub>3</sub> receptor-mediated [Ca<sup>2+</sup>]<sub>i</sub> increase was partially attenuated in the absence of extracellular Ca<sup>2+</sup> or in the presence of nickel, an inorganic Ca<sup>2+</sup> influx blocker. It was unaffected by



# Influence of different types of cyclization on certain biological activities of three structural types of bradykinin antagonists

Siegmond Reissmann,<sup>a</sup> Inge Agricola,<sup>a</sup> Torsten Steinmetzer,<sup>a</sup> Lydia Seyfarth,<sup>a</sup> Georg Greiner<sup>a</sup> and Inge Paegelow<sup>b</sup>

<sup>a</sup> Friedrich-Schiller University of Jena, Institute of Biochemistry and Biophysics, Philosophenweg 12, D-07743 Jena, FRG, <sup>b</sup>University of Rostock, Institute of Pharmacology and Toxicology, Schillingallee 70, D-18057 Rostock, FRG

In order to study conformational requirements for different types of bradykinin antagonists and different receptor types we systematically cyclized bradykinin analogs by formation of lactam bridges between side chains and modified peptide groups from the backbone. To gain a more detailed insight into conformational bioactivity we studied the influence of sequence position, type, direction and size of the lactam bridges.

## Results and Discussion

Cyclization between side chains in position 0 and 6 (**2**) and between the modified backbone residue at position 2 and the side chain at position 6 provides antagonists with the same or enhanced activity on the smooth muscle contraction (B<sub>2</sub> receptor) compared to lead structure or linear precursors. In these cases the cyclization seems to stabilize the bioactive conformation. In contrast to the lead structure **1** antagonistic potency is shifted by cyclization from GPI in favour of RUT (Table 1). The direction of the lactam bridge has a crucial effect on biological activity. While antagonistic compound **2** with the direction HN-CO is

Table 1. Biological activities of linear and cyclic bradykinin analogs.

No.	Structure*	RUT	GPI	LS
1	[DPhe <sup>7</sup> ]-BK	1.5%	pA <sub>2</sub> =4.9	pA <sub>2</sub> =4.46
2	cyclo(0-6)[Lys <sup>0</sup> ,Glu <sup>6</sup> ,DPhe <sup>7</sup> ]-BK	pA <sub>2</sub> =5.78	n.a	n.a
3	cyclo(0-6)[Glu <sup>0</sup> ,Lys <sup>6</sup> ,DPhe <sup>7</sup> ]-BK	n.a	n.a	-
4	[ΔPhe <sup>5</sup> ]-BK	170%	150%	95%
5	cyclo(0-6)[Glu <sup>0</sup> ,ΔPhe <sup>5</sup> ,Lys <sup>6</sup> ]-BK	n.a.	n.a.	-
6	[NMePhe <sup>2</sup> ]-BK	34.6%	4.2%	pA <sub>2</sub> =5.59
7	cyclo(0-6)[Lys <sup>0</sup> ,NMePhe <sup>2</sup> ,Glu <sup>6</sup> ]-BK	n.a.	n.a.	n.a.

• ΔPhe= dehydrophenylalanine, NMePhe= N-methylphenylalanine n.a.=inactive

more active than the linear precursor, the comparable compound **3** with the lactam bridge direction CO-NH is completely inactive. Comparison with other cyclic type-7-antagonists shows no dependence of the activity on side chain or backbone cyclization. Furthermore,

the results of the active antagonists give no evidence for an important role of ring size. Lactam rings with 20 or 27 and with 20 member gave nearly the same  $pA_2$  values. From our systematic studies on linear antagonists of  $B_2$ -receptor antagonists we assume the existence of different structure types. Apart from antagonists with an D-amino acids at position 7 [1] we found antagonists with  $\Delta$ Phe and its related analogs at position 5 [2] and with N-alkyl amino acids at position 2 [3]. Until now systematic lactamization was only performed at position 7 antagonists. First results of type-5- and type-2-antagonists show changed conformational requirements for both these structural types. Thus, in contrast to type-7-antagonists, in both cases agonistic and antagonistic activity is strongly reduced by lactam bridges in the N-terminus. Cytokine release from mononuclear cells induced by bradykinin antagonists prevents their use as a drug because of their own inflammatory action. In contrast, the inhibition of cytokine release favours their use as antiinflammatory agents. Systematic structure activity studies with linear antagonists have shown that the receptor on mononuclear cells has structural requirements quite different from the  $B_2$ -receptor [4]. Cyclization in the N-terminal part of type-7-antagonists shows a favourable effect. Agonistic activity is reduced whereas the inhibition of cytokine release is enhanced by 3 orders of magnitude. Structural requirements for histamine release from rat mast cells are also quite different from those for smooth muscle contraction and cytokine release [5]. Cyclization of bradykinin agonists and antagonists has no general effect on histamine release. Compared to bradykinin itself or to the linear precursors cyclization by lactam or disulfide bridges in the N-terminal sequence often enhances histamine releasing potency, whereas backbone modification strongly reduces that potency.

Thus, cyclizations in different sequence positions destroy activity in agonist whereas lactam bridges in the N-terminus of type-7-antagonists enhance antagonistic potency. While no difference could be observed between side chain or backbone cyclization, the direction of the lactam bridges is crucial for high potency or inactivity. The results indicate a turn structure in the N-terminal sequence of type-7-antagonists but give no evidence for a turn structure in the C-terminus.

## References

1. Stewart, J.M., *Biopolymers (Peptide Science)*, 37(1995)143.
2. Greiner, G. et al., *J. Pep. Sci.*, in press.
3. Reissmann, S. et al., *Immunopharmacology*, 33(1996)73.
4. Paegelow, I., Werner, H. and Reissmann, S., *Europ. J. Pharmacol.*, 279(1995)211.
5. Vietinghoff, G., Paegelow, I. and Reissmann, S., *Peptides*, 17(1996)1467.

# Antimicrobial peptides with activity against an intracellular pathogen

T. S. Yokum, P. H. Elzer and M. L. McLaughlin

Department of Chemistry, Louisiana State University, Baton Rouge, LA 70803, USA

Bacterial resistance to antibiotic therapy is increasing at an alarming rate [1]. The reduced effectiveness of current antibiotics arises from the reliance on only a few distinct mechanisms of action [1]. As a result, there is a need to develop new antibiotics with unique mechanisms. In addition to acquiring multi-drug resistance, intracellular pathogens pose an additional problem in that they are sequestered in a cell. The ability of *Brucella abortus*, an intracellular pathogen, to survive in macrophages allows it to quickly establish chronic infection [1]. The sequestered bacteria are not exposed to the compliment cascade, neutrophils, antibodies, or antibiotics. We report the *in vivo* and *in vitro* activities of a series of peptides against *Brucella abortus* and the proteolytic stability of these peptides using trypsin.

## Results and Discussion

The peptides presented can be grouped into four categories: naturally occurring antimicrobial peptides (1-3), simplified analogs of naturally occurring antimicrobial peptides (4-6), *de novo* amphipathic peptides (7-12), and *de novo* amphipathic peptides composed of 50-80%  $\alpha,\alpha$ -disubstituted amino acids (13-19) [1,2]. The sequences in Table 1 are listed using their one-letter codes for the proteinogenic amino acids and the  $\alpha,\alpha$ -disubstituted amino acids: B,  $\alpha$ -aminoisobutyric acid; X, 1-aminocyclohexane carboxylic acid; and J, 4-aminopiperidine-4-carboxylic acid.

All of the peptides, except peptides 15 and 18, show significant antimicrobial activity against *S. aureus* and *E. coli* bacteria with MIC activity ranging from 1-17  $\mu\text{M}$  [1,2]. In contrast, none of the peptides showed any significant direct antimicrobial activity against *Brucella abortus* at peptide concentrations up to 100  $\mu\text{M}$ . Even though these peptides show no direct activity against *Brucella abortus in vitro*, many of the peptides significantly reduce *Brucella abortus* levels in chronically infected BALB/c mice (Table 1). The doses were titrated down to the highest non-lethal dose. Toxicity observations at these doses were classified into 3 categories: none (no difference between peptide treated and saline treated mice), stress (mice show signs of distress), and toxic (some of the mice in the group died). *In vitro* testing of peptide toxicity against normal and infected macrophages reveals that only peptides 13, 14, 15 and 18 show significant selectivity of infected macrophage killing over normal macrophages. Because some of the peptides are expected to undergo proteolysis *in vitro*.

We treated the peptides *in vitro* with trypsin to test the proteolytic stability of these peptides [3]. All of the peptides composed solely of proteinogenic amino acids except for 1

and 5 showed no stability while all of the peptides containing  $\alpha,\alpha$ -disubstituted amino acids were completely stable (Table 1).

Table 1. *In vivo* peptide activity against *B. abortus* in BALB/c mice and proteolytic stability.\*

Peptide	Sequence	Dose ( $\mu\text{g}$ )	% Brucella Reduction	Toxicity	Stability
1	Melittin	25	50	none	partial
2	Cecropin B amide	500	53 <sup>a</sup>	none	none
3	Maganin 2 amide	500	54 <sup>a</sup>	none	none
4	Melittin analog	500	90	toxic	none
5	D-Melittin analog	500	65	stress	partial
6	Cecropin analog	1000	44 <sup>a</sup>	stress	none
7	(KFAKFAK) <sub>3</sub> -NH <sub>2</sub>	100	91	none	none
8	(KLAKLAK) <sub>3</sub> -NH <sub>2</sub>	100	51	none	none
9	(KLAKKLA) <sub>3</sub> -NH <sub>2</sub>	100	0 <sup>a</sup>	none	none
10	(KALKALK) <sub>3</sub> -NH <sub>2</sub>	100	63 <sup>a</sup>	none	ND
11	(KLGKKLG) <sub>3</sub> -NH <sub>2</sub>	500	18 <sup>a</sup>	stress	none
12	(KAAKAAA) <sub>3</sub> -NH <sub>2</sub>	1000	0 <sup>a</sup>	stress	ND
13	KBBKKBBKBBKBB-NH <sub>2</sub>	500	80	none	complete
14	KKBBKBBKBB-NH <sub>2</sub>	500	63	none	complete
15	Ac- KKBBKBBKBB-NH <sub>2</sub>	500	30	none	complete
16	KXXXXXXXKXX-NH <sub>2</sub>	100	33 <sup>a</sup>	none	complete
17	KKXXXXKXX-NH <sub>2</sub>	100	0 <sup>a</sup>	toxic	complete
18	BBJKBBKBB-NH <sub>2</sub>	500	90	none	complete
19	Ac- BBJKBBKBB-NH <sub>2</sub>	500	0 <sup>a</sup>	toxic	ND

\*Melittin analog = FALALKALKKALKKALKKAL-NH<sub>2</sub>, D-Melittin analog = D-(FALALKALKKALKKALKKALKKAL)-NH<sub>2</sub>; Cecropin analog = RWRLFRRIDRVGKQIKQIGILRAGPAIALVGDARAV-NH<sub>2</sub>. <sup>a</sup>not statistically significant

*Brucella abortus* has been reduced *in vivo* in BALB/c mice by selective killing of infected macrophages. This selective killing of infected macrophages may be applied to other intracellular pathogens.

## Acknowledgments

We gratefully acknowledge support via the NSF/EPSCoR Grant [(RII/EPSCoR)LEQSF(1992-96)-ADP—01].

## References

1. Yokum, T.S., Elzer, P.H., McLaughlin, M.L., J. Med. Chem., 39 (1996) 3603.
2. Javadpour, M.M., Juban, M.M., Lo, W.-C.J., Bishop, S.M., Alberty, J.B., Cowell, S.M., Becker, C.L., McLaughlin, M.L., J. Med. Chem., 39 (1996) 3107.
3. Wade, D., Boman, A., Wählin, B., Drain, C.M., Andreu, D., Boman, H.G., Merrifield, R.B., Proc. Natl. Acad. Sci. U.S.A., 87 (1990) 4761.

# Properties of cyclic peptides having inhibitory site of $\alpha$ -amylase inhibitor tendamistat

**Tomiya Hirano,<sup>a</sup> Shin Ono,<sup>a</sup> Hiroyuki Morita,<sup>a</sup> Toshiaki Yoshimura,<sup>a</sup>  
Hiroki Yasutake,<sup>b</sup> Tetsuo Kato<sup>b</sup> and Choichiro Shimasaki<sup>a</sup>**

<sup>a</sup>Department of Chemical and Biochemical Engineering, Faculty of Engineering, Toyama University, Gofuku 3190, Toyama, 930 Japan; <sup>b</sup>Department of Applied Microbial Technology, Kumamoto Institute of Technology, Kumamoto 860 Japan

*Streptomyces tendae* 4158 produces an extracellular protein, tendamistat, showing a strong inhibitory activity ( $K_i = \text{ca. } 0.2\text{nM}$ ) against porcine pancreatic  $\alpha$ -amylase [1]. Tendamistat is 74 amino acids long and consists of a small and a large loop (Cys<sup>11</sup>-Cys<sup>17</sup> and Cys<sup>45</sup>-Cys<sup>73</sup>, respectively) bridged by disulfide bonds. The three-dimensional structures of tendamistat and its complex with pancreatic alpha-amylase were determined by X-ray crystallographic and NMR spectroscopic techniques [2-5]. The small loop forms a  $\beta$ -turn connecting two strands of a  $\beta$ -sheet which contains an inhibitory site (Trp<sup>18</sup>-Arg<sup>19</sup>-Tyr<sup>20</sup>). So far, several  $\beta$ -turn model peptides have been designed and synthesized, and their conformation and inhibitory activities were investigated [6-10]. In this work, five short cyclic peptides having the inhibitory site, Ten(16-22), Ten(15-23), Ten(14-24), Ten(13-25), and Ten(12-26), were synthesized (Fig. 1). Their structures in an aqueous solution and TFE (trifluoroethanol) were examined by circular dichroism (CD) spectroscopy and their inhibitory activities for porcine pancreatic alpha-amylase were measured.

## Results and Discussion

All five peptides were synthesized manually by the solid phase method on Fmoc chemistry. We reported on the structures of four, Ten(15-23), Ten(14-24), Ten(13-25), Ten(12-26) which gave good agreement with their desired structure on MALDI-TOF-MS. Ten(16-22), however, gave a mass corresponding to the dimerized product. CD spectra of Ten(12-26), Ten(13-25), and Ten(14-24) in 20mM Tris-HCl buffer (pH 7.0) were relatively similar to each other (Fig. 2A), although their differences appeared random. The CD spectrum of Ten(15-23) with minimum at 218 nm differed from that of the other peptides. Ten (15-23) may take a partial  $\beta$ -sheet structure. The effect of TFE on the

**-Cys-Val<sup>12</sup>-Thr-Leu-Tyr-Gln-Ser-Trp-Arg-Tyr-Ser-Gln-Ala-Asp-Asn-Gly<sup>26</sup>-Cys-**

*Fig. 1. Amino acid sequence of the small loop of tendamistat.*

structure of the cyclic peptides was investigated (Fig. 2B). The CD spectra of Ten(12-26), Ten(13-25), and Ten(14-24) showed double minima at around 208 and 222 nm. This indicates that these three peptides predominantly form  $\alpha$ -helical structures in TFE. However, Ten(15-23) showed a CD spectrum with a minimum at 227nm in TFE.

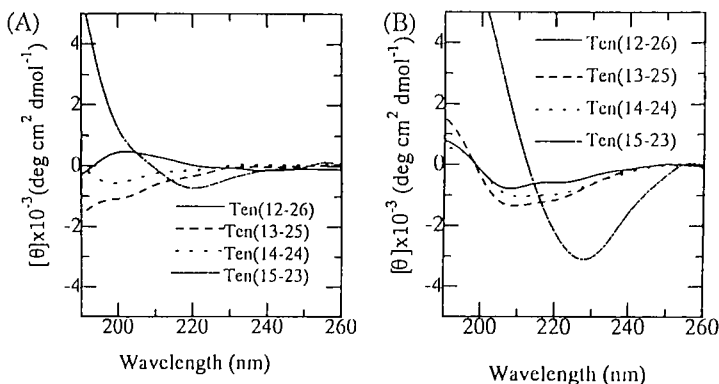


Fig. 2 CD spectra of the four cyclic peptides in 20 mM Tris-HCl buffer (pH7.0) (A) and TFE (B). The peptide concentrations were 10  $\mu$ M.

In conclusion, the CD spectral data in buffer and TFE suggested that the structural properties of Ten(15-23) differed from those of other peptides. In a preliminary work, Ten(15-23) showed the strongest inhibitory activity ( $K_i = 121 \mu$ M) among the four peptides, although its inhibition was weak. Therefore, the present results may imply a relationship between the structure and the inhibitory activity of short cyclic peptides.

## References

1. Vertesy, L., Oeding, V., Bender, R., Zepf, K. and Neesemann, G., *Eur. J. Biochem.*, 141 (1984)505-512.
2. Pflugrath, J. W., Wiegand, G., Huber, R. and Vertesy, L., *J. Mol. Biol.*, 189(1986)383.
3. Kline, A. D., Braun, W. and Wuthrich, K., *J. Mol. Biol.*, 189(1986)367-382.
4. Wiegand, G., Epp, O. and Huber, R., *J. Mol. Biol.*, 247(1995)99.
5. Oconnell, J. F., Bender, R., Engels, J. W., K.-P., Scharf, M. and Wuthrich, K., *Eur. J. Biochem.*, 220(1994)763.
6. Blanco, F. J., Jimenez, M. A., Rico, M., Santoro, J., Herranz, J. and Nieto, J. L., *Eur. J. Biochem.*, 200(1994)345.
7. Etzkorn, F. A., Guo, T., Lipton, M. A., Goldberg, S. D. and Bartlett, P. A., *J. Am. Chem. Soc.*, 116(1994)10412.
8. Matter, H. and Kessler, H., *J. Am. Chem. Soc.*, 117(1995)3347.
9. Blanco, F. J., Jimenez, M. A., Herranz, J., Rico, M., Santoro, J. and Nieto, J., *J. Am. Chem. Soc.*, 115(1993)5887.
10. Thin, Z. -Q. and Bartlett, P. A., *J. Am. Chem. Soc.*, 118(1996)943.

# Solid-phase synthesis of caged peptides containing photolabile derivatives of aspartic acid

Yoshiro Tatsu, Yasushi Shigeri, Shinji Sogabe, Noboru Yumoto, and Susumu Yoshikawa

Osaka National Research Institute, AIST, Midorigaoka, Ikeda, Osaka 563, Japan

Rapid release of biologically active substances from photolabile (caged) precursors is an important technique in the study of fast and local biological processes, such as in muscle fiber and in neuron. Recently we have developed a simple method for the synthesis of caged peptides using derivatives of tyrosine [1] and lysine of which side chains were protected with a photocleavable group. Here we report the development of a method to synthesize derivatives of aspartic acid residues.

## Results and Discussion

The side chain of aspartic acid was selectively protected by the complexation of  $\alpha$ -amino and carboxy groups with copper ion, in a manner similar to those of tyrosine and lysine.  $\beta$ -Carboxyl group of aspartic acid was protected with 2-nitrobenzyl or 2-nitro, 3, 4-dimethoxybenzyl group and the  $\alpha$ -amino group was then protected with Fmoc group (Fig.1). The derivatives of aspartic acid were used for solid phase synthesis of angiotensin II (DRVYIHPF) using an automated peptide synthesizer under the usual Fmoc chemistry.

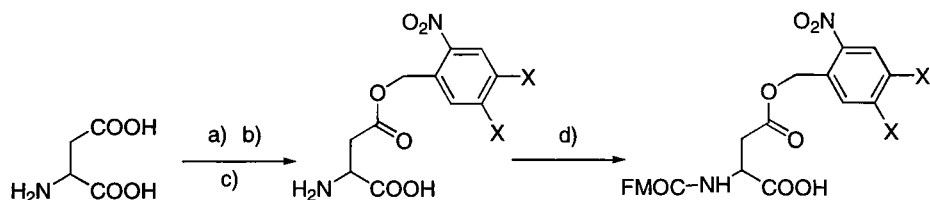
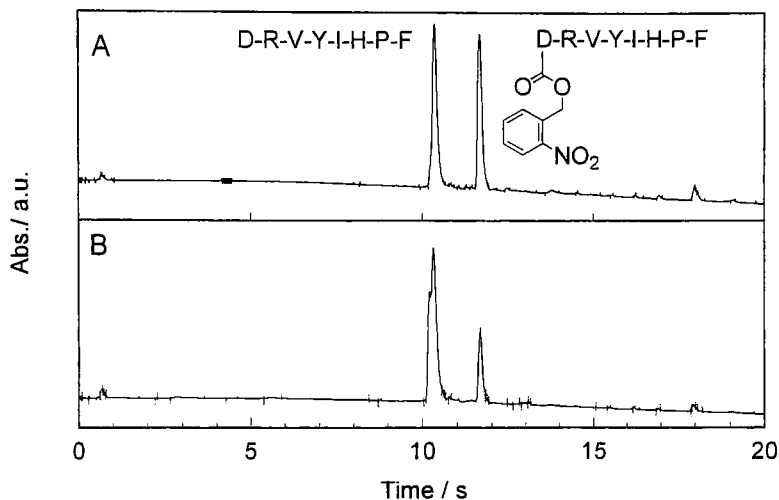


Fig. 1. Preparation of the photolabile derivatives of aspartic acid. a) Copper acetate, b) nitrobenzylbromide for  $X = H$  and nitrovertrylbromide for  $X = OCH_3$ , c) EDTA, d) Fmoc-OSu.

In the crude products of the peptide synthesis, two major peaks were found in  $C_{18}$ -RP-HPLC (Fig. 2A). The later peak was assigned to the nitrobenzyl angiotensin II by mass spectrometry: obs. 1184 and calcd. 1181. The earlier peak was assigned to the intact angiotensin II. The nitrobenzyl group of the peptide was also found to be stable for trifluoroacetic acid but not for piperidine, indicating that the nitrobenzyl group was partially cleaved during the removal of the Fmoc group.

When nitrobenzyl angiotensin II was irradiated with UV light by a hand lamp for TLC viewer for 30 min, production of the intact peptide was observed (Fig.2B). Similar results were observed for the peptide containing the nitroveratryl derivative of aspartic acid.



*Fig.2. HPLC analysis of the photolabile precursor of angiotensin II. The crude product of the peptide synthesis of the nitrobenzyl angiotensin II (A) and the photolytic products of the nitrobenzyl angiotensin II (B).*

In conclusion, photolabile peptides protected at aspartic acid residue were substantially obtained and can be used as caged peptides, although the photolabile group was partially removed during the peptide synthesis.

## References

1. Tatsu, Y, Shigeri, Y., Sogabe, S., Yumoto, N., and Yoshikawa, S., *Biochem. Biophys. Res. Commun.*, 227 (1996) 688.

# Induction of erectogenic activity in the human male by systemic delivery of a melanotropic peptide

M. Hadley<sup>a</sup> and V. J. Hruby<sup>b</sup>

*From the Departments of <sup>a</sup>Cell Biology & Anatomy and <sup>b</sup>Chemistry, University of Arizona, Tucson, AZ 85724, USA*

$\alpha$ -Melanocyte stimulating hormone ( $\alpha$ -MSH, Ac-Ser-Tyr-Ser-Met-Glu-His-Phe-Arg-Trp-Gly-Lys-Pro-Val-NH<sub>2</sub>), regulates melanin pigmentation of the skin in many animals, including humans. Ac-Nle-c[Asp-His-DPhe-Arg-Trp-Lys]-NH<sub>2</sub> (MT-II) is a superpotent, prolonged acting, enzyme resistant, melanotropic peptide analog of  $\alpha$ -MSH. This cyclic lactam-bridged peptide is a superagonist of peripheral (melanocyte) MC1Rs. Ac-Nle<sup>4</sup>-c[Asp<sup>5</sup>, DPhe<sup>7</sup>, Lys<sup>10</sup>]  $\alpha$ -MSH<sub>4-10</sub>-NH<sub>2</sub> is also a potent agonist of melanocortin 3, 4 and 5 brain receptors. When injected intracerebro-ventricularly in the mouse, the peptide inhibited feeding and the mice lose weight [1]. Most interestingly, MT-II also induced erections in human males, as discussed below.

## Results and Discussion

The cyclic peptide (MT-II) was chemically synthesized using solid phase synthesis based on previously published methods. The linear molecule was cyclized by coupling the side chain groups of Asp<sup>5</sup> and Lys<sup>10</sup> with BOP reagents, and the resultant cyclic lactam-bridged peptide, Ac-Nle<sup>4</sup>-c[Asp<sup>5</sup>-His<sup>6</sup>-DPhe<sup>7</sup>-Arg<sup>8</sup>-Trp<sup>9</sup>-Lys<sup>10</sup>]-NH<sub>2</sub>, was then purified by reverse-phase high-performance liquid chromatography as previously described [2].

Several normal white males were enrolled in this study after informed consent was obtained through a protocol approved by the Human Subjects Committee, Arizona Health Sciences Center, University of Arizona. The starting dose of MT-II was 0.01 mg/kg, which was less than one-tenth the dose safely administered to rodents in unpublished preclinical toxicity tests. The trial was single-blinded; the placebo, 0.9% NaCl, was given on alternate days so that MT-II was never administered on successive days. Each subject received a single daily subcutaneous injection for 5 days per week for two consecutive weeks. Thus, each subject received 5 injections of MT-II and 5 injections of saline over a 2-week period. The MT-II dose for each subject was escalated by 0.005 mg/kg increments. All three subjects developed an erection in response to MT-II to at least one of the concentrations administered. At a dose level of 0.025 mg/kg (3 escalations from baseline), spontaneous, non-painful penile erections were reported in all subjects. Satiety, flushing, yawning/stretching, gastrointestinal discomfort, and fatigue were transient side effects noted in some of the volunteers. None of the three subjects reported stretching and yawning or penile erections on any of the five days of saline injection [3]. Ten men with claimed erectile dysfunction of a psychogenic (non-organic/physiological) nature were then enrolled in a double-blind crossover vehicle-controlled study. Eight of the ten subjects developed erections to subcutaneous (non-penile)

injections of MT-II (0.025-0.157 mg) as monitored objectively by Rigiscan (penile tumescence meter). This device measures rigidity of both the tip and the base of the penis. The erections were deemed satisfactory for intercourse. Transient side effects (stretching and yawning, facial flushing, and nausea) were reported in 9/10 men administered MT II versus 4/10 on placebo. The side effects in the individuals so far studied were mild and no participants terminated participation because of the toxicity associated with the test compound. Nevertheless, at high doses the peptide can cause gastrointestinal discomfort such as cramping and/or vomiting. The peptide does not appear to enhance libido, but rather, causes a transient erectile response (an erection on demand). The peptide appears to be effective for the differential diagnosis of erectile dysfunction and for the treatment of psychological (idiopathic) erectile dysfunction.

To our knowledge, this is the first study to demonstrate that a melanotropic peptide administered by injection induces an erectile response in humans. Both  $\alpha$ -MSH and  $\beta$ -MSH, as well as ACTH have been injected into humans. Although other side effects were carefully documented, in no instance was induction of an erection reported. In fact, in the rat, it was reported that sexual responses such as penile erections can only be induced by direct intracerebro-ventricular injection of a melanotropic peptide [4]. Most interesting in the present study was the observation that, as in rodent studies, administration of a melanotropic peptide not only produced an erection, but also induced a form of stretching/yawning response ("syndrome", SYS). Since these responses originate in the brain, it suggests that most likely subcutaneous injection of the peptide with delivery to the systemic circulation results most likely in the passage of the peptide across the blood-brain barrier into the central nervous system. MT-II therefore represents a model for the development of peptide delivery to the brain. The peptide and related analogs are patented for use in the diagnosis and treatment of impotency of psychogenic origin.

## References

1. Fan, W., Boston, B.A., Kesterson, R.A., Hruby, V.J. and Cone, R.D. *Nature*, 385 (1997) 165.
2. Al-Obeidi, F., Hruby, V.J., Castrucci, A.M.L. and Hadley, M.E. *J. Med. Chem.*, 32 (1989) 2555.
3. Dorr, R.T., Lines, R., Levine, N., Xiang, L., Hruby, V.J. and Hadley, M.E. *Life Sci.*, 58 (1996) 1777.
4. Vergoni, A.V., Poggioli, R., Facchinetti, F., Bazzani, C., Marrama, D. and Bertolini, A. *Neuropeptides*, 14 (1989) 93.

# Design and synthesis of opioid mimetics containing pyrazinone ring and examination of their opioid receptor binding activity

Yoshio Okada,<sup>a</sup> Masaki Tsukatani,<sup>a</sup> Hiroaki Taguchi,<sup>a</sup> Toshio Yokoi,<sup>a</sup>  
Sharon D. Bryant<sup>b</sup> and Lawrence H. Lazarus<sup>b</sup>

<sup>a</sup>Faculty of Pharmaceutical Sciences, Kobe Gakuin University, Nishi-ku, Kobe 651-21, Japan and

<sup>b</sup>Peptide Neurochemistry, LMNI, National Institute of Environmental Health Sciences, Research Triangle Park, NC 27709, USA

Previously, a facile and convenient synthetic procedure for obtaining 2(1*H*)-pyrazinone derivatives from dipeptidyl chloromethyl ketones was developed [1]. This novel synthetic method can afford 2(1*H*)-pyrazinone derivatives substituted at positions 3 and 6 with the desired groups in high yield. Therefore, an amino group and/or a carboxyl group can be introduced at position 3 or 6 of the pyrazinone ring by using the appropriate amino acid residues. Our idea is to employ the above pyrazinone derivatives to prepare peptidomimetics. This paper deals with the synthesis of pyrazinone ring-containing tyrosine derivatives (Fig. 1), examination of their binding activity with opioid receptors and studies on structure-activity relationships.

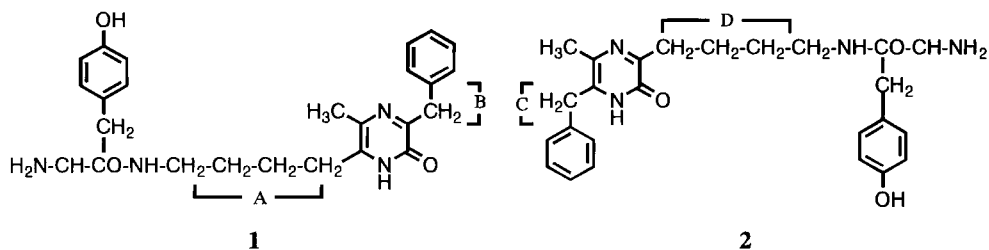


Fig. 1. Structures of Two Types of Tyrosine Derivatives.

## Results and Discussion

All pyrazinone ring-containing tyrosine derivatives were synthesized by our novel method. As shown in Fig. 1, two types of tyrosine derivatives containing pyrazinone rings were prepared. In order to study the structure-activity relationship of the tyrosine derivatives, parts A or D and B or C in 1 and 2 were modified. For the introduction of amino groups with different chain lengths at position 3 or 6 of a pyrazinone ring, lysine, ornithine, 2,4-diaminobutyric acid or 2,3-diaminopropionic acid was employed as a constituent amino acid of dipeptidyl chloromethyl ketone. For the introduction of phenyl groups with different chain lengths at position 3 or 6 of pyrazinone ring, phenylglycine, phenylalanine or homophenylalanine was employed as a constituent amino acid of dipeptidyl chloromethyl ketone. All tyrosine derivatives were purified with preparative HPLC and the purity of each compound was confirmed by analytical HPLC and FAB mass spectrometry.

The opioid activity profile of each compound was determined using a receptor binding assay based on displacement of  $^3\text{H}$ -DAGO [(D-Ala<sup>3</sup>,Gly-ol<sup>5</sup>)-enkephalin] ( $\mu$ -selective) and  $^3\text{H}$ -DPDPE [c(D-Pen<sup>2</sup>, D-Pen<sup>5</sup>)-enkephalin] ( $\delta$ -selective) from rat brain membrane binding sites [2]. Compound **1** exhibited binding activity with  $\delta$  receptor with a  $K_i$  value of 333 nM and with  $\mu$  receptor with a  $K_i$  value of 3909 nM. It was revealed that a benzyl moiety at position 3 of compound **1** was required to manifest binding activity with  $\delta$  receptor. Compound **2** exhibited binding activity with  $\delta$  receptor with a  $K_i$  value of 462 nM and with  $\mu$  receptor with a  $K_i$  value of 438 nM. These results show that the introduction of a Tyr residue at position 3 or 6 of the pyrazinone ring gives different opioid activity profiles.

In order to obtain more potent opioid mimetics, structure-activity relationships were studied. First the chain length of part A and/or B of compound **1** (Fig. 1) was changed to give various compounds. However, all compounds obtained exhibited much less binding activity with both  $\delta$  and  $\mu$  receptors compared with the parent molecule **1**. Next, the chain length of part C and/or D of compound **2** (Fig. 1) was changed. Of the various compounds prepared, only 5-methyl-6-phenethyl-3-tyrosylaminobutyl-2(1*H*)-pyrazinone (Fig. 2) exhibited binding activity at the  $\mu$  opioid receptor with a  $K_i$  value of 55.8 nM and  $\delta$  opioid receptor with a  $K_i$  value of 2165 nM.

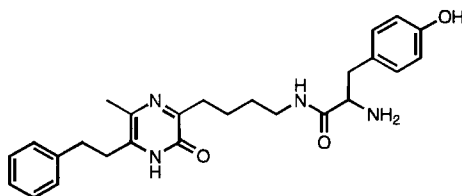


Fig. 2. Structure of  $\mu$  Selective Opioid Mimetic.

## References

1. Taguchi, H., Yokoi, T., Tsukatani, M. and Okada, Y., *Tetrahedron*, 51 (1995) 7361.
2. Salvadori, S., Attila, M., Balboni, G., Bianchi, C., Bryant, S.D., Crescenzi, O., Guerrini, R., Picone, D., Tancredi, T., Temussi, P.A. and Lazarus, L.H., *Molecular Medicine*, 1 (1995) 678.

# Intracellular third loop of galanin receptor as G-protein interaction site

Ursel Soomets and Ülo Langel

*Department of Neurochemistry and Neurotoxicology, Arrheniuslaboratories, Stockholm University, S-10691 Stockholm Sweden*

Galanin is a 29/30 amino acid long neuroendocrine peptide with widespread distribution in the endocrine, peripheral and central nervous systems [1]. It has a regulatory role in a variety of physiological processes including release of neurotransmitters and hormones, smooth muscle contractility, nociception, feeding, and memory-related and sexual behaviors [2]. Galanin triggers cellular responses by acting at seven transmembrane domain type galanin receptor(s). The first galanin receptor subtype, GalR1, was cloned from human melanoma cell line Bowes' in 1994[3]. Another galanin receptor subtype, GalR2, was cloned in 1997[4]. The effects of activated galanin receptors are mediated by G<sub>i1-3</sub>/G<sub>o</sub> subtypes of pertussis toxin ADP-ribosylable G-proteins[5]. Galaninergic effects mediated by different effector systems play a role in pathophysiological conditions involving pain signalling, cognitive and feeding disorders, and diabetes, which makes this system interesting as a potential drug target. Mutagenesis studies of different receptors have shown that the third intracellular loop is a major determinant for G-protein binding and activation. Synthetic peptides derived from the third intracellular loop of many receptors have been demonstrated to mimic the receptor G-protein interaction[6]. In this study, we have examined the effect of synthetic peptides corresponding to the sequences of the whole [GalR1(222-245)amide, KVLNHLHKKLKNMSKKSEAS KKKTamide] (whole ic3), N-terminus [GalR1(222-233)amide, KVLNHLHKKLKNamide] (N-ic3) and C-terminus [GalR1(235-245)amide, SKKSEASKKKTamide] (C-ic3) of the third intracellular loop of rat/human galanin receptor (GalR1) on galaninergic signal transduction in rat ventral hippocampal and Bowes' human melanoma cell membrane preparations.

## Results and Discussion

To study the involvement of the third intracellular loop of the human Bowes' galanin receptor in signal transduction, peptides with sequences from the third intracellular loop of rat/human galanin receptors were synthesized. Their influence on <sup>125</sup>I-galanin binding, basal activity of G-protein coupled adenylate cyclase and GTPase activity in membrane preparations from rat ventral hippocampal and Bowes' human melanoma cells were measured.

The IC<sub>50</sub> for the inhibition of basal adenylate cyclase activity in ventral hippocampus by the N-terminus and whole third intracellular loop were 115 nM and 393 nM, respectively. In the case of Bowes cell membrane preparations, all three synthetic peptides were able to inhibit adenylate cyclase activity. All synthetic peptides were found to be

nearly equipotent and the inhibitory effects of N-ic3, C-ic3 and whole ic3 at 10  $\mu\text{M}$  concentration were 24, 26 and 28%, respectively.

N-ic3 and whole ic3 had the ability to increase GTPase activity in ventral hippocampal membrane preparations. The maximal activity induced by the peptides were 32% and 28% higher than basal GTPase activity, with  $\text{EC}_{50}$  of  $2.8 \pm 0.7$  nM and  $4.8 \pm 1.4$  nM, respectively. The effects of N-ic3 on GTPase activity is characterized by relatively high affinity compared with that of whole ic3.

All three synthetic peptides inhibited  $^{125}\text{I}$ -galanin binding in rat ventral hippocampal and Bowes human melanoma cell membrane preparations. N-ic3 displaces  $^{125}\text{I}$ -galanin from Bowes cell membranes with a  $K_D = 16 \pm 3$   $\mu\text{M}$ , while whole ic3 had  $K_D = 72 \pm 18$   $\mu\text{M}$ , and C-ic3 had  $K_D = 187 \pm 35$   $\mu\text{M}$ . In the rat ventral hippocampal membranes, the  $K_D$  for whole ic3 =  $35 \pm 8$   $\mu\text{M}$  and for C-ic3 the  $K_D = 185 \pm 32$   $\mu\text{M}$ . All these inhibitory effects may be explained by the conformational changes in the receptor protein caused by the competition of the synthetic peptides and the receptor for the G-protein. This interaction could alter ligand recognition by the extracellular loops of the receptor.

In conclusion, the N-terminus [ $K_D$  GALR(222-233)amide] of the third intracellular loop of galanin receptor is responsible for receptor - G-protein interaction, causing changes in receptor coupled effector systems and also in ligand binding properties. Such mimicry of protein-protein interaction by short peptides could be used as a lead for drug design for disorders of signal transduction by galanin receptors. The role of the other intracellular loops of the galanin receptor in signal transduction remain to be clarified.

## Acknowledgments

This work was supported by grants from the Swedish Research Council for Engineering Sciences (TFR), from European Structural JEP 09270-95, from Swedish Institute and from Royal Swedish Academy.

## References

1. Bartfai, T., Hökfelt, T. and Langel, Ü., *Crit. Rev. Neurobiol.*, 7 (1993) 229.
2. Kask, K., Langel, Ü. and Bartfai, T., *Cell. Mol. Neurobiol.*, 15 (1995) 653.
3. Habert-Ortoli, E., Amiranoff, B., Loquet, I., Laburthe, M. and Mayaux, J.F., *Proc. Natl. Acad. Sci. U.S.A.*, 91 (1994) 9780.
4. Howard, A.D., Tan, C., Shiao, L.-L., Palyha, C., McKee, K.K., Weinberg, D.H.,
5. Feighner, S.D., Cascieri, M.A., Smith, R.G., Van Der Ploeg, L.H.T. and Sullivan, K.A., *FEBS Letters*, 405 (1997) 285.
5. Lorinet, A.M., Javoyagid, F., Laburthe, M. and Amiranoff, B., *Eur. J. Pharmacol.- Molec. Pharm.*, 269 (1994) 59.
6. Hayashida, W., Horiuchi, M. and Dzau V.J., *J. Biol. Chem.*, 271 (1996) 21985.



## **Session VIII**

### **Protease Inhibitors**



# Potent dipeptide HIV protease inhibitors containing the hydroxymethylcarbonyl isostere as an ideal transition-state mimetic

Yoshiaki Kiso,<sup>a</sup> Satoshi Yamaguchi,<sup>a</sup> Hikaru Matsumoto,<sup>a</sup> Tsutomu Mimoto,<sup>b</sup> Ryohei Kato,<sup>b</sup> Satoshi Nojima,<sup>b</sup> Haruo Takaku,<sup>b</sup> Tominaga Fukazawa,<sup>b</sup> Tooru Kimura<sup>a</sup> and Kenichi Akaji<sup>a</sup>

<sup>a</sup>Department of Medicinal Chemistry, Kyoto Pharmaceutical University, Yamashina-ku, Kyoto 607, Japan and <sup>b</sup>Bioscience Research Laboratories, Japan Energy Co., Toda 335, Japan

Based on the substrate transition state, we designed and synthesized a novel class of HIV protease inhibitors containing allophenylnorstatine [A<sub>pn</sub>s; (2*S*, 3*S*)-3-amino-2-hydroxy-4-phenylbutyric acid] with a hydroxymethylcarbonyl (HMC) isostere. Among them, the tripeptide KNI-272 was a highly selective and superpotent HIV protease inhibitor (K<sub>i</sub> = 5.5 pM) [1]. KNI-272 exhibited potent in vitro and in vivo antiviral activities with low cytotoxicity [2]. The NMR, X-ray crystallography and molecular modeling studies showed that the HMC group in KNI-272 interacted excellently with the aspartic acid carboxyl groups of HIV protease active site [3].

The hydroxyl group makes one hydrogen bond to Asp<sup>125</sup> oxygen and the carbonyl oxygen makes a hydrogen bond to the protonated oxygen of Asp<sup>25</sup> in the essentially the same manner as the transition state (Fig. 1). The *trans* conformation of the HMC-peptide bond at the P1-P1' site of KNI-272 was predominant due to the rigidity of the P1-P1' amide linkage. The *trans* conformer of KNI-272 fitted favorably to HIV-1 protease and was the bioactive conformation. Thus, KNI-272 was preorganized to bioactive conformation and constrained conformation of KNI-272 might be responsible for the high activity. These results imply that the HMC isostere is an ideal transition-state mimetic. Here, we report potent small-sized dipeptide inhibitors containing the HMC isostere.

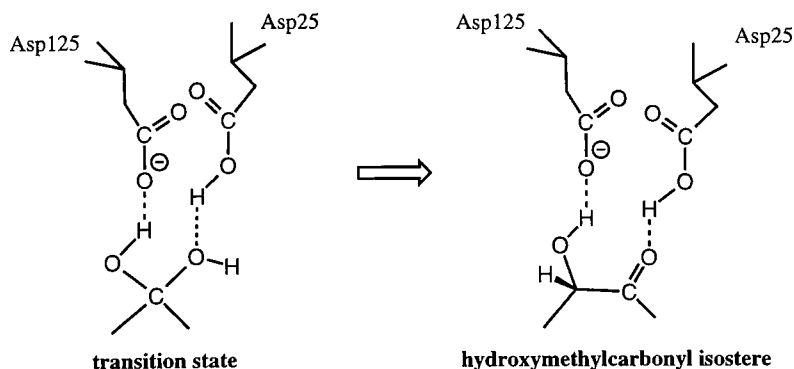


Fig. 1. Interaction of active site aspartic acids.

## Results and Discussion

HIV-1 develops *in vitro* a high level of resistance to KNI-272 by acquiring mutations in the protease-encoding gene, although it takes relatively a long time. The sensitivity of KNI-272 reduced 130-fold against mutant HIV-1 V32I/L33F/K45I/F53L/A71V/I84V. In order to overcome the resistance, the Apns-containing peptides were screened and KNI-241 (Fig. 2) was found to be active against both wild-type and resistant variants. The P3 moiety of KNI-241 is interacting with 53-Leu of the mutant protease [4].

Furthermore, we studied small-sized dipeptide inhibitors (Fig. 2). The solution, crystalline and complex structures of KNI-272 were similar except for P3 moiety [5]. Therefore, P3 was removed and P2 was replaced by several alkyl and hydrophilic groups. Among them, KNI-413 and -549 containing a dimethyl and a carboxyl groups exhibited HIV protease inhibitory activities [6].

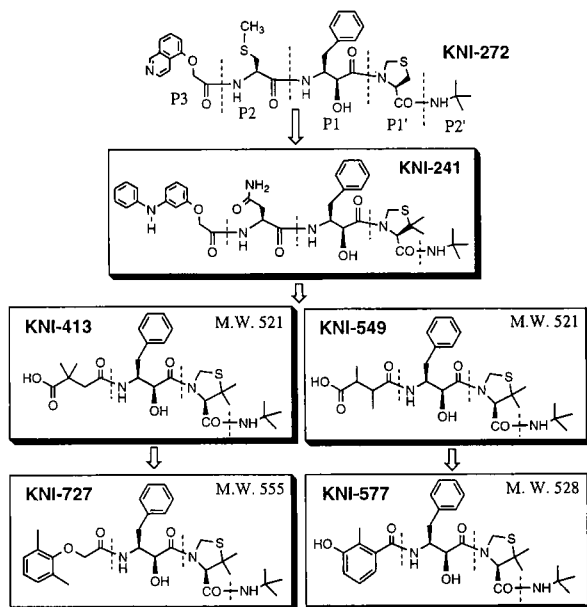


Fig. 2. Design of dipeptide HIV protease inhibitors.

In order to enhance the inhibitory activity, we carried out the optimization study of P2 moiety. At first, we introduced the dimethylphenoxyacetyl group in P2 position to give a potent HIV protease inhibitor KNI-727 (HIV protease inhibition = 95.9% at 50 nM; anti-HIV activity  $EC_{50}$  = 1.73  $\mu$ M in MT4 cells) [7]. Next, we cyclized P2 moiety in KNI-549 to give a potent HIV protease inhibitor KNI-577 (87.6% inhibition at 50 nM) which showed remarkable anti-HIV activity ( $EC_{50}$  = 0.02  $\mu$ M in CEM-SS cells). This antiviral activity of

KNI-577 was higher than that of the tripeptide KNI-272. KNI-577 had very low cytotoxicity and the bioavailability after intraduodenal administration in rats was 48%. The excellent antiviral activity and good pharmacokinetic properties of KNI-577 may be due to the constrained conformation and the good balance between hydrophilicity and lipophilicity caused by the cyclized P2 moiety.

The synthetic scheme of KNI-577 is simple and short as shown in Fig. 3. All couplings were performed by DCC/HOBt, and all deprotections by HCl.

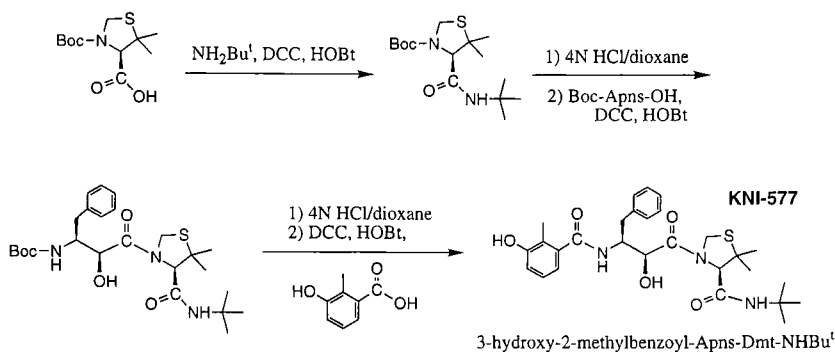


Fig. 3. Synthesis of KNI-577, a potent dipeptide HIV protease inhibitor.

In conclusion, the hydroxymethylcarbonyl isostere was an ideal transition-state mimetic in HIV protease inhibitor design. Small-sized dipeptides containing the hydroxymethylcarbonyl isostere exhibited potent HIV protease inhibitory activities. Among them, a dipeptide HIV protease inhibitor, KNI-577 exhibited potent antiviral activities, low toxicity and good pharmacokinetic properties. This study suggests that the small-sized dipeptide HIV protease inhibitors are good candidates for anti-HIV drugs.

## References

- Mimoto, T., Imai, J., Kisanuki, S., Enomoto, H., Hattori, N., Akaji, K. and Kiso, Y., *Chem. Pharm. Bull.*, 40 (1992) 2251.
- Kiso, Y., *Biopolymers*, 40 (1996) 235.
- Wang, Y. X., Freedberg, D. I., Yamazaki, T., Wingfield, P. T., Stahl, S. J., Kaufman, J. D., Kiso, Y. and Torchia, D. A., *Biochemistry*, 35 (1996) 9945.
- Tanaka, M., Mimoto, T., Anderson, B., Gulnik, S., Bhat, T. N., Yusa, K., Hayashi, H., Kiso, Y., Erickson, J. W. and Mitsuya, H., 11th Int. Conf. AIDS (1996) Abst. Tu.A.260.
- Ohno, Y., Kiso, Y. and Kobayashi, Y., *Bioorg. Med. Chem.* 4 (1996) 1565.
- Mitoguchi, T., Nakata, S., Enomoto, H., Kimura, T., Akaji, K., Hattori, N., Kato, R., Mimoto, T. and Kiso, Y., In Nishi, N. (Ed) *Peptide Chemistry 1995*, Protein Res. Found., Osaka, 1996, p. 373.
- Yamaguchi, S., Mitoguchi, T., Nakata, S., Kimura, T., Akaji, K., Nojima, S., Takaku, H., Mimoto, T. and Kiso, Y., In Kitada, C. (Ed) *Peptide Chemistry 1996*, Protein Res. Found., Osaka 1997, p.297.

# Rational design and synthesis of conformationally constrained inhibitors of human cathepsin D

Pavel Majer, Jack R. Collins, Wenxi Pan, Sergei V. Gulnik, Angela Lee, Elena Gustchina and John W. Erickson

Structural Biochemistry Program, SAIC, National Cancer Institute, Frederick Research and Development Center, Frederick MD, 21702-1201, USA

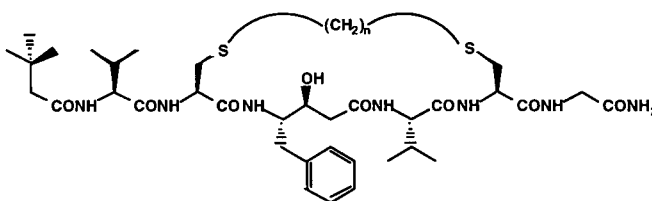
Cathepsin D, a ubiquitous lysosomal catabolic protease, has attracted increasing attention in the last few years. The enzyme plays an important yet not fully understood role in the pathophysiology of cancer, especially breast cancer [1]. It is involved in processes leading to the breakdown of basement membranes and eventually to metastatic spread of the disease [2]. Cathepsin D is also thought to be responsible for proteolysis of the soluble  $\beta$ -amyloid precursor and subsequent senile plaque formation in the brain of Alzheimer's patients [3]. The inhibition of overproduced cathepsin D may therefore be a promising approach to treatment of these diseases.

## Results and Discussion

Our lab recently solved the crystal structure of the tight binding ( $K_i$  in  $10^{-11}$  M range) complex of human cathepsin D with pepstatin A (IvaValValStaAlaSta-OH; a general inhibitor of aspartic proteases) [4] and a complex with a cyclic inhibitor **2**. In the present study we have used crystal structures of cathepsin D-inhibitor complexes as guides for the rational design of small molecule peptidomimetic inhibitors with the aim of avoiding inherent difficulties connected with the use of linear peptides as leads for drug development.

Table 1. Cyclic inhibitors with cycles connecting P2-P3' positions.

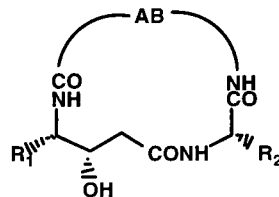
#	n	$K_i$ [nM]
1	2	2.0
2	3	1.5
3	4	0.1



We have prepared a series of cyclic inhibitors with bridges connecting P<sub>2</sub> and P<sub>3</sub>' positions. Introduction of these cycles into full size (ie. P<sub>4</sub> - P<sub>4</sub>' spanning) pepstatin A analogues led to a slight decrease of potency which was still in the  $10^{-10}$  M range (Table 1). Since a series of truncated linear inhibitors revealed a high sensitivity of pepstatin A to any size reduction we have chosen the cyclic series for further modifications.

Table 2. Truncated cyclic inhibitors.

#	R <sub>1</sub>	R <sub>2</sub>	A	B	K <sub>i</sub> [nM]
4	CH <sub>2</sub> Ph	iPr	-(CH <sub>2</sub> ) <sub>10</sub> -		20
5	CH <sub>2</sub> Ph	iPr	-(CH <sub>2</sub> ) <sub>11</sub> -		4
6	CH <sub>2</sub> Ph	iPr	-(CH <sub>2</sub> ) <sub>12</sub> -		6
7	CH <sub>2</sub> Ph	Me	-(CH <sub>2</sub> ) <sub>11</sub> -		46
8	iBu	iPr	-(CH <sub>2</sub> ) <sub>11</sub> -		125
9	iBu	Me	-(CH <sub>2</sub> ) <sub>11</sub> -		205
10	CH <sub>2</sub> Ph	iPr	-(CH <sub>2</sub> ) <sub>3</sub> CH <sub>3</sub>	CH <sub>3</sub> (CH <sub>2</sub> ) <sub>4</sub>	400



We assumed that the constraining influence of the ring would preorganize inhibitors and decrease the entropic penalty of binding. The extensive hydrophobic contact of the aliphatic bridge with the enzyme S2-S3' pocket might compensate for the binding energy losses caused by truncation. Removal of both exocyclic parts of **3** accompanied by an S => CH<sub>2</sub> replacement led to inhibitor **4** with a potency of 20 nM (Table 2). Extension of its cycle by one methylene increased potency to 4 nM (**5**), whereas further extension had a slightly negative effect (**6**). The importance of proper P1 and P2' side chains (R<sub>1</sub> and R<sub>2</sub>) is demonstrated by compounds **7**, **8** and **9** possessing the original pepstatin substituents. The superiority of our cyclization/truncation design over simple truncation is well illustrated by inhibitor **10**. This compound is approx. two orders of magnitude less active than cyclic inhibitors of comparable size.

## Conclusion

Using a cyclization/truncation design strategy based on the crystal structures of human cathepsin D-inhibitor complexes we prepared a novel series of peptidomimetic inhibitors with potencies as low as 4 nM. The inhibitors have molecular weights less than 500 and contain only three amide endocyclic bonds. These features make them promising lead compounds for development of potential drugs against cathepsin D associated disorders.

## References

1. (a) Tumminello, F.M.; Gebbia, A.; Pizzolanti, G.; Russo, A.; Bazan, V.; Leto, G., *Oncology*, 52(1995)237. (b) Liaudet, E.; Garcia, M.; Rochefort, H. *Oncogene* 9(1994)1145. (c) Cardiff, R.D. *Hum. Pathol.*, 25(1994)847-848.
2. Liotta, L.A., *Cancer Res.* 46(1986)1-7.
3. (a) Schwagerl, A.L.; Mohan, P.S.; Cataldo, A.M.; Vonsattel, J.P.; Kowall, N.W.; Nixon, R.A. *J. Neurochem.*, 64(1995)443-446. (b) Cataldo, A.M.; Hamilton, D.J.; Nixon, R.A., *Brain Res.*, 640(1994)68-80.
4. Baldwin, E.T.; Bhat, T.N.; Gulnik, S.; Hosur, M.V.; Sowder, R.C.; Cachau, R.E.; Collins, J.; Silva, A.M.; Erickson, J.W. *Proc. Natl. Acad. Sci. USA*, 90(1993)6796-6800.

# Discovery of a novel, selective, and orally bioavailable class of thrombin inhibitors incorporating aminopyridyl moieties at the P1 position

Dong-Mei Feng,<sup>a</sup> Roger M. Freidinger,<sup>a</sup> S. Dale Lewis,<sup>b</sup> Stephen J. Gardell,<sup>a</sup> Mark G. Bock,<sup>a</sup> Zhonggo Chen,<sup>c</sup> Adel Naylor-Olsen,<sup>d</sup> Richard Woltmann,<sup>e</sup> Elizabeth P. Baskin,<sup>e</sup> Joseph J. Lynch,<sup>e</sup> Robert Lucas,<sup>b</sup> Jules A. Shafer,<sup>b</sup> Kimberley B. Dancheck,<sup>f</sup> I-Wu Chen<sup>f</sup>, Joseph P. Vacca<sup>a</sup>

<sup>a</sup>Departments of Medicinal Chemistry, <sup>b</sup>Biological Chemistry, <sup>c</sup>X-Ray Crystallography Group, <sup>d</sup>Molecular Systems, <sup>e</sup>General Pharmacology, <sup>f</sup>Drug Metabolism, Merck Research Laboratories, West Point, PA 19486, USA

Recently, a new class of thrombin inhibitor was reported that has nanomolar potency. It contains a trans-4-aminocyclohexyl methyl moiety at the P<sub>1</sub> position (L-371,912), and is selective, but exhibits low oral bioavailability (1-10%) in rat and dog. Herein, we report novel amino aryl P<sub>1</sub> substituents varying in size and basicity, and identify aminopyridyl moieties as important replacements for the trans-aminocyclohexyl group at P<sub>1</sub> in the L-371,912 template. The lipophilic amino acids (D)-3,3-(Ph)<sub>2</sub>-Ala, (D)-3,3-(Chx)<sub>2</sub>-Ala or D-3,4-Cl<sub>2</sub>-Phe and a benzylsulfonyl group on the N-terminus were used as P<sub>3</sub> ligands.

## Results and Discussion

As illustrated in the table, L-371,912 has a K<sub>i</sub> for thrombin of 4.9nM (P<sub>ka</sub> 10.2, logP - 1.68), but exhibits low oral bioavailability (1-10%) in rat and dog. Aniline analog (1) was a low potency thrombin inhibitor with K<sub>i</sub> of 3.7μM (logP 2.34). The analog (2), which has the benzylsulfonyl on the N-terminus and D-3,4-Cl<sub>2</sub>Phe in the P<sub>3</sub> position, displayed a K<sub>i</sub> of 9 nM for thrombin (P<sub>ka</sub> 4.8, logP >3.68), a 400-fold increase in potency over corresponding analog (1). Analog (2) also showed 35% oral bioavailability in rats (Table). The greatly reduced pK<sub>a</sub> of P<sub>1</sub> in analog (2) might facilitate penetration of biological membranes by the uncharged form. The corresponding aminopyridine analog (3) was even more potent, displaying a K<sub>i</sub> for thrombin of 3.0 nM (P<sub>ka</sub> 6.3, logP 2.57). A SAR study therefore has been initiated to incorporate less basic 5 and 6-membered amino-heteroaryl moieties such as aminopyridyl, aminodimethylpyridyl, aminothiazolyl, or aminothiophene at P<sub>1</sub> and append lipophilic groups at P<sub>3</sub> in order to improve inhibitory activity and structural diversity and achieve better oral bioavailability. In the aminopyridine series, the most potent analog (4), which featured D-3,3-(Chx)<sub>2</sub>-Ala at P<sub>3</sub>, displayed a K<sub>i</sub> for thrombin of 0.82 nM (P<sub>ka</sub> 6.2, logP 2.21), 1500-fold selectivity against trypsin, and 76% oral bioavailability in rats. The corresponding N-Boc- analog (5) with a K<sub>i</sub> for thrombin of 3.0 nM (P<sub>ka</sub> 6.5, logP >3.35), had 60% oral bioavailability in rats. Aminopyridine analog (6), featuring D-3,3-(Ph)<sub>2</sub>-Ala at P<sub>3</sub> displayed a K<sub>i</sub> for thrombin of 12 nM. Analog (6) showed good absorption kinetics in beagle dogs. Following oral administration (5 mg/kg),

the drug reached a peak concentration ( $C_{max}$ ) in plasma of 7000nM in 20 minutes. Oral bioavailability was estimated to be 52%. When the compound was given intravenously (1mg/kg), the plasma concentration of **6** declined in a polyphasic manner. Plasma clearance, terminal  $t_{1/2}$  and volume of distribution were 7.3 ml/min/kg, 151 min and 1.20 l/kg, respectively.

Table 1. Oral Active Thrombin Inhibitors with Aminopyridyl Moieties.

NO.	R <sub>2</sub>	R <sub>1</sub>	R <sub>3</sub>	K <sub>i</sub> <sup>a</sup> (nM)		PKa	LogP	F <sup>d</sup> (%) in rats
				Thrombin <sup>b</sup>	Trypsin <sup>c</sup>			
L-371,912	Ph		CH <sub>3</sub>	4.9	11000	10.2	-1.68	1.0
1	Ph		Boc	3700	233000	ND	2.34	ND
2	3,4-Cl <sub>2</sub> -Ph		SO <sub>2</sub> CH <sub>2</sub> Ph	9.0	12000	4.8	>3.68	35
3	3,4-Cl <sub>2</sub> -Ph		SO <sub>2</sub> CH <sub>2</sub> Ph	3.0	430	6.3	2.57	12
4	(Chx) <sub>2</sub>		H	0.82	1200	6.2	2.21	76
5	(Chx) <sub>2</sub>		Boc	3.0	657	6.5	>3.35	60
6	(Ph) <sub>2</sub>		H	12.0	5400	ND	ND	52 <sup>e</sup>
7	(Ph) <sub>2</sub>		Boc	3.6	2500	ND	1.65	40

<sup>a, d</sup> The determinations of K<sub>i</sub> and F(%) are described in reference 11. <sup>b</sup>Human thrombin. <sup>c</sup> Bovine trypsin. <sup>e</sup> Beagle dogs.

In the aminodimethylpyridine series, the bioassay results showed that analog (**7**) (K<sub>i</sub> 3.6 nM, logP 1.65) featuring Boc-D-3,3-(Ph)<sub>2</sub>-Ala in the P3 position was 40% orally bioavailable in the rats. Analogs featuring Boc- D-3,3-(Chx)<sub>2</sub>-Ala or its corresponding free amino group in the P3 position have similar inhibitory activity (K<sub>i</sub>'s 2.2-3.9 nM).

Derivatives with dimethyl- substituted aminopyridyl groups appear to be more selective for thrombin versus trypsin than corresponding non-substituted analogs, and nanomolar potency was maintained. However, analogs with 5-membered-heteroaryl moieties such as aminothiazole and aminothiophene are much less potent. Presumably, a 6-membered aryl ring is preferred for hydrophobic binding in the S1 specificity pocket of thrombin. X-ray crystal structure data is consistent with this interpretation.

# Aminopeptidase A: Selective inhibition and physiological involvement in CCK<sub>8</sub> metabolism

Laurent Bischoff, Christelle David, Tarik Khaznadar, Valérie Daugé,  
Bernard Pierre Roques and Marie-Claude Fournié-Zaluski

INSERM U 266 - CNRS URA D 1500, Faculté des Sciences Pharmaceutiques et Biologiques, 4,  
avenue de l'Observatoire, 75006 Paris, France

Aminopeptidase A is a zinc metallopeptidase which is involved in the metabolism of peptides containing a N-terminal aspartate or glutamate. This specificity accounts for the *in vivo* degradation of cholecystokinin CCK<sub>8</sub> [1] and angiotensin II into angiotensin III [2].

Preliminary studies [3] of both S<sub>1</sub> subsite and catalytic site of APA have led to β-aminothiols H<sub>2</sub>N-CH(R)-CH<sub>2</sub>SH as selective inhibitors, but their affinities still remained too low. We anticipated that further interaction with S<sub>1</sub>' and S<sub>2</sub>' subsites would increase the affinities of the inhibitors. Thus, we wished to develop pseudotripeptides H<sub>2</sub>N-CH(R)-CH(SH)-CO-AA<sub>1</sub>-AA<sub>2</sub>, in which additional interaction with S<sub>1</sub>' and S<sub>2</sub>' subsites is brought about by the dipeptidic unit AA<sub>1</sub>-AA<sub>2</sub>.

## Results and Discussion

First, using combinatorial chemistry [Martin, L. et al, in preparation], we determined which were the best AA<sub>1</sub> and AA<sub>2</sub> for good recognition of APA. This work indicated that APA exhibited a marked preference for Ile (or Tyr) and Asp at S<sub>1</sub>' and S<sub>2</sub>' positions, respectively. We then focused on the synthesis of enantiomerically pure α-mercapto-β-amino acids. Thus, using a newly developed reagent [4] for the asymmetric electrophilic sulfenylation of chiral enolates, we prepared optically pure and suitably protected α-mercapto-β-amino acids containing functionalized side-chains. These compounds were subsequently coupled with peptide units and various inhibitors were obtained after deprotection of the functional groups. K<sub>i</sub> values measured on APA and APN for these compounds showed that both sulfonamide and carboxylate moieties could lead to potent and selective inhibitors. In each case, the (R,S) diastereomers were the most selective molecules.

Using the (2R,3S) sulfonamide CD 124A (entry 2), *in vivo* experiments were carried out. In this study [Khaznadar et al, British Association of Psychopharmacology Summer Meeting 13th-17th July 1997 - Cambridge, U.K.], administration of the compound was performed by microdialysis into the medial prefrontal cortex of freely moving rats. CCK<sub>8</sub> was titrated by a radioimmunoassay. Our first results were very promising, since the inhibitor increased the extracellular level of CCK-like immunoreactivity by 220% (Table 1). This confirmed that the inhibitor *in vivo* protected endogenous CCK<sub>8</sub> from degradation by APA. Until now, the implication of APA in CCK<sub>8</sub> degradation had only been observed *ex vivo* on brain slices or during *in vivo* binding experiments [1]. This is the first demonstration of the physiological role of APA *in vivo*.

Table 1. Inhibitory potencies of some inhibitors of aminopeptidase A.

entry	C <sub>2</sub> ,C <sub>3</sub>	structure	K <sub>i</sub> (nM)		selectivity
			APA	APN	
1	S,S		40 ± 5	2,900 ± 600	70
2	R,S		17 ± 4	4,900 ± 900	300
3	S,S		13 ± 3	120 ± 10	9
4	R,S		16 ± 4	5,000 ± 1000	320

## Conclusion

We have developed potent and selective inhibitors of aminopeptidase A. These inhibitors allowed a study of the *in vivo* degradation of CCK<sub>8</sub> in the brain, which is a major effect of this enzyme.

## Acknowledgments

We wish to gratefully acknowledge Dr. Catherine Llorens-Cortes and Nadia de Mota (INSERM U36, Collège de France) for determination of the inhibitory potencies on APA. We also thank Emmanuel Ruffet for determination of the inhibitory potencies on APN.

## References

1. Migaud, M.; Durieux, C.; Viereck, J.; Soroca-Lucas, E.; Fournié-Zaluski, M.-C. and Roques, B.P. *Peptides*, 17 (1996) 601.
2. Zini, S.; Fournié-Zaluski, M.-C.; Chauvel, E.; Masdehors, P.; Roques, B.P.; Corvol, P. and Llorens-Cortes, C. *Proc. Natl. Acad. Sci. USA*, 93 (1996) 11968.
3. a : Chauvel, E.N.; Coric, P.; Llorens-Cortes, C.; Wilk, S.; Roques, B.P. and Fournié-Zaluski, M.-C. *J. Med. Chem.* 37 (1994) 1339; b : *ibid.* 37 (1994) 2950.
4. Bischoff, L.; David, C.; Martin, L.; Meudal, H.; Roques, B.P. and Fournié-Zaluski, M.-C. *J. Org. Chem.* (1997) (in press).

# Synthetic proregion-related peptides of proprotein convertases, PC1 and furin, represent potent inhibitors of each protease

Ajoy Basak,<sup>a</sup> Dany Gauthier,<sup>a</sup> Nabil G. Seidah<sup>b</sup> and Claude Lazure<sup>a</sup>

<sup>a</sup>Neuropeptides Structure and Metabolism and <sup>b</sup>Biochemical Neuroendocrinology Laboratories, Clinical Research Institute of Montreal (Affiliated to University of Montreal), 110 Pine Ave W, Montreal, Quebec H2W 1R7, CANADA.

Proprotein convertases are Ca<sup>2+</sup>-dependent serine proteases related to yeast kexin and bacterial subtilases [1,2]. Members of this family, comprising PC1/3, PC2, furin, PC4, PACE4, PC5/6, PC7/8/LPC, specifically cleave the COOH-terminal to single or pairs of basic residues present in protein and peptide precursors of various hormones, growth and neurotrophic factors and viral envelope proteins. In order to better understand their mode of action and to develop specific inhibitors, we previously designed peptidyl inhibitors containing a COOH-terminal reactive moiety [3], a non-hydrolysable isostere bond [4], a chloromethylketone moiety [5] and non-natural amino acids [6]. However, these proteases were first synthesized as enzymatically inactive proforms. We, therefore, envisioned that peptides derived from the proregion could represent potent inhibitors as previously shown in the case of prosubtilisin [7] and procathepsin [8]. This hypothesis was further investigated to identify the optimum size and sequence of peptides for the highest inhibitory property towards furin and PC1. Here, we report the synthesis of 7 proPC1 and 3 profurin-related peptides plus 2 mutated forms along with their comparative inhibitory properties towards m(mouse)PC1 and h(human)furin.

## Results and Discussion

Based on sequence alignment and secondary structural analysis, a number of segments were selected. These peptides, listed in Table I, were all synthesized using the fastFMOC-solid phase synthesis protocol on a fully automated peptide synthesizer (ABI model 431A), purified by RP-HPLC and fully characterized through amino acid analysis and FAB-MS. Their inhibition properties were assayed using enzymatically active PC1 and furin obtained from the media of insect and mammalian cells infected with a recombinant baculovirus (bv) and vaccinia virus (vv), respectively.

Initial analysis of these peptides indicated that they behave as competitive inhibitors allowing the comparison of the apparent K<sub>i</sub> listed in Table I. Clearly, peptides corresponding to the proPC1 regions 77-110 and 66-89 as well as profurin 63-86 appear the most potent towards mPC1 and hfurin. However, prior incubation of the active mPC1 with some peptides in the absence of substrate leads to time-dependent inhibition of the enzyme indicating that some of these could act as slow-binding tight inhibitors. Interestingly, we showed recently that the proregion 1-98 is a potent (K<sub>i</sub>: 6nM) slow-binding tight inhibitor (Boudreault *et al.*, submitted) of mPC1. These findings support the

inhibitory role of particular segments within the proregion of either proPC1 or profurin and may lead to a better understanding of the interaction of the proregion with the rest of the molecule.

Table 1. Inhibition constant ( $K_i$ ) of Various proPC1 and profurin-related synthetic peptides.

Sequence positions	Amino acid sequence	Ki ( $\mu$ M)	
		MPC1	hfurin
<b>ProPC1-related peptides</b>		18.6*	31.6*
82-89	SALHITKR	22.1	13.0
82-89A	SALAITKR	18.2	2.3
77-89	RRSRRSALHITKR	15.4	0.7
66-89	NHYLFKHKSHPRRSRRSALHITKR	43.2	1.2
66-89A	NAYLFKHKSHPRRSRRSALHITKR	0.7	4.8
77-110	RRSRRSALHITKRLSDDDRVTWAEQQYEKERSKR	1.7	ND
82-110	SALHITKRLSDDDRVTWAEQQYEKERSKR	1.0	ND
91-110	SDDDRVTWAEQQYEKERSKR	1.7	ND
101-110		2.3	47.5
<b>Profurin-related peptides</b>			
78-86	SPHRPRHSR	37.5*	23.0*
72-86	VTKRSLSPHRPRHSR	36.0*	2.8*
63-86	DYYHFWHRGVTKRSLSPHRPRHSR	10.2*	0.9*

Note: ND, not determined. \* These values were computed from the IC50 values determined with  $[S]=3xK_m$  being 50  $\mu$ M and 15  $\mu$ M pERTKR-MCA for bv:mPC1 and vv:hfurin respectively

## References

1. Seidah, N.G., Chrétien, M. and Day, R., *Biochimie*, 76 (1994), 197.
2. Rouillé, Y., Duguay, S.J., Lund, K., Furuta, M., Gong, Q., Lipkind, G., Oliva, A.A., Chan, S.J. and Steiner, D.F., *Front. Neuroendocrinol.*, 16 (1995), 322.
3. Basak, A., Jean, F., Seidah, N.G. and Lazure C., *Int. J. Peptide Protein Res.*, 44 (1994) 253.
4. Basak, A., Schmidt, C., Ismail, A.A., Seidah, N.G., Chretien, M. and Lazure, C., *Int. J. Peptide Protein Res.*, 46 (1995), 228.
5. Jean, F., Boudreault, A., Basak, A., Seidah, N.G. and Lazure, C., *J. Biol. Chem.*, 270 (1995) 19225.
6. Jean, F., Basak, A., DiMaio, J., Seidah, N.G. and Lazure, C., *Biochem. J.*, 307 (1995) 689.
7. Gallagher, T., Gilliland, G., Wang, L. and Bryan, P., *Structure*, 3 (1995) 907.
8. Fox, T., de Miguel, E., Mort, J.S. and Storer, A.C., *Biochem.*, 31 (1992) 12571.

# “O, N-Acyl migration”-type prodrugs of dipeptide HIV protease inhibitors

Yoshiaki Kiso, Satoshi Yamaguchi, Hikaru Matsumoto, Tooru Kimura  
and Kenichi Akaji

*Department of Medicinal Chemistry, Kyoto Pharmaceutical University,  
Yamashina-Ku, Kyoto 607, Japan*

O, N-acyl migration is a well known side reaction of Ser- or Thr- containing peptides. The  $\beta$ -hydroxyl groups are acylated by an N $\rightarrow$ O shift under acidic conditions and the resulting O-acyl products can be readily converted to N-acyl compounds in aqueous buffer. The liberated ammonium ion enhances the solubility of O-acyl products in water. This feature is useful in prodrug design of less soluble compounds [1]. We have designed and synthesized an “O $\rightarrow$ N-acyl migration” type prodrug of KNI-272, which is a potent inhibitor containing hydroxymethylcarbonyl isostere as a transition state mimic [2-4]. Starting from KNI-272, dipeptide inhibitors having lower molecular weights were developed that were as potent as tripeptide inhibitors. These new compounds were hydrophobic and less soluble in water than KNI-272. In the present study, we applied the “O $\rightarrow$ N-acyl migration” type prodrug system to the dipeptide inhibitors.

## Results and Discussion

The dipeptide inhibitor, KNI-727 (Fig. 1) showed potent enzyme inhibition activity (95.9 % inhibition at 50 nM), but solubility in water was only 1.5  $\mu$ g/ml. In order to improve solubility, we synthesized prodrugs of the inhibitor. The esterification of Boc-Apns-Dmt-NHBU<sup>t</sup> (Apns=allophenylnorstatine, Dmt=5,5-dimethylthiazolidine-4-carboxylic acid) with 2,6-dimethylphenoxyacetic acid prepared from the corresponding phenol by DCC-dimethylaminopyridine gave N-Boc form of the prodrug. Deprotection of the Boc group by 4N HCl/dioxane afforded the desired prodrug without difficulty. A series of prodrugs containing a phenoxyacetyl moiety were prepared in the same manner. The aqueous solubilities of the prodrugs were determined by HPLC analysis of saturated solutions of the compounds (Fig. 1). The derivatization into prodrugs increased the solubilities more than 1000-fold.

The O $\rightarrow$ N-acyl migrations in phosphate buffered saline (pH 7.4) proceeded smoothly and no by-products were detected on HPLC. The conversion rate of this series of inhibitors ( $t_{1/2}$ =ca. 0.5 min) was higher than that of KNI-272 ( $t_{1/2}$ =1.2 min) (Fig. 1). This result was due to less steric hindrance of the acyl-components. At the different pH values, the conversion rates were also determined. The rate was lower at the lower pH (Fig. 2).

We further applied the prodrug concept to KNI-565 (benzoyl-Apns-Thz-NHBU<sup>t</sup>) (Thz=thiazolidine-4-carboxylic acid). In this case, water solubility increased about 10-fold.

The O→N-acyl migration proceeded through a stable intermediate, and the rate was very slow ( $t_{1/2}$ =ca. 6 h at pH 7.4) (Fig. 2).

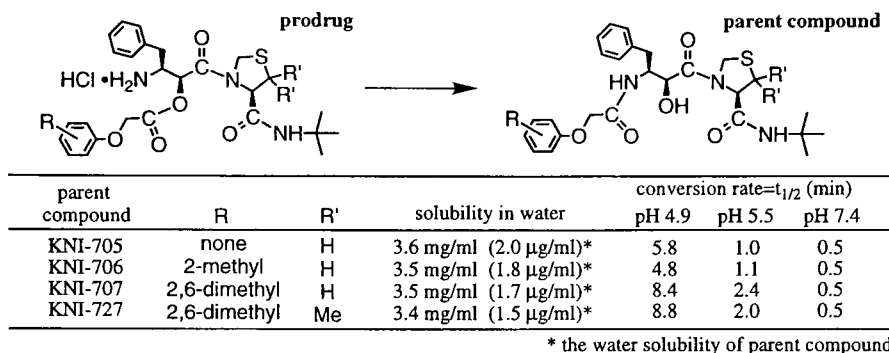


Fig. 1. Prodrugs of dipeptide HIV protease inhibitors.

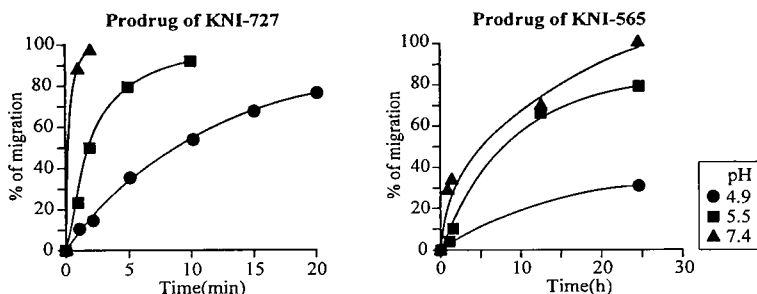


Fig. 2. Comparison of migration rate under different pH value.

In conclusion, we applied the "O→N-acyl migration" type prodrug system to dipeptide inhibitors. The prodrugs were prepared easily without racemization. Solubility was increased more than 1000-fold, and the acyl-migration of prodrug to the parent compound was smooth without forming by-products.

## References

- Hurley, T.R., Colson, C.E., Hicks, G. and Ryan, M.J., *J. Med. Chem.*, 36 (1993) 1496.
- Mimoto, T., Imai, J., Kisanuki, S., Enomoto, H., Hattori, N., Akaji, K. and Kiso, Y., *Chem. Pharm. Bull.*, 40, (1992) 2251.
- Kageyama, S., Mimoto, T., Murakawa, Y., Nomizu, M., Ford, Jr.H, Shirasaka, T., Gulnik, S., Erickson, J., Takada, K., Hayashi, H., Broder, S., Kiso, Y. and Mitsuya, H., *Antimicrob. Agent Chemother.*, 37 (1993) 810.
- Kiso, Y., Kimura, T., Ohtake, J., Nakata, S., Enomoto, H., Moriwaki, H., Nakatani, M., Akaji, K., In Kaumaya, P.T.P. and Hodges, R.S. (Eds.), *Peptides: Chemistry, Structure and Biology (Proceedings of the Fourteenth American Peptide Symposium)*, Mayflower Scientific Ltd, England, 1996, p.157.

# The crystal structure of $\alpha$ -thrombin with retro-binding inhibitor SEL2711

Igor Mochalkin and Alexander Tulinsky

Department of Chemistry, Michigan State University, E.Lansing, MI 48824, USA

Thrombin, a multifunctional serine protease, plays a central role in the blood coagulation cascade by performing both procoagulant and anticoagulant activities [1]. Most of the peptidic thrombin active site inhibitors bind to thrombin forming a short anti-parallel  $\beta$ -strand with residues Ser<sup>214</sup>-Glu<sup>217</sup>. However, the crystallographic structure of ternary SEL2711-hirugen-thrombin complex shows that SEL2711 (Fig.1), a member of a new class of combinatorially designed active site inhibitors of Factor Xa ( $K_i=3\text{nM}$ ), binds to thrombin ( $K_i=45\mu\text{M}$ ) in a retro-fashion forming a parallel  $\beta$ -strand with Ser<sup>214</sup>-Glu<sup>217</sup> similar to the N-terminal residues of the natural inhibitor hirudin [2], the synthetic Bristol-Myers Squibb inhibitor BMS-183507 [3], and the natural product Nazumamide A [4].

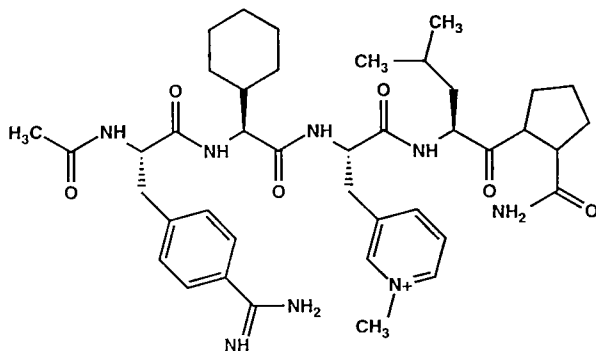


Fig.1. Molecular structure of SEL2711.

## Results and Discussion

The crystallographic structure of the ternary SEL2711-hirugen-thrombin complex, containing 137 water molecules, has been determined in a resolution range from 7.0 to 2.1 Å to the final R-value 15.5%. Its structure is isomorphous with that of hirugen-thrombin. The p-amidinophenylalanyl residue of SEL2711 has been fixed at the S1 site utilizing favorable ionic interactions between the nitrogen atoms of amidino group and the carboxylate oxygen atoms of Asp<sup>189</sup>. The Glu<sup>192</sup> residue adopts an open conformation that allows the "P3" cyclohexylglycyl residue to occupy the same site as the P3 aspartate of the thrombin platelet receptor peptide. The N-terminal acetyl and 3-(methyl pyridinium)alanyl of SEL2711 are located at the S2 and the S3 D-Phe sites of D-PheProArg chloromethyl

ketone bound to thrombin, respectively. The two C-terminal residues of SEL2711 (Leu and Pro) extend from the S3 site into the solvent space and are disordered (Fig.2).

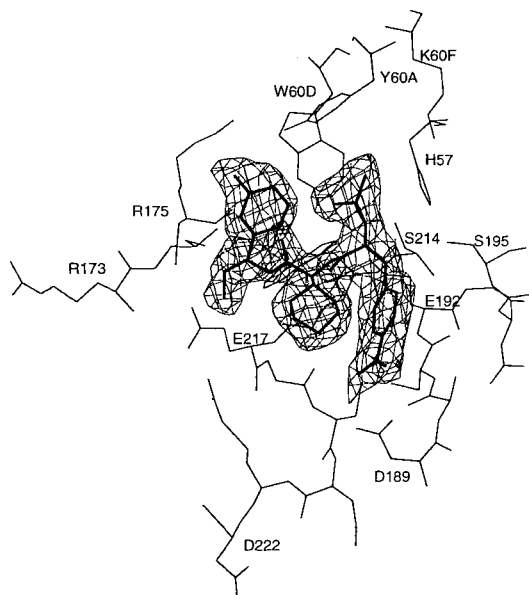


Fig.2. Stereoview of (2Fo-Fc) electron density of SEL2711 in its bound state (map is contoured at 1 sigma).

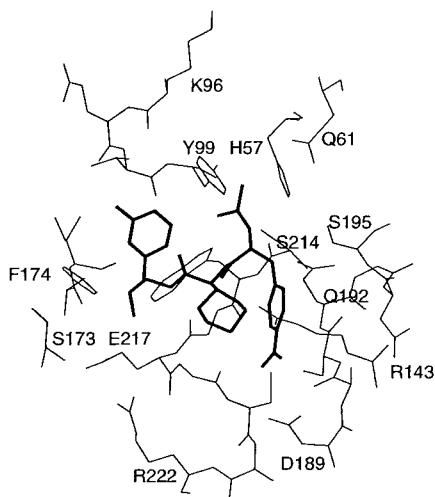


Fig. 3. Modeling of SEL2711 bound to Factor Xa.

Modeling of SEL2711 bound to Factor Xa also suggests a retro binding mode where the 3-(methyl pyridinium)alanyl adopts an orthogonal orientation to the aromatic rings of Tyr<sup>99</sup> and Phe<sup>174</sup> of Factor Xa in the D-Phe quanomorph S3 subsite (Fig.3). This most likely is a major contribution to the high specificity of SEL2711 for Factor Xa.

## Conclusion

SEL2711 is a new retro-binding inhibitor for thrombin. Modeling of SEL2711 bound to Factor Xa also suggests a retro-binding mode and explains the high specificity of SEL2711 for Factor Xa.

## Reference

1. Stubbs, M.T. and Bode, W., Thrombosis Research, 69(1993)1.
2. Rydel, T.J., Ravichandran, K.G., Tulinsky, A., *et al.*, Science, 249(1990)277.
3. Taberner, L., Chang, C.Y., Ohringer, S.L., *et al.*, J. Mol. Biol., 246(1995)14.
4. Nienaber, V.L. and Amparo, E.C., J. Am. Chem. Soc., 118(1996)6807.

# Novel peptide inhibitors for interleukin-1 $\beta$ processing in monocytes

Sándor Bajusz, Irén Fauszt, Klára Németh, Éva Barabás, Attila Juhász  
and Miklós Patthy

*Institute for Drug Research, PO Box 82, Budapest, H-1325, Hungary*

Interleukin-1 $\beta$  (IL-1 $\beta$ ), an inflammatory mediator released by human monocytes, is synthesized as a 269-mer precursor. It is cleaved by a cytoplasmic cysteine protease termed IL-1 $\beta$  converting enzyme (ICE) at Asp<sup>116</sup>-Ala<sup>117</sup> to produce the active cytokine. ICE and its homologues, which are responsible for apoptosis, appear to belong to a new cysteine protease family. Effective ICE inhibitors are peptidyl aspartals (Asp-H) and (acyloxy)methanes (Asp-CH<sub>2</sub>OAc) [1]. A recent study reported [2] that (i) the analog of the latter having the  $\beta$ -homo-aspartyl (hAsp) residue, NH-CH(CH<sub>2</sub>COOH)-CH<sub>2</sub>-CO, is inactive which indicates the key role of Asp  $\alpha$ -CO in P<sub>1</sub> recognition; (ii) ICE accepts both D- and L-Asp at the P<sub>1</sub> of both kinds of inhibitors. It is noted that epimerization occurs slowly at the P<sub>1</sub>-Asp and it is not known whether or not ICE catalyzes this process.

The mechanism of the inhibition of cysteine proteases by peptidyl halomethanes and (acyloxy)methanes assumes the thiolate can react directly with the C=O (*a*) as well as the adjacent halomethyl or (acyloxy)methyl group (*b*) [1]. In path *b*, one may expect that the thiolate (i) can contact the  $\alpha$ -proton of the temporarily bound P<sub>1</sub>-D-Asp and produce the L-Asp-thiomethane product via proton abstraction and asymmetric induction, and (ii) can also attack the  $\beta$ -CO of hAsp that results in reversible inhibition; lack of such interaction with the  $\beta$ -hAsp analog studied may be due to steric hindrance. Starting from these findings and speculations we compared the inhibiting activity of some peptide  $\beta$ -homo-aldehydes to their parent  $\alpha$ -aldehydes against ICE, papain, trypsin and thrombin.

## Results and Discussion

The peptide aldehydes and their homo- $\beta$ -aldehyde analogues that we studied were prepared by conventional procedures. ICE inhibiting activity was assessed in human whole blood stimulated by LPS; the release of IL-1 $\beta$  from the monocytes was measured by ELISA. Inhibition of the other proteases was determined by the amidolytic method assays using Z-Arg-Ile-Phe-AMC for papain and Tos-Gly-Pro-Arg-pNA for trypsin and thrombin.

Data presented in Table 1 indicate that tetrapeptide aldehydes *A* having L- $\alpha$ -aspartal and L- $\beta$ -homo-aspartal in the P<sub>1</sub> display similar ICE inhibiting activity with an L $\beta$ :L $\alpha$  IC<sub>50</sub> ratio of 1.55. The other L- $\beta$ -homo-aldehyde analogues, by contrast, are much less inhibitory than the parent  $\alpha$ -aldehydes, particularly against papain and trypsin with ratios of 587-929. Neither the thiolate of papain nor the serine-OH of trypsin and thrombin can react

Table 1. Protease inhibiting activity ( $IC_{50}$   $\mu$ M) of peptidyl L- and D- $\alpha$ -amino aldehydes compared with their L- $\beta$ -homo-aldehyde analogues.<sup>a</sup>

Protease	Peptide aldehyde		$P_1 = \alpha, -NH-CHR-CHO; \beta, -NH-CHR-CH_2-CHO^b$				
	$P_n$	$P_2$	L $\alpha$	L $\beta$	D $\alpha$	L $\beta$ :L $\alpha$	D $\alpha$ :L $\alpha$
ICE	A, Ac-Tyr-Val-Ala		1.170 $\pm$ 0.36	1.82 $\pm$ 0.79 <sup>c</sup>	ND <sup>d</sup>	1.55	-1 <sup>d</sup>
Papain	C, iBoc-Phe		0.130 $\pm$ 0.02	150.00 $\pm$ 5.00	12.50 $\pm$ 1.50	929	96
Papain	B, Z-Arg-Ile		0.070 $\pm$ 0.01	65.00 $\pm$ 0.08	8.50 $\pm$ 1.00	808	121
Trypsin	D, Boc-D-Phe-Pro		0.003 $\pm$ 0.0001	1.76 $\pm$ 0.08	1.79 $\pm$ 0.09	587	597
Thrombin	D, Boc-D-Phe-Pro		0.009 $\pm$ 0.001	0.19 $\pm$ 0.02	5.44 $\pm$ 1.50	21	604

<sup>a</sup>For determination of  $IC_{50}$  values see text. ND, not determined. <sup>b</sup>R =  $-CH_2COOH, C_6H_5CH_2-$  and  $-(CH_2)_3-NH-C(NH_2)=NH$  for A, B and C-D, respectively. <sup>c</sup>The D $\beta$  isomer was inactive at 100  $\mu$ M.

<sup>d</sup>Such diastereomeric inhibitor pairs have been found equipotent against ICE (cf. ref. 1).

with the  $\beta$ -CO of the inhibitors. The somewhat high antithrombin activity of Boc-D-Phe-Pro-hArg-H is due to the very high affinity of D-Phe-Pro for thrombin. While the peptidyl L- and D- $\alpha$ -aspartals have been found equipotent against ICE [1], A with P<sub>1</sub>-D- $\beta$ -homo-aspartal shows virtually no ICE inhibiting activity. Substitution of D- $\alpha$ -amino aldehydes for the L isomers in the P<sub>1</sub> of the peptides lowers the trypsin and thrombin inhibiting activities of D much better than the antipapain activity of B and C (D $\alpha$ :L $\alpha$   $IC_{50}$  ratios are ~600 vs. 96-121).

In conclusion, substrate related peptidyl  $\beta$ -homo-aspartals are approximately as inhibitory as the parent  $\alpha$ -aspartals against ICE and appear to be specific for the ICE/CED3 (caspase) family. Alkylation of ICE with peptidyl halomethanes and (acyloxy)methanes can occur either through the hemithioketal-episulfonium ion pathway (a) or via direct reaction with the halomethyl or (acyloxy)methyl (b), while papain can only be alkylated by mechanism b, i.e. via interaction between the catalytic thiolate and the  $\alpha$ -CO of the inhibitor. (iii) Trypsin and thrombin accept only L-residues at the P<sub>1</sub>, while papain shows tolerance for the P<sub>1</sub>-D- $\alpha$ -amino aldehyde residues apparently depending on their optical stability. (iv) It is the side chain rather than the  $\alpha$ -CO group of Asp that plays a key role in P<sub>1</sub> recognition for ICE.

## References

1. Thornberry, N.A., In Barrett, A.J. (Ed.), Meth. Enzymol. Academic Press, San Diego, USA 1994, Vol. 224, p 615. Otto, H-H. and Schirmeister, T., Chemical Reviews, 97(1997) 133.
2. Prasad, C.V.C., Prouty, C.P., Hoyer, D., Ross, T.M., Salvino, J.M., Awad, M., Graybill, T.L., Schmidt, S.J., Osifo, I.K., Dolle, R.E., Helaszek, C.T., Miller, R.E. and Ator, M.A., Bioorg. Med. Chem. Lett., 5(1995)315.

# Synthetic route to P<sub>1</sub>-argininals suitable for radiolabeling studies

Susan Y. Tamura,<sup>a</sup> J. Edward Semple,<sup>a</sup> David C. Rowley,<sup>a</sup> Paul McNamara,<sup>b</sup> Ruth F. Nutt<sup>a</sup> and William C. Ripka<sup>a</sup>

<sup>a</sup>Department of Medicinal Chemistry, Corvas International, Inc. 3030 Science Park Rd., San Diego, CA 92121, U.S.A. and <sup>b</sup>Chemical Research, Schering-Plough Research Institute, 2015 Galloping Hill Rd., Kenilworth, NJ 07033 USA

Peptidyl argininals which inhibit Factor VIIa, Factor Xa and thrombin, trypsin-like serine proteases involved in the coagulation cascade, are of current high interest as therapeutic targets for the treatment of thrombotic vascular disease [1,2]. A currently favored method for the synthesis of peptidyl argininals utilizes the late stage hydride reduction of a N $\epsilon$ -Cbz-arginine lactam intermediate [3]. However, this strategy is limited to substrates which are stable to lithium aluminum hydride and thus can not be applied to our targets containing incompatible functionalities. Argininal syntheses via semicarbazone intermediates have been reported using both solution [4,5] and solid phase methods [6].

A general synthetic route to targets possessing the P<sub>1</sub>-argininal moiety, whose methodology could be readily modified to a radiolabeled synthesis, was developed for the preparation of CVS 1123 and CVS 1778, and used in the preparation of <sup>14</sup>C-labeled CVS 1778. Our criteria for the radiolabeled synthesis of peptidyl argininals were the following: 1) a convergent route; 2) racemization is suppressed during all steps of the synthesis; 3) the final step to release the aldehyde moiety involves a simple reaction which can be easily monitored and rapidly quenched, and is highly selective in the presence of other sensitive moieties; 4) a common labeled intermediate would contain the arginine moiety, so that a variety of P<sub>4</sub>-P<sub>2</sub> segments could be coupled to it; 5) the guanidino moiety would be introduced with a guanylating reagent which can be easily prepared with a <sup>14</sup>C label.

## Results and Discussion

The N $\epsilon$ -nitro-argininal ethyl amination method [7] that was developed in our laboratories is well suited for large scale preparation of peptidyl P<sub>1</sub>-argininals. However, employment of argininol as synthon is our preferred method for the radiolabeled synthesis of peptidyl argininals (Fig. 1). The guanylation of N- $\alpha$ -Boc-ornithinol to give N- $\alpha$ -Boc-argininol is the cornerstone of our synthetic route. A modified procedure originally described by Bernatowicz et al. [8] produced the labeled reagent, 1H-pyrazole-1-carboxamide, by introducing the radiolabel with <sup>14</sup>C-cyanamide.

Boc-L-Orn(Cbz)-ol, which contained 5% of the D-isomer, was purified by preparative HPLC (Chiralpak AD<sup>TM</sup>). Coupling of the unprotected argininol proceeded smoothly after activation of the peptide with DCC/HOBt. The crude peptidyl argininol was purified using CBA cation exchange solid phase extraction, eluting with 0-0.1% aqueous acetic acid to

afford the acetate salt. Oxidation with pyridine•SO<sub>3</sub> [9], using the conditions described in Fig. 1 produced our final targets.

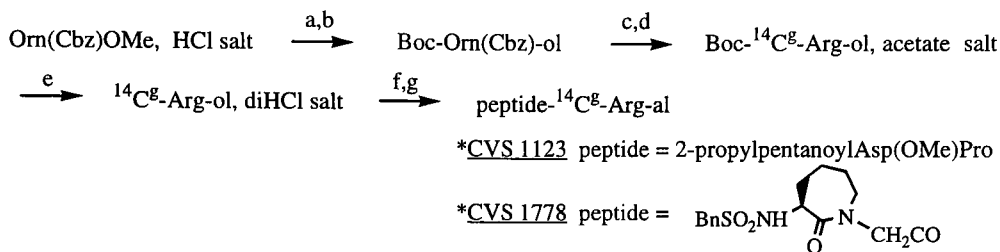


Fig 1. A general scheme for the preparation of radiolabeled P1-argininals. Reagents and conditions: a) Boc<sub>2</sub>O, NaHCO<sub>3</sub>, aq dioxane, 100%; b) LiBH<sub>4</sub>, EtOH, THF, 89%; c) H<sub>2</sub>, Pd/C, 88-94%; d) 1.0–1.1 eq <sup>14</sup>C-pyrazole carboxamidine, 84%; e) HCl, EtOH, 85%; f) peptide-OH, DCC, HOBt, NMM, 48-62%; g) 6 eq pyridine/SO<sub>3</sub>, 6-8 eq Et<sub>3</sub>N, DMSO, 10 min, rt; peptidyl argininol, pH 4-6, 20 min; H<sub>2</sub>O; prep RP-HPLC.

## Conclusion

We have developed a novel, efficient and general synthetic route to several peptidyl <sup>14</sup>C-argininal targets. Studies of these inhibitors have advanced from the laboratory to preclinical and clinical stages. The sequence in Fig. 1 was utilized in the successful preparation of radiolabeled CVS 1778.

## References

1. Scarborough, R. M.; Annual Reports in Medicinal Chemistry, Bristol, J.A.; ed., 30(1995)71.
2. Semple, J. E.; Rowley, D. C.; Brunck, T. K.; Ha-Uong, T.; Minami, N. K.; Owens, T. D.; Tamura, S. Y.; Goldman, E. A.; Siev, D. V.; Ardecky, R. A.; Carpenter, S. H.; Ge, Y.; Richard, B. M.; Nolan, T. G.; Håkanson, K.; Tulinsky, A.; Nutt, R. F.; Ripka, W. C. J. Med. Chem., 39(1996)4531.
3. Bajusz, S.; Szell, E.; Bagdy, D.; Garabas, E.; Horvath, G.; Dioszegi, M.; Fittler, Z.; Szabo, G.; Juhasz, A.; Tomori, E.; Szilagyi, G. J. Med. Chem., 33(1990)1729.
4. McConnell, R. M.; Barnes, G. E.; Hoyng, C. F.; Gunn, J. M. J. Med. Chem., 33(1990)86.
5. Webb, T. R., Dagnino, R., Jr. Tetrahedron Lett., 35(1994)2125.
6. Murphy, A. M.; Dagnino, R., Jr.; Vallar, P. V.; Trippe, A. J.; Sherman, S. L.; Lumpkin, R. H.; Tamura, S. Y.; Webb, T. R. J. Am. Chem. Soc., 114(1992)3156.
7. Tamura, S. Y.; Semple, J. E.; Ardecky, R. A.; Leon, P.; Carpenter, S.; Ge, Y.; Shamblin, B. M.; Weinhouse, M. I.; Ripka, W. C.; Nutt, R. F. Tetrahedron Lett, 37(1996)4091.
8. Bernatowicz, M. S.; Wu, Y.; Matsueda, G. R. J. Org. Chem., 57(1992)2497.
9. Parikh, J. R.; von E. Doering, W. J. Am. Chem. Soc., 89(1967)5505.

# Peptide vinyl sulfones: Inhibitors and active site probes for the study of proteasome function *in vivo*

Matthew Bogyo, John S. McMaster, Rickard Glas, Maria Gaczynska, Domenico Tortorella and Hidde L. Ploegh  
Center for Cancer Research, Massachusetts Institute of Technology,  
Cambridge, MA 20139, USA

The proteasome is a large, barrel shaped multi-subunit protein complex which is responsible for controlling the majority of catabolic events taking place within the cell (for reviews see [1, 2]). Crucial to understanding the diverse functions of the proteasome is the ability to inhibit its activity through the use of pharmacological agents. Recently, we have synthesized and characterized a new class of peptide based inhibitors of the proteasome [3]. These C-terminal peptide vinyl sulfones inhibit the catalytically active  $\beta$ -subunits of the proteasome by covalent modification of the active site threonine hydroxyl sidechain (Fig. 1). This type of irreversible inhibition allows for the use of this class of cell-permeable inhibitors as active site probes in living cells. Further, these reagents can be used to examine the results of pharmacological “knock-outs” generated by prolonged treatment of cells with these inhibitors.

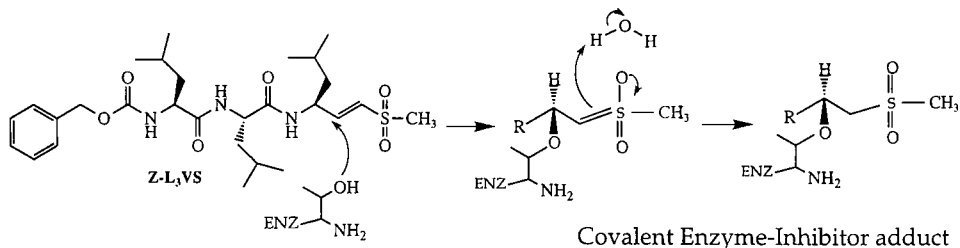


Fig. 1. Covalent modification of the catalytic threonine of the proteasome by a tri-peptide vinyl sulfone.

## Results and Discussion

Based on the finding that the peptide sequence Leu-Leu-Leu is a good substrate for the proteasome [4], we synthesized several tri-leucine peptide vinyl sulfones equipped with either a Cbz (Z-L<sub>3</sub>VS), biotin (Biotin-L<sub>3</sub>VS; for use in affinity purification), or nitro-phenol (NP-L<sub>3</sub>VS) moiety at the N-terminus. All three compounds were potent inhibitors of the three catalytic activities of the proteasome of which the greatest inhibition was of chymotrypsin-like activity. Treatment of several tissue culture cell lines with <sup>125</sup>I-NIP-L<sub>3</sub>VS (generated by iodination of NP-L<sub>3</sub>VS with Na<sup>125</sup>I) resulted in the labeling of multiple proteasomal  $\beta$ -subunits which could be resolved by 2D SDS-

PAGE (Fig. 2). These subunits could be identified using proteasome mutant cell lines lacking distinct subunits and based on the known 2D maps of the proteasome [3].

Prolonged treatment of cells with the tri-peptide vinyl sulfones resulted in cell death due to loss of proteasome function. However, this toxicity could be overcome at low concentrations of the inhibitor in distinct populations of cells. These cells were termed resistant and could sustain growth in the presence of doses of inhibitor which caused rapid death in normal cells. Although initially thought to be the result of genetic mutation or a drug-resistance phenomenon, we have ruled out these possible explanations and we have found that proteasome function in these cells is in fact blocked. In addition, it appears that at least one new proteolytic activity, distinct from the proteasome, is increased in adapted cells. Blocking of this activity with a tri-peptide chloromethyl ketone results in impaired cell growth of adapted but not normal cells, suggesting that this activity is, at least in part, responsible for compensation for the loss of proteasome function.

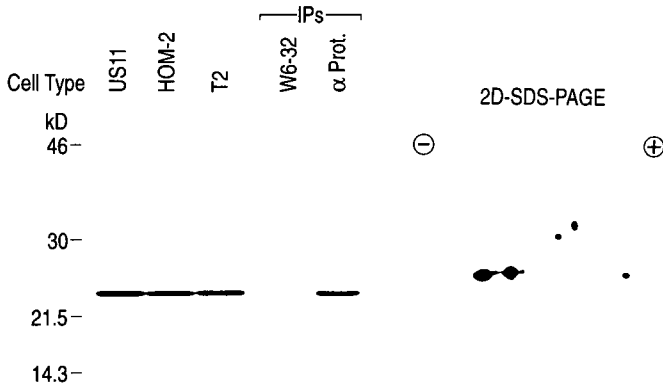


Fig 2. Labeling of intact cells with  $^{125}\text{I-NIP-L}_3\text{VS}$ . A) 1D SDS-PAGE of total cell lysates (US11, HOM-2, T2), immunoprecipitation with a proteasome specific antibody ( $\alpha$  prot.) and an irrelevant control antibody (W6-32) and B) 2D SDS-PAGE of total cell lysates.

## References

1. Coux, O., Tanaka, K. & Goldberg, A.L., *Annu. Rev. Biochem.*, 65(1996)801.
2. Rivett, A.J., *Biochem J.*, 291(1993)1.
3. Bogyo, M., McMaster, J.S., Gaczynska, M., Tortorella, D., Goldberg, A.L. & Ploegh, H., *Proc. Natl. Acad. Sci. USA*, 94(1997)6629.
4. Jensen, T.J., Loo, M.A., Pind, S., Williams, D.B., Goldberg, A.L. & Riordan, J.R., *Cell*, 83(1995)129.

# Synthesis of 3-(3-pyrrolidinyl)alanine and its derivatives as arginine peptidomimetics for incorporation into serine protease inhibitors

Darin R. Kent, Wayne L. Cody and Annette M. Doherty

Parke-Davis Pharmaceutical Research, Division of Warner-Lambert Company,  
2800 Plymouth Road, Ann Arbor, MI 48105, USA

Serine proteases are involved in many biological processes such as blood coagulation, digestion, and inflammation and are important therapeutic targets for a variety of diseases. Selectivity among the various serine proteases is an important consideration in the design of thrombin inhibitors. Thrombin is a trypsin-like serine protease consisting of a Ser<sup>195</sup>, His<sup>57</sup>, and Asp<sup>102</sup> catalytic triad that cleaves a polypeptide chain on the C-terminal side of a lysine or arginine residue. The basic side chains of these amino acids fit deep into a pocket in the protein surface (S<sub>1</sub>) and interact via hydrogen bonding interactions with an aspartic acid residue. Consequently, arginine and lysine residues are common groups that have been incorporated into many serine protease inhibitors. To confer activity, selectivity and proteolytic stability, many arginine peptidomimetics have been substituted into the P<sub>1</sub> position of serine protease inhibitors. This article describes the synthesis of 3-(3-pyrrolidinyl)alanine and its corresponding guanylated derivatives as pseudoisosteric replacements for arginine residues in serine protease inhibitors to potentially maintain potency while conferring selectivity.

## Results and Discussion

The 3-substituted pyrrolidine side chain was prepared according to the method described by Joucla *et al.* [1] via a 1,3-dipolar cycloaddition of the azomethine ylide, formed by condensing N-benzyl glycine and formaldehyde and subsequent decarboxylation of the imine with methyl acrylate to yield N-benzyl-3-carbomethoxy pyrrolidine (34%).

The methyl ester was reduced with lithium aluminum hydride providing the corresponding primary alcohol. The N-benzyl group was then removed by hydrogenolysis and the resulting secondary amine was converted to the urethane. The alcohol was then converted to the bromide according to the method of Corey *et al.* [2] and treated with sodium iodide to provide the iodide in 85% yield for the five step process.

The classical chiral auxiliary of Schöllkopf *et al.* [3] was used for alkylation with the iodide. The alkylation reaction was optimized using HMPA as a cosolvent to provide the desired product (66%). The alkylated dihydropyrazine was cleaved to form a mixture of D-valine methyl ester and the 3-substituted pyrrolidine amino acid methyl ester, which was Boc protected as a mixture and separated by flash chromatography to provide the 3-substituted pyrrolidine amino acid methyl ester (84%). The methyl ester was hydrolyzed (96%) and the resulting free acid was coupled to N,O-dimethylhydroxylamine

hydrochloride yielding the N,O-dimethylamides (quant.) to facilitate conversion into electrophilic ketones or aldehydes. The side chain Cbz protecting group was then quantitatively removed to complete the synthesis of the amino acid N<sup>α</sup>-Boc-3-(3-pyrrolidinyl)alanine-N,O-dimethylamide.

N<sup>α</sup>-Boc-3-(3-pyrrolidinyl)alanine-N,O-dimethylamide was guanylated using a methodology previously worked out in our laboratories [4]. Both the Mtr and the Pmc groups were incorporated as protecting groups for the guanidines. The Mtr or Pmc protected S-methylisothioureas were reacted with N<sup>α</sup>-Boc-3-(3-pyrrolidinyl)alanine-N,O-dimethylamide to provide the mono-protected guanylated amino acid derivatives in 67 % yield in both cases (Fig. 1).

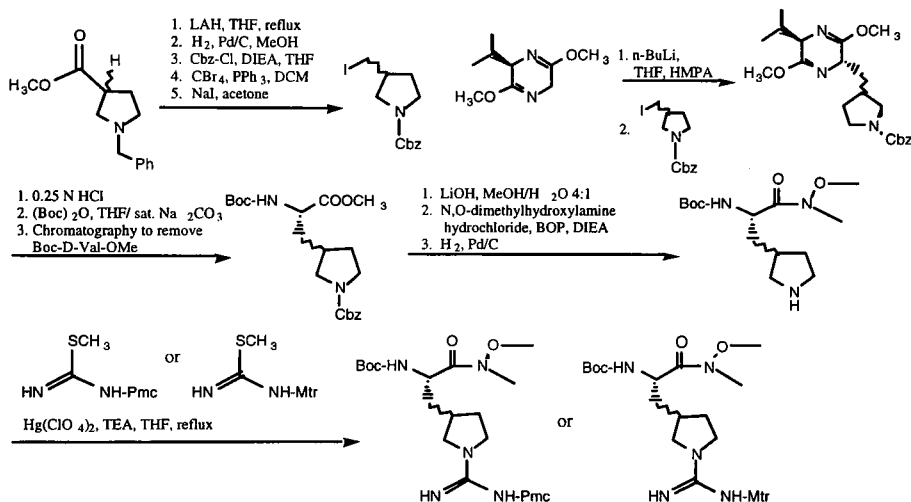


Fig. 1. Synthesis of N<sup>α</sup>-Boc-3-(3-pyrrolidinyl)alanine-N,O-dimethylamide and its guanylated derivatives.

The amino acid N<sup>α</sup>-Boc-3-(3-pyrrolidinyl)alanine-N,O-dimethylamide and its guanylated derivatives were synthesized. These amino acids are being coupled to a variety of template structures (e.g. Ac-D-Phe-Pro-OH) to yield inhibitors of a variety of serine protease's such as thrombin. The key step in the synthesis of the 3-substituted pyrrolidine side chain is a 1,3-dipolar cycloaddition reaction of methyl acrylate and an azomethine ylide, derived from the condensation of N-benzyl glycine and formaldehyde.

## References

1. Joucla, M., Mortier, J., Chem. Commun., (1985) 1566.
2. Corey, E. J., Fuchs, P. L., Tetrahedron Lett., (1972) 3769.
3. Schöllkopf, U., Groth, U., Deng, C., Angew. Chem. Int. Ed. Engl., 20 (1981) 798.
4. Kent, D. R., Cody, W. L., Doherty, A. M., Tetrahedron Lett., 37 (1996) 8711.

# Design of a protein-based inhibitor for proprotein convertase furin: Expression, purification and inhibition of furin substrates *in vivo* by an epitope-tag recombinant serpin $\alpha_1$ -PDX/hf

François Jean,<sup>a</sup> Kori Stella,<sup>b</sup> Craig J. Lipps,<sup>b</sup> James B. Hicks<sup>b</sup>  
and Gary Thomas<sup>a</sup>

<sup>a</sup>Vollum Institute, Oregon Health Sciences University, 3181 SW Sam Jackson Park Road,  
Portland, OR 97201 and <sup>b</sup>Hedral Therapeutics, Portland, OR 97201, USA

A small family of convertases which catalyze the *in vivo* proteolytic activation of proproteins and prohormones by cleavage of the substrates at single or pairs of basic amino acids was recently identified [1]. One of these convertases, furin, is a membrane-associated, calcium-dependent, serine endoprotease that cleaves a wide range of proproteins at the consensus sequence -Arg-X-Lys/Arg-Arg- in both the biosynthetic and endocytic pathways [2]. Mutational analysis showed that the minimal consensus furin cleavage site is -Arg-X-X-Arg- [3].

In addition to a large number of endogenous substrates, many pathogens require processing by furin to exert their virulence. For example, several viral fusion glycoproteins including HIV-1 gp160 and Measles virus F<sub>0</sub> [4] require processing at furin sites. Likewise a number of bacterial toxins including the anthrax toxoid and *Pseudomonas* exotoxin (PE) [5] require processing by furin for their activation.

Because of the central role of furin in the proteolytic activation of diverse human pathogens, the design of furin-specific inhibitors has become an important area of research for the development of novel therapeutics. Previously, we showed that genomic expression of a furin-directed  $\alpha_1$ -antitrypsin ( $\alpha_1$ -AT) variant,  $\alpha_1$ -PDX (reactive site mutated to -Arg-X-X-Arg- to inhibit furin), blocked the processing of several furin substrates including HIV-1 gp160 and measles virus F<sub>0</sub> and strongly inhibited the production of infectious virus [4,6]. To explore the use of recombinant  $\alpha_1$ -PDX as a protein-based therapeutic, a His- and FLAG-tagged  $\alpha_1$ -PDX,  $\alpha_1$ -PDX/hf, was constructed and expressed in bacteria.

## Results and Discussion

Recombinant  $\alpha_1$ -PDX/hf and  $\alpha_1$ -PIT/hf were isolated from bacterial extracts using Ni<sup>2+</sup> affinity chromatography followed by hydrophobic interaction chromatography. Analytical reversed-phase HPLC of each protein revealed a single molecule void of contaminants. The measured molecular masses of  $\alpha_1$ -PDX/hf and  $\alpha_1$ -PIT/hf obtained by electrospray mass spectrometry (46719 Da  $\pm$  3 Da and 46631 Da  $\pm$  3 Da, respectively) was in excellent agreement with the expected values (46727 Da and 46642 Da, respectively). The slow tight binding inhibition of furin by  $\alpha_1$ -PDX/hf was demonstrated using progress curve analysis (Fig. 1). In agreement with previous studies using serpins expressed in mammalian cells (6),  $\alpha_1$ -PIT/hf is a potent inhibitor of thrombin but not furin. By contrast, a single amino acid

substitution in the P4 position of the reactive site loop to generate  $\alpha_1$ -PDX/hf strikingly alters the selectivity of the serpin resulting in a potent and selective furin inhibitor.

As an important step toward the development of new strategies for attenuating the virulence of many microorganism and viruses whose pathogenesis is furin activity, we found addition of micromolar concentrations of exogenous  $\alpha_1$ -PDX/hf to cell cultures blocks PE-induced cytotoxicity in cultured cells (F. Jean, unpublished results).

In summary, the application of his- and FLAG-tag strategy has provided a means by which to purify rapidly an active recombinant serpin from bacterial cell extracts and follow efficiently the recombinant protein during the purification procedure. The availability and the extensive biochemical characterization of  $\alpha_1$ -PDX/hf will facilitate determination of the applicability of this protein-based inhibitor as a broad-based therapeutic.

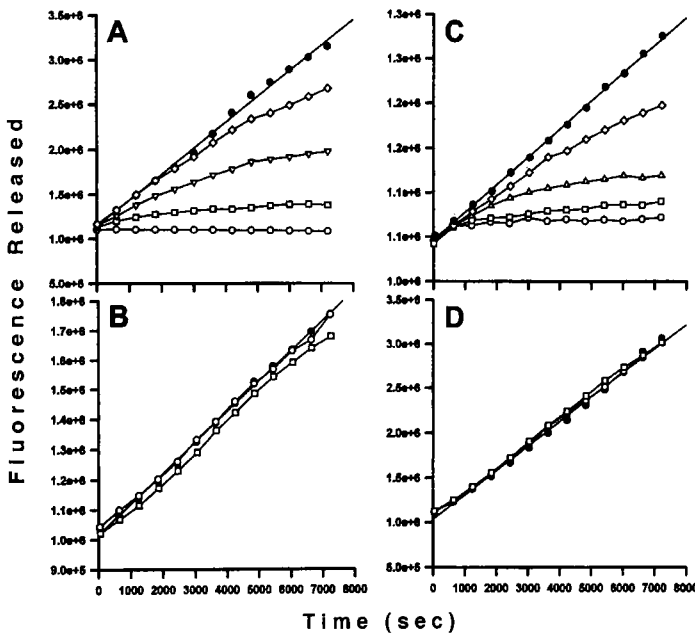


Fig.1. Progress curves for the slow-binding inhibition of furin and thrombin by engineered serpins. Each curve shows the time course of thrombin (panels A and B) or furin (panels C and D) inhibition either in the absence (black circles) or presence (open symbols) of increasing concentrations of added serpin ( $\alpha_1$ -PIT/hf, panels A and D;  $\alpha_1$ -PDX/hf, panels C and B). Each reaction was initiated by addition of enzyme to inhibitor and substrate. Serpin concentrations were either 7.5 nM (diamonds), 15 nM (triangles), 30 nM (squares) or 75 nM (circles).

## References

- Steiner, D.F., Smeekens, S.P., Ohagi, S., and Chan, S.J., *J. Biol. Chem.*, 267 (1992) 23435.
- Molloy, S.S., Thomas, L., VanSlyke, J.K., Stenberg, P.E., and Thomas, G., *EMBO J.*, 13 (1994) 18.
- Molloy, S.S., Bresnahan, P.A., Klimpel, K.R., Leppla, L., and Thomas, G., *J. Biol. Chem.* 267 (1992) 16936.
- Watanabe, M., Hirano, A., Stenglein, S., Nelson, J., Thomas, G., and Wong, T.C. *J. Virol.*, 69 (1995) 3206.
- Inocencio, N.M., Moehring, J. M., Moehring, T.J., *J. Biol. Chem.*, 269 (1994) 31831.
- Anderson, E.D., Thomas, L., Hayflick, J.S., and Thomas, G., *J. Biol. Chem.*, 268 (1993) 24887.



## **Session IX**

# **Glyco-, Lipo-, and Phospho Peptides**



# Multiphosphorylated synthetic peptides as antigens and immunogens in Alzheimer's disease paired helical filaments

Laszlo Otvos, Jr.,<sup>a</sup> Virginia M.-Y. Lee,<sup>b</sup> Susan Leight,<sup>b</sup>  
Peter Davies<sup>c</sup> and Ralf Hoffmann<sup>a</sup>

*<sup>a</sup>The Wistar Institute and <sup>b</sup>Department of Pathology and Laboratory Medicine, University of Pennsylvania, Philadelphia, PA 19104, U.S.A., and <sup>c</sup>Department of Pathology, Albert Einstein College of Medicine, Bronx, NY 10461, USA*

The major histopathological abnormalities that characterize the brains of patients with Alzheimer's disease (AD) include excess of neurofibrillary tangles (NFT), and senile plaques [1]. The NFT are composed of paired helical filaments (PHF) that likely develop from hyperphosphorylated forms of the low molecular weight microtubule-associated  $\tau$  protein, known as PHF- $\tau$  [2]. A major prerequisite for evaluating therapeutic and/or prevention strategies in AD would be the availability of valid biological markers of AD. However, currently there is no diagnostic biochemical test that can be used reliably to stage the cognitive status of AD patients. In this regard, it is significant that  $\tau$  levels are increased in the cerebrospinal fluid (CSF) of AD patients and that the CSF  $\tau$  levels correlate with clinical measures of dementia severity [3]. In our current study we used highly purified synthetic peptides, as well as single and double phosphorylated analogues to identify the binding sites on a large panel of frequently used or newly developed mAbs. In addition, we used these phosphopeptides to generate PHF-specific mAbs.

## Results and Discussion

One of the peptide families we used included the unphosphorylated (nP)  $\tau$  sequence 224-240 (KKVAVVRTPPKSPSSAK), two monophosphorylated analogs (231P and 235P) and a diphosphorylated version (231P, 235P). This region turned to be the recognition site of two of the three currently available mAbs that recognize PHF- $\tau$ , but do not recognize normal adult  $\tau$ , and just weakly label fetal- $\tau$ , or biopsy-originated  $\tau$  [4,5]. The latter two  $\tau$  variants are known to carry more phosphate groups than normal  $\tau$ , but less than PHF- $\tau$  [6]. Dependence of the antigen structure on antibody recognition was studied using our conformation-sensitive ELISA protocol [7]. Antigen conformational effects played roles in the peptide binding of both "true" PHF-specific mAbs, PHF-27 and TG3. The recognition of the major phosphorylation site Thr231 was considerably increased when the monophosphorylated peptide was plated to ELISA from TFE. While TG3 required a stabilized peptide structure to recognize the double phosphorylated peptide variant, the comparative ELISA indicated that for PHF-27 the best binding double phosphorylated peptide structure was already fully presented in water.

Phosphorylated Thr231 was also recognized by the widely used mAb, AT180. A similar set of peptides was used to map the binding sites of the third "true" PHF-specific mAb, AT10. MAb AT10 bound only to a Thr212, Ser214 diphosphorylated version of the

207-222 peptide family. No binding was detected to any monophosphorylated (Thr212P, Ser214P, or Thr217P), or any other diphosphorylated (212P, 217P, or 214P, 217P) peptides or to the unphosphorylated sequence.

Table 1. Peptide recognition of new anti-PHF antibodies that recognize PHF- $\tau$  but not normal  $\tau$ .

mAb	Binding to peptides							
	nP		231P		235P		231P, 235P	
	water	TFE	water	TFE	water	TFE	water	TFE
PHF-6	-	-	+++	++++	-	-	+++	++++
PHF-41	-	-	+++	++++	-	-	+++	++++
PHF-27	-	-	+	+++	-	-	+++	+++
TG3	-	-	+	+++	-	-	+/-	++
TG4	-	-	-	-	++	++	++	++
MC5	-	-	-	-	-	+/-	+++	++++
MC6	-	-	-	-	++	+++	+++	+++
MC15	-	-	-	-	+	++	+++	+++

Since two of the PHF-specific mAbs, PHF-27 and AT10 recognize multiphosphorylated peptide sequences, based on the distance between the two phosphate pairs, it is possible to design multiarm compounds that selectively bind to the abnormally hyperphosphorylated  $\tau$  fragments. Indeed, our preliminary results indicated that mixing  $\alpha$ - $\omega$ -diamines with the phosphopeptides prior to the ELISA assay reduced the strength of the antibody binding, and the extent of the reduction depended upon the distance between the two amino groups (Table 1). Nevertheless, this approach needs to be treated with caution because, for example, mAb MC5 also selectively recognizes multiphosphorylated peptide sequences, but does not discriminate PHF- $\tau$  from fetal  $\tau$  or biopsy- $\tau$ .

PHF- $\tau$  likely contains additional abnormal phosphate sites. Because some phosphoamino acids are immunodominant in the PHF- $\tau$  protein (brought about by increased stability and, consequently, increased presence of antigenic stimulus) [8] alternative strategies are needed for the production of mAbs specific for given sites. Antibodies against designed phosphopeptides offer considerably increased variety and specificity to hidden linear or conformational epitopes that may be singly or, more likely, multiply phosphorylated in PHF- $\tau$ , but not in normal adult  $\tau$ , fetal  $\tau$  or biopsy-originated  $\tau$ . To test this hypothesis, we immunized mice with a peptide construct consisting of the double phosphorylated 224-240 peptide, a turn-inducing spacer, and 31D, a major T-helper cell epitope of the rabies virus nucleoprotein. The anti-peptide antisera labeled PHF- $\tau$  but not normal  $\tau$  on ELISA and Western-blot. Fetal- $\tau$  was recognized at an intermediate level. After fusion of the splenocytes with hybridoma cells, some of the generated mAbs weakly labeled only PHF- $\tau$  (Fig. 1).

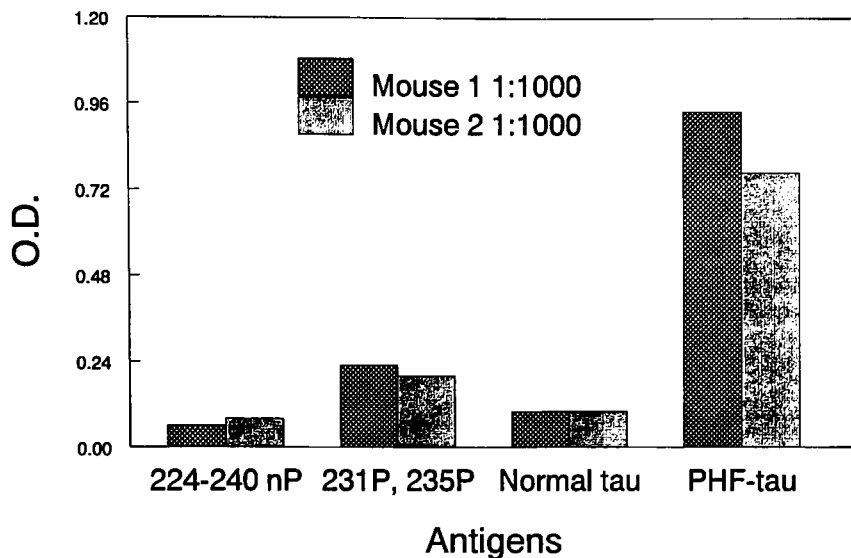


Fig 1. Phosphate specificity of anti-phosphopeptide antisera in 1:1000 dilution.

### Acknowledgments

The authors wish to thank A. Van de Voorde for mAb AT10 and AT180. This work was supported by NIH grants AG 10670, AG 10210, AG 06803 and MH 38623.

### References

1. Selkoe, D.J., Trends Neurosci., 16 (1993) 403.
2. Trojanowski, J.Q., Schmidt, M.L., Shin, R.-W., Bramblett, G.T., Goedert, M. and Lee, V.M.-Y., Clin. Neurosci., 1 (1994) 184.
3. Mock, C., Golombowski, S., Naser, W. and Muller-Spahn, F., Ann. Neurol., 3 (1995) 414.
4. Hoffmann, R., Lee, V.-M.Y., Leight, S., Varga, I. and Otvos, L., Jr., Biochemistry, in press.
5. Jicha, G.A., Lane, E., Vincent, I., Otvos, L., Jr., Hoffmann, R. and Davies, P. Submitted.
6. Matsuo, E.S., Shin, R.-W., Billingsley, M.L., Van de Voorde, A., O'Connor, M., Trojanowski, J.Q. and Lee, V.M.-Y., Neuron, 13 (1993) 1002.
7. Lang, E., Szendrei, G.I., Lee, V.M.-Y. and Otvos, L., Jr., J. Immunol. Meth., 170 (1994) 103.
8. Hoffmann, R., Vasko, M. and Otvos, L., Jr., Anal. Chim. Acta, in press.

# Synthesis of fluoroalkylated muramyldipeptide analogs with lipophilic character

Zheng-Fu Wang and Jie-Cheng Xu

Shanghai Institute of Organic Chemistry, Chinese Academy of Sciences, Shanghai 200032, China

N-Acetylmuramyl-L-alanyl-D-isoglutamine (MDP) has been shown to be the minimal structure of bacterial cell walls required essentially for immunoadjuvant activity[1]. Studies on the relationship between biological activity and chemical structure have indicated that the enhancement of lipophilicity may cause various important effects on the biological activity of MDP, leading to increased adjuvancy and decreased pyrogenicity. We report herein the synthesis of some analogs with lipophilic character by the introduction of perfluoroalkyl onto the C1 position of the sugar moiety or the C-terminal of peptidyl, or by the substitution of alanine with trifluoroalanine(i.e. trifluoromethylglycine,TFMGly).

## Result and Discussion

The MDP analogs containing perfluoroalkyl chain(s) were synthesized by solution method (Fig. 1). Protected D-isoglutamine and muramic acid were synthesized from D-Glu and N-

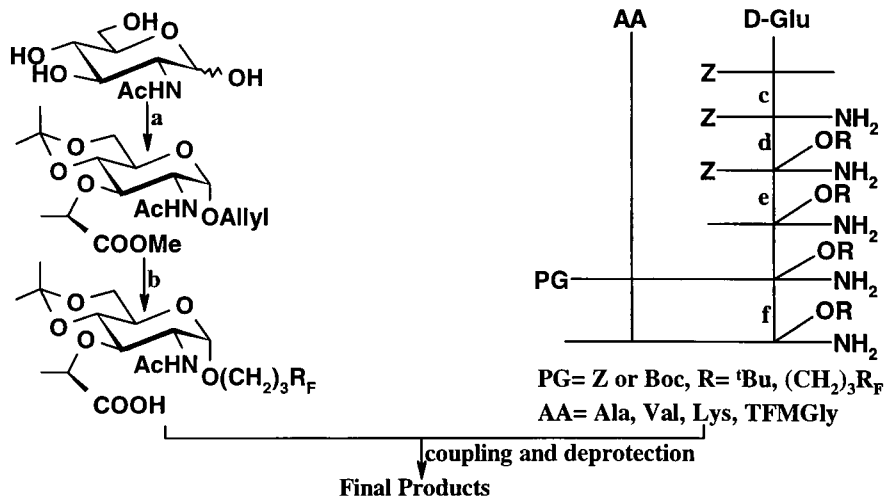


Fig. 1. A general scheme for the synthesis of the title compounds[2].

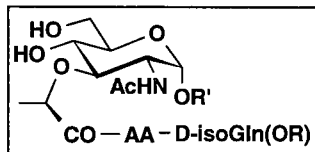
acetyl-D-glucosamine, respectively, followed by the introduction of the perfluoroalkyl group ( $R_F=(CF_2)_nCF_3$ ,  $n=5$  or  $7$ ) by sulfinatodehalogenation[3]. Ethyl N-benzyloxycarbonyl-

3,3,3-trifluoromethylglycinate was prepared by a new method developed by K.Uneyama[4] followed by resolution with subtilisin to afford Z-L-TFMGly. The dipeptides (Table 1) were synthesized using Z<sup>t</sup>Bu strategy *via* a new coupling reagent, benzotriazol-1-yloxy-bis(pyrrolidino)carbonium hexafluoro-phosphate[5].

The solution conformation of three typical compounds has been studied in DMSO-d<sub>6</sub> by NMR. The biological activity of most compounds was evaluated by analyzing the proliferation of T cells and B cells *in vitro*. These results will be published elsewhere.

Table 1. Fluorine-containing MDP analogs obtained in the final step.

AA	R	R
Ala	(CH <sub>2</sub> ) <sub>3</sub> (CF <sub>2</sub> ) <sub>5</sub> CF <sub>3</sub>	H
Ala	(CH <sub>2</sub> ) <sub>3</sub> (CF <sub>2</sub> ) <sub>7</sub> CF <sub>3</sub>	H
Ala	(CH <sub>2</sub> ) <sub>3</sub> (CF <sub>2</sub> ) <sub>5</sub> CF <sub>3</sub>	(CH <sub>2</sub> ) <sub>3</sub> (CF <sub>2</sub> ) <sub>5</sub> CF <sub>3</sub>
Ala	(CH <sub>2</sub> ) <sub>3</sub> (CF <sub>2</sub> ) <sub>7</sub> CF <sub>3</sub>	(CH <sub>2</sub> ) <sub>3</sub> (CF <sub>2</sub> ) <sub>7</sub> CF <sub>3</sub>
Ala	(CH <sub>2</sub> ) <sub>3</sub> (CF <sub>2</sub> ) <sub>7</sub> CF <sub>3</sub>	(CH <sub>2</sub> ) <sub>3</sub> (CF <sub>2</sub> ) <sub>5</sub> CF <sub>3</sub>
Ala	(CH <sub>2</sub> ) <sub>3</sub> (CF <sub>2</sub> ) <sub>5</sub> CF <sub>3</sub>	(CH <sub>2</sub> ) <sub>3</sub> (CF <sub>2</sub> ) <sub>7</sub> CF <sub>3</sub>
Ala	H	(CH <sub>2</sub> ) <sub>3</sub> (CF <sub>2</sub> ) <sub>5</sub> CF <sub>3</sub>
Ala	H	(CH <sub>2</sub> ) <sub>3</sub> (CF <sub>2</sub> ) <sub>7</sub> CF <sub>3</sub>
Val	(CH <sub>2</sub> ) <sub>3</sub> (CF <sub>2</sub> ) <sub>5</sub> CF <sub>3</sub>	H
Val	(CH <sub>2</sub> ) <sub>3</sub> (CF <sub>2</sub> ) <sub>7</sub> CF <sub>3</sub>	H
Lys(TFA)	(CH <sub>2</sub> ) <sub>3</sub> (CF <sub>2</sub> ) <sub>5</sub> CF <sub>3</sub>	H
Lys(TFA)	(CH <sub>2</sub> ) <sub>3</sub> (CF <sub>2</sub> ) <sub>7</sub> CF <sub>3</sub>	H
L-TFMGly	Allyl	H



## References

- (a) Ellouz, F., Adam, A., Ciorbaru, R. and Lederer, E., *Biochem. Biophys. Res. Commun.*, 59 (1974) 1317; (b) Kotani, S., Watanabe, Y., Kinoshita, F., et. al., *Biken J.*, 18 (1975) 105.
- Reagents: a.(i) allyl alcohol, AcCl; (ii) (CH<sub>3</sub>)<sub>2</sub>C(OEt)<sub>2</sub>, p-TsOH; (iii) NaH, DL-CH<sub>3</sub>CHClCOOH; (iv) K<sub>2</sub>CO<sub>3</sub>, MeI; b. (i) R<sub>F</sub>I, NaHCO<sub>3</sub>/Na<sub>2</sub>S<sub>2</sub>O<sub>4</sub>; (ii) H<sub>2</sub>, Pd/C; c. (i) trioxane, p-TsOH; (ii) NH<sub>4</sub>OH; d. for R= <sup>t</sup>Bu, see ref.6; for R=(CH<sub>2</sub>)<sub>3</sub>R<sub>F</sub>: (i) Cs<sub>2</sub>CO<sub>3</sub>, CH<sub>2</sub>CH=CH<sub>2</sub>Br; (ii) R<sub>F</sub>I, NaHCO<sub>3</sub>/Na<sub>2</sub>S<sub>2</sub>O<sub>4</sub>; (ii) H<sub>2</sub>, Pd/C; e. H<sub>2</sub>, Pd/C; f. H<sub>2</sub>, Pd/C for Z, TFA for Boc.
- Huang, W.Y., Huang, B.N. and Hu, C.M., *J. Fluorine Chem.*, 23 (1983) 193.
- Watanabe, H., Hashizumi, Y. and Uneyama, K., *Tetrahedron Lett.*, 33 (1992) 4333.
- Chen, S.Q. and Xu, J.C., *Tetrahedron Lett.*, 33 (1992) 647.
- Chevallet, P., Garrouste, P., Malawska, B. and Martinez, J., *Tetrahedron Lett.*, 34 (1993) 7409.

# Lipoderivatives of an immunodominant epitope of myelin basic protein increased T cell responsiveness in Lewis rats

Anna M. Papini,<sup>a</sup> Silvia Mazzucco,<sup>a</sup> Daniela Pinzani,<sup>a</sup>  
Massimo Biondi,<sup>a</sup> Mario Chelli,<sup>a</sup> Mauro Ginanneschi,<sup>a</sup>  
Gianfranco Rapi,<sup>a</sup> Benedetta Mazzanti,<sup>b</sup> Marco Vergelli,<sup>b</sup>  
Luca Massacesi<sup>b</sup> and Luigi Amaducci<sup>b</sup>

<sup>a</sup>Dipartimento di Chimica Organica "Ugo Schiff" and Centro di Studio sulla Chimica e la Struttura dei Composti Eterociclici e loro Applicazioni, Università di Firenze, Via Gino Capponi 9, I-50121 Firenze, Italy and <sup>b</sup>Dipartimento di Scienze Neurologiche e Psichiatriche, Università di Firenze, Viale Pieraccini 6, I-50131 Firenze, Italy

Because demyelination in multiple sclerosis (MS) is associated with chronic inflammatory lesions in central nervous system (CNS) white matter, it has long been suspected that the disease is determined by an autoimmune mechanism. Several observations have strengthened the hypothesis that CNS myelin protein reactive T cells may play a role in the pathogenesis of MS lesions [1]. Myelin basic protein (MBP) is the most deeply studied myelin antigen because of its intensive encephalitogenicity in experimental models and its role in post-infective and post-vaccine encephalomyelitis. Immunization of susceptible animals with MBP or with its immunodominant peptides induces experimental allergic encephalomyelitis (EAE), an animal model of MS. T cells specific for the immunodominant peptides of MBP can transfer the disease in syngeneic naive animals. As synthetic lipopeptides have been demonstrated to have immunoadjuvant properties both *in vitro* and *in vivo* [2,3], we investigated the T cell response to wild type and lipid-bound immunodominant MBP epitopes in Lewis rats.

## Results and Discussion

We undertook a comparative study of GpMBP(74-85) (MBP1), the immunodominant MBP epitope the in Lewis rat, and two lipopeptide derivatives with the palmitoyl residue (Palm) in two different positions of the sequence.

**R-Gln-Lys(R')-Ser-Gln-Arg-Ser-Gln-Asp-Glu-Asn-Pro-Val-NH<sub>2</sub>**  
MBP1: R=H, R'=H; MBP2: R=Palm, R'=H; MBP3: R=H, R'=Palm

The syntheses were performed by SPPS following the Fmoc/tBu strategy, in a standard synthetic protocol using the NovaSyn Gem continuous-flow synthesizer on TentaGel S RAM resin. We synthesized MBP3 introducing a N<sup>ε</sup>-palmitoyl lysine residue by Fmoc-Lys(Palm)-OH and MBP2 obtained by N-terminal modification of MBP1 with the pentafluorophenyl ester of palmitic acid. All the compounds were purified by RP-HPLC and characterized by FABMS and amino acid analysis.

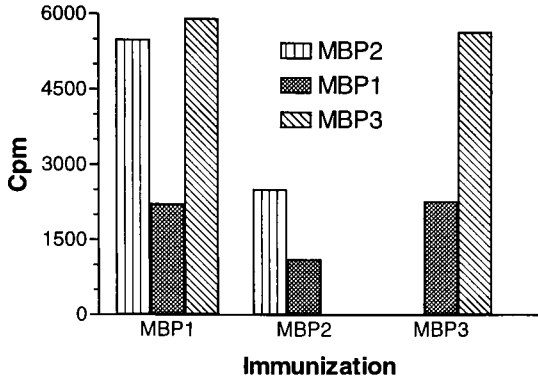


Fig. 1. Proliferative response of spleen cells isolated from Lewis rats immunized with GpMBP(74-85) and its lipoderivatives MBP2 and MBP3 to the wild type and the modified peptide derivatives. Data are expressed as cpm. Background proliferation was 630 cpm.

Lewis rats were immunized with MBP1 and its lipoderivatives MBP2 and MBP3. All the peptides induced EAE and the disease course and severity were comparable in the three groups (data not shown). Spleen cells were isolated from immunized animals at day 10 after immunization and tested in a proliferation assay to evaluate the response to the wild type and lipid-bound peptides. Regardless of the immunizing peptides, spleen cells proliferated more vigorously with the lipid-bound peptides compared to the lipid-free wild type analog (Fig. 1). Successively, we tested the *in vitro* activity of lipopeptides on the proliferative response of long-term CD4+ T cell lines generated from spleen cells of Lewis rats immunized with entire MBP and maintained in culture by periodic restimulation with the whole protein. The large majority of T cell lines (TCL) obtained from Lewis rats immunized with entire MBP proliferated in response to the immunodominant MBP1 peptide. When the proliferative response to lipoderivatives was compared it turned out that the lipid-bound analogs exerted an increased stimulatory activity compared to the lipid-free peptide. Proliferation started at lower antigen concentrations and the overall response was more intense (Fig. 2).

In order to rule out the possibility that this "superagonist" activity of the lipopeptides was due to an unspecific mitogenic activity, the proliferative response of a protein purified derivative-specific (PPD-specific) TCL was tested for these antigens. No response to the lipid-conjugate peptides was observed suggesting that the stimulatory activity of lipid-bound MBP peptides was specific for MBP-reactive T cells (data not shown).

Finally, we could demonstrate that the increased responsiveness of T cells to the lipopeptide required a stable coupling of the two components. The proliferative response of TCL to MBP1 was not increased when an equimolar amount of  $N^{\epsilon}$ -palmitoyl lysine was added during the proliferation assay (data not shown).

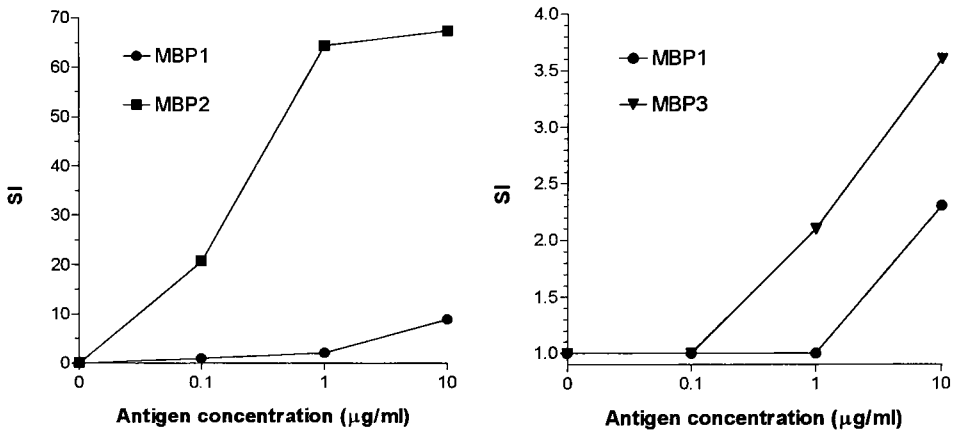


Fig. 2. Proliferative response of two GpMBP(74-85) specific TCL to different concentrations of the wild type peptides and its lipoderivatives MBP2 and MBP3. Data are expressed as SI (stimulation index) =  $cpm$  (stimulated culture)/ $cpm$  (unstimulated culture).

Different hypothesis can be formulated to explain the increased T cell responsiveness of the lipid-bound peptides. A costimulatory activity of the lipophilic moiety can be hypothesized. It has been recently demonstrated that a single modification of a relatively long peptide by a lipophilic aminoacid with a long hydrocarbon chain results in the ability to reproducibly induce without immunoadjuvant a relevant virus-specific CTL response *in vivo* [3]. The mechanisms of this immunoadjuvant activity are not well understood. However a recent study showed that lipoproteins can provide costimulatory signals to CD4+ and CD8+ T lymphocytes to produce pro-inflammatory cytokines required for their differentiation [4]. Alternatively, an increased affinity to the MHC molecule and/or TCR of responding T cells as well as a more favourable antigen presentation could explain the lipopeptide "superagonist" activity.

In conclusion this study demonstrate that lipopeptides may represent a new efficient tool for the study of T cell responses to myelin proteins in MS.

## References

1. Martin, R., McFarland, H.F. and McFarlin, D.E., *Annu. Rev. Immunol.* 10 (1992) 153.
2. Schild, H., Deres, K., Wiesmüller, K.H., Jung, G. and Rammensee, H.G., *Eur. J. Immunol.*, 21(1991) 2649.
3. BenMohamed, L., Gras-Masse, H., Tartar, A., Daubersies, P., Brahimi, K., Bossus, M., Thomas, A. and Druilhe, P., *Eur. J. Immunol.* 27 (1997) 1242.
4. Knigge, H., Simon, M.M., Meuer, S.C., Kramer, M.D. and Wallich R., *Eur. J. Immunol.*, 26 (1996) 2299.

# Antibacterial insect glycopeptides: Synthesis, structure and activity

Laszlo Otvos, Jr.,<sup>a</sup> Philippe Bulet,<sup>b</sup> Istvan Varga<sup>a</sup> and Ralf Hoffmann<sup>a</sup>

<sup>a</sup>The Wistar Institute, Philadelphia, PA 19104, U.S.A., <sup>b</sup>Institut de Biologie Moleculaire et Cellulaire, UPR 9022 du CNRS, Strasbourg 67084, France

Insects are remarkably resistant to bacterial infection. The resistance is explained in part by the rapid synthesis, following bacterial infection or injury of a battery of small cationic peptides [1]. Three of them, pyrrocoricin, drosocin and dipterocin carry O-linked carbohydrate moieties that are necessary for the full biological activity [2-4]. The N-terminal regions of these glycopeptides show a great deal of amino acid and carbohydrate homology. While only one sugar chain is attached to the shorter peptides, drosocin and pyrrocoricin, the longer dipterocin carries carbohydrates at both its N-terminal, proline-rich, and C-terminal glycine-rich domains. We decided to synthesize all three peptides without and with sugars by using a step-by-step solid-phase technique.

## Results and Discussion

The synthesized peptide sequences are as follows (glycosylated threonines are marked with asterisks):

Pyrrocoricin: V<sup>1</sup>DKGSYLP<sup>RPT\*</sup>11PPRPIYNRN<sup>20</sup>

Drosocin: G<sup>1</sup>KPRPYS<sup>RPT\*</sup>11SHPRPIRV<sup>19</sup>

Diptericin N-term. D<sup>1</sup>EKPKLIL<sup>PT\*</sup>10PAPPNLPQLVG<sup>21</sup>

(G<sup>22</sup>GGGNR<sup>KD</sup>GFGVSVDAHQK<sup>V</sup>WTSD<sup>45</sup>)

Diptericin C-term. N<sup>46</sup>GRHSIGVT<sup>\*54</sup>PGYSQHLGGPYGNSR<sup>PDYRIGAGYSYNF</sup>82

The peptides and glycopeptides were purified until homogeneity by reversed-phase HPLC and their integrity was verified by MALDI-mass spectroscopy.

The anomeric configuration of sugars in insects is not known, but we suggest it is Gal( $\beta$ 1 $\rightarrow$ 3)-GalNAc( $\alpha$ 1 $\rightarrow$ O), as our synthetic drosocin with this sugar and the isolated drosocin show indistinguishable antibacterial activity, and HPLC retention time. The antibacterial activity of drosocin in a liquid assay is increased approximately 100 times when the sugar is added [5], and this activity pattern is very similar to that of pyrrocoricin. In spite of the relatively minor sequence alterations between drosocin (or pyrrocoricin) and the N-terminal domain of dipterocin during identical assay conditions, this latter peptide was inactive both glycosylated and without sugar, as were the C-terminal dipterocin domain pair and mixtures of the N- and C-terminal fragments. Even more surprisingly, a partially purified batch of synthetic full-sized, unglycosylated dipterocin

exhibited some antibacterial activity in both types of assays, while a recombinant version of this peptide (small protein) did not.

Very little is known about the mode of action of these glycopeptides. Unglycosylated drosocin, made up from all D-amino acids, is considerably less potent than drosocin made up from L-amino acids [5], indicating that this family of antibacterial peptides, unlike other families, may act on the gram-negative bacteria through a stereospecific target. The role of the attached carbohydrate chain maybe either stabilization of a given secondary structure or provision of resistance to circulating proteases. Based on CD, addition of the disaccharide to drosocin, pyrrococin, and the N- or C-terminal dipterocin fragments did not considerably alter the conformation of the peptides. Drosocin with or without sugar exhibited identical stability in human serum during the entire 45 min to 4 h period of the study (Table 1). The peptide degradation in mammals or in insects likely proceeds through a different pathway and this may explain why drosocin was inactive in mice *in vivo*. While the peptides were almost fully degraded after 4 h in human serum, a recent mass spectroscopy study of the hemolymph composition of a single insect demonstrated that glycosylated drosocin lost one of its sugar moieties during circulation, but the second sugar remained attached to the peptide even after several weeks. Many of the remaining questions will be answered when the synthetic double glycosylated dipterocin 1-82 is available for analysis.

Table 1. Stability of drosocin peptides in 25% human serum (n=3).

Peptide	0 min	Remaining (%) after		
		45 min	120 min	240 min
Drosocin no sugar	100 ± 2	59 ± 4	20 ± 2	2 ± 2
Drosocin Gal-GalNAc	100 ± 3	59 ± 1	24 ± 5	5 ± 2

## Acknowledgments

This work was supported by NIH grant GM 45011.

## References

1. Hultmark, D., Trends Genet., 9 (1993) 178.
2. Bulet, P., Dimarcq, J.-L., Hetru, C., Legueux, M., Charlet, M., Hegy, G., van Dorsselaer, A. and Hoffmann, J.A., J. Biol. Chem., 268 (1993) 14893.
3. Cociancich, S., Dupont, A., Hegy, G., Lanot, R., Holder, H., Hetru, C., Hoffmann, J.A. and Bulet, P., Biochem. J., 300 (1994) 567.
4. Bulet, P., Hegy, G., Lambert, J., van Dorsselaer, A., Hoffmann, J.A. and Hetru, C., Biochemistry, 34 (1995) 7394.
5. Bulet, P., Urge, L., Ohresser, S., Hetru, C. and Otvos, L. Jr., Eur. J. Biochem., 238 (1996) 64.

# 1997 ABRF Peptide synthesis research committee study on a peptide containing a phosphorylated tyrosine

Lynda F. Bonewald,<sup>a</sup> Lisa Bibbs,<sup>b</sup> Steven A. Kates,<sup>c</sup> Ashok Khatri,<sup>d</sup>  
Katalin F. Medzihradzsky,<sup>e</sup> John S. McMurray<sup>f</sup> and Susan T. Weintraub<sup>a</sup>

<sup>a</sup>Univ. Of Texas Health Science Center, San Antonio, TX 78284; <sup>b</sup>Research Institute of Scripps Clinic, La Jolla, CA 92037; <sup>c</sup>PerSeptive Biosystems, Inc., Framingham, MA 01701;

<sup>d</sup>Massachusetts General Hospital, Boston, MA 02114; <sup>e</sup>Univ. Of California, San Francisco, CA 94143; <sup>f</sup>Univ. Of Texas M.D. Anderson Cancer Center, Houston, 77030, USA

Post-translational modifications of proteins create important changes in protein structure resulting in dramatic changes in function. Phosphorylation and dephosphorylation is a major mechanism for controlling a variety of cellular processes from cell movement to cell growth. Tyrosine phosphorylation is especially important in many receptor-mediated events [1]. Covalently modified synthetic peptides representative of *in vivo* post-translational modifications have become critical tools for examining numerous cell functions [2].

Because tyrosine phosphorylation has become the focus of an increasing number of investigations on protein/protein interactions [3], the present study was initiated to introduce phospho-peptide chemistry to the member laboratories and to assess their synthesis capabilities. The Peptide Synthesis Research Committee of the Association of Biomolecular Resource Facilities (ABRF) conducts anonymous studies to introduce and evaluate the ability of ABRF member laboratories to synthesize and characterize test peptides [4]. For the 1997 ABRF study, the Peptide Synthesis Research Committee requested that its member facilities synthesize and submit a crude sample of the following phosphotyrosine peptide for analysis: H-Glu-Asp-Tyr-Glu-Tyr(PO<sub>3</sub>H<sub>2</sub>)-Thr-Ala-Arg-Phe-NH<sub>2</sub>.

## Results and Discussion

In preparation for this study, the committee members synthesized and analyzed four variations of the tyrosine-containing sequence: non-phosphorylated, Tyr(PO<sub>3</sub>H<sub>2</sub>)<sup>3</sup>, Tyr(PO<sub>3</sub>H<sub>2</sub>)<sup>5</sup>, and Tyr(PO<sub>3</sub>H<sub>2</sub>)<sup>3,5</sup>. The following observations were made concerning these reference peptides. Analytical and microbore HPLC, as well as capillary electrophoresis, revealed that the peptides were distinctly separated in the following elution order: first Tyr(PO<sub>3</sub>H<sub>2</sub>)<sup>3,5</sup>, then Tyr(PO<sub>3</sub>H<sub>2</sub>)<sup>5</sup>, followed closely by Tyr(PO<sub>3</sub>H<sub>2</sub>)<sup>3</sup>, and finally Tyr(OH)<sup>3,5</sup>. Mass spectrometric analysis (electrospray and MALDI-TOF) provided the calculated masses for each peptide. As anticipated no differences were observed by amino acid analysis. The phosphotyrosine (pY) was easily detected by Edman degradation sequence analysis with an elution position 1-2 minutes before Asp. In addition, the pY<sup>3</sup> and pY<sup>5</sup> peptides could be easily distinguished by MALDI-PSD. The MALDI-TOF MH<sup>+</sup> for the non-phosphorylated peptide was found to be more intense than the MH<sup>+</sup> for phosphorylated peptide in the negative mode when loaded in

a 1:1 mixture.

Submitted peptides were analyzed by amino acid composition, sequence analysis, RP-HPLC, and electrospray and MALDI-TOF mass spectrometry as described previously [5]. Mass spectrometric analysis of the 33 samples submitted indicated that all but 4 contained the correct product. By HPLC analysis, 10 samples contained greater than 70% correct product when quantified using a wavelength of 230 nm; 20 contained greater than 75% correct product and 4 contained between 50 and 75% correct product when quantified at 275 nm, whereas 4 had no correct product at either wavelength. All samples submitted were synthesized using Fmoc chemistry. No correlation was found between coupling time and percent correct product. A correlation might exist between increased yield of correct product and the use of non-protected phosphotyrosine because 15 of the 20 samples with greater than 75% correct product used non-protected phosphotyrosine.

While the majority of submitted samples contained the desired peptide, deletion sequences of the phosphotyrosine and/or the preceding amino acid were observed in 7 of the 33 submitted samples. One sample contained Thr in place of Tyr, one sample was synthesized backwards, one had a +1 mass, one contained mainly acetylated-TARF-NH<sub>2</sub> and one contained what appeared to be acetylated-TARF-NH<sub>2</sub> plus a t-butyl protecting group.

A singly charged ion at *m/z* 535.5 was detected in 6 of the submitted samples by ESI/MS, but was not observed by MALDI-TOF. It was suspected that this ion represents an acetylated-TARF-NH<sub>2</sub> truncated peptide. This truncated peptide could be generated if the peptide had been capped with acetic anhydride prior to phosphotyrosine addition. This hypothesis was tested by synthesizing the acetylated, truncated peptide and showing that it exhibited the 535.5 ion by ESI/MS and had an elution position by HPLC that was identical to the unknown peak in samples shown to contain this ion.

## Conclusion

Overall, the success rate for synthesis of the requested phosphopeptide by member facilities was quite good, as 61% of the samples had greater than 75% correct peptide, and 73% containing greater than 50% correct peptide. The use of non-protected phosphotyrosine may yield a greater amount of correct product than the use of protected phosphotyrosine.

## References

1. Heldin, C.H., *Cancer Surveys*, 27 (1996) 7.
2. Eck, M.J., Shoelson, S.E., and Harrison, S.C., *Nature*, 362 (1993) 87.
3. Waksman, G., Shoelson, S.E., Pant, N., Cowburn, D., and Kuriyan, J. *Cell*, 72 (1993) 779.
4. Angeletti, R.H., Bonewald, L.F., and Fields, G.G., *Methods in Enzymology* (in press).
5. Angeletti, R.H., Bibbs, L., Bonewald, L.R., Fields, G.B., Kelly, J.W., McMurray, J.S., Moore, W.T., and Weintraub, S.T., In *Techniques in Protein Chemistry VIII*, D.Marshak (Ed), Academic Press, Chapter 4, (in press).

# Targeting a hydrophobic patch on the surface of the GRB2-SH2 domain leads to high-affinity phosphotyrosine-containing peptide ligands

H. Fretz, P. Furet, J. Schoepfer, C. Garcia-Echeverria, B. Gay, J. Rahuel  
and G. Caravatti

*Oncology Research, Novartis Pharma Inc., CH-4002 Basel, Switzerland*

Growth factor receptor binding protein 2 (Grb2) is an important element of mitogenic signal transduction and therefore an attractive target for intervention in the process cell growth regulation. Recently, the X-ray crystal structure of its SH2 domain in complex with a high-affinity heptapeptidic ligand (KPFpYVNV) was determined [1]. In contrast to all other published structures of SH2 domain-peptide complexes, where the ligands are bound in an extended conformation, this structure revealed that the bound peptide ligand adopts a  $\beta$ -turn type I conformation. This unique binding mode and an observed hydrophobic patch on the surface of the protein can be utilized to design and synthesize specific Grb2-SH2 ligands.

## Results and Discussion

The X-ray crystallographic structure of the Grb2-SH2 domain complexed with a synthetic phosphopeptide ligand revealed that the hydrocarbon side chains of Lys $\beta$ D6 and Leu $\beta$ D'1 formed a lipophilic area on the surface of Grb2-SH2 [1]. On the basis of this structural information, a series of pTyr-containing peptides of the general structure Ac-pTyr-Xxx-Asn-NHR were designed, wherein R represented hydrophobic moieties such as, 3-(2-hydroxy-naphthalen-1-yl)-propyl (Fig. 1) and Xxx is either Ile of the pTyr<sup>1068</sup> sequence of the EGF receptor or the  $\beta$ -turn promoting Ac<sub>6</sub>c.

The peptides were assembled on a Rink amide MBHA resin applying Fmoc/ tBu chemistry (Fig. 2). Fmoc-Asp-OAll was coupled through its side chain to the linker. Fmoc-Tyr(PO<sub>3</sub>Me<sub>2</sub>)-OH was used as building block for the introduction of pTyr. Pd (0)-catalyzed allyl ester cleavage was performed on the complete peptide resin. TPTU activation was used for the amidation of the C( $\alpha$ ) carboxylic acid of Asn with various amines (NHR<sub>1</sub>R<sub>2</sub>, NH<sub>2</sub>R). The phosphate methyl groups were cleaved on the peptidyl resin employing TMSI in MeCN prior to TFA-mediated side-chain deprotection and release of the peptide from the support [2].

The results presented are in agreement with our design criteria. Grb2-SH2 binds these modified peptides with high affinity (Table 1). The marked gain in affinity of peptides 1 and 6 can obviously be explained by the large hydrophobic interaction of the naphthyl ring with the protein. This unique hydrophobic patch interaction further improved the selectivity of our compounds towards the Grb2-SH2 domain.

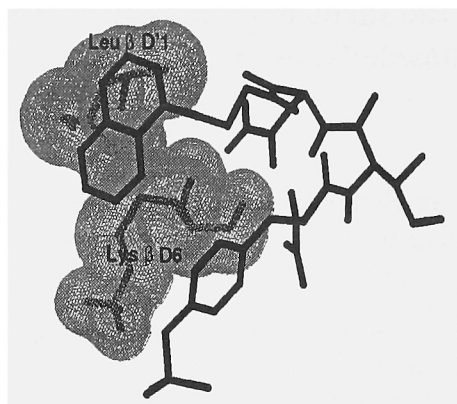


Fig. 1. Model of peptide 1 bound to the Grb2-SH2 protein.

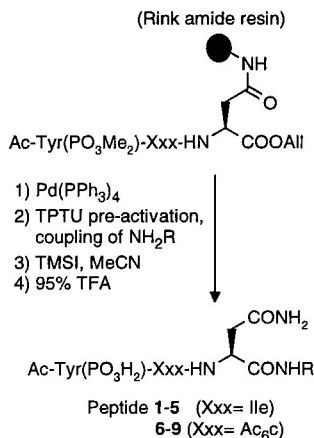


Fig. 2. Synthesis of C-terminally modified phosphopeptides.

Table 1. Binding affinities of phosphopeptides to Grb2-SH2.

Ac-Tyr (PO <sub>3</sub> H <sub>2</sub> )-Ile-Asn-NHR			Ac-Tyr (PO <sub>3</sub> H <sub>2</sub> )-Ac <sub>6</sub> c-Asn-NHR		
Peptide	R	IC <sub>50</sub> [μM]	Peptide	R	IC <sub>50</sub> [μM]
1		0.29	6		0.011
2		2.3			
3		3.1			
4	Ethyl	5.8			
5	H	8.7	7	H	0.21

## References

1. Rahuel, J., Gay, B., Erdmann, D., Strauss, A., García-Echeverría, C., Furet, P., Caravatti, G., Fretz, H., Schoepfer, J. and Grütter, M.G., *Nature Struct. Biol.*, 3 (1996) 586.
2. H. Fretz, *Lett. Pept. Sci.*, 3 (1996) 343.

# Synthesis and purification of unphosphorylated and phosphorylated Phospholamban

Holger Schmid,<sup>a</sup> Sjouke Hoving,<sup>a</sup> Stefan Vetter,<sup>a</sup> Thomas Vorherr<sup>b</sup> and Ernesto Carafoli<sup>a</sup>

<sup>a</sup> Institute of Biochemistry, Swiss Federal Institute of Technology Zürich, CH-8092 Zürich, Switzerland, <sup>b</sup> Bachem AG, CH-4416 Bubendorf, Switzerland

Phospholamban (PLN) is an oligomeric 52 residue membrane spanning protein that regulates the Ca<sup>2+</sup>-ATPase of the cardiac sarcoplasmic reticulum. PLN binds to and inhibits the enzyme. The inhibition is reversed by phosphorylation by Protein kinase A at Ser<sup>16</sup> and by a Ca<sup>2+</sup>-Calmodulin (CaM) dependent protein kinase at Thr<sup>17</sup>, respectively. PLN contains a very hydrophobic membrane spanning the C-terminal portion and a hydrophilic cytosolic N-terminal portion containing the phosphorylation sites. PLN can be isolated from canine hearts, can be expressed in either yeast or in the baculovirus system or can be obtained by chemical synthesis [1]. The chemically synthesized material is identical to the isolated biological material [2]. Enzymatic phosphorylation of PLN does not produce a uniform product, but a mixture of different phosphorylation states [3].

PLN forms pentamers in SDS-PAGE which can be disrupted by boiling in SDS. Phosphorylated PLN runs with lower mobility in SDS-PAGE than unphosphorylated PLN. A mutant of PLN with Cys<sup>41</sup> in the transmembrane region replaced by Phe<sup>41</sup> does not form pentamers on SDS-PAGE and is monomeric in chloroform/methanol 1/1 (v/v).

## Results and Discussion

The 52mer peptide was synthesized manually in the monophosphorylated and bisphosphorylated forms using Fmoc-chemistry by incorporation of Fmoc-Ser(POOBzlOH)-OH and Fmoc-Thr(POOBzlOH)-OH that we synthesized ourselves (data not shown). In the first step the Fmoc amino acids were coupled in three fold excess using TPTU/collidine and in the second step with one equivalent Fmoc amino acid using HATU/ collidine as activating reagents. In the third step we capped unreacted aminogroups with acetic anhydride and DIPEA. Tentagel S resin (Rapp Polymers, Tübingen, FRG) with a HMPB linker (4-(4-Hydroxymethyl-3-methoxyphenoxy)-butyric acid) was used. Oxydized Met residues were reduced with trimethylbromosilane as described by Beck and Jung [4].

Purification was performed by cation exchange HPLC using a gradient of chloroform/methanol/water 4/4/1 (v/v/v) as solvent A, and 0.4 M ammonium acetate in A was used as solvent B. The phosphorylated forms of PLN also showed retention on the TSK carboxymethyl column, but eluted at lower salt concentrations.

The peptides were checked by MALDI-TOF-MS for purity (Fig. 1). The measurements were performed in the positive mode using  $\alpha$ -cyano-4-hydroxy-cinnamic acid as matrix. The bisphosphorylated PLN required very high laser energy to ionize so that fragmentation of the

product could occur. Because of the chemical introduction of the phosphate groups we could purify uniformly phosphorylated PLN with one (Ser<sup>16</sup> or Thr<sup>17</sup>) or two phosphorylations (Ser<sup>16</sup> and Thr<sup>17</sup>) in mg amounts.

In SDS-PAGE the phosphorylated PLN forms pentamers with lower mobility than the unphosphorylated PLN. No differences in aggregation behaviour could be observed in SDS-PAGE between the different forms of PLN using bifunctional crosslinkers (data not shown).

The biological properties of the three phosphorylation states of PLN will be tested by reconstitution of PLN with SR-Ca<sup>2+</sup>-ATPase in liposomes and by measuring Ca<sup>2+</sup>-uptake and/or ATPase activity. The chemical synthesis enabled us to obtain sufficient amounts of both unphosphorylated and phosphorylated PLN to undertake detailed structural studies using NMR spectroscopy.

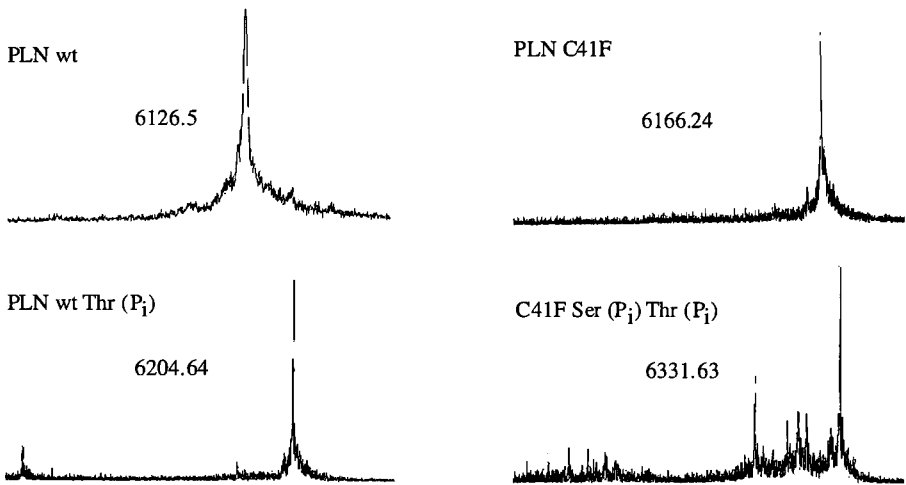


*Fig. 1. MALDI-TOF-MS of the different PLN forms*

## References

1. Vorherr, T., Wrzosek, A., Chiesi, M. and Carafoli, E., *Protein Science*, 2 (1993) 339.
2. Mayer, E.J., Mc Kenna, E., Garsky, V.M., Burke, C.J., Mach, H., Middaugh, C.R., Sardana M., Smith, J. and Johnson R.G.jr., *J. Biol. Chem.*, 271 (1996) 1669.
3. Jackson, W.A. and Colyer J., *Biochem. J.*, 316 (1996) 201.
4. Beck W. and Jung G., *Letters in Peptide Science*, 1 (1994) 31.

# **Design and synthesis of controlled oligomeric neo-C-glycopeptides as multivalent inhibitors of carbohydrate protein interactions**

**Johanne Roby, Robert N. Ben, Kristina Kutterer, Huiping Qin,  
George K. H. Shimizu, Michael Barnes and Prabhat Arya**

*Steacie Institute for Molecular Sciences, National Research Council of Canada, Ottawa,  
ON, Canada, K1A 0R6*

Interactions between cell surface glycoconjugate ligands (e.g. glycolipids, glycoproteins) and protein receptors form the basis of recognition events which are fundamental to a vastly diverse range of biological and pathological processes [1-4]. Unlike non-covalent protein-protein and nucleotide-protein interactions, individual non-covalent carbohydrate-protein interactions are weak. In order to compensate for the weak binding forces, both nature, and subsequent attempts by various research groups to mimic nature, have employed multivalency (co-operativity) as a tool to augment individual ligand-receptor interactions [5-6]. Well defined mimics of cell surface glycoconjugates having biological stability and stronger bindings to pathogenic protein receptors are crucial for understanding recognition processes and for the development of new diagnostics and preventive therapeutics.

## **Results and Discussion**

Towards the goal of mimicking cell surface glycoconjugates, our group is developing a flexible and control-oriented model as a probe for studying carbohydrate-protein interactions. This model illustrates the multivalent presentation of the terminal saccharides which couples the intrinsic structural variation provided by a peptide backbone with the enhanced enzymatic stability offered by C-glycosidic linkages [7]. Our strategy is to display the stable mimics of terminal saccharides (i.e. replacement of anomeric oxygen by carbon) as recognition elements on a peptide backbone as shown schematically in Fig. 1.

Optimization of spacers to display the terminal saccharides on a peptide template could play an important role in designing the inhibitors of carbohydrate-binding proteins. Our approach offers: (i) systematic building block assembly using solid phase chemistry or solid phase approach to the glycosylation of pseudo-peptide template, (ii) highly controlled, yet broad, structural variation, (iii) secondary interactions with adjacent amino acid residues which may further augment binding, and (iv) the incorporation of markers (e.g. biotin) either at the N- or C-terminal of the peptide backbone.

## C-Analogs of Exposed Saccharides Crucial for Recognition

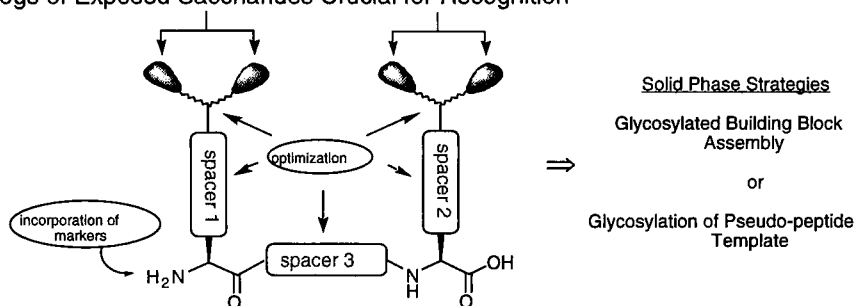


Fig. 1. Strategy of displaying the stable mimics of terminal saccharides.

## Conclusion

Using  $\alpha$ -galactose as a terminal sugar, various neo-C-glycopeptides have been obtained using a building block assembly or glycosylation of pseudo-peptide templates on a solid phase. Applications of neo-C-glycopeptides towards the understanding of carbohydrate-protein interactions is under investigation.

## References

1. Varki, A., *Glycobiology*, 3 (1993) 97.
2. Sharon, N., Lis, H., *Sci. Am.*, (1993), 82.
3. Lee, Y.C. and Lee, R.T., *Acc. Chem. Res.*, 26 (1995) 323.
4. Sears, P. and Wong, C.-H., *Proc. Natl. Acad. Sci. U.S.A.*, 93 (1996) 12086.
5. Roy, R., *Curr. Opin. Struct. Biol.*, 6 (1996) 692.
6. Kiessling, L.L. and Pohl, N.L., *Chem. Biol.*, 3 (1996) 71.
7. Arya, P., Dion, S. and Shimizu, G.K.H., *Biorg. & Med. Chem. Lett.*, 1997 (in press).

# Structural analysis of peptide substrates for O-glycosylation

L. Kirnarsky,<sup>a</sup> O. Prakash,<sup>b</sup> S.M. Vogen,<sup>a</sup> Y. Ikematsu,<sup>a</sup> N. Johnson Kaufman,<sup>a</sup> S.D. Sanderson,<sup>a</sup> H. Clausen,<sup>c</sup> M.A. Hollingsworth<sup>a</sup> and S. Sherman<sup>a</sup>

<sup>a</sup>*Eppley Cancer Institute, University of Nebraska Medical Center, Omaha, NE 68198, USA;*

<sup>b</sup>*Department of Biochemistry, Kansas State University., Manhattan, KS 66506, USA;*

<sup>c</sup>*Faculty of Health Sciences, School of Dentistry, University of Copenhagen, DK-2200 Copenhagen N, Denmark*

O-linked glycosylation is an important post-translational modification of many proteins. In the human mucin, MUC1, which is a heavily O-glycosylated glycoprotein, an N-acetylgalactosamine moiety is attached by N-acetyl-galactosaminyltransferase to the side chains of specific Thr/Ser residues within the 20-residue tandem repeat core. Three distinct N-acetyl-galactosaminyltransferases (designated as GalNAc-T1, -T2, and -T3), which were recently cloned and expressed [1-3], exhibit more complicated substrate specificities [4] than were previously known.

In order to study the molecular mechanisms involved in the specificity of the O-glycosylation reaction, the conformational features of two peptide substrates, RPAPGSTAPPAHGV and PPAHGVTSAPDTRPA, which comprise the sequence of the tandem repeat core of MUC1 and include both glycosylated (underlined) and non-glycosylated sites for all three GalNAc transferases, were analyzed by NMR and computational methods.

## Results and Discussion

The peptides were synthesized by standard Fmoc solid-phase methodologies on an Applied Biosystems Model 430A synthesizer. Side-chain deprotection and cleavage from the resin were achieved in a single-step acidolysis reaction. The peptides were purified by analytical and preparative reverse phase-HPLC on columns packed with C<sub>18</sub>-bonded silica and characterized by amino acid compositional analysis as described previously [5, 6].

The 1D and 2D <sup>1</sup>H-NMR experiments were performed at 500 MHz on a 11.5T Varian UNITY plus spectrometer. All NMR spectra were recorded in pure H<sub>2</sub>O and in a mixture of ddH<sub>2</sub>O with 30% TFE at different temperatures 30°C and 20°C, to resolve CaH-NH cross peaks that overlapped with the strong water signal. NMR data were collected in hypercomplex phase sensitive mode. Water peak suppression was obtained by low-power irradiation of the H<sub>2</sub>O peak during relaxation delay. The data were processed and analyzed using Varian NMR software. Sequence-specific proton resonance assignments were established from two-dimensional proton-proton total chemical shift correlation spectroscopy experiments and confirmed by comparison with cross peaks in 2D NOESY spectra acquired for the peptides under similar experimental conditions. Inter- and intra-residue NOE intensities were measured in 100, 200, 300, and 400 ms mixing time NOESY experiments.

The NMR data were used to retrieve conformational constraints for structure calculations. Newly developed programs and procedures [7] were applied to increase a number of stereospecific assignments and to narrow the torsional angle constraints. These data were used in NMR structure calculations by the DIANA program [8].

A comparative analysis of the structural and kinetic data allowed us to develop a structural model that may explain certain features of the O-linked glycosylation reaction. We propose that the reactive Thr/Ser residue and several flanking residues are in an extended, polyproline II-like conformation, which provides recognition and binding to an active site of the enzyme through interactions with amide protons and carbonyl oxygens on the acceptor substrate. In contrast, the non-glycosylated Thr residue within the APDTR fragment has demonstrated the tendency to be involved in more twisted, compact substructure determined by salt bridge formation between side chains of the flanking Asp and Arg residues. The structural impact of the primary glycosylation of the Thr on the subsequent glycosylation of the adjacent Ser residues was studied by molecular dynamics simulations.

### Acknowledgements

This work was supported by NIH grant CA69234 (to M.A.H.). The Molecular Modeling Core Facility of the UNMC/Eppley Cancer Center was used in these studies. The facility is partially supported by Cancer Center Support Grant CA36727 from the National Cancer Institute.

### References

1. White, T., Bennett, E.P., Takio, K., Sorensen, T., Bonding, N. and Clausen, H., *J. Biol. Chem.*, 270 (1995) 24156.
2. Sorensen, T., White, T., Wandall, H.H., Kristensen, A.K., Roepstorff, P. and Clausen, H., *J. Biol. Chem.*, 270 (1995) 24166.
3. Bennett, E.P., Hassan, H. and Clausen, H., *J. Biol. Chem.*, 271 (1996) 17006.
4. Wandall, H.H., Hassan, H., Mirgorodskaya, E., Kristensen, A.K., Roepstorff, P., Bennet, E.P., Nielsen, P.A., Hollingsworth, M.A., Burchell, J., Taylor-Papadimitriou, J. and Clausen, H., *J. Biol. Chem.*, in press.
5. Ember, J.A., Sanderson, S.D., Taylor, S.M., Kawahara, M. and Hugli, T.E., *J. Immunol.*, 148 (1992) 3165.
6. Nishimori, I., Johnson, N.R., Sanderson, S.D., Perini, F., Mountjoy, K.P., Cerny, R., Gross, M.L. and Hollingsworth, M.A., *J. Biol. Chem.*, 269 (1994) 16123.
7. Kirmarsky, L., Shats, O. and Sherman, S., *THEOCHEM*, in press.
8. Güntert, P. and Wüthrich, K., *J. Biomol. NMR*, 1 (1991) 447.

# Phosphopeptide models of the C-terminal basic domain of p53

**Ralf Hoffmann,<sup>a</sup> Randall E. Bolger,<sup>b</sup> Zhi Quan Xiang,<sup>a</sup> Magdalena Blaszczyk-Thurin,<sup>a</sup> Hildegund C.J. Ertl<sup>a</sup> and Laszlo Otvos, Jr.<sup>a</sup>**

*<sup>a</sup>The Wistar Institute, Philadelphia, PA 19104, USA, and <sup>b</sup>PanVera Corporation, Madison, WI 53711, USA*

The tumor suppressor p53 protein plays a central role in regulating cell growth, G1/S boundary arrest, transactivation and apoptosis. Phosphorylation of p53 is generally thought to modify the properties of the protein [1]. Because of the bias introduced by the use of specific cell lines and the expression of mutated proteins, published reports are contentious and contradictory on the subject of p53 properties with or without phosphorylation. Due to the domain structure of p53, synthetic peptides and phosphopeptides are promising candidates to investigate various functions of the protein [2]. We directly studied the effects of phosphorylation on the non-specific DNA-binding, conformation and stability of the C-terminal, basic domain with synthetic peptides. The peptides corresponded to amino acids 371-393 or 361-393 of human wild-type p53 and were either unphosphorylated or phosphorylated at the protein kinase (PKC) site, Ser378 or diphosphorylated on both the PKC site and the casein kinase II (CKII) site, Ser378 and Ser392. We also used the peptides as immunogens to generate monoclonal antibodies (mAbs).

## Results and Discussion

A fluorescence polarization analysis revealed that recombinant p53 protein was more potent than any of the long peptides in binding to the target DNA fragment. Phosphorylation at the PKC site significantly decreased double stranded DNA binding and addition of a second phosphate group at the CKII site almost completely abolished binding [3]. CD spectroscopy showed that all three long peptides (361-393) assumed identical unordered structures in a DNA-binding buffer. The unmodified peptide changed conformation in the presence of DNA. The Ser378 phosphorylated peptide either did not bind to DNA or binding did not result in a conformational change. The inherent ability of the unphosphorylated peptide to form an  $\alpha$ -helix could be detected when the CD spectra were recorded in trifluoroethanol. Phosphorylation of the PKC site broke the helix structure and addition of the second phosphate to the CKII further enhanced this effect.

Independent observations have suggested that variations in the phosphorylation status might affect the half-life of wild-type p53 [1]. Since p53 is suggested to follow a ubiquitin-dependent degradation pathway [4], examination of the phosphorylation of p53 on its ubiquitination and subsequent degradation may provide an explanation. Alternatively, a direct effect of phosphorylation on peptide stability can be examined by exposing the peptides to mixtures of proteases. As a first attempt to obtain information about stability changes in the peptides, we incubated the three short peptides (371-393) with diluted

human serum. The phosphopeptides exhibited considerably increased serum stability, with no difference in the stability of the two phosphopeptides (Fig. 1).

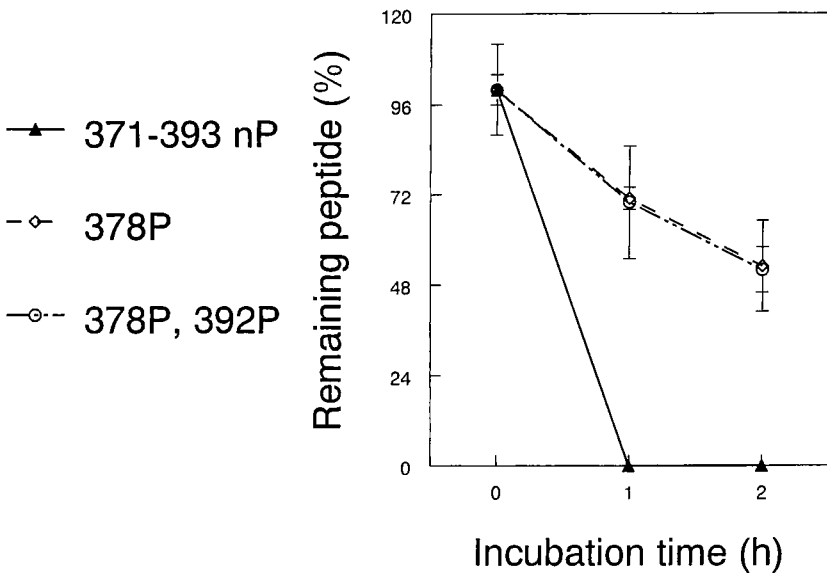


Fig. 1. Stability of C-terminal human p53 peptides in 25% human serum.

Phosphorylation of the PKC site was reported to inhibit the protein recognition of polyclonal antibody 421 [5]. Our results with the short synthetic peptides indicated that the Ser378 phosphorylated peptide was recognized much less efficiently than the unphosphorylated analog, but because antibody 421 bound weakly to the peptides, this finding needs to be treated with caution. The synthetic phosphopeptides, however, can be used to generate monoclonal antibodies. We immunized mice with the short double phosphorylated peptide co-synthesized with a turn-inducing spacer and 31D, a T-helper cell epitope. After fusion, a number of mAbs, variable in their sensitivity and phosphate specificity were obtained. MAb p53-18, an IgM, albeit phosphate independent, labeled p53 in ELISA and Western-blot considerably stronger than antibody 421. In fact, our mAb p53-18 is more sensitive to the p53 protein than the currently available antibodies.

## References

1. Steengena, W.T., van der Eb, A.J. and Jochemsen, A.G., *J. Mol. Biol.*, 263 (1996) 103.
2. Sakamoto, H., Kodama, H., Higashimoto, Y., Kondo, M., Lewis, M.S., Anderson, C.W., Appella, E. and Sakaguchi, K., *Int. J. Peptide Protein Res.*, 48 (1996) 429.
3. Hoffmann, R., Bolger, R.E. and Otvos, L.Jr., Submitted.
4. Ciechanover, A., DiGiuseppe, J.A., Bercovich, B., Orian, A., Richter, J.D., Schwartz, A.L. and Brodeur, G.M., *Proc. Natl. Acad. Sci. USA*, 88 (1991) 139.
5. Ullrich, S.J., Mercer, W.E. and Appella, E., *Oncogene*, 7 (1992) 1635.

# Solid phase synthesis of N- and O-glycopeptide by Boc-strategy

Tadashi Teshima, Saeko Oikawa, Kumiko Y. Kumagaye,  
Kiichiro Nakajima and Tetsuo Shiba

Peptide Institute Inc., Protein Research Foundation, 4-1-2 Ina, Minoh, Osaka 562, Japan

Glycoproteins show important biological activity and play essential roles in the living body. To elucidate the function of the carbohydrate portion, a method is needed for the synthesis of the glycopeptide. The linkage between carbohydrate and protein can be classified into two categories, an N-glycosidic bond linked to an Asn residue and an O-glycosidic bond linked to a Ser or Thr residue. In this study, we tried to synthesize a glycopeptide with one N-acetylglucosamine (GlcNAc) and N-acetylgalactosamine (GalNAc) unit. As the N-glycoside bond of GlcNAc and the O-glycoside bond of GalNAc seemed to be stable against HF treatment from the results of the structural study of the glycoprotein [1] as well as the synthetic study [2], we used one-step HF treatment for the final deprotection. We were able to successfully synthesize N-acetylglucosaminylated and N-acetylgalactosaminylated peptide by the usual solid phase peptide synthesis using Boc strategy (Fig. 1).

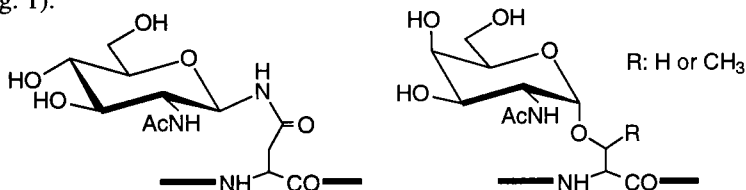


Fig. 1. Structure of N-acetylglucosaminylated and N-acetylgalactosaminylated peptide.

## Results and Discussion

In our strategy, the benzyl group was used to protect hydroxyl groups on the sugar moiety. To introduce the glycosylated amino acid, Boc-Asn(O-Bzl<sub>3</sub>GlcNAc)-OH and Boc-Ser(O-Bzl<sub>3</sub>GalNAc)-OH were synthesized from GlcNAc and GalNAc, respectively.

We chose the peptide sequence (60-71) of CD2 with one GlcNAc residue as a model peptide of the N-glycosylated peptide as shown in Fig. 2. Asn<sup>65</sup> is glycosylated with a high mannose type polysaccharide in the native glycoprotein, whose saccharide part plays an important role in the binding with CD58 [3]. Trp<sup>63</sup> and Cys<sup>59</sup> derivatives as well as the original sequence were also synthesized to demonstrate the versatility of this strategy.

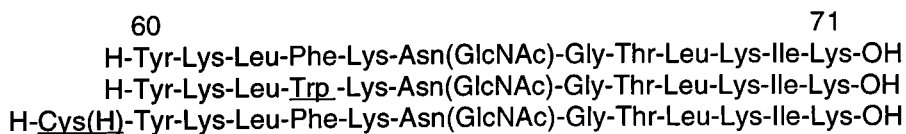


Fig. 2. Sequences of CD2 (60-71), [Trp<sup>63</sup>]-CD2 (60-71), and [Cys(H)<sup>59</sup>]-CD2 (59-71).

Peptide synthesis was carried out by solid phase synthesis. Amino acids other than Boc-Asn(O-Bzl<sub>3</sub>GlcNAc)-OH were introduced by an automated procedure, while Boc-Asn(O-Bzl<sub>3</sub>GlcNAc)-OH was coupled manually by monitoring the free amino group by the Kaiser test. Final deprotection was carried out by normal one-step HF treatment to give crude glycopeptide, which was purified by HPLC. NMR, mass spectrometry, and amino acid analysis data were consistent with the structures of the synthetic glycopeptides.

As model peptides of the O-glycopeptide, we chose suppressin A and desgalactosyl suppressin B (Fig. 3). Suppressin is the glycopeptide which was isolated as a suppressor of phytoalexin production secreted by a pea pathogen, *Mycosphaerella pinodes* [4].

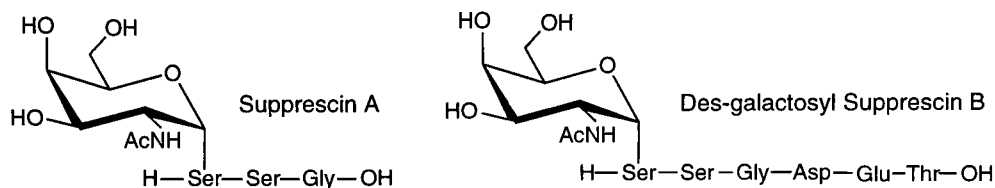


Fig. 3. Structures of suppressin A and desgalactosyl suppressin B.

O-Glycopeptide was also synthesized in the same manner as N-glycopeptide. One-step HF treatment of the protected peptide resin gave the crude glycopeptide, which was purified by HPLC. The structure of the peptide with the O-glycosyl bond was also confirmed by NMR, MALDI-mass spectrometry, and amino acid analysis.

## Conclusion

From this study, we were able to develop a facile strategy for synthesizing N-acetylglucosaminylated and N-acetylgalactosaminylated peptides, which can be used to modify the physical properties of biologically active peptides and can also be used as substrates for enzymatic elongation of carbohydrate chains.

## Acknowledgments

We thank Dr. Hitoshi Yamamoto and Dr. Susumu Yoshikawa, Osaka National Research Institute, AIST, MITI, and Mr. Makoto Nakata, Peptide Institute Inc., for measuring the MALDI-MASS spectra. The present work was supported in part by the New Energy and Industrial Technology Development Organization (NEDO).

## References

1. Mort, A.J. and Lamport, D.T.A., *Anal. Biochem.*, 82 (1977) 289.
2. Unverzagt, C., Kelm, S. and Paulson, J.C., *Carbohydr. Res.*, 251 (1994) 285.
3. Wyss, D.F., Choi, J.S., Li, J., Knoppers, M.H., Willis, K.J., Arulanandam, A.R.N., Smolyar, A., Reinherz, E.L. and Wagner, G., *Science*, 269 (1995) 1273.
4. Shiraishi, T., Saitoh, K., Kim, H.M., Kato, T., Tahara, M., Oku, H., Yamada, T. and Ichinose, Y., *Plant Cell Physiol.*, 33 (1992) 663.

# Novel Dde-protected glycoamino acids and glycoazido acids in saccharopeptide synthesis

Gyula Dekany, Bruno Drouillat, Barrie Kellam and Istvan Toth

Department of Pharmaceutical and Biological Chemistry, School of Pharmacy, University of London, 29-39 Brunswick Square, London, WC1N 1AX, UK

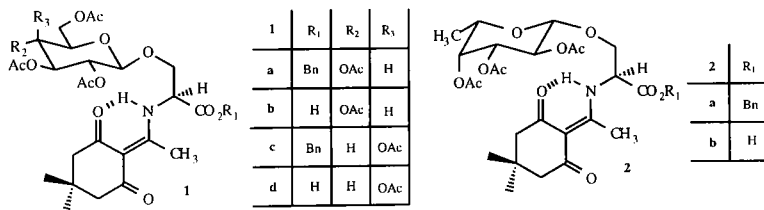
Glycoamino acids are glycosylated amino acids or modified monosaccharides carrying properly protected amino and carboxyl functional groups. The importance of carbohydrate recognition in biological events [1] and the growing interest in the use of synthetic *O*- and *N*-linked glycopeptides and saccharopeptides [2] has demanded the synthesis of glycoamino acids. Since the *O*-glycosidic bond of the glycopeptides is labile to both strong acidic and basic conditions, only the *N*-Fmoc protecting group could be exploited to date. Here, we report the synthesis and application of the *N*-Dde protected *O*- and *N*-glycoamino acids and glycoazido acids, which are suitable for solid phase peptide or saccharopeptide synthesis.

## Results and Discussion

The hydrazine labile 1-(4,4-dimethyl-2,6-dioxocyclohexylidene)ethyl (Dde) protecting group has been successfully employed in solid phase peptide synthesis [3] and its mild deprotection conditions has made it an attractive protection strategy for glycopeptide synthesis.

### 1. Synthesis of *N*-Dde protected *O*-glycoamino acids.

*N*-Dde L-serine was synthesized from L-serine and 2-acetyldimedone [3] in ethanol. The protected amino acid was then regioselectively benzylated using  $\text{Cs}_2\text{CO}_3$ /benzyl bromide in DMF. The fully protected glycoamino acids **1a**, **1c** and **2a** were subsequently prepared from *N*-Dde-L-serine benzyl ester and methyl peracetylated ( $\beta$ -D-gluco-,  $\beta$ -D-galacto- and  $\beta$ -L-fuco-)-1-thio-glycopyranosides *via* dimethyl(methylthio)sulphonium triflate (DMTST) promoted glycosylation reactions. The benzyl deprotection was achieved by Pd/C catalyzed hydrogenation affording the *N*-Dde protected *O*-glycoamino acids **1b**, **1d** and **2b** in high yield.



## 2. Synthesis of *N*-Dde protected *N*-glycoamino acids

Peracetylated-D-glucose **3a** was reacted with trimethylsilylazide in the presence of SnCl<sub>4</sub> affording β-D-glucopyranosyl azide **3b**, (Fig. 1). Glycosylamine **3c** was prepared by catalytic reduction of the azido function and subsequently coupled to Boc-Asp-OBn using DCC, affording glycoconjugate **4a**. Catalytic hydrogenolysis generated free acid **4b** and Boc deprotection afforded the glycoamino acid **4c**. The free amine was then reprotected as the *N*-Dde derivative **4d**.

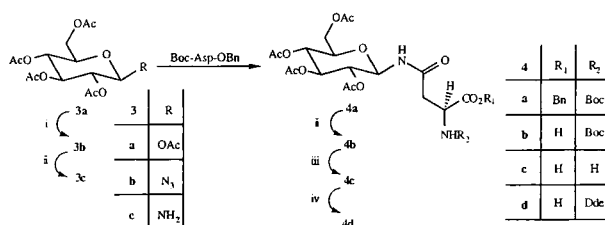


Fig. 1. Reagents and conditions; i) TMSN<sub>3</sub>, SnCl<sub>4</sub>, ii) Pd/C, H<sub>2</sub>, III) TFA, iv) Dde-OH, EtOH, Δ

Carbohydrate based azido acids can act as masked amino acids for the construction of saccharopeptides *via* a novel solid phase route, Fig. 2.

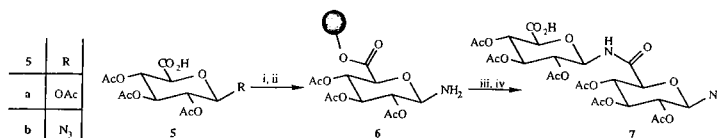


Fig. 2. Reagents and conditions; i) 2-Clt resin, DIEA, ii) PDT, Et<sub>3</sub>N, iii) 5b, HBTU, HOBT, DIEA, iv) TFA.

Glucuronic acid was acetylated with acetic anhydride in the presence of iodine [4] to generate the β-acetate **5a**. The anomeric azide **5b** was then prepared from **5a** by reaction with an excess of trimethylsilyl azide and SnCl<sub>4</sub>. The glycoazido acid was immobilized on a 2-chlorotrityl resin and the azide reduced *in situ* using propane-1,3-dithiol to generate the resin bound glycosylamine **6**. Coupling of **5b** to the immobilized glycoamino acid **6** was achieved using an HBTU/HOBT/DIEA coupling strategy to afford the disaccharopeptide **7**, which was subsequently released from the resin by treatment with TFA.

## References

- Varki, A., *Glycobiology*, 3 (1993) 97.
- Fugedi, P., Peto, C.S. and Wang, L. (1996), Abstract BO 013 at XVIII International Carbohydrate Symposium, Milano, Italy.
- Bycroft, B.W., Chan, W.C., Chhabra, S.R. and Hone, N.D., *J. Chem. Soc. Chem. Commun.* (1993) 778.
- Kartha, R.P.K., Aloui, M. and Field, R.A. 1996, Abstract BP 271 at XVIII International Carbohydrate Symposium, Milano, Italy.

**Session X**

**Peptide Biology**



# Design of novel melanotropin antagonists and agonists for the recently discovered MC3, MC4 and MC5 receptors and their use to determine new biological roles

Victor J. Hruby,<sup>a</sup> Guoxia Han,<sup>a</sup> Wei Yuan,<sup>a</sup> Sejin Lim,<sup>a</sup> Carrie Haskell-Luevano,<sup>a</sup> Roger D. Cone,<sup>c</sup> George Kunos<sup>d</sup> and Mac E. Hadley<sup>b</sup>

<sup>a</sup>Department of Chemistry and <sup>b</sup>Cell Biology & Anatomy, University of Arizona, Tucson, AZ 85721; <sup>c</sup>The Vollum Institute, Oregon Health Sciences University, Portland, OR 97201;

<sup>d</sup>Department of Pharmacology and Toxicology, Virginia Commonwealth University, Richmond, VA 23298-0613, USA

The human genome project has raised many expectations for understanding the basis for health and disease. One false concept that seems to have arisen in the popular press and in scientific journals is the one disease-one gene concept. Nature is much more clever, often utilizing single genes for multiple roles. Control can occur at several levels including the nucleic acid level (alternate splicing, *etc.*), or at the protein product level (posttranslational modification, alternate processing, *etc.*) providing many new opportunities for chemists. A good example of such a system is the proopiomelanocortin (POMC) gene which produces by alternate processing the peptide hormones and neurotransmitters ACTH,  $\alpha$ -melanotropin ( $\alpha$ -MSH),  $\gamma$ -melanotropin ( $\gamma$ -MSH), and  $\beta$ -endorphin ( $\beta$ -End) among others. The major biological activities identified for these peptides (Table 1) include pigmentation ( $\alpha$ -MSH), adrenal function (stress, fear-flight; ACTH) and pain ( $\beta$ -End) [1]. Recently, the receptors for two of these ligands have been sequenced and cloned: the MSH pigment cell receptor (MC1R) and the ACTH adrenal receptor (MC2R). In addition, three other receptors have been identified, their structures determined, and cloned: the MC3R and MC4R found primarily in the brain, and the MC5R found throughout the body [1]. A major question and opportunity arises. What are the biological functions controlled and/or modulated by these multiple ligands and receptors?

## Results and Discussion

To examine the roles of previously unknown peptide receptors in biological systems it is necessary to develop peptide agonist and antagonist analogues with specific properties including high potency, high selectivity for the receptors, and high stability for use *in vitro* and *in vivo* studies. We are developing such agonist and antagonist ligands for the MC1, MC3, MC4 and MC5 receptors.

$\alpha$ -MSH (Ac-Ser-Tyr-Ser-Met-Glu-His-Phe-Arg-Trp-Gly-Lys-Pro-Val-NH<sub>2</sub>) has a rich history of structural-activity studies [2]. A major development was [Nle<sup>4</sup>, DPhe<sup>7</sup>]  $\alpha$ -MSH (2, MT-I, NDP-MSH) [3] which was shown to have numerous favorable biological and biochemical properties, including high potency (Table 2), no ACTH-like activity, prolonged biological activity *in vitro* and *in vivo*, high stability against biodegradation, no

toxicity, extended half-life in circulation, good bioavailability transdermally and even

*Table 1. Proposed Classical and New Discovered Biological Roles for Melanocortin Peptides.*

I. Classical Biological Role	
A. ACTH	- Adrenal Function; Stress; Anti-inflammatory - Peripheral MC2R - Fear-flight; Learning - Central MC2R?
B. $\alpha$ -MSH	- Pigmentation - Peripheral MC1R Learning; Temperature Control - Central CM1R Receptor?
C. $\beta$ -Endorphin	- Pain - Opioid Receptors
II. New Biological Roles	
A. $\alpha$ -MSH	- Feeding Behavior; Anti-obesity - Central MC4R - Sexual Behavior; Erectile Function - Unknown MC Receptor - Temperature Control - Use Central MC3(or 4)R - Cardiovascular Function; Blood Pressure; Heart Rate - Central MC3R/MC4?

orally and, in human clinical trials, the ability to stimulate pigmentation without sun [reviews 2,4]. A more potent cyclic analogue was discovered more recently, Ac-Nle<sup>4</sup>-c[Asp<sup>5</sup>, DPhe<sup>7</sup>, Lys<sup>10</sup>] $\alpha$ -MSH(4-10)-NH<sub>2</sub> (**3**, MT-II) [5]. In addition to its smaller size MT-II is more potent, more stable (not hydrolyzed by any proteolytic enzyme), and provides a useful template for the design of agonists and antagonists. Data from studies in our laboratories are shown in Table 2. Clearly,  $\alpha$ -MSH, NDP- $\alpha$ -MSH, and MT-II bind potently to all the new melanocortin receptors, with **3** generally being the most potent. A further key finding was the discovery of a potent and selective melanotropin antagonist, Ac-Nle<sup>4</sup>-c[Asp<sup>5</sup>, DNal(2'), Lys<sup>10</sup>] $\alpha$ -MSH (**4**, Table 2), whereas the DPhe(p-F)<sup>7</sup>-substituted analogue **5** (Table 1) is a highly potent agonist at all melanocortin receptors. The major significance of the discovery of **4** was its potent antagonist activities at both MC4 and MC3 receptors and selectivity (about 12 fold) for the MC4R. Interestingly, the DNal(1')<sup>7</sup>-containing analogue of **4** is an agonist at these receptors (data not shown).

The availability of **4** provided a unique opportunity to investigate the role of melanotropins and new melanocortin receptors in critical biological functions. Animals that express large quantities of agouti, an antagonist protein of  $\alpha$ -MSH at the MC1 receptor, has been speculated to be involved in obesity. To test this hypothesis MT-II was used as an MC4R agonist and SHU-9119 (**4**, Table 2) as an antagonist. Administration of MT-II given i.c.v. or peripherally led to inhibition of feeding for both normal and obese animals, and could be reversed by **5** [6]. These effects are mediated by central MC4 receptors. Next the possibility that melanocortin peptides and melanocortin receptors might be involved in cardiovascular control was examined using agonists and **4** as an antagonist. The agonist MT-II, either alone or in combination with the antagonist SHU-9119, was microinjected into the medullary dorsal-vagal complex. The agonist caused a decrease in blood pressure and in heart beat which was specifically blocked by SHU-9119 [7]. In another series of experiments, the potent agonist MT-II was given intramuscularly to over

a dozen normal and impotent male volunteers. It was determined in double blind placebo controlled studies that very small amounts of **3** could elicit an erection in normal and psychogenic impotent males. Further studies on other roles of melanocortins and melanotropin receptors are in progress. Finally, in a search for new templates we have

Table 2. Biological Activities of Melanotropin Agonists and Antagonist at Melanocortin Receptors.

Compound	Biological Activities <sup>2</sup>			
	MC1R	MC3R	MC4R	MC5R
<b>1</b> $\alpha$ -MSH	0.3 (RP); 2.0 (H)	.67 (H)	.21 (H)	.80 (M)
<b>2</b> [Nle <sup>4</sup> ,D-Phe <sup>7</sup> ] $\alpha$ -MSH (MT-I)	0.01 (RP); 0.5 (H)	.13 (H)	.017 (H)	ND
<b>3</b> Ac-Nle <sup>4</sup> -c[Asp <sup>5</sup> ,DPhe <sup>7</sup> ,Lys <sup>10</sup> ] $\alpha$ -MSH(4-10)-NH <sub>2</sub> (MT-II)	0.01 (AC) 0.6 (RP); 0.2 (H)	0.27 (R)	0.057 (M)	ND
<b>4</b> Ac-Nle <sup>4</sup> -c[Asp <sup>5</sup> ,DNal(2') <sup>7</sup> ,Lys <sup>10</sup> ] $\alpha$ -MSH(4-10)-NH <sub>2</sub> (SHU-9119)	pA <sub>2</sub> >10.5 (RP) 0.036 (H)	Antag. pA <sub>2</sub> 8.3	Antag. pA <sub>2</sub> 9.7	0.43 (M)
<b>5</b> Ac-Nle <sup>4</sup> -c[Asp <sup>5</sup> ,DPhe(p-F),Lys <sup>10</sup> ] $\alpha$ -MSH(4-10)-NH <sub>2</sub>	0.016 (H)	0.19 (H)	0.019 (H)	1.4 (M)
<b>6</b> DPhe-c[Cys-His-DPhe-Arg-Trp-DCys]-Thr-NH <sub>2</sub>	0.10 (RP)	ND	ND	ND

<sup>1</sup> Biological potencies taken from several different published studies in our laboratories.

<sup>2</sup> RP = *Rana pipiens*; AC = *Anolis carolinensis*; H = human receptor; M = mouse receptor; R = rat receptor

examined whether the somatostatin template could be used to design potent and receptor selective melanotropin receptor agonists and antagonists. As shown in Table 2, we have been very successful in obtaining highly potent ligands for the MC1R, e.g. **6** (Table 2), which is almost equipotent to MT-II.

## References

1. The Melanotropin Peptides, Ann. N.Y. Acad. Sci., 680 (1993) 687.
2. For a review see Hruby, V.J., Wilkes, B.C., Cody, W.L., Sawyer, T.K. and Hadley, M.E., Peptide Protein Rev., 3 (1984) 1.
3. Sawyer, T.K., SanFillippo, P.J., Hruby, V.J., Engle, M.H., Howard, C.B., Burnett, J.B. and Hadley, M.E., Proc. Natl. Acad. Sci. USA, 77 (1980) 5754.
4. Hruby, V.J., Sharma, S.D., Toth, K., Jaw, J.J., Al-Obeidi, F., Sawyer, T.K. and Hadley, M.E., Ann. N.Y. Acad. Sci., 681 (1995) 51.
5. Al-Obeidi, F., Hruby, V.J., Pettitt, B.M. and Hadley, M.E., J. Am. Chem. Soc., 111 (1989) 3413.
6. Fan, W., Boston, B.A., Kesterson, R.A., Hruby, V.J. and Cone, R.D., Nature, 385 (1997) 165.
7. Li, S.J., Varga, K., Archer, P., Hruby, V.J., Sharma, S.D., Kesterson, R.A., Cone, R.D. and Kunos, G., J. Neurosci., 16 (1996) 5182.

# Cellular import of functional peptides

**Jacek Hawiger**

*Department of Microbiology and Immunology, Vanderbilt University Medical Center, A 5321 MCN  
Nashville, TN 37232, USA*

Ten thousand proteins expressed in an average mammalian nucleated cell are engaged in signal transduction, gene transcription, and intracellular trafficking from one subcellular compartment to another. To look at their intracellular interactions as the blueprint for their functions, we need non-invasive approaches to import peptides and other probes for structure-function analysis. Functional genomics will undoubtedly utilize methods based on cellular import of peptides representing newly discovered cellular proteins for their intracellular structure-function analysis.

The non-invasive methods employed for cellular import of peptides include the use of peptide encoded by *Antennapedia* homeobox, peptide based on signal sequence hydrophobic (h) region, peptide with myristate group, HIV Tat protein or the so called loligomers made of polylysine-branched peptide. Because of intolerable cytotoxicity of the loligomers and significant side effects of the Tat protein of HIV, the use of both methods seem limited, [for review see 1].

A non-invasive method of importing functional peptides into intact cells based on hydrophobic motif of the signal peptide comprises the main focus of this paper.

## Results and Discussion

In collaboration with Dr. Yao Zhong Lin, we developed a new non-invasive method of importing peptides into a cell a signal peptide [2]. We reasoned that the hydrophobic sequence of the signal peptide known to translocate through cell membrane and phospholipid vesicles can be used as a leading edge to carry peptides into cells. The hydrophobic core (h) region was identified in 126 signal sequences ranging in length from 18 to 21 residues [3]. The h region made of 7-15 non-conserved amino acid residues is the dominant structure determining membrane-translocating function of signal sequence.

The concept of utilizing hydrophobic sequence of signal peptide for the outside-in import of evolves from realization that most of synthetic peptides cannot cross impermeable membrane barrier if specific membrane receptor is not involved. However, synthetic peptides carrying signal sequence will cross cell membrane. To test this hypothesis we used two distinct signal sequences derived from Kaposi Fibroblast Growth Factor and from integrin  $\beta_3$ . We deleted the amino-terminal positively charged N region and the carboxy-terminal cleavage site. The remaining hydrophobic (h) region constitutes Membrane Permeable Sequences (MPS). We attached to the carboxy-terminal end of MPS a functional cargo containing an epitope tag to detect the imported peptides in intracellular compartments with monospecific anti-peptide antibodies. Signal sequence hydrophobic peptide import is independent of a cell type [1]. The

latter characteristics distinguishes it from cell type-dependent import of *Antennapedia* peptide [4].

The list of cells competent for import of signal sequence-engineered peptides tested by us includes five human cell types: monocytic, endothelial, T lymphocyte, fibroblast and erythroleukemia and two murine lines (Table 1). The imported peptides carrying functional cargo change the intracellular signaling pathways of these cells in a significant way. Analysis of two different signaling pathways illustrate the power of cell permeable peptide import applied by us to identify a new functional domain of integrins involved in intracellular signaling and a common pathway of nuclear import of four transcription factors in inflammatory and immune cells.

*Table 1. Functional studies of intracellular protein-protein interactions employing cell-permeable peptide import based on hydrophobic (h) region of signal sequences.*

Membrane Permeable Sequence (MPS)	Functional Domain	Cell Line
AAVALLPAVLLALLAP	Nuclear localization sequence of NF- $\kappa$ B p50 wild type 10 residues idem (mutant 2/10) idem (mutant 7/10); NLS of SV40 T antigen wild type idem (mutant)	Human monocytic THP-1 cells Murine endothelial LE-II cells Human T lymphocytes Jurkat
	NLS of FGF-1	Murine NIH 3T3 cells
VTVLALGALAGVGVG	Integrin $\beta_3$ cytoplasmic domain Integrin $\alpha_{IIb}$ cytoplasmic domain	Human erythroleukemia HEL cells and endothelial ECV 304 cells
	Integrin $\beta_1$ cytoplasmic domain	Human fibroblast cell line

Integrins are major two-way signaling receptors responsible for the adhesion of cells to the extracellular matrix and for cell-cell interaction mediated by adhesive blood proteins such as fibrinogen, fibronectin, and vitronectin. Integrins "integrate" signals from extracellular matrix with intracellular signaling pathways [5]. To conduct structure-function analysis of intracellular sequence of integrins we prepared a series of synthetic peptides representing overlapping sequences of the cytoplasmic tail of integrin  $\beta_3$  [6]. They were covalently bound via peptidyl bond to the hydrophobic region of the signal peptide of integrin  $\beta_3$ . Such peptides were tested for their inhibitory effect on adhesion of human erythroleukemic (HEL) cells to immobilized fibrinogen after stimulation with phorbol myristate acetate. Only cell-permeable peptide  $\beta_3$ -IS spanning residues 747-762 of the cytoplasmic segment of integrin  $\beta_3$  inhibited adhesion of HEL cells measured by cell ELISA [6].

A mutant peptide was prepared to reproduce in our experimental system "an experiment

of nature", namely a loss of function mutation Ser752Pro responsible for a bleeding disorder, Glanzmann thrombasthenia, Paris 1 [6]. Indeed, cell permeable peptide carrying the same mutation was not active in our system. Using other mutant peptides we established that two tyrosines 747 and 759 form a functional tandem within the sequence 747-762. We identified and termed this intracellular region of integrin  $\beta_3$  as the Cell Adhesion Regulatory Domain (CARD) and established that a similar sequence in integrin  $\beta_1$  cytoplasmic tail is active in blocking adhesion of human fibroblast mediated by  $\beta_1$  integrins [6]. Because different integrins play a role in tumor metastasis, progression of atherosclerosis and thrombosis underlying heart attacks and strokes, and in immune and inflammatory responses, cell-permeable peptides offer a new tool to interrupt from within adhesive function of integrins.

Many inflammatory and immune responses involve signaling from cell membrane to the nucleus. Such a signaling in T lymphocytes results in import of transcription factors into the nucleus where they activate transcription of a large subset of genes [7]. The nuclear import of karyophilic protein involves recognition of a nuclear localization sequence (NLS) within the protein by a cytoplasmic NLS receptor [8]. Initially, we focused on designing a cell-permeable peptide with a functional cargo containing NLS from p50 subunit of transcription factor NF- $\kappa$ B. NF- $\kappa$ B is a transcription factor most readily responding to inflammatory and immune stress [9]. We hypothesized that cell-permeable peptide containing NLS from the NF- $\kappa$ B p50 subunit introduced to human monocytic and endothelial cells will block translocation of NF- $\kappa$ B in response to proinflammatory agonists, lipopolysaccharide and tumor necrosis factor (TNF) $\alpha$ . Indeed, the effective blockade of nuclear import of transcription factor NF- $\kappa$ B was achieved by cell-permeable peptide containing homologous NLS [2]. We extended these experiments to human T lymphocytes by testing the hypothesis postulating that nuclear import of not one but four transcription factors NF- $\kappa$ B, AP1, NFAT and STAT involves a common pathway sensitive to inhibition by one type of NLS [10]. Thus, cell-permeable peptides blocking nuclear import of NFAT and other key transcription factors offer a novel approach to immunosuppressive and antiinflammatory therapy.

The cell-permeable peptide import we have developed provides a vast array of applications in peptide biology [1, 2, 6, 11]. A wide range of cell types, the speed and ease of translocation across the plasma membrane, free movement to cytoplasmic target proteins, low immunogenicity and easy detectability of cell-permeable peptide overcome the inherent limitations of currently used invasive and some non-invasive methods. Thus, cellular import of bioactive peptides and hopefully peptide and non-peptide mimetics will help not only in verifications of currently known intracellular targets but in structure-function analysis of newly sequenced cellular proteins flowing from the Human Genome Initiative. Moreover, new ways to target subcellular compartments besides nucleus are becoming feasible to study normal and abnormal function of mitochondria, lysosomes, and peroxisomes. There is also a need to unravel not only fundamental mechanism of peptide import across cell membrane but also transendothelial and transepithelial transport of cell-permeable peptides to establish a firm basis for their bioavailability and selectivity *in vivo*. These parameters will expand the cellular import of functional peptides and nonpeptides mimetics to their *in vivo* delivery.

## Acknowledgements

I thank Ann Colosia, John Donahue, Xue-Yan Liu, Yao Zhong Lin, Sheila Timmons, Troy Torgerson, Ruth Ann Veach, and Song Yi Yao whose collaborative efforts contributed to the recent experimental work discussed in this review. The assistance of Traci Castleman in the preparation of this manuscript is also acknowledged. It was supported by the NIH NHLBI Merit Award HL-30647 and grants HL 45994 and HL 30648.

## References

1. Hawiger, J., *Current Opinion in Immunology*, 9 (1997) 189.
2. Lin, Y.Z., Yao, S.Y., Veach, R.A., Torgerson, T.R. and Hawiger, J., *J. Biol. Chem.*, 270 (1995) 14255.
3. Prabhakaran, M., *Biochem. J.*, 269 (1990) 691.
4. Joliot, A.H., Triller, A., Volovitch, M., Pernelle, C. and Prochiantz, A., *New Biologist*, 3 (1991) 1121.
5. Clark, E.A. and Brugge, J.S., *Science*, 268 (1995) 233.
6. Liu, X.-Y., Timmons, S., Lin, Y.-Z. and Hawiger, J., *Proc. Natl. Acad. Sci. USA*, 93 (1996) 11819.
7. Crabtree, G.R. and Clipstone, N.A., *Annu. Rev. Biochem.*, 63 (1994) 1045.
8. Gorlich, D. and Mattaj, I.W., *Science*, 271 (1996) 1513.
9. Baeuerle, P.A. and Baltimore, D., *Cell*, 87 (1996) 13.
10. Torgerson, T.R., Colosia, A.D., Donahue, J.P., Lin, Y.Z. and Hawiger, J., *J. Immunol.*, Submitted (1997).
11. Lin, Y.Z., Yao, S.Y. and Hawiger, J., *J. Biol. Chem.*, 271 (1996) 5305.

# Novel highly potent bradykinin antagonists containing pentafluorophenylalanine

Lajos Gera and John M. Stewart

*Department of Biochemistry, University of Colorado School of Medicine,  
Denver, Colorado 80262, USA.*

Bradykinin (BK) is a linear nonapeptide having the sequence Arg-Pro-Pro-Gly-Phe-Ser-Pro-Phe-Arg. It has a broad range of biological activities in both normal physiology and pathophysiology. Because of its role in the inflammatory responses, developing bradykinin antagonists is of great interest. The first antagonist to receive wide application, NPC-349 (DArg-Arg-Pro-Hyp-Gly-Thi-Ser-DPhe-Thi-Arg), was developed by Stewart and Vavrek in 1984 [1]. The key modification was replacement of L-proline at position 7 by D-phenylalanine. The second generation of BK antagonists began with the Hoechst HOE-140, in which DPhe was replaced by its ringclosure analog (DTic) at position seven, and it was modified further at position eight (Oic) [2]. Investigators at Cortech [3] crosslinked a cysteine-containing first generation antagonist with hexamethylene-*bis*-maleimide to yield CP-0127 (Bradycor), a dimer that shows good potency and persistence of action *in vivo*. Nova investigators reported analogs of NPC-349 containing 4-*n*-propoxy- or 4-phenylthio-proline at position seven [4]. In 1995 "third generation" BK antagonists containing the novel amino acid  $\alpha$ -(2-indanyl)-glycine (Igl) were developed in our laboratories [5]. One of the most potent peptides, B9430 (DArg-Arg-Pro-Hyp-Gly-Igl-Ser-DIgl-Oic-Arg), is orally active, extremely potent at both B1 and B2 receptors and has extremely long duration of action *in vivo*. It is active in models of acute and chronic inflammation. We have now introduced pentafluorophenylalanine (f5f) into BK antagonists, and have found several which have greater potency than any known antagonists. On isolated rat uterus the most potent of these is B10056, which is a full order of magnitude more potent than B9430.

## Results and Discussion

Peptides (Table 1) were synthesized by standard solid phase methods [6], purified by CCD and/or HPLC and characterized by HPLC, TLC, LDMS and amino acid analysis. DCC was used for coupling of normal amino acids, and BOP-HOBT, TBTU or HATU were used for sterically hindered residues. For N-terminal guanylation, peptide-resin was treated with a 4-fold excess of N,N'-*bis*-guanylpiperazine in DMF at room temperature. Analogs B10118 and B10158 were synthesized by treatment of peptide-resin with dodecanedioyl dichloride and DIEA in DCM. B10236 was synthesized by treating the free peptide overnight with 0.55 equiv. of EGS (ethylene glycol-*bis*-[succinimidylsuccinate]) and DIEA in DMF. Boc-D- and L-f5f were purchased from Advanced ChemTech. The reduced peptide bond for analog

Table 1. Structures and Activities of Bradykinin Antagonists.

NUMBER	STRUCTURE										ACTIVITY	
	0	1	2	3	4	5	6	7	8	9	UTERUS pA <sub>2</sub>	ILEUM pA <sub>2</sub>
B9340	DArg	Arg	Pro	Hyp	Gly	Thi	Ser	Dlgl	Oic	Arg	I(7.9)	I(8.0)
B9430	DArg	Arg	Pro	Hyp	Gly	Igl	Ser	Dlgl	Oic	Arg	I(8.5)	I(7.9)
B10044	DArg	Arg	Pro	Hyp	Gly	Igl	Ser	Df5f	Oic	Arg	I(8.1)	I(8.4)
B10056	DArg	Arg	Pro	Hyp	Gly	Igl	Ser	Df5f	Igl	Arg	I(9.5)	I(8.0)
B10058	DArg	Arg	Pro	Hyp	Gly	Igl	Ser	Df5f	Thi	Arg	I(8.2)	I(7.9)
B10112	DArg	Arg	Pro	Hyp	Gly	Igl	Ser	Df5f	NchG	Arg	21%	I(7.6)
B10116	DArg	Arg	Pro	Pro	Gly	Thi	Ser	Df5f	Oic	Arg	I(8.2)	I(7.8)
B10150	DArg	Arg	NMF	Hyp	Gly	Igl	Ser	Df5f	Oic	Arg	I(8.1)	I(7.9)
B10164	DArg	Arg	Pro	Hyp	Gly	f5f	Ser	Dlgl	Oic	Arg	I(8.0)	I(7.2)
B10166	DArg	Arg	Pro	Hyp	Gly	Thi	Ser	Df5f	f5f	Arg	I(8.1)	I(8.0)
B10172	DArg	Arg	Pro	Hyp	Gly	Thi	Ser	Df5f	Leu	Arg	I(8.3)	I(7.3)
B10174	DArg	Arg	Pro	Hyp	Gly	Igl	Ser	Df5f	Leu	Arg	I(8.1)	I(8.2)
B10180	DArg	Arg	Pro	Hyp	Gly	Igl	Ser	Df5f	Chg	Arg	I(8.2)	I(8.1)
B10186	DArg	Arg	Pro	Hyp	Gly	Cpg	Ser	Df5f	Cpg	Arg	I(8.1)	I(7.4)
B10196	DArg	Arg	Pro	Hyp	Gly	Igl	Ser	Df5f	Cpg®	Arg	I(7.9)	I(4.9)
B10206	DArg	Arg	Pro	Hyp	Gly	Igl	Ser	Df5f	Nc7G	Arg	I(8.9)	I(7.8)
B10208	DArg	Arg	Pro	Hyp	Gly	Thi	Ser	Df5f	NchG	Arg	14%	I(8.7)
B10210	DArg	Arg	Pro	Hyp	Gly	f5f	Ser	Dlgl	Oic	Arg	I(8.0)	I(7.8)
B10214	DArg	Arg	Pro	Igl	Gly	Igl	Ser	Df5f	Oic	Arg	I(8.2)	I(8.1)
B10274	DArg	Arg	Pro	Hyp	Gly	f5f	Ser	Df5f	f5f	Arg	I(8.2)	I(8.1)
B10232	DArg	Arg	Pro	Hyp	Gly	Igl	Ser	Df5f	f5f	Arg	I(8.1)	I(7.7)
B10148	Lys	Arg	Pro	Hyp	Gly	Igl	Ser	Df5f	Oic	Arg	I(7.2)	I(6.0)
B10154	Aca	Arg	Pro	Hyp	Gly	Igl	Ser	Df5f	Oic	Arg	I(8.2)	I(7.9)
B10156	Gun <sub>2</sub> bApp	Arg	Pro	Hyp	Gly	Igl	Ser	Df5f	Oic	Arg	I(8.3)	I(7.9)
B10118	α-DDD(Lys)	Arg	Pro	Pro	Gly	Thi	Ser	Df5f	Oic	Arg <sub>2</sub>	I(8.1)	I(8.3)
B10158	α-DDD(Lys)	Arg	Pro	Hyp	Gly	Igl	Ser	Df5f	Oic	Arg <sub>2</sub>	I(8.5)	I(8.0)
B10236	EGS (Arg)	Arg	Pro	Hyp	Gly	Igl	Ser	Df5f	f5f	Arg <sub>2</sub>	I(7.7)	I(7.4)

B10196 was introduced by reductive alkylation of Arg(Tos)-resin with Boc-cyclopentylglycine aldehyde by the procedure of Sasaki and Coy [7]. Peptides were assayed on rat uterus and guinea pig ileum by standard methods [5].

## Conclusion

These f5f BK analogs explore a new class of bradykinin antagonists. B10056 has a potency one order of magnitude higher in rat uterus than our earlier most potent B9340 or B9430. Heretofore Oic at position 8 has given the most potent antagonists, with various residues at position 7. Among these new 7-Df5f antagonists, analogs having f5f (B10232), Chg (B10180), Cpg (B10186), Leu (B10172 and B10174) and Thi (B10058) at position 8 have potency as high as the Oic analog (B10164). The 7-Df5f analog with Nc7G at position 8 (B10208) has high ileum antagonist potency ( $pA_2=8.7$ ), but is an *agonist* on uterus. Some of these new antagonists show long term inhibition on rat blood pressure following a bolus injection. The new highly potent, very stable, long-lasting B10056 and B10206 are good candidates for anti-inflammatory drug development.

## Acknowledgments

This work was aided by grants from the U.S. NIH (grant HL-26284) and from Cortech Pharmaceutical Corp. We thank Vikas C. Dhawan and Paul A. Bury for assistance with chemistry, and Frances Shepperdson for the assays. We thank G.R. Matseuda for a gift of N,N'-*bis*-Cbz-1-guanylpyrazole.

## References

1. Vavrek R.J. and Stewart J.M., *Peptides*, 6 (1985) 161.
2. Lembeck F., Griesbacher T., Eckhardt M., Henke S., Breipohl G. and Knolle J., *Brit. J. Pharmacol.*, 102 (1991) 297.
3. Cheronis J.C., Whalley E.T., Nguyen K.T., Eubanks S.R., Allen L.G., Duggan M.J., Loy S.D., Bonham K.A. and Blodgett J.K., *J. Med. Chem.*, 35 (1992) 1563.
4. Kyle D.J., Martin J.A., Burch R.M., Carter J.P., Lu S., Meeker S., Prosser J.C., Sullivan J.P., Togo J., Noronha-Blob L., Sinsko J.A., Walters R.F., Whaley L.W. and Hiner R.N., *J. Med. Chem.*, 34 (1991) 2649.
5. Stewart J.M., Gera L., Hanson W., Zuzack J.S., Burkard M., McCollough R. and Whalley E.T., *Immunopharmacology*, 33 (1996) 51.
6. Stewart J.M. and Young J.D., *Solid Phase Peptide Synthesis*. Rockford, IL: Pierce Chemical Co., 1984.
7. Sasaki Y. and Coy D.H., *Peptides*, 8 (1987) 119.

# Application of cell-permeable peptides to the functional analysis of EGF-induced mitogenic signaling pathways

**Mauricio Rojas, SongYi Yao, John P. Donahue and Yao-Zhong Lin**

*Department of Microbiology and Immunology, Vanderbilt University, Nashville, TN 37232, USA*

Epidermal growth factor (EGF)-stimulated mitogenic pathways require the intrinsic tyrosine kinase activity of its transmembrane receptor [1]. *Ras*/MAP kinase activation cascade originating from the EGFR comprises a number of protein-protein interactions involving a *Grb2*/Sos-1 signaling protein complex. The *Grb2* protein, which functions as an adaptor, binds to tyrosine-phosphorylated EGFR either directly by its SH2 domain or indirectly via the *Shc* protein. To determine the functional consequence of disrupting the EGFR/*Grb2* or *Shc*/*Grb2* protein-protein associations *in vivo*, we delivered peptides containing either the EGFR Tyr1068- [2] or the *Shc* Tyr317-containing region [3] into intact cells using a nondestructive cell-permeable peptide import method [4].

## Results and Discussion

To influence EGF-induced EGFR/*Grb2* interaction, we designed a peptide comprised of a cell permeable sequence at its N-terminus (underlined) and the phosphotyrosine 1068-containing site of EGFR at its C-terminus, AAVALLPAVLLALLAPLPVPE<sub>p</sub>YINQSV (SP1068 peptide). In EGF-stimulated SAA cells (NIH 3T3 cells overexpressing EGFR), the phosphorylated EGFR was coprecipitated with *Grb2* (Fig. 1A). However, the amount of associated EGFR was significantly reduced in cells pretreated with SP1068 peptide (Fig. 1A). Neither non-cell-permeable P1068 nor cell-permeable unphosphorylated SY1068 peptide treatment showed any significant inhibition. Peptide-mediated disruption of the EGFR/*Grb2*/Sos-1 cascade led to reduced *Ras* activation (Fig. 1B) and MAP kinase activation (not shown) in EGF-stimulated cells.

We also delivered cell-permeable peptides carrying *Shc* Tyr317-containing region into SAA cells, AAVALLPAVLLALLAPFDDPSYVNVQNL. The EGF-induced *Shc*/*Grb2* association was inhibited substantially in the cells treated with phosphorylated SP317 peptide (Fig 2A). Interestingly, this association was also inhibited by unphosphorylated SY317 peptide. In contrast, the non-cell-permeable *Shc* peptide (P317) and cell-permeable SY1068 peptide were without significant effect (Fig. 2A). To verify that the *Grb2*-binding activities of non-phosphorylated SY317 peptide do not result from *in vivo* phosphorylation of the peptide, we used an *in vitro* peptide-protein binding assay. Fig. 2B showed that *Grb2* SH2 protein could bind both phosphorylated and unphosphorylated *Shc* peptides, but not an unphosphorylated SY1068 peptide derived from the EGFR. This finding represents the first paradigm of the functional interaction between an unphosphorylated tyrosine-containing motif and an SH2 domain.

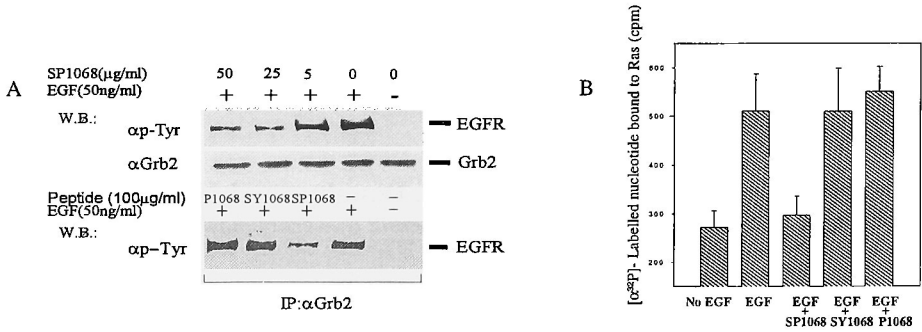


Fig. 1. A. *In vivo* inhibition of EGF-induced EGFR/Grb2 association by cell-permeable SP1068 peptide. B. EGF-induced guanine nucleotide exchange on Ras can be inhibited by SP1068 peptide.

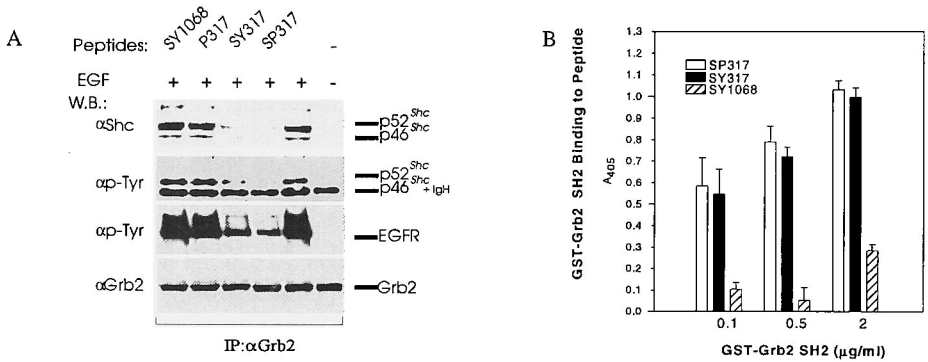


Fig. 2. A. *In vivo* inhibition of EGF-induced Shc/Grb2 association by both phosphorylated and unphosphorylated cell-permeable SP317 and SY317 Shc peptides. B. *In vitro* binding of SP317 and SY317 peptides to Grb2 SH2. Peptides coated on a microplate were incubated with GST-Grb2 SH2 fusion protein. The peptide-bound protein was detected in ELISA using anti-GST antibodies.

**Acknowledgments**

This work was supported by NIH grant GM52500 and ACS grant RD-392.

**References**

1. Pawson, T., Nature, 373 (1995) 573.
2. Rojas, M., Yao, S., and Lin, Y. Z., J. Biol. Chem., 271 (1996) 27456.
3. Rojas, M., Yao, S., Donahue, J. P., and Lin, Y. Z., Biochem. Biophys. Res. Commun., 234 (1997) 675.
4. Lin, Y. Z., Yao, S., Veach, R. A., Torgerson, T. R., and Hawiger, J., J. Biol. Chem., 270 (1995) 14255.

# Biological functions of synthetic peptides derived from the laminin alpha 1 chain G domain

**Motoyoshi Nomizu, Yuichiro Kuratomi, Woo Ho Kim, Sang-Yong Song, Matthew P. Hoffman, Hynda, K. Kleinman and Yoshihiko Yamada**

*CDBRB, National Institute of Dental Research, NIH, Bethesda, Maryland 20892, USA*

Laminin, a major component of the basement membrane matrix, is a heterotrimeric molecule with at least eleven isoforms. Laminin-1 consists of  $\alpha 1$ ,  $\beta 1$  and  $\gamma 1$  chains which have similar domain structures except for a unique C-terminal globular domain (G domain) on the  $\alpha 1$  chain. Laminin-1 has multiple biological activities including promotion of cell adhesion, spreading, growth, neurite outgrowth, tumor metastasis, and collagenase IV secretion. Several active sites have been identified using proteolytic fragments, recombinant proteins and synthetic peptides [1]. Our goal is to understand the biological role of laminin in development and disease using laminin-derived synthetic peptides to identify its cell adhesion sites [2]. By systematically screening the G-domain with 113 overlapping synthetic peptides we identified five peptides (AG-10, AG-22, AG-32, AG-56 and AG-73) that showed cell attachment activities with cell-type specificities. These were evaluated for direct cell attachment, spreading and inhibition of cell spreading to a laminin-1 substrate using several cell lines. The minimum active sequences of AG-10, AG-32 and AG-73 were determined to be SIYTTRF, IAFQRN and LQVQLSIR, respectively. These sequences are highly conserved among the different species and different laminin  $\alpha$  chains, suggesting that they play critical roles in biological functions and in interactions with cell surface receptors [3]. Cell spreading on AG-10 and AG-32 was inhibited by  $\beta 1$  and  $\alpha 6$  integrin antibodies. In contrast, cell adhesion and spreading on peptide AG-73 was not inhibited by these antibodies. AG-10 and AG-32 were found to promote tumor cell invasion by stimulating invadopodial activities via an  $\alpha 6\beta 1$  integrin signaling mechanism [4]. Here, we describe biological functions of AG-73 (RKRLQVQLSIRT), one of the most biologically active peptides in the laminin  $\alpha 1$  chain G domain.

## Results and Discussion

We studied the attachment of B16-F10 cells to laminin-1, the E-3 fragment and AG-73. In attachment assays AG-73 did not inhibit cell attachment to laminin-1, but significantly inhibited cell attachment to E3 and to AG73. The scrambled peptide, AG-73T (LQRRSVLRTKI) showed no effect on cell attachment to any of the substrates. Cell attachment to AG73, the E3 fragment, and laminin-1 was inhibited by EDTA. These results suggest that cell attachment to AG-73 and to E3 is mediated by a cation-dependent receptor(s).

We determined the effects of the AG-73 peptide on tumor metastasis and growth. *In vitro* studies showed that AG-73 enhanced tumor cell adhesion, migration, invasion, and

gelatinase production, and blocked laminin-1 mediated cell migration. We tested the *in vivo* effects of AG-73 on lung colonization in C57BL6/N mice intravenously injected with B16-F10 melanoma cells. Control animals had a mean of 116.5 ( $\pm$  11.2) lung colonies while mice receiving 1 mg or 2 mg of AG-73 intraperitoneally developed more lung colonies with means of 142.2 ( $\pm$  15.7) and 171.3 ( $\pm$  30.3) colonies, respectively. Unexpectedly, many of the mice treated with AG-73 peptide developed hepatic metastases, whereas the control mice did not. Mice receiving 1 mg AG73 developed 2.6 ( $\pm$  1.2) liver metastases and mice receiving 2 mg AG73 developed 16.3 ( $\pm$  5.5) liver metastases. The effect of extrapulmonary metastases was not previously reported with another metastasis-promoting laminin-derived peptide, IKVAV. AG-73 and the control peptide, AG-73T, were each coinjected subcutaneously with B16-F10 melanoma cells into mice with the basement membrane matrix Matrigel. AG-73 was able to stimulate tumor growth significantly over that observed in the absence of the peptide. AG-73T peptide did not enhance tumor growth. The culture of a human submandibular salivary gland cell line (HSG) on laminin-1 induced acinar cell differentiation. HSG cells formed multicellular spherical structures with polarized nuclei and a central lumen [6]. When peptides from the G-domain were added only AG-73 inhibited acinar formation. When HSG cells were cultured directly with AG73, morphological organization into acinar-like structures occurred, although the cells did not polarize. These data suggest that AG73 is an important site on laminin-1 for HSG cell acinar differentiation. AG73 also promoted neurite outgrowth [5]. Three neuronally derived cell lines were used, all of which extended neurites when cultured on laminin-1. All three cell lines bound to AG73 but only two of the cell lines extended neurites on AG73, suggesting cell type specificity for AG73 stimulated neurite outgrowth.

Most of the biologically active sequences of laminin-1 contain an arginine or lysine positively charged residue, that appears to be critical for interaction with cell surface receptors. The minimum active sequence of the AG-73 peptide (LQVQLSIR) in the mouse laminin  $\alpha$ 1 chain also contains an arginine. This sequence is conserved in the human laminin  $\alpha$ 1 chain, the human laminin  $\alpha$ 2 chain, the mouse laminin  $\alpha$ 2 chain and the *Drosophila* laminin  $\alpha$  chain. Thus, the minimal active sequence of AG-73, LQVQLSIR, could be an important biologically active site on laminin-1.

## References

1. Yamada, Y. and Kleinman, H.K., *Curr. Opin. Cell Biol.*, 4 (1992) 819.
2. Nomizu, M., Kim, W.H., Yamamura, K., Utani, A., Song, S.Y., Otaka, A., Roller, P.P., Kleinman, H.K. and Yamada, Y., *J. Biol. Chem.*, 270 (1995) 20583.
3. Nomizu, M., Song, S.Y., Kuratomi, Y., Tanaka, M., Kim, W.H., Kleinman, H.K. and Yamada, Y., *FEBS Letters*, 396 (1996) 37.
4. Nakahara, H., Nomizu, M., Akiyama, S.K., Yamada, Y., Yeh, Y. and Chen, W.T., *J. Biol. Chem.*, 271 (1996) 27221.
5. Richard, B.L., Nomizu, M., Yamada, Y. and Kleinman, H.K., *Exp. Cell Res.*, 228 (1996) 98.
6. Hoffman, M.P., Kibbey, M.C., Letterio, J.J. and Kleinman, H.K., *J. Cell Sci.*, 109 (1996) 2013.

# Competitive antagonists of the corticotropin releasing factor (CRF) scanned with a i-(i+3) Glu Lys Bridge

A. Miranda,<sup>a</sup> S. Lahrichi,<sup>b</sup> J. Gulyas,<sup>b</sup> C. Rivier,<sup>b</sup> S. Koerber,<sup>b</sup> C. Miller,<sup>b</sup> A. Corrigan,<sup>b</sup> S. Sutton,<sup>b</sup> A. Craig,<sup>b</sup> W. Vale<sup>b</sup> and J. Rivier<sup>b</sup>

<sup>a</sup>Department of Biophysics, Universidade Federal de São Paulo, C.P. 20.388, 04034-020, São Paulo, SP, Brazil; <sup>b</sup>Clayton Foundation Laboratories for Peptide Biology, The Salk Institute, 10010 N. Torrey Pines Road, La Jolla, CA 92037, USA.

CRF [1] is involved in a wide spectrum of central nervous system (CNS)-mediated effects, suggesting that this peptide plays an important role within the brain, especially in response to stressful stimuli [2]. Systematic SAR investigations have resulted in the development of CRF antagonists such as  $\alpha$ -helical CRF<sub>(9-41)</sub> [3], members of the [DPhe<sup>12</sup>,Nle<sup>21,38</sup>] r/hCRF<sub>(12-41)</sub> (standard) family [4] and conformationally restricted analogs [5] that are effective in the CNS. Those results, predictive methods and physicochemical measurements have suggested that CRF and its family members (urotensins and sauvagine) assume an  $\alpha$ -helical conformation when interacting with the CRF receptors. To further test this hypothesis, we have scanned the whole rat/human CRF<sub>(9-41)</sub> sequence with an i-(i + 3) bridge consisting of the Glu-Xaa-Xbb-Lys scaffold which we and others had shown to be compatible with maintenance or enhancement of  $\alpha$ -helical structure in at least some unpredictable cases.

## Results and Discussion

CRF analogs [6] were tested for antagonist activity in an *in vitro* assay measuring alteration of CRF-induced release of ACTH by rat anterior pituitary cells in culture. From this series we have identified seven analogs that are either equipotent to (cpds **2**, **5** and **11**), or up to three times more potent (cpds **3**, **6**, **7**, and **8**) than the standard in addition to cyclo(30-33)[DPhe<sup>12</sup>, Nle<sup>21,38</sup>, Glu<sup>30</sup>, Lys<sup>33</sup>]r/hCRF<sub>(12-41)</sub> (astressin **9**) that is 32 times more potent than the standard in blocking ACTH secretion *in vitro* (see Table 1). Because the corresponding linear analogs (cpds **4** and **10**) are significantly less potent, our interpretation of the increased potency of the cyclic analogs is that the introduction of the side-chain to side-chain bridging element (at positions 30-33, and to a lesser extent at positions 14-17, 20-23, 23-26, 26-29, 28-31, 29-32, and 33-36) induces and stabilizes in the receptor environment a putative  $\alpha$ -helical bioactive conformation.

These results, although unpredictable, confirm the importance of a systematic hypothesis-driven and rational approach to the design of peptide antagonists and illustrate dramatically the role that secondary and possibly tertiary structures may play in modulating biological signaling through specific protein ligand interactions.

Sequence of Rat/Human-CRF:



Table 1. Most potent CRF cyclic antagonists of the Glu Lys *i*-(*i*+3) bridge scan.

No.	Compound	Relative Potency <i>in vitro</i>
1.	[DPhe <sup>12</sup> ,Nle <sup>21,38</sup> ]r/hCRF <sub>(12-41)</sub>	1.0 (standard)
2.	cyclo(14-17)[DPhe <sup>12</sup> ,Glu <sup>14</sup> ,Lys <sup>17</sup> ,Nle <sup>21,38</sup> ]r/hCRF <sub>(12-41)</sub>	1.3 ( 0.14-8.8)
3.	cyclo(20-23)[DPhe <sup>12</sup> ,Glu <sup>20</sup> ,Lys <sup>23</sup> ,Nle <sup>21,38</sup> ]r/hCRF <sub>(12-41)</sub>	2.9 ( 1.3-6.7)
4.	linear [DPhe <sup>12</sup> ,Glu <sup>20</sup> ,Lys <sup>23</sup> ,Nle <sup>21,38</sup> ]r/hCRF <sub>(12-41)</sub>	0.31 ( 0.14-0.65)
5.	cyclo(23-26)[DPhe <sup>12</sup> ,Nle <sup>21</sup> ,Glu <sup>23</sup> ,Lys <sup>26</sup> ,Nle <sup>38</sup> ]r/hCRF <sub>(12-41)</sub>	1.8 ( 0.67-4.5)
6.	cyclo(26-29)[DPhe <sup>12</sup> ,Nle <sup>21</sup> ,Glu <sup>26</sup> ,Lys <sup>29</sup> ,Nle <sup>38</sup> ]r/hCRF <sub>(12-41)</sub>	2.8 ( 0.35-3.4)
7.	cyclo(28-31)[DPhe <sup>12</sup> ,Nle <sup>21</sup> ,Glu <sup>28</sup> ,Lys <sup>31</sup> ,Nle <sup>38</sup> ]r/hCRF <sub>(12-41)</sub>	3.1 ( 1.1-10)
8.	cyclo(29-32)[DPhe <sup>12</sup> ,Nle <sup>21</sup> ,Glu <sup>29</sup> ,Lys <sup>32</sup> ,Nle <sup>38</sup> ]r/hCRF <sub>(12-41)</sub>	3.4 ( 1.2-12)
9.	cyclo(30-33)[DPhe <sup>12</sup> ,Nle <sup>21</sup> ,Glu <sup>30</sup> ,Lys <sup>33</sup> ,Nle <sup>38</sup> ]r/hCRF <sub>(12-41)</sub>	32 (12-82)
10.	linear [DPhe <sup>12</sup> ,Nle <sup>21</sup> ,Glu <sup>30</sup> ,Lys <sup>33</sup> ,Nle <sup>38</sup> ]r/hCRF <sub>(12-41)</sub>	0.10 (0.06-0.16)
11.	cyclo(33-36)[DPhe <sup>12</sup> ,Nle <sup>21</sup> ,Glu <sup>33</sup> ,Lys <sup>36</sup> ,Nle <sup>38</sup> ]r/hCRF <sub>(12-41)</sub>	0.8 (0.40-1.7)

## Acknowledgments

This work was supported in part by NIH grant No. DK-26741, The Hearst Foundation, the Foundation for Research, California Division, FAPESP-Brazil. Drs. W.W. Vale, C.L. Rivier and A.G. Craig are FR investigators. We thank Dr. C. Hoeger and Ms. L. Cervini for constructive comments and C. Miller, R. Kaiser, T. Goedken and Y. Haas for technical assistance.

## References

- Vale, W., Spiess, J., Rivier, C. and Rivier, J., *Science*, 213 (1981) 1394.
- Taché, Y. and Rivier, C. (Eds.), *Corticotropin-Releasing Factor and Cytokines: Role in the Stress Response*, Proceedings of the Hans Selyé Symposium on Neuroendocrinology and Stress, The New York Academy of Sciences, New York, 1993, p. 296.
- Rivier, J., Rivier, C. and Vale, W., *Science*, 224 (1984) 889.
- Hernandez, J.-F., Kornreich, W., Rivier, C., Miranda, A., Yamamoto, G., Andrews, J., Taché, Y., Vale, W. and Rivier, J., *J. Med. Chem.*, 36 (1993) 2860.
- Miranda, A., Koerber, S. C., Gulyas, J., Lahrichi, S., Craig, A. G., Corrigan, A., Hagler, A., Rivier, C., Vale, W. and Rivier, J., *J. Med. Chem.*, 37 (1994) 1450.
- Miranda, A., Lahrichi, S. L., Gulyas, J., Koerber, S. C., Craig, A. G., Corrigan, A., Rivier, C., Vale, W. and Rivier, J., *J. Med. Chem.*, (1997) submitted.

# Cytocidal effect of custom antibacterial peptides on leukemia cancer cells

Hueih Min Chen, Wei Wang, David Smith and Siu-Chiu Chan

Department of Biochemistry, Hong Kong University of Science and Technology, Clear Water Bay, Kowloon, Hong Kong, China

Natural cecropin B (CB) [1-3], consisting of 35 amino acids, possesses the highest anti-bacterial activity [4] in the cecropin family. The cell killing ability of these peptides is shown by their helical conformation. However, the detailed mechanism of cell lysis by cecropin peptides is not yet clearly known but is believed to involve the formation of an ion-channel or pore prior to cell death [5]. Another proposed model is through the "Non-pore" mechanism. The "carpet like" formation of the peptide leads to the disintegration of the membrane [6].

In this study, we synthesized cecropin B-1 (CB-1) by replacing the C-terminal segment of CB from positions 26 to 35 with the sequence of CB from positions 1 to 10. This customized CB-1 with five more positive amino acids was used to test the peptide's anticancer activity. In addition, another similar custom peptide, CB-2, with the same sequence as CB-1 but including an extra pair of Gly-Pro inserted at position 24 was generated. CB-2 was used to test the effect of an extended flexible linker and to compare the results to those obtained from CB-1. The natural cecropin A (CA) was also synthesized and used as a reference to compare its anticancer activity to that of CB, CB-1 and CB-2.

## Results and Discussion

The  $IC_{50}$  of CA and CB obtained from the plot of cell survival (%) versus the concentration of the peptides in killing HL-60 cells are 39.1  $\mu$ M and 14.3  $\mu$ M, respectively. The ability of these

Table 1. Measurements of  $IC_{50}$  of the peptides, CB, CB-1 and CB-2, on various cell lines.

Species	$IC_{50}$ ( $\mu$ M)		
	CB	CB-1	CB-2
<u>Leukemia cells</u>			
CCRF-CEM	12.3 $\pm$ 0.8	8.6 $\pm$ 0.5	7.0 $\pm$ 0.6
Jurkat (E6-1)	8.0 $\pm$ 0.4	2.4 $\pm$ 0.3	3.1 $\pm$ 0.3
K-562	17.6 $\pm$ 1.7	10.2 $\pm$ 0.7	11.1 $\pm$ 1.5
HL-60	14.1 $\pm$ 1.3	7.5 $\pm$ 0.5	9.2 $\pm$ 0.8
<u>Fibroblast cells</u>			
3T3	>50	>50	>50
3T6	>50	>50	>50
<u>Blood cells</u>			
erythrocyte	>200	>200	>200

two peptides to kill cells seems to be similar to that of antibacterial activity at which CB is larger than CA [4]. For Killing HL-60 cells, CB analog  $IC_{50}$  are 7.5  $\mu\text{M}$  for CB-1 and 9.6  $\mu\text{M}$  for CB-2. These results indicate that the anticancer activities of the peptide analogs, CB-1 and CB-2, are greater than that of the natural cecropin, CB. Similar experiments using these peptides on other cells including other leukemia cell lines, fibroblast cells and erythrocyte are summarized in Table 1. In general, the cancer cells were obtained from leukemia patients differing in age, sex and race. These differences cause different cell growth rates and life cycles. Their characteristics vary with cell line and consequently resistance to each peptide is varied, CB having the weakest. Both CB-1 and CB-2 are about two times more potent than natural CB. For Jurkat (6E-1) leukemic cells, the killing ability of CB-1 and CB-2 is around three times than that of CB. This suggests that the cationic amino acids (five lysine residues) located in the C-terminus of the peptides enhance its ability to lyse cancer cells. Insertion of Gly-Pro into the flexible region of CB-1 (to create CB-2) decreases lethality except for CCRF-CEM cancer cells. All the peptides have a much higher  $IC_{50}$  in lysing normal fibroblast cells such as 3T3 and 3T6 (over 50  $\mu\text{M}$ ) and blood cells such as erythrocytes (over 200  $\mu\text{M}$ ). A possible reason for the difference between the activity on eukaryotic cancer cells and other eukaryotic cells may be that tumor cell membranes have a greater susceptibility to cationic lytic peptides. Transformed cells usually have more exposed anionic lipids or a larger accessible surface.

## Conclusion

The difference in potency of the peptides (CB, CB-1 or CB-2) could reflect different cell lysis mechanisms. The extra cationic segment of the analogs (CB-1 and CB-2) may allow a more effective mechanism of cell lysis than that allowed by the hydrophobic segment of natural CB.

## References

1. Steiner, H., Hultmark, D., Engstrom, A., Bennich, H. and Boman H.G., Nature, 292 (1981) 246.
2. Boman, H.G. and Hultmark, D., Ann. Rev. Microbiol., 41 (1987) 103.
3. Lee, J.Y., Boman, I.A., Sun, C., Andersson, M., Jornwall, H., Mutt, V. and Boman H.G., Proc. Natl. Acad. Sci., USA, 86 (1989) 9159.
4. Hulmark, D, Engstrom, A., Bennich, H., Kapur, R. and Boman, H.G., Eur. J. Biochem., 127 (1982) 207.
5. Christensen, B., Fink, J., Merrifield, R.B. and Mauzerall D., Proc. Natl. Acad. Sci. USA, 85 (1988) 5072.
6. Pouny, Y., Rapaport, D., Mor, A., Nicolas, P. and Shai, Y., Biochemistry, 31 (1992) 12416.

## ***In vitro* and *in vivo* properties of NSL-9511, a novel anti-platelet hexapeptide without an RGD sequence**

**Jun Katada, Yoshio Hayashi, Yoshimi Sato, Michiko Muramatsu, Yoshimi Takiguchi, Takeo Harada, Toshio Fujiyoshi and Isao Uno**

*Life Science Research Center, Advanced Technology Research Laboratories, Nippon Steel Corporation, 3-35-1 Ida Nakahara-ku, Kawasaki 211, Japan*

Integrins are heterodimeric cell surface receptor molecules and are thought to be particularly important mediators of cell adhesion to extracellular matrix proteins, cell migration, cell-to-cell contact, etc. Many of them, such as platelet GpIIb/IIIa (fibrinogen receptor), vitronectin receptor  $\alpha_v\beta_3$  and fibronectin receptor  $\alpha_5\beta_1$ , recognize the Arg-Gly-Asp sequence (RGD) as a common recognition motif within their putative ligands [1,2]. Because the RGD sequence has been found in many types of proteins, there are apparent redundancies in integrin-ligand interactions. These redundancies are interesting aspects of integrin receptors and may be beneficial to cell functions.

We are developing small peptides which are specific for each integrin as a tool for investigating ligand-integrin interactions and as agents for therapeutic uses. In this study, we have found a novel motif sequence which exhibited potent and highly specific GpIIb/IIIa antagonistic activity. *In vivo* and *in vitro* properties of one of these motif peptides are examined and discussed.

### **Results and Discussion**

In a previous study [3], we found that an RGD-containing hexapeptide, PSRGDW, was an unexpectedly potent inhibitor of human platelet aggregation ( $IC_{50} = 0.79 \mu M$ ), although it was not specific for platelet GpIIb/IIIa. A replacement of the Arg residue with a neutral amino acid residue, such as norvaline, proline or hydroxyproline, resulted in a slight increase in anti-platelet activity, suggesting that the Arg residue of the RGD site is not necessary for the anti-platelet activity of this peptide. We also synthesized N-acetyl PSPGDW, in which the imino group of the N-terminal Pro residue was blocked. Because we found that the acetylation of the imino group resulted in a complete loss of platelet inhibition this free imino group is probably essential to the anti-platelet activity of the peptide. These results suggest that binding of PSRGDW to GpIIb/IIIa is mediated by the N-terminal imino group and the  $\beta$ -carboxyl group of the Asp residue as ionic interaction sites. Among the peptides we have synthesized, PS-hydroxyPro-GDW (NSL-9511) was one of the most potent inhibitors of platelet aggregation ( $IC_{50} = 0.40 \mu M$ ). Results of the structure-activity relationship studies of this motif peptide were described in detail by Hayashi et al. in this volume.

To investigate the selectivity of NSL-9511 towards integrins, we performed a competitive enzyme-linked immunosorbent assay using purified human platelet GpIIb/IIIa

and purified placental  $\alpha_v\beta_3$ , both of which have the same  $\beta$  subunit ( $\beta_3$ ), and found that it was highly specific for platelet GpIIb/IIIa. The binding specificity was also examined in a cell adhesion assay in which ECV304 cells, originating from human umbilical vein endothelial cells, adhered to immobilized vitronectin and fibronectin via integrin receptors. NSL-9511 did not inhibit the adhesion of ECV 304 cells to immobilized fibronectin and vitronectin up to 1000  $\mu\text{M}$ .

Flow cytometric studies showed that NSL-9511 competed with FITC-labelled RGD peptide upon binding to activated human platelets, suggesting that this peptide may share the same binding site on GpIIb/IIIa with an RGD peptide alternatively, their binding sites may be so close that RGD and NSL-9511 are mutually exclusive. Conformational analysis of the motif peptide indicated that the imino group of the Pro residue can occupy the same conformational space as that of the guanidino group of the Arg residue of the RGD sequence, suggesting that the imino group may substitute for the role of the guanidino group as a basic interaction site.

The *in vivo* anti-thrombotic activity of NSL-9511 was examined in a guinea pig arterio-venous shunt model. NSL-9511, administered by infusion, inhibited thrombus formation in a dose-dependent manner, and no thrombus was formed during infusion at a dose of 10 mg/kg/hr. This anti-thrombotic activity disappeared quickly after termination of the infusion. Therefore, NSL-9511 has potential for clinical uses, especially as an anti-thrombotic drug at an acute phase that will not cause serious bleeding.

In conclusion, we found a novel hexapeptide sequence with anti-platelet activity. This peptide was a specific antagonist of the platelet fibrinogen receptor (GpIIb/IIIa) and upon binding to GpIIb/IIIa this peptide and the RGD peptide were mutually exclusive. It also inhibited platelet-rich thrombus formation *in vivo*, thus suggesting potential therapeutic applications.

## References

1. Humphries, M.J., *J. Cell Sci.*, 97 (1990) 585.
2. Ruoslahti, E. and Pierschbacher, M.D., *Science*, 238 (1987) 491.
3. Hayashi, Y., Sato, Y., Katada, J., Takiguchi, Y., Ojima, I. and Uno, I., *Bioorg. Med. Chem. Lett.*, 6 (1996) 1351.

# Model peptides of interstitial collagens: hydrolysis by matrix metalloproteinases

**Kathleen Tuzinski,<sup>a</sup> Ken-ichi Shimokawa,<sup>b</sup> Hideaki Nagase<sup>b</sup>  
and Gregg B. Fields<sup>a</sup>**

*<sup>a</sup>Dept. Lab Medicine and Pathology and The Biomedical Engineering Center, Univ. Minnesota, Minneapolis, MN 55455, USA., and the <sup>b</sup>Dept. Biochemistry and Molecular Biology, Univ. Kansas Medical Center, Kansas City, KS 66103, USA*

The matrix metalloproteinase (MMP) family plays an integral role in both normal connective tissue remodeling and in a variety of disease states involving unbalanced degradation of extracellular matrix components. Obtaining selective substrates for these MMPs, modeled after the sequences surrounding the cleavage site in collagen, would allow the design of specific inhibitors. The sequences targeted by these MMP members have been identified, and a model collagenase cleavage site in types I-III collagen has been proposed [1]. We have constructed triple-helical peptide (THP) models of the MMP-1 cleavage site in types I and II collagen by methods previously described in our laboratory [2,3]. The THPs incorporate either the  $\alpha 1(\text{I})772\text{-}786$  sequence Gly-Pro-Gln-Gly-Ile-Ala-Gly-Gln-Arg-Gly-Val-Val-Gly-Leu-Hyp or the  $\alpha 1(\text{II})772\text{-}783$  sequence Gly-Pro-Gln-Gly-Leu-Ala-Gly-Gln-Arg-Gly-Ile-Val.

For these studies, we wished to compare THP hydrolysis specifically with several MMP family members. Most MMPs have a similar tripartite structures including a propeptide domain, a  $\text{Zn}^{2+}$ -dependent catalytic domain, and a hemopexin/vitronectin-like domain [4]. MMP-1, MMP-3, and MMP-13 are three members of the MMP family that have such domains, although they differ in their collagenolytic behavior due to variances in their C-terminal domain. For these studies, we utilized the full-length MMP-1, MMP-3, and MMP-13 along with the C-terminal-truncated forms of MMP-1 and MMP-3.

## Results and Discussion

In this study we were concerned with the suitability of our synthetic substrates (THPs) as peptide models of the native collagens. We found that cleavage of the substrates did occur with MMP-1, and only at the Gly~Ile and Gly~Leu loci corresponding to the sites in native collagens (Fig. 1). From these results we can assume that the THPs contain all the necessary information to direct enzyme binding and proteolysis. The  $\alpha 1(\text{I})772\text{-}786$  THP maintained its triple-helicity at 37°C, since no cleavage was observed at that temperature in the presence of MMP-3, whereas MMP-3 is capable of cleaving the same single-stranded substrate [4]. MMP-13 cleaved the  $\alpha 1(\text{I})772\text{-}786$  THP at the same locus as MMP-1.

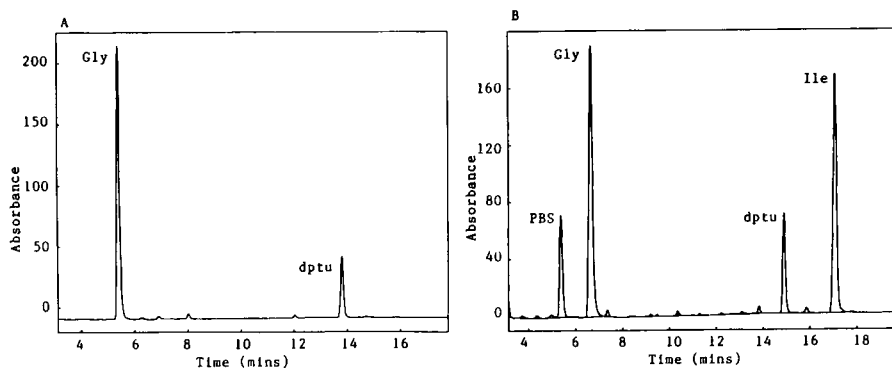


Fig. 1. First cycle of Edman degradation sequence analysis of: A)  $\alpha 1(I)772-786$  THP; B) MMP-1 hydrolysis of  $\alpha 1(I)772-786$  THP.

It has been shown that the ability of collagenases to cleave native interstitial collagens is lost when the C-terminal domain is removed [5]. In this study, however, cleavage of the THP did occur with enzyme concentrations as low as 20 nM of the C-terminal-truncated MMP-1 at the same bond that is cleaved by the full length MMP-1. Hydrolysis of single-stranded collagen analogs by MMP-1 showed no significant differences between activities of the intact enzyme and the C-terminal-truncated enzyme [4]. The specificity of MMP-1 in that case appeared to be determined by the catalytic domain with little contribution from the C-terminal domain. From these observations, we propose that the C-terminal domain is necessary for orienting the whole, native collagen molecule but not necessary for binding to and cleaving the THP.

### Acknowledgements

Supported by NIH grants AR39189, KD44494, and AR01929 and Pfizer, Inc. Central Research Division.

### References

1. Fields, G.B., *J. Theor. Biol.*, 153 (1991) 585.
2. Fields, C.G., Lovdahl, C.M., Miles, A.J., Matthias Hagen, V.L. and Fields, G.B., *Biopolymers*, 33 (1993) 1695.
3. Grab, B., Miles, A.J., Furcht, L.T., and Fields, G.B., *J. Biol. Chem.*, 271 (1996) 12234.
4. Review: Nagase, H. and Fields, G.B., *Biopolymers*, 40 (1996) 3994.
5. Murphy, G. and Knäuper, V., *Matrix Biol.*, 15 (1997) 511.

# Serum amyloid A and its related peptides modulate endothelial cells proliferation and prostaglandin I<sub>2</sub> production

Liana Preciado-Patt,<sup>a</sup> Ruth Shainkin-Kestenbaum<sup>b</sup> and Mati Fridkin<sup>a</sup>

<sup>a</sup>*Department of Organic Chemistry, The Weizmann Institute of Science, Rehovot, 76100 Israel, and*

<sup>b</sup>*Biochemical Laboratory, Meir Hospital, Sapir Medical Center, Kfar-Saba, 44281 Israel*

Serum amyloid A (SAA), the acute phase HDL apolipoprotein, is produced mainly in the liver following stimulation by the cytokines IL-1, TNF and IL-6 [1-2]. A recent study in mice demonstrated that SAA enhances the binding of HDL<sub>3</sub> to mouse macrophages during inflammation, concomitantly with a decrease in the capacity of HDL<sub>3</sub> to bind hepatocytes [3]. Previous studies suggest the involvement of SAA in regulating various acute phase events, including inhibition of platelet aggregation, attenuation of hypothalamic PGE<sub>2</sub> induction by IL-1 or TNF [4]. We have examined the involvement of SAA in the regulation of basal or cytokine-induced endothelium PGI<sub>2</sub> production. Furthermore, we studied the effect of SAA on endothelial cell proliferation. Towards identification of putative active domains within SAA, the effects of amyloid A (AA), i.e. the pathological proteolytic product of SAA (SAA1-76), and of synthetic SAA-related peptides on endothelial cell proliferation were evaluated.

## Results and Discussion

To study the effect of human SAA on induction of PGI<sub>2</sub> production by BAEC, cells were incubated with SAA in the presence and absence of the inflammatory cytokine TNF. SAA induced significant PGI<sub>2</sub> production following a 24h incubation period (Fig. 1). To identify the active domain in the SAA molecule which induces PGI<sub>2</sub> production, four synthetic peptides, SAA1-14 (RSFFSFLGEAFDGA), SAA29-33, SAA29-42 and SAA77-104, were tested. Among these, only SAA1-14 expressed PGI<sub>2</sub> inducing activity similar to SAA (Fig. 1a). As shown in Fig. 1b, the PGI<sub>2</sub>-inducing effect exerted by TNF on BAEC was more pronounced but was significantly inhibited by SAA (50µg/ml). The effect of SAA on endothelial cell proliferation was studied in combination with the angiogenic agent FGF. In cells chronically cultured with FGF, SAA inhibits cell proliferation in a dose-dependent manner (see Fig. 2). The effect of amyloid A (AA) and the synthetic peptides SAA1-14, SAA29-33, SAA29-42 and SAA77-104, on BAEC proliferation was evaluated. Amyloid A (SAA2-82) inhibited cell proliferation similarly to the intact SAA molecule (Fig. 2) while enhanced proliferation was observed in the presence of SAA29-33. SAA29-42, SAA77-104 and SAA1-14 did not have any significant effect on BAEC proliferation (not shown).

## Conclusion

Our findings suggest that there is a physiological role for the HDL-associated acute phase protein apo-SAA in regulating endothelial cell proliferation and PGI<sub>2</sub> synthesis. SAA may

contribute to the known protective effect of HDL in atherosclerosis and cardiovascular diseases. Moreover, under pathological conditions when cytokine and SAA levels are concomitantly increased, SAA may act as an anti-cytokine and anti-inflammatory agent.

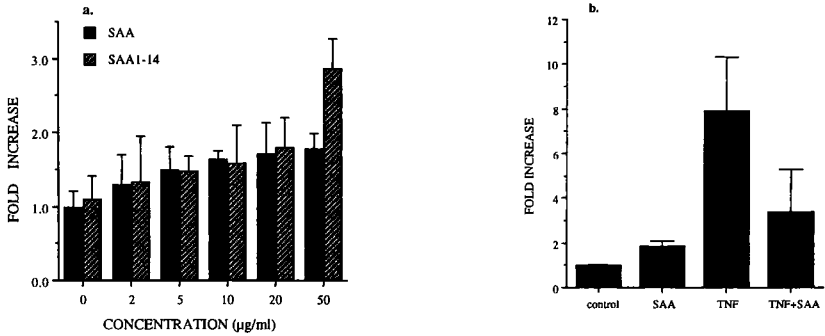


Fig. 1. PGI<sub>2</sub> (6-keto PGF<sub>1α</sub>) production by BAEC. a. PGI<sub>2</sub> production determined following 24 h incubation with different concentrations of highly purified SAA and the synthetic peptide SAA1-14. b. The combined effect of SAA (50µg/ml) and TNF (1ng/ml) on PGI<sub>2</sub> (6-keto PGF<sub>1α</sub>) production was determined following 24 h induction. Data are presented as means of fold increase ± SEM.

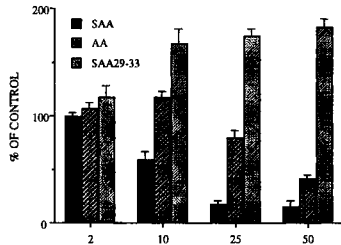


Fig. 2. Regulation of endothelial cell proliferation by SAA and SAA related fragments. BAEC chronically cultured with FGF were incubated with indicated concentrations of SAA and its related fragments for 24h after which [<sup>3</sup>H]thymidine tracer was added for another 24h. Cells were harvested and radioactivity was measured. Each value represents mean ± SEM % of control of 7 experiments.

## References

1. Baumann, H. and Gauldie, J., Immunology Today, 15 (1994) 74.
2. Coetzee, G.A., Strachan, A.F., van der Westhuyzen, D.R., Hoppe, H.C., Jeenah, M.S. and deBeer, F.C., J. Biol.Chem., 261 (1986) 9644.
3. Kisilevsky, R. and Subrahmanyam, L., Lab.Invest., 66 (1992) 778.
4. Conti, P., Bartle, L., Barbacane, R.C., Reale, M., Placido, F.C. and Sipe, J., Immunol Invest., 24 (1995)523.

# A new paradigm for fish antifreeze protein binding to ice

Michael Houston, Jr.,<sup>a</sup> Heman Chao,<sup>a</sup> Michèle C. Loewen,<sup>b</sup> Frank D. Sönnichsen,<sup>c</sup> Cyril M. Kay,<sup>a</sup> Brian D. Sykes,<sup>a</sup> Peter L. Davies<sup>b</sup>  
and Robert S. Hodges<sup>a</sup>

<sup>a</sup>Protein Engineering Network of Centres of Excellence, University of Alberta, Edmonton, Alberta, T6G 2S2, Canada. <sup>b</sup>Department of Biochemistry, Queen's University, Kingston, Ontario, K7L 3N6, Canada; <sup>c</sup>Department of Physiology and Biophysics, Case Western Reserve University, Cleveland, OH 44106-4970, USA

The Type I antifreeze proteins are long  $\alpha$ -helical, alanine rich peptides found in flounder and sculpin [1]. The most abundant isoform, HPLC-6, is 37 amino acids long and contains three 11 amino acid repeats consisting of of Thr-X<sub>2</sub>-Asx-X<sub>7</sub> where X is generally alanine. This *i*, *i*+11 spacing allows for Thr and Asx residues to be regularly aligned on one face of the helix and spaced 16.5 Å apart [2, 3], which closely matches the 16.7 Å distance between accessible oxygens along the 01-12 direction of the {20-21} binding plane [4]. This match suggested a plausible mechanism for protein/ice interaction whereby the side chains of Thr and Asx can hydrogen bond to oxygen atoms in the ice lattice [5, 6]. In order to probe the contribution of Thr residues to ice binding, systematic substitutions were made to two or three threonine residues and the resulting variants were assayed for thermal hysteresis activity.

## Results and Discussion

Substitution of the putative ice binding residues Thr13 and Thr24 to Ser (peptide S2) and Val (peptide V2) were accomplished by SPPS. A third peptide (V3) was synthesized where Thr13, Thr24 and Thr35 were replaced by Val. For all variants the CD spectra were indistinguishable from that of the wild type peptide with helical contents approaching 100% at 1 °C. Sedimentation equilibrium analysis indicated that substitutions did not affect the oligomerization state of the proteins and that all proteins were monomeric at concentrations up to 6.5 mg/mL.

The thermal hysteresis activity of the wild type protein shown in Fig. 1 was identical to that of the protein isolated from flounder serum. Substitution of Ser for Thr, which should not have unduly altered the H-bonding potential of this peptide, resulted in a protein which was substantially less active (10% active, Fig. 1) than the WT protein. At high peptide concentrations the ice crystal was morphologically identical to that obtained with the WT protein indicating that the peptide was binding to the same prism plane as the WT protein. Surprisingly, replacing the two Thr residues with Val, which is similar in size and exhibits similar side-chain rotamer preferences, yielded a protein that was 80 to 90% as active as the wild type protein (Fig. 1). Further Val substitution (V3) resulted in a peptide that was 60% as active as the wild type protein (Fig. 1). For both Val mutants ice crystal morphology was identical to the WT protein.

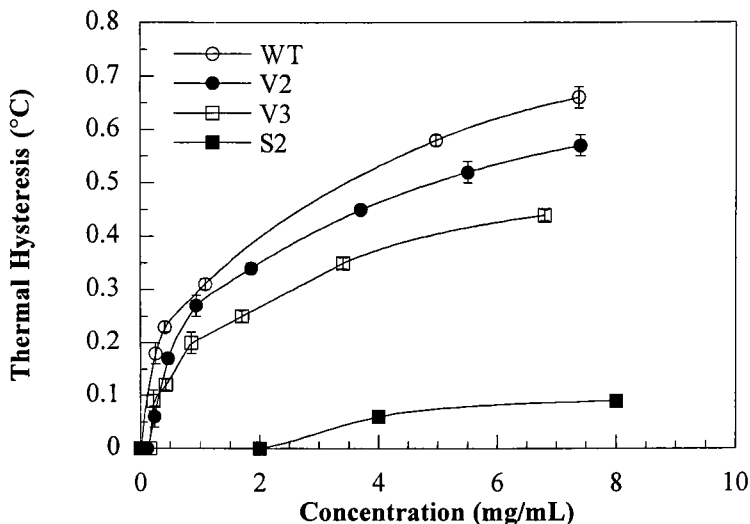


Fig. 1. Antifreeze activity of Type I AFP and its variants in 0.1 M  $\text{NH}_4\text{HCO}_3$ , pH 7.9.

## Conclusion

Taken together, these variants demonstrate the importance of the  $\gamma$ -methyl group to AFP interaction with ice. This result calls into question the hypothesis that the AFP/ice interaction is largely driven by hydrogen bonding interactions and forms the basis of a new paradigm for protein/ice interactions in which van der Waals and entropic contributions play a major role.

## References

1. Davies, P. L. and Hew, C. L., *FASEB J.*, 4 (1990) 2460.
2. Yang, D. S. C., Sax, M., Chakrabarty, C. L. and Hew, C. L., *Nature*, 333 (1988) 232.
3. Sicheri, F. and Yang, D. S. C., *Nature*, 375 (1995) 427.
4. Knight, C. A., Cheng, C. C. and DeVries, A. L., *Biophys J.*, 64 (1991) 409.
5. Wen, D. and Laursen, R. A., *J. Biol. Chem.*, 267 (1992) 14102.
6. DeVries, A. L. and Lin, Y., *Biochem. Biophys. Acta*, 495 (1977) 388.

# Neuropeptides and skin cell function: VIP and stearyl-[Nle<sup>17</sup>]VIP effects on HaCaT cells

Ruth Granoth,<sup>a,b</sup> Mati Fridkin<sup>a</sup> and Illana Gozes<sup>b</sup>

*Departments of Organic Chemistry<sup>a</sup>, The Weizmann Institute of Science, Rehovot 76100, and Clinical Biochemistry<sup>b</sup>, Sackler School of Medicine, Tel-Aviv University, Tel-Aviv 69978, Israel*

Vasoactive intestinal peptide (VIP) is a multifunctional peptide in the central nervous system and periphery. It has been implicated in regulation of growth, proliferation and survival of many cell types, sometimes operating in an autocrine. VIP and pituitary adenylate cyclase activating peptide (PACAP) share a high degree of homology, although they are derived from different precursor proteins. Distinct receptors for the VIP and PACAP have been cloned, all of which are G-protein coupled, stimulating adenylate cyclase activity [3-5]. Stearyl-Nle<sup>17</sup>-VIP (SNV) is a super agonist of VIP, in which the Met at position 17 was replaced by Nle and a fatty acid moiety was attached to the N-terminal. SNV exhibits higher potency, stability and penetration through physiological barriers compared to VIP, as well as selectivity to high affinity, cAMP independent, VIP receptors [1, 2]. To explore possible proliferative effects of VIP, PACAP-27 and SNV on keratinocytes, the primary cells in human epidermis, we utilized a human keratinocytic model cell line, HaCaT [6]. Since a mitogenic effect was obtained, we further aimed to identify receptors that might be involved in this effect.

## Results and Discussion

The proliferative effect of VIP and the related peptides was examined on HaCaT cells, using the [<sup>3</sup>H]thymidine incorporation. VIP and PACAP-27 were moderate mitogens for HaCaT, with their effect manifested at sub-nM concentrations (Fig. 1a). As this result with VIP indicated association with high affinity VIP receptors, SNV was tested. SNV is highly active as a mitogen, manifesting both greater potency and efficacy (Fig. 1a). This superiority over VIP is paralleled in other systems, e.g., for neuronal survival promoting activity [2]. To assess possible receptors mediating the proliferative effect, displacement experiments utilizing <sup>125</sup>I-VIP were carried out (Fig. 1b). VIP and PACAP-27 displaced the tracer with identical affinities, indicating that there is a common VIP/PACAP receptor. SNV also yielded a similar curve. Further molecular identification of VIP1R mRNA was achieved using specific primers by RT-PCR. Messenger RNAs obtained from HaCaT cells and human keratinocytes responded positively (not shown). In order to test whether VIP is an autocrine or paracrine modulator, mRNAs from HaCaT, human keratinocytes and NCI-H727 (NSCLC, positive control) were examined for VIP expression by RT-PCR. No PCR product was obtained from keratinocytes (not shown). Thus, VIP, released from sensory nerve endings is likely to be a paracrine mitogen for keratinocytes.

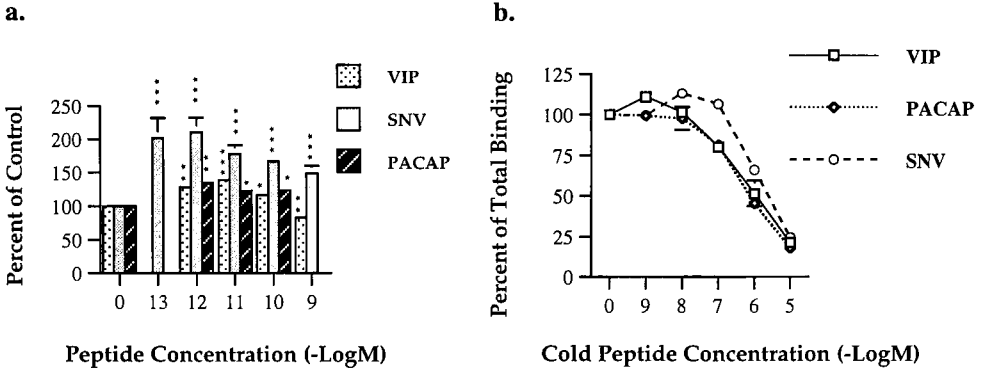


Fig.1. a. The proliferative effect of VIP, PACAP-27 and SNV on HaCaT cells evaluated by [ $^3$ H]thymidine incorporation, following 48 h cell starvation. (n=5). \*,  $P < 0.05$ ; \*\*,  $P < 0.005$ ; \*\*\* $P < 0.00005$  by Student's *t*-test. b. Competitive displacement experiments by PACAP-27 and SNV, using  $^{125}$ I-VIP as a tracer, on HaCaT cells. Data is presented as mean  $\pm$  SEM.

The large mismatch between affinity attributed to VIP1R and the actual concentration at which VIP is mitogenic for HaCaT, as in neuronal survival, is puzzling. We suspect the effect is mediated *via* an alternative high affinity VIP receptor, operating through a non-cAMP signal transduction mechanism. The superiority of SNV in this system further supports this idea.

## Conclusion

Our findings indicate that HaCaT keratinocytes maintain responsiveness to VIP, operating in a paracrine fashion that is manifested in increased cell proliferation. Both HaCaT and human keratinocytes have VIP1 receptors on their surface. SNV, the lipophilic analog of VIP, constitutes a potent mitogenic factor for keratinocytes. Thus, it may enable artificial manipulation in medical situations requiring enhanced keratinocyte proliferation, such as for wounds and burns.

## References

1. Gozes, I. and Fridkin, M., *J. Clin. Invest.*, 90 (1992) 810.
2. Gozes, I., *et al.* *J. Pharmacol. Exp. Ther.*, 273 (1995) 161.
3. Ogi, K., *et al.* *Biochem. Biophys. Res. Comm.*, 196 (1993) 1511.
4. Sreedharan S.P., *et al.*, *Biochem. Biophys. Res. Comm.*, 193 (1993) 546.
5. Lutz E.M., *et al.*, *FEBS Lett.*, 334 (1993) 3.
6. Boukamp P. *et al.*, *J. Cell. Biol.*, 106 (1988) 761.
7. We would like to thank Prof. N.E. Fusenig of the German Cancer Research Center for kindly donating the HaCaT cell line for this study.

# Inhibiting dimerization and DNA binding of c-Jun

S. Q. Yao, E. I. Pares-Matos, M. L. Brickner and J. A. Chmielewski

*Department of Chemistry, Purdue University, West Lafayette, IN 47907, USA*

The proto-oncoproteins c-Fos and c-Jun are members of the class of dimeric bZip proteins which contain a transactivating domain, a basic region with specific DNA (AP-1) binding activity and a C-terminal dimerization domain composed of a leucine zipper in the form of a coiled-coil [1, 2]. Heterodimers of Fos and Jun and homodimers of Jun mediate a myriad of cellular responses to serum, growth factors, and tumor-promoting phorbol esters, as well as to the protooncogenes c-Ha-ras, c-src, and c-mos [3]. Malignant cell transformation has been attributed to disruption of Fos and Jun dimers either by mutations which disrupt phosphorylation of Jun [4] or by deregulation of protein expression [5], both of which lead to increased DNA binding and expression of genes under AP-1 regulation.

Since the oncogenic transcription factors Fos and Jun are only active in their homodimeric or heterodimeric forms, inhibition of dimerization presents itself as a means of blocking the transforming ability of these DNA binding proteins. In this work a strategy is outlined in which regulation is accomplished by targeting peptide agents to the dimerization interface of the transcription factor Jun, thereby inhibiting protein dimerization and subsequent DNA binding.

## Results and Discussion

The structure of Jun consists of a highly basic region which binds into the major groove of DNA in a helical conformation and an amphiphilic helical leucine zipper which forms the coiled-coil dimerization interface either with itself or Fos. Peptides corresponding to the leucine zipper region of Fos (Fig. 1), which does not effectively form homodimers, were explored as agents to inhibit the dimerization and DNA binding of Jun.

Fos-32	TDTLQAETDQLEEKSA	LQTEIANLLLKEKKEKL
Fos-N25	TDTLQAETDQLEEKSA	LQTEIANL
Fos-N18	TDTLQAETDQLEEKSA	
Fos-C25		TDQLEEKSA
Fos-C18		LQTEIANLLLKEKKEKL
Fos-15	LQAETDQLEEKSA	
Fos-14	LQAETDQLEEKSA	

*Fig. 1. Sequence of synthetic Fos leucine zipper peptides.*

DNA binding was monitored by gel mobility shift assays with *in vitro* synthesized Jun and an oligonucleotide containing the AP-1 sequence (TGACTCA), to which Fos peptides were added that contained either the full length or the variously truncated leucine zipper (Fig. 1). All of the Fos peptides inhibited Jun DNA binding, although Fos-32 and Fos-N25

were the most effective with  $IC_{50}$  values of 11  $\mu$ M (Table 1). Truncation of the leucine zipper at the N-terminus was highly detrimental to inhibition of Jun DNA binding, whereas truncations at the C-terminus were better accommodated. Surprisingly, removing three N-terminus residues from Fos-N18 (Fos-15) restored the inhibition to levels obtained with Fos-32.

Table 1. Inhibition of *c-Jun* DNA binding to AP-1.

Inhibitor	$IC_{50}$ $\mu$ M
Fos-32	11
Fos-N25	12
Fos-N18	62
Fos-C25	105
Fos-C18	400
Fos-15	11
Fos-14	105

Protein crosslinking was used to confirm that the Fos peptides inhibited Jun dimerization. Jun was crosslinked with bis(sulfosuccinimidyl)suberate, and the monomer and crosslinked dimer were separated by SDS PAGE. Adding increasing amounts of Fos-32 to Jun prior to the crosslinking reaction led to a decrease in the amount of crosslinked dimer formed, with complete inhibition of dimer crosslinking obtained with 50 eq. of Fos-32 as compared to Jun. These results indicate that the dimerization of Jun is blocked with Fos peptides leading, to a loss of high affinity DNA binding.

The ability of Fos-32, Fos-15 and Fos-14 to inhibit AP-1 transcription within cells was assayed using a reporter plasmid containing the firefly luciferase gene under control of three TRE sequences (AP-1) [6, 7]. MCF-7 cells (breast cancer) were transfected with the reporter plasmid using the Tfx<sup>TM</sup>-50 (Promega) cationic lipofect reagent. After 8 hrs, the peptides were delivered to MCF-7 cells with the Tfx<sup>TM</sup>-50 reagent. Firefly luciferase production was quantitated using the substrate beetle luciferin which bioluminescences upon product formation. Fos-32 and Fos-15 both decreased firefly luciferase transcription approximately two fold, whereas Fos-14, which has the highest  $IC_{50}$  value of the three peptides, had little effect on luciferase production. Within the MCF-7 cells, therefore, both Fos-32 and Fos-15 are able to reduce AP-1 related transcription.

## References

1. Alber, T., Current Opinion in Genetics and Development, 2 (1992) 205.
2. Glover, J.N.M. and Harrison, S.C., Nature, 373 (1995) 257.
3. Angel, P. and Karin, M., Biochimica et Biophysica Acta, 1072 (1991) 129.
4. Morgan, I.M. *et al.*, Oncogene, 9 (1994) 2793.
5. Schütte, J., Minna, J. and Birrer, M., Proc. Natl. Acad. Sci. U.S.A., 86 (1989) 2257.
6. Alam, J. and Cook, J.L., Analytical Biochemistry, 188 (1990) 245.
7. Pazzagli, M., Devine, J.H., Peterson, D.O. and Baldwin, T.O., Analytical Biochemistry, 204 (1992) 315.

# Inhibition of E-cadherin-mediated cell-cell adhesion by cadherin peptides

**K. L. Lutz, D. Pal, K. L. Audus and T. J. Siahaan**

*Department of Pharmaceutical Chemistry, The University of Kansas, Lawrence, KS 66047, USA*

The objective of this work was to evaluate modulation of E-cadherin-mediated cell-cell adhesion by cadherin peptides using: a) cell aggregation, b) cell dissociation, and c) FITC-dextran (MW = 4,400) transport assays. Bovine-brain microvessel endothelial cell (BBMECs) monolayers were used as a model for the blood-brain barriers. Previously, several peptide sequences that are responsible for cadherin-cadherin interactions have been identified, including His-Ala-Val (HAV) and calcium binding sequences (*i.e.*, DQNDN) [1].

*Table 1. Inhibition of E-cadherin mediated cell-cell aggregation by cadherin peptides.*

Peptide	Sequence	Origin	IC <sub>50</sub> μM
<b>1</b>	LRAHAVDVNG-NH <sub>2</sub>	<sup>a</sup> m-N-cadherin	450
<b>2</b>	LYSHAVSSNG-NH <sub>2</sub>	m-E-cadherin	31
<b>3</b>	Ac- <b><u>DR</u></b> ERIATYTLFSHAVSSNGNAVED-NH <sub>2</sub>	<sup>b</sup> <sub>h</sub> -E-cadherin	0.008
<b>4</b>	Ac-AHAVDV-NH <sub>2</sub>	m-N-cadherin	NA
<b>5</b>	Ac-SHAVSS-NH <sub>2</sub>	m-E-cadherin	20
<b>6</b>	Ac-SHAVKS-NH <sub>2</sub>	m-E-cadherin	NA
<b>7</b>	Ac-SHAVFS-NH <sub>2</sub>	m-E-cadherin	NA
<b>8</b>	Ac-SHAVDS-NH <sub>2</sub>	m-E-cadherin	600
<b>9</b>	Ac-D <b><u>Q</u></b> NDN-NH <sub>2</sub>	m-E-cadherin	800
<b>10</b>	p(ClCH <sub>2</sub> CH <sub>2</sub> ) <sub>2</sub> N-Phe-Glu-OH	unrelated	NA

<sup>a</sup>m = mouse; <sup>b</sup>h = human; NA = no activity; bold letter = conserved sequence; underline = Ca<sup>2+</sup>-binding sequence.

## Results and Discussion

*A. Inhibition of E-cadherin-mediated BBMECs aggregation:* E-cadherin-mediated cell aggregation of BBMECs was inhibited by cadherin peptides (Table 1). Peptide **3** was the most potent HAV peptide to inhibit cell aggregation; this selectivity was due to its sequence and conformation. Peptides **1** and **2** were derived from N- and E-cadherin sequences, respectively; peptide **2** was more potent than peptide **1**. Peptides **4** and **5** were derived from peptides **1** and **2**, respectively. E-cadherin peptide **5** had biological activity similar to that of the parent peptide **2**; however, N-cadherin peptide **4** did not inhibit BBMEC aggregation. These results suggest that the E-cadherins on BBMECs can selectively recognize E-cadherin peptides over N-cadherin peptide. To evaluate the role of flanking residues to the HAV sequence, Ser5 of peptide **5** was mutated with Lys5, Phe5,

and Asp5, respectively to give peptides 6, 7 and 8. Peptides 6 and 7 did not have any inhibitory activity; however, peptide 8 maintained some inhibitory activity. These results suggest that the Ser5 residue is important for the selectivity of E-cadherin peptide. Peptide 9, from the Ca<sup>2+</sup>-binding sequence of E-cadherin, inhibited cell-cell aggregation at higher concentration than peptide 5. This suggests that the calcium binding sequences have a role in cadherin-cadherin interactions. The dipeptide *p*(ClCH<sub>2</sub>CH<sub>2</sub>)<sub>2</sub>-N-Phe-Glu-OH (10), a negative control, did not inhibit cell-cell aggregation.

**B. Dissociation of preconfluent BBMECs:** The cell dissociation assay was performed to evaluate the ability of cadherin peptides to dissociate cell-cell adhesion; unlike the single cells in the aggregation assay, the BBMECs have already acquired initial cell-cell contact and are approaching confluency. The near confluent BBMECs were treated for 8 h with anti-E-cadherin and peptides 2, 3 and 5, respectively; cell dissociation was scored and photographed. Significant cell dissociation was observed on BBMECs treated with anti-E-cadherin antibody and peptides 3 and 5; however, the cells treated with peptide 2 did not show any dissociation. The anti-E-cadherin antibody and peptides 3 and 5 can dissociate the BBMECs by inhibiting cadherin-cadherin interactions. Peptide 2 cannot dissociate BBMECs, presumably due to degradation by aminopeptidase during the experiment.

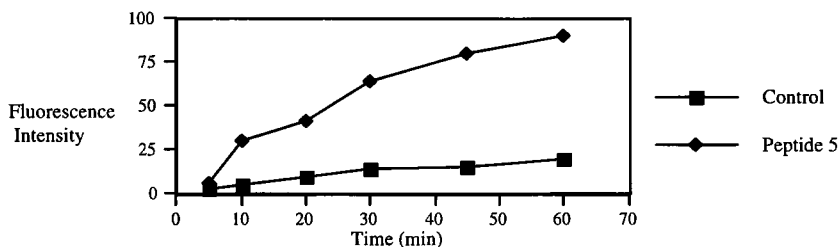


Fig. 1. Time dependent permeation of FITC-dextran 4400 in the presence (◆) and absence (■) of peptide 5.

**C. FITC-Dextran transport assay:** This experiment was performed to evaluate the ability of peptide 5 to improve paracellular permeation of marker molecules through BBMEC monolayers. The apical-to-basolateral flux of FITC-dextran 4400, a marker of the paracellular pathway, was measured across BBMEC monolayers using the fluorescence intensity. BBMEC monolayers were incubated with peptide 5 simultaneously from the apical and basolateral sides for 5 h; as a negative control, no peptide was added to the BBMEC monolayers. FITC-dextran was added to the apical side, and samples were drawn from the basolateral side at different time points. Improved permeation of FITC-dextran was observed for the peptide-treated BBMEC monolayers compared to the non-treated BBMECs (Fig. 1). The increased in flux of FITC-dextran was due to the modulation of intercellular junctions by cadherin peptide 5.

## References

1. Lutz, K.L., Szabo, L.A., Thompson, D.L. and Siahaan, T.J., *Pept. Res.*, 9 (1996) 233.

# Discovery and structure-activity relationship studies of a novel and specific peptide motif, Pro-X-X-X-Asp-X, for platelet fibrinogen receptor recognition

Yoshio Hayashi, Jun Katada, Yoshimi Sato, Katsuhide Igarashi, Takeo Harada, Michiko Muramatsu, Emiko Yasuda and Isao Uno

*Life Science Research Center, Advanced Technology Research Laboratories, Nippon Steel Corporation, 3-35-1 Ida, Nakahara-ku, Kawasaki 211, Japan*

## Introduction

Many integrins recognize the Arg-Gly-Asp (RGD) sequence as a common recognition motif within their putative ligands [1]. Upon recognition of ligands, some integrins show apparent redundancy [2]. Therefore, most linear RGD peptides show very low specificity among many types of integrins including platelet GpIIb/IIIa (fibrinogen receptor),  $\alpha_v\beta_3$  (vitronectin receptor) and  $\alpha_5\beta_1$  (fibronectin receptor) [3]. However, some cyclic RGD peptides with conformationally constrained structures show relatively high specificity [4]. One of our interests is to develop small linear peptides which are specific for each integrin. Here we report the discovery and the structure-activity relationship (SAR) studies of a novel hexapeptide motif, Pro-X-X-X-Asp-X, for GpIIb/IIIa recognition.

## Results and Discussion

In previous studies [5], we found that an RGD containing hexapeptide, PSRGDW **1**, was a very potent inhibitor of platelet aggregation (Table 1). The N-terminal Pro residue with a free imino group is essential for this high potency, since the modification of this residue, such as N-acetylation (**2**) or the replacement of the nitrogen atom with an oxygen atom, decreased the inhibitory activity by 20 to 60 times compared to that of **1**. These results suggest that this Pro residue is responsible for other interactions between **1** and GpIIb/IIIa besides the guanidino group and the  $\beta$ -carboxyl group of the RGD site. However, **1** is not specific to platelet integrin GpIIb/IIIa.

In order to acquire linear oligopeptides with high specificity toward one integrin such as GpIIb/IIIa, it was thought that the common RGD structure in the integrin-recognizing peptides should be partially changed. In particular two ionic functional groups that associate with integrins were specific targets. The exceptionally potent activity of **1** led us to the idea of elimination of the basic guanidino group from the Arg residue. We synthesized Pro-Ser-Nva-Gly-Asp-Trp, **3**, in which the Arg residue in **1** was replaced with a norvaline (Nva) residue by Fmoc-based SPPS and its activity was evaluated.

**3** showed not only a slight increase in both anti-platelet activity and inhibition of fibrinogen binding to GpIIb/IIIa, but also high specificity toward GpIIb/IIIa (IC<sub>50</sub> value of  $\alpha_v\beta_3$  ELISA was >100  $\mu$ M). This result suggests that the Arg residue of the RGD motif is

not necessary for GpIIb/IIIa recognition and that the elimination of guanidino function can elucidate its specificity toward GpIIb/IIIa.

*Table 1. Inhibitory effects of synthetic peptides on human platelet aggregation and the fibrinogen binding to human GpIIb/IIIa*

Compound No.	Peptide	Platelet aggregation <sup>a</sup> IC <sub>50</sub> (μM)	GpIIb/IIIa ELISA IC <sub>50</sub> (μM)
1	PS-Arg-GDW	0.87	0.051
2	N-Ac-PS-Arg-GDW	50	1.8
3	PS-Nva-GDW (NSL-9507)	0.59	0.030
4	PS-Pro-GDW (NSL-9510)	0.77	0.017
5	PS-ΔPro-GDW	0.30	0.018
6	N-Ac-PSPGDW	> 1000	> 1000
7	PSPG-Glu-W	> 1000	> 1000
8	PSPG-Ala-W	> 1000	80

<sup>a</sup>Collagen (5 μg/ml)-induced platelet aggregation using human platelet-rich plasma.

Encouraged by the discovery of novel peptide **3**, we have synthesized a series of peptides whose Nva residue is substituted with neutral amino acids with different types of side chains, or more rigid cyclic structures. When L-proline, which has a 5-membered ring structure, was introduced (**4**), potent anti-platelet activity was also obtained. Peptide **5**, which has a L-3,4-dehydropoline residue (ΔPro), was the most potent among the more than 100 peptides we synthesized.

Modification of the imino group of the N-terminal Pro residue (**6**) resulted in complete loss of activity, although peptides with the same iminogenic modification in **1** showed anti-platelet activity, suggesting that the N-terminal Pro residue with a free imino group is essential to peptides without the Arg residue. The Asp residue at the fifth position was also essential because substitution of this residue for a Glu or an Ala residue resulted in almost complete loss of activity(**7,8**). These results lead to a common motif sequence, Pro-X1-X2-X3-Asp-X4, in which X1 to X4 are L-α-amino acids.

Results of the SAR studies at each X position suggest that (1) small amino acid such as Ser, Ala or Gly are preferable at X1 position, (2) X2 may be any amino acid, (3) X3 must be a small amino acid with a residue such as Gly, or a cyclic amino acid such as Pro, and (4) X4 prefers an amino acid with an aromatic side chain.

In conclusion, it is proposed that Pro-X1-X2-X3-Asp-X4 is a newly discovered peptide motif which functions as a platelet aggregation inhibitor. These new motif peptides, which exhibit potent binding activity and high specificity for GpIIb/IIIa, can be a useful tool in integrin research as well as agents in anti-thrombotic therapy.

## References

1. Ruoslahti, E. and Pierschbacher, M.D., *Science*, 238 (1987) 491.
2. Hynes, R.O., *Cell*, 68 (1992) 11.
3. Ruggeri, Z.M., Houghten, R.A., Russell, S.R. and Zimmerman, T.S., *Proc. Natl. Acad. Sci. U.S.A.*, 83 (1986) 5708.
4. Cheng, S., Craig, W.S., Mullen, D., Tschopp, J.F., Dixon, D. and Pierschbacher, M.D., *J. Med. Chem.*, 37 (1994) 1.
5. Hayashi, Y., Sato, Y., Katada, J., Takiguchi, Y., Ojima, I. and Uno, I., *Bioorg. Med. Chem. Lett.*, 6(1996)1351.



**Session XI**

**Peptide Vaccines/Immunology/Viruses**



# **Synthetic combinatorial libraries for the study of molecular mimicry: Identification of an all D-amino acid peptide recognized by an anti-carbohydrate antibody**

**Clemencia Pinilla, Jon R. Appel, Jaime Buencamino, Gretchen D. Campbell, Jutta Eichler, Neil S. Greenspan<sup>a</sup> and Richard A. Houghten**

*Torrey Pines Institute for Molecular Studies, San Diego, CA 92121, USA*

*<sup>a</sup>Institute of Pathology, Case Western Reserve University, Cleveland, OH 44106, USA*

A current area of immunodiagnostic research is the identification of synthetic mimics that are recognized by the antibody, regardless of whether the mimic retains any resemblance to the immunogen. Combinatorial libraries represent a new advance over previous epitope mapping methods in that antigenic mimics of proteins, as well as carbohydrates, DNA, and RNA, can be explored. One approach, soluble synthetic combinatorial libraries (SCLs), composed of millions of individual, nonsupport-bound peptide sequences, has been used to correctly and rapidly identify antigenic determinants recognized by monoclonal antibodies [1]. In the current study, the specificity of a monoclonal antibody that binds to N-acetyl-D-glucosamine (GlcNAc) [2] was examined with a D-amino acid hexapeptide positional scanning SCL (PS-SCL). The identification of an all D-amino acid peptide that is recognized by mAb HGAC 39.G3 with high affinity clearly illustrates the advantage of using SCLs to identify antigenic mimics. This approach can also be used to identify mimics recognized by other carbohydrate-specific proteins (lectins) that are involved in cellular recognition and growth.

## **Results and Discussion**

The D-amino acid hexapeptide PS-SCL was prepared using the simultaneous multiple peptide synthesis approach as previously described [3]. The PS-SCL is made up of 120 peptide mixtures having one position individually defined with one of 20 D-amino acids and the remaining five positions as mixtures. Thus, each peptide mixture is made up of nearly 2 million hexapeptides for a PS-SCL totaling more than 52 million different peptide sequences. Each of the 120 peptide mixtures of the PS-SCL was screened using competitive ELISA. Activity was measured as the percent inhibition of mAb HGAC 39.G3 binding to GlcNAc-BSA adsorbed to the microtiter plate relative to antibody binding in the absence of peptide mixture. Based on the library screening results, amino acids in each of the six positions were selected to prepare 27 different peptides. The concentration necessary to inhibit 50% ( $IC_{50}$ ) of mAb HGAC 39.G3 binding to GlcNAc was determined for each peptide. The most active peptide (Ac-yryygl-NH<sub>2</sub>,  $IC_{50}$ =300nM) inhibited the GlcNAc-mAb HGAC 39.G3 interaction approximately 500 times better than GlcNAc (Fig. 1).

Since the first three positions of the hexapeptide were specific in the screening, the tripeptide Ac-yry-NH<sub>2</sub> was synthesized and assayed for activity. It was found to be as active as GlcNAc, but nearly 200-fold less active than Ac-yryygl-NH<sub>2</sub>, suggesting that more than these three residues are required for high affinity recognition. The L-amino acid version, namely Ac-YRYYGL-NH<sub>2</sub>, was not recognized by mAb HGAC 39.G3 at the highest concentration tested (IC<sub>50</sub>>1mM), indicating stereospecificity for Ac-yryygl-NH<sub>2</sub>. Substituting each tyrosine residue of this peptide for phenylalanine revealed that the third position was highly specific, whereas positions 1 and 4 could be replaced with phenylalanine without a significant loss of activity.

Multimeric forms of Ac-yryygl-NH<sub>2</sub> were synthesized on various linear and branched lysine scaffolds in an effort to increase peptide antigenicity. Molecules containing two, three, and four copies of Ac-yryygl-NH<sub>2</sub> were recognized with significant increases in affinity (IC<sub>50</sub>=5-20 nM). These results suggest that this peptide represents a high affinity mimic of GlcNAc, and illustrate how combinatorial libraries can be used to identify ligands to antibodies or other acceptor molecules having higher affinities and different chemical characteristics than their known ligands.

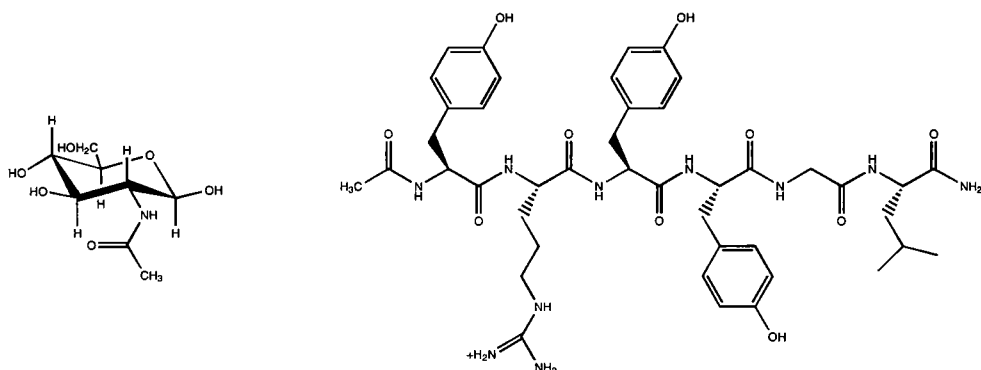


Fig. 1. Structural comparison of GlcNAc and its peptide mimic, Ac-yryygl-NH<sub>2</sub>.

## Acknowledgments

Supported by Trega Biosciences, Inc. and grant DAMD17-94-J-4110 from USAMRDC.

## References

1. Pinilla, C., Appel, J., Blondelle, S., Dooley, C., Dörner, B., Eichler, J., Ostresh, J. and Houghten, R.A., *Peptide Science*, 37 (1995) 221.
2. Greenspan, N.S. and Davie, J.M., *J. Immunol.*, 134 (1985) 1065.
3. Pinilla, C., Appel, J.R., Blanc, P. and Houghten, R.A., *Biotechniques*, 13 (1992) 901.

# Processing of peptide antigens in EBV-transformed B cells and in an *in vitro* system

Hubert Kalbacher,<sup>a</sup> Hermann Beck,<sup>a</sup> Christian J. Schröter,<sup>a</sup> Martin Deeg,<sup>a</sup> Helmut. E. Meyer<sup>b</sup> and Thomas Halder<sup>a</sup>

<sup>a</sup>Medical and Natural Sciences Research Center, University of Tübingen, D-72074 Tübingen,

<sup>b</sup>Institute for Physiological Chemistry, University of Bochum, D-44780 Bochum, Germany

Major histocompatibility complex (MHC) class II molecules are heterodimeric glycoproteins which present intracellularly generated peptides derived from exogenous antigens or endogenous self proteins to CD4<sup>+</sup> T helper cells. They are expressed on antigen-presenting cells (APCs), such as dendritic cells, macrophages, and B cells. APCs are able to internalize peptide and protein antigens by receptor-mediated endocytosis or to a lesser extent via pinocytosis and phagocytosis. Previous studies have indicated that acidic cysteine and aspartic proteinases in the endosomal-lysosomal compartments, cathepsins B, L, S and D, play a critical role in the proteolytic processing of internalized proteins to generate the antigenic peptides presented to the immune system (for review see [1,2]).

We describe a method to detect very low amounts of processed peptide antigens in specialized cellular compartments after pulsing APCs with a defined peptide antigen.

## Results and Discussion

*Peptide and peptide-antigen labeling.* As peptide antigens we used an extended form of the immunodominant epitope (78-106) of the myelin basic protein (MBP) which was specifically labeled with the fluorophore AMCA (7-amino-4-methyl-coumarin-3-acetic acid) in position 91 via the ε-amino group of the lysine residue [3].

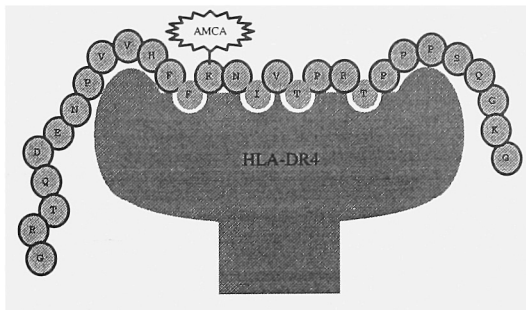


Fig. 1. Sequence and interaction of the MBP peptide ("MPuls") with the HLA-DR4 molecule. The fluorophore AMCA was introduced in a position which points away from the MHC binding groove.

Binding studies show that specific binding pockets of this DR molecule interact with peptide side chains in position i, i+3, i+5 and i+8 (Fig. 1). As APC we used the Epstein

Barr Virus (EBV)-transformed B cell line BSM, expressing the HLA-DR4 (DRB1\* 0401) molecule. Recent studies demonstrate that the native MBP protein can be presented by recycling of the cell surface MHC II molecules [4].

*In vitro digestion of peptide antigens with cathepsin B,L,D, and S.* Processing studies of the antigen were performed with the cathepsins B,L,S, and the cathepsin D and with cellular endosomal or lysosomal fractions obtained by differential centrifugation [5,6]. All proteolytic products were characterized by LC-MS using a Finnigan MAT 700. Interestingly, all enzymes and cellular fractions except cathepsin B cleave the peptide in a central region that is an integral part of the peptide binding core interacting with the MHC molecule which is destroyed by the proteases (Fig. 2).

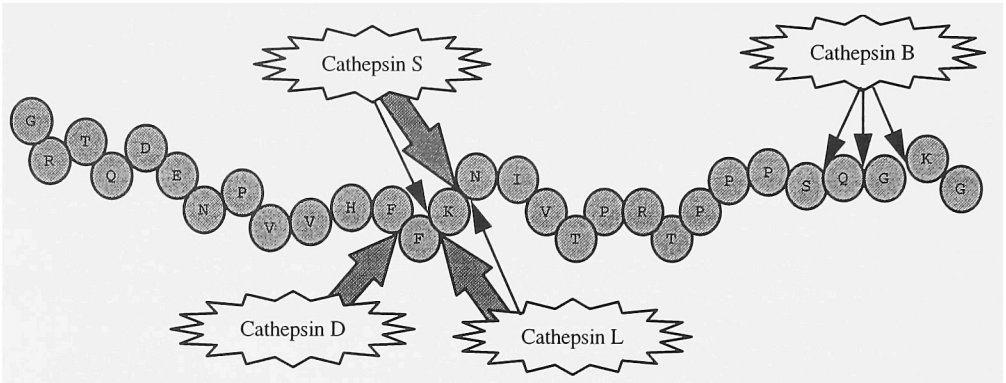
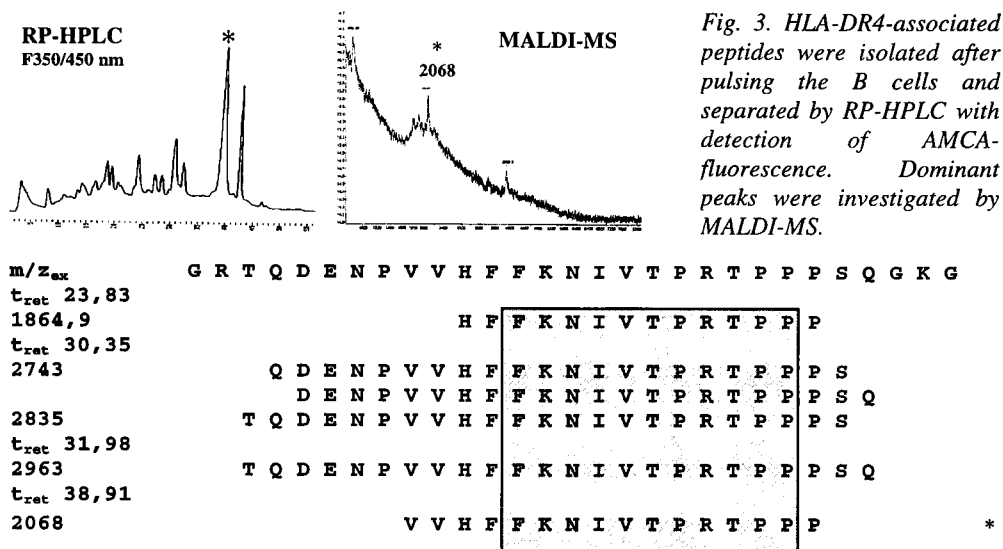


Fig. 2. Cleavage sites of the MPuls peptide with the main lysosomal proteases.

*In vitro digestion of the MHC:peptide complex.* A preformed MHC:peptide complex was treated with cathepsin D. In contrast to the non-associated peptide, which was cleaved specifically between F89/F90, the peptide in the complex was completely stable to the endoprotease. The MHC molecule therefore protects the immunodominant binding region [5,6].

*Pulsing of the APC with peptide antigen and isolation of processed peptides.* 2mg of MPuls-peptide was pulsed with  $5 \times 10^9$  cells of the EBV-transformed B cell line BSM for 2 hr followed by a 2hr chase. Peptides of the endosomal and of the lysosomal fraction were isolated and investigated by LC-MS. The endosomal fraction mainly contained unprocessed antigen and very short peptides, and only a small amount of processed peptides with intact binding core regions. In lysosomal fractions only completely digested antigen could be detected. In a second experiment, the MHC:peptide complexes were purified by cyclic immunoaffinity chromatography using the anti HLA-DR monoclonal antibody L243 [7]. Elution of MHC-associated peptides was achieved by addition of TFA/H<sub>2</sub>O, pH 2.0. After ultrafiltration, the self peptide pool was separated by RP-HPLC using a C<sub>18</sub>/2mm column with detection of AMCA fluorescence. Dominant peaks were collected and investigated by ESI-MS, MALDI-MS, and Edman sequencing (Fig. 3). All

isolated peptides contained the intact binding core region but were N- and C-terminally trimmed as already described for MHC class II-associated self peptides [1].



We conclude that our investigated peptide antigen will be degraded mainly in an endosomal compartment leading to a preprocessed peptide that can readily associate with the appropriate MHC class II molecule. Binding to the MHC class II molecule protects the bound peptide from proteolysis of the immunodominant region. We exclude the possibility that lysosomal enzymes, such as cathepsin D, are able to generate readily processed T cell epitopes able to bind to the MHC. Trimming of the bound peptide may occur in an endosomal/lysosomal compartment or most likely after presentation of the MHC:peptide complex on the cell surface by exopeptidases.

## References

1. Rammensee, H.-G., Friede, T. and Stevanovic, S., *Immunogenetics*, 41 (1995) 178.
2. Wolf, P.R. and Ploegh, H.L., *Annu. Rev. Cell. Dev. Biol.*, 11 (1995) 267.
3. Kalbacher, H., Max, H. and Kropshofer, H., In Schneider, C.H. and Eberle (Eds), *Peptides: 1992 (Proceedings of the Twenty-Second European Peptide Symposium)*, ESCOM, LEIDEN, The Netherlands, 1993, p. 131.
4. Vergelli, M., Pinet, V., Vogt, A.B., Kalbus, M., Malnati, M., Riccio, P., Long, E.O. and Martin, R., *Europ. J. Immunol.*, 27 (1997) 941.
5. Beck, H., Schröter, C.J., Halder, T. and Kalbacher, H., *Immunogenetics*, 24 (1997) 4.
6. Schröter, C.J., Schmid, H., and Kalbacher, H., *Immunogenetics*, 24 (1997) 92.
7. Halder, T., Pawelec, G., Kirkin, A., Zeuthen, J., Meyer, H.E., Kun, L. and Kalbacher, H., *Cancer Research*, (1997) in press.

# New ligands for MHC molecules based on activity patterns of peptide libraries

**Karl-Heinz Wiesmüller,<sup>a</sup> Burkhard Fleckenstein,<sup>b</sup> Peter Walden,<sup>c</sup>  
Roland Martin<sup>d</sup> and Günther Jung<sup>b</sup>**

*<sup>a</sup>Naturwissenschaftliches und Medizinisches Institut an der Universität Tübingen, 72762 Reutlingen, FRG; <sup>b</sup>Institut für Organische Chemie, Universität Tübingen, 72076 Tübingen, FRG; <sup>c</sup>Dermatologische Klinik, Charité, 10117 Berlin, FRG; <sup>d</sup>Neuroimmunology Branch, National Institute of Neurological Disorders and Stroke, National Institutes of Health, Bethesda, MD, USA*

Peptides from self or foreign protein sources are cleaved by proteasomes and cross the membrane of the endoplasmatic reticulum. They are displayed on the surface of cells in association with MHC class I or MHC class II molecules for recognition by receptors of cytotoxic T cells or T helper cells. Peptide libraries in the positional scanning format [1] were applied to determine favorable and nonfavorable amino acids in each sequence position of octa-, nona- and undecapeptides in MHC class I stabilization assays [2], in induction of cell lysis by killer cells [3], in competition assays with MHC class II molecules [4], in T cell proliferation assays [5] and for stabilizing binding to TAP [6]. Activity patterns of the peptide libraries support the design of new ligands and are useful as a database for prediction algorithms [7]. The fully automated synthesis of these libraries was optimized to achieve close to equimolar representation of the individual peptides. The peptide mixtures were analyzed by pool sequencing and electrospray mass spectrometry. The influence of every individual amino acid at the 11 sequence positions of peptides binding to HLA-DR2b (MHC class II) was investigated and summarized in an allele-specific activity pattern.

## Results and Discussion

The undecapeptide amide libraries and the defined peptides were prepared by solid phase peptide synthesis using Fmoc/tBu chemistry and Rink amide MBHA polystyrene resins. For the introduction of randomized sequence positions, double couplings were performed with equimolar mixtures of Fmoc-L-amino acids which were used in an equimolar ratio with respect to the coupling sites of the resins. For coupling of defined sequence positions a 5-fold molar excess of Fmoc-L-amino acids was used. Characteristics of this premix method are extended coupling times, double coupling, an initially high concentration of dichloromethane and evaporation of dichloromethane during coupling. The peptide library and peptide sublibraries O/X<sub>n</sub> were cleaved off the resins, and side chains were deprotected with TFA/Reagent K.

For evaluation of the premix method, defined peptides were synthesized using the chemfile for library synthesis and results from HPLC and ES-MS confirmed the quality of the method. To identify missing individual peptides in a complex peptide mixture

generated by the premix method, a collection of 361 peptides with a subcollection of 19 individual peptides carrying the "mass tag" SE<sub>4</sub> has been designed. This series of XRRLKLWSE<sub>4</sub> peptides was simultaneously synthesized with XXRLKLWN peptides using the premix method for the introduction of X positions. Fig. 1 shows the ES-MS spectrum of 19 individually synthesized peptides (HPLC purity > 80%) that were mixed by weighing equal amounts. This spectrum is compared to the ES-MS of the same peptides shifted to higher mass from the remaining collection XXRLKLWN (342 peptides) and the expected peptides were identified. Due to the restrictions for measuring highly diverse compound collections, these preliminary results do not represent quantitative peptide distributions.

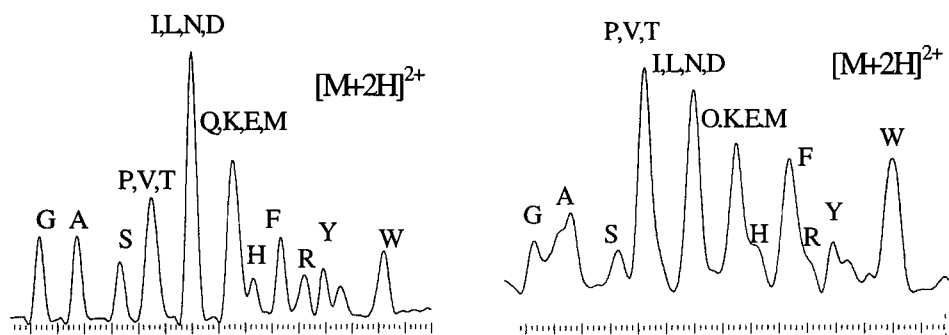


Fig. 1. ES-MS of a mixture of 19 individually synthesized peptides differing in one amino acid residue (A-Y)RRLKLWSE<sub>4</sub> (left) and the same peptides shifted from a 361 peptide collection X(19aa)X(19aa-R)RLKLWN / X(19aa)RRLKLWSE<sub>4</sub>.

The peptide mixtures investigated for binding to HLA-DR2b consist of the completely randomized X<sub>11</sub> library and 220 sublibraries (11 positions x 20 amino acids, cysteine replaced by  $\alpha$ -aminobutyric acid). Sublibraries contained ten randomized positions and one defined amino acid moving across the 11 sequence positions. Each of the 220 O/X<sub>10</sub> sublibraries is calculated for 20<sup>10</sup> different peptides and they were investigated in competition assays [4]. Peptide mixtures and the fluorescein-labeled HLA-DR2b-specific AMCA-EAEQLRAYLDGTGVE peptide amide were incubated with isolated HLA-DR2b at 37°C for 48h. MHC protein was subsequently separated by HPLC, UV-intensities of the MHC signal were measured, and competition C of a given sublibrary was compared to that of the X<sub>11</sub> library resulting in a relative competition (rel C = C<sub>sublib</sub>/C<sub>X11</sub>). Biological activity of a sublibrary is governed only by the defined sequence position. In positions interacting with the HLA-DR2b molecule we identified residues contributing strongly to MHC-binding as well as residues with unfavorable effect is on the interaction (Table 1). In other positions, however, defined amino acid residues showed a more or less neutral influence on MHC binding. A wide variety of side chains are accepted by the HLA-DR2b protein and also the allele-specific pockets in the binding groove show favorable

interactions to several amino acid residues, clearly demonstrating the degenerated peptide binding to class II molecules.

*Table 1. Activity pattern of O/X<sub>11</sub> defined by competition experiments. (A) amino acids unfavourable for competition (rel C: 0 - 0.70), (B) amino acids favourable for competition (rel C: 1.4 - 2.07) residues with intermediate contribution to competition for HLA-DR2b are not shown.*

Pos.	1	2	3	4	5	6	7	8	9	10	11
A	-	D E N Q T S K	D H G P R W S	P	D S N E G K P	D G E	E	E F D W	D E I	D E	W
B	-	B M V I	V L I	I	F I L W M Y	F Y	Y	N S	N S	M B	

The average of the competition values for all 20 sublibraries of a position can be considered as a measure of its tolerance to amino acid variations. Positions 2 and 5 were shown to be widely intolerant to amino acid exchanges. The complete activity pattern supports the design of defined peptides binding to HLA-DR2b.

In conclusion, the use of mass tags for the optimization of procedures for library synthesis confirmed the high quality of the premix method developed for automated synthesis of peptide libraries. The influence of individual amino acids in 11 sequence positions of peptides binding to HLA-DR2 could be defined and the code for the construction of new MHC binding or non-binding peptides was summarized in an activity pattern of the library. Our approach is useful for characterizing the binding pockets of any MHC allele within short time.

## References

1. Pinilla, C., Appel, I.R., Blanc, P. and Houghten, R.A., *Biotechniques*, 13 (1992) 901.
2. Udaka, K., Wiesmüller, K.-H., Kienle, S., Jung, G. and Walden, P., *J. Biol. Chem.*, 720 (1995) 24130.
3. Gundlach, B.R., Wiesmüller, K.-H., Junt, T., Kienle, S., Jung, G. and Walden, P., *J. Immunol.*, 156 (1996) 3645.
4. Fleckenstein, B., Kalbacher, H., Muller, C.P., Stoll, D., Halder, T., Jung, G. and Wiesmüller, K.-H., *Eur. J. Biochem.*, 240 (1996) 71.
5. Hemmer, B., Fleckenstein, B., Vergelli, M., Jung, G., McFarland, H., Martin, R. and Wiesmüller, K.-H., *J. Exp. Med.*, 185 (1997) 1651.
6. Uebel, S., Kraas, W., Kienle, S., Wiesmüller, K.-H., Jung, G. and Tampé, R., *Proc. Natl. Acad. Sci., USA*, in press.
7. Fleckenstein, B., Jung, G. and Wiesmüller, K.-H., in: Brown, F., Burton, D., Doherty, P., Mekalanos, J., Norrby, E. (Eds.), *Vaccines 97*, Cold Spring Harbour Laboratory Press, in press.

# Transformation of a L-peptide epitope into a D-peptide analog

Achim Kramer and Jens Schneider-Mergener

Institut für Medizinische Immunologie, Universitätsklinikum Charité,  
Humboldt-Universität zu Berlin, Schumannstr. 20-21, 10098 Berlin, Germany

A major problem in the use of short synthetic peptides as vaccines or therapeutic agents is their rapid *in vivo* degradation by endogenous proteases. To overcome this limitation we developed a strategy for the systematic transformation of L-amino acid peptides into D-amino acid analogs with comparable biological properties, *i.e.* binding affinity and specificity, but considerably higher stability.

The transformation is performed by subsequent substitutions of each epitope residue by D-amino acids followed by antibody binding studies [1]. In the first step each single residue of the L-peptide is substituted by all 19 D-amino acids plus glycine. From antibody binding studies a peptide containing one D-amino acid is selected for a further substitutional analysis. Then, a peptide containing two D-amino acids serves as starting point for the next step. In repeating this step-by-step procedure one ends up with the identification of a complete D-peptide.

## Results and Discussion

Each single residue of the 11meric peptide epitope GATPQDLNTML, recognized by the anti-p24 (HIV-1) monoclonal antibody CB4-1, was substituted by 19 D-amino acids plus glycine. The substitution analogs were prepared by spot synthesis on a continuous cellulose membrane support [2] and consist of one D-amino acid and 10 L-amino acids at this first transformation step.

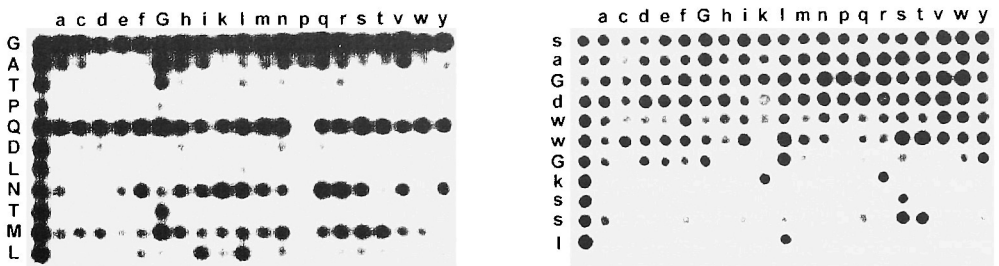


Fig. 1. Substitutional analyses of the L-peptide GATPQDLNTML (left) and the D-peptide saGdwwGkssl (right) prepared by spot synthesis. All spots in the left columns are identical and represent the original peptides. Each position of the peptides is substituted by all 19 D-amino acids plus glycine (rows). Lower-case letters are D-amino acids.

Binding studies with CB4-1 (Fig. 1, left) revealed proline 4, aspartic acid 6 and leucine 7 as positions which cannot be substituted by D-amino acids without loss of binding, whereas for the other positions D-amino acids (including glycine) can be selected. For the following substitutional analysis the peptide GATPQDLkTML was chosen comprising D-lysine at position 8. This procedure was repeated 10 times ending up with the D-peptide saGdwwGkssl (Fig. 2).

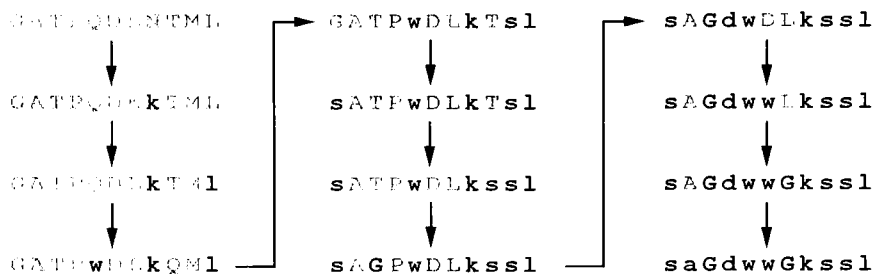


Fig. 2. Transformation of the L-peptide GATPQDLNTML into the D-peptide saGdwwGkssl.

The specificity of CB4-1 binding of this D-peptide was demonstrated by the identification of key binding residues for this kind of interaction (Fig. 1, right). The substitutional analysis revealed that the C-terminal part of the peptide is responsible for specificity, since D-serine 9 and D-leucine 11 cannot be substituted at all and D-lysine 8 only by the physicochemically similar D-amino acid arginine.

In conclusion, this approach should be a helpful tool for the creation of novel, biologically more stable compounds starting from a given peptide. Furthermore, binding studies using complete sets of substitution analogs at each transformation step provide interesting insights into the molecular basis of this type of cross reactivity.

## References

1. Stigler, R., Rüker, F., Katinger, D., Elliott, G., Höhne, W., Henklein, P., Ho, J., Keeling, K., Carter, D., Nugel, E., Kramer, A., Porstmann, T. and Schneider-Mergener, J., *Prot. Eng.*, 8 (1995) 471.
2. Kramer, A. and Schneider-Mergener, J., *Meth. Mol. Biol.*, 87 (1997) in press.

# Production of potent specific antigens and effective immunogens using sequential oligopeptide carriers (SOC<sub>n</sub>)

**Constantinos Sakarellos,<sup>a</sup> Vassilios Tsikaris,<sup>a</sup> Eugenia Panou-Pomonis,<sup>a</sup> Charalampos Alexopoulos,<sup>a</sup> Maria Sakarellos-Daitsiotis,<sup>a</sup> Constantinos Petrovas,<sup>b</sup> Panagiotis G. Vlachoyiannopoulos<sup>b</sup> and Haralampos M. Moutsopoulos<sup>b</sup>**

<sup>a</sup>*Department of Chemistry, University of Ioannina, 45110 Ioannina, GREECE.*

<sup>b</sup>*Department of Pathophysiology, Medical School, National University of Athens, 75 M. Asias St., 11527 Athens, GREECE.*

We report a class of peptide carriers containing lysine residues for anchoring antigenic peptides in a well defined spatial position and designed so as to present a predetermined conformation. Our support, formed by the repetitive Lys-Aib-Gly moiety, named SOC<sub>n</sub>, aims at providing carriers with regular secondary structure, in which the antigenic peptides attached to the Lys sidechain amines would not interact with each other or with the carrier. They would thus retain their original active conformation. On the other hand, the PPGMRPP sequence present in a variety of copies in the Sm and U1RNP autoantigens constitutes the main target of anti-Sm and anti-U1RNP antibodies found in patient sera characterized with systemic lupus erythematosus (SLE) and mixed connective tissue disease (MCTD).

## Results and Discussion

The immunoreactivity of PPGMRPP-NH<sub>2</sub> and PPGMRPP conjugated to a pentameric Sequential Oligopeptide Carrier (SOC<sub>5</sub>) [1] was investigated by testing sera (ELISA) with various antibody specificities. Their conformational properties were examined by 1D and 2D <sup>1</sup>H-NMR spectroscopy. Three main conformers were found for the free PPGMRPP, including an extended one that also identified for PPGMRPP-NH<sub>2</sub> and the (PPGMRPP)<sub>5</sub>-SOC<sub>5</sub>. This behavior can be ascribed to the conversion of the C-terminal carboxylate group to the amide form and consequently to the absence of an ionic bridge between the Arg-guanidinium and the carboxylate groups. When the protonated carboxyls are not available for an ionic interaction, the Arg-guanidinium is characterized by a triplet at about 7.65 ppm (N<sup>ε</sup>H proton). When a guanidinium-carboxylate interaction occurs, the N<sup>ε</sup>-H resonance shifts downfield to 10 ppm. From the NMR data, we can conclude that: (i) the main PPGMRPP-NH<sub>2</sub> conformer (>95%) adopts a completely extended conformation, similar to that found for the minor conformer of PPGMRPP, (ii) the arginine side-chain is not involved in the structural stabilization of the PPGMRPP-NH<sub>2</sub>, resulting to a reduced number of conformers, (iii) all the X-Pro peptide bonds of the main PPGMRPP-NH<sub>2</sub> conformer are found in the trans form. Evaluation of the NMR data for PPGMRPP-NH<sub>2</sub>

Table 1. Antigenic properties and conformational characteristics of the PPGMRPP, PPGMRPP-NH<sub>2</sub>, (PPGMRPP)<sub>5</sub>-SOC<sub>5</sub> peptides.

Peptide	anti-U1RNP(+) anti-S <sub>m</sub> (-) anti-Ro(SSA)(-) anti-La(SSB)(-)	anti-S <sub>m</sub> (+) anti-U1RNP(+) anti-Ro(SSA)(-) anti-La(SSB)(-)	anti-Ro(SSA)(+) anti-La(SSB)(+) anti-S <sub>m</sub> (-) anti-U1RNP(-)	% <sup>o</sup> RNεH <sup>a</sup> (ppm)
PPGMRPP	17/24	4/5	12/30	10.51 10.57 7.63
PPGMRPP-NH <sub>2</sub>	4/6	6/8	4/22	7.62
(PPGMRPP) <sub>5</sub> -SOC <sub>5</sub>	18/29	12/12	1/42	7.77

<sup>a</sup>Chemical shift values in DMSO-d<sub>6</sub>

peptide and the PPGMRPP conjugated to the SOC<sub>5</sub> indicates a very close similarity of almost all the chemical shift values between (PPGMRPP)<sub>5</sub>-SOC<sub>5</sub> and PPGMRPP-NH<sub>2</sub> (Table 1). The existence of multiple conformers of the Sm-epitope may explain the observed cross reactivity with the anti-U1RNP, anti-S<sub>m</sub>, anti-Ro (SSA) and anti-La (SSB) positive sera [2]. This hypothesis is further supported by the fact that when the heptapeptide PPGMRPP was anchored by its C-terminal carboxylate to the sequential oligopeptide carrier (SOC)<sub>n</sub> or converted to its amide form, their recognition by the anti-U1RNP and anti-S<sub>m</sub> positive sera was enhanced, while anti-Ro(SSA) and anti-La (SSB) positive sera were not recognized.

It is concluded that the antigenic specificity of the PPGMRPP-NH<sub>2</sub> peptide and (PPGMRPP)<sub>5</sub>-SOC<sub>5</sub> is mainly induced by conformational changes, resulting from the conversion of the C-terminal carboxylate group to its amide form.

## Acknowledgments

This work was supported by the European Union and the Greek Secretariat for Research and Technology.

## References

1. Tsikaris V., Sakarellos C., Cung M.T., Marraud M., and Sakarellos-Daitsiotis M., *Biopolymers* 38, 1996, 291.
2. Tsikaris V., Vlachoyiannopoulos P., Panou-Pomonis E., Marraud M., Sakarellos C., Moutsopoulos H., and Sakarellos-Daitsiotis M., *Int. J. Pept. Protein Res.* 48, 1996, 319.

# Cross-immunogenicity of topological mimics of peptide antigens

**Maria Rossi, Antonio Verdoliva, Menotti Ruvo and Giorgio Fassina**

*Protein Engineering, TECNOGEN S.C.p.A., Parco Scientifico,  
81015 Piana di Monte Verna (CE), Italy.*

Peptide side chain topology plays a central role in peptide antigenicity. Antibody recognition is preserved with peptide mimics resembling the parent peptide's original side chain stereochemical arrangement [1]. Recent work from our group suggested that peptide antigens could be sequence-simplified while maintaining at least part of the antigenic properties of the parent peptide. Synthetic variants of antigenic peptides, one lacking the side chains in the sequence odd position and the other in even position, prepared by replacing amino acid residues in the parent peptide with glycine residues alternately in the sequence, cross-reacted to a significant extent with antibodies raised against the parent peptide [2]. In order to extend our ongoing investigation on the mechanisms responsible for peptide antigenicity, polyclonal antibodies were raised in rabbits against two sequence simplified variants and their ability to recognize the parent antigen was examined by direct and competitive ELISA assays, by plasmon resonance experiments, and by affinity chromatography.

## Results and Discussion

The two sequence simplified peptides used in this study were derived from the parent peptide **P15 (VRLGWLLAPADLDAR)** [3] by replacing parent peptide residues with glycine in the sequence odd position (**-P15, GRGGGLGAGAGLGAG**) or in the even position (**+P15, VGLGWGLGPGDGDGR**). Peptides were conjugated to **KLH** via glutaraldehyde mediated cross-linking and induced a strong immunogenic response in rabbits even after the first boost. Sera were then purified by affinity chromatography on columns prepared by immobilizing the corresponding sequence-simplified antigen. Purified antibodies against **-P15** and **+P15** peptides were characterized first by ELISA assays for their ability to recognize the parent peptide **P15**. Both polyclonal antibodies recognized the parent peptide to a similar extent, and binding was specific since it could be inhibited by the parent peptide or the corresponding sequence-simplified antigen in a dose dependent manner. Cross-immunogenicity was further confirmed by plasmon resonance experiments on cuvettes derivatized with the parent peptide, where both antibodies against the sequence-simplified antigens displayed similar affinities. Additional evidence of antigenic mimicry was provided by affinity chromatography experiments, since columns prepared with the parent peptide proved useful for the purification of antibodies raised against the two sequence-simplified variants. A schematic representation of the cross-antigenic and cross-immunogenic properties of sequence-simplified variants of parent

peptide antigens is shown in Fig. 1. Results cumulatively suggest the possibility of redesigning peptide antigens in two variants which could preserve antigenicity as well as immunogenicity similar to the parent peptide.

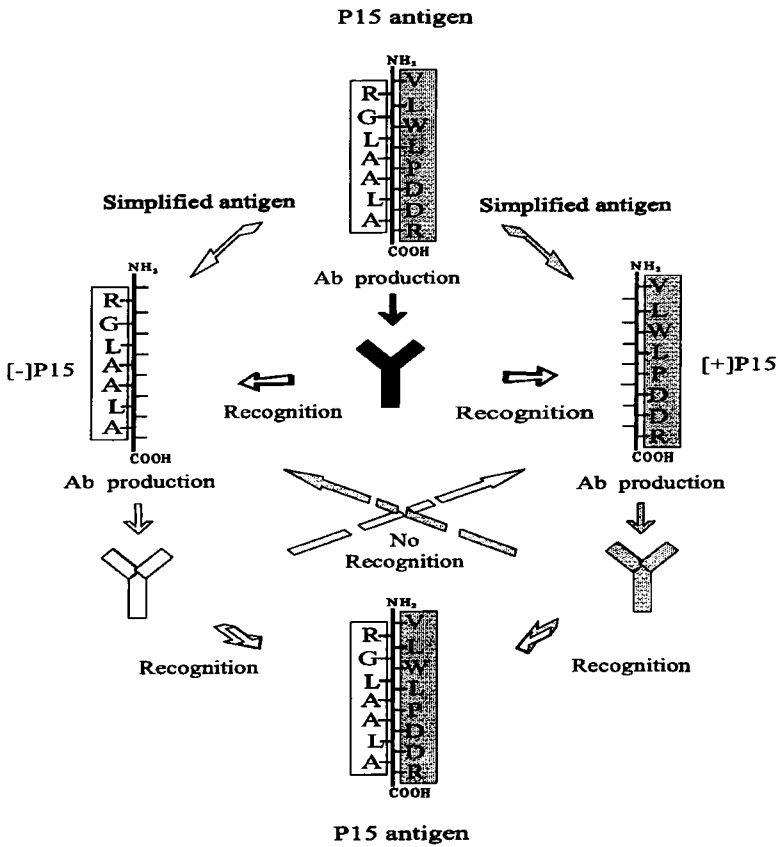


Fig. 1. Schematic representation of cross-antigenicity and cross-immunogenicity relationships between sequence-simplified antigens, parent peptides and corresponding antibodies.

## References

1. Guichard, G., Benkirane, N., Zeder-Lutz, G., Van Regenmortel, M.H.V., Briand, J.-P. and Muller, S., Proc. Natl. Acad. Sci. USA, 91 (1994) 9765.
2. Verdoliva, A., Ruvo, M., Cassani, G. and Fassina, G. J., Biol. Chem., 270 (1995) 30422.

# Searching for dominant linear antigenic region of hepatitis B surface antigen with human immune sera against phage-displayed random peptide library

Zhi-Jian Yao,<sup>a</sup> Lay-Hian Ong,<sup>a</sup> Lily Chan<sup>a</sup> and Maxey C. M. Chung<sup>a,b</sup>

*<sup>a</sup>Bioprocessing Technology Centre and <sup>b</sup>Department of Biochemistry, National University of Singapore, Singapore 119260, Republic of Singapore.*

Human sera and other body fluids are a rich sources of information reflecting health or disease, including the constitution of immunoglobulins directly linked to the repertoire of humoral immune responses. This reflects the immune system's defense mechanisms against invasive pathogens. On the other hand, a random peptide library or combinatorial peptide libraries [1] provide a comprehensive potential for identifying the binding sites of proteins. Therefore, it is reasonable to suggest that by using immunoglobulins isolated from the patient's body fluids to screen against the repertoire of a random peptide library, the resulting binding peptide sequence(s) that correspond to an epitope or a mimotope of the pathogenic protein would be region(s) of great interest in pathogenesis.

## Results and Discussion

The use of polyclonal antiserum as selection ligate is known to pose background ("noise") problems. An efficient method to eliminate these high background problems when using polyclonal antiserum as ligate is to preselect the antibody by the target antigen [2]. In this study, purification was done by incubating a recombinant HBsAg solution on a polystyrene surface of a Petri dish and recovering the purified "mono-specific" antibody by elution. 10 µg of recombinant hepatitis B surface antigen was sufficient for preparing the ligate used in three rounds of biopanning.

Biopanning yields of pVIII15x library between rounds showed positive enrichment of phage carrying inserts bound to the selection ligate. Thirty-five clones were randomly selected from the third round output of both biopannings. In the sequencing of the 35 inserts from the 15-mer library, one deduced amino acid sequence was directly picked up by the search program, Blitz, which showed similarity to residues 113-125 of HBsAg. When the 113-125 region was further compared to the aforementioned 35 sequences, five other similar sequences were found.

Based on the results of biopanning and prediction algorithm [3], several peptides were synthesized to compare their binding with antibody. To increase sensitivity, all of the peptides were synthesized as their branched form [4]. The binding of these peptides with pooled positive and negative sera shows that P2 (113-125 of HBsAg, ayw), P6 (107-126, ayw) and P7 (107-126, adw) exhibited observable differences between positive and negative sera, the readings of P6 and P7 being higher than P2. Another interesting observation was the result for peptide P8, in which residues 121-125 from P6 had been omitted. This peptide showed almost no obvious binding to positive sera, indicating that

the cysteine-rich region of the protein was essential for forming the antigenic determinant. The contribution of the cysteine-rich region was further confirmed by alanine-scanning. A panel of peptides, in which each amino acid was successfully replaced by alanine, was synthesized. Binding tests revealed that about 85% of the binding affinity was lost when each of the residues 121/124 (cysteine) or 120 (the flanking proline) had been replaced (Fig.1).

The most interesting point is that the mapping results focused directly on the region of residues 110-150, which had been suggested as the major antigenic/immunogenic structure of HBsAg by other approaches in the past twenty years. Therefore, it supports the observation [5] that a combinatorial peptide library can result in a higher probability of locating the most dominant antibody binding site(s) of a protein.

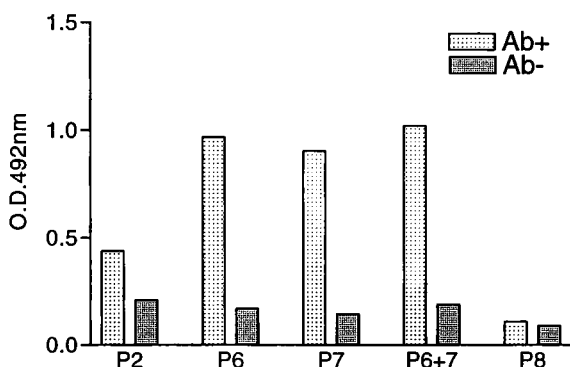


Fig. 1. Binding of peptides to serum. P2: SSTTSTGPCRTCM (ayw) 113-125 (MAP x 8). P6: CPLIPGSSTTSTGPCRTCMT (ayw) 107-126 (MAP x 4). P7: CPLIPGSTTTSTGPKCTCTT (adw) 107-126 (MAP x 4). P8: CPLIPGSSTTSTGP (ayw) 107-120 (MAP x 4). Ab+: Pooled anti-HBsAg positive serum. Ab-: Pooled anti-HBsAg negative serum.

## References

1. Scott, J.K. and Smith, G.P. *Science*, 249 (1990) 386.
2. Yao, Z.-J., Kao, M.C.C. and Chung, M.C.M. *J. Protein Chem.*, 14 (1995) 161.
3. Rost, B., *Methods in Enzymology*, 266 (1996) 525.
4. Tam, J.P., *Proc. Natl. Acad. Sci. USA*, 85 (1988) 5409.
5. Yao, Z.-J., Chan, M.-C., Kao, M.C.C. and Chung, M.C.M. *Int. J. Peptide Protein Res.*, 48 (1996) 477.

# Comparative immunological properties of lipidated HIV-1 gp41 fragments on various structural templates

Artur Pedyczak, Dave McLeod, Olive James, Michel Klein,  
and Pele Chong

Research Centre, Pasteur-Mèrieux-Connaught Canada, 1755 Steeles Avenue West, North York,  
Ontario, M2R 3T4, CANADA

The transmembrane protein (gp41) of human immunodeficiency virus type 1 (HIV-1) plays a key role in both virus infection and virus-mediated cell-cell fusion. Previous studies revealed that linear peptides containing Katinger's epitope ELDKWA [1] failed to elicit neutralizing antibodies in animal models. It is well established that the HIV envelope gp41 moiety forms an oligomeric structure in the virus[2]. Therefore, one can hypothesize that the neutralization epitopes may exist in the context of the gp41 oligomeric form, which cannot be mimicked by a linear peptide. In the present work, we report the results of an immunogenicity study performed with different MAPs containing the cross-neutralization epitope ELDKWA [1] of HIV-1 gp41:

GPKEPFRDYVDRFYKDAASDLELDKWASLWNWF AAAARSS (CLTB-166)

GPKEPFRDYVDRFYKGPGLLELDKWASLWNWFDITNWLWYIKSS (CLTB-165)

GPKEPFRDYVDRFYKGPGEKNEQELLELDKWASLWNWFDITNWLWYIKSS  
(CLTB-164)

## Results and Discussion

The above linear peptides were incorporated in bi- and tetravalent lipidated templates, as shown in Fig. 1. The branched peptides were synthesized using combined t-Boc and Fmoc strategies.

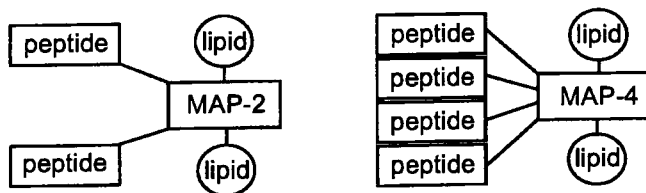


Fig. 1. Schematic representation of the synthetic peptides. MAP-2 =  $\beta$ Ala-Lys-Ser-Ser-lys-Lys- $\beta$ Ala-NH<sub>2</sub>, MAP-4 =  $\beta$ Ala-Lys- $\beta$ Ala-Lys[ $\beta$ Ala-Lys]Ser-Ser-lys-Lys- $\beta$ Ala-NH<sub>2</sub>, lipid = CH<sub>3</sub>(CH<sub>2</sub>)<sub>14</sub>CO-, peptide = CLTB-164, CLTB-165, CLTB-166.

Guinea pigs were immunized with 3x200µg of MAP constructs, and their sera were analyzed by immunoassay against both immunized peptides and recombinant gp160. The highest titers were obtained with MAP-4 containing the CLTB-166 sequence, [CLTB-166]<sub>4</sub>-[MAP-4]-L<sub>2</sub> (L=CH<sub>3</sub>(CH<sub>2</sub>)<sub>14</sub>CO-). However, none of the anti-MAP antisera reacted with recombinant gp160 and had no viral neutralization activity.

CD measurements showed that all the studied peptides were predominantly  $\alpha$ -helical (Fig. 2). The highest mean residue ellipticity of the  $\alpha$ -helix specific bands (210, 220 nm) was observed for [CLTB-166]<sub>4</sub>-[MAP-4]-L<sub>2</sub>, the peptide with the best immunological properties in the series. This could be a consequence of intramolecular peptide chain association, leading to the formation of a parallel, 4- $\alpha$ -helix bundle-like structure which may present the epitope better to the immune system.

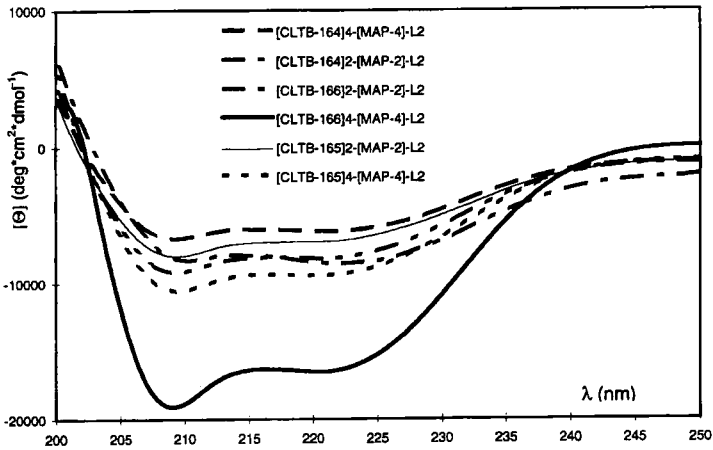


Fig.2. CD spectra of the studied peptides in 50% methanol.

## References

1. Muster, T., Guinea, R., Trkola, A., Purtschner, M., Klima, A., Steindl, F., Palese, P., Katinger, H., *Journal of Virology*, June 1994, 4031-4034.
2. Matthews, T.J., Wild, C., Chen, C-H., Bolognesi, D., Greenberg, M., *Immunological Reviews*, 1994, No. 140.

# Biological effects of peptide antibodies raised to HER-2/neu. Implications for therapy of human breast cancer

Donna Woodbine,<sup>b,c</sup> Naveen Dakappagari,<sup>g</sup> Pierre Triozzi,<sup>d, e</sup> Vernon Stevens<sup>a,c</sup> and Pravin T.P. Kaumaya<sup>a,b,c,f</sup>

<sup>a</sup>College of Medicine, <sup>b</sup>Comprehensive Cancer Center, <sup>c</sup>Dept. of OB/GYN, <sup>d</sup>Division of Hematology and Oncology, <sup>e</sup>Dept. of Internal Medicine, <sup>f</sup>Medical Biochemistry and Microbiology, <sup>g</sup>Dept. of Microbiology, The Ohio State University, Columbus, OH 43210 USA

Cancer is the second leading cause of death in the United States. In breast cancers, about one quarter overexpress the erbB-2 oncogene, which encodes a 185kD growth factor receptor, HER-2/neu. Because its overexpression correlates with poor prognosis [1], the ability to control the expression of this protein could favorably reduce the number of cancer related deaths. HER-2 is composed of 4 domains: an extracellular cysteine rich domain, a transmembrane sequence, a tyrosine kinase domain and the C-terminal tyrosine autophosphorylation sites. The extracellular accessibility of HER-2 makes it an ideal candidate for antibody therapy. Antibodies can cause receptor internalization, tumor retardation and differentiation to the mature state [2, 3]. Our studies involve generating antibodies to conformational epitopes by peptide immunization, thus giving antibodies of defined specificity. No ligand has yet been found for HER-2. Studies have shown that its action is mediated by heterodimerization with the other three members of the epidermal growth factor receptor family: EGFR, HER-3 and HER-4. This dimerization engages its tyrosine kinase (TK) activity, signalling a cascade of intracellular events which result in aberrant growth. Monoclonal antibodies can modulate this TK activity and thus tumor progression. Peptide candidates from HER-2/neu were studied by computer-aided analysis. B cell epitopes were synthesized colinearly with a "promiscuous" T cell epitope, MVF 288-302. We have raised a panel of peptide antibodies capable of affecting the biology of HER-2: DW1MVF (376-395), MVFDW4 (628-647), DW5MVF (115-136), and DW6MVF (410-429). The effect of peptide antibody on tyrosine phosphorylation and cell proliferation was studied. The anti-tumor effects of these peptide antibodies were tested in the BALB/c nude mouse model. Mice are injected with ( $3 \times 10^6$ ) HER-2 overexpressing cells and infused with 1.5 - 2mg of anti-HER2 antibodies.

## Results and Discussion

Our studies show that peptide antibodies can have as profound a biological effect as monoclonals. The *in vivo* and *in vitro* immune responses to the peptide were studied in outbred New Zealand white rabbits (Table 1). Antibody (Ab) titers against the peptide immunogen increased steadily as early as the primary immunization. Peptide antibodies caused receptor downregulation and reduced tumor volume *in vivo*. A [<sup>3</sup>H] thymidine proliferation assay revealed the ability of anti-peptide antibodies to reduce proliferation *in vitro*.

*Table 1. Comparative effects of anti-peptide antibodies in various assays.*

<b>Antibody</b>	<b>Reduce</b> 1) phosphorylation	2) <i>in vivo</i> prolif.	3) <i>in vitro</i> prolif.
<b>DW1MVF</b>	-	+	++
<b>MVFDW4</b>	+++	+++	++
<b>DW5MVF</b>	-	+++	++
<b>DW6MVF</b>	+++	+	-
<b>mAb-2</b>	+++	ND	-

### References

1. Slamon, D.J. Clark, G.M., Wong, S.G., Levin, W.J., Ullrich, A., McGuire, W.L. *Science*, 235(1987)177.
2. Bacus, S., Stancovski, I., Huberman, E., Chin, D., Hurwitz, E., Mills, G.B., Ullrich, A., Sela, M., Yarden, Y. *Cancer Research*, 52(1992)2500.
3. Drebin, J.A., Link, V.C., Stern, D.F., Weinberg, R.A., Greene, M.I. *Cell*, 41(1985)695.

# **A multiple branch peptide construction derived from a conserved sequence of the envelope glycoprotein gp41 inhibits human immunodeficiency virus infection**

**Jean-Marc Sabatier,<sup>a</sup> Maxime Moulard,<sup>b</sup> Emmanuel Fenouillet,<sup>a</sup> Hervé Rochat,<sup>a</sup> Jurphaas Van Rietschoten<sup>a</sup> and Kamel Mabrouk<sup>a</sup>**

<sup>a</sup>Laboratoire de Biochimie, CNRS UMR 6560, IFR Jean Roche, Faculté de Médecine Nord, Bd Pierre Dramard, 13916 Marseille Cédex 20, France, <sup>b</sup>Centre d'Immunologie Marseille-Luminy, Case 906, 13288 Marseille Cédex 9, France.

We have recently reported some anti-HIV properties of SPC3 [1-3], a gp120 V3 loop-derived synthetic polymer construction [4, 5] which is currently under phase II clinical trials in HIV-1-infected humans. Due to the importance of both gp120 and gp41 envelope glycoproteins in the virus-cell and cell-cell fusion processes [6], we have chemically synthesized a series of other multiple branch peptides (SPCs) derived from the conserved sequences of gp41 [7, unpublished results]. The gp41-derived SPCs have been tested *in vitro* for their ability to inhibit i) syncytium formation induced either by a recombinant vaccinia virus-expressing HIVLai Env or various HIV strains, and ii) infection of human peripheral blood lymphocytes by laboratory strains and clinical isolates of both HIV-1 and HIV-2.

## **Results and Discussion**

Among the gp41-derived SPCs, only multiple branch peptide [RQGYSP]<sub>8</sub>-K<sub>4</sub>-K<sub>2</sub>-K-βA, derived from the gp41 consensus sequence 714-720, was found to inhibit virus-induced syncytium formation, with a full blockade (IC<sub>100</sub>) obtained at about 10 μM peptide concentration. This SPC also inhibited in a dose-dependent manner infection of human peripheral blood lymphocytes by both HIV-1 (Table 1) and HIV-2 with 50% inhibitory activity (IC<sub>50</sub>) obtained at peptide concentrations ranging from 0.1 to 1 μM depending on the virus tested, i.e. T-cell line adapted strains (e.g. Hx10, LAV-2/B) or clinical isolates of HIV (e.g. JRFL, JRCSF, W5A2A9, P16/B6, P16/C9, ...). The gp41-derived SPC was found to act synergistically with the V3 loop-derived SPC3; however, its mode of action remains to be determined. In contrast, the monomeric form of the SPC, i.e. peptide RQGYSP, was inactive in these tests. Interestingly, the RQGYSP sequence is highly conserved among the diverse HIV-1, HIV-2, and SIV viruses, but does not share full homology with any other known protein structures.

*Table 1. Inhibition (%) of the HIV-1 clinical isolates infectivity by the multiple branch peptide [RQGYSP]<sub>8</sub>-K<sub>4</sub>-K<sub>2</sub>-K-βA. Example shown is the W5A2A9 isolate. Experiments were performed with 1:10 diluted virus solution. The state of infection of the human peripheral blood lymphocytes was determined 10 days post-infection with the virus -in the presence or absence of the peptide- by both reverse transcriptase assay and p24 production in culture supernatants.*

Peptide (μM)	5	1	0.5	0.1	0.05
[RQGYSP] <sub>8</sub> -K <sub>4</sub> -K <sub>2</sub> -K-βA	100	100	100	45	0
[GPGKTL] <sub>8</sub> -K <sub>4</sub> -K <sub>2</sub> -K-βA (control peptide)	0	0	0	0	0

## Conclusion

The multiple branch peptide [RQGYSP]<sub>8</sub>-K<sub>4</sub>-K<sub>2</sub>-K-βA showed neither cellular toxicity at active concentration nor lethal activity when injected by the intracerebroventricular route in mice. Therefore, because of its potent antiviral activity against both HIV-1 and HIV-2, it represents a novel candidate chemotherapeutic drug against HIV infection.

## References

1. Yahi, N., Fantini, J., Mabrouk, K., Tamalet, C., De Micco, C., Van Rietschoten, J., Rochat, H. and Sabatier, J.M., *J. Virol.*, 68 (1994) 5714.
2. Yahi, N., Sabatier, J.M., Baghdiguian, S., Gonzalez-Scarano, F. and Fantini, J., *J. Virol.*, 69 (1995) 320.
3. Yahi, N., Fantini, J., Baghdiguian, S., Mabrouk, K., Tamalet, C., Rochat, H., Van Rietschoten, J. and Sabatier, J.M., *Proc. Natl. Acad. Sci. U.S.A.*, 92 (1995) 4867.
4. Tam, J.P., *Proc. Natl. Acad. Sci. U.S.A.*, 85 (1988) 5409.
5. Fantini, J., Yahi, N., Mabrouk, K., Rochat, H., Van Rietschoten, J. and Sabatier, J.M., In Fantini, J. and Sabatier, J.M. (Eds.) *Perspectives In Drug Discovery and Design*, ESCOM Science Publishers B.V., 1996, p. 243.
6. Moore, J.P., Bradford, A., Jameson, A., Weiss, R.A. and Sattentau, Q.J., In Bentz, J. (Ed.) *Viral Fusion Mechanisms*, CRC, Boca Raton F.L., 1993, p. 233.
7. Sabatier, J.M., Mabrouk, K., Moulard, M., Rochat, H., Van Rietschoten, J. and Fenouillet, E., *Virology*, 223 (1996) 406.

# Antigenic domains of *Shigella* virulence proteins

**Kevin R. Turbyfill and Edwin V. Oaks**

*Department of Enteric Infections, Walter Reed Army Institute of Research  
Washington, D.C. 20307, USA*

*Shigella* are gram-negative, nonmotile bacteria that have the ability to invade and multiply within the colonic epithelium of higher primates, eventually leading to bacillary dysentery. Invasion by shigellae requires the expression and secretion of the "invasion plasmid antigens", or Ipa proteins, which are actively involved in the induced phagocytic event that initiates the invasiveness process [1,2,3]. Upon infection, the host immune system produces antibodies against IpaB, IpaC, IpaD, and IpaH as well as another virulence protein, VirG [4]; however, the significance of the serum antibody response to the Ipa proteins is not clear.

Using the Geysen multipin technology our lab has identified three regions of clustered peptide epitopes on IpaC that were recognized by shigellae-infected monkeys [5]. In this report, a similar strategy was used to characterize the epitopes of IpaD, VirG, and two forms of IpaH. In addition, soluble, overlapping synthetic peptides representing the 3 IpaC epitope regions were used to further evaluate the immune response in a large population of infected monkeys. By characterizing the epitopic domains of each Ipa protein we hope to identify regions of the protein that are immunodominant and likely involved in the protective immune response.

## Results and Discussion

The surface localization of these crucial virulence determinants makes them suitable targets for neutralization by the host immune response. Epitope analysis of IpaC, IpaD, IpaH, and VirG with serum antibodies from 13 shigellae-infected monkeys revealed distinct epitope domains within each protein (see Table 1). The epitope domains were generally localized in the amino terminal half of the protein and were in regions containing high antigenic indices, high surface probability, and predominantly hydrophilic amino acids. Interestingly, each infected animal had a unique epitope pattern within the epitope domains, suggesting that a heterogenous antibody response had occurred, most likely due to their individual genetic makeup.

Using epitope mapping data from previous studies [5], overlapping synthetic peptides representing epitope Regions I, II, and III of IpaC were used in an ELISA to further characterize the immune response in a large population of animals infected with *S. flexneri* [6]. Out of 44 infected monkeys producing antibodies reactive with purified IpaC, 39 were positive in the IpaC peptide ELISA for Regions I, II, or III. Because some animals reacted with the whole IpaC protein but were not positive in the peptide ELISA, either IpaC epitopes other than those represented by the Region I, II, and III synthetic peptides were

Table 1. Epitope domains of *Shigella* virulence proteins.

Protein	Immunodominant Region*	No. of Animals Responding	Surface Exposed
IpaC	CI (1-61)	6/13	Yes
	CII (177-257)	12/13	Partial
	CIII (298-307)	7/13	Not Determined
IpaD	(14 - 77)	10/13	Yes
IpaH 4.5	Unique N-terminal half (1-251)	8/13	Not Determined
VirG	GI (67-191)	11/13	Partial
	GII (951-962)	4/13	Not Determined

\*First and last amino acid residue number of the region is in parentheses.

recognized by the infected monkeys or conformational epitopes found in the purified protein may not be present in the synthetic peptides.

Not only is the multipin technique useful for identifying epitopes but we have also used this approach to identify epitopes that are exposed on the shigellae surface. Using anti-IpaD or anti-VirG antibodies affinity-purified against intact virulent shigellae coupled with the multipin procedure it was possible to identify surface-accessible epitopes on the invasive organism. Surface-exposed peptide epitopes identified in IpaD and VirG were located in the amino-terminal region of the protein. Other IpaD or VirG epitopes located in the carboxyl-terminal half of the proteins were not exposed on the organism's surface.

## Conclusion

Epitope mapping of the *Shigella* Ipa proteins has identified immunodominant domains of each protein within which are numerous unique epitopes. Furthermore, by coupling the multipin technique with antibodies affinity-purified against surface epitopes of shigellae surface proteins, protein domains that are accessible to antibodies on the intact organism have been identified.

## References

1. Buysse, J., Stover, C., Oaks, E., Venkatesan, M., et al, *J. Bacteriol.*, 169(1987)2561.
2. Andrews, G.P., Hromockyj, A.E., Coker, C. and Maurelli, A.T., *Inf. Immun.*, 59(1991)1997.
3. Venkatesan, M.M., Buysse, J.M. and Oaks, E.V., *J. Bacteriol.*, 174(1992)1990.
4. Oaks, E.V., Hale, T.J. and Formal, S.B., *Infect. Immun.*, 53(1986)57.
5. Turbyfill, K.R., Joseph, S.W. and Oaks, E.V., *Infect. Immun.*, 63(1995)3927.

# Characterization and immune response of a novel synthetic peptide vaccine for HTLV-I

Melanie Frangione<sup>b</sup> and Pravin T.P. Kaumaya<sup>a,b,c,d</sup>

<sup>a</sup>The College of Medicine, <sup>b</sup>Departments of Obstetrics and Gynecology, <sup>c</sup>Medical Biochemistry, and <sup>d</sup>Microbiology, The Ohio State University, Columbus, Ohio 43210, USA

Human T-cell lymphotropic virus type I (HTLV-I) is the causative agent of adult T-cell leukemia (ATL) and the neurological disorder, tropical spastic paraparesis/HTLV-I associated myelopathy (TSP/HAM). In our continuing efforts to develop and engineer conformational epitopes for the human T-lymphotropic virus type I (HTLV-I), we have synthesized a novel construct, designated MVFMF1, consisting of the envelope gp46 sequence, 229-257, linked by a four residue sequence (Gly-Pro-Ser-Leu) to a "promiscuous" T-cell epitope from the measles virus fusion protein (seq 288-302). This site represents a region of considerable complexity both in terms of secondary/tertiary structure potential (loop, turn, glycosylation, disulfide bond) as well as immunological reactivity (sero-reactivities from HTLV-I patients are: 209-231, 48%; 211-233, 18%; 224-244, 81%; 230-244, 50%, 242-257, 100%) [1]. Computer algorithms of Hopp and Woods (hydrophilicity), Kyte and Doolittle (hydropathy), Fraga, Hopp (acrophilicity), Welling (antigenicity), Fauchere and Pliska, and Novotny (accessibility) were utilized, focusing on accessibility scales.

The structural characteristics of this new construct, MVFMF1, and various intermediate sequences within this construct (MF1a, residues 229-257, MF1b, residues 234-257, MF1c, residues 242-257) were determined by CD for the purpose of comparing structural characteristics to immunological properties.

## Results and Discussion

Antibody titers were determined by direct ELISA after weekly collection of sera. The MVFMF1 construct elicited high-titer antibodies against MVFMF1, MF1a, and the recombinant HTLV-I protein RE3 (env 165-306). Antibodies were also shown to bind to the construct MF1b at lower titers and did not react to MF1c (Fig. 1). Sera were also analyzed by competitive ELISA. When plates were coated with the immunogen MVFMF1 and its intermediate construct MF1a, both were able to compete for antibody binding. The recombinant protein RE3, however, was ineffective as an inhibitor. When RE3 was used to coat the plates, MF1a and RE3 inhibited antibody binding, but the immunogen MVFMF1 did not.

Circular dichroism indicated that MVFMF1 has moderate  $\alpha$ -helical character and, as shown in Table 1, the  $\alpha$ -helical character decreased for the intermediate constructs MF1a, MF1b, and MF1c as the length of the peptide decreased. Structural characterization and immune data taken together indicate that  $\alpha$ -helical character is important for the binding of antibodies to these constructs and that the ability of antibodies to bind decreases as secondary structure is

lost. (This work was supported by NIH grants AI40302 and AI0D40302-01 to PTPK).

*Table 1. Mean residue ellipticity ( $[\theta]_{M, \lambda}$ ) values for peptide constructs in water or 50% trifluoroethanol (TFE). Ellipticities are expressed in  $\text{deg}\cdot\text{cm}^2/\text{dmol}$ . Values show an increase in  $\alpha$ -helicity as the length of the peptide increases. Antibody binding to these constructs correlates with  $\alpha$ -helicity.*

Peptide	Sequence	$[\theta]_{M,208}$ in Water	$[\theta]_{M,208}$ in 50% TFE	$[\theta]_{M,222}$ in Water	$[\theta]_{M,222}$ in 50% TFE
MVFMF1	MVF 288-302 env 229-257	5726.34	12704.3	2037.69	8953.19
MF1a	env 229-257	8200.74	10042.48	3642.83	5417.54
MF1b	env 234-257	7432.05	7496.43	3240.15	4392.07
MF1c	env 242-257	8565.79	5676.88	3849.08	4213.87

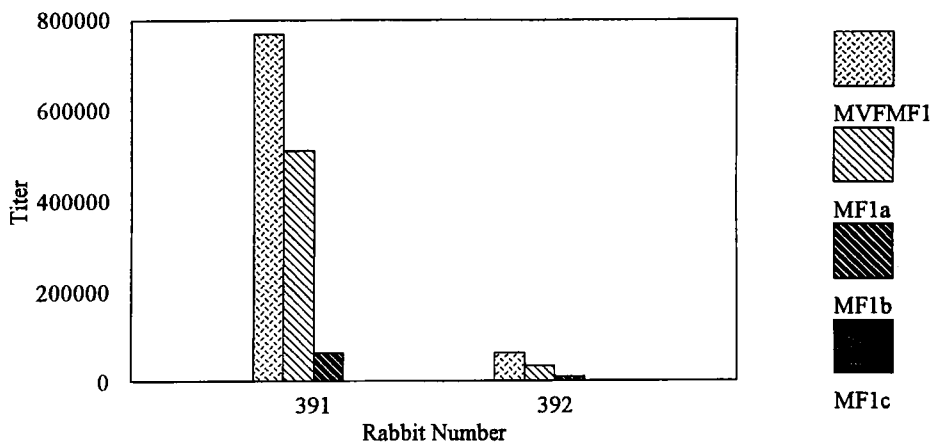


*Fig.1. Anti-MVFMF1 antibody binding to constructs MF1a, MF1b, and MF1c. Data indicate that antibodies specific for MVFMF1 bind the intermediate constructs, but to a lesser degree. Antibodies do not bind the MF1c construct.*

## References

1. Lal, R., Rudolph, D., Lairmore, M.D., Khabbaz, R., Garfield, M., Coligan, J. and Folks, T., J. *Infect. Dis.*, 161 (1991) 41.

# Mapping of the immunodominant B- and T-cell epitopes of the outer membrane protein D15 of *H. influenzae* type b using overlapping synthetic peptides

**Pele Chong, Olive James, Yan-Ping Yang, Charles Sia, Sheena Loosmore, Dave McLeod and M. Klein**

*Research Centre, Pasteur Merieux Connaught Canada, 1755 Steeles Ave. West, Willowdale, Ontario, Canada. M2R 3T4.*

Although current *Haemophilus influenzae* type b (Hib) capsular polysaccharide conjugate vaccines protect against Hib infection, they do not protect against other invasive typeable and non-encapsulated strains which are a common cause of otitis media in children. Recent studies [1,2] indicate that antibodies raised against the outer membrane protein D15 are protective in the infant rat model of bacteremia. Therefore, the use of D15 or its immunodominant epitopes as both additional immunogens and carriers for PRP represents a promising strategy to develop new conjugate Hib vaccines with enhanced protective ability and autologous T-cell priming. Thus, the purpose of this study was to map the antigenic determinants of D15 using overlapping synthetic peptides, and assess their immunogenicity for possible inclusion in a cross-protective synthetic *H. influenzae* vaccine.

## Results and Discussion

To identify the B-cell linear epitopes of D15, rabbits, guinea pigs and mice were immunized with chromatographically purified recombinant D15 (rD15) emulsified in Freund's adjuvant. After two immunizations, all animals generated strong D15-specific antibody responses as judged by both ELISA and immunoblots. Thirty six peptides covering the entire D15 sequence were synthesized and tested for their reactivities with the various anti-D15 antisera in peptide-specific ELISAs as previously described [3]. *Bordetella pertussis* peptides were used as negative controls. Two immunodominant linear B-cell epitopes recognized by rabbit anti-D15 antibodies were mapped to residues 304-323 and 769-798 of the mature D15 sequence. Similarly, residues 45-74 and 180-209 and residues 180-209, 219-249, 241-270, and 554-582 were identified as guinea pig and BALB/c mouse immunodominant B-cell epitopes, respectively.

Peptides containing T-cell epitopes were characterized by their ability to stimulate the proliferation of BALB/c mouse T-lymphocytes primed with rD15 in a standard *in vitro* T-cell proliferation assay [4]. Eleven synthetic peptides corresponding to residues 114-143, 219-249, 262-291, 282-312, 390-416, 410-435, 554-582, 577-602, 596-625, 725-750 and 745-771 were found to be capable of stimulating the proliferation of D15-primed T-cells. These results indicate that peptides corresponding to residues 219-249 and 554-582 comprise both BALB/c mouse T- and B-cell epitopes. The identification of these immunodominant B-

and T-cell epitopes represents a first step towards the rational design of a potentially cross-protective Hib vaccine.

### **Acknowledgements**

We thank S-P. Shi, and T. Olivier for their excellent technical assistance. This work was partially supported by IRAP grant# CA103-9-1423 from the National Research Council Canada.

### **References**

1. Thomas, W.R., Collow, M.G., Dilworth, R.J. and Andesho, A.A. *Infect. Immun.*, 58(1990) 1090.
2. Flack, F.S., Loosmore, S., Chong, P. and Thomas, W.R. *Genes*, 156(1995) 97.
3. Chong, P., Sydor, M., Wu, E., Zobrist, G., Boux, H. and Klein, M. *Molec. Immunol.*, 28 (1991) 239.
4. Sia, D.Y. and Chou, J.L. *Scand. J. Immunol.*, 26 (1987) 683.

# A novel bovine antimicrobial peptide of the cathelicidin family

Renato Gennaro,<sup>a</sup> Marco Scocchi,<sup>a,b</sup> Laura Merluzzi,<sup>a</sup>  
Shenglun Wang<sup>b</sup> and Margherita Zanetti<sup>a,b</sup>

<sup>a</sup>Department of Biomedical Sciences and Technology, University of Udine, I-33100 Udine

<sup>b</sup>National Laboratory CIB, AREA Science Park, I-34012 Padriciano-Trieste, Italy

Antimicrobial peptides are a first line of defense against pathogens widely distributed among animal species. In mammals they have been found in epithelial surfaces and in professional phagocytes. The latter are equipped with different sets of peptides which fall within one of two major groups: the Cys-rich  $\alpha$ - and  $\beta$ -defensins and the heterogeneous group of the cathelicidin-derived peptides. The cathelicidins are a family of antimicrobial peptide precursors characterized by a highly conserved preproregion and by a variable antimicrobial domain [reviewed in 1].

## Results and Discussion

The bovine cathelicidin gene family consists of at least eleven members. They are made of four exons, three of them encoding the conserved preproregion and a fourth specifying the antimicrobial domain. The bovine members identified are Bac5, Bac7, cyclic dodecapeptide (two copies), indolicidin (two copies), BMAP-27 and BMAP-28, a novel functional cathelicidin gene (BMAP-34), and two presumed nonfunctional genes (Bac4 and CATHLP).

Exon four of the novel functional gene encodes the last four residues of the cathelicidin proregion and a putative 34-residue cationic peptide that was named BMAP-34 from Bovine Myeloid Antimicrobial Peptide. The deduced amino acid sequence contains several charged residues (9 Arg, 3 Lys, 2 Glu and 2 Asp) and a C-terminal glycine corresponding to a putative amidation signal. Northern blot analysis of bovine bone marrow total RNA reveals a transcript of approximately 0.7 kb, indicating expression of this gene in myeloid cells.

A C-terminally amidated peptide corresponding to this sequence was synthesized by the solid phase method using the Fmoc strategy, purified by RP-HPLC and characterized by ES-MS. CD analysis shows that the peptide undergoes a conformational transition from a random coil in aqueous buffer to an  $\alpha$ -helical conformation on addition of trifluoroethanol (50–60% helical content at 30–45% TFE), indicating the amphipathic nature of the helix.

BMAP-34 displays considerable antibacterial activity *in vitro* against several strains of both Gram negative (e.g. *Escherichia coli*, *Serratia marcescens*, *Salmonella typhimurium* and *enteritidis*) and Gram positive bacteria (e.g. *Staphylococcus epidermidis*, *Bacillus megaterium*, and *Staphylococcus aureus*, including methicillin-resistant strains), with minimum inhibitory concentration (MIC) values in the 1–12  $\mu$ M range. The peptide is also active against the fungus *Cryptococcus neoformans* (MIC of 3  $\mu$ M), but not against

*Candida albicans* nor does it show any lytic activity on human red blood cells, even at concentrations much higher than those that are antimicrobial (<2% hemolysis at 50  $\mu$ M peptide).

Sequencing of Bac4, one of the two nonfunctional genes, shows it is a highly similar to the corresponding exon and intron regions of Bac7. In particular, if translated, exon four would reveal a Pro- and Arg-rich sequence of 36 amino acid residues with 61% identity and 80% similarity (with a 10 residue gap) to the corresponding Bac7 region. This similarity induced us to chemically synthesize the peptide and to test its antimicrobial activity, although an in-frame translation termination codon in the putative exon 1 suggests that this gene should not be translated. At variance with Bac7 and with the fragment Bac7(1-35) of similar length [2], Bac4 is virtually inactive against all the bacterial and fungal strains mentioned above (MIC values of >96  $\mu$ M) when the antimicrobial assay is carried out in Mueller-Hinton broth, and displays poor activity against *E. coli* only when tested in a low ionic strength buffer.

## Conclusion

Characterization of the bovine cathelicidin gene family has allowed the identification of a congener with a 3' sequence encoding a novel antimicrobial peptide. This peptide belongs to the linear  $\alpha$ -helical peptide group and displays potent activity against antibiotic-resistant pathogens such as methicillin-resistant *S. aureus*, a major problem in hospital-acquired infections, and against opportunistic pathogens infecting immunosuppressed patients, such as *C. neoformans*. For these reasons BMAP-34 could represent a good candidate as a lead for developing new antiinfective agents.

In addition to BMAP-34, another peptide was deduced from a cathelicidin-related genomic sequence and named Bac4. Although inactive, this peptide is of interest due to its high similarity to Bac7, a well known antimicrobial peptide isolated from bovine neutrophils. In fact, using a systemic substitution approach, Bac4 can help in structure/activity relationship studies, being a useful starting point to identify residues that are essential for Bac7 activity.

## Acknowledgements

This study was supported by grants from the National Research Council (CNR) and the Italian Ministry for University and Research (MURST 40% and 60%).

## References

1. Zanetti, M., Gennaro, R. and Romeo, D., FEBS Lett., 374(1995)1.
2. Gennaro R., Scocchi, M., Skerlavaj, B., Tossi, A. and Romeo D, In Hodges, R.S. and Smith, J.A. (Eds.), Peptides: Chemistry, Structure and Biology (Proceedings of the 11th American Peptide Symposium), ESCOM, Leiden, The Netherlands, 1994, p. 461.

# On the reaction kinetics of peptide: Antibody binding in the “BIAcore™” biosensor

**Robert M. Wohlhueter, Sunan Fang, Thomas W. Wells  
and Danny L. Jue**

*National Center for Infectious Diseases, Centers for Disease Control and Prevention, 1600 Clifton Road, Mailstop G36, Atlanta, GA 30333, USA*

Real-time biosensors based on surface plasmon resonance have gained wide acceptance among scientists studying the kinetics of biomolecular interactions. The *BIAcore™* instrument (BIAcore, Inc., Piscataway, NJ) uses a continuous flow system in which one reactant is immobilized on the sensor surface, while the second reactant is directed over that surface in a mobile phase. Analysis of the binding kinetics is typically carried out with curve-fitting procedures which assume a simple, bimolecular reaction mechanism; the software distributed with the instrument is based on this assumption. Critical publications, [1,2] however, have noted that the simple model does not seem to account well for the data, and have suggested that mass transport of mobile-phase ligand into the dextran phase supporting the immobilized ligand may limit the rate of association and complicate estimation of dissociation.

One obstacle to validating conformity to a specific model is the experimental difficulty of varying the concentration of the immobilized ligand. In the experiments reported here we used a biotinylated peptide, and monoclonal antibody specific to it, to generate a wide range of immobilized ligand concentrations. The experiments demonstrate that, at immobilized ligand concentration in excess of about  $1 \times 10^{-5}$  M (in dextran phase), the assumption of a simple, bimolecular model does not pertain. Computer simulations and use of the *Clamp3*<sup>®</sup> software to fit more complicated models globally to the data suggest approaches to remedy the problem.

## Results and Discussion

We generated a series of “immobilized ligand” concentrations by repeatedly injecting biotinyl-KK(NANP)<sub>4</sub> onto a streptavidin surface. At each level of biotinyl-peptide, a near-saturating concentration of anti-peptide IgG was injected. A pulse of chaotropic salt stripped off antibody, to make way for the next round of peptide immobilization. The initial velocity of antibody:peptide binding (Fig. 1) was proportional to peptide concentration only to about  $1 \times 10^{-5}$  M in dextran space (= 150 resonance units of saturation with IgG). Above  $1 \times 10^{-4}$  M, the association reaction showed zero-order kinetics with respect to immobilized peptide. The association reaction was first-order with respect to mobile ligand (cf. inset) over a wide range.

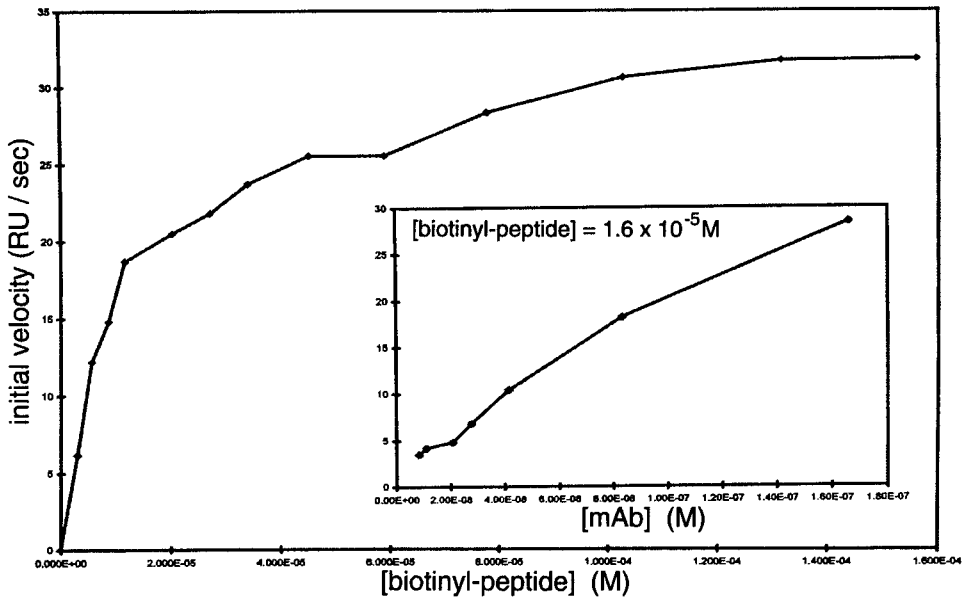


Fig. 1. Immobilized ligand concentration on the sensor surface was varied by consecutive injections of biotinyl-peptide, and initial velocities of binding measured with near-saturating concentrations of monoclonal antibody. Inset shows kinetic dependence of binding on mobile-phase ligand at one of several concentrations tested.

Such experiments suggest that a precursor reaction, dependent only on mobile ligand concentration, asserts rate limitation on the over-all process recorded by the biosensor:  $L_0 = L_i + I = LI$ ; where  $L_0$  and  $L_i$  are mobile-phase ligand outside and inside the dextran phase,  $I$  is immobilized ligand, and  $LI$  is the signal-generating complex. Computer simulations of this model, and use of *Clamp3*<sup>®</sup> [4] to fit real data (none shown), indicate that, for example, at an immobilized peptide concentration of  $6.8 \times 10^{-4}$  M, the velocity of the mass-transport step is 0.17x velocity of the bimolecular association step. Obviously, under such experimental conditions the analysis of *BIAcore*<sup>™</sup> data in terms of the simple, bimolecular model leads to serious faulty estimations of kinetic parameters.

## References

1. Wohlhueter, R.M., Parek, K., Udhayakumar, V., Fang, S. and Lal, A.A., *J. Immunol.*, 153 (1994) 181.
2. Schuck, P. and Minton, A.P., *Analytical Biochem.*, 240 (1996) 262.
3. Myszka, D.G, Morton, T.A., Doyle, M.L. and Chaiken, I.M. *Biophys. Chem.*, 64 (1997) 127.
4. Roden, L.D. and Myszka, D.G., *Biochem. Biophys. Res. Comm.*, 225 (1996) 1073. The *Clamp3*<sup>®</sup> computer program is available at [www.hic.utah.edu/cores/biacore](http://www.hic.utah.edu/cores/biacore)

# V3-mediated neutralization of primary isolates. Serology with synthetic V3 peptides demonstrates deficiencies in anti-V3 response

**R. Pipkorn,<sup>a</sup> A. Lawoko,<sup>b,c</sup> B. Johansson,<sup>d</sup> B. Christenson,<sup>e</sup> B. Ljungberg,<sup>e</sup> U. Dietrich,<sup>f</sup> L. Alkhalili,<sup>g</sup> E-M. Fenyö<sup>g</sup> and J. Blomberg<sup>b</sup>**

<sup>a</sup>Deutsches Krebsforschungszentrum, Heidelberg Germany. <sup>b</sup>Sec.Virology,Dept.of Infec. Diseases and Med. Microbiology, Uppsala, Sweden; <sup>c</sup>Sec.Virology,Dept. Med. Microbiology, Lund Sweden; <sup>d</sup>Dept.of Infectious Diseases, Hålsingborg Sweden; <sup>e</sup>Dept.of Infectious Diseases, Lund, Sweden; <sup>f</sup>Georg Speyer Haus, Frankfurt Germany; <sup>g</sup>Microbiology and Tumor Biology Center, Karolinska Inst., Stockholm Sweden

We wanted to know why the humoral anti-V3 response does not suffice to control viral replication. Initially, we used 92 overlapping decameric, and pentadecameric HIV1MnV3 peptides and 47 singly substituted variants of a south Swedish consensus V3 synthetic peptide with Tanzanian and Swedish HIV-1 infected sera to identify the structures most important for V3 antigenicity in a south cohort. They were located in the N-terminus of the V3 loop, including the motif -TRKRIHIGPG-. Five synthetic tetrameric V3 peptides with sequences derived from the N-terminal half of the V3 loops of primary isolates from four patients in the cohort were then used to immunize rabbits. The four isolates were chosen from patients whose quasispecies had been shown to contain V3 variants to which autologous IgG antibodies were not detectable in EIA's using synthetic V3 peptides [1]. Rabbit antisera and patient autologous sera were used in neutralization assays with the four named primary isolates. The V3 sequences of viruses emerging from the neutralization pressures exerted by such sera were studied.

## Results and Discussion

In three of four cases, there were only low titers (less than 1/40) of neutralizing antibodies found in autologous sera. In one case, the titers were 1/80. This correlates with the demonstrated lack of autologous anti-V3 IgG in this serum. All rabbit antisera were neutralizing (including both autologous and heterologous combinations) to at least 2/4 isolates, meaning that antibodies to the V3 are capable of neutralizing primary isolates. However, rabbit anti-V3 to the apparently B-cell anergic synthetic V3 peptides neutralized autologous isolates in only two of four cases. The V3 sequences of variants emerging from neutralization pressure were studied by RT-PCR and direct sequencing, while those of proviral DNA were studied by PCR, cloning and sequencing randomly selected clones. The following information was revealed:

a) The amino acid sequences of the variant to which autologous IgG antibodies were not detectable in EIAs (B-cell anergic) were in 2/4 cases the majority sequence in proviral DNA. In the third case the majority proviral V3 sequence was one to which autologous IgG

antibodies had been demonstrated. An aberrant, B-cell anergic sequence obtained from the proviral DNA of this latter isolate, containing the sequence, -TRKRMTMGPG-, was not demonstrable in freely cultured virus. In the fourth case a single amino acid substitution - TRKGIHIGPG- to TRKGIHMGPG-, differentiated the B-cell anergic variant from the predominant proviral one.

b) In three of four cases the majority V3 sequence in the supernatant of freely cultured virus was the same as that of the proviral DNA. In two of these cases the relevant sequence was B-cell anergic. Thus, in these latter cases there was a deficient humoral response to the V3 region represented in the predominant HIV quasispecies. In one of these two cases, the same sequence emerged from under 95% neutralization with autologous serum, indicating that the lack of IgG to this particular V3 may have afforded the variant neutralization evasion capacity.

c) When the V3 sequences of variants emerging from the neutralization pressure of rabbit antisera on the synthetic peptide variant with sequences from the same isolate were studied, mutations were found in the V3 region that, were determined to be important for antigenicity in both such cases, further confirming this finding.

## Conclusion

Anti-V3 antibodies are capable of neutralizing primary isolates on their own. B-cell anergy towards the principal neutralization determinant of HIV-1 variants infecting an individual may in part be an explanation for apparent immunotolerance to infection, while their isolates are often susceptible to neutralization by heterologous sera. EIAs with singly substituted variants of south Swedish consensus N-terminal V3 peptides showed that antigenicity of the V3 loop (PND) of HIV-1 is determined to a great extent by structures in the amino terminal half corresponding to the HIV1MN-TRKRIHIGPG- motif.

## Reference

1. Lawoko, A., Johansson, B., Dash, R., Falck, L., Dietrich, U., Pipkorn, R., Nilehn, B. and Blomberg, J., *J. Infec. Dis.*, 172 (1995) 682.

# Conformational mapping of a neutralizing epitope of the C4 region of HIV-1 gp120 with cyclic and bicyclic peptides

Ruoheng Zhang,<sup>a</sup> Yuan Xu,<sup>a</sup> Gerald R. Nakamura<sup>b</sup>,  
Philip W. Berman<sup>b</sup> and Arnold C. Satterthwait<sup>a</sup>

<sup>a</sup>*Department of Molecular Biology, The Scripps Research Institute, La Jolla, CA 92037, U.S.A and*

<sup>b</sup>*Genentech, Inc., South San Francisco, CA 94080, USA*

A series of murine monoclonal antibodies (1024, 1091, 1096, 1097, 1110, 1112, 1127) bind gp120 on HIV-1 and block reaction with the CD4 receptor [1]. Mabs 1024 and 1127 potently neutralize HIV-1(MN), rivaling those directed to the V3 loop[1]. While each Mab requires K429 in the C4 region for binding and Mab 1024 binds a recombinant C4 fragment [1], the identification of fine structure and conformational specificity is required for synthetic vaccine design[2]. In this study, we identify the epitope recognized by these Mabs and test a new strategy for conformational mimicry using monocyclic and bicyclic disulfide loops.

## Results and Discussion

Peptides were synthesized with an ACT-350 multiple peptide synthesizer using Fmoc chemistry. Disulfide loops were prepared by linking two free cysteines in 10% DMSO/H<sub>2</sub>O, pH 4 [3]. Bicyclic peptides were formed by linking two free cysteines and then two protected Cys-Acm with iodine in 10% acetic acid. Peptides were purified by HPLC, confirmed by MS and monitored for stability by HPLC before and after ELISAs.

Acetyl-KQIINMWQKVGKAMYAPPIEGQIRC-NH<sub>2</sub> from the C4 region was coupled to maleimide-activated BSA. Each Mab from the series with the possible exception of Mab 1024 bound the peptide-BSA in an ELISA. Shortening the C4 peptide from its C-terminus identified PPI as one end of the epitope. Shortening acetyl-KQIINMWQKVGKAMYAPPIE from its N-terminus identified acetyl-KVGKAMYAPPI-NH<sub>2</sub> as the shortest peptide that binds each of the Mabs. Mab 1024 binds this peptide much better than the longer peptides in the ELISA. Although this region of gp120 is known to be exposed, efforts to raise neutralizing antibodies to corresponding peptides have failed, presumably reflecting a conformational requirement [4]. To begin defining and mimicking the conformation of the C4 epitope, the following strategy was pursued.

First, an L-alanine scan of Ac-KVGKAMYAPPIEC-NH<sub>2</sub> (the two Ala were scanned with Gly) using an ELISA showed that all amino acids except V, M and E bind each of the Mabs with the most critical residues being the two Ks and I. A competition ELISA was used to fine tune these results for Mabs 1024 and 1127. Substitution of M and E with L-Ala may slightly improve binding. Replacing V with L-Ala reduces binding several-fold. Replacing either of the terminal K or I residues with L-Ala reduces affinity more than 1000-fold. Interestingly, substitution of Gly with D-Ala improves affinity, suggesting that the Mabs bind either KVGK or VGKA as a reverse turn [5].

Second, all possible disulfide loops that could be found by replacing non-critical amino acids with L-Cys, replacing Gly with D-Cys and using L-Cys and in some cases D-Cys at the termini of the epitope were synthesized. Relative affinities of the disulfide loops for Mabs 1024 and 1127 were measured in competition ELISAs (Table 1). The data is approximate. Mabs 1024 and 1127 showed similar profiles (Table 1). Although a range of affinities was observed, no cyclic peptide binds better than its' corresponding linear peptide. However, acetyl-[CKVKGAMYAPPIC]-NH<sub>2</sub> shows only a 4-8 fold reduction in affinity relative to acetyl-GKVGKAMYAPPIG-NH<sub>2</sub>. This observation is significant since the terminal K and I residues are critical for binding. Together with the scanning data, it strongly implies that the epitope is a well exposed loop that positions the N- and C-terminal amino acids, K and I, close together in the Mab binding pocket.

Table 1. Competition ELISAs of Peptides for C4 Mabs.

Peptides	MAb 1024 IC <sub>50</sub> (10 <sup>-7</sup> M)	MAb 1127 IC <sub>50</sub> (10 <sup>-7</sup> M)
Ac-GQKVGKAMYAPPIG-NH <sub>2</sub>	5	0.2
Ac-KVGKAMYAPPIEG-NH <sub>2</sub>	5	0.2
Ac-[CQKVGKAMYAPPIC]-NH <sub>2</sub>	20	1.5
Ac-GKVGKA[CYAPPIEC]-NH <sub>2</sub>	520	40
Ac-GKV[XKAMYAPPIEC]-NH <sub>2</sub>	105	20
Ac-GKV[XKAC]YAPPIEG-NH <sub>2</sub>	90	3
Ac-[CQKV[XKAC]YAPPIC]-NH <sub>2</sub>	5	0.8

X= D-Cys. Brackets delineate disulfide loops.

Third, we tested several bicyclic disulfide loops built on the best binding loops. One of the bicyclic peptides, acetyl-[CQKV[(D-Cys)KAC]YAPPIC]-NH<sub>2</sub> showed improved affinity relative to the monocyclic peptides and affinity similar to the corresponding linear peptide for both Mabs 1024 and 1127 (Table 1). This implies that the Mabs bind a complex loop with multiple turns that is partially mimicked by the bicyclic peptide.

This research was supported by NIH AI37512. This is publication 11041-MB from The Scripps Research Institute.

## References

1. Nakamura, G.R., Byrn, R., Wilkes, D.M., Fox, J.A., Hobbs, M.R., Hastings, R., Wessling, H.C., Norcross, M.A., Fendly, B.M. and Berman, P.W., *J. Virol.*, 67 (1993) 6179.
2. Satterthwait, A.C., Cabezas, E., Dovalsantos, E.Z., Zhang, M.Z. and Zhang, R., this volume
3. Tam, J.P., Wu, C.R., Liu, W., and Zhang, J.W., *J. Am. Chem. Soc.* 113 (1991) 6657.
4. McKeating, J.A., Moore, J.P., Ferguson, M., Mardsden, H.S., Graham, S., Almond, J.W., Evans, D.J. and Weiss, R.A., *AIDS Res. and Human Retrovir.*, 8 (1992)451.
5. Degrado, W.E., *Adv. Prot. Chem.*, 39 (1988) 51.

## **Further characterization of anchor and non-anchor residues on deca- and undeca-peptides in addition to nona-peptides, which bind to the HLA Class I molecules (HLA-B\*3501)**

**Kiyoshi Nokihara,<sup>a</sup> Christian Schönbach<sup>b</sup> and Masafumi Takiguchi<sup>b</sup>**

*<sup>a</sup>Shimadzu Scientific Research Inc., Kanda Nishikicho 1-3, Chiyodaku, Tokyo 101 Japan, <sup>b</sup>Institute of Medical Science, University, of Tokyo, Shirokanedai, Minato-ku, 108 Tokyo, Japan*

HLA-I binds endogenously processed self or viral peptides and presents them to CTL. Interactions between ligand peptides and MHC molecules are strictly governed by a motif [1]. HLA-I binding peptides carry anchor residues which are a minimum requirement for recognition, but residues other than anchors are also important in binding nona-peptides [2]. An efficient quantitative assay method has been developed using flow cytometry with the RMA-S cells transfected with the HLA gene [3]. Binding of peptides to HLA-I can be quantitated using this assay system and statistical residue-pocket analysis of binding for the 9-mer peptides has been successfully carried out [2, 4]. In the present report, further characterization of the binding of 10- and 11-mer peptides is described and compared with 9-mer peptides.

### **Results and Discussion**

Highly efficient solid-phase syntheses of more than 400 nona~undeca peptides related to virus proteins (HIV-1, HTLV-1, -2, HCV, HPV) were performed. Synthetic peptides were characterized by HPLC and MALDI-MS. Binding affinity was classified into four different classes with score values between 3 and 0. The results indicate that all binding peptides have two anchor residues at the C-terminus (Y, L, I, F or M) and a 2nd position (P) as an additional anchor, which are minimum requirements. The positive and negative influence of amino acid side-chain functions at non-anchor positions has been statistically analyzed to evaluate the binding features (detail in [5]). In the case of 10 mers, aromatic bulky residues at position 1 and aliphatic hydrophobic residues at positions 3, 5 and 8 enhanced binding but positively charged side-chains at positions 6 and Pro at position 8 gave negative effects. In the case of 11 mers, positions 1 and 3 are similar to 10 mers and acidic or polar residues at positions 4, 8 and 10 enhanced binding but negative effects were observed for small residues carrying small side chains at position 1 and positively charged residues at positions 3, 5 and 7. The forecasting of binding peptides was carried out using *ca* 30 peptide fragments independently chosen from EBV and HCV to confirm the prediction based on the present results. The effects of residue change are summarized in Fig. 1.

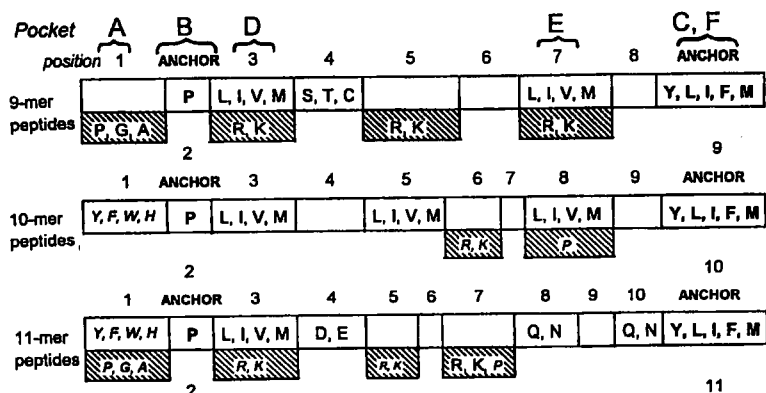


Fig. 1. Refined HLA-B\*3501 binding motif for nona-, deca-, and undeca-peptides. Hatched residues in the lower panel are associated with low affinity to HLA-B\*3501 and residues in the upper panel significantly enhance binding to HLA-B\*3501. Blank boxes in the upper panel are permissive to all residues. Small italicized residues were associated with low (lower panel) or high (upper panel) binding.

## Conclusion

The refined HLA-B\*3501 peptide binding motifs enhanced the screening of T-cell epitopes. The disparity between positive effects at the middle and C-terminal part (positions 5-8 and 10) of 11-mers and shorter peptides supports the extrusion of 11-mer residues at positions 5, 6 and 7, away from the HLA-B\*3501 binding cleft. These binding peptides were mixed with the lipopeptide and immunized to HLA-B\*3501 transgenic mice. After *in vitro* stimulations, several peptides showed a CTL response [6]. These results indicate that the peptides are possible vaccine candidates.

## References

1. Reviewed in: Ramensee, H-G., Friede, T. and Stevenovic, S., *Immunogenetics*, 41 (1995) 178.
2. Schönbach, C., Ibe, M., Shiga, H., Takamiya, Y., Miwa, K., Nokihara, K. and Takiguchi, M., *J. Immunology*, 154 (1995) 5951.
3. Takamiya, Y., Nokihara, K., Ferrone, S., Yamaguchi, M., Kano, K., Egawa, K. and Takiguchi, M., *Int. Immunol.*, 6 (1994) 255.
4. Nokihara, K., Yamaguchi, M., Schönbach, C., Ibe, M., Shiga, H. and Takiguchi, M., in Kaumaya, P.T.P. and Hodges, R.S. (Eds), *Peptides: Chemistry, Structure and Biology* (Proceedings of the Fourteenth American Peptide Symposium), Mayflower Scientific Ltd., Birmingham, UK, 1996, p. 820.
5. Schönbach, C., Miwa, K., Ibe, M., Shiga, H., Nokihara, K. and Takiguchi, M., *Immunogenetics*, 45 (1996) 121.
6. Schönbach, C., Nokihara, K., Bangham, C.R.M., Kariyone, A., Karaki, S., Shiga, M., Takatsu, T., Egawa, K., Wiesmüller, K-H. and Takiguchi, M., *Virology*, 226 (1996) 102.

## **Delivery of peptide epitopes for HTLV-I using biodegradable microspheres**

**Melanie Frangione,<sup>b</sup> Travis Rose,<sup>d</sup> Steven P. Schwendeman,<sup>e</sup> Vernon C. Stevens<sup>b</sup> and Pravin T.P.Kaumaya<sup>a,b,c,d</sup>**

*<sup>a</sup>College of Medicine, <sup>b</sup>Departments of Obstetrics and Gynecology, <sup>c</sup>Medical Biochemistry, and <sup>d</sup>Microbiology, and <sup>e</sup>College of Pharmacy, Division of Pharmaceutics, The Ohio State University, Columbus, Ohio 43210, USA.*

Peptide epitopes, being poorly immunogenic, require efficient delivery protocols as well as the co-administration of an appropriate adjuvant to enhance the immune response. New peptide delivery formulations that optimize the interaction of antigen with immune system cells are urgently required for the design of new vaccines. Thus far, one of the most promising antigen delivery systems appears to be biodegradable polymer microspheres of poly(lactide-co-glycolide) (PLGA). This polymer has the advantage of being approved by the FDA as safe for human use. Furthermore, biodegradable microspheres can provide the prolonged and sometimes pulsatile release that can effectively mimic and possibly replace conventional immunization protocols.

In an effort to develop peptide vaccines for the human T-lymphotropic virus type I (HTLV-I), a new peptide construct has been synthesized and encapsulated in biodegradable microspheres. This construct, denoted MVFMR4, consists of the viral envelope glycoprotein 46 (env gp46) sequence of 175-218 linked C-terminal to the promiscuous T-cell epitope, MVF, of the measles virus fusion protein (aa 288-302). The gp46 sequence was chosen because of the presence of an immunodominant region (aa190-209) [1], a major T-cell epitope (aa194-210) [2], predicted CTL epitopes [3], and the ability of the sequence 190-209 to elicit high-titered antibodies specific for the native envelope protein [4]. We also previously demonstrated that a similar sequence (SP4exMVF) of HTLV-I elicited high titers of anti-peptide antibodies in both mice and rabbits that recognized the recombinant proteins RE3 (env 165-306) and MTA-1 (env 162-209). In this work we compare the immune responses of rabbits immunized with i) encapsulated peptide with adjuvant (nor-muramyl dipeptide), ii) encapsulated peptide without adjuvant, and iii) non-encapsulated peptide with adjuvant.

### **Results and Discussion**

A novel encapsulation procedure using trifluoroacetic acid as the polymer carrier solvent was used to encapsulate the peptide construct MVFMR4 with high loading. Sera were collected weekly and analyzed by direct ELISA. Rabbits showed moderate to high titers after five weeks. Initial responses indicated that the presence of nor-MDP had no apparent effect. However, after six weeks, titers clearly demonstrated the effects of adjuvant and indicated a synergistic effect with the encapsulated peptide. The response of the encapsulated peptide without adjuvant suggests that the microspheres are adjuvant-active. Cross reactivity data, as

shown in Fig. 1, indicate that the antibodies also bind to the HTLV-I recombinant protein, RE3 (aa165-306). Antibodies raised to MVFMR4 were shown to not significantly bind MVF. Rabbit sera were also studied by competitive ELISA. The immunogen MVFMR4 was shown to inhibit antibody binding to both MVFMR4 and to the recombinant protein RE3. Results indicated that the affinities of the antibodies for MVFMR4 and RE3 are similar. This demonstrates that the peptide construct is effectively mimicking the native protein.

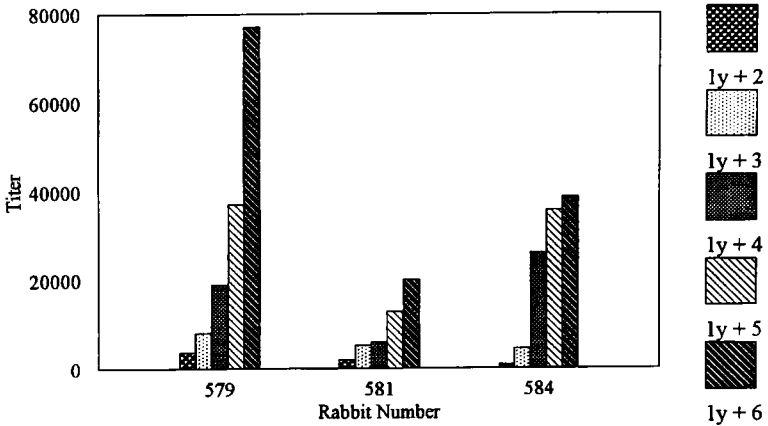


Fig. 1. Antibodies titered against the recombinant HTLV-I protein RE3 by direct ELISA. Rabbit 579 was immunized with encapsulated MVFMR4 and adjuvant, rabbit 581 with encapsulated MVFMR4, and rabbit 584 with free MVFMR4 and adjuvant.

In conclusion, the ability of the polymer microspheres to potentiate the immune response has been demonstrated. Furthermore, antibodies raised to the MVFMR4 epitope were highly specific for the native protein. The effectiveness of the immunogen will be evaluated by syncytia inhibition assay and viral challenge of the immunized rabbits with HTLV-I infected cells. (This work was supported by grants AI40302 and AI0D40302-01 to PTPK).

## References

1. Palker, T., Tanner, M., Scarce, R., Strleim, R., Clark, M., and Haynes, B., *J. Immunol.*, 142 (1989) 971.
2. Baba, E., Nakamura, M., Tanaka, Y., Kuroki, M., Itoyama, Y., Nakano, S. and Niho, Y., *J. Immunol.*, 151 (1993) 1013.
3. Pique, C., Connan, F., Levilain, J., Choppin, J. and Dokhelar, M., *J. Virol.*, 70 (1996) 4919.
4. Lairmore, M.D., DiGeorge, A.M., Conrad, S.F., Trevino, A.V., Lal, R.B. and Kaumaya, P.T.P., *J. Virol.*, 69 (10) (1995) 6077.

## **Session XII**

### **Analytical Methods**



# Differences in encephalitogenicity in MBP peptide 68-88 due to histidine racemization

**P. L. Jackson,<sup>b</sup> M. Villain,<sup>a</sup> F. S. Galin,<sup>a</sup> N. R. Krishna<sup>b</sup> and J. E. Blalock<sup>a</sup>**

*<sup>a</sup>Dept. Physiology and Biophysics, <sup>b</sup>Dept. Biochemistry & Mol. Genetics, University of Alabama at Birmingham, Birmingham, Al, 35294, USA*

Experimental allergic encephalomyelitis (EAE), a demyelinating disease affecting the central nervous system, can be actively induced in rats and mice by immunization with myelin basic protein (MBP) or MBP peptides. Residues 68-88 of guinea pig myelin basic protein (MBP68-88) (GSLPQKSQRSQDENPVVHF) is an encephalitogenic epitope in the Lewis rat. In the synthesis of this peptide by Fmoc SPPS, we encountered a second product (Comp2) which, unlike MBP 68-88, had weak, if any, encephalitogenic activity. This was not a complete surprise, since specific amino acid substitution or N-terminal acylation of MBP peptides has been shown to affect their encephalitogenic properties [1,2]. Different analytical techniques were used to characterize the two compounds and NMR analysis showed that a racemization of His<sup>87</sup> had occurred during the synthesis. The presence of a D-His in Comp2 was confirmed by carboxypeptidase A digestion. In this report, we show that not only can racemization of the L-His to D-His at position 87 alter the encephalitogenicity of the MBP68-88 peptide but can also protect animals from EAE induced by the native peptide.

## Results and Discussion

After standard Fmoc SPPS using OPfp/HOAt amino acid, TFA cleavage and ether precipitation, C18 RP-HPLC analysis of crude MBP 68-88 peptide showed the presence of two products in a ratio of 2 to 3. The two compounds were purified by SemiPrep RP-HPLC. The purified products maintained a different retention time after lyophilization. MALDI-TOF mass spectrometry showed an essentially identical mass for both products (Comp1 2153.78 Da, Comp2 2154.63 Da). Amino acid analysis and sequencing gave the expected amino acid composition. CD spectra in the 190-280 nm region showed no secondary structure for either compound. NMR analysis was used to elucidate the difference between the two compounds. Magnitude mode correlation experiments (COSY) were done in 100% D<sub>2</sub>O at pH 6.3 on a Bruker WH-400. The COSY indicated differences in the His<sup>87</sup> ring (H) proton chemical shifts. Correlation Experiments (TOCSY, 70msec) and ROESY (rotating Frame Overhauser experiment, 150 msec) were done on 1mM peptide samples in 90% H<sub>2</sub>O/10% D<sub>2</sub>O pH 6.3 on a Bruker AM-600. Small chemical shift changes were seen in NH of His<sup>87</sup> and Phe<sup>88</sup>. Small downfield shifts were also seen for Val<sup>86</sup> beta and methyl protons, consistent with the deshielding expected for D-L compounds [3]. These differences indicate the presence of LVal<sup>86</sup> and DHis<sup>87</sup> in Comp2. For this synthesis we used FmocHis(Trt)OPfp/HOAt, which theoretically should protect the His from its natural tendency to racemize. To further confirm these findings the two compounds were digested using Carboxypeptidase A. The products

were purified by HPLC and analyzed by MALDI-TOF. As expected, due to the presence of Pro<sup>84</sup>, digestion of Comp1 stopped at Val<sup>85</sup> (Carboxypeptidase A is unable to cleave Pro-X sequences). Comp2 was unaffected by the enzyme and no cleavage was detected. Carboxypeptidase A is stereoselective for L amino acids.

To determine whether racemization of His<sup>87</sup> would affect the encephalitogenicity of the peptide, Lewis rats were immunized in the hind foot pads with 100 µg of either the L or D-containing MBP68-88 peptide, emulsified in complete Freund's adjuvant (CFA). The native peptide (Comp1) was effective in inducing EAE, in that 80% (4/5) of the animals showed clinical signs of disease after day 10 with a mean clinical score (MCS) of 1.2. However, in the group that received Comp2 only, one of five animals showed any signs of the disease and in that animal the severity was low (Grade 1). Animals receiving PBS/CFA alone showed no signs of disease. Two weeks after the animals in group one recovered, all the animals were challenged with Comp1. In Lewis rats, native MBP68-88 peptide induces an acute monophasic form of EAE that cannot be reinduced. Therefore, as expected, the animals initially immunized with Comp1 showed no sign of EAE (MCS 0) as compared to the PBS controls in which 80% (4/5) got EAE with a MCS of 2. Interestingly, only 1/5 (20%) of the animals immunized with Comp2 prior to challenge with Comp1 got a mild form of EAE (MCS of 0.2)(Table 1).

*Table 1. Each group consisted of 5 animals. 100 µg/animal were used for both peptides.*

Group	First injection with:	MCS at day 13	Second injection with:	MCS at day 42
1	87L MBP68-88	1.2	87L MBP68-88	0
2	87D MBP68-88	0.2	87L MBP68-88	0.2
3	PBS control	0	87L MBP68-88	2.0

Collectively, these results suggest that racemization of His<sup>87</sup> from L to D conformation can suppress the encephalitogenic activity of the peptide. Moreover, this peptide seems to have therapeutic potential in that it can prevent active induction of EAE by the native form.

## Reference

1. Zhao, W., Wegmann, K.W., Trotter, J.L., Ueno, K. and Hickey, W.F., *J Immunol.*, 153 (1994) 901.
2. Gaur, A., Boehme, S.A., Chalmers, D., Crowe, P.D., Pahuja, A., Ling, N., Brocke, S., Steinman, L. and Conlon, P.J., *J. Neuroimmunol.*, 74 (1997) 149.
3. Halpern B., Chew L.F. and Weinstein B., *J. Am. Chem. Soc.*, 89 (1967) 5051.

# TFA/HCl mixture as an alternative to the standard propionic acid/HCl mixture for aminoacyl- and peptidyl-resin hydrolysis

**G.N. Jubilut, A. Miranda, E. Oliveira, E.M. Cilli,  
M. Tominaga and C.R. Nakaie**

*Departamento de Biofísica, Universidade Federal de São Paulo  
Rua 3 de Maio, 100 - São Paulo, SP 04044-020, Brazil.*

For decades, the propionic acid/12 N HCl (1:1, v/v) mixture at 130 °C [1] or 160 °C [2] has been used as the standard solution for aminoacyl- or peptidyl-resin hydrolysis. However, no further systematic study has been carried out concerning the applicability of this hydrolysis protocol to other resins introduced later in the SPPS field. In this regard, we have recently demonstrated that much longer hydrolysis time than reported in the literature is necessary for quantitative cleavage of aminoacyl- or peptidyl-groups from most resins used in the Boc-strategy [3]. The hydrolysis times necessary for complete cleavage of Phe resin are 100 h (at 130 °C) or 30 h (at 160 °C) for benzhydrylamine-resin (BHAR) and 30 h (at 130 °C) or 18 h (at 160 °C) for p-methyl-benzhydrylamine- (MBHAR) and 4-(oxymethyl)-phenylacetamidomethyl-resin (PAMR). In order to propose a more accelerated hydrolysis protocol, the present report describes a comparative time-course hydrolysis study of aminoacyl- and dipeptidyl-resins using a trifluoroacetic acid (TFA)/12 N HCl hydrolysis mixture in different proportions. The Gly and Phe residues and the corresponding dipeptide sequences (Ala-Gly and Ala-Phe) coupled to PAMR, BHAR, MBHAR and also to chloromethyl-resin (CMR) were studied as models for this alternative hydrolysis condition at 160 °C.

## Results and Discussion

Initially, the hydrolysis rates of Phe-BHAR in several 12 N HCl solutions containing increasing amounts of TFA (from 9:1 to 1:1, v/v) were measured. The fastest cleavage of the resin-bound aminoacyl group was obtained at a 1:3 ratio of TFA to HCl. This binary solution was therefore selected for comparative time-course hydrolysis studies with the propionic acid/HCl mixture.

As seen in Table 1, irrespective of the resin or the nature of the resin-bound group, the hydrolysis rate with the TFA/HCl mixture was always higher than with the standard propionic acid/HCl solution. For instance, in the stable Phe-BHAR or Ala-Phe-BHAR samples, reaction times necessary for complete hydrolysis at 160 °C decreased from 30 to 20 h and from 24 to 15 h, respectively. These findings suggest that, similar to findings concerning the hydrolysis of proteins [4], the 12 N HCl solution containing TFA is a more efficient mixture to accelerate cleavage of any resin-bound aminoacyl- or peptidyl- groups.

Table 1. The approximate time necessary for complete hydrolysis of aminoacyl- and peptidyl-resins in: (A), propionic acid:12 N HCl (1:1, v/v) and (B), TFA:12 N HCl (1:3, v/v) at 160 °C.

	CMR		PAMR		MBHAR		BHAR	
	A	B	A	B	A	B	A	B
	Time (h)							
Gly-R	--	--	8	2	10	4	15	8
Phe-R	--	--	15	5	15	5	30	20
Ala-Gly-R	0.5	0.3	3	1	3	1	5	3
Ala-Phe-R	7	1	8	3	10	4	24	15

Confirming previous results [3], regardless of the hydrolytic solution Phe was more stable than Gly towards acid cleavage, and the hydrolysis rate from the resin was higher when their comparative N-terminal portions were acylated with another aminoacyl group (Ala). Finally, in comparative studies of resins, the following order of decreasing acid stability was observed: BHAR (MBHAR = PAMR) CMR.

### Acknowledgments

Financial support from FAPESP, CNPq and FINEP, from Brazil, is gratefully acknowledged.

### References

1. Scotchler, J., Lozier, R. and Robinson, A.B., *J. Org. Chem.*, 35 (1970) 3151.
2. Westall, F.C. and Hesser, H., *Anal. Biochem.*, 61 (1974) 610.
3. Jubilut, G.N., Marchetto, R., Cilli, E.M., Oliveira, E., Miranda, A., Tominaga, M. and Nakaie, C.R., *J. Braz. Chem. Soc.*, 8 (1997) 65.
4. Tsugita, A. and Scheffler, J.J., *Eur. J. Biochem.*, 124 (1982) 585.

# Investigation of aggregation and binding of $\beta(12-28)$ using NMR spectroscopy

Dimuthu A Jayawickrama and Cynthia K. Larive

Department of Chemistry, University of Kansas, Lawrence, KS 66045, USA

Aggregation is a common problem associated with the purification, analysis, stability and activity of proteins and peptides. Hydrophobic interactions often play an important role in stabilizing these aggregates in aqueous solutions. This has been investigated using a model peptide, a 17 residue fragment  $\beta(12-28)$ , VHHQKLVFFAEDVGSNK, of the Alzheimer's associated  $\beta$ -amyloid peptide at low pH in aqueous solution. Previous studies have shown that  $\beta(12-28)$ , like the parent 39-42 residue peptide, undergoes amyloid fibril formation *in vitro* above pH 4[1]. At low pH the NOESY spectrum of  $\beta(12-28)$  shows strong unusual cross peaks in the aromatic region defined by hydrophobic residues 17-21[2] that suggest formation of aggregates. Pulsed-field gradient nuclear magnetic spectroscopy is used to determine the diffusion coefficient of the peptide [3]. Since the diffusion coefficient is inversely proportional to the size, an increase in size will result in a decrease in the diffusion coefficient. The concentration dependence of the  $\beta(12-28)$  diffusion coefficient is indicative of self-association, consistent with a monomer-dimer equilibrium.

Chemical additives such as beta-cyclodextrin ( $\beta$ -CD), trimethylsilylpropionic acid (TSP) and naphthylalanine (NapAla) have also been used to probe the role of hydrophobic and  $\pi$ - $\pi$  interactions in aggregation. Furthermore, the relaxation rates and rotational correlation times ( $\tau_c$ ) of hydrophobic groups of the peptide and chemical additives can be used to evaluate the degree and site of binding. The use of capillary electrophoresis was examined for the measurement of peptide aggregation and binding to these and other chemical agents, although in our hands these results were unsuccessful.

## Results and Discussion

The change in chemical shifts of Val<sup>18</sup>, Leu<sup>17</sup>, Phe<sup>19</sup> and Phe<sup>20</sup> with  $\beta$ -CD concentration (Fig. 1.) suggests complex formation involving this region of the amino acid sequence. The changes in chemical shifts of the Val<sup>18</sup> methyl groups are the most pronounced, indicating binding of the  $\beta$ -CD to the Val<sup>18</sup> side chain. Alternatively, complexation of one of the nearby phenyl rings or a change in the conformation of the peptide could also result in a change in the Val<sup>18</sup> methyl proton chemical shifts due to a change in the local chemical environment. In Fig. 1, similar changes are observed for both the Phe<sup>20</sup> and Leu<sup>17</sup> proton chemical shifts.

TSP appears to interact strongly with the  $\beta(12-28)$  peptide at low pH. In solutions of TSP and the peptide the linewidth of TSP increases significantly as shown in Table 1. TSP

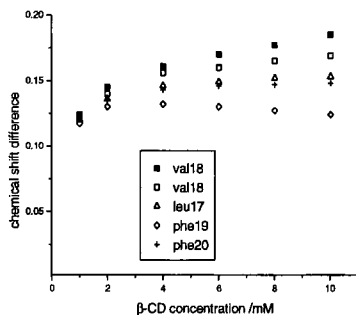


Fig. 1. The change in chemical shifts of Val<sup>18</sup>, Leu<sup>17</sup>, Phe<sup>19</sup> and Phe<sup>20</sup> with  $\beta$ -CD concentration.

can provide a strong hydrophobic face with its three methyl groups and, therefore, interact with the hydrophobic region of the peptide. Electrostatic interactions of the negatively charged TSP with the positively charged peptide may also stabilize this interaction. In addition, a significant decrease in the diffusion coefficient of TSP (Table 1) is indicative of binding to the peptide.

Table 1. Results of the TSP titration of 1.48 mM  $\beta$ (12-28).

[TSP]	linewidth	$D_{\text{TSP}} \times 10^6$
0.20 mM	40.47 Hz	
1.53	34.37	
1.94	34.59	3.4 cm <sup>2</sup> s <sup>-1</sup>
2.54	34.59	3.8
2.75	31.86	4.6
3.33	31.29	
4.25	28.64	

In conclusion, hydrophobic contacts can be probed with NMR by measuring the effect of small molecules with a hydrophobic and/or aromatic nature. Chemical shifts, linewidths and diffusion coefficients all can be used as analytical parameters to investigate these non-polar intermolecular interactions.

## References

1. Krischner, D.A., Indouye, H., Duffy, L.K., Sinclair, A., Lind, M. and Selkoe, D., J. Proc. Natl. Acad. Sci. U.S.A., 84(1987)6953.
2. Jayawickrama, D., Zink, S., Vander Velde, D., Effiong, R. L. and Larive, C.K., J. Biomol. Struct. Dyn., 13(1995)229.
3. Wu, D., Chen, A., Johnson, C. S., Jr., J. Magn. Reson. A., 115(1995)260.

# ESI-MS and MALDI-MS analysis, and amino acid sequencing of three multiple-antigen peptides (MAPs)

Robert R. Becklin<sup>a</sup> and Dominic M. Desiderio<sup>a,b</sup>

*Charles B. Stout Neuroscience Mass Spectrometry Laboratory, Departments of <sup>a</sup>Biochemistry & <sup>b</sup>Neurology, University of Tennessee, Memphis, Memphis, TN 38163, USA*

ESI-MS and MALDI-MS were used to determine the MWs and amino acid sequencing was used to determine the sequences of three MAPs whose peptide sequences were derived from the cloned rat delta-opioid receptor (DOR). MAPs are synthetic compounds that contain multiple copies (eight in our case) of a peptide attached to an oligomeric, branched lysine core matrix and are used as immunogens for the production of antibodies. The inherent advantage of the MAP approach over the traditional peptide-carrier protein approach is that the immunogen is a small structural unit that is amenable to characterization prior to immunization. Such characterization allows full confidence in the interpretation of results gained from the use of anti-MAP antisera.

## Results and Discussion

Each MAP was purified by RP-HPLC prior to ESI-MS, MALDI-MS and amino acid sequencing. Table 1 shows the amino acid sequence of each peptide that is coupled to the MAP core matrix via its carboxy terminus and the calculated and observed MW for each MAP. An AutoSpecQ instrument (VG-Fisons) was used for ESI-MS and a Voyager Biospectrometry workstation (PerSeptive Biosystems) was used for MALDI-MS. The ESI-MS spectrum (Fig. 1A) and the MALDI-MS spectrum (Fig. 1B) of B3 MAP each shows a multiply protonated ion series. Therefore, MAPs act much like proteins and peptides during ionization as a range of multiply charged ions is generated. Similar results were obtained for B2 MAP and B4 MAP. HPLC purification significantly improved the MALDI-MS mass resolution of each MAP. MALDI-MS appears to be an easier approach for MAP characterization and is not as susceptible to impurities as is ESI-MS, although mass accuracy better in ESI-MS. Edman-based sequencing determined the full, correct amino acid sequence of each peptide on each MAP.

The combination of HPLC, MS and amino acid sequencing proved to work very well for the identification and characterization of each MAP and will also likely prove to be a powerful method for the characterization of other MAPs.

Table 1. Amino acid sequence, calculated MW and observed MW of B2, B3 & B4 MAPs.

	Amino Acid Sequence	Calculated MW	ESI observed MW	MALDI observed MW
B2 MAP	SGSPGARSASS-	8,553.0	8,540 (0.2%)	8,497 (0.7%)
B3 MAP	MEPVPSARAEL-	10,444.3	10,455 (0.1%)	10,380 (0.6%)
B4 MAP	GQEPGSLRRPRQ-	11,893.5	11,976 (0.7%)	11,862 (0.3%)

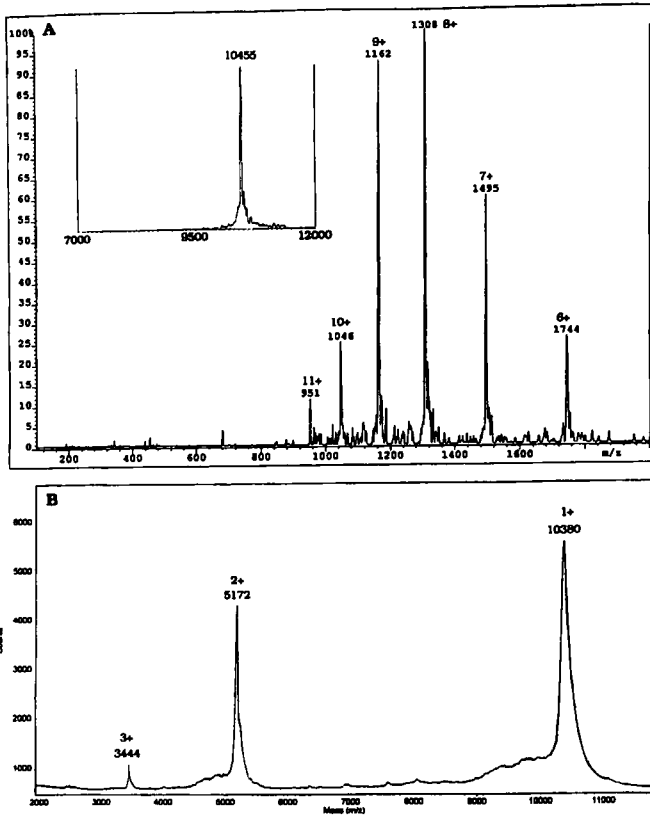


Fig. 1. A) ESI-MS spectrum and B) MALDI-MS spectrum of HPLC-purified B3 MAP. The insert in A) contains the transformed ESI-MS spectrum.

# Stability studies on peptide aldehyde enzyme inhibitors

Patricia A. Messina, John P. Mallamo, and Mohamed A. Iqbal  
*Cephalon, Inc. West Chester, PA 19380, USA*

Peptide aldehydes are reversible [1,2], competitive [3], highly potent and specific inhibitors of cysteine [4,5], serine [6], and aspartyl proteases [7,8]. Although peptide aldehydes may not be ideal drug candidates due to their short half-life in biological systems, they are very often useful in optimizing the structural requirements of protease inhibitors.

Instability of peptide aldehydes is observed under several conditions and frequently arises from hydration [10] and oxidation of the aldehyde functional group and, in some cases, by an internal cyclization [11,12] leading to a hemiaminal. During the synthesis and design of protease inhibitors, we observed the cyclization and dehydration of dipeptide aldehydes. In order to study the structural and environmental factors which govern by-product formation, we carried out a systematic study. Of several dipeptide aldehydes exposed to neutral and acidic conditions, the results suggest that stability is increased in the presence of a bulky residue at P1, enantiomeric configurations at P1 and P2, and a tosyl protecting group.

## Results and Discussion

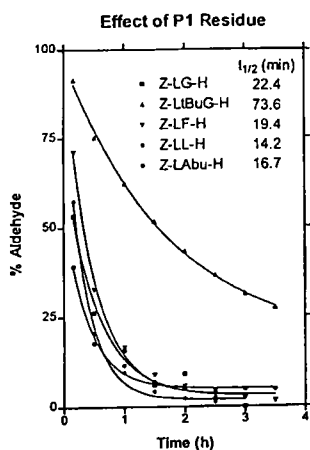


Fig. 1

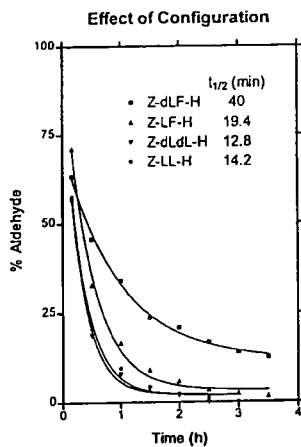


Fig. 2

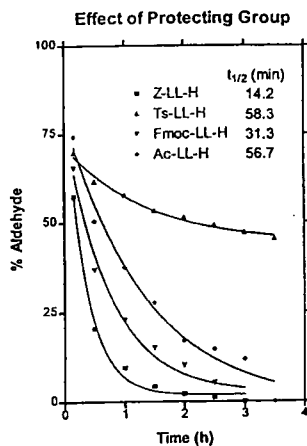


Fig. 3

The selected compounds did not show any cyclization under neutral conditions. Under acidic conditions the following results were obtained. Dipeptide aldehyde analogues containing Gly, Abu, Leu, tBuG, and Phe at the P1 position were studied. The results indicate that the bulky sidechain in tBuG enhances the stability of the structure (Fig. 1.).

To analyze the effect of configuration, four dipeptides (Z-D-Leu-Phe-H, Z-Leu-Phe-H, Z-D-Leu-D-Leu-H, and Z-Leu-Leu-H) were studied. The peptide with the D-configuration at P2 (Z-D-Leu-Phe-H) is more stable than the other three peptides. As expected, the Z-D-Leu-D-Leu-H peptide behaves similarly to the Z-Leu-Leu-H peptide (Fig. 2.). The four peptides, Z-Leu-Leu-H, Tosyl-Leu-Leu-H, Fmoc-Leu-Leu-H, and Ac-Leu-Leu-H were studied to examine the effect of the protecting group. The results indicate that the tosyl group was more effective in stabilizing the linear structure in comparison to the other compounds (Fig. 3.).

### Acknowledgments

We would like to thank Dr. Sankar Chatterjee, Mr. Bruce Dembofsky, Ms. Bethany K. Paxson, and Dr. Ming Tao for supplying several compounds. Also, we would like to thank Drs. James C. Kauer and Mark A. Ator for their critical review and Dr. Jeffry L. Vaught for his continuing support.

### References

1. Hanzlik, R. P., Jacober, S. P. and Zygmunt, J., *Biochim. Biophys. Acta.*, 1073 (1991) 33.
2. Thompson, R. C., *Biochemistry.*, 12 (1973) 47.
3. Westerik, J. O. and Wolfenden, R., *J. of Biol. Chem.*, 247 (1972) 8195.
4. Graybill, T. L., Dolle, R. E., Helaszek, C. T., Miller, R. E. and Ator, M. A., *Int. J. Pep. Prot. Res.*, 44 (1994) 173.
5. Iqbal, M., Messina, P. A., Freed, B., Das, M., Chatterjee, S., Tripathy, R., Tao, M., Josef, K. A., Dembofsky, B., Dunn, D., Griffith, E., Siman, R., Senadhi, S. E., Biazzo, W., Bozyczko-Coyne, D., Meyer, S. L., Ator, M. A. and Bihovsky, R., *Bioorg. Med. Chem. Lett.*, 7 (1997) 539.
6. Sandler, M., Smith, H. J., (Eds.) *Design of Enzyme Inhibitors as Drugs*, Oxford University Press, 1989, p. 596.
7. Sarubbi, E., Seneci, P. F., Angelastro, M. R., Peet, N. P., Denaro, M. and Islam, K., *FEBS Lett.*, 319 (1993) 253.
8. Fehrentz, J., Heitz, A., Castro, B., Cazaubon, C. and Nisato, D., *FEBS Lett.*, 167 (1984) 273.
9. Gold, V. (Ed.) *Advances in Physical Organic Chemistry*, Academic Press, 1966, p.1.
10. Okada, Y., Taguchi, H. and Yokoi, T., *Tet. Lett.*, 37 (1996) 2249.
11. Nishikata, M., Yokosawa, H. and Ishii, S., *Chem Pharm. Bull.*, 34 (1986) 2931.
12. Bajusz, S., Szell, E., Bagdy, D., Barabas, E., Horvath, G., Dioszegi, M., Fittler, Z., Szabo, G., Juhasz, A., Tomori, E. and Szilagyi, G., *J. Med. Chem.*, 33 (1990) 1729.

# The selectivity of C18 reversed-phase for peptides depends on the type of silanes linked to the silica matrix

Paul J. Kostel, Yan-Bo Yang and William H. Campbell

Vydac, 17434 Mojave Street, Hesperia, CA 92345, USA

A new “monomeric” bonded C18 reversed-phase HPLC packing provides alternative selectivity for peptide separation. Exploiting selectivity differences between reversed-phase columns assists in analysis and purification of peptides. Changing the TFA concentration in the mobile phase is another means of altering peptide selectivity.

## Results and Discussion

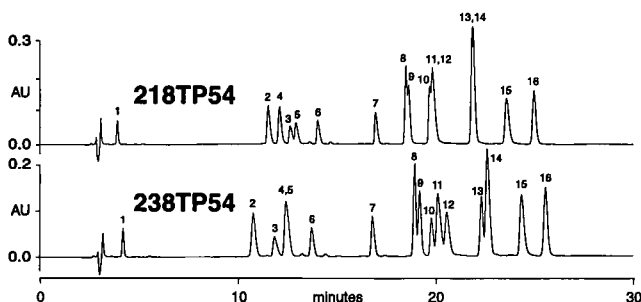


Fig. 1. Synthetic peptides on two 300Å C18 silica reversed-phase columns. Note the greater resolution of components in the 18-26 minute range on the 238TP54 column. The 218TP54 column, however, gives better selectivity for at least two components emerging at 10-15 minutes. Both columns were 4.6 mm ID x 250 mm L. Chromatographic conditions were identical. Conditions: 1.0 mL/min, absorbance at 220 nm, gradient from 10% to 40% ACN with 0.1% TFA (w/v) over 30 minutes. Sample: Mixture of standard peptides, listed with peak identification: 1>GY, 2>VYV, 3> neurotensin fragment 1-8 (pELYENKPR), 4>acRGGGGLGLGK-NH<sub>2</sub>, 5>RGAGGLGLGK-NH<sub>2</sub>, 6>acRGAGGLGLGK-NH<sub>2</sub>, 7>acRGVGGGLGLGK-NH<sub>2</sub>, 8>oxytocin (CYIQNCPLG-NH<sub>2</sub>), 9>met enkephalin (YGGFM), 10>bradykinin (RPPGFSPFR), 11>acRGVVGLGLGK-NH<sub>2</sub>, 12>neurotensin fragment 8-13 (RRPYIL), 13>angiotensin II (DRVYIHPF), 14>leu enkephalin (YGGFL), 15>neurotensin (pELYENKPRRPYIL), and 16>angiotensin I (DRVYIHPFHL).

Vydac TP is a high-purity 300Å pore-size silica produced from purified organic silicates. Historically, protein/peptide reversed-phase adsorbents produced from TP silica have had “polymeric” bonded phases – synthesized from polyfunctional silanes which produce crosslinking of the hydrophobic phase on the silica surface. This produces columns with very long lifetimes and no measurable stationary phase leaching. Vydac 218TP is a C18

reversed-phase adsorbent produced in this way. More recently a “monomeric” C18 adsorbent based on the same silica has been produced. Called 238TP, it is mono-silane bonded and exhaustively end-capped.

It can be seen from the chromatograms (Figs. 1. and 2.) that under identical operating conditions 218TP and 238TP exhibit comparable retention of peptides, but subtle differences in selectivity. This can help in separating peptides that are not resolved or incompletely resolved if only one type of reversed-phase column is tried.

Changing the concentration of TFA modifier in the mobile phase (Fig. 2.) is another way to change selectivity. For reproducible runs it is important that THE TFA concentration be clearly specified (v/v or w/v) and carefully controlled.

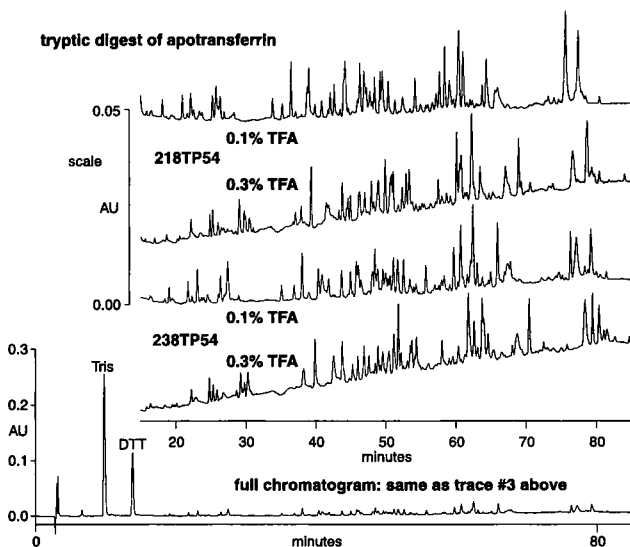


*Fig. 2. Effects of reversed-phase column type and TFA concentration. The bottom trace is a complete chromatogram. The upper traces show the region from 15 to 85 minutes, in which virtually all tryptic peptides emerge, for four individual runs with the vertical scale expanded to facilitate comparison. Samples identical for all runs. Conditions: 1.0 mL/min, absorbance at 215 nm, TFA concentration (w/v) as indicated, gradient from 0% to 50% ACN over 100 minutes. Both columns were 4.6mm ID x 250mm L. Sample: Tryptic digest of apotransferrin.*

# Purification of a crude synthetic peptide by strong cation exchange: Breaking up hydrophobic complexes prior to reversed-phase

**Paul Kostel**

*Vydac, 17434 Mojave Street, Hesperia, CA 92345, USA*

In peptide syntheses, hydrophobic contaminants often accumulate from condensation of side chain protectants and scavenger reagents. These contaminants complex with peptides and bind to reversed-phase columns, interfering with peptide purification by reversed-phase chromatography. A two-stage purification including ion-exchange chromatography with a chaotropic solvent in the mobile phase followed by reversed-phase chromatography overcomes these difficulties and provides several advantages.

## Results and Discussion

Including a chaotrope in the mobile phase for ion-exchange chromatography favors ionic retention and breaks up hydrophobic complexes. In this work, an ion-exchange separation (Fig. 1.) in the presence of the chaotrope, 25% acetonitrile, was used for initial purification of a crude synthetic peptide. The ion-exchange column provides an ideal first step because of its high loading capacity. In addition, uncharged hydrophobic contaminants that can interfere with reversed-phase separation are not retained and are removed by the ion exchange step. Reversed-phase analysis of the crude synthetic peptide (Fig. 2.) does not clearly indicate a main peak. In this case, running ion exchange with organic solvent helps

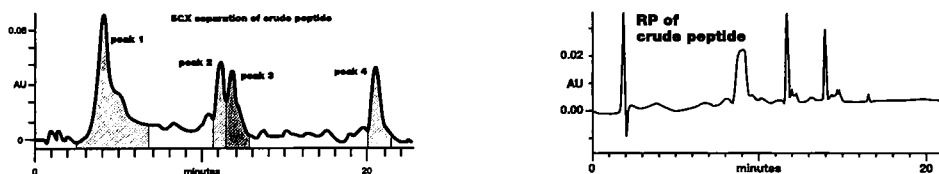


*Fig. 1 (left). Strong cation-exchange (SCX) separation of crude peptide. Sample: crude 23-mer containing met, but no cys or trp. Column: Vydac 400VHP575 sulfonic acid polymer cation exchange, 5 $\mu$ m, 7.5mm ID x 50 mm L. Conditions: 1mL/min. 220 nm. Buffer A= 0.1% TFA (w/v) in 25% ACN. Buffer B = A + 500 mM NaCl. Gradient = 0 to 60%B in 30 minutes.*

*Fig. 2 (right). Reversed-phase chromatography of crude peptide. Column: Vydac 218TP54 C18, 5 $\mu$ m, 4.6mm ID x 250mm L. Conditions: 1.5 mL/min. 220nm. Gradient = 20-60% ACN over 30 min in 0.1% TFA (w/v). Note that a broad, irregular peak is present at about 9 minutes, and there is no 19 minute peak in this run.*

identify the desired product. For charged synthetic peptides, failure sequences will have equal or lesser charges. The target peptide will normally be in the longest-retained ion-exchange peak. Reversed-phase of selected fractions from the ion exchange separation (Figs. 3 - 6) succeeds in isolating the desired product (Fig. 6.). For synthetic peptides, the chemically resistant polymer-based ion-exchange column removes HF and TFA reagents and prevents them from attacking the silica-based reversed-phase column. The differing selectivities of ion exchange and reversed phase produce a high degree of purification. The procedure can also be used for purifying proteins and peptides from other sources.

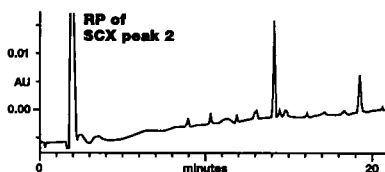
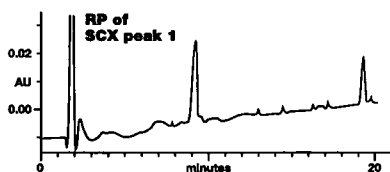


*Fig. 3 (left). Reversed-phase of SCX Peak 1. Column and conditions as described for Fig. 2. This run shows that SCX peak 1 contained the small molecules present in the broad, irregular peak and a 19 minute peak that was not present in the reversed-phase separation of the crude peptide because the molecules ran as a complex which eluted with an earlier retention time. The 25% ACN in the SCX run broke up this complex.*

*Fig. 4 (right). Reversed-phase of SCX Peak 2. Column and conditions as described for Fig. 2. This SCX peak contained both the 14 minute peak that was present in the reversed-phase separation of the crude peptide and the 19 minute peak that was not present in the crude run. This complex was also broken up by the 25% ACN in the SCX run.*

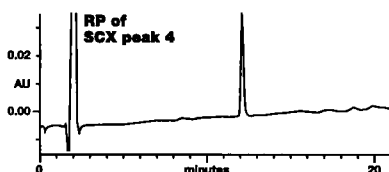
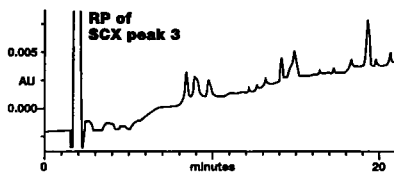


*Fig. 5 (left). Reversed-phase of SCX Peak 3. Column and conditions as described for Fig. 2. This SCX peak contains a variety of small peaks as well as the 19 minute peak. This is a good example of ion exchange simplifying the subsequent reversed-phase isolation. Unless the 19 minute peak is important, all of this material is best removed by SCX prior to the reversed-phase step.*

*Fig. 6 (right). Reversed-phase of SCX Peak 4. Column and conditions as described for Fig. 2. This peak was predicted to be the full length peptide, and this was confirmed. Doing an initial SCX step in a large scale purification of this peptide is very efficient because the C18 load contains only this fraction. All the material that eluted in Figures 3, 4 and 5 would never be loaded onto the prep C18 column.*

# Molecular recognition using a peptide combinatorial library and its detection by surface plasmon resonance spectroscopy

Hiroshi Taniguchi,<sup>a</sup> Koji Inai,<sup>b</sup> Takahisa Taguchi<sup>a</sup>  
and Susumu Yoshikawa<sup>a</sup>

<sup>a</sup>*Osaka National Research Institute, AIST, Ikeda, Osaka 563, Japan*

<sup>b</sup>*Medical Development Group, Kararay Co., Ltd., Kurashiki 710, Japan*

Although peptides are potent molecules for specific molecular recognition of some small compounds, there are many difficulties in detecting these molecular complexes directly, since the affinity interactions are too small to detect without using specific labels, such as fluorescent probes. For this purpose, we developed a new methodology using surface plasmon resonance spectroscopy for sensitive detection of small molecules without using any label.

## Results and Discussion

To find a pair of molecules with specific binding affinity, we used a pentapeptide library method for the porphyrin derivative, tetracarboxylic phenyl porphyrin, TCPP. The 5 residue peptide library consisted of 19 natural amino acids, but not cysteine, attached on a polymer matrix via a spacer, with a diameter of about 300 $\mu$ m. It was prepared by the split and pool method, giving one peptide on one bead. The TCPP molecules (1 $\mu$ g/ml) were added to this library (50 mg). After reaction for 1 hour at room temperature, these beads were washed with PBS. The reacted beads were colored by the TCPP. To determine the peptide sequence, the colored bead were removed one by one from the unreacted beads under microscopic observation. The reacted beads were washed with 6M guanidine hydrochloride and DMSO to remove the receptor complex, and then the peptide sequence on each bead was determined by protein sequencer (model 473A, Perkin Elmer). Peptides with the selected sequence (Table 1) were synthesized after which GGC sequence was attached to these sequences for SPR measurement. These peptides had a good binding affinity for TCPP. The synthesized peptide (Table 1) was immobilized on the silver coated BK-7, an optical glass. This peptide monolayer was reacted with TCPP and monitored by SPR.

## Conclusion

Surface plasmon resonance spectroscopy is quite promising for the sensitive detection of small molecules by peptide combinatorial library. The dose-dependence of TCPP was observed over a concentration range of 1 to 100 $\mu$ M. One micromolar of TCPP was detectable within 5 minutes.

*Table 1. Amino acid sequences of peptides binding TCP, synthesized peptides and their binding affinities.*

Peptide	Sequence of peptide	Sequence of synthesized peptide	Binding affinity
BMP-1	HRFHR	HRFHRGGC	-
BMP-2	MRWNF	MRWNFGGC	+
BMP-3	MIDFR	MIDFRGGC	++
BMP-4	VLIRF	VLIRFGGC	+
BMP-5	LFFAN	LFFANGGC	n.o.
BMP-6	QRRSG	QRRSGGGC	+
BMP-7	WRSTR	WRSTRGGC	+
BMP-8	WRINP	WRINPGGC	n.o.
BMP-9	FRRAQ	FRRAQGGC	-

*n.o.: not observed -: weak +: medium ++: strong*

## References

1. Yoshikawa, S., In Japan Combinatorial Chemistry Focus Group (Eds.), Combinatorial Chemistry, Kagakudojin, Japan, 1997, p. 44.
2. Yoshikawa, S., In the Japanese Soc. Spectroscopy (Eds.), Proceedings of the SPR Symposium, Tokyo, 1996, p. 31.

# Preliminary mapping of conformational epitopes on the HPV16 E7 oncoprotein

**Julio C. Calvo, Katia C. Choconta, Diana Diaz, Oscar Orozco, Fabiola Espejo, Fanny Guzman and Manuel E. Patarroyo**

*Instituto de Inmunología, Hospital San Juan de Dios, Universidad Nacional de Colombia, Av. 1 # 10-01, Bogota D.C., Colombia.*

Cervical cancer is one of leading causes of cancer deaths in women. Increasing evidence supports the hypothesis that human papillomaviruses (HPVs) are involved in cervical cancer. Papillomaviruses are small DNA viruses that infect the epithelial cells and induce skin lesions. 60 types of HPVs have been identified and about 20 of these are known to infect epithelial cells that comprise the genital mucosa. These HPVs are subdivided into two groups: the low-risk HPVs (e.g., HPV-6, HPV-11) and the high-risk HPVs (e.g., HPV-16, HPV-18). HPV-16 is the most prevalent HPV type and is found in more than 50% of patients. Genetic studies performed with a variety of rodent fibroblast cell lines showed that E7 high-risk protein is necessary and sufficient for the transformation of established rodent fibroblasts [1-2]. A previous work, using linear peptide mapping of 20-mer peptides with a window of six amino acids, showed very low or no reactivity. These results indicated that when antibodies were raised against the HPV-16 E7 oncoprotein, they were formed against conformational epitopes. We took advantage of the Satterthwait methodology for synthesizing conformational epitopes [3].

## Results and Discussion

As predicted by the algorithm of Garnier, structural features of the HPV-16 E7 oncoprotein show three  $\alpha$ -helical structures in segments encompassing residues 11 through 17, 27-38 and 75-83, and a loop-like structure between 54-70. In order to identify conformational epitopes on the HPV-16 E7 oncoprotein, the following peptides were synthesized by the Fmoc strategy :

helix-1	JLAZ-----TLHEYMLDLQ-----GGG	residues 7-16
linear-1A	MHGDTPTLHEYMLDLQPETT	residues 1-20
helix-2	JLAZ-----QLNDSSEEEDEI---GGG	residues 27-38
linear-2	QLNDSSEEEDEI	residues 27-38
loop-4	VTFCKCDSTLRLCVQ	residues 55-70
linear-4	VTFCKCDSTLRLCVQ	residues 55-70
linear-5A	RLCVQSTHVDIRTLEDLLMG	residues 66-85

Peptides were purified by reverse-phase HPLC and their molecular weights were verified by MALDI-TOF mass spectrometry. Structure determination by NMR showed the

prospective helix-1 having a real  $\alpha$ -helix conformation. 1072 serum showed a strong positive reaction with helix-1, no reaction with helix-2 and low reaction with loop-4, linear-1A, linear-4 and linear-5A peptides (Fig.1).

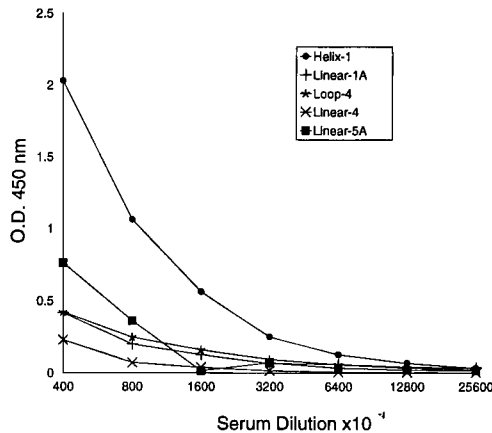


Fig. 1. Titers of 1072 human serum against modeled helix-1 and loop-4 and linear-1A, -4 and -5A peptides from HPV-16 E7 oncoprotein.

Helix-1, linear-1A, loop-4, linear-4 and linear-5A peptides were tested by ELISA with a set of 32 human serum samples (22 sera from patients with invasive carcinoma, 5 sera from normal patients and 5 sera from children) diluted 1:1000. 50% of sera containing antibodies against HPV exhibited strong reactivity to helix-1 and 9% of them exhibited reactivity to linear-5A. Sera from normal patients and children showed no reaction with peptides.

## Conclusion

The results obtained suggest that a large improvement in antigenicity can be achieved by using folded peptides and that the helix-1 peptide sequence contains a conformational epitope.

## References

1. Zur Hausen, H., *Science*, 254(1991)1167.
2. Munger, K. and Phelps, W.C., *Biochim.Biophys.Acta*, 155(1993)111.
3. Chiang, L.C., Cabezas, E., Calvo, J.C. and Satterthwait, A.C., In Hodges, R.S. and Smith, J.A. (Eds.), *Peptides: Chemistry, Structure and Biology* (Proceeding of the Thirteenth American Peptide Symposium), ESCOM, Leiden, The Netherlands, 1994, p.278.

## **Session XIII**

### **Drug Delivery**



# Synthesis, characterization and use of novel non viral vectors for gene delivery

Gerardo Byk, Catherine Dubertret, Bertrand Schwartz, Marc Frederic, Gabrielle Jaslin and Daniel Scherman

UMR-133 Rhône-Poulenc Rorer Gencell/CNRS, 13 Quai Jules Guesde B.P. 14, 94403-Vitry sur Seine, France

As an alternative to viral vectors, synthetic DNA delivery agents are of crucial interest for gene therapy since they display potentially less risk in terms of immunogenicity and propagation. Among synthetic DNA delivery agents, cationic lipids represent the most developed approach. Cationic lipids are composed of a lipophilic moiety (usually dialkyl or cholesteryl) linked to a cationic head through various linkers. First generation cationic heads were quaternary ammonium salts or tertiary amines [1]. A significant improvement was introduced by the use of a polyamine derivative of spermine, leading to increased *in vitro* transfection activity by lipopolyamine DOGS (dioctadecylglycylcarboxyspermine) [2]. Subsequently, other spermine containing lipopolyamines such as Lipofectamine [1] were introduced and, more recently, other derivatives.

## Results and Discussion

We have synthesized compound **4** related to DOGS by direct modification of the carboxyspermine building block **1**, and compound **6** derived from bis-aminopropyl propylene diamine **5** (Fig. 1).

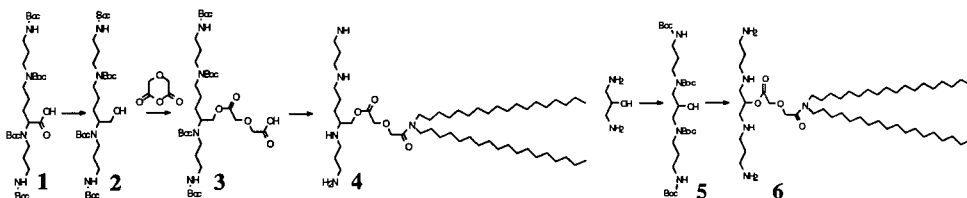


Fig. 1. Synthesis of novel cationic lipids for gene delivery.

We have found that **6** undergoes intramolecular rearrangement to give the cyclized product **7** during HPLC purification or when left in water solution. When arginine was placed as spacer in product **8**, the cyclized product was not isolated and the expected product was obtained after purification (Fig. 2). In a first study products **4** and **7** were assayed *in vitro* on the NIH 3T3 cell line. Product **7** displays increased transfection activity ( $16 \times 10^4$  RLU/ $\mu\text{g}$  prot) as compared to DOGS ( $8 \times 10^4$  RLU/ $\mu\text{g}$  prot) or to **4** ( $8 \times 10^4$  RLU/ $\mu\text{g}$  prot).

prot). In a second study products **7** and **8** were assayed *in vitro* on NIH 3T3 and rabbit smooth muscle cell lines and compared to Lipofectamine (see Table 1).

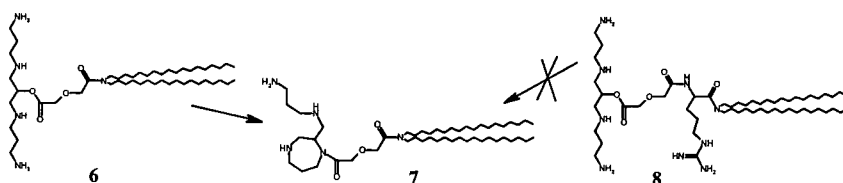


Fig. 2. Intramolecular rearrangement of cationic lipid **6**.

Table 1. Expression of luciferase on two cell lines \*RLU: Relative Light Units.

Product	$\mu\text{gDNA/well}$	$\text{nmol lipid } / \mu\text{g}$ DNA	NIH3T3 [ $10^9 \text{ RLU}/\mu\text{g prot}$ ]	Rabbit SMC [ $10^5 \text{ RLU}^*/\mu\text{g prot}$ ]
Lipofectamine	2	6	$12 \pm 0.5$	$9.2 \pm 0.7$
<b>7</b>	2	6	$1.2 \pm 0.4$	$22 \pm 0.4$
<b>8</b>	2	6	$43 \pm 0.5$	$130 \pm 0.5$

Results indicate that the introduction of arginine in the linker position in compound **8** leads to increased transfection activities for both cell lines as compared to Lipofectamine. Compound **7** displayed increased activity in rabbit smooth muscular cells, whereas transfection activity was decreased in NIH3T3 cells compared to Lipofectamine. Finally, compound **7** is able to promote luciferase gene expression ( $2.7 \times 10^4 \text{ RLU/tumor}$ ) *in vivo* in Lewis Lung carcinoma, whereas naked DNA is inefficient in that model.

## Conclusion

The introduction of a novel polyamine into cationic lipids promotes increased *in vitro* and *in vivo* gene expression as compared to other cationic lipids. The increased transfection activity after the introduction of a substituted amino acid in the linker position illustrated in the arginine-containing compound **8** allows us to consider the introduction of short peptides into cationic lipids for a specific tissue/organ targeting.

## References

1. Felgner, P.L., Gadek, T.G., Holm, M., Roman, R., Chan, H.W., Wenz, M., Northrop, J.P., Ringold, G.M. and Danielsen, M. Proc. Natl. Acad. Sci. USA., 84 (1987) 7413.
2. Behr, J., Demeneix, B., Loeffler, J. and Perez-Mutul, J. Proc. Natl. Acad. Sci. USA., 86 (1989) 6982.

# Prodrug strategies to enhance the permeation of peptides through the intestinal mucosa

**Ronald T. Borchardt**

*Department of Pharmaceutical Chemistry, The University of Kansas, Lawrence, KS 66047, USA*

Recent dramatic advances in molecular biology and modern synthetic chemistry have generated new methodologies that permit the production of large quantities of structurally diverse peptides possessing a wide range of pharmacological effects. The clinical development of drugs in this structural class, however, has been restricted because of their unfavorable permeation across important biological barriers, including the intestinal mucosa, and their susceptibility to enzyme-mediated degradation. The hydrophilic, charged nature of peptides generally leads to poor permeability across the intestinal mucosa, resulting in low oral bioavailabilities (typically less than 1–2%) [1–4].

The successful design of peptides as orally bioavailable drugs represents a major challenge to pharmaceutical scientists. To develop an orally bioavailable peptide drug having high pharmacological specificity and potency *in vivo*, it is necessary to incorporate structural features that optimize the pharmacological (*e.g.*, receptor binding), pharmaceutical (*e.g.*, solubility) and biopharmaceutical (*e.g.*, membrane permeability, metabolic stability) properties of the molecule. Alternatively, unfavorable pharmaceutical and/or biopharmaceutical properties of the molecule have to be transiently modified using prodrug approaches. Recently, Oliyai [5] and Gangwar *et al.* [6] published comprehensive reviews of prodrug strategies for peptides. This presentation will be restricted to strategies for a bioreversible cyclization of the peptide backbone as a novel means of altering the physico-chemical properties of peptides so as to enhance their membrane permeability and to stabilize them to metabolism.

## Results and Discussion

In recent years, our laboratory has developed several novel ‘chemical linkers’ that can be used to make cyclic prodrugs of peptides. Possible advantages of this cyclization strategy, from a membrane permeation perspective, include: a) reduction in the overall charge of the molecule; b) possible creation of unique solution structures that reduce the molecule’s hydrogen bonding potential; and c) possible reduction in the molecule’s size [1,7]. Recently, our laboratory has described methodologies for linking the N-terminal amino group to the C-terminal carboxyl group of peptides using an acyloxyalkoxy promoiety (Fig. 1a) [8] or a 3-(2’-hydroxy-4’,6’-dimethylphenyl)-3,3-dimethylpropionic acid (Fig. 1b) [9]. Similarly, Professor Binghe Wang and his colleagues (North Carolina State University) have used coumaric acid (Fig. 1c) [10,11] as a chemical linker to make cyclic opioid peptides (unpublished data). All three chemical linkers were designed to be susceptible to esterase metabo-

lism (slow step), leading to a cascade of chemical reactions and resulting in release of the peptide (Fig. 1).

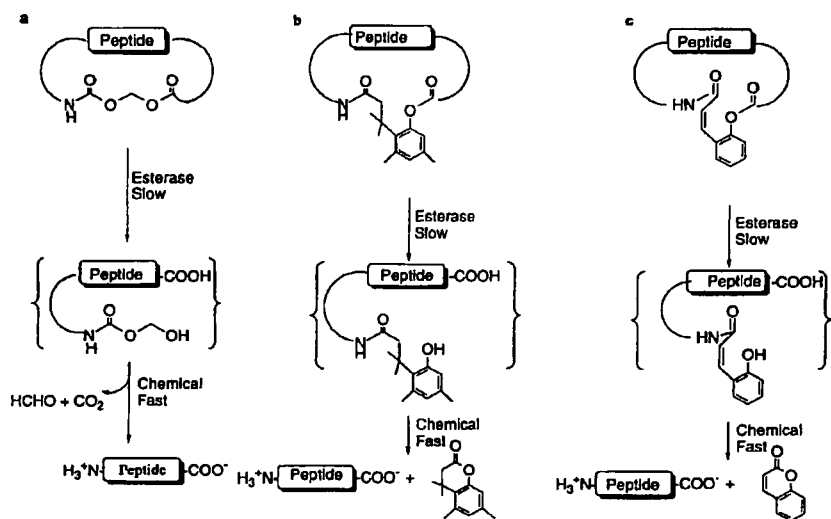


Fig. 1. Strategies for preparing cyclic prodrugs of peptides.

Recently, our laboratory has shown that an acyloxyalkoxy cyclic prodrug [12] and a phenylpropionic acid prodrug [13] of a model hexapeptide are converted to the parent peptide more rapidly in human blood than in physiological buffer, supporting the involvement of esterases in their bioconversion. In addition, in transport studies conducted using Caco-2 cell monolayers, an *in vitro* model of the intestinal mucosa, both cyclic prodrugs were shown to permeate at least 70 times better than the parent hexapeptide [12,13]. The enhanced permeation of the acyloxyalkoxy cyclic prodrug could be explained by formation of unique solution structures that reduced the molecule's hydrogen bonding potential [14].

More recently, in collaboration with Professor Binghe Wang's laboratory, our laboratory synthesized coumaric acid-based cyclic prodrugs of [Leu<sup>5</sup>]-enkephalin (H-Tyr-Gly-Gly-Phe-Leu-OH) and DADLE (H-Tyr-D-Ala-Gly-Phe-D-Leu-OH) and have characterized their chemical and enzymatic stability and their cellular permeability characteristics (O.S. Gudmundsson, G.M. Pualetti, W. Wang, D. Shan, H. Zhang, B. Wang and R.T. Borchardt, unpublished data). In physiological buffer, the cyclic prodrugs were shown to degrade slowly and stoichiometrically to (Leu<sup>5</sup>)-enkephalin and DADLE. In human plasma, the conversion of the prodrugs to the opioid peptides was significantly faster. When applied to Caco-2 cell monolayers, [Leu<sup>5</sup>]-enkephalin rapidly underwent degradation catalyzed by peptidase whereas DADLE was stable. In contrast, the cyclic prodrugs of [Leu<sup>5</sup>]-enkephalin and DADLE were stable enzymatically and were shown to be approx. 665 and

30 times, respectively, more able to permeate this cell monolayer than were the parent peptides. This enhanced cell membrane permeability of the opioid peptide cyclic prodrugs could be related to their increased lipophilicity and the formation of unique solution structures (O.S. Gudmundsson, S.D.S. Jois, D.G. Vander Velde, T.J. Siahaan, D. Shan, W. Wang, H. Zhang, B. Wang and R.T. Borchardt, unpublished data).

Through a better understanding of the physicochemical properties (*i.e.*, charge, hydrophilicity) that restrict cell membrane permeation of peptides, it has been possible to develop strategies to make prodrugs that have more favorable membrane permeation characteristics. Some of the most dramatic enhancements in cell permeation appear to occur when cyclic prodrug strategies are employed. Ultimately, these strategies could lead to cyclic peptide prodrugs having oral bioavailabilities acceptable for clinical use.

### Acknowledgments

The author's research in this area was supported by grants from the U.S. Public Health Service (DA-09315, GM-51633, GM-088359), Glaxo Wellcome, Inc., and Costar Company.

### References

1. Borchardt, R.T., In Kaumaya, P.T.P. and Hodges, R.S. (Eds.), *Peptides: Chemistry, Structure and Biology* (Proceedings of the Fourteenth American Peptide Symposium), Mayflower Scientific, Ltd., Leiden, The Netherlands, 1996, p. 902.
2. Pauletti, G.M., Gangwar, S., Knipp, G.T., Nerurkar, M.N., Okumu, F.W., Tamura, K., Siahaan, T.J. and Borchardt, R.T., *J. Controlled Release*, 41(1996)3.
3. Burton, P.S., Conradi, R.A., Ho, N.F.H., Hilgers, A.R. and Borchardt, R.T., *J. Pharm. Sci.*, 85(1996)1336.
4. Pauletti, G.M., Okumu, F.W. and Borchardt, R.T., *Pharm. Res.*, 14(1997)164.
5. Oliyai, R., *Adv. Drug Del. Rev.*, 19(1996)275.
6. Gangwar, S., Pauletti, G.M., Wang, B., Siahaan, T.J., Stella, V.J. and Borchardt, R.T., *Drug Discovery Today*, 2(1997)148.
7. Okumu, F.W., Pauletti, G.M., Vander Velde, D.G., Siahaan, T.J. and Borchardt, R.T., *Pharm. Res.*, 14(1997)169.
8. Gangwar, S., Pauletti, G.M., Siahaan, T.J., Stella, V.J. and Borchardt, R.T., *J. Org. Chem.*, 62(1997)1356.
9. Wang, B., Gangwar, S., Pauletti, G.M., Siahaan, T.J. and Borchardt, R.T., *J. Org. Chem.*, 62(1997)1363.
10. Wang, B., Zhang, H. and Wang, W., *Bioorg. Med. Chem Lett.*, 6(1995)945.
11. Wang, B., Wang, W., Zhang, H., Shan, D. and Smith, T.D., *Bioorg. Med. Chem. Lett.*, 6(1996)2823.
12. Pauletti, G.M., Gangwar, S., Okumu, F.W., Siahaan, T.J., Vander Velde, D.G., Stella, V.J. and Borchardt, R.T., *Pharm. Res.*, 13(1996)1615.
13. Pauletti, G.M., Gangwar, S., Wang, B. and Borchardt, R.T., *Pharm. Res.*, 14(1997)11.
14. Gangwar, S., Jois, S.D.S., Siahaan, T.J., Vander Velde, D.G., Stella, V.J. and Borchardt, R.T., *Pharm. Res.*, 13(1996)1657.

# Characterization of a stable leuprolide formulation for one year in an implantable device

**Cynthia L. Stevenson, Cynthia A. Corley, Matt Cukierski, Corinne A. Falender, Steven C. Hall, Paul Johnson, J. Joe Leonard, Mandy M. Tan and Jeremy C. Wright**

*ALZA Corporation, Palo Alto, CA 94304, USA*

Leuprolide is an LHRH agonist used for the palliative treatment of prostate cancer. Cancer patients are living longer and sustained release dosage forms may increase their quality of life. Although leuprolide has been demonstrated to be fairly stable, it is also known to gel at high concentrations [1-4]. The DUROS<sup>TM</sup> osmotic implant is approximately 4 mm x 45 mm and is implanted under the skin on the inside of the upper arm, with a local anesthetic. One end contains a semi-permeable membrane which controls the rate at which water is taken up by the osmotic engine. As the engine swells, a piston slides forward, releasing drug from the orifice located at the opposite end of the device. The drug reservoir holds ~150  $\mu$ l formulation and is isolated from the engine compartment, as well as the surrounding body fluid. The limited size of the drug reservoir requires a highly concentrated formulation. Accordingly leuprolide was formulated at 370 mg/ml to allow a continual therapeutic dose for 12 months. This paper provides a summary of leuprolide stability data in an implantable osmotically driven system.

## Results and Discussion

Stability studies were performed at 37°C, 50°C, 65°C and 80°C for two years in both aqueous and non-aqueous excipients. The samples were assayed by RP-HPLC and SEC and fit to apparent pseudo first-order kinetics (Fig. 1). The resulting activation energies for both formulations were similar ( $E_a=21-23$  kcal/mol), but only the aqueous formulation was observed to gel with time. The aqueous gels were highly birefringent and marked by an increase in  $\beta$ -sheet structure, at  $1632\text{ cm}^{-1}$ , by FTIR. The aqueous gelled and non-gelled formulations demonstrated similar chemical and physical stability, indicating that gelation did not accelerate the degradation process. Leuprolide formulated in the non-aqueous excipient formed an unstable random coil/ $\alpha$ -helix conformation that did not easily refold into a  $\beta$ -sheet structure and therefore did not gel. Subsequently, the non-aqueous formulation was chosen for development, and demonstrated 93% solution stability after 18 months at 37°C.

The effect of leuprolide concentration, moisture content and temperature on the degradation rate of the non-aqueous formulation were also explored. Leuprolide stability was observed to increase with increasing leuprolide concentration (50 mg/ml to 400 mg/ml) at 80°C for 6 months (Fig. 2). This increase in stability was primarily due to a

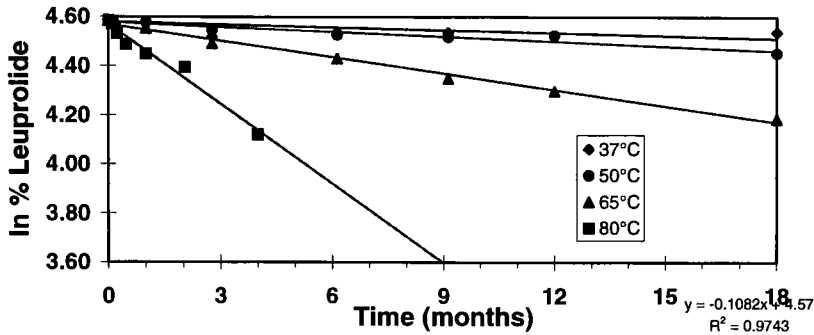


Fig. 1. Pseudo first-order fit of a non-aqueous leuprolide formulation.

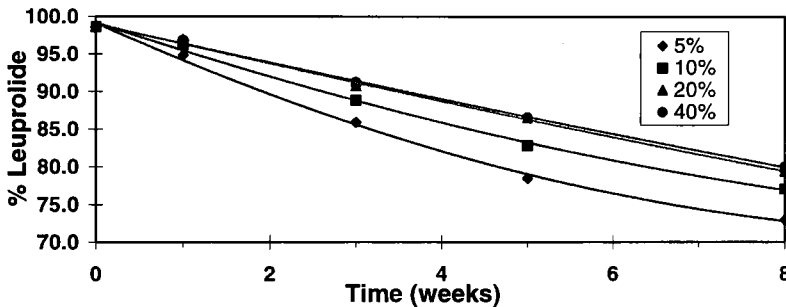


Fig. 2. Effect of leuprolide concentration at 80°C (n=3).

decrease in hydrolysis. Leuprolide degradation products could be categorized into four major degradation pathways by LC/MS: isomerization, hydrolysis, oxidation and aggregation. Degradation products were similar in the aqueous and non-aqueous formulations; however, more oxidation products were found in the non-aqueous formulation. For example, Trp<sup>3</sup> was observed to oxidize to a mono-oxidized tryptophan, N-formylkynurenine and kynurine. Conversely, the aqueous formulation degradation products were primarily obtained from hydrolysis reactions at the C-terminal to pGlu<sup>1</sup>, His<sup>2</sup>, Trp<sup>3</sup>, Ser<sup>4</sup> and Tyr<sup>5</sup>. The leuprolide non-aqueous formulation was also spiked with moisture (5% to 15% H<sub>2</sub>O). Samples containing more water were observed to degrade faster, where chemical degradation products were observed to increase (Fig. 3), but aggregate content remained constant. Temperature was observed to affect not only the rate of degradation, but also the ratio of degradation products in the non-aqueous formulation. At 65°C and 80°C, oxidation was the major chemical degradation pathway. However, at 37°C and 50°C, hydrolysis and isomerization degradation routes were predominant. This was to be expected since the activation energy for hydrolysis reactions is generally higher than that of

oxidation reactions. Secondly, the increased oxidation rate at lower temperatures may be accelerated by the increased solubility of oxygen with decreasing temperature.

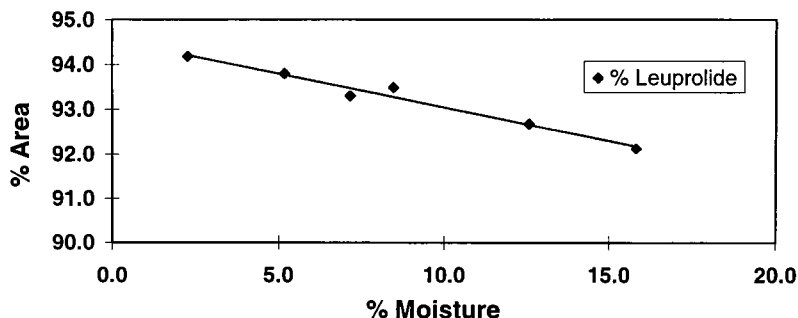


Fig. 3. Effect of moisture content on leuprolide stability after 6 months at 50°C (n=3).

Release rate studies were followed for one year and delivered the target dose of ~125 µg/day. Both *in vitro* and *in vivo* pumping rate and leuprolide stability (>90%) studies showed good correlation. DUROS™ leuprolide devices were implanted into dogs and serum testosterone levels remained suppressed for one year, compared to control animals. Finally, a human placebo “wearing” study was completed, showing no adverse reaction to insertion, wearing and removal of the system.

## Conclusion

Leuprolide formulated at 370 mg/ml in a DUROS™ implantable osmotic device demonstrated better than 90% stability for 18 months at 37°C. The systems also continued to release drug at the target dose for 12 months at 37°C both *in vitro* and *in vivo*. An IND has been filed and Phase I/II trials are ongoing.

## References

1. Adjei, A.L., and Hsu, L., In Wang, Y.J. and Pearlman, R. (Eds.), Stability and Characterization of Protein and Peptide Drugs, Plenum Press, New York, 1993, p. 159.
2. Powell, M.F., Sanders, L.M., Rogerson, A. and Si, V., Pharm. Res., 8(1991)1258.
3. Helm, V.J. and Muller, B.W., Pharm. Res., 7 (1990) 1253.
4. Okada, J., Seo, T., Kasahara, F., Takeda, K. and Kondo, S., J. Pharm. Sci., 80(1991) 167.

## Oligopeptide transport systems in eukaryotes

Jeffrey M. Becker,<sup>a</sup> Mark Lubkowitz<sup>a</sup> and Fred Naider<sup>b</sup>

<sup>a</sup>*Departments of Microbiology and Biochemistry, Cellular, and Molecular Biology, University of Tennessee, Knoxville, TN 37996, U.S.A. and* <sup>b</sup>*Department of Chemistry, College of Staten Island, CUNY, Staten Island, NY 10314, USA*

The transport of peptides across cellular membranes against a concentration gradient has been observed in a wide variety of cells [1]. Used as a means to provide a source of amino acids, nitrogen, and carbon for growth, peptide transport systems may also serve a number of other functions such as transporting antibiotics from the intestinal lumen into the circulatory system [2]. Although components of peptide transport systems from prokaryotic cells have been known for many years [3], only recently have studies focused on the molecular components of eukaryotic peptide transport systems. Cloning and sequencing has led to the identification of membrane proteins from several eukaryotic cell types that mediate the translocation of peptides across the plasma membrane [4, 5]. In addition, components involved in the regulation of peptide transport systems have been enumerated in yeast [6]. In this report we describe our recent studies that have identified two transporters that co-exist in a variety of eukaryotic cells: a di-/tripeptide transporter and an oligopeptide transporter.

### Results and Discussion

Genes encoding a di- and tripeptide transporter were cloned first from the yeast *Saccharomyces cerevisiae* [4] and from rabbit intestinal cells [5]. Discovery of a whole family of such di-/tripeptide transporters named the PTR family soon followed [7]. Although the rabbit intestinal transporter was called an oligopeptide transporter, all of the peptide transport proteins whose genes had been cloned prior to 1997 mediate the uptake of di- and tripeptides, not larger peptides. An interesting aspect of these systems is the coupling of H<sup>+</sup> ions to allow concentrative peptide uptake. In fact, the di-/tripeptide transporters of eukaryotic cells are the only known eukaryotic transport systems that use the H<sup>+</sup> gradient as the energy source for substrate translocation.

It had been known for some time that the pathogenic yeast *Candida albicans* was sensitive to toxic tetrapeptides [8]. Thus, we reasoned that an oligopeptide transport gene could be cloned using a host cell that was not able to use tetrapeptides but was able to express a foreign gene. In this manner, the host cell was thereby conferred with a new phenotype by the foreign DNA. We used a *C. albicans* genomic library as the DNA source and *S. cerevisiae* as the recipient cell. The scheme for accomplishing the cloning of the *C. albicans* oligopeptide transport gene is shown in Fig. 1.

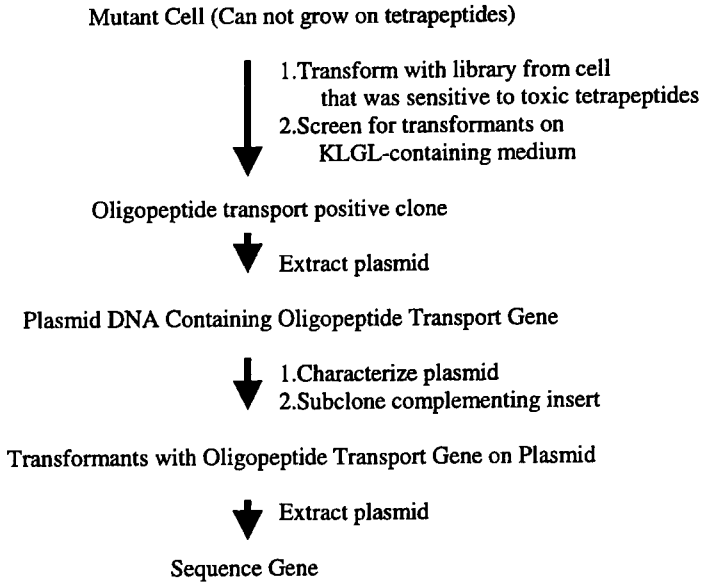


Fig.1. Scheme for cloning an oligopeptide (KLGL) transport gene.

The characterization of this gene revealed that it belonged to a new family of transport proteins we have tentatively named the OPT family[9]. These proteins have an amino acid motif found only in this group of proteins and not elsewhere in the entire protein database. The oligopeptide transporters appear to have 12 to 14 transmembrane domains by Kyte-Doolittle hydrophobicity plots, but their number and orientation have not been established experimentally. Comparison of some of the characteristics of the three major families of peptide transporters cloned to date are shown in Table 1.

## Conclusion

We have identified and cloned a gene encoding an oligopeptide transport protein of *C. albicans*. Using database searches, we have also identified three additional putative homologues of this gene and several plant ESTs as well. These proteins represent the first members of a new peptide transport family called the OPT family. Additional members may be found in other kingdoms, but it is also possible that this family has uniquely evolved to perform specific functions in plants and fungi. Future studies will determine the physiological role(s) of these and other peptide transport systems found throughout the living world.

Table 1. Characteristics of peptide transport families.

Family Name	Acronym	Transport Substrates	Amino Acid Motif	Members	Energy Source
Peptide Transporters of <u>A</u> TP- <u>B</u> inding <u>C</u> assette superfamily	ABC	Di-/tripeptides and some oligopeptides	Walker motifs (ATP-binding) in cytoplasmic domains	Found only in prokaryotes	ATP
<u>P</u> eptide <u>T</u> ransport	PTR	Di-/tripeptides	FYxxINxG(S/A) (L/F) in fifth transmembrane domain	About 12 members identified to date ranging from prokaryotes to humans	H <sup>+</sup> (protonmotive force)
<u>O</u> ligo <u>P</u> eptide <u>T</u> ransport	OPT	Oligopeptides (3-5 residues)	SPYxEVRxxVx xxDDP(T/S) (cytoplasmic domain?)	Four members cloned to date from fungi plus a number of plant ESTs identified	H <sup>+</sup> (preliminary data)

## References

1. Taylor, M. D and Amidon, G.L. (Eds.) Peptide-based drug design: controlling transport and metabolism, ACS Professional Reference Books, American Chemical Society, Washington, DC, 1995.
2. Kramer, W., Girbig, F., Gutjahr, U., and Kowalewski, S., In Taylor, M. D. and Amidon, G. L., (Eds.) Peptide-based drug design: controlling transport and metabolism, ACS Professional Reference Books, American Chemical Society, Washington, DC, 1995, p. 149.
3. Payne, J. W. In Taylor, M. D. and Amidon, G. L., (Eds.) Peptide-based drug design: controlling transport and metabolism, ACS Professional Reference Books, American Chemical Society, Washington, DC, 1995, p. 341.
4. Perry, J.R., Basrai, M., Stiner, H.-Y., Naider, F., and Becker, J.M. Mol. Cell. Biol., 14(1994)104.
5. Fei, Y.-L., Kanai, Y., Nussberger, S., Ganapathy, V., Leibach, F.H., Romero, M., Singh, S.K., Boron, W.F., and Hediger, M.A. Nature ,368(1994)563.
6. Island, M.D., Perry, J.R., Naider, F., and Becker, J.M. Curr. Genet., 20(1991)457.
7. Steiner, H.-F., Naider, F., and Becker, J.M. Mol. Microbiol. 16(1995)825.
8. Basrai, M., Zhang, H.-L., Miller, D., Naider, F., and Becker, J.M. J. Gen. Microbiol., 138(1992)2353.
9. Lubkowitz, M., Hauser, L., Breslav, M., Naider, F., and Becker, J.M. Microbiology UK, 143(1997)387.

# Brain delivery and targeting of thyrotropin-releasing hormone analogs by covalent packaging and sequential metabolism

Laszlo Prokai, Katalin Prokai-Tatrai, Whei-Mei Wu, Jiaxiang Wu,  
Xudong Ouyang, Ho-Seung Kim, Alevtina Zharikova,  
James Simpkins and Nicholas Bodor

Center for Drug Discovery, College of Pharmacy, University of Florida,  
Gainesville, FL 32610-0497, USA

The blood-brain barrier (BBB) has been the major obstacle to the development of peptide neuropharmaceuticals. Most neuropeptides and their synthetic analogs are hydrophilic, do not have a specific transport system and thus do not enter the central nervous system (CNS) in pharmacologically significant amounts. Peptide delivery to the CNS must, therefore, be addressed to exploit the biological diversity and promise of these biomolecules as a future generation of neuropharmaceuticals [1]. Recently we reported a novel strategy to deliver and target peptides into the brain by covalently attaching lipophilic functional groups (a 1,4-dihydrotrigonellyl, DHT, attached to the N-terminal part of the peptide via a spacer and a C-terminal lipophilic ester, OCho) [2]. These moieties are designed to carry the peptide across the BBB by passive transport and, once in the CNS, to convert the molecule to an ionic trigonellyl derivative that furnishes retention at the target site. The biologically active peptide is then obtained by sequential metabolism. We have adapted this method to peptides without apparent functional groups that allow covalent attachment of lipidizing and targeting moieties, such as selected analogs of thyrotropin-releasing hormone (TRH) showing selective CNS-effects (pGlu-Xaa-Pro-NH<sub>2</sub>, where Xaa is a hydrophobic residue such as Leu [3]), by considering Gln-Xaa-Pro-Gly as their progenitor sequence [4] (Fig. 1). Peptidyl glycine  $\alpha$ -amidating monooxygenase (PAM) converts Gly to carboxamide, and glutaminyl cyclase produces pGlu. For the latter reaction, a directed endopeptidase (post-proline cleaving enzyme, PPCE) cleavage was found to be optimal for removing the trigonellyl+spacer part and exposing the N-terminal Gln.

## Results and Discussion

*In vitro* studies have indicated that the conversion of C-terminal Gly to carboxamide by PAM takes place in the brain, but is not prevalent in the systemic circulation. Metabolic (PPCE) release of the Gln-terminated peptide in the brain has also been confirmed *in vitro* (incubation of the appropriate peptide conjugate in brain homogenate followed by electrospray ionization mass spectrometry). We have also demonstrated by an *in vivo* cerebral microdialysis study that the TRH analog significantly increases brain acetylcholine levels. As a consequence, the pharmacological evaluation of the chemical targeting systems for pGln-Leu-Pro-NH<sub>2</sub> using the drug-induced cholinergic hypofunction paradigm in mice indicated a statistically significant improvement of the CNS effect compared to the

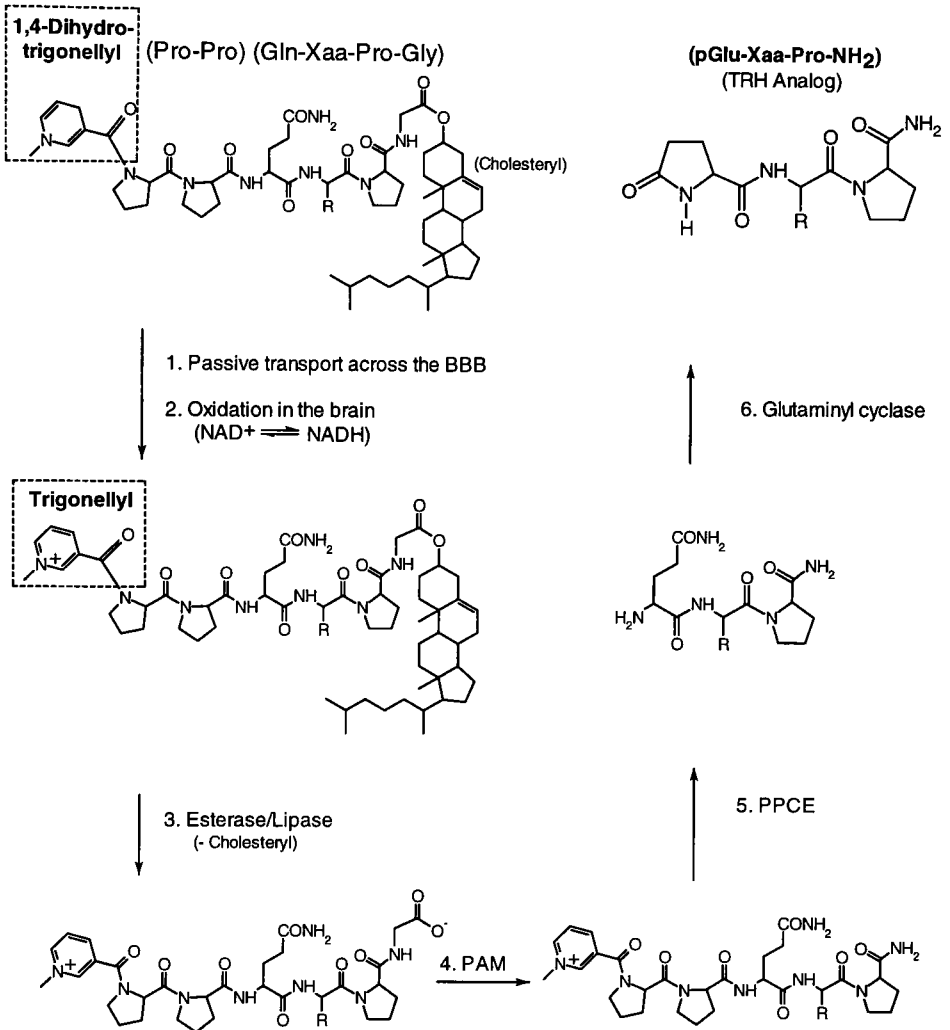


Fig. 1. Covalent “packaging” and sequential metabolism for the CNS-targeting of TRH analogs.

unmodified analogs (Table 1). We have also made modifications in the peptide sequence based on its structure-activity relationship [3, 5]. Upon replacing [Leu<sup>2</sup>] with [Nva<sup>2</sup>], which reportedly further increased the CNS effect in rats, the corresponding CDS was not significantly different in analeptic activity from the chemical CNS-targeting system for the [Leu<sup>2</sup>]-analog at 10  $\mu$ mol/kg body weight dose in mice.

Table 1. Pentobarbital-induced sleeping time in mice after intravenous administration (10  $\mu$ mol/kg)

*an unmodified TRH analog versus that of chemical CNS-targeting systems for TRH analogs.*

Treatment	Sleeping Time (min, mean $\pm$ standard error)
Control	94.2 $\pm$ 2,5
PGlu-Leu-Pro-NH <sub>2</sub>	79.2 $\pm$ 4.9
DHT-Pro-Pro-Gln-Leu-Pro-Gly-OCho	50,9 $\pm$ 2.5
DHT-Pro-Pro-Gln-Nva-Pro-Gly-OCho	49.8 $\pm$ 7.8
DHT-Pro-Pro-Gln-Nva-Pip-OCho	41.4 $\pm$ 2.6

Because the -Pro-NH<sub>2</sub> obtained from the -Pro-Gly precursor by PAM was susceptible to deamidation by PPCE (a.k.a. TRH deamidase, a competitive reaction to the PPCE-cleavage of the spacer-Gln peptide bond), the Pro-Gly residues in the covalently packaged [Nva<sup>2</sup>]-analog were replaced by a single L-pipecolic acid (Pip) residue [5] to yield a [Nva<sup>2</sup>][Pip<sup>3</sup>]-analog by sequential metabolism without the involvement of PAM. This novel TRH analog accommodates a C-terminal carboxyl and, unlike the analogs containing Pro-NH<sub>2</sub>, is not subject to deactivation by deamidation. Consequently, the CNS effect is further increased (Table 1).

## Conclusion

A rational approach to deliver and target TRH analogs to the CNS has been demonstrated to increase central nervous system effects significantly in an animal model. The evolution of this strategy clearly highlights the importance of controlling transport and metabolism in peptide-based drug design.

## Acknowledgment

This project was supported by a grant from the National Institute on Aging (PO1 AG10485).

## References

1. Prokai, L., *Exp. Opin. Ther. Patents*, 7(1997)233.
2. Bodor, N., Prokai, L., Wu, W.-M., Jonnalagadda, S., Farag, H., Kawamura, T. and Simpkins, J., *Science*, 257(1992)1698.
3. Szirtes, T., Kisfaludy, L., Palosi, E. and Szporny, L., *J. Med. Chem.*, 27(1984)741.
4. Prokai, L., Ouyang, X., Wu, W.-M. and Bodor, N., *J. Am. Chem. Soc.*, 116(1994)2643.
5. Nutt, R.F., Holly, F.W., Homnick, C., Hirschman R. and Veber, D.F., *J. Med. Chem.*, 24 (1981)692.

# A novel lipoamino acid based system for delivery of Leu-enkephalinamide derivatives through the blood-brain barrier

Barrie Kellam, Mike S. Starr, Temitope G. Lamidi and Istvan Toth

Department of Pharmaceutical and Biological Chemistry, The School of Pharmacy, University of London WC1N 1AX, UK

The blood-brain barrier (BBB) is a crucial element in the regulation and constancy of the brain's internal environment. The presence of tight junctions and lack of aqueous pathways between cells greatly retard the movement of polar solutes between the capillary lumen and the cerebral tissue [1]. Peptides are one such group of polar solutes which exert multiple biological actions within the CNS and are therefore extremely attractive targets for neuropharmaceuticals [2]. However, their lack of penetration through the BBB and rapid degradation by luminal and abluminal peptidases [3] remain major obstacles which must be addressed before their clinical application becomes feasible. We reasoned that introduction of lipoamino acids (LAA's) [4] into the structure of a bioactive peptide could both increase the overall molecular lipophilicity, while imparting a degree of peptidase resistance due to the atypical nature of the amino acids incorporated [5]. We chose the analgesic peptide, Leu-enkephalinamide, as an initial candidate to investigate this hypothesis. The *in vitro* activity and preliminary *in vivo* data is presented for a series of C- and N-terminal modified LAA-conjugates.

## Results and Discussion

The following series of C-terminal (**1**) and N-terminal (**2**) diastereomeric LAA-modified Leu-enkephalinamides were synthesized *via* standard Boc SPPS conditions using an MBHA resin (Table 1).

Table 1. C-Terminal (**1**) and N-terminal (**2**) modified Leu-enkephalinamides synthesized.

Compound No.	m	n
<b>1a</b>	1	8
<b>1b</b>	2	8
<b>1c</b>	1	10
<b>1d</b>	2	10
<b>1e</b>	1	12
<b>1f</b>	2	12
<b>1g</b>	1	16
<b>1h</b>	2	16
<b>2a</b>	1	8
<b>2b</b>	1	10
<b>2c</b>	1	12
<b>2d</b>	2	12
<b>2e</b>	2	14
<b>2f</b>	1	18

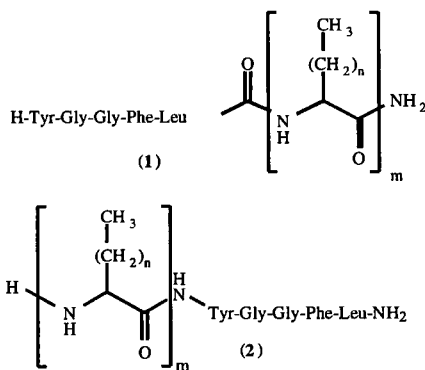


Table 2. Guinea pig ileum (GPI) and mouse vas deferens (MVD) assays of the active C- and N-terminal LAA-conjugates of Leu-enkephalinamide.

Compound No	GPI		MVD	
	IC <sub>50</sub> [μM] <sup>a</sup>	Rel. Potency	IC <sub>50</sub> [μM] <sup>a</sup>	Rel. Potency
<b>1a</b>	1.8 ± 0.41	0.97 ± 0.22	0.18 ± 0.01	1.58 ± 0.1
<b>1b</b>	not active	not active	7.0 ± 0.35	0.04 ± 0.002
<b>1c</b>	3.0 ± 0.67	0.18 ± 0.04	2.3 ± 0.35	0.12 ± 0.01
<b>1e</b>	6.0 ± 1.30	0.09 ± 0.02	2.55 ± 0.23	0.11 ± 0.01
<b>1g</b>	60 ± 4.0	0.009 ± 0.0006	14 ± 2.1	0.02 ± 0.003
<b>2a</b>	0.92 ± 0.12	0.60 ± 0.08	0.50 ± 0.02	0.55 ± 0.02
<b>2b</b>	2.16 ± 0.52	0.25 ± 0.06	1.08 ± 0.25	0.26 ± 0.06
<b>2c</b>	7.71 ± 1.10	0.07 ± 0.01	2.15 ± 0.66	0.13 ± 0.04
<b>Leu-Enkephalinamide</b>	0.54 ± 0.16	1.0	0.26 ± 0.07	1.0

<sup>a</sup> Mean of three determinations ± SEM.

Following RP-HPLC purification, the individual diastereomeric LAA-peptide conjugates were investigated for intrinsic activity using both guinea pig ileum (GPI) and mouse vas deferens (MVD) assay (Table 2). The *in vitro* data indicated one conjugate (**1a**) exhibited a greater activity than that of the native peptide. The *in vivo* data for this particular compound is currently under evaluation. The compounds **1c**, **1e**, **2a**, and **2b** were utilized in a series of hot plate tests on pre-dosed rats.

The *in vivo* results obtained for the above mentioned compounds demonstrated higher activity in the C-terminal LAA-modified enkephalins than in the N-terminal conjugates. However, it is worth taking note that in most cases, the activity was not as marked as that displayed by the native peptide. The exception was monomer **1c**, which possessed an activity comparable to that of Leu-enkephalinamide. Brain dialysis experiments using radiolabelled compounds are currently being undertaken to quantify CNS uptake.

As further future work, we are focusing attention on the C<sub>8</sub> and C<sub>10</sub> modified structures and investigating whether a degradable pro-drug linkage or a stable peptide bond isostere will provide the most potent and long acting enkephalin derivative.

## References

1. For reviews see: a) Begley, D.J. *J. Pharm. Pharmacol.*, 48 (1996) 136. b) Zlokovic, B.V. *Pharm Res.*, 12 (1995) 1395. and references cited there in.
2. Partridge, W.M. *Peptide Delivery to the Brain*, Raven Press, New York, (1991), pp 23-52.
3. Brownson, E.A., Abbruscato, T.J., Gillespie, T.J., Hruby, V.J. and Davis, T.P. *J. Pharmacol. Exp. Ther.*, 270 (1994) 675.
4. Gibbons, W.A., Hughes, W.A., Charalambous, M., Christodoulou, M., Szeto, A., Aulabaugh, A.E., Mascagni, P. and Toth, I. *Liebigs Ann. Chem.*, (1990) 1175.
5. Toth, I., Flinn, N., Hillery, A.M., Gibbons, W.A. and Arthursson, P. *Int. J. Pharm.*, 105 (1994a) 241.

# Hydrophobic peptides: Synthesis and interaction with model membranes

Francesca Reig,<sup>a</sup> Isabel Haro,<sup>a</sup> Patricia Sospedra<sup>b</sup>  
and M. Asunción Alsina<sup>b</sup>

<sup>a</sup>*Department of Peptides, CID-CSIC, Jordi Girona 18, 08034-Barcelona, Spain*

<sup>b</sup>*Unity of Physicochemistry, Faculty Pharmacy, Av. Joan XXIII, 08028- Barcelona, Spain*

Targeting of drugs, particularly with toxic molecules, is a key point in the treatment of several diseases. The side effects of cytostatics can be reduced using liposomes as carriers. Specific delivery of cytostatics to tumor cells can increase its efficacy resulting in a reduction of therapeutic doses.

Attachment of peptides to the surface of vesicles can be carried out by several methods, the simplest one being the use of hydrophobic peptide/protein derivatives.

Following this approach several laminin YIGSR peptide derivatives have been synthesized and their physicochemical characteristics as well as their incorporation into lipid vesicles determined.

## Results and Discussion

The parent peptide was synthesized by Fmoc/tBut methodology, using a Rink Amide MBHA resin. Fatty residues incorporated to the amino terminal group were stearoyl (S-P1), myristoyl (M-P1) and decanoyl (D-P1). Hydrophobic peptides were characterized by amino acid analysis, mass spectrometry and RP-HPLC (C<sub>8</sub>); peptides were purified when necessary by preparative HPLC.

Physicochemical characterization was carried out studying several parameters: HPLC capacity factors, surface activity, compression isotherms of monomolecular layers, insertion in DPPC monolayers spread at 10 mN/m, binding to DPPC vesicles and modification of DPPC vesicle microviscosity. As a reference, decanoic and myristic acid were also included in the protocols. As a general trend results of physicochemical studies are highly dependent on the polarity of the media. Experiments that involve peptide organic solutions, such as HPLC and monomolecular layers compression isotherms, showed a clear profile dependence on the length of the alkyl chain (Fig. 1).

Surface activity and insertion into monolayers of DPPC indicated a maximum activity for D-P1 and M-P1 derivatives, respectively, but that of S-P1 was negligible. This behavior could be due to some type of aggregate formation in aqueous media. The stability of these structures, probably micelles, would reduce the incorporation of peptide derivatives both to the air /water interface and DPPC monolayers.

The interaction of these peptides with phospholipid bilayers was determined using polarization fluorescence techniques. After incubation of liposomes with P-1 and P-2 no changes in the microviscosity of bilayers were detected in the range of 25-50°C. On the

contrary, the presence of D-P1, M-P1 and S-P1 in the incubation media had a soft rigidifying effect (Fig. 1). Moreover, water dispersions of these peptides mixed with DPH were fluorescent. This fact indicates the presence of aggregates that provide hydrophobic holes able to accommodate DPH molecules and is in agreement with the results previously described with monolayers.

The possibility of incorporating hydrophobic peptides to the surface of liposomes was determined following two approaches. Peptides D-P1, M-P1 and S-P1 were either mixed in organic media with DPPC at the beginning of the liposomal preparation process or incubated with DPPC liposomes. Results indicate that when peptides are incorporated at the beginning of the process yields are slightly better than after incubation with preformed liposomes. Moreover, in this case the higher hydrophobicity of M-P1 compared to D-P1 had a beneficial effect on its incorporation into the liposomal surface. The same experiments carried out with S-P1 resulted in aggregation of vesicles as well as the formation of amorphous deposits.

In summary, the optimal hydrophobic-hydrophilic balance has to be determined in order to obtain a maximal incorporation of hydrophobic peptides to the surface of liposomes.

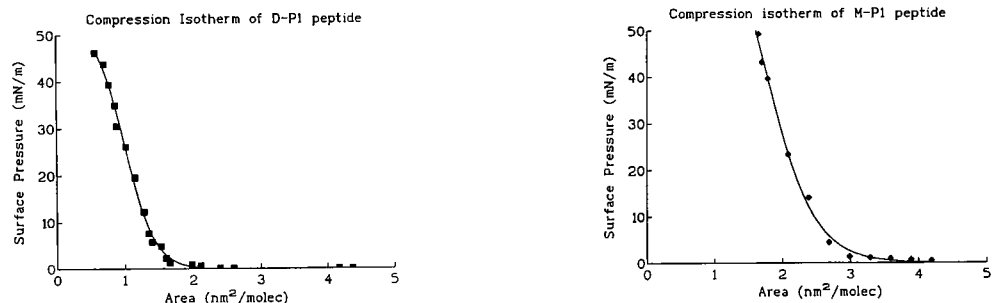


Fig. 1. Pressure-area isotherms of peptides D-P1 and M-P1.

## Acknowledgements

This work was supported by a Grant SAF93-0063 from CICYT, Spain.

# Importance of hydrophobic region in cationic peptides on gene transfer

Naoya Ohmori<sup>a</sup>, Takuro Niidome<sup>a</sup>, Taira Kiyota<sup>b</sup>, Sannamu Lee<sup>b</sup>,  
Gohsuke Sugihara<sup>b</sup>, Akihiro Wada<sup>c</sup>, Toshiya Hirayama<sup>c</sup>, Tomomitsu  
Hatakeyama<sup>a</sup> and Haruhiko Aoyagi<sup>a</sup>

<sup>a</sup>Faculty of Engineering, Nagasaki University, Nagasaki 852, Japan, <sup>b</sup>Faculty of Science, Fukuoka University, Fukuoka 814-80, Japan and <sup>c</sup>Institute of Tropical Medicine, Nagasaki University, Nagasaki 852, Japan

Gene transfer techniques represent important advances in the treatment of both inherited and acquired diseases. For the purpose of gene therapy, many nonviral gene transfer techniques have been studied, particularly the use of cationic lipid and polycation such as polylysine [1,2]. However, these gene transfer techniques have some problems, *e.g.*, transfection efficiency, reproducibility, and cytotoxicity. We have previously reported that an amphiphilic  $\alpha$ -helical peptide containing basic amino acid residues efficiently made the target gene transfect into cultivated cells [3]. In this study, to clarify the importance of the hydrophobic region of an amphiphilic structure on gene transfer, we synthesized five Hel peptides, which have different hydrophobic region widths and examined the correlation between their structural features and their gene-transfer abilities.

## Results and Discussion

The synthetic peptides (Fig. 1) contain Leu and Lys residues in ratios of 13:5, 11:7, 9:9, 7:11, and 5:13, respectively, the width of hydrophobic region therefore decreasing in this

Hel 13-5	:	H-KLLKLLLKLWLKLLKLLL-OH
Hel 11-7	:	H-KLLKLLLKLWKKLLKLLK-OH
Hel 9-9	:	H-KLLKKLLKLWKKLLKCLK-OH
Hel 7-11	:	H-KKLKLLKKWKKLLKCLK-OH
Hel 5-13	:	H-KKLKLLKKKWKLLKCLK-OH

Fig. 1. The primary structures of Hel peptides.

order. We investigated DNA-binding ability of the peptides by agarose gel electrophoresis. Among the peptides, Hel 13-5, which has the widest hydrophobic region, most strongly bound to DNA. The order of binding abilities was Hel 13-5 > Hel 11-7, Hel 9-9 >> Hel 7-11, Hel 5-13. The results of CD spectra measurements of the five peptides showed that Hel 13-5 and Hel 11-7 formed  $\alpha$ -helical structures, while the other three peptides mainly took a

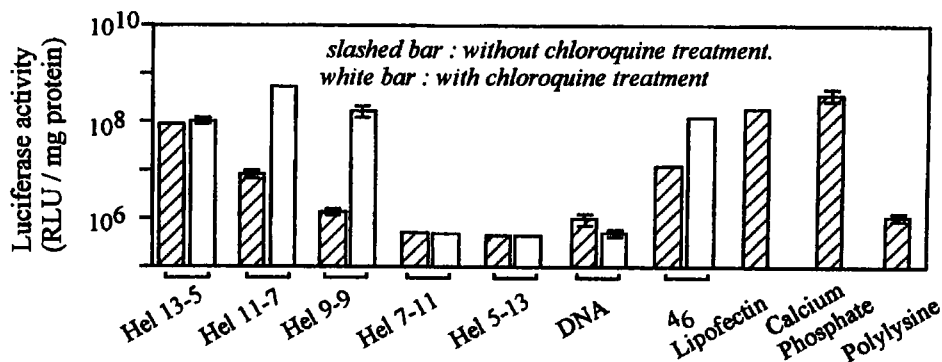


Fig.2. Gene-transfer efficiency of Hel peptides.

random structure in the absence of DNA. In the presence of DNA, Hel 13-5 and Hel 11-7 showed different CD patterns compared with those in the absence of DNA, suggesting that the conformations of these two peptides were largely changed by forming a complex with DNA. These results indicated that binding ability of the peptide was correlated with its secondary structure. The gene-transfer efficiency of these peptides was tested with the plasmid DNA which contains a reporter gene encoding firefly luciferase (Fig. 2). Hel 13-5 showed the highest transfection ability. The order of transfection efficiency was Hel 13-5 > Hel 11-7 > Hel 9-9. Hel 7-11 and Hel 5-13 did not have transfection efficiency. The efficiency depended on the width of their hydrophobic region. Concurrent treatment with chloroquine increased the gene-transfer efficiencies of Hel 13-5, Hel 11-7, and Hel 9-9, suggesting that the internalization of the peptide-DNA complex could be mediated by an endocytosis pathway.

In this study, we clarified that the width of the hydrophobic region in  $\alpha$ -helical structure of peptides is important for binding to DNA and efficient gene-transfer. It is expected that peptides with high potential as functional gene carriers will be constructed.

## References

1. Plank, C., Oberhauser, B., Mechtler, C., Koch, C. and Wagner, E., *J. Biol. Chem.*, 269(1994)12918.
2. Hara, T., Kuwasawa, H., Aramaki, Y., Takada, S., Koike, K., Ishidate, K., Kato, H. and Tsuchiya, S., *Biochim. Biophys. Acta*, 1278(1996)51.
3. Niidome, T., Ohmori, N., Ichinose, A., Wada, A., Mihara, H., Hirayama, T. and Aoyagi, H., *J. Biol. Chem.*, 272(1997)15307.

# A novel lipoamino acid based system for peptide delivery: Application for administering tumor selective somatostatin analogues

Nicholas S. Flinn,<sup>a</sup> Judit Erchegyi,<sup>b</sup> Aniko Horvath,<sup>b</sup> Gyorgy Keri<sup>b</sup>  
and Istvan Toth<sup>a</sup>

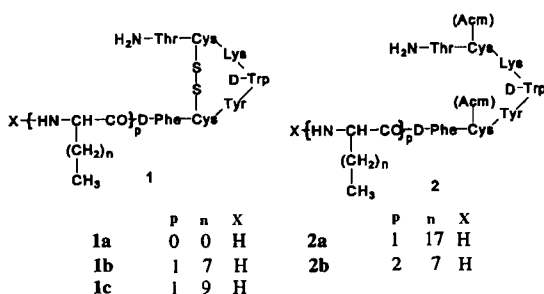
<sup>a</sup>Dept. Of Pharmaceutical and Biological Chemistry, The School of Pharmacy, University of London, 29-39 Brunswick Square, London WC1N 1AX. U.K.; <sup>b</sup>Institute of Biochemistry, Semmelweis University of Medicine, 1444 Budapest 8, POB 260. Hungary.

Incorrectly or over-expressed signals generated by hormones and growth factors that control tumor development have become established areas for anti-tumor research. The anti-tumor activity of the hormone somatostatin has long been known and several somatostatin analogues are already in clinical practice as anti-secretory hormones. However, their use as anti-tumor agents is limited due to their lack of selectivity for cancer cells and their poor delivery and biological instability, which is common to peptides.

One such somatostatin analogue, TT-232 (1a) [1], has been conjugated to a drug/peptide delivery system based on lipoamino acids, which are alpha amino acids with long alkyl side chains of varying lengths at the alpha-carbon. These lipoamino acids have previously been shown to enhance oral bioavailability and the biological stability of peptide hormones.[2].

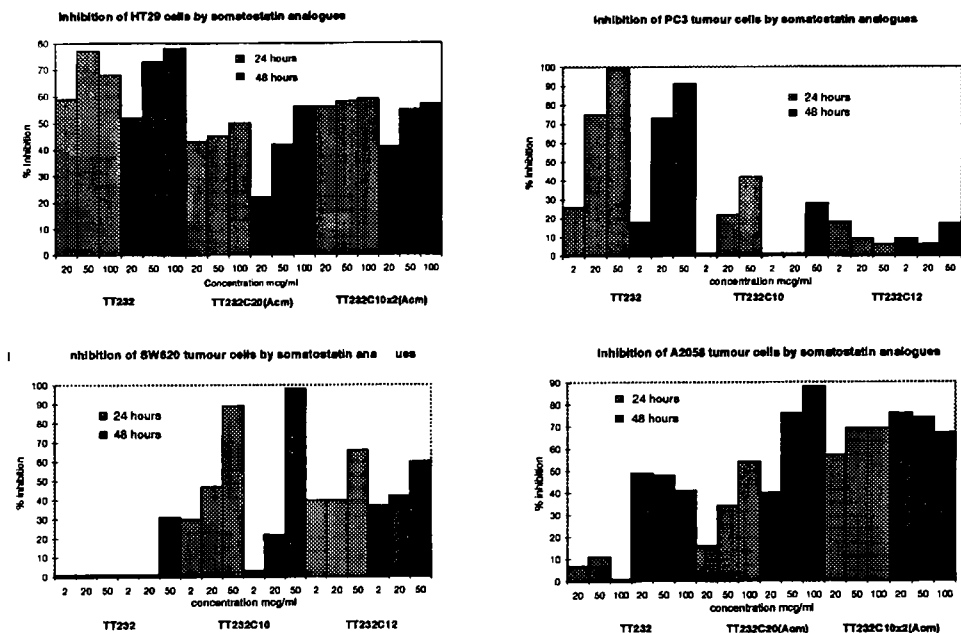
## Results and Discussion

The somatostatin analogue, 1a, was synthesized using Boc/Benzyl protection and HBTU coupling methodology and was extended on its N-terminus with either one or two lipoamino acids having side chains of varying lengths. The compounds were used in either their oxidized (cyclic) form or as the linear (Ac<sub>m</sub> protected) derivative. The cyclizations were performed off-resin using 20-30eq. of iodine in 95% acetic acid (aq.).



The above analogues were then incubated with various tumor cell lines for 24 and 48 hours

at varying concentrations. Visualization of the anti-tumor activity was achieved by employing a spectrophotometric assay using a tetrazolium salt (MMT), [3], which is converted to a colored derivative (Formazan) only by surviving cells and not those killed by the somatostatin analogues. The OD of the Formazan produced was measured at 570nm. The tumor cell lines used were HT29 (colonic), PC3 (prostatic), SW620 (colonic) and A2058(melanoma) cells.



In the SW620 cells **1a** has less effect than the **1b** and **1c** cyclic analogues which show very strong activity in a dose dependant manner. However, **1a** has a kill rate of almost 100% in PC3 cells while the lipid analogues have very little activity towards this cell line. Similar selectivity is seen with the linear **2a** and **2b** lipopeptides in A2058 and HT29 cells.

## References

1. Keri, G., Erchegeyi, J., Horvath, A., Mezo, I., Idei, M., Vantus, T., Balogh, A., Vadasz, Z., Bokonyi, G., Seprodi, J., Teplan, I., Csuka, O., Tejada, M., Gaal, D., Szegedi, Z., Szende, B., Roze, C., Kalthoff, H. and Ullrich, A., Proc. Natl. Acad. Sci. U.S.A., 93 (1996) 12513.
2. Flinn, N., Coppard, S. and Toth, I., Int. J. Pharm., 137 (1996) 33.
3. Hansen, M., Nielsen, S. and Berg, K., J. Immunol. Methods, 119 (1989) 203.

# Aerosol delivery of peptide immuno-modulators to rodent lungs

**Ronald J. Pettis and Anthony J. Hickey**

*School of Pharmacy, University of North Carolina at Chapel Hill, Beard Hall, Chapel Hill, N.C. 27599, U.S.A. "Current affiliation: Becton Dickinson Research Center, 21 Davis Drive, Research Triangle Park, N.C. 27709, USA*

The lung is a primary and metastatic site for a variety of tumors due to the entrapment potential of the alveolar capillary bed [1]. One approach to treatment is to stimulate the local immune system to destroy cells with metastatic potential prior to formation of secondary tumors. Alveolar macrophages (AM) are the first line of defense in cell-mediated immunity of the lung. Immunomodulators can enhance the activity of these cells by stimulating phagocytosis, enhancing the production of cytokines and degradative enzymes, and recruiting additional macrophages to the site [2]. Delivery of aerosolized immunomodulators directly to the lung by inhalation can localize the drug at the site of action and minimize systemic side effects. Our preliminary studies have been performed to evaluate indicators of alveolar macrophage activation following treatment of rodents with the peptide immunomodulator, muramyl dipeptide (MDP) [3].

## Results and Discussion

*Cellular Morphology.* Aerosolized solutions of MDP (100 µg/ml, 10 min exposure) were administered to guinea pig lungs *in vivo* by inhalation. The estimated dosage to each animal was 10-20 µg of MDP. After specified survival intervals, AM were

*Table 1. Morphological changes in Guinea pig alveolar macrophages after MDP exposure.*

Survival Time after MDP Aerosol (h)	MDP Exposure	
	<i>In Vivo</i>	<i>In Vivo + In Vitro</i>
0 <sup>a</sup>	-	+/-
6	+/-	+/-
24	+	++
48	+/-	+
48 <sup>b</sup>	++	++

a. Saline treated control animals.

b. Two *in vivo* exposures on successive days.

- ≤ 10% cytoplasmic spreading
- +/- 10-20% spreading, some visible extension of pseudopodia
- + 20-35% spreading, numerous cells with pseudopodia or elongated morphology
- ++ >35% spreading or altered morphology

harvested by broncho-alveolar lavage (BAL), and examined by light microscopy. AM from MDP exposed animals began to show morphological indicators of activation, such as cytoplasmic spreading [4], within six hours after exposure (Table 1). These effects became more pronounced at 24 h, and had begun to diminish by 48 h. Cells treated *in vitro* with a second MDP stimulus (100  $\mu$ l of 100  $\mu$ g/ml for 1 h) exhibited a higher percentage of activated cells in all cases. The total number of AM recovered from the lungs of treated animals was elevated 3-8 fold above that of saline-treated controls, indicating cellular recruitment to the administration site. Recovered BAL fluid also showed elevated levels for enzymatic markers of AM activation (alkaline phosphatase, N-acetyl- $\beta$ -D-glucosaminidase, and total protein).

**Nitric Oxide (NO) Synthesis.** To correlate morphological changes with cytostatic potential, production of the reactive chemical species NO was investigated *in vitro*. AM were harvested from untreated and MDP-aerosol treated (24 h survival) rats and cultured in the presence of a second immunomodulator stimulus, either MDP or lipopolysaccharide (LPS) for 24 h. NO levels in the culture supernate were colorimetrically quantitated (Greiss reagent) as nitrite. AM from control and MDP-treated animals show low basal levels of NO production (Fig. 1, control bars). Untreated AM show a concentration dependent response to *in vitro* LPS or MDP. AM from *in vivo* MDP-aerosol treated animals are refractory to a secondary *in vitro* challenge of MDP, but show an elevated response to LPS. Morphological, numerical and NO synthase activity studies of AMs exposed to MDP aerosols indicate activation of these cells. Further studies are required to address the potential for lung cancer therapy.

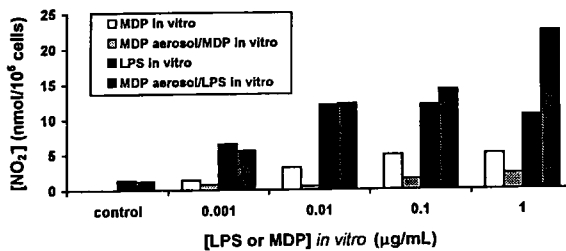


Fig. 1. NO production of untreated and MDP-aerosol treated AM in response to a immunomodulator stimulus.

## References

1. Pulmonary Disease, J.P. Lipincott Philadelphia, 1994, p. 524 Saldana, M.J., Sridhar, K.S. and Thurer, R.J., In Saldana, M.J. (Ed.) Pathology of Pulmonary Disease, J. P. Lipincott Philadelphia, 1994, p. 524.
2. Adam, A., Petit, J.F., Lefrancier, P. and Lederer, E., Molec. Cell. Biochem., 41 (1981) p. 27
3. Pettis, R.J., Hall, I. and Hickey, A.J., Pharm. Res., 13 (1996) S166.
4. Donaldson, K., Bolton, R.E., Brown, D. and Douglas, A., Immunol. Comm., 13 (1984) p. 229.

## AUTHOR INDEX

- Abel, P.W., 597  
Agner, E.K., 178  
Agricola, I., 650  
Aguilar, M.-I., 194, 485  
Ahn, J.-M., 293, 619  
Aida, C., 295  
Aimoto, S., 475, 491  
Akaji, K., 333, 667, 678  
Akamatsu, Y., 121  
Albericio, F., 38, 68, 307, 339  
Albert, A.D., 424  
Alberts, D., 178, 192  
Alderfer, J.L., 424  
Alexopoulos, C., 771  
Alfaro-Lopez, J., 145, 214  
Aligue, R., 605  
Alkhalili, L., 793  
Alsina, J., 38  
Alsina, M.A., 839  
Alvarez, V., 60  
Amaducci, L., 700  
Amato, M.A., 426  
Amblard, M., 101  
Anantharamaiah, G.M., 410  
Andersen, N.H., 408  
Andersen, P.H., 635  
André, F., 111  
Angell, Y.M., 223, 339  
Annis, I., 343  
Antohi, O., 428  
Aoyagi, H., 627, 841  
Appel, J.R., 761  
Aramini, J.M., 609  
Arendt, A., 424  
Arshava, B., 309, 428  
Asari, T., 216  
Attila, M., 473  
Audus, K.L., 753
- Bab, I., 607  
Bajusz, S., 682  
Balachandran, G.K., 147  
Balanov, A., 50  
Balasubramaniam, A., 578  
Balasubramanian, P., 569  
Balboni, G., 603  
Baldwin, M., 285
- Ball, H.L., 285  
Bankaiti-Davis, D., 32  
Barabás, É., 682  
Barany, G., 38, 68, 157, 226, 271, 273,  
275, 277, 339, 343, 495  
Barbier, J.-R., 599  
Barbone, F.P., 501  
Barchi, J.J., 582  
Bardají, E., 307  
Barford, D., 183  
Barnes, M., 711  
Baron, R., 181  
Basak, A., 676  
Baskin, E.P., 672  
Baum, J., 463  
Baumruk, V., 481  
Baxter, A.D., 204  
Beaton, G., 32  
Beausoleil, E., 151  
Beck, H., 763  
Becker, J.M., 309, 428, 831  
Becklin, R.R., 809  
Bednarek, M.A., 303  
Behar, V., 447  
Bekker, T., 285  
Bélichard, P., 101  
Ben, R.N., 711  
Ben-Aroya, N., 621  
Benckhuijsen, W.E., 56  
Berezowska, I., 514  
Berg, R.H., 89, 169  
Bergé, G., 101  
Berman, P.W., 795  
Bernd, M., 465  
Bernhagen, J., 394, 400  
Beyer, B.M., 381  
Beyermann, M., 239  
Bhatnagar, P.K., 178, 192  
Bhatt, D., 381  
Bhawasari, N., 424  
Bhowmick, N., 584  
Bianchi, C., 473, 603  
Bianchi, E., 86, 396  
Bibbs, L., 705  
Bienert, M., 239, 289  
Binstead, R.A., 149  
Biondi, B., 611

- Biondi, M., 700  
 Bischoff, L., 674  
 Bisello, A., 392, 439, 479  
 Bishop, B.M., 109  
 Bitan, G., 451  
 Bjergarde, K., 32  
 Blalock, J.E., 255, 803  
 Blaszczyk-Thurin, M., 715  
 Blazyk, J., 385  
 Blomberg, J., 793  
 Blondelle, S.E., 605  
 Blumenstein, M., 567  
 Blundell, T., 381  
 Boatman, P.D., 212  
 Bock, K., 46  
 Bock, M.G., 672  
 Bodo, B., 435  
 Bodor, N., 834  
 Bogyo, M., 686  
 Boileau, A.J., 508  
 Bolger, R.E., 715  
 Bonewald, L.F., 705  
 Bonk, I., 553  
 Bonner, G.G., 633  
 Bontcheva, M., 155  
 Borchardt, R.T., 825  
 Borin, G., 611  
 Brader, M.L., 406  
 Bradley, M., 54  
 Brex, V., 200  
 Brehm, E., 265, 605  
 Breipohl, G., 181  
 Breslav, M., 309, 428  
 Briand, J., 178  
 Brickner, M.L., 461, 751  
 Briskin, M.J., 204  
 Broto, P., 181  
 Broxterman, Q.B., 375  
 Brunner, H., 400  
 Bryan, H., 43  
 Bryan, W.M., 43  
 Bryant, S.D., 473, 603, 660  
 Bucala, R., 394, 400  
 Buencamino, J., 761  
 Bukhtiyarova, M., 381  
 Bulet, P., 703  
 Burgess, J.L., 192  
 Burke, Jr., T.R., 183  
 Burkhart, B.M., 389  
 Burkhart, F., 449  
 Burley, S.K., 619  
 Burritt, A., 293  
 Bursavich, M.G., 329  
 Burton, J.A., 253  
 Butcher, D.J., 139  
 Byk, G., 48, 823  
 Cabezas, E., 202, 441  
 Cai, C., 241  
 Calderan, A., 611  
 Callahan, J.F., 178, 192  
 Calvo, J.C., 208, 819  
 Camarero, J.A., 62, 387  
 Cameron, P., 66  
 Campbell, G.D., 761  
 Campbell, W.H., 813  
 Câmpian, E., 35  
 Canne, L.E., 301, 643  
 Carafoli, E., 709  
 Caravatti, G., 555, 707  
 Carpenter, G., 520  
 Carpenter, K.A., 514  
 Carpino, L.A., 239  
 Carter, J.M., 60  
 Cavalieri, F., 186  
 Cavelier, F., 111  
 Cervini, L., 637  
 Chaddha, M., 410  
 Chan, L., 775  
 Chan, S.-C., 739  
 Chan, W.Y., 127  
 Chance, W.T., 578  
 Chao, H., 747  
 Chelli, M., 345, 700  
 Chen, C.C., 432  
 Chen, H.M., 739  
 Chen, I.-W., 672  
 Chen, L., 192, 275  
 Chen, S.-T., 414  
 Chen, V.J., 615  
 Chen, Y., 607  
 Chen, Z., 672  
 Cheng, J.-W., 565  
 Cheng, L.L., 127  
 Cheung, C.P., 511, 613  
 Chi, K., 341  
 Chittur, K.K., 410  
 Chmielewski, J.A., 366, 461, 751  
 Choconta, K.C., 819  
 Choksi, S., 493, 517, 609  
 Chong, P., 777, 787  
 Chorev, M., 392, 402, 439, 447, 451, 479,  
 541, 607  
 Christensen, D.H., 251  
 Christenson, B., 793  
 Chung, M.C.M., 775  
 Chung, N.N., 514  
 Cilli, E.M., 805

- Cirillo, R., 186  
 Clark, P.L., 349  
 Clark-Pierce, L., 549  
 Clausen, H., 713  
 Cochran, N.A., 204  
 Cody, W.L., 335, 688  
 Cohen, I., 50  
 Coleman, C., 60  
 Collins, J.R., 670  
 Cone, R.D., 723  
 Conte, B., 186  
 Cooper, P.S., 603  
 Corey, D.R., 299  
 Corley, C.A., 828  
 Cornille, F., 398, 535  
 Corrigan, A., 737  
 Cowburn, D., 157  
 Coy, D.H., 526, 559  
 Craig, A., 737  
 Crisma, M., 375, 378, 435  
 Cronin, N., 381  
 Crozet, Y., 29  
 Cubbon, R., 66  
 Cukierski, M., 828  
 Cummings, R., 66  
 Cung, M.-T., 437  
 Cussac, D., 398, 535  
 Cuthbertso, A.S., 178  
 Cypess, A.M., 511  
 Czajkowski, C., 508  
  
 D'Andrea, L.D., 92  
 D'Auria, G., 92  
 Daffix, I., 101  
 Dakappagari, N., 779  
 Dancheck, K.B., 672  
 Danho, W., 539  
 Daugé, V., 674  
 David, C., 674  
 Davies, P., 695  
 Davies, P.L., 747  
 Davis, P., 145, 214, 617  
 De Falco, S., 537  
 De Farnesco, R., 396  
 De Fatima Fernandez, M., 237  
 De Jonge, N., 165  
 Deber, C.M., 125, 355  
 Deeg, M., 763  
 DeGrado, W.F., 95  
 Dekany, G., 719  
 del Fresno, M., 38  
 Deschamps, J.R., 633  
 Desiderio, D.M., 809  
 Diaz, D., 208, 819  
  
 Dickinson, C., 580  
 Dietrich, U., 793  
 DiMarchi, R.D., 615  
 Dodey, P., 101  
 Dodge, J.A., 133  
 Doherty, A.M., 210, 335, 688  
 Donahue, J.P., 733  
 Donaldson, C., 637  
 Donella-Deana, A., 611  
 Dong, J.Z., 541  
 Dorey, M., 424  
 Dörner, B., 58  
 Dovalsantos, E.Z., 202  
 Dower, W.J., 501, 569  
 Drakopolou, E., 86  
 Dreveny, I., 443  
 Drijfhout, J.W., 56  
 Drouillat, B., 719  
 Duax, W.L., 389  
 Dubertret, C., 823  
 Due, Y.-C., 575  
 Dumy, P., 155  
 Dunn, B.M., 381  
  
 Echner, H., 283  
 Eden, P., 578  
 Edling, A.E., 517, 609  
 Edwards, P.J., 297  
 Eguchi, M., 212  
 Eichler, J., 761  
 Eissenstat, M.A., 317  
 El-Faham, A., 239  
 Eliot, G.S., 631  
 Elzer, P.H., 595, 652  
 Enjalbal, C., 111  
 Erchegyí, J., 843  
 Érchegyí, J., 190  
 Erickson, B.W., 109, 141, 147, 149, 161,  
 163  
 Erickson, J.W., 670  
 Ertl, H.C.J., 233, 715  
 Espejo, F., 208, 819  
 Evers, A.R., 508  
  
 Falender, C.A., 828  
 Fan, C.-X., 337  
 Fang, S., 791  
 Fann, Y.C., 504  
 Farrell, F.X., 501  
 Fassina, G., 537, 773  
 Fauszt, I., 682  
 Feng, D.-M., 672  
 Fenouillet, E., 781

- Fenyő, E.-M., 793  
 Fergus, J., 173  
 Fields, G.B., 287, 523, 743  
 Figliozzi, G.M., 643  
 Fincham, C.I., 186  
 Fiori, S., 315  
 Fischle, W., 394  
 Fjerdingsstad, H., 178  
 Fleckenstein, B., 766  
 Flentke, G.R., 223  
 Flinn, N.S., 843  
 Flippen-Anderson, J.L., 435, 633  
 Flippen-Andeson, J.L., 378  
 Flora, D.B., 615  
 Floreani, A.A., 549  
 Formaggio, F., 435  
 Formagigo, F., 375, 378  
 Foster, M.C., 109  
 Fouchère, J.-L., 176  
 Fourny, D., 315  
 Fournié-Zaluski, M.-C., 398, 674  
 Fowler, C.B., 586  
 Frangione, M., 785, 799  
 Frederic, M., 48, 823  
 Freidinger, R.M., 672  
 Fretz, H., 555, 707  
 Fridkin, M., 621, 745, 749  
 Frieden, A., 38  
 Friedman, A.R., 327  
 Friedman, T.M., 517, 609  
 Frigo, T.B., 253  
 Fry, D., 539  
 Fujii, T., 475  
 Fujita, I., 623  
 Fujiwara, H., 295  
 Fujiwara, Y., 333  
 Fujiyoshi, T., 741  
 Fukazawa, T., 667  
 Fukuda, M., 321  
 Fukuhara, S., 648  
 Funakoshi, S., 307  
 Furet, P., 555, 707  
 Furka, Á., 35  
 Fuselier, J., 526  
 Futaki, S., 295, 321  
  
 Gaál, D., 561  
 Gaczynska, M., 686  
 Gadek, T., 181  
 Galaktionov, S., 361  
 Galatkionov, S., 477  
 Galin, F.S., 803  
 Gallant, D.L., 204  
 Galoppini, C., 571  
  
 Gambarini, A.G., 641  
 Gantz, I., 198, 580  
 Gao, J., 493, 517, 609  
 Garbay, C., 535  
 Garbow, J.R., 428  
 Garcia-Echeverria, C., 707  
 García-Echeverría, C., 555  
 Gardell, S.J., 672  
 Gardner, B.S., 212  
 Gaudino, J.J., 32  
 Gautam, N., 504  
 Gauthier, D., 676  
 Gauthier, T.J., 325, 595  
 Gay, B., 555, 707  
 Gazit, A., 190  
 Gazit, D., 607  
 Gellman, S.H., 159  
 Gennaro, R., 789  
 George, C., 378, 435, 633  
 Gera, L., 730  
 Germann, M.W., 609  
 Gershengoru, M.C., 52  
 Ghirlanda, G., 95  
 Ghosh, I., 366  
 Gierasch, L.M., 349  
 Ginanneschi, M., 700  
 Ginanneshci, M., 345  
 Giulianotti, A., 265  
 Giulianotti, M.A., 25, 58  
 Glas, R., 686  
 Goodman, B.A., 32  
 Goodman, M., 80, 259, 455, 469, 588  
 Goodman, S.L., 206  
 Gordon, T.D., 275  
 Gourvest, J.F., 181  
 Gozes, I., 749  
 Graham, H.D., 141  
 Graham, Jr., H.D., 141  
 Granoth, R., 749  
 Greeley, D., 539  
 Greenberg, Z., 607  
 Greenspan, N.S., 761  
 Gregson, K.S., 167  
 Greiner, G., 650  
 Griffin, P., 66  
 Griffith, J.D., 161  
 Gröger, S., 291  
 Groissman, E., 489  
 Gross, C.M., 495  
 Grouzmann, E., 625  
 Guerassina, T.A., 317  
 Guerrini, R., 473, 603  
 Gulnik, S.V., 670  
 Gulyás, E., 561

- Gulyas, J., 737  
 Guo, G., 364  
 Guo, L., 297  
 Gururaja, T.L., 483  
 Gustchina, E., 670  
 Guzman, F., 819  
 Guzmán, F., 208  
  
 Hadas, E., 50  
 Hadley, M., 658  
 Hadley, M.E., 198, 723  
 Haehnel, W., 107, 165  
 Hal, X.-L., 337  
 Halder, T., 763  
 Hall, D.A., 329  
 Hall, S.C., 828  
 Hamashin, V.T., 25, 265  
 Hammer, J., 385  
 Hammer, R.P., 117, 237, 595  
 Hammonds, G.R., 181  
 Han, G., 293, 723  
 Han, H., 22  
 Han, S.J., 420  
 Han, X., 517  
 Han, Y., 241, 273, 339  
 Hancock, R.E.W., 153  
 Hanly, A.M., 416  
 Hannah, A.L., 25  
 Hansen, B.S., 635  
 Hanson, P., 435  
 Hara, S., 631  
 Harada, T., 216, 741, 755  
 Haraux, F., 111  
 Hargittai, B., 271, 273  
 Hargrave, P.A., 424  
 Haro, I., 839  
 Harris, S.M., 408  
 Harvey, A.L., 593  
 Haskell-Luevano, C., 198, 580, 723  
 Hatakeyama, T., 627, 841  
 Hawiger, J., 726  
 Hayashi, Y., 216, 741, 755  
 He, J.X., 335  
 He, Z., 233  
 Hearn, M.T.W., 194  
 Heerding, D., 178, 192  
 Heires, A.J., 549  
 Henklein, P., 239  
 Hennard, C., 247  
 Hermes, J., 66  
 Herrera, C.J., 32  
 Herrera, R., 173  
 Hessler, G., 449, 465  
 Hickey, A.J., 845  
  
 Hicks, J.B., 690  
 Hiebl, J., 178  
 Hiemstra, H.S., 56  
 Higgins, K.A., 194  
 Hindsgaul, O., 557  
 Hine, B.M., 615  
 Hines, W., 68  
 Hirano, E., 623  
 Hirano, T., 654  
 Hirayama, T., 841  
 Hirschman, R., 11  
 Ho, J.C., 629  
 Hodges, R.S., 83, 135, 153, 467, 557,  
     639, 747  
 Hoey, K., 501  
 Hoffman, M.P., 735  
 Hoffmann, J.A., 615  
 Hoffmann, R., 233, 695, 703, 715  
 Hoffmüller, U., 70, 545, 551  
 Hojo, H., 121, 321  
 Holland, D., 173  
 Hollingsworth, M.A., 713  
 Hollósy, F., 190  
 Holm, A., 251  
 Hone, N., 204  
 Horstman, D., 520  
 Horvath, A., 843  
 Horváth, A., 190  
 Hosohata, K., 145, 214  
 Houghton, R.A., 25, 58, 265, 605, 761  
 Houston, Jr., M., 747  
 Houston, Jr., M.E., 467  
 Hoving, S., 709  
 Howl, J., 601  
 Hoyt, D.W., 372  
 Hruby, V.J., 145, 198, 214, 241, 293, 404,  
     619, 633, 658, 723  
 Hsieh, K.-H., 64  
 Hu, B.-H., 123  
 Hu, X., 573  
 Hua, Q., 369, 471  
 Huang, Z., 139, 493, 517  
 Hubbell, S., 173  
 Huffman, W.F., 43, 178, 192  
 Humblet, 173  
 Hung, Z., 609  
 Hurley, L.H., 383  
 Husbyn, M., 178  
 Hussain, R., 543, 571  
 Hvilsted, S., 89, 169  
  
 Idei, M., 190  
 Igarashi, K., 755  
 Iijima, K., 216

- Ikematsu, Y., 713  
 Ilag, L.L., 70  
 Inai, K., 817  
 Inui, T., 593  
 Ionescu, D., 239  
 Iqbal, M.A., 811  
 Irvin, R.T., 557
- Jablonski, J.-A., 323  
 Jackson, P.L., 255, 803  
 Jain, R., 526  
 James, O., 777, 787  
 Janda, K.D., 22  
 Janes, R.W., 358  
 Jarosinski, M., 305  
 Jaslin, G., 823  
 Jayawickrama, D.A., 807  
 Jean, F., 690  
 Jefferson, E.A., 80  
 Jelokhani-Niaraki, M., 153  
 Jensen, K.J., 38  
 Jernigan, K.A., 214  
 Jhon, J.S., 420  
 Ji, Q.-S., 520  
 Jiang, X., 455, 588  
 Jiang, Y., 491  
 Johansen, N.L., 635  
 Johansson, B., 793  
 John, D.M., 141  
 Johnson Kaufman, N., 713  
 Johnson, D.L., 501  
 Johnson, P., 828  
 Johnson, W.T., 615  
 Jolliffe, L.K., 501  
 Jonczyk, A., 206  
 Jones, L.M., 196  
 Jubilut, G.N., 805  
 Jue, D.L., 791  
 Juhász, A., 682  
 Jung, G., 766  
 Juvvadi, P., 497, 645
- Kahn, M., 212  
 Kalbacher, H., 763  
 Kaljuste, K., 249  
 Kálnay, A., 561  
 Kamphuis, J., 375  
 Kang, Y.K., 420  
 Kao, J., 489  
 Kappel, J.C., 237  
 Kapurniotu, A., 394, 400  
 Kari, U.P., 196  
 Karle, I.L., 104  
 Karlström, A.H., 244
- Katada, J., 216, 741, 755  
 Kates, S.A., 38, 68, 273, 705  
 Katipally, R., 299  
 Kato, R., 667  
 Kato, T., 654  
 Kaumaya, P.T.P., 779, 785, 799  
 Kay, C.M., 135, 467, 747  
 Kay, J., 381  
 Kazmierski, W., 633  
 Kearns, A.E., 385  
 Keidelring, T.A., 481  
 Keiderling, T.A., 375, 416  
 Kellam, B., 719, 837  
 Kelley, M.A., 68  
 Kelly, M., 545  
 Kemp, D.S., 445, 457  
 Kent, D.R., 688  
 Kent, S.B.H., 301, 643  
 Keri, G., 843  
 Kéri, G., 190  
 Kessler, H., 206, 449, 465  
 Khatir, A., 705  
 Khaznadar, T., 674  
 Kikelj, D., 188  
 Kim, H.-O., 212  
 Kim, H.-S., 834  
 Kim, W.H., 735  
 Kimura, M., 627  
 Kimura, T., 333, 593, 667, 678  
 King, A.G., 178, 192  
 King, C.R., 582  
 King, D., 285  
 Kinoshita, M., 121  
 Kirby, D.A., 52  
 Kimarsky, L., 416, 713  
 Kishida, M., 333  
 Kiso, Y., 333, 667, 678  
 Kisselev, O., 504  
 Kitagawa, K., 295  
 Kiyota, S., 641  
 Kiyota, T., 841  
 Kleemann, R., 400  
 Klein, M., 777, 787  
 Kleinjung, J., 437  
 Kleinman, H.K., 735  
 Klis, W.A., 127  
 Knolle, J., 181  
 Koch, U., 517, 609  
 Koch, Y., 621  
 Kochan, J., 539  
 Kodaira, K.-I., 475  
 Kodama, H., 623  
 Koerber, S., 637, 737  
 Kohn, W.D., 135

- Kondejewski, L.H., 153, 467, 639  
Kondo, M., 623  
Köpke, A.K.E., 553  
Korngold, R., 493, 517, 609  
Kostel, P., 815  
Kostel, P.J., 813  
Kowalska, M.A., 139  
Kowalski, J.A., 218  
Kramer, A., 769  
Krause, E., 289  
Kremmer, T., 561  
Kriauciunas, A., 615  
Krishna, N.R., 255, 803  
Kroll, M., 161  
Krstenansky, J.L., 619  
Kubiak, T.M., 327  
Kucken, A., 508  
Kumagaye, K.Y., 717  
Kunos, G., 723  
Kuratomi, Y., 735  
Kurth, M.J., 58  
Kutscher, B., 465  
Kutterer, K., 711
- Labbe, T.A., 117  
Lacassie, E., 481  
Lacey, D.L., 631  
Lahrichi, S., 737  
Lamaty, F., 176  
Lamer, S., 289  
Lamidi, T.G., 837  
Langel, Ü., 662  
Langs, D.A., 389  
Larive, C.K., 807  
Larsen, B.D., 251  
Larsen, M.J., 327  
Lauer, J.L., 523  
Lavigne, P., 83, 467  
Lawoko, A., 793  
Lazaro, R., 176  
Lazarus, L.H., 473, 603, 660  
Lazure, C., 676  
Lee, A., 670  
Lee, G.M., 408  
Lee, S., 841  
Lee, T.-H., 485  
Lee, V.M.-Y., 695  
Lehmann, C., 453  
Leight, S., 695  
Lemieux, C., 514  
Lemon, S.M., 147  
Lenoir, C., 398, 535  
Lenz, D.M., 32, 631  
Leonard, D.M., 210  
Leonard, J.J., 828  
Lester, C.C., 422  
LeVine, H., 586  
Levine, M.J., 483  
Lewis, G.S., 32  
Lewis, R.N.A.H., 639  
Lewis, S.D., 672  
Li, C., 123  
Li, H., 455  
Li, S., 139, 493, 517, 609  
Li, X., 573  
Li, Y.-J., 422  
Liao, C.-Y., 565  
Liao, S., 145, 241  
Lim, A., 161  
Lim, S., 723  
Lin, J., 241  
Lin, Y., 619  
Lin, Y.-Z., 733  
Liolitsas, C., 437  
Lipps, C.J., 690  
Lipton, M.A., 218  
Liu, B., 325  
Liu, C.-F., 235  
Liu, C.F., 291  
Liu, L.-P., 125, 355  
Liu, Z., 408  
Liu, Z.P., 349  
Livnah, O., 501  
Ljungberg, B., 793  
LoCastro, S., 178, 192  
Loewen, M.C., 747  
Lombardi, A., 92, 95  
Lomize, A.L., 530  
Loosmore, S., 787  
Lou, B.-S., 582  
Lovas, S., 412, 561  
Løvhaug, D., 178  
Lowis, D.R., 361  
Lowther, W.T., 381  
Lozano, J.M., 208  
Lu, J., 563  
Lu, N., 631  
Lu, Y.-A., 229  
Lu, Z., 139  
Lubell, W.D., 151  
Lubkowitz, M., 831  
Lucarini, J.-M., 101  
Lucas, R., 672  
Lund-Katz, S., 410  
Lung, F.-D.T., 547, 582  
Lunney, E.A., 173  
Luo, Z., 139  
Lutz, K.L., 753

- Lynch, J.J., 672  
Lynch, P., 68
- Ma, K.-Y., 575  
Ma, W., 133  
Mabrouk, K., 781  
MacDonald, D.L., 196  
MacDonald, M.T., 196  
Maddukuri, S.R., 196  
Madison, V., 539  
Madsen, K., 635  
Maglio, O., 92  
Majer, P., 317, 670  
Majerová, E., 317  
Makara, G.M., 281  
Makhov, A.M., 161  
Makofske, R., 539  
Malak, H., 430  
Mallamaci, M., 539  
Mallamo, J.P., 811  
Mallik, I., 257  
Mallik, S., 257  
Maloy, W.L., 196, 385  
Mamadou Sow, 176  
Mamalaki, A., 437  
Mammi, S., 439, 447, 479  
Manning, M., 127  
Maretto, S., 402, 439, 479  
Marks, J., 173  
Marletta, M.A., 167  
Marshall, G.R., 64, 281, 361, 432, 477, 489, 504  
Marti, R.E., 305  
Martin, L., 398  
Martin, L.M., 123  
Martin, M.S., 305  
Martin, R., 766  
Martire, M., 625  
Mascagni, P., 285  
Massacesi, L., 700  
Mathieu, M., 98  
Matinez, J., 101  
Matsueda, G.R., 567  
Matsumoto, H., 333, 667, 678  
Mattern, R.-H., 469  
Mayer, J.P., 32, 291, 631  
Mayfield, L., 299  
Mazaleyrat, J.-P., 378  
Mazzanti, B., 700  
Mazzucco, S., 345, 700  
McDowell, J.H., 424  
McElhaney, R.N., 639  
McInnes, C., 372  
McLaughlin, M.L., 325, 329, 331, 595, 652  
McLeod, D., 777, 787  
McMahon, F.J., 501  
McMaster, J.S., 686  
McMullen, T.P.W., 639  
McMurray, J.S., 705  
McNamara, D.J., 210  
McNamara, P., 684  
Mechnich, O., 465  
Medzihradsky, K.F., 705  
Meldal, M., 41, 46  
Mendel, D., 319  
Merluzzi, L., 789  
Merrifield, R.B., 497, 511, 613, 645  
Merslavič, I., 188  
Messina, P.A., 811  
Meyer, H.E., 763  
Meyer, J.-P., 25  
Meyer, T.J., 149  
Mező, I., 561  
Miao, Z., 491  
Middleton, S.A., 501  
Mierke, D.F., 392, 402, 439, 451  
Mihara, H., 137, 627  
Mihara, H., 131  
Miki, S., 121  
Miller, C., 737  
Miller-Lindholm, A., 549  
Millhauser, G.L., 435  
Mimoto, T., 667  
Min S. Lee, 212  
Miranda, A., 737, 805  
Miranda, M.T.M., 641  
Mishra, V.K., 410  
Mitaritonna, N., 119  
Miyazaki, M., 623  
Miyazaki, S., 623  
Mochalkin, I., 680  
Mokotoff, M., 311  
Molla, A., 176  
Monaco, V., 435  
Monteagudo, E., 186  
Moore, C., 633  
Moore, M.L., 43  
Morales, G.A., 325  
Moreau, J.-P., 541  
Morgan, B.A., 275, 541  
Morgan, E.L., 549  
Morita, H., 654  
Morley, P., 599  
Moroder, L., 313, 315  
Mosberg, H.I., 167, 530, 586, 629  
Moulard, M., 781

- Mousigian, C.A., 629  
 Moutsopoulos, H.M., 771  
 Muhrad, A., 607  
 Muir, T., 459  
 Muir, T.W., 62, 387  
 Mukai, H., 648  
 Mulcahy, L.S., 501  
 Munekata, E., 648  
 Muramatsu, M., 741, 755  
 Murphy, R.F., 412, 561  
 Murphy, W.A., 526  
 Mutoh, M., 547  
 Mutter, M., 155, 453, 625  
  
 Naganogowda, G.A., 483  
 Nagase, H., 743  
 Nägele, T., 313  
 Naider, F., 309, 428, 831  
 Nakagawa, S.H., 369, 471  
 Nakai, T., 129  
 Nakaie, C.R., 805  
 Nakajima, K., 717  
 Nakamoto, C., 479, 541  
 Nakamura, G.R., 795  
 Nakamura, Y., 121  
 Nakanishi, H., 212  
 Nakhle, B.M., 163  
 Nambiar, K.P., 115  
 Narayan, P., 584  
 Nardi, E., 345  
 Nastri, F., 92  
 Naylor-Olsen, A., 672  
 Nefzi, A., 25, 265  
 Neidigh, J.W., 408  
 Németh, K., 682  
 Nettleton, M., 539  
 Newlander, K.A., 43  
 Neyton, J., 86  
 Nielsen, O.F., 251  
 Niewiarowski, S., 139  
 Niidome, T., 627, 841  
 Nikiforovich, G.V., 361, 453, 477, 487  
 Nischiuchi, Y., 593  
 Nishio, H., 593  
 Nishizawa, N., 333  
 Niwa, M., 321  
 Nojima, S., 667  
 Nokihara, K., 797  
 Nomizu, M., 735  
 Nutt, R.F., 684  
  
 O'Connor, P.M., 547  
 O'Connor-McCourt, M., 372  
 O'Donnell, M.J., 319  
  
 Oaks, E.V., 783  
 Oda, K., 381  
 Odawara, O., 129  
 Oesterhelt, D., 313  
 Ohmori, N., 841  
 Oikawa, S., 717  
 Ojima, I., 216  
 Okada, H., 660  
 Okada, T., 475  
 Oliveira, E., 805  
 Olma, A., 127  
 Ong, L.-H., 775  
 Ono, S., 654  
 Ôrfi, L., 190  
 Orlewski, P., 437  
 Orozco, O., 819  
 Osada, S., 623  
 Oschkinat, H., 545, 551  
 Oslick, S., 445  
 Ostresh, J.M., 25, 58  
 Ötvös, F., 561  
 Otvos, Jr., L., 233, 695, 703, 715  
 Ouyang, X., 834  
 Owens, R.A., 615  
 Oyama, S., 641  
  
 Paegelow, I., 650  
 Pal, D., 753  
 Palgunachari, M.N., 410  
 Palleschi, A., 378, 426  
 Pályi, I., 561  
 Pan, W., 670  
 Pancoska, P., 481  
 Pangborn, W.A., 389  
 Panou-Pomonis, E., 771  
 Papini, A.M., 345, 700  
 Paquet, J.-L., 101  
 Para, K.S., 173  
 Pares-Matos, E.I., 751  
 Park, Y.-W., 66  
 Patarroyo, M.E., 208, 819  
 Patel, H.V., 565  
 Pató, J., 561  
 Patthy, M., 682  
 Pauletto, L., 447  
 Pavel, J., 62, 387  
 Pavone, V., 92, 95  
 Pease, A.M., 233  
 Pedone, C., 92  
 Pedyczak, A., 777  
 Peggion, E., 439, 447, 479  
 Pekar, S.K., 631  
 Pellegirni, M., 402  
 Pellegrini, M., 392, 451

- Pelus, L.M., 178, 192  
 Peng, F., 578  
 Peng, J.-L., 422  
 Pérez-Payá, E., 605  
 Perini, F., 416  
 Perlmutter, P., 485  
 Pessi, A., 86, 396  
 Petrovas, C., 771  
 Pettis, R.J., 845  
 Peyman, A., 181  
 Phillips, M.C., 410  
 Pietanza, M., 459  
 Piha-Paul, S.A., 329  
 Pinilla, C., 761  
 Pinna, L.A., 611  
 Pinzani, D., 700  
 Pipkorn, R., 793  
 Pispisa, B., 186, 378, 462  
 Planas, M., 307  
 Ploegh, H.L., 686  
 Plummer, M.S., 173  
 Podduturi, S., 569  
 Pogozheva, I.D., 530  
 Polese, A., 375  
 Pons, J.-F., 176  
 Porreca, F., 145, 617  
 Potier, E., 186  
 Povšič, L., 188  
 Powers, E.T., 445  
 Powers, S.P., 323  
 Prabhat Arya, 711  
 Prakash, O., 416, 713  
 Prasad Kari, U., 385  
 Preciado-Patt, L., 745  
 Prenner, E.J., 639  
 Préville, P., 335  
 Prokai, L., 834  
 Prokai-Tatrai, K., 834  
 Pruneau, D., 101  
 Prusiner, S.B., 285  
 Puett, D., 584  
  
 Qin, H., 711  
 Qiu, W., 241  
  
 Radford, S.E., 352  
 Rahuel, J., 555, 707  
 Raju, B.G., 253  
 Raman, P., 223  
 Ramanujam, P.S., 89, 169  
 Rao, C., 235  
 Rao-Naik, C., 381  
 Rapi, G., 345, 700  
 Rapp, W.E., 56  
  
 Rasmussen, P.H., 89, 169  
 Ratzkin, B., 631  
 Rau, H.K., 107, 165  
 Razaname, A., 625  
 Rebuffat, S., 435  
 Reddy, H.K., 115  
 Reig, F., 839  
 Reineke, U., 533  
 Reissmann, S., 650  
 Reißmann, S., 261  
 Remmer, H.A., 287  
 Rennard, S.I., 549  
 Renold, P., 445  
 Rich, D.H., 223  
 Ripka, W.C., 684  
 Rivier, C., 737  
 Rivier, J., 637, 737  
 Rivier, J.E., 52  
 Rizo, J., 349  
 Roby, J., 711  
 Rocco, G., 119  
 Rochat, H., 781  
 Roeske, R.W., 297  
 Rogers, H.M., 416  
 Rojas, M., 733  
 Roller, P.P., 547, 582  
 Romanovskis, P., 29, 319  
 Romeo, D., 119  
 Romoff, T.T., 259  
 Roques, B., 535  
 Roques, B.P., 398, 674  
 Rose, T., 799  
 Rosenblatt, M., 392, 402, 439, 447, 479,  
     541  
 Ross, V., 599  
 Rossi, M., 773  
 Rossowski, W.J., 526  
 Rothwarf, D.M., 422  
 Rotondi, K.S., 349, 645  
 Rottenberger, C., 70  
 Rovera, G., 233  
 Rovero, P., 571  
 Rowan, E.G., 593  
 Rowley, D.C., 684  
 Royo, M., 38, 402  
 Rubin, J.R., 173  
 Ruddon, R.W., 416  
 Rudolph-Böhner, S., 313  
 Rühmann A., 553  
 Rutar, A., 188  
 Ruvo, M., 537, 773  
 Ruzza, P., 611  
  
 Saatchi, T., 517

- Sabat, R., 533  
 Sabatier, J.-M., 781  
 Saderholm, M.J., 147, 161, 163  
 Saha, S., 597  
 Sakakibara, S., 1, 593  
 Sakarellos, C., 437, 771  
 Sakarellos-Daitsiotis, M., 437, 771  
 Salazar, L.M., 208  
 Saltiel, A.R., 173  
 Saltmarsh, J., 257  
 Salvadori, S., 473, 603  
 Sanderson, S.D., 549, 713  
 Saneii, H.H., 35  
 Santolini, J., 111  
 Sastry, L., 582  
 Sato, Y., 741, 755  
 Satoh, T., 609  
 Satterthwait, A.C., 202, 441, 795  
 Savva, M., 311  
 Sawyer, T.K., 173, 198  
 Sawyer, W.H., 127  
 Scarallo, A., 537  
 Scarborough, P.E., 381  
 Schaible, U., 289  
 Schaschke, N., 315  
 Scheer, H., 107  
 Scheibler, L., 155  
 Schenck, H.L., 159  
 Schenk, M., 313  
 Scheraga, H.A., 422  
 Scherman, D., 48, 823  
 Scheunemann, K.H., 181  
 Schievano, E., 439, 479  
 Schiller, P.W., 430, 514  
 Schmid, H., 72, 709  
 Schmidt, M.A., 267, 269  
 Schmidt, R., 430  
 Schmitt, J.S., 206  
 Schneider-Mergener, J., 70, 533, 545,  
 551, 769  
 Schoepfer, J., 555, 707  
 Scholten, J.D., 210  
 Schönbach, C., 797  
 Schoner, C.C., 25, 58, 265  
 Schröter, C.J., 763  
 Schwartz, B., 823  
 Schweinitz, A., 261  
 Schwendeman, S.P., 799  
 Schwender, C.F., 204  
 Scocchi, M., 789  
 Scott, W.C., 319  
 Sebolt-Leopold, J.S., 210  
 Segre, A.L., 426  
 Segrest, J.P., 410  
 Seibel, G., 178  
 Seidah, N.G., 676  
 Semple, J.E., 684  
 Seyfarth, L., 261, 650  
 Shafer, J.A., 672  
 Shahripour, A., 173  
 Shainkin-Kestenbaum, R., 745  
 Shan, S., 139, 493  
 Shen, J., 573  
 Shenderovich, M.D., 145, 214, 361, 404  
 Sheriff, S., 578  
 Sherman, S., 416, 713  
 Shiba, T., 717  
 Shigeri, Y., 656  
 Shimasaki, C., 475, 654  
 Shimizu, G.K.H., 711  
 Shimokawa, K.-I., 743  
 Shin Ono, 475  
 Shobana, N., 297  
 Shpritzer, R., 323  
 Shroff, H.N., 204  
 Shteyer, A., 607  
 Shuler, K.R., 210  
 Sia, C., 787  
 Siahaan, T.J., 753  
 Siani, M.A., 643  
 Siddiqui, M.A., 335  
 Sigalat, C., 111  
 Siligardi, G., 543, 571  
 Silva, R.A.G.D., 416, 481  
 Simmons, C., 299  
 Simon, R.J., 301, 643  
 Simpkins, J., 834  
 Singleton, J., 60  
 Sisto, A., 186  
 Skinner, S.R., 275  
 Slate, C.A., 149  
 Smart, O.S., 410  
 Smiley, D.L., 615  
 Smith, D., 739  
 Smith, D.D., 416, 597  
 Smith, H.K., 54  
 Smrcina, M., 317  
 Snigula, H., 107  
 Sogabe, S., 656  
 Sogawa, K., 321  
 Song, S.-Y., 735  
 Sönnichsen, F.D., 747  
 Soomets, U., 662  
 Sospedra, P., 839  
 Spatola, A.F., 29, 133, 319, 617  
 Spetzler, J.C., 41  
 Spiess, J., 553  
 Spindler, J., 70

- Srinivasan, A., 267, 269  
 St. Hilaire, P.M., 46  
 Štalc, A., 188  
 Stankovic, C.J., 173  
 Stark, R.E., 428  
 Starr, M.S., 837  
 Steer, D.L., 194  
 Steinkühler, C., 396  
 Steinmetzer, T., 261, 650  
 Stella, K., 690  
 Stevens, V., 779  
 Stevens, V.C., 799  
 Stevenson, C.L., 828  
 Stewart, J.M., 730  
 Stilz, H.U., 181  
 Stoev, S., 127  
 Striplin, D.R., 149  
 Strome, P., 60  
 Stropova, D., 214  
 Stucky, R.D., 615  
 Stura, E.A., 501  
 Stürzebecher, J., 261  
 Subo Liao, 214, 404  
 Sugihara, G., 841  
 Suguang Sun, 257  
 Sukumar, M., 349  
 Sutton, S., 737  
 Swistok, J., 539  
 Sykes, B.D., 372, 641, 747  
 Szántó, G., 190  
 Szegedi, Z., 190  
 Szende, B., 190
- Tachiki, A., 216  
 Taguchi, H., 660  
 Taguchi, T., 817  
 Takahashi, E., 605  
 Takahashi, T., 131  
 Takahashi, Y., 137  
 Takaku, H., 333, 667  
 Takata, J.S., 178  
 Takiguchi, M., 797  
 Takiguchi, Y., 741  
 Tam, J.P., 19, 229, 231, 235, 247, 249,  
 263, 422  
 Tamura, S.Y., 684  
 Tan, M.M., 828  
 Tang, Y., 143, 491  
 Tani, N., 129  
 Taniguchi, H., 817  
 Tanner, H.R., 35  
 Tao, Z., 578  
 Tarantino, C., 119  
 Tarazi, M., 335
- Tarlton, C.M., 32  
 Tarpley, J.E., 631  
 Tatsu, Y., 656  
 Taylor, J., 463, 578  
 Taylor, J.E., 275, 526, 559  
 Taylor, J.W., 364, 563  
 Teichberg, S., 394  
 Teplán, I., 190, 561  
 Terracciano, R., 186  
 Teshima, T., 717  
 Thalji, M.K., 117  
 Thannhauser, T.W., 422  
 Thøgersen, H., 635  
 Thomas, G., 690  
 Thompson, D.A., 301, 643  
 Thompson, P.E., 194  
 Tian, G.-L., 337  
 Tiraboschi, G., 535  
 Tomatis, R., 473  
 Tominaga, M., 805  
 Tong, H., 408  
 Toniolo, C., 375, 378, 435  
 Torotrella, D., 686  
 Tossi, A., 119  
 Tóth, G., 561  
 Toth, I., 719, 837, 843  
 Tourwé, D., 200  
 Townsend, R., 609  
 Tran, T.-A., 259, 469  
 Trifilieff, E., 443  
 Triozzi, P., 779  
 Tripet, B., 83  
 Trivedi, D., 619  
 Trudelle, Y., 481  
 Tsang, K.Y., 457  
 Tseitin, V.M., 361, 487  
 Tsikaris, V., 437, 771  
 Tsukatani, M., 660  
 Tu, G., 143  
 Tuchscherer, G., 98, 625  
 Tulinsky, A., 680  
 Tullai, J., 501  
 Tungaturthi, P.K., 331  
 Turbyfill, K.R., 783  
 Tuzinski, K., 743  
 Tzartos, S.J., 437  
 Tzeng, S.-R., 565
- Ueno, A., 131, 137  
 Undén, A.E., 244  
 Uno, I., 216, 741, 755  
 Unson, C.G., 511, 613  
 Urbani, A., 396  
 Urry, D.W., 76

- Vacca, J.P., 672  
Vachet, R.W., 109  
Vale, W., 637, 737  
Van Betsbrugge, J., 200  
Van Rietschoten, J., 781  
Vandersteen, A.M., 22  
Varga, I., 703  
Venanzi, M., 186, 378, 426  
Verdoliva, A., 537, 773  
Verducci, J., 111  
Vergelli, M., 700  
Verheyden, P., 200  
Vestal, T.L., 163  
Vetter, S., 72, 709  
Viallefont, P., 176  
Vidson, M., 607  
Villain, M., 255, 803  
Vincze, B., 561  
Vita, C., 86  
Viviani, W., 641  
Vlachoyiannopoulos, P.G., 771  
Voelte, W., 283  
Voelter, W., 394  
Vogel, D., 29  
Vogel, H., 155  
Vogel, K.M., 461  
Vogen, S.M., 713  
Vogt, T., 424  
Volk, H.-D., 533  
Volkmer-Engert, R., 545  
Vorherr, T., 709  
Vunnam, S., 497, 645
- Wachtveitl, J., 313  
Wada, A., 841  
Wagschal, K.C., 83  
Wakselman, M., 378  
Walden, P., 766  
Wallace, B.A., 358  
Wang, C., 355  
Wang, D., 297  
Wang, K.-T., 414  
Wang, R., 573  
Wang, S., 183, 582, 789  
Wang, W., 739  
Wang, Z.-F., 698  
Watts, C.R., 412  
Waugh, D.J.J., 597  
Wehner, V., 181  
Weintraub, S.T., 705  
Weiss, M.A., 369, 471  
Wellenhofer, G., 70  
Wells, T.W., 791  
Welniak, L., 549
- Weltrowska, G., 514  
Wenschuh, H., 239, 289  
Westlin, J., 381  
Weston, B.F., 349  
Westphal, V., 41  
Wheatley, M., 601  
Whitfield, J.F., 599  
Whoriskey, J.S., 631  
Wiegandt-Long, D.L., 617  
Wiesmüller, K.-H., 766  
Wilhelm, R.R., 269  
Wilken, J., 643  
Wilkes, B.C., 430, 514  
Willick, G.E., 599  
Wilson, I.A., 501  
Winther, J.R., 41  
Wirth, H.-J., 485  
Wo, N.C., 127  
Wohlhueter, R.M., 791  
Woltmann, R., 672  
Wong, W.Y., 557  
Woodbine, D., 779  
Woodward, C., 495  
Wright, D.E., 279  
Wright, J.C., 828  
Wrighton, N.C., 501, 569  
Wu, B., 463  
Wu, B.Y., 383  
Wu, C.-R., 511, 613  
Wu, C.-Y., 414  
Wu, J., 834  
Wu, L., 183  
Wu, W.-M., 834  
Wyslouch-Cieszynska, A., 263  
Wysong, C.L., 117
- Xiang, Z.Q., 715  
Xie, H.-B., 337  
Xinhua Qian, 404  
Xu, J.-C., 698  
Xu, Q., 157  
Xu, X., 143, 491  
Xu, Y., 795
- Yagami, T., 295  
Yahalom, D., 621  
Yakubu-Madus, F.E., 615  
Yamada, Y., 735  
Yamaguchi, S., 667, 678  
Yamaguchi, T., 623  
Yamamura, H.I., 145, 214  
Yamauchi, K., 121  
Yamazaki, Y., 311  
Yan, B., 305

- Yan, X., 183  
Yan, Y., 161  
Yang, C.M.C., 557  
Yang, J.J., 113  
Yang, L., 341  
Yang, W., 113  
Yang, Y.-B., 813  
Yang, Y.-K., 580  
Yang, Y.P., 787  
Yao, S.-Y., 733  
Yao, S.Q., 366, 751  
Yao, Z.-J., 183, 775  
Yasuda, E., 755  
Yasuda, T., 129  
Yasutake, H., 654  
Ye, B., 183  
Ye, Y.-H., 337  
Yeagle, P.L., 424  
Yin, Q., 569  
Yoder, G., 375  
Yokoi, T., 660  
Yokum, T.S., 329, 331, 595, 652  
Yoo, B., 497  
Yoshikawa, S., 656, 817  
Yoshimura, T., 475, 654  
Yoshinaga, S.K., 631  
Yu, C., 277, 364  
Yu, Q., 231  
Yuan, W., 723  
Yumoto, N., 656  
Yusuf, C., 461  
Zaccaro, L., 95  
Zamborelli, T.J., 631  
Zanetti, M., 789  
Zanotti, G., 426  
Zelent, B., 430  
Zhang, D.-Y., 337  
Zhang, J., 32, 291  
Zhang, L., 19, 422  
Zhang, M., 463  
Zhang, R., 143, 795  
Zhang, W.-J., 489  
Zhang, Z.-Y., 183  
Zhao, H., 183  
Zhao, M., 369, 471  
Zharikova, A., 834  
Zheng, J., 157  
Zheng, S., 66  
Zhenwei Miao, Z., 143  
Zhou, C., 319

## SUBJECT INDEX

- Abelson kinase, 157  
ABRF, 705  
acetylcholine receptor, 437  
acid chloride, 239  
activation, 11  
adaptor protein, 535  
adhesion, 204  
aerosol delivery, 845  
Ag<sup>+</sup> ion, 19  
aggregation, 394, 807  
agonist, 502  
Aib, 473  
Aib-based peptides, 426  
alkylation, 58, 244  
alkyloxyaryl-keto side chain function, 303  
all D-amino acid peptide, 761  
allelespecific activity pattern, 766  
allophenylnorstatine, 667  
 $\alpha,\alpha$ -disubstituted amino acids, 329  
 $\alpha$ -amino-*n*-butyric acid, 226  
 $\alpha$ -aminoisobutyric acid, 473, 542  
 $\alpha$ -amylase inhibitor, 654  
 $\alpha$ -carbon alkylation, 319  
 $\alpha$ -conotoxin, 226  
 $\alpha$ -endorphin, 284  
 $\alpha$ -helical coiled coil, 141, 147  
 $\alpha$ -helicity, 497  
 $\alpha$ -helix, 115, 131, 137, 361, 364, 461, 463  
 $\alpha$ -helix nucleation, 202  
Alzheimer's disease, 695  
amidation, 249  
amino acid analogues, 253  
amino acid chloride, 239  
amino acid fluorides, 239  
amino acid scanning, 62  
amino acid sequencing, 809  
aminoacyl-resin hydrolysis, 805  
aminolysis, 249  
aminopeptidase A, 674  
aminopyridyl moieties, 672  
amphipathic, 119, 498  
amphipathic  $\alpha$ -helical domains, 595  
amphipathic  $\alpha$ -helical, 119  
amphipathic  $\beta$  strand, 418  
amphipathic peptides, 652  
amphiphilic  $\beta$ -sheet, 563  
amyloid, 137, 353  
analog, 281  
angiotensin, 64  
angiotensin II, 573  
antagonist to VLA-4, 455  
antagonists, 603  
anthracene, 131  
anthranilic acid effect, 555  
anti-adhesin, 557  
anti-carbohydrate antibody, 761  
anti-parallel, 383  
anti-platelet hexapeptide, 741  
anti-V3 response, 793  
antibacterial activity, 703  
antibacterial peptides, 153, 739  
antibody binding, 791  
antidiuretic potencies, 127  
antifreeze proteins, 747  
antigenic domains, 783  
antigenic region, 775  
antigens, 695  
antimicrobial, 385  
antimicrobial activities, 196, 489  
antimicrobial peptides, 119, 497, 652  
antiproliferative drugs, 535  
antitumor activity, 561  
apamin, 226  
apolipoprotein B-100, 418  
apoptosis, 190  
appetite controlling drugs, 578  
arginine peptidomimetics, 688  
asialo-GM<sub>1</sub> receptor, 557  
aspartic acid residues, 656  
aspartic proteinase, 381  
asymmetric Michael-like addition, 241  
14-atom hydrogen bond rings, 106  
ATP-synthase, 111  
automation, 12  
autophosphorylation, 611  
AVP(4-8), 575  
azatide, 23  
azobenzene, 313  
azobenzene-containing peptides, 91, 169  
B<sub>2</sub> BKR agonist, 602  
bacteriophage  $\phi$ K, 475

- bended conformation, 315  
benzodiazepines, 508  
 $\beta$  (12-28), 807  
 $\beta$ -sandwich, 161  
 $\beta$ -structure, 349  
 $\beta$ -casomorphin analogs, 430  
 $\beta$ -cyclodextrin, 807  
 $\beta$ -Dde protecting group, 269  
 $\beta$ -elimination, 307  
 $\beta$ -foldamer, 105  
 $\beta$ -helix conformation, 389  
 $\beta$ -methyl aspartic acids, 293  
 $\beta$ -ribbon, 383  
 $\beta$ -sheet, 159, 383, 394  
 $\beta$ -sheet peptide, 153  
 $\beta$ -sheet protein, 161  
 $\beta$ -sheet/ $\beta$ -turn structure, 154  
 $\beta$ -structure, 137  
betidamino acids, 52  
BIAcore biosensor, 791  
bicyclic structures, 364  
binding, 511  
binding interactions, 543  
binding of peptides to HLA-I, 797  
binding sites, 510  
bioactive peptides, 202, 337  
biodegradable microspheres, 799  
biogenic herbicide, 111  
biological activity, 542  
biosensors, 155  
bipyridine ligands, 109  
BK analog, 602  
Boc strategy, 717  
bovine antimicrobial peptide, 789  
bovine pancreatic trypsin inhibitor (BPTI), 226, 495  
bradykinin, 601  
bradykinin antagonists, 650, 730  
breast cancer mucin antigen, 60  
bromination with NBS, 241  
*Brucella abortus*, 595, 652  
Bruton's tyrosine kinase, 565
- c-Abl, 459  
C-C bond, 345  
c-Crk, 62  
C-glycopeptides, 449  
C-glycosidic linkages, 711  
c-Jun, 751  
C-terminal amides, 327  
cadherin, 113  
cadherin peptides, 753  
caged peptides, 656  
calcineurin, 96  
calcium channel, 321  
calcium-binding, 113  
calmodulin, 167  
calmodulin antagonists, 605  
calmodulin mimetics, 95  
cancer, 210  
cancer vaccine, 60  
*Candida albicans*, 557  
carbohydrate-protein interactions, 711  
carboxy-terminus, 545  
carboxyfluorescein, 289  
cardiotoxin, 414  
carrier, 315  
cathelicidin, 119, 789  
cathepsin D, 670  
cation exchange, 815  
cationic lipids, 823  
cationic peptides, 841  
CCK<sub>8</sub> metabolism, 674  
CD, 115, 121, 151, 392, 416, 447, 479, 543  
CD spectrum, 383, 445  
CD4, 517  
CD4 D1 domain CC' loop mimic, 609  
CD4 functional epitopes, 609  
CD4-MHC class II interaction, 609  
Cdk/Cyclin, 547  
cecropin A-melittin hybrids, 645  
cecropin B-1, 739  
cell adhesion, 113  
cell surface glycoconjugates, 711  
cell-cell adhesion, 753  
cell-permeable peptides, 733  
cell-surface receptors, 141  
cellular import of peptides, 726  
channels, 498  
chaotrope, 815  
charge-transfer complex, 187  
chaybotoxin/zinc-finger chimera, 86  
chemical diversity, 52  
chemical ligation, 301, 333  
chemical synthesis, 414  
chemokine-sized proteins, 643  
Chimeras, 508  
chimeric peptides, 601, 621  
chimeric receptor, 584  
chimeric TASP, 155  
cholecystokinin (CCK)-39, 295  
cholesterol, 639  
circular dichroism, 143, 349, 475, 481  
circular protein, 387  
cis-proline rotamer, 422  
cleavable handles, 307  
cleavage, 278

- coiled-coils, 135  
collagen-mimetic, 80  
combinatorial chemistry, 22, 38, 216  
combinatorial libraries, 25, 54, 58, 265, 605, 761  
combinatorial synthesis, 51  
combinatorial synthetic libraries, 50  
combizymes, 22  
conformational energy, 362  
computational procedure, 362, 487  
computer modeling, 414  
computer simulations, 447  
configuration, 200  
conformation, 143, 202, 402, 428, 439, 447, 479  
conformational analysis, 449, 455, 465, 469  
conformational analysis by fluorescence spectroscopic, 430  
conformational and photophysical study, 378  
conformational calculations, 426, 453  
conformational energy calculations, 420  
conformational epitopes, 819  
conformational flexibility, 325  
conformational mapping, 795  
conformational studies, 392, 491  
conformational switch, 461  
conformational template, 457  
conformations, 143, 202, 439  
congener breaking sets, 253  
conotoxin, 271  
consolidated ligands, 157  
constrained amino acids, 281  
constrained dipeptides, 489  
constrained structures, 378  
convergent solid-phase peptide synthesis, 307  
copper(II)-induced folding, 161  
corticotropin-releasing factor, 553, 737  
coupling reagents, 337  
CRF antagonists, 737  
cross-immunogenicity, 773  
crystal structure of  
  [Lys<sup>17,18</sup>,Glu<sup>21</sup>]glucagon, 620  
crystal structure of  $\alpha$ -thrombin, 680  
crystal structures of glucagon, 619  
cyanylation, 327  
cyclic, 19  
cyclic octapeptide *Axinastatin*, 465  
cyclic peptide libraries, 29  
cyclic peptides, 153, 176, 229, 235, 249, 607, 611, 654  
cyclic peptoids, 206  
cyclic prodrugs of peptides, 825  
cyclization, 19, 43, 50, 223, 280, 291, 387, 439  
cyclization of EDNEYTA, 611  
cyclized bradykinin analogs, 650  
cyclo (CNSNQIC), 609  
cyclodextrin, 315  
cyclohexylalanine, 541  
cyclopeptide, 449  
cyclopropanol, 229  
cyclosporin, 223  
[2,3-cyclopropane amino acids]fMLP analogs, 623  
cysteine, 339  
cysteine-knot motif, 229  
cysteinyl-peptides, 313  
cytotoxic effect, 739  
cytokine, 400, 571  
cytotoxicity, 394  
  
D-amino acid hexapeptides, 605  
D-peptide analog, 769  
D-proline, 159  
de novo design, 83, 95, 145, 155, 165, 173  
de novo protein, 107  
decamer template, 453  
 $\delta$ -opioid receptor, 145  
deltoid protein, 147  
deltorphin, 473  
demyelination in multiple sclerosis, 700  
denaturation, 481  
*Dendroaspis augusticeps*, 593  
*Dendroaspis polylepis polylepis*, 593  
dendrotoxin I, 593  
des-DTPA peptide, 268  
desamino His<sup>7</sup> GLP-1, 615  
desgalactosyl suppressin B, 718  
design, 159, 461  
2,6-diaminopimelic acid, 311  
Difference Minimum Energy  
  Ramachandran Plot (DMER-Plot), 253  
difficult coupling, 223  
difficult sequences, 255  
digestion of peptide antigens, 764  
diketopiperazines, 38, 176  
5-dimethylproline, 422  
dimeric peptide agonists, 569  
dimerization, 101, 751  
dimerization of the EB, 501  
1-(4,4-dimethyl-2,6-dioxocyclohexylidene)ethyl (Dde)  
  protecting group, 719

- diptericin, 703  
discontinuous epitopes, 533  
discrete, 271  
distance geometry, 451, 530  
distance geometry calculations, 479  
disubstituted amino acids, 117  
disulfide bonds, 412  
disulfide bridges, 226, 400  
disulfide-mispaired isomers, 271  
DKP, 38  
dmt-tic  $\delta$  antagonists, 604  
DNA interactions, 131  
DNA-binding peptides, 123  
DNA-encoded library, 50  
2DNMR, 573, 575  
domain structure of p53, 715  
domains, 157  
DPDPE, 214, 404  
drosocin, 703  
DTPA-containing peptides, 268  
dynorphin A, 284  
dynorphin B, 284
- EBV-transformed B cells, 763  
Edman bead sequencing, 56  
electron transfer, 165  
electrophilic azidation, 241  
electrophilic substitution, 303  
Ellman's reagents, 344  
encephalitogenicity, 803  
encoded libraries, 68  
end capping, 115  
endothelial cells, 745  
endothelin-A receptor, 584  
energy calculations, 361  
engineering, 414  
enkephalin, 291  
enkephalin analog, 218  
envelope glycoprotein gp41, 781  
enzymatic assays, 66  
enzymatic specificity, 381  
epidermal growth factor (EGF), 372, 733, 412  
epitope ELDKWA, 777  
epitopes, 551  
epitopes of D15, 787  
EPO insufficiency, 569  
EPOR, 569  
erectile dysfunction, 658  
erectogenic activity, 658  
erythropoietin, 501  
erythropoietin binding protein, 501  
erythropoietin receptor, 569  
ESI-MS, 809
- ESR spectra, 573  
1,2-ethanedithiol, 309  
eukaryotes, 831  
exodus, 643
- F<sub>2</sub>Pmp, 2, 183  
factor X<sub>a</sub>, 261  
fibrin clots, 567  
fibrinogen, 216  
fish antifreeze protein, 747  
fluorescence, 289, 349, 426  
fluorescence spectroscopy, 325  
fluorescent, 331  
fluorescent quenched substrates, 41  
fluoroalkylated muramyl dipeptide analogs, 698  
Fmoc solid phase synthesis, 269  
Fmoc-2-aminopalmitic acid, 345  
Fmoc-solid-phase peptide synthesis, 287, 321  
folding, 135, 143, 349, 352, 369, 443  
formylation, 65  
Fourier transform infrared (FTIR), 481  
Fourier-transform infrared (FTIR) spectroscopy, 385, 418  
furin, 676  
furin substrates, 690  
fusogenic activity, 628  
Fv antibody fragment, 437
- G protein, 511  
G-protein coupled receptors (GPCR), 504, 530, 601  
G-protein interaction site, 662  
GABA<sub>A</sub> receptor, 508  
galanin receptor, 662  
 $\gamma$ -amino acids, 317  
gastric acid release, 526  
gastrin, 315  
gene delivery, 823  
gene transfer, 841  
genome sequence data, 643  
GHRP-6 analogues, 635  
Glanzmann thrombasthenia, 728  
glucagon action, 613  
glucagon amides, 613  
glucagon analogues, 619  
glucagon binding affinity, 614  
glucagon receptor, 511  
glucagon-like peptide-1, 615  
glycoamino acids, 719  
glycopeptide, 46  
glycosylated hydroxylysine, 287  
glycosylation, 287

- GnRH conjugates, 561  
GnRH-endothelin chimeras, 621  
gonadotropin releasing hormone, 621  
gp120, 477  
GPIIb/IIIa antagonists, 195  
GpIIb/IIIa recognition, 755  
gramicidin, 389, 489  
gramicidin S, 153  
gramicidin S and lipid bilayers, 639  
Grb2, 535  
GRB2-SH2, 555, 707  
Grb2-SH2 domain, 582  
Grb2-SH2 domain binding peptide, 582  
green fluorescent protein, 7  
growth factor receptor binding protein 2, 707  
guanylation, 207  
guinea-pig bronchi, 186
- H-bonding, 530  
*H. influenzae* vaccine, 787  
HaCaT cells, 749  
HATU, 297  
HBTU, 297  
hCG folding, 416  
Heck reaction, 279  
HEL cell adhesion, 176  
helical oligoproline, 149  
3<sub>10</sub>-helical peptides, 378  
4 $\alpha$ -helical bundle, 99  
helical structure, 385  
helix dipole, 497  
3<sub>10</sub> helix formation, 375  
helix forming tendency, 125  
helix stabilization, 115  
helix-loop-helix, 95  
hematopoiesis, 178  
hematopoietic synergistic factor (HSF), 192  
hemateregulatory, 192  
heme, 165  
hemoprotein, 92  
hemtoregulatory, 178  
hepatitis B, 537  
hepatitis B surface antigen, 775  
hepatitis C virus, 396  
hepatitis delta antigen, 147  
HER-2/neu, 779  
heregulin, 631  
heterocyclic, 265  
heterocyclic libraries, 25  
heterodimerization, 467  
hexamer, 406  
HF adduct, 65
- hGRF 1-29-NH<sub>2</sub> agonist, 637  
hGRF 1-29-NH<sub>2</sub> antagonists, 637  
hindered bases, 339  
hindered systems, 240  
histidine containing peptides, 257  
histidine racemization, 803  
histocompatibility complex (MHC) class II, 517  
HIV co-receptors, 477  
HIV protease inhibitors, 667, 678  
HIV-1, 441, 781  
HIV-1 gp120, 795  
HIV-1 gp41 fragments, 777  
HIV-1 protease, 333  
HIV-2, 781  
HLA Class I molecules, 797  
hMCI R-binding pocket, 581  
HOE 140 bradykinin antagonists, 101  
Hofmann rearrangement, 218  
holographic, 89  
holographic data storage, 169  
hospopeptides, 424  
HPLC, 370, 486  
HPV16 E7 oncoprotein, 819  
HTLV-I, 785, 799  
human breast cancer, 561, 779  
human bronchial epithelial cells, 549  
human C5a anaphylatoxin, 549  
human CD8, 493  
human endothelin, 358  
human fibroblast growth factor-1, 641  
human immune sera, 775  
human parathyroid hormone, 402  
human parathyroid hormone analogs, 541  
human SRIF receptors, 559  
human- $\alpha$ -Calcitonin gene-related peptide, 597  
hybrid resins, 56  
hydantoin, 329, 331  
hydrolysis, 805  
hydrophobic contaminants, 815  
hydrophobic effect, 409  
hydrophobic folding and assembly, 76  
hydrophobic patch, 707  
hydrophobic peptides, 355, 839  
hydrophobic region, 841  
hydrophobic-hydrophilic balance, 840  
hydrophobic-induced pK<sub>a</sub> shifts, 78  
hydrophobicity scale, 355  
hydroxymethylcarbonyl isostere, 667, 678
- i to i+4 lactam, 451  
ice binding residues, 747

- IgE-mediated diseases, 539  
IgE-receptor, 539  
IL-8, 549  
iminodiacetic acid, 129  
immobilizing phosphatidylcholine, 485  
immunodominant MBP epitopes, 700  
immunogens, 695  
immunoglobulins, 86  
immunologically active component, 188  
immunomodulators, 188  
immunotherapeutics, 517  
implantable device, 828  
inhibition of c-Jun DNA binding, 752  
inhibition of cysteine proteases, 682  
inhibition of nitric oxide synthase, 167  
inhibitors, 204, 262, 335  
Inogatran, 335  
insect glycopeptides, 703  
insulin, 369, 406  
insulin analogs, 471  
insulinotropic, 296  
integrin antagonists, 181  
integrins, 206, 455, 523, 727, 741, 755  
integrins  $\beta_3$ , 726  
interaction, 475  
intercalator, 131  
interleukin-10, 533  
interleukin-1 $\beta$ , 682  
interlocking, 271  
interstitial collagens, 743  
intestinal mucosa, 825  
intracellular pathogen, 652  
intracellular signal transduction, 648  
intracellular signalling pathways, 555  
intramolecular cyclization, 277  
intramolecular disulfide bonds, 343  
ion channels, 410  
iron(II)-braced, 163  
IS4, 491  
islet amyloid, 394  
islet amyloid polypeptide, 394  
isomerization, 314  
isopeptide cleavage, 312  
isopeptides, 311
- JUDY-Procoil, 141
- Kaposi Fibroblast Growth Factor, 726  
kinase inhibitory activity, 547  
kinetics of biomolecular interactions, 791
- L-peptide epitope, 769  
labeling, 290  
lactam, 235, 439  
lactam bridges, 463, 650  
lactam scan, 637  
lactam-type cyclization, 451  
laminin, 735  
lanthionine, 291, 455  
lathyrus odoratus, 46  
leucine zippers, 467  
leukemia cancer cells, 739  
leukocytes, 204  
leuprolide formulation, 828  
Lev-enkephalinamide derivatives, 837  
LHRH agonist, 828  
libraries, 19, 46, 48, 55, 66  
libraries from libraries, 265  
lifetime, 149  
ligands for MHC molecules, 766  
light-absorbing proteins, 107  
lipoamino acid, 837, 843  
lipopeptides, 345, 702  
liposomes, 461  
locked-in fold, 98, 100  
lutropin receptor, 584
- macrocylic, 29  
macrophage migration inhibitory factor, 400  
macrotorials, 29, 133  
MAdCAM-1, 204  
main immunogenic region, 437  
malaria vaccines, 208  
MALDI-MS, 809  
MALDI-TOF, 68  
MALDI-TOF mass spectrometry, 46, 369  
MAP characterization, 809  
marine sponge, 465  
matrix metalloproteinases, 312, 743  
MDP, 188  
melanocortin peptides, 724  
melanocortin receptors, 198, 293, 580  
melanocyte stimulating hormones (MSH), 198  
melanotropin antagonists, 723  
Meldrum's acid, 317  
melittin, 485  
14-membered ring, 104  
membrane associating function, 541  
membrane model, 485  
membrane-interactive, 125  
metal binding, 129  
metal ion-assisted, 249  
metal ion-binding, 135  
metalloprotease, 398  
methionine, 231  
MHC class I binding, 493

- microbial adherence, 557  
midkine, 6  
migration, 269  
Migration Inhibitory Factor (MIF), 301, 400  
mimetic peptide, 503  
mimetics, 212, 279  
mimics, 233  
mimochromes, 92  
minimal functional epitope, 501  
miniprotein, 86  
misfolding, 352  
mitogenic signaling pathways, 733  
Mitsunobu conditions, 341  
mixed connective tissue disease, 771  
mixed  $\mu$  agonist/ $\delta$  antagonist, 430  
model membranes, 639, 839  
model of the human MC1R, 580  
models for partially folded intermediates, 495  
molecular design, 118  
molecular docking, 437  
molecular dynamics, 410  
molecular dynamics simulation, 412  
molecular mechanics study, 431  
molecular mimicry, 761  
molecular modeling, 404, 453  
molecular recognition, 817  
molecular structure of SEL2711, 680  
monoclonal antibody 4A5, 567  
multiphosphorylated synthetic peptides, 695  
muramyl dipeptide, 188  
muscarinic receptors, 586  
mutations, 233  
myasthenia gravis, 437  
myelin, 443  
myelin basic protein, 700, 803  
myristoylation, 537  
  
N-carboxyanhydrides, 259  
N-Dde protected N-glycoamino acids, 720  
N-Dde protected O-glycoamino acids, 719  
N-glycopeptides, 449  
N-glycosylated peptide, 717  
N-methylated amino acids, 341  
N-methylated peptides, 341  
N-terminally truncated, 460  
nanotubes, 104  
naphthylalanine, 807  
native chemical ligation, 459  
natural motif, 139  
  
NDF, 631  
NDF isoforms, 631  
nematode neuropeptide, 327  
nested, 271  
neurokinin receptor, 648  
neurokinin-1 receptor, 432  
neuropeptide Y, 625  
neuropeptides, 749  
N<sub>g</sub>-nitro-argininal ethyl aminal method, 684  
NILIA-CD, 543  
NIR-FT Raman spectroscopy, 251  
NK-1 receptor antagonists, 186  
NLPR, 575  
NLPR binding, 576  
NMR, 392, 402, 409, 416, 422, 426, 432, 439, 447, 451, 479, 483, 489, 505, 567  
NMR spectroscopy, 92, 428, 807  
NMR structure, 441  
NMR structure determination, 372, 463  
NOE analysis, 372  
non viral vectors, 823  
non-immobilised ligand interaction assay, 571  
non-peptide, 216, 517  
non-peptide mimetic, 145, 214  
non-peptide antagonists, 173  
NPY, 578  
NSL-9511, 741  
  
O-glycopeptide, 718  
O-linked glycosylation, 713  
OGP analogues, 607  
oligomers, 169  
oligopeptide substrates, 381  
oligopeptide transport systems, 831  
O $\rightarrow$ N-acyl migrations, 678  
on-resin synthesis, 264  
opiate peptides, 279  
opiates, 514  
opioid, 603  
opioid agonists, 514  
opioid analogues, 617  
opioid compounds, 430  
opioid  $\delta$  receptor, 404  
opioid mimetics, 660  
opioid peptide ligands, 214  
opioid peptides, 284  
opioid receptors, 530, 629, 633  
opioidmimetic peptides, 473  
optical storage, 89  
oral bioavailability, 672  
organophosphorus compounds, 337

- orphanin FQ, 284  
orthogonal ligation, 229, 231, 235, 247  
osteogenic growth peptide, 607  
osteoporosis, 599  
overlapping synthetic peptides, 547  
5-oxazolidinones, 305  
oxytocic agonists, 127  
oxytocin, 226
- p-benzoylphenylalanine, 309  
p21<sup>Cip1/Waf1</sup>, 547  
p53 protein, 715  
paranitroanilide, 297  
parathyroid hormone, 392, 439  
parathyroid hormone analogue, 599  
parathyroid hormone related protein, 451  
PC1, 676  
PDZ domains, 545  
PEGA-resin, 41  
Pelizaeus-Merzbacher disease, 443  
penile erections, 658  
pentafluorophenylalanine, 730  
pepstatin A analogues, 670  
peptide agonist, 145  
peptide aldehyde enzyme inhibitors, 811  
peptide aldehydes, 263  
peptide and peptide-antigen labeling, 763  
peptide antibodies, 779  
peptide antigens, 763, 773  
peptide bond mimic, 200  
peptide bonds, 11  
peptide combinatorial library, 817  
peptide delivery, 843  
peptide epitopes, 799  
peptide epitopes on IpaC, 783  
peptide hapten interactions, 70  
peptide helices, 445  
peptide hydrazides, 39  
peptide immuno-modulators, 845  
peptide libraries, 35, 41, 43, 72, 123, 545, 551, 766  
peptide mapping, 493  
peptide mimetics, 22, 208  
peptide nucleic acids (PNAs), 233, 299  
peptide P115, 571  
peptide separation, 813  
peptide substrates, 713  
peptide synthesis, 259, 285  
Peptide Synthesis Research Committee, 705  
peptide templates, 143  
peptide thioester, 321  
peptide transport families, 833  
peptide vinyl sulfones, 686  
peptide-bilayer interactions, 125  
peptides, 117, 428, 432, 523, 539  
peptidomimetic, 190, 192, 198, 205  
peptidomimetic inhibitors, 670  
peptidomimetic scaffolds, 32  
peptidomimetic Vitronectin receptor antagonists, 181  
peptidomimetics, 15, 32, 194, 463  
peptidyl argininals, 684  
peptidyl-resin hydrolysis, 805  
peptoid, 80, 469  
PGLa, 385  
PH-30 $\alpha$ , 627  
phage display, 70  
phage display library, 70  
phage libraries, 60, 582  
pharmacophore, 192  
pharmacophore model, 178  
Phe-His (i,i+4) helical stabilization, 457  
phosphatase binding peptides, 72  
phosphatase binding sequence, 73  
phosphinate amino acid, 238  
Phospholamban, 709  
phospholipase C- $\gamma$ 1, 520  
phospholipid vesicle binding, 563  
phospholipid-peptide interactions, 639  
phosphoramidate, 237  
phosphonopeptides, 237  
phosphopeptide models, 715  
phosphorazo-method, 297  
phosphorylated PLN, 709  
phosphorylated tyrosine, 705  
phosphorylation of p53, 715  
phosphotyrosine-containing peptide ligands, 707  
photolabile derivatives, 656  
pipecolic acids, 281  
platelet fibrinogen receptor, 755  
platelet integrin receptor, 567  
pleiotrophin, 7  
PNA-peptide chimera, 299  
PNA-peptide conjugates, 299  
point mutations, 443  
polyamines, 48, 54  
polyethylene glycol-polystyrene (PEG-PS), 68  
polyproline, 151  
positional scanning, 25, 58  
pre-sequence, 251  
prediction, 410  
prediction of intramembrane regions, 487  
prion, 285  
Pro-Leu-Gly, 1

- Pro-Pro-Gly, 3  
Pro-X-X-X-Asp-X, 755  
prodrug strategies, 825  
profurin-related peptides, 677  
proline, 151  
proline-containing peptides, 420  
proline-II, 163  
ProPC1-related peptides, 677  
proprotein convertase, 676, 690  
proregion-related peptides, 676  
prostaglandin I<sub>2</sub> production, 745  
prostate cancer, 828  
protease, 396  
protease inhibitors, 238  
proteasme function, 686  
protecting groups, 244, 277  
protection, 11  
protein, 352, 459, 475  
protein binding assays, 46  
protein design, 98  
protein disulfide isomerase, 41  
protein engineering, 76  
protein folding, 139, 471, 495  
protein stability, 83  
protein synthesis, 13, 235  
protein tyrosine kinases, 611  
protein-based inhibitor, 690  
protein-based polymers, 76  
protein-peptide interactions, 533  
protein-protein interactions, 545  
protein-tyrosine phosphatase inhibitors, 183  
proteolipid protein, 443  
PSD/CID, 69  
pseudodipeptide, 29  
pseudopeptides, 29, 208, 607  
PTH, 133  
PTH-related protein, 447  
PTH-related protein (PTHrP), 479  
pyrazinone ring, 660  
pyrrolicin, 703  
pyrrolidinone, 317
- QSAR, 253
- racemization, 259, 323, 339  
radiolabeled derivatives, 561  
radiolabeled LH-RH, 37  
radiolabeling, 684  
RAMP, 141  
random peptide library, 775  
Ras farnesyl transferase, 210  
rat brain sodium ion channel, 491  
rational design, 405  
receptor-bound conformation, 516  
receptors, 257  
recognition, 257  
recombinant serpin  $\alpha$ -1-PDX/hf, 690  
redox, 107  
redox potentials, 313  
redox-separated state (rss), 149  
reductive amination, 329  
refolding, 285  
retro-inverso, 186  
reverse turns, 281  
reversed amide bond, 449  
reversed-phase high performance liquid chromatography, 355  
reversed-phase HPLC packing, 813  
RGD, 216  
RGD-mimetic, 176  
rhGM-CSF, 571  
rhIL-3, 571  
rhodopsin, 424, 504  
ribonuclease A, 422  
ring constrains, 325  
ring opening reactions, 305  
rodent lungs, 845  
Rop protein, 129  
rotational-echo double resonance, 428  
RP-HPLC, 285  
ruthenium (II) complexes, 109
- S,N-acyltransfer, 231  
S-methylation, 232  
S-protected, 277  
S-Xanthenyl, 273  
saccharopeptide synthesis, 719  
salivary statherin, 483  
scaffolds, 52  
scavenger receptor, 121  
Schwesinger base, 319  
screening, 55  
secondary structure, 208, 409, 428  
SEL2711-hirugen-thrombin complex, 680  
selective enzyme inactivation, 645  
selective ligand binding, 586  
self-assembly, 155  
self-encoded library, 63  
self-replicating, 366  
separation of crude peptide, 815  
sequence assisted peptide synthesis (SAPS), 251  
sequential ligations, 301  
sequential oligopeptide carriers, 771  
serine protease inhibitors, 688  
serine proteases, 335

- serum amyloid A, 745  
serum apolipoprotein B-100, 563  
SH2 domains, 459, 520  
SH3 domains, 62, 151, 565  
*Shigella*, 783  
shigella flexneri, 86  
side reactions, 244, 309  
side-chain anchoring, 273  
side-chain hydrophobicities, 84  
side-chain linkages, 364  
signal transduction, 523  
silica reversed-phase columns, 813  
single bead FT-IR, 305  
single-stranded DNA, 475  
SK&F, 178  
SK&F 107647, 192  
skin cell function, 749  
small molecule, 183  
solid phase, 301  
solid phase approach, 43  
solid phase assay, 46  
solid phase organic synthesis, 32  
solid phase peptide syntheses, 38, 233, 337  
solid phase synthesis, 273, 297, 319, 341  
somatostatin, 588  
somatostatin agonists, 559  
somatostatin analogs, 275, 469, 633, 843  
somatostatin receptor, 276  
somatostatin receptor antagonists, 526  
somatostatin receptor-ligand complexes, 588  
somatostatins, 200  
sperm-egg fusion protein, 627  
spin labeling, 573  
spot synthesis, 533, 545  
SPPS, 268, 283, 295, 308, 323, 443  
Src homology, 157  
Src SH2 domain, 173  
SRIF octapeptide analogs, 559  
stabilities, 467  
stabilization, 463  
stepwise solid-phase synthesis, 339  
stereoselectivity, 293, 318  
*Streptomyces tendae*, 654  
structural diversity, 64  
structural template, 139  
structure, 489  
structure control, 117  
structure-activity, 253  
structure-activity relationship, 154, 196  
structure-function analyses, 483  
substitution analogs, 769  
substrate, 396  
sulfamated, 445  
sulfated peptide, 295  
suppressin A, 718  
surface plasmon resonance, 155  
surface plasmon resonance spectroscopy, 817  
synthesis, 289, 432  
synthetic peptide libraries, 56  
synthetic peptide mapping, 609  
synthetic peptide vaccine, 785  
systemic lupus erythematosus, 771  
  
T → R conformational transition, 471  
t-Boc-benz[f]tryptophan, 331  
T-cell epitopes, 787  
TBTU, 323  
template, 445  
template assembled synthetic proteins (TASP), 98, 107, 143, 453, 625  
tendamistat, 654  
tentoxin, 111  
tert-butylproline, 151  
tetanus, 398  
TFA/HCl mixture, 805  
theoretical analysis, 493  
thermal hysteresis activity, 747  
thiazolidine-based phenacyl, 247  
thioester, 19, 121  
thioester couplings, 283  
thioester ligation, 247, 321  
thioester resin, 263  
threshold hydrophobicity, 125  
thrombin, 335  
thrombin inhibitors, 672  
thrombin inhibitory activity, 212  
thyrotropin releasing hormone (TRH), 52  
thyrotropin-releasing hormone analogs, 834  
TMH VII, 586  
Topliss tree, 210  
topological mimics, 773  
4-trans-aminomethylcyclohexanecarboxylic acid, 617  
transducin, 504  
transforming growth factor alpha, 372  
transition state mimic, 678  
transmembrane helices, 487  
transport of peptides, 831  
transthioesterification, 231  
tri-t-butyl-DTPA, 267  
trimethylsilylpropionic acid, 807  
triple helical, 80, 523  
triple helical state, 122

- tripod protein, 163
- trisulfide, 275
- trisyl azide, 241
- trityl resins, 261
- TRNOE, 504
- tropane, 194
- truncated bacteriorhodopsin, 586
- tryptophan, 325
- tumor, 190
- tumor cell interactions, 523
- tumor therapy, 555
- two-stranded  $\alpha$ -helical coiled-coil, 83
- type 2 SRIF receptor, 526
- tyrosine derivatives, 660
- tyrosine kinase, 66
- tyrosine kinase inhibitors, 190
- tyrosine O-sulfate, 295
- tyrosine phosphorylation, 520, 705
  
- UNCA, 259
- unnatural peptide synthesis, 319
- unnatural peptides, 123
- unphosphorylated PLN, 709
- unprotected peptide, 247, 301
- unusual hydrogen bond rings, 105
- urea herbicides, 70
- ureas, 218
  
- ureidopeptides, 218
- urocortin, 553
- uronium salts, 283, 323
  
- V<sub>1a</sub>-selective VPR antagonist, 602
- V<sub>2</sub> agonists, 127
- V3 loop, 441, 477
- V3 peptides, 793
- varied lipopolyamines, 48
- vasoactive intestinal peptide, 749
- vasodilator, 597
- vasopressin, 127, 601
- vibrational CD, 375
- viral protein domains, 537
  
- WW domains, 2, 387, 551
  
- X-linked agammaglobulinemia, 565
- X-ray structure, 358
- xanthenyl group, 343
  
- Y-1 NPY receptor antagonists, 578
- Y2 receptor, 625
  
- zinc, 406
- zinc endopeptidase, 398
- zinc-finger, 86

---

# Peptides

## Frontiers of Peptide Science

Proceedings of the Fifteenth American Peptide Symposium

James P. Tam and Pravin T.P. Kaumaya (Eds.)

This volume contains the proceedings of the Fifteenth American Peptide Symposium (15APS) held in Nashville, Tennessee, on June 14-19, 1997. This biennial meeting was jointly sponsored by the American Peptide Society and Vanderbilt University. The American Peptide Symposium is the most important international peptide meeting, and attracts the largest number of attendees and attention. The attendance of 1,081 participants from 37 countries was lower than the two previously held symposia. However, the number of participating countries was the largest. Thus, it was gratifying to see that this meeting retained both its international flavor and participant loyalty at a time when there are many more symposia held each year on similar subjects.

The scientific program was comprised of 124 oral and 550 poster presentations. These presentations together with those from selected poster presentations are included in this proceedings volume. Together they constitute the most up-to-date advances in peptide science.

KLUWER/ESCOM

